Cyclic Polymers
(second edition)

Edited by J. Anthony Semlyen

CYCLIC POLYMERS

CYCLIC POLYMERS
(Second edition)

Edited by

J. ANTHONY SEMLYEN

University of York, U.K.

Created in the United States of America

Visit Kluwer Online at: http://kluweronline.com
and Kluwer's eBookstore at: http://ebooks.kluweronline.com

CONTENTS

PREFACE

The first edition of "Cyclic Polymers" was published by Elsevier Applied Science Publishers in 1986. It consisted often chapters reviewing the advances that had been made in a new area of Polymer Science, where macromolecules are based on large ring molecules rather than long chain molecules. There have been important developments in the subject since then and this second edition of "Cyclic Polymers" describes many of them in sixteen chapters dealing with both synthetic and biological cyclic polymers.

In this second edition, some of the developments in cyclic polymer chemistry over the past forty years are outlined in Chapter 1 and fundamental differences between the properties of large ring molecules and long chain molecules are discussed. In the following three chapters, the importance of cyclic structures in biological macromolecular science is strikingly demonstrated by detailed reviews of circular DNA, cyclic peptides and cyclic oligosaccharides and polysaccharides. The preparation and properties of synthetic cyclic polymers are covered in a series of chapters on cyclic polysiloxanes, large cyclic ethers and ether-esters and other organic cyclic polymers. The importance of ring-opening polymerization reactions to produce commercially valuable linear polymers is emphasised in chapters on cyclic polycarbonates and cyclic polyesters and on cyclic oligomers used to prepare high performance polymers. Cyclic inorganic oligomers and polymers are described in a separate chapter. A fundamental difference between large ring and long chain molecules is the ability of the rings to form catenanes and rotaxanes and advances in both these are described in separate chapters in this book. Two techniques that have been found to be particularly useful for investigating synthetic cyclic polymers are neutron scattering and nuclear magnetic resonance spectroscopy and a chapter is devoted to outlining the applicability of both these methods. Another chapter describes the role of cyclization in network formation. Finally, theoretical aspects of cyclic polymer properties are reviewed in the last chapter of the book.

Two aspects of the subject of large ring molecules and cyclic polymers are especially noteworthy. The first is its multidisciplinary nature, so that cyclic polymers may be based on organic, inorganic or biological macromolecules and subjects such as chemistry, physics, biology, materials science, engineering and computer science are all involved. The second aspect results from the unique topology of large ring molecules, which has been exploited so effectively by nature (for example with circular DNA, which supercoils, catenates and forms permanent knots in different natural living systems).

A most encouraging feature of this new, rapidly developing subject of cyclic polymers has been the world-wide cooperation it has engendered. The editor of this book alone has had the privilege of working with over 150 coworkers and coauthors drawn from five continents. The authors contributing to this book come from Algeria, Canada, England, France, Japan, Roumania, the United States of America and Wales. Scientific research is one activity where co-operation rather than competition can result not only in greater material achievement but also it can enhance international understanding.

The editor of this book would like to thank all the authors who have contributed to it so effectively, as well as his coworkers at York, Dr Barry Wood and Dr Caroline Hamilton, for their dedicated help in its final preparation.

With more and more large ring molecules and cyclic polymers being prepared, characterised and investigated year by year in biological as well as synthetic macromolecular systems, the future of the subject of cyclic polymers seems well assured as we advance into the twentyfirst century.

J Anthony Semlyen
University of York 1999

CONTRIBUTORS

Chapter 1
Dr J A Semlyen
Department of Chemistry
University of York
York YO10 5DD
UK

Chapter 2
Professor Alexander Vologodskii
New York University
Department of Chemistry
New York
NY 10003
USA

Chapter 3
Dr John S Davies
University College Swansea
Department of Chemistry
Singleton Park
Swansea
W Glamorgan SA2 8PP
Wales

Chapter 4
Professor Shinichi Kitamara
Kyoto Prefectural University
Department of Agricultural Chemistry
606 Shimogamo
Kyoto
Japan

Chapter 5
Dr Stephen J Clarson
College of Engineering
644 Baldwin Hall
University of Cincinnati
OH 45221-0018
USA

x

Chapter 6   Dr Daniel J Brunelle
GE Corporate Research & Development
General Electric Company
Bldg CEB, Room 130
PO Box 8
Schnectady
NY 12301
US

Chapter 7   Dr Colin Booth and Professor Colin Price
Department of Chemistry
University of Manchester
Oxford Road
Manchester
M13 9PL
UK

Chapter 8   Dr Barry R Wood and Dr S Caroline Hamilton
Department of Chemistry
University of York
York YO 10 5DD
UK

Chapter 9   Professor Allan S Hay and Dr Yong Ding
Department of Chemistry
McGill University
801 Sherbrook St W
Montreal
PQ H3A 2K6
Canada

Chapter 10   Professor Jacques Roovers
Institute for Environmental Chemistry
National Research Council of Canada
Ottawa K1A 0R6
Canada

Chapter 11   Dr Peter C Griffiths
School of Chemistry and Applied Chemistry
University of Wales Cardiff
PO Box 912
Cardiff CF1 3TB
Wales

Chapter 12   Professor Harry W Gibson and Dr Eric J Mahan
              Department of Chemistry
              Virginia Polytechnic Institute and State University
              Blacksburg
              VA 24061-0212
              USA

Chapter 13   Dr David A Leigh and Mr Richard Smith
              Department of Chemistry
              University of Warwick
              Coventry
              CV4 7AL
              UK

Chapter 14   Professor Ionel Haiduc
              Facultatea de Chimie
              Universitatea "Babes-Bolyai"
              RO-3400
              Cluj-Napoca
              Roumania

Chapter 15   Professor R F T Stepto and Dr David J R Taylor
              Manchester Materials Science Centre
              University of Manchester & UMIST
              Grosvenor Street
              Manchester
              M1 7HS
              UK

Chapter 16   Professor Ulrich Maschke
              Laboratoire de Chimie Macromoleculaire
              UA-CNRS No 351
              Université des Sciences et Technologies de Lille
              F-59655 Villeneuve d' Ascq Cedex
              France

              Professor Mustapha Benmouna
              University Aboubakr Belkaid
              Institute of Physics
              Bel Horizon BP119
              13000 Tlemcen
              Algeria

Contributors Biographies

Authors are listed in the order in which they appear in the book

J Anthony Semlyen was a Gibbs Scholar, Salters Scholar and Domus Senior Scholar at Merton College, Oxford until 1962 and a Research Lecturer at Christ Church, Oxford in 1963 and 1967. He obtained his MA, BSc and DPhil degrees at Oxford under the supervision of Dr Courtenay S G Phillips. From 1964 to 1966, he was a Fulbright Scholar with Professor Paul J Flory at Stanford University, California. Since 1967, he has been at the University of York. He has edited *Cyclic Polymers* (Elsevier Applied Science, 1986), co-edited *Siloxane Polymers* (Prentice Hall, 1993) with Dr Stephen J Clarson and edited *Large Ring Molecules* (John Wiley & Sons, 1996). His research interests are large ring molecules and cyclic polymers and he has published research papers, reviews and books on these topics with the active collaboration of over 150 co-workers and co-authors drawn from five continents

Alexander Vologodskii received his PhD in Molecular Biophysics at Moscow Physical Technical Institute in 1975. He spent the next 16 years in the Institute of Molecular Genetics, Moscow. In 1985 he received the higher Russian scientific degree, Doctor of Science, at Moscow University. He was a visiting scientist at University of California at Berkeley in 1992-1993 and now is Research Professor in the Department of Chemistry at New York University. His research interests include conformational properties of nucleic acids, particularly properties of circular DNA molecules. He authored the book *Topology and Physics of Circular DNA* (1992) and more than 70 research papers.

John S Davies received his BSc and PhD degrees from the University of Wales, Swansea, before post-doctoral work with John C Sheehan at MIT, Cambridge Massachusetts. He returned to Swansea as junior lecturer in 1964, joining the research team of Professor Cedric Hassall on peptide antibiotics and general peptidomimetic work. This led to setting up his own research group on the synthesis/modifications of cyclic peptides and cyclodepsipeptides, carbohydrate derivatives on amino acids, and an interest in the chiral analysis of peptides. He has reviewed annually for a number of years, the literature on cyclopeptides and cyclodepsipeptides for the Royal Society of Chemistry's Specialist Periodical Reports on *Amino Acids, Peptides and Proteins.* He is currently the Senior Editor of

this Specialist Periodical Report, and Senior Lecturer in the Department of Chemistry at Swansea.

Shinichi Kitamura received his PhD in Agricultural Chemistry from Kyoto University in 1984. From 1985 to 1987 he was a Postdoctoral Fellow at Yale University with Professor Julian M Sturtevant. He is now Lecturer in Chemistry of Biological Macromolecules at Kyoto Prefectural University. His research interests include bioactive carbohydrates, protein-carbohydrate interactions, and biochemical applications of calorimetry.

Stephen J Clarson is a Yorkshireman by birth but currently resides in the Cincinnati area with his wife, their two daughters, four Himalayan Persians and two Mini Lops. He obtained his DPhil in Chemistry at the University of York, England in 1985 where he studied with Dr Tony Semlyen. He then spent the summer at the Institute of Macromolecular Chemistry, Prague before taking up a postdoctoral appointment with Professor James Mark. In the spring of 1988 he joined the faculty of the Department of Materials Science and Engineering at the University of Cincinnati and is currently Assistant Dean for Educational Development in the College of Engineering. Dr Clarson has received numerous awards for his teaching including the Neil Wandmacher Excellence in Teaching Award in 1993 for 'Most Outstanding Teacher in the College of Engineering', the TEXNIKOI Award in 1992 for 'Outstanding Teaching and Service to the College of Engineering' and the Engineering Tribunal Award, for the 'Outstanding Teacher of the Quarter', Spring Term, 1992 and Spring Term, 1995. Dr Clarson has also published over one hundred technical articles and co-authored the text 'Siloxane Polymers' with Dr Tony Semylen, which was published in 1993. Due for publication in 1999 is the text 'Silicones and Silicone-Modified Materials'. The research carried out in his group has led to a number of inventions and he holds three US patents. His current scientific research interests include polymer synthesis, organosilicon chemistry, cardiovascular biomaterials and plasma polymerization.

Daniel J Brunelle received a BS degree from Emory University in 1970. He received his MS and PhD degrees from The John Hopkins University in 1972 and 1974. He then carried out postdoctoral research on total synthesis and synthetic methodology with Professor E J Corey at Harvard University for two years. After joining GE Corporate Research and Development in 1977, he began work on a number of organic and polymer-chemistry problems. Specific areas of interest include synthesis and ring-opening polymerization of cyclic oligomers, high temperature phase transfer catalysis, mechanisms of catalysis, and new methods of polymer formation, with special emphasis on polycarbonates, and polyetherimides. He is an inventor on over 75 patents, has published more than 70 research papers, and was the editor of the volume "*Ring Opening Polymerization,*" published in 1993.

Colin Booth completed his PhD in Chemistry under the direction of Professor Geoffrey Gee at the University of Manchester in 1956. After working with R L Scott at UCLA he spent four years with Shell Chemical Co, Synthetic Rubber Division, California, before returning to Manchester as Research Fellow, subsequently to join the teaching staff. His present position is Reader in Polymer Science. He was editor, with Colin Price of Volume 1 (Polymer Characterisation) and 2 (Polymer Properties) of Comprehensive Polymer Science (1989), reflecting his lifelong interest in this area. His present research interests include the aqueous solution properties of block copolyethers (including the gel state), particularly the effect of block and chain architecture, and the solid state properties of uniform cyclic oligo(oxyethylene)s (large unsubstituted crown ethers) and of cyclic poly(oxyethylene)s.

Colin Price obtained his PhD in Chemistry from the University of Manchester in 1964. He then joined the teaching staff at Manchester where he is now Professor of Polymer Chemistry and Head of the Department of Chemistry. He has published some 200 papers on polymer synthesis, characterisation and properties. He is the joint editor of Volumes 1 and 2 of Comprehensive Polymer Science. For his work on the microstructure, supramolecular structure and phase behaviour of block copolymers in bulk and solution, and for studies on rubber elasticity, he received the 1991 RSC Award for Macromolecules and Polymers. His present extensive programme of research on copolymers is carried out in collaboration with other members of the Manchester Polymer Centre, and with groups in industry and other universities, both in the UK and abroad. He is also engaged in research on new routes to aqueous polymer dispersions including water borne zirconium ionomers.

Barry R Wood graduated in 1986 with a BSc (Hons) degree in Applied Chemistry from Thames Polytechnic (now the University of Greenwich). He obtained an MSc degree in Polymer Science at North London Polytechnic (now the University of North London) and a PhD degree from Brunel University in 1990 working with Professor Michael Folkes on electrically conducting colloidal dispersed gold-polymer composites. He has spent the last nine years as a research fellow at the University of York working with Dr J A Semlyen preparing and studying large cyclic esters and ether-esters.

S Caroline Hamilton gained her first degree in Chemistry at the University of York and an MSc with distinction in Materials Technology from Napier University in Edinburgh. She spent six months at BNFL, Springfields in the solid oxide fuel cell group. She obtained her DPhil degree at the University of York, where she investigated large ring esters and ether-esters under the supervision of Dr Tony Semlyen. Her hobbies include playing field hockey and computers. With Dr Barry Wood, she runs a part-time computer business ("Ecky Thump Computers").

Allan S Hay was born in Edmonton, Alberta, Canada. Dr Hay received a BSc and MSc in Chemistry from the University of Alberta (1950, 1952). In 1955 he received his PhD in Organic Chemistry from the University of Illinois and then joined the staff of the GE Research

Laboratory in Schenectady, NY. In 1956 he discovered a new method of polymerization, "polymerization by oxidative coupling" which afforded high molecular weight poly(phenylene oxide)s by direct catalytic oxidation of phenols at room temperature. This led to the development of GE's **PPO®** and **Noryl®** thermoplastic resins. These polymers today are manufactured by several companies worldwide with annual sales above $1 billion per year. In 1968 he became manager of the Chemical Laboratory in the Research and Development Center of GE. In 1980 he was appointed to the position of Research and Development Manager, Chemical Laboratories where he directed the work of 220 scientists and engineers engaged in exploratory chemistry, process chemistry, chemical engineering, polymer physics and engineering, electrochemistry, biotechnology, and electronic materials. In September 1987, Dr Hay accepted the GE/NSERC Industrial Research Chair of Polymer Chemistry at McGill University. Research on oxidative coupling chemistry has continued, however, the major focus of the research has been: (1), synthesis of amorphous, thermooxidatively stable polymers with very high glass transition temperatures which remain soluble and processable; (2), the development of novel methods for crosslinking these soluble polymers to make them insoluble, which makes them attractive as materials for use in the aerospace and electronic industries; (3), synthesis of novel cyclic precursors to some of these high performance polymers, which potentially makes them attractive as high temperature adhesives, coatings, and as matrix resins for advanced composites. Dr Hay was elected a Fellow of the Royal Society of London in 1981 and received the Society of Plastics Engineers International Award in 1975. In 1971 he was elected a Coolidge Fellow of General Electric. In 1984 he received the Achievement Award of the Industrial Research Institute and in 1985 was made a Chemical Pioneer of the American Institute of Chemists. He received the Carothers Award in 1985. In 1987 he was awarded an honorary DSc degree from his alma mater, the University of Alberta. In 1992 he was made an Honorary Professor, Dalian University of Science and Technology, Dalian, China. In 1997 he was awarded the Tomlinson Chair in Chemistry. He is the author of more than 250 publications and patents.

Yong Ding is a polymer scientist at Innovative Membrane Systems, Praxair Inc, Norwood, MA. He obtained his PhD degree in Polymer Chemistry with Professor Allan S Hay from McGill University. Then he moved to the University of Arizona, working with Professor H K Hall Jr as a postdoctoral fellow. His research activities include the synthesis, characterization and application of polymers, and oligomers.

Jacques Roovers received his PhD in Polymer Chemistry from the University of Louvain with G Smets (1962). After postdoctoral work with S Bywater in Ottawa and at the University of Louvain, he joined the National Research Council in Canada in 1966. In 1977-1978, he took a sabbatical with W W Graessley at Northwestern University. He did work on anionic polymerization and is interested in the use of anionic polymerization for the synthesis of model polymers with long-chain architectural features. Emphasis is placed on the relation between the large-scale structure of polymers and its effect on their dilute solution

properties and melt theology. He is presently also adjunct professor at the University of Athens.

Peter Griffiths obtained his BSc(Hons) degree in Chemistry from the University College of North Wales in 1988. He then moved to Bristol and under the guidance of Professor T Cosgrove, undertook his PhD degree in the area of polymer diffusion. After postdoctoral periods in Bristol and then at the Royal Institute of Technology, Stockholm working with Professor P Stilbs, he took up his present position in Cardiff in 1985. His research interests include polymer solutions, polymer-surfactant interactions and the structure and dynamics of adsorbed polymer layers.

Harry W Gibson was born in Syracuse, NY, USA and grew up in the Adirondack Mountains of northern New York State, close to the Canadian border and ca 60 miles from Montreal. He received his BS (1962, with distinction) and PhD (1966) degrees in Chemistry from Clarkson University where his thesis under the direction of Professor Frank D Popp was based on alkaloid syntheses. From 1965-66 he was a postdoctoral research associate of Professor Ernest L Eliel at the University of Notre Dame (IN), where he carried out stereochemical studies, primarily on acyclic molecules. From 1966-69 he was employed as a research chemist at Union Carbide Corporation in Tarrytown, NY, where he did research on uses of formic acid and carried out kinetic and mechanistic studies of reactions of alcohols with epoxides. From 1969-1984 he advanced up the technical ladder to Senior Scientist at Xerox Corporation in Webster, NY and was involved in studies of liquid crystals, triboelectric charging, photoconduction and dark conduction and the synthesis of materials for use in these technologies. In 1984 he joined Signal Corporation in Des Plaines, IL, which later merged to become Allied Signal, as Senior Research Scientist; there he was concerned with polymers for printed wiring boards and membranes. In 1986 he assumed his present position as Professor of Chemistry at VPI&SU. Professor Gibson has published more than 275 original research papers, chapters and reviews, is listed as inventor on 32 US patents and has delivered more man 145 invited lectures worldwide. Currently his research interests include rotaxanes, polyrotaxanes, hyperbranched and dendritic polymers, self assembly processes, liquid crystalline materials and "living" radical polymerizations. During his 12 years in academia Professor Gibson has supported and supervised the research of 26 undergraduates, 12 PhD, 8 MS graduates and 16 postdoctoral fellows in his laboratories. Currently 1 undergraduate, 3 PhD students and 2 postdoctoral fellows work under his direction.

David Leigh carried out his PhD studies on novel macrocyclic trichothecenes in the research group of J Fraser Stoddart at the University of Sheffield from 1984-1987. He then spent two years investigating carbohydrate-protein interactions as a Research Associate with David Bundle at the National Research Council of Canada (NRC) laboratories in Ottawa before returning to the UK to a Lectureship at the University of Manchester Institute of Science and Technology (UMIST) in 1989. In 1996 he was promoted directly to Reader and in October 1998 he simultaneously took up the Chair in Synthetic Chemistry and an EPSRC

Advanced Research Fellowship in the Centre for Supramolecular and Macromolecular Chemistry at the University of Warwick. His research interests include novel molecular architectures and their applications in materials.

Richard A Smith obtained his BSc(Hons) degree in Chemistry from the University of York in 1996. He men joined the research group of Professor David Leigh at the University of Manchester Institute of Science and Technology (UMIST) to begin his PhD on developing a synthetic route towards a "true" polycatenane ([n]catenane). In 1998 he moved to the University of Warwick with Professor Leigh to complete his final year.

Ionel Haiduc is Professor at "Babes-Bolyai" University, in Cluj-Napoca, Roumania. He obtained his PhD in Moscow with Professor K A Andrianov with a thesis in Organosilicon Chemistry, was a Fulbright Postdoctoral Fellow with Professor Henry Gilman at Iowa State University (1966-1968) and with Professor R Bruce King at the University of Georgia, Athens, Georgia (1971-1972). He was Visiting Professor at Instituto de Quimica, Universidad Nacional Autonoma de Mexico (1993-1994), University of Texas at El Paso (1997) and Universidad de Santiago de Compostela, Spain (1998). He received a Humboldt Fellowship for a reasearch visit at Universitat Magdeburg, Germany (1997) and the Gauss Professorship of the Akademie der Wissenschaften in Gottingen, Germany (1998). He also received visiting grants from the National Science Foundation (USA, 1992), European Community (Spain 1993) and British Council (United Kingdom, 1995) and a NATO Cooperative Research Grant (United Kingdom, 1997). He authored or co-authored several books (including *The Chemistry of Inorganic Ring Systems, 1970, The Chemistry of Inorganic Homo- and Heterocycles, 1987; Basic Organometallic Chemistry, 1985, Organometallics in Cancer Chemotherapy, 1989, 1990 and Supramolecular Organometallic Chemistry, 1998 in press)* and more than 250 research papers and several chapters in some multi-authored books. His interests cover inorganic ring systems, Main Group Organometallic and coordination chemistry, organophosphorus and organoarsenic ligands and Supramolecular Organometallic chemistry. He participated in an extensive international collaboration with colleagues from United Kingdom, Germany, Spain, Mexico, Belgium, United States of America, Brazil, Canada, France, which resulted in numerous joint publications. After the anti-communist revolution in Roumania (December 1989) he was elected and served as Rector (President) of "Babes-Bolyai" University (1990-1993), and in 1998 was elected Vicepresident of the Roumanian Academy.

Robert Stepto obtained his BSc degree in Chemistry (with Special Honours in Physical Chemistry) and his PhD degree studying the Diffusion of Polymers in Solution from the University of Bristol. He moved to UMIST in 1961 as a Research Fellow in Polymer Crosslinking in the Department of Polymer and Fibre Science. He was subsequently appointed to the teaching staff and eventually to Professor of Polymer Science in the Materials Science Centre, UMIST. He was awarded a DSc

by the University of Manchester in 1987 for his work on Statistical Studies in Polymer Science. Robert Stepto's research activities are in the area of the physical chemistry of polymers including polymerisation statistics, intramolecular reaction and gelation; the formation, structure and properties of polymer networks; polymer solutions and mixtures, covering diffusion, scattering, phase behaviour and intrinsic viscosity; computational studies of polymer chain behaviour; and the thermoplastic processing of starch and starch materials. He has well over 200 research publications to his name and has recently edited a book on Polymer Networks. He received an Interphex Award for Innovation in production in the Pharmaceutical Industry for his work on starch processing. He is currently the European Editor of Computational and Theoretical Polymer Science, Secretary of the Polymer Networks Group, Chairman of the IUPAC Commission on Macromolecular Nomenclature and Vice-President of the Macromolecular Division of IUPAC.

David Taylor earned a BSc(Hons) in Polymer Science and Technology (Chemistry) at the University of Manchester Institute of Science and Technology (UMIST). During a subsequent period of employment in the plastics processing industry, David also continued his theoretical research into the molecular origins of elastomeric behaviour, eventually leading to the award of an MSc degree in 1995. He then returned to UMIST as a Research Associate, and has since been engaged in theoretical studies of polymer network formation, structure and properties, under the guidance of Professor Bob Stepto. In 1996 David was a visiting scientist in the Polymer Group at Biosym/MSI (now Molecular Simulations Inc) in San Diego.

Ulrich Maschke studied Chemistry at the University of Mainz (Germany) where he received his Diploma in 1989 working on miscibilities of polymer mixtures. In 1992 he finished his PhD thesis (Static and dynamic properties of polymer melts studied by neutron scattering) at the Max-Planck-Institut für Polymerforschung in Mainz with Professor B Ewen and Professor E W Fischer. In the fell of 1992 he joined the French National Center of Scientific Research (CNRS) as a Research Associate (Chargé de Recherche) at the laboratory of macromolecular chemistry at the University of Lille, France. His current research interests include the synthesis and analysis of materials composed of liquid crystals and polymers (polymer dispersed liquid crystals). He is working together with Professor Mustapha Benmouna and his group of the University of Tlemcen (Algeria).

Mustapha Benmouna earned a BS degree in Physics at the University of Algiers in 1969 and in Electrical Engineering in 1971 in Paris. He obtained a Master's degree in 1977 and a PhD in 1979 at the University of Michigan (Ann Arbor, USA) in 1979 with Professor Ziya A Akcasu. In 1984, he earned a PhD in Physics at the University of Strasbourg (France) with Professor Henri Benoit working on the static and dynamic scattering properties of polymer mixtures and copolymers. He joined the University of Tlemcen in Algeria in 1981 as an associate professor and was appointed full professor in 1986. He was visiting professor of several universities in Europe (University of East Anglia, England, 1986;

University of Konstanz, Germany, 1987; University of Strasbourg, France, regularly from 1984 – to date, University of Lille, France, 1996 and 1998) and United States (University of Michigan, 1986; National Institut of Standards and Technology, Gaithersburg, Maryland and the University of Maryland, 1995, Tulane University, New Orleans, 1995). Since 1990, he became a regular visiting professor of the Max-Planck-Institut für Polymerforschung (Mainz, Germany) collaborating with Professor E W Fischer, Professor Thomas A Vilgis, Professor Bernd Ewen and Professor Adam Patkowski. Recently, he joined the group of Professor Kurt Kremer as a visiting professor. Since 1995, he became interested in the properties of polymer dispersed liquid crystals and started a programme of collaboration between the University of Tlemcen and the University of Lille collaborating with Dr Ulrich Maschke and Professor Xavier Coqueret. This collaboration is supported by both the CNRS in France and the Ministry of Education in Algeria.

CHAPTER 1
INTRODUCTION : CYCLIC POLYMERS - THE FIRST 40 YEARS

J. Anthony Semlyen,
University of York, UK

1.1 Preparation and characterisation of cyclic oligomers and polymers

1.1.1 Early investigations of large cyclics

Some 40 years ago in November 1959, the author was given a tutorial assignment on synthetic polymers. His tutor at Merton College, Oxford, Dr. Courtenay Phillips recommended Paul Flory's book *"The Principles of Polymer Chemistry"*[1]. The book describes how polymeric materials such as plastics, rubbers and fibres are constructed from long chains of covalently bound atoms. The resultant long chain molecules may consist of tens of thousands or even hundreds of thousands of atoms. This was established by Hermann Staudinger in his macromolecular hypothesis, despite the opposing views that polymeric materials were either ring molecules or were colloidal aggregates of smaller molecules held together by secondary forces in micellar structures (see, for example, Ref [1] [2]). While reading *"The Principles of Polymer Chemistry"*, the author noticed that the largest well characterised ring molecules described in the book had only 24 skeletal bonds. Further reading showed that there was a gap in chemistry waiting to be developed, namely the preparation, characterisation, investigation and possible application of large ring molecules with more than 30 skeletal bonds as well as synthetic cyclic polymers with more than 100 skeletal bonds. The author's main aim in chemistry since that time was to try and establish this new subject area both in collaboration with and alongside other research chemists in this general area. The first edition of *"Cyclic Polymers"* was published some 27 years later in 1986 [3]. In the book, 14 authors described the advances that had been made in the chemistry of both synthetic and biological cyclic polymers.

The subject of cyclic polymers effectively began with a paper by Jacob and Wollman [4] about 40 years ago in 1958, who concluded that the genetic map of bacterial chromosomes of Escherichia coli showed circularity. Further evidence for the existence of circular DNA was soon established [5] [6] and final confirmation came from electron microscopy of øX174 DNA [7] (see chapter 7 in Ref. [3]). The discovery of large cyclic molecules in natural biological systems is described in Ref. [3] as well as in a more recent book [8] in chapters by Andrzej Stasiak, Harold Scheraga and David Brant and also in this book.

2

At the time when the first papers on circular DNA molecules were being published, there was an upper limit of about 30 skeletal bonds for well characterised large synthetic ring molecules. The pioneering researches of Wallace Carothers on high polymeric substances is described in his collected papers [9]. They show how important new polymers including linear polyamides and linear polyesters were prepared and characterised. In addition, a number of large ring molecules were prepared for the first time such as many-membered cyclic esters and anhydrides. An example of the largest is the macrocyclic ester, decamethylene octadecanedioate (Figure 1), which has 30 skeletal bonds.
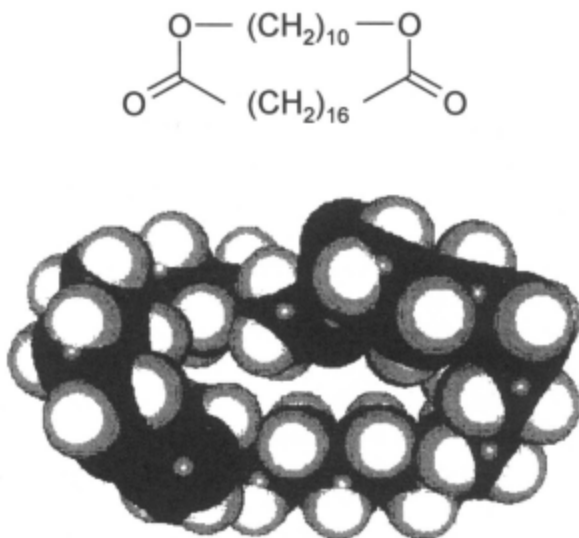

Figure 1 - The chemical structure and model of decamethylene octadecanedioate.

In 1962, a review of the stereochemistry of many-membered rings was published [10] describing a wide range of large ring molecules including a 30-membered macrocyclic polyene [11] (Figure 2) and the first catenane with its interlocked ring system [12] (Figure 3).

Despite the important advances that had been made in the chemistry of large organic ring molecules following the characterisation of benzene as the first ring compound in 1865 (Figure 4), it was developments in siloxane and polysiloxane chemistry and in chromatographic techniques that resulted in the preparation of narrow molar mass fractions of the first cyclic polymer, allowing for detailed investigations of its properties.
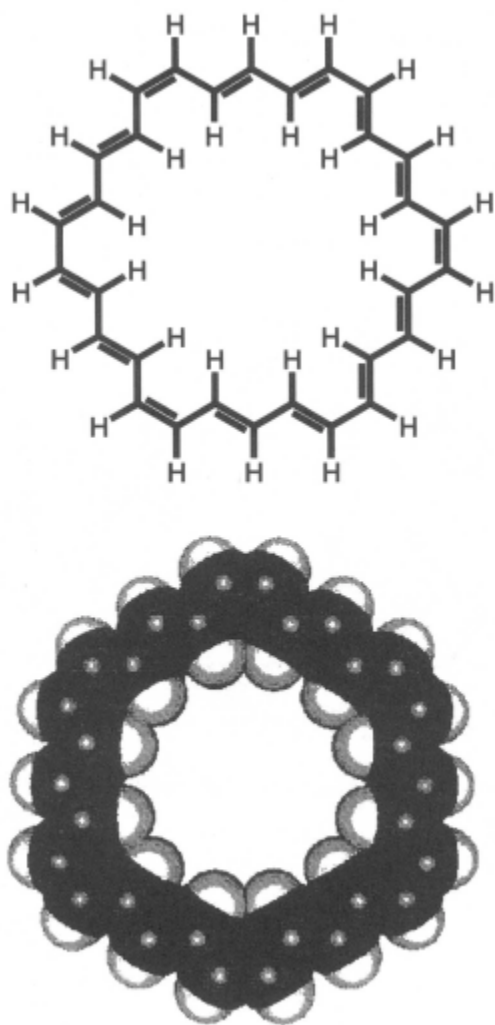
Figure 2 - The chemical structure and molecular model of a 30 membered macrocyclic polyene
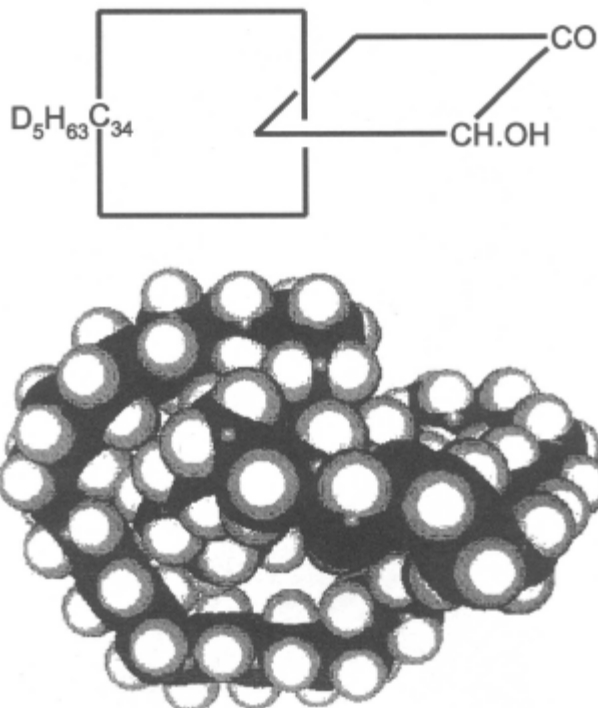
4

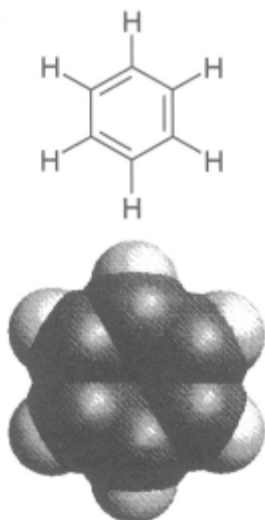**Figure 3 -** **The chemical structure and molecular model of the first catenane.**

Figure 4 - **The chemical structure and molecular model of the benzene ring.**

1.1.2 Large rings in polysiloxane systems

The first report on the production of ring and chain species in poly(dimethylsiloxane) (PDMS) ring-chain equilibrates was made by Scott [13] in 1946 and in 1962 Hartung and Camiolo [14] published measured values for the concentrations of the cyclics $[(CH_3)_2SiO]_x$ (with $x = 3-9$) in PDMS equilibration reactions in solution in xylene. Carmichael and his coworkers [15][16] extended these studies and were able to analyse cyclic dimethylsiloxanes with values of $x = 4-25$ using gas-liquid chromatography. All these investigations culminated in the work of Brown and Slusarczuk [17] who carried out PDMS ring-chain equilibration reactions in the bulk and in solution in toluene. In their base catalysed solution reaction, the siloxane concentration was 222 g dm^{-3} and the temperature was 383 K.

Under the conditions used by Brown and Slusarczuk nearly all the material obtained is cyclic, with only small amounts of high molar mass chains and the latter are well separated from the cyclic species. Furthermore, for this reaction, in principle the individual cyclic concentrations produced should be calculable by application of the Jacobson-Stockmayer theory [18] and the distribution of linear species by the Flory relationships for linear condensation polymers (see Ref. 1). Thus, the Brown and Slusarczuk reaction in toluene gave an opportunity for the preparation of narrow molar mass fractions of cyclic polymers with an average up to 1000 skeletal bonds, provided that suitable analytical and preparative techniques were available. From the point of view of characterisation, it would also be an advantage to calculate the individual concentrations of cyclic and linear species in such equilibrates and this was also undertaken [19].

Early experiments on gas-liquid chromatography (GLC) were carried out by James and Martin [20] and the first book on the subject of gas chromatography was written by Courtenay Phillips [21]. The technique became so well developed that it could be used to analyse cyclics $[(CH_3)_2SiO]_x$ with up to 100 skeletal bonds, when OV17 from the Field Instrument Company is used as the stationary liquid phase and Embacel is used as the solid support [22]. An example of the GLC analysis of a cyclic fraction is shown in Figure 5.
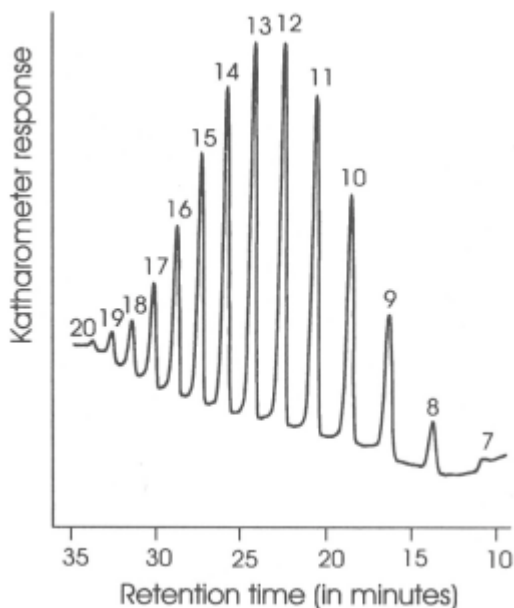
Figure 5 - Gas-liquid chromatogram of a dimethyl siloxane fraction consisting of cyclics $[CH_3)_2SiO]_x$ (with x=7-20).

For dimethylsiloxane rings with numbers of skeletal bonds in the range 100-1000, the resolution of individual cyclics by GLC is not possible and so cyclic fractions were analysed in the author's laboratory using the technique of analytical gel permeation chromatography (GPC) (otherwise known as size exclusion chromatography). This technique was first described by Moore [23] and preparative GPC was developed shortly afterwards (see, for example, Ref. [24]). The preparative GPC instrument used to obtain cyclic fractions of PDMS at York was designed and constructed by David Sympson [25]. The results of a typical fractionation are shown in Figure 6 and the dispersities of the individual fractions were all in the range $1.03 < M_w/M_n < 1.06$. In the higher molar mass fractions obtained by preparative GPC, appreciable amounts of linear species are present but the rings can be separated from the chains very effectively, as described in Ref. [25], Once a whole range of narrow fractions of PDMS cyclics had been obtained, these first cyclic polymers could be characterised and their properties investigated. This was done in collaboration with 20 other University research groups and with Dow Corning Ltd., resulting in a range of publications (see, for example, Ref. [26] [27]). Some of these properties will be described later in the chapter.
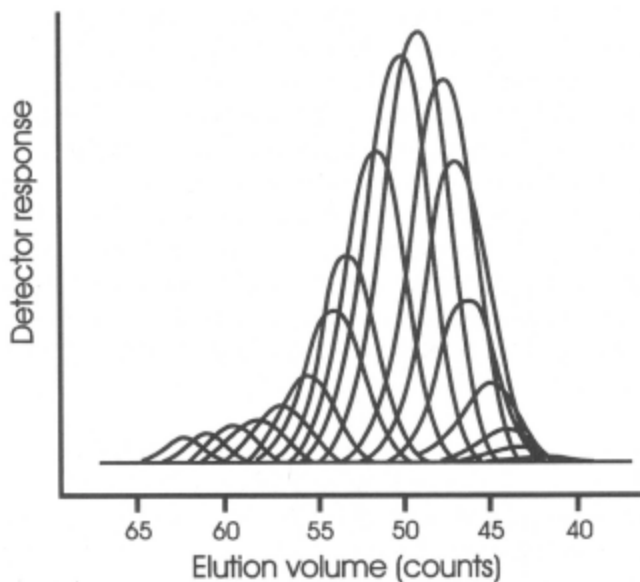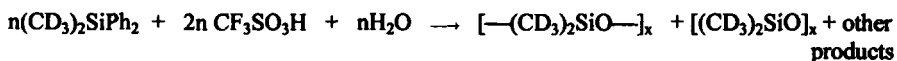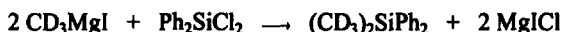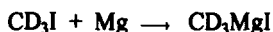
Figure 6 - Analytical gel permeation chromatography of the individual fractions of cyclic dimethyl siloxanes obtained by preparative GPC. The number average number of skeletal bonds in the fractions range from 40 to 1270.

Figure 7 - Molecular model representation of a cyclic $[(CH_3)_2SiO]_{50}$ with 100 skeletal bonds.

Cyclic dimethylsiloxanes can also be conveniently produced in cationic polymerizations as have been described by JulianChojnowski [28] [29]. The polymerization of the cyclic trimer $[(CH_3)_2SiO]_3$ with trifluoromethanesulphonic acid CF_3SO_3H ('triflic' acid) in solution in n-heptane at concentrations of 40wt% may be kinetically or thermodynamically controlled. Chains corresponding to the cyclics D_{3m} are found to obey Gaussian statistics in solution for n > 6, resulting in gradients close to the theoretical values of -1.5 and -2.5 in the log $[D_{3n}]$ versus log 3n plots for the kinetically and thermodynamically controlled reactions respectively [29]. Other cyclic polysiloxanes have been prepared at York using ring-chain equilibration reactions. These systems have included the cyclics $[R(CH_3)SiO]_x$ (where $R = H$ [22], CH_3CH_2 [22], $CH_3CH_2CH_2$ [22], $CF_3CH_2CH_2$ [22], $CH_2=CH$ [30] and C_6H_5 [31] [32]).

Recently, a range of per-deuterated cyclic dimethylsiloxanes $[(CD_3)_2SiO]_x$ have been obtained in our laboratory by a modification and extension of a preparation described by Beltzung and coworkers [33]. The reaction scheme is as follows [34] [35]:

$$CD_3I + Mg \longrightarrow CD_3MgI$$

$$2\ CD_3MgI + Ph_2SiCl_2 \longrightarrow (CD_3)_2SiPh_2 + 2\ MgICl$$

$$n(CD_3)_2SiPh_2 + 2n\ CF_3SO_3H + nH_2O \longrightarrow [-(CD_3)_2SiO-]_x + [(CD_3)_2SiO]_x + \text{other products}$$

The large cyclics were fractionated by preparative GPC, giving the first examples of fully deuterated cyclic polymers. The fractions are suitable for fundamental conformational and topological investigations by, for example, neutron scattering and field gradient nuclear magnetic resonance spectroscopy. They were characterised by infrared (IR), nuclear magnetic resonance (NMR) and mass spectroscopic techniques [34] [35].

Following the preparation and characterisation of linear block copolymers of polystyrene (PS) and PDMS by several groups (see, for example, Ref. [36] [37]), Frank Jones set out to prepare the corresponding cyclic block copolymers in the author's laboratory [38]. Taking advantage of the reactive nature of the PDMS blocks, the linear block copolymers were used for ring-chain equilibration reactions in toluene solution following methods used by Peter Wright for PDMS alone [39]. Following solution fractionation and GPC and NMR spectroscopic analysis, Jones concluded that one of the fractions was cyclic in nature. Reference [40] describes a recent synthesis of macrocyclic PS-PDMS block copolymers.

1.1.3 Preparation of some organic cyclic polymers

The preparation and characterisation of cyclic PDMS was followed by reports in 1980 of the preparation of cyclic polystyrene by Geiser and Höcker [41] [42], who polymerized styrene using sodium naphthalene as the initiator and tetrahydropyran as the solvent. Intramolecular cyclization of the resultant 'living' polymers was carried out using **α, α'-dichloro-p-xylene.** Chains in the product were separated from the cyclic material by reacting the former with high molar mass 'living' polystyrene in intermolecular reactions. Finally, the ring polystyrenes were isolated by fractionation giving cyclic fractions with number-average molar masses up to ca. 24000. Variations in the preparation of cyclic polystyrene material by a number of different authors (see, for example, Ref. [43] [44]) have been reviewed by Helmut Keul and Hartwig Höcker [45]. Some of the problems associated with the preparation and investigation of high molar mass cyclic polystyrene have been discussed by McKenna and hiscoworkers [46]. In recent years, a range of different organic cyclic polymers have been obtained by a variety of different experimental approaches [45]. These include cyclic alkanes C_nH_{2n} with up to 300 skeletal bonds [47] [48], cyclic polybutadiene [49] and cyclic poly (2-chloroethyl vinyl ether) [50]. Other organic cyclic oligomers and polymers are reviewed in detail in this book and some are now commercially available, including cyclic polystyrene and cyclic poly(methylmethacrylate).

1.1.4 Characterisation of cyclic oligomers

Large ring compounds can be produced in many chemical reactions but it was only when powerful investigative techniques were developed that it became possible to characterise large cyclics and establish their identities. These techniques include chromatographic methods such as GLC, GPC and HPLC (high performance liquid chromatography) as well as spectroscopic methods including IR, NMR and several types of mass spectroscopy. Most of these techniques are now used routinely in chemical research. Their power and sophistication have increased steadily over the past 40 years and this has proved a major factor in the continuing preparation and characterisation of new large ring compounds and cyclic polymers. Some examples of how these techniques are applied will now be given. In a recent investigation of the preparation and characterisation of mixtures of cyclic oligomers ofpoly(butylene terephthalate) (PBT), a number of state-of-the-art techniques were applied to the cyclics $[CO.C_6H_4.CO.O.(CH_2)_4.O]_x$ where $x \geq 2$ [51]. These cyclics were prepared by solution ring-chain reactions of PBT in 1, 2-dichlorobenzene usingdibutyl tin oxide as the catalyst. The largest rings observed by the analytical techniques had

Figure 8 shows a GPC of the PBT cyclic oligomers that were recovered from the ring-chain reaction by filtering off the insoluble linear polymer and then removing the solvent [51]. The columns used for the separation were four PL-gel **3μm** mixed-E columns supplied by Polymer Laboratories Ltd. By contrast with the SX-1 Bio-bead columns (obtained from Biorad Laboratories) used in much earlier investigations [52][53], the new mixed E-columns allow GPC analysis to proceed much faster as well as producing better resolution. In the poly(decamethylene adipate) system, such columns have been used to analyse individual cyclic oligomers up to 200 skeletal bonds [54].
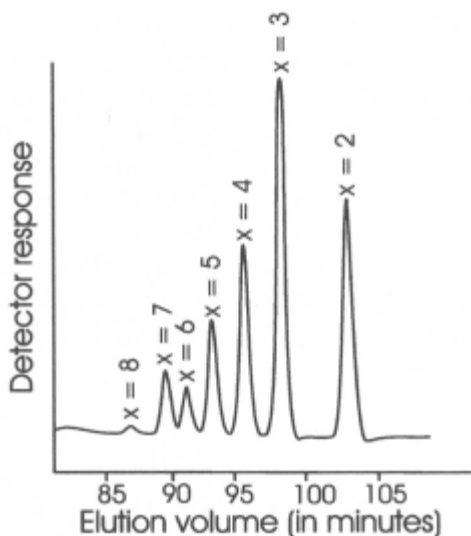

Figure 8 - GPC of cyclics $[CO.C_6H_4.CO.O.(CH_2)_4.O]_x$ (with x = 2-8) using a Shimadzu RID-6A refractive Index detector [51].

An alternative chromatographic technique to GPC is HPLC and Figure 9 shows the trace obtained for the PBT cyclic oligomers prepared as described above [51]. The HPLC column was a spherisorb S3 0DS2 column with a two solvent eluent: water (0.1% ethanoic acid) and acetonitrile (0.1% ethanoic acid) at a flow rate of **0.9 ml min⁻¹**. The instrument was fitted with an ultraviolet detector functioning at a wavelength of 240 nm. When analysing a mixture of cyclic oligomers it is important to establish the identity of the first member of the series.
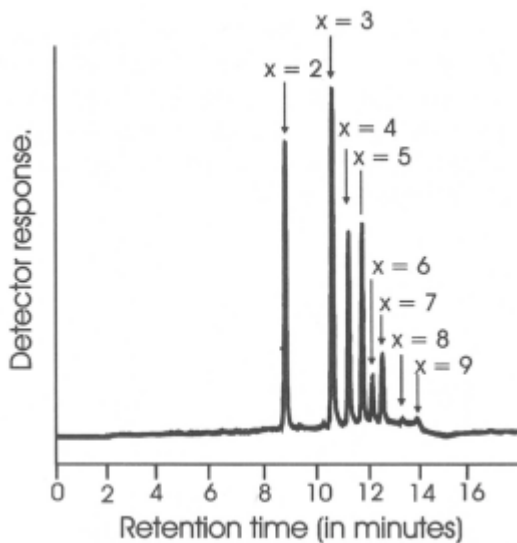
Figure 9 - HPLC of cyclics $[CO.C_6H_4.CO.O.(CH_2)_4.O]_x$ (with x = 2-9) [51].

In the case of the PBT system, the cyclic dimer was isolated using column chromatography and its identity confirmed by X-ray crystallography [51] (see Figure 10).
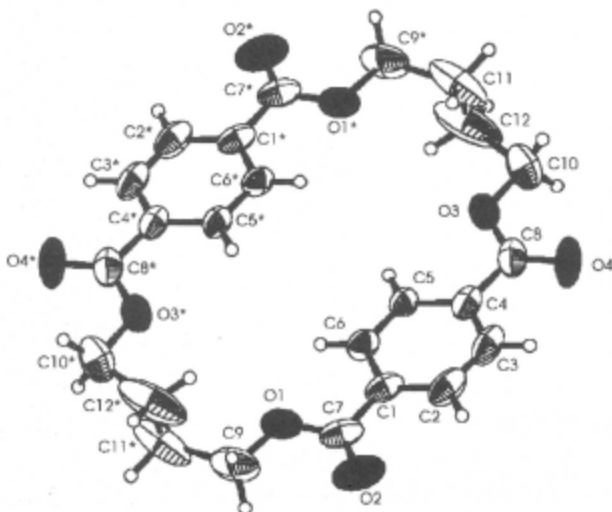

Figure 10 - Representation of the crystal structure of the cyclic dimer
$[CO.C_6H_4.CO.O.(CH_2)_4.O]_2$

There are a range of spectroscopic techniques available for characterising cyclic oligomer populations, including NMR and mass spectroscopy. For the PBT rings, two examples of mass spectra are shown in Figure 11 and Figure 12 [51]. Liquid chromatography tandem mass spectroscopy and 500 MHz NMR spectroscopy are particularly useful for characterising mixtures of cyclic oligomers.
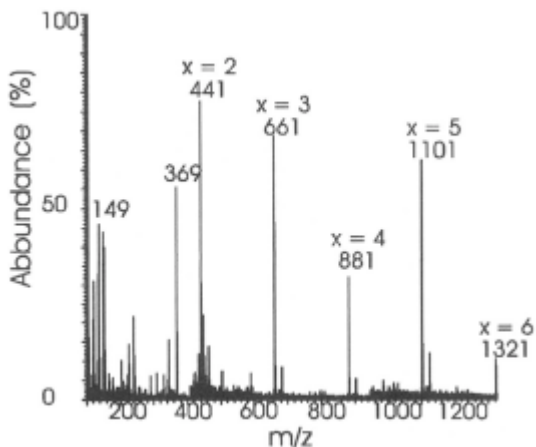

Figure 11 - Fast atom bombardment mass spectrum of cyclic PBT oligomers showing spectral lines (M+) corresponding to the exact multiples of the repeat unit [CO.C$_6$H$_4$.CO.O.(CH$_2$)$_4$.O] [51].
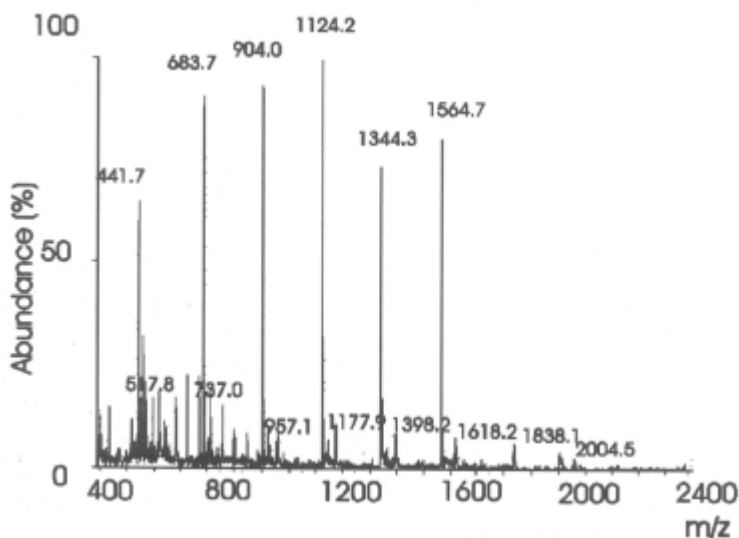

Figure 12 - Matrix assisted laser desorption ionization mass spectrum of cyclic PBT oligomers showing ions (M+Na)$^+$ from the species [CO.C$_6$H$_4$.CO.O.(CH$_2$)$_4$.O]$_x$. Some linear species are also present in the sample.

1.1.5 Cyclics produced in ring-chain equilibration reactions

Between 1969 and 1976, the author and his coworkers published a series of 14 papers describing large cyclics produced by ring-chain equilibration reactions [55]. Equilibrium cyclic concentrations were then related to the statistical conformations of the corresponding open chain molecules as described in section 1.3. Following the preparation of cyclic siloxanes $[R(CH_3)SiO]_x$ (as described above), an example of a family of cyclic paraffin-siloxanes was investigated [56] by GLC and GPC. The equilibrium concentrations of cyclics $[(CH_3)_2Si-(CH_2)_4-(CH_3)_2Si-O]_x$ with $x = 1-6$ were determined in this way. The study illustrated that the conformational characteristics of many chain molecules (in this case short paraffin chains) can be investigated provided that suitable labile groups are incorporated into the molecular structure (in this case, dimethyl siloxane units).

Monomer-polymer equilibria can be set up in polyether systems (see, for example, Ref. [57] [58]). Poly(tetrahydrofuran) monomer-polymer equilibria were found to produce no cyclic oligomers under the conditions used in Ref. [59]. By contrast, a full range of cyclics $[CH_2OCH_2CH_2O]_x$ with $x = 1-8$ were found to be present in monomer-polymer equilibrates of poly(1, 3-dioxolane) [60]. Bulk and solution polymerisations were carried out by adding boron trifluoride diethyl etherate to the monomer (1,3-dioxolane) alone or to the monomer in solution in dichloroethane. The equilibrates were quenched in diethylamine and the cyclics extracted and analysed by GLC, IR, NMR and mass spectroscopy.

Following earlier investigations [61], the concentrations of the cyclics $[NH(CH_2)_5CO]_x$ with $x = 1-6$ were determined for melt equilibrates of nylon.6 [62]. The cyclic oligomers were analysed by GPC using sephadex columns from Pharmacia Ltd. and glacial ethanoic acid/water as the solvent.

Equilibrium ring concentrations were also measured in two aliphatic polyester [53] and one aromatic polyester system [52] some 25 years ago. Further studies have been carried out more recently (see, for example, Ref. [54] [63] [64]).

Potentially, there is a huge range of large ring compounds that could be prepared in polyether, polyamide and polyester systems. Some of these cyclics could be obtained as pure compounds by preparative GPC or preparative HPLC. It is expected that in the years ahead many new large organic ring compounds will be made available to chemists in this way.

Ring-chain equilibria can also be set up in purely inorganic systems and two examples are sodium phosphate melts and liquid sulphur. Sodium phosphate $NaPO_3$ (known as Graham's salt [65]) may be prepared by heating sodium dihydrogen phosphate at high temperatures and then rapidly quenching the molten polymer [66]. The water-soluble product consists of long linear polyphospbate chains terminated by hydroxyl groups [67] together with 10% w/w cyclics $[NaPO_3]_x$ with $x = 3\text{-}7$. The equilibrium concentrations of cyclics in such melts have been measured using paper chromatography as the main analytical technique [68] [69] [70].

It is well established that ring-chain equilibria can be set up in liquid sulphur [71] [72]. Above a critical transition temperature of 432K, polymeric sulphur chains are formed in the molten element [71]. Below this temperature, liquid sulphur consists of cyclooctasulphur S_8 and a mixture of other cyclics S_x (called S_π). Using IR and Raman spectroscopy and HPLC, Steudel and his coworkers [73] [74] have established the main constituents of S_π at 388K. It is a mixture of cyclics containing the small rings S_6 and S_7 (as ca. 3.5% by weight) and ca. 1.5% of larger cyclics S_x with $x > 8$; the remaining 95% by weight being cyclooctasulphur [73]. It is S_π that gives rise to the well-known self-depression of the freezing point of elemental sulphur discovered by Gernez [75]. Although it was shown that large rings with at least 34 atoms are present at equilibrium in liquid sulphur below 432K, only three have so far been isolated from the molten element and these are S_{12} [76] [77], S_{18} [77] and S_{20} [77]. From his detailed investigations of the unique properties of liquid sulphur, Steudel [74] has concluded that the theory of Tobolsky and Eisenberg [72] does not provide a full explanation of the behaviour of the element on heating to its boiling-point. Bond rearrangements involving the formation of four-centre transition states are well known in inorganic chemistry (see, for example, Ref. [78] [79] [80] [81] [82] [83]). Such bond interchange reactions in liquid sulphur could lead to ring-ring equilibria in addition to the ring-chain equilibria. Further detailed experimental studies of this fascinating element would be most welcome (see Section 1.3).

Some of the results of the experimental investigations of cyclic concentrations in polymeric ring-chain equilibrates outlined in this section will be discussed from a theoretical point of view in Section 1.3. This describes the calculation of equilibrium ring concentrations in a range of systems in terms of the statistical conformations of the corresponding open chains.

1.1.6 Alternative routes to cyclic oligomers

In the first edition of *Cyclic Polymers* [3], the author reviewed three methods for preparing mesocyclics that were established more than 50 years ago.

The first is the dilution method of Ruggli [84], in which the reaction system is diluted so as to favour kinetically-controlled ring formation. An example is the Thorpe-Ziegler reaction [85] [86].

A second method is the thermal depolymerization route of Carothers and his coworkers [9]. For example, cyclics with up to 30 skeletal bonds were obtained by heating polymeric esters at 270 °C and 1 mmHg using a tin catalyst.

A third method developed by Stoll and Rouvé [87] is believed to involve cyclization on a surface, such as the acyloin condensation on sodium metal.

Over the past 40 years, a wide range of cyclic oligomers have been prepared in kinetically-controlled reactions. Some examples are as follows: large cyclic carbonates [88] [89], large cyclic ethers [90] [91], large cyclic esters [51] [92] [93] [94] [95] [96], large cyclic ether-esters [97] [98] and macrocyclic oligomers as intermediates for the preparation of high performance polymers [99] [100]. Many of these cyclics will be discussed in detail in this book.

Cyclic structures are of great importance in biological chemistry as has been emphasised in books previously edited by the author [3] [8]. Merrifield was awarded a Nobel prize for his synthetic methods in polypeptide chemistry [101], which can be used to synthesise cyclic peptides on solid-phase polymeric supports, that are usually cross-linked polymer gels. Mutter [102] has discussed the influence of peptide residue sequences on polypeptide cyclization reactions, as described by Alan Tonelli in Ref. [3]. Synthetic procedures for preparing cyclic oligo-and poly-saccharides are beginning to be established (see, for example, Ref. [103]). An example of a DNA cyclization is phage **λDNA** studied by Wang and Davidson [104] [105]. Many more examples of large ring molecules and cyclic polymers in biological systems will be described in this book.

1.2 Differences between the properties of cyclic and linear oligomers and polymers

Large ring molecules and long chain molecules are topologically distinct species and so there are fundamental differences between the properties of cyclic and linear oligomers and the properties of cyclic and linear polymers. Some examples are outlined in this section and many will be covered in more detail in other chapters in this book.

(i) Cyclic oligomers and cyclic polymers have no end-groups, so they can be represented by simple structural formulae and names. For example, cyclic poly(dimethylsiloxane) is an exact name, whereas in the case of linear poly(dimethylsiloxane) end-groups should be specified. The properties of linear polymers can be markedly affected by the nature of their end-groups, for example with linear poly(dimethylsiloxane) the surface properties can be different depending on whether the end-groups are $(CH_3)_3Si$- or HO-. For some applications, it may be an advantage to have no end-groups in the polymeric material. In this connection, many forms of DNA are circular [3] [8], thus preventing any possible reactions or interactions with chain ends. Two examples are shown in Figure 13 [131] [132] and Figure 14 [132] [133].
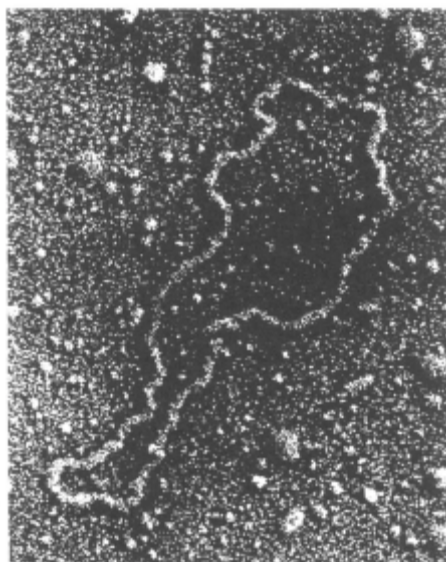

Figure 13 - An electron micrograph of a plasmid, which is a circular molecule of DNA about 3μm in circumference. It exists apart from the chromosome in a bacterium and replicates on its own [131].
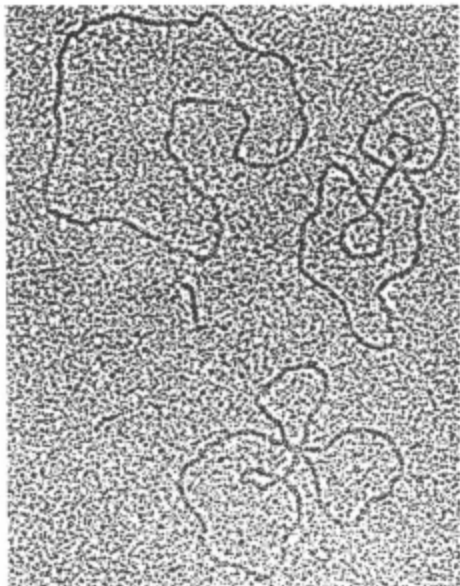
Figure 14 - An electron micrograph of three closed loops of DNA, each of which is a double helix. One strand of each loop is the natural single strand DNA of the bacterial virus ♦X174 and each loop contains about 5500 base pairs [133].

There are examples of cyclic polypeptides and loops in proteins [3] [8] and recently large ring molecules have been observed in some polysaccharide systems, as shown in Figure 15 [134].
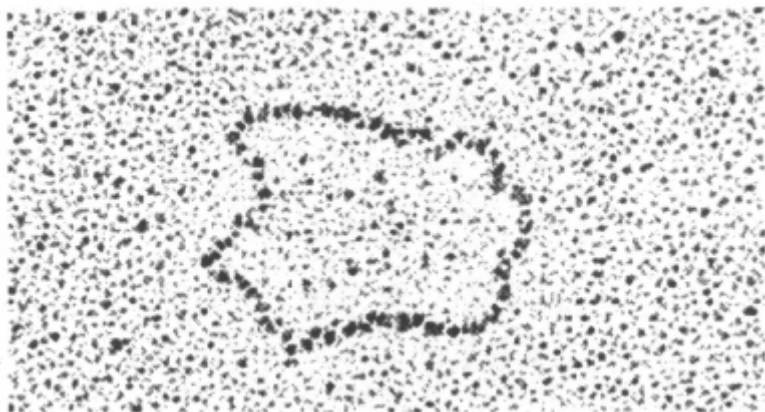

Figure 15 - An electron micrograph of a fully ordered cyclic structure of iotacarrageenan.

(ii) The difference between the topologies of cyclic and linear polymers is illustrated when a single bond in the polymer is broken. A large ring gives a chain with a similar molar mass, whereas the long chain will give two short chains (see Figure 16). Such differences have been discussed by Kelen and his coworkers for the poly (1,3 dioxolane) system [134].
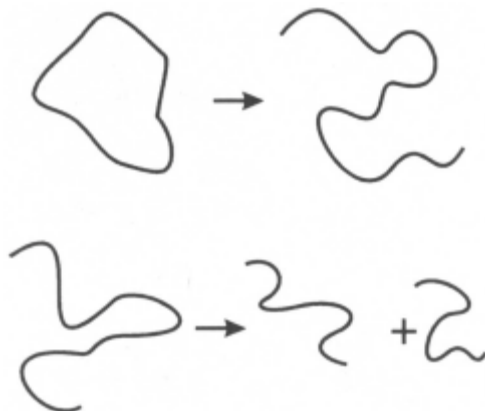

Figure 16 - Cleavage of a single skeletal bond in a cyclic and linear molecule.

(iii) Skeletal bond interchange reactions of cyclics and linears (as discussed in Ref. [82] [83]) result in very different consequences, as illustrated in Figure 17. Intramolecular bond interchange of a single ring molecule results in two smaller rings, whereas intermolecular bond interchange reactions between two ring molecules results in the formation of one larger ring. Bond interchange reactions between two long chain molecules always result in no change in the number of chemical species.
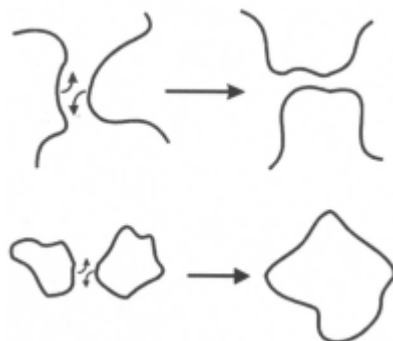

Figure 17 - Skeletal bond Interchange reactions of cyclic and linear molecules.

(iv)   The linking together of long chain molecules with reactive groups along their length can result in a whole range of chemical species, whereas bond formation between two of the corresponding cyclic molecules can give only a single dimer (as illustrated in Figure 18).
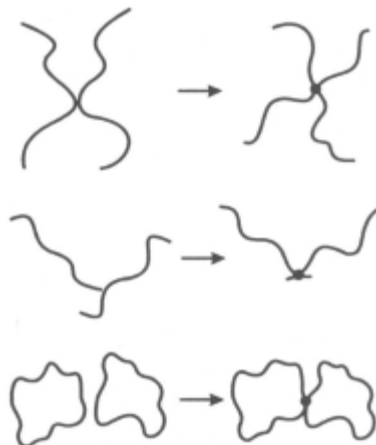

Figure 18 - Linking reactions of linear and cyclic molecules (see text).

(v)   Ring-opening polymerization (ROP) reactions are an important application of large ring molecules. The process is illustrated in Figure 19. This shows the opening of a large cyclic to form the corresponding linear polymer, which in turn reacts with another large cyclic to produce a long, linear chain. Such reactions have been investigated in detail and have found applications, for example, in polycarbonate andpolyester chemistry [88] [89] [136]. They are proving to be a useful route to very high molar mass linear polymers.
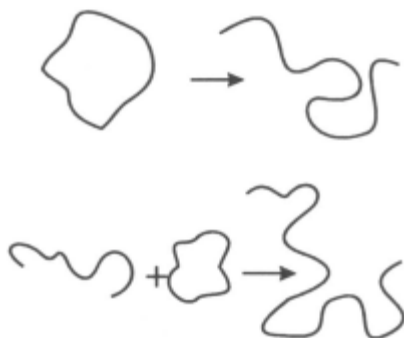

Figure 19 - An illustration of the ring opening polymerisation process.

(vi)   Differences between the bulk viscosities of large rings and long chains are shown in Figure 20 for the PDMS system [137] [138]. Smaller rings are more viscous than shorter chains and the reverse is the case for the largest species studied. The cross-over occurs at about 100 skeletal bonds. The lower bulk viscosities of cyclics above the critical molar mass for entanglements M_c are contrary to the expectations of reptation theory [139] [140], but may result from fewer entanglements between cyclic molecules as opposed to linear molecules in the melt (as illustrated in Figure 20). There are also marked differences between the activation energies for viscous flow between ring and chain PDMS species [137].
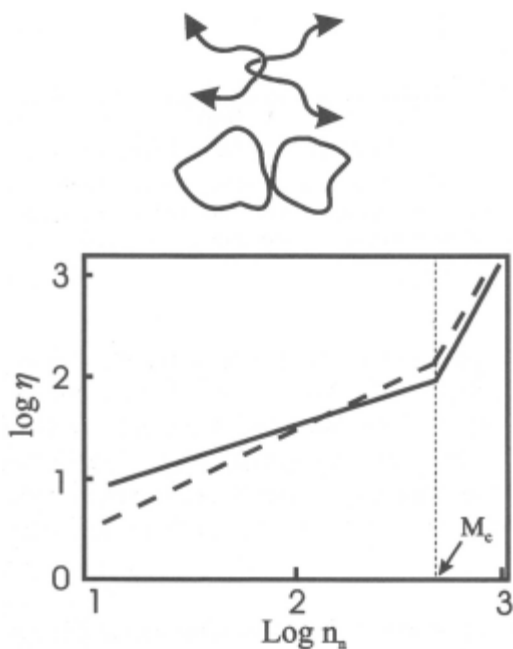
Figure 20 - The plot shows the logarithm of the bulk viscosity η as a function of the logarithm of the number-average number of skeletal bonds n_n for the PDMS system for rings (—) and chains (- - -) [138].

(vii)   Another consequence of the different topologies of ring and chain molecules is that mixtures of cyclic and linear polymers can have higher bulk viscosities than either component. This is illustrated in Figure 21 for PDMS blends. The effect is believed to be the result of some threading of large rings by long chains creating temporary cross-links in the melt [138]. It has also been observed in polystyrene systems [141].

Figure 21 - Ratio (%) of PDMS ring and chain bulk viscosities η (experimental values divided by values calculated assuming that no threading occurs) for blends shown as a function of the number average number of skeletal bonds [141].
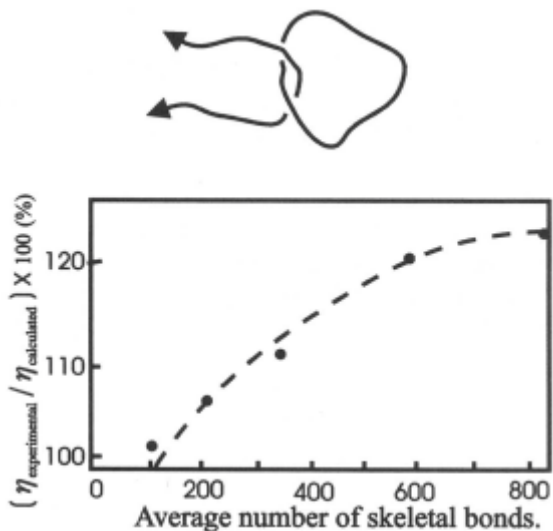
(viii) Topological trapping of large cyclics in networks was outlined in Section 1.1.7(c). When PDMS networks are formed in the presence of large PDMS rings, some of the latter become topologically entrapped as shown in Figure 22 [126]. Increasing quantities of cyclics are entrapped as the sizes of the rings increase, so that 95% of cyclics with 500 skeletal bonds are incorporated into the network without the formation of chemical bonds.

(ix) Catenation is a possibility for large ring molecules and cyclic polymers. The first example of a man-made catenane is depicted in Figure 3 [12]. The chemistry and topology of catenanes has been discussed previously by Schill [143] and by Jean-Pierre Sauvage and his coworkers in Chapter 5 of Ref. 8. A poly[2] catenane with topological bonds in a polymer main chain has been reported recently [144]. Figure 23 shows an electron micrograph of catenated DNA molecules of a virus, illustrating how nature can catenate biological macromolecules. No comparable structures are possible for chain molecules.
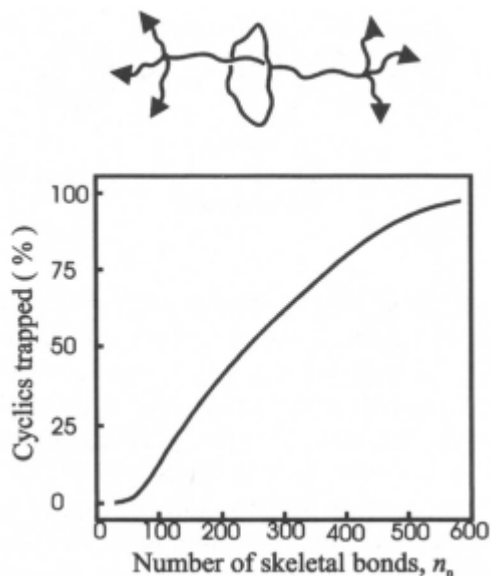
Figure 22 - Percentage uptake of PDMS rings in a PDMS network as a function of the
number of cyclic skeletal bonds.
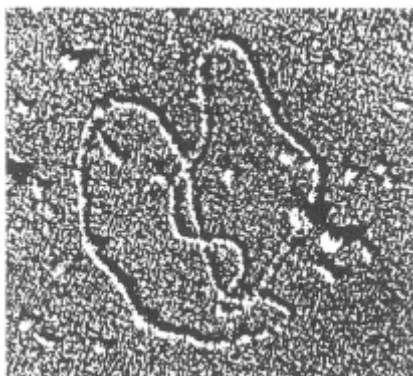
Figure 23 - A biological catenane (see p249 in Ref (3)).

(x) Rotaxane formation is another possibility for large ring molecules and cyclic
polymers that is denied to the linear species. In these structures, large
cyclics are threaded on to linear molecules without the formation of covalent
bonds. End-stoppers are often used to stabilise the structures (as illustrated
in Figure 24). Rotaxanes have been reviewed previously by Schill [143] and
by Harry Gibson in Chapter 6 of Ref. 8. It is interesting to note that even
cyclodextrins have been incorporated into rotaxane structures as reported by
Akira Harada in Chapter 11 of Ref. 8.

Figure 24 - A line diagram showing the basic structure of a rotaxane molecule with end stopper groups.

(xi) The possibility of large ring molecules and cyclic polymers having knots in their structures has been reviewed by a number of authors (see, for example, Ref. [12] [44] [143] [145]). It has been estimated that the smallest cycloalkane $[CH_2]_n$ that can exist as a knotted structure has about 50 methylene units in the ring [12] [143]. Discussions of the topologies of knotted chemical structures include those by Frisch and Wasserman [146] and by Jean-Pierre Sauvage and his coworkers (see Chapter 5 of Ref. 8). In Figure 25, an example of a knot that is observed in genes by electron microscopy is illustrated by a drawing of a knotted circular DNA structure. Permanent knots are another structural feature denied to chain molecules.

Figure 25 - A knotted circular DNA structure.

(xii) An electron micrograph of a DNA ring in a relaxed and supercoiled state is shown in Figure 26. The supercoiled state is of higher energy than the relaxed state. This phenomenon of supercoiling of circular DNA has important biological consequences and it has been reviewed by James Wang (Chapter 7 in Ref. 3), by Andrzej Stasiak (Chapter 2 in Ref. 8) and by Alexander Vologodskii [147]. There have been no reports of supercoiled states in synthetic cyclic polymer chemistry.
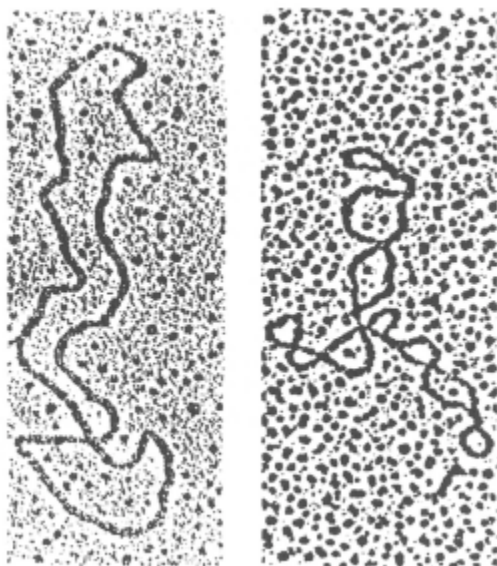
Figure 26 - An electron micrograph of a DNA ring in a relaxed and a supercoiled state (see p235 in Ref[3]).

(xiii) The role of large ring molecules in rotaxane and catenane structures has been discussed by Fraser Stoddart and his coworkers [149] [150] in relation to their future use as molecular switches and shuttles and even molecular computers.

(xiv) A most important aspect of cyclic oligomer chemistry is the ability of some large ring structures to complex with metal ions. The discovery of these phenomena resulted in the award of Nobel prizes to Pederson [151] and Cram [152]. The complexation of inorganic cations by crown ethers and cryptands and by calixarenes has been reviewed by George Gokel (Chapter 7) and by David Gutsche (Chapter 8) of Ref. [8] respectively.

In general, the field of molecular recognition by macrocyclic compounds is so large that it will not be discussed here. A review of the area has been published by Anthony Davis as Chapter 13 of Ref. [8]. Large ring molecules have been used as catalytic cavities and even to carry out chemical reactions within them. It is noted that the relatively new area of molecular imprinting using large cyclics is described in a recent article [153].

(xv) The volumes of the domains of synthetic cyclic polymers in dilute solution are considerably smaller than those of the corresponding linear polymers. Both have been shown to adopt random-coil conformations obeying Gaussian statistics in the limit of large ring size or long chain length (see, for example, Ref. [1] [154] [155]). It follows that the radius of gyration of a random-coil linear polymer $\langle s^2 \rangle_l$ is related to its mean-square end-to-end distance $\langle r^2 \rangle_l$ in the limit of high chain length by the relationship [156]:

$$\langle s^2 \rangle_l = \langle r^2 \rangle_l \; / \; 6 \tag{1}$$

The ratio of the radius of gyration of a random-coil cyclic polymer $\langle s^2 \rangle_r$ to that of the corresponding linear polymer $\langle s^2 \rangle_l$ for high molar masses at the Θ-point has been shown theoretically to be as follows [115] [116] [117]:

$$\frac{\langle s^2 \rangle_l}{\langle s^2 \rangle_r} = 2 \tag{2}$$

This prediction was confirmed experimentally by neutron scattering [114].

The differences between the volumes of the domains occupied by cyclic and linear polymers in dilute solution leads to marked differences in properties including GPC elution volumes [106], viscosities [111], translational friction coefficients [118], α expansion factors [157], neutron scattering functions ([158], see also Chapter 5 in Ref. [3]) and lower critical solution temperatures [159].

(xvi) Apart from the differences between the properties of cyclic and linear oligomers and polymers already discussed in this section, a number of differences have been observed in other properties. For example, for dimethylsiloxanes, these include densities and refractive indices [141] [160], dipole moments [161], glass transition temperatures [162], ultrasonic relaxation properties [163], surface properties [164] [165] and silicon-29 NMR spectra [166].

Similarly, differences between the properties of rings and chains have been found for other siloxane systems $[R(CH_3)SiO]_x$, where $R = H$ [26], C_6H_5 [31] [32] [167] [168] [169], $CH_2 = CH$ [30] and liquid crystal mesogens [170].

In conclusion, the differences between the properties of ring and chain

oligomers and polymers discussed in this section (1.2) demonstrate the potential for commercial applications, as well as providing theoretical information which is useful for a deeper understanding of molecular behaviour and polymer properties.   In the next section, one such theoretical application will be considered, namely the calculation and interpretation of equilibrium cyclic concentrations in polymeric systems.

1.3 Calculation of cyclic concentrations in ring-chain equilibrates

13.1 Ring-chain equilibration reactions

In section 1.1.5, some experimental investigations of the concentrations of cyclics in a range of polymeric ring-chain equilibrates were outlined. These systems included a paraffin-siloxane, a polyether, a polyamide, a polyphosphate and aliphatic and aromatic polyesters. There is a direct relationship between equilibrium ring concentrations in such equilibrates and the statistical conformations of the corresponding open chain molecules   as will now be outlined. All these ring-chain equilibrates can be represented as follows [55] [171]:

$$- M_y - \quad \Leftrightarrow \quad - M_{y-x} - \; + \; M_x \tag{3}$$

where M_x represents an x-meric cyclic in equilibrium with chain species containing y   and y-x monomeric units.   The molar cyclization equilibrium constant K_x of an individual cyclic is given by:

$$K_x = \frac{[-M_{y-x}-][M_x]}{[-M_y-]} \tag{4}$$

with a most probable distribution of chain species in the linear polymer, the relationship derived by Paul   Flory [1] can be applied so that:

$$K_x = \frac{[M_x]}{p^x} \tag{5}$$

The factor p can be obtained experimentally from the number average molar mass of the polymer [1]. It is often close to unity, so for many practical purposes, K_x values for ring molecules that are not too large:

$$K_x \cong [M_x] \tag{6}$$

1.3.2 Theoretical molar cyclization equilibrium constants

It is now well established that synthetic linear polymers adopt random-coil conformations in solution and in the melt [1] and, provided that they are of sufficient length and flexibility, they should obey Gaussian statistics [172] [173]. As a result, the probability of end-to-end closure of an x-meric chain should be given by:

$$W_x(\underline{O}) = \left(\frac{3}{2\pi \langle r^2 \rangle} \right)^{3/2} \tag{7}$$

where $\langle r^2 \rangle$ is the mean-square end-to-end distance and $W_x(\underline{O})$ is the density of end-to-end vectors $\underline{r}$ in the region corresponding to the close approach of chain ends, where $\underline{r} \approx \underline{O}$.

The Jacobson and Stockmayer cyclization theory [18] gives the following expression for the molar cyclization equilibrium constant K_x of an x-meric ring in a ring-chain equilibrate:

$$K_x = \frac{W_x(\underline{O})}{N_A \; \sigma_{RX}} \tag{8}$$

where N_A is the Avogadro constant and σ_{RX} is a symmetry number corresponding to the number of skeletal bonds that can be opened in the cyclic M_x in the reverse reaction of equation (3).

Application of equations 7 and 8 to real polymer systems assumes no enthalpy change in equation 3, which will be the case for large, unstrained cyclics but may not be so for smaller rings. Correlations between the termini of chains with their ends close for ring formation have been discussed in detail by Paul Flory and his coworkers [19] [174] [175] [176] and will not be considered further in this section. Any such correlations are best dealt with using direct computational methods, which are described in the next section.

Figures 27-32 show examples of experimental molar cyclization equilibrium constants K_x for cyclics (with x monomeric units or n skeletal bonds) measured by the York group (see section 1.1.5). They are compared with theoretical values calculated using the Jacobson and Stockmayer cyclization theory (equations 7 and 8). Theoretical values are shown by the unbroken lines and experimental values by the broken lines joining experimental K_x values (shown as open circles). The mean-square end-to-end distances of open chains corresponding to the cyclic species were assumed to be unperturbed by excluded volume effects and $\langle r^2 \rangle_o$ values calculated by the matrix algebraic methods of Flory and Jernigan [177] [178] using rotational isomeric state models as described in Ref. [19] [52] [53] [56] [60] [62]. Good agreement between experiment and theory is found for large rings in all the systems apart from poly(ethylene terephthalate). Further investigations of this latter system may result in an explanation for the observed discrepancies.

Figure 27 - Poly(dimethyl siloxane) system [19]
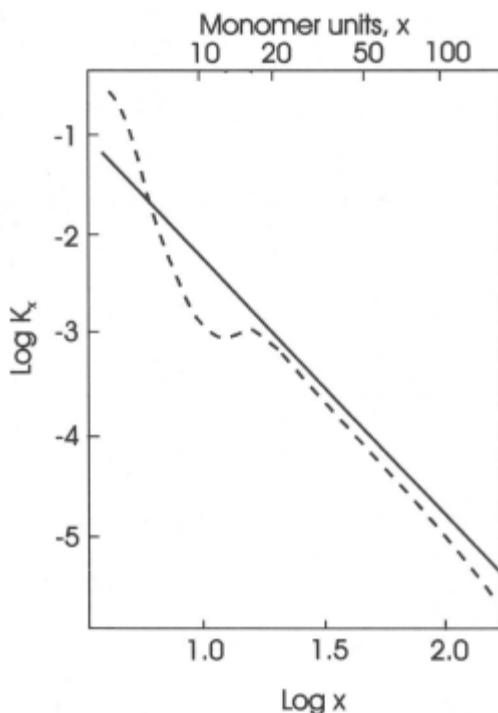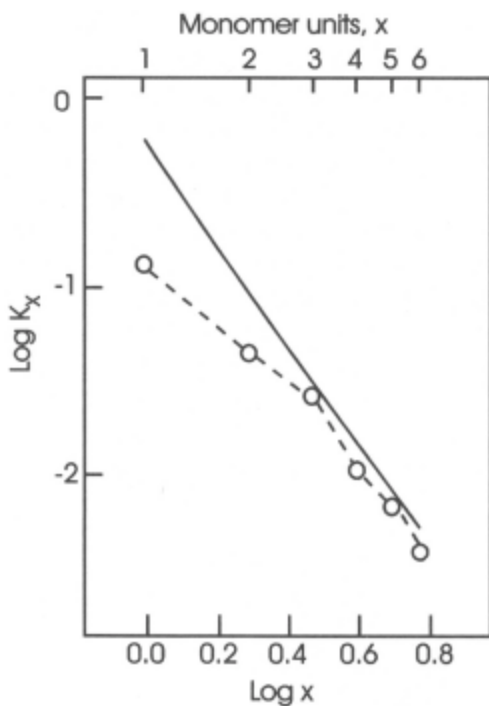
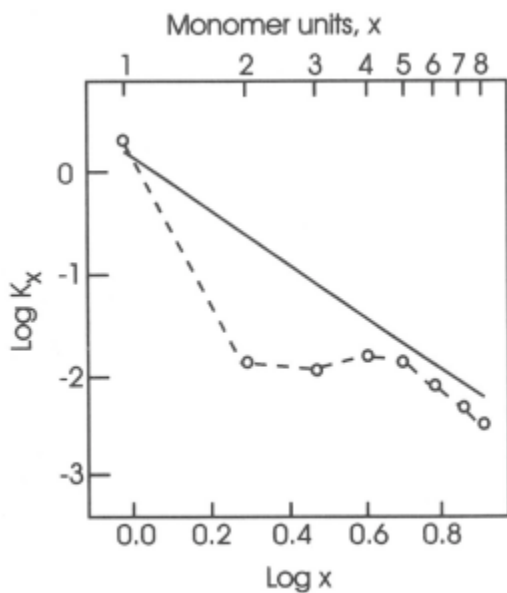Figure 28 - Paraffin-siloxanes $[(CH_3)_2Si-(CH_2)_4-(CH_3)_2Si-O]_x$ [56].

Figure 29 - Poly(1,3-dioxolane) system [60].
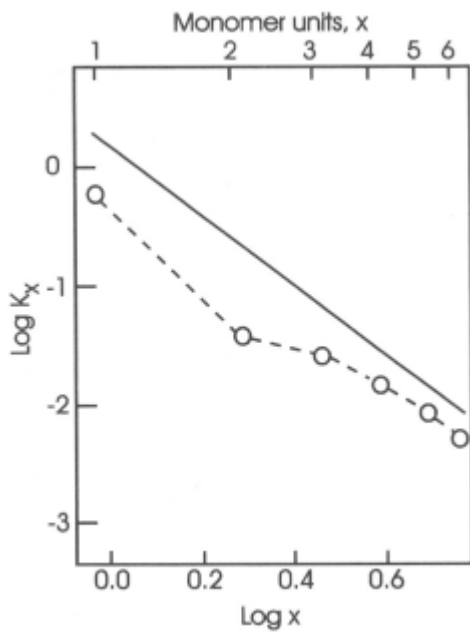
Figure 30 - Nylon.6 system [62].
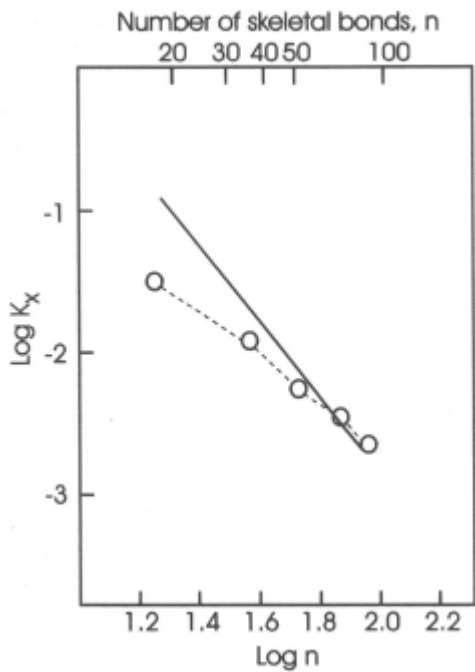
Figure 31 - Poly(decamethylene adipate) system [53].
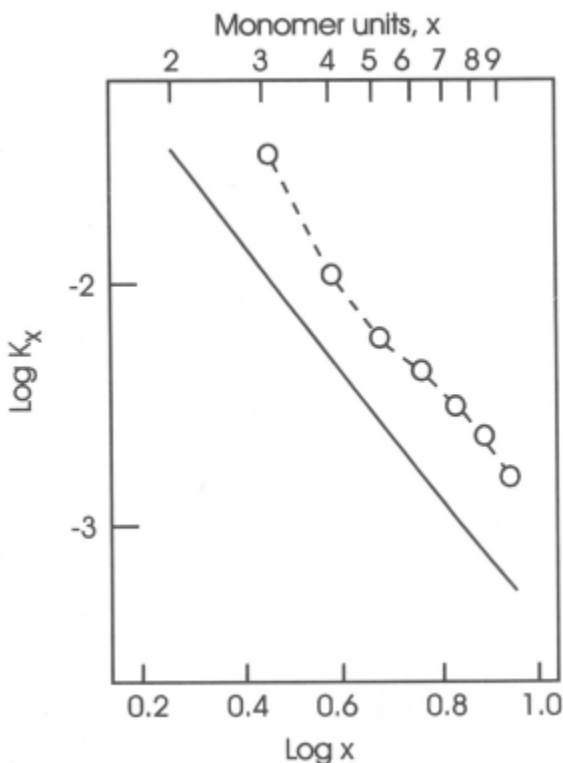
Figure 32 - Poly(ethylene terephthalate) system [52].

1.3.3 The direct computational method for calculating equilibrium cyclic concentrations

A direct computational method can be applied [179] [180] [181] to calculate cyclic concentrations in polymer systems, when the corresponding open chain molecules do not obey the Gaussian expression (equation 7) for the probability of intramolecular cyclization. This method is now illustrated for liquid sulphur which, as described in section 1.1.5, has been found to contain a range of large cyclics S_x with $x > 8$. A rotational isomeric state (RIS) model [154] [182] for sulphur chains [181] [183] [184] [185] was used as the basis of these calculations. All the individual conformations of sulphur chains defined by the RIS model were generated and full account was taken of excluded volume effects.

Individual molar cyclization equilibrium constants K_x were then calculated using the following expression:

$$K_x \approx \frac{z}{Z\,(4/3)\,\pi\;r^3 N_A \sigma_{RX}} \qquad \qquad \textbf{(9)}$$

where Z represents the total sum of the statistical weights of all the individual conformations defined by the RIS model for an x-meric chain and z represents the sum of the statistical weights of those conformations that have the centres of their terminal atoms separated by less than a reaction distance r. The quantity N_A is the Avogadro constant and σ_{RX} is a symmetry number, which is x for S_x rings.

The RIS model for polymeric sulphur is based on all the available structural data and it has been reviewed by the author in previouspublications [3] [181] [183] [184] [185]. The S-S bond length 1 is assigned the value 0.206 nm and the bond angle supplement Θ is assigned the value 74°. Each bond in a sulphur chain is assigned to one of two discrete rotational isomeric states located at internal rotation angles $\emptyset = + 90°$ (a + state) or $\emptyset = - 90°$ (a - state). A statistical weight parameter σ given by a Boltzmann factor takes account of the energy difference ΔE between the states +- (or - +) and + + (or - -). Initially σ was assigned a value of unity for the calculations to follow.

An excluded volume corresponding to each sulphur atom in the chain having a finite volume was taken into account as follows. When the distances d between the centres of non-bonded sulphur atoms (with the exception of terminal pairs) were less than 0.3 nm, the conformations were not included in the calculation. Ring formation was assumed when the reaction distance r was less than 0.3 nm.

Values of z and Z required for the application of equation 8 are listed in Table 1 and it can be seen that the cyclics S_x with x > 8 that should be present in greatest amounts in liquid sulphur are S_{12}, S_{18} and S_{20} [186]. These are the only three large cyclics that have been recovered from the liquid element [76] [77]. Individual conformations of chains corresponding to rings are shown in Table 2 [186].

Some of the cyclics $(S_9,\ S_{10},\ S_{11},\ S_{13},\ S_{14},\ S_{15}\ \textbf{and}\ S_{16})$ are predicted by the model to be absent from the molten element. Steudel and his coworkers reported detecting all these cyclics by HPLC but some such as S_{11} and S_{13} were present in only trace quantities [73]. If cyclic concentrations are equated with molar cyclization equilibrium constants, the total ring content from S_9 to S_{26} is calculated to be 0.7% by weight, compared with Steudel's estimate of 1.5% by weight for cyclics from S_9 up to S_{34}.

Table 1

Value of x in S_x	Number of conformations corresponding to ring formation z	Total number of conformations Z
9	0	48
10	0	88
11	0	162
12	4	298
13	0	536
14	0	980
15	0	1790
16	0	3270
17	4	5974
18	16	10896
19	10	19832
20	68	36144
21	44	65724
22	74	119644
23	236	217716
24	248	395672
25	298	719284
26	634	1307670
27	1424	2376558
28	2134	4317352

Table 2 - S_x conformations predicted to cyclize for $8 < x < 20$.

S_x	Conformation	No of Conformations
S_{12}	+ - - ++ - - ++[a]	4
S_{17}	+++ - ++ - - + - - - - +	4
S_{18}	++++ - - ++ - - - - - ++	4
	+ - - ++ - +++ - ++ - - +[b]	2
	+ - - ++ - - - - - ++ - - +	2
	+ - - - - - ++ - - +++++	4
	+ - - ++ - - - - + - - ++ -	4
S_{19}	++++ - ++++ - ++++ - +	4
	+++ - ++++ - ++++ - ++	4
	- ++++ - ++++ - ++++ -	2

[a] Conformation corresponding to the crystal structure of S_{12}.
[b] Conformation corresponding to the crystal structure of α-S_{18}.

The effect of changing the structural and statistical weight parameters of the RIS model has been explored [186]. A value of 1.4 for σ is believed to be the best estimate for this parameter [183] and it was used when exploring the effect of changing the values of $\varnothing$, r and d (which are all defined above). When $\varnothing$ was changed by just + 10° or - 10°, the cyclic S_{12} was predicted to be absent from the sulphur melt, contrary to experiment. When r was changed from 0.3 nm to 0.35 nm, S_{17} and S_{19} were predicted to be present in larger concentrations than S_{18} and S_{20}, again contrary to experiment. When the excluded volume distance d was increased by only 0.03 nm, all the conformations became excluded. When d was decreased by only 0.035nm, substantial quantities of S_{13} were predicted, once again contrary to experimental findings. In conclusion, it is the original RIS model for polymeric sulphur that gives large ring concentrations in good agreement with all the available experimental information. The success of the model gives encouragement for future attempts to correlate large cyclic concentrations in polymeric systems with the statistical conformations of the corresponding open chain molecules. Progress in this enterprise has already been achieved, for example for cyclic dimethylsiloxanes [187] [188], sodium metaphosphates [189] and large ring esters [190]. More progress still is to be expected in the future with the increasing sophistication and power of computational methods for modelling the conformations of both synthetic and biological macromolecules.

Appendix

Polymer Chemistry and Chemical Education

At the American Chemical Society Meeting in Las Vegas in September 1997, distinguished American chemists reported that there was still considerable opposition to the incorporation of polymer chemistry into undergraduate chemistry degree courses in the USA [191]. Some of these difficulties may be associated with the historical development of the subject, as will now be outlined.

Chemistry can be considered to be a single, indivisible subject, which is easily defined as the science of the chemical elements and the compounds and materials derived from them. All attempts to divide the subject into separate parts have either ended in failure or, in the end, may have created more problems that they have solved.

Fundamental differences of approach by some of the alchemical religious philosophers (such as Isaac Newton [192]) and medical and technical alchemists (such as Paracelsus [193]) were resolved by the establishment of modern chemistry as a unified subject, following the publication of Robert Boyle's *"Sceptical Chymist"* in 1661 [194]. Later attempts to divide chemistry by distinguishing between chemicals with a 'vital force' and those without were shown to be erroneous by FriedrichWoehler's laboratory synthesis of urea in the middle of the 19th Century [195].

However, as the subject developed later in the 19th Century, it became subdivided into three main branches. These were Organic Chemistry (arising from the work of Jakob Berzelius early in the century), Inorganic Chemistry (as illustrated by the publication of *"A System of Inorganic Chemistry"* in 1891) and Physical Chemistry (associated with the founding of the journal *"Zeitschrift für Physikalische Chemie"* by Wilhelm Ostwald and Jacobus Van't Hoff [196] in 1887).

Although these three branches were a useful and effective division of the whole subject at the beginning of the 20th Century, a major problem arose later on with the establishment of synthetic and biological macromolecular chemistry, initially by Hermann Staudinger in the 1920's [197][198] [199]. Large molecule chemistry is as much a part of the subject as small molecule chemistry but it is multidisciplinary in nature and often uses different experimental techniques, so it does not fit neatly into any of the three traditional branches. In fact, the

multidisciplinary nature of the chemistry of large ring molecules and cyclic polymers was illustrated by a recent book [8], in which all the main branches of the subject were involved (organic, inorganic, physical, biological, polymer, analytical and theoretical chemistry).

The resistance to the establishment of macromolecular chemistry by eminent small molecule chemists, such as Wolfgang Ostwald [200] and Adolph von Baeyer resulted in a slower incorporation of large molecule chemistry into chemistry first degree courses than might otherwise have been the case. To this day, most undergraduate chemistry courses in the USA are traditional and do not teach macromolecular chemistry. Much large molecule chemistry is instead being taught in Polymer Science, Engineering and Biochemistry Departments. This is despite the fact that many important advances are being made in polymer chemistry, which are of considerable value to the chemical industry; as well as in biological chemistry, which are central to an understanding of life processes. In this connection, our Chemistry Department at York may be ahead of its time by fully incorporating both synthetic and biological polymer chemistry in its undergraduate courses [201].

As Brian Fender has commented, the divisions into inorganic, physical and organic chemistry may have outlived their usefulness [202]. The beginning of the 21st Century could be the right time to reorder our subject in a more integrated way, so that it may be taught with a proper balance between large and small molecule chemistry in all undergraduate chemistry courses.

Acknowledgements

References

1. P. J.Flory, *Principles of Polymer Chemistry,*Cornell University Press,Ithaca,NY, 1953.

2. J.M.G.Cowie,*Polymers: Chemistry and Physics of Modern Materials,*Blackie,Chapman and Hall,London,1973 and 1991.

3. J.A.Semlyen (ed.),*Cyclic Polymers,*Elsevier Applied Science,London,1986.

4. F.Jacob and E.L.Wollman, Symp.Soc.Exp.Biol.,**12**,75(1958).

5. W.Fiers and R.L.Sinsheimer,J.Mol.Biol.,**5**,408(1962).

6. W.Fiers and R.L.Sinsheimer,J.Mol.Biol.,**5**,4214(1962).

7. D.Freifelder,A.K.Kleinschmidt and R.L.Sinsheimer,Science,**146**,254(1964).

8. J.A.Semlyen(ed.),*Large Ring Molecules*, John Wiley & Sons Ltd.,Chichester,New York, 1996.

9. H.Mark and G.S.Whitby,*Collected Papers of Wallace Hume Carothers on High Polymeric Substances,* Interscience Publishers,New York, 1940.

10. P.B.D.de la Mare and W.Klyne(eds.),*Progress in Stereochemistry*,Butterworths, Washington, 1962.

11. F.Sondheimer,R.Wolovsky and Y.Gaoni,J.Amer.Chem.Soc.,**82**,755(1960).

12. E.Wasserman,J.Amer.Chem.Soc.,**82**,4433(1960).

13. D.W.Scott,J.Amer.Chem.Soc.,**68**,2294(1946).

14. H.A.Hartung and S.M.Camiolo,Division of Polymer Chemistry, 141st National Meeting of the Amer.Chem.Soc.,Washington D.C., March 1962.

15. J.B.Carmichael and R.J.Winger,J.Poly.Sci., **A3**,971(1965).

16. J.B.Carmichael,D.J.Gordon and F.J.Isackson,J.Phys.Chem.,**71**,2011(1967)

17. J.F.Brown and G.M.J.Slusarczuk,J.Amer.Chem.Soc.,**87**,931(1965).

18. H.Jacobson and W.H.Stockmayer.J.Chem.Phys., **18,**1600(1950).

19. PJ.Flory and J.A.Semlyen,J.Amer.Chem.Soc.,**88**,3209(1966).

20. A.T.James and A.J.P.Martin,Analyst,**77**,915(1952).

21. C.S.G.Phillips,*Gas Chromatography,*Butterworths, London, 1956.

22. P.V.Wright and J.A.Semlyen,Polymer,**11**,462(1970).

23. J.C.Moore,J.Polym.Sci.,**A2**,835(1 964).

24. M.F. Vaughan and R.Dietz in *Chromatography of Synthetic and Biological Polymers,* edited by R.Epton,volume 1,Ellis Horwood,Chichester,1978.

25. K.Dodgson,D.Sympson and J.A.Semlyen,Polymer,**19**,1285, (1978).

26. S.J.Clarson and J.A.Semlyen(eds.),*Siloxane Polymers*,Prentice Hall,Englewood Cliffs, N.J.,1993,Chapter3.

27. J.A.Semlyen and coworkers,Studies of Cyclic and Linear Poly(dimethylsiloxanes),Parts 1-33,Polymer(1977-98).

28. J.Chojnowski,M.Scibiorek and J.Kowalski,Makromol.Chem.,**178**,1351(1977).

29. J.Chojnowski in Ref.26,Chapter 1.

30. T.R.Formoy and J.A.Semlyen,Polymer Comm.,**30**,86(1989).

31. M.S.Beevers and J.A.Semlyen,Polymer,**12**,373(1971).

32. S.J.Clarson and J.A.Semlyen,Polymer,**27**,1633(1986).

33. M.Beltzung,C.Picot,P.Rempp and J.Herz,Macromolecules,**15**,1594(1982).

34. A.C.Dagger and J. A.Semlyen,Polymer,**39**,2621 (1998).

35. A.C.Dagger and J.A.Semlyen,to be published.

36. M.Morton,A.A.Rembaum and E.E.Bostick,J.Appl.Polym.Sci.,**8**,2707(1964).

37. J.C.Saam,D.J.Gordon and S.Lindsey,Macromolecules,**3**,l(1970).

38. F.R.Jones,European Polymer J.,**10**,249(1974).

39. P.V.Wright,J.Polym.Sci.,Polym.Physics Edition,**11**,51(1973).

40. R.Yin,E.J.Amis and T.E.Hogenesch,Macromolecular Symposia,**85**,217(1994).

41. D.Geiser and H.Höcker,Polym.Bull.,**2**,591(1980).

42. D.Geiser and H.Höcker,Macromolecules,**13**,653(1980).

43. B.Vollmert and J.X.Huang,Makromol.Chem.,Rapid Commun.,**2**,467(1981).

44. J.Roovers and P.M.Toporowski,Macromolecules, **16**,843(1983).

45. H.Keul and H.Höcker in *Large Ring Molecules,* edited by J.A.Semlyen,John Wiley & Sons Ltd.,Chichester,New York, 1996.

46. G.B.McKenna,B.J.Hostetter,N.Hadjchristidis,L.J.Fetters and D.J.Plazek, Macromolecules **22**,1834(1989).

47. K.S.Lee and G.Wegner,Makromol.Chem.,Rapid Commun.,**6,**203(1985).

48. K.S.Lee and G.Wegner,Polymer,**28**,889(1987).

49. R.P.Quirk and J.Ma,Polym.Prep.,**33**,976(1992).

50. M.Schappacher and A.Deffieux,Macromol.Chem.,Rapid Commun.,**12**,447(1991).

51. J.J.L.Bryant and J.A.Semlyen,Polymer,**38**,4531(1997).

52. D.R.Cooper and J.A.Semlyen,Polymer,**14**,185(1973).

53. F.R.Jones,L.E.Scales and J.A.Semlyen,Polymer,**15**,738(1974).

54. B.R.Wood,J.A.Semlyen and P.Hodge,Polymer,**38**,191(1997).

55. J.A.Semlyen and coworkers, Equilibrium ring concentrations and the statistical conformations of polymer chains ,Parts l-14,Polymer(1969-76).

56. M.S.Beevers and J.A.Semlyen,Polymer,**13**,523(1972).

57.   K.J.Ivin and J.Leonard,Polymer,**6**,621 (1965).

58.   D.Vofsi and A.V.Tobolsky,J.Polym.Sci.,**A3**,2361(1965).

59.   J.M.Andrews and J.A.Semlyen,Polymer,**12**,642(1971).

60.   J.M Andrews and J.A.Semlyen,Polymer,**13**,141(1972).

61.   H.Spoor and H.Zahn, Z.Analyst.Chem.,**168**,190(1959).

62.   J.M.Andrews,F.R.Jones and J.A.Semlyen,Polymer,**15**,420(1974).

63.   J.A.Semlyen,J.J.L.Bryant,S.C.Hamilton and B.R.Wood,Abstracts of papers of the
        Amer.Chem.Soc.,**214**,**2**,54(1997).

64.   J.J.L.Bryant, D.Phil.thesis,University of York, 1997.

65.   T.Graham,Phil.Trans.R.Soc., **A123**,253(1833)

66.   J.R.van Wazer,*Phosphorus and its Compounds,*Vol.1,Interscience,NY, 1958.

67.   W.D.Treadwell and F.Leutwyler,Helv.Chim.Acta.,**20**,931(1937).

68.   J.F.McCullough,J.R.van Wazer and E.J.Griffith,J.Amer.Chem.Soc.,**78**,4528(1956).

69.   J.R.van Wazer and E.Karl-Kroupa,J.Amer.Chem.Soc.,**78**,1772(1956).

70.   E.Thilo and U.Schulke,Z.Anorg.Allgem.Chem.,**341**,293(1965).

71.   G.Gee,Trans.Faraday Soc.,**48**,515(1952).

72.   A.V.Tobolsky and A.Eisenberg,J.Amer.Chem.Soc.,**81**,780(1959).

73.   R.Steudel,H.-J.Mäusle,D.Rosenbauer,H.Möckel and T.Freyholdt,Angew.Chem.Int.Ed.,
        20,4,394(1981).

74.   R.Steudel in *Inorganic Ring Systems*,ed.by F.L.Boschke,Springer-Verlag,Berlin,1982.

75.   M.D.Gernez,Compt.rend.,**82**,115(1876).

76.   M.Schmidt and H.D.Block,Angew.Chem.,**79**,944(1967).

77.   R.Steudel and H.-J.Mäusle,Angew.Chem.Int.Ed.,**18,2**,152(1979).

78.   T.H.Thomas and T.C.Kendrick,J.Polym.Sci.,A2,**8**,537(1969).

79.   T.H.Thomas and T.C.Kendrick,J.PoIym.Sci.,A2,**8**,1823(1970).

80.   N.Grassie and I.G.MacFarlane,Eur.Polymer J.,**14**,875(1978).

81.   M.Blazso,G.Garzo,K.A.Andrianov,N.N.Makarova,A.I.Chernavsk and
        I.M.Petrov,J.Organometallic Chem.,**165**,273(1979).

82.   E.Thilo in *Advances in Inorganic Chemistry and Radiochemistry,*Academic
        Press,NY, 1962,Vol.4.

83.   A.Eisenberg,Inorganic Macromol.Rev.,**1**,75(1970).

84.   P.Ruggli,Liebigs Ann.,**392**,92(1912).

85.   K.Ziegler and R.Aurnhammer,Liebigs Ann.,**513**,43(1934).

86.   K.Ziegler,H.Eberle and H.Ohlinger, Liebigs Ann.,**504**,94(1933).

87.   M.Stoll and A.Rouvé,Helv.Chim.Acta,**30**,1822(1947).

88.   D.J.Brunelle and T.G.Shannon, Macromolecules,**24**,3035(1991).

89.   D.J.Brunelle.H.O.Krabbenhoff and D.K.Bonauto,Macromol.Symposia,**77**,l 17(1994).

90.   G.E.Yu,P.Sinnathamby,C.Price and C.Booth,Chem.Comm.,31(1996).

91.   Z.G.Yan,Z.Yang,C.Price and C.Booth,Makromol.Chem.Rapid Commun.,**14**,725(1993).

92.   M.Melissen,H.Keul and H.Höcker,Makromol.Chem.and Phys.,**l96,5**,1645(1995).

93.   B.R.Wood,J.A.Semlyen and P.Hodge,Polymer,**38**,191(1997).

94.   S.C.Hamilton and J.A.Semlyen,Polymer,**38**,1685(1997) .

95.   J.J.L.Bryant and J.A.Semlyen,Polymer,**38**,2475(1997).

96.   S.C.Hamilton and J.A.Semlyen,Polymer,**39**,3241(1998) .

97.   B.R.Wood,J.A.Semlyen and P.Hodge,Polymer,**38**,2287(1997).

98.   B.R.Wood,S.C.Hamilton and J.A.Semlyen,Polym.Int.,**44**,397(1997).

99.   Y.F.Wang,K.P.Chan and A.S.Hay,Reactive and Functional Polymers,**30**,1-3,205(1996).

100.   Y.F.Wang and A.S.Hay,Macromolecules,**30**,**2**,182(1997) .

101.   R.B.Merrifield,J.Amer.Chem.Soc.**85**,2149(1963).

102.   M.Mutter,J.Amer.Chem.Soc.,**99**,8307(1977).

103.   H.Driguez and J.-P.Utille,Carbohydr.Lett,**l**,125(1994).

104.   J.C.Wang and N.Davidson,J.Mol.Biol.,**15**,l 11(1966).

105.   J.C.Wang and N.Davidson,J.Mol.Biol., **19**,469(1966).

106.   J.A.Semlyen and P.V.Wright in R.Epton(ed.),*Chromatography of Synthetic Polymers and Biopolymers,* Ellis Horwood,Chichester, 1977, Vol. 1.

107.   P.J.Flory and J.A.Semlyen,J.Amer.Chem.Soc.,**88**,3209(l966).

108.   J.E.Mark and P.J.Flory,J.Amer.Chem.Soc.,**86**,138(1964).

109.   V.Crescenzi and P.J.Flory,J.Amer.Chem.Soc.,**86**,141(1964).

110.   P.J.Flory,V.Crescenzi and J.E.Mark,J.Amer.Chem.Soc.,**86**,146(1964).

111.   K.Dodgson and J.A.Semlyen,PoIymer,**18,**1265(1977).

112.   V.Bloomfield and B.H.Zimm,J.Chem.Phys.,**44**,315(1966).

113.   M.Fukatsu and M.Kurata,J.Chem.Phys.,**44**,4539(1966).

114.   J.S.Higgins,K.Dodgson and J.A.Semlyen,Polymer,**20**,553(1979).

115.   H.A.Kramers,J.Chem.Phys.,**14**,415(1946).

116.   B.J.Zimm and W.H.Stockmayer, J.Chem.Phys.,**17**,1301(1949).

117.   E.F.Casassa,J.Polym.Sci.,Part A,**3**,605(1965).

118.   C.J.C.Edwards,R.F.T.Stepto and J.A.Semlyen, Polymer,**21**,781(1980).

119.   M.Kumbar,J.Chem.Phys.,**55**,5046(1971).

120.   M.Kumbar,J.Chem.Phys.,**59**,5620(1973).

121.   E.F.Casassa and Y.Tagami, Macromolecules,**2,**14(1969).

122.   E.F.Casassa,Sep.Sci.,**6,**305(1971).

123.   E.F.Casassa,Macromolecules,**9**,182(1976).

124.   L.Garrido, J.E.Mark,S. J.Clarson and J. A.Semlyen,Polym.Commun.,**26**,43(1985).

125.   L.Garrido,J.E.Mark,S.J.Clarson and J.A.Semlyen,Polym.Commun.,**26**,55(1985).

126.   S.J.Clarson,J.E.Mark and J.A.Semlyen,Polym.Commun.,**27**,244(1986).

127.   T.J.Fyvie,H.L.Frisch,J.A.Semlyen,S.J.Clarson and J. E.Mark,J.Polym.Sci.,Polym. Chem.Ed.,**25**,2503(1987).

128.   S.J.Clarson,J.E.Mark and J. A.Semlyen,Polymer Commun.,**28**,151 (1987).

129.   W.Huang,H.L.Frisch,Y.Hua and J.A.Semlyen,J.Polym.Sci.,Polym.Chem.Ed.,**28**, 1807(1990).

130.   S.J. Joyce,R.E.Hubbard and J.A.Semlyen,Euro.Polym.J.,**29**,305(1993).

131.   S.N.Cohen,Scientific American,July(1975).

132.   J.A.Semlyen,Chemistry in Britain, **18,10**,704(1982).

133.   A.Kornberg,Scientific American, October 1968.

134.   R.M.Abeysekera,E.T.Bergström,D.M.Goodall,I.T.Norton and A.W.Robarts, Cabohydrate Research,**248**,225(1993).

135.   T.Kelen.D.Schlotterbeck and V.Jaacks.IUPAC Conference on Macromolecules,Boston, (1971).

136.   D.J.Brunelle(ed.),*Ring-Opening Polymerization (Mechanisms, Catalysis, Structure, Utility)*,Hanser Publications,Munich,Vienna,New York,Barcelona,(1993).

137.   K.Dodgson.D.J.Bannister and J.A.Semlyen,Polymer,**22**,663(1980).

138.   D.J.Orrah,J.A.Semlyen and S.B.Ross-Murphy,Polymer,**29**,1452(1988).

139.   M.Doi and S.F.Edwards,*The Theory of Polymer Dynamics,Oxford* University Press, Oxford,(1986).

140.   W.W.Graessley,Faraday Symp., **18**,7(1983).

141.   D.J.Orrah,J.A.Semlyen and S.B.Ross-Murphy,Polymer,**29**,1455(1988).

142.   G.B.McKenna and P.J.Plazek,Polym.Commun.,**27**,304(1986).

143.   G.Schill,*Catenanes, Rotaxanes and Knots* (translated by J. Boeckmann),Academic Press,New York,London,(1971).

144.   D.Muscat,A.Witte,W.Köhler,K.Müllen and Y.Geerts,Macromol.Rapid Commun.,**18**,233 (1997).

145.   F.Brochard and P-G De Gennes, Macromolecules,**10**,1157(1977).

146.   H.L.Frisch and E.Wasserman,J.Amer.Chem.Soc.,**83**,3789(1961).

147.   A.V.Vologodskii,*Topology and Physics of Circular DNA.Physical Approaches to DNA.* CRC Press,Boca Raton,FL,(1992).

148.   J.C.Wang, Trends in Biochem.Sci.**5**,219(1980).

149.   F.Stoddart,Chemistry in Britain,**27**,714(1991).

150.   D.Amabilino and F.Stoddart,New Scientist, 19 Feb.l994,p.25.

151.   C.J.Pederson,Angew.Chem.Int.Ed.Engl.,**27**,1021 (1988)(Nobel lecture).

152.   D.J.Cram,Angew.Chem.Int.Ed.Engl.,**27**,1009(1988)(Nobel lecture).

153.   E.Vulfson,C.Alexander and M.Whitcombe,Chemistry in Britain,Jan. 1997,p.23.

154.   P.J.Flory,*Statistical Mechanics of Chain Molecules,*Interscience Publishers,New York, London,(1969).

155.   H. Yamakawa, *Modern Theory of Polymer Solutions,* Harper and Row,New York, London, (1971).

156.   P.Debye,J.Chem.Phys.,**14**,636(1946).

157.   C.J.C.Edwards,R.F.T.Stepto and J.A.Semlyen,Polymer,**23**,869(1982).

158.   C.J.C.Edwards,R.W.Richards,R.F.T.Stepto,K.Dodgson,J.S.Higgins and J.A.Semlyen, Polymer,**25**,365(1984).

159.   J.-M.Barbarin,I.A.McLure,S.J.Clarson and J.A.Semlyen,Polymer Commun.,**28**,212 (1987).

160.   D.J.Bannister and J.A.Semlyen,Polymer,**22**,377(1981).

161.   M.S.Beevers, S.J.Mumby, S.J.Clarson and J.A.Semlyen,Polymer,**24**,1565(1983).

162.   S.J.Clarson, K.Dodgson and J.A.Semlyen,Polymer,**26**,930(1985).

163.   D.J.Orrah, J.A.Semlyen, K.Dodgson and R.A.Pethrick,Polymer Commun.,**31**,25(1990).

164.   S.Granick,S.J.Clarson,T.R.Formoy and J.A.Semlyen,Polymer,**26**,925(1985).

165.   A.Patel,T.Cosgrove and J.A.Semlyen,Polymer,**32**,1313(1991).

166.   B.J.Burton, R.K.Harris, K.Dodgson, C.J.Pellow and J.A.Semlyen, Polymer Commun.,**24**,278(1983).

167.   S.J.Clarson and J.A.Semlyen, Polymer,**28**,189(1987).

168.   S.Granick,D.J.Kuzmenka,S.J.Clarson and J.A.Semlyen,Langmuir,**5**,144(1989).

169.   S.Granick,D.J.Kuzmenka,S.J.Clarson and J.A.Semlyen,Macromolecules,**22**,1878 (1989).

170.   R.D.C.Richards, W.D.Hawthorne, J.S.Hill,M.S.White,D.Lacey, J. A.Semlyen,G.W.Gray and T.C.Kendrick,Chem.Commun.95(1990).

171.   J.A.Semlyen, Adv.Polym.Sci.,**21**,41(1976).

172.   W.Kuhn,Kolloid-Z.,**76**,258(1936).

173.   W.Kuhn,Kolloid-Z., **87**,3(1939).

174.   P.J.Flory,U.W.Suter and M.Mutter,J.Amer.Chem.Soc.,**98**,5733(1976).

175.   U.W.Suter,M.Mutter and P.J.Flory,J.Amer.Chem.Soc.,**98**,5740(1976).

176.   M.Mutter.U.W.Suter and P.J.Flory,J.Amer.Chem.Soc.,**98**,5745(1976).

177.   P.J.Flory,Proc.Natl.Acad.Sci.,USA,**51**,1060(1964).

178.   P.J.Flory and R.L.Jernigan,J.Chem.Phys.,**42**,3509(1965).

179.   M.A.D.Fluendy,Trans.Faraday Soc.,**59**,1681(1963).

180.   J.B.Cannichael and J.B.Kinsinger,Canad.J.Chem.,**42**,1996(1964).

181.   J.A.Semlyen,Trans.Faraday Soc.,**63**,2342(l967).

182.   W.L.Mattice and U.W.Suter,*Conformational Theory of Large Molecules,*John Wiley & Sons Ltd.,Chichester,New York (1994).

183.   J.A.Semlyen,Trans.Faraday Soc.,**63**,743(1967).

184.   J.A.Semlyen,Trans,Faraday Soc.,**64**,1396(1968).

185.   J.A.Semlyen,Polymer,**12**,383(1971).

186.   K.Dodgson,R.E.Heath and J.A.Sonlyen, Polymer, 40,3995 (1999).

187.   M.S.Beevers and J.A.Semlyen,Polymer,**13**,385(1972).

188.   L.E.Scales and J.A.Semlyen,Polymer,**17**,601(1976).

189.   D.R.Cooper and J.A.Semlyen,Polymer,**13**,414(1972).

190.   R.E.Heath,B.R.Wood and J.A.Semlyen, to be published.

191.   M. Jaffe and W.H.Daly(Organisers),Symposium on Aspects of Graduate Training in Polymer Science, American Chemical Society Meeting in Las Vegas, September 7-11 (1997).

192.   E.N.da C.Andrade, *Sir Isaac Newton,* Fontana Books, London(1961).

193.   F.Sherwood Taylor, *The Alchemists,* Granada Publishing Ltd., St. Albans (1976).

194.   R-Boyle, *The Sceptical Chymist,* J.Cadwell,London(1661).

195.   B.Jaffe, *Crucibles,*Jarrods Publishers,London(1931), chapter 10.

196.   E. von Meyer, *A History of Chemistry,* translated by G.McGowan, Macmillan&Co.Ltd, New York(1898).

197.   H.Staudinger,Ber.,**53**,1073(1920).

198.   H.Staudinger,Ber.,**57**,1203(1924).

199.   H.Staudinger,Ber.,**59**,3019(1926).

200.   Wolfgang Ostwald, *An Introduction to Theoretical and Applied Colloid Chemistry,* 2nd American edition, translated by M.H.Fischer,John Wiley & Sons Ltd.New York(1922).

201.   J.A.Semlyen,Polymer News,**21,10**,350(1996).

202.   R.Stevenson,Brian *Fender - H E reaching new heights*, Chemistry in Britain, 30
        December (1996).

CHAPTER 2

CIRCULAR DNA

Alexander V. Vologodskii,

New York University, USA

In 1963 by Dulbecco and Vogt [l] and Weil and Vinograd [2] discovered that double-stranded DNA of the polyoma virus exists in a closed circular form. At present it is generally acknowledged that this form is typical of bacterial DNA and of cytoplasmic DNA in animals. Furthermore, giant DNA molecules in higher organisms form loop structures held together by protein fasteners in which each loop is largely analogous to closed circular DNA. The distinctive feature of closed circular molecules is that its topological state cannot be altered by any conformational rearrangement short of breaking DNA strands. This topological constraint is the basis for the characteristic properties of closed circular DNA which have fascinated biologists, physicists and mathematicians for the past 35 years. In this chapter we concentrate our attention on physical properties of circular DNA which understanding is necessary for the successful analysis of the biological effects connected with this form of DNA.

2.1 DNA supercoiling

2.1.1 Basic concepts

2.1.1.1 Closed circular DNA and linking number

Two forms of circular DNA molecules are extracted from the cell; they were designated as form I and form II. The more compact form I was found to turn into form II after a single-stranded break was introduced into one chain of the double helix. Subsequent studies performed by Vinograd et al. [3] linked the compactness of form I, in which both DNA strands are intact, to supercoiling. Form I came to be called the closed circular form. In this form each of the two strands that make up the DNA molecule is closed in on itself. A diagrammatic view of closed circular DNA is presented in Figure 1.

The two strands of the double helix in closed circular DNA are linked. In topological terms, the link between the strands of the double helix belong to the torus class. The quantitative description of such links is called the linking number (Lk), which may be determined in the following way (Figure 2).

One of the strands defines the edge of an imaginary surface (any such surface gives the same result). The Lk is the algebraic (i.e., sign-dependent) number of intersections between the other strand and this spanning surface. By convention, the Lk of a closed circular DNA formed by a right-handed double helix is

47

positive. *Lk* depends only on the topological state of the strands and hence is maintained through all conformational changes that occur in the absence of

Figure 1 - Diagram of dosed circular DNA. The Unking number of the complementary, *Lk,* strands is 11.
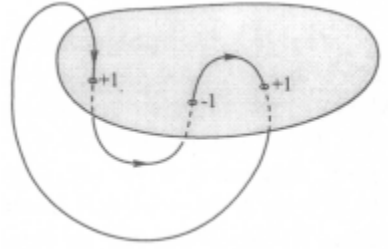

Figure 2 - Definition of the linking number of two closed contours. An imaginary surface is drawn up on one contour, then one calculates the algebraic number of intersections between this surface and the other contour. *Lk=1* for this example.

strand breakage. Its value is always integral. *Lk* can be also defined through the Gauss integral,

$$Lk = \oint_{C_1} \oint_{C_2} \frac{(d\mathbf{r}_1 \times d\mathbf{r}_2)\mathbf{r}_{12}}{r_{12}^3} , \tag{1}$$

where $\mathbf{r}_1$ and $\mathbf{r}_2$ are vectors whose ends run, upon integration, over the first and second contours, $\mathbf{C}_1$ and $\mathbf{C}_2$ respectively, $\mathbf{r}_{12} = \mathbf{r}_2 - \mathbf{r}_1$ (see Figure 3).

Quantitatively, the linking number is close to N/γ, where N is the number of base pairs in the molecule and γ is the number of base pairs per double-helix turn in linear DNA under given conditions. However, these values are not exactly equal one to another, and the difference between *Lk* and N/γ (which is also denoted as Lk_o) defines most of the properties of closed circular DNA.
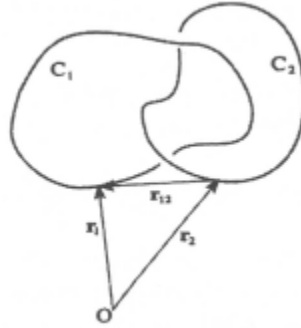
Figure 3 - Notation of vectors in the calculation of the Gauss integral.

2.1.1.2 Linking number difference and superhelix density. Topoisomers

The fact that closed circular DNA has a topological invariant gives rise to a new physical parameter which characterizes this form and determines many of its properties. This parameter, **ΔLk,** is called the *linking number difference* and is defined as

$$\Delta Lk = Lk - N/\gamma \qquad (2)$$

There are two inferences to be made from the above definition.

1. The value of **ΔLk** is not a topological invariant. It depends on the solution conditions which determine γ. Even though γ itself changes very slightly with changing ambient conditions, these changes may substantially alter **ΔLk,** as the right-hand part of Eq. (2) is the difference between two large quantities that are close in value.

2. The linking number Lk is by definition an integer, whereas **N/γ** should not be an integer. Hence **ΔLk** is not an integer either. However, the values of **ΔLk** for a closed circular DNA with a particular sequence can differ by an integer only. This simply follows from the fact that, whatever the prescribed conditions, all changes in **ΔLk** can only be due to changes in Lk, since the value of **N/γ** is the same for all molecules (Of course any change of Lk would involve a temporary violation of the integrity of a double-helix strand).

Molecules that have the same chemical structure and differ only with respect to *Lk* are called topoisomers.

It often proves more convenient to use the value of superhelical density, σ, which is N/γ normalized for Lk_o:

$$\sigma = \Delta Lk / Lk_o = \gamma \cdot \Delta Lk / N. \tag{3}$$

Whenever $\Delta Lk \neq 0,$ closed circular DNA is said to be supercoiled. Clearly, the entire double helix is stressed in supercoiled condition. This stress can either lead to a change in the actual number of base pairs per helix turn in closed circular DNA or cause regular spatial deformation of the helix axis. The axis of the double helix then forms a helix of a higher order (Figure 4). It is this deformation of the helix axis in closed circular DNA that gave rise to the term "superhelicity" or "supercoiling" [3]. Circular DNA extracted from cells turns out to be always (or nearly always) negatively supercoiled and has a σ between -0.03 and -0.09, but typically near the middle of this range [4].

2.1.1.3 Twist and writhe

Supercoiling can be structurally realized in two ways: by deforming the molecular axis and by altering the twist of the double helix. This can be ascertained by means of a simple experiment involving a rubber hose. Take a piece of hose and a short rod that can be pushed into the hose with some effort. The rod can be used to join together the ends of the hose and thus rule out their reciprocal rotation around the hose axis. If before joining the two ends one turns one of them several times around the axis, i.e. if one twists the hose, it will shape itself into a helical band once the ends are joined. If one draws longitudinal stripes on the hose prior to the experiment, it will be clear that reciprocal twisting of the ends also causes the hose's torsional deformation. There is very important quantitative relationship between the deformation of the DNA axis, its torsional deformation and *Lk* of the complementary strands of the double helix. The first mathematical of treatment the problem was presented in 1961 by Calugareanu, who found the basic relationship between the geometrical and topological properties of a closed ribbon [6]. The theorem in its current form was first proved by White in 1969 [7]. Two years later, Fuller specifically suggested how the theorem can be applied to the analysis of circular DNA [8].

According to the theorem, the *Lk* of the edges of the ribbon is the sum of two values. One is the twist of the ribbon, *Tw,* a well known concept, and the second, a new concept, writhe *Wr.* Thus,

$$Lk = Tw + Wr. \tag{4}$$

Tw is a measure of the number of times one of the edges of the ribbon spins about its axis. The *Tw* of the entire ribbon is the sum of the *Tw* of its parts. The value of *Wr* is defined by the spatial course of the ribbon axis; i.e., it is a
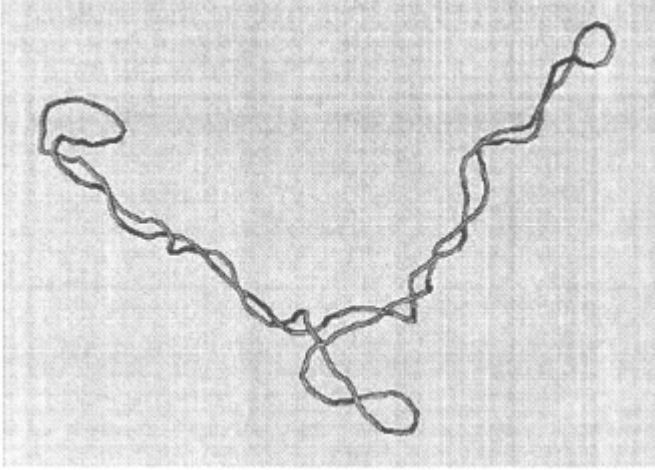

Figure 4 - A typical conformation of supercoiled DNA. The picture obtained by computer simulation of supercoiled molecule 3500 base pairs in length, σ = -0.06, for physiological ionic conditions [5].

characteristic of a single closed curve, unlike *Lk* and *Tw* which are properties of a closed ribbon. Thus *Lk* can be represented as a sum of two values that characterize the available degrees of freedom: the twist around the ribbon axis and the deformation of this axis. To apply the theorem to circular DNA, the two strands of the double helix are considered as edges of a ribbon.

Let us consider the most important properties of *Wr* (see [8-11] for more detailed reviews). *Wr* is completely specified by the geometry of DNA axis and is equal to the Gauss integral (see Eq. (1)) in which integration is performed both times along the same contour - the ribbon axis. *Wr* can be thought as a measure of a curve's net right-handed or left-handed asymmetry, i.e., its chirality, and is equal to zero for a planar curve. Unlike *Lk*, which can only be an integer, a curve's *Wr* can have any value. It changes continuously with the curve's deformation that does not involve the intersection of segments. A curve's *Wr* does not change with a change in the curve's scale and depends solely on its shape.

Consider *Wr* of an almost flat 8-shaped curve (Figure 5). As it turns out, the *Wr* of such a curve is -1 if the curve is a fragment of a right-handed helix (the case in Figure 5), and +1 if the crossing corresponds to a left-handed helix. This result does not depend on the shape or size of the two loops of the "8", or

on the angle between the curve segments in the crossing area. In general, for nearly flat curves Wr is equal to the algebraic sum of the contributions of all "crossings"[8].
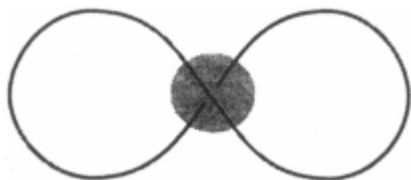

Figure 5 - The nearly flat "eight" figure. Only the gray-circled part of the contour juts out of plane. For such a curve Wr approaches -1.

Another important property of Wr holds not only for the "quasi-flat" curve but for an arbitrary curve as well. When the curve is deformed in such a way that one of its parts passes through another, the writhe value experiences a leap by 2 (or -2 for the opposite direction of the pass). This property helped greatly in the analysis of the action mechanisms of topoisomerases [12].

The main result of the ribbon theory, expressed in Eq. (4), is that Lk can be structurally realized in two different ways. The first way consists in changing the twist of the double helix, the second lies in the deformation of the helix axis, giving rise to a certain writhe.

Fuller was the first who made simple theoretical analysis of the shape of supercoiled DNA [8]. He calculated the Wr of two possible form, simple and interwound helices (Figure 6).

Figure 6 - Diagram of simple (left) and interwound helices (right). The helix winding angles (a) are shown. The number of helical turns equals 4 and 8, correspondingly.
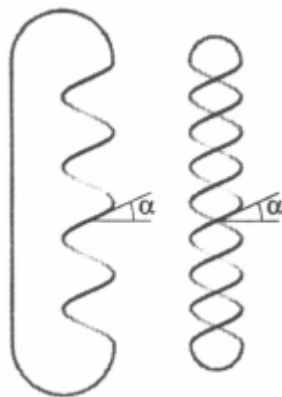
By neglecting the ends of the helices, he concluded that the Wr of a simple right-handed helix is given by

$$Wr = n(1 - \sin \alpha) \qquad (5a)$$

and that the Wr of an interwound right-handed helix has the form

$$Wr = -n \sin \alpha \qquad (5b)$$

where n is the number of helical turns and α is the winding angle. As either helix is extended, the value of α increases thereby decreasing the curvature of the rod and its bending energy. It follows from Eqs. (5), that as α increases, the $|Wr|$ of a simple helix diminishes, whereas that of an interwound helix increases. The torsional deformation will be less, then, for the interwound form. Therefore, the interwound superhelix should be favored over a simple one from an energetic point of view. Indeed, all available experimental and theoretical data indicate interwound conformations for supercoiled DNA (reviewed in [13]).

2.1.2 Basic questions

Eq. (4) expresses that there are at least two ways of structural realization of supercoiling. So the questions arises:

1. How is DNA supercoiling distributed between different possible ways of its structural realization?

2. How does this partitioning depend on σ and on solution conditions?

3. How does DNA sequence affect the partitioning?

Mathematical analysis of supercoiling described in the previous section suggested that supercoiling causes only elastic torsional and bending deformation of the double helix. However, sufficiently high negative supercoiling can also cause disruptions of the regular DNA structure, (nonelastic deformation). Such disruptions come out as opened base pairs, cruciforms, Z and H forms of DNA. We will consider the issue later in this chapter.

Today we know a lot about conformational changes caused in DNA by supercoiling. Essential part of this knowledge was obtained by experimental methods specific for supercoiled DNA. These methods are very powerful and often open unique opportunities to study general properties of the double helix. Therefore we first consider specific experimental approaches to study DNA supercoiling.

2.1.3 Experimental methods specific for supercoiled DNA

2.1.3.1 Measuring ΔLk

The value of DNA supercoiling is specified by ΔLk and thus experimental determination of ΔLk is the first problem to be solved. Two different experimental approaches to the problem are based on the fact that supercoiling makes DNA more compact, increasing its mobility in gel or the sedimentation constant. The first method developed in the pioneering studies of Vinograd and coworkers uses the titration of supercoiling by an intercalating dye [14]. This approach is applicable only to negatively supercoiled DNA. The molecules of some dyes have the ability to intercalate themselves between base pairs in the double helix on binding to DNA, thus reducing the helical rotation angle between the base pairs. As an increasing number of these molecules bind themselves to negatively supercoiled DNA, the tensions within the DNA molecule are gradually removed and conformations of the double-helix axis becomes less compact. This causes a decrease in the molecule's mobility, which can be registered experimentally (Figure 7).
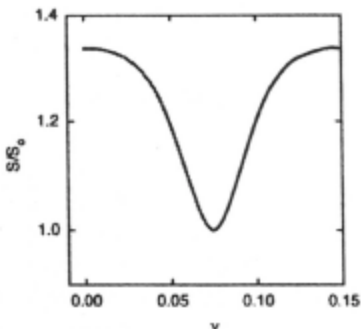
Figure 7 - Dependence of the sedimentation constant for closed circular DNA on the amount of bound ligand molecules. The ratio of the sedimentation constants of supercoiled and opened circular forms is plotted.

Then, after the number of bound ligand molecules per base pair, v, exceeds the value

$$v = 360\Delta Lk / (\varphi N) \tag{6}$$

where φ corresponds to the change of angle, in degrees, between adjacent pairs upon the integration of a ligand molecule between them, the tensions in DNA will start growing again. This will increase the molecule's mobility. As a result, DNA mobility has a minimum. Having found the value of v at the minimum one

can find ΔLk from Eq. (6) if the value of φ is known. For ethidium bromide, which is most often used for titration supercoiled DNA, $\varphi = -26°$ [15]. The number of bound ligand molecules can be found with the help of spectral methods.

In 1975 Keller proposed the second approach to determining the linking number difference in closed circular DNA [16], This approach is based on the fact that the values of ΔLk in any mixture of DNA topoisomers can differ by an integer only. The electrophoretic mobility of DNA is so sensitive to conformational changes, that under appropriate experimental conditions molecules with a difference in ΔLk of 1 produce separate bands in the electrophoretic pattern. If DNA sample contains all possible topoisomers with ΔLk from 0 to some limiting value and they are all well resolved with respect to mobility, one can find the value of ΔLk corresponding to each band simply by band counting (Figure 8).

One can then scan the gel to find the relative amount of DNA at each band. The band that corresponds to $\Delta Lk \approx 0$ (since ΔLk is not an integer we should talk about the closest to 0 possible value) can be identified through a comparison with the band for the nicked circular form. One should bear in mind the fact that topoisomer mobility is determined by the absolute value of ΔLk only, so the presence of topoisomers with both negative and positive ΔLk can make interpreting the electrophoresis more difficult. Another restriction of the method lies in the saturation of molecular mobility growth with increasing $|\Delta Lk|$.
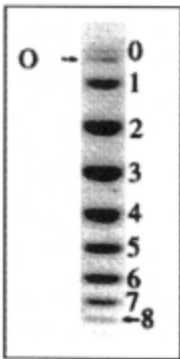

Figure 8 - Gel electrophoretic separation of topoisomers of pUC19 DNA. The mixture of topoisomers covering the range of $\boxed{\Delta Lk}$ from 0 to -8 was electrophoresed from a single well in 1% agarose from top to bottom. The topoisomer with $\boxed{\Delta Lk} = 0$ has the lowest mobility: it moves slightly slower than the opened (nicked) circular DNA (OC). The value of ($-\boxed{\Delta Lk}$) for each topoisomer is shown. (Illustration provided by M. Vologodskaia.)

A very elegant and effective way to overcome these shortcomings, two-dimensional gel electrophoresis, was proposed in [17]. A mixture of DNA topoisomers is loaded into a well at top left corner of a slab gel, and electrophoresed along left side of the gel. The bands corresponding to topoisomers with large ΔLk values merge into one spot. After that the gel is

transferred in a buffer containing the intercalating ligand chloroquine and electrophoresed in the second, horizontal direction (Figure 9).

The mobility of topoisomers in the second direction no longer be determined by ΔLk, but by the value $(\Delta Lk - N\nu\varphi/360)$, which can be regarded as the effective linking number difference. We can say that the distribution of ΔLk for the second direction is shifted by a positive value. As a result the mobilities of topoisomers with opposite values of ΔLk are different in the second direction and the topoisomers with large negative ΔLk which had identical mobility in the first direction move with different speed in the second direction. The number of topoisomers that can be resolved almost doubles in the case of two-dimensional electrophoresis.
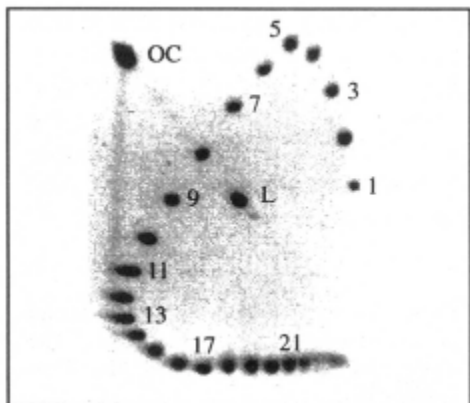
Figure 9 - Separation of pUC19 DNA topoisomers by two-dimensional gel electrophoresis. Topoisomers 1-4 have positive supercoiling, the rest have negative supercoiling. After electrophoresis was performed in the first direction, from top to down, the gel was saturated with ligand intercalating into the double helix. Upon electrophoresis in the second direction, from left to right, the 12th and 13th topoisomers turned out to be relaxed. The spot in the top left corner corresponds to the nicked circular form (OC), the spot in the middle of the gel corresponds to the linear DNA (L). (Illustration provided by M. Vologodskaia.)

The separation of DNA topoisomers in a gel has proved to be one of the most potent techniques in DNA research. This method and its two-dimensional version have led to a whole series of remarkable experimental studies (reviewed in [11, 18]).

It is important to emphasize here that ΔLk depends on the ambient conditions in solution. A temperature increase of 30° causes σ to increase by approximately 0.01, since the double helix unwinds with rising temperature [19-22]. The increase constitutes about 20% of the characteristic σ for a closed circular DNA isolated from the cell. The double helix winds itself up with

increasing the ion concentration, and a change of σ resulting of changing ionic conditions can be as large as 0.01 [23, 24].

2.1.3.2 Obtaining DNA with a preset ΔLk

To obtain a DNA with a preset superhelical density closed circular DNA molecules are treated with an enzyme called topoisomerase I. The action of this enzyme can alter the value of Lk in closed circular DNA as it introduces a single-stranded break into the double helix and then, after a while, "heals" it [25]. In between these two events the DNA may undergo changes in axial twist and shape, so that Lk gradually relaxes to its equilibrium value for the given conditions, i.e. the value corresponding to the minimum stress in closed circular DNA. This equilibrium value of Lk can be changed within a wide range by adding various ligands which alter the helical rotation angle of the double helix upon binding to it. Thus, by adding varying amounts of an intercalating dye (usually ethidium bromide), one can obtain, after enzyme treatment and removing both ligand and enzyme from the solution, closed circular DNA with a certain required negative superhelicity. It was difficult to obtain positively supercoiled DNA in this way until recently, when a protein was found which increases Lk_o upon binding with the double helix [26].

It is important that by such a way we always obtain a distribution of DNA topoisomers with Lk distributed around a mean value rather than one topoisomer (if DNA is longer than 500 base pairs). This distribution is analyzed in detail in the next section.

2.1.4 Equilibrium distribution of topoisomers

2.1.4.1 Free energy of supercoiling

Closed circular DNA molecules with a ΔLk value other than zero have additional free energy, which is called supercoiling free energy, $G(\Delta Lk)$. Precise knowledge of $G(\Delta Lk)$ is very important for successful analysis of many problems related with DNA supercoiling. Here we will consider one of two known ways of the experimental determination of $G(\Delta Lk)$. In 1975 Depew and Wang [21] and Pulleyblank et al. [27] studied the equilibrium thermal distribution of closed circular DNA over topoisomers. The distribution was obtained by the same treatment of circular closed DNA with topoisomerase I, in the absence of any ligands. As we have said above, the enzyme can alter the value of Lk in closed circular DNA by breaking and men restoring one strand in the double helix. This treatment causes the distribution of molecules with respect to Lk to relax towards the equilibrium form. Large DNA molecules adopt a lot of different conformations in solution with comparable probability and these conformations correspond to different values of Tw and Wr, and consequently ΔLk. Therefore the equilibrium distribution of topoisomers contains in comparable amounts more than one topoisomer if DNA length exceeds 500 bp.

The distributions were analyzed by gel electrophoresis. Figure 10 presents typical result of such experiment. The maximum of the equilibrium distribution always corresponds to $\Delta Lk = 0$. It is also clear that molecules with close absolute values of ΔLk must have close mobility, hence be next to each other in the gel. Distributions of the kind presented in Figure 10, where molecules having positive and negative ΔLk values are separated, are the result of electrophoresis conditions that differ from those used for the topoisomerase reaction. The change in conditions means that γ in Eq. (2) needs to be replaced by a different value, γ', while Lk remains unchanged. As a result the entire distribution will shift by the value $\Delta Lk - \Delta Lk' = N(1/\gamma - 1/\gamma')$, and for a large enough value of this difference all the topoisomers will be well separated.
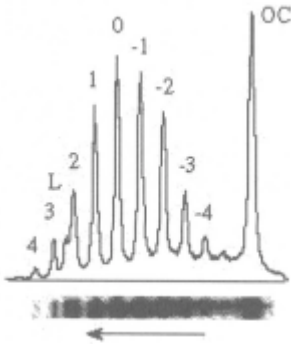
Figure 10 - Equilibrium topoisomer distribution of circular DNA 7,000 base pairs in length. A photograph of the gel is shown together with its quantitative scan. Adjacent peaks correspond to topoisomers that differ by 1 in the Lk value. (The illustration provided by V. Rybenkov.)

The experiments demonstrated [21, 27, 28] that the resulting distribution is always a normal one and thus can be specified by its variance, $\left\langle (\Delta Lk)^2 \right\rangle$:

$$P(\Delta Lk) = A\exp\left[-\frac{(\Delta Lk)^2}{2\left\langle (\Delta Lk)^2 \right\rangle} \right], \qquad (7)$$

where A is the normalization factor, and the brackets $\langle\ \rangle$ correspond to an averaging over the equilibrium distribution of DNA conformations. On the other hand, there is general relationship between the probability of a state and the

corresponding free energy. Thus the equilibrium distribution $P(\Delta Lk)$ can be expressed as

$$P(\Delta Lk) = A \exp\left[-G(\Delta Lk)/RT\right]. \qquad (8)$$

Experiments showed (Figure 11) that $\left\langle(\Delta Lk)^2\right\rangle$ is proportional to DNA length if $N > 2500$ [21, 27,28]:

$$\left\langle(\Delta Lk)^2\right\rangle = N/2K \qquad (9)$$
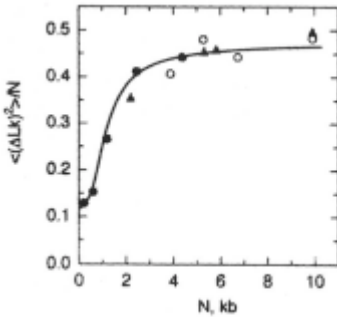
where K is a constant.

Figure 11 - Dependence of the variance, $\left\langle(\Delta Lk)^2\right\rangle$, of the equilibrium topoisomer distribution on the DNA length, N, measured in thousands of base pairs. The variance values have been normalized for N. The experimental data are from refs. [21] (○), [27] (▲), [28] (●).

Note that $\left\langle(\Delta Lk)^2\right\rangle$ diminishes faster when $N < 2500$ (Figure 11). Comparing (6), (7) and (8) one concludes that

$$G(\Delta Lk) = KRT(\Delta Lk)^2 / N, \quad \text{if} \quad N > 2500. \qquad (10)$$

It was predicted theoretically[29] and recently shown experimentally [24] that the value of K depends on ionic conditions. For ionic conditions close to physiological ones (0.2 M NaCl or 10 mM $MgCl_2$) $K = 1100$ if $N > 2500$ [21, 24, 27, 28].

In spite of its intrinsic elegance, the method of finding $G(\Delta Lk)$ based on the equilibrium distribution of topoisomers is not without its shortcomings. Most important is that this method allows $G(\Delta Lk)$ to be determined only for $|\sigma| < 0.01$, whereas it is the -0.07 -0.03 range that is of the greatest interest in physical and biological terms. Recent theoretical calculations of $G(\Delta Lk)$ showed that although the quadratic dependence on ΔLk is kept until $|\sigma| < 0.06$ for physiological ionic conditions, it is not the case for lower ion concentrations [5, 13]. Another approach to $G(\Delta Lk)$ determination based on titration of supercoiling by an intercalating ligand, pioneered by Bauer and Vinograd [30], seems more appropriate in this case (see also [31])

2.1.4.2 Further analysis of the equilibrium distribution of topoisomers

It is important to understand well the nature of the equilibrium distribution of topoisomers considered above, so we are continuing its discussion. The experimentally observed equilibrium fluctuations in the ΔLk are made up of fluctuations in the twist, Tw, and writhe, Wr, of the double helix. In a circular DNA with a single-stranded break torsional (changing of Tw) and bending (changing of Wr) fluctuations occur independently from each other (this is an assumption which should be considered as a good first approximation). The enzyme-assisted rejoining of the DNA strand at the break point occurring at a random moment in time fixes the momentary value of the sum $Tw + Wr$, i.e. Lk. It is clear that the average values of Lk and Tw are equal to Lk_o and the average value of Wr is zero. So random values ΔLk, $\Delta Tw = Tw - Lk_o$, and Wr will have zero averages and their variances can be expressed as $\langle (\Delta Lk)^2 \rangle$, $\langle (\Delta Tw)^2 \rangle$, and $\langle (Wr)^2 \rangle$, correspondingly. Independence of the random fluctuations of Tw and Wr allows us to write the following equation:

$$\langle (\Delta Lk)^2 \rangle = \langle (\Delta Tw)^2 \rangle + \langle (Wr)^2 \rangle. \tag{11}$$

Since the value of $\langle (\Delta Lk)^2 \rangle$ has been found experimentally (see above), and $\langle (Wr)^2 \rangle$ can be calculated (see below), Eq. (10) makes it possible to determine $\langle (\Delta Tw)^2 \rangle$ and thus to find torsional rigidity of the double helix since a simple equation relates $\langle (\Delta Tw)^2 \rangle$ to DNA torsional rigidity, C:

$$\langle (\Delta Tw)^2 \rangle = NlkT / \pi^2 C, \tag{12}$$

where l is the separation between adjacent base pairs along DNA axis ($l = 0.34$ nm), and k is the Boltzmann constant [32].

Although DNA double helix is very rigid molecule in the scale of a few base pairs, long DNA molecules are flexible regarding their thermal fluctuations (see [33], for example). Thus a circular DNA longer than a few hundreds base pairs adopts very different conformations in solutions (Figure 12). Each of these conformations have certain value of Wr. To evaluate $\langle (Wr)^2 \rangle$ we can simulate the equilibrium distribution of DNA conformations for a particular DNA length and calculate $\langle (Wr)^2 \rangle$ over the simulated set of conformations [34, 35]. Refining the DNA model and computational programs for such simulations allowed to compute $\langle (Wr)^2 \rangle$ for different DNA lengths with good accuracy (see

Wr= 2.64   Wr= 0.36   Wr=-1.97
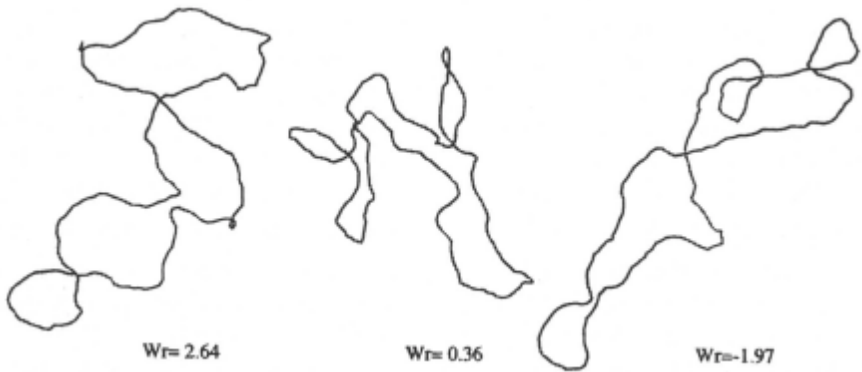
Figure 12 - Typical conformations of nicked circular DNA 3500 base pairs in length. The illustration was obtained by computer simulation of the equilibrium conformational set [29]. The values of Wr for each simulated conformation are shown.

[29] and refs. therein). The simulation results showed that $\langle (Wr)^2 \rangle$ is proportional to N if $N > 2500$. However, $\langle (Wr)^2 \rangle$ drops faster for shorter DNA molecules, since their typical conformations are becoming more and more flat as the length decreases (Wr of a flat conformation equals zero). The difference between the experimentally determined value $\langle (\Delta Lk)^2 \rangle$ and the

calculated value $\langle (Wr)^2 \rangle$, however, is proportional to N over the whole range of N studied, $250 < N < 10000$, in full agreement with Eq. (11). The $\langle (\Delta Tw)^2 \rangle$ found in this way made it possible to determine the torsional rigidity of the double helix on the basis of Eq. (11). The value of C obtained in this treatment equals $3 \cdot 10^{-19}$ erg·cm [29].

The above treatment also gave an answer to the other questions about conformations of supercoiled DNA: what are the relative contributions of Wr and Tw in the structural realization of supercoiling? The data show that about 3/4 of ΔLk are realized in the form of bending deformation for the molecules with more than 2500 base pairs and for ionic conditions close to physiological ones. Although this conclusion was obtained for very low supercoiling which corresponds to the thermal fluctuations, further studies showed that the answer is correct for all range of supercoiling where the DNA secondary structure remains intact [5, 36-39].

2.1.5 Conformations of supercoiled DNA

Electron microscopy (EM) is the most straightforward way to study conformations of supercoiled DNA. This method has been used extensively since the discovery of DNA supercoiling by Vinograd and coworkers in 1965 [3]. They found that supercoiled DNA has a compact, interwound form. This conclusion was conformed in many EM studies which also brought quantitative information about DNA supercoiling [36, 37, 40, 41]. The data obtained include the measurements of $\langle Wr / \Delta Lk \rangle$ and the average superhelix radius as a function of σ, and the branching frequency of the superhelix axis. It became clear, however that labile DNA conformations may change during sample preparation for EM (see [13] for details). A serious problem for interpreting EM results is that the ionic conditions on the grid are not specified. The DNA is exposed to several different solutions and dried before being viewed, and it is unknown when in the procedure the DNA is "fixed". Cryoelectron microscopy and atomic force microscopy are free from some of the disadvantages of more conventional EM since in these methods DNA is viewed in solution or in a thin layer of vitrified water without shadowing or staining. It was shown by these methods that conformations of supercoiled DNA depend greatly on ionic conditions [36, 42, 43]. Still, independent solution studies are required to confirm conclusions of the methods about this very flexible object.

The solution methods, like hydrodynamic and optical ones, do not give direct, model-independent information about the three-dimensional structure of supercoiled DNA. These methods do, however, measure structure-dependent features of supercoiled DNA in well-defined solutions while perturbing conformation only minimally. The methods turned out to be very productive in

the studies of DNA supercoiling when used in combination with computer simulation of supercoiled molecules. The strategy of these studies is simple: using a model of the double helix one has to calculate measurable properties of supercoiled DNA, measure the properties for the actual molecules and compare the results with the simulation data. If the results are in agreement we can assume that simulated and actual conformations look similar as well.

The efficiency of this approach originates from the simple elastic rod model that can be used for the quantitative calculations of DNA conformational properties [5]. The bending and torsional rigidities of this model are known from numerous independent studies. The third and last parameter of the model, DNA effective diameter, specifies the electrostatic interaction between DNA segments. It is the diameter of an uncharged elastic rod which mimics the conformational properties of actual electrically charged DNA [44]. Its value depends strongly on ionic conditions and can be several times greater than the geometric diameter of the double helix [24, 44-48]. The electrostatic repulsion between DNA segments is very important for properties of tight conformations of supercoiled DNA, and therefore the effective diameter is very essential parameter of the model. Using this model one can simulate a random set of conformations that corresponds to the equilibrium distribution of DNA conformations. Monte Carlo method is usually used to prepare the set [5, 49, 50]. The constructed set allows to determine the mean and distribution of different superhelix parameters such as Wr, the average number of branches, or sedimentation coefficient [38]. There is an analogy between this computer approach and EM which can also be considered as a Monte-Carlo method, because conclusions are drawn from a limited statistical sample. Of course, a much larger set can be generated computationally.

Let us consider the study of the equilibrium formation of DNA catenanes between supercoiled and nicked circular DNA as an example of this approach [39]. Catenanes were formed by cyclizing linear DNA with long cohesive ends in the presence of supercoiled molecules. The efficiency of the catenation depends on the distance between opposing segments of DNA in the interwound superhelix. The fraction of cyclizing molecules that becomes topologically linked with the supercoiled DNA is the product of the concentration of the supercoiled DNA and a proportionality constant, B, that depends on conformations of supercoiled DNA. The values of B were measured for different ionic conditions and supercoiling. In parallel with the experiments, the values of B were calculated using Monte Carlo simulations of the equilibrium distribution of DNA conformations. Very good agreement between measured and simulated values of B was found in this study over a broad range of σ and ionic conditions (Figure 13).

Taking into account that there were no adjustable parameters in the simulation the agreement between experimental and simulation results is striking. Very good agreement between experimental and simulated results were obtained in other studies of supercoiled DNA based on the comparison of solution measurements and computer simulations [38, 51]. This allowed to conclude that the simulations predict conformations of the supercoiled DNA extremely well and can be used to study properties of the supercoiled molecules which are hard to measure directly. We conclude this section by a picture of typical simulated conformations of supercoiled molecules for two different ionic conditions and $\sigma = -0.06$ (Figure 14). Although the conformations for both ion concentrations clearly correspond to branched interwound superhelices, there is
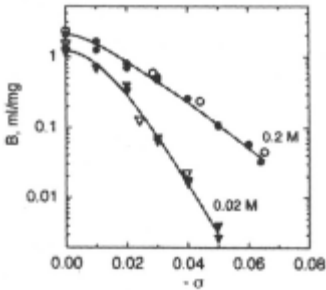
Figure 13 - Probing conformations of supercoiled DNA. Measured and simulated equilibrium constants of catenation, B, are shown as a function of supercoiling at NaCl concentration of 0.2 M (circles) and 0.02 M (triangles). The experimental values of B (open symbols) are shown together with calculated results (filled symbols). The solid lines are the best fits to the calculated data.

a large difference between them. This difference explains a big effect of ionic conditions on the equilibrium constant of catenation shown in Figure 13.
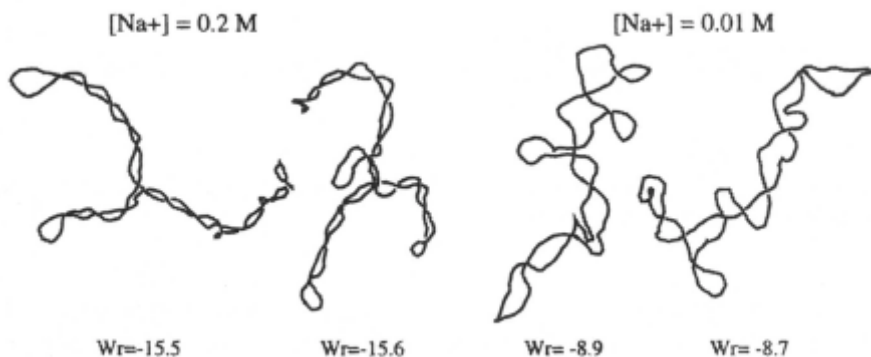
Figure 14 - Typical simulated conformations of supercoiled DNA in solution containing 0.2 M NaCl (left) and 0.01 M NaCl (right). The conformations of the model chains correspond to DNA 3.5 kb in length and $\sigma = -0.06$.

2.1.6 Formation of noncanonical structures

2.1.6.1 General consideration

So far we considered properties of circular DNA which do not involve disruptions of the regular structure of the double helix. However, with sufficiently high negative supercoiling such disruptions become inevitable. In effect, such disruptions are a way of structural realization of supercoiling. In contrast torsional and bending deformations, which are distributed along the whole circular DNA molecule, disruptions in the regular structure have a local character, while their type and location depend on the DNA sequence. All these alternative structures have a smaller (compared with the canonical B-form of DNA) interwinding of one strand of the DNA relative to the other.

The simplest type of structures induced by negative supercoiling are melted or opened regions where DNA strands are not interwoven in the relaxed state (Figure 15). Such regions appear first of all in the DNA sections enriched with AT base pairs because melting of such pairs requires less free energy than does the melting of GC pairs.

Figure 15 - Formation of the opened region in double-stranded DNA. Complementary strands are not interwoven, in average, in such region.

In palindromic regions of DNA, cruciform structures may occur (Figure 16). Again, the complementary strands of DNA are not twisted relative to each other in the cruciform structures. At the same time, a large part of the cruciform's nucleotides are involved in the helical structure, which means that their free energy corresponds to the free energy of a regular linear double helix. That is why formation of a long enough cruciform structure must be preferable to the formation of opened sections of the same size.

Figure 16 - Formation of cruciform in double-stranded DNA. (A) Example of a palindromic sequence. The symmetrical parts of the sequence are shaded. (B) Diagram of the B-DNA - cruciform transition.

The maximum release of negative superhelical stress per base pair causes formation of the Z-form [52], where the strands are twisted into a left-handed helix with a helical repeat of 12 base pairs per turn (Figure 17). The left-handed form predominantly occurs in DNA regions with a regular alternation of purines and pyrimidines, first of all G and C.

Figure 17 - Formation of the left handed Z form inside B-DNA segment.

Another type of noncanonical structure occasioned by negative supercoiling is the H form, which may occur in DNA sections where one strand comprises only purine and the other only pyrimidine bases [53]. The main element of the H form is a triple helix stabilized by Watson-Crick and Hoogsteen base pairs (Figure 18). Topologically, the H form is equivalent to an opened section or a cruciform structure: the complementary strands of DNA in the H form are not twisted relative to each other. The development of the H form is stimulated by the reduction of pH of the solution
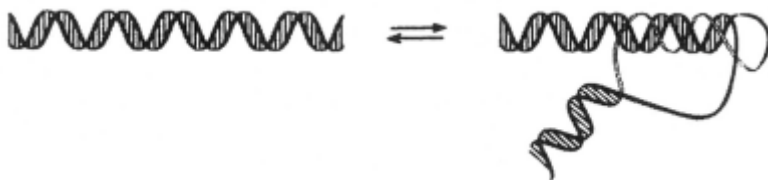
Figure 18 - Formation of the H form inside B-DNA segment. The pyrimidine strand and half the purine strand make up a triple helix; the other half of the purine strand is free. Only Watson-Crick base pairs are shown. The CGC triplets are protonated in this structure.

One more structure where the double helix is somewhat unwound compared to B-DNA is A-DNA. The difference in the angles of helical rotation for these two forms is so small, however, that negative supercoiling cannot by itself induce the transition of any DNA section from the B into the A form in usual solution conditions.

It is worth emphasizing once again that the formation of all the above noncanonical structures is thermodynamically wasteful in linear DNA in near-physiological conditions, and it is only negative supercoiling that allows them to evolve under such conditions.

2.1.6.2 Experimental detection of noncanonical structures

All the existing methods of studying noncanonical DNA structures occasioned by negative supercoiling can be divided into two groups. The first group brings together the methods based on the registration of local changes in DNA sections where a structural modification has taken place. In principle, these methods can be used just as effectively to register local structural changes in linear molecules, too. We shall refer to this group as methods of localization of

structural transitions. The second group of methods is based on the measurement of integral properties of DNA. As it is, only one method in this group, which is based on the use of the specific properties of closed circular DNA, is truly effective. On the formation of a noncanonical structure under the impact of negative supercoiling, superhelical stress itself decreases and so does the absolute writhe value which determines the electrophoretic mobility of DNA molecules in gel. This change in mobility lies at the core of the second approach. The method does not provide any information on where exactly the conformational change has happened, but allows one to obtain quantitative characteristics of the transition observed. The method offers an absolutely unique opportunity of reliable quantitative registration of conformational changes in a region that accounts for about 1% of the total length of the molecule. No other physical method registering integral properties of DNA (UV-spectroscopy, circular dichroism, infra-red spectroscopy, NMR) makes it possible to monitor changes affecting such a small fraction of DNA base pairs.

2.1.6.2.1 Methods of localization of structural transitions

Most methods of localization of structural transitions are based on breaking DNA at the site of the formation of a noncanonical structure with the subsequent mapping of these breaks. The breaks can be introduced by special enzymes, endonucleases, which specifically hydrolyze single-stranded DNA. These endonucleases are sensitive even to minor irregularities in the helical structure of DNA. In cruciform structures they cause breaks in the loops of the hairpins [54, 55]. There are sites sensitive to these endonucleases in the areas of Z and H forms and, naturally, in opened regions of DNA. In supercoiled DNAs there are also other areas of increased sensitivity to such endonucleases, though the nature of structural changes in such areas is not clear yet. Although after the application of the first single-strand break noncanonical structures in DNA soon disappear as a result of the relaxation of superhelical stress, the enzymes often go on to cut the second strand of the DNA, opposite the first break. That is why a considerable fraction of the molecules end up in the linear form after the treatment with endonucleases.

Another way of applying breaks in the areas of the formation of noncanonical structures is by using chemical agents which modify DNA bases at the spots which in the regular B form are screened off by the double helix structure. Further chemical treatment of such a selectively modified DNA leads to a break-up of the sugar-phosphate chains at the sites of primary modification.

Restriction analysis is used for rough preliminary mapping of the breaks. DNA molecules converted into the linear form by way of nuclease or chemical cutting are treated with some restriction endonuclease to obtain a set of restriction fragments. This set is compared by way of electrophoretic separation with a reference set obtained by treatment of the original circular DNA with the same restriction endonuclease. If the cutting at the point of structural

deformation occurred in one DNA region, two additional bands should appear in the electrophoresis of the first set of fragments, compared with the reference set. Besides, one of the lines of the calibration set should be missing in the first set of fragments or become much less intensive. By gauging the length of the additional fragments according to the graduation of the gel and knowing localization within the sequence of the cut fragments, it is possible to find two possible sites of structural deformation. After the preliminary localization of the site of specific cleavage, it is possible to obtain the picture of the distribution of cuts at the nucleotide level. By this method Lilley and Panayotatos and Wells discovered the formation of cruciform structures in natural supercoiled DNAs [54, 55].

2.1.6.2.2 Method of two-dimensional gel electrophoresis

This very elegant and effective method of analyzing local conformational changes in supercoiled DNA was first suggested by Wang and coworkers [56]. The method allows one to obtain, as a result of a single experiment, the complete dependence of the probability of the formation of an alternative structure on σ. Besides, it yields important information on the changing equilibrium number of turns of one DNA strand relative to the other, which is associated with this transition. Two-dimensional electrophoresis is the most informative and accurate method of quantitative analysis of local conformational transitions in supercoiled DNA.

The electrophoretic mobility of DNA molecules increases monotonously with the growth of the absolute value of ΔLk. This is due to the fact that topoisomers with a larger $|\Delta Lk|$ must have a greater $|Wr|$ and, consequently, a more compact conformation. This, however, is true only as long as the molecule undergoes no conformational changes which reduce superhelical stress and, consequently, $|Wr|$. DNA topoisomers which have undergone the transition will have lower mobility compared to what it would have been in the absence of the transition. As a result, the monotonous rise in the mobility of molecules with the growing ΔLk may be disrupted. A one-dimensional electrophoresis of the mixture of topoisomers will show a pattern of irregular bands by which it will be hard to identify specific topoisomers. Two-dimensional electrophoresis helps to identify the bands with specific topoisomers. Electrophoresis in the first direction is performed under ordinary conditions, along one of the edges of a flat gel. This results in the distribution of topoisomers which was described above. Before the electrophoresis in the second direction the gel is saturated with an intercalating ligand. As a result of the ligand binding the superhelical stress in DNA is no longer determined by ΔLk but by the value $(\Delta Lk - \nu\phi N / 360)$, where ν is the number of bound ligand molecules per base pair, ϕ is the angle of unwinding of the double helix upon the binding of a single ligand molecule $(\phi < 0)$, and N is the number of base pairs in DNA. The concentration of the

ligand is selected in such a way that the remaining superhelical stress should be insufficient for the formation of a noncanonical structure in the topoisomer set. In this case, the mobility of topoisomers monotonously depends on $|\Delta Lk - \nu\phi N / 360|$. That is why after the completion of electrophoresis in the second direction, correlating spots with specific topoisomers is not difficult at all (Figure 19). The mobility of the 17th topoisomer in Figure 19 is close to that of the 12th during the first direction of the electrophoresis. It means that these topoisomers have the same Wr and, consequently, the same torsional stress. The torsional stress is defined by the same deviation in the strands' twist from the equilibrium value and therefore

Figure 19 - Cruciform extrusion in palindromic region $d[CCC(AT)_{16}GGG]$ of circular DNA 3000 bp in length. The mobility of topoisomers in the course of the first, vertical electrophoresis leaps sharply between the 14th and 15th, which becomes clear after the completion of electrophoresis in the second, horizontal direction. This mobility leap is associated with the cruciform formation in the palindromic region. (Illustration provided by M. Vologodskaia.)
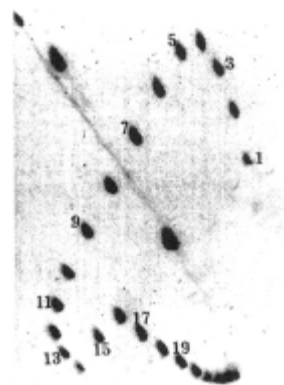
the deviations have to be same as well. Consequently, the whole difference in $|\Delta Lk|$ in these topoisomers is compensated with the change of the equilibrium twist during the transition, δTw, which equals 5 in this case. For some reasons for cruciform structures the observed δTw value is often 1 to 1.5 turns larger than the estimated value.

2.1.6.3 Thermodynamic analysis

Let us consider a simple thermodynamics of the formation of noncanonical structures in closed circular DNA (more advanced version of this analysis can be found in ref. [13]). The analysis is very useful for comprehending the main regularities of the formation of noncanonical structures in supercoiled DNA, although it leaves out the important fact that in real DNA a multitude of states may occur with a comparable probability, so in general one has to use the statistical-mechanical approach for quantitative analysis.

The analysis is based on the generally accepted assumption that the free energy of the formation of noncanonical structures can be presented in the form of two terms [35, 56, 57]. One of these terms corresponds to the transition-related change in the free energy of supercoiling, and the second is the change in the free energy of linear DNA upon the conformational transition. As long as DNA remains in regular B form, it torsional stress and, consequently, the free energy of supercoiling is defined by ΔLk (see Eq. (10)). We assume that the energy of supercoiling will continue to depend only on the DNA's elastic deformation after the formation of a of noncanonical structure. The magnitude of elastic deformation will be defined now by $(\Delta Lk - \delta Tw)$ rather than by ΔLk, where δTw is the change in the equilibrium twist at the transition of m base pairs from the B form to the alternative structure. The δTw value can easily be expressed through the number of base pairs per turn of the double helix in the B form, γ_B, and the number of base pairs per turn of one strand around the other in the alternative structure, γ_{alt}:

$$\delta Tw = m(1/\gamma_{alt} - 1/\gamma_B) \tag{13}$$

Thereby the energy of supercoiling can now be expressed in the form:

$$G = KRT(\Delta Lk + m\kappa/\gamma_B)^2 / N, \tag{14}$$

where we introduced $\kappa = 1 - \gamma_B/\gamma_{alt}$. The value of κ specifies the change of DNA twist per base pair associated with a particular transition. Accordingly, the change in the free energy of supercoiling δG equals:

$$\delta G = KRT\left[(\Delta Lk + m\kappa/\gamma_B)^2 - (\Delta Lk)^2\right]/N \tag{15}$$

It is often more convenient to express δG as a function of σ;

$$\delta G = AN\left[(\sigma + m\kappa/N)^2 - \sigma^2\right], \tag{16}$$

where $A = KRT/\gamma_B^2$. This equation formally implies that the formation of any structure with a lesser Tw of the strands than in the B form of DNA reduces the energy of supercoiling (for a negative σ) and, consequently, must be stimulated by negative supercoiling. This, of course, is true only under the condition that this structure forms in a comparatively short DNA fragment, so that the $m\kappa/\gamma_B$ value does not exceed $|\Delta Lk|$. It should be noted here that Eqs. (15) and (16) assume the square dependence of the free energy of supercoiling on ΔLk. Generalization of the equations for any other dependence $G(\Delta Lk)$ is straightforward, however.

The change in the free energy of linear DNA upon the conformational transition can be calculated as $\sum_{i=1}^{m}\Delta F_i + 2F_j$, where ΔF_i is the free energy change associated with base pair i, and F_j is the free energy of each boundary between B form and the alternative structure. At the transition point, σ_{tr}, the full free energy change must be zero:

$$\delta G + \sum_{i=1}^{m}\Delta F_i + 2F_j = 0. \tag{17}$$

Let us consider application of this analysis to two types of alternative structures.

Cruciform structures. Of the energy parameters, ΔF_i and F_j, in the case of cruciforms the ΔF_i values must be assumed to be zero. Indeed, the cross grows in size at the expense of the destruction of two base pairs in the main helix and the formation of two identical pairs in the hairpins. This should not change the free energy of the structure, because the number of paired bases and all border elements of the structure remain as they were. This means that the formation of cruciform structures must be characterized by a single energy parameter F_j (only the $2F_j$ value has a physical meaning in this case). Thus Eq.(17) is reduced to

$$-\sigma_{tr} = F_j / (Am) + m / (2N). \tag{18}$$

We accounted here that for cruciform structures the parameter κ is equal to 1. Indeed, in cruciform structures the complementary strands are not twisted relative to each other ($\gamma_{alt} = \infty$). It follows from Eq. (18) that the absolute value of σ_{tr} decreases when m increases, since the last term in Eq. (18) is relatively small. Experimental studies show that cruciform extrusion at typical palindromic regions 25-30 bp in length takes place at σ_{tr} of (-0.04) ÷ (-0.06) [58]. Taking $A = 10RT$, one can evaluate F_j from these data which is around 10 kcal/mol.

Left-handed Z form. The transition of a DNA fragment from a right-handed B-helix into a left-handed Z-helix ($\gamma_Z = -12$) provides the maximum release of superhelical stress compared to other noncanonical structures:

$$\kappa = 1 - 10.5 / (-12) = 1.87. \tag{19}$$

Although the transition was initially observed for $d(CG)_n \cdot d(CG)_n$ and $d(AC)_n \cdot d(GT)_n$ inserts in supercoiled DNA, many others sequences can be converted into the Z form as long as the superhelical stress is high enough. For

DNA regions with a regular alternation of purines and pyrimidines $\Delta F_{GC} = 0.33$ kcal/mol and $\Delta F_{AT} = 1.15$ kcal/mol, F_j is close to 5 kcal/mol [59-61]. More general analysis of Z DNA formation for an arbitrary DNA sequence can be found in [61-63].

2.1.6.4 Mutual influence of structural transitions

There is strong mutual influence between different transitions in closed circular DNA, caused by negative supercoiling. The primary reason for this is that any such transition reduces the superhelical stress in DNA, a driving force for other transitions. This mutual influence has to be taken into account in a

Figure 20 - Changing equilibrium twist of DNA upon the B-Z transition in two identical inserts, d(CG)$_{12}$·d(CG)$_{12}$, within the 4400-bp plasmid [66]. The theoretical curve is shown alongside the experimental data (O).
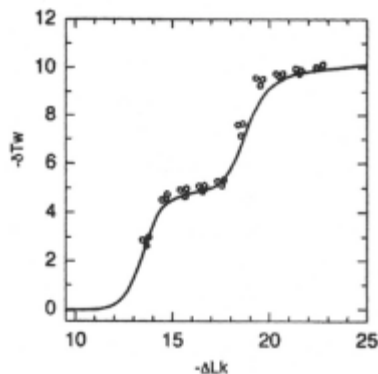
quantitative analysis of conformational changes in supercoiled DNA. The phenomena has been studied in details both experimentally and theoretically [11, 64-67]. Here we only illustrate it by one graphic example, B-Z transitions in a plasmid containing two d(CG)$_{12}$·d(CG)$_{12}$ inserts separated by a certain distance. With the growth of negative supercoiling in that DNA two cooperative transitions are observed, corresponding to B-Z transitions in both inserts (Figure 20). Since the inserts are identical, it is impossible to say which of them undergoes the transition earlier and which later, but the transition in one of them reduces the superhelical stress and holds back the formation of the Z helix in the other insert. Such a picture of conformational transitions was observed experimentally and obtained theoretically by accounting all possible states of the inserts [66]. It is important to emphasize that this kind of behaviour is essentially impossible in linear DNA where two such transitions occur independently and simultaneously.

2.2 Knots and links in DNA

As a linear DNA molecule links into a circle, it ends up in a specific topological state. Until now we examined different topological states associated with the linking number of the complementary strands of the double helix. The strands' linking number, however, is not the only topological characteristic of circular DNA. As it links into a circle, any polymeric chain may finish up in an unknotted state or form a knot of a certain type. In the case of the DNA double-helix attention has to be focused on the type of the knot formed by the axis of the double helix (an unknotted closed chain is considered as a trivial knot). With all conformational rearrangements of the chains the type of the knot must remain unchanged. This factor must influence the conformational properties of closed chains, which have to depend on their topology.

Just as different types of knots may form through the ring closure of single chains, a closed pair or a larger number of polymeric chains may form links of different types, or catenanes. We have already considered special type of links formed by the complementary strands of a double helix in a closed circular DNA. In this section, however, the double helix will be treated as a simple polymer chain. Linked DNA molecules occur quite frequently in nature and can be obtained in lab conditions too. As it is, links of two chains, even as knots in isolated molecules, come in an infinitely large number of topologically non-equivalent types. The notion of linking number which was extensively used above is good only for characterizing links of a certain class (torus links) forming in closed circular DNA. The overall picture is much more complicated.

Knots and links often form in living cells and in the course of various laboratory manipulations with DNA. Different aspects of these issues are discussed in reviews [68-70].

2.2.1 Types of knots and links

For the classification knots and links have to be deformed to obtain the standard form of their projection on a plane. A standard form of a knot (link) projection is such an image thereof when the minimum number of intersections on the projection is achieved. One must be always careful, though, that there should be no self-intersection of chains in the course of such reduction. Deformations of this kind are known in topology as isotopic deformations. Two knots (or links) which can be transformed into each other by way of isotopic deformation belong to the same isotopic type.

Knots can be simple or composite. A knot is composite if there is an unlimited surface crossed by the knot at two points, which thus divides it into two knots. This definition is graphically presented in Figure 21. The simplest knot has three intersections in the standard form and is called a trefoil.

Figure 21 - A composite knot The shaded unbounded surface intersects this knot at two points only. By contracting these points into one along the surface, we obtain two trefoils.
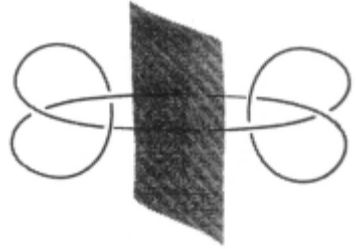
Figure 22 shows the initial part of the table of simplest knots - namely, all knots with less than six intersections in the standard form.

3_1 (Trefoil) 4_1 5_1 5_2 6_1 6_2 6_3
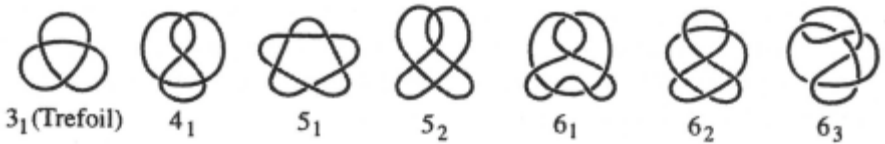
Figure 22 - Table of simple knots with less than seven intersections in the standard form.

A knot and its mirror image are considered to belong to the same type of knot, although they may belong to the same or different isotopic types. In particular, the trefoil and its mirror image cannot be transformed into each other by way of continuous deformation without self-intersection, and therefore belong to different isotopic types. The figure eight knot (4_1) and its mirror image belong to the same isotopic type. The table of knots is, in fact, a table of knot types, for it features only one representative of mirror pairs. With the growth of the number of intersections the number of types of simple knots grows very fast. As it turns out, there are 49 types of simple knots with nine intersections, 165 with ten and about 552 types of knots with eleven intersections [71, 72].

The tables of two-contour links are based on the same principle as the table of knots [71]. The initial part of the table of link types is shown in Figure 23. Although three links in this table, 2_1, 4_1 and 6_1, belong to the torus class which corresponds to the links of the complementary strands of the double helix in closed circular unknotted DNA, the fraction of torus links between more complex links is very small.
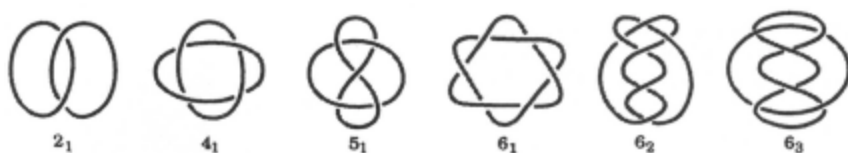
Figure 23 - Table of links with less than seven intersections in the standard form.

2.2.2 Topological equilibrium

It was discussed earlier that long DNA molecules adopt many different conformations in solution and their properties have to described in terms of the probability distribution (**2.1.4.2**). Between many possible distributions one is very important, the distribution which corresponds to thermodynamic equilibrium. We have considered the equilibrium distribution of Wr in nicked circular DNA (**2.1.4**). Another example is the distribution of the end-to-end distance in linear molecules. As a result of thermal motion the distributions of these and other properties always relax to their equilibrium form. So after some time we will always have an equilibrium distribution of conformational properties of our molecules in solution.

Distributions of topological states of circular molecules are different. These distributions are not changed as long as the molecule backbones stay intact. For example, if all our circular DNAs form left-handed trefoils, they will keep this state (and it will affect all other their conformational properties). The system of circular molecules does not relax to the equilibrium distribution of topological states. The concept of the equilibrium distribution is very useful, however, in this case as well.

A formal definition of the equilibrium distribution of topological states of circular molecules is not different from the equilibrium distributions of properties of linear molecules. This is the most probable distribution which has to reached by random exchange between different states in solution. This distribution minimizes the free energy of the molecule set. We would get the equilibrium distribution of topological states if our circular molecules had phantom backbones, so their segments could pass one through another during the thermal motion. Thus, to calculate the distribution we should forget about forbidden exchange between different topological states and use the usual rules of statistical mechanics.

Although exchange between different topological states is impossible in solution of circular DNAs, we can obtain the topological equilibrium by slow cyclization of linear molecules (reviewed in [11, 18]). The cyclization can be provided by cohesive ends of DNA. If the cohesive ends are long enough (about a dozen nucleotides or longer), a circular form is stable at room temperature; for shorter cohesive ends ligation is required to seal at least one of two single stranded brakes. Sometime we can also use enzymes, DNA topoisomerases, which catalyze the strand passage reaction between DNA segments, to obtain the equilibrium distribution. The second approach can shift the distribution from its equilibrium form, however, if the enzyme consume the free energy of ATP hydrolysis catalyzing strand passage reaction [73].

2.2.3 Equilibrium probabilities of knots in circular molecules

Let us first consider very diluted solution of opened circular DNA so the probability of links between two of them is negligible. In this case the equilibrium distribution of topological states is reduced to the probabilities of unknotted circles and various knots. The first question is what is the probability of any knot for a circular DNA of a particular length? The main problem to study the question is how to distinguish between unknotted circular molecules and knots of various types. Let us first consider theoretical aspect of this problem.

How to analyze the topology of a particular closed chain configuration, or how to determine the knot type to which this configuration belongs? Let us imagine that we have a heavily entangled circular cord and we want to find out whether it is knotted or not. The fact that persistent attempts to untangle the cord have produced no result cannot be taken as a proof that we are dealing with a knot. What is needed for resolving this problem is a single-valued algorithm of verification of the topological identity of the configuration in question. The construction of such algorithms belongs to the realm of a branch of mathematics known as topology [72]. Topologists developed invariants of the topological states, characteristics thereof which remain unchanged with any deformations of the chains, which are possible without the disruption of their integrity. The simplest topological state invariant is the Gauss integral which defines the linking number of two chains (reviewed in [10, 11]. Of course, for classifying the state of chains with a topological invariant, the latter must assume different values for different topological states. Not a single topological invariant meets this requirement in full measure, but there are very powerful ones among them which help identify many elementary types of knots (links) and distinguish them from more complex ones. The Gauss integral is a fairly weak topological invariant and is of no use for distinguishing many linked states of chains from unlinked states. Still the integral is very useful for analysis of DNA supercoiling, since it identifies all links of the torus class. Another very useful invariant is the Alexander polynomial which is convenient in computer simulation (reviewed in [10]). It is a polynomial of one variable in the case of knots and of two variables

in the case of links. The invariant was used in all studies dealing with the computer calculation of the equilibrium distribution of topological states.

Starting from 1974, about a dozen studies have been devoted to computer calculations of the equilibrium probability of knots (reviewed in [10, 74]; see also [75] and refs. therein). The results show that equilibrium probability of knotted circular molecules increases with their length (Figure 24).

Figure 24 - Equilibrium probability of the simplest knots in circular DNA. Results of computer simulations [48], solid lines, are shown together with experimental measurements [47, 48], symbols. The data correspond to the physiological ionic conditions.
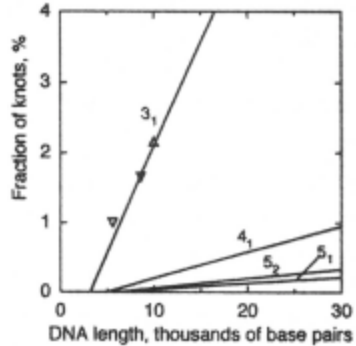
The figure shows that for DNA molecules a thousands base pairs in length the equilibrium fraction of knots is rather small, although the fraction of the simplest knots, trefoils, can be measured with good accuracy. Computer calculations of the equilibrium probabilities of knots showed, that the probabilities reduce dramatically when the thickness of the molecule increases [76]. In the case of DNA their effective thickness is defined not only by the geometrical diameter of the double helix, but also by electrostatic repulsion of the DNA segments. Therefore comparison between calculated and measured equilibrium fraction of trefoils allowed to determine electrostatic repulsion between DNA segments for different ionic conditions by comparing measured and calculated equilibrium probability of knotting [24, 47, 48].

Knots and links of different types formed by circular DNA molecules have different electrophoretic mobility in gel, which makes it possible to separate them by electrophoresis (Figure 25). The method requires special calibration, for it is impossible to say in advance what position a particular topological structure must occupy relative to the unknotted circular DNA form. A sufficiently large body of experiment results on the mobility of various topological structures has been accumulated by now [68, 77]. To separate knotted and linked DNA molecules by gel electrophoresis they must have single-strand breaks, for otherwise mobility will also depend on the double helix's linking number.

Figure 25 - Electrophoretic separation of knotted (right lane) and linked (left lane) DNA molecules 4363 bp length. Each band corresponds to knots or links with a specific number of intersections in the standard form. These numbers are shown next to each band. All links belong to the torus family. OC dimer is opened circular DNA molecule of double length. (Illustration provided by E. M. Shekhtman and D. E. Adams.)
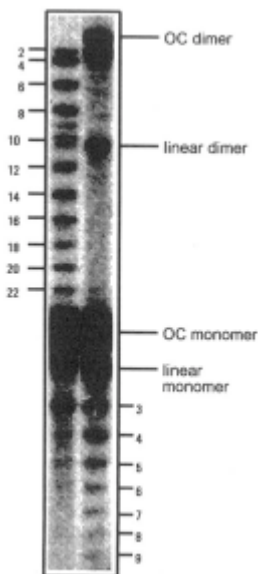
2.2.4 Equilibrium probabilities of links

If the concentration of DNA molecules during their random cyclization in solution is not too small, some fraction of the molecules will form catenanes at thermodynamic equilibrium. Let us suggest that the concentration is still small enough so most of circular molecules are not linked with others at equilibrium; in this case links of 3 and more molecules can be neglected. In this case we can consider the formation of catenanes as a bimolecular reaction which is characterized by its equilibrium constant, B. Equilibrium concentration of linked DNA molecules, c_{cat}, can be found from the equation

$$c_{cat} = B(c - c_{cat})^2 \approx Bc^2, \qquad (20)$$

where c is the total concentration of circular molecules. The value of B depend on DNA length and ionic conditions in solutions. Dependence of B on DNA length for physiological ionic conditions is shown in Figure 26.

We can also consider topological equilibrium for a system which includes two types of circular DNAs (A and B). Such a system was used to probe conformations of supercoiled molecules (described in **2.1.5**). It consisted of supercoiled molecules of one length (molecules A) and cyclizing molecules of

another length (molecules B). The system was prepared in such a way that there was only partial topological equilibrium: there were no AA catenanes although the concentration of molecules A was rather high but there was equilibrium regarding AB links. Since the goal was to measure the equilibrium constant for AB links, such partial equilibrium simplified the analysis of various products in this system. It is interesting that a similar approach to measure equilibrium catenation was used by Wang and Schwarz more than 30 years ago [78].
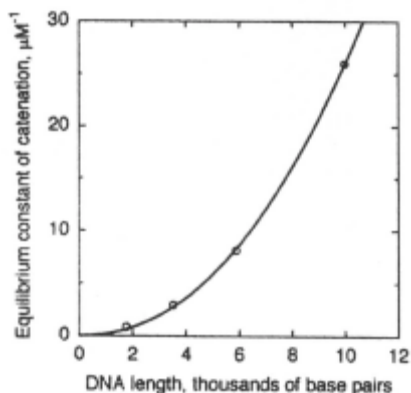
Figure 26. - Equilibrium constant of catenation of two identical circular DNAs. The data obtained by computer simulation for the physiological ionic conditions [76].

We have considered here different distributions of topological states: distributions of topoisomers of supercoiled DNA, distributions of knots and links. All these distributions have one very important advantage in comparison with distributions of other DNA conformational properties. They are not changed during all manipulations with DNA which are required for quantitative analysis of these distributions. Conditions under which the distributions were analyzed are not important since the molecules keep their circular form. It differs in distributions of topological states from the distribution of many other conformational properties which are so easy to disturb. This advantage of distributions topological states was widely used in studies of conformational properties of DNA molecules per se and action of enzymes which are capable of changing DNA topology (see [68, 69] for reviews of some biological applications).

References

1.. R. Dulbecco and M. Vogt, *Proc. Natl. Acad. Sci. USA*, **50**, 236 (1963).

2. R. Weil and J. Vinograd, *Proc. Natl. Acad. Sci. USA*, **50**, 730 (1963).

3. J. Vinograd, J. Lebowitz, R. Radloff, R. Watson and P. Laipis, *Proc. Natl. Acad. Sci. USA*, **53**, 1104 (1965).

4. W.R. Bauer, F.H.C. Crick and J.H. White, *Sci. Am.*, **243**, 100 (1980).

5. A.V. Vologodskii, S.D. Levene, K.V. Klenin, M.D. Frank-Kamenetskii and N.R. Cozzarelli, *J. Mol. Biol.*, **227**, 1224 (1992).

6. G. Calugareanu, *Czech. Math. J.*, **11**, 588 (1961).

7. J.H. White, *Am. J. Math.*, **91**, 693 (1969).

8. F.B. Fuller, *Proc. Natl. Acad. Sci. USA*, **68**, 815 (1971).

9. F.B. Fuller, *Proc. Natl. Acad. Sci. USA*, **75**, 3557 (1978).

10. M.D. Frank-Kamenetskii and A.V. Vologodskii, *Sov. Phys.-Usp.*, **24**, 679 (1981).

11. A.V. Vologodskii, *Topology and physics of circular DNA*, CRC Press, Boca Roton, 1992.

12. P.O. Brown and N.R. Cozzarelli, *Science*, **206**, 1081 (1979).

13. A.V. Vologodskii and N.R. Cozzarelli, *Ann. Rev. Biophys. Biomol. Struct.*, **23**, 609 (1994).

14. W. Bauer and J. Vinograd, *J. Mol. Biol.*, **33**, 141 (1968).

15. J.C. Wang, *J. Mol. Biol.*, **89**, 783 (1974).

16. W. Keller, *Proc. Natl. Acad. Sci. USA*, **72**, 4876 (1975).

17. C.H. Lee, H. Mizusawa and T. Kakefuda, *Proc. Natl. Acad. Sci. USA*, **78**, 2838 (1981).

18. J.C. Wang, in *Cyclic Polymers*, ed. by Semlyen, J.A., Elsevier Appl. Sci. Publ. Ltd, Essex, England, 1986.

19. J.C. Wang, *J. Mol. Biol.*, **43**, 25 (1969).

20. W.B. Upholt, H.B. Gray Jr. and J. Vinograd, *J. Mol. Biol.*, **62**, 21 (1971).

21. R.E. Depew and J.C. Wang, *Proc. Natl. Acad. Sci. USA*, **72**, 4275 (1975).

22. M. Duguet, *Nucl. Acids Res.*, **21**, 463 (1993).

23. P. Anderson and W. Bauer, *Biochemistry*, 17, 594 (1978).

24. V.V. Rybenkov, A.V. Vologodskii and N.R. Cozzarelli, *Nucl. Acids Res.*, **25**, 1412 (1997).

25. J.C. Wang, *Ann. Rev. Biochem.*, **65**, 635 (1996).

26. W.A. LaMarr, K.M. Sandman, J.N. Reeve and P.C. Dedon, *Nucl. Acids Res.*, **25**, 1660 (1997).

27. D.E. Pulleyblank, M. Shure, D. Tang, J. Vinograd and H.P. Vosberg, *Proc. Natl. Acad. Sci. USA*, **72**, 4280 (1975).

28. D.S. Horowitz and J.C. Wang, *J. Mol. Biol.*, **173**, 75 (1984).

29. K.V. Klenin, A.V. Vologodskii, V.V. Anshelevich, V.Y. Klisko, A.M. Dykhne and M.D. Frank-Kamenetskii, *J. Biomol. Struct. Dyn.*, **6**, 707 (1989).

30. W. Bauer and J. Vinograd, *J. Mol. Biol.*, **47**, 419 (1970).

31. T.S. Hsieh and J.C. Wang, *Biochemistry*, **14**, 527 (1975).

32. A.V. Vologodskii, V.V. Anshelevich, A.V. Lukashin and M.D. Frank-Kamenetskii, *Nature*, **280**, 294 (1979).

33. C.R. Cantor and P.R. Schimmel, *Biophysical chemistry*, W. H. Freeman and Company, New York, 1980.

34. C.J. Benham, *J. Mol. Biol.*, **123**, 361 (1978).

35. A.V. Vologodskii, A.V. Lukashin, V.V. Anshelevich and M.D. Frank-Kamenetskii, *Nucleic Acids Res.*, **6**, 967 (1979).

36. M. Adrian, t.H.-B. B., W. Wahli, A.Z. Stasiak, A. Stasiak and J. Dubochet, *EMBO J.*, **9**, 4551 (1990).

37. T.C. Boles, J.H. White and N.R. Cozzarelli, *J. Mol. Biol.*, **213**, 931 (1990).

38. V.V. Rybenkov, A.V. Vologoskii and N.R. Cozzarelli, *J. Mol. Biol.*, **267**, 299 (1997).

39. V.V. Rybenkov, A.V. Vologodskii and N.R. Cozzarelli, *J. Mol. Biol.*, **267**, 312 (1997).

40. J.M. Sperrazza, J.C. Register III and J. Griffith, *Gene*, **31**, 17 (1984).

41. C.H. Laundon and J.D. Griffith, *Cell*, **52**, 545 (1988).

42. J. Bednar, P. Furrer, A. Stasiak, J. Dubochet, E.H. Egelman and A.D. Bates, *J. Mol Biol.*, **235**, 825 (1994).

43. Y.L. Lyubchenko and L.S. Shlyakhtenko, *Proc. Natl. Acad. Sci. USA,* **94**, 496 (1997).

44. D. Stigter, *Biopolymers*, **16**, 1435 (1977).

45. A.A. Brian, H.L. Frisch and L.S. Lerman, *Biopolymers*, **20**, 1305 (1981).

46. E.G. Yarmola, M.I. Zarudnaya and Y.S. Lazurkin, *J. Biomol. Struct. Dyn.*, **2**, 981 (1985).

47. S.Y. Shaw and J.C. Wang, *Science*, **260**, 533 (1993).

48. V.V. Rybenkov, N.R. Cozzarelli and A.V. Vologodskii, *Proc. Natl. Acad. Sci. USA*, **90**, 5307 (1993).

49. K.V. Klenin, A.V. Vologodskii, V.V. Anshelevich, A.M. Dykhne and M.D. Frank-Kamenetskii, *J. Mol. Biol.*, **217**, 413 (1991).

50. J.A. Gebe, S.A. Allison, J.B. Clendenning and J.M. Schurr, *Biophys. J.*, **68**, 619 (1995).

51. M. Hammermann, C. Stainmaier, H. Merlitz, U. Kapp, W. Waldeck, G. Chirico and J. Langowski, *Biophys. J*, **73**, 2674 (1997).

52. A. Rich, A. Nordheim and A.H.-J. Wang, *Annu. Rev. Biochem.*, **53**, 791 (1984).

53. S.M. Mirkin and M.D. Frank-Kamenetskii, *Ann. Rev. Biophys. Biomol. Struct.*, **23**, 541 (1994).

54. D.M. Lilley, *Proc. Natl. Acad. Sci. USA*, **77**, 6468 (1980).

55. N. Panayotatos and R.D. Wells, *Nature*, **289**, 466 (1981).

56. J.C. Wang, L.J. Peck and K. Becherer, *Cold Spring Harbor Symp. Quant. Biol.*, **47**, 85 (1983).

57.   C.J. Benham, *Proc. Natl. Acad. Sci. USA.*, **76**, 3870 (1979).

58.   A.I.H. Murchie and D.M.J. Lilley, *Methods in Enzymology*, **211**, 158 (1992).

59.   L.J. Peck and J.C. Wang, *Proc. Natl. Acad. Sci. USA.*, **80**, 6206 (1983).

60.   M.J. Ellison, R.J. Kelleher 3d., A.H. Wang, J.F. Habener and A. Rich, *Proc. Natl. Acad. Sci. USA.*, **82**, 8320 (1985).

61.   S.M. Mirkin, V.I. Lyamichev, V.P. Kumarev, V.F. Kobzev, V.V. Nosikov and A.V. Vologodskii, *J. Biomol. Struct. Dyn.*, **5**, 79 (1987).

62.   P.S. Ho, M.J. Ellison, G.J. Quigley and A. Rich, *EMBO. J.*, **5**, 2737 (1986).

63.   V.V. Anshelevich, A.V. Vologodskii and M.D. Frank-Kamenetskii, *J. Biomol. Struct. Dyn.*, **6**, 247 (1988).

64.   C.J. Benham, *Cold Spring Harbor Symp. Quant. Biol.*, **47**, 219 (1983).

65.   M.J. Ellison, M.J. Fenton, P.S. Ho and A. Rich, *EMBO J.*, **6**, 1513 (1987).

66.   R.J. Kelleher 3d., M.J. Ellison, P.S. Ho and A. Rich, *Proc. Natl. Acad. Sci. USA*, **83**, 6342 (1986).

67.   F. Aboul-ela, R.P. Bowater and D.M.J. Lilley, *J. Biol. Chem.*, **267**, 1776 (1992).

68.   S.A. Wasserman and N.R. Cozzarelli, *Science*, **232**, 951 (1986).

69.   W.M. Stark and M.R. Boocock, in *Mobile genetic elements*, ed. by Sherratt, D.J., ARL Press, Oxford Univ. Press, Oxford, 1995.

70.   C.J. Ullsperger, A.V. Vologodskii and A.V. Cozzarelli, *Nucl. Acids and Mol. Biol.*, **9**, 115 (1995).

71.   D. Rolfsen, *Knots and Links*, Publish or Perish, Inc., Berkeley, CA, 1976.

72.   C.C. Adams, *The knot book*, Freeman, New York, 1994.

73.   V.V. Rybenkov, C. Ullsperger, A.V. Vologodskii and N.R. Cozzarelli, *Science*, **277**, 690 (1997).

74.   J.P.J. Michels and F.W. Wiegel, *Proc. Roy. Soc. London A.*, **403**, 269 (1986).

75.   T. Deguchi and K. Tsurusaki, *Phys. Rev. E*, **55**, 6245 (1997).

76.   K.V. Klenin, A.V. Vologodskii, V.V. Anshelevich, A.M. Dykhne and M.D. Frank-Kamenetskii, *J. Biomol. Struct. Dyn.*, **5**, 1173 (1988).

77.   A.V. Vologodskii, N.J. Crisona, B. Laurie, P. Pieranski, V. Katritch, J. Dubochet and A. Stasiak, *J. Mol. Biol.*, **278**, 1 (1998).

78.   J.C. Wang and H. Schwartz, *Biopolymers*, **5**, 953 (1967).

John S. Davies
University of Wales, Swansea, UK

3.1 Introduction

The coverage in this Chapter reflects the recent interest in these molecules, as (i) structures evolved by Nature which have been useful templates of biological activity, as either antibiotics or cytotoxic peptides, or (ii) the development of cyclic peptide analogues of naturally-occurring peptides as a means of introducing conformational constraints, to improve receptor interaction and reduce the biodegradability of peptides by enzymes. The latter approach represent key steps in the pharmaceutical industry's quest for peptidomimetic structures for drug development. The nomenclature used in the discussion will rely heavily on the three-letter amino-acid notation and IUPAC Rules [1], with the terms, cyclic homodetic peptides representing peptides where all the cyclic backbones comprise peptide bonds, while cyclic heterodetic peptides refer to cyclic backbones bearing other functional groups, e.g. ester bonds or Nature's own cyclic constraint, the disulfide link. Comprehensive coverage of the topics highlighted can be obtained from review articles produced annually [2], or as expert updates of specific areas [3].

Whether it be for proof of structure, or for studying the conformation of the constrained cyclic peptides, most of the modern physical methods have been applied to this field. Structural elucidation is now often all-encompassing, in that high-field nmr techniques, X-ray studies and other methods appear in one publication. Some of the very early applications of X-ray crystallography were on the cyclodepsipeptide family related to valinomycin. Recent investigations [4] of new crystalline forms within this family, reflect the power of this technique. The full potential of 2D-nmr technology has been fully explored by the Kessler group [3g][5], and consensus conformations (l)-(3) for a large number of cyclo-penta, -hexa and -heptapeptides have been elucidated. Although cyclic constraints limit the number of conformers, the energy minimised forms can be quite flexible species. The consensus structure usually seen therefore in cyclopentapeptides is a combination of the **β** and **γ-turn** (1), in cyclohexapeptides transannular H-bonding favours two **β-turns** (2) while the cycloheptapeptides show a **β-bulge,** two **β-turns** and one bifurcated H-bond as in (3).

In cyclic homodetic peptides the macrocyclisation of the last peptide bond is the yield-determining step, which even at high dilution is not always a high yielder. If grammes of material are needed, as in cases where there is a pharmaceutical demand, it would still be advantageous to synthesise the linear precursor using solution phase techniques ending up with fully protected precursors, capable of cyclisation by carboxyl activation according to **Scheme 1.**

(1)   (2)   (3)

(i) e.g. EDCI, HATU, BOP. TBTU, HAPyU.
(ii) usually trifluoroacetic acid or $H_2/Pd/C$ depending on protecting groups.
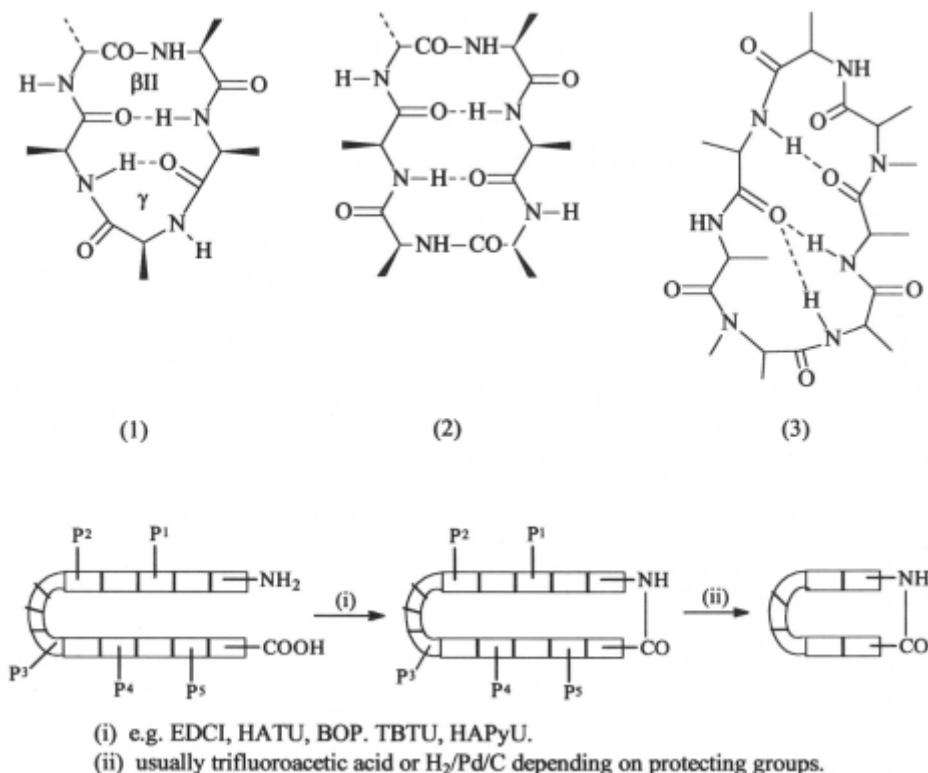
Scheme 1

Carboxyl activation in the solution phase is often a 'test it and see' approach, and it is difficult to generalise. In a series of three demanding thymopentin-derived sequences **H-Arg(NO₂)**-Lys(Z)-Asp(OBn)-Val-Tyr-OH, H-Arg(Tos)-Lys(Z)-Asp(OBn)-Val-Tyr(Bn)-OH and H-Val-Arg(H⁺)-Lys(Ac)-Ala-Val-Tyr-OH, the reagents[*], HAPyU, PyAOP, HATU, TBTU, BOP, PyBOP and DPPA were compared [6] for their efficiency in cyclomonomer, cyclodimer and epimerisation (of activated C-terminal residue). HAPyU gave yields of 55%, 25% and 8.8% under the various categories and seemed to have the edge over

---

the others. In the cyclisation to form cyclo[Tyr(Bzl)-Asp(OBzl)-Phe-Phe-Ser-**(Bu^t)-D-Ala]**, utilising various cyclising positions, TBTU/HOBt proved highly efficient, although DPPA gave 100% yield, but took a longer time [7]. Soluble carbodiimides such as EDCI [l-(3-dimethylaminopropyl)-3-ethylcarbodiimide] [8], and pre-formed active esters, e.g. *p*-nitrophenyl or pentafluorophenyl esters have all had their supporters. Cyclisation under high dilution conditions is not always necessary [9], and one of the best methods under more concentrated conditions is DPPA/solid base **(NaHCO$_3$ or K$_2$HPO$_4$) [5]**.

The essence of **Scheme 1** can also be carried out from protected linear precursors released under very mild conditions from the polymer used for solid phase peptide synthesis. This approach necessitates that a linker be attached between peptide and polymer, which can release protected precursor peptides under mild acid conditions, without removing sensitive side chain protecting groups. Two linkers, the 2-chlorotrityl resin [5] and the 4-hydroxymethyl-3-methoxyphenoxybutyric acid MBHA resin [10] have been successful in this context. Kaiser's oxime-based linker attached to the resin [11], allows direct cyclisation on the resin, by changing the conditions to acetic acid after removal of the last residue to be added, as illustrated in **Scheme 2**.

(i) HOAc/Et$_3$N
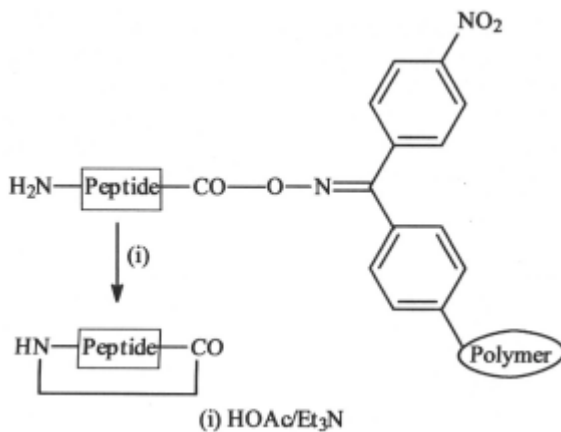
Scheme 2

Another recent development involves cyclisation of the pre-assembled peptide without removal from the resin. This approach [12], as given in the example in **Scheme 3** requires as the first step, the side-chain attachment (usually *via* the side chain of Asp, Glu or Lys) of the first residue to the resin, and then each protected amino acid is added sequentially while the **α-COOH** group of the first residue is protected with a suitable ester protecting group. Removal of this protecting group and release of a free amino group at the other end, provides the means for a coupling agent to undertake the cyclisation on resin. Finally cleavage of the side-chain from the resin releases a completely de-protected cyclic peptide.

Fmoc—Xxx—D—Leu—Val—D—Pro—Asp—OFm

(i)(ii)

Xxx—D—Leu—Val—D—Pro—Asp

(iii)

Xxx—D—Leu—Val—D—Pro—Asp

Xxx = Ala, Phe, Tyr or Trp

(i) 20% piperidine
(ii) BOP or HOAt
(iii) HF
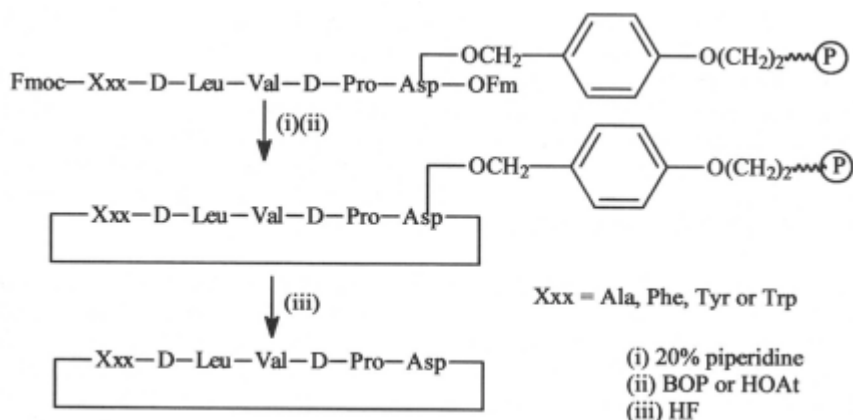
Scheme 3

Mainly *via* the work of Tam's group [13], it is now possible to cyclise unprotected linear peptides, *via* the orthogonal coupling strategies outlined in **Scheme 4** (parts (a) and (b)). The final product is not completely homodetic, but as it is useful, for the larger peptides, the small degree of heterodicity does not affect properties. In approach (b) it has been found that **Ag⁺ ions** can assist lactamisation. Even with this variety of approaches available it is not easy to predict which approach should be taken. However in most cases, quite complicated mixtures have to be purified, and unless preparative hplc units are available, extensive periods of recycling can be the norm.

(a)

(i) aq. IO_4^-/pH 6.8

(b)

(i) $(HOOCCH_2CH_2)_3P$, pH 7.4

Scheme 4
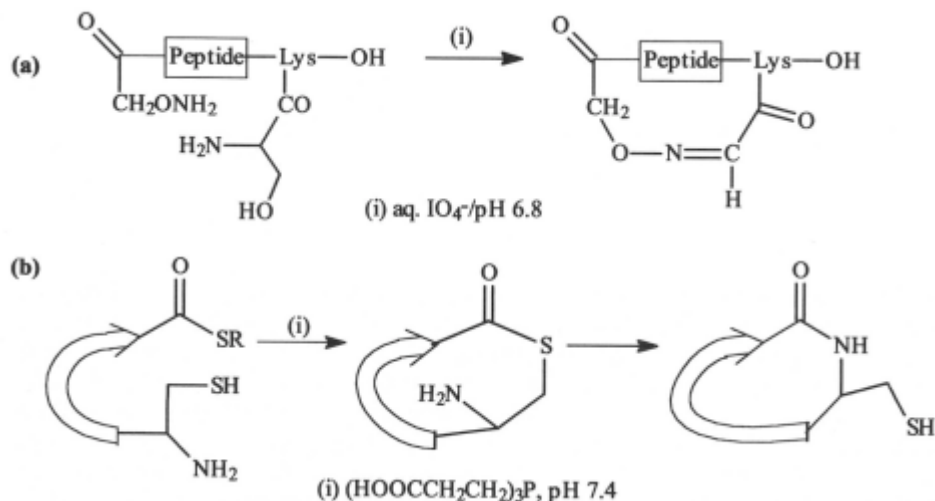
As there are 20 coded amino acids available in Nature, the number of cyclic combinations possible are enormous, yet the vast majority characterised

fall in the range cyclic dipeptides to cyclic dodecapeptides. These, together with highly modified cyclic heterodetic peptides, will be the focus for the remainder of the Chapter. However the great wealth of structures and literature on them, necessitates severe pruning and selecting of examples to highlight the frontiers reached under each sub-category.

3.2 Cyclic Homodetic Peptides

3.2.1 Cyclic Dipeptides (Dioxopiperazines)

Though its structure is totally unrepresentative of cyclic peptides (it has two *cis* amide bonds, and a flagpole boat conformation, in contrast to *trans* amide bonds generally) it has generated an immense amount of conformational [14][15] and mass spectral [16] interest. It is a structure not always welcomed in synthetic circles [17], since any free dipeptide ester auto-cyclises to dioxopiperazines, a principle utilised for cleavage of peptides off resins [18]. The tendency to cyclise however can be minimised by judicious selection of protecting groups [19].

Ever since Inoue and co-workers recognised cyclo (L-His-L-Phe) (4) as an asymmetric catalyst for cyanohydrin synthesis (hydrocyanation of aldehydes), the mechanism of action has generated much interest [20].

(4)   (5)   (6)
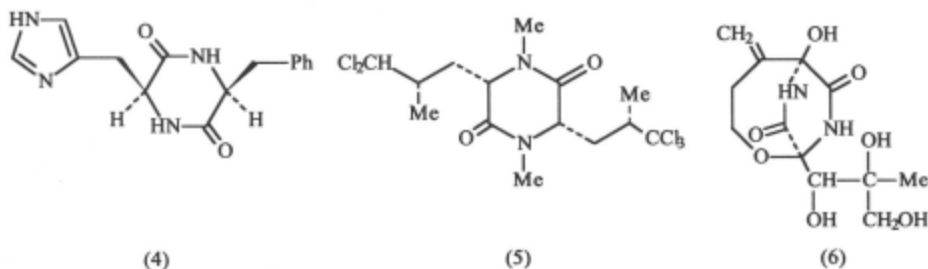
Methylated modifications of the dioxopiperazine ring are not so catalytically efficient lending support to recent evidence [21],[22] that a highly ordered supramolecular complex of the dioxopiperazine acts as catalyst.

Some years have gone by since Nature's catalogue of dioxopiperazine rings was compiled [23], and is in need of updating. Some of the more recent diverse structures characterised include: dysamide D (5) [24]; cyclo(-Trp-Phe) a plant growth regulator [25]; chitinase inhibitor cyclo(-Arg-D-Pro) [26]; bicyclomycin (6) [27]; dioxopiperazine (7) from the sponge *Calyx cf. podatypa* [28]; maremycins A and B (8) [29].
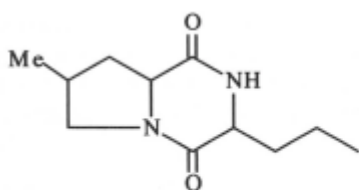
(7)
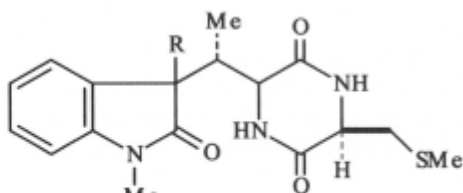
(8) R = ---OH or ▬OH

3.2.2 Cyclotripeptides

In contrast to the wide distribution of cyclic dipeptides, cyclotripeptides are very much a minority interest. It is quite difficult to construct all L-cyclotripeptides from **α-amino** acids. Very often in their synthesis, the cyclodimer, i.e. cyclohexapeptides are the main products. However, head to side-chain 'extended' cyclic tripeptides do have potential, e.g. (9) as endothelin receptor antagonist [30], the 12-membered ring (10) as a helix-turn-helix motif [31], and (11) as cyclic **β** casomorphin-5 analogues [32].

H–Lys—Trp·Asp

BocNH ... NH—CO₂Me

H–Tyr—Xaa—Phe-D—Pro
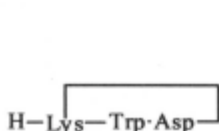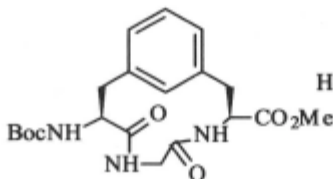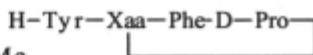
Xaa = Lys, Orn or A₂bu

(9)　　　　　(10)　　　　　(11)

3.2.3 Cyclotetrapeptides

The synthesis of all L-cyclotetrapeptides remains a problem in this series, and often an appropriately substituted D-residue or N-alkylated amino acid residue assists in conformational flexibility. The 'strain' in an all L-cyclotetrapeptide is even manifested in C-terminal residues undergoing enantiomerisation to a D-residue before cyclisation. An example [33] has shown that attempts to synthesise cyclo(Pro-Val-Pro-Tyr) yielded 31% of cyclo(Pro-Val-Pro-D-Tyr), and the main products were cyclooctapeptides rather than Cyclotetrapeptides. This has raised a query on the configurations of the residues in the three cancerostatic all L-cyclotetrapeptides, cyclo(Pro-Leu-Pro-Leu), cyclo(Pro-Val-Pro-Val) and cyclo(Pro-Phe-Pro-Phe) derived from tunicate *Cystodytes delle chiajei* [34]. Proline residues offer the flexibility advantage of *cis* or *trans* imide bonds but positioning of residues is still important in achieving synthesis. Using DPPA for activation of a series of diastereoisomeric tetraprolines [35], cyclo(D-Pro-D-Pro-L-Pro-L-Pro) could only be obtained from **DLLD-Pro₄** as precursor. A reflection of the strain in the cyclic structure is its quantitative ring opening in trifluoroacetic acid at room

temperature. Prediction of sequence best able to cyclise is crucial in this series, so modelling calculations for predicting cyclisation [36] are welcomed. For the 4-Ala-chlamodycin analogue cyclo(Aib-Phe-D-Pro-Ala) the GenMol programme predicted the best linear precursor to be H-Ala-Aib-Phe-D-Pro-OPh. In a real comparison test [37] for the synthesis of cyclo(Arg-Gly-Asp-Phg) on a Kaiser oxime resin, **Table 1** summarises the results.

Table 1

AA$_4$	AA$_3$	AA$_2$	AA$_1$	Monomer %	Dimer %
1. Arg(Tos)	Gly	Asp(cHex)	Phg*	75	20
2. Phg	Arg(Tos)	Gly	Asp(cHex)	50	25
3. Asp(cHex)	Phg	Arg(Tos)	Gly	70	40
4. Gly	Asp(cHex)	Phg	Arg(Tos)	10	not detected

* Phg = phenylglycine

Physical methods have been extensively used to determine the conformations of cyclotetrapeptides. Molecular mechanics calculations (CHARMM programme) [38] reveal that most *cis/trans* transitions are hindered by barriers of >30kcal/mol. In cyclo(L-Pro-D-Pro-L-Pro-D-Pro) four *cis/trans* isomerisations could be identified as **ctct → cttt → tttc → tctt → tctc.** X-ray analysis showed **cyclo(DDLLPro$_4$)** to be a strained **C$_i$** symmetrical conformation with alternating *cis-trans* bonds [35]. Similarly for cyclo(D-Phe-Pro-Sar-Gly), X-ray showed alternating *cis-trans* bonds, but nmr studies in solution found *trans-cis-trans-cis* also [39]. Conformation of cyclo**(γ-Abu-Pro-γ-Abu-Pro)** has been shown by nmr, ir and cd to be solvent dependent, but in most solvents a *cis-trans-cis-trans* arrangement was detected [40].

Nature's assortment include cyclo(Pro-Tyr-Pro-Val), a strong inhibitor of mushroom tyrosinase [41], clamydocin (12) and analogues [42], apicidin (13) and analogues from *Fusarium pallidoroseum* [43], and cytotoxic cyclocinamide A (14) from marine sponge *Psammocinia* [44].

3.2.4 Cyclopentapeptides

This category has been the most highly investigated series in recent years. 'State of the art' can best be revealed from a 231-reference review [5] [*Angew.Chem.Int.Ed.Engl.*, **36,** 1374 (1997)] of the central role of cyclo-pentapeptides in the evolution of cyclomimetics based on the Arg-Gly-Asp motif. The restrictions to this motif offered by a cyclopentamer appears to be the ideal conformation for interaction with the receptors (integrins, e.g $\alpha_v\beta_3$ integrin). Many of the analogues [5] produced exhibit antagonist activity in the nanomolar range and suppress tumour induced angiogenesis. Cyclo(Arg-Gly-Asp-D-Phe-Val) appears as one of the most selective inhibitors for $\alpha_v\beta_3$. Studies on this group of analogues have been accompanied by detailed nmr work to determine the ideal spatial structures. Structure (1) in the introduction to this Chapter summarises the consensus conformation. While the Kessler

(12)

(13)

(14)
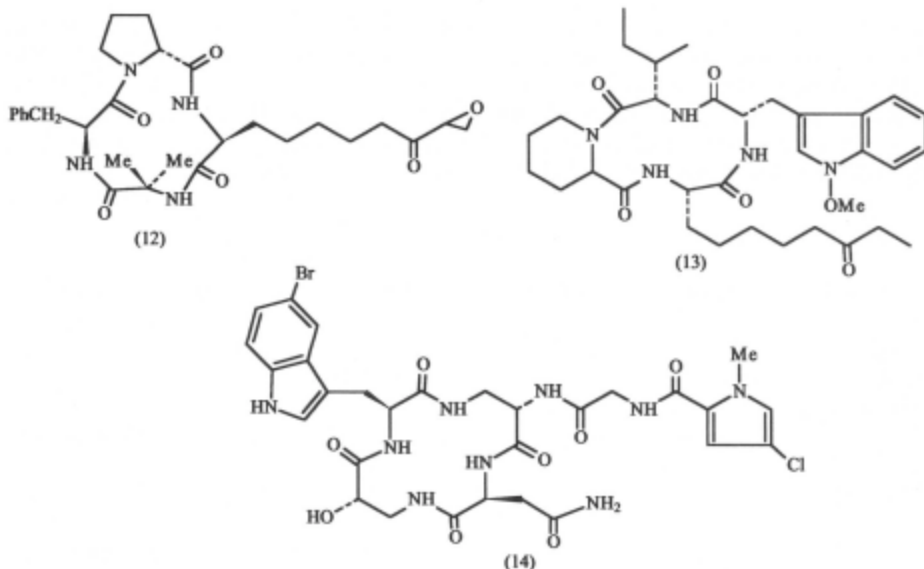
group have used many options in their synthetic work, their most recent protocol utilises the DPPA/solid base method for macrocyclisation. The use of cyclopentapeptide Arg-Gly-Asp analogues as antagonists of blood platelet aggregation has assumed relevance in medical imaging [8], and cyclic heterodetic versions of the motif have shown promise *in vivo* [9] as antithrombotic imagers. Non-peptidic mimics of the motif are also well documented by the pharmaceutical industry, and include potent fibrinogen receptor antagonists [45] where the Arg-Gly-Asp has been constrained *via* a

disulfide link as in **Ac-Pen-Arg-Gly-Asp-Cys-OH** .

Endothelin, the vasoconstrictor associated with impaired cardiovascular and renal function, has been a focussed molecule for pharmaceutical exploration for some years, and recently much information on endothelin receptors has been obtained. The discovery of naturally occurring receptor antagonists in the form of BQ123, cyclo(D-Trp-D-Asp-Pro-D-Val-Leu) [46], BE18257A cyclo(D-Glu-Ala-D-Val-Leu-D-Trp) and BE18257B cyclo(D-Glu-Ala-D-alle-Leu-D-Trp) [47] have justified intensive activity mainly on BQ123, and its analogues. For example, cyclo(D-Trp-D-Asp-Pro-D-Val-Leu) inhibits ^{125}I-endothelin-l binding to aortic smooth muscle membranes with an **IC_{50} = 22nM,** but only weakly inhibits binding to porcine cerebellum membranes **(IC_{50} = 18µM)** [48]. Synthesis of BQ123 has been carried out on up to a l00g scale [46], and its availability has initiated a number of conformational studies such as nmr and molecular modelling studies [49]. Peptide backbone conformations were well defined as type II **β-turns** at Leu-D-Trp and a **γ'-turn** at proline. In a structure-activity relationship study [50] it appears that a DDLDL chirality sequence is critical. Cyclo[D-Trp-D-**Cys(SO₃⁻Na⁺)-Pro-D-Val-Leu],** another potent antagonist, exists as a type II **β-turn** around **D-Val-Leu-D-Trp-Cys(SO₃⁻Na⁺)** and a **γ-turn** around D-Val-Pro-

D-Cys(SO₃⁻Na⁺) [51]. With a similar conformation confirmed for BQ123 and cyclo(D-Asp-Pro-D-Val-Leu-D-Trp), the proposition is that these antagonists mimic the C-terminus of endothelin [52].

Viomycin (15), capreomycin (16) and tuberactinomycin (17), peptide antibiotics from *Streptomyces* species have been known for some years and already used as tuberculostatic agents. But in this era of methillicin resistant *Staphylococcus aureus* (MRSA), renewed interest has been shown [53] in modification of these naturally-occurring cyclopentapeptides. Substitutions for the dehydroureido positions in the form of 3'4'-dichlorophenyl amino and 4'-cyclohexylphenylamino groups have yielded compounds with activity against *Pasteurella spp* MRSA and vancomycin-resistant *enterococci*. The plant *Aster tataricus* (Compositae) has proved a rich source of cyclopenta-
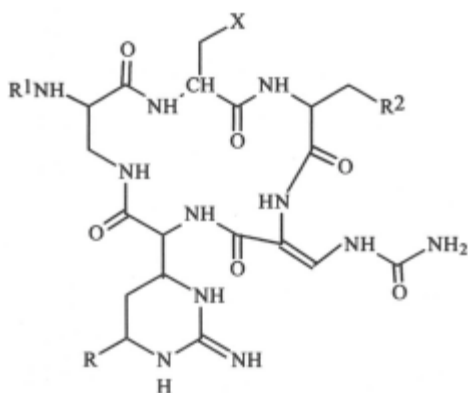
(15) R = X = OH, R2 = OH
   R2 = NH₂(CH₂)₃CH(NH₂)CH₂CO
(16) R = R1 = H, X = NH₂
   R2 = NHCOCH(NH₂)(CH₂)₃NH₂
(17) R = H, X = OH, R2 = OH
   R1 = NH₂(CH₂)₃CH(NH₂)CH₂CO
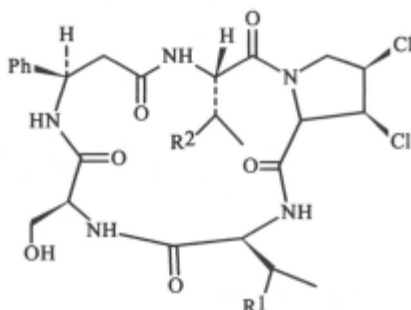
(18) R1 = H, R2 = OH
(19) R1 = OH, R2 = H
(20) R1 = H, R2 = H

peptides, amongst them astins A (18), B (19) and C (20) which have antitumour activity [54]. Nmr studies confirm that the acyl-prolyl bond is in the *cis* conformation. *Vaccaria segetalis* is another plant that contains cyclic peptides in its seeds and some of them segetalin B, cyclo(Gly-Val-Ala-Trp-Ala), segetalin G, cyclo(Ala-Gly-Val-Lys-Tyr), and H cyclo(Arg-Phe-Ser-Gly-Tyr) have estrogen-like activity [55]. Their backbone structure [56] determined by distance geometry calculation and restrained energy minimisation from nmr data showed segetalin G with a **βII-turn** at **Tyr⁴-Ala⁵** and segetalin H to contain a **βII'-turn** at Gly-Tyr and a **γ-turn** at Arg-Phe-Ser. Cyanobacterium *Oscillatoria agardhii* (NIES-204) is another rich source, as exemplified by anabaenopeptins E (21), F (22) [57] and oscillamide Y (23), and analogues which on synthesis [58] have shown no evidence of chymotrypsin inhibition as thought earlier.
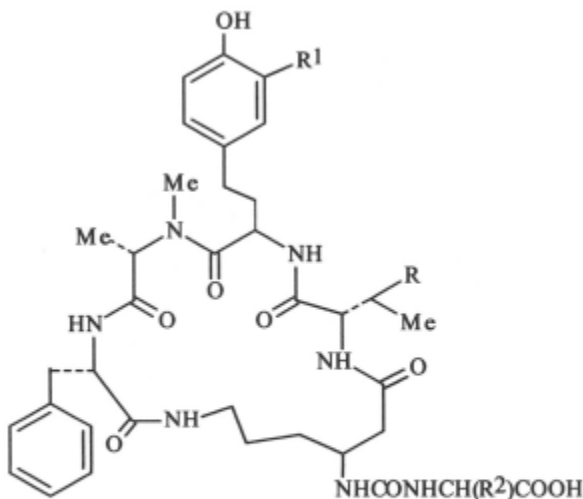
(21) R = R^1 = Me, R^2 = (CH$_2$)$_3$NH(=NH)NH$_2$
(22) R = Et, R^1 = H, R^2 = (CH$_2$)$_2$NH(=NH)NH$_2$
(23) R = Et, R^1 = H, R^2 = CH$_2$-Ph(OH)

3.2.5 Cyclohexapeptides

For two decades or more, the Cyclohexapeptides with their potential for two **β-turn** structures (2), have been the testing ground for numerous physical techniques and for synthetic conditions conducive to high yields at the macrocyclisation step. Rather than rely on Nature's output, many of the cyclic peptides have been custom-built to highlight certain factors governing conformation. Cyclo(Val-Pro-D-Ala-Val-Pro-D-Ala) which exhibits **C$_2$** symmetry in the crystalline state [59] with *cis* amide links between Val-Pro residues, would be a good example and the nmr derived solution conformation of cyclo(D-Ala-Phe-Val-Lys(Z)-Trp-Phe) has been simulated by molecular dynamics calculations [60]. For the synthesis [61] of cyclo(Leu-Tyr-Leu-Glu-Ser-Leu) using the **Leu^6-Leu^1** bond for the final link, and using the azide method for macrocyclisation, varying each residue for a D-residue in turn, the yield did not seem to vary much from a 55% average. However an all L-equivalent only gave a 1% yield, so both for synthesis and to stabilise the **β-turns** a favourable cyclohexapeptide structure should contain at least one Gly, Pro or D-residue. A series of substitutions in cyclo(Xxx-Pro-Gly-Yyy-Pro-Gly), where Xxx = Yyy = Glu; Xxx = Arg, D-Arg, Yyy = Tyr; or Xxx = Lys, **Yyy = Glu,** have given nmr spectra which show that cyclo(L-L-Gly-L-L-Gly) sequences display two conformers, one being the bis-*cis* conformer, while the minor one contained two **β-turns.** For cyclo(D-L-Gly-L-L-Gly) one *cis* and one *trans* X-Pro was seen and one type **II β-turn** [62]. Contained in a mini-review [63] on conformational mobility of cyclic oligopeptides is a constrained

distance geometry search of the isomeric cyclo(Pro-Arg-Gly-Asp-Gly-D-Pro) and cyclo(Pro-Arg-Gly-Asp-D-Pro-Gly). The role of Pro in defining **β-turn** conformation has been studied [64] using 2D nmr and restrained molecular dynamics simulations on cyclohexapeptides containing L- and D-Pro. An optimised 'designer' cyclohexapeptide, cyclo(D-Pro-Phe-Ala-Trp-Arg-Tyr) [65] showed inhibition of **α-amylase** with a K_i of **14-32μM,** as a structural mimic of a distorted type I **β-turn** in tendamistat protein known to be an **α-amylase** inhibitor.

Many studies in this section have been part of the initiative to find an efficient way of restricting Arg-Gly-Asp in a biologically active form, **Cyclo(Arg-Gly-Asp)₂** and cyclo(Arg-Gly-Asp-Arg-Gly-D-Asp) have been synthesised on solid phase by side chain attachment of Asp to a Wang resin [66], but were less active than cyclopentapeptide counterparts in binding assays with **αII$_b$/β$_3$** fibrinogen and **αVβ$_3$** vitronectin interactions. Stronger binding to the fibrinogen receptors were achieved from the designed examples, cyclo(Phe-Asp-Gly-Arg-Gly-Phe), cyclo(D-Ser-Asp-Gly-Arg-Gly-Phe) and cyclo(D-Ser-Asp-Gly-Arg-D-Phe) [67].

Nature's most important contribution under this category is probably the availability of the potent anti-tumour cyclohexapeptide RA-VII (24) and its congener deoxybouvardin (25). The extra cyclic ring involves the linking up of

(24) R = Me, (25) R = H

(26) R = H, R¹ = H
(27) R = H, R¹ = Me
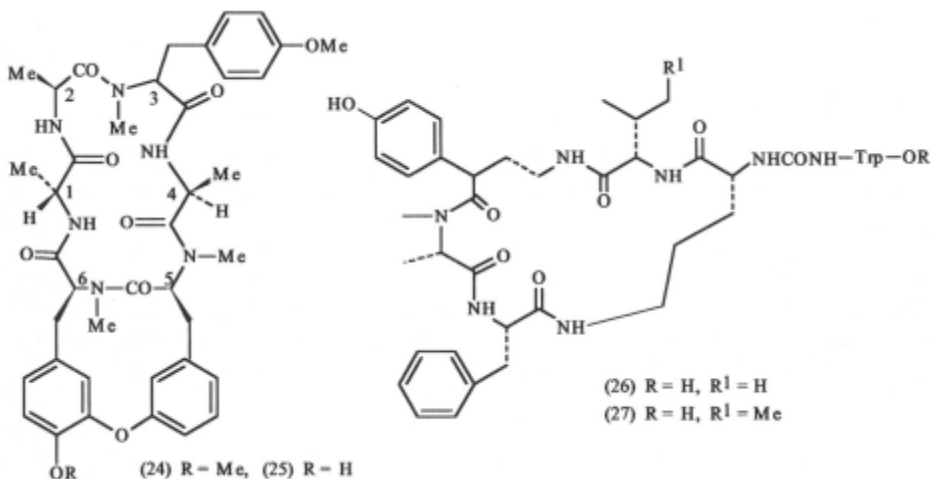
two phenolic rings, the latter feature proved quite difficult to synthesise in early attempts. Eventually an Ullmann reaction proved successful [68] for producing the diaryl ether, subsequently augmented by methodology involving **S$_N$Ar** reactions and by thallium trinitrate mediated oxidation [69]. The final macrocyclisation was carried out with DPPA. In a very interesting discussion between the Japanese [70] and American [71] groups who have totally synthesised RAVII, it has emerged that the latter group's methodology [69] gives a facile epimerisation at positions in a diaryl ether precursor. The

conformation [72] of the *cis* N-methylamide bond between **Tyr^5** and **Tyr^6** was deemed to be critical but has recently been disputed [73]. The continuing interest in RAVII reflects its cytotoxic propeties which has justified its entry into clinical trials.

Somatostatin is a heterodetic cyclic peptide with a **Cys^3-Cys^14** disulfide bridge, and is used clinically for neuroendocrine tumours, etc., often as its analogue an octapeptide, octreotide. However biological lifetimes have been a problem and many attempts have been made to produce mimetics of somatostatin action. A potent analogue is cyclo(Pro^6-Phe^7-D-Trp^8-Lys^9-Thr^10-**Phe^11**) [74]. Confirmation of the significance of the Phe^11-Pro^6 to biological activity as a *cis* bond requirement has also been made [75].

Cyanobacteria, *Microcystis aeriginosa*, have yielded cyclic peptides, ferintoic acids A (26) and B (27) [76]. Bioactive cyclic peptides from plants is becoming a buoyant source, e.g. dichotomins A-D from the roots of *Stellaria dichotoma L var lanceolata Bges* having structures A, cyclo(Gly-Thr-Phe-Leu-Tyr-Val), B, cyclo(Gly-Thr-Phe-Leu-Tyr-Thr), C, cyclo(Gly-Thr-Phe-Leu-Tyr-Ala) and D, cyclo(Gly-Val-Gly-Phe-Tyr-Ile) respectively [77]. Roots of *Stellaria yunnanensis* have yielded stellarin B cyclo(Gly-Ser-HOIle-Phe-Phe-Ala) and C, cyclo(Gry-Ser-HOIle-Phe-Phe-Ser) [78]. Seeds of *Vaccaria segetalis* have given rise to segetalin A cyclo(Trp-Ala-Gly-Val-Pro-Val) which has estrogen-like activity [79] and a conformation determined as two **β-turns** both by X-rays and nmr [80].

3.2.6 Cycloheptapeptides

On reaching this size of cyclopeptide the thrust of the research is totally focussed on structural elucidation/synthesis of products derived from Nature, and quite a wealth of structures have been discovered *via* screening for various biological activities. Space does not allow detailed discussion of any one member, but the diversity of structure is well represented in **Table 2.** Large scale isolation of the water bloom *Microcystis spp* have added greatly to the constituent members of the microcystin LR family whose basic structure is represented by (28) [89]. Viroisin (29) has the same biological function as phalloidin (30), from the toxic mushroom *Amanita phalloides* although the structures are different [90]. In solution (29) seems to have a well-ordered conformation, with functional groups orientated for interaction with target proteins. Nmr and X-ray techniques have confirmed that evolidine, cyclo(Ser-Phe-Leu-Pro-Val-Asn-Leu) has a type I **β-turn** (Leu-Ser), and a type VIa incorporating the *cis* Leu-Pro, giving two **β-turns** and backbone bulge [91] as depicted in structure (3) of the introduction. Similar structures exist in pseudostellarin D [92], axinastatins [93], yunnanin A [94] and segetalins D and E [95].

Table 2

Name		Cycloheptapeptide	Source		Ref
Hymenamide	A	c(Pro-Pro-Val-Pro-Phe-Trp-Arg)	*Hymeniacidon sponge*		81
"	B	c(Pro-Pro-Asn-Phe-Val-Glu-Phe)	"	"	81
"	C	c(Trp-Pro-Phe-Gly-Pro-Glu-Leu)	"	"	81
"	D	c(Ile-Pro-Tyr-Asp-Pro-Leu-Ala)	"	"	81
"	E	c(Phe-Pro-Thr-Thr-Pro-Tyr-Phe)	"	"	81
"	F	c(Leu-Arg-Pro-Pro-Ala-Val-Met)	"	"	81
Phakellistatin	1	c(Pro-Ile-Pro-Ile-Phe-Pro-Tyr)	*Phakellia costata*		82
"	2	c(Tyr-Pro-Phe-Pro-Ile-Ile-Pro)	" *carteri*		82
"	3	c(Phe-Gly-Pro-Thr-Leu-Y*-Pro)	*Phakellia carteri*		82
"	5	c(Met-Ala-Ile-Pro-Phe-Asn-Ala)	*Phakellia costata*		82
Axinastatin	1	c(Asn-Pro-Phe-Val-Val-Pro-Val)	*Axinella cf. carteri*		83
"	2	c(Asn-Pro-Phe-Val-Leu-Pro-Val)	" " "		83
"	3	c(Thr-Pro-Leu-Trp-Val-Pro-Leu)	" " "		83
"	4	c(Trp-Val-Pro-Leu-Thr-Pro-Leu)	" " "		83
Nairaiamide	A X = Val	c(Ile–Ile–Pro–X–Thr–Ile–Pro)	*Lissoclinum bistratum*		84
	B X = Ile	$\overset{\mid}{\text{CMe}_2\text{CH=CH}_2}$	"	"	84
Stylostatin		c(Leu-Ala-Ile-Pro-Phe-Asn-Ser)	*Stylotella aurantum*		85
Segetalin	C	c(Gly-Leu-His-Phe-Ala-Phe-Pro)	*Vaccaria segetalis*		86
"	D	c(Gly-Leu-Ser-Phe-Ala-Phe-Pro)	" "		86
"	E	c(Gly-Tyr-Val-Pro-Leu-Trp-Pro)	" "		86
Yunnanin	A	c(Gly-Tyr-Gly-Gly-Pro-Phe-Pro)	*Stelloria yunnensis*		87
"	C	c(Gly-Ile-Gly-Phe-Tyr-Ser-Pro)	" "		87
"	D	c(Gly-Ile-Ser-Phe-Arg-Phe-Pro)	" "		87
Agardiheptin A		c(His-Gly-Trp-Pro-Trp-Gly-Leu)	*Oscillatoria agardhii* (NIES 204)		88

Y* = oxidised Trp

(28)

$\rightarrow$Ala^5 — SMeTrp^6 — HO$_3$Leu^7
HO$_2$Pro^4 ← Ser^3 ← Thr^2 ← Val^1

(29)

Ala^5 Trp^6 HOLeu^7
CH$_3$
CH_3CH—$CONH$—CH—$CONH$—$CHCH_2$-C-OH
NH   CH$_2$ CO   CH$_2$OH
CO   NH
CHMe
N—CO—CHNHCOCHNHCO Ala^1
Hyp^4 Cys^3 CHCH$_3$
HO   OH D-Thr^2

(30)
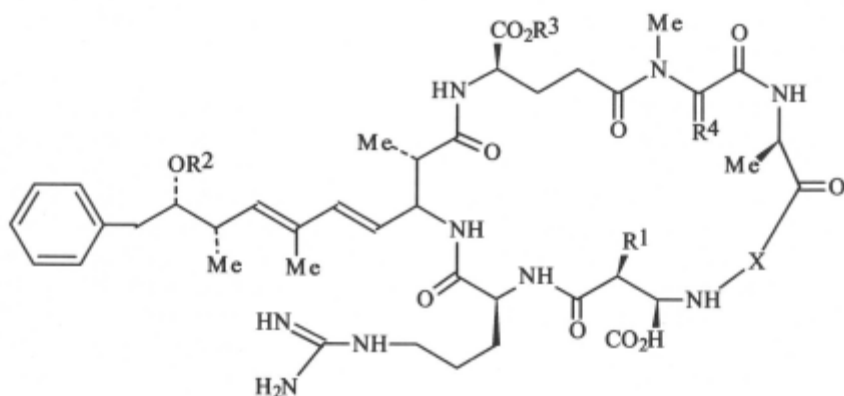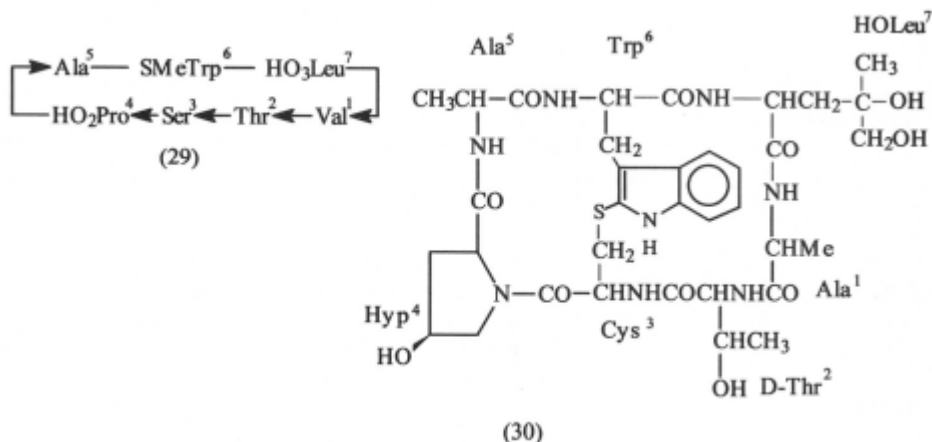
3.2.7 Cyclooctapeptides

Apart from the interest in naturally-occurring examples under this category, metal complexing properties have been identified, and model compounds designed to complex diastereoisometrically. Thus **cyclo(Phe-Pro)₄** and DL-noradrenaline hydrochloride form a complex which retains a **C₂-symmetric** conformation [96]. Calcium complexes of cyclo(Ala-Leu-Pro-**Gly)₂** have also been determined by X-ray techniques [97]. The cyclooctapeptide has a 2-fold symmetry very similar to antamanide complexes. Hymenistatin I, cyclo(Pro-Pro-Tyr-Val-Pro-Leu-Ile-Ile) contains a **βVIa** turn **(Ile⁸-Tyr³)** and includes a **Pro¹-Pro²** *cis* bond, with a **β-turn** at **Val⁴-Ile⁷** [98]. The ability of **cyclo(Phe-Pro-Gly-Pro)₂** to distinguish between the D- and L-enantiomer of Phe-OMe(HCl) is superior to **cyclo[(Phe-Pro)₂-(Gly-Pro)₂]** [99]. Phe-OMe(HCl) in its D-form is transported through an organic liquid membrane complexed either to cyclo[Lys(Z)-Lys(Z)-Gly-Phe-Phe-X-Sar-X] (X = Gly or Sar) or cyclo[Glu(Bzl)-Glu(Bzl)-Gly-Phe-Phe-Sar-Sar-Sar), more efficiently than the L-analogue [100]. Two **β-turns** (over Pro-Phe residues) in cyclo(Ala-Gly-Pro-Phe-Ala-Gly-Pro-Phe), makes it similar in conformation to **cyclo(Cys-Gly-Pro-Phe)₂** [101].

Cyclooctapeptides have recently been found to be plentiful in various parts of higher plants. Thus the roots of *Stellara delavayi* have yielded stelladelins B and C with structures cyclo(Gly-Ile-Pro-Pro-Ala-Tyr-Asp-Leu) and cyclo(Val-Pro-Tyr-Pro-Pro-Phe-Tyr-Ser) respectively [102]. *Stellaria dichotoma var* roots have yielded dichotomin H, cyclo(Ala-Pro-Thr-Phe-Tyr-Pro-Leu-Ile) and I, cyclo(Val-Pro-Thr-Phe-Tyr-Pro-Leu-Ile) [103], while the seeds of *Annona squamosa* have given annosquamosin A, cyclo(Pro-Met(O)-Thr-Ala-Ile-Val-Gly-Tyr) [104]. The latex of *Jatropha gossypifolia* (Euphorbiaceae) contains cyclogossine B cyclo(Val-Gly-Gly-Trp-Leu-Ala-Ala-Ile) [105], while the *Jatropha curcas* variety has yielded curcacycline A, cyclo(Gly-Leu-Leu-Gly-Thr-Val-Leu-Leu) [106]. Stellarin G, cyclo(Gly-Ala-

Gly-Ser-Pro-Trp-Phe-Pro) has been found in the roots of *Stellaria yunnanenis* [107]. Pseudostellarins A-G have been characterised [108], from the roots of *Pseudostellaria heterophylla*, and a few of the family have turned out to be cyclooctapeptides: B, cyclo(Gly-Ile-Gly-Gly-Gly-Pro-Pro-Phe), C, cyclo(Gly-Thr-Leu-Pro-Ser-Pro-Phe-Leu), F, cyclo(Gly-Gly-Tyr-Leu-Pro-Pro-Leu-Ser) and G, cyclo(Pro-Phe-Ser-Phe-Gly-Pro-Leu-Ala).

While most of the cyclic peptides from higher plants conform strictly to a cyclic homodetic peptide structure, marine organisms tend to produce more complicated and modified structures, which under the cyclooctapeptide category can be represented by aciculitins A-C (31-33), from the lithistid sponge *Aciculites orientalis* [109].

(31) R = C_5H_{11}
(32) R = C_6H_{13}
(33) R = C_7H_{15}
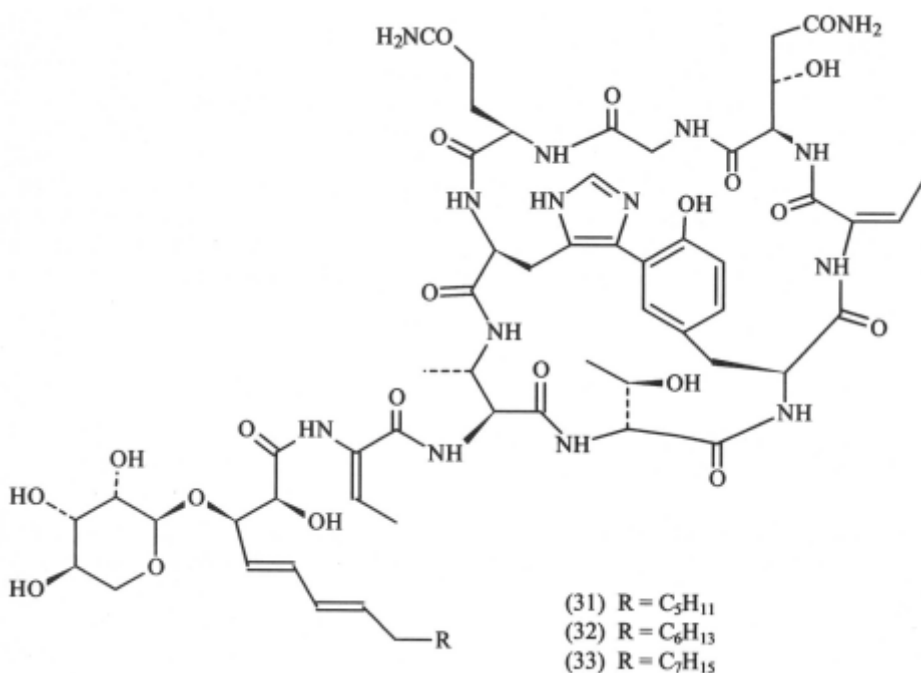
3.2.8 Cyclononapeptides

Activity on compounds in this sub-section have been dominated over the years by interest in the cytotoxic properties and immunosuppressive activity of cyclolinopeptide A, (CLA) cyclo(Pro-Pro-Phe-Phe-Leu-Ile-Ile-Leu-Val) isolated from linseed oil. In this ring size the conformation is flexible [110] and requires high field nmr techniques to rationalise the conformation. In acetonitrile solution the backbone contains a *cis* Pro-Pro bond with all other amide bonds *trans*. **Ba²⁺** ions complex tightly to CLA, and the complex

changes to an all *trans* peptide bond conformation, with a type **1 6→3β-turn** and a **3→1 γ-turn** giving an overall bowl shape. Insertion of amino isobutyric acid (Aib) into the sequence giving cyclo(Pro-Pro-Phe-Phe-Aib-Aib-Ile-D-Ala-Val) constrains effectively the conformational flexibility in the molecule [111]. The Phe residues in CLA have also been replaced [112], with **[D-Phe⁹]** CLA showing the highest biological activity and best conformational comparison with CLA. A new cyclolinopeptide B, cyclo(Pro-Pro-Phe-Phe-Val-Ile-Met-Leu-Ile) has been isolated [113] from the seeds of *Linum usitatissimum* which shows comparable immunosuppressive activity to CLA. Cyclolinopeptide B's rotamase activity can be enhanced by curcacycline B, cyclo(Leu-Gly-Ser-Pro-Ile-Leu-Leu-Gly-Ile) from *Jatropha curcas* [114].

The higher plant *Leonuris heterophyllus* has yielded [115] in its fruits (used by the Chinese to invigorate blood circulation), three proline rich cycloleonuripeptides A-C, cyclo(Gly-Pro-Pro-Pro-Tyr-Pro-Pro-Met-Ile), cyclo-(Gly-Pro-Pro-Pro-Tyr-Pro-Pro-Met(O)-Ile) and its isomer respectively [115]. The backbone structures of all three consist of two **β-turns,** a **βVI-turn** at **Pro³-Pro⁴** and a **βI-turn** at **Pro⁷-Met⁸**, with a transannular **4→1** H-bond between **Tyr⁵NH** and **Pro²CO,** and two H-bonds between **Gly¹NH** and **Pro⁶CO** and between **Ile⁹NH** and **Pro⁹CO,** thus completing a **β-bulge** conformation [116]. Two cyclic nonapeptides have come to the fore as selective endothelin type B receptor antagonists. The structures of RES-701-1 and RES-701-2 are as shown in (34) and (35) respectively [117]. Two cyclononapeptides which show

$$\overline{}$$
Gly—Asn—Trp—Gly—Thr—Ala—Pro—Asp—R
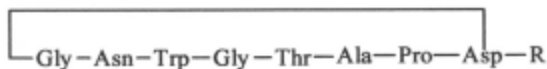
(34) R = Trp-Phe-Phe-Asn-Tyr-Tyr-Trp-OH
(35) R = Trp-Phe-Phe-Asn-Tyr-Tyr-Htp-OH   Htp = 7 hydroxytryptophan

moderate cyclo-oxygenase activity have been characterised from the roots of *Stellaria dichotoma L. var laceolata Bge* as dichotomins F, cyclo(Val-Leu-Pro-Ser-Val-Tyr-Pro-Tyr-Phe) and G, cyclo(Ser-Pro-Leu-Pro-Ile-Pro-Pro-Phe-Tyr) [118].

3.2.9 Cyclodecapeptides

The dominant structure that has been truly representative of this sub–section for 40 years or more is gramicidin S, **cyclo(Val¹-Orn²-Leu³-D-Phe⁴-Pro⁵-Val¹ˊ-Orn²ˊ-Leu³ˊ-D-Phe⁴ˊ-Pro⁵ˊ)** which has activity against Gram-positive organisms. Synthetic methodology, conformational work using a variety of techniques, and structure-activity relationships have all at one time or another been weaned or tried out on gramicidin S from *Bacillus brevis.* Quite early work deduced [119] the two **β-turn** and **β-sheet** structure as (36). **[L-Lys²,²ˊ]-**

(36)
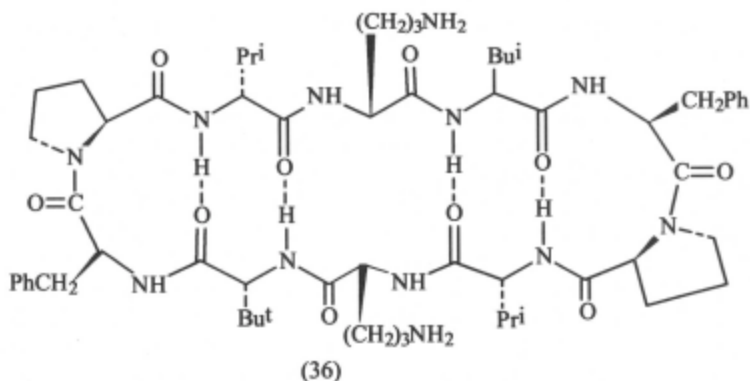
Gramicidin S has been shown to have same activity as parent molecule, but if configuration of residues are changed [120] to [D-Lys$^{2,2'}$]- or [D-Lys^2,L-Lys$^{2'}$]-gramicidin S, the cd spectra showed β-turns but the analogues had weak or no activity against Gram-positive micro-organisms. L-α-Aminomyristic acid(Amy) with its lipophilic $C_{12}H_{25}$ side chain, as incorporated into [Amy$^{3,3'}$]-gramicidin S [121], enhances affinity for membranes without conformational change in the backbone (cd and nmr). The Kaiser oxime on-resin method has found utility [122] in making [D-pyrenylalanine$^{4,4'}$]-gramicidin S, an analogue which can be used as a fluorescent probe, and L-1-pyrenylalanines to explore involvement of β-sheets with amphiphilic character. The biosynthesis of gramicidin S involves linking a Leu residue to GS synthetase followed by formation of a pentapeptide which then cyclodimerises. As mimics of this process, pentapeptide active esters based on N-hydroxysuccinimide have been synthesised [123], and only the 'natural' sequence, H-D-Phe-Pro-Val-Orn-Leu-ONSu gave the cyclic pentapeptide monomer and cyclodimer (gramicidin S) in 15 and 38% yields respectively. This confirms the 'existence' of sequence features that promote cyclisation. Similar features seem to affect the synthesis of a series of pentapeptides cyclised with water soluble carbodiimide and HOBt coupling agents as summarised in **Table 3** [124]. Also included in **Table 3**

Table 3

Cyclodimerisation to GS derivatives

	semi GS	:	GS(derivatives)
H-Val-Orn(Z)-Leu-D-Phe-Pro-OH	10	:	90
H-Orn(Z)-Leu-D-Phe-Pro-Val-OH	56	:	44
H-Leu-D-Phe-Pro-Val-Orn(Z)-OH	97	:	3
H-D-Phe-Pro-Val-Orn-(Z)-Leu-OH	65	:	35
H-Pro-Val-Orn(Z)-Leu-D-Phe-OH	58	:	42
H-D-Phe-Pro-Val-Orn-Leu-ONSu	28	:	72

(line 6) is the one example of success when four linear precursor with changes at **Phe^4** and **Val$^{1'}$** were cyclised using active esters [125]. Reducing the size of the gramicidin S ring reduces antibiotic activity but when residues were added

[126], as in cyclo(Val-Orn-Leu-Leu-D-Phe-Pro-Val-Orn-Leu-D-Phe-Pro) the activity doubled.

In contrast to the poisonous principles in *Amanita* mushrooms, they also contain an antitoxic principle, antamanide, which counteracts the lethal action of phalloidin and α-amanitin. Antamanide has been characterised as **cyclo(Val[1]-Pro[2]-Pro[3]-Ala[4]-Phe[5]-Phe[6]-Pro[7]-Pro[8]-Phe[9]-Phe[10])** since 1968 [127]. Its first synthesis followed in 1969 [128] *via* the cyclisation of a linear decapeptide. Antamanide and cyclolinopeptide A (see earlier) share the same postulated active sequence -Pro-Pro-Phe-Phe so a recent synthesis [129] of **cyclo[Pro-Phe-Phe-Ala-Glu(OBu')₂]₂,** together with X-ray and nmr studies have shown a conformation which allows all amides in backbone to be *trans* with two **β-turns,** and the compound has similar biological activity to cyclolinopeptide A.

The puwainaphycins contain some members within the family which are cardioactive cyclic peptides, e.g. C and D, now augmented by puwainaphycins A, B and E with structures (37-39) respectively [130]. Blue green algae, *Calothridx fusca* yielded calophycin (40) very similar to the

(37) R = (CH₂)₉CO(CH₂)₃CH₃   X = OH
(38) R = (CH₂)₉CO(CH₂)₃CH₃   X = H
(39) R = (CH₂)₁₁CH₃   X = OH

$$Me \quad C_{11}H_{23}$$

(R)

OH

Pro—HN (R)

O

Val-Ala—D-Asp

MeAsn ← Arg ← Gly ← Gln ← Asn ←

(40)
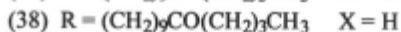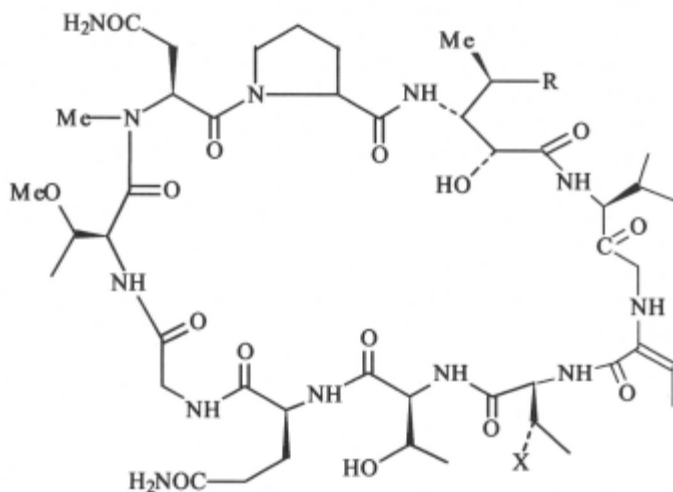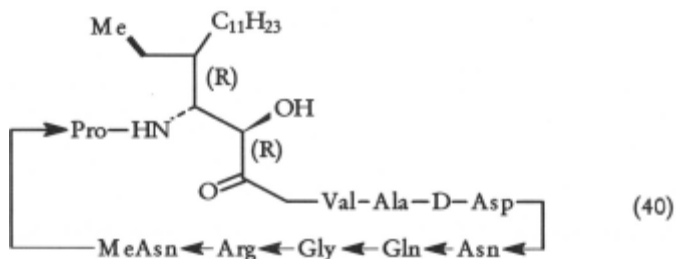
puwainophycins but in contrast it has strong antifungal properties [131]. A marine worm from Papua New Guinea, has yielded [132] a potent Gram-positive antibiotic cyclo(Val-Orn-Leu-Tyr-Pro-Phe-Phe-Asn-Asp-Trp) which in preliminary studies inhibited some of the worst of the resistant bacteria in the laboratory (e.g. MRSA). The proline-rich cycloleonuripeptide D, cyclo(Ser-Pro-Pro-Pro-Tyr-Phe-Gln-Thr-Pro-Ile) from fruits of *Leonurus heterophyllus*, has been studied [133] in solid state and in solution. In its conformation it has a type **I β-turn(Pro-Ile),** type **III β-turn** (Pro-Tyr), and a transannular **4→1** H-bond between PheNH and ProCO, and a Pro-Pro bond judged to be *cis,* very similar to **[Phe⁴,Val⁶]**-antamanide. A similar conformation to antamanide has also been revealed [134] in the crystal conformation of cyclo(Pro-Pro-Ile-Phe-Val-Leu-Pro-Pro-Tyr-Ile), while the symmetrical cyclolinopeptide A analogue, **cyclo(Pro-Phe-Phe-Aib-Leu)₂** in solid and solution [135], showed all *trans* amide bonds, six intramolecular H-bonds and four turns (3 type I, and one type III).

3.2.10 Other Higher Cyclic Peptides

While cycloundecapeptides to cyclododecapeptides might qualify for a subsection themselves, in the main, only sporadic examples of such structures have been characterised. Hence the broader sub-section title to encompass some commercially important compounds, as well as the more routine.

With an estimated 20,000 publications already written, cyclosporin A (41) takes pride of place as the molecule which has been instrumental in improving our understanding of immunosuppression. Detailed nmr studies [136] have been critical to this understanding, as it has been possible to study cyclosporin A when it is complexed to the protein receptor cyclophilin (a 17.7kDa protein with peptidyl-prolyl isomerase activity) [137]. The con–formation of the bound cyclopeptide is very different from the X-ray structure and nmr derived conformation in solution, and it is critical to have a *trans* conformation at **MeLeu⁹-MeLeu¹⁰** [138]. With so many N-methylated amide

(41)
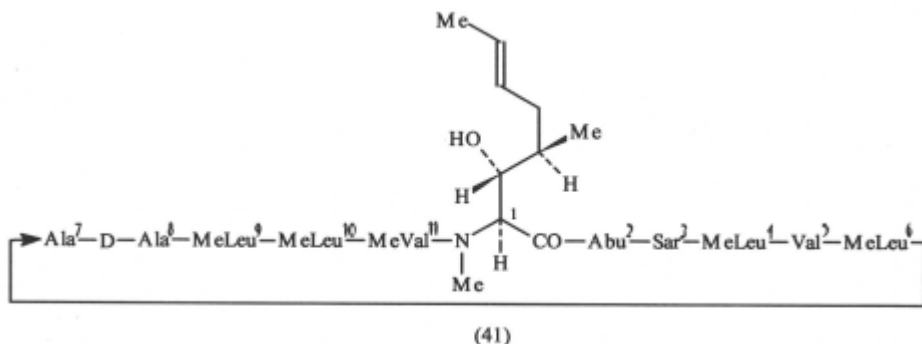
bonds in the molecule *cis-trans* rotational isomeism is possible at many centres, and also creates steric hindrance problems at many stages in its synthesis. Thus it was a welcomed development in 1995, that Rich's group had synthesised cyclosporin A on solid phase [139]. The availability of activating agents HOAt and HATU, and utilising double couplings ultimately proved successful. In order to synthesise a diversity of analogues a detailed study [140] of the coupling stages have been made. A number of links proved difficult to achieve, e.g. 10/11, 9/10, 6/5 and 11/1. The last pair proved very difficult, so the best synthetic strategy proved to be to start at MeVal^{11} and assemble the linear peptide to reach MeBmt^1, and then cyclise with the BOP reagent. The difficulties in synthesising the molecule has made structure-activity studies a daunting task, but with serendipity in some cases (e.g. [141] where **Sar^3** could be stereochemically modified *via* Li enolates and electrophiles), modifications have been carried out. **[D-MeSer^3, 4(OH)MeLeu^4]-cyclosporin** A, has a higher affinity for cyclophillin A, but lacks immunosuppressing activity [142]. [5-Hydroxynorvaline^2]-cyclosporin A, has lower binding with cyclophillin A [143] but a combination of changes at positions 3, 7 and 8 as in **[D-MeAla^3,Phe^7,D-Ser^8]-cyclosporin** A [144] bound more tightly. However most aspects of MeBmt (residue 1) are required for biological activity. Even a change of OH to OMe is detrimental [145]. A **β-turn** constraint has been inserted to replace **Ala^7-D-Ala^8** [146], an area of the cyclopeptide not involved in binding. With this constraint the affinity for cyclophilin was 3 times that of cyclosporin A.

The marine sponge *Theonella sp.* produces a family of cytotoxic bicyclic peptides whose structures vary according to **Figure 1** [147]. The blue-
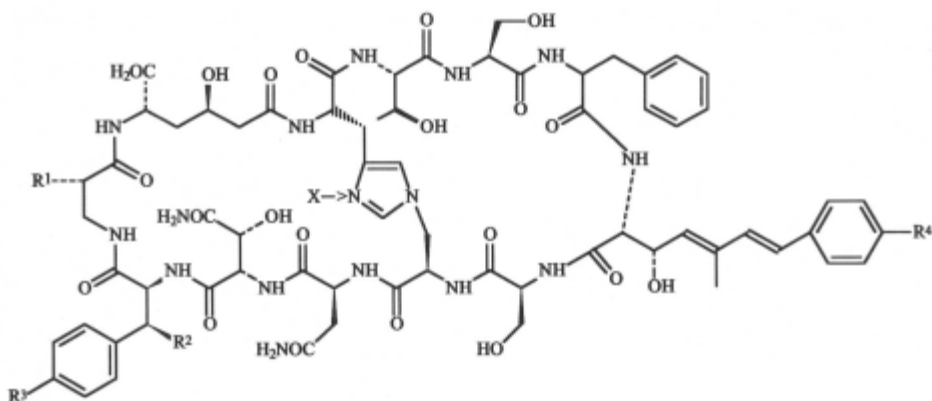
	R¹	R²	R³	R⁴	X
Theonellamide F	H	H	Br	Br	-
" B	OH	Me	Br	H	-
" C	H	H	H	Br	-
" A	OH	Me	Br	H	β-D-Gal
" D	H	H	Br	Br	β-L-Ara
" E	H	H	Br	Br	β-D-Gal

Figure 1

green algae *Anabaena laxa* FK-1-2 have yielded a mixture of antifungal and cytotoxic peptides, known as laxaphycins. Two separate research groups [148] have proven the structures to be A(42), E(43), B(44) and O (45). It is only

(42) R = H
(43) R = Et

(44) R = E
(45) R = H
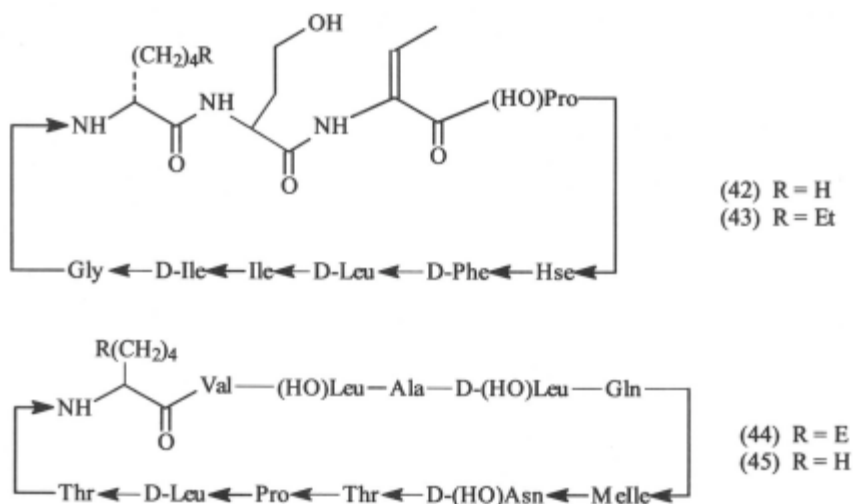
when A and B are mixed that they show antifungal activity. Cyanobacterium, *Microcystis-aureginosa* (NIES-88), already known as a source of microcystins has also yielded kawaguchipeptin A (46) and B which is cyclo(Trp-Ser-Thr-

Pro-Trp-Leu-Asn-Gly-Asp-Asn-Asn), with the latter showing antibacterial activity.

(46)
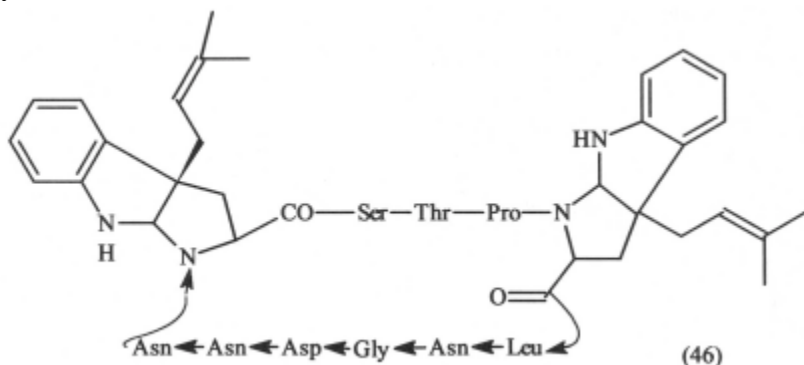
The conformational preferences of cycloleonurinin, cyclo(Gly-Pro-Thr-Ghi-Tyr-Pro-Pro-Tyr-Tyr-Thr-Pro-Ala) from the fruits of *Leonurus hetero-phyllus* [150], have been narrowed to a uniquely determined conformation of a **βVI** turn at **Pro⁶-Pro⁷** and a **βI-turn** at **Pro¹¹-Ala¹²** with the two Pro residues *cis*. Transannular **4→1** H-bonds constructed two **β-turns,** with two H-bonds between **Tyr⁹(NH)** and **Pro⁷CO**, between **Thr¹⁰(NH) and Tyr⁸CO** constructing **γ-turns,** together with H-bonds between **Ala¹⁴(NH)** and **Thr¹⁰(OH)** were observed. Gratisin, the cyclododecapeptide equivalent to gramicidin S, having the structure **cyclo(D-Phe-Pro-D-Tyr-Val-Orn-Leu)₂,** and also having antibiotic properties, is only formed *via* a biomimetic synthesis [151] from a peptide with a sequence H-D-Phe-Pro-D-Tyr-Val-Orn-Leu-ONSu. Both gramicidin S and gratisin therefore need a C-terminal Leu to trigger off biomimetic synthesis. It has been reported earlier in this Chapter that higher homologues of gramicidin S inhibit bacterial growth with high potency. However, while cyclo(Leu-Orn-**Leu-Orn-D-Phe-Pro)₂** and **cyclo(Leu-Orn-Leu-Orn-Leu-D-Phe-Pro)₂** fit this pattern, analogues with Lys of Orn showed no antimicrobial activity although their conformation was the same [152].

3.3 Cyclo Heterodetic Peptides

Here the discussion turns to cyclic peptides which contain features in the macrocycle, other than amide bonds made up from **αNH** and CO groups of amino acids. This allows a wide variety of inserts into the macrocycle, but the field of interest is usually dictated by the wealth of diverse structures produced by Nature.

3.3.1 Cyclopeptides with Disulfide Bridges

Many biologically active peptides and proteins contain disulfide links. These probably evolved as a means of stabilising bioactive conformations, but space here only allows discussion of the intra-chain bridged species. The disulfide bridge has also been introduced into many bioactive motifs to

constrain the motif into less flexible bioactive conformations. Coverage of this category of cyclopeptides has produced a vast literature, and it is highly recommended that access to the literature should be made *via* authoritative reviews [153-156].

Many of the naturally occurring examples have become medicinal 'household' names as they are hormones with very important control properties in biological systems. The molecules (47-52) are representative. The salmon calcitonin (47) is the analogue used in therapy for osteoporosis and the treatment of Paget's disease for 25 years or more [157]. This particular analogue, available by chemical synthesis is several times more potent than the human variety, and has benefitted from solid phase synthetic techniques on a large scale. Recently details of its receptors have been published [158]. Atrial Natriuretic Peptide (48) belongs to a family of endogenous peptide diuretics, which also causes vasodilation, and is part of a counter regulatory system to the renin-angiotensin system. Its potential therapeutic use has been reviewed [159]. Endothelin 1 (49) is a 21-amino acid peptide with potent vasopressor and vasoconstrictive properties, and possibly influences steroid hormone production [160], but the attention has moved to studies on the antagonists of the endothelin receptors which have been identified. Amongst the most successful antagonists have been analogues of the cyclopentapeptide BQ123 cyclo(D-Trp-D-Asp-Pro-D-Val-Leu) (see earlier in this Chapter).

Oxytocin (50) and vasopressin (52) were amongst the first hormones to be synthesised by the du Vigneaud group in the 1950's. Since then, hundreds of analogues have been synthesised [162]. Oxytocin is widely used to promote uterine contractions in labour, while vasopressin, especially as its prolonged action super-potent analogue, desmopressin (53) are used as antidiuretics [163].

H—Cys—Ser-Asn-Leu—Ser-Thr-Cys—Val—Leu—Gly—Lys—Leu—Ser—Gln—Glu—Leu—His—

—Lys—Leu—Gln—Thr-Tyr—Pro—Arg—Thr-Asn-Thr—Gly—Ser—Gly—Thr-Pro—NH$_2$

(47) Calcitonin (Salmon)

H—Ser—Leu—Arg-Arg-Ser—Ser—Cys—Phe—Gly—Gly—Arg—Met—Asp—Arg—Ile—Gly—Ala—

Gln—Ser—Gly—Leu—Gly—Cys—Asn—Ser^{25}—Phe—Arg—Tyr—OH

(48) Atrial Natriuretic Peptide

H—Cys—Ser—Cys—Ser—Ser—Leu—Met⌐

HO◄Trp◄Ile◄Ile◄Asp◄Leu◄His-Cys◄Phe-Tyr◄Val◄Cys◄Glu◄Lys◄Asp◄⌐

(49) Endothelin-1

H—Cys—Tyr—Ile—Gln—Asn—Cys—Pro—Leu—Gly—NH$_2$

(50) Oxytocin

H—Ala—Gly—Cys—Lys—Asn—Phe—Phe—Trp—Lys—Thr—Phe—Thr—Ser—Cys—OH

(51) Somatostatin

H—Cys—Tyr—Phe—Gln—Asn—Cys—Pro—Arg—Gly—NH$_2$

(52) Vasopressin

S(CH$_2$)$_2$CO—Tyr—Phe—Gln—Asn—Cys—Pro—D-Arg—Gly—NH$_2$

(53)

Somatostatin (51) exerts negative control over both growth hormone and thyroid stimulating hormone synthesis and excretion. However the therapeutic potential of somatostatin is limited by its short biological half-life of approx. 2 minutes, and explains why the octapeptide, sandostatin or octreotide (54) with a much longer half-life has been used [164]. Octreotide only retains four of the essential amino acid residues essential for activity, with the incorporation of N-terminal Phe, a C-terminal alcohol, D-tryptophan and a disulfide bridge improving resistance to metabolic breakdown.

H—D—Phe—Cys—Phe—D—Trp—Lys—Thr—Cys—Thr—ol

(54)
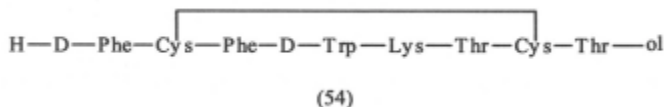
Most of the syntheses [153] involve pre-assembly of the peptide sequences using protected cysteine derivatives, both in the solution and solid phase. In the simplest examples, the disulfide bridges can be constructed by oxidation of free or protected sulfhydryls. The regioselective pairing to form the bridge can take place spontaneously but tend to need high dilution conditions to minimise scrambling and dimerisation. In their review [153] Barany et al. have listed the following protecting groups used on the sulfhydryl group of cysteine:-

S-xanthyl, S-trimethoxybenzyl, S-monomethoxytrityl, S-trityl, S-monomethoxy-benzyl, S-methylbenzyl, S-t-butyl, S-acetamidomethyl, S-phenylacetamido-methyl, S-fluorenylmethyl, S-S-t-butyl, S-S-methoxycarbonyl, S-S-nitropyridyl.

These are either removed to release sulfhydryl groups which then can be oxidised by air oxidation, oxidation in redox buffers, dimethyl sulfoxide or with potassium ferricyanide. Alternatively many of the S-protected species above can be oxidised directly, e.g. using iodine, thallium III trifluoroacetate and chlorosilane-sulfoxide. For the more complicated multiple disulfide bridges graduated orthogonal deprotection and/or co-oxidation of pairwise half-cystines is needed [165].

3.3.2 Cyclodepsipeptides

This sub-division covers cyclic peptides containing ester bonds (depsides) as part of the backbone. The nomenclature can also include esters formed between the side-chains of serine and threonine and the main backbone carboxyls (macrocyclic lactones). Again Nature is a rich source of the most fascinating Cyclodepsipeptides, and the biological significance of incorporating the depside bond is not clear, but appears to be essential for biological activity, since all-amide analogues of the Cyclodepsipeptides are often inactive. In their syntheses, it has been well-recognised that the depside bond is more difficult to form than amides, and tends to be incorporated prior to the macrocyclisation step which is usually carried out at a suitable amide position. The depside link also provides more flexible conformational properties as it lacks the rotational barrier and H-bonding characteristics of the amide link.

The best known structures under this category belong to the ion-selective antibiotics valinomycin, **cyclo(Val-D-Hyiv-D-Val-L-Lac)₃** where Hyiv = **α-Hydroxyisovaleric** acid and Lac represents lactic acid, and the closely related enniatin family: enniatin A, **cyclo(D-Hyiv-MeIle)₃;** B, cyclo(D-Hyiv-**MeVal)₃;** C, **cyclo(D-Hyiv-MeLeu)₃;** D, cyclo(D-Hyiv-MeLeu-D-Hyiv-MeVal-D-Hyiv-MeVal); E, cyclo(D-Hyiv-MeIle-D-Hyiv-MeLeu-D-Hyiv-MeVal); F, cyclo(D-Hyiv-MeLeu-MeIle-D-Hyiv-MeIle) [166]. The bracelet structures of the ion-complexes were worked out from X-ray and nmr studies in the 1960's, but are still proving of interest [4]. The most recent activity on the synthesis comes from three reports [167] on the synthesis of valinomycin and analogues. Macrocyclisation was carried out at 90°C at a C-terminal Hyiv carboxyl group activated as a pentafluorophenyl ester.

The initial burst of structural and synthetic activity on the actinomycins goes back to the 1960's, but their known ability to intercalate with the DNA double-helix has revived interest in them. Thus analogues of actinomycin D (55) with structures (56-59) have been synthesised [168] to study antibody interaction. None of the changes made significant differences to the nmr data.
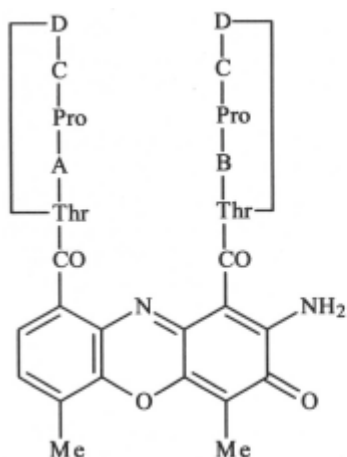
	A	B	C	D
(55)	D-Val	D-Val	Sar	MeVal
(56)	D-Val	D-Val	Sar	MeLeu
(57)	D-Val	D-Val	Meg	MeVal
(58)	D-Val	D-Thr	Sar	MeVal
(59) {	D-Thr	D-Val	Sar	MeVal
	D-Val	D-Thr	Sar	MeVal

Analogue (56) appeared to bind more strongly to DNA and had 100 times the antitumour activity, but only half the antimicrobial activity.

In the last decade the dominant source of complex cyclodepsipeptides, often with cytotoxic properties have been marine organisms. None more so than the sea hare *Dolabella auricularia*, whose rich source has been reviewed [169]. Not all the dolastatins produced by this species are cyclodepsipeptides but representative members are:- dolastatin 16 (60) [170]; dolastatin 11 (61) [171]; dolastatin D (62) [172]. All marine cytotoxic peptides suffer from difficulties of extraction and scarcity at source, and if their properties are to be utilised by the pharmaceutical industry, efficient synthesis is a pre-requisite. Dolastatin 11 (61) was recently synthesised [171] and all stereogenic centres confirmed.

(60)   (61)   (62)
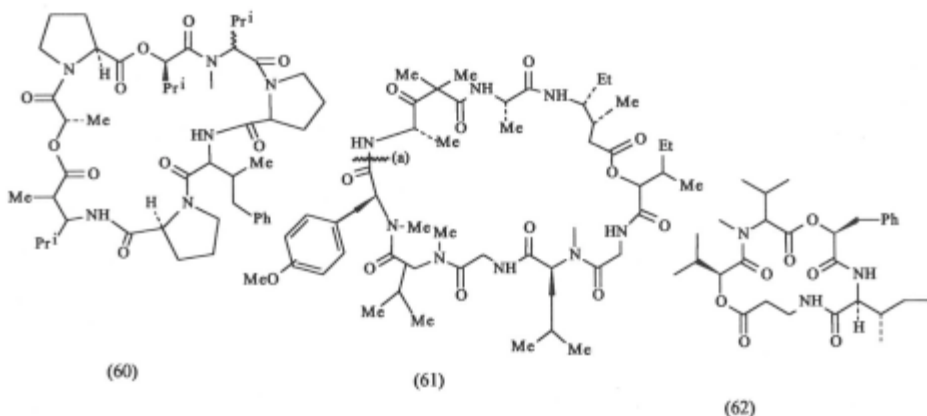
The final cyclisation point was at (a) in (61) using HBTU or BOP-C1 for cyclisation. Other cyclodepsipeptides recently isolated from *Dolabella auricularia* also include doliculide [173], dolastatin G and nordolastatin G [174].

A decade's intensive survey of marine tunicates *Tridemnum solidum* and *Alidium albicans* [175] have yielded a family of structures summarised in **Table 4.** Decigram quantities of didemnins A-C have been synthesised [176].

Table 4

	A			**A**
Didemnin A	H	Didemnin	G	CHO
"	B	Pro-Lac	"	M	Pro-Lac-Gln-pGlu
"	C	Lac	"	N	Pro-Lac
"	D	Pro-Lac-(Gln)₂pGlu	"	X	Pro-Lac-(Gln)₃-Hydec
"	E	Pro-Lac-(Gln)₂pGlu	"	y	Pro-Lac-(Gln)₄-Hydec

Didemnin A has become a prime target for synthesis, as other members of the family are congeners based on side-chain differences. Two approaches to synthesis have been reported [177]. Macrocyclisation was carried out between Pro- and **Me₂Tyr** using HATU/HOAt in 28% yield, which is useful since didemnin B has undergone phase II clinical trials for antitumour activity. Hapalosin (63), the multi-drug resistance reverser is experiencing intense

(63)

(64) R = PhCH–CH–   (65) R = PhCH–

structure-activity studies [178]. Comparisons between (63) and its des-N-methyl analogue have confirmed that it is the *cis* N-methyl conformation that occurs in (63) [179]. Enantiospecific total syntheses of the potent antitumour macrolides cryptophycin 1 (64) and 8 (65) have been reported [180] with

further members of the family being found in trace amounts in *Nostoc sp.* GSV224 [181].

The destruxins are a family of cyclodepsipeptides represented by the structures (66-70) for destruxins A-E, isolated from *Metarrhizium anisopliae*
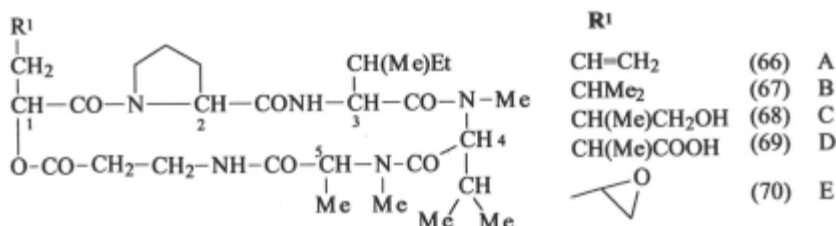
and *Oospora destruktor* (Hyphomycetes) which have been searched for anti-hepatitis B virus agents [182]. For activity in this context it is concluded that the destruxins require hydrpphobic residues in position 1 and 3, the N-Me and lactose groups being essential, since all-amide analogues are inactive [183]. An efficient synthesis of destruction B (67) from (3+3) fragments has been reported [184]. A calcium blocker, leualacin (71) has been isolated from *Hapsidospora irregularis* and its structure confirmed by synthesis [185], by macrocyclisation involving the non-hindered amino group of one of the leucyl residues.
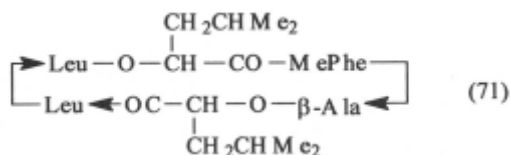
This sub-section is only a glance and Nature's complex families of cyclodepsipeptides Space does not allow further highlighting, but further reading on jaspanamide [186], virginiamycin [187], viscosin [188], micropeptins [189] fusaricidins [190], geodiamolides [191], acirilide [192], arenastatins [193] and discokiolides [194] would still be representative of contemporary 1990's research.

3.3.3 Cyclopeptides with "Modified" Side-Chains in the Macrocycle.

Nature seems to have evolved, mainly in marine species, the five-membered thiazole and oxazole rings as a means of imposing severe conformational restrictions on cyclic peptides [195]. These rings emanate from a condensation between side-chain cysteine thiols or threonyl/seryl hydroxy groups and the neighbouring amide bond. **Figure 2** depicts the possible origin

(72)
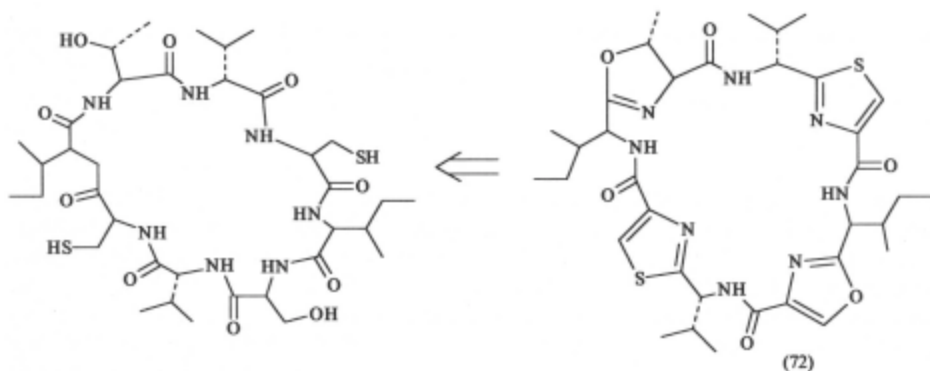
of a typical thiazoline/oxazoline cyclopeptide (72) which would be a highly constrained pseudo-boat or saddle-shaped macrocycle. Natural examples have been found in the genus *Lissoclinum*, an ascidian which has been extensively investigated [196]. Representative of the structures identified [197] and synthesised [198] are patellamide F (73) and lissoclinamide 4 (74). The sea hare *Dolabella auricularia* has also been a rich source of these modified cyclopeptides especially the dolastatins [199] while the *Theonella* marine sponge has generated many novel compounds bearing this type of modification

(73)

(74)
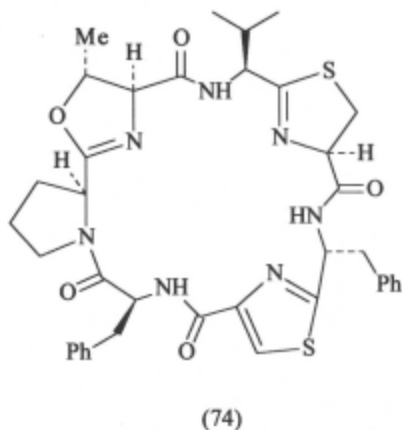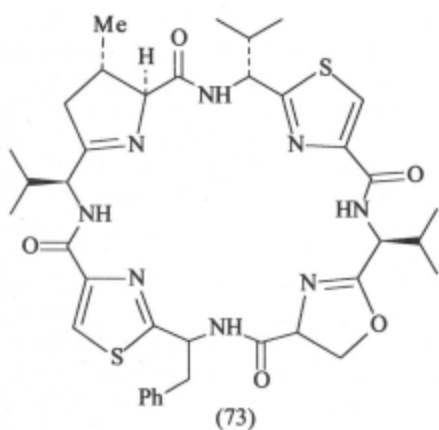
[200]. An excellent review [201] on synthetic aspects of the thiazole/oxazole cyclopeptides is an invaluable compilation on marine sources.

Side-chain modifications where sulfur bridges are built in *via* meso-lanthionine (75) or *threo* **β-methyllanthionine** (76) are widely distributed as
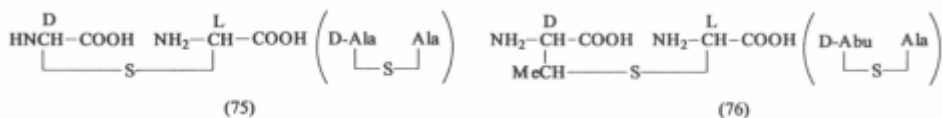
antibiotics within *Staphylococcus, Lactococcus, Bacillus* and *Streptomyces.* Probably the best known member is nisin (77) from *Streptococcus lactis*, widely used as a food preservative because of its activity against *Clostridium botulinum.* Nisin has been synthesised by Shiba's group [202]. The 'lantibiotic' family members can be divided into two sub-types - Type A (nisin related), which includes subtilin, epidermin, gallidermin, mersacidin and actagardin, and type B (duramycin type) which includes cinnamycin **(R$_o$090198),** lanthiopeptide, duramycin and ancovenin.
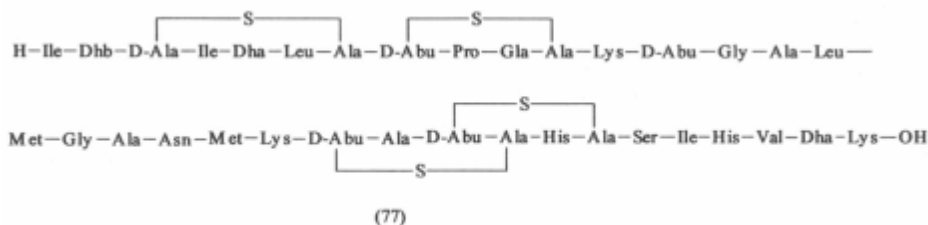
Finally, we reach a very important class of antibiotics and antitumour compounds whose heterodetic character involves coupled aromatic rings either as biphenyl linkages or as biphenyl ether bridges. The simplest form of the latter is manifested in the potent antitumour compounds RAVII (24) and deoxybouvardin (25) discussed in section 3.2.5. These side chain modifications are seen at their 'best' in the glycopeptide antibiotics represented by vancomycin (78), proliferated by *Streptomyces orientalis.* Vancomycin was used in hospitals in the late 1950's against penicillin-resistant staphylococci, but lost out, mainly due to its toxicity, to the semi-synthetic penicillins. However, it has re-emerged as a 'last resort' armour against the increasing problem of methicillin resistant *Staphylococcus aureus.* There is also the worry that vancomycin resistance is now strongly established in hospitals and hence the drive towards finding analogues and alternatives to vancomycin. From a structural point of view the task of analogue studies cannot be more difficult, so the demanding challenge of a total synthesis is fully justified. After years of intensive work by many groups (see Ref. 206 for list of relevant references), the year 1998 saw the pinnacle of achievement by the groups of Evans [204] and Nicolaou [205] reporting successful total syntheses of the vancomycin
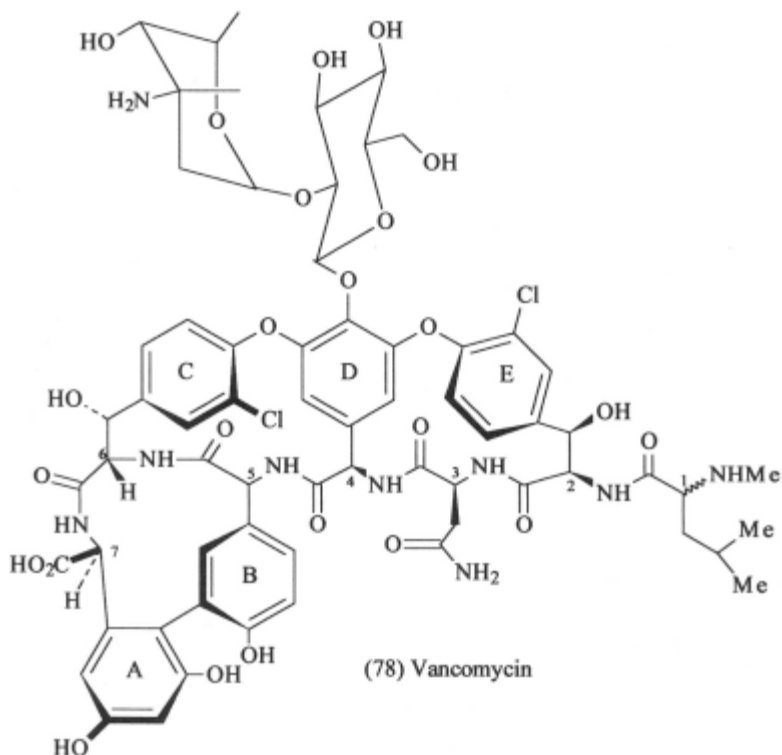
(78) Vancomycin

aglycone. The vancomycin skeleton contains three stereochemical elements of atropisomerism as a consequence of hindered rotation around diphenyl and diaryl ether links. The A-B diphenyl link was accomplished by Evans's group using vanadyl trifluoride oxidative cyclisation, while the diphenyl ethers were constructed by **S$_N$Ar** fluoride displacement reactions of nitro substituted aryl rings (also used for an earlier synthesis of orienticin C aglycone [206]). Construction of the A-B system in Nicolaou's approach was effected by the Suzuki conditions **[Pd(Ph$_3$P)$_4$]/Na$_2$CO$_3$** for coupling an iodo-aryl compound to a boronic acid aryl group, while the CDE biaryl linkages was accomplished *via* the in-house triazene-based technology [207].

Fundamental to the thrust towards new antibiotics is the understanding as to why vancomycin is able to interact with bacteria which have mutated to include D-Ala-D-Lac-OH moieties in their cell wall rather than D-Ala-D-Ala usually seen in **β-lactam** sensitive bacteria. Nmr techniques have been at the fore [208] in elucidating the basis of the mode of action of the glycopeptide antibiotics and in a simplified form (without including the fact that most bind as dimers) a model for the interaction has been proposed **(Figure 3)**.

Figure3

X = NH or O
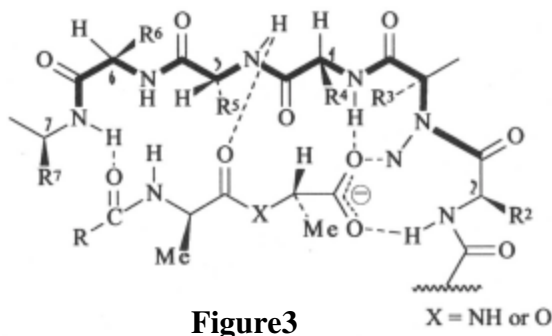
At the end of the millennium, therefore, quite a few of Nature's cyclopeptide secrets are being unravelled. No doubt new challenges will be ahead in the **21st** century.

References
1. Eur.J.Biochem, **148**, 9(1984); IntJ.PeptProtein Res, **24**, 84(1984); J.Biol.Chem., **260**, 14(1985)
2. J.S.Davies in *Amino Acids, Peptides and Proteins,* ed. J.S.Davies, Royal Society of Chemistry SPR, **25**, 246(1994); **26**, 235(1995); **27**, 230(1996), **28**, 233(1997); **29**, 262(1998); **30,** in press (1999).
3. (a) C.Blackburn and S.A.Kates, *Methods EnzymoL.*, **289** (Solid Phase Peptide Synthesis), 175(1997); (b) A.F.Spatola and P.Romanovskis, in *Comb.Pept.Nonpept.Libr.,* ed. G.Jung, 327(1996); (c) A.G.Beck-Sickinger, Methods Mol.Biol, **73**, 61(1997); (d) J.Eichler and R.A.Houghten, *Protein Pept.Lett.,* **4,** 157(1997); (e) I.Annis, B.Hargittai and G.Barany, *Methods EnzymoL,* **289** (Solid Phase Peptide Synthesis), 198(1997); (f) M.Qabor, J.Urban, C.Sia, M.Klein and M.Kahn, Letters in PeptSci, **3**, 25(1996); (g) H.Kessler, R.Gratias, G.Hessler, M.Gurrath and G.Muller, Pure Appl.Chem., **68**, 1201(1996); (h) P.Wipf, Chem.Rev., **95**, 2115(1995); (i) J.Gante, Angew.Chem.IntEd.Eng., **33**, 1699(1994); (j) G.V.Nikiforovich, IntJ.PeptProtein Res., **44**, 513(1994).
4. V.Z.Pletnev, V.T.Ivanov, D.A.Langs, B.M.Burkhart and W.L.Duax, Biopolymers, **42**, 645(1997); V.Z.Pletnev, S.N.Ruzeinikov,. I.N.Tsigannik, V.T.Ivanov, S.V.Pletnev, D.A.Langs and W.L.Duax, *ibid.,* **42**, 651(1997); H.Rapaport, I.Kuzmenko, K.Kjaer, P.Howes, W.Bowman, J.Als-Nielsen, L.Leiserowitz and M.Lahav, J.Amer.Chem.Soc., **119**, 11211(1997).
5. R.Haubner, W.Schmitt, G.Holzemann, S.L.Goodman, A.Jonczyk and H.Kessler, J.Amer.Chem.Soc., **118**, 7881(1996); G.Mueller, Angew.Chem.Int.Ed.Engl., **35**, 2767(1996); ; E.Graf Von Roeden, E.Lohof, G.Hessler, M.Hofrnann and H.Kessler, J.Am.Chem.Soc., **118**, 10156(1996); S.Behrens, B.Mathä, G.Bitan, C.Gilon and H.Kessler, Int.J.Pept.Protein Res, **48**, 569(1996); R.Haubner, D.Finsinger and H.Kessler, Angew.Chem.Int.Ed.Engl., **36**, 1374(1997); J.Wermuth, S.L.Goodman, A.Jonczyk and H.Kessler, J.Am.Chem.Soc., **119**, 1328(1997); O.Mechnich, G.Hessler, H.Kessler, M.Bernd and B.Kutscher, Helv.Chim.Acta, **80**, 1338(1997).
6. A.Ehrlich, H-U.Heyne, R.Winter, M.Beyermann, H.Haber, L.A.Carpino and M.Bienert, J.Org.Chem., **61**, 8831(1996).
7. S.Zimmer, E.Hofftnann, G.Jung and H.Kessler, Liebigs.Ann.Chem., 497(1993).

8. J.S.Davies, J.Howe, J.Jayatilake and T.Riley, Lett.Pept.Sci., **4**, 441(1997).
9. L-h.Zhang, J.A.Pesti, T.D.Costello, P.J.Sheeran, R-Uyeda, P.Ma, G.S.Kauffman, R.Ward and J.L.McMillan, J.Org.Chem., **61**, 5180; T.D.Harris, M.Rajopadhye, P.R.Damphousse, S.J.Heminway, J.Lazewatsky, T.Mazoika and T.R.Carroll, Bioorganic.Med.Chem.Lett., **6**, 1741(1996); A.C.Bach II, J.R.Espina, S.A.Jackson, P.F.W.Stouten, J.L.Duke, S.A.Mousa and W.F.Degrado, J.Amer.Chem.Soc., **118**, 293(1996).
10. D.Lim and K.Burgess, J.Am.Chem.Soc., **119**, 9632(1997).
11. H.Mihara, J.Hayashida, H.Hasegawa, H.I.Ogawa, T.Fujimoto and N.Nishimo, J.Chem.Soc.Perkin Trans. 2, 517(1997); N.Nishimo, M.Xu, H.Mihara, T.Fujimoto, M.Ohba, Y.Ueno and H.Kumagai, J.Chem.Soc.Chem.Commun., 180(1992).
12. A.F.Spatola, K.Darlak and P.Romanovskis, Tetrahedron Lett, **37**, 591(1996); S.A.Kates, N.Sole, F.Albericio and G.Barany, Peptides, 39(1994); J.Alsina, F.Rabanal, F.Alboicio and G.Barany, Tetrahedron Lett, **35**, 9633(1994).
13. T.D.Pallin and J.P.Tam, J.Chem.Soc.Chem.Commun., 2021(1995); J.P.Tam and Y-A.Lu, Tetrahedron Lett, **38**, 5599(1997); L.Zhang and J.P.Tam, Tetrahedron Lett, **38**, 4375(1997); J.Am.Chem.Soc., **119**, 2363(1997).
14. D.Apperley, M.North and R.B.Stokoe, Tetrahedron:Asymmetry, **6**, 1869(1995); P.Speers, C.Chan, R.Wilcock and K.T.Douglas, Amino Acids, **12**, 49(1997); G.Impellizzeri, G.Pappalatdo, E.Rizzarelli and C.Tringali, J.Chem.Soc.Perkin Trans. 2, 1435(1996).
15. C.L.L.Chai, A.R.King and D.C.R-Hockless, Acta Crystallogr.Sect C:Cryst.Struct.Commun., **C51**, 1836(1995); M.Szkaradzinska, M.Kubicki and P.W.Codding, ibid., **C50**, 565(1994).
16. M.Henczi and D.F.Weaver, Rapid Commun.Mass Spectrom. **9,** 800(1995).
17. P.M.Fischer, M.Solbakken and K.Undheim, Tetrahedron, **50**, 2277(1994); K.A.Carpenter, G.Weltrowska, B.C.Wilkes, R-Schmidt and P.W.Schiller, J.Am.Chem.Soc., **116**, 8450(1994).
18. A.M.Bray, N.J.Maeji, R.M.Valerio, R.A.Campbell and H.M.Geysen, J.Org.Chem, **56**, 6559(1991).
19. J.Alsina, E.Giralt and F.Albericio, Tetrahedron Lett, **37**, 4195(1996).
20. M.North, Synlett, 807(1993).
21. J.Thoen and M.A.Lipton, Tetrahedron.-Asymmetry, **8**,1987(1997).
22. C.R-Noe, A.Weigand, S.Pirker and P.Liepert, Monatsch Chem., **128**, 301(1997).
23. P.G.Sammes, Forstschr.Chem.Org.Naturst., **32**, 51(1975)
24. X.Fu, L-M.Zeng, J-Y.Su and M.Pais, J.Nat.Prod., **60**, 695(1997).
25. Y.Kimura, K.Tani, A.Kojima, G.Sotoma, K.Okada and A.Shimada, Phytochemistry, **41**, 665(1996).
26. H.Izumida, M.Nishyima, T.Takedera, A.M.Nomoto and H.Sano, J.Antibiotics, **49**, 829(1996).
27. A.Santillan Jr., H-g.Park, X.Zhang, O-S.Lee, W.R.Widger and H.Kohn, J.Org.Chem., **61**, 7756(19%); H-g.Park, X.Zhang, W.R.Widger and H.Kohn, ibid., **61**, 7764(1996).
28. M.Adanczeski, A.R.Reed and P.Crews, J.NatProd., **58**, 201(1995).
29. W.Balk-Bindseil, E.Helmke, H.Weyland and H.Laatsch, Liebigs Ann.Chem., 1291(1995).
30. C.Flouzat, F.Marguerite, F.Croizet, M.Percebois, A.Monteil and M.Combourieu, Tetrahedron Lett., **38**, 1191(1997).
31. J.M.Travins and F.A.Etzkorn, J.Org.Chem., **62**. 8387(1997).
32. D.Vogel, R.Schmidt, K.Hartung, H-U.Demuth, N.N.Chung and P.W.Schiller, Int.J.Pept.Protein Res, **48**, 495(1996).
33. U.Schmidt and J.Langner, J.Pept.Res., **49**, 67(1997).
34. J-M.Aracil, A.Badre, M.Fadli, G.Jeanty, B.Banaigs, C.Francisco, F.Lafargue, H.Heitz and A.Aumelas, Tetrahedron Lett., **22**, 2609(1991).

35. W.Maestle, U.Link, W.Witschel, U.Thewalt, T.Weber and M.Rothe, Biopolymers, **31**, 735(1991).

36. F.Cavalier-Frontin, G.Pèpe, J.Verducci, D.Siri and RJacquier, J.Am.Chem.Soc., **114**, 8885(1991).

37. N.Nishori, M.Xu, H.Mihara, T.Fujimoto, Y.Ueno and H.Kumugai, Tetrahedron Lett, **33**, 1479(1992).

38. U.Link, W.Mästle and M.Rothe, Int.J.Pept.Protein Res, **42**, 475(1993).

39. D.S.S.Jois, S.Suresh, M.Vijayan and K.R.K.Easwaran, Int.J.Pept.Protein Res, **48**, 12(1996).

40. M.Tamaki, S.Komiya, M.Yabu, E.Watanabe, S.Akabori and I.Muramatsu, J.Chem.Soc.Perkin Trans. 2, 3497(1997).

41. M.J.Bogusky, S.F.Brady, J.T.Sisko, R.F.Nutt and G.M.Smith, Int.J.Pept.Protein Res, **42**, 194(1993).

42. S.Gupta, G.Peiser, T.Nakajima and Y-S.Hwang, Tetrahedron Lett., **35**, 6009(1994).

43. S.B.Singh, D.L.Zink, J.D.Polishook, A.W.Dombravski, S.J.Darkin-Rattay, D.M.Schmatz and M.A.Goetz, Tetrahedron Lett, **37**, 8077(1996).

44. W.D.Clark, T.Corbett, F.Valeriote and P.Crews, J.Am.Chem.Soc., **119**, 9285(1997).

45. M.J.Bogusky, A.M.Naylor, M.E.Mertzman, S.M.Pitzenberger, R.F.Nutt, S.F.Brady, C.D.Colton and D.F.Veber, Biopolymers, **33**, 1287(1993).

46. T.Fukami, T.Nagase, T.Mase, A.Naya, K.Fujita, K.Niiyama and K.Ishikawa, Bioorg.Med.Chem.Lett, **4**, 1613(1994); J.X.He, W.L.Cody and A.M.Doherty, Lett. Pept.Sci., **1**, 25(1994); I.Vlatas, J.Dellureficio, R.Dunn, I.I.Sytwu and J.Stanton, Tetrahedron Lett., **38**, 7321(1997).

47. S.Nakajima, K.Niiyama, M.Ihara, K.Kojiri and H.Suda, J.Antibiotics, **44**, 1348(1991).

48. K.Ishikawa, T.Fukami, T.Nagase, K.Fujita, T.Hayama, K.Niyama, T.Mase, M.Ihara and M.Yano, J.Med.Chem., **35** 2139(1992).

49. N.C.Gonnella, X.Zhang, Y.Jin, O.Prakash, C.G.Paris, I.Kolossvary, W.C.Guida R.S.Bohacek, I.Vlattas and T.Sytwu, Int.J.Pept.Protein Res, **43**, 454(1994); J.W.Bean, C.E.Peishoff and K.D.Kopple, Int.J.Pept.Protein Res, **44**, 223(1994).

50. T.Fukami, T.Nagase, K.Fujita, T.Hayama, K.Niiyama, T.Mase, S.Nakajima, I.Fukuroda, T.Saeki, M.Nishikibe, M.Ihara, M.Yano and K.Ishikawa, J.MedChem., **38**, 4309(1995).

51. M.J.Bogusky, S.F.Brady, J.T.Sisko, R.F.Nutt and G.M.Smith, Int.J.Pept.Protein Res, **42**, 194(1993).

52. M.Coles, V.Sowemimo, D.Scanlon, S.L.A.Munro and D.J.Craik, J.Med.Chem., **36**, 2658(1993).

53. J.P.Dirlam, A.M.Belton, N.C.Birsner, R.R.Brooks, S-P.Chang, R.Y.Chandrasekaran, J.Clancy, B.J.Cronin, B.P.Dirlam, S.M.Finegan, S.A.Froshauer, A.E.Girard, S.F.Hayashi, R.J.Howe, K.C.Kane, B.J.Kamicker, S.A.Kaufman, N.L.Kolosko, M.A.LeMay, R.G.Lind II, J.P.Lyssikatos, C.P.MacLelland, T.V.Magee, M.A.Massa, S.A.Miller, M.L.Minich, D.A.Perry, J.S.Petitpas, C.P.Reese, S.B.Seibel, W.-G.Su, K.T.Sweeney, D.A.Whipple and B.V.Yang, Bioorg.Med.Chem.Lett., **7**, 1139(1997); R.C.Linde II, N.C.Birsner, R.Y.Chandrasekaran, J.Clancy, R.J.Howe, J.P.Lyssikatos, C.P.MacLelland, T.V.Magee, T.W.Petitpas, J.P.Rainville, W-G.Su, C.B.Vu and D.A.Whipple, Bioorg.Med.Chem.Lett., **7**, 1149(1997).

54. H.Morita, S.Nagashima, K.Takeya and H.Itokawa and Y.Iitaka, Chem.Pharm.Bull., **41**, 992(1993), Tetrahedron, **51**, 1121(1995).

55. Y.S.Yun, K.Takeya, H.Itokawa and K.Yamada, Tetrahedron, **51**, 6003(1995).

56. H.Morita, Y.S.Yun, K.Takeya and H.Itokawa, Bioorg.Med.Chem., **5**, 2063(1997).

57. H.J.Shin, H.Matsuda, M.Murakami and K.Yamaguchi, J.Nat.Prod., **60**, 139(1997).

58. I.R.Marsh, M.Bradley and S.J.Teague, J.Org.Chem., **62**, 6199(1977).

59.   K.K.Bhandary and K.D.Kopple, Acta Crystallogr.Sect.C:Cryst.Struct.Commun., **C47**, 1280(1991).
60.   D.Mierke and H.Kessler, J.Am.Chem.Soc., **113**, 9466(1991).
61.   H.Kessler and B.Haase, Int.J.Pept.Protein Res, **39**, 36(1992).
62.   A.F.Spatola, M.K.Anwer and M.N.Rao, Int.J.Pept.Protein Res, **40**, 322(1992).
63.   K.D.Kopple, J.W.Bean, K.K.Bhandary, J.Briand, C.A.D'Ambrosia and C.E.Peishoff, Biopolymer, **33**, 1093(1993).
64.   G.Mueller, M.Gurrath, M.Knuz and H.Kessler, Proteins:Struct.Funct., Genet, **15**, 235(1993).
65.   F.A.Etzkorn, T.Guo, M.A.Lipton, S.D.Goldberg and P.A.Bartlett, J.Am.Chem.Soc., **116**, 10412(1994).
66.   K.Burgess, D.Lim and S.A.Mousa, J.Med.Chem., **39**, 4520(1996).
67.   A.Lender, W.Yao, P.A.Sprengeler, R.A.Spanevello, G.T. Furst, R.Hirschmann and A.B.Smith III, Int.J.Pept.Protein Res, **42**, 509(1993).
68.   D.L.Boger, D.Yohannes, J.Zhou and M.A.Patane, J.Am.Chem.Soc., **115**, 3420(1993).
69.   D.L.Boger, J.Zhou, R.M.Borzilleri, S.Nukii and S.L.Castle, J.Org.Chem., **62**, 2054(1997); T.Inoue, T.Inaba, I.Umezawa, M.Yuasa, H.Itokawa, K.Ogura, K.Komatsu, H.Hara and O.Hoshino, Chem.Pharm.BuIl., **43**, 1325(1995).
70.   T.Inoue, T.Sasaki, H.Takayanagi, Y.Harigaya, O.Hoshino, H.Hara and T.Inaba, J.Org.Chem., **61**, 3936(1996).
71.   D.L.Boger and J.C.Zhou, J.Org.Chem., **61**, 3938(1996).
72.   D.L.Boger and J.Zhou, J.Am.Chem.Soc., **117**, 7364(1995).
73.   Y.Hitotsuyanagi, S.Lee, K.Takeya and H.Itokawa, J.Chem.Soc.Chem.Commun., 503(1996).
74.   Y.B.He, Z.Huang, K.Raynor, T.Reisine and M.Goodman, J.Am.Chem.Soc., **115**, 8066(1993).
75.   N.G.J.Deleat, P.Verheyden, B.Velkeniers, E.L.Peters-Hooghe, C.Burns, D.Tourwe and G.Van Binst, Pept.Res., **6**, 24(1993); S.F.Brady, W.J.Palevada Jr., B.H.Arison, R.Saperstein, E.J.Brady, K.Raynor, T.Reisine, D.F.Veber and R.M.Freidinger, Tetrahedron, **49**, 3449(1993).
76.   D.E.Williams, M.Craig, C.F.B.Holmes and R.J.Andersen, J.Nat.Prod., **59**, 570(1996).
77.   H.Morita, T.Kayashita, A.Shishido, K.Takeya, H.Itokawa and M.Shiro, Tetrahedron **52**, 1165(1996).
78.   Y.Zhao, J.Zhou, X.Wang, H.Wu, X.Huang and C.Zou, Chin.Chem.Lett., **5**, 127(1994).
79.   H.Morita, Y.S.Yun, K.Takeya and H.Itokawa, Tetrahedron Lett, **35**, 9593(1994)
80.   H.Morita, Y.S.Yun, K.Takeya, H.Itokawa and M.Shiro, Tetrahedron, **51**, 5987(1995); **51**, 6003(1995).
81.   J.Kobayashi, M.Tsuda, T.Nakumara, Y.Mikami and H.Shigemori, Tetrahedron, **49**, 2391(1993); M.Tsuda, H.Shigemori, Y.Mikami and J.Kobayashi, Tetrahedron, **49**, 6785(1993); J.Kobayashi, T.Nakamura and M.Tsuda, Tetrahedron, **52**,6355(1996).
82.   G.R.Pettit, Z.Cichacz, J.Barkoczy, A.C.Dorsaz, D.L.Herald, M.D.Williams, D.L.Doubek, J.M.Schmidt and P.L.Tackett et al., **56**, 253(1993); G.R.Pettit, R.Tan. M.D.Williams, P.L.Tackett, J.M.Schmidt, R.L.Cerny and J.N.A.Hooper, Bioorg.Med.Chem.Lett, **3**, 2869(1993); G.R.Pettit, R.Tan, D.L.Herald, M.D.Williams, and R.L.Cerny, J.Org.Chem., **59**, 1593(1994).
83.   G.R.Pettit, F.Gao and R.Cerny, Heterocycles, **35**, 711(1993); O.Mechnich, G.Hessler, H.Kessler, M.Bemd and B.Kutscher, Helv.Chim.Acta, **80**, 1338(1997).
84.   M.P.Foster and C.M.Ireland, Tetrahedron Lett, **34**, 3871(1993).
85.   G.R.Pertit, J.K.Srirangam, D.L.Herald, K.L.Ericksen, D.L.Doubek, J.M.Schmidt, L.P.Tackett and G.J.Bakus, J.Org.Chem., **57**, 7217(1992).

86. Y.S.Yun, K.Takeya, H.Itokawa and K.Yamada, Tetrahedron, **51**, 6003(1995); M.Horishi, Y.S.Yun, K.Takeya, H.Itokawa and O.Shirota, Phytochemistry, **42**, 439(1996).
87. H.Morita, M.Shimomura, K.Takeya and H.Itokawa, J.Nat.Prod., **59**, 280(1996); H.Morita, T.Kayashita, K.Takeya, H.Itokawa and M.Shiro,Tetrahedron, **53**, 1607(1997).
88. H.J.Shin, H.Matsuda, M.Murakami and K.Yamaguchi, Tetrahedron, **52**, 13129(1996).
89. N.Namikoshi, F.Sun, B.W.Choi, K.L.Rinehart, W.W.Carmichael, W.R.Evans and V.R.Beasley, J.Org.Chem., **60**, 361(1995).
90. R.Bhaskaran and C.Yu, Int.J.Pept.Protein Res, **43**, 393(1994); H.Kessler and T.Wein, Liebigs.Ann.Chem., 179(1991).
91. D.S.Eggleston, P.W.Baures, C.E.Peishoff and K.D.Kopple, J.Am.Chem.Soc., **113**, 4410(1991).
92. H.Morita, T.Kayashita, K.Takeya, H.Itokawa and M.Shiro, Tetrahedron, **51**, 12539(1995).
93. O.Mechnich, G.Hessler, H.Kessler, M.Bemd and B.Kutscher, Helv.Chim.Acta, **80**, 1338(1997).
94. H.Morita, T.Kayshita, K.Takeya, H.Itokawa and M.Shiro, Tetrahedron, **53**, 1607(1997).
95. H.Morita, Y.S.Yun, K.Takeya and H.Itokawa, Chem.Pharm.Bull., **45**, 883(1997).
96. T.Ishizu, J.Hirayama and S.Noguchi, Chem.Pharm.Bull., **42**, 1146(1994).
97. D.S.Jois, G.S.Prasad, M.Bednarek, K.R.K.Easwaran and M.Vijayan, Int.J.Pept.Protein Res, **41**, 484(1993).
98. R.K.Konat, D.F.Mierke, H.Kessler, M.Bernd, B.Kutscher and R-Voegeli, Helv.Chim.Acta, **76**, 1649(1993).
99. M.Pohl, D.Ambrosius, J.Grötzinger, T.Kretzchmar, D.Saunders, A.Wollmer, D.Brandenburg, D.Bitter-Suermann and H.Höcker, Int.J.Pept.Protein Res, **41**, 362(1993).
100. H.Kataoka, T.Hanawa and T.Katagi, Chem.Pharm.Bull., **40**, 570(1992).
101. K.K.Bhandary,Acta Crystallogr.Sect.C:Cryst.Struct.Commun. **C47**,1483(1991).
102. Y.R.Zhao, J.Zhou, X-K.Wang, H-M.Wu, X-L.Huang and C.Zou, Phytochemistry, **46**, 709(1997).
103. H.Morita, K.Takeya and H.Itokawa, Phytochemistry, **45**, 841(1997).
104. L.Chao-Ming, T.Hing-Hua, M.Qing, Z.Hiu-Lan and H.Xiao-Jiang, Phytochemistry, **45**, 521(1997).
105. C.Auvin-Guette, C.Baraguey, A.Bland, J-L.Pousset and B.Bodo, J.Nat.Prod, **60**, 1155(1997).
106. A.J.J.van den Berg, S.F.A.J.Horsten, J.J.Kettenes-van den Bosch, B.H.Kroes, C.J.Beukelman, B.R.Leeflang and R-P.Labadie, FEBS Lett., **358**, 215(1995).
107. Y-R.Zhao, X-K.Wang, J.Zhou, C-X.Cheng, X-L.Huang, H-M.Wu, Chin.J.Chem., **13**, 552(1995).
108. H.Morita, T.Kayashita, H.Kobata, A.Gonda, K.Takeya and H.Itokawa, Tetrahedron, **50**, 6797(1994); ibid, **50**, 9975(1994); H.Morita, H.Kobata, K.Takeya and H.Itokawa, Tetrahedron Lett., **35**, 3563(1994).
109. C.A.Bewley, H.He, D.H.Williams and J.D.Faulkner, J.Am.Chem.Soc., **118**, 4314(1996).
110. T.Tancredi, E.Benedetti, M.Grimaldi, C.Pedone, P.A.Temussi and G.Zanotti, Biopolymers, **31,** 761(1991).
111. B.D.Blasio, F.Rossi, E.Benedetti, V.Pavone, M.Saviono, C.Pedone, G.Zanotti and T.Tancredi, J.Am.Chem.Soc., **114**, 8277(1992); M.Saviono, F.Rossi, M.Filizola, B.DiBlasio and C.Pedone, Acta Crystallogr., Sect.C:Cryst.Struct.Commun., **C51**, 663(1995).
112. M.Cebrat, M.Lisowski, I.Z.Siemon and Z.Wieczorek, Pol.J.Chem., **71**, 1401(1997).
113. H.Morita, A.Sishido, T.Matsumoto, K.Takeya, H.Itokawa, T.Hirano and K.Oka, Bioorg.Med.Chem.Lett., **7**, 1269(1997).

114. C.Auvin, C.Baraguey, A.Bland, F.Lezenven, J-L.Pousset and B.Bodo, Tetrahedron Lett, **38**, 2845(1997).

115. H.Morita, A.Gonda, K.Takeya and H.Itokawa, Bioorg.Med.Chem.Lett., **6**, 767(1996).

116. H.Morita, A.Gonda, K. Takeya, H.Itokawa and O.Shirota, Chem.Pharm.Bull., **45**, 161(1997).

117. K.Yano, M.Yamasaki, M.Yoshida, Y.Matsuda and K.Yamaguchi, J.Antibiot **48**, 1368(1995); J.X.He, W.L.Cody, M.A.Flynn, K.M.Welch, E.E.Reynolds and A.M.Doherty, Bioorg.Med.Chem.Lett., **5**, 621(1995).

118. H.Morita, A.Shishido, T.Kayashita, K.Takeya and H.Itokawa, J.NatProd, **60**, 404(1997).

119. A.Stern, W.A.Gibbons and L.C.Craig, Ptoc.Nat.Acad.Sci., USA, **61**, 734(1968); R.Schwyzer and U.Ludescher, Helv.Chim.Acta, **52**, 2033(1969); M.Ohnishi and D.W.Urry, Biochem.Biophys.Res.Comm., **36**, 194(1969).

120. M.Tamaki, S.Akabori and I.Muramatsu, Bull.Chem.Soc.,Jpn., **64**, 583(1991).

121. H.Mihara, N.Nishino, H.I.Ogawa, N.Izumiya and T.Fujimoto, Bull.Chem.Soc.,Jpn., **65**, 228(1992).

122. M.Xu, N.Nishino, H.Mihara, T.Fujimoto and N.Izumiya, Chem.Lett., 191(1992); H.Mihara, J.Hayashida, H.Hasegawa, H.I.Ogawa, T.Fujimoto and N.Nishino, J.Chem.Soc.Perkin Trans. 2,517(1997).

123. M.Tamaki, S.Akabori and I.Muramatsu, J.Am.Chem.Soc., **115**, 10492(1993).

124. M.Tamaki, S.Akabori and I.Muramatsu, Bull.Chem.Soc.Jpn., **66**, 3113(1993).

125. M.Tamaki, S.Komiya, S.Akabori and I.Muramatsu, Bull.Chem.Soc.,Jpn., **70**, 899(1997).

126. M.Tamaki, I.Arai, S.Akabori and I.Muramatsu, Int.J.Pept.Protein Res, **45**, 299(1995).

127. T.Wieland, G.Lüben, H.Ottenheym, J.Faesel, J.X.DeVries, A.Prox and J.Schmid, Angew.Chem.Int.Ed.Engl., **7**, 204(1968).

128. T.Wieland, J.Faesel and W.Kanz, Annalen,**722**, 179(1969).

129. G.Zanotti, F.Rossi, M.Saviano, T.Tancredi, G.Saviano, A.Maione, M.Filizola, B.DiBlasio and C.Pedone, J.Am.Chem.Soc., **117**, 8651(1995).

130. J.M.Gregson, J-L.Chen, G.M.L.Pattereon and R.E.Moore, Tetrahedron, **48**, 3727(1992).

131. S.S.Moon, J.L.Chen, R.E.Moore and G.M.L.Patterson, J.Org.Chem., **57**, 1097(1992).

132. J.Gerard, P.Haden, M.T.Kelly and R.J.Andersen, Tetrahedron Lett, **37**, 7201(1996).

133. H.Morita, A.Gonda, K.Takeya, H.Itokawa and Y.Iitaka, Tetrahedron, **53**, 1617(1997).

134. D.L.Herald, G.L.Cascarano, G.R.Pettit and J.K.Srirangam, J.Am.Chem.Soc., **119**, 6962(1997).

135. F.Rossi, M.Saviano, P.DiTalia, B.DiBlasio, C.Pedone, G.Zanotti, M.Mosca, G.Saviano, T.Tancredi, K.Ziegler and E.Benedetti, Biopolymers, **40**, 465(1997).

136. H.Kessler, D.F.Mierke, D.Donald and M.Furber, Angew.Chem.Int.Ed.Eog., **30**,954(1991).

137. S.W.Fesik, R.T.Gampe Jr., H.L.Eaton, G.Gemmeker, E.T.Olejniczak, P.Neri, T.F.Holzman, D.A.Egan, R.Edalji, R.Simmer, R.Helfrich, J.Hochlowski and M.Jackson, Biochemistry, **30**, 6574(1991); C.Weber, G.Wider, B.von Freyberg, R.Traber, W.Braun, H.Widmer and K.Wüthrich, Biochemistry, **30**, 6563(1991).

138. P.Verhayden, H.Jaspers, E.deWolf and G.Van Binst, Int.J.Pept.Protein Res, **44**, 364(1994).

139. Y.M.Angell, T.L.Thomas, G.R.Flentke and D.H.Rich, J.Am.Chem.Soc., **117**, 7279(1995).

140. S.Y.Ko and R.M.Wenger, Helv.Chim.Acta, **80**, 695(1997).

141. D.Seebach, A.K.Beck, H.G.Bossler, C.Gerber, S.Y.Ko, C.W.Murtiashaw, R.Naef, S.Shoda, A.Thaler, M.Krieger and R.Wenger, Helv.Chim.Acta, **76**, 1564(1993).

142. C.Papageorgiou, J.J.Sanglier and R.Traber, Bioorg.Med.Chem.Lett, **6**, 23(1996).

143. V.Mikol, C.Papageorgiou and X.Borer, J.Med.Chem., **38**, 3361(1995).

144. M.-K-Hu, A.Badger and D.H.Rich, J.Med.Chem., **38**, 4164(1995).

145. M.K.Eberle and F.Nuninger, Tetrahedron Lett, **35**, 6477(1994).

122

146. D.G.Alberg and S.L.Schreiber, Science, **262**, 248(1993).
147. S.Matsunga and N.Fusetani, J.Org.Chem., **60**,1177(1995).
148. W.P.Frankmolle, G.Knubel, R.E.Moorc and G.M.L.Patteson, J.Antibiot., **45**, 1458(1992); W.P.Frankmolle, L.K.Larsen, F.R.Caplan, G.M.L.Patterson, G.Knubel, I.A.Levine and R.E.Moore, ibid, **45**, 1451(1992); I.Bonnard, M.Rolland, C.Francisco and B.Banaigs, Letters in Pept.Sci., **4**, 289(1997).
149. K.Ishida, H.Matsuda, M.Murakami and K.Yamaguchi, J.Nat.Prod, **60**, 724(1997); Tetrahedron, **52**, 9025(1996).
150. H.Morita, A.Gonda, KTakeya, H.Itokawa, T.Hirano, K.Oka and O.Shirota, Tetrahedron, **53**, 7469(1997).
151. M.Tamaki, S.Komuja, S.Akabori and I.Muramatsu, J.Chem.Soc.Perkin Trans. 1, 2045 (1997).
152. S.Ando, M.Nishihama, H.Nishikawa, H.Takiguchi, S.Lee and G.Sugihara, Int.J.Pept.Protein Res, **46**, 97(1995).
153. I.Annis, B.Hargittai and G.Barany in *Methods in Enzymology,* **289** (Solid Phase Synthesis), Academic Press, Chapter 10,198(1997).
154. D.Andreu, F.Albericio, N.A.Solé, M.C.Munson, M.Ferrer and G.Barany in *Methods in Mol.Biol - Peptide Synthesis Protocols,* eds. M.W.Penningten and B.M.Dunn, Humana Press, Totowa, N.Jersey, **35**, 91(1994).
155. Y.Kiso and H.Yajima in *Peptides - Synthesis, Structures and Applications,* ed B.Gutte, Academic Press, 35(1995).
156. L.Moroder, D.Besse, H.J.Musiol, S.Rudolph-Böhner and F.Siedler, Biopolymers, **40**, 207 (1996).
157. M.Azria, D.H.Copp and J.M.Zanelli, Calcified Tissue Intl., **57,** 405 (1995); A.N.Semenov and I.V.Lomonoseva, Bioorg.Khim., **19**, 182(1993); Int.J.Peptide Protein Res., **43**, 113 (1994).
158. R.Muff, W.Born and J.A.Fischer, Eur.J.Endocrinol., **133**,17(1995).
159. G.McDowell, C.Shaw, K.D.Buchanan and D.P.Nicholls, Eur.J.Clinical Invest, **25**, 291(1995).
160. Q.Li, L.Grimclius, A.Hoog, H.Johansson, M.Kjellmann and A.Larsson, Histochem and Cell Biol., **111**, 33(1990).
161. H.Nishiuchi, K.Akaji and Y.Kiso, Pept.Chem., 225 (1994).
162. V.J.Hruby and C.W.Smith in *The Peptides,* ed. C.W.Smith, Academic Press, Vol. 8, Chapter 4 (1987).
163. A.F.Bristow in *Polypeptides and Protein Drugs,* eds. R.C.Hider and D.Barlow, Ellis Harwood, Chapter 3, p.54 (1991).
164. D.F.Veber, R.M.Friedinger, R.Schwenk-Perlaw *et al.,* Nature, **292**, 55(1981); L.E.Rosenthal, D.J.Yamashiro, J.Rivier, *et al.,* J.Clin.Invest, **71**,840(1983).
165. M.C.Munson and G.Barany, J.Am.Chem.Soc., **115**, 10203(1993).
166. H.Tomoda, H.Nishida, X.H.Huang, R.Masuma, Y.K.Kim and S.Omura, J.Antibiot., **45**, 1207(1992).
167. Y.L.Dory, J.M.Mellor and J.F.McAleer, Tetrahedron, **52**, 1343(1996); J.R.Dawson, Y.L.Dory, J.M.Mellor and J.F.McAleer, ibid, **52,** 1361(1996); Y.L.Dory, J.M.Mellor and J.F.McAleer,ibid, **52**,1379(1996).
168. A.B.MaugerandO.A.Stuart, J.Med.Chem., **34**,1297(1991)
169. G.R.Pettit, Prog.Chem.Org.Nat.Prod **70**, 1(1997); K.Yamada and H.Kigoshi, Bull.Chem. Soc.-Jap., **70**, 1479(1997).
170. G.R.Pettit, J-p.Xu, F.Hogan, M.D.Williams, D.L.Doubek, J.M.Schmidt, R.L.Cerny and M.R.Boyd J.Nat.Prod, **60**, 752(1997).

171. R.B. Bates, K.G. Brusoe, J.J.Burns, S.Caldera, C.Sriyani, W.Cui, S.Gangwar, M.R.Gramme, K.J.McClure. G.P.Rouen, H.Schadow, C.C.Stessman, S.T.Taylor, V.H.Vu., G.V.Yarik, J.Zhang, G.R.Pettit and R-Bontems, J.Am.Chem.Soc., **119**, 2111(1997).

172. H.Sone, T.Nemoto, B.Ojika and K.Yamada, Tetrahedron Lett.,, **34**, 8447(1993).

173. H.Ishiwata, T.Nemoto, M.Ojika and K.Yamada, J.Org.Chem., **59**, 4710(1994).

174. T.Mutou, T.Kondo, M.Ojika and K.Yamada, J.Org.Chem., **61**, 6340(1996).

175. R.Sakai, K.L.Rinehart, V.Kishore, B.Kundu, G.Faircloth, J.B.Gloer, J.R.Carney, M.Namikoshi, F.Sun, R.G.Hughes Jr., D.G.Gravalos, T.G.DeQueseda, G.R.Wilson and R.M.Heid, J.Med.Chem., **39,** 2819(1996); E.Abou-Mansour, A.Boulanger, A.Badre, I.Bonnard, B.Banaigs, G.Combaut and C.Francisco, Tetrahedron, **51,** 12591(1995).

176. U.Schmidt, M.Kroner and H.Griesser, Synthesis, 294(1991).

177. G.Jou, I.Gonzalez, F.Albericio, P.Lloyd-Williams and E.Giralt, J.Org.Chem., **62**, 354(1997).

178. T.Q.Dinh, C.D.Smith and R. W.Armstrong, J.Org.Chem., **62**, 790(1997).

179. T.Q.Dinh, X.Du and R.W.Armstrong, J.Org.Chem., **61**, 6606(1995); A.K.Gosh, W.M.Liu, Y.B.Xu and Z.Chen, Angew.Chem.Int.Ed.Engl., **35**, 75(1996).

180. K.M.Gardinier and J.W.Leahy, J.Org.Chem.,, **62**, 7098(1997).

181. G.V.Subbarju, T.Golakoti, G.M.L.Patterson and R.E.Moore, J.Nat.Prod, **60**, 302(1997).

182. S.F.Yeh, W.Pan, G.T.Ong, AJ.Chiou, C.C.Chuang, S.H.Chiou and S.H.Wu, Biochem.Biophys.Res.Comun., **229**, 65(1996).

183. F.Cavalier, RJacqauier, J-L.Mercadier and J.Verducci, Tetrahedron, **52**, 6173(1996).

184. D.E.Ward, R.Lazny and M.S.C.Pedras, Tetrahedron Lett, **38**, 339(1997).

185. K.Hamano, M.Kinoshita, K.Tanzawa, K.Yoda, Y.Ohki, T.Nakamura and T.Kinoshita, J.Antibiot., **45**, 906 (1992); U.Schmidt and J.Langner, J.Chem.Soc.Chem.Commun., 2381 (1994).

186. R.Jansen, B.Kunze, H.Reichenbach and G.Hofle, Liebigs Annalen, 285(1996).

187. R.H.Schlessinger and Y-J.Li, J.Am.Chem.Soc., **118**, 3301(1996); F.Tavares, J.P.Lawson and A.I.Meyers, ibid, **118**, 3303(1996); D.A.Entwhistle, S.I.Jordan, J.Montgomery and G.Pattendedn, J.Chem.Soc.Perkin Trans. 1,1315(1996).

188. J.Gerard, R-Lloyd, T.Borsby, P.Haden, M.T.Kelly and R.J.Anderson, J.NatProd, **60**, 223 (1997).

189. K.Ishida, H.Matsuda, M.Murakami and K.Yamaguchi, J.Nat.Prod, **60**, 184(1997).

190. Y.Kajimura and M.Kaneda, J.Antibiotics, **50**, 220(1997).

191. T.Shioiri, T.Imaeda and Y.Hamada, Heterocycles, **46**, 421 (1997).

192. K.Suenaga, T.Mutou, T.Shibata, T.Itoh, H.Kigoshi and K.Yamada, Tetrahedron Lett., **37**, 6771(1996).

193. M.Kobayashi, W.Wang, N.Ohyabu, M.Kurosu and I.Kitagawa, Chem.Pharm.Bull., **43**, 1598(1995).

194. H.Tada, T.Tozyo, Y.Terui and F.Hayashi, Chem.Lett., 431(1992).

195. G.Abbenante, D.P.Fairlie, L.R.Gahan, G.R-Hanson, G.K.Pierens and A.L. van den Brank, J.Am.Chem.Soc., **118**,10384(1996).

196. A.R.Carroll, J.C.Coll, D.J.Bourne, J.K.McLeod, T.M.Zabriskie, C.M.Ireland and B.F.Bowden, Aust.J.Chem., **49**, 659(1996).

197. M.A.Rashid, K.R.Gustafson, J.H.Cardellina II and M.R.Boyd, J.Nat.Prod, **58**, 594(1995).

198. C.D.J.Boden and G.Pattenden, Tetrahedron Lett., **36**, 6153(1995).

199. H.Sone, H.Kigoshi and K.Yamada, Tetrahedron, **53**, 8149(1997).

200. J.Kobayashi, F.Itagaki, H.Shigenori, T.Takao and Y.Shimonishi, Tetrahedron, **51**, 2525(1995).

201. P.Wipf, Chem.Rev., **95**, 2115(1995).

202. K.Fukase, M.Kitazawa, A.Sano, K.Shimbo, H.Fujita, S.Horimoto, T.Wakamiya and T.Shiba, Tetrahedron Lett, **29**, 795(1988).
203. G.Jung and H.G.Sahl, *Nisin and Novel Lantibiotics,* ESCOM Leiden (1991).
204. D.A.Evans, M.R.Wood, B.W.Trotter, T.I.Richardson, J.C.Barrow and J.L.Katz, Angew.Chem.Int.Ed.Engl., **37**, 2700(1998); D.A.Evans, C.J.Dinsmore, P.S.Watson, M.R.Wood, T.I.Richardson, B.W.Trotter and J.L.Katz, ibid., **37**, 2704(1998).
205. K.C.Nicolaou, S.Natarajan, H.Li, N.F.Jain, R.Hughes, M.E.Solomon, J.M.Ramanjulu, C.N.C.Boddy and M.Takayanagi, Angew.Chem.Int.Ed.Engl., **37**, 2708(1998); K.C.Nicolaou, N.F.Jain, S.Natarajan, R.Hughes, M.E.Solomon, H.Li, J.M.Ramanjulu, M.Takayanagi, A.E.Koumbis and T.Bando, ibid., **37**, 2714(1998); K.C.Nicolaou, M.Takayanagi, N.F.Jain, S.Natarajan, A.E.Koumbis, T.Bando, J.M.Ramanjulu, ibid, **37**, 2717(1998).
206. D.A.Evans, C.J.Dinsmore, A.M.Ratz, D.A.Evrard, J.C.Barrow, J.Am.Chem.Soc., **117**, 3417 (1997); D.A.Evans, J.C.Barrow, P.S.Watson, A.M.Ratz, C.J.Dinsmore, D.A.Evrard, K.M.DeVries, J.A.Ellman, S.D.Rychnovsky and J.Lacour, ibid, **119**, 3419(1997).
207. ICC.Nicolaou, C.N.C.Boddy, S.Natarajan, T.Y.Yue, H.Li, S.Bräse and J.M.Ramanjulu, J.Am.Chem.Soc., **119**, 3421(1997).
208. D.H.Williams, Natl.Prod.Reports, 469(1996).

CHAPTER 4
CYCLIC OLIGOSACCHARIDES AND POLYSACCHARIDES

Shinichi Kitamura,
Kyoto Prefectural University, Japan.

4.1 Introduction

It is well known that the products resulting from the action of the extracellular microbial enzyme cyclodextrin glucosyl transferase(CGTase) (E.C. 2.4.1.19) on starch and its components are cyclic oligosaccharides, composed of **α-(1→4)-linked** D-glucopyranose unit, i.e., cyclodextrins [1-3]. Although cyclodextrins which contain more than nine glucose units are found in the reaction mixture, the so-called **α-, β-, γ-cyclodextrins** with six, seven and eight sugars, respectively, are the most common. These cyclodextrins are commercially available and are industrially useful. Considerable information on preparation, structures, properties and applications has been accumulated to date. Several monographs have recently appeared that review historical and current aspects of cyclodextrin science and technology [4-12]. Cyclodextrins are best known for their ability to incorporate a variety of organic compounds into their cavity and for the fact that they exhibit catalytic activity.

Most recently, larger cyclodextrins having degrees of polymerization (dp) up to several hundreds have been found in the reaction mixture of recombinant potato D-enzyme(EC 2.4.1.25) on linear amylose [13]. It has also been reported that **α-, β- and γ- cyclodextrins** are not the major cyclic glucans produced by the initial action of CGTase on amylose [14]. The initial products appear to be cyclodextrins with dps in excess of 60. Crystal structures of large CDs have been reported [15-17]. These findings open new fields in cyclodextrin science and will stimulate further research in this fascinating area of cyclic polymers.

In addition to cyclodextrins, a large number of cyclic oligo- and polysaccharides have been recently discovered in nature and have been synthesized chemically and enzymatically [18-20]. Among these, cyclic **β-** glucans produced by bacteria of the family *Rhizobiaceae* have been studied extensively because of the possibility that they may play important roles in biological functions, such as the maintenance of the osmotic potential of the periplasm [21] and the phytopathogenicity of these bacteria [18].

Although in this review, the preparation and biological functions of cyclic oligosaccharides will be touched on, emphasis will be placed on establishing the conformations and physical properties of cyclic glucans,

THEORETICAL ASPECTS OF CYCLIC POLYMERS: EFFECTS OF EXCLUDED VOLUME INTERACTIONS

Mustapha Benmouna[a)] and Ulrich Maschke[b)]

a) Université Aboubakr Belkaïd, Institut de Physique et Chimie, Bel Horizon, BP119,13000 Tlemcen, Algeria

b) Université des Sciences et Technologies de Lille, Laboratoire de Chimie Macromoléculaire, CNRS UPRESA N° 8009, Bâtiment C6, 59655 Villeneuve d'Ascq Cedex, France

16.1. Introduction

Cyclic polymers provide the ideal conditions for studying the statistics of long polymer chains. Terminal ends in linear chains introduce defects from the statistical point of view since the translational invariance along the chain is suddenly interrupted. This is not the case for ring polymers where all the monomers are identical. This translational invariance along ring homopolymers is very attractive from the theoretical point of view and attributes to this class of polymers with special features as compared to their linear counterparts [l]-[2]. These features were the subject of intensive investigations both from the theoretical [3]-[8] and the experimental [9]-[13] points of view. It has been recognized long time ago that the theta temperature of dilute solutions of ring polymers undergoes a shift downward due to chain closure [11]. The second virial coefficient obtained either from light scattering or osmotic pressure is found to be positive at the ordinary theta temperature $(T=\Theta)$ corresponding to linear chains where normally it should be zero [11] [12] [14] [15]. The size of a ring polymer such as the radius of gyration is more than 40% lower than its linear counterpart for the same molecular weight and temperature only because of chain closure. Under good solvent conditions however, some models predict that cyclic polymers swell more than linear chains. Interestingly enough, many properties of cyclic chains are found to be similar to those of branched polymers. This observation may indicate that the reason for discrepancies between cyclic and linear chains should be the same than that distinguishing linear from branched polymers of the same molecular weight [17]. Since the relatively higher monomer density around the center of mass for branched polymers is responsible for discrepancies with the linear chains, the same interpretation should hold for cyclic polymer systems where the monomer density is slightly higher around the center of mass. This is supported by similarities observed between the properties of cyclic and branched polymers as compared to linear chain systems. The argument of enhanced density used to explain discrepancies between linear and cyclic polymers has been disputed by others who support rather the point of view that such discrepancies are due to

especially large cyclodextrins and cyclosophorans, in aqueous solution. The methods used to study these conformational properties, molecular modeling and small-angle-X-ray scattering (SAXS), will be described, and the application of these techniques to some specific examples will be presented with respect to cyclosophorans and cyclodextrins [22,23]. Complex formation of large cyclodexrins with iodine in aqueous solution will be focused on as examples of the functional properties of new cyclodextrins in comparison with common CDs [24]. Lastly we will attempt to interpret the functional properties of these molecules in terms of their conformation in solution.

4.2 Source and Nomenclature

Table 1 summarizes the structure and sources of cyclic glucans which consist of solely glucose units with different linkages. A large number of cyclic oligosaccharides which contain sugar units other than glucose are not listed here, but are described later in this chapter. The table also does not cover cyclic glucans which have been chemically synthesized. The reader is referred to an excellent review for these synthetic cyclic glucans [20].

Table1
Linkage types, sources, and degree of polymerization of cyclic glucans

Linkage type	Common name	Representative enzyme or bacterial species	dp
α-D-Glucans			
1→4	Cyclodextrin	CGTase, D-enzyme	6<
1→6	Cycloisomalto-Oligosaccharide	*Bacillus* sp. T-3040	7-9
1→3, 1→6	Alternan	Altanase	4
β-D-Glucans			
1→2	Cyclosophoran	*Agrobacterium, Rhizobium*	17-40
1→3	Cycloraminaran	*Rhizobium melilote* TY7	10
1→2, 1→6		*Xanthomomus campestris*	16
1→3, 1→6		*Bradyrhizobium japonicum*	11-13

Cyclodextrins (cycloamyloses, cyclomaltooligosaccharides)   were discovered in 1891 by Viliers, and their preparation was first described by Schardinger [1]. Thus, they are often also referred to as Schardinger dextrins. However, the term cycloamylose is now preferred for designating higher

homologs of CD, e.g. cyclodextrins which contain 17 to several hundred glucose residues [13,17,25]. However, in this article we use cyclodextrin or its abbreviated designation CD for all cyclic **(1→4)–α-D-glucans,** irrespective of the degree of polymerization. A complete and unanimous nomenclature has been proposed by Lichtenthaler and Immel [26,27]. Based on their suggestion, when the individual CD is shown, we use **CD$_n$** where n represents the degree of polymerization. Thus, **α-, β- and γ-cyclodextrins** are abbreviated **CD$_6$, CD$_7$** and **CD$_8$** rather than **α-CD, β-CD and γ-CD.** For the case of the recently synthesized **cyclo-α(1→4)-glucopentaosides** [28], the minimum size of cyclodextrin, this is referred to as **CD$_5$.**

The preparation of cyclodextrins has been improved to a considerable extent [29]. CGTase is produced by a large number of bacteria such as *Bacillus macerans, Bacillus circulans, Bacillus megaterium, Klebsiella pneumoniae,* and so on [3]. The **CD$_6$, CD$_7$, and CD$_8$** molecules are produced on an industrial scale and are commercially available. Genetic engineering has provided more active enzymes, and probably, in the future, these enzymes will be used extensively for industrial CD production [29, 30]. Recent improvements in the production of larger CDs by recombinant D-enzyme and amylomaltase from *Themus aquaticus* permit the production of larger amounts of larger CD [31].

All species from the family *Rhizobiaceae* have been shown to synthesize periplasmic cyclic **β-glucans** [18]. Cyclic **(1→2)-β-D-glucans,** which are produced by *Agrobacterium* and *Rhizobium* species, are also often referred to as cyclosophorose or cyclosophoran. Here cyclosophoran or the abbreviated designation CS will be used. The dp of CS isolated from culture broth is dependent on the bacterial strain [32], and typical dps range from 17 to 24 [33]. The largest molecular weight reported corresponds to dp 40 [34,35]. The large scale production of cyclosophorans has been also examined [36]. However, these products are not presently commercially available. Bundle et al. [37] reported that the mammalian pathogens *Brucella* spp. synthesize cyclosophorans essentially identical to those synthesized by members of the *Rhizobiaceae. Xanthomonas campestris* produces a cyclic hexadecaglucoside containing 15 **β-(1→2)-linkages** and one **α-(1→6)–linkage** [38].

Bradyrhizobium japonicum synthesizes cyclic **(1→3, 1→6)-β-glucans** composed of 11 to 13 glucosyl residues, rather than **(1→2)–β–glucans** [39]. Molecules with various proportions of **β-(1→3)** and **β-(1→6)** linkages have also been observed and usually these linkages are included in the main chain [18]. An exception is the cyclic decasaccharide(cyclohexakis-**(1→3)–β–D-**glucosyl) which has been isolated from a recombinant strain of a *Rhizobium melilote* TY7, a cyclic **(1→2)-β-glucan** mutant carrying a locus specifying **(1→3,1→6)** glucan syntheses from *Bradyrhizobium japonicum* USDA110 [40].

One of the residues of this molecule is substituted at its 6-position with **β-laminarabiose**.

Alternase from *Leuconostoc mesenteroides* NRRL B-1355 produces **(1→3, 1→6)-α-glucans,** known as alternan [41]. Cyclic **(1→6)-α-glucans** are produced from dextran by the enzymatic action of *Bacillus* species [42].

4.3 Sample isolation and molecular weight determination

In the laboratory, isolation of the individual compounds from mixtures of cyclic glucans is usually performed by HPLC. An example is shown in
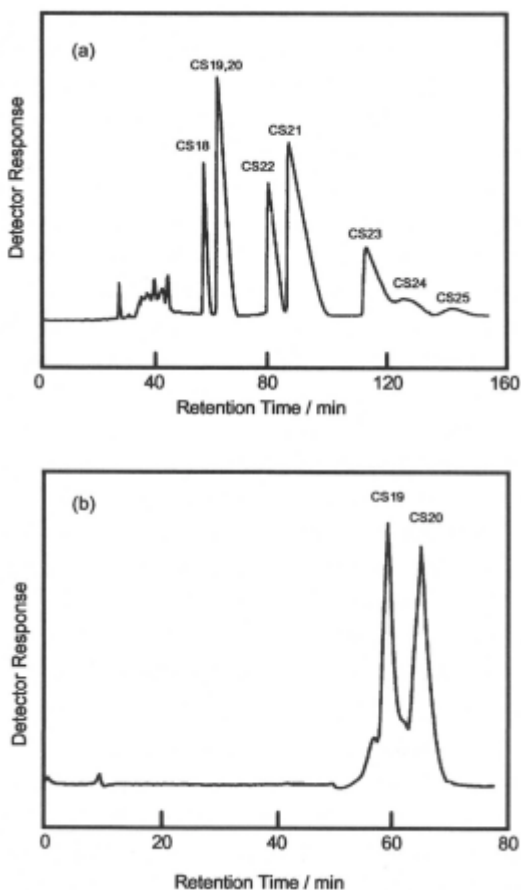
Figure 1 - Two step HPLC separation of cyclosophoran. (a) Preparative HPLC of a mixture of cyclosophrans(A-23-9) on an ODS column, (b)HPLC separation of **CS$_{19}$** and **CS $_{20}$** on an **NH$_2$-bonded** column [22].
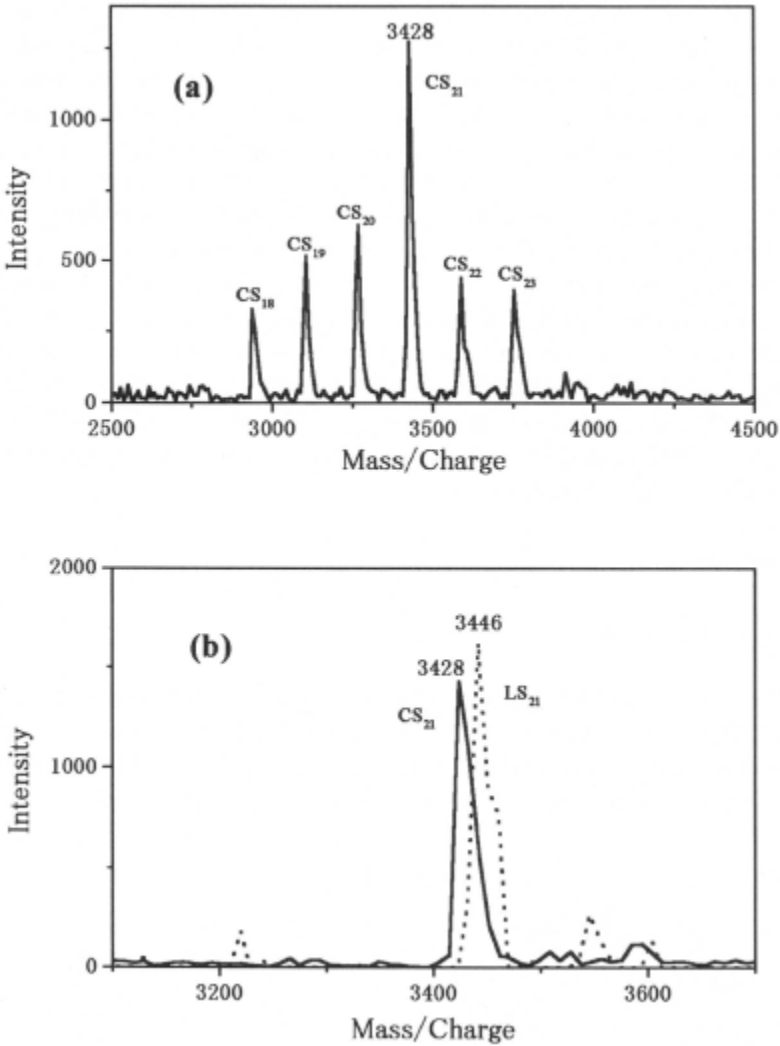
Figure 2 - MALD-TOF spectra of a CS mixture(a), an isolated CS$_{21}$ (b) and a linear sophoran LS$_{21}$. The samples were dissolved in 7:3 water-MeOH containing 100 mM 2,5-dihydroxybenzoic acid. Approximately 1 μL of this mixture was applied to a MALD probe and dried under vacuum. MALD-TOF spectra were recorded with a KOMPACT MALDI IV (Shimadzu/Kratos) spectrometer operating at 20 kV accelerating voltage.

Figure 1 [22]. A sample consisting of a mixture of cyclosophorans produced by *Rhizobium phaseoli* AHU1133 was first fractionated into seven cyclosophoran

peaks by HPLC on two sequentially connected ODS columns. Since **CS$_{19}$** and **CS$_{20}$** were not separated with the ODS columns, the fraction containing both **CS$_{19}$** and **CS$_{20}$** was further fractionated by HPLC using a Polyamine II column. Anomalies in the order of elution of the mixture of CS found in the ODS chromatogram indicate that glucans of certain ring sizes bind strongly to hydrophobic C-18 resins. It should be noted that CD mixtures, which are produced by the action of D-enzyme and CGTase on linear amylose, can be separated into each isolated CD up to 33 using an ODS column.

The molecular weights of cyclic oligosaccharides isolated from the mixture were determined by fast atom bombardment mass spectroscopy [43,44] and more recently by matrix-assisted laser-desorption time of flight spectroscopy (MALD-TOF) [13,23]. Figure 2 shows MALD-TOF spectra of a mixture of CS and an isolated CS showing **ions(M+Na)$^+$** from the CS species of the mixture and isolated CS. The figure also includes a spectrum of linear sophoran having a dp of **21(LS$_{21}$).**

4.4 Conformation

4.4.1 Crystal structures

Structural features of CDs have been addressed using data derived from X-ray crystallographic analysis of solid-state structures [17,45,46]. In a recent review, Saenger and collaborators examined the structures of the common cyclodextrins, as well as larger analogues, **CD$_{10}$, CD$_{14}$,** and **CD$_{26}$** [17].
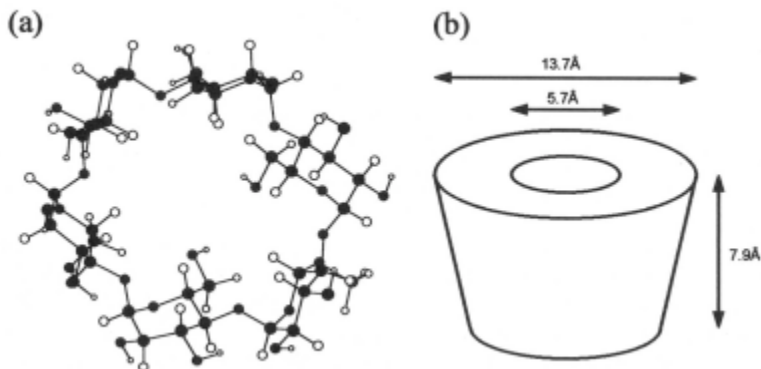
Figure 3- Structure of CD6(a) and its schematic representation(b).

Figure 3 shows the structure and schematic representation of **CD$_6$**. In which glucose units adopt $^4C_1$ chair conformation. As shown in the figure, **CD$_6$**

has a toroidal structure with a hydrophilic exterior and the inside is lined largely by H-3 and H-5 of the glucose rings and inter-unit oxygen atoms which together generate a hydrophobic environment. The diameters of the cavity of the common cyclodextrins are known to be, respectively, 4.7-5.3 Å for CD_6, 6.0-6.5 Å for CD_7, and 7.5-8.3 Å for CD_8. Thus, these CDs possess a hydrophobic central cavity suitable for the inclusion of a wide variety of organic compounds. Recent publications on the crystalline structure of larger cyclodextrins [15-17], especially, CD_{26} [17], is of interest and is related to main topics of this review article. The structure contains $(CD_{26})_2/78$ H_2O in the triclinic unit cell. As shown Figure 4, the CD_{26} molecule adopts the shape of a figure eight in which each half consists of two left-handed, single helical turns with six glucoses per repeat. At the "upper" and" lower" sides, the short helices are connected by two stretches of three glucoses containing one band flip each. The two short single helices contain channel-like cavities with a similar width as is found in CD_6 [47,48].

Sophisticated computer-aided visualization of molecular lipophilicity patterns of CD_6 [26, 49] and CD_{26} [50] provides information on the possible regions where guest molecules can interact. Figure 5 shows the MOLCAD-program [51] mediated color-coded projection [52] of the molecular lipophilicity patterns (MLPs) [53] onto the contact surfaces [54] of the solid-state structures of CD_6 [48] and CD_{26} [50]. The color-code applied ranges from dark blue for the most hydrophilic surface areas to full yellow, corresponding to the most hydrophobic regions. On the left, the solid-state structure of CD_6 is shown, and on the right the crystal geometry of CD_{26}; the upper models display the "front-side" of the closed surfaces, whereas in the bottom row the front half of the molecular surfaces is cut off and a ball-and-stick model inserted in order to visualize the molecular orientation and the "back-side" surface properties. The model of CD_6 displays the extensively hydrophilic (deep blue) front OH-2/OH-3 side of the torus (top left), whereas the half-opened surface (bottom left) provides a view onto the most hydrophobic surface areas around the primary OH-6 groups and the central cavity. For CD_{26}, the linked arrangement of the two six-fold, CD_6-analog helices is visualized. The anti-parallel alignment of the helices causes both the hydrophilic secondary OH-2/OH-3 groups of one helix, and the more hydrophobic CH_2OH side of the other helix to be visible in the top right model. In the center, the linking glucose units between the two helices are involved in the band-flips. In contrast to cyclodextrin, crystal structures for cyclosophorans have not yet been reported.
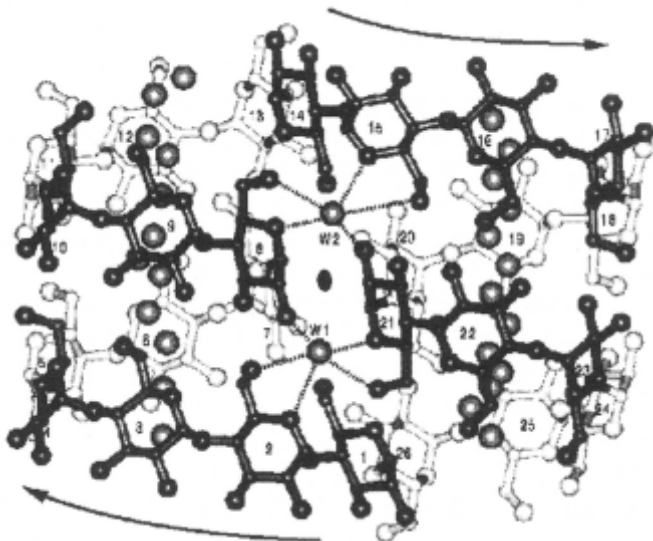
Figure 4 - Folding of the **CD₂₆** showing pseudo-2-fold rotation symmetry with the axis vertical to the plane of the paper at the oval.Glucoses are numbered 1 through. Band flips occur between glucose residues 13,14 and 26,1. The arrows indicate left-helical V-amylose turns with six glucoses per pitch. Hydrogen bonds are shown only for water(W1 and W2) [17].
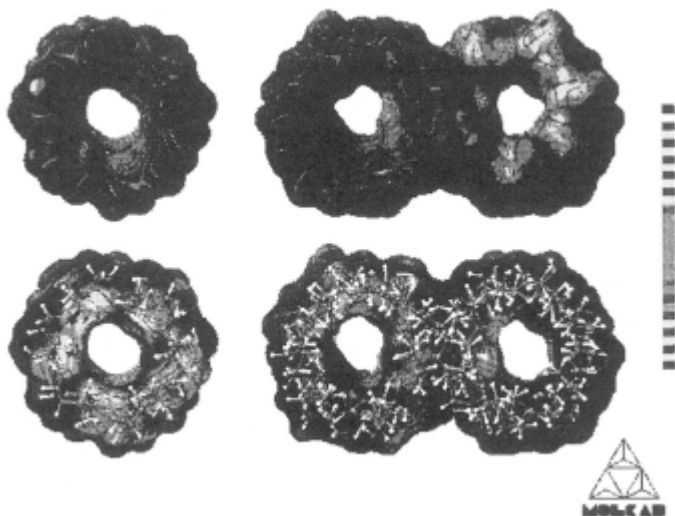
Figure 5 - MOLCAD-generated lipophilic surface of **CD₆(left)** and **CD₂₆(right)** provided from Immel and Lichtentarler [50].
(See also http://caramel.oc.Chemie.tu-darmstadt.de/~lemmi/molcad/Gallery.html for more examples and additional Information.)

4.4.2 Conformational energy map

The flexibility of a glucan chain is mainly the result of rotation about the bonds of the glycosidic linkages, since a pyranose ring is rather rigid [55]. Figure 6 shows a disaccharide unit of cyclosophoran, **2-O-β-glucopyranosyl-D-glucopyranose**. The conformation of this disaccharide unit is largely determined by non-bonded interactions between the two glucose residues. It is thus possible to represent all the conformations available for the disaccharide as a contour map in the space of the glycosidic torsion angles φ and ψ. Two examples of the conformational map for the disaccharide are shown in Figure 7, where the open areas are too high in energy to be of interest, due to steric repulsion [22,56]. Only van der Waals and electrostatic interactions between the two glucose residues of the disaccharide are considered. Although the fine structure of the contour depends on the energy function and geometry of the pyranose ring employed for the calculation, each energy map reported, as can be seen in Figure 7, showed that the preferred range of rotational angles for the glycosidic linkage is restricted within narrow limits.
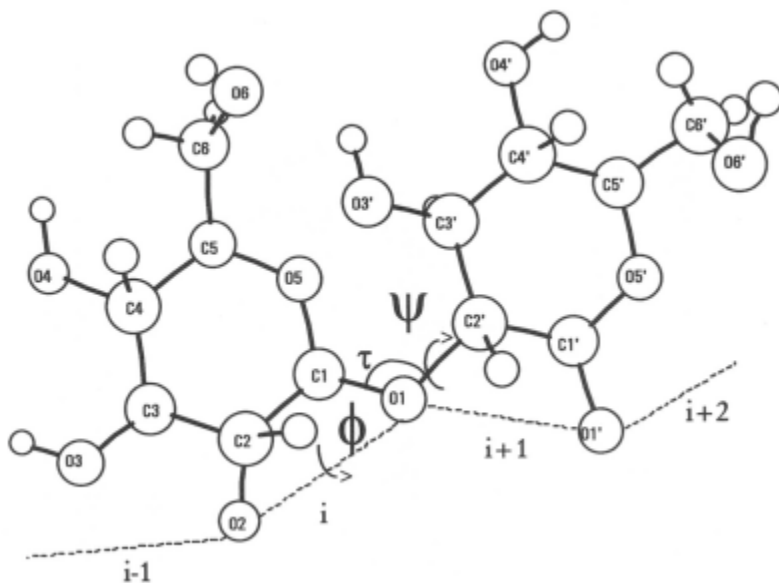
Figure 6-A dimeric skeletal segment of cyclosophoran, i.e., 2-Oβ-D-glucopyranosyl-D-glucopyranose. The two dihedral angel about the glucosidic linkage, φ and ψ, are defined as φ = θ[H-1,C-1, O-1, C-2'] and ψ = θ[C-1,O-1, C-2', H-2']. Virtual bonds i and i+1 are shown by broken lines.
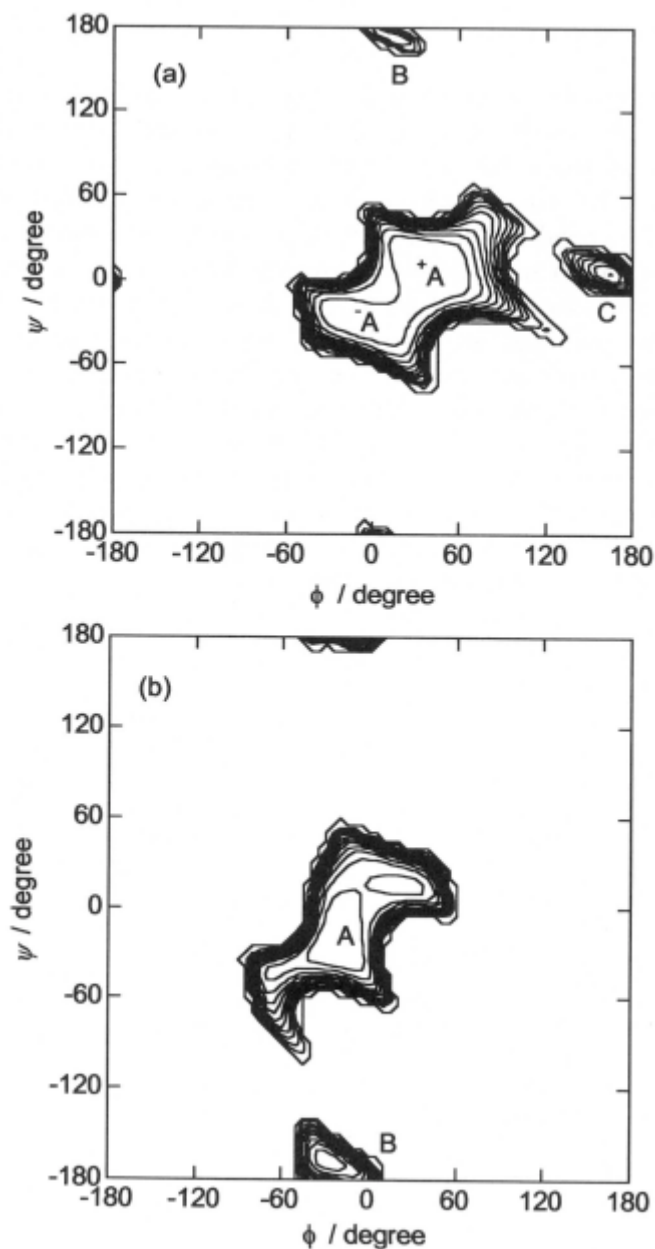
Figure 7 - Conformational energy maps for **2-O-β-D-glucopyranosyl-D-glucopyranose, β-sophorobiose** [22](a)and **4-O-α-D-glucopyranosyl-D-glucopyranosem, α-maltose** [56] (b). Contours are shown at Intervals of 1.0 kcal mol⁻¹for energies less than 10 kcal mol⁻¹.

It is also possible to include the flexibility of the sugar rings and rotational flexibility of the exocyclic -OH and **-CH₂OH** groups in the conformation analysis [57,58]. For comparison, a flexibility conformation map which was calculated by commercial molecular mechanics software (MM3) [59] is shown in Figure 8. It is clear that the attainable conformation areas in terms of the potential energy at each point specified by a pair of ϕ and ψ angles are much wider in the flexible map than in the rigid map shown in Figure 7-b. These conformational maps are useful in searching for the solution and crystalline conformation of related cyclic glucans. Crystalline structures of common CDs show that all the ϕ and ψ angles are located in region A. In contrast to these small CDs, two pairs of ϕ and ψ for the glucosidic linkages between 13 and 14, and 26 and 1 of **CD₂₆** in crystalline form are located in region B of the conformation map [17]. However, it should be noted that in solution the rotational angles can fluctuate within an allowed area.
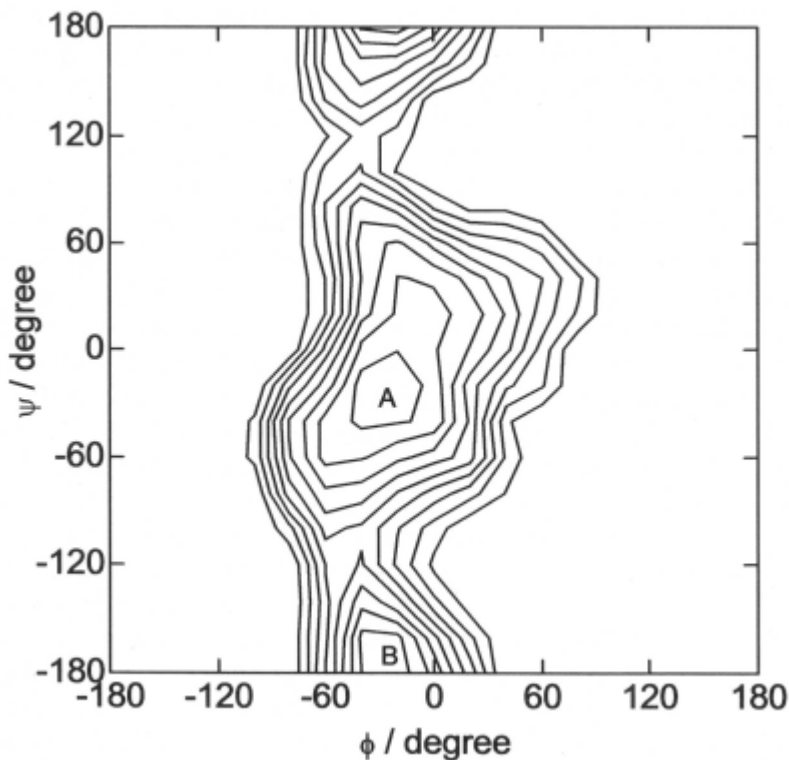
Figure 8 - MM3-generated relaxed-residue steric energy maps of **α-maltose.** Contours are shown at Intervals of 1.0 kcal **mol⁻¹** for energies less than 10 kcal **mol⁻¹.**

4.4.3 Molecular modeling based on Monte Carlo methods

Monte Carlo methods have been used for the simulation of solution conformation of linear and cyclic glucans [22,23,56,60-63]. Glucan chains were generated in conformations consistent with the disaccharide conformational energy map by the Monte Carlo methods. Here the glucose residue is assumed to be rigid and is replaced with a virtual bond connecting the neighboring oxygen atoms of the glycosidic linkages. It should be noted that the virtual bond for the **β-(1→2)-linkage** is much shorter than that of the **α-(1→4)-linkage.** The energy map for **α-maltose,** shown in Figure 7-b, has been refined so as to yield chain dimensions including the mean square end-to-end distance, the mean square radius of gyration [64], and the scattering function [56], as observed for malto-oligosaccharides and amylose in solution. The occurrence probability for a given ϕ and ψ pair was obtained by normalizing the Boltzmann factor associated with each pair by the sum of all such Boltzmann factors, thus normalizing the energy with respect to the total energy over the two-dimensional energy map. The normalized radial distribution function $W_x(r)$ of the end-to-end distance r was evaluated from 100,000 chains of length x by counting the number of chains whose end-to-end distances were found to be in the interval dr between r and $r + dr$.

Figure 9 shows the dp-dependence of the probability that the terminal units of a simulated **(1→4)–α-glucan** chain approach one another within a certain distance (4 Å). The highest probability is seen in the dp range from six to eight for a **(1→4)–α-glucan** chain. This is clearly related to the likelihood that the polymer will exist in a cyclic form. Rings which contain 6 - 8 sugar units predominate in the distribution of common CDs prepared from starch. It was shown that a simulated **(1→2)-β–glucan** chain has the highest probability at dp ranging from 15 to 40 [22]. This result is evidently correlated with the occurrence in nature of cyclosophorans containing from 17 to 40 glucose residues.

Among the generated chains in the Monte Carlo sample for a given dp, those with an end-to-end distance less than 1.5 Å were considered to be examples of cyclic glucans and a representative model chain among these was selected for examination, based on agreement of the calculated and observed R_G. Further refinements have been performed, in order to connect non-reducing and reducing ends by examining the orientation of the two ends. After connection, molecular mechanics minimization is carried out for the models. Figure 10 represents examples of CD_{21} and CD_{26} generated by the method described above.
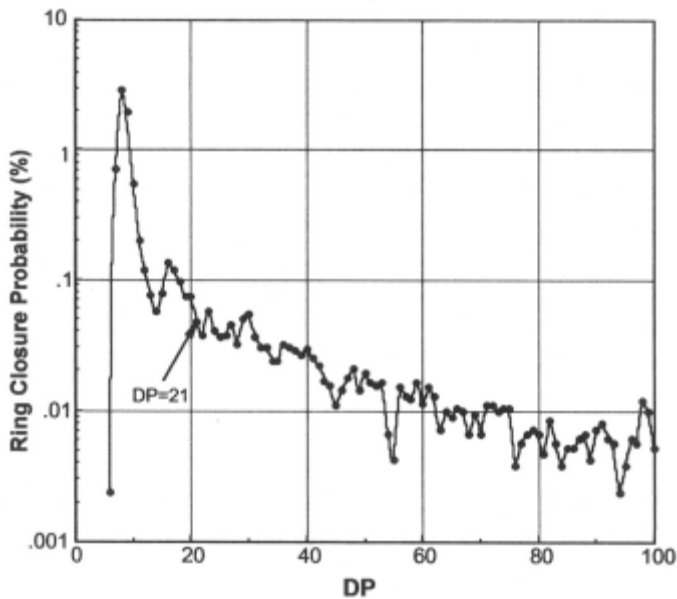
Figure 9 - The probability that terminal segments of a amylosic chain of dp segments will approach one another within a distance of 4 Å.

CD$_{21}$ CD$_{26}$
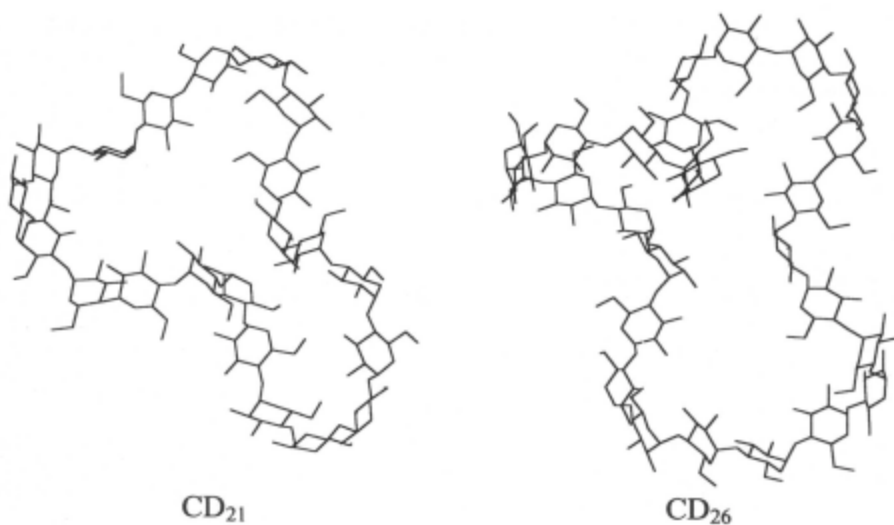
Figure 10 - Representative cycloamylose chains, CD$_{21}$ and CD$_{26}$ generated by Monte Calro methods. Hydrogen atoms are not shown.

4.4.4 Molecular modeling based on a wire model

Shimada constructed several helical models for cyclic amylose based on a wire model [25]. For a single helical model he formed a single helical pathway of a radius r and k turns deformed around a large circle of radius R, assuming $2\pi R = nD_z$, where D_z is the axial rise per residue and $n=dp$. Having established the positions of the oxygens, the rigid glucose units were then positioned such that the V-shape of the C-O-C glycosidic linkage was aligned with the curvature of the wire. A slight mismatch in the chain ends was compensated by distributing this distance equally into each unit.

For the double helical model we assumed two types of anti-parallel double helices:one with a radius 5.1 Å, a pitch 18.6 Å and eight residues per turn, while the other has a radius 2.989 Å, a pitch 21.2 Å and six residues per turn [65,66]. A simple continuous elastic wire model was introduced to assist the atomic modeling of foldbacks. This model is assumed to be composed of a regular arrangement of glycosidic oxygens along a smoothly varying elastic string. The local elastic energy reaches a minimum in the regular helical form with the above radius and pitch. Glucose units were placed as described above. The number of glucose residues in the terminal loops was varied at around eight. Table 2 summarizes the geometrical parameters used for single and double helical models of CD_{21}. The strain in the structures thus built was removed by energy minimization *in vacuo* for which a simple distance-dependent dielectric constant was used to mimic the electrostatic shielding of the surrounding water.

Table 2
Geometrical parameters for generating various initial model structures for CD_{21}[23]

Code	Form	Radius (Å)	D_z (Å/res)	Loop size
a	3-turn single	2.971	3.543	
b	3-turn single	3.658	2.971	
c	3-turn single	4.05	2.77	
d	3-turn single	4.6	2.6	
e	2-turn single	5.1	3.3	
f	2-turn single	6.0492	2.718	
g	double	5.185	2.33	8 + 9
h	double	2.989	3.43	8 + 7
i	double	5.185	2.33	8 + 7

b (R_G=11.6Å)   e (R_G=13.6Å)

h (R_G=11.7Å)   i (R_G=10.2Å)
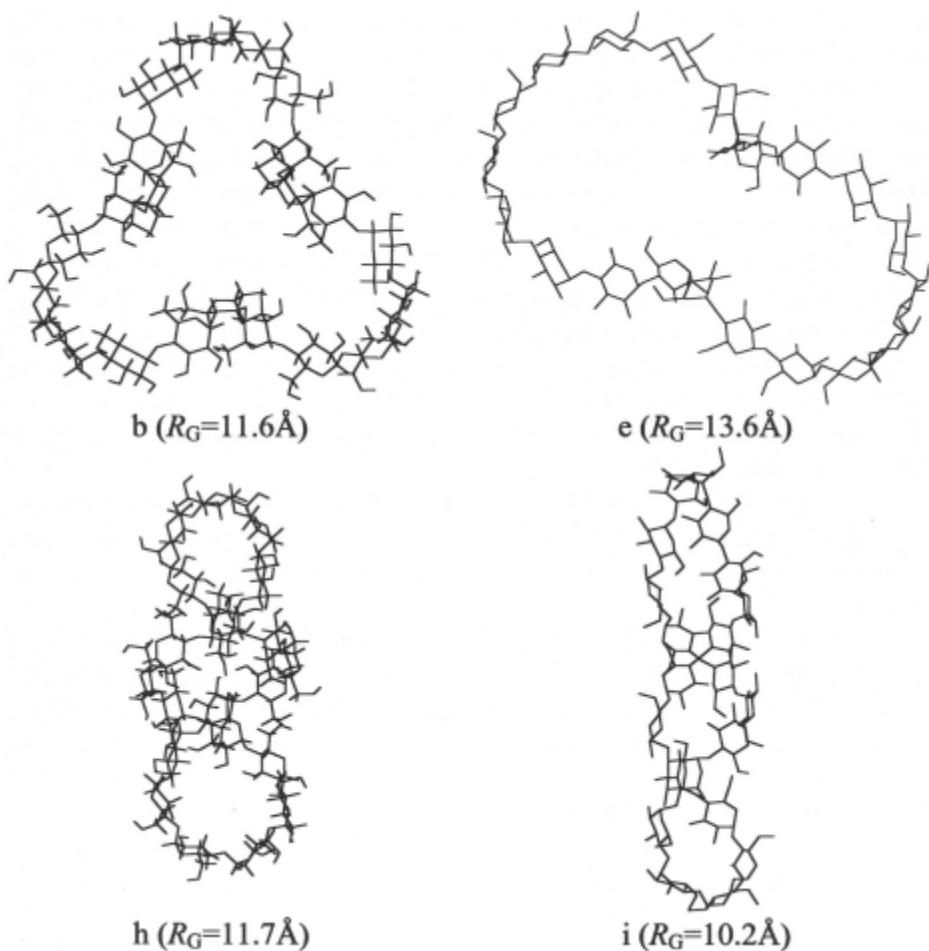
Figure 11 - Conformations b, e, h, and i generated with the corresponding parameter codes given in Table 2.

4.4.5 NMR study on cyclic glucans

Previous conformational analysis of the cyclosophorans [67-72] by molecular modeling and NMR has been somewhat inconclusive [19]. The structural model for **CS$_{17}$** proposed by Serrano et al. [68] involves an alternation of the low energy conformation A (low energy region in the conformation map in Figure 7-a with an energetically unfavorable conformation. This model yields a rather symmetric macrocycle with an internal diameter of about 15 Å. Metropolis Monte Carlo investigations [70] suggest a relatively symmetric structure with a small polar cavity for **CS$_{18}$** to

CS$_{24}$. In contrast to these symmetric geometry models, Andre et al. [72] reported that MM3 molecular mechanics calculations predict a non-symmetric conformer with a small cavity of 3.7 Å in diameter as the lowest energy form. Fair agreement was found between NMR experimental data and the corresponding average values predicted by molecular modeling [72]. York [70] suggested that ring closure in these cyclic glucans could be achieved by interrupting a perfectly alternating **$^+$A$^-$A** pattern of linkage conformations(**$^+$A,** and $^-$A regions are given in energy map of Figure 7-a) with two "frame shifts" at which the alternating pattern is broken. A feature common to all of these models is the requirement, at any given instant in time, that the ϕ and ψ values for the glycosidic linkage must vary from glucose residue to residue. Only six ^{13}C and seven ^{1}H NMR peaks are observed for CS in aqueous solution, indicating that the microenviroments of individual glucosidic residues interconvert on the NMR time scale.

Simple NMR spectra for unmodified CDs have also been reported [16,73-75]. Increasing the macrocyclic size mainly affects signals of the Cl and C4 atoms, while resonances of the other carbons are only marginally influenced

Although the NMR method has been widely employed for studies of the conformation and mobility of cyclic glucans [76], the method can generally only provide information about the time average geometry of molecules which undergo rapid conformational interconversion.

4.5 SAXS study on cyclic glucans

4.5.1 Radii of gyration

In this section, the advantages of scattering methods for the study of cyclic glucans which contain only one type of glycosidic linkage will be presented [22,23,77]. The method consists of small angle X-ray scattering measurements using a synchrotron radiation source in conjunction with molecular modeling. Small angle X-ray scattering provides structural information of the order of a few angstroms to a few thousand angstroms [78]. The primary parameter obtained for the case of cyclic oligosaccharides is the radius of gyration **R_G.**

The excess scattering intensity $I(q)$ was evaluated by subtracting the scattering intensity of the solvent from that of the solution. The $I(q)$ at small scattering angles can be approximated according to Guinier [79] as

$$I(q) \propto exp\ (-R_G^2 q^2/3) \qquad\qquad (1)$$

with a single parameter R_G defined as the radius of gyration of a solute molecule, where $q = (4\pi/\lambda)\sin(q/2)$ is the magnitude of the scattering vector, while q and λ represent the scattering angle and wavelength of the incident X-rays respectively. Equation (1) implies that the radius of gyration of compact molecules is determined from the initial slope of $I(q)$ plotted against q^2 which is referred to as a Guilder plot in this review. Figure 12-a shows Guinier plots
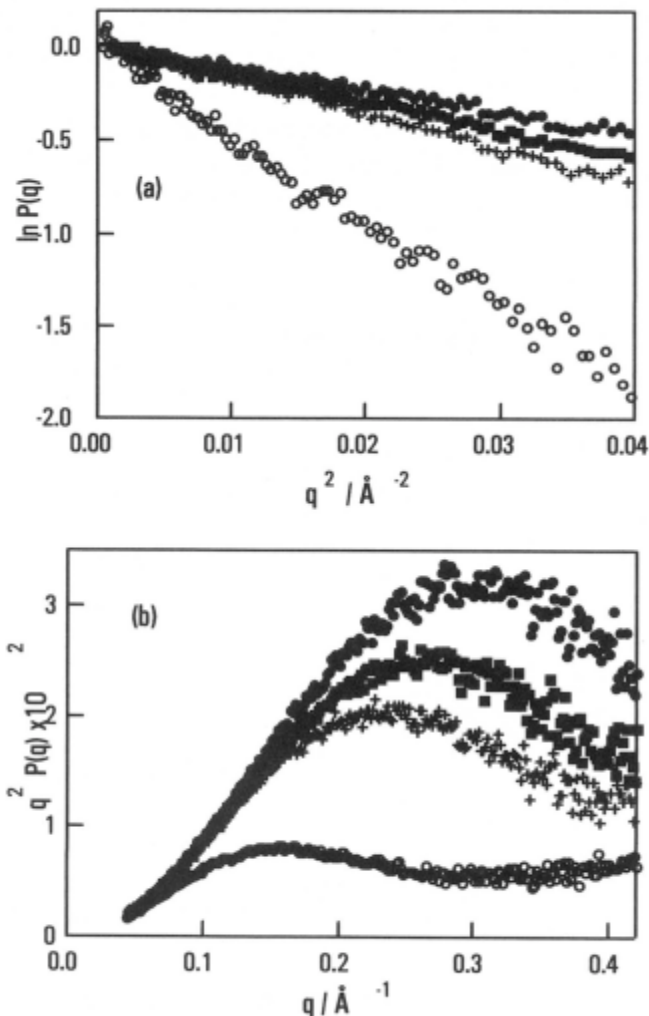
Figure 12 - SAXS profiles of cyclodeitrins in terms of (a) Guinier plots[In$P(q)$ versus q^2 and (b) Kratky plots[$q^2P(q)$ versus q]; $CD_6(\bullet)$, $CD_7(\blacksquare)$, $CD_8(+)$, and $CD_{21}(O)$.

for CD_6, CD_7, and CD_{21} in water. The plots are represented using the particle scattering function $P(q)$ thus allowing all the data to be compared in the same figure. The $P(q)$, is defined by $P(q) = I(q) / I(0)$, where $I(q)$ is the scattered intensity at scattering vector q and $I(0)$ is the corresponding intensity extrapolated to $q=0$. The radius of gyration R_G was evaluated by extrapolating to $c=0$ for different glucan concentrations. However, it was found that the dependence of R_G on concentration is not large. For example, the apparent R_G of CD_{21} was estimated to be 11.5, 11.4, and 11.3 Å for the polymer concentrations of 3.1, 9.3, and 18.7 mg/mL, respectively, indicating that R_G is virtually independent of CD concentration.

Table 3 summarizes the R_G values for CS and CD together with corresponding linear glucans. Compared to the same DP, the value of R_G for CD_{21} is larger than CS_{21} by 1.9 Å. As predicted from theory, CD and CS has a smaller R_G than corresponding linear glucans.

Table 3
R_G for cyclic and linear oligosaccharides determined by SAXS[a]

Dp	R_G (Å)			
	CS	LS	CD	LD
6	-	-	6.0	6.7
7	-	-	6.7	7.3
8	-	-	7.3	8.1
17	7.8	-	-	-
18	8.1	-	-	-
19	8.5	11.1	-	-
20	8.3	-	-	-
21	8.6	12.0	11.5	-
22	8.4	-	-	-
23	8.9	-	-	-
24	10.6	-	-	-
26	-	-	19.6	-

[a] Measured in water at 25 °C.

4.5.2 Experimental and theoretical particle scattering function

Attempts were made to construct a molecular model which yields a particle-scattering factor similar to that observed by SAXS. The molecular conformations of CA and CS are comparably discussed from the results of the molecular model and the SAXS observation [22,23].

The scattering profile $I(q)$ was calculated as a function of the magnitude of the scattering vector q from the atomic coordinates of the molecular model chains according to the Debye formula [80]:

$$I(q) = \sum_{i=1}^{n} f_i^2 g_i^2(q) + 2\sum_{i=1}^{n-1} \sum_{j=i+1}^{n} f_i f_j g_i(q) g_j(q) \frac{\sin d_{ij} q}{d_{ij} q} \qquad (2)$$

where, f_i is an atomic scattering factor, and d_{ij} is the distance between the ith and jth atoms, and 1 and q are the wavelength of the incident beam and the scattering angle, respectively. The form factor for a single atom $g_i(q)$ is assumed to be given by the form factor of a sphere which possesses a radius equivalent to the van der Waals radius of the ith atom as

$$g_i(q) = \frac{3[\sin(R_i q) - (R_i q)\cos(R_i q)]}{(R_i q)^3} \qquad (3)$$

with R_i being the van der Waals radius of the ith atom. The radii of carbon and oxygen atoms are taken to be 1.67 Å and 1.50 Å, respectively. The simulated scattering profiles are directly compared with those observed by SAXS by normalizing with respect to the scattered intensity at the zero angle.

Comparison of measured and theoretical $P(q)$ values was made in plots of $q^2 P(q)$ vs. q (Kracky plot), since this plot is known to show marked differences between linear and cyclic species which are of the same physical dimensions [81]. Figure 13 shows a Kracky plot for a CS_{21} and for CD_{21}. For comparison, SAXS data for the linear $(1 \rightarrow 2)-\beta-D-glucan(LS21)$ are also shown.

Figure 14 shows that reasonable agreement exists for the simulated scattering profile for CS_{21} with that observed by SAXS, where the scattering profiles calculated from two elementary models, a rigid ring [81] and flexible Gaussian ring [82,83], are shown for comparison. The observed SAXS profiles of CS_{21} exhibit a degree of chain stiffness in comparison with the profiles calculated from the flexible Gaussian ring, where the conformational freedom is suppressed by end to end linking. The deviation from the observed profile at $u(\equiv q R_G) > 3$ can be reduced by introducing a smaller apparent scattering unit in Eq.(3), but its physical significance cannot be explained precisely at this stage. It should be noted that similar deviations at large q have been observed for the simulation of other linear glucans [56,63].
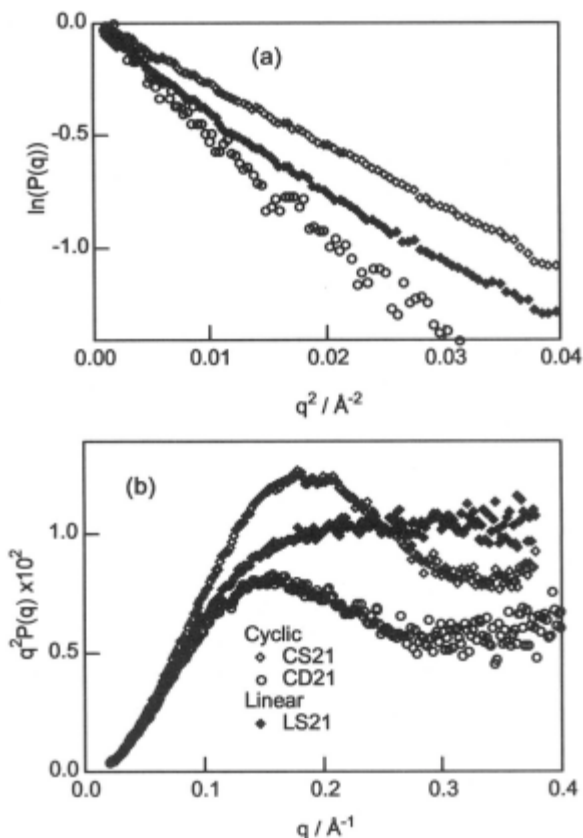
Figure 13 – SAXS data for CD21, CS21, and for the linear sophoran with dp 21(LS21). (a) A plot of $qP(q)$ vs. q. (b) A plot of $q2P(q)$ vs. q.

Typical conformations of the simulated cyclic CS_{17} and CS_{21} chains are shown in Figure 15. The shape is an irregular doughnut-like ring for both molecules. Since the β-(1→2) linkage produces a rather thick cylindrical conformation, the cavity in a cyclosophoran chain may be too small to form inclusion complexes with relatively large molecules. In fact, the diameter of the ring annulus for CS_{21} is only about 4-5 Å. All the glycosidic linkage torsion angles are found within region A of the conformational energy map of Figure 7-a. Thirteen of 20 linkages are in region ^+A, and seven are in region *A. No special mode of arranging ^+A and ^-A can be observed. The present model is very similar to Andre's model [72] in terms of the asymmetrical nature of the molecules, i.e; a small cavity size, and the distribution of dihedral angles of glucosidic linkage. It should be noted that R_G calculated from the
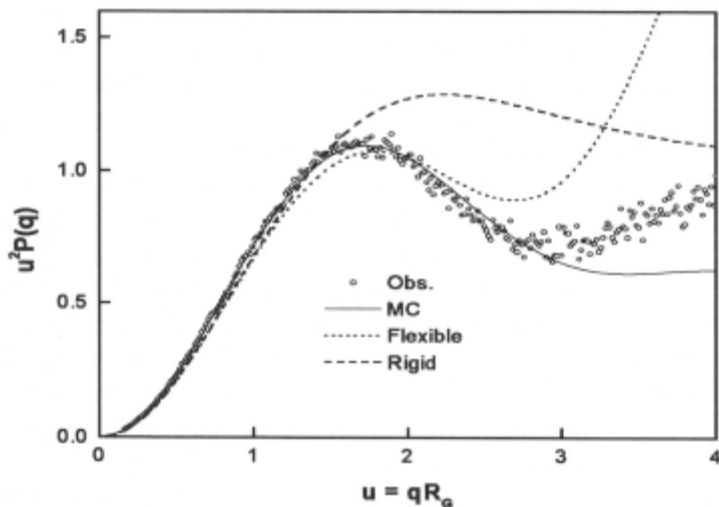
Figure 14 - A normalized Kratky plot of SAXS for CS21 along with curves calculated for the Monte Carlo chains, the rigid ring and the flexible ring, respectively. Open circles represent the observed data.
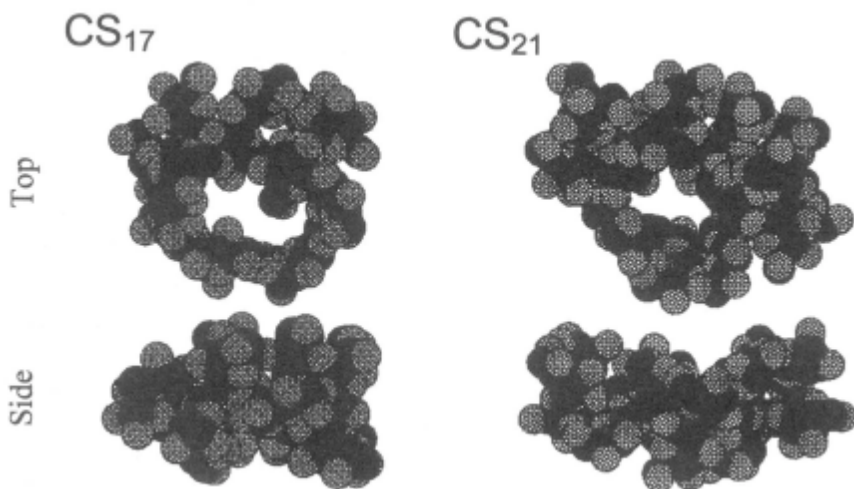
Figure 15 - Space filling models of "cyclosophoran" based on Monte Carlo simulation: CS$_{17}$ (left) and CS$_{21}$ (right). The model chains have an end-to-end distance of less than 1.5 Å. Hydrogen atoms are not shown [22].

atomic coordinates of the Serrano model [68] for CS_{17} is 9.4 Å while the measured R_G for this cyclosophoran is just 7.8 Å. We should also note that the evaluation of various models proposed previously in the light of the SAXS data may be an appropriate topic for further research.

Similar simulation for cyclodextrins is shown in Figure 16. "Pseudo-cyclic glucans" from Monte Carlo generated linear $(1\rightarrow4)$-α-D-glucan chains whose ends are separated by less than 1.5 Å were collected, and a representative model chain was selected from the collection of pseudo-cyclic glucans based on the consistency of the calculated and observed R_G. It can be seen that the scattering profile calculated from the atomic coordinate is in reasonable agreement with that observed by SAXS. The figure also includes the scattering profile for CD_{21} model constructed from pseudo-cyclic model.

The experimental SAXS profile is further compared with those calculated from several models derived from the wire model mentioned above. Among the models shown in Figure 12, the most satisfactory result is obtained from a three-turn single helical chain (model b). The two double helix models (h and i) yield less satisfactory results with respect to the scattering profile (Figure 17). Although the radii of gyration evaluated from the double helix chains are in good agreement with the observed values by SAXS, the deviation in scattering profile becomes apparent, even at $q = 0.1$ Å^{-1}.
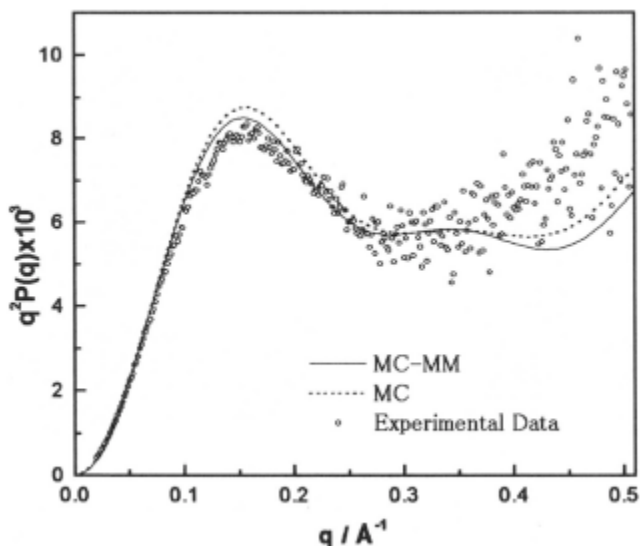
Figure 16 - Kratky plots of SAXS experimental data along with theoretical scattering profiles calculated from a pseudo cyclic chain(MC), and from a cyclic chain constructed from the pseudo cyclic chain using molecuar mechanics(MC-MM).
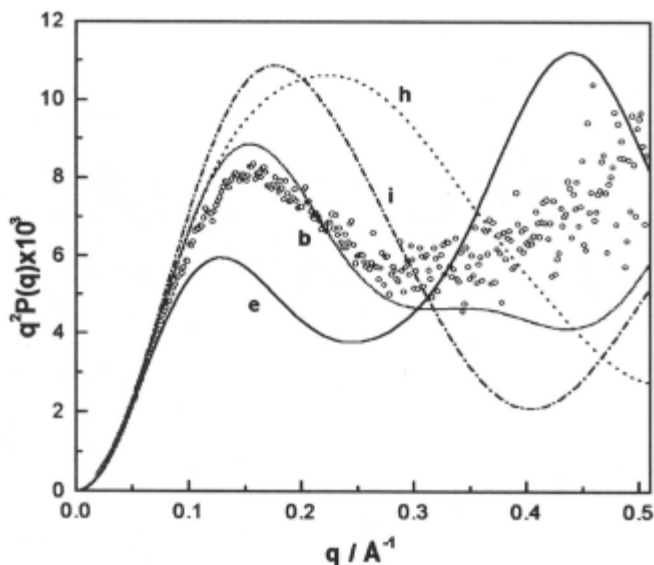
Figure 17 - Scattering profiles of some molecular models(b, e, h, and I). This figure includes the experimental profiles (o) [23].

4.5.3 SAXS and molecular dynamics simulation

Molecular dynamics simulations of CD_{21} were carried out as previously described [25,84]. A CD_{21} molecule was immersed in a large water sphere, having a radius of about 25 Å (1999 water molecules), and simulations were carried out for at least 100 ps with a time step of 2fs at 300K. The results beyond 100 ps were used for the calculation of the scattering function. All bond lengths were constrained by applying the SHAKE procedure with a tolerance of 10^{-10} [85]. GROMOS parameters [86] and TIP3P water model [87] were used and the temperature was controlled by the Nose-Hoover scheme [88,89]. Thre escape of water molecules from the sphere was prevented by applying a weak central force beyond 1.5 Å separation [25]. For each conformation shown in Figure 13, for the best-fit model b, the simulation was further extended to 400 ps. Figure 18 shows the scattering profiles between 100 to 400 ps at 30 ps intervals. It can be seen that the scattering profile fluctuates, reflecting a conformational fluctuation of the molecule with time. During this period, R_G fluctuates in the range of 0.7 Å around its mean. The scattering profile of an initial regular structure deformed slightly with time, as seen from Figure 17 (curve b) and Figure 18. This slight deformation may be as a
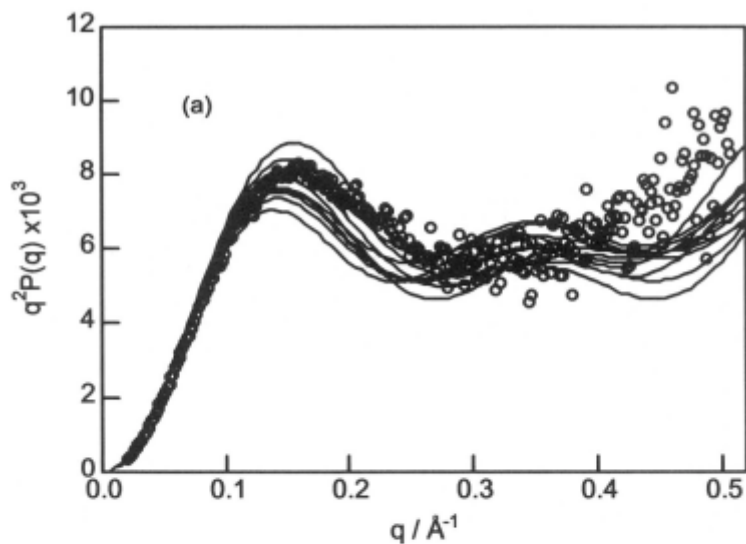
Figure 18 - **Superposition of the scattering profiles calculated for 12 consecutive 100,130, 160, 180, 190, 220, 250, 280, 310, 340, 370, 400 ps atomic coordinate sets from the dynamic model of CD$_{21}$ (model b), whose superimposed snapshots are shown in (b)[23][50].**
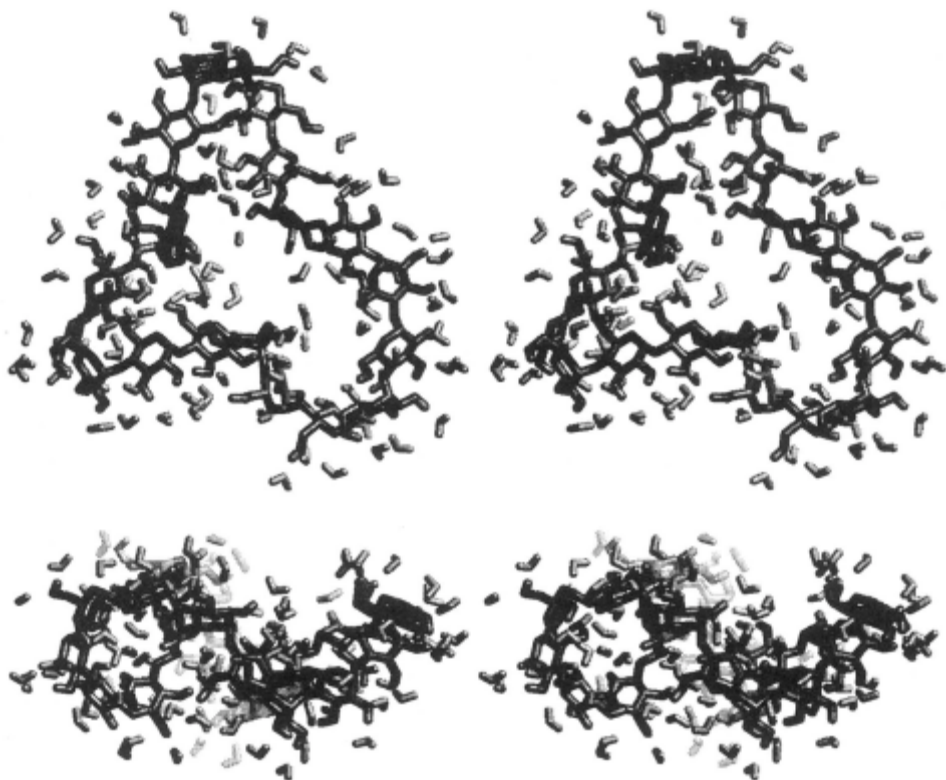
Figure 19 - Stereoview of the snapshot of CD$_{21}$ with hydrogen-bonded water molecules. This view was obtained by a 180 ps molecular dynamic simulation in water at 300 K Right and left views are separated by 36 Å along the horizontal direction [23].

reflection of the process of randomization of the regular helical conformation. However it is important to note that the essential feature of the starting scattering profile is maintained during the simulation.

One may wonder whether the scattering profile of the double-helical models might approach the observed profile by simulation. However, each double-helical model shrinks considerably by simulation, decreasing its R_G by about 1-2 Å. As a result, the agreement became even worse than that with the starting conformation with respect to both R_G and the scattering profile. It may be helpful to note a general tendency that the first peak of the scattering profile is more enhanced with decreasing R_G.

Figure 19 shows a CD$_{21}$ molecule where water molecules are incorporated and hydrogen bonding is introduced. Here water molecules are regarded as being hydrogen-bonded, provided the following three conditions are satisfied: (i) the donor-acceptor distance is smaller than 3.4 Å, (ii) the

hydrogen-acceptor distance is smaller than 2.4 Å, and (iii) the donor-H-acceptor angle is larger than 150 deg [90]. The number of such water molecules is about 100 (96 for this snapshot), indicating that approximately 4.6 water-glucose hydrogen bonds are formed per glucose unit. Intramolecular hydrogen bonds were also observed for about 30 % of 21 consecutive O-2 and O-3'pairs. Its frequency is intermediate between simulated results for cyclodextrins (nearly 100%) [91] and maltose (3%) [92]. Two to four water molecules were observed in the inner cavity, although this determination is somewhat arbitrary for this molecule.

4.6 Complex formation of large cyclodextrins with guest molecules

One of the remarkable properties of typical cyclodextrins is their ability to include small molecules within their cyclic structure to form inclusion compounds. The types of materials which form inclusion complexes are numerous, ranging from iodine to aliphatic and aromatic acids, esters and many other aromatic compounds, in which the aromatic ring lies within the cyclic structure and substituents interact with the carbohydrate hydroxyl groups via hydrogen bonding. Numerous crystal structures of CD inclusion compounds have been determined and have been summarized in two reviews [93] [46]. In addition, all of the thermodynamic data for complex formation involving CD_6, CD_7, and CD_8 with a wide variety of compounds can be found in a table of a recent review written by Rekharsky and Inoue [94]. These data are current as of October, 1997.

In contrast to CD_{6-8}, only a few papers on inclusion complexes of large-ringed CDs has been published [95-97], and these are reviewed in this article. These large CDs have the potential to function as host molecules for a variety of organic reagents and iodine in a manner which is different from common cyclodextrins, since the large CDs may have a cavity geometry which is different from that of CD_{6-8}. CD_9 was found to have a significant effect on the solubility of digitoxin and spironolactone which have a steroidal framework, suggesting that inclusion complex formation occurs with these drugs [95]. Most recently, a water-soluble complex of a fullerene C_{70} with CD_9 which had higher aqueous solubility than that of the complex between C_{70} and CD_8 was reported [97]. Using capillary electrophoresis, the binding constants of inclusion complexes formed with CD_9 to CD_{13} have been determined [96]. Although the binding constant is dependent on the type of guest molecules, CD_9 and CD_{10} are the weakest complex formers. The complex forming ability of CD_{10} to CD_{13} increased with increasing size of the ring structure and CD_{13} displayed inclusion complex formation constants comparable to those of CD_8.

What happens to theCD's inclusion ability if their dp becomes larger than 20? An answer to this question will be presented here to demonstrate the interaction of iodine ions with CD_{26}. As already mentioned before, if the dp is sufficient to allow the molecule to behave as a flexible chain, the local conformation may be similar to that of a long linear amylose chain. In this review, we describe complex formation of these large CDs with iodine in aqueous solution as studied by isothermal titration calorimetry [24].

We emphasize here that isothermal titration calorimetry, in which the affinity constant and binding entalphy are directly and simultaneously determined by using the data at a constant temperature, has considerable advantages over other methods, in which thermodynamic quantities are determined from the vant Hoff equation, assuming an invariant heat capacity over the temperature range employed [94,98]. The titration calorimetry described here was performed with an MCS titration microcalorimeter (Micro Cal., Inc., MA) at the constant temperature of 20 °C. The calorimeter has two cells, a reaction cell and reference cell, each of which is approximately 1.3 mL in volume. An aqueous solution containing I_2 and KI is injected into the reaction cell from a syringe which simultaneously functions as a stirrer. 35-7µL injections, spaced at 270 sec intervals are used for CD_{26}, and 25-10 µL injections for CD_6. Figure 20-a shows heat signals for CD_6 and CD_{26} titrated with the iodine solutions. Manufacturer-supplied software (ORIGIN, MicroCal, Inc) is used for the integration of heat signals, and nonlinear regression analysis of the data. Figure 20-b shows the plotted results for CD_6 and CD_{26}. The titration curve for CD_6 is consistent with a 1:1 complex. Association constants of $1.45 \pm 0.02 \times 10^5 \, M^{-1}$, and enthalpy of binding of -28.2 ± 0.04 kJ mol^{-1} were obtained for the CD_6-iodine system. In contrast to the CD_6-iodine system, the titration curves obtained for CD_{26} with iodine cannot be analyzed by a model based on a single set of identical sites, but, rather, by a model assuming 1 : 2 complex formation with identical interacting sites. For the two interacting but identical sites, the binding constants K_1 and K_2, and the binding enthalpies ΔH_1 and ΔH_2 are defined relative to the progress of saturation. The K_1 and K_2 for CD_{26} are determined to be $3.29 \pm 0.05 \times 10^3 \, M^{-1}$ and $16.4 \pm 0.16 \times 10^3 \, M^{-1}$, respectively. The ΔH_1 and ΔH_2 are -13.0 ± 0.54 and -136.4 ± 0.67 kJ mol^{-1}, respectively. The values of $T\Delta S_2$ for CD_{26} is calculated to be 112.8 $kJmol^{-1}$. Thus, "enthalpy-entropy compensations" [99] are observed for the system. The enthalpy-entropy compensation signifies that changes in free energy are much smaller in magnitude than the corresponding changes in enthalpy and entropy. A similar enthalpy-entropy compensation was obtained, not only for common CDs [94], but also protein-ligand interactions such as the Fab of an antibody and the binding of the epitope [98]. This phenomena have
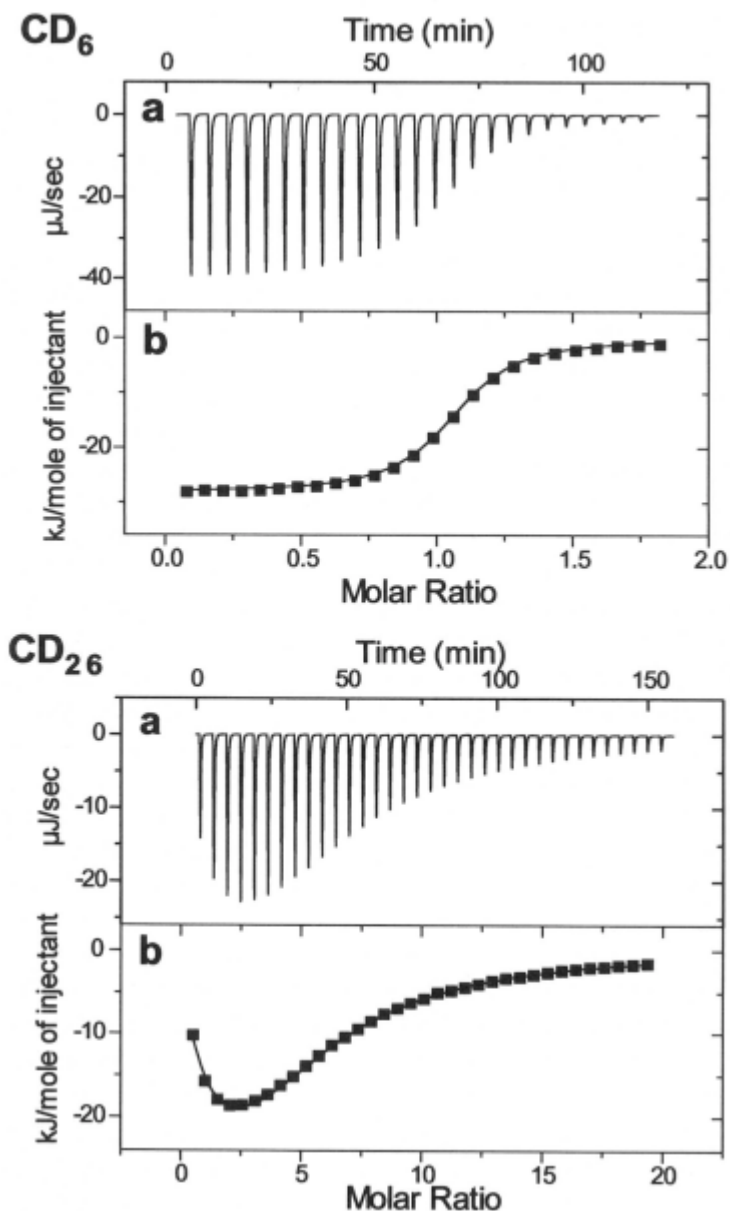
Figure 20 - Experimental data for titrations of 5 mM I_2 containing 200 mM Kl Into 0.6 mM CD_6 (upper panel) and 0.05 mM CD_{26} (lower panel) in aqueous solution containing 200 mM KI solution. CD_6: 25-10 μL injections, iodine solution at 4.5 min intervals. CD_{26}: 35-7 μL injections of iodine solution at 4.5 min intervals. (b): data points obtained by integration of injection peaks, and the titration curve obtained by fitting the data points.

been interpreted in terms of release of structural water molecules from the interacting surfaces and the formation of weaker hydrogen bonds in bulk water. The magnitudes of the enthalpy and entropy changes for this process are roughly equal. However, the entropy term should contain other contributions, such as a decrease in conformational flexibility of the CD chain. The large values of $-T\Delta S_2$ obtained for CD_{26} could be attributed to a large decrease in conformational flexibility of the CD which accompanies the complex formation [100]. The thermodynamic data obtained could be interpreted in terms of the crystalline structure of CD_{26} in Figure 4. CD_{26} has two cavities and each could include an iodine ion, indicating a 1:2 complex formation of CD_{26} and iodine ions. However, our preliminary result derived from SAXS data on an aqueous solution of CD_{26} shows that solution conformation cannot be simulated by the solid state structure, but rather by a circularized single helical structure with a somewhat larger R_G, as shown in Figure 10. The folding of CD_{26} from a single helical structure to a more compact structure, such as the crystalline structure shown in Figure 4 leads to entropy loss in terms of conformational flexibility.

For a larger CD having weight-average dp 115, we obtained $K = 1.33 \times 10^6$ M^{-1} and $\Delta H = -65.3$ kJ mol^{-1} using a model assuming independent bindings of iodine molecules to identical N sites of the chain sequence of the CD molecule. These values of K and ΔH are similar to those obtained for a long linear amylose [101].

Another unusual property of large CDs is their high solubility in water, unlike linear amylose which is usually only slightly soluble. An aqueous solution (3 %) of a large CD is stable at least for three months.

4.7 Biological function of the cyclic β-glucans

The cyclic β-glucans are major cell envelope constituents of all members of the *Rhizobiaceae* family. A recent review [18] covers progress in identifying and characterizing the genetic loci and enzyme systems involved in cyclic β-glucan, their biochemical functions, and possible industrial applications. Membrane associated glycosyl transferase activity, which is capable of catalyzing the formation of cyclic glucans from UDP-glucose has been identified for members of the *Rhizobium*, *Agrobacterium*, and *Bradyrhizobium* genera [102]. Two genes (*ndv*A and *ndv*B) from *Rhizobium* and (*chv*A and *chv*B) from *Agrobacterium* which code for the synthesis and transport of cyclosophoran have been identified [103-105]. In some cases *in vitro* synthesis of cyclic oligosaccharides identical to those isolated from bacterial cultures has been achieved [106,107]. It has been suggested that these glucans play a role in the hypo-osmotic adaptation of bacteria to changes in

environmental osmolality by regulating the osmotic balance between the cytoplasm and the periplasmic space [21]. Under certain conditions, non-reducing oligosaccharides can constitute as much as 20% of the dry weight of the bacterial cells. Studies with mutants of *R. meliloti* and *A. tumefaciens* have provided the most direct evidence that periplasmic cyclic **β-glucans** function during hypoosmotic adaptation [108,109]. The growth of these mutants has been shown to be specifically impaired in hypoosmotic media, and growth is restored to wild-type levels on the addition of solutes to the growth medium. In addition, several studies have shown that the biosynthesis of cyclic **β-glucans** is osmotically regulated in a wide variety of *Rizobium*, *Agrobacterium*, and *Bradyrhizobimu* strains, with the highest levels of synthesis occurring during growth in low-osmolarity media [18]. However, the growth of some strains of *R. leguminosarum* and *R. meliloti strain* GR4 is independent of growth medium osmolarity [110], suggesting that the mechanism of osmo-reguration may be more complicated.

The possibility that these compounds mediate bacterium-plant host interactions during infection of the host [18,111,112] has also been suggested as an alternate function. The behavior of cyclic **β-glucan-deficient** mutants during infection of the host plant has been examined and found to be defective in terms of their ability to infect plants [103,113].

Morris et al. [114] proposed a biological role for cyclic glucans in accumulating naringenin, which is ascribed to the possibility that these cyclic **β-glucans** may bind the ligand in the annular space in a manner analogous to the behavior of a CD. Naringenin is a flavonoid which induces nodulation by *R. leguminosarum.* It has been suggested that the cyclic glucan acts to accumulate naringenin by enhancing the solubility of naringenin in the periplasmic space, thus allowing these molecules to partition into the cytoplasmic membrane where specific binding to the NodD protein occurs, thus activating this protein.

Bacterial species of *Bradyrizoba* secrete cyclic glucans that contain both **β-(1→3)** and **β-(1→6)** linkages instead of **(1→2)** linkage and have both smaller DP and range of dp, ranging between 10 and 13 [39]. These structurally different molecules appear to be functionally equivalent to cyclosophrans [115-117].

In addition to the common functions of **β-cyclic** glucans it has been reported that cyclic glucans composed of **β-(1→3)** and **β-(1→6)** linkages are capable of blocking the elicitor function of fungal glucans [118].

4.8 Other cyclic oligosaccharides and polysaccharides

A few examples of cyclic oligosaccharides which contain sugar units other than glucose, and which have more complex structures than the typical homo cyclic glucans found in nature exist. For example, cyclic heteropolysaccharides were identified as a component of the entrobacterial common antigen of *Enterobacteriaceae* [119]. The structure of this family of oligosaccharide from *Yersina pestis* is reported to be:

cyclo[→4)-β-D-Man*p*2NAcA-(1→4)-α-D-Glc*p*2NR-(1→3)-α-D-Fuc*p*4NAc-(1→]$_n$

$$6$$
$$\uparrow$$
$$R'$$
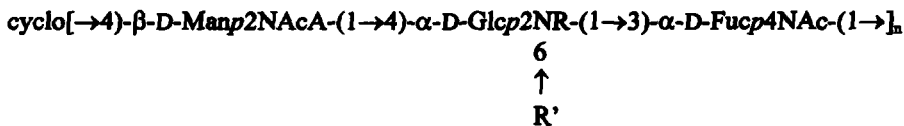
where R is Ac or H(approximately 1:1), R' is Ac or H (approximately 1:4), and **n=4(major),** 3,5(minor) [120].

Digestion of inulin with *Bacillus circulans* fructrotransferase leads to the production of cyclofructins [121]. The major product was identified as cyclofructohexaoside **(CF$_6$)** composed of six **β-(1→2)-linked** D-fructofuranose residues. Small amounts of the larger cyclic hepta- and octafructosides were also isolated [122]. The solid-state structure of the **CF$_6$-trihydrate** was reported [123], and **CF$_6$, CF$_7$** and **CF$_8$** are capable of complexing with metal cations. A computer modeling study on a series of this type of cyclic fructins predicts that **CF$_9$** and **CF$_{10}$** are capable of forming inclusion complexes with organic materials [27].

Synthetic chemical procedures for the preparation of cyclic oligosaccharides have recently been summarized [20]. Since the total chemical synthesis of **CD$_6$** reported in 1985 [124], a number of procedures have been developed for synthetically producing other synthetic cyclic oligosacharides. A recent review [20] on this subject systematizes the currently available information on the different approaches to constructing synthetic cyclic oligosaccharides, as well as on their structural characterization. Synthetic cyclic oligosaccharides are listed in this review, as well.

In addition to covalently linked cyclic polysaccharides, a new class of cyclic polysaccharides, whose structure is stabilized by non-covalent interactions between the chains comprising multiple helix, has emerged [125-131], Circular triple helical structure has been found in anti-tumor **(1→6)** branched **(1→3)-β-D-glucans** which had been subjected to a denaturation-renaturation cycle [127,132]. Cyclic structures, stabilized by non-covalent bonds, are also observed for **ι-carrageenan** and gellan under certain conditions [128,129]. This topic is reviewed by Brant and McIntire [19].

Further screening of bacteria and developments in enzymatic and chemical synthesis will almost certainly lead to the production of new cyclic oligosaccharides and polysaccharides. Although this review does not cover all of the topics in cyclic oligosaccharides and polysaccharides, readers will understand that structural analysis offers the most fundamental knowledge in our understanding of the functions of cyclic oligosaccharides and polysaccharides. The structural and conformational diversity of cyclic oligosaccharides and polysaccharides shows great potential for the study of aspects such as host-guest chemistry and related important biological events.

Acknowledgements

References
1. D.French,Advan.Carbohydr.Chem.,**12**,189(1957).
2. J.A.Thoma and L.Stewart,in *Starch, Chemistry and Technology* I, ed. by R.L. Whistler and E.F.Paschall,Academic Press,New York, 1965.
3. S.Kitahata,in *Handbook of Amylases and Related Enzymes,* ed. by The Amylase Research Society of Japan.Pergamon Press,New York, 1988.
4. T.Kuge,Biophysics(Jpn),**17**,29(1977).
5. M.L.Bender and M.Komiyama,*Cyclodextrin Chemistry*,Springcr-Verlag,1978.
6. K.Kainuma,in *Starch,* ed. by R.L.Whistler,J.N.BeMiller and E.F.Paschall, Academic Press,Orlando,1984
7. J.Szejtli,*Cyclodextrin Technology*,Kluwer Academic Publisher,Dordrecht,1988.
8. J.Szejtli,Carbohydr.Polym.,**12**,375(1990).
9. S.Li and W.C.Purdy,Chem.Rev.,**92**,1457(1992).
10. A.Harada, in *Large Ring Molecules*,ed.by J.A.Semlyen, Wiley,London,1996.
11. K.A.Connors,Chem.Rev.,**97**,1325(1997).
12. Cyclodextrins,ed.by V.T.D'souza and K.B.Lipkowitz,Chem.Rev.,**98**(1998).
13. T.Takaha,M.Yanase,H.Takata,S.Okada and S.M.Smith,J.Biol.Chem.,**271**,2902(1996).
14. Y.Terada.M.Yanase,H.Takata,T.Takaha and S.Okada,J Biol.Chem.,**272**,15729(1997).
15. K.Harata,T.Endo,H.Ueda and T.Nagai,Supermolecular Chem.,**9**,143(1997).
16. J.Jacob,K.Gessler,D.Hoffmann,H.Sanbe,K.Koizumi,S.M.Smith,T.Takaha and W.Saenger,Angew.Chem.Int.Ed.,**110**,606(1998).
17. W.Saenger,J.Jacob,K.Gessler,T.Steiner,D.Hoffmann,H.Sanbe,K.Koizumi,S.M.Smith and T.Takaha,Chem.Rev.,**98**,1787(1998);K.Gessler,I.Usòn,T.Takaha,N.Krauss,S.M.Smith, S. Okada, G.M.Sheldrick and W.Saenger,Proc.Natl.Acad.Sci.USA,**96**,4246(1999).
18. M.W.Breedveld and K.J.Millen,Microbiol.Rev.,,**June**, 145(1994).
19. D.A.Brant and T.M.McIntire,in *Large Ring Molecules,*ed.by J.A.Semlyen, Wiley,London, 1996.
20. G.Gattuso,S.A. Nepogodiev and J.F.Stoddart,Chem.Rev.,**98**,1919(1998).
21. K.J.Miller,E.P.Kennedy and V.N.Reinhold,Science,**231**,48(1986).
22. M.Mimura,S.Kitamura,S.Goto,K.Takeo,H.Uehara and K.Kajikawa,Carbohydr.Res.,**289**,25(1996).
23. S.Kitamura,H.Isuda,J.Shimada,T.Takada,T.Takaha,S.Okada,M.Mimura and K.Kajiwara,Carbohydr.Res.,**304**,303(1997).
24. S.Kitamura,K.Nakatania,T.Takaha and S.Okada,Abstracts of papers of XIXth International Carobohydrate Synposium,DP032(1998);*Macromol. Rapid Commun.,* in press.
25. J.Shimada,S.Handa,H.Kaneko and T.Takada,Macromolecules,**29**,6408(1996).
26. F.V.Lichtenthaler and S.Immel,Tetrahedron Asymmetry,**5**,2045(1994).
27. S.Immel and F.W.Lichtenthaler,Carbohyd.Res.**313**,91(1998).
28. T.Nakagawa,K.Ueno,M.Kashiwa and J.Watanabe,Tetrahedron Lett.,**35**,1921(1994).
29. J.Szejtli,Chem.Rev.,**98**,1743(1998).
30. A.Nakamura and K.Yamane,in *Enzyme Chemistry and Molecular Biology of Amylases and Realted Enzymes* ed. by The Amylase Research Society of Japan, CRC Press,1995.
31. Y.Terada,K.Fujii,T.Takaha and S.Okada, Appl.Environ.Microbiol.,in press (1999).
32. M.Hisamatsu,A.Amemura,K.Koizumi,T.Utamura and Y.Okada,Carbohydr.Res.,**121**,31(1983).
33. K.Koizumi,Y.Okada,S.Horiyama,T.Utamura,M.Hisanatsu and A.Amemura,J.Chromatogr.,**265**,89(1983).
34. K.Koizumi,Y.Okada,T.Utamura,M.Hisamatsu and A.Amemura,J.Chromatogr.,**299**,215(1984).
35. K.Koizumi,Y.Kubota,T.Tanimoto and Y.Okada,J.Chromatogr.,**45**,303(1988).

36.   T.Higashiura,M.Ikeda,M.Okubo,M.Hisamatsu,A.Amemura and
       T.Harada,Agric.Biol.Chem.,**49**,1865(1985).
37.   D.R.Bundle,J.W.Cherwonogrodzky and M.B.Perry,Infect.Immun.,**56**,1101(1988).
38.   A.Amemura and J.Cabrera-Crespo,J.Gen.Microbiol.,**132**,2443(1986).
39.   D.B.Rolin,P.E.Pfeffer,S.F.Osman,B.S.Szwergold,F.Kappler and
       A.J.Benesi,Biochim.Biophys.Acta.,**1116**,215(1992).
40.   P.E.Pfeffer,S.F.Osman,A.Hotchkis,A.A.Bhagwat,D.L.Keister and
       K.M.Valentine,Carbohydr. Res., **296**,23(1996).
41.   G.L.Cote and P.Biely,Eur.J.Biochem.**226**,641(1994).
42.   T.Oguma,T.Horiuchi and M.Kobayashi,Biosci.Biotech. Biochem., **57**,1225(1993).
43.   A.Dell.W.S.York,M.McNeil,A.G.Darvill and
       P.Albersheim,Carbohydr.Res.,**117**,185(1983).
44.   J.E.Harris,F.A.Mellon,V.J.Morris,K.R.Parsley,B.J.H.Steven and
       K.R.J.Austin,Carbohydr.Polym.,**16**,321(1991).
45.   W.Saenger,Angew.Chem.,Int.Ed.Engl.,**19**,344(1980).
46.   K.Harata,Chem.Rev.,**98**,1803(1988).
47.   P.C.Manor and W.Saenger,J.Am.Chem.Soc.,**96**,3630(1974).
48.   K.K.Chacko and W.Saenger, J.Am.Chem.Soc.,**103**,1708(1981).
49.   F.W.Lichtenthaler and S.Immel,Liebigs Ann.,**9**,27(1995).
50.   S.Immel and F.W.Lichtenthaler, personal communications.
51.   J.Brickmann,*MOLCAD-MOLecular Computer Aided Design,*Darmstadt University
       of Technology,Darmstadt,1997.
52.   M.Teschner,C.Henn,H.Vollhardt,S.Reiling and
       J.Bricksmann,J.Mol.Graphics,**12**,98(1994).
53.   W.Heiden,G.Moeckel and J.Brickmann,J.Comput.-Aided Mol.Des.,**7**,503(1993).
54.   M.L.Connolly,J.Appl.Cryst,**16**,548(1983).
55.   D.A.Brant,Q.Rev.Biophys,**9**,527(1976).
56.   M.Mimura,H.Urakawa,K.Kajiwara,S.Kitamura and K.Takeo,
       Macromol.Symp.,**99**(1995).
57.   M.K.Dowd,J.Zeng,A.D.French and P.J.Reilly,Carbohydr.Res.,**230**,223(1992).
58.   M.K.Dowd,A.D.French and P.J.Reilly,Carbohydr.Res.,**233**,15(1992).
59.   N.L.Allinger,Y.H.Yuh and J.H.Lii,J.Am.Chem.Soc.,**111**,8293(1989).
60.   R.C.Jordan,D.A.Brant and A.Cesàro,Biopolymen,**17**,2617(1978).
61.   B.A.Burton and D.A.Brant,Biopolymers,**22**,1969(1983).
62.   S.Kitamura,T.Okamoto,Y.Nakata,T.Hayashi and T.Kuge,Biopolymers,
       26,537(1987).
63.   S.Kitamura,T.Minami,Y.Nakamura,H.Isuda,H.Kobayashi,M.Mimura,H.Urakawa,
       K.Kajikawa and S.Ohno,J. Mol. Struct.,**395-396**,425(1997).
64.   Y.Nakata,S.Kitamura,K.Takeo and T.Norisuye,Poym.J.,**26**,1085(1994).
65.   W.Hinrichs,G.Buettner,M.Steifa,C.Betzel,V.Zabel,B.Pfannemueller and
       W.Saenger,*Science,***238**,205(1987).
66.   W.Schulz,H.Sklenar,W.Hinrichs and W.Saenger,Biopolymers,**33**,363(1993).
67.   A.Palleschi and V.Crescenzi,Gazz.Chim.Ital.,**115**,243(1985).
68.   A.M.G.Serrano,G.Franco-Rodrigues,I.Gonzalez-Jimenez,P.Tejero-
       Mateo,M.M.Molina,J.A.Dobado,M.Megias and M.J.Romeo,
       J.Mol.Struct.,**301**,211(1993).
69.   L.Poppe,W.S.York and H.V.Halbeek,J.Biomol.NMR,**3**,81(1993).
70.   W.S.York,J.U.Thomsen and B.Meyer,Carbohydr.Res.,**248**,55(1993).
71.   W.S.York,*Carbohydr.Res.,***278**,205(1995).
72.   I.Andre,K.Mazeau,F.R.Travel and I.Tvaroska,*Int.J.Biol.Macromol.,***17**,189(1995).

73. K.Takeo,K.Hirose and T.Kuge,Chem.Lett.,1233(1973).
74. Y.Inoue,Annual reports on NMR spectroscopy **27**,60(1993).
75. T.Endo,H.Nagase,H.Ueda,A.Shigihara and S.Kobayashi,Chem. & Pharm. Bull.,**46**,1840(1998).
76. H.-J.Schneider,F.Hacket and V.Ruediger,Chem.Rev.,**98**,1755(1998).
77. K.Kajiwara and T.Miyamoto, in *Polysaccharides,* ed. by S.Dumitriu,Marcel Dekker,New York, 1998.
78. K.Kajiwara and Y.Hiragi,in *Applications of Synchrotron Radiation to Materials Analysis,*ed. by H.Saisho and Y.Gohshi,Elsevier,Tokyo,1996.
79. G.Porod,in *Small Angle X-ray Scattering,* ed. by O.Glatter and O.Kratky,Academic Press,London,1982.
80. O.Glatter,*Acta Phys.Austr.,***52**,243(1980).
81. W.Burchard,in *Cyclic Polymers,* ed. by J.A.Semlyen,Elsevier Applied Science Publishers,London,1986.
82. E.F.Casassa,*J.Polym.Sci.,***A-3**,605(1965).
83. W.Burchard and M.Schmid,*Polymer,***21**,745(1980).
84. J.Shimada,H.Kaneko and T.Takada,J.Comput.Chem.,**15**,28(1994).
85. M.P.Allen and D.J.Tildesley, *Computer Simulation of Liquids,*Oxford Univ.Press,Oxford,1987.
86. J.E.H.Koehler,W.Saenger and W.F.von Gunsteren,Eur.Biophys.J.,**16**,197(1987).
87. W.L.Jorgensen and J.Tirado-Rives,J.Am.Chem.Soc.,**110**,1657(1988).
88. S.Nose,J.Chem.Phys.,**81**,511(1988).
89. W.G.Hoover,Phys.Rev.,**A31**,1695(1985).
90. W.F.von Gunsteren and M.Karplus,Macromolecules,**15,**1528(1982).
91. J.E.H.Koehler.W.Saenger and W.F.von Gunsteren,J.Mol.Biol.,**203**,241(1987).
92. K.H.O.a.B.Meyer,Carbohydr.Res.,**281**,11(1996).
93. K.Harata,in *Comprehensive Supramolecular Chemistry* vol.3, ed.by J.L.Atwood,J.E.D.DavisD.D.Vogtle,Pergamon,Oxford,1996,
94. M.V.Rekharsky and Y.Inoue,Chem.Rev.,**98**,1875(1998).
95. I.Miyazawa,H.Ueda,H.Nagase,T.Endo,S.Kobayashi and T.Nagai,Eur.J.Pharm.Sci. **3**,153(1995).
96. K.L.Larsen,T.Endo,H.Ueda and W.Zimmermann,Carbohydr.Res.,**309**,153(1998).
97. T.Furuishi,T.Endo,H.nagase,H.Ueda and T.Nagai,Chem.Parm.Bull.,**46**,1658(1998).
98. D.R.Bundle and B.W.Sigurskjold,Method in Enzymology,**247**,288(1994).
99. R.Lumry and S.Rajender,Biopolymers,**9**,1125(1970).
100. M.S.Searle and H.W.Dudley,J.Am.Chem.Soc.,**114,**10690(1992).
101. K.Takahashi and S.Ono,J.Biochem.,**72**,1041(1972).
102. J.L.Cohen and K.J.Miller,J.Bacteriol.,**173**,4271(1991).
103. C.J.Douglas,RJ.Staneloni,R.A.Rubin and E.W.Nester,J.Bacteriol.,**161**,850(1985).
104. T.Dylan,L.Ielpi,S.Stanfield,L.Kashyap,C.Douglas,M.Yanofsky,E.Nester, D.R.Helinski and G.Ditta,Proc.Natl.Acad.Sci.,**83**,4403(1986).
105. G.A.Cangelosi,L.Hung,V.Puvanesarajah,G.Stacey,D.A.Ozga,J.A.Leigh and E.W.Nester,J.Bacteriol.,**169**,2086(1987).
106. R.A.Dedonder and W.Z.Hassid,Biochim.Biophys.Acta,**90**,239(1964).
107. A.Amemura,Agric.Biol.Chem.,**48**,1809(1984).
108. G.A.Cangelosi,G.Martinetti and E.W.Nester,J.Bacteriol.,**172**,2172(1990).
109. T.Dylan,D.R.Helinski and G.S.Ditta,J.Bacteriol.,**172**,1400(1990).
110. M.J.Sato,V.Lepek,J.Olivares and N.Toro,Mol.Plant-Microbe Interact,**6**,11(1993).
111. M.Abe,A.Amemura and S.Higashi,Plant Soil,**64**,315(1982).

160

112. S.W.Stanfield,L.Ielpi,D.O'Brochla,D.R.Helinski and
     G.S.Ditta,J.Bacteriol.,**170**,3523(1988).
113. T.Dylan,P.Nagpal,D.R.Helinski and G.S.Ditta,J.Bacteriol.,**172**,1409(1990).
114. V.J.Morris,G.J.Brownsey,G.R.Chilvers,J.E.Harris,A.P.Gunning and
     B.H.J.Stevens,Food Hydrocoll.,**5**,185(1991).
115. KJ.Miller and R.S.Gore,Curr.Microbiol.,**24**,101(1992).
116. R.E.Tully,D.L.Keister and K.C.Gross,Appl.Environ.Microbiol.,**56**,1518(1990).
117. A.A.Bhagwat,K.C.Gross,R.E.Tully and D.L.Keister,J.Bacteriol.,**178**,4635(1996).
118. A.Mithofer,A.A.Bragwat,M.Feger and J.Ebel,Planta,**199**,270(1996).
119. G.Acker,D.Bitter-Suermann,U.Meiier-Dieter,H.Peters and H.Mayer,J.Bacteriol.,
     186,348.
120. E.V.Vinogradov,Y.A.Knirel,J.E.Thomas-Oates,A.S.Shashkov and
     V.L.L'vov,Carbohydr.Res.,**258**,223(1994).
121. M.Kawamura,T.Uchiyama,T.Kuramoto,Y.Tamura and
     K.Mizutani,Carbohydr.Res.,**192**,83(1989).
122. M.Kawamura and T.Uchiyama,Biosci.Biotech.Biochim.,**57**,343(1993).
123. M.Sawada,T.Tanaka,Y.Takai,T.Hanafusa,T.Taniguchi,M.Kawamura and
     T.Uchiyama,Carbohydr.Res.,**217**,7(1991).
124. T.Ogawa and Y.Takahashi,Carbohydr.Res.**138**,C5(1985).
125. B.T.Stokke,A.Elgsaeter,D.A.Brant,T.Kuge and S.Kitamura,Macromolecules,
     24,6349(1991).
126. B.T.Stokke,A.Elgsaeter,D.A.Brant and S.Kitamura,in *Physical Chemistry of Colloids
     and Interfaces in Oil Production*,Technip,Paris,1992.
127. B.T.Stokke,A.Elgsaeter,D.A.Brant,T.Kuge and S.Kitamura,Biopolymers,
     33,193(1993).
128. B.T.Stokke,A.Elgsaeter and S.Kitamura,Int.J.Biol.Macromolecules,**14**,63(1993).
129. R.M.Abeysekera,D.M.G.E.T.Bergstrom,I.T.Norton and
     A.W.Robards,Carbohydr.Res.,**248**,225(1993).
130. T.M.McIntire and D.A.Brant,Biopolymers,**42**,133(1997).
131. T.M.McIntire and D.A.Brant,J.Am.Chem.Soc.,**120**,6909(1998).
132. S.Kitamura,T.Hirano,K.Takeo,H.Fukada,K.Takahashi,B.H.Falch and
     B.T.Stokke,Biopolymers,**39**,407(1996).

CHAPTER 5
CYCLIC POLYSILOXANES

Stephen J. Clarson
University of Cincinnati, USA

5.1   Introduction

Polymers molecules may be prepared with a variety of architectural structures such as linear, ring, star, branched, ladder and dendritic chains and they may also be three dimensional network structures. Some of these molecular forms are illustrated in Figure 1. The first synthetic cyclic polymers to be prepared and characterized were the poly(dimethysiloxanes) (PDMS) which were reported in 1977 [1]. Since that time a number of other cyclic polymers have been synthesized which include cyclic polystyrene [2,3,4], cyclic poly(phenylmethylsiloxane) [5], cyclic poly(2-vinylpyridine) [6], cyclic polybutadiene [7] and cyclic poly(methylvinylsiloxane) [8].
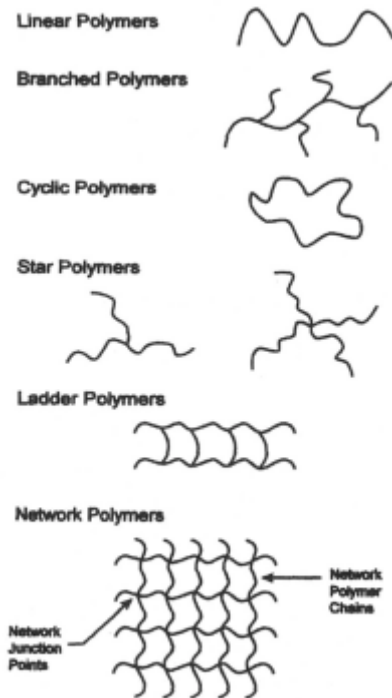
Figure 1. Typical structures for polymer molecules

161

In this overview, we will discuss some selected properties of cyclic polysiloxanes, particularly where large differences are seen when compared to the linear polymeric analogs. The area of topological entrapment of ring polymers into networks structures will also be described, which is an area that is not accessible to linear polymers unless they undergo end-cyclizing chemistry. This concept of topological threading is somewhat general for ring molecules as it may also be utilized in the preparation of catenanes and rotaxanes.

5.2   Preparation of Cyclic Poly(dimethysiloxanes)

A distribution of cyclic PDMS $[(CH_3)_2SiO]_x$ may be isolated from PDMS ring-chain equilibration reactions carried out either in the bulk state or in solution. The successful utilization of such reactions for preparing large ring molecules is largely due the extensive experiments performed on this system [9,10,11] and also a good theoretical understanding of the reactions through the Jacobson-Stockmayer cyclization theory [12] used in conjunction with the rotational isomeric state model for PDMS [13]. Vacuum fractional distillation and preparative gel permeation chromatography (GPC) may be used to prepare sharp fractions of the cyclic siloxanes having narrow molar mass distributions. Such methods allow the preparation of cyclic PDMS samples containing up to 1000 skeletal bonds, on average, on a gram scale. The molar mass for each polymer and the polydispersity may then be characterized using techniques such as gas chromatography, HPLC and analytical GPC.

5.3   Solution Properties of Cyclic Poly(dimethysiloxane)

5.3.1   Intrinsic Viscosities

Many solution properties of cyclic PDMS have been investigated and compared both to their linear analogs and with the predictions of theory [14]. One property which illustrates the behaviour of the cyclic polymers in solution is their intrinsic viscosities $[\eta]$. The results for cyclic and linear PDMS in bromocyclohexane - a θ-solvent at 301 K - are shown as a function of their weight-average molar molar mass in Figure 2 [15]. The results are in agreement the theoretically predicted ratio for intrinsic viscosities for ring (r) and linear polymers (1) of $[\eta]_r/[\eta]_l = 0.66$ [16,17,18]. These results are also in agreement with the ratio measured for cyclic and linear PDMS in another θ-solvent - methyl ethyl ketone [1].
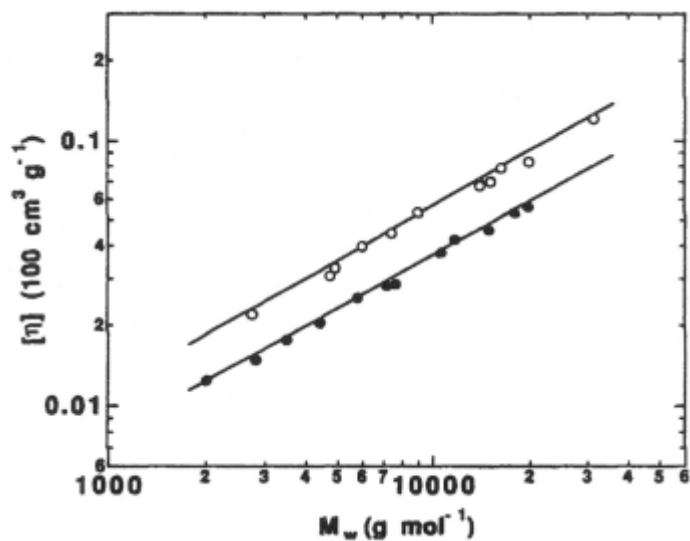
Figure 2. Intrinsic viscosities [η] for cyclic (●) and linear (o) poly(dimethylsiloxane) in bromocyclohexane at 301 K plotted against their weight-average molar masses M_W [15]

5.3.2 Mean Square Radius of Gyration

Small-angle neutron scattering has been used to obtain the z-average mean square radius of gyration for a series of cyclic and linear PDMS sharp fractions.
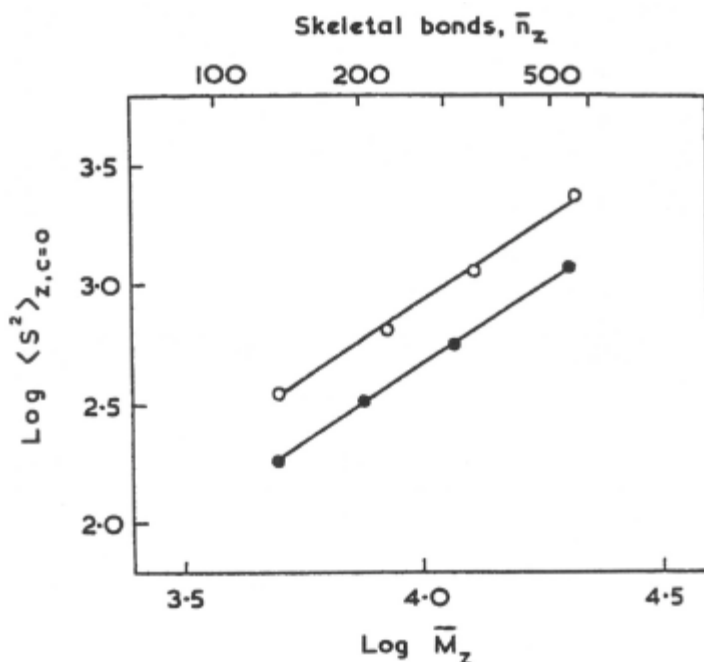
Figure 3. Plots of the logarithms of the z-average mean square radii of gyration$<s^2>_{z,c=0}$ at zero concentration of the linear (o) and cyclic (●) PDMS fractions against their z-average molar masses M_z hi benzene-d6 at 292K by SANS [19]

As can been seen in Figure 3., the solution measurements in **benzene-d6** gave a ratio $<s^2>_{z,l} / <s^2>_{z,r} = 1.9 \pm 0.2$. This ratio agrees with the theoretically predicted value of 2.0 for flexible high molar mass polymers unperturbed by excluded volume effects [14,19].

5.3.3 Critical Point Behaviour of Cyclic Polysiloxanes

One of the key underlying assumptions in the solution measurements described above is that the θ-temperatures for rings and chains are the same. In order to address this assumption, the phase behaviour of binary mixtures of cyclic poly(dimethylsiloxane) (PDMS) and linear poly(phenylmethylsiloxane) (PPMS) chains were investigated using a static wide angle light scattering technique [20]. Evidence for the effect of a component's molecular architecture

/ topology (cyclic or linear) on the phase separation of blends was investigated by cloud point measurements and examining the composition dependence of the resulting phase diagram. The cyclic-linear blend exhibited an upper critical solution temperature (UCST) and showed a dependence on the molecular architecture / topology in that the critical temperature T_C for the cyclic-linear blend was lower than expected when compared with PDMS-PPMS blends in which both components had a linear polymer structure. The interaction energy density parameter Λ_{12} for the polymers was evaluated via the Flory-Huggins treatment for the thermodynamics of mixing of two polymers. The blending of cyclic PDMS led to a lower Λ_{12} when compared with the corresponding linear-linear binary blend - again due to the chain architecture / topology effect. For this UCST system, it thus appears that PDMS cyclics are more soluble / compatible than their linear analogs of the same degree of polymerization.

The findings described above are consistent with the current, but very limited, experimental data in the literature for large ring systems. For example, the phase separation kinetics studies on blends containing high molar mass cyclic polystyrene [21] and star-shaped polystyrene [22] with linear poly(vinylmethylether) PVME have been studied. In both these studies a lower critical solution temperature (LCST) was seen however, the cyclic polystyrene was observed to phase separate 7-8°C above the PS-PVME linear-linear blend, where the components had the same molar mass. This result is consistent with a previous study [23] in which phase diagrams of the lower critical solution temperature (LCST) were shown for cyclic and linear PDMS in tetramethylsilane and neopentane solution. In all cases the cyclic polymers were found to show a higher LCST by up to 2.5°C when compared with the linear polymers of the same molar mass.
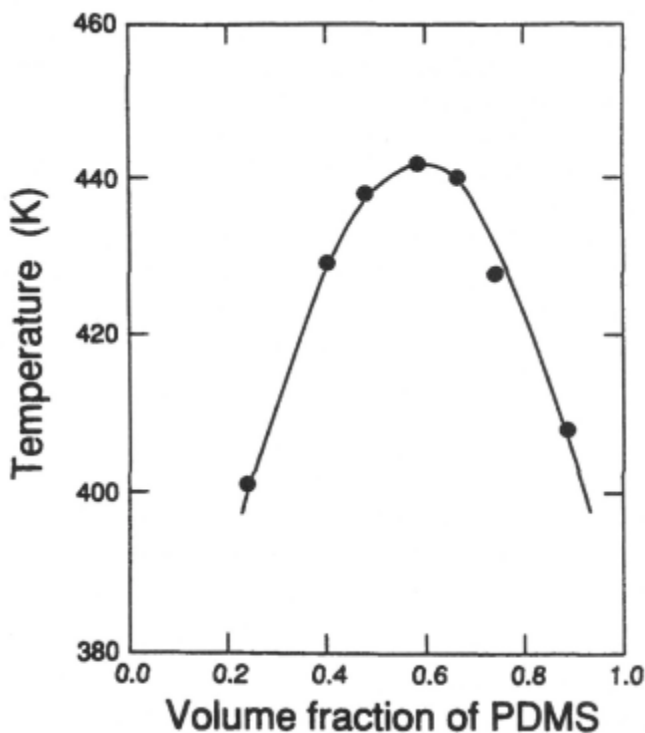
Figure 4. Cloud point temperatures of homopolymer mixtures of cyclic PDMS and linear PPMS. The cyclic PDMS had a molar mass of **1420 g mol⁻¹** and the linear PPMS had a molar mass of **1890 g mol⁻¹**. The experimental cloud points are designated by the filled circles and the fit represents the binodal phase boundary for the system [20].

5.4   Bulk Properties of Cyclic Poly(dimethysiloxane)

5.4.1   Glass Transition Temperatures

Many bulk properties of cyclic PDMS have also been investigated and compared both to their linear analogs and with the predictions of theory [14]. Of fundamental importance in polymer science is the temperature at which an amorphous or semi-crystalline polymer becomes a glass. For the effect of chain length upon the glass transition temperature T_g, a number of relationships have been proposed which account for the behaviour observed for linear polymers. These predict T_g to show a linear dependence on reciprocal number-average molar mass M_n and are of the form [24,25]

$$T_g = T_{g\,(\infty)} - \frac{K}{M_n} \qquad (1)$$

$$\frac{1}{T_g} = \frac{1}{T_{g\,(\infty)}} + \frac{K^1}{M_n} \qquad (2)$$

where $T_{g\,(\infty)}$ represents the glass transition temperature at infinite molar mass and K and K^1 are constants.

The glass transition temperatures of cyclic poly(dimethylsiloxane) in the molar mass range $370 \leq M_n \leq 24500$ g mol^{-1} were measured by differential scanning calorimetry (DSC) and were the first values for ring polymers to be reported [26]. The cyclic polymers showed remarkable behaviour in that their T_g values were found to increase with decreasing molar mass M_n (see Figure 5). This was unanticipated, as the T_g values of the cyclic polymers, having no end-groups, would not be expected to show any dependence on molar mass using a simple free volume theory [24,25]. Following these experimental findings, the first theoretical model for the glass formation of noncatenated ring polymers was developed by Di Marzio and Guttman [27] and was based on a configurational entropy theory [28,29]. As the configurational entropy of a ring polymer is always less than that of its linear analog [30], the ring system will clearly always have a higher T_g [26]. At infinite molar mass, however, the glass transition temperatures $T_{g(\infty)}$ for cyclic and linear polymers should be the same, as was observed experimentally for cyclic and linear PDMS [26]. The theoretical treatment was then developed by incorporating the effect of flexes on the configurational entropy of cyclic and linear molecules [27].
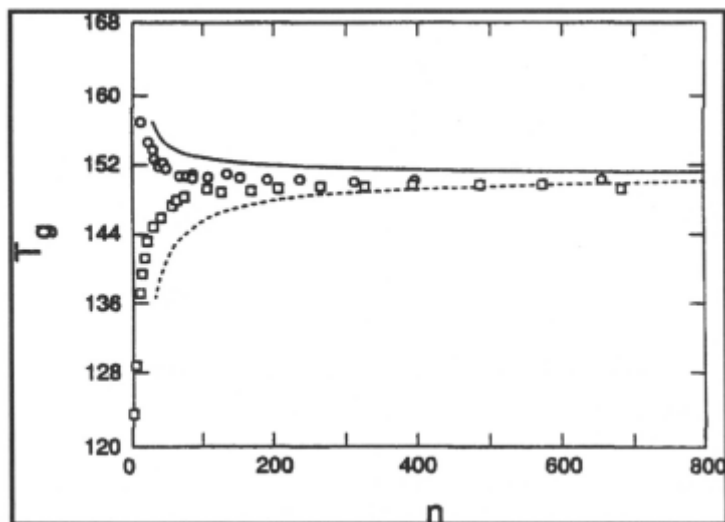
Figure 5. Glass transition temperatures T_g of cyclic (o) and linear (□)
poly(dimethylsiloxane) plotted against their number-average number of skeletal bonds n_n.
The theoretical lines are from the Di Marzio and Guttman theory using the maximum term
method [27].

The results of this approach are strikingly elegant in that the two input
parameters - the hole energy E_h and the flex energy $\Delta\varepsilon$ - can first be selected to
fit the T_g data for the linear polymers and the resulting values for the ring
analogues are then essentially based on a no-parameter prediction. The Di
Marzio and Guttman theory [27] successfully predicts that the glass transition
temperature of a ring molecule system increases as the molar mass is lowered,
while the glass transition temperature of a linear polymer system decreases with
decreasing molar mass, as was observed for the cyclic and linear
poly(dimethylsiloxane) (see Figure 5) [26].

5.4.2 Crystallisation Behaviour

Of the various low molar mass dimethylsiloxanes, only the six (D3) and
sixteen (D8) membered rings are solids at room temperature. From structural
studies of the small cyclic structures, the six membered ring
hexamethylcyclotrisiloxane (D3) is known to be highly strained and has thus
been widely investigated and used in both anionic and cationic ring-opening
polymerization reactions. The small cyclic compounds all exhibit higher
melting points than their linear analogs. As will be shown below however, high
molar mass cyclic and linear PDMS show similar melting characteristics.

Two endothermic peaks are typically exhibited in the measured DSC thermograms of high molar mass cyclic and linear [26] poly(dimethylsilloxanes), as can be seen in Figure 6. Multiple endothermic peaks are frequently observed for a variety of polymeric materials that have been studied by differential scanning calorimetry (DSC) [31,32]. Three possible causes of this phenomenon could be (i) differences in crystallite size distribution, (ii) melting-recrystallization of the original crystallites and their subsequent melting and (iii) different crystalline forms of the polymer. In DSC studies of PDMS model networks however, only one crystalline melting peak was observed suggesting that the junction points inhibit the melting-recrystallization of the original crystallites and that this is therefore the likely source of the double endothermic melting peaks commonly observed for linear PDMS [26,68]. This is also consistent with the fact that only one type of crystal structure has been reported for linear PDMS [33], which is monoclinic, with a helix conformation and having six structural units per primitive cell. The measured crystallographic parameters are $\mathbf{a} = 13.0$ Å, $\mathbf{b} = 8.3$ Å (helix axis), $\mathbf{c} = 7.75$ Å and $\boldsymbol{\beta} = 60^{\mathbf{o}}$ [33,34]. These data give a theoretical density of fully crystallized PDMS $\boldsymbol{\rho} = 1.07 \text{ g cm}^{-3}$.

Friedrich and Rabolt have reported detailed Raman scattering studies of linear PDMS at 296 K and 6K [35]. The spectra at these temperatures were seen to be quite similar in all regions except for those bands near 490 cm^{-1}. This band has been assigned to the symmetric Si-O stretching vibration $\mathbf{v_S(Si\text{-}O)}$. The changes observed in the Raman spectrum at 6K have been attributed to the semicrystalline nature of the material with $\mathbf{v_S(Si\text{-}O)}$ in the amorphous region being assigned to the peak at 486 cm^{-1} and that at 466 cm^{-1} being the corresponding crystalline component. Little change was observed in the bandwidth of either the 486 cm^{-1} or 466 cm^{-1} Raman peaks until the polymer is considerably above $\mathbf{T_g}$. The collapse onto one Raman band having the same frequency and bandwidth then occurs in the range -60 to -40°C temperature range - which corresponds to the crystalline melting range of linear PDMS.

It has been shown previously that high molar mass linear PDMS materials are highly crystalline and do not show a glass transition when they are cooled at rates of less than about 1 K min^{-1} [36]. As described above, pure low molar mass cyclic and linear dimethylsiloxanes form molecular crystals. Cyclic dimethylsiloxane sharp fractions having number-average numbers of skeletal bonds $\mathbf{n_n}$ in the range $24 \leq \mathbf{n_n} \leq 79$ showed only a glass transition when investigated over the temperature range 103 K to 298 K [26]. The fact that such materials are completely amorphous presumably results from these medium

size rings not being able to be incorporated into the polymer lamellar structures, whereas the PDMS rings with $84 \leq n_n$ clearly form the same polymer crystals as high molar mass linear PDMS [26].
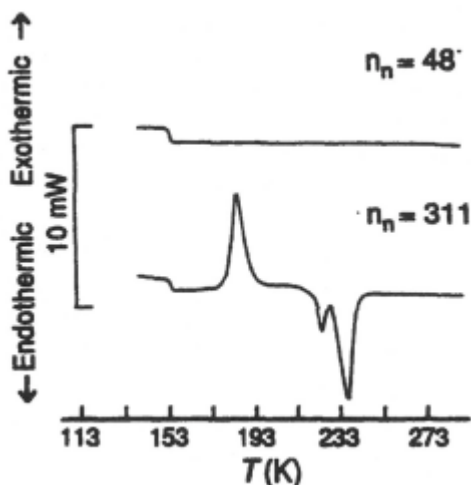
Figure 6. DSC Thermograms of cyclic PDMS [37].

In order to confirm the non-crystallization of these cyclics, studies of the low temperature Raman spectra [37] have been carried out. The Raman spectrum clearly showed a splitting of the band near 491 cm^{-1} into two peaks upon cooling for a cyclic PDMS fraction with 311 skeletal bonds, as has been described above for high molar mass linear PDMS [35]. For the cyclic with 48 skeletal bonds however no splitting of this band was observed at temperatures below the T_m of PDMS, thus suggesting that the material was completely amorphous [37].

Investigations of the mobility of fluorescent probes in cyclic PDMS at subambient temperatures have also been carried out in order to investigate the conformational mobility of cyclic PDMS and also to confirm the noncrystallisation of the medium sized PDMS rings [38].
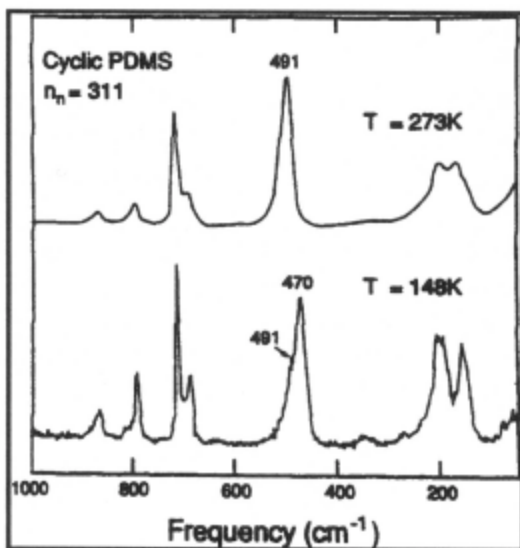
Figure 7. Raman spectra of high molar mass cyclic PDMS $(n_n= 311)$ as a function of temperature [37].
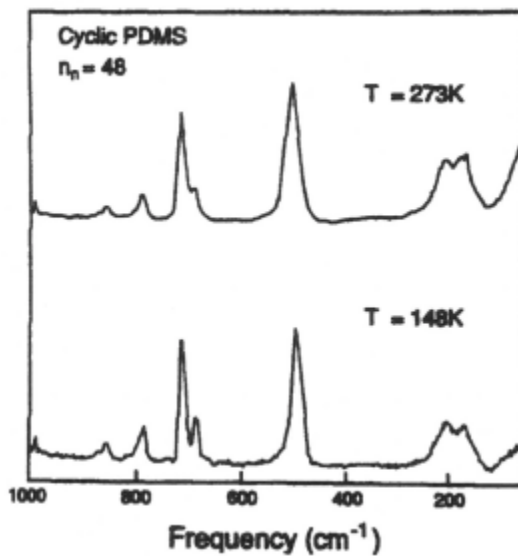
Figure 8. Raman spectra of cyclic PDMS $(n_n= 48)$ as a function of temperature [37].

5.4.3   Melt Viscosities

The work of Dodgson, Bannister and Semlyen gave bulk viscosity ratios at 298 K in the range $0.45 < \eta_r / \eta_l < 0.51$ for cyclic and linear PDMS samples with molecular weights in the range $16,000 < M_w < 24,000$ g mol^{-1}[39]. These values agree well with the theoretically predicted ratio of 0.5 obtained by Bueche for 'flexible' chains below the critical entanglement molecular weight [14]. The values were expanded to include samples higher than the critical entanglement molecular weight for PDMS by Orrah and coworkers [40]. Somewhat surprisingly, these latter results indicated similar entanglement behaviour for the cyclic and linear PMDS.
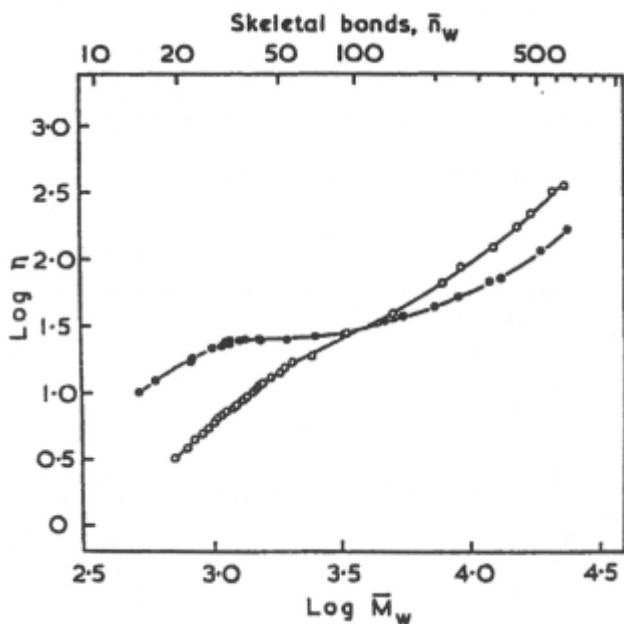
Figure 9. Plots of the logarithms of the bulk viscosities η of the cyclic ($\bullet$) and linear (o) PDMS fractions at 298 K against the logarithms of their weight average molecular weights M_w [39].

5.5   Topological Trapping of Cyclic Poly(dimethysiloxane)

Figure 10. Topological trapping of cyclic molecules by linear chains which pawed through them prior to end-linking to form a tetrafunctional network structure [44].

If relatively large cyclic molecules of poly(dimethylsiloxane) (PDMS) are present when linear PDMS chains are end-linked, then some are permanently trapped by one or more network chains threading through them prior to network formation [41-45] (see Figure 10).

As would be expected, the % trapped depends markedly on the size of the cyclic. Some typical experimental results [42] are shown in Figure 11. As can be seen, the smaller ring siloxanes having degrees of polymerization DP<20 (n_n<40) are not trapped at all, presumably due to the effective "hole" being too small for a linear PDMS chain to pass through. For the large rings DP$\geq$250 essentially all the cyclics are threaded by chains and are thus topologically incorporated into the resulting network structure. These experimental results have been successfully interpreted using models [41] based on Monte Carlo generation of typical spatial configurations of the cyclic of interest using conformational information available from the rotational isomeric state analysis of PDMS chains. Geometric examination of these configurations then gives "hole" sizes which can be compared to the cross sections of the linear PDMS chain, to gauge the probability that cyclics of the specified size will be threaded and trapped. This method thus shows considerable promise for elucidating the configurations of linear and cyclic molecules in the bulk state.
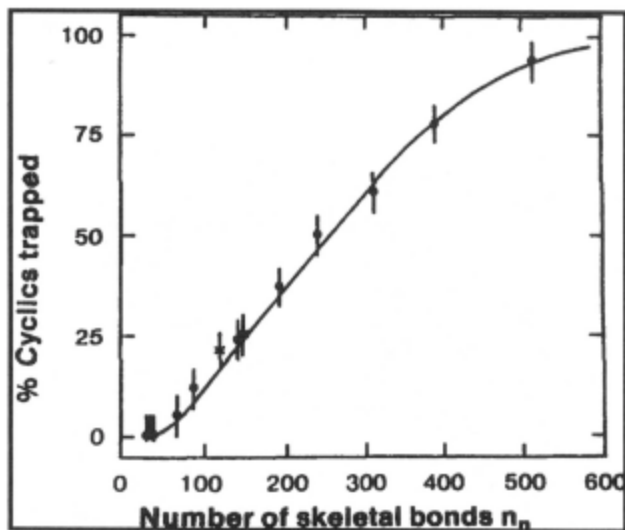
Figure 11. Percentage of PDMS cyclics trapped in the PDMS network shown as a function of the number of bonds n_n in the cyclic. The symbols(●) and (X) correspond to cyclics trapped Into PDMS chains systems having different cure chemistry for the network formation [42].

An alternate model for the topological trapping of cyclics was presented by Galiatsatos and Eichinger [46]. In this work a power law for the trapping probability was formulated which gave results that revealed that the cross-sectional area of the PDMS cyclics is fractal in length, with a fractal dimension 1.81. This model was found to be in good agreement with the experimental results for rings containing up to ~300 skeletal bonds.

The incorporation of cyclic molecules into a network by threading results in an elastomer having a more complex topology. As many of the modern theories of rubberlike elasticity are concerned with topological constraints - for example the Flory-Erman treatment [47-49] and the slip-link model of Edwards and coworkers [50] - it is of interest to determine the equilibrium stress-strain properties of PDMS networks containing topologically trapped PDMS cyclics. Some small but significant increases in the low deformation modulus have in fact been observed [51,52]. This topological approach has also been utilized to incorporate PDMS cyclics into a thermoplastic network material, poly(2,6-dimethyl-1,4-phenylene oxide) [45,53]. In this case the cyclic PDMS can act as a plasticizer that is intermediate to the usual external (dissolved) and internal (copolymerized) varieties. Interesting changes in the mechanical and swelling properties have been observed in materials of this type [45].

It may also be possible to use the techniques described above to form polymeric network structures having no chemical cross-links whatsoever. Mixing difunctionally terminated linear chains with large amounts of cyclic polymer and then cyclizing them by end-linking could give sufficient cyclic interlinking to yield an "Olympic" or "chain mail" network [44,54-56]. Such materials are expected to have highly unusual equilibrium and dynamic mechanical properties and attempts to prepare them are in progress.

5.6   Other Cyclic Polysiloxanes

As described above, the most investigated siloxane ring system to date is cyclic poly(dimethysiloxane) PDMS, however many properties of the cyclic poly(phenylmethylsiloxane) [5] and cyclic poly(methylvinylsiloxane) [6] have been reported. A number of key properties of each of these three systems are given below in Tables 5.1, 5.2 and 5.3, respectively.

Table 5.1 Selected Properties of the Cyclic Poly(dimethylsiloxanes) (r) and Their Properties Compared to the Linear Poly(dimethylsiloxanes) (l)

Properties	Values
Characteristic Ratio $<r^2>/nl^2$ Derived from Molar Cyclization Equilibrium Constants in the Bulk State at 383 K	6.8
Density at 298 K (x = 95)	971.67 kg m^{-3}
Glass Transition Temperature $T_{g\,(\infty)}$	149.8 K
Melting Point T_{m1} (M_n= 24,370 g mol^{-1})	227.0 K
Melting Point T_{m2} (M_n= 24,370 g mol^{-1})	237.8 K
Raman Absorption v_s (Si-O) Crystalline Region	466 cm^{-1}
Raman Absorption v_s (Si-O) Amorphous Region	486 cm^{-1}
Activation Energy for Viscous Flow $E_{visc\,(\infty)}$	15.5 kJ
Static Dielectric Permittivity ε_O at 298 K (x = 95)	2.757
Root Mean Square Dipole Moment $10^{30}<\mu^2>^{1/2}$ at 298 K (x = 95)	14.3 C m
Refractive Index (632.8 nm) at 298 (x = 95)	1.4025
Refractive Index (436.0 nm) at 298 (x = 95)	1.4140
Onset temperature for thermal depolymerization under N_2	623 K
Intrinsic Viscosities $[\eta]_r/[\eta]_l$ in Butanone (θ-solvent) at 293 K	0.67
Intrinsic Viscosities $[\eta]_r/[\eta]l$ in Cyclohexane at 298 K	0.58
Intrinsic Viscosities in $[\eta]_r/[\eta]_l$ in Bromocyclohexane (θ-solvent) at 301 K	0.66
Diffusion Coefficients D_r/D_l in PDMS Networks at 296 K	1.18 ± 0.03
Diffusion Coefficients D_l/D_r in Toluene at 298 K	0.84 ± 0.01
Means Square Radius of Gyration $<s^2>_{z,l}/<s^2>_{z,r}$ in Benzene d_6 at 292 K	1.90
Translational Friction Coefficients f_r/f_l in Toluene at 298K	0.83 ± 0.01
Number-Average Molar Masses of PDMS Rings and Chains With The Same GPC Retention Values M_r/M_l	1.24 ± 0.04
Melt Viscosities η_r/η_l for M_w = 24,000 g mol^{-1}	0.45 ± 0.02

5.6.1 Cyclic Poly(phenylmethylsiloxanes)

The molar cyclization constants from ring-chain equilibration reactions of poly(phenylmethylsiloxane) (PPMS) in both the bulk state and in solution were investigated in detail by Beevers and Semlyen [71]. Based upon these studies Clarson and Semlyen [75] have described the scaling up such reactions to successfully isolate cyclic poly(phenylmethylsiloxanes) $-[(C_6H_5)(CH_3)SiO]_x-$ from ring-chain equilibration reactions carried out in toluene solution at 383 K. Following fractionation, a variety of investigations of their physical properties of these cyclic polymers have be carried out and have also been compared with their linear polymer analogs. It should be noted that the large rings are atactic due to the equilibration used in their preparation. It is possible to obtain the stereoisomers of the small rings for this system, however. Although a rotational isomeric state model has been developed for the PPMS system by Mark and Ko, no detailed calculations of the properties of the rings using this model have been described so far.

Table 5.2 Selected Properties of the Cyclic Poly(phenylmethylsiloxanes) (r) and Their Properties Compared to the Linear Poly(phenylmethylsiloxanes) (l)

Properties	Values
Characteristic ratio $<r^2>/nl^2$ derived from molar cyclization equilibrium constants in the bulk state at 383 K	10.7
Characteristic ratio $<r^2>/nl^2$ derived from molar cyclization equilibrium constants in toluene at 383 K	10.4
Critical Dilution Point in Toluene at 383 K (% Volume Polymer)	52%
Glass Transition Temperature T_g ( )	244.9 K
Characteristic ratio $<r^2>/nl^2$ derived from GPC in toluene at 292 K	8.8
Means Square Radius of Gyration $<s^2>_{z,l}/<s^2>_{z,r}$ in benzene d6 at 292 K	2.0
Dipole Moment μ^2 (x=5)	5.01 (10^{-31} Cm)
Number-Average Molar Masses of PDMS Rings and Chains With The Same GPC Retention Values M_r/M_l in toluene at 292 K	1.25 ± 0.05
Enthalpy Change for the Formation of the *cis*-Trimer	27 kJ mol^{-1}
Enthalpy Change for the Formation of the trans-Trimer	22 kJ mol^{-1}
Enthalpy Change for the Formation of the *cis*-Tetramer	8 kJ mol^{-1}

The major application of cyclic PPMS is the ring-opening polymerization of small rings to give linear PPMS high polymers. Copolymerization with other siloxane small rings is also used to give copolymers of controlled composition. Cyclic and linear PPMS samples are viscous fluids having good thermal stability. Certain stereoisomers of the small rings, when highly pure, [70,71,75] are solids at room temperature.

5.6.2 Cyclic Poly(vinylmethylsiloxanes)

The cyclic poly(vinylmethylsiloxanes) **-[(CH$_2$=CH)(CH$_3$)SiO]$_x$-** are an interesting cyclic polymer system in that they contain a reactive pendent group [81,82]. Thus possible chemistries include hydrogenation which yields cyclic poly(ethylmethylsiloxane) **-[(CH$_3$CH$_2$)(CH$_3$)SiO]$_x$-** (this route has also been used to deuterate the rings for neutron scattering investigations - **[(CH$_3$CHD)(CH$_2$D)SiO]$_x$-).**

Table 5.3 Selected Properties of the Cyclic Poly(vinylmethylsiloxanes) (r) and Their Properties Compared to the Linear Poly(vinylmethyl-siloxanes) (l)

Properties	Values
Characteristic ratio $<r^2>/nl^2$ Derived from Molar Cyclization Equilibrium Constants in 50% Toluene Solution at 383K	7.8
Intrinsic Viscosities $[\eta]_r/[\eta]_l$ in toluene at 298 K	0.69
Density at 298 K (M_n= 5,430 g mol^{-1} and M_n/M_n= 1.06)	1006.0 kg m^{-3}
Refractive Index (589.3 nm) at 298 K (M_n= 5,430 g mol^{-1} and M_n/M_n= 1.06)	1.4458
Refractive Index (589.3 nm) at 303 K (M_n= 5,430 g mol^{-1} and M_n/M_n= 1.06)	1.4421
Refractive Index (589.3 nm) at 313 K (M_n= 5,430 g mol^{-1} and M_n/M_n= 1.06)	1.4380
Refractive Index (589.3 nm) at 298 K (M_n= 11,440 g mol^{-1} and M_n/M_n= 1.14)	1.4465
Refractive Index (589.3 nm) at 303 K (M_n= 11,440 g mol^{-1} and M_n/M_n= 1.14)	1.4427

Refractive Index (589.3 nm) at 313 K (M_n= 11,440 g mol^{-1} and M_n/M_n= 1.14)	1.4385
Glass Transition Temperature T_g (M_n= 5,430 g mol^{-1} and M_n/M_n= 1.06)	144.5 K
Glass Transition Temperature T_g (M_n= 11,440 g mol^{-1} and M_n/M_n= 1.14)	144.7 K
Melt Viscosity $10^3\eta_r$ at 298 K (M_n= 5,430 g mol^{-1} and M_n/M_n= 1.06)	75.9 kg m^{-1} s^{-1}
Activation Energy for Viscous Flow (M_n= 5,430 g mol^{-1} and M_n/M_n= 1.06)	16.75 kJ

Other useful reactions are with molecules containing terminal or pendant Si-H groups which can readily be attached by hydrosilation chemistry. This functional ring system also shows that one can directly prepared elastomeric network structures having none of the usual network defects (dangling chain ends, etc.).

Although there are a limited number of studies of these novel functional rings to date, the large rings have been successfully isolated from ring-chain equilibration reactions carried out in solution. Following fractionation, some investigations of their physical properties of these cyclic polymers have be carried out and have also been compared with their linear polymer analogs [83-86].

Major applications of cyclic vinylmethylsiloxane rings include ring-opening polymerization of small rings to give linear PVMS high polymers. Copolymerization with other siloxane small rings are also used to give copolymers of controlled composition. Both the homopolymers and copolymers are widely used for preparing silicone elastomers. The cyclics polymers are viscous fluids at room temperature that have good thermal stability.

References

1. K. Dodgson and J. A. Semlyen, Polymer 18, 1265 (1977)

2. G. Hild, A. Kohler and P. Rempp, European. Poly. J. **16**, 525 (1980)

3. D. Geiser and H. Hocker, Polym. Bull 2, 591 (1980); Macromolecules **13**, 653 (1980)

4. J. Roovers and P. M. Toporowski, Macromolecules **16**, 843 (1983)

5. S. J. Clarson and J. A. Semlyen, Polymer **27**, 1633 (1986)

6. T. R. Formoy and J. A. Semlyen, Polymer Communications **30**, 86 (1989)

7. T. E. Hogen-Esch and W. Toreki, Polymer Preprints (Am. Chem. Soc. Div. Polym. Chem.) **30(1)**, 129 (1988)

8. J. Roovers, Macromolecules **21**, 1517 (1988)

9. J. F. Brown and G. M. J. Slusarczuk, J. Am. Chem. Soc. **87**, 931 (1965)

10. J. A. Semlyen and P. V. Wright, Polymer **10**, 543 (1969)

11. P. V. Wright, in 'Ring Opening Polymerization', (K. J. Ivin and Saegusa, T. Eds.), Elsevier, New York, **Vol 2**, 324 (1984)

12. H. Jacobson and W. H. Stockmayer, J. Chem. Phys. **18**, 1600 (1950)

13. P. J. Flory and J. A. Semlyen, J. Am. Chem. Soc. **88**, 3209 (1965)

14. C. J. C. Edwards and R. F. T. Stepto, R. F. T. in 'Cyclic Polymers' (J. A. Semlyen, Ed.), Elsevier, Barking, UK, pp135-165 (1986)

15. S. J. Clarson, J. A. Semlyen, J. Horska and R. F. T. Stepto, Polymer Communications **27**, 31 (1986)

16. V. Bloomfield, and B. H. Zimm, J. Chem. Phys. **44**, 315, (1966)

17. M. Fukatsu and M. Kurata, J. Chem. Phys. **44**, 4359 (1966)

18. H. Yu and H. Fujita, work cited by H. Yamakawa, in 'Modern Theory of Polymer Solutions', Harper and Row, New York (1971)

19. J. S. Higgins, K. Dodgson and J. A. Semlyen, Polymer **20**, 553 (1979)

20. C. M. Kuo, S. J. Clarson and J. A. Semlyen, Polymer, **35**, 4623 (1994)

21. M. M. Santore, C. C. Han and G. B. McKenna, Macromolecules **25**, 3416 (1992)

22. B. J. Factor, T. P. Russell, B. A. Smith, L. J. Fetters, B. J. Bauer and C.C.Han, Macromolecules **23**, 4452 (1990)

23. J. -M. Barbarin-Castillo, I. A. McLure, S. J. Clarson, and J. A. Semlyen, Polymer Communications, **28**, 212 (1987)

24. R. J. Roe, in 'Encyclopedia of Polymer Science and Engineering', 2nd Ed, Wiley, New York, Vol. **6**, 531 (1986)

25. G. B. McKenna, in 'Comprehensive Polymer Science', G. Allen, J. C. Bevington, C. Booth, and C. Price, (Eds.), Pergamon Press, Oxford, UK, **Vol 2**, 311 (1989)

26. S. J. Clarson, K. Dodgson and J. A. Semlyen, Polymer **26**, 930 (1985)

27. E. A. Di Marzio and C. M. Guttman, Macromolecules **20**, 1403 (1987)

28. J. H. Gibbs and E. A. Di Marzio, J. Chem. Phys. **28**, 373 (1958)

29. E. A. Di Marzio, Ann. N. Y. Acad Sci. **371**, 1 (1981)

30. N. Go, Macromolecules **19**, 2054 (1986)

31. L. Mandelkern, 'Crystallization of Polymers', McGraw-Hill, New York, (1963)

32. R. Alamo and L. Mandelkern, J. Polym. Sci.: Polym. Phys. Ed **24**, 2087, (1986)

33. G. Damaschun, Kolloid-Z. **180**, 65, (1962)

34. G. Feio, G. Buntinx and J. P. Cohen-Addad, J. Polym. Sci.: Polym. Phys. Ed. **27**,1 (1989)

35. J. Friedrich and J. F. Rabolt, Macromolecules **20**, 1975 (1987)

36. J. D. Helmer and K. E. Polmanteer, J. Appl. Polym. Sci. **13**, 2113 (1969)

37. S. J. Clarson and J. F. Rabolt, Macromolecules, **26**, 2621 (1993)

38. C. Pham-Van-Cang, L. Bokobza, L. Monnerie, S. J. Clarson, J. A. Semlyen, J. Vandendriessche and F. C. De Schryver, Polymer, **28**, 1561 (1987)

39. K. Dodgson, D. J. Bannister and J. A. Semlyen, Polymer **21**, 663 (1980)

40. D. J. Orrah, J. A.Semlyen and S. B. Ross-Murphy, Polymer **29**, 1455-1458 (1988)

41. L. C. DeBolt, and J. E. Mark, Macromolecules **20**, 2369 (1987).

42. S. J. Clarson, J .E. Mark, and J. A. Semlyen, Polym. Communications **28**, 151 (1987).

43. S. J. Clarson, J. E. Mark and J. A. Semlyen, Polym. Communications **27**, 244 (1986).

44. L. Garrido, J. E. Mark, S. J. Clarson and J. A. Semlyen, Polym. Communications **26**, 53 (1985).

45. T. J. Fyvie, H. L. Frisch, J. A. Semlyen, S. J. Clarson and J. E. Mark, J. Polym. Sci.: Polym. Chem. Ed. **25**, 2503 (1987).

46. V. Galiatsatos, and B. E. Eichinger, Polym. Communications **28**, 183 (1987)

47. P. J. Flory, J. Chem. Phys. **66**, 5720 (1977)

48. P. J. Flory, and B. Erman, Macromolecules **15**, 800 (1982)

49. B. Erman, and P. J. Flory, Macromolecules **15**, 806 (1982)

50. R. C. Ball, M. Doi. and S. F. Edwards, Polymer **22**, 1010 (1981)

51. L. Garrido, J. E. Mark, S. J. Clarson and J. A. Semlyen, Polym. Communications **26**, 55 (1985).

52. S. J. Clarson and J. E. Mark, unpublished results

53. W. Huang, H. L. Frisch, Y. Hua and J. A. Semlyen, J. Polym. Sci.: Polym. Chem. Ed. **28**, 1807 (1990).

54. P. G. de Gennes, 'Scaling Concepts in Polymer Physics', Cornell University Press, Ithaca, New York (1979)

55. P. G. de Gennes, Private communication and unpublished theoretical calculations (1991)

56. E. Raphael, C. Gay and P. G. de Gennes, 'Progressive Construction of an Olympic Gel', Manuscript in preparation

57. C. J. C. Edwards, R. F. T. Stepto and J. A. Semlyen, Polymer, **21**, 781-786 (1980)

58. D. J. Bannister and J. A. Semlyen, Polymer **22**, 377-381 (1981)

59. C. J. C. Edwards, R. F. T. Stepto and J. A. Semlyen, Polymer, **23**, 865-868 (1982)

60. C. J. C. Edwards, R. F. T. Stepto and J. A. Semlyen, Polymer, **23**, 869-872 (1982)

61. C. J. C. Edwards, S. Bantle, W. Burchard, R. F. T. Stepto and J. A. Semlyen, Polymer, **23**, 873-876 (1982)

62. M. S. Beevers, S. J. Mumby, S. J. Clarson and J. A. Semlyen, Polymer, **24**, 1565 (1983)

63. L. Garrido, J. E. Mark, S. J.Clarson and J. A. Semlyen, Polymer Communications, **25**, 218 (1984)

64. S. Granick, S. J. Clarson, T. R. Formoy and J. A. Semlyen, Polymer, **26**, 925 (1985)

65. L. Garrido, J. E. Mark, S. J.Clarson and J. A. Semlyen, Polym. Communications **26**, 53 (1985)

66. S. J. Clarson, New Journal Chem. **17**, 711 (1993)

67. A. A. Goodwin, M. S. Beevers, S. J. Clarson and J. A. Semlyen, Polymer, **37(13)**, 2603-2607 (1996)

68. C. R. Snyder, H. Marand and S. J. Clarson, Macromolecules, in press (1999)

69. S. J. Clarson, Macro Group UK Bulletin (RSC), **49**, 16-18 (1998)

70. H. J. Hickton, A. Holt, J. Homer and A. W. Jarvie, J. Chem. Soc. (C) 149 (1966)

71. M. S. Beevers and J. A. Semlyen, Polymer **12**, 373-382 (1971)

72. M. S. Beevers, D. Phil. Thesis, University of York (1972)

73. J. E. Mark and J. H. Ko, J. Polym. Sci. Polym. Phys. Ed **13**, 2221 (1975)

74. S. J. Clarson, D. Phil. Thesis, University of York (1985)

75. S. J. Clarson and J. A. Semlyen, Polymer **27**, 1633-1636 (1986)

76. J. A. Semlyen, Makromol. Chem., Macromol. Symp. **6**, 155-163 (1986)

77. S. J. Clarson, K. Dodgson and J. A Semlyen, Polymer **28**, 189-192 (1987)

78. S. J. Clarson, J. A. Semlyen and K. Dodgson, Polymer **32**, 2823 (1991)

79. Siloxane Polymers', (Ed. S. J. Clarson and J. A. Semlyen), Prentice Hall, Englewood Cliffs, NJ (1993)

80. A. A. Goodwin, M. S. Beevers, S. J. Clarson and J. A. Semlyen, Polymer **37(13)**, 2597-2602 (1996)

81. S. W. Kantor, R. C. Osthoff, and D. T. Hurd, J. Am. Chem. Soc. **77**, 1685 (1955)

82. J. F. Hampton, US Patent 3,465,016

83. T. R. Formoy, D. Phil. Thesis, University of York (1985)

84. J. A. Semlyen, Makromol. Chem., Macromol. Symp. **6**, 155-163 (1986)

85. T. R. Formoy and J. A. Semlyen, Polymer Comm. **30**, 86-89 (1989)

86. J. A. Semlyen, in 'Siloxane Polymers', (Ed S. J. Clarson and J. A. Semlyen), Prentice Hall, Englewood Cliffs, NJ (1993)

This page intentionally left blank

CHAPTER 6
CYCLIC OLIGOMERS OF POLYCARBONATES AND POLYESTERS

Daniel J. Brunelle
GE Corporate Research and Development
Schenectady, NY USA

6.1   Introduction

Cyclic oligomers of condensation polymers such as polycarbonates and polyesters have been known for quite some time. The cyclics are found in commercial grades of polyester and polycarbonate at levels of 0.25-2.0%, being formed either under kinetic conditions (e.g. in phosgenation reactions), or in their equilibrium concentration from melt polymerization reactions. The cyclic oligomers have been separated from the polymers and characterized by several groups, and synthesis of many discrete cyclics has also been reported using classical high dilution techniques. Most of the early work was of academic interest, due to the fact that syntheses were inefficient and purification of products was always necessary.

Chemistry has recently been developed for the facile preparation of large quantities of *mixtures* of cyclic oligomeric polycarbonates and polyesters (dimer, trimer, tetramer, etc). Through use of specific *pseudo*-high dilution techniques in kinetically controlled reactions, cyclic oligomer mixtures can be prepared in yields as high as 90%, and with excellent selectivity over the formation of linear oligomers. High selectivity of cyclic over linear oligomers was necessary because the presence of linears would limit the ultimate molecular weights achievable upon ring-opening polymerization (ROP) of the cyclics. Furthermore, these reactions were designed specifically for *high productivity* synthesis, and have been scaled to hundreds of kilograms per batch. With the advent of this cyclic oligomer synthesis technology, use of ROP of the cyclic oligomers for preparation of high molecular weight polyesters and polycarbonates became a commercial possibility.

The use of ROP reactions for the preparation of polyesters and polycarbonates was a very appealing technology for several reasons. During ring-opening, low molecular weight precursors led to very high molecular weight polymers without formation of by-products. Thus no diffusion-limited removal of by-products or polymer purification were necessary. Because the molecular weight of the product polymer in a ROP reaction of a pure cyclic was controlled only by the amount of initiator, extremely high molecular weights could be attained. The use of cyclic oligomers differed from conventional

185

polymerization reactions, in that the cyclics have low viscosities during processing, facilitating a number of processing techniques, such as filtration, high flow, resin transfer molding (RTM), or composite fabrication (Scheme 1). This chapter describes the chemistry involved in the preparation and ROP of two classes of engineering thermoplastics, cyclic oligomeric polycarbonates and polyesters. Polycarbonates are highly ductile amorphous polymers, and polyesters are crystalline, solvent-resistant materials.
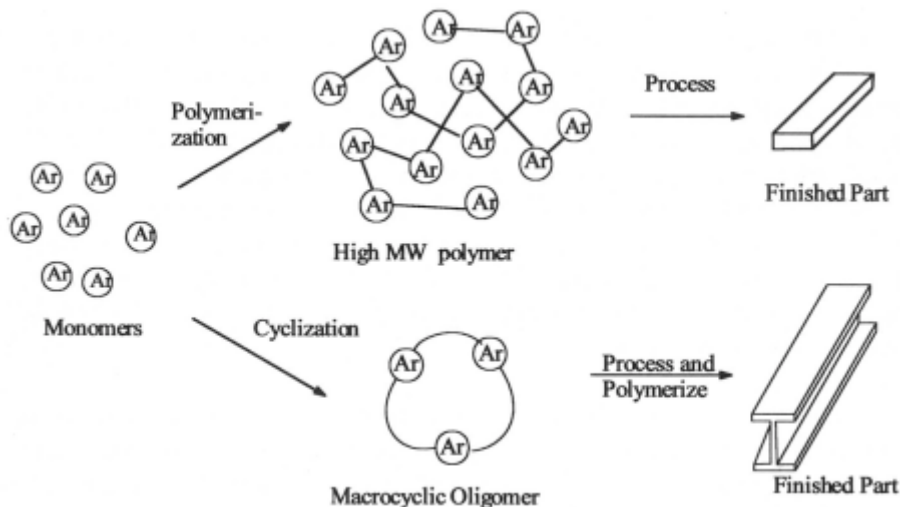
Scheme 1. Conversion of monomers to low viscositymacrocyclics (bottom) allows processing and polymerization to be carried out simultaneously. Conventional polymerization (top) forms viscous polymers, which may be difficult to process.

6.2 Preparation and polymerization of cyclic carbonate oligomers

6.2.1 History

In 1962, Schnell and Bottenbruch reported the preparation of the cyclic tetrameric carbonate of bisphenol A (4,4'-isopropylidene diphenol; BPA) [1][2][3]. They found that the cyclic tetramer could be formed in about 21% isolated yield via slow addition over 8 hours of equimolar amounts of BPA and its bischloroformate to pyridine in CH_2Cl_2 at a final monomer concentration of 0.05M. After isolation by chromatography and purification by multiple recrystallizations, the cyclic tetramer had a mp of 375°C, and the oligomer could be polymerized at its melting point either with or without catalyst, affording high molecular weight polycarbonate. Cyclic tetramer carbonates of other bisphenols were also reported from similar reactions.

cyclic tetramer ~20% yield
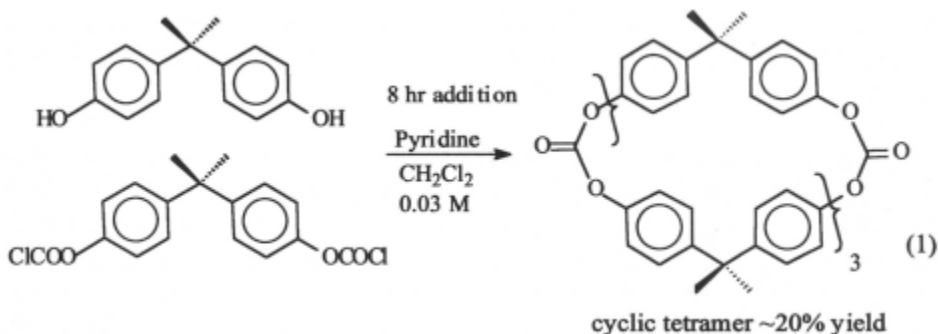
Prochaska was granted a patent on the preparation of cyclic dimers and trimers of various bisphenols, although only the preparation of the cyclic trimer of BPA was described [4]. Moody reported an improved process at about the same time [5]. Whereas Prochaska used direct phosgenation of dilute BPA in **CH₂Cl₂** using pyridine as base, Moody described the slow addition of BPA bischloroformate to pyridine containing a small amount of water, thereby effecting a high dilution reaction with a final concentration of 0.03M monomer units and with a reaction time of 1.75 hr.

Brunelle and Shannon [6] have reported an uniquivocal synthesis of low molecular weight linear and cyclic oligomeric BPA carbonates (dimer to pentamer linears and trimer to hexamer cyclics). Linear oligomers were built up in a series of steps starting from a mono-protected BPA. Classical high dilution condensation using triethylamine as base gave yields of individual cyclic oligomers of 35-60%. Their repetition of the earlier work, but using modern high pressure liquid chromatography (HPLC) to analyze the reaction products indicated that none of the reactions using pyridine as the base were selective toward formation of cyclic oligomers over linears. In fact, unless stringent measures were taken to keep the reactions dry, linear oligomers were the predominant products. Separation and isolation of cyclic oligomers was facilitated only because they are much more crystalline than the linear oligomers, with the tetramer typically having the highest melting point.

6.2.2 Preparation of mixtures of cyclic carbonate oligomers

A variety of techniques have been reported for preparation of aromatic cyclic oligomeric carbonates, including classical high dilution reactions of BPA with its bischloroformate, use of phase transfer catalysis to achieve dilution, or use of other activated species such as phosgene or bis-(2,4-dinitrophenyl)-carbonate [6]. However, selective formation of cyclic oligomers, even when

mixtures of ring sizes were obtained, was not possible; contamination with significant amounts of linear oligomers always occurred, as well as varying amounts of higher molecular weight polymer.

In 1989, Brunelle, et al. reported the selective preparation of mixtures of cyclic oligomers by use of a novel hydrolysis/condensation procedure [6][7][8]. According to that procedure, a 1.0 M solution of BPA-bischloro-formate in CH_2Cl_2 was added to a rapidly stirred mixture of aqueous NaOH, Et_3N, and CH_2Cl_2 over a 30 minute reaction time, concurrently adding Et_3N and NaOH to maintain a constant amine/CH_2Cl_2 concentration and constant pH. Total reaction time was 30-45 minutes, and the final product concentration was 0.5-1.0 M. The crude, isolated product (after separation of phases and washing with HCl) was comprised of 85-90% cyclic oligomers and 10-15% high molecular weight polymer (Mw ~ 45,000). Typical levels of linear oligomers in the reaction product were from 0.01 to 0.05%, indicating a selectivity toward cyclic vs linear oligomer formation of greater than 10,000 to 1. Because long reactions times and high dilution were not necessary, the procedure was easily scaled to multi-kilogram quantities.
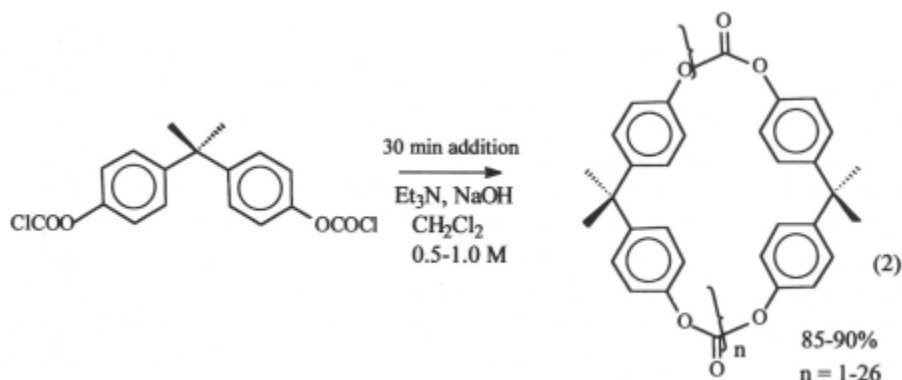
The mixture of cyclics obtained from the Brunelle procedure [6] was composed of a wide range of ring sizes, ranging from dimer to oligomer of n = 26, representing ring sizes from 24 atoms to over 300 atoms. Using HPLC analysis, both the distribution of ring sizes and the selectivity of cyclic/linear were easily observed. All of the cyclic oligomers but dimer have 254/285 nm area ratios of about 50, whereas the linear oligomers area ratios vary from 0.4 to about 2 (depending on the ratio of phenol end group to number of aromatic rings in the oligomer). The majority of cyclic oligomers had low degrees of polymerization, with >90% of the material having DP < 10. A typical distribution was composed of 5% dimer, 18% trimer, 16% tetramer, 12%

pentamer, 9% hexamer, and 25% higher cyclics. Cyclic dimer, which had never before been observed was the only oligomer with significant ring strain. Cyclic dimer, trimer, and tetramer were isolated and their properties reported [9]. The cyclic dimer has a *cis-trans* configuration about the carbonyl. A crystal structure has been reported, along with NMR and FTIR data which indicate the degree of ring strain (shifts in ^{13}C carbonyl peak and in FTIR C=O stretch). The structures of the BPA-cyclic tetramer and of diphenyl carbonate were reported in the same paper; both have *trans-trans* configurations about the carbonyl, although the cyclic shows two distinct rotamers. The tetramer carbonate macrocycle is a large, flexible ring, with an inside diameter of 14-16Å, and an outside diameter of about 21 Å. The carbonyl carbons on opposing sides of the ring are 14.92 and 13.8 Å apart.

Removal of high molecular weight polymer (and of cyclics with DP > 15) could be achieved by washing the crude product with acetone; the cyclics were soluble, but the polymer did not dissolve. Due to the presence of a *mixture* of cyclics, the melting point of the oligomers was much lower than those previously observed for the discrete cyclics, with softening beginning about 140°C, and complete melting observed by 200°C, although that melting point may be lowered to about 150°C by the incorporation of certain bisphenols substituted with long chain aliphatic groups, which seem to disrupt the cyclics' crystallinity [10].

Due to their low molecular weight, and lack of chain entanglements, the cyclic oligomeric carbonates have melt viscosities significantly lower than conventionally prepared polycarbonate (Figure 1). This lowered melt viscosity is the property most useful in subsequent applications of the cyclic oligomers. At their melting point the mixture of cyclic oligomers have significant flow, and have a greater degree of penetration and wetting of fibers in composite applications.
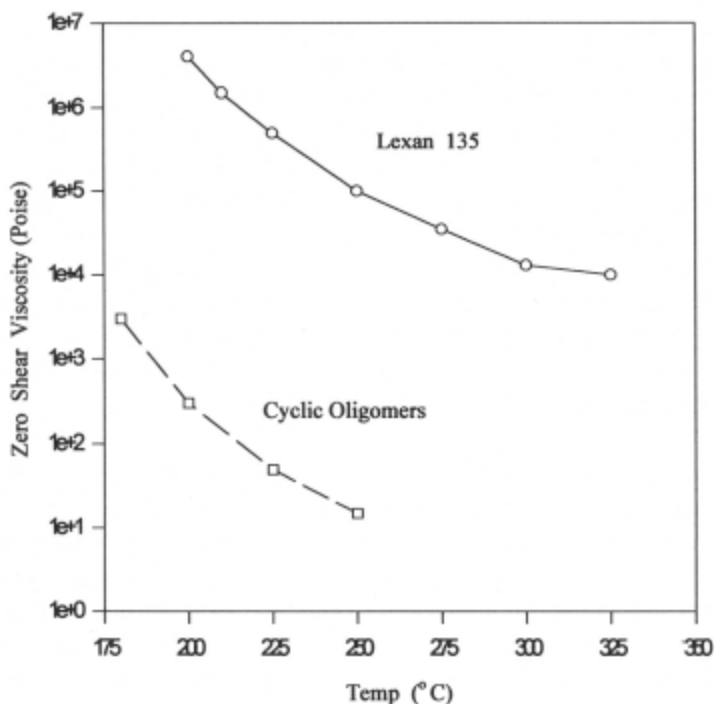
Figure 1. Comparison of zero-shear melt viscosities of commercial Lexan®135 to cyclic oligomers.

A study of the reaction variables which control selection of cyclics was carried out with the following optimum conditions: concentration-- maximum of 0.6 M monomer units at end of reaction; addition time-- 30-45 min; temperature-- reflux gave best results; NaOH concentration-- not important as long as pH was maintained at about 10-12; stirring-- good interfacial stirring recommended; catalyst-- triethylamine preferred with an amine concentration in **CH₂Cl₂** of 1.0-1.5% by volume maintained.

Although most work has been reported with BPA, this procedure was applicable to a variety of other bisphenols, either in formation of mixed cyclics with BPA or homocyclics [10]. Some of the representative bisphenols are summarized in Table 1. Generally, most bisphenols having a pKa similar to

BPA could be cyclized using the same general procedure. Many other types of oligomeric bisphenols having diverse functionalities such as ester, sulfone, ketone, amide, and urethane have also been converted to cyclic carbonates [10][12]. The carbonate functionality serves both as the key for forming a macrocycle and the reactive site for ring-opening polymerization. Some oligomeric bisphenols which have been converted to cyclic carbonates and then subjected to ring-opening polymerization are included in Table 2.

Table 1. Cyclic Oligomers of Various Bisphenols
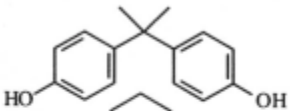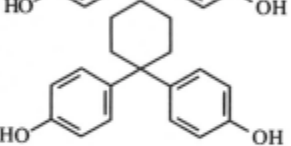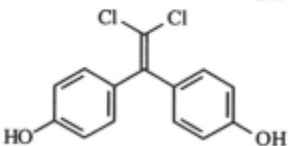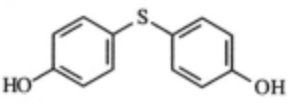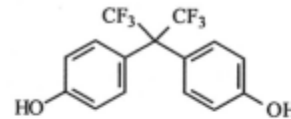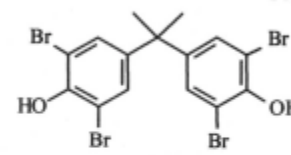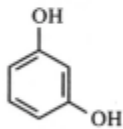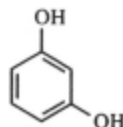
Bisphenol (% with BPA)	mp	Polymer Tg	Polymer M$_W$
	200	148	145,000
	217	165	87,000
	203	165	45,200
	215	115	insoluble
	192	167	121,800
(30%)	182	178	110,000
(30%)	190	152	88,000
(50%)	180	145	30,000

Table 2. Mixed Functionality Cyclics and Polymers

Cyclic	Cyclic Yield	Polymer
	80% (75% ester, 25% carb)	Mw = 67,00 Tg = 167°C
	95%	Mw = 48,00 Tg = 154°C
	90%	Mw = 48,00 Tg = 169°C
	92%	Mw = 88,00 Tg = 165°C
	88%	Mw = 48,00 Tg = 128°C

6.2.3 Mechanism of oligomeric cyclic carbonate formation

The mechanism for the selective formation of cyclic carbonates from bischloroformates has been the object of some interest [11][12][13]. Aromatic chloroformates react rapidly and reversibly with tertiary amines to form acyl ammonium salts (Equation 3). The acyl ammonium salt can decompose to a urethane (Equation 4), can be hydrolyzed to a phenoxide (equation 5), or undergo condensation with a phenol to form a carbonate (equation 6). In order for BPA-BCF to be converted to cyclic oligomeric products, both hydrolysis and condensation reactions must occur. Controlling the ratio of hydrolysis to condensation reactions is crucial, since an excessive hydrolysis rate will lead to recovery of BPA, or to oligomeric linears. Conversely, if the rate of hydrolysis is too slow, then the concentration of BPA-BCF will increase in the reactor, ultimately leading to conditions which favor *inter*molecular reactions rather than *intra*molecular reactions, and forming polymer. Selection of the optimum amine structure in the catalyst and controlling the reaction conditions to maintain the correct hydrolysis/condensation ratio, were the keys to successful high-yielding and selective cyclization.

$$\text{ArOC-Cl} + \text{R}_3\text{N} \; \underset{k_{-1}}{\overset{k_1}{\rightleftharpoons}} \; \text{ArOC-NR}_3^{\oplus} \; \text{Cl}^{\ominus} \tag{3}$$

$$\text{ArOC-NR}_3^{\oplus} \; \text{Cl}^{\ominus} \; \overset{k_2}{\longrightarrow} \; \text{ArOC-NR}_2 \; {}^{+} \; \text{R-Cl} \tag{4}$$

$$\text{ArOC-NR}_3^{\oplus} \; \text{Cl}^{\ominus} + \text{HO}^{\ominus} \; \overset{k_3}{\longrightarrow} \; \text{ArO}^{\ominus} + \text{NR}_3 \tag{5}$$

$$\text{ArOC-NR}_3^{\oplus} \; \text{Cl}^{\ominus} + \text{Ar'OH} \; \overset{k_4}{\longrightarrow} \; \text{ArOC-OAr'} \; + \text{R}_3\text{N-HCl} \tag{6}$$

The structure of the amine catalyst is the primary factor controlling the selectivity of cyclic vs linear oligomer formation. Replacing triethylamine with pyridine in an otherwise identical reaction leads to selective formation of *linear* oligomers, to the near-total exclusion of cyclic oligomeric products. Use of

other amines, bases, or phase transfer catalysts can give linear oligomers, cyclic oligomers, high molecular weight polymer, no reaction, or mixtures (Table 3). The sensitivity of the reaction outcome to the structure of the amine catalyst is best exemplified by comparing **Et₃N** and **Et₂NMe** in Table 3 below. A seemingly trivial change in the structure of the amine catalyst resulted in a reaction product with entirely different characteristics. These effect of various amine structural effects on the reaction outcome suggests that the amine catalyst operates by forming acyl ammonium salt intermediates during reaction.

Table 3. Variation of Products in Attempted Cyclization Reactions with Various Amines

Catalyst	% Cyclics	Products
Et₃N	85	Cyclics, polymer, <.05% linears
Et₂NMe	27	polymer, cyclics, linears
pyridine	0	linears and BPA
Me₂NBu or quinuclidine	<5	linears and polymer
(i-Pr)₂NEt	0	starting materials
n-Bu₄NOH or Bu₄NBr	0	starting materials
n-BuN₃	50	cyclics, polymer, .1% linears

Source: Ref. 6.

The equilibrium positions for the reversible formation of acyl ammonium salts via reaction of phenyl chloroformate with various amines have been measured (Equation 4) [11]. The amount of acyl ammonium salt present at equilibrium in CH_2Cl_2 solution correlates with the optimum amounts of amine necessary for efficient formation of cyclics. For example, approximately 3 times the level of tributylamine as triethylamine is necessary for highest yields of cyclics in standardized cyclization reactions, reflecting the difference in the equilibrium constants (Table 4).

Recently, the rate at which acyl ammonium salts form, their rates of decomposition to urethanes, and the rates of carbonate formation have been measured, using a stopped-flow apparatus coupled with FTIR spectroscopy (Table 4) [14][15][16][17][18]. Again, good correlation of these results with the expectations from cyclization reactions was evident. For example, the rate of acylammonium salt formation with diethylmethylamine was at least 400 times faster than with triethylamine. In cyclization reactions, the amount of diethyl-methylamine must be at least 50 times lower than triethylamine to obtain good yields of cyclics. The rates of decomposition of acylammonium salts to urethane were approximately the same for all types of amines studied. Surprisingly, the rates of condensation of acyl ammonium salts from various

amines with p-isopropylphenol to form a diaryl carbonate were also very similar. This fact suggests that approach of the amine to the carbonyl chloride suffers steric control, while attack of nucleophiles on the acyl ammonium salt, either via S_N2 reaction (to form urethane), or via S_NAc (to form carbonate) are subject to little steric effect.

Table 4. Equilibrium Constants for Acyl Ammonium Salt Formation and Rates of Acyl Ammonium Salt Formation, Urethane Formation, and Carbonate formation[a]

Amine	K, L mol^{-1} k_1/k_{-1} (Eq. 3)	k_1, L mol^{-1} s^{-1} (Eq. 3)	k_2, x10^4 s^{-1} (Eq. 4)	k_4, L mol^{-1} s^{-1} (Eq. 6)
n-Bu$_3$N	400	9 ± 1	2.6 ± 0.5	32 ± 12
Et$_3$N	1570	24 ± 3	$2.4 \pm .9$	28 ± 8
Et$_2$NMe	>50,000	>4000	1.0 ± 0.6	38 ± 6

[a]Source: Ref. 18.

A mechanism consistent with formation of cyclics controlled by the level of acyl ammonium salt formation is shown in Scheme 2. The figures schematically depict an oligomeric species, which is necessary for cyclization, since formation of cyclic monomer is not possible. The pathway leading to cyclic oligomers is seen arising from conversion of a bischloroformate to a mono-acyl ammonium salt, followed by hydrolysis to a phenoxide. Formation of a second acyl ammonium salt gives an intermediate with oppositely charged ends, which should cyclize rapidly. If that species does not cyclize, but rather reacts intermolecularly, to form a higher oligomeric bischloroformate, then the pathway starts again from the top, and an opportunity is again presented for cyclization.

The pathways which lead to linears involve extensive hydrolysis, usually because a bis-acyl ammonium salt is formed. By avoiding conditions of excessive hydrolysis (for example, use of pyridine or methylamines as catalysts), formation of linear oligomers can be prevented. Finally, the formation of polymer can arise from decomposition of an acyl ammonium salt to a urethane. Since that reaction has the slowest rate of any measured, polymer formation via that pathway is minimized. Pseudo-high dilution conditions require that starting materials be introduced at such a rate that concentrations of reactive functionalities do not increase, whereas the final product concentration can be quite high. Use of such conditions allows the selectivity of cyclic oligomers over higher molecular weight polymer. *Pseudo-*high dilution chemistry breaks down when the addition rate of bischloroformate is too fast, for example with addition times of less than 15 minutes. Ultimately,

the ideal conditions were found to be addition times of 30-45 minutes and final product concentrations of 0.5-1.0 molar. These conditions remained appropriate for reaction on a scale of 300 kg.
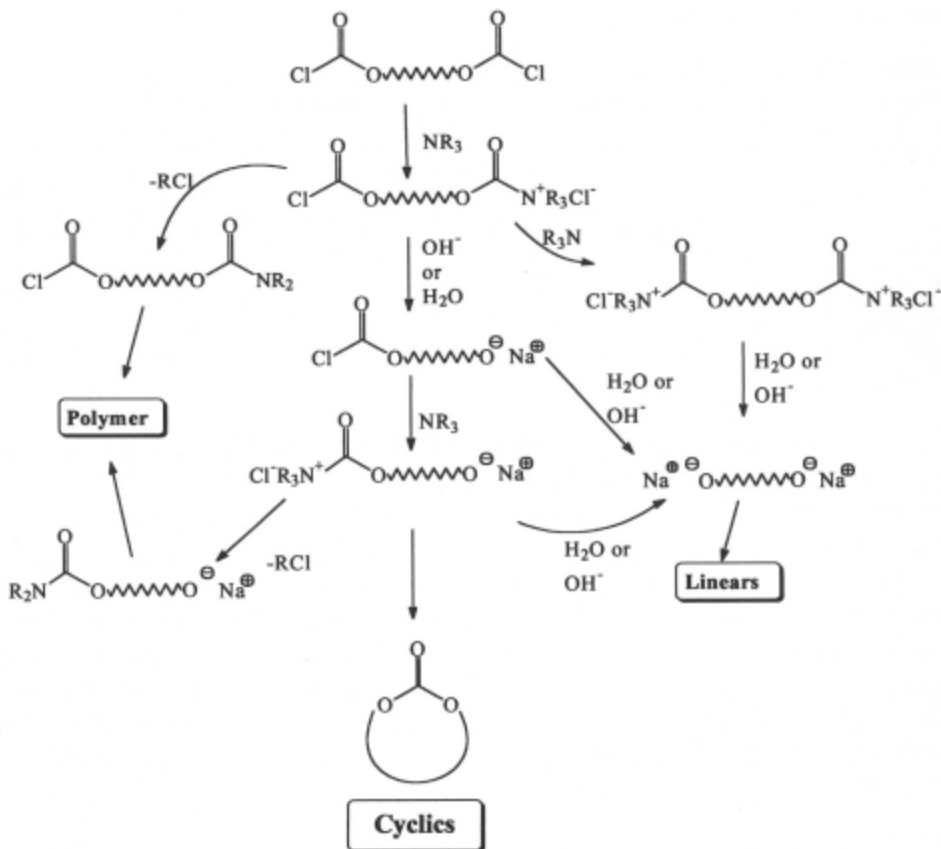
Scheme 2. Mechanism for formation of Cyclics, Linears, and Polymer, invoking intermediacy of acyl ammonium salts.

6.2.4 Polymerization of oligomeric cyclic carbonates

Ring opening polymerization of cyclic oligomers is a novel method for formation of polycarbonates. Because no byproducts which must be removed from the polymer are formed, there are no mass-transfer limitations on polymerization. As a consequence, if levels of linear impurities and initiator are low, extremely high molecular weight polymers can be produced [6][19][20]. Unlike most conventional ring-opening polymerization reactions, many of which are practiced commercially on very large scales, the

polymerization of macrocyclic oligomers is *not* normally driven by enthalpy release due to release of ring strain. Because of the large size of the rings and their flexibility, little ring strain is present, except in some cases for the smallest oligomers (for example, BPA cyclic carbonate dimer). Because the rate of ring-opening will be approximately the same as the rate of chain transfer (i.e. attack on a cyclic and attack on a linear chain are essentially energetically equivalent), total *ring-chain equilibrium is normally achieved during polymerization.* The shape and structure of the molecule, and the proximity of the chain ends will control the amount of cyclics present at equilibrium in most cases. Thus, the *entropy increase* is the controlling factor in polymerization of these macrocyclic oligomers. This rationale is verified by the fact that the amount of cyclics remaining from polymerization of oligomeric cyclic polycarbonates is approximately the same as seen in polycarbonate prepared via melt polycondensation.

When the polymerization of oligomeric cyclic carbonates was initiated by various catalysts, very high molecular weight polycarbonates could be generated (Table 5) [6][19][20]. Precipitation of the polycarbonate into acetone and analysis of the soluble portion by HPLC indicated that only about 0.25% cyclics remained after polymerization, the equilibrium amount of cyclics. The heat of reaction has been measured by differential scanning calorimetry, and has been found to be about -1.2 kJ/mole. This slight exotherm could be roughly correlated to the release of ring strain in opening of the cyclic dimer. The exotherm on polymerization of pure cyclic dimer was clearly evident in the DSC [9]. First heating showed a melting endotherm at 336°C, followed by an exotherm. Second heating showed only a glass transition temperature for polycarbonate. Pure cyclic trimer showed only a very small exotherm following the melting endotherm at 353°C, although only a glass transition temperature was seen on second heating. This indicated that polymerization occurred, even in the absence of an exotherm. Cyclic tetramer showed no exotherm on heating, although again, complete polymerization was observed. Thus, the reaction seems to be driven toward formation of linear polymer by an increase in entropy. The dispersivity of the product polymer approaches 2.0 (Table 5). This fact, along with the nearly thermoneutral nature of the reaction indicate that complete ring-chain equilibration occured during the polymerization.

The polymerization of cyclic carbonate oligomers has been achieved in the melt at 200-300°C, or in solution under various conditions, including reaction in **DMSO/CH$_2$Cl$_2$** at ambient temperature. A variety of catalysts have been investigated, including Bronsted and Lewis acids and bases, and various metallic compounds [6][19][20]. Proton acids were ineffective, and the only

Lewis acids which were effective initiators had nucleophilic ligands . Many types of basic species were very effective, including alkali phenoxides, quaternary ammonium hydroxides, and various metal acetylacetonates. One of the most effective initiators was **n-Bu₄NBPh₄,** an organic-soluble nucleophilic base. The effects of various initiators on the melt polymerization of BPA macrocyclic carbonates has been studied using a rheokinetic model. Polymerizations were carried out in a reactor designed to measure the increase in torque as a function of time. Although the melt viscosity is a function of many variables, a comparison of isothermal polymerizations with constant stirring speeds allowed a relative ranking of various initiators. The order of reactivity for various initiators was: **n-Bu₄NBPh₄ >> Al(acac)₃ > Fe(acac)₃ > Cu(acac)₃ > PhCH₂COOLi ~ LiOPh.**

The relative rates for sodium phenoxide-initiated polymerization were measured at several temperatures, and an Arrhenius plot constructed [21]. An activation energy of about 52.3 kJ/mole was calculated from the plot, a number which corresponds with the activation energy of diaryl carbonate transester-ification [22]. Since the activation energy of viscous flow for polycarbonate is about 98.0 kJ/mol, the lower polymerization activation energy indicates that it is not limited to the diffusion of the reactive end groups through the polymer melt; transesterification reactions are indiscriminate with regard to cyclics or linear chains, and do not require diffusion over long distances.

Table 5. Polymerization of BPA Cyclic Oligomeric Carbonates[a]

Initiator	Amt. (M %)	M_W	M_W/M_n	I.V. (dL/g)
none	--	17,400	2.8	0.12
Ti(Oi-Pr)₂ (acac)₂	0.05	248,000	2.5	2.2
LiOPh	0.20	60,190	2.3	0.6
Al(O-iPr)₂ (Etacac)₂	0.10	282,000	2.3	2.7
Bu₄NBPh₄	0.10	280,000	2.2	2.7
Sodium Benzoate	0.10	222,700	12.7[b]	--
p-Toluenesulfonic Acid	0.5	1500	1.5	--
Lithium Stearate	0.10	60,200	2.5	0.6
n-Oct₂SnO	0.20	119,000	20.3[c]	--

[a]All reactions were carried out at 300°C for 0.5 hr.

The polymerization of macrocyclic carbonates possess some, but not all of the characteristics of a living polymerization. Initiation occurs when a nucleophile opens a ring at the carbonate linkage, affording a linear oligomer with a new carbonate (assuming phenoxide as nucleophile) and a reactive chain end. In propagation steps, the active chain ends (phenoxides) continue to attack cyclic oligomers, making longer chains until the supply of cyclics is depleted (Scheme 3). In this regard, the polymerization is living-like, because the ultimate molecular weight achieved will be the determined by the molar ratio of initiator to cyclic (Mn = g cyclic/moles initator). When a polymerization was carried to completion at a certain cyclic/initiator level, and then additional cyclic added, polymerization continued to a higher molecular weight. Termination only occured upon addition of a quenching agent such as acid or an alkyl halide. Of course, the viscosity of the polymer must be taken into account in such studies, since mixing in the melt may be difficult after polymerization ensues. Because nucleophilic attack on a carbonate moiety in a ring is very nearly equal in energy to attack on a carbonate in a linear chain, total equilibration occurs, if the reaction is allowed to proceed to completion. Due to the size and conformation of the monomer units, the reaction products typically contain <0.25% macrocycles. Chain-chain equilibration concomitant with propagation necessitates that dispersivities will approach 2.0.

The molecular weight of the polymer has been controlled by the use of bisphenols or diphenyl carbonate as chain transfer agents [19]. Addition of various levels of diphenyl carbonate to cyclic oligomer polymerizations provided polycarbonates terminated with phenyl carbonate end groups comparable to commercial polycarbonate grades. The properties of polycarbonates so generated have been measured, and are essentially equivalent to commercial polycarbonate (Table 6). Use of bisphenol A as a chain transfer agent leads to polycarbonate with phenol end groups. When the molar ratio of BPA to cyclic oligomer monomer units was relatively low (0.02-0.03) and the ratio of initiator to BPA was also low, then reasonable molecular weights of hydroxy-terminated polycarbonate were obtained. This material, which is difficult to generate by other means, is useful for preparation of polycarbonate copolymers.

200

Initiation
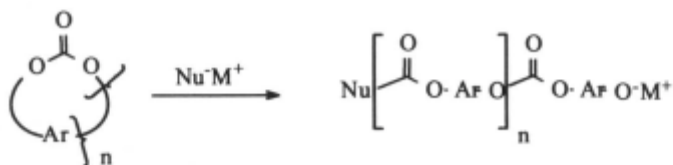
Propagation
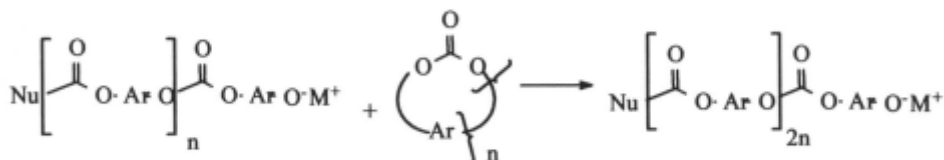
Termination
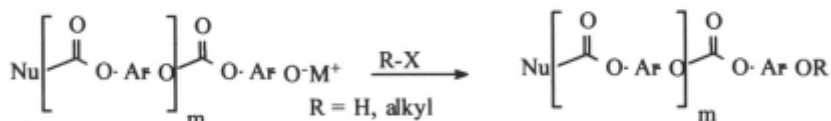
Chain Transfer
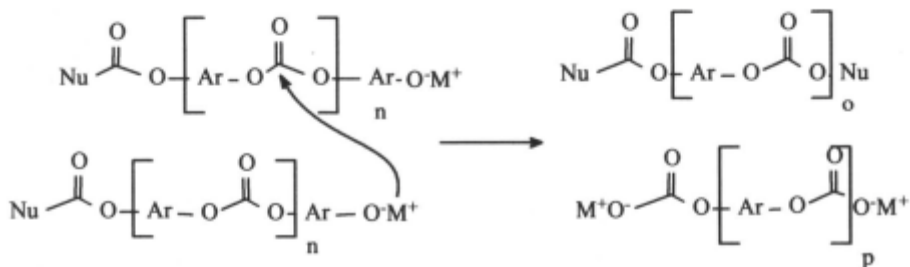
Scheme 3. Living-like polymerization of oligomeric carbonate cyclics, accompanied by chain-transfer reactions.

The low melt viscosity of the oligomeric cyclic carbonates made them attractive for a variety of processing/polymerization techniques [23]. The basic patent on polymerization of mixtures of cyclic oligomers covers many melt techniques such as casting, pultrusion, resin transfer molding, and reaction injection molding [24]. Polycarbonate composites have been fabricated from the cyclic oligomers with a variety of reinforcements, including glass, carbon, and polyimide fibers. With their low viscosity, wetting and consolidation of

the composite parts is enhanced, even at low resin pressures (<700kPa). Fiber loadings in excess of 70% have been demonstrated with final polymer molecular weights of >50,000.

Table 6. Mechanical Properties of Polycarbonate Derived from Cyclic Oligomers[a]

Property	Value
IV (dL/g)	1.0
DTUL (° C)	135.8
Tensile Yield (psi)	9024
Tensile Break (psi)	10,230
% Elongation	74
Flexural Yield (psi)	13,640
Flexural Modulus(psi)	317,400
Notched Izod (ft-lbs/in)	19.1

[a]Source: Ref. 19.

6.2.5 Polycarbonate copolymers from oligomeric cyclic carbonates.

The cyclization and polymerization chemistry which had been developed and optimized for bisphenol A is fairly general, and has been used for a variety of bisphenols [10]. Copolymers have been made by a variety of techniques, for example by preparation of co-cyclics with more than one type of bisphenol, or via polymerization of mixtures of cyclics. In addition, various functionalized polycarbonates have been prepared by incorporation of other functional groups such as ester, amide, ketone, sulfone, and urethane groups into a bisphenol monomer or oligomeric monomer [25][26]. Conversion to the bischloroformate and cyclization of these materials generally led to good yields of cyclic carbonate oligomers; in some cases, yields were excellent, since the formation of a cyclic directly from the monomer was possible. Subsequent polymerization under similar conditions to those described above afforded the functionalized high molecular weight polycarbonate copolymers (Equation 7).

X = SO2, ester, amide, imide,
    urethane, C=O, ether

n = 1-10

m = 20-50

(7)
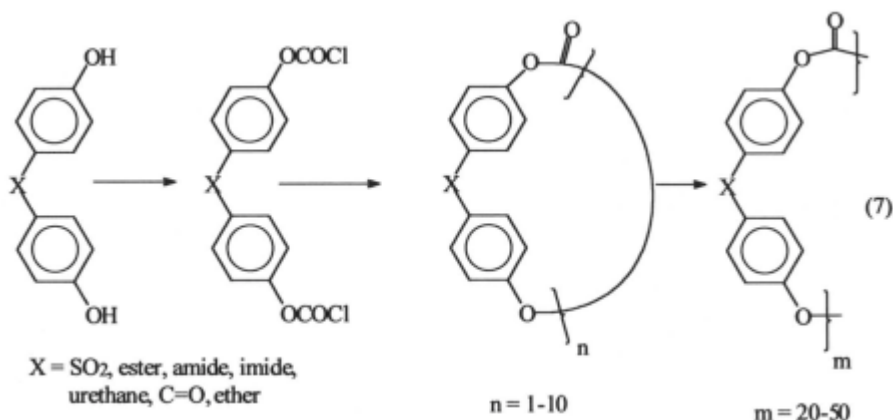
An interesting monomer which has been used for the preparation of macrocyclic carbonates is the spirobiindane bisphenol **1** (SBI). Due to its rigid structure, which forces the phenol functionalities into close proximity (7.00 Å vs 9.3 Å in BPA), cyclization reactions proceed more easily, with higher yields obtained; a 95% yield of macrocyclic carbonates was obtained, with cyclic dimer the major oligomer identified (Eq. 8) [27]. Because SBI is a chiral structure, diastereomers are observed among the cyclic oligomers. The rigid spirobiindane system also increases the glass transition temperature of the product polycarbonates which result from ring-opening polymerization: a 50:50 mixture of SBI and BPA affords a polymer with $T_g = 200°C$. However, the spirobiindane's propensity to form cyclics can also be a disadvantage. Polymerization of 100% SBI macrocyclic carbonates affords an equilibrated mixture with 9% cyclics present. Admixture with BPA disrupts the equilibrium, and fewer than 1% cyclics are found in 1:1 BPA:SBI copolymers.

1) $COCl_2$

2) Et_3N, NaOH
   CH_2Cl_2

(8)

1
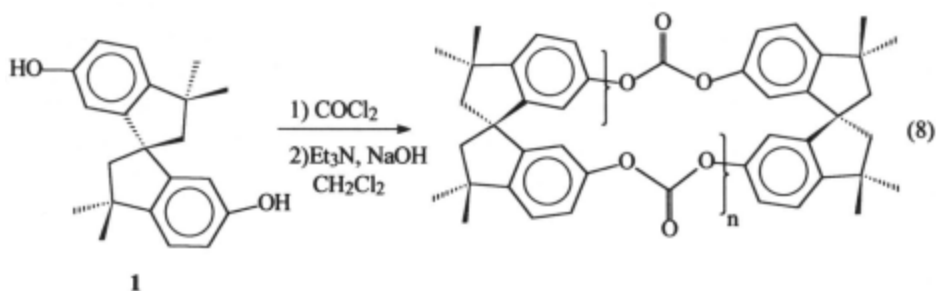
A cocyclic composition which led to polycarbonates with commercially interesting properties has been obtained from mixtures of BPA and hydro-quinone (HQ) [28][29][30][31]. Mixtures of BPA- and HQ-bischloroformates could be converted to cyclics in high yield, if the pH of the reaction mixture

was carefully controlled (Eq. 9). Control of pH was necessary to avoid extensive hydrolysis of the water-soluble hydroquinone oligomers. Although HQ cannot be incorporated into polycarbonate at levels greater than 10% using standard interfacial polymerization protocols, co-cyclics of HQ and BPA with up to 70/30 ratios of HQ/BPA remained soluble in CH_2Cl_2, and could be prepared in good yield. The mixtures of HQ/BPA bischloro-formates used as starting material could be prepared via an interfacial phosgenation reaction. Independently prepared hydroquinone *linear* oligomers had very low solubility in CH_2Cl_2 even at $DP = 2$, and were completely insoluble at $DP = 3$.

(9)

HQ-BPA Copolymer
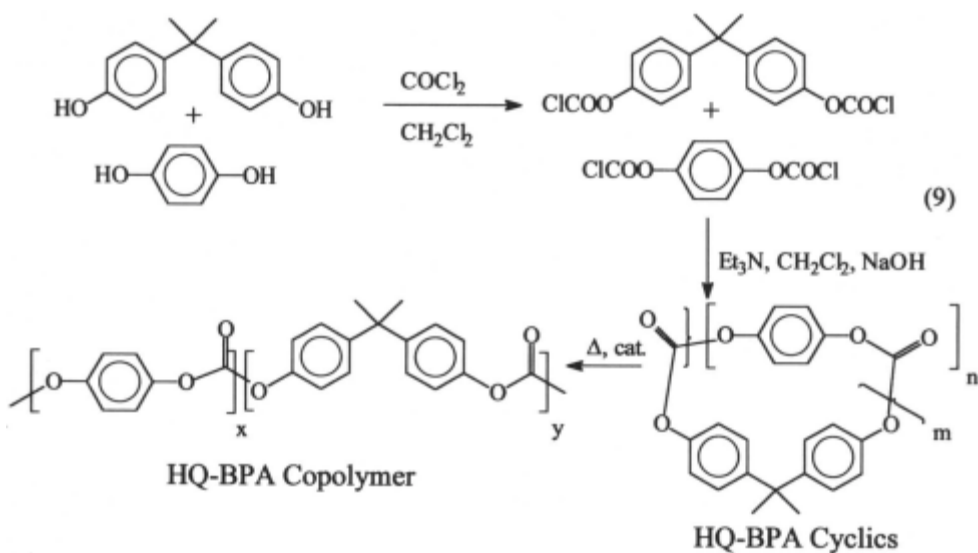
HQ-BPA Cyclics

Polymerization of the HQ/BPA co-cyclics afforded high molecular weight polycarbonates which showed dramatically increased solvent resistance. For example, molded bars of a 50/50 HQ-BPA copolymer formed in this manner retained their impact properties after immersion in Hess Hi-test gasoline, while being stressed in a 1% strain jig. Normal BPA-polycarbonate lost its impact properties after such immersion. The solvent resistance of the copolymers was observed at ratios of HQ / BPA > 40/60. These polymers were insoluble in CH_2Cl_2 or THF, although soluble in refluxing trichlorobenzene. At HQ/BPA ratios of over 60/40, some crystallinity could be observed by DSC. These HQ/BPA copolymers had glass transition temperatures of about 154°C, and a weak T_m of 313°C (11.0 J/g).

Several techniques were possible for copolymer formation, including:

1) co-polymerization of two different ring systems, 2) polymerization of a co-cyclic made from a mixture of two bisphenols, 3) use of a polymeric macroinitiator to ring-open cyclic polycarbonates, or 4) polymerization of cyclic carbonates, leaving an active chain end, which can initiate a second polymerization reaction. Copolymerization of two different cyclic aromatic carbonates leads to random copolycarbonates, assuming complete equilibration. In some cases, it was possible to combine cyclics of different functional types. For example, aromatic polycarbonate cyclics and polyarylate cyclics could be combined and copolymerized to form a polyestercarbonate [32]. Initiation of a 1:1 mixture of the cyclics by a tetraalkyltitanate provided a polymer with M_w = 66,000, M_n= 18,100, and T_g = 159°C. In another example, cyclic polycarbonates were co-polymerized with pivalolactone, using aluminum isopropoxide as the catalyst (Eqn. 10) [33]. The block copolymer had a glass transition temperature of 120°C, and a crystalline melting point of 232°C. Similar reaction with caprolactone led to a random polyester/carbonate.

(10)
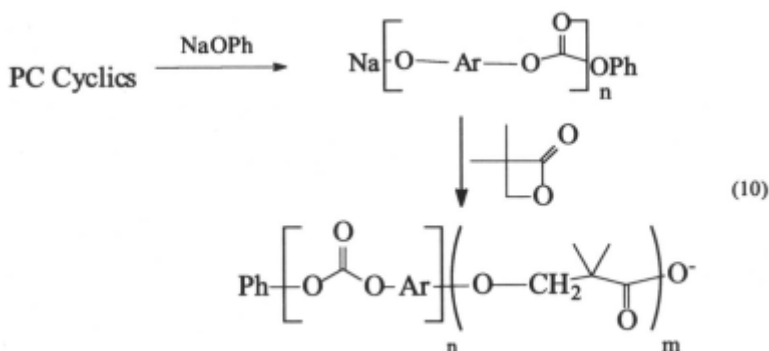
BPA poycarbonate-co-siloxanes have been prepared by several techniques [34][35]. Direct Copolymerization in the melt of mixtures of BPA cyclic carbonate oligomers with dimethylsiloxane cyclic tetramer led to a random copolymer, with 52-58% of the siloxane incorporated, but with no change in the polymer Tg (Tg = 148°C). Alternatively, the macroinitiator from either a cyclic siloxane polymerization or from a cyclic carbonate polymer-ization could be used to initiate polymerization of the other cyclic oligomer. The latter proved more effective, since the conditions for carbonate polymer-ization are more harsh than those required for siloxane polymerization, and more scrambling of the blocks occurred. Block copolymers were most effectively prepared by using an OH-terminated polycarbonate prepared from reaction of cyclic oligomers with BPA (Eqn. 11). Reaction with a chlorosilane-terminated siloxane oligomer led to block polycarbonate-co-siloxane with good

clarity, low glass transition temperature $(Tg = 110°C)$, and good mechanical properties.

$$(11)$$
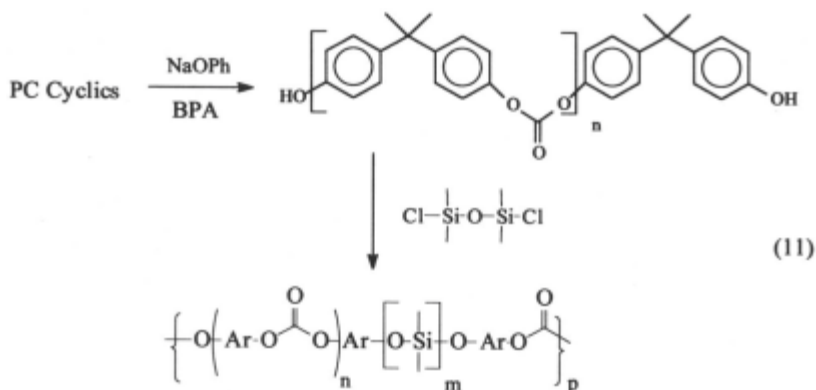
A variety of other copolymers have also been prepared using BPA cyclic oligomeric carbonates as starting materials. Phenoxide-terminated poly (2,6-dimethylphenylene oxide) has been used to initiate polymerization leading to a polycarbonate-co-polyphenylene oxide block copolymer (Eqn. 12) [36]. Epoxide/polycarbonates, polyimidecarbonates [37], copolyamidecarbonates [38], and copolyurethanecarbonates [39] have also been prepared.

$$(12)$$
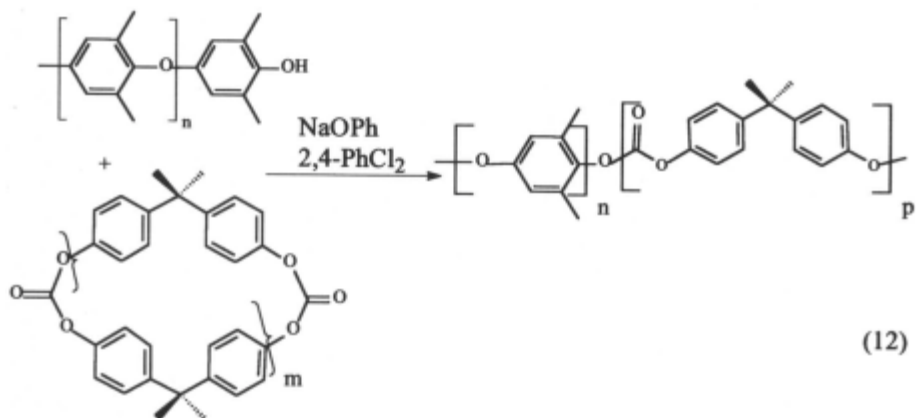
Cyclic oligomeric carbonates have also proven useful for preparation of highly branched or crosslinked polycarbonates. Although polycarbonate with low degrees of branching can be prepared via conventional techniques, highly branched or crosslinked structures cannot be formed by either interfacial or melt polycondensation. Because polymerization and processing occur nearly

simultaneously using ROP, branching and crosslinking are possible. Krabbenhoft and Boden have reported that 0.3 to 1.5 mol% of a trifunctional phenol such as 1,1,1-tris(4-hydroxyphenyl)ethane can be copolymerized in an extruder with BPA carbonate cyclics [40]. The polymer which results has a greatly enhanced shear sensitivity, varying by as much as 660% relative to linear polycarbonate resin. The greatest increases in shear sensitivity were seen at the lowest initiator levels (which also had the highest final molecular weights).

Crosslinked polycarbonates have been prepared by a variety of techniques. Rosenquist and Fontana reported crosslinking via copolymerization of a bis-cyclic carbonate (2) with BPA cyclic oligomers, using conventional initiators, resulting in a highly crosslinked resin (96% gel) and with a low swelling factor [41]. The copolymerization of BPA cyclic oligomers with polyfunctional epoxides was reported in the same paper. Brunelle and Shannon have reported the preparation and polymerization of macrocyclic polycyclics made by the co-cyclization of BPA-bischloroformate with tri- or tetraphenols (Eqn. 13) [10][42]. Incorporation of several mole percent of tetraphenols such as resorcinol sulfide was possible without formation of gel during the cyclization reaction. Upon anionic ROP, complete gelation occurred, leading to highly crosslinked polycarbonates (>99% gel) with elevated glass transition temperatures **(Tg = 171°C).** The same authors have reported crosslinking of high Tg systems such as SBI/BPA, and of the use of additives which lower the melting point (and therefore the processing temperature) of the cyclics.

2

$$(13)$$

Mixed Cyclic, mp = 175°

100% Crosslinked Polymer
Tg = 149° C
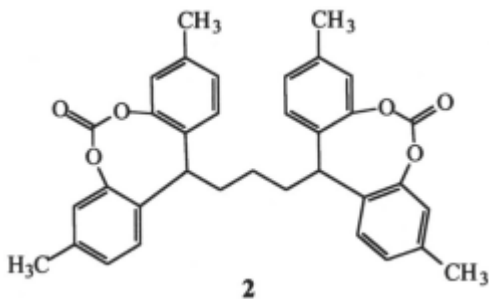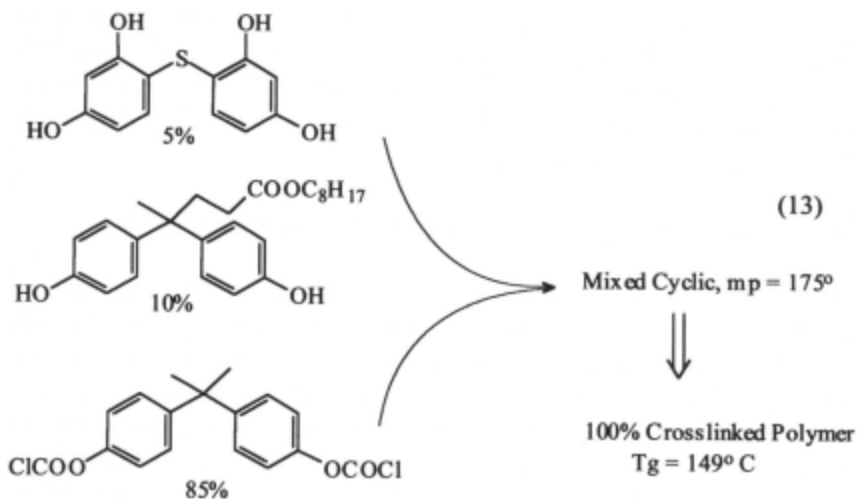
6.3 Preparation and polymerization of polyester cyclic oligomers

6.3.1 History

Alkylene phthalate polyesters such as poly[ethylene terephthalate] (PET) and poly[butylene terephthalate] (PBT) are commercial materials with a wide range of markets ranging from engineering thermoplastics to fibers. Both PET and PBT are semi-crystalline polymers with Tm's of 265°C and 225°C, respectively. Cyclic alkyl aryl esters based on iso- or terephthalic acid and aliphatic diols have been known for some tune. The cyclic oligomers are present in commercial polymers, and have been isolated by a variety of extraction techniques, typically antisolvent precipitation or soxhlet extraction followed by chromatography. The cyclic (3+3) trimer of poly (ethylene terephthalate) was first isolated in 1954 [43], and the dimer in 1969 [44]. An extensive study reporting the incidence of cyclic polyesters in 13 types of alkylene iso- and terephthalates was detailed by Wick and Zeitler in 1983 [45]. Various other authors have also studied cyclic oligomers obtained by extraction methods or melt equilibration methods [46][47][48][49].

Macrocyclic alkylene phthalates have been prepared by various low-productivity, classical high dilution techniques, involving multistep reactions. Zahn, et al., for example prepared macrocyclic oligomers via reaction of oligomeric diols with oligomeric diacid chlorides, according to Scheme 4 [50][51]. Very high dilution is typically necessary (< 0.003 M), with an increase in concentration to 0.01 M reducing isolated yields of cyclic to only

1.5-7.9%. A crystal structure of the macrocyclic (2+2) dimer of butylene terephthalate has been published [52]. Despite the previous work on oligomeric cyclic alkylene phthalates, no reports of direct formation of cyclics via reaction of monomeric phthalate derivatives with monomeric diols could be found until the recent report of Brunelle, et al [53].

6.3.2   Preparation of polyester cyclic oligomers from acid chlorides

It seemed reasonable to assume that PBT cyclics could be prepared by a routine extension of the earlier *pseudo*-high dilution chemistry used for the preparation of cyclic carbonate oligomers. The reaction of terephthaloyl chloride (TPC) with diols such as 1,4-butanediol was expected to be fast enough to ensure that the concentration of acid chlorides did not build up during condensation, which would favor polymer formation. Thus, slow addition of equimolar amounts of TPC and butanediol to an amine base under anhydrous conditions should form cyclic oligomers. However, when such reactions were carried out using triethylamine, pyridine, or even 4-dimethylaminopyridine as bases only small amounts of cyclic oligomers (<5% by HPLC analysis) were formed. (The products were identified by comparison to authentic materials isolated from commercial PBT by the method of Wick) [53].
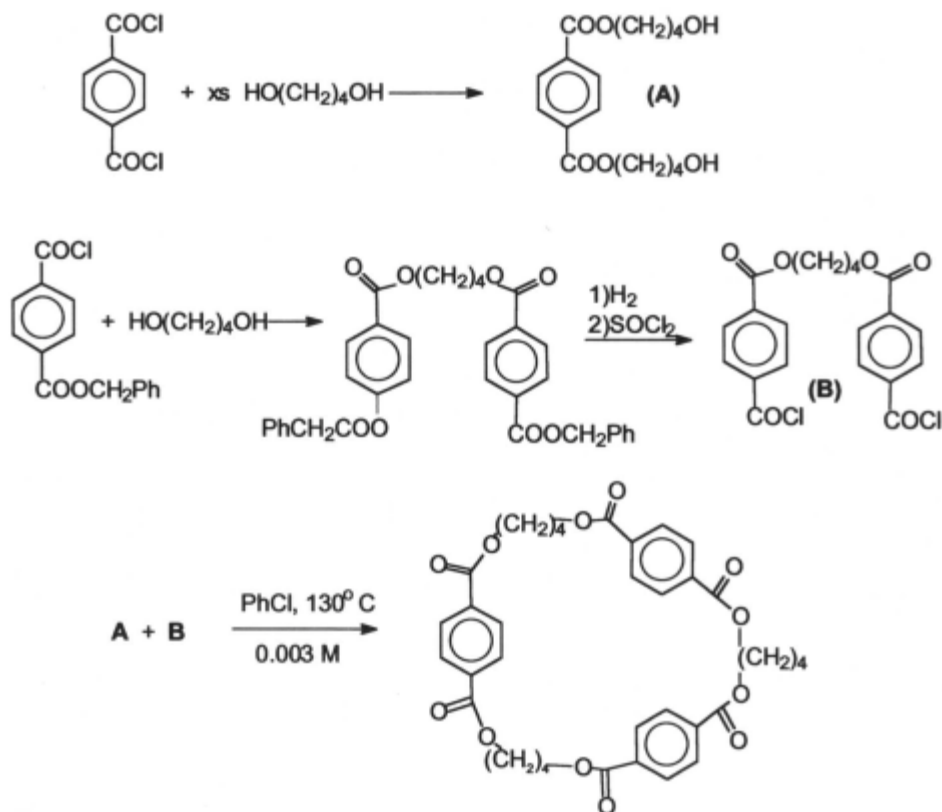
Scheme 4. Preparation of cyclic PBT oligomers via high dilution condensation of oligomers.

Investigation of model reactions revealed that the reaction of aromatic acid chlorides with diols such as butanediol or ethylene glycol was too slow to be useful for kinetically-controlled *pseudo*-high dilution reactions carried out at low temperatures (0-40°C). For example, reaction of butanediol with benzoyl chloride using stoichiometric pyridine or triethylamine as base provided only 5% or 11% butylene dibenzoate, respectively, after one hour at ambient temperature. Although monobenzoate formed rapidly, complete conversion to dibenzoate required 24 hrs reaction, even using a two-fold excess of pyridine. A variety of amines were tested using this model system, showing that most conventional amines gave poor yields of dibenzoate (Table 7). However, it was noticed that less hindered amines gave higher yields. In fact, very unhindered amines such as diazabicyclo[2.2.2]octane (DABCO) or quinuclidine have very fast reactions and a quantitative yield of dibenzoate was formed within 15 minutes at ambient temperature.

Table 7. Reaction of benzoyl chloride with butanediol using amine bases

$$2 \text{ PhCOCl} + \text{HO}(CH_2)_4OH + 2 \text{ amine} \rightarrow$$
$$\text{PhCOO-}(CH_2)_4\text{OCOPh} + 2 \text{ amine-HCl}$$
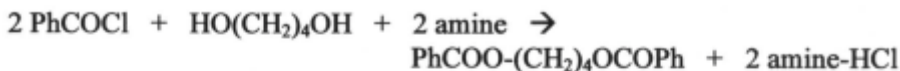
Amine	Solvent	time	% dibenzoate
Et₃N	THF	24 hr	30
"	CH₂Cl₂	3 hr	30
Pyridine	CH₂Cl₂	3 hr	46
"	THF	3 hr	12
"	dioxane	3 hr	22
"	EtOAc	3 hr	21
4-DMAP	CH₂Cl₂	3 hr	22
Me₂N-octyl	CH₂Cl₂	3 hr	67
MePyrrolidine	CH₂Cl₂	1 hr	75
DABCO	CH₂Cl₂	15 min	99
Quinuclidine	CH₂Cl₂	15min	97

Source: Ref. 53.

Cyclization reactions were carried out by concurrent addition of equimolar amounts of isophthaloyl chloride or TPC in CH_2Cl_2 and butanediol in dry THF to a slight stoichiometric excess of DABCO or quinuclidine in CH_2Cl_2 over one hour, with a final product concentration of 0.2 M [53]. HPLC analysis of the THF-soluble portion of the product indicated cyclic oligomers as the major products, with small amounts of linear oligomers (< 2%) also present. Isophthalate cyclics were isolated in 45% yield, and PBT cyclics in 30% yield, after filtration to remove insoluble polymer and flash chromato-graphy to remove linear oligomers. This was the first example of the direct formation of alkylene terephthalate cyclics from reaction of monomeric diols and diacid chlorides. The major cyclic formed in both cases was the 2+2 dimer, which accounted for 40-65% of the total cyclic yield, with diminishing amounts of higher cyclics. The highest oligomer observed by HPLC had **DP = 7.** Linear oligomers were present in amounts of 0.1-2%. Cyclic dimer, trimer, and tetramer were separated by column chromatography and were shown to be identical to authentic cyclics which had been isolated from commercial PBT using literature techniques. Linear oligomers were compared to oligomers prepared by reaction of dimethyl terephthalate with excess butanediol.

With the first demonstration of direct cyclic polyester oligomer synthesis, a significant amount of work was carried out in attempts to increase the reaction yield and to eliminate unwanted linear oligomers. Three side reactions which interfere with synthesis of cyclics were identified: reaction of the amine with acid chloride to form an acyl ammonium salt, followed by decomposition to an amide (Eqn. 14); reaction with CH_2Cl_2 to form a salt (Eqn. 15); and hydrolysis of the acid chloride, forming carboxylate via catalysis with the amine via the acyl ammonium salt (Eqn. 16). The first two reactions could be avoided by minimizing contact time between the reagents, and the third by carefully drying all reagents. Use of dry solvent was found to be particularly important, since even 100 ppm of water in the solvent will hydrolyze 3.7% of the acid chloride in a reaction carried out at 0.2 M monomer concentration. When hydrolysis of acid chloride occurred, either anhydride or carboxylic acid-containing polymers would be formed, products which would interfere with polymerization. Furthermore, hydrolysis would remove acid chloride from the reaction, damaging control of balanced stoichiometry.

(14)

(15)

(16)
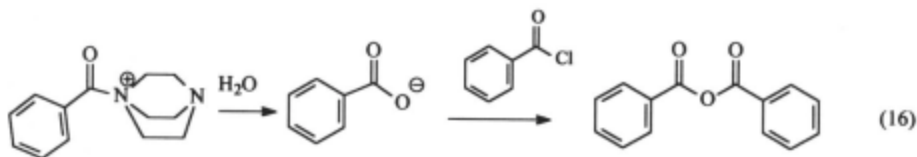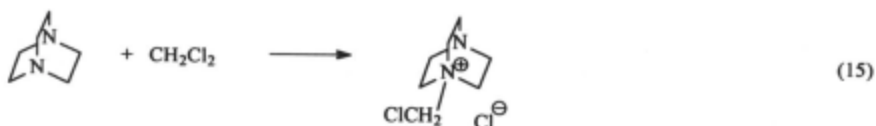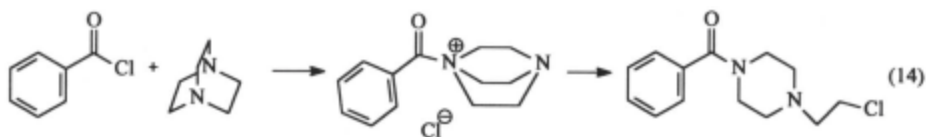
Ultimately, only catalytic amounts (2.5-10%) of unhindered amine were used, with Et_3N making up the remainder of the organic base, minimizing unwanted reactions of the very reactive unhindered amines. Also, a means for delivering neat butanediol was devised, avoiding the need to use THF, which was also a potential source of water. Incorporating these changes into the process allowed the formation of PBT cyclics in 0.25 M reactions carried out in one hour, with yields as high as 85% and linear oligomer levels under 1.0%

(Eqn. 17). The remainder of material was higher molecular weight polymer, which was insoluble in the reaction medium, and could be removed directly by filtration.

Cyclics 80% (17)
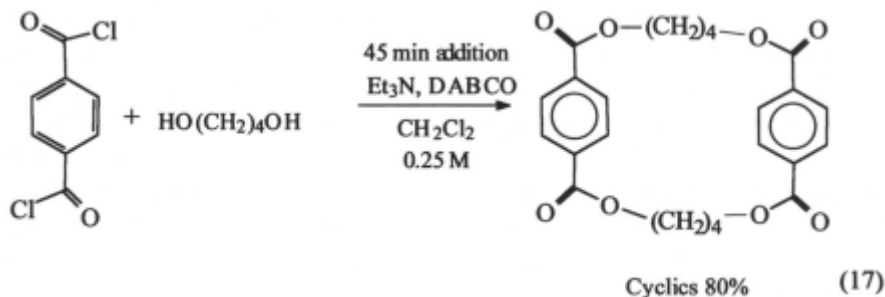
Removal of the traces of linear oligomer proved to be important, since even the presence of 1% linear oligomer limited the molecular weight achievable upon ROP. An in-situ cleanup procedure was developed in which a slight excess of diacid chloride was added at the end of the reaction, converting any hydroxy-butyl-terminated linear oligomers to acid chloride-terminated oligomer. Upon quenching with water, hydrolysis to the carboxylic acid occurred, making the linears insoluble in CH_2Cl_2, and easily removed by the same filtration used to remove polymer (Eqn. 18). Traces of cyclic oligomeric anhydrides which had been formed by incidental hydrolysis of acid chlorides were removed by treatment of the crude product solution with NH_4OH, which converted them into amide-acid oligomers, which also were removed in the filtration step (Eqn. 19). Typically, the linear oligomer level by quantitative HPLC was less than 0.2%. Once optimized, the reaction of terephthaloyl chloride with butanediol was easily scaled to several liters, then to a 100-gal reactor, which was capable of producing 10 kg of cyclic PBT oligomers per batch in a 45 minute reaction at 0.25 M.

(18)

(19)
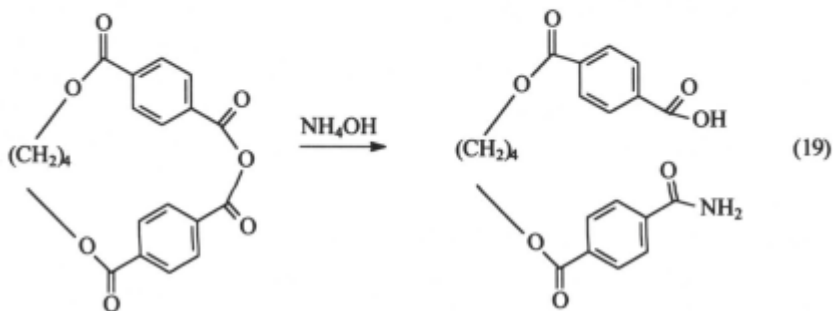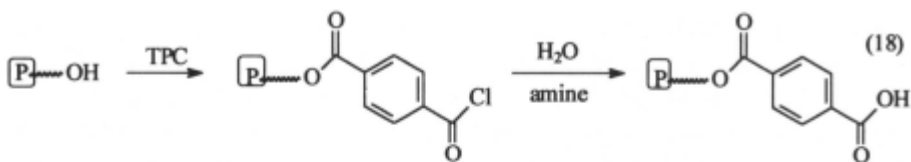
Using similar procedures, a variety of alkylene phthalate cyclics were prepared in high yields via direct reaction of diols with diacid chlorides (Table 2) [53]; other than 100% PBT and 5% PET/PBT (molar) co-cyclic oligomers, these reactions were not optimized. The yields of cyclic oligomers from terephthaloyl chloride were somewhat lower than those from isophthaloyl chloride using either ethylene glycol or neopentylene glycol. In the former case, only a trace of cyclic (2+2) dimer was present, due to ring strain, and cyclic (3+3) trimer was the predominant species; a correspondingly higher amount of polymer was formed. It is not surprising that the isophthalates, which have a bent conformation, were formed more readily than the terephthalates.

6.3.3   Polyester cyclic oligomers via ring-chain equilibration

Formation of cyclic esters via ring-chain equilibration of polymers in dilute solution (depolymerization) has been known since the pioneering work of Carothers, *et al.* in the 1930's [54][55][56]. This procedure is particularly effective for the preparation of small-ring esters and carbonates, such as caprolactone, which are volatile and easily removed from the reaction vessel. With the non-volatile macrocycles required as precursors to engineering thermoplastics such as PBT, the primary limitations for commercial exploitation have been the long reaction times, and the large amounts of solvent necessary to achieve high yields. For example, equilibration of linear oligomers at 0.07 M in m-terphenyl required a reaction time of 24 hours, with continuous removal of butanediol, under vacuum [57]. A Japanese patent [58]

reports the depolymerization of poly(ethylene terephthalate) [PET] to cyclic PET, requiring reaction at 240-280°C in **α-methylnaphthalene,** using 1.0 wt percent of PET for an unspecified time, with an unspecified amount of catalyst. Attempts to depolymerize PBT polymers under such conditions afforded poor results, with mixtures of cyclics, linear oligomers, and polymer being formed. According to Jacobsen-Stockmayer theory, ring-chain equilibration of a polymer will lead to a mixture of cyclic oligomers and polymer in which a critical monomor concentration (CMC) can be defined for each monomer structure [59]. At concentrations below the CMC, only cyclics will be present, while above that concentration, mixtures of cyclics and polymer will be present.

Table 8. Preparation of Alkylene Phthalate Cyclic Oligomers[a]

Cyclic[b]	% Yield[c]	FTIR[d] (cm^{-1})	^{1}H NMR[e] (ppm)	Cyclic ratio[f]
PEI	80	3021, 1725, 1296, 1206	4.17-4.73 (4H) 8.11-8.14 (4H)	74, 13, 6, 2
PET	60	3021, 1725, 1286, 1209	4.65-4.77 (4H) 7.51-8.93 (4H)	39, 21, 14, 10, 7, 3, 1
PBI	85	3021, 1720, 1306, 1212	1.93-2.08 (4H) 4.39-4.50 (4H) 7.49-8.65 (4H)	63, 19, 8, 7, 3, 1
PBT	82	3022, 1718, 1274, 1206	1.96-2.18 (4H) 4.34-4.42 (4H) 7.83-8.11 (4H)	51, 26, 11, 8, 2, 2
PHI	75	3021, 1718, 1307, 1216	1.56-1.86 (8H) 4.34-4.42 (4H) 7.47-8.65 (4H)	59, 23, 11, 6
PHT	55	3025, 1717, 1274, 1209	1.55-1.85 (8H) 4.35-4.42 (4H) 8.07-8.11 (4H)	33, 18, 9, 5, 3, 1
PNI	80	3022, 1721, 1278, 1208	1.06-1.34 (6H) 4.25-4.38 (4H) 7.19-8.60 (4H)	62, 26, 12
PNT	53	3021, 1721, 1278, 1208	1.14-1.46 (6H) 4.27-4.97 (4H) 7.67-8.21 (4H)	68, 10, 2
PDI	53	3024, 1724, 1306, 1206	3.81-3.94 (4 H) 4.42-4.44 (4H) 7.18-8.47 (4H)	83, 14, 1
PDT	49	3021, 1719, 1278, 1216	3.78-3.87 (4H) 4.43-4.49 (4H) 7.95-7.98 (4H)	58, 26, 8

[a]Cyclic oligomers prepared from IPC or TPC and diol; purified by filtration through celite to remove polymer and flash chromatography to remove linears. [b]I - isophthalate, T = terephthalate, E = ethylene, B = butylene, H = hexylene, N = neopentylene, D = diethylene glycol. [c]Isolated yield after removing polymer and linears. [d]Solution FTIR in CHCl$_3$. [e]CDCl$_3$ solvent. [f]Ratio of peaks on HPLC.
Source: Ref. 53.

The first efficient preparation of alkylene phthalate cyclic oligomers via ring-chain equilibration appeared in the patent literature in 1995 (Eqn. 20) [60]. Laboratory studies were carried out in glassware in o-dichlorobenzene, since PBT is quite soluble at its reflux temperature, and reaction rates were also reasonable at that temperature. Larger-scale work was carried out in either 1-L or 8-L stainless steel autoclaves, using o-xylene as the solvent, since use of non-chlorinated solvents was preferred. Most of the early work was carried out using tin catalysts of various types. Early results indicated that tin catalysts were far more effective than titanates for the ring-chain equilibration reaction. Cyclic stannoxanes **3** or **4**, prepared from **Bu₂SnO** and ethylene glycol or 2,2-dimethyl-1,3-propanediol were used in most of the early reactions, while scoping the conditions necessary for depolymerization. Equilibration in refluxing o-dichlorobenzene took about 30 min to 2 hrs, depending on reactant and catalyst concentrations.
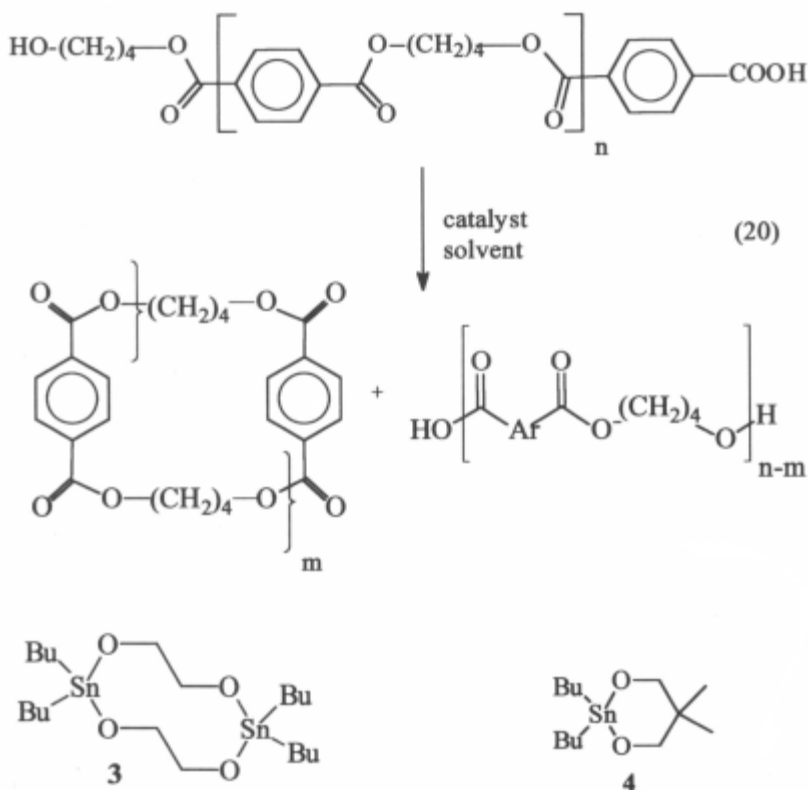
Efficient use of titanate catalysts for the preparation of PBT cyclics via depolymerization in a continuous reactor was patented in 1997 by Brunelle, et al [61]. At about the same time, Bryant and Semlyen began publishing a series of papers on preparation of cyclics via ring-chain equilibration [62][63][64]. Brunelle concentrated on efficient throughput reactions to form mixtures of cyclics with careful attention paid to avoid linear oligomers, in order to utilize the cyclics for ROP reactions. Bryant and Semlyen concentrated on isolation and characterization of the oligomers by fast atom bombardment mass spectrometry, tandem HPLC-MS, and X-ray crystallography. Bryant and Semlyen, et al. also published papers on a variety of other cyclic ester and ether ester oligomers using the same technology, including tetraethyleneglycol iso- and orthophthalates, decamethylene phthalates, and polyethylene terephthalates.

Depolymerization reactions were carried out by Brunelle, et al. simply by dissolving commercial PBT in dry o-DCB at reflux, then adding the equilibration catalyst [60]. Surprisingly, extremely dilute solutions were not necessary to form reasonable yields of cyclic oligomers. Using Valox® 315 (which has a weight average Mw of about 100,000 relative to polystyrene standards) as the starting material, about 50% cyclics were detected by GPC in reactions carried out at 0.10 M (1.68 wt percent) in o-DCB. Decreasing the concentration to 0.050 M gave an increase to about 90%, and increasing the concentration to 0.15 M gave a decrease to 33% yield of cyclics (see Table 8). Figure 2 compares the level of cyclics on a molar, weight percent, or yield basis as a function of reaction concentration. Note that as the reaction concentration dropped, the yield increased to near 100%, as predicted from theory. However, the amount of cyclic PBT on a molar or weight percent basis remained constant at the critical monomer concentration, which is about 0.050 M, regardless of reaction concentration. In fact, if one calculates the amount of cyclic present in the melt (1-2%), it fits on the curve, at about 0.05 M cyclic. *The same amount of cyclic was generated via the ring-chain equilibration process regardless of the reaction concentration*; only the amount of polymer which remains as a byproduct differed, and hence the overall yield (i.e. cyclics divided by [cyclics + polymer]). Unfortunately, the theory breaks down at very low reaction concentrations, since some "polymer" must always be formed, because the starting material has end groups; thus a 100% yield of cyclic can never be achieved.

Table 9. Effect of Depolymerization Concentration on Yield of Cyclic PBT[a]

Conc. (M)	% Cyclic PBT
0.05	89.7
0.075	61.1
0.10	50
0.15	32.9
0.20	25.9
0.30	15

[a]Reaction in o-DCB at reflux using 1.0 mole % cyclic stannoxane **1** (2% tin).
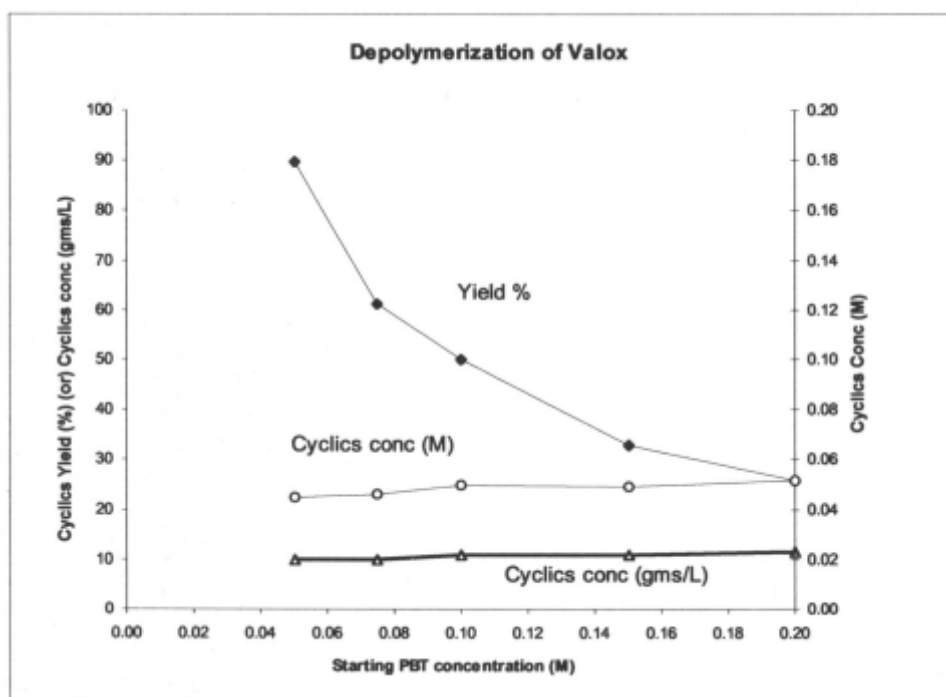
Figure 2. Amount of Cyclic as a Function of Reaction Concentration

Figure 3 shows the progress of reactions carried out at various concentrations at reflux in o-DCB using 2 mole % of cyclic stannoxane **3** as catalyst. Most reactions, except the most dilute, reached equilibrium in about one hour at that temperature. As the concentration of polymer and of catalyst were reduced, kinetics require that the rate to achieve equilibrium will be slower. Reaction temperature seemed to have only a slight effect on the equilibrium position, with similar yields being obtained from reaction in

slower.   Reaction temperature seemed to have only a slight effect on the equilibrium position, with similar yields being obtained from reaction in dichlorotoluene at 180° C or 200° C, or in trichlorobenzene at 214°C; the equilibrium was achieved more rapidly at the higher temperatures, as expected. Solubility of the starting polymer in the chosen solvent was very important. Reaction rates were depressed whenever the polymer was not completely dissolved at the reaction temperature.
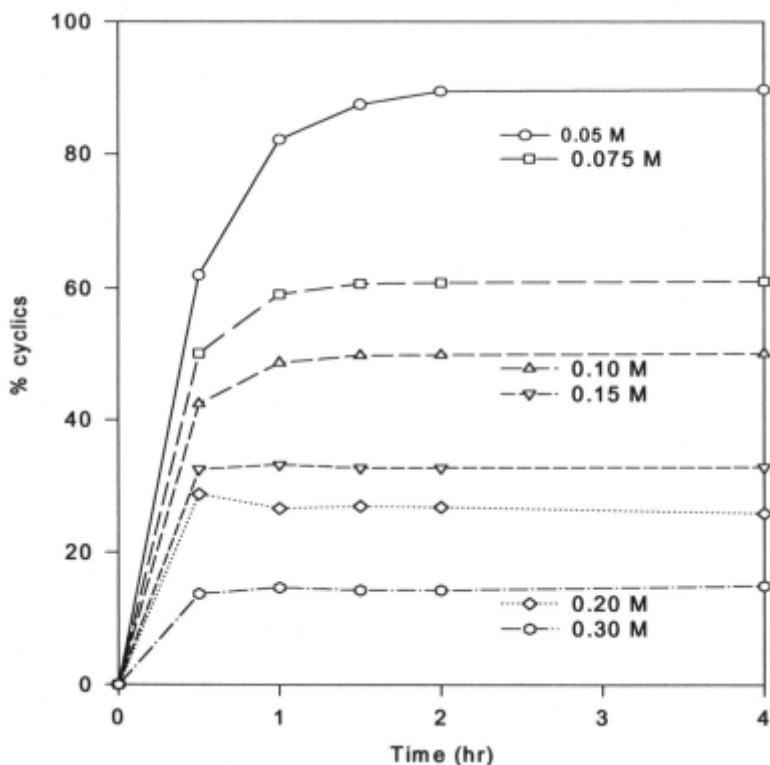
Figure 3. Depolymerization of Valox 315

Use of scrupulously dry solvents was necessary when using titanates as catalysts, to prevent their hydrolysis [61]. The tin catalysts are more robust and less sensitive to water than the titanates, since hydrolysis of a stannoxane leads to dibutyl tin oxide, which can react with a diol to cleave water and re-form a stannoxane, whereas hydrolysis of a titanate affords titanium dioxide,   which

cannot be regenerated into an active catalyst. However, removal of traces of tin catalyst before isolation was necessary, to prevent premature polymerization, and proved to be cumbersome, so the easily quenchable titanates became the catalysts of choice. Brunelle, et al. also found that hydroxybutyl-terminated oligomers could be eliminated from the reaction products by carrying out the depolymerization reaction at elevated temperatures. Back-biting of the hydroxybutyl chains forms tetrahydrofuran and a carboxylic acid-terminated oligomer, which was easily removed from the product solution by filtration (Eqn. 21) [61].
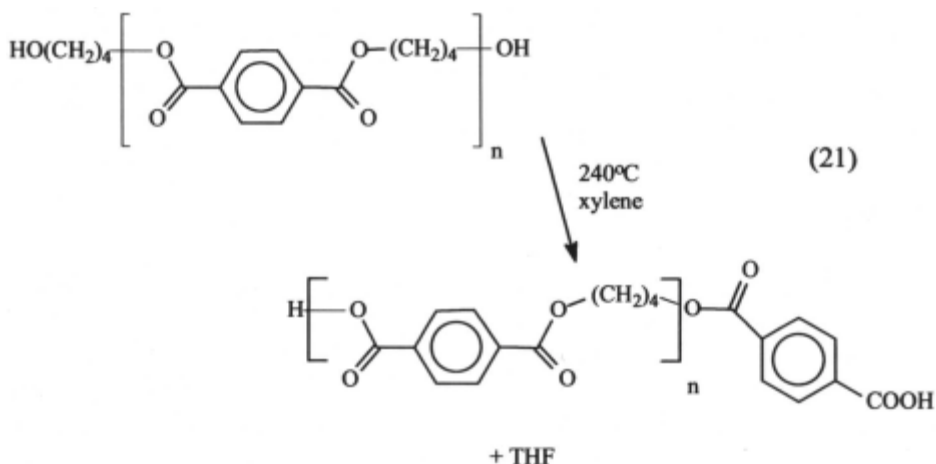
Initially, analyses for cyclics was carried out using a standard GPC column (Varian TSK columns), integrating the high vs low Mw sections. However, clean separation of polymer from cyclics was not possible. Furthermore, that method did not distinguish between oligomeric linear and cyclic materials. An HPLC method was developed, using an internal standard for accurate quantification of cyclics. In this method, an inert standard with a high molar absorbtivity, which had been calibrated against a standard solution of PBT cyclics, was added to the depolymerization reaction. HPLC analysis, integrating the standard vs the 6 cyclic peaks (dimer through heptamer) gave the yield of cyclics. This method was quite accurate, and also allowed quantification of the level of linear oligomers formed in the process, but required separation of the byproduct polymer before analysis. A faster method utilized GPC analysis, using a special low molecular weight column (Polymer Labs mixed E) which afforded near baseline separation of cyclics from polymer. Crude samples could simply be dissolved in **HFIP/CHCl$_3$** and injected directly. Although resolution of linear oligomers was not possible

using the GPC method, it was found not to be necessary since production of linears was essentially eliminated at high temperatures. As the concentration of polymer in the depolymerization reaction was increased, the yield of product decreased, as mentioned above. The nature of the remaining polymer also changed, with higher molecular weight polymer being recovered at higher concentrations. The amount of linear oligomer did not seem to vary in reactions carried out in o-DCB (Table 10).

Table 10. Effect of Depolymerization Concentration on Cyclics and Polymer

Conc.	% Cyclics (GPC)	% linears (hplc)	Polymer M_w	Polymer M_n
0.20	26		14,700	10,200
0.10	50	1.3	10,500	7000
0.75	65	1.4	6100	2600
0.05	89	1.1	3800	2040

6.3.4 Mechanism for formation of cyclics via depolymerization

The mechanism for cyclic formation via depolymerization is basically a transesterification mechanism, as outlined in Scheme 5. Metal alkoxides such as tetraalkyl titanates or dibutyl tin alkoxides have proven to be the most efficient catalysts for such reactions. The metal alkoxides function by activating a carbonyl via complexation, then transferring an alkoxide ligand. Thus, a linear polymer will interact with a metal alkoxide catalyst to tranfer an alkoxide onto the polymer chain, forming a species such as **I**, and releasing a linear alkoxide which is terminated with the transferred ligand (**II**). The original polymer chain length (n) will be decreased by m units in such a reaction. The metal terminated polymer **I** can then react either by chain-chain transfer (polymerization reaction), or by a back-biting reaction to form cyclics. The degree of cyclization vs polymerization can only be controlled by the concentration of species **I** in solution. Dilute solutions favor *intra-* rather than *inter*molecular reactions. Cyclization to cyclics with degreee of polymerization $p+1$ releases another linear polymer chain terminated with a metal (**Ia**), which is shorter in length by $p+1$ units, and which can continue to react to form cyclics. Eventually, equilibrium is reached, and the linear chains (**I, Ia, II**) react degenerately at the same rate as they form cyclics. Active intermediate **I** could also be formed by direct reaction of an alcohol-terminated polymer with the metal alkoxide, with loss of free alcohol, but this event is far less likely than reaction at the interior of a chain, because the number of end groups is small by comparison. In this regard, metal alkoxides have the advantage over Bronsted acids, which can only catalyze reactions of chain ends (i.e. attack of **RCH$_2$OH**

on a chain end of an ester via backbiting, using acid catalysis).
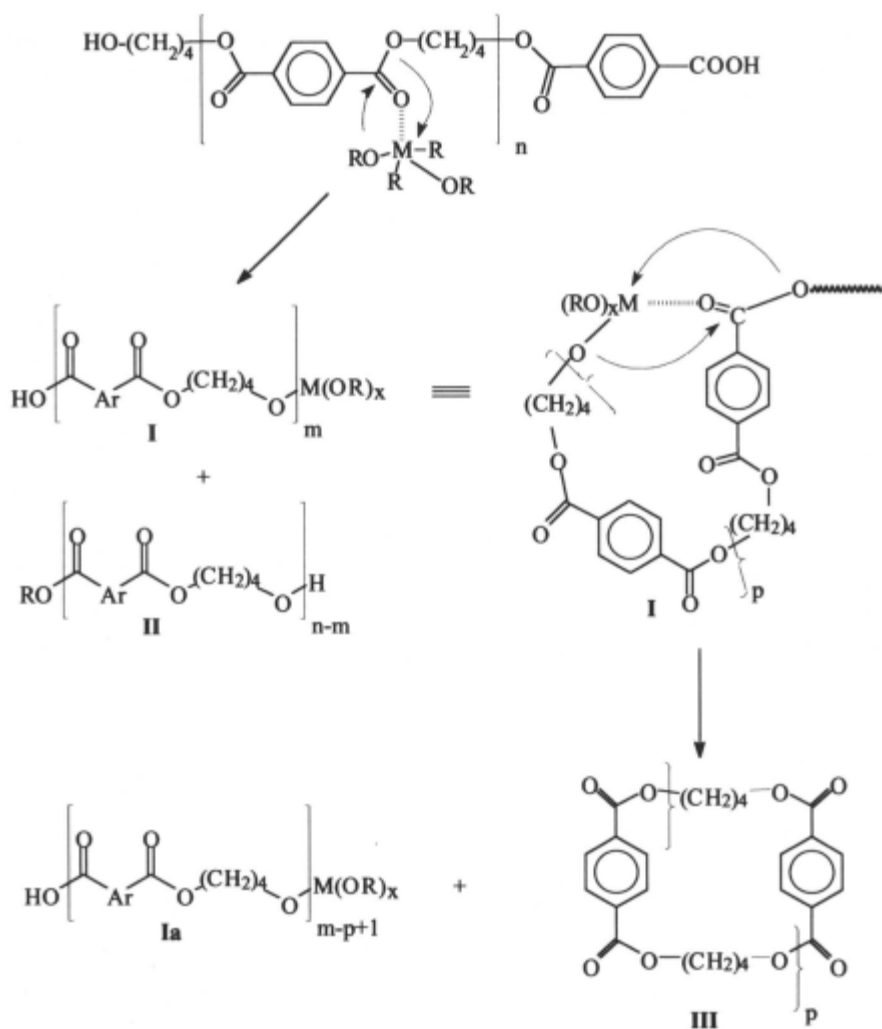
Scheme 5. Mechanism for metal alkoxide catalyzed formation of cyclics via depolymerization.

Figure 4 shows the distribution of cyclics formed in a typical reaction as a function of time. It can be seen that initially the levels of longer chains are higher than at the end of reaction. Initially many long polymer chains are present in solution from which cyclics can form. As the reaction proceeds, not only are the linear chains reduced in size, but also the cyclics themselves can be

attacked by the metal alkoxide. Such an attack forms a short polymer chain such as **I** or **Ia**, which can react to make a smaller cyclic. Entropy favors the formation of the smallest cyclics, as long as ring-strain is not involved. An attempt at correlation of the experimental results with theory has been presented by Hubbard, Brittain, et al [65].
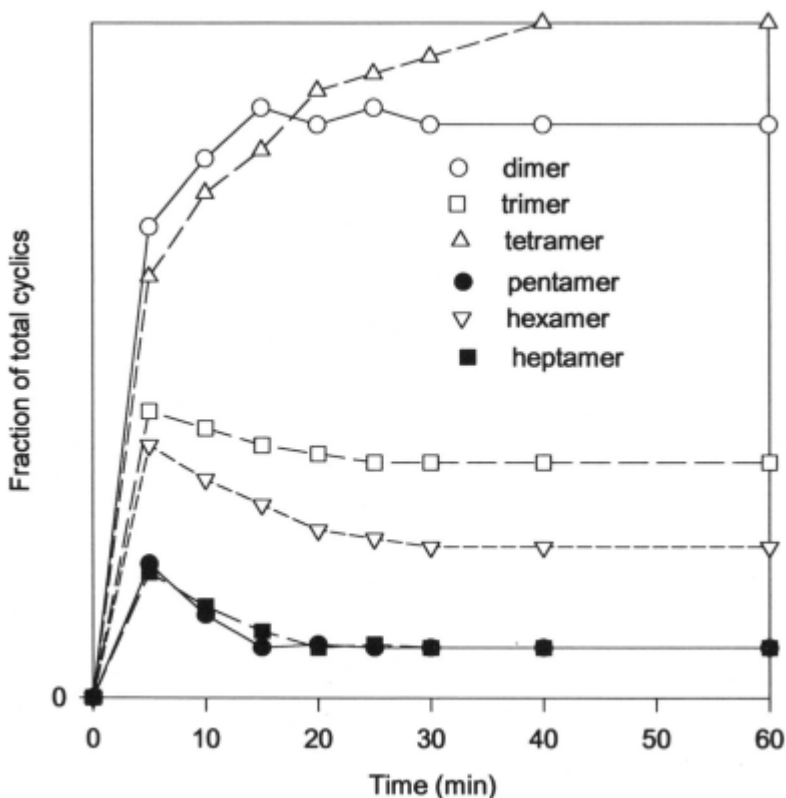
Figure 4. Cyclics distribution with time during depolymerization.

6.3.5 Polymerization of oligomeric ester cyclics

With a supply of oligomeric cyclic phthalates readily available from two routes, the study of bulk ring opening polymerization became feasible. Because reactive processing applications were most appealing, and because PBT or PET cyclics led to crystalline, insoluble polymers, melt polymerizations were the method of choice. Additionally, the extremely low melt viscosity of

PBT cyclics (about 30 cP at 190°C) [66] made melt processing extremely attractive. Visually, the mixture of PBT cyclic oligomers began to melt at about 140°C, and was completely molten at 160-190°C. DSC showed a broad melting range (100-175°C), with peaks at 130°C and 160°C; the total melting endotherm was 68 J/g. Upon a second heating DSC indicated some crystallization occurring before remelting with a peak temperature of 163°C (ΔH = 32 J/g) [53]. It appears that the nature and amount of crystallinity in the cyclics can be a function of the isolation technique (melt vs antisolvent).

Polymerization of PET cyclic oligomers at 275-310°C has been reported by Goodman and Nesbitt [46]. They claimed that a linear polyester was formed when the macrocycles are heated with a catalyst neat or in 2-methylnaphthalene at 240°C. They also stated that scrupulously dried material does not polymerize in the presence of antimony oxide under dry nitrogen, suggesting that a second initiating substance (presumabley water) was necessary. Polymerization was also reported with tetramethyl titanate, lead oxide, or calcium oxide, but not with p-toluene sulfonic acid. PBT cyclics melt substantially lower than the PET cyclics, and also, it has been shown that polymerization can be carried out below the melting point of the product polyester, and therefore the polymerization reaction was studied in some detail [53].

Although many types of compounds can initiate polymerization of oligomeric cyclic esters, certain tin and titanium initiators were most effective (Table 10). Either commercially available titanates [tetrakis-(2-ethylhexyl)-titanate {TOT} or **Ti(Oi-Pr)$_4$**] or cyclic stannoxanes such as **3** were effective initiators for polymerization at levels of 0.05-1.0 mole % based on monomer units [53]. These initiators operate via the same Lewis acid activation-insertion mechanism described above under depolymerization (Section 6.3.4).

The mechanism is similar in principle to the ring opening of cyclic carbonates described in Section 6.2.4, in that it involves initiation to form an active chain end, followed by propagation reactions continuing until all the cyclic oligomers are depleted and the ring-chain equilibration becomes degenerate. In this case, the initiator becomes built into the polymer, which is not terminated unless quenched. The titanate initiator becomes a star point from which polymer chains can grow in four directions. Again, due to their size, the cyclic oligomers are nearly strain-free, and the polymerization is almost thermoneutral, leading to complete equilibration of ester groups (i.e. initiation, propagation, and chain transfer have nearly the same rates). Polydispersivities therefore approach 2.0, and were typically in the range of

2.0-3.0, as in conventional polycondensation of DMT with butanediol (Commercial Valox® 315 has $M_w/M_n \sim 2.3$). GPC traces are typically monomodal, with a small amount (1-3%) of cyclics remaining, presumably the equilibrium amount. DSC analysis of a mixture of cyclic oligomers containing stannoxane **3** showed only the melting endotherm **($\Delta H = 68$ J/g),** with no exotherm evident. Cooling showed the crystallization of the polymer, and the second heating showed only the melting point of the PBT polymer at 213°C **($\Delta H = 54$ J/g);** the polymer had **$M_w = 117,000$,** and was 97% polymerized by GPC.

Initiation:
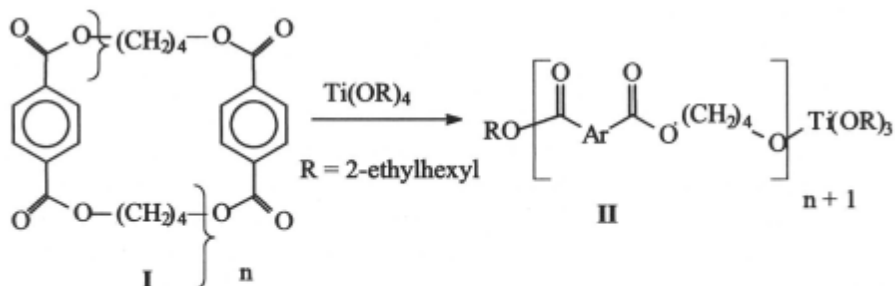
Propagation:
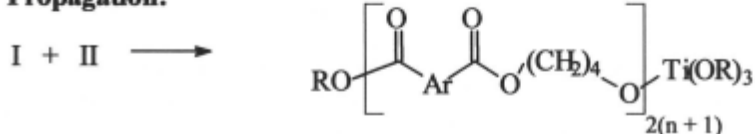
Scheme 6. Ring opening polymerization of oilgomeric PBT cyclics.

As in living ring-opening polymerizations, the molecular weight of the polymer was controlled by the molar ratio of cyclic esters to linear functionalities. Low molecular weight linear oligomers such as 1,4-bis-(4-hydroxybutyl) terephthalate or its oligomers limited the ultimate molecular weight achieved, hence the precautions taken for their removal. Furthermore, some initiators (such as TOT) introduced monomers (2-ethylhexanol) which also limited the molecular weight. Thus, as the level of titanate initiator (which contains 4 alcohol groups) was decreased, higher molecular weights were observed. Conversely, as the amount of linear oligomers was decreased, the polymer molecular weight increased. Unlike the titanates, when cyclic stannoxane **3** was used as the initiator, no decrease in molecular weight was observed with increasing catalyst level, because no end groups were introduced; the tin should be built into a macrocyclic polymer which is more stable to GPC conditions than the titanate esters. The GPC characteristics of

the stannoxane-initiated polymerizations were quite different from those of the titanate-initiated systems (much higher M_w's and lower apparent dispersivities). These effects are delineated in Table 11.

Table 11. Polymerization of 5% molar ratio PET/PBT Co-cyclic Oligomers[a]

Initiator[b] (mole %)	Temp (°C)	Time (min)	% Polym.	Mw x 10⁻³ (vs PS)	Mn x 10⁻³ (vs PS)	Mw/Mn
Bu₂Sn=O (0.5)	275	10	97	58.9		
Ti(Oi-Pr)₄ (0.2)	190	6	98	115	55	2.1
TOT (0.1)	190	20	99	352	167	2.1
TOT (0.2)	190	20	98	117.1	52	2.25
TOT (0.3)	190	6	95	95	39.7	2.4
TOT (0.3) + 0.5% linear[c]	190	6	96	75.6	26.7	2.8
TOT (0.3) + 1.0% linear[c]	190	6	95	61.2	22.1	2.8
TOT (0.3) + 2.0% linear[c]	190	10	98	25.4	11.4	2.2
TOT (0.4)	190	20	97	62.1	19.6	3.2
TOT (0.5)	190	6	99	53.2	22.7	2.3
Stannoxane 1 (0.05)	190	20	91	401	303	1.3
Stannoxane 1 (0.1)	190	20	95	344	177	1.9
Stannoxane 1 (0.2)	190	20	95	445	286	1.55
Stannoxane 1 (0.4)	190	20	98	330	171	1.9
Stannoxane 1 (0.2)		10	97	117	51.9	2.25
NaOEt (1.0)	225	10	41	5.3		
Sn(OMe)₂ (1.0)	250	10	54	36		
Comm. (Valox® 315)	NA	NA		111	48.7	2.3

[a]Polymerizations were carried out neat by adding catalyst in a minimum amount of solvent to molten cyclic oligomers at the temperature shown. [b]Mole percent relative to monomer units. [c]bis-(4-hydroxybutyl)terephthalate added at level shown.
Source: Ref. 53

The polymerization reaction was typically carried out at 180-200°C, well below PBT's melting point of ~225°C. Regardless, complete polymerization with only 1-3% cyclic remaining (by GPC) could be achieved. Three factors controlled the completeness of polymerizations: 1) purity of the monomers (see above), 2) complete mixing of initiator before polymerization caused the viscosity to increase to the point where mixing stopped (the initiator needs to be intimately mixed with the molten cyclic), and 3) Polymerization at a high enough rate that it was essentially complete before crystallization occurred. For most fast initiators, polymerization at 190°C using mechanical stirring at 300-500 rpm was ideal for effecting complete conversion to polymer. In some cases, premature crystallization (temperatures below 185°C) or inefficient mixing of the initiator led to incomplete polymerization and recovery of cyclics along with polymer.

Polymers prepared from cyclic oligomers showed higher levels of crystallinity than conventionally prepared polyester (60-80 J/g vs 35-50 J/g for commercial materials of similar molecular weights [53]). The cause of such excess crystallinity is under investigation [67].   One possibility is that more order exists in the polymer since polymerization only requires breaking and making ester bonds, rather than removal of condensation byproducts such as methanol or butanediol and the vigorous mixing which that process requires. The crystallinity of the polymer could be controlled by incorporation of low levels of another monomer (such as ethylene glycol) into the cyclics. A co-cyclic prepared by mixing reactants melted at a significantly lower temperature than a physical mixture of PET and PBT cyclics which had been prepared separately. Much of the processing work was carried out using the 5% (molar) PET/PBT co-cyclics.

Conversion of cyclic oligomers to composite structures via Resin Transfer Molding (RTM) and Reaction Injection Molding (RIM) techniques has been demonstrated, and will be the subject of subsequent publications. Glass loadings as high as 70% and composite tensile moduli of 3 million psi are routinely achieved [68].

6.4 Conclusion

Recent chemistry has been developed for the efficient preparation of oligomeric cyclic esters and carbonates. The current techniques have made it possible to prepare hundreds of kilograms of the cyclic oligomers per batch, and have made these materials available for study. Both methods of synthesis have been studied mechanistically. Purification to polymerization quality has been simply achieved in both cases, with selective reactions for removal of linear oligomers. The cyclic oligomers melt at 130-180°C (polyesters) or 180-200°C (polycarbonates), and have melt viscosities about 4 orders of magnitude lower than the parent high molecular weight polymers. Polymerization of the cyclic oligomers has been achieved with a variety of initiators, and using various techniques. Polymerization can be complete within minutes, and leads to very high molecular weight polyesters or polycarbonates without formation of byproducts, and with essentially no exotherm.   The ring opening chemistry facilitates a variety of new copolymer reactions, and has made the fabrication of composite structures with very high fiber loadings possible.

Acknowledgements

References:
1. H. Schnell, L. Bottenbruch, Ger. Pat. 1,229,101 (1966).
2. H. Schnell, L. Bottenbruch, Belg. Pat., 620 620, (1960).
3. H. Schnell, L. Bottenbruch, Makromol. Chem., **57**, 1 (1962).
4. R. J. Prochaska, U. S. Pat. 3,274,214 (1966).
5. L. S. Moody,   U. S. Pat, 3,155,683 (1964).
6. D. J. Brunelle, T. G. Shannon, Macromolecules, **24**, 3035 (1991).
7. D. J. Brunelle, T. L. Evans, T. G. Shannon, E. P. Boden, et al., Polym. Prepr., **30** (#2), 569 (1989).
8. D. J. Brunelle, E. P. Boden, T. G. Shannon, J. Am. Chem. Soc., **112**, 2399 (1990)
9. D. J. Brunelle and M. F. Garbauskas, Macromolecules, **26**, 2724 (1993).
10. D. J. Brunelle, Makromol. Chem., Macromol. Symp., **64**, 65 (1992).
11. D. J. Brunelle and E. P. Boden, Polym. Prepr., **31**, 399 (1991).
12. D. J. Brunelle and E. P. Boden, Makromol. Chem., Macromol. Symp., **54/55**, 397 (1992).
13. E. P. Boden and D. J. Brunelle, *Contemporary Topics in Polymer Science*, Vol. **7**, pp. 21-34, J. C. Salamone and J. S. Riffle, Eds, Plenum Press: New York (1992).
14. E. Aquino, W. J.Brittain, D. J. Brunelle, Polym. Prepr., **33** (#1), 1185 (1992).
15. E. Aquino, W. J. Brittain, D. J. Brunelle, Macromolecules, **25**, 3827 (1992)
16. E. Aquino, W. J. Brittain, D. J. Brunelle, Polym. Prepr. **34**, (#1): 865 (1993).
17. E. A. Aquino, W. J. Brittain, D. J. Brunelle, Polymer International, **33**, 161 (1994).
18. E. C. Aquino, W. J. Brittain, D. J. Brunelle, Jour. Poly. Sci: Part A: Poly. Chem., **32**, 741 (1994).
19. T. L. Evans, C. B. Berman, J. C. Carpenter, D. Y. Choi, D. A. Williams, Polym. Prep., **30** (#2), 573 (1989).
20. D. J. Brunelle and T. L. Evans, *Contemporary Topics in Polymer Science,* Vol. **7**, pp 5-19, J. C. Salamone and J. Riffle, Eds., Plenum Press, New York (1992).
21. K. R. Stewart, Polym. Prepr., **30** (#2), 140 (1989).
22. J. E. Bartmess, R. L. Hays, G. Caldwell, J. Am. Chem. Soc., **103**, 1338 (1981).
23. T. L. Evans, D. J. Brunelle, A. J. Salem, K. R. Stewart, Polymer Preprints, **32**, (# 2), 176 (1991).
24. D. J. Brunelle, T. L. Evans, M. A. Vallance, K. R. Stewart, T. G. Shannon, D. A. Williams, D. J. Patterson, N. R. Rosenquist, W. Hilakos, U. S. Patent **4,740,583** (1988).
25. D. J. Brunelle and T. G. Shannon, Polymer Preprints, **31** (# 1), 14 (1990).
26. D. J. Brunelle and T. G. Shannon, Makromol. Chem., Macromol. Symp., **42/43**, 155 (1991).
27. D. J. Brunelle, T. L. Guggenheim, J. A. Cella, T. L. Evans, et al., U. S. Patent **4,980,453** (1990).
28. D. J. Brunelle and D. K. Bonauto, U. S. Patent **4,920,200** (1990).
29. D. J. Brunelle, H. O. Krabbenhoft, and D. K. Bonauto, Polym. Prepr., **34** (#1), 73 (1993).
30. D. J. Brunelle, H. O. Krabbenhoft, and D. K. Bonauto, Macromol. Symp.**, 77,** 117-124 (1994).
31. D. J. Brunelle, Trends in Polymer Science, **3**, 154 (1995).

32. T. L. Guggenheim, J. M. Fukuyama, J. J. Kelly, Eur. Pat. Appl., 402676 (1990); CA, **114**:208077k.
33. T. L. Evans, U. S. Patent **4,699,974** (1987).
34. [1] T. L. Evans and J. C. Carpenter, Polym. Prepr., **31** (#1): 18 (1990). (b) T. L. Evans and J. C. Carpenter, Makromol. Chem. Macromol. Symp., **42/43**: 177 (1991).
35. T. L. Evans and J. C. Carpenter, Makromol. Chem. Macromol. Symp., **42/43**, 177 (1991).
36. T. L. Evans, T. J. Shea, C. B. Wasserman, J. R. Campbell, U. S. Patent **5,010,143** (1991).
37. T. L. Evans, N. R. Rosenquist, E. E. Bostick, U. S. Patent **4,746,724** (1988).
38. T. L. Evans, Eur. Pat. Appl., EP 249,809 (1987); CA **108**:187816j.
39. T. Takekoshi, P. P. Anderson, U. S. Patents **4,695,612** and **4,766,199** (1988).
40. H. O. Krabbenhoft, E. P. Boden, Polym. Prep., **31** (#1), 16 (1990).
41. N. R. Rosenquist, L. P. Fontana, Polym. Prep., **30** (#2), 577 (1989)
42. D. J. Brunelle and T. G. Shannon, U. S. Patents **4,755,586** (1988), **4,794,160** (1988), **4,888,411** (1989), and **4,972,039** (1990).
43. S. D. Ross, E. R. Coburn, W. A. Leach, W. B. Robinson, J. Polym. Sci., **13,** 406 (1954).
44. E. Repin and E. Papanikolau, J. Polym. Sci.,A-1, **7**, 3426 (1969).
45. G. Wick and H. Zeitler, Angew. Makromol. Chem., **112**, 59 (1983).
46. I. Goodman and B. F. Nesbitt, Polymer, 1, 384 (1960).
47. L. H. Peebles, M. W. Huffman, C. T. Ablett, J. Polym. Sci. (A-1), **7**, 479 (1969).
48. G. C. East, A. M. Girshab, Polymer, **23**, 323 (1982).
49. G. Montaudo, C. Puglisi, F. Samperi, *Polymer Degradation and Stability,* **42**, 13 (1993).
50. E. Meraskentis and H. Zahn, Chem. Ber., **103**, 3034 (1970).
51. F.-J. Muller, P. Kusch, J. Windeln, H. Zahn, Makromol. Chem., **184**, 2487 (1983).
52. Y. Kitano, A. Ishitani, T. Ashida, Polymer Journal, **23**, 949 (1991).
53. D. J. Brunelle, J. E. Bradt, J. Serth-Guzzo, T. Takekoshi, T. L. Evans, E. J. Pearce, Macromolecules, **31**, 4782 (1998).
54. J. W. Hill, W. H. Carothers, J. Am. Chem. Soc., **55**, 5031 (1933).
55. W. H. Carothers, J. W. Hill, *J. Am. Chem. Soc.,* **55**, 5043 (1933).
56. E. W. Spanagel, W. H. Carothers, J. Am. Chem. Soc., **57**, 929 (1935).
57. G. L. Warner, D. J. Brunelle, P. R. Wilson, U. S. Patent **5,446,122** (1995).
58. Nippon Gijutsu Boeki Co., Japanese Patent **21873** (1971).
59. H. Jacobson, W. H. Stockmayer, J. Chem. Phys., **18**, 1600 (1950).
60. D. J. Brunelle and T. Takekoshi, U. S. Patent **5,407,984** (1995).
61. D. J. Brunelle, G. Kailasam, J. Serth-Guzzo, P. Wilson, U. S. Patent **5,668,186** (1997).
62. J. J. L. Bryant and J. A. Semlyen, Polymer, **38**, 2475 (1997).
63. J. J. L. Bryant and J. A. Semlyen, Polymer, **38**, 4531 (1997).
64. S. C. Hamilton, J. A. Semlyen, and D. M. Haddleton, Polymer, **39**, 3241 (1998).
65. P. A. Hubbard, W. J. Britain, W. L. Mattice, D. J. Brunelle, Macromolecules, **31**, 1518 (1998).
66. Measurement taken using a Brookfield viscometer, Carbone, J. and Pearce, E. J., personal communication.
67. Kambour, R.P., personal communication.
68. T. L. Evans, D. J. Brunelle, J. E. Bradt, E. J. Pearce, P. R. Wilson, U. S. Patent **5,466,744** (1995).

LARGE CROWN ETHERS, CYCLIC POLYETHERS
and CYCLIC BLOCK COPOLYETHERS

Colin Booth and Colin Price
University of Manchester, UK

*Dedicated to the memory of Dr. Richard H. Mobbs,
expert in polyether chemistry.*

7.1   Introduction

Accounts of the preparation and properties of cyclic ethers invariably start with Pedersen's preparation of dibenzo-18-crown-6 and subsequently of a range of substituted and unsubstituted crown ethers, as reported in 1967 [1]. This reflects Pedersen's recognition of their potential as complexing agents rather than prior discovery, since cyclic oligomers of ethylene oxide were already known in the 1950s [2] [3], and similar compounds had been reported as early as 1937 [4]. The smallest crown is 1,4,7-trioxacyclononane, 9-crown-3, and the commonly encountered members of the series are 12-crown-4 and 18-crown-6.

Our purpose here is not to retrace this familiar ground, which is already comprehensively reviewed [5]-[8], but to summarise recent work on: (i) large unsubstituted crown ethers, i.e. uniform cyclic oligomers of ethylene oxide containing at least ten oxyethylene units; (ii) non-uniform cyclic poly(oxyethylene)s, i.e. cyclic polymers with narrow distributions of chain length, which the polymer community might call monodisperse; (iii) related cyclic polyethers, e.g. poly(oxypropylene) and poly(oxybutylene); and (iv) cyclic block copolymers with hydrophilic and hydrophobic polyether components. As befits our interests, emphasis is placed upon the properties of the cyclic polymers in the bulk state, particularly the crystalline state, and upon the association properties of the block copolymers in aqueous solution. Application of large crown ethers in forming rotaxanes is covered in another review in this volume.

7.2   Large crown ethers

7.2.1   Preparation and characterisation

For large crown ethers as for small, the preparative methods are based on the Williamson reaction. The many variations have been reviewed [5]-[8] In a useful procedure suggested by Okahara *et al.* [9] [10] an oligoethylene glycol

is mixed with tosyl chloride (*p*-toluenesulphonyl chloride) in solution in the presence of powdered dispersed potassium hydroxide. The monotosylate forms *in situ*, and immediately reacts intramolecularly to form the crown:

$$K(OCH_2CH_2)_m)OK + TsCl \rightarrow K(OCH_2CH_2)_m)OTs + KCl$$
$$\rightarrow \boxed{(OCH_2CH_2)_m)} + KOTs$$
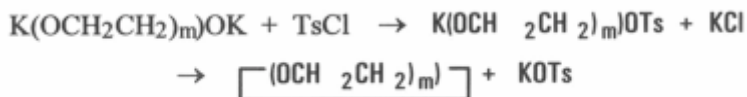
Intermolecular reaction leads to chain extension before eventual cyclisation.

Okahara reported the preparation of 18-crown-6 in 75% yield.[9] The same method was used by Vitali and Masci [11], who prepared 15-crown-5 to 30-crown-10 in 40-60% yield, with small yields (<8%) of higher crown ethers formed from chain-extended by-products,. More recently, we have used Okahara's method to obtain *ca.* 70% conversions to target crown ether in the preparation of 54-crown-18 and 81-crown-27 [12] [13], and a somewhat lower conversion (*ca.* 50%) in the preparation of 108-crown-36 [14].

Considering that competition between cyclisation and chain extension is always a problem, an important consideration is the concentration of the glycol and tosyl chloride in the reaction mixture. In our work [12] [13], very high dilution is achieved by adding a dilute solution of glycol (*ca.* 0.01 mol dm^{-3}) in 50 cm^3 tetrahydrofuran (THF), plus tosyl chloride in approximately equimolar proportion, to a similar volume of solvent with dispersed powdered KOH. Very slow addition from a syringe pump takes place over a period of two or three days. We estimate an effective glycol concentration in the reaction mixture of *ca.* 10^{-5} mol dm^{-3}, which greatly favours the intramolecular reaction.

A major step in this route to large crown ethers is the preparation of a pure sample of precursor oligoethylene glycol. A useful procedure, first described by Bomer *et al.*[15], is controlled chain extension by reaction of the ditosylate of an oligoethylene glycol with the monopotassium salt of the same glycol to obtain a product of three times the chain length. For example, starting from tetraethylene glycol (**E₄, E = oxyethylene**), to form first **E₁₂** and then **E₃₆** [14]. Pure oligoethylene glycols as long as **E₄₅** have been isolated in our laboratory [16]-[19], and, using similar methods, up to **E₅₄** by Kinugasa *et al.* [20] [21]. A feature of these preparations was careful monitoring and purification at each stage, the methods of choice being analytical and preparative gel permeation chromatography (GPC), the latter taking place on Sephadex LH20 gel with ethanol eluent. Confirmation of molar mass was by [13]**C NMR** spectroscopy and, in Japan [20] [21], additionally by vapour pressure

osmometry and light scattering.

Attention to monitoring and purification by analytical and preparative GPC carries over into the cyclisation stage of our work [12]-[14]. Figures 1 and 2 give an indication of the quality of the final products of the process. The analytical GPC curves shown in Figure 1 were obtained for samples of cyclic and linear oligo(oxyethylene)s both with 18 E units, the linear oligomer being the dimethyl ether of the glycol used in preparing 54-crown-18 [13]. The width of the peaks is that expected for uniform samples, i.e. consistent with instrumental spreading in the GPC system. Minor peaks in the GPC curve of the crown are from 36-crown-12 and 72-crown-24, both derived from E_{12} impurity in the precursor. The shift in elution volume, from **26.0 cm^3** (linear) to 27.3 **cm^3** (crown) reflects the lower hydrodynamic volume of the cyclic oligomer, effectively caused by forcing a zero end-to-end distance.
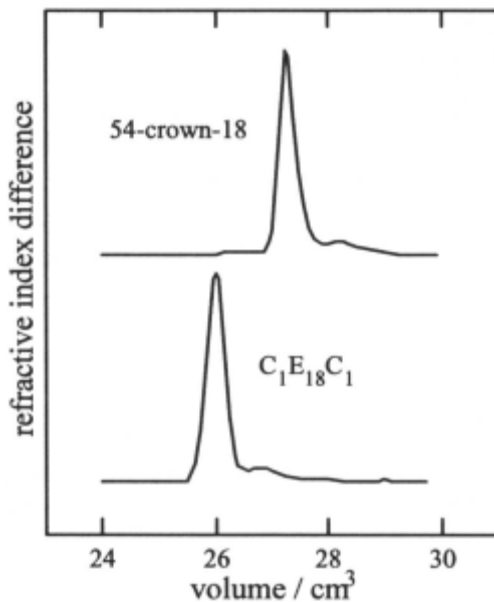
Figure 1 - GPC curves of purified cyclic and linear oligo(oxyethylene)s. Adapted with permission from J. Chem. Soc., Faraday Trans., 93, 4033 (1997).

The NMR spectra in Figure 2 confirm high conversion to cyclic product: i.e. resonances from **CH$_2$CH$_2$OH** and **CH$_2$CH$_2$OH** at $\delta_c = 61.5$ and 72.5 ppm respectively (spectrum b) are not seen in the spectrum of the crown, even at high expansion (spectrum a).

Chênevert and D'Astous [22], using a method previously reported by Greene [23], reacted an oligoethylene glycol ditosylate with a second glycol in the presence of base to form large crown ethers.

$$K(OCH_2CH_2)_aOK + Ts(OCH_2CH_2)_bOTs$$
$$\rightarrow \quad \left[(OCH_2CH_2)_{a+b}\right] + 2\ KOTs$$
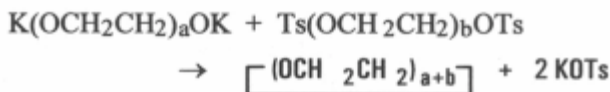
Ring size was determined by CI and FAB mass spectrometry. Gibson and co-workers [24] also used this method, again making us of mass spectroscopy for determination of ring size. Chromatographic methods were not used [22]-[24].
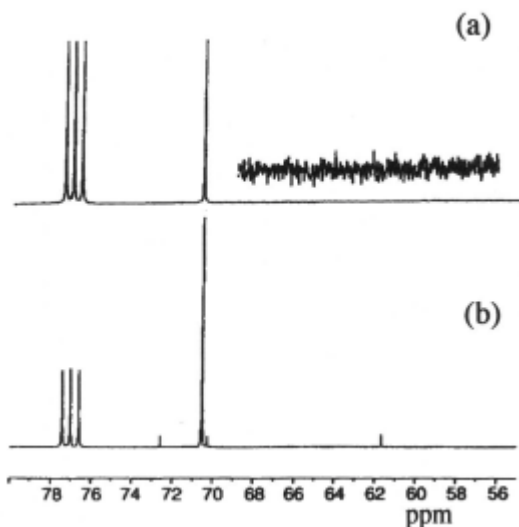
Figure 2 - ^{13}C NMR spectra of (a) 81-crown-27 and (b) its linear oligoethylene glycol precursor. The expansion confirms the absence of the resonance from end group carbon at 61.5 ppm. Adapted with permission from J. Chem. Soc., Faraday Trans., 92, 3173 (1996).

We have worked with the group at Virginia Polytechnic Institute [24] to characterise their products by analytical GPC, and found evidence of chain extension [25] [26]. Figure 3 compares GPC curves obtained using the same system for 81-crown-27 [12], cyclised polyethylene glycol $M_n = 2000\ \text{g mol}^{-1}$ (PEG2000, see Section 3) and sample "42-crown-14" prepared from tetra- and triethylene glycol precursors, as described by Gibson *et al.* [24] [26]. The GPC curve obtained for cyclised PEG2000 corresponds to M_w/M_n 1.04, i.e. approaching a Poisson distribution. That for "42-crown-14" is much wider, and contains very large rings eluting at the exclusion limit of the columns in use: i.e.

3 ∞ 30 cm³ columns packed with Styragel HR1-HR3, exclusion limit for linear poly(oxyethylene) **15000 g mol⁻¹**. We estimate a range from 63-crown-21
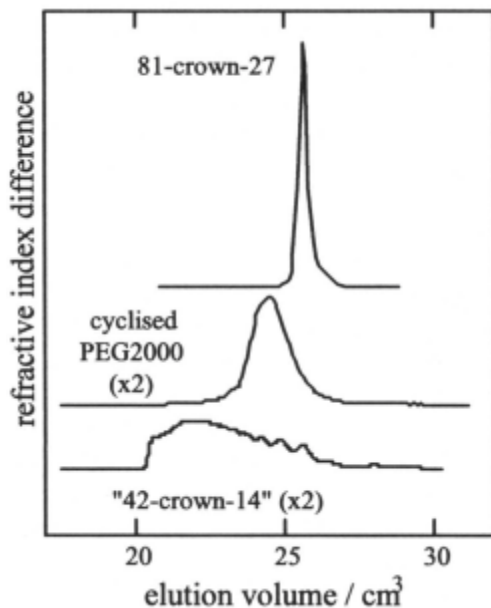
Figure 3 - GPC curves of cyclic oligo(oxyethylene)s, as indicated
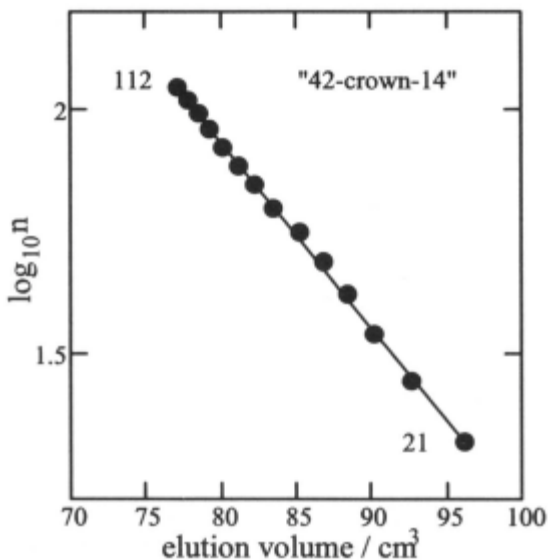
Figure 4 - Log(ring size) *versus* GPC elution volume for "42-crown-14".Minimum and maximum values of n are shown.

to beyond 750-crown-250, with very little of the target 42-crown-14. Peaks corresponding to the smaller crowns can be seen in the GPC curve in Figure 3: the chemistry dictates that they correspond to 3n-crown-n with n in steps of 7. Better resolution of these peaks was obtained using a second GPC system: $4 \infty 30$ cm^3 columns packed with mixed-bed type E PL-gel, exclusion limit for linear poly(oxyethylene) 10000 g mol^{-1}. Results from this system are shown in Figure 4 as a plot of log(n) against elution volume: the points range from 63-crown-21 to 336-crown-112.

7.2.1.1 Effect of reactant concentration

Chain extension preceding cyclisation can be traced to experiments carried out at relatively high concentrations. In Table 1 we compare conditions used in preparing large crown ethers. Both the concentration of glycol in the added solution and the addition time are important variables determining the concentration of reactants in the pot, and so the extent of conversion to the target crown. Table 1 illustrates the significant differences in conditions between various preparations of large crowns. In these terms, the large difference in conversion to target crown between, for example, Yang's preparation of 81-crown-27 (*ca.* 70%) and Gibson's preparation of "42-crown-14" (almost zero) can be readily understood.

Table 1 - Preparation of unsubstituted crown ethers

Reference	[Glycol][a] mol dm^{-3}	Volumes[b] cm^3	Addition time[a]/ min	Estimated reactant conc.[c] / mol dm^{-3}
Chênevert [22]	0.04	125 Ø 250	120	$2\infty10^{-3}$
Vitali [11]	0.4	20 Ø 70	100	$2\infty10^{-2}$
Gibson [24]	0.8	2400 Ø 3100	120	$8\infty10^{-3}$
Yang [12]	0.008	50 Ø 100	3000	$1\infty10^{-5}$

(a)   Concentration of glycol in the solution added over the given time
(b)   Volumes of solutions: added Ø total
(c)   Concentration estimated assuming 10 min residence time in all cases.

7.2.1.2 Product separation

The final mix of crowns in a given product depends not only on preparative conditions, but also on the purification step. A separation technique is needed even for preparations at very high dilution, for example preparative GPC monitored by analytical GPC [12] [13] or fractional distillation monitored

by gas-liquid chromatography [11]. These methods have limitations: preparative GPC on Sephadex LH20 with ethanol eluent [12] [13] has an exclusion limit at or about 150-crown-50.

7.2.1.3 Melting temperatures

In the absence of chromatographic information across the range of preparations, an indication of the composition of a sample can be obtained from comparison of its melting point with those reported for samples demonstrated to be pure by analytical GPC combined with ^{13}C NMR. Figure 5 shows such a comparison. The evidence available [13] is that the melting temperatures of pure crown ethers across the range **n = 10-27** are not greatly dependent on ring size: the dotted lines define the range $T_m = 41\pm3$ °C. The higher values of T_m reported for some crowns prepared by Vitali and Masci **(n = 16)** [11], by Chênevert and D'Astous **(n = 16)** [22], and by Gibson *et al.* **(n = 12)** [24], can be ascribed to the presence of very large rings. The crystallinity and melting behaviour of large crown ethers, including the low value of $T_m = 28$ °C seen for 51-crown-17 in Figure 5, are reviewed in detail in the next Section.
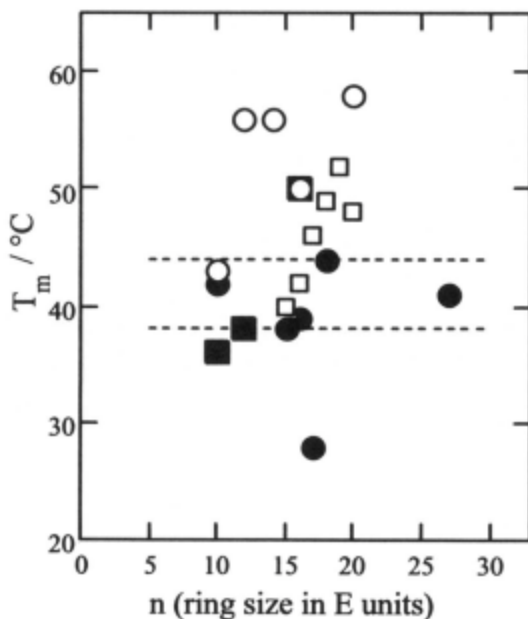
Figure 5 - Melting temperatures reported for unsubstituted crown ethers: data from (■) [11], (●) [13], (□) [22], and (○) [24].

7.2.2 Crystallinity of large crown ethers

7.2.2.1 30-crown-10

The crystal structure of a pure sample of 30-crown-10 has been determined by Bheda *et al.* [27]. Among other methods [24], the purity of the sample was checked by analytical GPC [25]. As with 18-crown-6 [28], water of crystallisation is possible, and the crystal structure of the complex, 30-crown-10.4H$_2$0, has also been determined [27]. Here we concentrate on the anhydrous crown, which forms crystals with an orthorhombic unit cell (*Pbca*) and density **1.234 g cm^{-3}**. The ring conformation is two trans-planar stems, each of three E units, connecting folds of two units with rotational angles

$$g\ t\ t\ g^-\ g^-\ t \qquad \text{for the bond sequence} \qquad \text{C–C–O–C–C–O–C}$$

There is no cavity in the centre, in sharp contrast to crystalline anhydrous 18-crown-6 [29] [30]. The folded rings pack parallel to each other in tilted layers, as shown in Figure 6. The long spacing of the unit cell, **d = 33.3 Å,** is for the two-layer repeat.
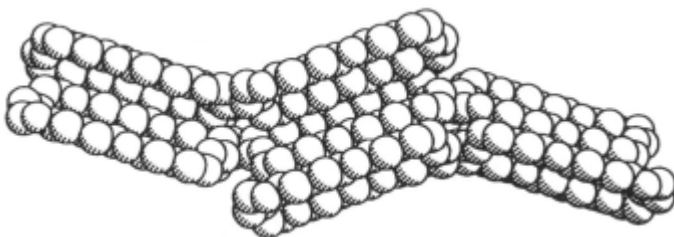
Figure 6 - Layer structure of crystalline 18-crown-6. Reproduced with permission from J. Org. Chem., 59, 1694 (1994). Copyright 1994 Am. Chem. Soc.

7.2.2.2 Large crown ethers

Structural information is not available for 33-crown-11 to 42-crown-14, but there is useful information thereafter. Figure 7 shows wide-angle X-ray scattering (WAXS) patterns obtained [13] for 45-crown-15 to 54-crown-18 and, for comparison, a sample of linear poly(oxyethylene) M_n = 2000 g mol^{-1}. All samples were crystallised at 20 °C. The pattern found for 54-crown-18 is essentially identical with that of the linear polymer, while those of the lower crowns differ. The WAXS pattern of crystalline 81-crown-27 (not shown) is also essentially identical with that of poly(oxyethylene) [12]. WAXS patterns obtained for 51-crown-17 (not shown in Figure 7) contained broad peaks with

only limited evidence of the poly(oxyethylene) pattern [13]. This is attributed to formation of mixed crystals, implying similar energetics of formation for the two types of crystallisation at room temperature. Leaving aside this transitional case, it is clear that 54-crown-18 and higher crowns must crystallise with two parallel stems of the ring in helical conformation.

The crystal structure of a closely related ring, dibenzo-54-crown-18, has been determined by van Eerden *et al.* [31]. The unit cell is monoclinic **(P2₁/c),** the
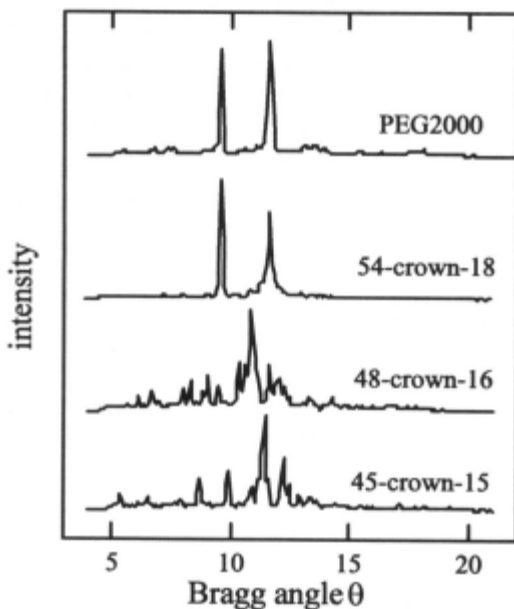
Figure 7 - WAXS patterns for crown ethers and linear PEG2000. Adapted with permission from J. Chem. Soc, Faraday Trans., 93, 4033 (1997).

density is **1.28 g cm⁻³** at 161 K, where the long spacing is 27.4 Å. The two benzo groups are incorporated in two folds, each equivalent to two E units, which are connected by two parallel helical stems, each of seven E units. The rotational angles in the stems follow the familiar sequence for helical poly(oxyethylene) [32], i.e.

$$t\,g\,t \quad \text{for the bond sequence} \quad O\text{--}C\text{--}C\text{--}O$$

The two stems are right and left handed helices, thus allowing similar packing to that in crystalline poly(oxyethylene). A corresponding structure calculated by Colquhoun for 54-crown-18 using Molecular Simulations software and energy minimisation has each fold equivalent to three E units [33]. Linear poly(oxyethylene) crystallises in the 7/2 helical conformation [32] so, whatever

238

the details of the fold conformation, it is reasonable that 54-crown-18 is the smallest unsubstituted crown to form stable crystals with the poly(oxyethylene) structure. We suppose that all the higher crown ethers will do the same, at least in the anhydrous state. Certainly this has been shown to be so for 81-crown-27 (WAXS, 12], for which additional conformation comes from Raman spectroscopy [12]. making use of the assignments of Matsuura *et al.* [34]-[36].

Further information on the crystal structure has come from measurement of long spacings (*d*) by small-angle X-ray scattering (SAXS): see Table 2. Also in the table are frequencies of the whole molecule longitudinal vibration (LAM-1 frequency, *v*) obtained from Raman spectroscopy. Comparison with the same quantities measured for linear dimethyl ethers, and with molecular contour lengths (*l*) calculated for the 7/2-helical conformation assuming 2.85 Å per E unit [37], indicates that the helical stems in the crown ethers are normal to the fold-planes of the layer crystal.

Table 2 - Long spacing (*d*) from SAXS

Sample	*d* / Å	*v* / cm^{-1}	*l* / Å	ref.
81-crown-27	39	26	77	[12]
54-crown-18	27	—	51	[13]
C_1-E_{27}-C_1	81	12.1	80	[12]
C_1-E_{18}-C_1	50	—	54	[38]

7.2.2.3 Energetics of chain folding

Chain folding in linear polymers is a topic of some importance in polymer science. There is considerable advantage in using oligomers in detailed studies [39]. For crystallisation at a given temperature, chains fold once in their layer crystals only when they exceed a critical length. For oxyethylene oligomers crystallised at room temperature, the critical length is *ca.* 170 chain atoms (approaching 60 E units) [40], very similar to that found for long n-alkanes [39] [41]. An advantage with cyclic oligomers is that each molecule must fold twice in the layer crystal: see Figure 8. Such chain folding in large crown ethers with poly(oxyethylene)-like crystal structure (54-crown-18 or greater) provides an ideal model for chain folding in linear poly(oxyethylene).
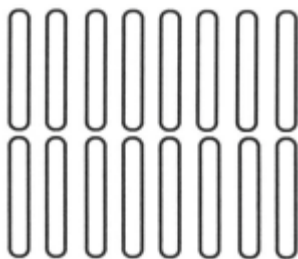
Figure 8 - Schematic showing two folds per molecule in a crystalline cyclic compound.

For layer crystals, the measured enthalpy of fusion per chain unit conforms to

$$\text{fus}H = \text{fus}H^0 - \frac{2\eta_e}{z} \qquad (1)$$

where $\text{fus}H^0$ is the thermodynamic enthalpy of fusion in J **(mol chain units)$^{-1}$** i.e. the enthalpy of fusion of perfect crystal with no chain-end or fold defects, η_e is the enthalpy of formation of the chain-end or fold plane of the layer crystal from perfect crystal, measured in J **(mol crystal stems)$^{-1}$**, and z is the chain length (or half-chain length if folded) in E units. Figure 9 shows enthalpies of fusion, measured by differential scanning calorimetry (DSC) and corrected to a common temperature of 40 °C [42], plotted against reciprocal z. The straight line through the points for the linear dimethyl ethers gives $\text{fus}H^0$ = 8.4±0.2 kJ mol^{-1} at 40 °C. The slope of the line gives η_e = 3.9±1.6 kJ mol^{-1}, indicating only a small excess energy in the chain-end plane compared with bulk crystal.

The corresponding analysis for the crowns is based on just two data points, but the natural extrapolation of the line through those points meets the ordinate at the value of $\text{fus}H^0$ found for the linear oligomers. The slope leads to η_e 18 kJ mol^{-1}. Since each fold involves two crystal stems, this means an enthalpy of formation of a fold from perfect crystal of *ca.* **36 kJ mol^{-1}** at 40 °C. Similar treatment of the melting temperatures of the linear and cyclic oligomers gives related values of the entropy and Gibbs energy of fold formation: details are in ref. 13.
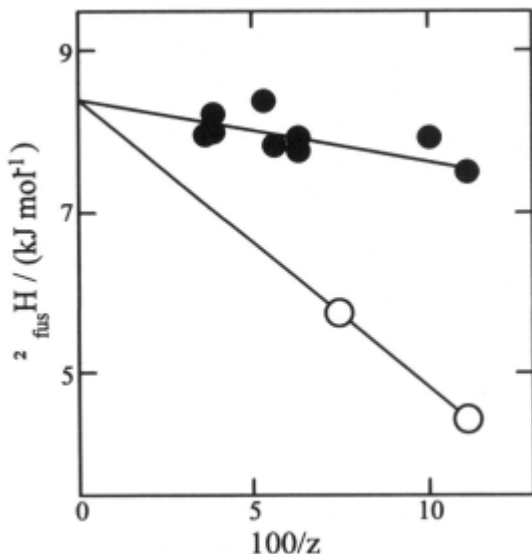
Figure 9 - Enthalpy of fusion at 40 °C *versus* (●) reciprocal chain length (E units) for linear dimethyl ethers and (O) reciprocal half-chain length (E units) for crown ethers. Adapted with permission from J. Chem. Soc., Faraday Trans., 93, 4033 (1997).

7.3. Cyclic poly(oxyethylene)s

7.3.1 Preparation

The method of ring closure by reaction of a polyethylene glycol with tosyl chloride at high dilution in the presence of solid KOH (as described in Section 2.1) has been used to prepare cyclic poly(oxyethylene)s with number-average molar mass up to 6000 g mol^{-1} [43] [44]. Okahara *et al.* cyclised PEG200 in this way [10]. Vitali and Masci cyclised PEG200, 300, 400, 600 in 30-60% yield, but PEG1000 in much lower yield, reported as 8% [11]. Under more favourable conditions (i.e. very high dilution, *ca.* 10^{-5} mol dm^{-3} glycol) we have obtained 80% conversion of PEG1000 and 50% conversion of PEG6000 to the corresponding cyclic polymers [44]. Our attempts to cyclise PEG10000 by this route have been less successful, conversions to the target cyclic being rather low (<20%).

A second method used in our laboratory [45] [46] is the reaction of a polyethylene glycol with dichloromethane (DCM) at high dilution (again *ca.* 10^{-5} mol dm^{-3} glycol) in the presence of solid KOH, to attain ring closure *via* an acetal linkage. In this case the reactions are:

$$K(OCH_2CH_2)_mOK + CH_2Cl_2 \rightarrow K(OCH_2CH_2)_mOCH_2Cl + KCl$$

$$\rightarrow \left[\begin{array}{c} (OCH_2CH_2)_m \\ CH_2O \end{array} \right] + KCl$$
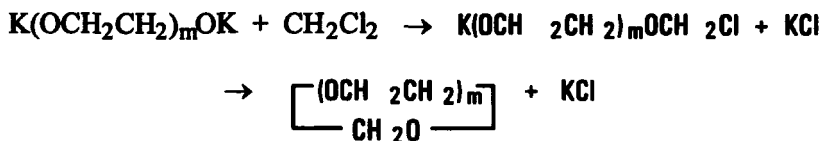
Conversions to cyclic polymer approaching 95% have been obtained [46]. The greater efficiency of the acetal route reflects the extremely high reactivity of the chloroether, which ensures very rapid reaction in the second step under conditions of high dilution.

Table 3 summarises our preparations to date. In both procedures, as in the preparation of crown ethers described in Section 2.1, a proportion of chain extension could not be avoided, but this polymer could be eliminated by a simple fractional precipitation procedure, as described below. Given this precaution, the narrow molar mass distributions of the precursor polymers, prepared by anionic polymerisation, carry over to the cyclic products. The conversion to target cyclic given in Table 3 were calculated as the area under the major peak in the GPC curve relative to the total area (see Section 3.2). Loss of material in the fractionation process reduced the final yield by *ca.* 25%.

Ishizu and Akiyama have reported the cyclisation of polyethylene glycol by reaction of its sodium salt with 1,4-dibromobutane [47]. Interestingly they report cyclisation with no chain extension even at relatively high concentrations of glycol (10^{-2} to 10^{-3} mol dm^{-3}). We have tried to repeat their procedure without success, finding almost complete recovery of precursor glycol. If there is little or no linking, the absence of evidence of chain extension in the GPC curves of the products is explained. Unfortunately Ishizu and Akiyama did not use spectroscopic methods to characterise their products.

Table 3 - Cyclic poly(oxyethylene)s

Acetal linked		Ether linked	
M_n / g mol^{-1}	Conversion-%	M_n / g mol^{-1}	conversion-%
400	90	—	—
600	90	—	—
1000	85	1000	80
1500	85	1500	75
2000	85	2000	75
3000	93	3000	75
4000	80	4000	48
6000	82	6000	50
10000	63	10000	5
20000	35	—	—

7.3.1.1 Fractionation

Figure 10 shows GPC curves of PEG 10000 precursor, the product of cyclisation by acetal closure, and the fractionated product. The dotted lines emphasise the shift to higher elution volumes which results from cyclisation. ^{13}C NMR was used (see below) to confirm 100% conversion of hydroxyl groups to acetal links. The tail of material eluting at low volumes is assigned to large cyclics formed by chain extension. Generally, fractionation was by precipitation of the large cyclics from dilute solution in toluene by addition of heptane, followed by equilibration by slowly raising and lowering the temperature [43] [45] [46]. With the larger rings, crystallisation of the precipitate could complicate the fractionation process, and precipitation from dilute solution in DCM by adding heptane, which yielded a liquid precipitate, was preferred [44].

7.3.1.2 Characterisation

^{13}C NMR was used to confirm the absence of OH end groups and, in the case of the acetal linked products, to confirm that the number of oxyethylene units per acetal link in the final product was equivalent, within experimental
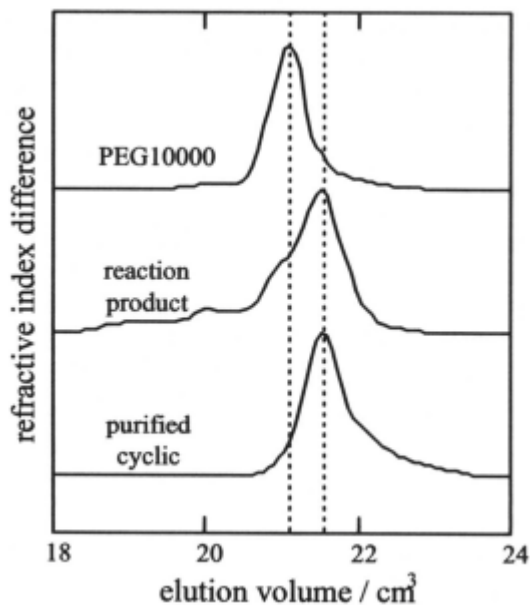
Figure 10 - GPC curves illustrating stages in the purification of cyclic poly(oxyethylene) prepared from PEG10000. Adapted with permission from Chem. Commun., 31 (1996).
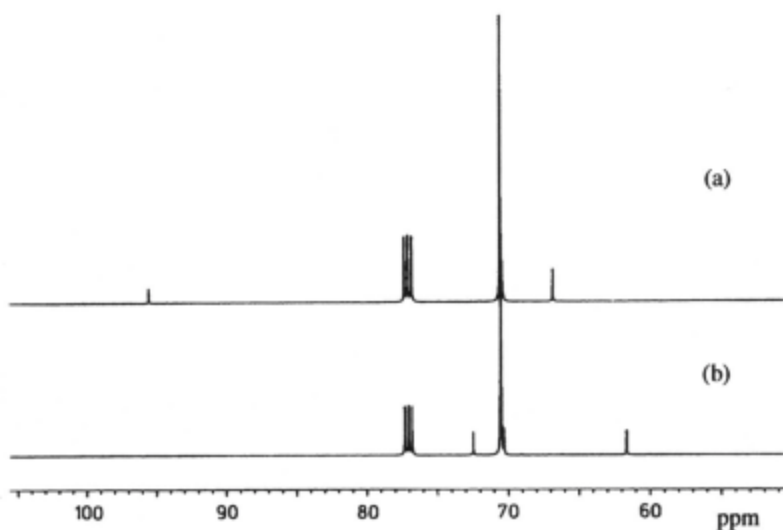
Figure 11 - ^{13}C NMR spectra of (a) cyclised PEG1000 and (b) PEG1000 precursor. Adapted with permission from Makromol. Chem., Rapid Commun., 14, 725 (1993).

error, to the number per two hydroxyl end groups in the PEG precursor. As an example, ^{13}C NMR spectra of cyclised PEG 1000 and its precursor are shown in Figure 11: the significant features are no signals from chain end carbons at δ_c = 61.3 ppm **(OCH$_2$CH$_2$OH)** and 72.3 ppm **(OCH$_2$CH$_2$OH),** and signals from acetal-link carbons at δ_c = 66.8 **(CH$_2$OCH$_2$OCH$_2$)** and 95.5 **(CH$_2$OCH$_2$OCH$_2$).**

      Calibration of the GPC system with both cyclic and linear polymers gave the expected [48] shift of the data points for cyclic polymers towards higher elution volume: see Figure 12. Use of these calibration curves confirmed almost identical molar-mass distribution widths, i.e. almost identical values of the ratio of mass-average to number-average molar mass for precursor and cyclic product alike, the range being $M_w/M_n = 1.07 \pm 0.03$.
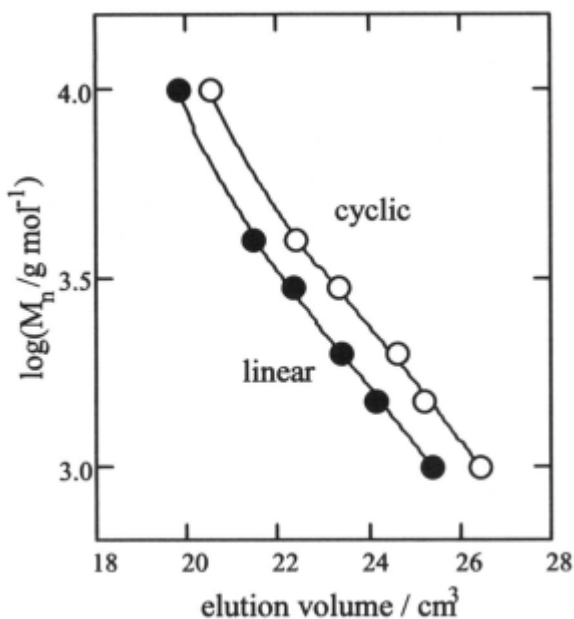
Figure 12 - GPC calibration for cyclic and linear poly(oxyethylene)s. Three μ-Styragel columns (HR1 to HR3) with THF eluent. Adapted with permission from Macromolecules, 31, 3030 (1998).

7.3.1.3 Notation

For the cyclic poly(oxyethylene)s we use the notation RE and RA for cyclics with ether closure or acetal closure, and combine this with an indication of the number-average molar mass of the polymer. Thus samples PEO-6000RA and PEO-6000RE derive from PEG6000 and, within experimental error, have the same molar mass and molar mass distribution. Comparison of properties is made with corresponding polyethylene glycols and their dimethyl ethers, for which we use, for example, PEG6000 (as usual) and PEO-6000LM.

7.3.2   Crystallinity of cyclic poly(oxyethylene)s

The crystallinity of cyclic poly(oxyethylene)s with M_n 1000 g mol^{-1} has been investigated. As might be expected considering the results presented in Section 2.2, all the cyclics crystallise with the poly(oxyethylene) structure, i.e. with a monoclinic sub-cell $(P2_1/c)$ with alternating right and left-hand 7/2 helices, as described by Takahashi and Tadokoro [32]. This has been confirmed by WAXS [44] [49] and by Raman spectroscopy [44] [49] [50].

Figure 13 shows typical SAXS results, the plots being either of (a) log intensity or of (b) Lorentz-corrected intensity against scattering vector $q = (4/\lambda)\sin\theta$, where θ is the Bragg angle. In this notation, Bragg's Law is $d = (2n/q)$, where n is the order of scattering. The scattering peaks seen in Figure 13 are equally spaced, as expected for lamellar structures. Figure 13a shows the equivalence of SAXS from crystalline cyclic PEO-3000RE and linear PEO-1500LM [49]. Figure 13b shows scattering from linear PEO-6000LM crystallised at 54 °C (unfolded) and 20 °C (once-folded) and from cyclic PEO-6000RA. The peak maxima for the once-folded linear polymer and the cyclic polymer coincide.
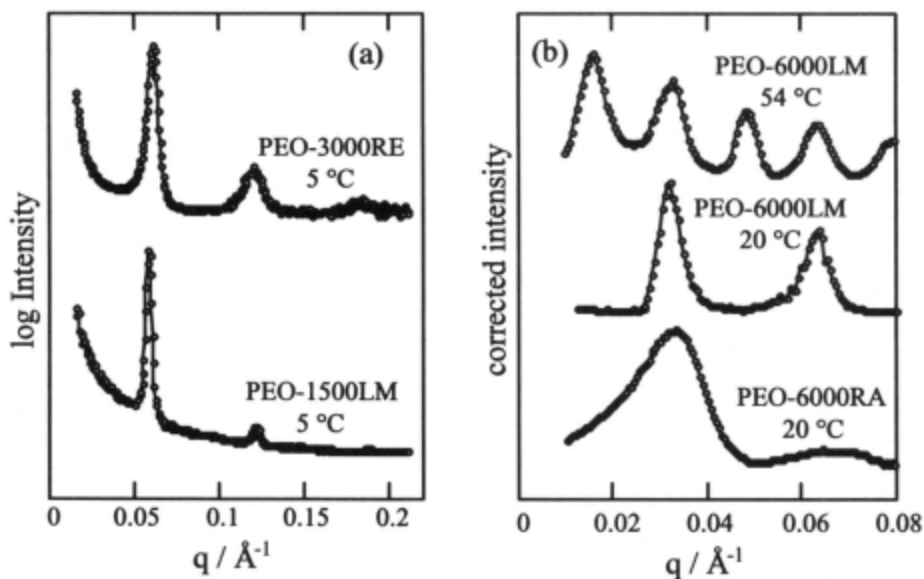
Figure 13 - SAXS from cyclic and linear poly(oxyethyiene)s. Samples crystallised by cooling at 10 °C min⁻¹ from the melt to the temperatures indicated. Adapted with permission from Polymer, 38, 35 (1997) and Macromolecules, 31, 3030 (1998).

Table 4 lists the lamellar spacings (d) obtained by SAXS for the range of cyclic oligomers prepared by acetal closure and crystallised from the melt at the temperatures shown. Also listed are the contour lengths of the molecules (l) calculated assuming 2.85 Å per E unit [38], and the numbers of folds per molecule calculated $f = l/d$ and rounded to the nearest integer. Values of f found for cyclic poly(oxyethylene)s prepared by ether closure (up to PEO-6000RE) were identical [43] [44] [49]. Values of the LAM-1 frequency from Raman spectroscopy (ν_1, inversely proportional to d) confirm the SAXS results [44] [49] [50]. Crystallisation from the melt at room temperature resulted in the expected conformation with two folds for all cyclic poly(oxyethylene)s up to $M_n = 6000$ g mol⁻¹, i.e. up to *ca* 200 chain atoms in the half-molecule. The same conformation was obtained on slowly crystallising PEO-10000RA at high temperature. However, rapid crystallisation from the melt at T_c 49 °C resulted in a four-times folded conformation. Two possibilities are depicted in Figure 14.

Table 4 - Lamellar spacings, LAM-1 frequencies, and numbers of folds

Sample	T_c / °C	d / Å	l / Å	ν_1/ cm^{-1}	f	Ref.
PEO-1000RA	20	37	66	27.7	2	[49]
PEO-1500RA	20	52	98	20.5	2	[49]
PEO-2000RA	20	67	130	16.1	2	[49]
PEO-3000RA	20	107	195	9.5	2	[49]
PEO-4000RA	20	129	260	8.3	2	[44]
PEO-6000RA	20	193	390	6.0	2	[44]
PEO-10000RA	20-49	164	649	7.4	4	[44]
PEO-10000RA	55	331	649	3.9	2	[44]

7.3.2.1 Enthalpy of fusion

In Figure 15, enthalpies of fusion corrected to 70 °C are plotted against reciprocal chain length, (or half-chain length for cyclics) in E units for low molar mass poly(oxyethylene)s for which chain folding is not a consideration (M_n 3000 g mol^{-1}). In contrast to Figure 8, which is the corresponding plot for uniform oligomers, data points for both linear and cyclic samples fall on the same line. Using eqn. (1), the ordinate intercept is **9.3±0.5 kJ mol^{-1}** at 70 °C, which corresponds to **8.8±0.5 kJ mol^{-1}** at 40 °C [42], in agreement with the value of **8.4±0.2** derived for uniform oligomers. From eqn. (1), the slope of the line through the points gives η_e = **30±4 kJ mol^{-1}**, almost ten-times the value found for uniform linear dimethyl ethers and twice the value found for uniform crown ethers (see Section 2.2.3).
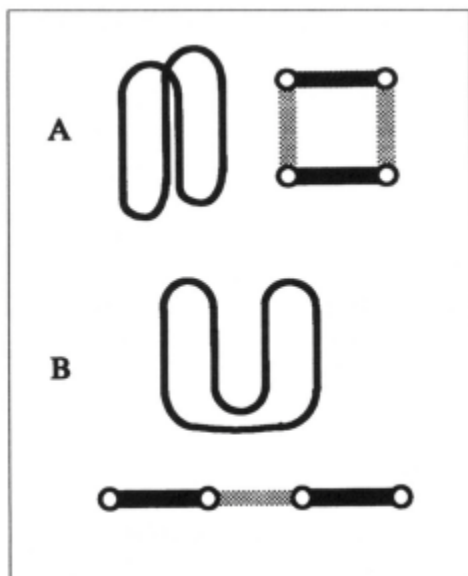
Figure 14 - Schematic showing two possible conformations of cyclic PEO-10000RA in its four-times folded conformation. Views along and normal to the crystal stems are shown. In the former the stems are indicated by circles and the folds by shading. Reproduced with permission from Macromolecules, 31, 3030 (1998).
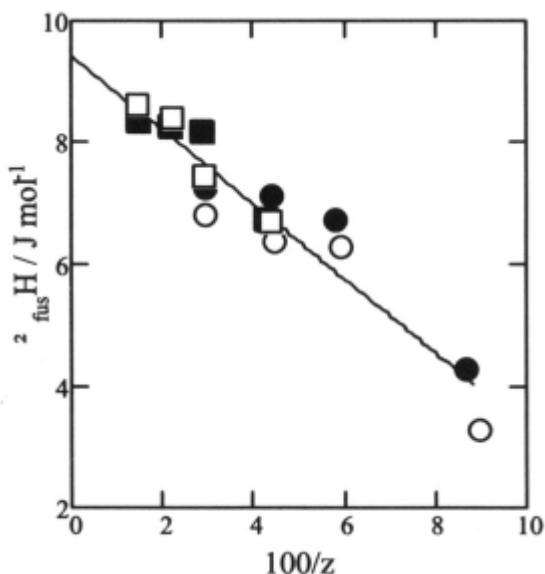
Figure 15 - Molar enthalpies of fusion (corrected to 70 °C) of linear and cyclic poly-(oxyethylene)s: (■) hydroxy-ended or (□) methoxy-ended linear polymer; (●) aceta-linked or (○) ether-linked cyclic polymers. Adapted with permission from Polymer, 38, 35 (1997).

The high value of the enthalpy of end-surface formation is a consequence of polydispersity. The narrowest distribution possible in an ideal anionic polymerisation (i.e. instantaneous initiation and no termination) is a Poisson distribution. For a linear poly(oxyethylene) of number-average chain length 45 E units (corresponding to M_n = 2000 g mol^{-1}), the standard deviation of the (Poisson) chain length distribution is 6 [51]. Assuming rapid crystallisation (no fractionation), and considering both chain ends, 12 of the chain units cannot be in the ordered crystalline layers of the lamellae, but must be in disordered lamellar surface layers. The consequence for lamellar crystal formation, whether of linear or cyclic poly(oxyethylene) 2000, is illustrated schematically in Figure 16. Since the disordered layer is essentially noncrystalline no matter what the chain architecture, the similarity of the enthalpy of surface formation is explained, as is the high value of η_e, which corresponds to fusion of four chain units per chain end, or 8 chain units per fold.
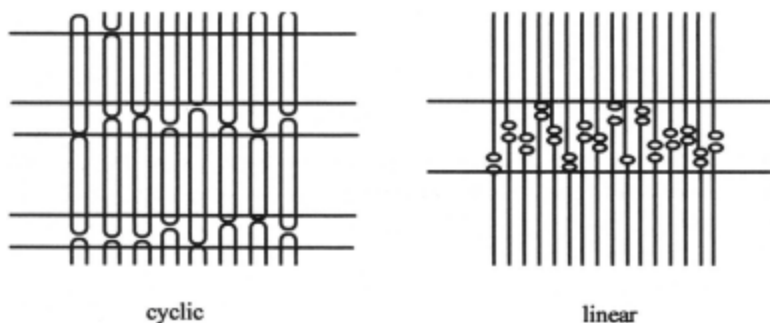
cyclic   linear

Figure 16 - Schematic representation of polydisperse cyclic and linear chains in lamellar crystals.

7.3.2.2 Melting temperature

Corresponding to Figure 15, melting temperatures of the low molar mass poly(oxyethylene)s are plotted against reciprocal z in Figure 17. Given similar enthalpies of fusion, the higher melting points found for the small cyclics can be attributed to lower entropies of fusion, through

$$T_m = \frac{\Delta_{fus}H}{\Delta_{fus}S} \tag{2}$$

The effect would be expected, since the linear and cyclic polymers are similarly conformationally restricted in the crystalline state but the cyclic polymer is more conformationally restricted (compared with a linear polymer of the same

length) in the melt state. The result is that $\Delta_{fus}S$ is lower for the cyclic polymers, hence T_m is higher.
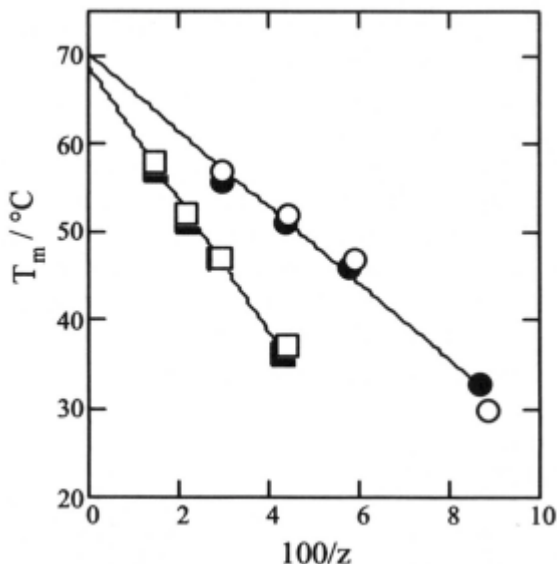
Figure 17 - Melting temperatures of linear and cyclic poly(oxyethylene)s: (■) hydroxy-ended or (□) methoxy-ended linear polymer; (●) acetal-linked or (○) ether-linked cyclic polymers. Adapted with permission from Polymer, 38, 35 (1997).

7.3.3   Solution properties

Sample PEO-10000RA has been used by Griffiths *et al.* in a comparative study by pulse-gradient spin-echo NMR of the self diffusion of cyclic and linear polymers in dilute aqueous solution [52]. Hydrodynamic radii derived *via* the Stokes-Einstein equation fitted the expected relationship: i.e. $(r_{h,L}/r_{h,C})^2 = 1.9\pm0.1$. This work is described in Chapter 11.

The same sample of PEO-10000RA has been spread as a surface film at the air-water interface and studied by surface quasielastic (dynamic) light scattering (SQELS) [53]. It was thought that differences in surface properties (surface tension, dilational modulus, and their associated viscosities) might arise because of lack of free ends in the cyclic molecule. In fact, the concentration dependences of surface tension found for the cyclic and linear (PEO-10000LM) were very similar, both reaching a constant value of 64-66 mN m^{-1} at a surface concentration of 0.4-0.6 mg m^{-2}, symptomatic of a full monolayer. The concentration dependences of the other surface properties were also identical at low concentration, but they differed in the full-monolayer

region . With increase in concentration of linear polymer above 0.4-0.6 mg m^{-2}, the dilational modulus and dilational viscosity rose and the transverse shear modulus fell, whereas steady values were recorded for the cyclic polymer. This difference in properties must originate in difference in molecular structure, and may relate to penetration of the subphase by free ends of the linear polymer.

7.4. Cyclic poly(oxypropylene) and poly(oxybutylene)

Yu *et al.* have described the preparation of cyclic poly(oxypropylene), $M_n = 2000$ g mol^{-1}, by acetal closure [54]. Starting from PPG2000, 60-75% conversions to the target cyclic were achieved in replicate experiments. Because of the ready solubility of poly(oxypropylene) in a wide range of solvents, preparative GPC (ethanol and Sephadex LH20, see Section 7.2.1) was used to separate PPO-2000RA from chain-extended products. Analytical GPC gave $M_w/M_n = 1.04$ (precursor 1.03) and ^{13}C NMR gave $M_n = 2060$ g mol^{-1} (precursor 1970 g mol^{-1}).
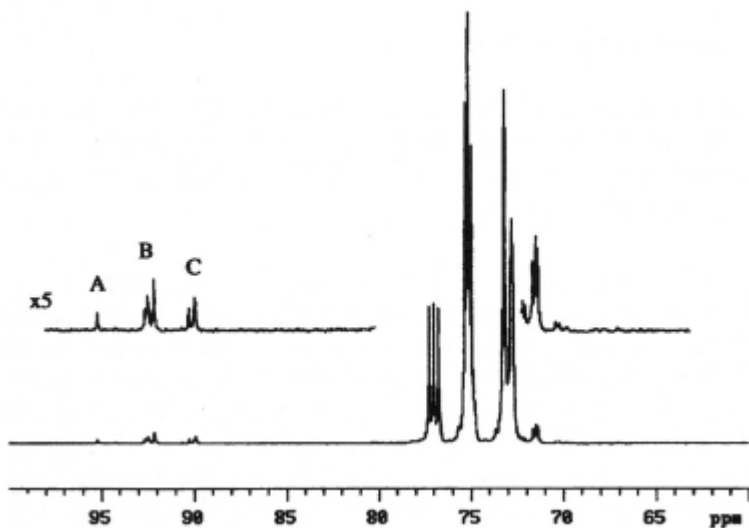
Figure 18 - ^{13}C NMR spectrum of cyclised PPG2000 showing resonances (A-C) originating from single, double and triple acetal links. See text for details. Adapted with permission from Macromol. Rapid Commun., 18, 1085 (1997).

In contrast to the ^{13}C NMR spectra of the acetal-linked poly(oxyethylene)s, which showed a single resonances at $\delta_c = 66.8$ and 95.5 ppm assigned to $\underline{C}H_2OCH_2O\underline{C}H_2$ and $CH_2O\underline{C}H_2OCH_2$ respectively, that of PPG-2000RA gave evidence of more than one acetal group in the link: see Figure 18. DEPT and ^{1}H-coupled NMR were used to show that the resonances in the range 90-95

ppm (labelled A to C in Figure 18) could be assigned as follows

single link	$CH(CH_3)OCH_2OCH(CH_3)$	B
double link	$CH(CH_3)OCH_2OCH_2OCH(CH_3)$	C (part)
triple link	$CH(CH_3)OCH_2OCH_2OCH_2OCH(CH_3)$	A and C (part)

The integrals indicate: single link, 77%; double link, 12%; triple link, 11%.

Recently successful cyclisation reactions (acetal route, conversions 60 to 80%, purification by preparative GPC) have been carried out starting with polybutylene glycols (PBG400 to PBG3000), i.e. chains with secondary hydroxyls hindered by ethyl rather than methyl groups [55]. The ^{13}C NMR spectra of the cyclic polymers also show complex resonances associated with multiple acetal links. Exact assignments have yet to be determined.

Attempts to form ether-linked cyclic poly(oxypropylene)s and poly(oxybutylene)s by Okahara's route (see Sections 2.1 and 3.1) have been largely unsuccessful [54] [55].

7.5. Cyclic block poly(ethers)

Cyclic block copolyethers have been prepared by the acetal route (see Section 3.1), combining an oxyethylene block with different hydrophobes, either oxybutylene $\{cyclo\text{-}B_nE_m, \ B = OCH_2CH(C_2H_5)\}$ or oxypropylene $\{cyclo\text{-}P_nE_m, P = OCH_2CH(CH_3)]\}$.

In early work, Yan *et al.* [45] described the preparation of $c\text{-}B_8E_{40}$ starting from triblock copolymer $E_{20}B_8E_{20}$, and also their failure to cyclise the reverse triblock, $B_4E_{40}B_4$, under similar conditions. In fact our later work (see Section 4) shows that cyclisation of polyethers with secondary hydroxyl end groups is possible. Subsequently cyclic copolymers $c\text{-}B_8E_{42}$ [56] $c\text{-}B_{27}E_{144}$ [57] and $c\text{-}P_{34}E_{104}$ [58] have been used in studies of the effect of molecular architecture on association properties (micellisation and gelation) in aqueous solution, and copolymer $c\text{-}B_{15}E_{206}$ [59] has been used in a study of effects of molecular architecture on adsorption at the solid/liquid interface. Acetal closure has also been used to prepare related copolymers with an alkylene hydrophobic block, i.e. $cyclo\text{-}E_mC_{10}, C = CH_2, m < 100$ [60].

7.5.1 Preparation and characterisation of cyclic block copolymers

As an example we describe the preparation of $c\text{-}B_{27}E_{144}$ from its linear precursor, $E_{72}B_{27}E_{72}$ [57]. Vacuum line and ampoule techniques were used in order to rigorously exclude moisture in its preparation by sequential anionic polymerisation. The polymerisation of dry 1,2-butylene oxide was initiated by 1,2-butanediol, partly in the form of its potassium salt,. A sample of the

resulting difunctional poly(oxybutylene) gave $M_w/M_n = 1.04$ (GPC) and 27 B units (NMR), equivalent to $M_n = 1940$ **g mol^{-1}.** An appropriate amount of dry ethylene oxide was added and polymerised in the second stage. The resulting copolymer had M_w/M_n 1.08 (GPC) and 84.2 mol-% E (NMR), corresponding to 144 E units. Overall, NMR gave $M_n = 8280$ **g mol^{-1}.** Comparison of the integrals of the resonances of the end-group carbons, which were all **OCH$_2$CH$_2$OH,** with those associated with BE junctions indicated little if any homopoly(oxyethylene) in the product.

The cyclisation of the triblock copolymer followed the acetal-linking procedure described in Section 3.1. Conversion of triblock copolymer **$E_{72}B_{27}E_{72}$** to its cyclic counterpart was 85%. Chain-extended products were separated by fractional precipitation, as described in Section 3.1.1. The GPC curves obtained (not reproduced here) were essentially similar to those illustrated for the cyclisation of PEG10000 in Figure 10. The ^{13}C NMR spectrum of the purified product showed the expected resonances from the acetal link ($\delta_c = 66.8$ and 95.5 ppm) and no signals attributable to end groups **($\delta_c = 61.3$ ppm).** The integrals confirmed the same composition as the precursor copolymer.

7.5.2 Micellisation and micelle properties

Examples of experimental results obtained for cyclic copolymers and their linear triblock precursors are shown in this Section.

7.5.2.1 Dynamic light scattering

Dynamic light scattering (DLS) is an excellent technique for confirming the formation of micelles in dilute solution. Because the intensity of scattered light is z-weighted ($z = wM$) the method is very sensitive. Allied with CONTIN analysis [61], it gives the distribution of hydrodynamic radius (i.e. the hydrodynamically-equivalent hard-sphere radius) for the micelles, as well as the intensity average hydrodynamic radius.

Intensity-fraction distributions of **$\log_{10} r_{h,app}$** (apparent because of the finite concentration) are shown in Figure 19 for 13 g **dm^{-3}** solutions at 25 °C of **c-$B_{27}E_{144}$** and its precursor, **$E_{72}B_{27}E_{72}$.** The narrow distributions centred on **$r_{h,app}$** 10 nm are characteristic of spherical micelles formed by a closed association process [62]. The weak broad peak centred on 60-70 nm seen in the distribution obtained for the cyclic copolymer, but not for the linear copolymer, is attributed to a small proportion of multiblock cyclic copolymer causing micellar linking, much as found for **$B_nE_mB_n$** block copolymers [63] [64]. The

254

proportion by mass of this material is very small, probably less than 0.1 wt-%, and must originate from chain extension before cyclisation (as expected, see Sections 2.1 and 3.1). Small multiblock rings formed in this way would not be removed from the distribution by fractional precipitation. In our experience, this linking effect is generally found for micellar solutions of cyclic block copolymers of concentration greater than 1 wt-% [56]-[58].
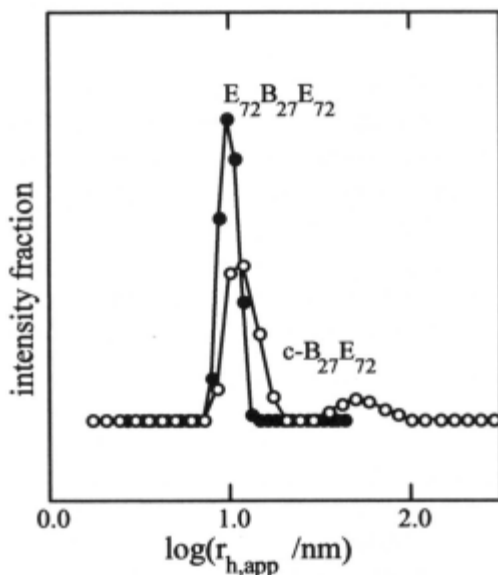
Figure 19 - Intensity-fraction distribution of log(apparent hydrodynamic radius) for aqueous micellar solutions of linear and cyclic oxyethylene/oxybutylene block copolymers, as indicated. Adapted with permission from J. Chem. Soc, Faraday Trans., 92, 5021 (1996).
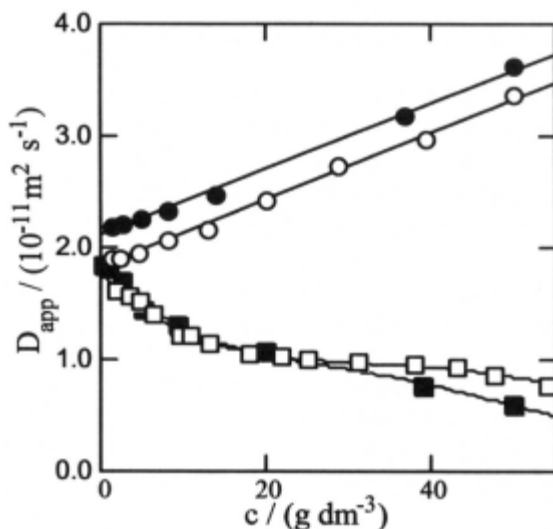
Figure 20 - Concentration dependence of the apparent mutual- (circles) and self- (squares) diffusion coefficients for micelles of cyclic (unfilled) and linear (filled) oxyethytene/oxybutylene block copolymers (c-B27E144 and $E_{72}B_{27}E_{72}$) in aqueous solution. Adapted with permission from J. Chem. Soc, Faraday Trans., 92, 5021 (1996).

The apparent hydrodynamic radius and the apparent mutual diffusion coefficient $(D_{m,app})$ are related through the Stokes-Einstein equation. Values of $D_{m,app}$ for solutions of c-$B_{27}E_{144}$ and $E_{72}B_{27}E_{72}$ at 25 °C, obtained by integrating over intensity distributions ignoring any linked-micelle peaks, are plotted against concentration in Figure 20. Positive slopes of $D_{m,app}$ against c are expected for micelles acting as hard spheres, in this case spheres of hydrodynamic radius $r_h = 12\text{-}13$ nm (infinite dilution).

7.5.2.2 Diffusion coefficient by PGSE-NMR

In related experiments, values of the apparent self-diffusion coefficients $(D_{s,app})$ were obtained for solutions at 22 °C by pulse-gradient spin-echo NMR. These values are compared with those of $D_{m,app}$ from DLS in Figure 20. As expected [65], the concentration dependence of $D_{s,app}$ differs from that of $D_{m,app}$, but (allowing for the difference in temperature between the two experiments) the same value of D is obtained at infinite dilution.

7.5.2.3 Critical micelle temperature and concentration

Critical micelle conditions in aqueous systems are determined either by increasing the concentration of copolymer in solution at a given temperature, when the critical micelle concentration (*cmc*) is that at which micelles are first detected, or by increasing the temperature of a solution of given concentration, when the critical micelle temperature (*cmt*) is that at which micelles are first detected. Light scattering (for *cmt* and *cmc*) and surface tensiometry (for *cmc*) are techniques of choice [56]-[58]. Generally light scattering is more satisfactory, and results from this technique are illustrated in Figure 21.

Plots of light scattering intensity from copolymer solution, relative to that from benzene, against temperature are shown in Figure 21a for solutions of cyclic copolymer *c*-$P_{34}E_{104}$ and its linear triblock precursor $E_{72}P_{34}E_{72}$. The *cmts* are the temperatures at which the intensities depart from the established baselines. Plots of excess light scattering (over that from solvent) are shown in Figure 21b for solutions of cyclic copolymer *c*-$P_{34}E_{104}$ at various temperatures The *cmcs* are the concentrations at which the excess intensities extrapolate to meet the curve established for unassociated molecules of similar composition (shown dashed in Figure 22).

Values of the *cmc* at given *T* and of *cmt* at given *c* are complementary data which can be plotted together as the logarithm of concentration *versus* inverse temperature. This form of the plot comes from application of the van't Hoff equation to the molecule/micelle equilibrium [66]. An example is shown in Figure 22. The plot allows *cmc* and *cmt* data to be smoothed and interpolated. Given certain restrictions [67] [68] the slope of the line gives the standard enthalpy of micellisation, $\Delta_{mic}H^o$.
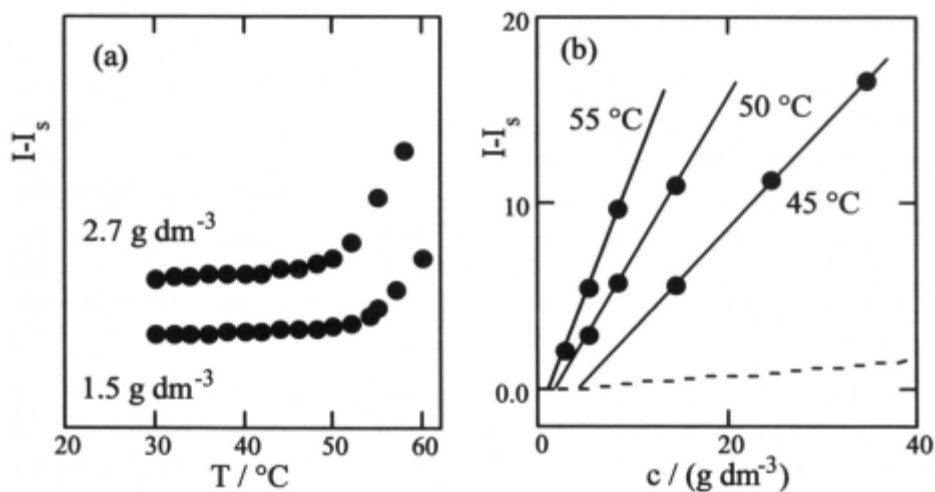
Figure 21 - Excess light scattering intensity relative to that from benzene versus (a) temperature and (b) concentration for aqueous solutions of block copolymer c-$P_{34}E_{104}$. Adapted with permission from Langmuir, 14, 2278 (1998).
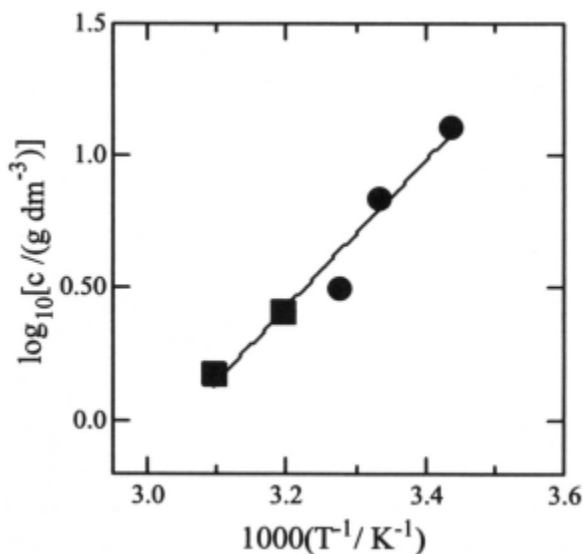
Figure 22 - Critical conditions for micellisation of cyclic block copolymer c-B_8E_{42}. The data points are from (●) light scattering and (■) surface tension. Adapted with permission from Macromolecules, 29, 8479 (1998).

7.5.2.4 Micelle mass and radius

Debye plots for solutions at 25 °C of copolymers c-$B_{27}E_{144}$ and $E_{72}B_{27}E_{72}$ are shown in Figure 23. Angular correction is unnecessary since the micelle diameters are small compared to the wavelength of light. Micellar dissociation is negligible, i.e. there is no significant upturn in Kc/R_{90} in the Debye plots at low concentrations (0.3 g dm^{-3}). This is consistent with very low *cmcs* for these two copolymers (see Section 5.3). Bearing this in mind, the concentration of micelles $(c_{mic} = c\text{–}cmc)$ is equated to c itself with negligible error.

The plots in Figure 23a are restricted to the concentration range $c < 6$ g dm^{-3}, and these data are well fitted by straight lines, so giving precise values of the mass-average molar mass (M_w) and the second virial coefficient (A_2). Given M_w, A_2 can be related directly to the excluded volume (u) [69], and thereby to the thermodynamic volume $(v_t = u/8)$ and the thermodynamic radius (r_t).
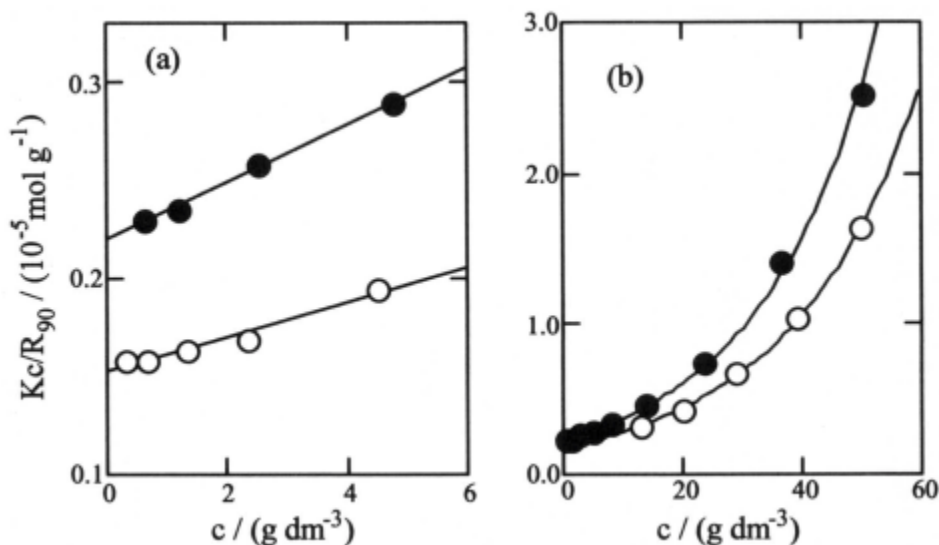
Figure 23 - Debye plots for micellar solutions of copolymers (i) c-$B_{27}E_{144}$ and (¢) $E_{72}B_{27}E_{72}$. Adapted with permission from J. Chem. Soc., Faraday Trans., 92, 5021 (1996).

Because the intensity of light scattered from solutions of the cyclic copolymer can be affected by micellar-linking (see Section 5.1.2), an alternative analysis was also employed. Where possible, the DLS data were used to determine the contribution to the scattering intensity from micellar clusters, the

SLS data for solutions of c-$B_{27}E_{144}$ were corrected, and the corrected data were used to construct the Debye plot seen in Figure 23b. The curves, which are based on scattering theory for hard spheres, fit the data well, and yield micellar properties (M_w, r_t) similar to those from the more conventional Debye plot (Figure 23a), The conformity to scattering theory indicates that the micelles are essentially unchanged in mass, size and shape over the concentration range investigated.

7.5.3   Effect of cyclisation on micellisation and micelle properties

7.5.3.1 Critical micelle concentration

Comparing cyclic copolymers with their linear triblock precursors, the available evidence (see Table 5) favours slightly lower *cmc*s for the cyclic copolymer [56]-[58]. In contrast, a linear diblock copolymer of the same composition has a *cmc* at least ten-times lower than the cyclic. This last result can be understood as linear diblock copolymers have one block junction located in the core/fringe interface of their spherical micelles, whereas cyclic diblock copolymers have two (as illustrated in Figure 24), with a corresponding entropy penalty in the Gibbs energy of micellisation.

Table 5 - Critical micelle concentrations of cyclic and linear block copolymers in aqueous solution

	$T/°C$	cmc / g dm^{-3}	$_{mic}H^o$ / kJ mol^{-1}	Ref.
c-$P_{34}E_{104}$	50	2.1	130±40	[58]
$E_{52}P_{34}E_{52}$	50	2.6	190±20	[58]
$E_{102}P_{37}$	50	0.05	210±20	[70]
c-B_8E_{42}	40	ca. 3	55±10	[56]
$E_{21}B_8E_{21}$	40	ca. 3	95±20	[71]
$E_{41}B_8$	40	0.11	80±10	[72]
c-$B_{27}E_{144}$	25	<0.005	—	[57]
$E_{72}B_{27}E_{72}$	25	<0.01	—	[57]

The temperature dependence of the *cmc* is represented in Table 5 by $\Delta_{mic}H^o$. Positive values of $\Delta_{mic}H^o$ reflect the fact that the temperature coefficient of the *cmc* is negative in these systems, as demonstrated in Section

5.2.3. Values of $\Delta_{mic}H^{o}$ are seen to be low for cyclic copolymers compared to their linear counterparts. This effect has been attributed to reduced exposure of the hydrophobic block to water when a cyclic copolymer is in its unassociated molecular state [56].

7.5.3.2 Micelle properties

Micelle properties are set out in Table 6. In this table, the quantity N_w is the mass-average association number of the micelles calculated as

$$N_w = \frac{M_w(micelle)}{M_w(molecule)}$$

Since high temperature ensures that the copolymers achieve essentially complete micellisation, the comparison in Table 6 is made for solutions in the range 40-55 °C. As can be seen, at these temperatures the association numbers and radii (both hydrodynamic and thermodynamic) of cyclic copolymers are larger than those of their linear triblock counterparts. The micelles of the linear diblock copolymers are much larger sizes than either. This stems directly from the longer effective length of the hydrophobic block in the comparable linear diblock copolymer see Figure 24. To a fair approximation the radii of the micelles formed from the linear diblock copolymers are twice those of the micelles of their cyclic and triblock counterparts, so matching the double length of the hydrophobic block.

Table 6 - Micelle properties of cyclic and linear block copolymers in aqueous solution

	T °C	M_w 10^5 g mol^{-1}	N_w	r_t nm	r_h nm	Ref.
c-P$_{34}$E$_{104}$	50	1.0	14	4.6	7.8	[58]
E$_{52}$P$_{34}$E$_{52}$	50	0.8	11	4.4	7.5	[58]
E$_{102}$P$_{37}$	45	4.6	67	10.2	13.7	[70]
c-B$_8$E$_{42}$	50	0.4	16	2.9	4.4	[56]
E$_{21}$B$_8$E$_{21}$	50	0.15	6	2.2	4.0	[71]
E$_{41}$B$_8$	50	1.1	44	4.9	7.1	[72]
c-B$_{27}$E$_{144}$	40	5.6	62	10.4	12.8	[57]
E$_{72}$B$_{27}$E$_{72}$	40	4.5	49	10.0	11.3	[57]

It is clear from the brief discussion above that the overriding consideration in determining micelle size is geometrical. Developing this further, there is a strong correlation between the maximum-possible length of the hydrophobic core-forming block and the core radius (r_c). We suppose that the statistical weighting of accessible conformations maintains the cyclic copolymer in a more extended conformation in the micelle than is the case for the triblock copolymer, i.e. maintains the hydrophobic block in a hairpin-like conformation. For a given hydrophobic-block length, the effect is to increase the micelle-core radius for the cyclic copolymer compared to that of its precursor triblock copolymer. This is illustrated in Figure 24. There is theoretical support for this effect in the results of Linse's calculations [73] which show a higher association number for a PEP copolymer (loop in the micelle fringe) than for an EPE copolymer (loop in the micelle core). However, we know of no theoretical study of micelle properties of cyclic block copolymers which would provide a direct physical interpretation of their larger size compared with their triblock precursors.
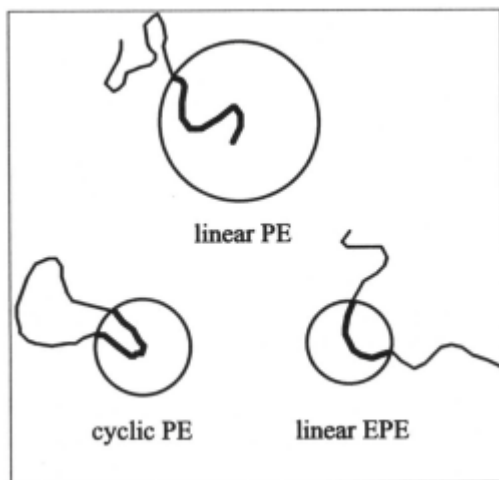
Figure 24 - Representation of chain conformations in micelles of linear diblock, cyclic diblock and linear triblock oxyethylene/oxypropylene block copolymers with the same overall chain length and composition. Reproduced with permission from Langmuir, 14, 2278 (1998).

7.5.4   Gelation

Moderately-concentrated micellar solutions of block copolymers may gel. These materials have been of interest for some time, particularly for pharmaceutical use, possibly as vehicles for drug solubilisation and controlled

release [74] [75]. For drug release from a gel formed on subcutaneous injection, the requirement is a mobile sol at room temperature and a hard gel at body temperature. Block copolyethers are uniquely suited to this application: as an example a phase diagram indicating the hard gel region of aqueous micellar solutions of diblock copolymer $E_{41}B_8$ is shown in Figure 25a [76]. The part sol-gel diagram shown in Figure 25b for solutions of cyclic copolymer c-$P_{34}E_{104}$ and its precursor $E_{52}P_{34}E_{52}$ indicates similar behaviour one to the other, and to solutions of copolymer $E_{41}B_8$. (The amount of cyclic copolymer available did not permit determination of a full phase diagram.)
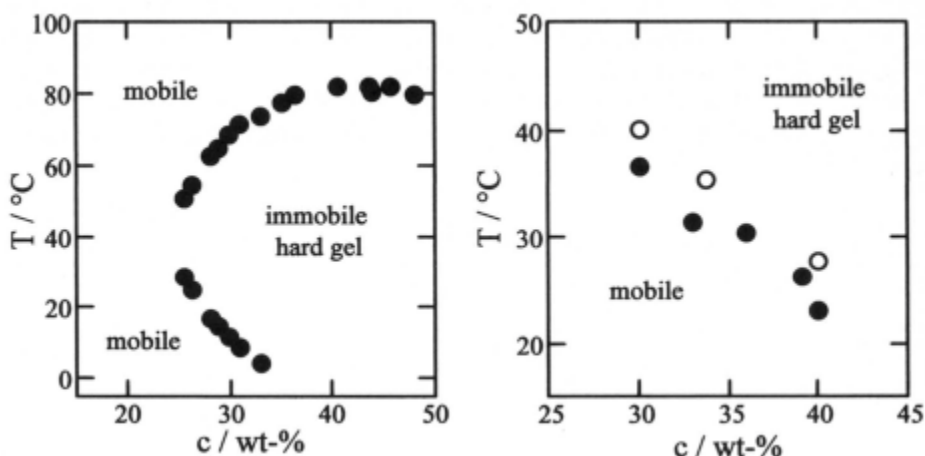
Figure 25 - Gel-sol diagrams for aqueous micellar solutions of: (a) copolymer $E_{41}B_8$ and (b) copolymers (¢) $E_{52}P_{34}E_{52}$ and (í) c-$P_{34}E_{104}$. Adapted with permission from Macromolecules, 29, 8479 (1998) and Langmuir, 14, 2278 (1998).

Hard gels of this type comprise packed spherical micelles acting as hard spheres. The usual structure is body-centred cubic (bcc), and the dynamic elastic modulus can approach 10^5 Pa [76]-[78]. Because of the structural information, it is possible to closely predict the gelation behaviour from known micellar properties. In a bcc gel, the water-swollen spherical micelles must fill a volume fraction 0.68 effectively as hard spheres. The quantity r_t, available from static light scattering (see Section 7.5.3.2, Table 6) is the effective hard sphere radius of a micelle. An expansion (swelling) factor (δ) can be defined as the ratio of the thermodynamic (hard-sphere) volume (v_t) of a micelle to its anhydrous volume, the latter being calculated as $v_a = M_w/\rho_a N_A$, where ρ_a is the density of the anhydrous copolymer $(g\ cm^{-3})$ and N_A is Avogadro's constant. In terms of δ, the critical gel concentration (cgc) at given temperature is given by [79] [80]:

$$cgc \, / \, (\text{g dm}^{-3}) \; = \; 680\rho_a \, /\delta$$

For example, at 50 °C a *cgc* of 272 g **dm⁻³** (*ca.* 26.5 wt%) is predicted from the data in Table 6. Considering the expected shape of the hard-gel region (see Figure 25a), this is as found experimentally.

A cyclic copolymer micellises with loops in the fringe (see Figure 23), and it is possible that enhanced solubilisation might result: e.g. similar to that found with large crown ethers [81]. Moreover, the hydrophobic/hydrophilic nature of the copolymer may transfer useful adsorption properties to a solubilised drug in a drug-copolymer complex. These ideas have not been explored, but the finding that cyclic block copolymers closely mimic the micellisation and gelation behaviour established for linear block copolymers is a useful first step.

7.5.5 Effect of cyclisation on adsorption

7.5.5.1 Air-water interface

Surface tensiometry has been used to study adsorption of c-B_8E_{42} at the air/water interface [56]. The area per molecule in the full Gibbs monolayer (*a*) was obtained by use of the Gibbs adsorption isotherm in the usual way [82]. In Table 7, values of a are compared for aqueous solutions at 40 °C of c-B_8E_{42}, its triblock precursor ($E_{21}B_8E_{21}$) and a linear diblock analogue ($E_{41}B_8$). Also included in Table 7 are values of the surface tension characteristic of the full monolayer (γ). The similarity of the surface properties of the cyclic copolymer and its triblock precursor is in keeping with the similarity of their association properties (see Section 7.5.3).

Table 7 - Surface properties of cyclic and linear block copolymers

Copolymer	$a \, / \, \text{nm}^2$	$\gamma \, / \, \text{mN m}^{-1}$	Ref.
c-B_8E_{42}	1.6	35	56
$E_{21}B_8E_{21}$	1.5	33	70
$E_{41}B_8$	1.2	38	71

7.5.5.2 Solid/liquid interface

Copolymers are used extensively to enhance the stability of colloids To stabilise a hydrophobic colloid in an aqueous systems, the requirement is a

hydrophobic block which will adsorb on the hydrophobic surface (anchor block) and a lengthy hydrophilic block (buoy block) to ensure a positive (repulsive) Gibbs energy of interaction when two particles collide and the adsorbed layers overlap. Oxyethylene/oxybutylene block copolymers are well suited to this application, since a B unit is very hydrophobic, e.g. some six-times the hydrophobicity of an oxypropylene (P) unit, and even a short B block will anchor an E chain to a hydrophobic surface [83].

There is a clear difference in the structure of adsorbed films of linear and cyclic copolymers, in that the buoy blocks of linear diblock E_mB_n and triblock $E_mB_nE_m$ copolymers have tails, whereas those of cyclic copolymers have only loops. The possible consequences of this difference in structure has been examined in a comparative study of the adsorption of copolymers c-$B_{15}E_{206}$, its triblock precursor $E_{103}B_{15}E_{103}$, and two related linear diblock copolymers $E_{106}B_{16}$ and $E_{210}B_{16}$ [59]. The micellisation and association properties of the linear copolymers have been determined [84] [85], and their critical micelle concentrations are known to be very low (diblock copolymers <0.005 g dm^{-3}, triblock copolymer < 0.5 g dm^{-3}, at 25 °C).

Adsorption isotherms (25 °C) for the four copolymers on deuterated poly(styrene) latex particles in aqueous solution were determined by a conventional depletion method. Small-angle neutron scattering (SANS) experiments were carried with sufficient copolymer in solution to attain the plateau region. Table 8 lists the surface area per adsorbed molecule (a, an average of values determined by depletion and SANS), and the root-mean-square thickness of the adsorbed layer determined by SANS (d_{rms}).

Table 8 - Adsorption of block copolymers at a solid/liquid interface

Copolymer	a / nm^2	d_{rms} / nm	r_E / nm
c-$B_{15}E_{206}$	14	3.3	4.8
$E_{103}B_{15}E_{103}$	13	3.1	4.8
$E_{106}B_{16}$	6.2	5.6	4.9
$E_{210}B_{16}$	11	6.7	6.7

It apparent from the parameters listed in Table 8 that the adsorption behaviour of a cyclic copolymer is very similar to that of its triblock precursor. Volume fraction profiles, giving more detail of layer structure, are also remarkably similar for the two copolymers [59]. The major difference lies between triblock and cyclic diblock copolymers on the one hand, and linear

diblock copolymers on the other. In this the adsorption behaviour parallels the association behaviour described in Section 5.3.

Root-mean-square unperturbed end-to-end distances of E chains (r_E) of the same length as the E blocks (or half-length for the cyclics) are listed in Table 2. These were calculated using a value of $C = 5.2$ [86] [87], and a bond length of 0.12 nm [88]. Since the rms radius of gyration approximates $r_E/6$, r_E approximates twice the radius of gyration. Using this quantity for comparison, only the shorter linear diblock copolymer $(E_{106}B_{16})$ is found to be stretched in the adsorbed layer.

7.6.   Concluding remarks

Our work on cyclic oligoethers and polyethers has taken us from a lower bound of conventional crown ether chemistry to an upper bound of relatively large molecules: $M_n = 20000$ g mol^{-1}, i.e. an average of some 1400 backbone atoms in the ring. The basis has been adaptation of the Williamson reaction to achieve efficient cyclisation of glycols, principally through carrying out the reactions at high dilution (ca. 10^{-5} mol dm^{-3} of glycol), but also by accepting the more efficient acetal linking where necessary. Equally important has been our close monitoring of reaction products at all stages by a combination of GPC and ^{13}C NMR.

Concerning physical properties, whether of the solid or the solution state, the overriding feature is a similarity of behaviour of cyclics and their linear precursors across a wide range of ring size: from c-E_{18} (54-crown-l8) to cyclic E_{227} (PEO-10000RA), including cyclic block copolymers. This is seen in crystal structure and extent of chain folding of homo-oligomers and homo-polymers, in adsorption of homopolymers and block copolymers at the air-water and solid-water interfaces, in self association (micellisation) of block copolymers in aqueous solution, and in gelation of concentrated micellar solutions. Of all the properties examined, only the melting points of the smaller rings show significant differences from those of their linear counterparts, an effect related to conformational entropy in the melt state.

Our studies will be extended to microphase separation in block copolymer melt and semicrystalline states where, because of conformational restriction, significant differences would be expected between linear and cyclic analogues.

The cyclics we have prepared have not been used in examination of complexation, whether with chain molecules (rotaxanes) or with large compact molecules (e.g. in solubilisation of certain drugs). In this regard we draw attention to Figure 3, and note that the ring size distributions in preparations from conventional linear polyglycols can be significantly narrower than the those of products prepared by other routes, but which have been used with success in some applications (e.g. solubilisation, modification of thermal properties). In this respect acetal-linked cyclics are of interest, since their function would be pH sensitive.

7.7   Acknowledgements

7.8   References

1.   C.J. Pedersen, J. Am. Chem. Soc., **89**, 2495, 7017 (1967).

2.   D.J. Worsfold and A.M. Eastham, J. Am. Chem. Soc., **79**, 900 (1957); G.A. Latremouille, G.T. Merrall and A.M. Eastham, J. Am. Chem. Soc., **82**,120 (1960); J. Dale, K. Daasvatn and T. Grønneberg, Makromol. Chem., **178**, 873 (1977).

3.   S. Penczek and S. Slomkowski in *Comprehensive Polymer Science, Vol. 3, Chain Polymerisation*, ed. by G.C. Eastmond, A. Ledwith, G. Russo and P. Sigwalt, Pergamon, Oxford, 1989, Ch. 47.

4.   D.G. Stewart, D.Y. Waddan and E.T. Burrows, Brit. Pat. 785 229 (1957).

5.   A. Luttringhaus and K. Ziegler, Liebigs. Ann. Chem., **528**, 155 (1937).

6.   G.W. Gokel in *Large Ring Molecules*, ed. by J.A. Semlyen, Wiley, New York, 1996.

7.   *Crown Ethers and Analogues*, ed. by S. Patai and Z. Rappaport, Wiley, New York, 1989.

8.   J.S. Bradshaw, R.M. Izatt, A.V. Bordunov, C.Y. Chu and J.K. Hathaway in *Comprehensive Supramolecular Chemistry. Vol. 1, Molecular Recognition: Receptors for Catiuonic Guests,* ed. by G.W. Gokel, Pergamon, Oxford, 1996.

9.   P.L. Kuo, M. Miki and M. Okahara, J. Chem. Soc., Chem. Commun., 296 (1979).

10.   P. L. Kuo, N. Kawamura, M. Miki and M. Okahara, *Bull. Chem. Soc. Jpn,* **53,** 1689 (1980).

11. C. A. Vitali and B. Masci, Tetrahedron, **45**, 2201 (1989).

12. Z. Yang, G.-E. Yu, J. Cooke, K. Viras, A. J. Ryan and C. Booth, J. Chem. Soc., Faraday Trans, **92**, 3173 (1996).

13. Z. Yang, J. Cooke, K. Viras, P. A. Gorry, A. J. Ryan and C. Booth, J. Chem. Soc., Faraday Trans., **93**, 4033 (1997).

14. T. Yonemitsu, Z. Yang and C. Booth, to be published.

15. B. Börner, W. Heitz and W. Kern, J. Chromatogr., **53**, 51 (1970).

16. A. Marshall, R. H. Mobbs and C. Booth, Eur. Polym. J., **16**, 881 (1980).

17. H. H. Teo, R. H. Mobbs and C. Booth, Eur. Polym. J., **18**, 541 (1982).

18. S. G. Yeates, H. H. Teo, R. H. Mobbs and C. Booth, Makromol. Chem., **185**, 1559 (1984).

19. J. R. Craven, R.H. Mobbs, C. Booth, E. J. Goodwin and D. Jackson, *Makromol Chem.,* **190**, 1207 (1989).

20. S. Kinugasa, H. Hayashi and S. Hattori, Polymer J., **22**, 1059 (1990).

21. S. Kinugasa, A. Takatsu, H. Nakanishi, H. Nakahara and S. Hattori, Macromolecules, **25**, 4848 (1992).

22. R. Chênevert and L . D'Astous, J. Heterocyclic Chem., **23**, 1785 (1986).

23. R.N. Greene, Tetrahedron Lett, **18**, 1793 (1972).

24. H.W. Gibson, M.C. Bheda, P. Engen, Y.X. Shen, J. Sze, H. Zhang, M.D. Gibson, Y. Delaviz, S.H. Lee, S. Liu, L. Wang, D. Nagvekar, J. Rancourt and L.T. Taylor, J. Org. Chem., **59**, 2186 (1994).

25. Z. Yang, P. Hodge, C. Booth and H.W. Gibson, unpublished work.

26. See, e.g., C. Gong, Q. Ji, C. Subramaniam and H.W. Gibson, Macromolecules, **31**, 1814 (1998), footnote 13.

27. M.C. Bheda, J.S. Merola, W.A. Woodward, V.J. Vasudevan and H.W. Gibson, J. Org. Chem., **59**, 1694 (1994).

28. K. Fukuhara, K. Ikeda and H. Matsuura, J. Mol. Struct, **224**, 203 (1990).

29. J.D. Dunitz, and P. Seiler, Acta Crystallogr, **B30**, 2739 (1974).

30. E. Maverick, P. Seiler, W.B. Schweizer and J.D. Dunitz, Acta Crystallogr., **B36**, 615 (1980).

31. J. van Eerden, A. Roos, S. Harkema, P.D.J. Grootenhuis and D.N. Reinhoudt, Acta. Crystallogr., **B43**, 799 (1987).

32. Y. Takahashi and H. Tadokoro, Macromolecules, **6**, 881 (1973).

33. H.M. Colquhoun, private communication.

34. H. Matsuura and T. Miyazawa, Bull. Chem. Soc. Jpn., **42**, 372 (1969).

35. H. Matsuura and K. Fukuhara, J. Mol. Struct, **126**, 251 (1985).

36. H. Matsuura and K. Fukuhara, J. Phys. Chem., **91**, 6139 (1987).

37. J.R. Craven, H. Zhang and C. Booth. J. Chem. Soc., Faraday Trans, **87**, 1183 (1991).

38. J. Cooke, PhD Thesis, UMIST (1998).

39. G. Ungar, J. Stejny, A. Keller, I. Bidd and M.C. Whiting, Science, **229**, 386 (1985).

40. S.G. Yeates and C. Booth, Makromol. Chem., **186**, 2663 (1985).

41. G Lieser, K.-S. Lee and G. Wegner, Colloid Polym. Sci., **266**, 419 (1988).

42. C. Campbell, K. Viras, M.J. Richardson, A.J. Masters and C. Booth, Makromol. Chem., **194**, 799 (1993).

43. T. Sun, G.-E. Yu, C. Price, C. Booth, J. Cooke and A.J. Ryan, Polymer Commun., **36**, 3775 (1995).

44. J. Cooke, G.-E. Yu, T. Sun, K. Viras, P. A. Gorry, A. J. Ryan, C. Price and C. Booth, Macromolecules, **31**, 3030 (1998).

45. Z.-G. Yan, Z. Yang, C. Price and C. Booth, Makromol. Chem., Rapid Commun., **14,** 725 (1993).

46. G.-E. Yu, P. Sinnathamby, C. Price and C. Booth, Chem. Commun., 31 (1996).

47. K. Ishizu and Y. Akiyama, Polymer, **38**, 491 (1997).

48. P.V. Wright and M.S. Beevers in *Cyclic Polymers*, ed by J.A. Semlyen, Elsevier, London, 1986, Ch. 3.

49. G.-E. Yu, T. Sun, Z.-G.Yan, C. Price, C. Booth, J. Cooke, A.J. Ryan and K. Viras, Polymer, **38**, 35 (1997).

50. K. Viras, Z.-G. Yan, C. Price, C. Booth and A.J. Ryan, Macromolecules, **28**, 104 (1995).

51. C. Booth in *Comprehensive Polymer Science, Vol. 1, Polymer Characterisation*, ed. by C. Booth and C. Price, Pergamon, Oxford, 1989, p. 66.

52. P.C. Griffiths, P. Stilbs, G.-E. Yu and C. Booth, J. Phys. Chem., **99**, 16752 (1995).

53. C. Booth, R. W. Richards, M. R, Taylor and G.-E. Yu, J. Phys. Chem., **102**, 2001 (1998).

54. G.-E. Yu, P. Sinnathamby, T. Sun, F. Heatley, C. Price and C. Booth, Macromol. Rapid Commun., **18**, 1085 (1997).

55. C. Chaibundit, F. Heatley, S.-M. Mai, T. Sun and C. Booth, to be published.

56.   G.-E. Yu, Z. Yang, D. Attwood, C. Price and C. Booth, Macromolecules, **29**, 8479 (1996).

57.   G.-E. Yu, Z.-K. Zhou, D. Attwood, C. Price, C. Booth, P.C. Griffiths and P. Stilbs, J. Chem. Soc., Faraday Trans., **92**, 5021 (1996).

58.   G.-E. Yu, C.A. Garrett, S.-M. Mai, H. Altinok, D. Attwood, C. Price and C. Booth, Langmuir, **14**, 2278 (1998).

59.   P.C. Griffiths, T. Cosgrove, J. Shar, S.M. King,, G.-E. Yu, C. Booth and M.Malmsten, Langmuir, **14**,1799 (1998).

60.   M. Pollard, PhD Thesis, University of Manchester, 1999.

61.   S.W. Provencher, Makromol. Chem., **180**, 201 (1979).

62.   H.-G. Elias in *Light Scattering from Polymer Solutions* ed. by M.B. Huglin, Academic Press, London, 1972.

63.   Y.-W. Yang, Z. Yang, Z.-K. Zhou, D. Attwood and C. Booth, Macromolecules, **29**, 670 (1996).

64.   Z. Yang, Y.-W. Yang, Z.-K. Zhou, D. Attwood and C. Booth, J. Chem. Soc., Faraday Trans., **92**, 257 (1996).

65.   H. Vink, J. Chem. Soc., Faraday Trans. 1, **81**,1725 (1985).

66.   D. Attwood and A.T. Florence, *Surfactant Systems,* Chapman and Hall, London, 1983, p. 101.

67.   D.G. Hall in *Nonionic Surfactants, Physical Chemistry, Surfactant Science Series, Vol 23.* ed. by M.J. Schick, Marcel Dekker, New York, 1987.

68.   X.-F. Yuan, A.J. Masters and C. Price, Macromolecules, **25**, 6876 (1992).

69.   P.J. Flory, *Principles of Polymer Chemistry,* Cornell UP, New York, 1953, p. 532.

70.   H. Altinok, G.-E. Yu, S. K. Nixon, P.A. Gorry, D. Attwood and C. Booth, Langmuir, **13**, 5837 (1997).

71.   Z. Yang, S. Pickard, N.-J. Deng, R.J. Barlow, D. Attwood and C. Booth, Macromolecules, **27**, 2371 (1994).

72.   G.-E. Yu, Z. Yang, M. Ameri, D. Attwood, J.H. Collett, C. Price and C. Booth, J. Phys. Chem., Part B, **101**, 4394 (1997).

73.   P. Linse, Macromolecules, **26**, 4437 (1992).

74.   I.R. Schmolka, J. Biomed. Mater. Res., 6,571 (1972): I.R. Schmolka in *Polymers for Controlled Drug Delivery*, (ed. by P. Tarcha) CRC, Boca Raton, FL, 1991, p. 189.

75.   M.W. Edens in *Nonionic Surfactants, Polyoxyalkylene Block Copolymers, Surfactant Science Series Vol. 60,* ed. by V.M. Nace, Marcel Dekker, New York, 1996, p. 185.

76. H. Li, G.-E. Yu, C. Price, C. Booth, E. Hecht and H. Hoffmann, Macromolecules, **30,** 1347(1997).

77. K. Mortensen and J.S. Pedersen, Macromolecules, **26,** 805 (1993).

78. I. W. Hamley, K. Mortensen, G.-E. Yu and C. Booth, Macromolecules, **31,** 6958 (1998).

79. N.-J. Deng, Y.-Z. Luo, S. Tanodekaew, N. Bingham, D. Attwood and C. Booth, J. Polym. Sci., Part B, Polym. Phys., **33,** 1085 (1995).

80. Y.-W. Yang, Z. Ali-Adib, N.B. McKeown, A.J. Ryan, D. Attwood and C. Booth, Langmuir, **13,** 1860(1997).

81. Y.-X. Shen, D. Xie and H.W. Gibson, J. Am. Chem. Soc. **116,** 537 (1994).

82. D. Attwood and A.T. Florence, *Surfactant Systems*, Chapman and Hall, London, 1983, p. 12.

83. K. Schillen, P.M. Claeson, M. Malmsten, P. Linse and C. Booth, J. Phys. Chem., Part B, **101,** 4238 (1997).

84. A. Kelarakis, V. Havredaki, G.-E. Yu, L. Derici and C. Booth, Macromolecules, **31,** 944 (1998)

85. A. Kelarakis, V. Havredaki, L. Derici, G.-E. Yu, C. Booth and I. W. Hamley, J. Chem. Soc., Faraday Trans., **94,** 3639 (1998).

86. D.R. Beech and C. Booth, J. polym. Sci., Part A-2, **7,** 575 (1969).

87. A. Abe in *Comprehensive Polymer Science, Vol. 2, Polymer Properties*, ed. by C. Booth and C. Price, Pergamon, Oxford, 1989, p. 55.

88. P.J. Flory, *Statistical Mechanics of Chain Molecules,* Interscience, New York, 1969, p. 165.

CHAPTER 8.
LARGE CYCLIC ESTERS AND ETHER-ESTERS

Barry R. Wood and S. Caroline Hamilton
Department of Chemistry, University of York, UK.

Introduction

Cyclic polyesters were some of the earliest cyclic polymers to be prepared. Vorlander[1] in the 1890's prepared the cyclic dimer of ethylene succinate and Carothers[2] experimented with a range of 17 bond cyclic esters in an attempt to produce artificial musk for the perfume industry. Since then many cyclic esters have been synthesised. The synthetic approach to these cyclic polymers is outlined in the following section. The study of cyclic ether-esters is a newer field, with considerable work having been carried out by Bradshaw and co-workers in the 1970's. The synthesis of ether-esters is very similar to that of the esters as is shown in the following section. The characterisation of cyclic esters and ether-esters is discussed in relation to those polymers recently and currently being produced at the University of York, U.K. Finally, the application of cyclic esters and ether-esters is reviewed briefly and possible future applications are postulated.

8.1 Large Ring Ester and Ether-Ester Synthetic Methods

There are a number of different methods of polyester macrocycle synthesis.

8.1.1 - From dibasic acids or diesters and glycol or diols.

The earliest reported macrocyclic compound prepared from a dibasic acid was cyclic dimeric ethylene succinate which was described by Vorlander in 1894 [1]. This reaction is shown below in Figure 8.1.1-1. The same compound has subsequently been prepared by others [2,3,4].

HOOCCH$_2$CH$_2$COOH + HOCH$_2$CH$_2$OH $\xrightarrow{\Delta}$
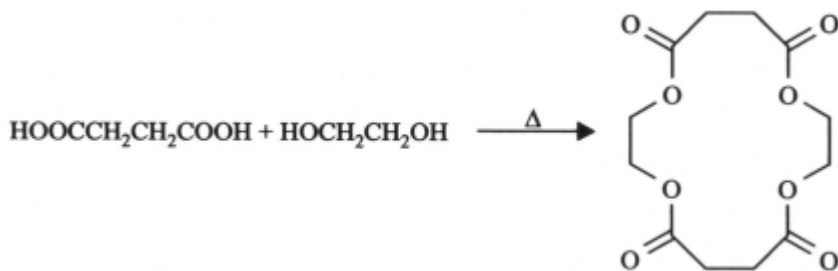
Figure 8.1.1-1 - The first macrocycle prepared by Vorlander [1].

Since then, a variety of macrocyclic diesters have been made from the dibasic acid or open chain diesters [5,6]. Vögtle and Neumann have prepared some macrocyclic di- and tetraesters from m-phenylenediacetic acid and various glycols [7], as is shown in Figure 8.1.1-2.
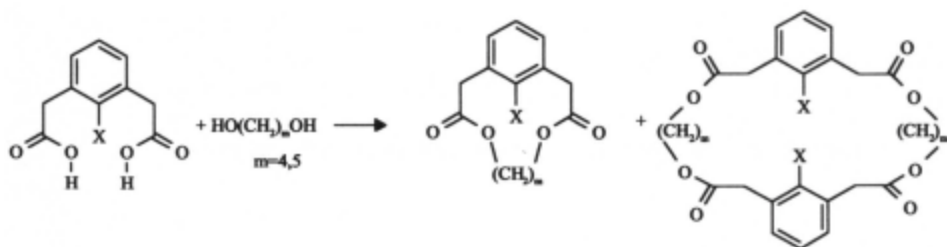
Figure 8.1.1-2 - The macrocyclic di- and tetra-esters of Vögtle and Neumann [7].

Hahn and coworkers have prepared two unusual macrocycles, "Paddleanes" with four ester units from the reaction of either 1,4-bis(hydroxymethyl)bicyclo[2.2.2.]octane and sebacoyl chloride or 1,4-dicarboxylbicyclo[2.2.2.]octane and 1,10-decandiol [8], as shown in Figure 8.1.1-3.
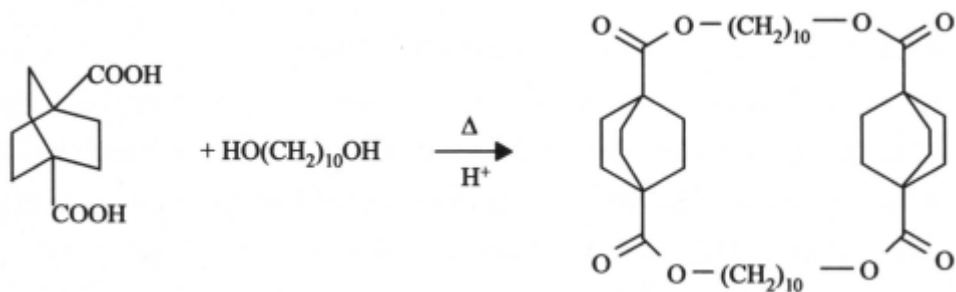
Figure 8.1.1-3- Hahn's Paddleanes [8].

By reacting various glycols with aliphatic dibasic acids, Stoll and Rouvé obtained both cyclic one-to-one (monomeric) and two-to-two (dimeric) adducts [9] as shown in Figure 8.1.1-4.

274
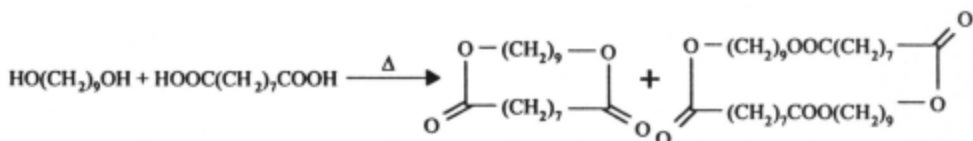
Figure 8.1.1-4 - The monomeric and dimeric adducts of Stolle and Rouvé

Stueben isolated a macrocyclic tetraester containing the cyclobutane unit when he polymerised trans-1,2-cyclobutanecarboxylic acid and ethylene glycol [10], as shown in Figure 8.1.1-5.
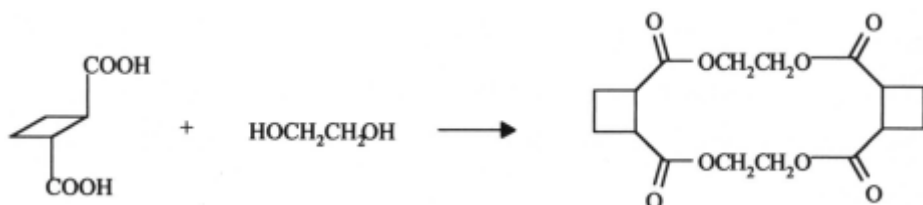
Figure 8.1.1-5 - Steuben's macrocyclic tetraester containing the cyclobutane unit [10].

8.1.2 - From Salts of Dibasic Acids and Alkyl Dihalides

Drewes and coworkers have prepared a number of macrocyclic di- and tetraesters by reacting the salts of dibasic acids with various dihalides [11-15]. When dipotassium phthalate was used, they obtained the dimer shown in Figure 1.12-1 where **n=2,3,7,9** and 11 and monomer where **n=4,5,6,8,10** and 12 [12].
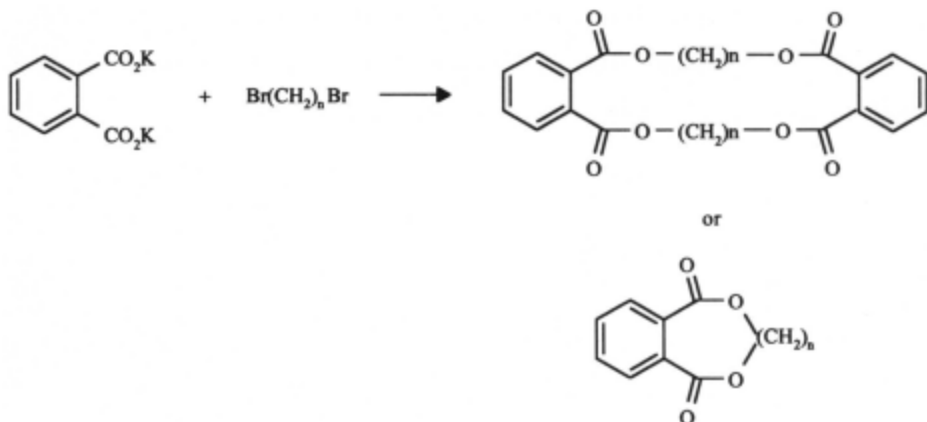
Figure 8.1.2-1 - Drewes pioneered the synthetic route using salts of dibasic adds and alkyl dihalides [11-15].

The rings contained even numbers in all cases except where **n=5.** Drewes suggested that for intermediate rings (size 8 to 18), odd numbered rings are more difficult to prepare than the even numbered owing to greater interferences during ring closure [12]. Spanagel and Carothers also observed this general phenomenon in their synthesis of macrocyclic diesters [16]. One steric factor that seems to control ring formation is the incorporation of a rigid structure compromising four atoms in a plane with angles of 120° [17]. The macrocyclic phthalates that Drewes prepared[11,12] are good examples of this requirement. Baker, McOmie and Ollis suggested that orthodisubstituted benzene derivatives should easily form 8-, 12-, 16- and higher membered ring systems[17]. That the rigid structure is an important factor in ring formation was shown by the work of Pedersen when he obtained dibenzo-18-crown-6 in 40% yield while 18-crown-6 was obtained in only 2% yield [18] (see Figure 8.1.2-2). The unsubstituted 18-crown-6 has since been obtained in high yields and ring closure reactions to obtain the ring compounds seem to be controlled more by a complexation or template effect than by other factors [19].

The rigid structure effect for ring formation is also shown by the synthesis of macrocyclic compounds from o-dibromoxylene and the salts of various aliphatic dibasic acids [15] as shown in Figure 8.1.2-3.

Dibenzo-18-Crown-6   18-Crown-6
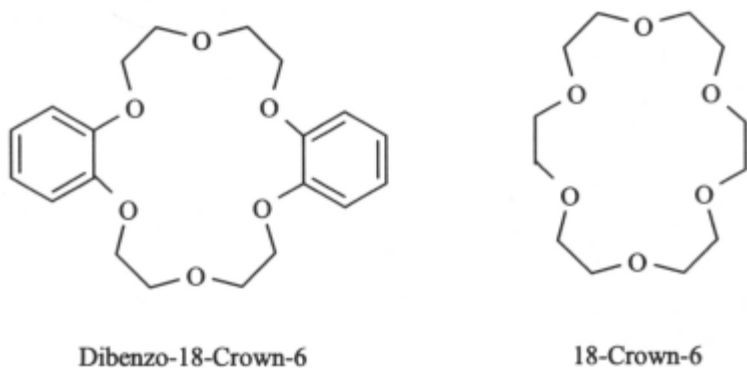
Figure 8.1.2-2 - Dibenzo-18-crown-6 and 18-crown-6.
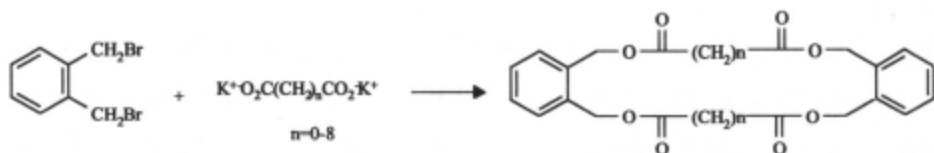
Figure 8.1.2-3 - More evidence of the rigid structure effect.

The work of Drewes and Riphagen showed that ring sizes of 16, 20, 28 and 32 were most easily prepared as suggested by Baker and co-workers [17]. The other even numbered ring systems (sizes 18-30) were also isolated, but in much diminished yields i.e. 0.6% for the 18 membered ring compound versus 35.3% and 16% for the 16- and 20-membered rings respectively [15]. The same workers also prepared macrocyclic tetraester compounds from dipotassium maleate (as shown in Figure 8.1.2-4), citraconate and phthalate with diacetylenic bromides [14]. These compounds were all either 20- or 24-membered rings.
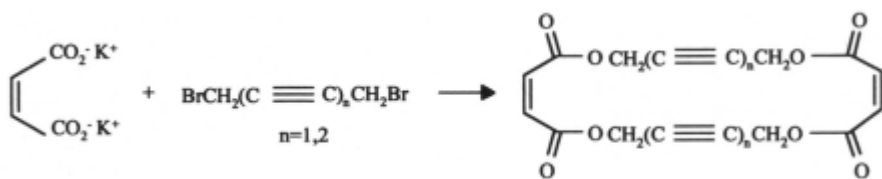
Figure 8.1.2-4 - Tetraester compound from dipotassium maleate prepared by Drewes [14].

The steric effect of rigid structures did not operate in a two step synthesis of macrocyclic diphthalates [13] (Figure 8.1.2-5)
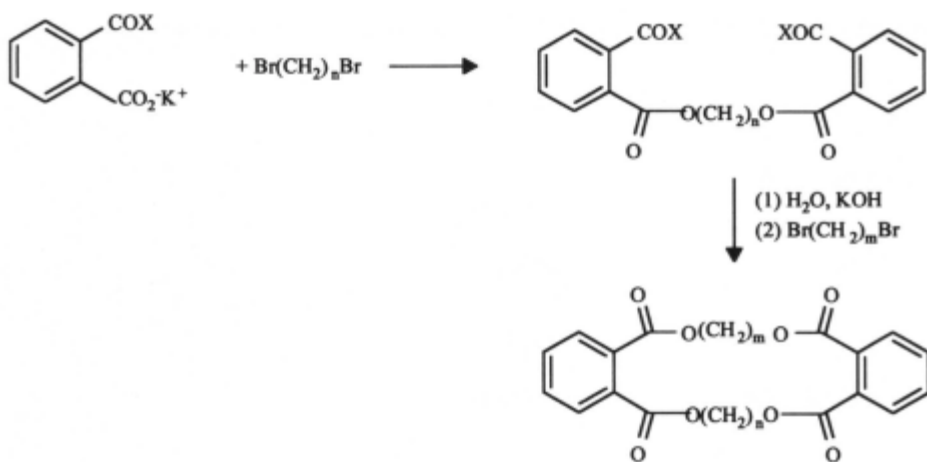
Figure 8.1.2-5- Drewes phthalate macrocycles [13].

The yields of all rings, both even and odd numbered were 10% or below except 19-, 20- and 22-membered rings where the yields were slightly higher. One noticeable exception to these low yields was found in the synthesis of the 20-membered ring shown in Figure 8.1.2-6, where the yield was 31.7%. This compound has a new rigid group in the form of a double bond [13].
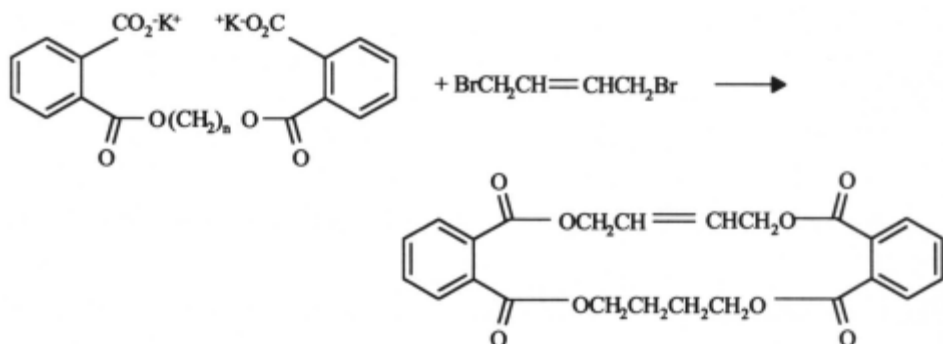
Figure 8.1.2-6 The rigid group here is a double bond [13].

Kaplan and Truesdale prepared p-xylene-1,4-benzenediacetate by heating the disilver salt with dibromo-p-xylene[20]. This scheme is shown in Figure 8.1.2-7.
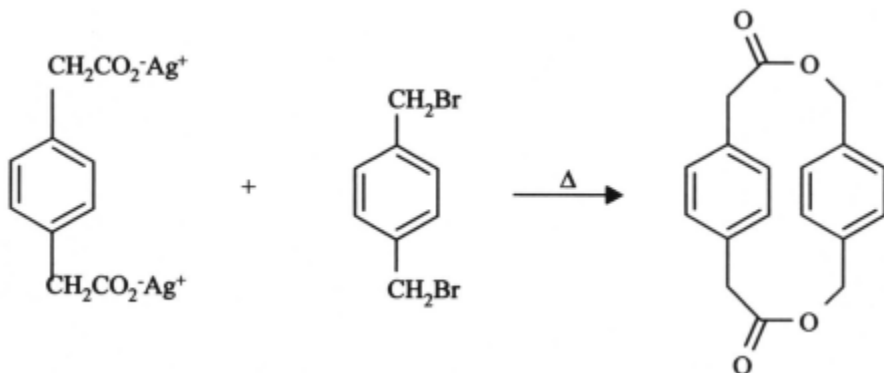
Figure 8.1.2-7 - Macrocycle synthesis using silver salts [20].

8.1.3 - By Depolymerisation of Linear Polyesters

The most interesting early development in the synthesis of macrocyclic diester compounds was the discovery by Carothers and co-workers that linear polyesters could be depolymerised using certain metal catalysts to yield the cyclic monomeric and dimeric adducts [16,21]. The latter adducts prevailed

when the unit lengths were 8-11 and the monomeric cyclic adducts for unit lengths of 13 or greater. For example when polymeric trimethylene succinate (unit length 9 atoms) was depolymerised, a 46% yield of a crude distillate was isolated which contained 9% of the cyclic monomer and 89% of the cyclic dimer; whereas with oxymethylene succinate (unit length 14 atoms), the crude distillate contained 55% monomer and only 5% dimer [16]. This is illustrated in Figures 8.1.3-1 and 8.1.3-2.
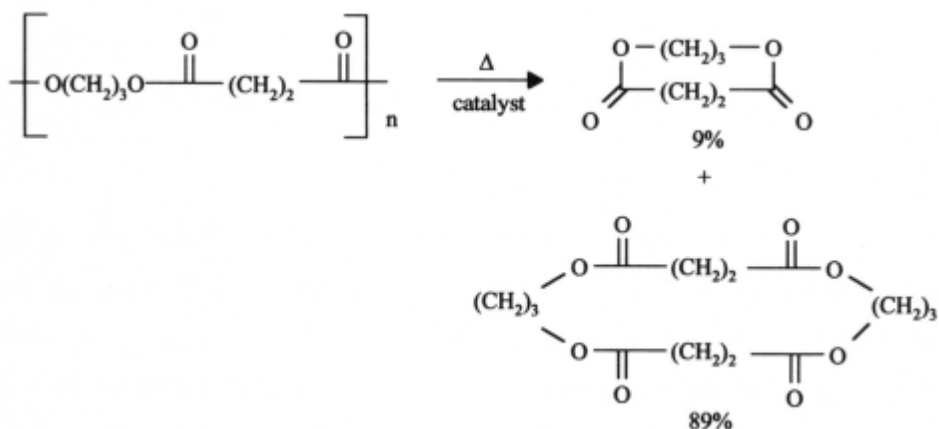
Figure 8.1.3-1 - The depolymerisation of polymeric trimethylene succinate [16].
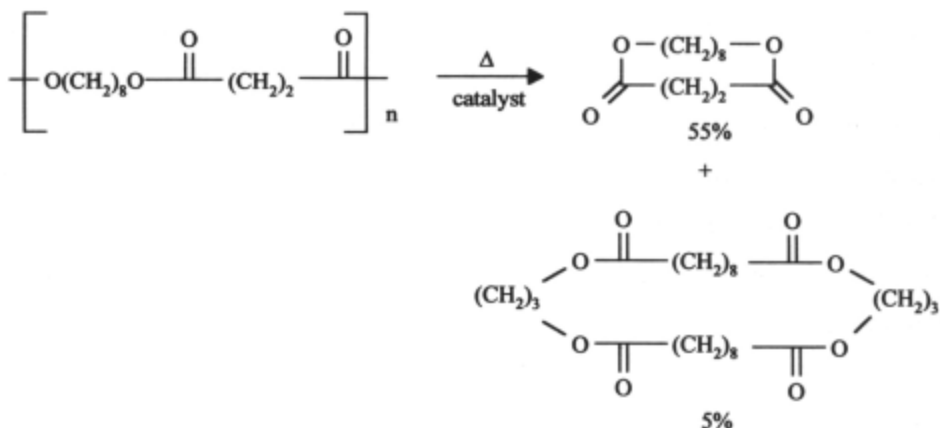
Figure 8.1.3-2 - The depolymerisation of oxymethylene succinate [16].

The best depolymerisation catalysts found were the divalent salts of tin, iron, manganese and cobalt [16]. Spanagel and Carothers also observed that the odd-membered rings were relatively more difficult to prepare [16]. This alternating effect of yields was also noted by Hill and Carothers in the preparation of macrocyclic anhydrides [22] and by Ziegler and Aurnhammer in the synthesis of large cyclic ketones [23].

A typical procedure to prepare the cyclic di or tetraester is to first synthesise the polyester by heating an equivalent amount of the dibasic acid (or diester) and diol until the water (or alcohol) is completely removed The polyester is then mixed with 1-2% of the catalyst and heated to around 270 °C at 1mm Hg pressure. The cyclic monomer or dimer then slowly distils from this mixture. The distillate is then purified usually by recrystalisation from alcohol [6,24]. Many different macrocyclic di- and tetraesters have been prepared using this method, either from the polyester or from reaction mixtures containing various oligomers and polymers. The glycols used in these reactions were

mostly the oligo(methylene glycols). The dibasic acid includes carbonic [21], oxalic [21,25,26], malonic [21], succinic [3,16,21], glutaric [16,27], adipic [16,27] and the higher alkanedicarboxylic acids [16,21,27] as well as phthalic [28] and resorchinol and hydroquinone diacetic acids [24]. This field tends to use the old nomenclature, so for clarification the structures of the groups mentioned are detailed in Figure 8.1.3-3.
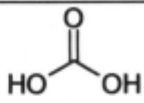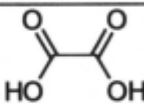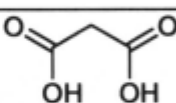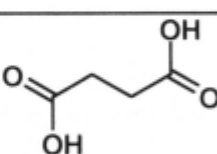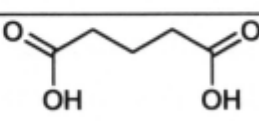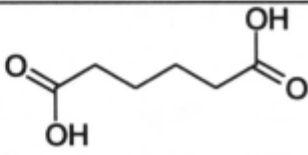
Old nomenclature of Dibasic acids	Structure
Carbonic	
Oxalic	
Malonic	
Succinic	
Glutaric	
Adipic	

Figure 8.1.3-3 - Structures and old nomenclature.

8.1.4 - From Diacid Chlorides and Glycols

Although esters are often easier to prepare from acid chlorides, only in the 1980's had this technique been generally used to synthesise macrocyclic diester compounds. Zahn and co-workers in 1970 reported the preparation of macrocyclic terephthalates and bis(terephthalates) from terephthaloyl chloride [29,30]. Sakamono and Oki described the synthesis of a series of hetero-p-cyclophanes from substituted 1,4-phenyldiacetyl chloride and various glycols [31-35] They studied the interesting correlations among the nmr spectra, size and rigidity of the paracyclophane rings.
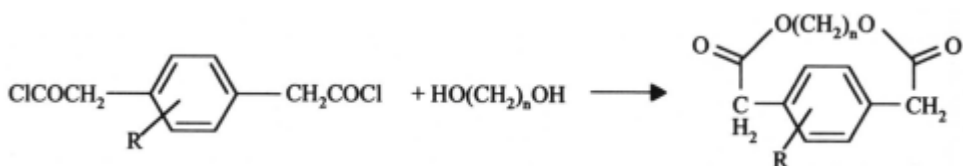
Figure 8.1.4-1 - Paracyclophane rings as prepared by Sakamono and Oki [31-35].

Bradshaw and co-workers have described a variety of compounds prepared from diacid chlorides. Their work has concerned the synthesis of macrocyclic multidentate polyether-diester compounds from various diacid chlorides and oligo(ethylene glycols), some of which contain sulphur atoms. Their first compounds were prepared from aliphatic diacid chlorides and oligo(ethylene glycols) (Figure 8.1.4-2) These include examples of oxalates [26], malonates [36-39], succinates [5,38,39], glutarates [38,39] and adipates [39]. More than 25 of these compounds have been prepared.
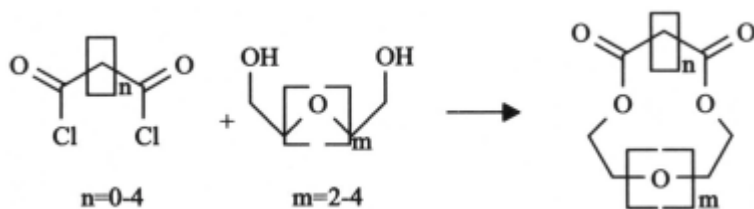
Figure 8.1.4-2 - Bradshaw's prolific method of macrocycle synthesis [26, 36-39,5].

Another series of compounds have been prepared from the diglycol and thiodiglycol chlorides and various oligo(ethylene glycols), some of which contain sulphur atoms [36,40,41] Some 15- and 18-membered rings in this series which contain two or four methyl substituents have also been prepared [42].
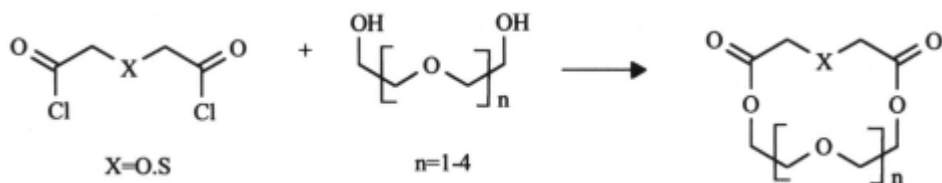
Figure 8.1.4-3 - Heteroatom inclusion in macrocyles.

A third series of macrocyclic diesters comprising more than 25 compounds have been prepared from aromatic diacid chlorides, the general methodology of which is shown in Figure 8.1.4-4.
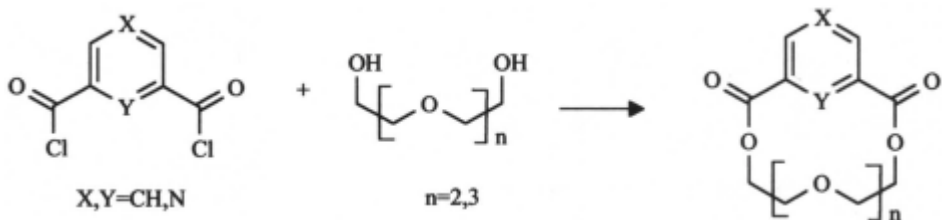
Figure 8.1.4-4 - General diacid chloride route.

Compounds have been prepared from the following aromatic diacids: 3,5-pyridinedicarboxylic [40,41,43], phthalic [44,45], isophthalic [46] and terephthalic acids [46]. Vögtle and co-workers have also prepared some of these compounds [47].

8.1.5 - By Oxidative Coupling of Diacetynes Containing a Diester Unit

Oxidative coupling of diacetylinic compounds containing a diester unit has been used by Nakagawa and Toda [48,49], Eglington and Galbraith [50,51] and Bohlmann and co-workers [52] to prepare macrocyclic diester-diacetyenic compounds. Nakagawa and Toda [48,49] found 2,2-dibenzofuranyl as a by-product in their preparation of cyclic derivatives of o,o-dihydroxydiacetylene, as shown in Figure 8.1.5-1.
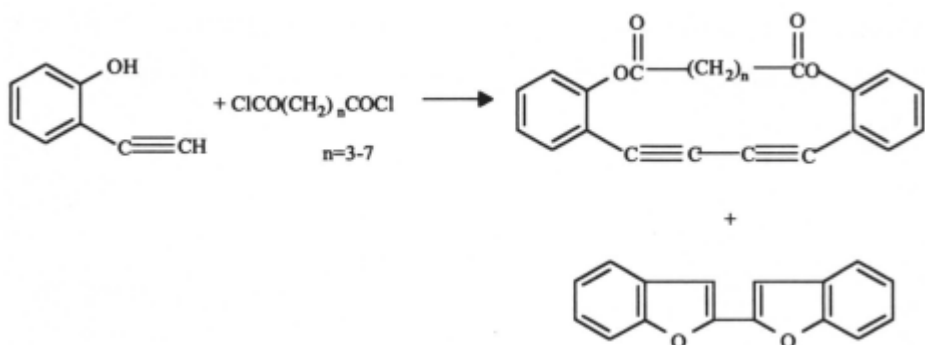
Figure 8.1.5-1 - Toda's preparation of cyclic derivatives of o,o-dihydroxydiacetylene [49,50].

It is interesting to note that even though this system is highly strained, the 16-membered ring **(n=4)** was isolated in a relatively high yield (40% vs. 21% or less for the other rings).

Eglington and Galbraith prepared 20-membered cyclic monomers and 40-membered cyclic dimers when they coupled diacetylenic compounds containing diester groups [50,51] (Figure 8.1.5-2).
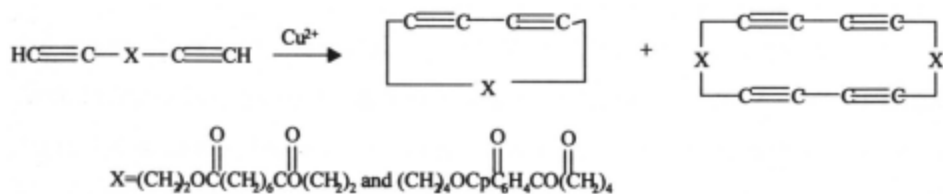
Figure 8.1.5-2 - Oxidative coupling by Eglington and Galbraith [50,51].

Again it is interesting to note that Eglington and Galbraith could not isolate products where **n=1** or 2.

Bohlmann and co-workers also isolated a highly unsaturated macrocyclic diester compound by the diacetylene process [52], and this is shown in Figure 8.1.5-3.
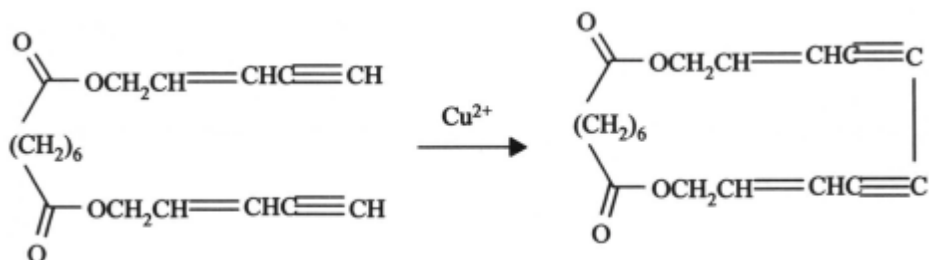
Figure 8.1.5-3 - Bohlmann isolated a highly unsaturated macrocycle by the diacetylene process [52].

8.1.6 - Polymer Supported Method

This method was pioneered in the early 1990s by Wood, Semlyen and Hodge [53,54,55]. It involved ionically binding the reactant monomer to a polystyrene polymer support. On heating the monomers would polymerise by an intramolecular alkylation reaction. When an intramolecular alkylation reaction occurs, a cyclic is formed which is then freed from the polymer support. Because the linear species are still attached to the polymer support, the cyclics can easily be separated. Wood, Semlyen and Hodge prepared cyclics in this way from bromoundecanoic acid and terephthalic acid mono-2 bromoethyl ester. The mechanism for the polymerisation of bromoundecanoic acid is shown in Figure 8.1.6-1 below.
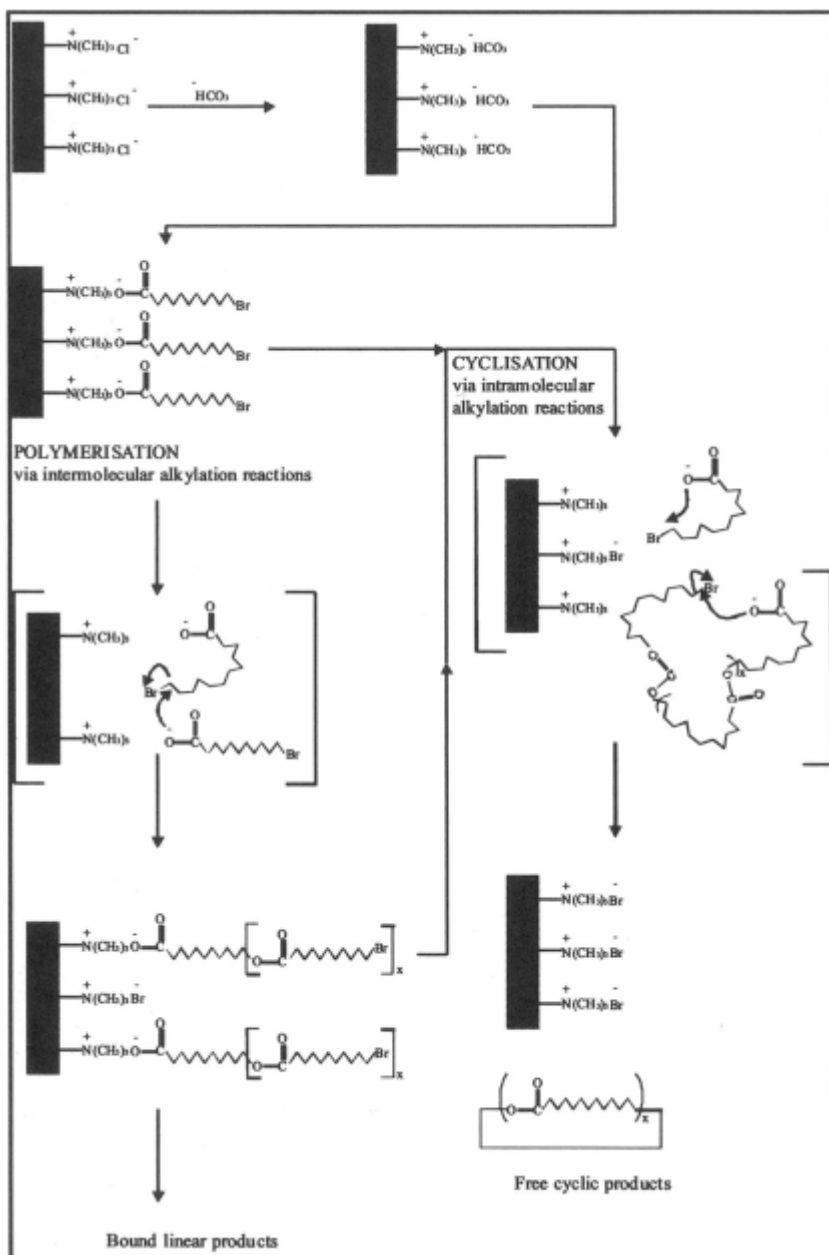
Figure 8.1.6-1 - The Polymer supported method investigated by Wood,Hodge and Semlyen [53,54,55].

8.1.7 - Miscellanious methods

A few macrocyclic diesters have been prepared by oxidative reactions of alkenes, dienes and glycols. Yukawa and Sakai reported that styrene reacts with lead bis(dicarboxylate) to form a cyclic diester [56], as shown in Figure 8.1.7-1.

$$Pb(O_2C(CH_2)_nCO_2)_2 + C_6H_6CH = CH_2 \longrightarrow \begin{array}{c} C_6H_5CH - CH_2 \\ | \qquad\qquad | \\ O_2C(CH_2)_nCO_2 \end{array}$$

n=7,8
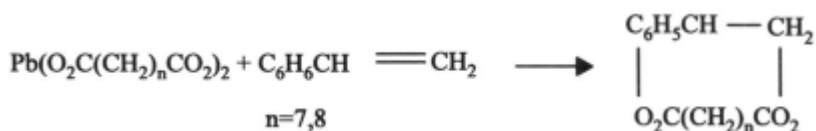
Figure 8.1.7-1 - The cyclic diester prepared by Yukawa and Sakai [56].

Kammerer and Pachta have shown that 2,2-azobisisobutyronitrile reacts with a diene which contains two ester groups to form two macrocyclic diesters [57,58] (Figure 8.1.7-2).
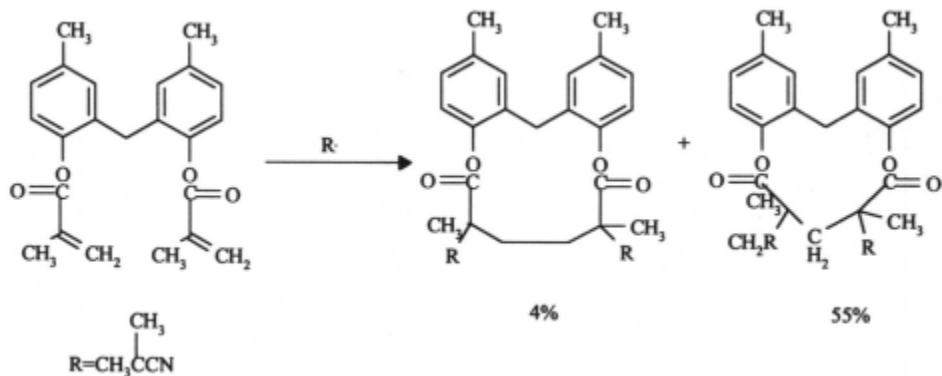
Figure 8.1.7-2 - Kammerer and Pachta's reaction [57,58]

Another oxidative process to form cyclic diesters was reported by Suga and Matsuura [59]. They isolated a cyclic diester when trans-1,2-cyclohexanediol was oxidised with tert-butyl chromate (Figure 8.1.7-3).
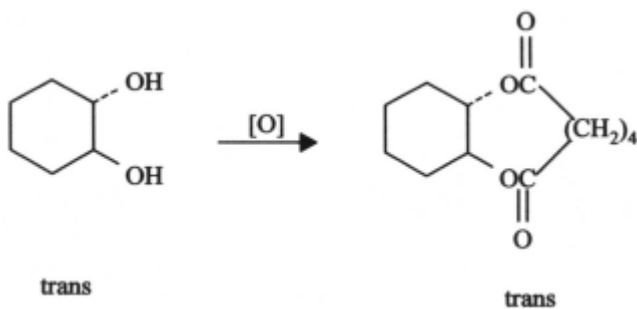
Figure 8.1.7-3 - Suga and Matsuura's cyclic diester [59].
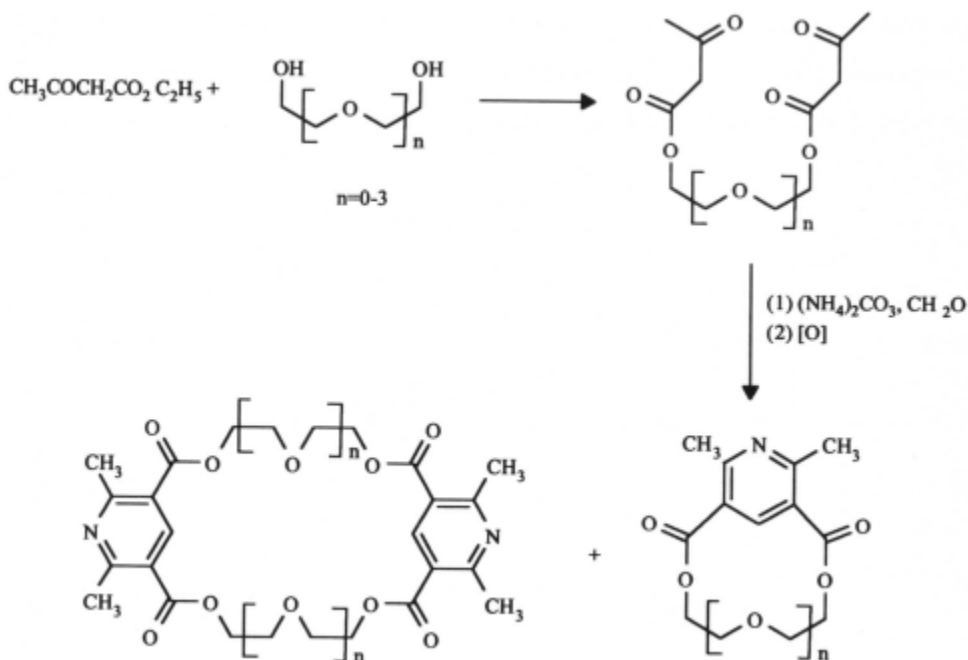
Figure 8.1.7-4 - van Bergen and Kellog's synthesis of macrocycles containing pyridine moieties.

Van Bergen and Kellog were able to prepare macrocyclic polyether-diester compounds containing one or two pyridine moieties by reacting the bis(acetoacetic) ester of various oligo(ethylene glycols) with ammonium carbonate and formaldehyde [60] (Figure 8.1.7-4).

8.2 Recent investigations.

At York, many cyclic ester and ether-esters have been prepared using dilute solution ring-chain transesterification reactions (Figures 8.2-1 and 8.2-2). This preparative method was used in preference to other preparative methods because it enabled a distribution of ring sizes to be prepared. The method also has the benefit that the reactions can readily be scaled up and the solvent could be easily recycled. As with all branches of polymer chemistry, characterization is very important. We have used a variety of instrumental techniques in the investigation of cyclic polymers, such techniques include gel permeation chromatography, mass spectroscopy, nuclear magnetic resonance spectroscopy, light scattering, neutron scattering and X-ray diffraction. Of these techniques gel permeation chromatography and mass spectroscopy have been routinely used to characterize cyclic esters and ether-esters.
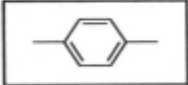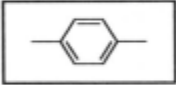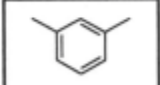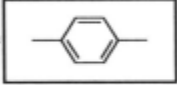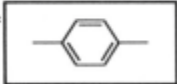
$[O(CH_2CH_2O)_p\text{-CO-R-CO}]_x$

P = 1,	R = -CH=CH-	ethyleneglycol maleate (EGM)
P = 4,	R = -CH=CH-	tetraethyleneglycol maleate (TGM)
P = 4,	R = -CH₂-	tetraethyleneglycol malonate (TGN)

P = 1, R = [benzene ring] ethylene terephalate (PET)

P = 4,	R = -CH₂CH₂-	tetraethyleneglycol succinate (TGS)
P = 5,	R = -CH₂CH₂-	pentaethyleneglycol succinate (PGS)
P = 6,	R = -CH₂CH₂-	hexaethyleneglycol succinate (HGS)

P = 4,	R = -(CH₂)₁₀-	tetraethyleneglycol dodecanedioate (TGD)
P = 4,	R = -(CH₂)₂₂-	tetraethyleneglycol tetracosonate (TGTCOS)
p = 5,	R = -(CH₂)₂₂-	pentaethyleneglycol tetracosonate (PGTCOS)
p = 6,	R = -(CH₂)₂₂-	hexaethyleneglycol tetracosonate (HGTCOS)

p = 4, R = [benzene ring para] tetraethyleneglycol terephalate (TGT)

p = 4, R = [benzene ring meta] tetraethyleneglycol isophalate (TGI)

p = 4, R = [benzene ring ortho] tetraethyleneglgol orthophalate (TGO)

$[O(CH_2)_qO\text{-CO-R-CO}]_x$

q = 10,	R = -CH₂CH₂CH₂CH₂-	decamethylene adipate (PDA)

q = 10, R = [benzene ring] decamethylene terephalate (PDT)

q = 4, R = [benzene ring] butylene terephalate (PBT)

q = 10,	R =10	decamethylene dodecandioate (PDD)
q = 10,	R = 22	decamethylene tetracosonate (PDTCOS)

Figure 8.2-1 Selected cyclic esters and ether-esters prepared at the University of York, U.K.
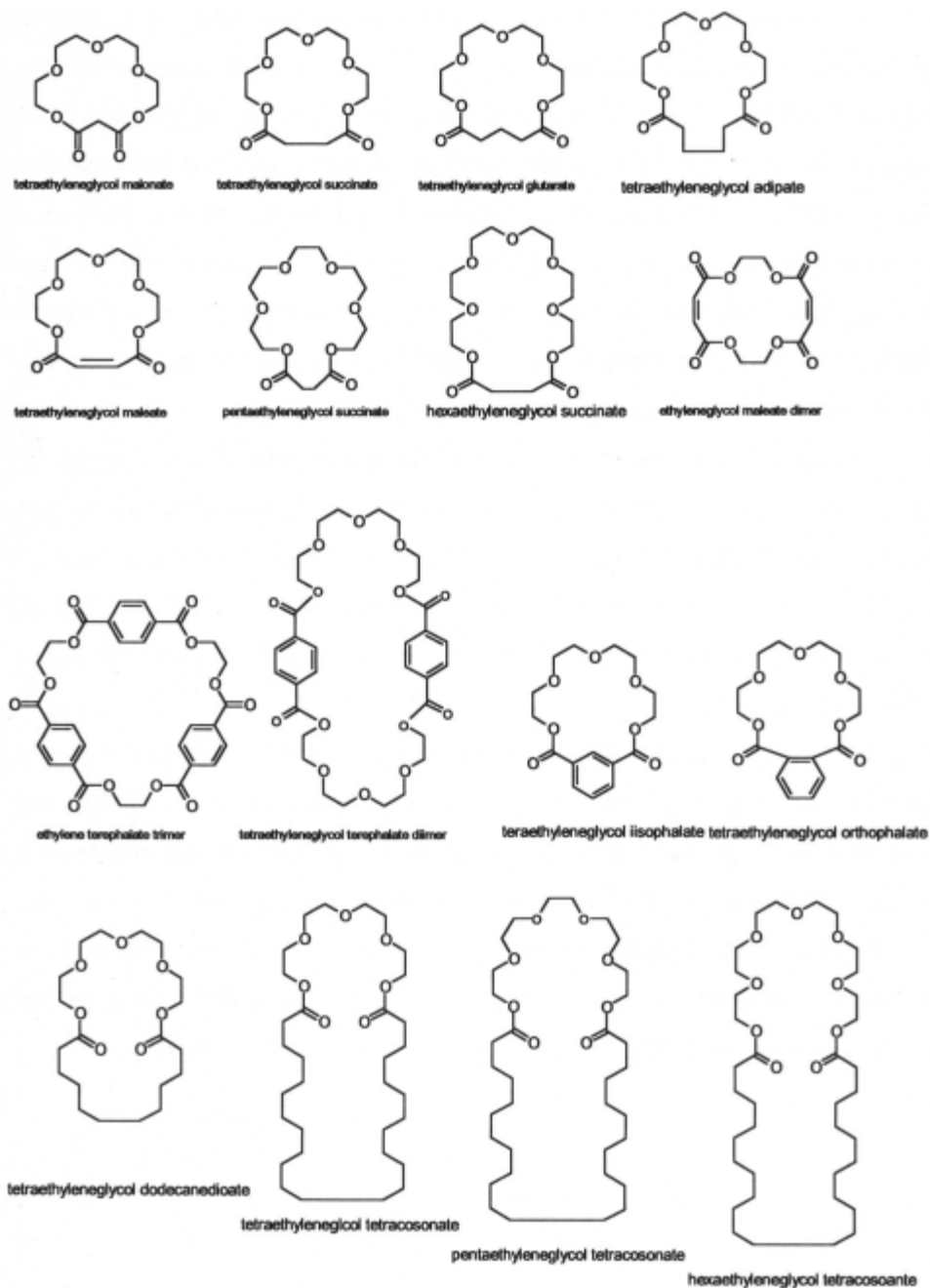
Figure 8.2-2 Schematic representation of the cyclic ether-esters prepared at the University of York (the smallest ring compounds formed are depicted).

Recent advances in GPC/HPLC column and detector technology have enabled the separation of cyclic oligomers comprising up to twelve repeat units (see Figures 8.2-3 and 8.2-4). This high resolution along with the high sensitivity of modem detectors has enabled the progress of ring-chain transesterification reactions to be followed with time. Small samples from the reaction flask were removed at regular intervals and injected straight on to the columns (see Figure 8.2-5). Such studies are useful to enable the optimization of the cyclization reactions. Also, the individual ring concentrations can be calculated from the chromatograms and compared to predicted values from theory.

Mass spectroscopy has also been of major importance in the characterization of cyclic esters and ether-esters. Fast atom bombardment mass spectroscopy and matrix assisted laser desorption ionization spectroscopy have been used to identify cyclic oligomers with 7 repeat units (see Figures 8.2-6 and 8.2-7). Maldi mass spectroscopy offers superior resolution as can be seen by the clarity of the mass spectra.

Preparative GPC has been used to obtain sharp fractions and single ring size samples (see Figure 8.2-8). The use of sharp fractions should enable the properties of cyclic esters and ether-esters to be investigated as a function of ring size. For example, the complexation of ether-ester rings with various metal ions (Figure 8.2-9). Crystallization of some of these sharp fractions has enabled the X-ray crystal structure of some cyclic oligomers to be determined, giving direct evidence for the shape of these rings (Figures 8.2-10 and 8.2-11).
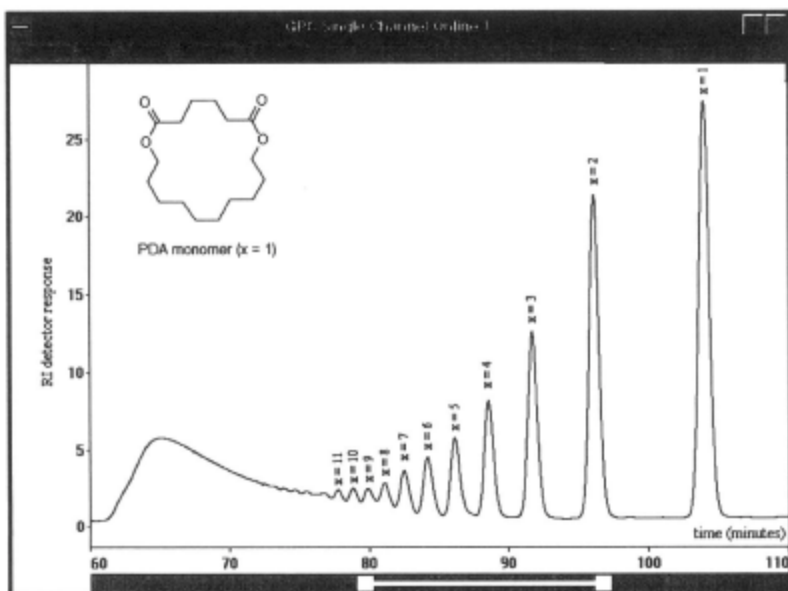
Figure 8.2-3 Gel Permeation chromatogram for the dilute solution ring-chain reaction products from the preparation of cyclicdecamethylene adipates (individual cyclic oligomers are labelled).
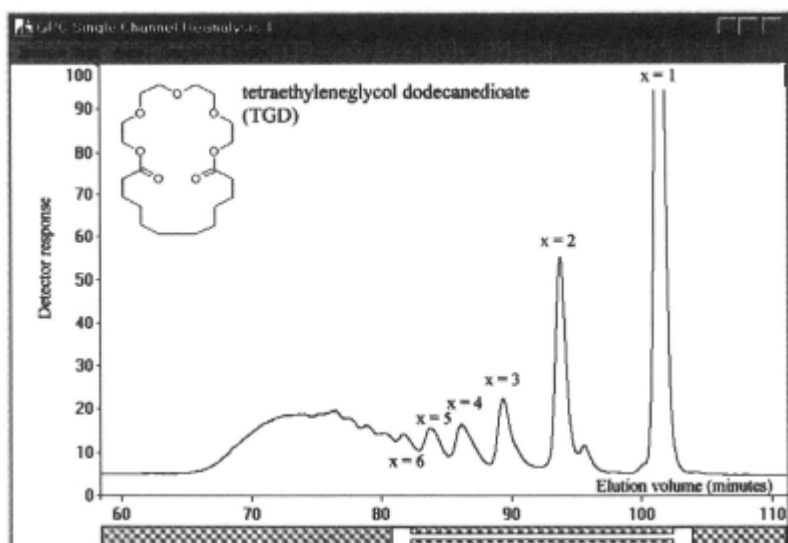
Figure 8.2-4 Gel Permeation chromatogram for the dilute solution ring-chain reaction products from the preparation of cyclic tetraethyleneglycol dodecanedioates (individual cyclic oligomers are labelled).
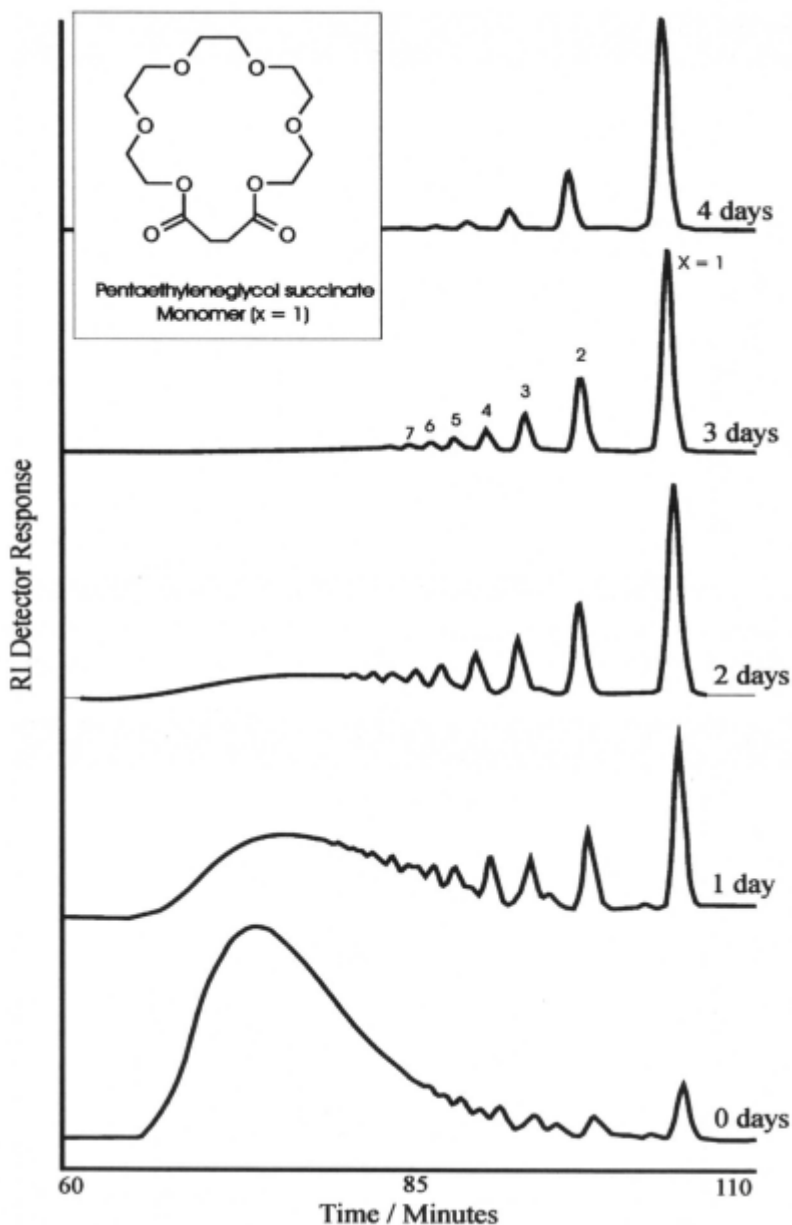
Figure 8.2-5 Gel permeation chromatograms showing the progress of ring formation for the dilute solution ring-chain transesterification reaction of poly (pentaethyleneglycol succinate).
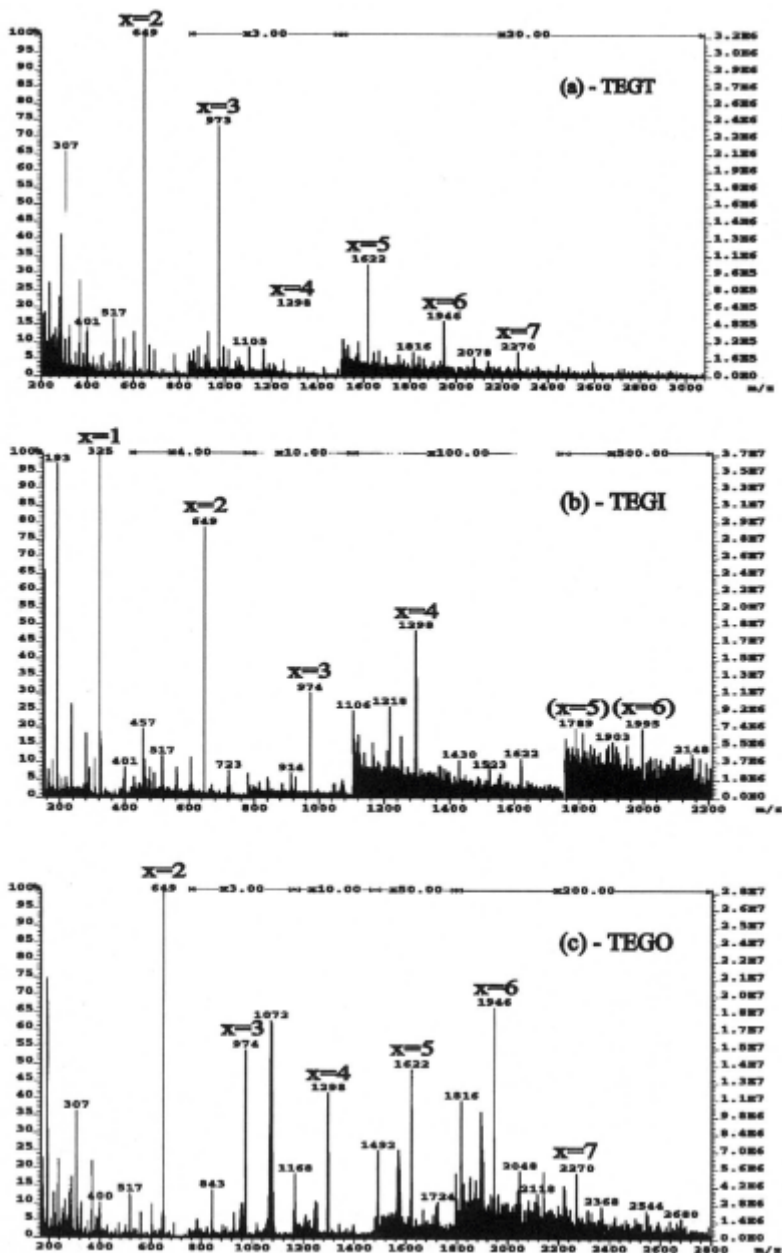
Figure 8.2-6 FAB-mass spectra of cyclic oligomers of (a) tetraethyleneglycol terephthalate, (b) tetraethyleneglycol isophthalate and (c) tetraethyleneglycol orthophthalate (cyclic oligomers with x-repeat units are identified).

298
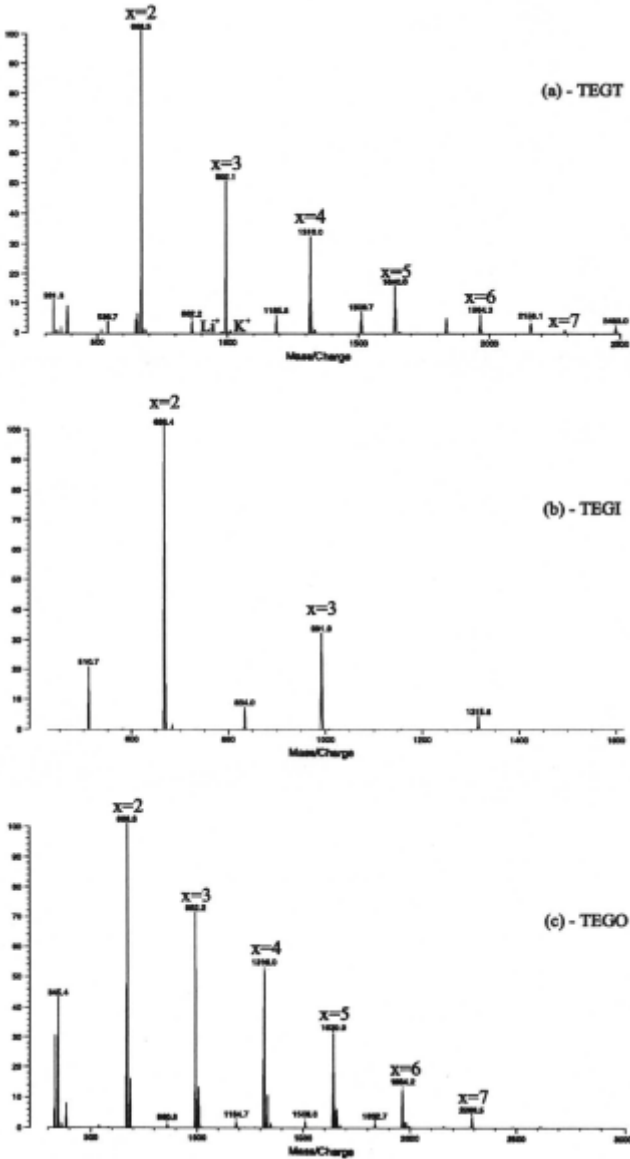
Figure 8.2-7 MALDI-mass spectra for the cyclic oligomers of (a) tetraethyleneglycol terephthalate, (b) tetraethyleneglycol isophthalate and (c) tetraethyleneglycol orthophthalate.
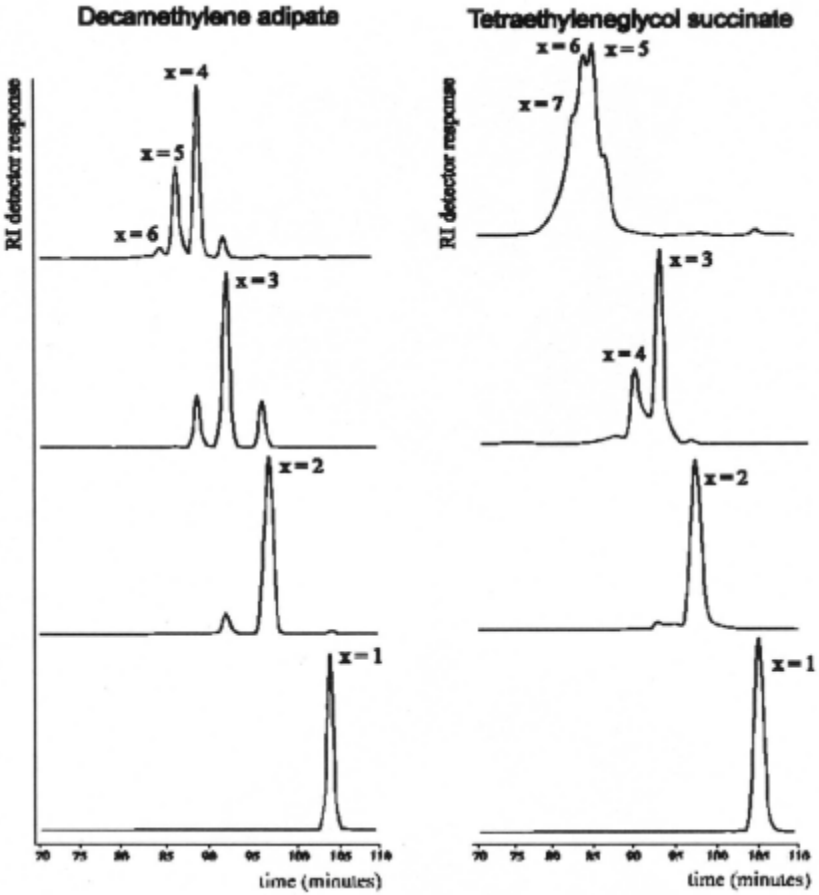
Figure 8.2-8 Gel permeation chromatograms showing the fractionation by preparative GPC of cyclic oligomers of decamethylene adipate and tetraethyleneglycol succinate (individual cyclic oligomers with x-repeat units are labelled).
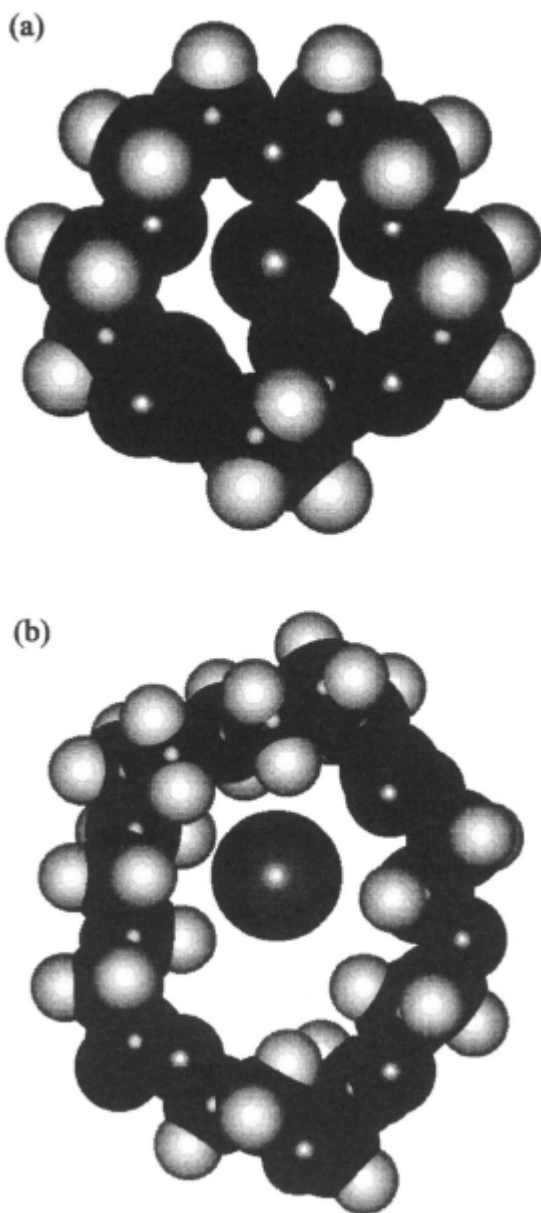
Figure 8.2-9 Molecular models of cyclic compounds complexed with metal ions; (a)tetraethyleneglycol succinate-lithium, (b) tetraethyleneglycol dodecanedioate-sodium.
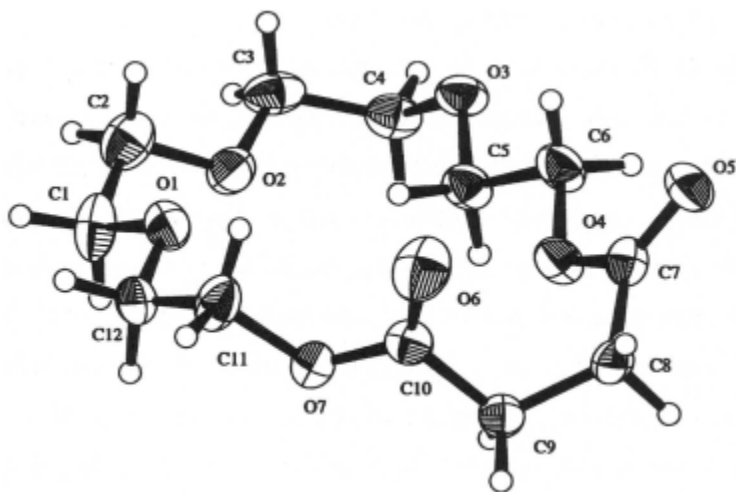
Figure 8.2-10 X-ray crystallographic structure for the cyclic monomer oftetraethyleneglycol succinate.
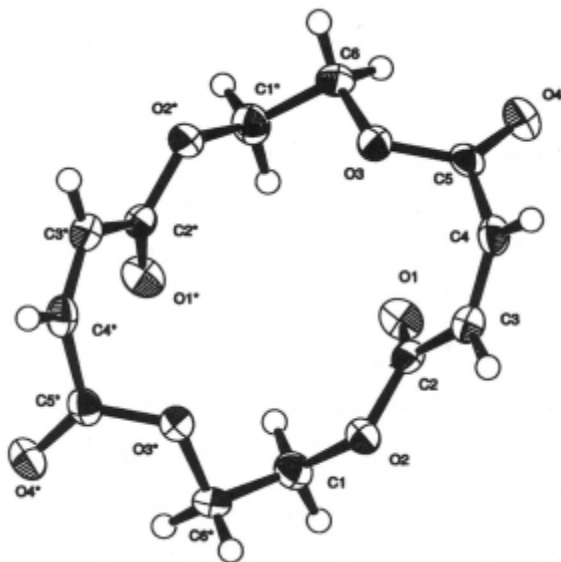
Figure 8.2-11 X-ray crystallographic structure of the cyclic dimer of ethyleneglycol maleate.

8.3 Uses of cyclic esters and ether-esters.

Although cyclic esters have been investigated for many years they have been mainly of academic interest. However, there are two notable exceptions. The first of these is in the application of ring-opening polymerization where the low melt viscosity of cyclic oligomers enables complicated moulds to filled relatively easily and then polymerized in-situ to give high molecular weight artefacts. This work is discussed in greater depth in chapter 6 of this book.

Cyclic esters have also been postulated for use as plasticizers, where the low diffusion characteristics of cyclic oligomers and the increase in molecular entanglements, should produce artefacts that do not have harmful, leachable materials.

The uses and possible uses of cyclic ether-esters are mainly due to their complexing behaviour in a similar way to crown ethers. Bradshaw has demonstrated that the complexation of cyclic monomers and dimers of a variety of cyclic ether-esters are significantly superior to that of crown ethers, as indicated by measurement of stability constants. The exciting part about cyclic ether-esters is that the preparative methods are very versatile and rings comprising different functional groups can be readily prepared (see Figures 8.2.1 and 8.2.2). Rings possessing both hydrophilic and hydrophobic groups have been prepared. It has been postulated that such amphiphilic compounds could be used as conducting polymers. It has been shown that enhanced conductivity occurs where supramolecular structures form and provide channels through which ions can travel. Cyclic ether-esters possessing amphiphilic character should form supramolecular structures when complexed with lithium salts (see Figure 8.3-1).
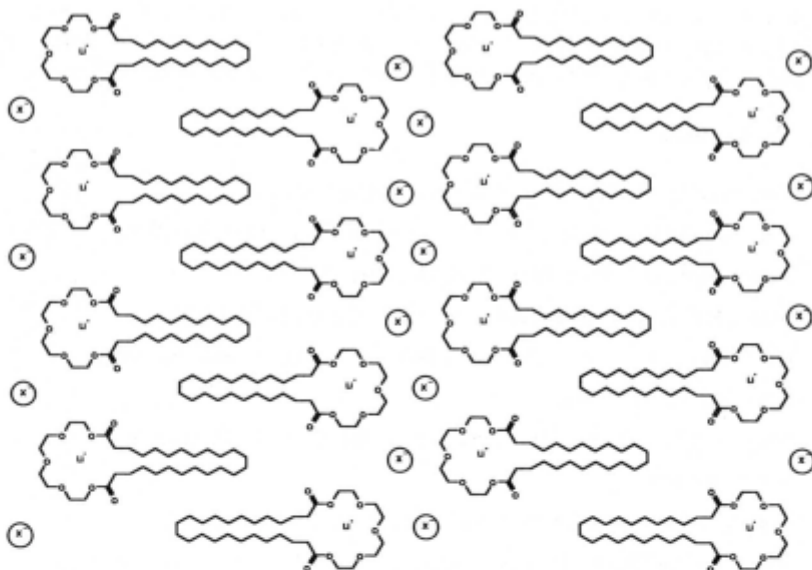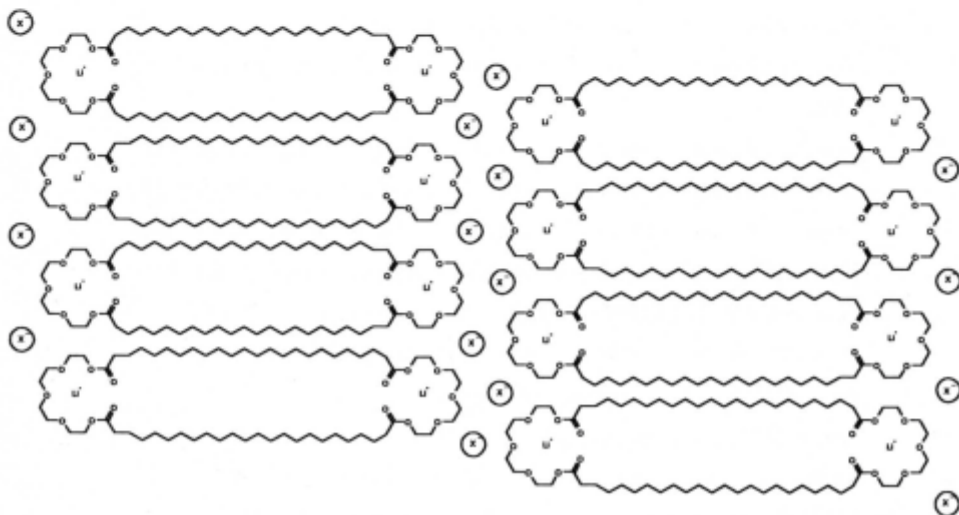
Figure 8.3-1 Schematic representation of possible structures formed by thecomplexation of (a) cyclic monomers and (b) cyclic dimers of tetraethyleneglycol tetracosonate with lithium salts.

304

8.4   References

1.   Vorländer, D., *Justus Lieblig Ann. Chem*., 1894, **280**, 167.

2.   Carothers, W.H. and Dorough, G.L., *J.Am.Chem.Soc*., 1930, **52**, 3292.

3.   Tilitschejew, M., *J.Russ.Phys.Chem.Soc,* 1925, **57**, 143.

4.   Assay, R.E. and Bradshaw, J.S., *J.Hetrocycl.Chem*., 1977, **14**, 85.

5.   Flory, P.J., *"Principles of Polymer Chemistry",* 1953, Cornell University Press, Ithaca, New York.

6.   Higgins, R.A., *"Properties of Engineering Materials",* 1994, Edward Arnold, London.

7.   Vögtle, F. and Newmann, P., *Tetrahedron Letters,* 1970, 115.

8.   Hahn, E.H. and Bohm, H., *Tetrahedron Letters,* 1973, 507.

9.   Stoll, M. and Rouvé, *Helv.Chim.Acta*., 1936, **19**, 253.

10.   Stueben, K.C., *J.Polym.Sci.Part 1-A*, 1966, **4**, 829.

11.   Crawford, L.M.R, Drewes, S.E. and Sutton, D.A., *Chem.Ind.(London)*, 1361.

12.   Drewes, S.E. and Coleman, P.C., *J.Chem.Soc.Perkin Trans.,* 1972, **1**, 2148.

13.   Drewes, S.E. and Coleman, P.C., *J.Chem.Soc.Perkin Trans*., 1974, **1**, 2578.

14.   Drewes, S.E. and Riphagen, B.G., *J.Chem.Soc.Perkin Trans*., 1974, **1**, 1908.

15.   Drewes, S.E. and Riphagen, B.G., *J.Chem.Soc.Perkin Trans.*, 1974, **1**, 323.

16.   Spanagel, E.W. and Carothera, W.H., *J.Am.Chem.Soc*., 1935, **57**, 929.

17.   Baker, W., McOmie, J.F.W. and Ollis, W.D., *J.Chem.Soc*., 1955, 200.

18.   Pedersen. C.J., *J.Am.Chem.Soc*., 1967, **89**, 7017.

19.   Greene. R.N., *Tetrahedron Letters*, 1972, 1793.

20.   Kaplan, M.L. and Truesdale, E.A., *Tetrahedron Letters*, 1975, 3665.

21.   Hill, J.W. and Carothers, W.H, *J.Am.Chem.Soc.*, 1933. **55**, 5031.

22.   Hill, J.W. and Carothere, W.H., *J.Am.Chem.Soc*., 1933. **55**, 5025.

23.   Ziegler, K. and Aurnhammer, R., *Justus Liebigs Ann.Chem*., 1934, **43**, 513.

24.   Spanagel, E.W. and Carothers, W.H., *J.Am.Chem.Soc*., 1935, **57**, 953.

25.   Carothers, W.H., Arvin, J.A. and Dorough, G.L., *JAm.Chem.Soc*., 1930, **52**,   3292

26.   Fore, P.E, Bradshaw, J.S. and Nielsen, S.F., *J.Hetrocycl.Chem*., 1978, **15**, 935.

27.   Dale, J., *J.Chem.Soc.*, 1965, 72.

28.   Ehrhart, W.A., *J.Org.Chem.*, 1968, **33**, 2930.

29.   Meraskentis, E. and Zahn, H.. *Chem.Ber.*, 1970, **103**, 3034.

30.   Zahn, H. and Repin, J.F., *Chem.Ber.*, 1970 **103**, 3041.

31.   Sakamoto, K. and Oki, M., *Tetrahedron Letters*, 1973, 3989.

32.   Sakamoto, K. and Oki, M., *Chem.Lett.*, 1974, 1173.

33.   Sakamoto, K. and Oki, M., *Bull.Chem.Soc.Jpn.*, 1974, **47**, 2739.

34.   Sakamoto, K. and Oki, M., *Chem.Lett.*, 1975, 615.

35.   Sakamoto, K. and Oki, M., *Bull.Chem.Soc.Jpn.*, 1976, **49**, 3159.

36.   Izat, R.M. and Bradshaw, J.S., *J.Am.Chem.Soc*, 1977, **99**, 2365.

37.   Bradshaw, J.S., J.Chem.Soc., *J.Chem.Soc.Chem.Comm.*, 1975, 874.

38.   Bradshaw, J.S., *J.Chem.Soc.Perkin Trans.*, 1976, **1**, 2505.

39.   Thompson, M.D. and Bradshaw, J.S., *Tetrahedron*, 1977, 33, 3317.

40.   Izat, R.M. and Bradshaw, J.S., *J.Am.Chem.Soc*, 1977, **99**, 6134.

41.   Maas, G.E. and Bradshaw, J.S., *J.Org.Chem.*, 1977, **42**, 3937.

42.   Bradshaw, J.S.,

43.   Bradshaw, J.S., *J.Heterocycl.Chem.*, , 1978, **15**, 825.

44.   Thompson, M.D. and Bradshaw, J.S., *Tetrahedron*, 1977, 33, 3317.

45.   Bradshaw, J.S. and Thompson, M.D., *J.Org.Chem.*, 1978, **43**, 2456.

46.   Frensch, K. and Vögtle, *Tetrahedron Letters*, 1977, 2573.

47.   Drewes, S.E. and Riphagen, B.C., *J.Chem.Soc.Perkin Trans.*, 1976, **1**, 2574.

48.   Nakagawa, M. and Toda, F., *Chem.Ind.(London)*, 1959. 458.

49.   Toda, F. and Nakagawa, M., *Bull.Chem.Soc.Jpn.*, 1960, **33**, 223.

50.   Eglington, G. and Galbraith, A.R., *Chem.Ind.(London)*, 1959, 548.

51.   Eglington, G. and Galbraith, A.R., *J.Chem.Soc.*, 1959, 889.

52.   Bohlmann, F., *Chem.Ber.*, 1964, **97**, 794.

53.   Wood, B.R., Hodge, P. and Semlyen, J.A., *Polymer*, 1993, **34**, 3052.

54.   Wood, B.R., Joyce, S.J., Scrivens, G., Semlyen, J.A., Hodge, P. and O'Dell, R., *Polymer*, 1993, **34**, 3059.

55.   Wood, B.R., Semlyen J.A. and Hodge, P., *Polymer,* 1994, **35**, 1542.

56.   Yukawa, Y. and Sakai, M., *Bull.Chem.Soc.Jpn.,* 1963, **36**, 761.

57.   Kammerer, H., *Naturwissenschaften,* 1974, **61**, 325.

58.   Kammerer, H. and Pachta, J., *Makromol.Chem.*, 1977, **178**, 1659.

59.   Suga, T. and Matsuura, T., *Bull.Chem.Soc.Jpn*., 1965, **38**, 1503.

60.   van Bergen, T.J. and Kellog, R.M., *J.Chem.Soc.Chem.Comm*., 1976, 964.

61.   van Bergen, T.J. and Kellog, R.M., *J.Am.Chem.Soc*., 1977, **99**, 3882.

CHAPTER 9
CYCLOMER TECHNOLOGY FOR HIGH PERFORMANCE POLYMERS

Yong Ding, Allan S. Hay
McGill University, Canada

9.1. Introduction

Cyclomer technology, ring-opening polymerization (ROP) of cyclic oligomers, has received increasing attention [1] since the pioneering work on the synthesis of cyclic carbonates by Brunelle *et. al.* at GE.[2-7] This technology is also of current research interest in the high performance polymers area and significant advances have been made.[8-12] In general, cyclomer technology has the advantage of avoiding the problem of extremely high melt viscosity associated with high molecular weight linear polymers since cyclic oligomers have much lower melt viscosities.[13] ROP of cyclic oligomers provides high molecular weight polymers in a short time without the evolution of low molecular weight volatile byproducts. This feature potentially enables the manufacture of high-performance composites free of voids and residual stress.   Additionally, cyclomer technoloy provides opportunities for polymer chemists to tailor the final products by varying the amount and type of suitable cyclic oligomers for specific applications.

This chapter describes the synthesis, characterization, and ROP of cyclic(arylene ether) and cyclic(arylene thioether) oligomers.   Cyclic arylates[14, 15] and cyclic aramides[16, 17] are not dealt with here and interested readers are referred to the original refrences.

9.2. Synthesis of cyclic(arylene ether)s.

9.2.1. Synthesis of cyclic(arylene ether)s by a nucleophilic substitution reaction

The most commonly used method to prepare high molecular weight poly(arylene ether)s is the nucleophilic substitution reaction between a bisphenol and an activated dihalo compound, which was first studied by Johnson et. al.[18, 19] For amorphous polymers, such as polysulfone, the

polymerization reaction can be carried out in a polar solvent, for example, N,N-dimethylacetamide (DMAc), dimethyl sulfoxide (DMSO), or N-methylpyrrolidinone (NMP). A base is added (NaOH, KOH or anhydrous **K₂CO₃** are the most commonly used) to the reaction mixture containing the monomers and the reaction mixture is dehydrated by removal of the water formed by azeotropic distillation. The polymerization then proceeds at a relatively low temperatures (140 - 200 °C).[20, 21] Sulfolane (tetramethylene sulfone), diphenylsulfone, or benzophenone have been used for highly insoluble polymers or highly crystalline polymers where the reaction has to be carried out around 300 °C or even higher.[22, 23]
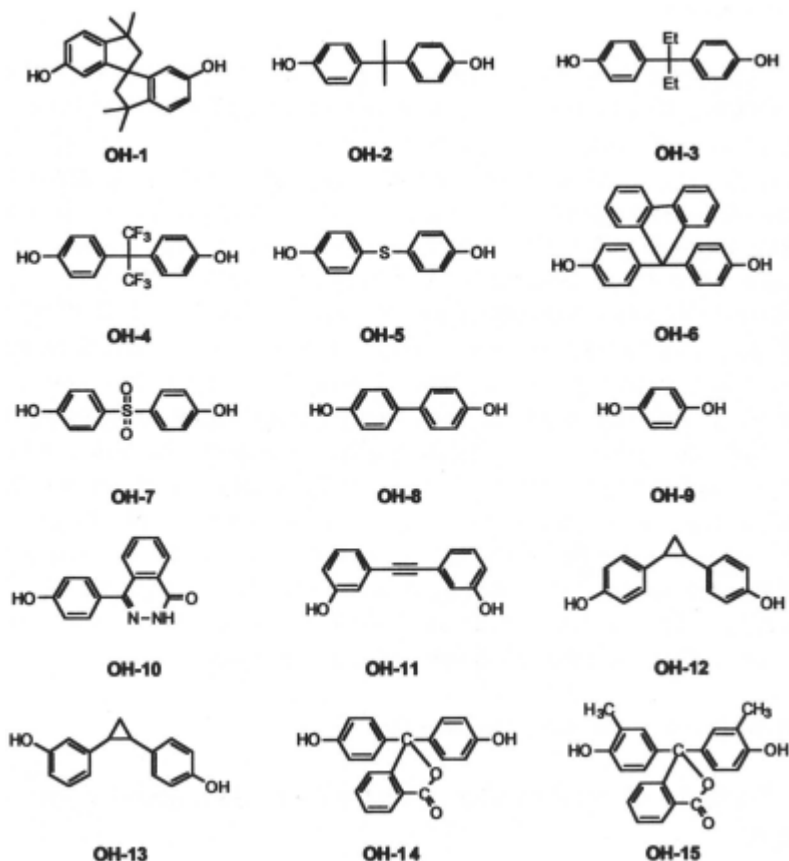
Scheme 1. Commonly used dihydroxy compounds.

The nucleophilic substitution reaction is also the most commonly used reaction for the synthesis of cyclic(arylene ether)s. The basic principle in the synthesis of cyclomers is the use of high dilution conditions under which the first order intramolecular cyclization will be favored relative to the second-order intermolecular polycondensation.[24, 25]   The reaction between an activated dihalo compound and a dihydroxy compound in the presence of a base has generally been used. Some commonly used dihydroxy compounds are listed in Scheme 1.

n = 2, 3, 4, 5, ...
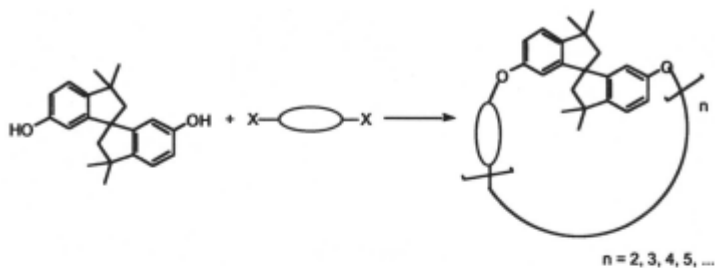
$\overline{}$	X	Cyclic yield*
Cy1.1	F	47
Cy2.1	F	45
Cy3.1	F	48
Cy4.1	F	40
Cy5.1	Cl	52

* The yields were determined by HPLC and GPC

Scheme 2.

Cella et. al. prepared a series of cyclic(arylene ether)s by using the nucleophilic substitution reaction (Scheme 2).[26] The reaction was carried out in DMSO with the highly bent and rigid diol OH-1, 2,2'3,3'-tetrahydro-

3,3,3',3'-tetramethyl-1,1'-spiro(1H-indene)-6,6'diol (SBI), which was used to facilitate the formation of cyclic oligomers. The reaction time was four hours. Even with the use of SBI, the yield of cyclic oligomers was low and they were contaminated with large amounts of high molecular weight linear oligomers.
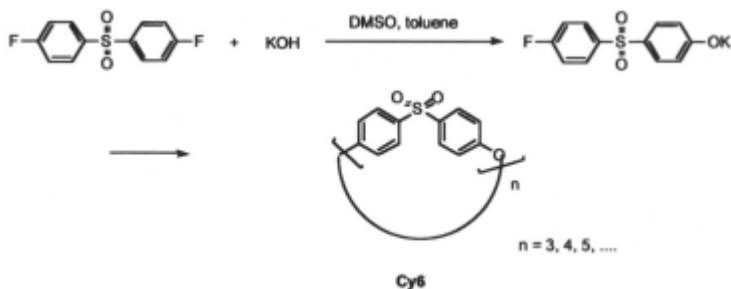
Schemes 3

Researchers at Dow Chemical Co. subsequently prepared a series of cyclic(arylene ether) oligomers under high dilution conditions.[8, 9] Reactants were added to the reaction flask slowly and the water formed during the reaction was removed by azeotropic distillation. DMSO was used as the solvent for the preparation of cyclic oligomers starting from AB monomers. A difluoro compound, bis(4-fluorophenyl)sulfone, and a KOH solution (2 M in water) were used.[9] In this case, the hydroxide initially displaces a fluorine in the difluoro monomer to form an AB monomer which subsequently forms cyclic oligomers (Scheme 3). The addition time used for the reaction was 60 hours followed by an additional time of reflux of 48 hours. Individual cyclomers with 3 and 4 repeat units are extremely high melting point solids (trimer, 447 °C; tetramer, > 450 °C). However, the mixture of these cyclic oligomers is amorphous and begins to flow at around 250 °C.

Other cyclic(arylene ether)s have been prepared using the same strategy, except that DMAc and anhydrous potassium carbonate were used.[8, 9] The optimum reaction temperature is 130 - 140 °C. At temperatures higher than 140 °C, side reactions take place and the yield is reduced. Cyclic(arylene ether)s prepared at Dow Chemical Co. are shown in Scheme 4.

We have used a modified method for the preparation of cyclic(arylene ether)s.[11, 12, 27] Typically, DMF and toluene were used as

the solvents in the presence of a large excess of anhydrous **K₂CO₃.** The reactants, dihydroxy compounds and difluoro compounds (equivalent amounts), were added to the reaction vessel through a syringe pump over a period of 8 hours, followed by an additional 8 hours at reflux temperature to ensure complete reaction. The slow addition of the reactants creates a pseudo high-dilution condition, which maintains the reactive species at very high dilution to favor the formation of cyclic oligomers. The use of the low boiling point DMF (combined with toluene) limits the reaction temperatures and ensures that the cyclic oligomers stay intact daring the reaction. In the presence of base, ring-opening polymerization would occur at temperatures higher than 140 °C.[8] DMF itself is also considerablely more stable than DMAc in the presence of base. The latter tends to form aldol condensation products under prolonged heating in the presence of base.[11]

312
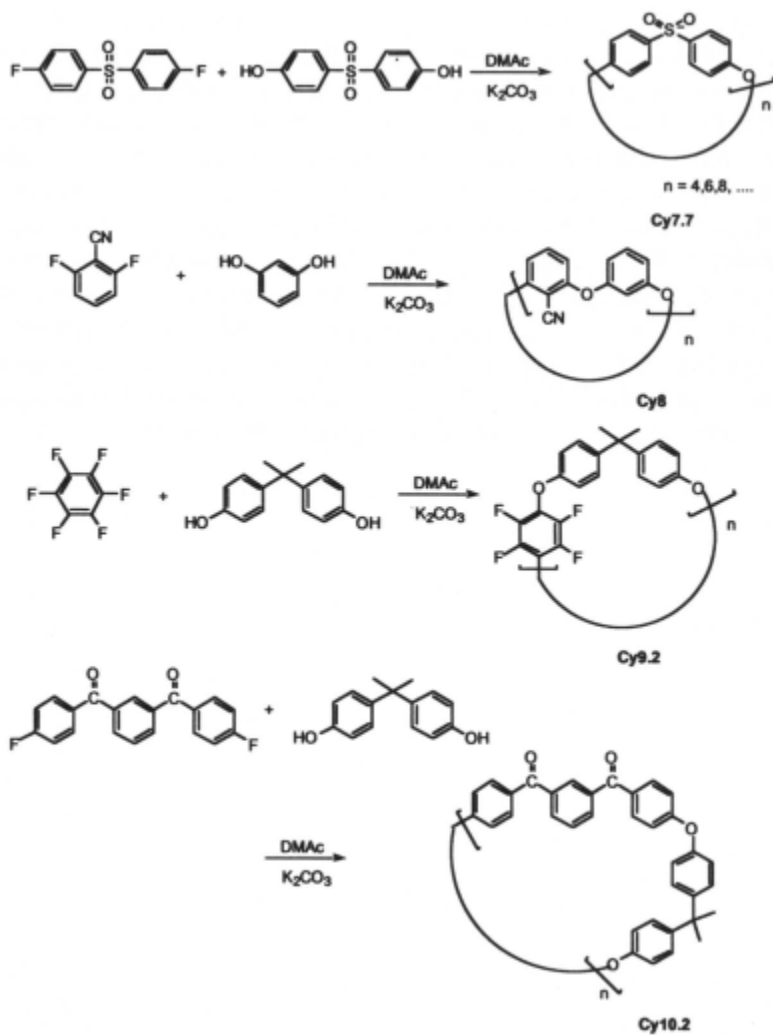
Scheme 4.

Table 1. Cyclomers prepared.[11-13, 27-33]
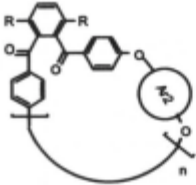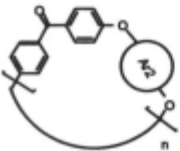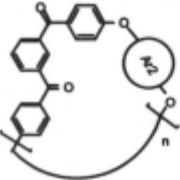
Cyclooligomers	HO—Ar2—OH	Denotation
	OH-1	R – H Cy11.1 R – Ph Cy12.1
	OH-2	R – H Cy11.2 R – Ph Cy12.2
	OH-3	R – H Cy11.3 R – Ph Cy12.3
	OH-4	R – H Cy11.4 R – Ph Cy12.4
	OH-5	R – H Cy11.5 R – Ph Cy12.5
	OH-6	R – H Cy11.6 R – Ph Cy12.6
	OH-10	R – H Cy11.10 R – Ph Cy12.10
	OH-11	R – H Cy11.11 R – Ph Cy12.11
	OH-12	R – H Cy11.12 R – Ph Cy12.12
	OH-13	R – H Cy11.13 R – Ph Cy12.13
	OH-2	Cy1.2
	OH-5	Cy1.5
	OH-10	Cy1.10
	OH-12	Cy1.12
	OH-14	Cy1.14
	OH-15	Cy1.15
	OH-2	Cy10.2
	OH-5	Cy10.5

314
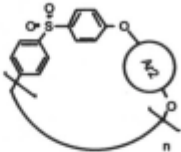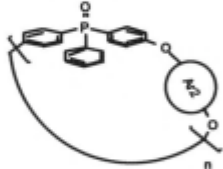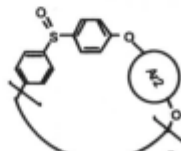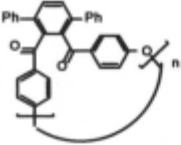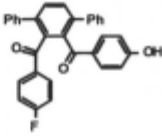
Table 1. (contd).

Cyclooligomers	HO–(Ar2)–OH	Denotation
	OH-10	Cy7.10
	OH-11	Cy7.11
	OH-12	Cy7.12
	OH-13	Cy7.13
	OH-14	Cy7.14
	OH-2	Cy13.2
	OH-5	Cy13.5
	OH-6	Cy13.6
	OH-8	Cy13.8
	OH-10	Cy13.10
	OH-4	Cy14.4
	OH-5	Cy14.5
	OH-6	Cy14.6
	OH-8	Cy14.8
	OH-9	Cy14.9
	OH-10	Cy14.10

Table 1. (contd.)

Cyclooligomers	HO—(Ar2)—OH	Denotation
		Cy15

Our process for the synthesis of cyclic(arylene ether)s is shown in Scheme 5. The final concentration of the products can be as high as 40 mM based on the repeating units. The products are formed in essentially quantitative yield and consist of low molecular weight cyclic oligomer mixtures.[11] Based on GPC analysis, the average degree of polymerization (dp) of the products was around three. **^{1}H-, ^{13}C-** and **^{19}F-NMR** spectrocopy gave no indication of the presence of any fluoro or phenolic end groups, which suggested that the low molecular weight oligomers are cyclomers.. This is a general procedure and high yields of cyclomers can be obtained with different difluoro compounds, even dinitro compounds[28c], and different dihydroxy compounds. Table 1 summarizes the cyclomers synthesized by this process. This process has also been used to synthesize novel cyclic(arylene ether sulfoxides) which were subsequently reduced to cyclic(arylene ether thioether)s (vide infra).

Scheme 5.

316
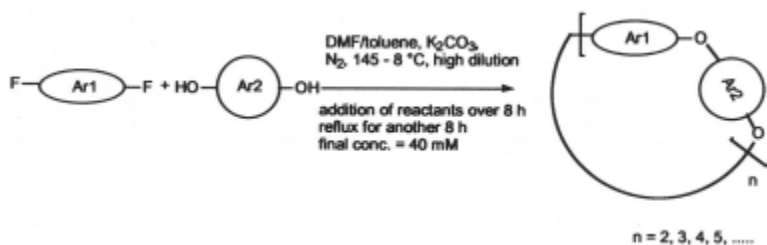
Table 2. Random cocyclomers prepared.[11, 29, 33, 34]
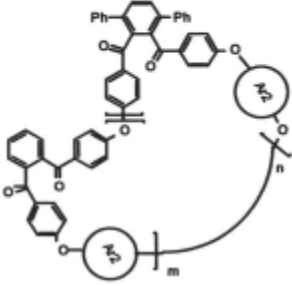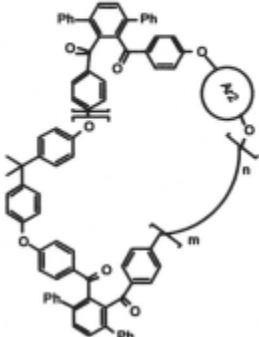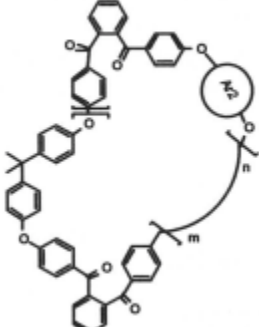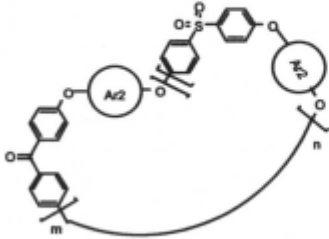
Cyclooligomers	HO—(Ar2)—OH	Denotation
	OH-2	Cy16.2
	OH-4	Cy16.4
	OH-5	Cy16.5
	OH-6	Cy16.6
	OH-2	Cy17.2
	OH-4	Cy17.4
	OH-5	Cy17.5
	OH-6	Cy17.6
	OH-12	Cy18

Table 2. (contd.)
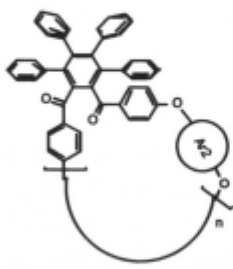
Cyclooligomers	HO—(Ar2)—OH	Denotation
	OH-10	Cy19.10
	OH-11	Cy19.11

A major problem that arose during work was the extremely high melting points of some of the cyclic products, even though the products were cyclomeric mixtures, which made the ROP reaction difficult. The high melting points and insolubility of the cyclomers, in particular the lower members, would make it difficult to consider a ring-opening polymerization in the melt. To tackle this problem, random cocyclomers were synthesized by using either different difluoro compounds with the same dihydroxy compound or different dihydroxy compounds with the same difluoro compounds.[11, 29, 30, 34] If necessary, random cocyclomers can be prepared with several different dihydroxy compounds or difluorocompounds, as long as both of them are introduced in equivalent amounts. Random cocyclomers synthesized are summarized in Table 2. DSC studies indicated that the random cocyclomers have much lower melting points and some of them are even even amorphous which facilitates the ROP reaction.

A variation of the aforementioned process was developed for the synthesis of cyclomers derived from 1,2-bis(4-fluorobenzoyl)-3,4,5,6-tetraphenylbenzene which has very low solubility in suitable solvents at room temperature which makes the delivery of the reactants using a syringe pump impossible.[32] Instead of using a syringe pump, the reactants were added into the reaction flask in 10 portions in solid form over a period of 9 hours followed by an additional 8 hours at reflux to ensure the completion of the reaction. If the reactants were added in one portion under these reaction conditions, significant amounts of linear, high molecular weight polymers were produced. Cyclomers prepared by this strategy are summarized in

Table 3. Although these cyclomers have extremely high melting points, they can undergo ROP when different cyclomers are mixed together which significantly lowered the melting points.[35]

Table 3. Cyclomers containing the tetraphenylbenzene moiety

Cyclooligomers	HO—(Ar2)—OH	Denotation
	OH-1	Cy20.1
	OH-2	Cy20.2
	OH-3	Cy20.3
	OH-4	Cy20.4
	OH-5	Cy20.5
	OH-6	Cy20.6
	OH-7	Cy20.7
	OH-8	Cy20.8
	OH-9	Cy20.9

Gibson has focussed on the preparation of single membered ring cyclics in order to address the problem encountered with cyclomer mixtures contaminated with very small amounts of linear oligomers.[36-40] They first prepared a long armed difunctional molecule and then this molecule was reacted with a suitable small molecule under high dilution conditions to selectively form single sized macrocyclic molecules. This approach has the drawback that it is a tedious procedures and gives low yields.

The single-sized cyclic(arylene ether)s synthesized are summarized in Table 3 and the long armed difunctional molecules are listed in Scheme 6. Single sized cyclics generally have extremely high melting points which preclude their possibility for ROP. For example, Cy21 has a melting point above 500 °C. To tackle this problem, some single-sized cocyclo oligomers

were synthesized and they showed lower melting points and readily underwent ROP to form high molecular weight polymers.[38]

Table 4. Single sized macrocycles.[36–40]
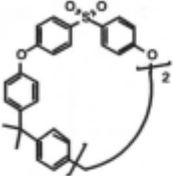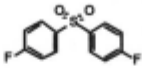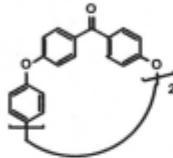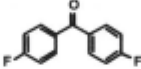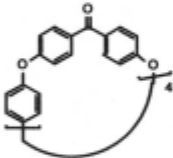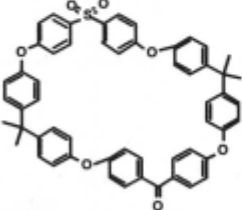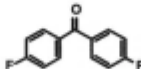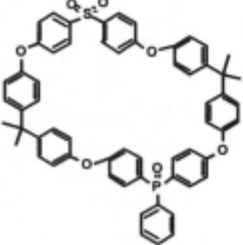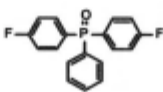
Cyclooligomer	Reactants	Yield (%)	Denotation
	OH-14 + 	67	Cy21
	OH-16 + 	27	Cy22
	OH-16 + F-3	66	Cy23
	OH-14 + 	68	Cy24
	OH-14 + 	44	Cy25

Table 4. (contd.)
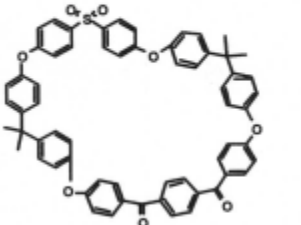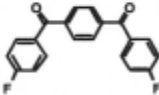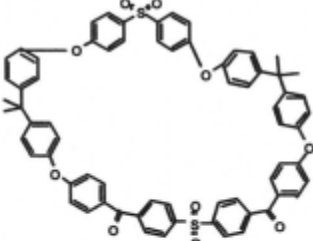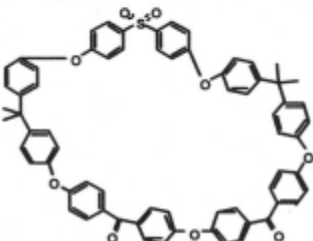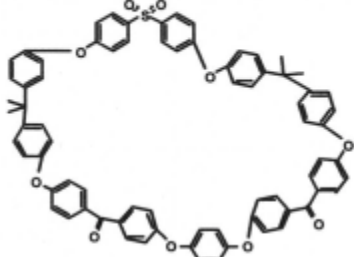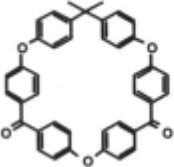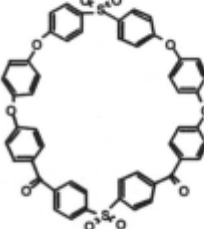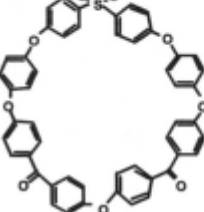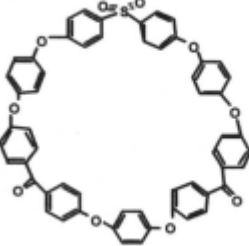
Cyclooligomer	Reactants	Yield (%)	Denotation
	OH-14 + 	83	Cy26
	OH-14 + F-1	44	Cy27
	OH-14 + F-2	75	Cy28
	OH-14 + F-3	63	Cy29

Table 4. (contd.)

Cyclooligomer	Reactants	Yield (%)	Denotation
	OH-2 + F-2	66	Cy30
	OH-2 + F-3	80	Cy31
	OH-15 + F-1	21	Cy32
	OH-15 + F-2	82	Cy33
	OH-15 + F-3	76	Cy34
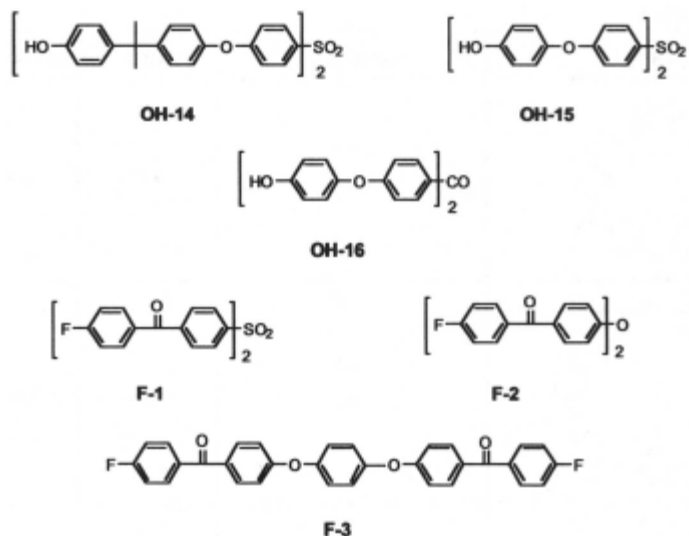
Scheme 6. Long armed difunctional molecules[38-40]
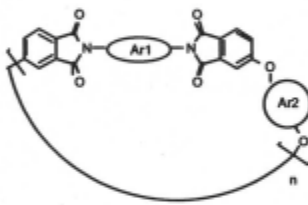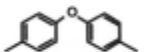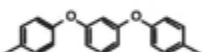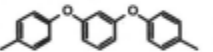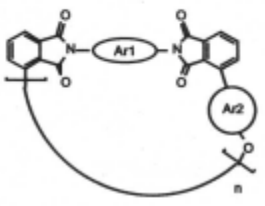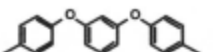
A novel process employing a thermally stable phase transfer catalyst to synthesize cyclic(arylene ether imide)s which was disclosed by Brunelle in a patent application,[41] is schematically shown in Scheme 7. The reactants, due to their insolubility, were added to the reaction flask in 10 portions over 30 minutes.
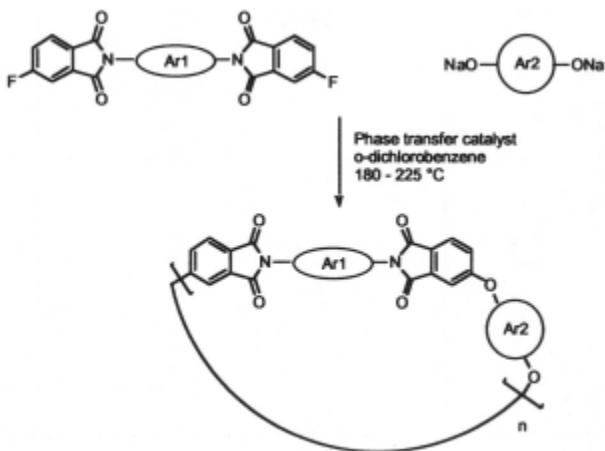
Scheme. 7.

Another process was reported by Takekoshi and Terry to prepare cyclic(arylene ether imide)s.[42] Their approach used the polymerization reaction developed by Kricheldorf, that is the polymerization reaction between a bis(trimethylsilyl ether) of bisphenol and a difluoro compound in the presence of a catalytic amount of cesium fluoride.[43, 44]   The cyclization reaction is shown in Scheme 8. In the conventional cyclization reactions mentioned above, an inorganic salt is formed as the side product which may cause, particularly in the case of cesium fluoride, the problem of ring-chain equilibration. However, for this process, a volatile trimethylsilyl fluoride is formed which vaporizes during the reaction. Thus, the isolation and purification of the cyclic products become simpler. The cyclomers prepared by this process are listed in Table 5.
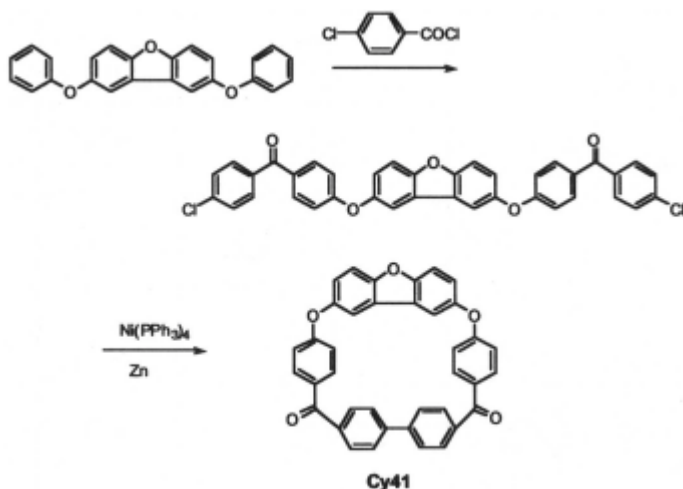
Table 5. Cyclic(arylene ether imide) oligomers

Cyclooligomer	—(Ar1)—	—(Ar2)—	Denotation
			Cy35
			Cy36
			Cy37
			Cy38
			Cy39
			Cy40
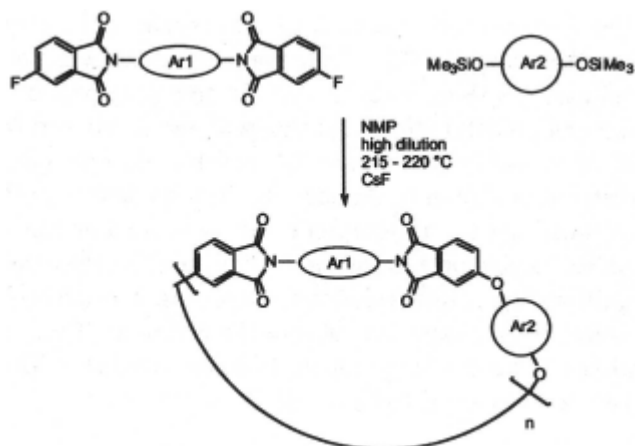
Scheme 8

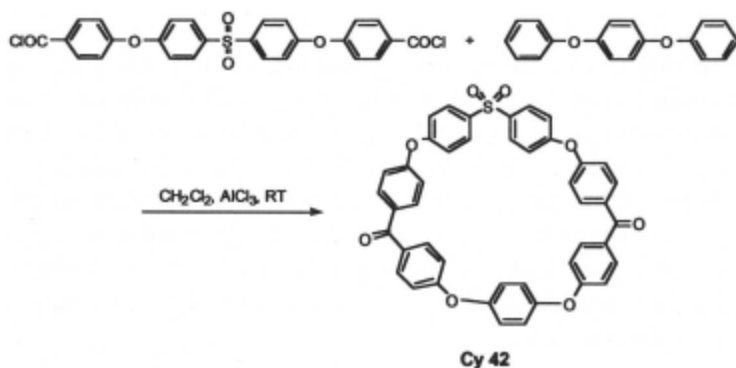## 9.2.2. Synthesis of cyclic(arylene ether)s by a nickel coupling reaction

Scheme 9 Synthesis of Cy41 by a nickel coupling reaction.

The only example for the synthesis of a large ring cycle by a nickel coupling reaction was reported by Colquhoun et al in 1990.[45] The single-sized macrocycle Cy41 was obtained in 40 % yield under high dilution conditions (Scheme 9). Due to the relative insolubility of Cy41 compared

with the linear coupled product, Cy41 can be easily isolated by recrystallization of the crude products with toluene.
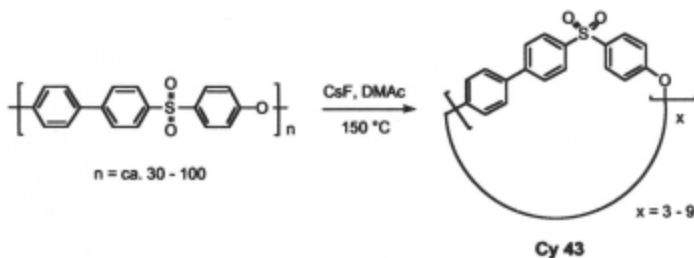
9.2.3. Synthesis of cyclic(arylene ether)s by a Friedel - Crafts reaction

The Fiedel - Crafts reaction is one of the classic reactions used to prepare high performance polymers. Poly(ether sulfone)s and poly(ether ketone)s have been synthesized by this route.[46,47] Gibson has synthesized a novel macrocycle under Friedel-Crafts conditions (Scheme 10).[48] The reaction was carried out under high dilution conditions with excess amount of anhydrous **AlCl₃** in **CH₂Cl₂.** A long armed diacyl chloride was used to facilitate the formation of a monodisperse cyclomer. The isolated yield of Cy42 was 21 %.

Scheme 10 Synthesis of cyclic(arylene ether) by a Friedel-Crafts reaction.

9.2.4. Synthesis of cyclic(arylene ether)s by a depolymerization reaction
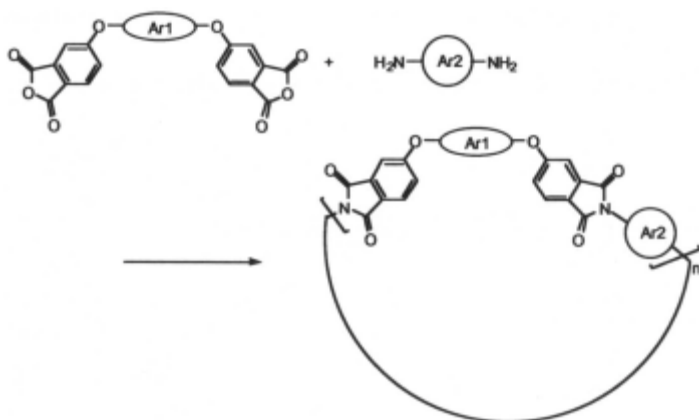

Scheme 11   Synthesis of cyclic(arylen ether) by ring-closing depolymerization of a poly(arylene ether).

A very interesting method to prepare cyclomers by ring-closing depolymerization of poly(arylene ether)s was developed by Colquhoun and coworkers.[49] It is well established that poly(arylene ether)s undergo transetherification at high temperatures in the presence of strong nucleophiles such as fluoride ion which can be used as the initiator for anionic ROP of cyclic(arylene ether) and cyclic(arylene thioether)s (vide infra). [10, 50] At high concentrations, this transetherification will result in a broad molecular weight distribution in the resulting polymers.[51, 52] However, under high dilution conditions, poly(arylene ether)s will also depolymerize to cyclomers (Scheme 11). This process is one that one can potentially be used for recycling of high performance polymers to form cyclomers.
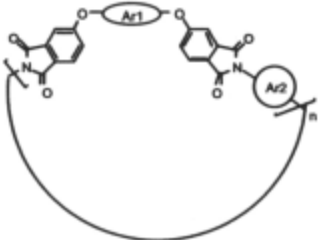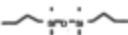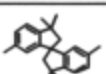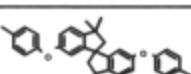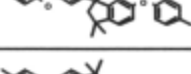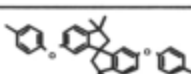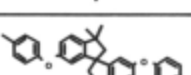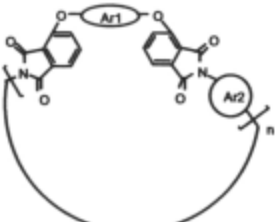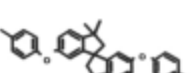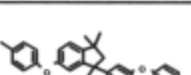
9.2.5. Other synthetic methods for cyclic(arylene ether)s

Theoretically speaking, any cyclization reaction utilizing a building block containing an arylene ether linkage is a potential synthetic method for cyclic(arylene ether)s. Among them, an imidization reaction has been used to synthesize cyclic(arylene ether imide)s (Scheme 12).[26] The cyclic(arylene ether imide)s synthesized by the imidization reaction are summarized in Table 6. Compared with the nucleophilic substitution reaction processes, this method has the drawback of low reaction rate for the imidization reaction and cyclomers can only be prepared in reasonable yield for very special monomers.

Scheme 12 Synthesis of cyclic(arylene ether) oligomers by the imidization reaction.

Table 6. Cyclic(arylene ether imide) oligomers

Cyclooligomer	Ar1	Ar2	Denotation
			Cy44
			Cy45
			Cy46
			Cy47
			Cy48
			Cy49
			Cy50
		—O—	Cy51
		—S—	Cy52
	—O—		Cy53
	—S—		Cy54

Cyclomers are generally produced as side products in condensation type polymerization reactions and small amounts of cyclomers have been separated from commercial high performance polymers and identified. Cyclic PEEK oligomers were isolated from commercial PEEK products[53] and a BPA type dimer was isolated from polysulfone.[54] Cyclic iso-PEK oligomers were also isolated from related polymer products and later were synthesized.[55]

Table 7. Cyclic(ether phthalazine)s and cyclic(ether isoquinoline)s*

	Cyclooligomers	Cyclic(arylene ketone) precusors
Cyclic(ether phthalazine)s	Cy55.1	Cy11.1
	Cy55.2	Cy11.2
	Cy55.5	Cy11.5
	Cy56.1	Cy20.1
	Cy56.2	Cy20.2
	Cy56.3	Cy20.3
	Cy56.4	Cy20.4
	Cy56.6	Cy20.6
	Cy56.7	Cy20.7
	Cy56.8	Cy20.8
	Cy56.9	Cy20.9
Cyclic(ether isoquinoline)s	Cy57.1	Cy11.1
	Cy57.2	Cy11.2
	Cy57.5	Cy11.5

* For structures, see Table 1 and Table 3.
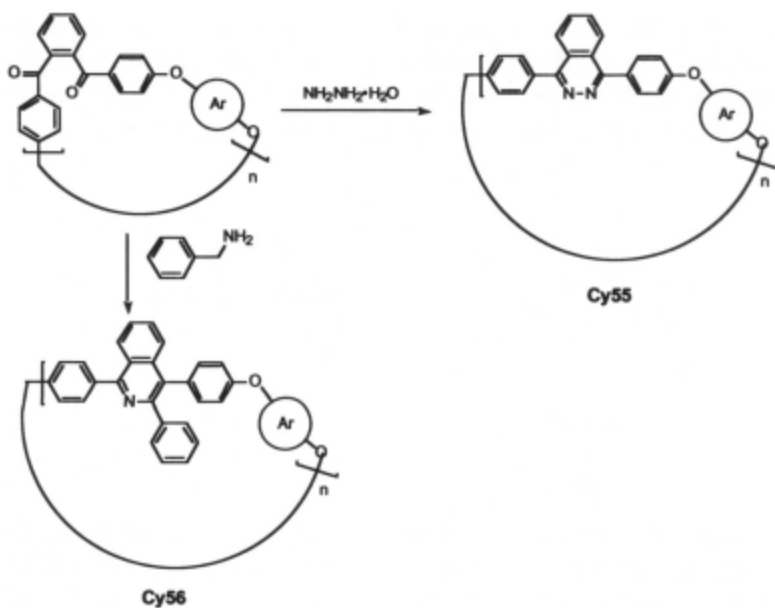
Scheme 13 Transformation of cyclic(arylene ether)s into phthalazines and isoquinolines.

By reacting with hydrazine or benzylamine, cyclic(arylene ether)s containing the 1,2-dibenzoylbenzene moiety can be quantitatively transformed into cyclic(arylene ether)s containing phthalazine or isoquinoline moieties (Scheme 13 and Table 7).[11, 32]

9.3. Synthesis of cyclic(arylene thioether)s.

9.3.1. Synthesis of cyclic(arylene thioether)s by a nucleophilic substitution reaction

Starting from a dihalocompound, cyclic(arylene thioether)s have been synthesized from an arylenedithiol or sodium sulfide. Cyclic(PPS) oligomers were synthesized by reaction between p-dichlorobenzene[56] or bis(4-bromophenylthio)-l,4-benzene with sodium sulfide under high dilution

conditions.[57]   These cyclomers have also been separated from commercial PPS products.[58]   Cy58 was synthesized in 38 % yield from reaction of 4,4'-difluorobenzophenone and sodium sulfide[59]   and Cy59 was synthesized from 4,4'-difluorobenzophenone and 1,3-benzenedithiol in 72 % yield.

Cy58   Cy59
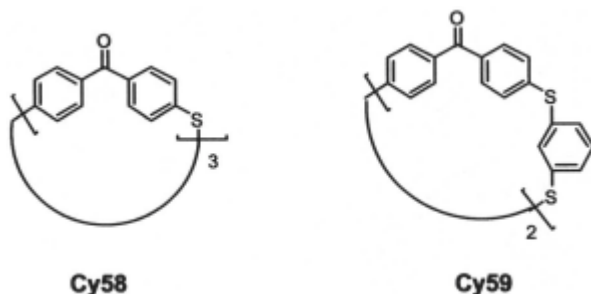
Arylenedithiols are generally oxidatively unstable and their purification is difficult.   A modified polymerization process has been developed to synthesize high molecular weight poly(arylene thioether)s starting from a N-n-propylcarbamate protected arylenedithiol[60] and this reaction has been used to synthesize cyclic(arylene thioether)s.[61]   The cyclization   reaction   shown   in   Scheme   14   utilizes   bis(4-fluorophenyl)sulfoxide as the building block.

Cy60-a
Cy60-b
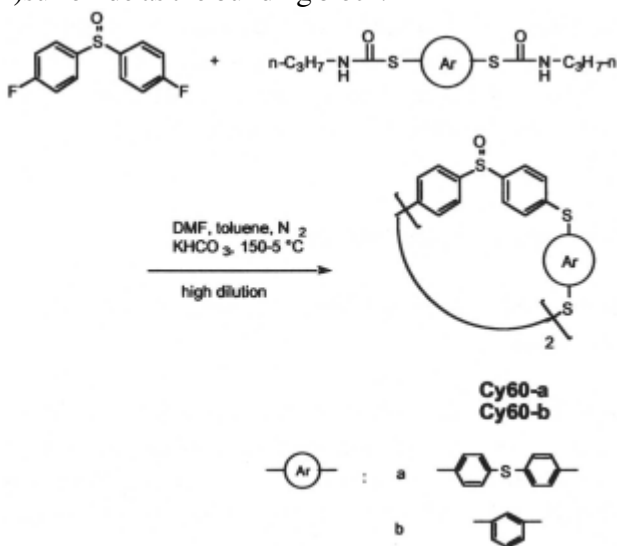
Scheme 14   Synthesis of cyclic(arylene thioether)s starting from N-n-propylcarbamate protected arytenedithiol.

9.3.2. Synthesis of cyclic(arylene thioether)s by an electron-transfer mechanism

The copper(I) salt of 4-bromophenylthiolate undergoes a cyclization reaction to form cyclomers in quinoline at 195 - 200 °C under high dilution conditions (Scheme 15).[62] The reaction mechanism for the polymerization reaction has been described as a single electron transfer reaction(SET).[63, 64]
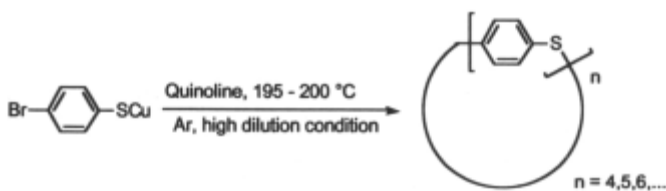
Scheme 15

9.3.3. Synthesis of cyclic(arylene thioether)s by the reduction of cyclic(arylene sulfoxide)s

Since bis(4-fluorophenyl)sulfoxide is highly reactive in nucleophilic substitution reactions, high molecular weight poly(arylene sulfoxide)s can be readily obtained by reaction with bisphenates. Therefore, the reduction of the sulfoxide group to a thioether linkage is an attractive method for the synthesis of poly(arylene thioether)s.[65] The high reactivity of bis(4-fluorophenyl)sulfoxide enabled it to be used in the synthesis of cyclic(arylene sulfoxide)s (see 2.1). With these cyclic(arylene sulfoxide) in hand, a series of cyclic(arylene thioether) were readily synthesized by the reduction of the sulfoxide group (Scheme 16).[61, 62, 66, 67] Cyclic(arylene thioether)s synthesized by the reduction of sulfoxide group are listed in Table 8.
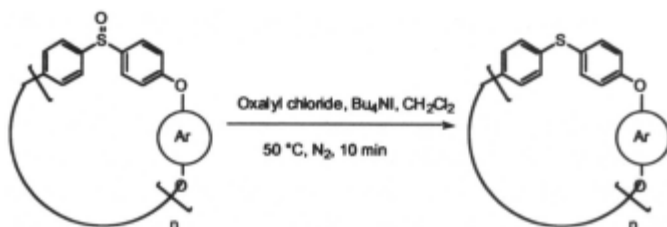
Scheme 16

Table 8. Cyclic (arylene thioether) oligomers*

Cyclic (arylene thioether)s	Cyclic (arylene sulfoxide) precursors
Cy61.4	Cy14.4
Cy61.5	Cy14.5
Cy61.6	Cy14.6
Cy61.8	Cy14.8
Cy61.9	Cy14.9
Cy61.10	Cy14.10
Cy62-a	Cy60-a
Cy62-b	Cy60-b

* For structures, see Table 1 and Scheme 12

9.3.4. Synthesis of cyclic(arylene thioether)s by an oxidative polymerization reaction.

Diphenyl disulfide undergoes an oxidative polymerization reaction to form cyclic PPS oligomers under high dilution conditions (Scheme 17).[68] The reaction was carried out in acidic dichloromethane solution with an equimolar amount of 2,3-dichloro-5,6-dicyano-p-benzoquinone (DDQ) as the oxidant. The diphenyldisulfide was added to the reaction vessel over two days with a final concentration of less than 0.05 M.
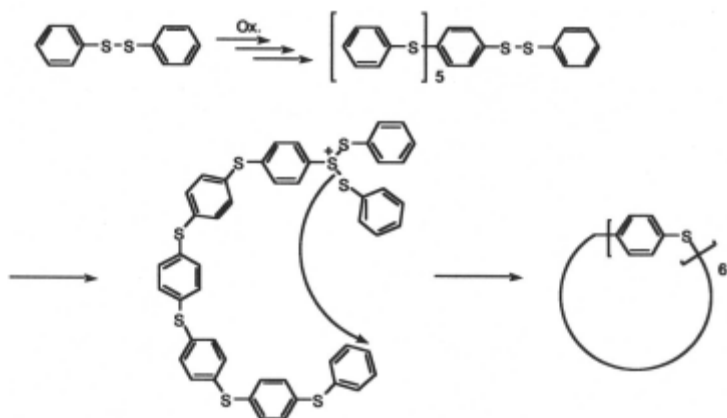
Scheme 17

9.4. Characterization of cyclic(arylene ether)s and cyclic(arylene thioether)s.

9.4.1. Gel permeation chromatography (GPC)

GPC has been commonly used for analyzing cyclomers to provide molecular weight information as well as to measure the amounts of cyclic vs. linear products formed. With the cyclomers it is important to ensure that there is complete solubility since the lower cyclics, in particular, are often very insoluble and therefore the results could be misleading. GPC analysis has been used to determine the cyclic contents in a product mixture[26] and to optimize cyclization conditions.[11] The GPC profiles of a sample containing linear oligomers and the corresponding cyclomers are shown in Figure 1.

334
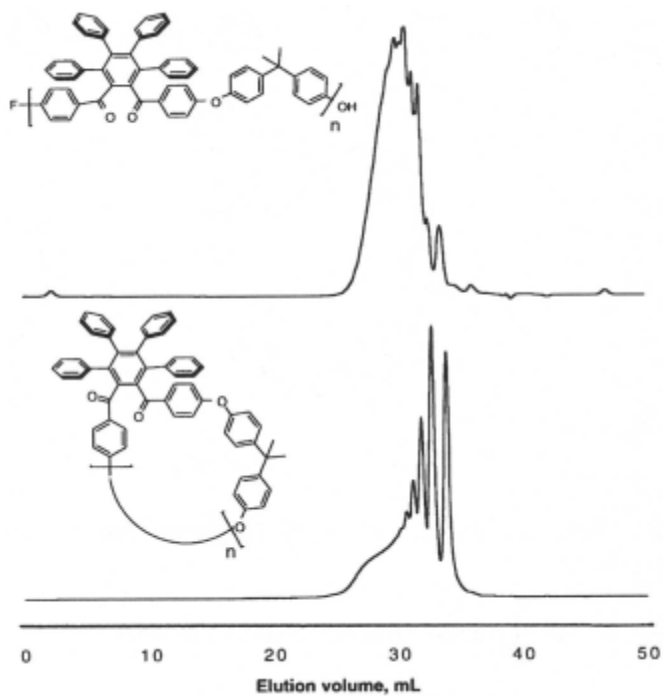
Figure 1. GPC profiles of Cy20.2 and its linear analog with comparable molecular weight.
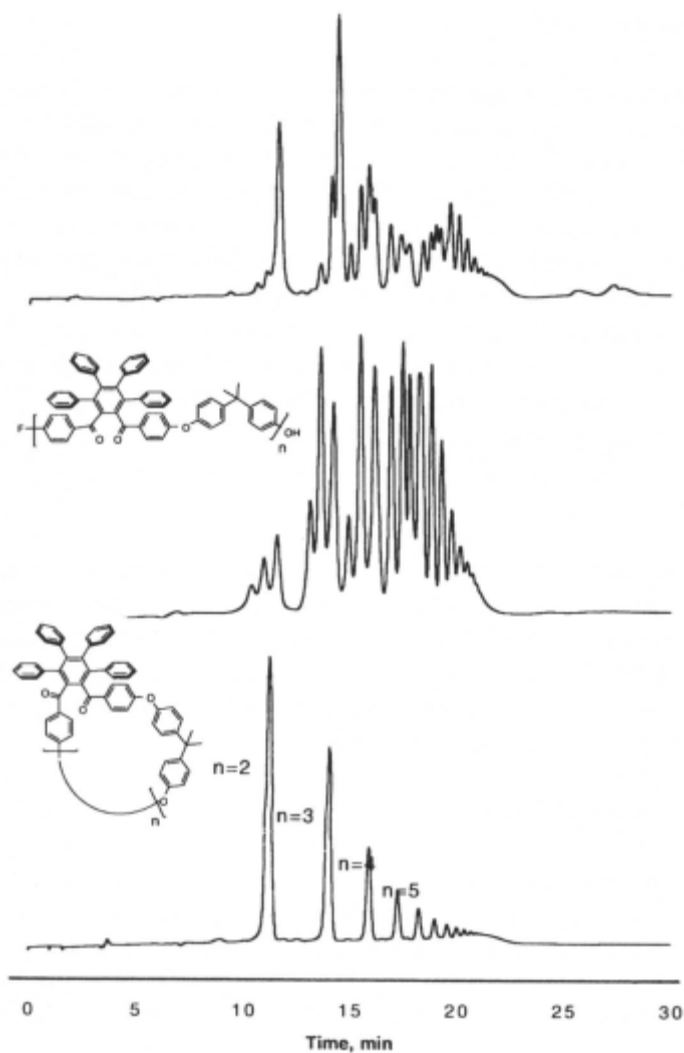
Figure 2. Gradient HPLC profiles of Cy20.2 and its linear analog with comparable molecular weight. (The top curve shows the mixture of the cyclomers and linear oligomers).

9.4.2. Gradient HPLC

Gradient HPLC has been found to be a very effective technique for the analysis of cyclomers since it provides excellent resolution of each of the individual cyclomers as well as the overall composition of cyclomer mixtures.[11, 27, 32] Gradient HPLC can provide information about the purity of the cyclomers, i.e. the amounts of contamination with linear oligomers.[69] Figure 2 shows the gradient HPLC profiles obtained with THF and water as eluents for Cy20.2, its linear analog with comparable molecular weight, and the mixture of equivalent amounts of Cy20.2 and the linear oligomer. Note that the low molecular weight linear oligomers contain three kinds of species, F-Ar-F, HO-Ar-OH and HO-Ar-F, and all of them are clearly resolved by HPLC.

9.4.3. NMR

High resolution NMR has been used principally to detect any residual groups in the cyclomer products due to the contamination with linear oligomers. Typically, for cyclomers obtained by a nuceophilic substitution reaction, one can detect the presence of -OH by ^{1}H-NMR and the presence of -F end groups by ^{19}F-NMR.[11] Their presence would indicate the presence of linear oligomers.

9.4.4. X-ray crystal structure

Many single sized cyclomers have been isolated and their x-ray structures have been resolved to confirm their cyclic properties. Among all of the cyclic(arylene ether) and cyclic(arylene thioether)s which have been synthesized, the x-ray stuctrures of cyclic dimers of Cy11.5[70], Cy21,[54] Cy22,[39], Cy41,[45] Cy42,[48] and Cy43[49] were determined.

9.4.5. FAB-MS

FAB-MS spectrometry has been used for the characterization of cyclic(arylene ether) and cyclic(arylene thioether) oligomers.[40, 55] However, this technique generally can only provide masses for cyclomers lower than 2000 Da.

9.4.6. MALDI-TOF-MS

Matrix assisted laser desorption ionization-time of flight-mass spectroscopy (MALDI-TOF-MS) is a new, very effective, technique for the characterization of cyclomers. This technique is characterized by its extreme sensitivity and accuracy. It is rapid and provides absolute molecular masses for the individual cyclomers along with any linear impurities. For general application of MALDI-TOF-MS in polymeric materials, readers are referred to some original papers and reviews. [71-73]   In MALDI analysis, the sample to be analyzed is mixed uniformly with a matrix, which absorbs light at the laser wavelength used (337 nm). The sample absorbs the laser energy which vaporizes along with the substrate to be analyzed which undergoes ionization. A cationization agent is generally added to the sample so that the mass observed is that of the cyclomer plus the cation, e.g. Li^+, Na^+ or Ag^+ and, in addition any possible linear oligomers.[l 1, 27, 30, 32, 66] Figure 3 shows the MALDI-TOF mass spectra for Cy20.2 and the linear analog with comparable molecular weight. Each individual peak coresponding to a specific ring size can be observed. As shown in Figure 3, the MALDI-TOF mass spectrum clearly shows the three different kinds of species in the linear oligomers, F-Ar-F, HO-Ar-OH and HO-Ar-F.

A: Cyclooligomer Cy20.2

B: Linear analog of cyclooligomer Cy20.2
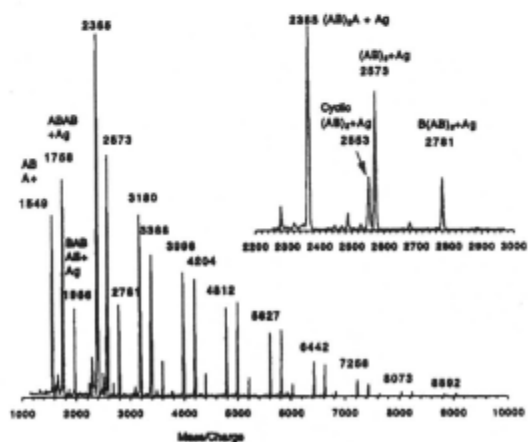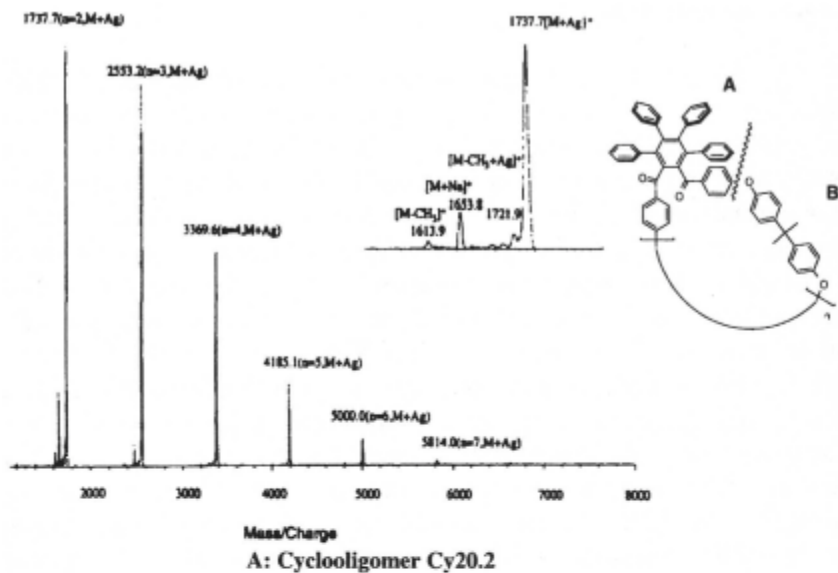
Figure 3. MALDI-TOF mass spectra of cyclomer Cy20.2 and the linear analog.
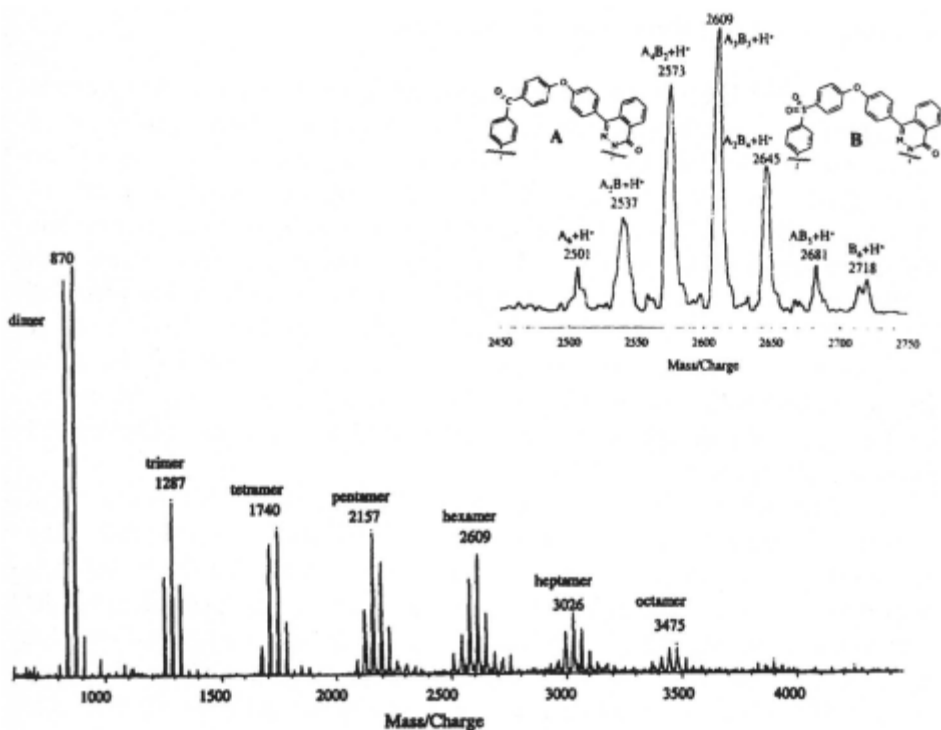
Figure 4. MALDI-TOF mass spectrum of cocyclomer Cy19.10.

Figure 4 shows the MALDI-TOF mass spectrum of cocyclomer Cy19.10. The spectrum allows us to define the composition of each set of cyclomers. The inset in Figure 4 shows the region of molecular mass range of 2450 to 2750 Da, corresponding to cyclic hexamers. The signal at 2501 Da corresponds to the protonated cyclic hexamer A_6, signal at 2537 Da corresponds to cyclic A_5B, the signal at 2573 Da corresponds to A_4B_2, the signal at 2609 Da corresponds to A_3B_3, the signal at 2645 Da corresponds to A_2B_4, the signal at 2681 Da corresponds to AB_5, and the signal at 2718 Da corresponds to B_6.

9.5. Ring-opening polymerization reactions.

There is little or no ring strain present in the cyclic arylene ethers or thioethers that have been synthesized. There is a ring - chain equilibrium in these reactions and the amount of cyclics present generally depends on the concentration of the poly(aryl ether)s in the reaction. Small amounts of cyclics are formed during high polymer formation at high concentration and the same equilibrium is reached by ring - opening polymerization of cyclomers at an equivalent concentration. Many initiators have been studied for the ROP of cyclic(arylene ether)s and cyclic(arylene thioether)s. Both of the systems can be initiated by a suitable base, providing that the ether linkage is activated by a neighboring electron withdrawing group. However, cyclic(arylene thioether)s can also undergo ROP with cationic initiators and free-radical initiators.

One precondition for the study of ROP of cyclomers is that cyclomers should be free from any residual salts and linear oligomers. The former condition can be met either by passing the cyclomer solution through a strong acid ion exchange column[8] or simply by precipitating the cyclomers from 0.2 M HCl solution.[28] It is also important that the cyclomer mixtures should have reasonable melting points or softening points. If the melting points are higher than 400 °C and they are insoluble because of their high crystallinity then they are difficult or impossible to polymerize, particularly in the melt, and unlikely to find any useful application in ROP technology.

9.5.1. Anionic ring-opening polymerization reaction

The anionic ROP is facilitated by the presence of a neighboring electron withdawing group and high molecular weight linear polymers are readily attainable. Cesium fluoride, sodium sulfide, sodium phenoxide, and sodium thiophenoxide are initiators that were used initially.[8, 10, 45] The effects of different initiators for ROP of Cy11.2 have been studied.[28] It was found that the polymerization rate in the melt increases in the order of $Cs^+ < Na^+ < K^+$ for the alkali phenoxides and in the order of $PhPhO^- < PhOPhO^- < PhO^- < {}^-OPhPhO^-$ for the phenolates. In comparison, the ROP in an aprotic dipolar solvent (DMF) is faster in the presence of cesium phenoxide than in the presence of potassium phenoxide. Studies on the single sized large ring cycle Cy24 also confirmed that potassium salts give the best results in terms of conversion.[38] Model studies on single sized ring cycle Cy24 suggested that there are two distinct stages for the ROP of

cyclomers.[38]   In the first stage (0 - 3 min), the rate of monomer consumption was very fast, 63 % of the macrocycle was consumed during a 3 minute period. However, the reaction in the second stage was slow, and only 2 % of the macrocycle was consumed during the last 30 minutes of reaction. The molecular weight built up rapidly and almost independent of reaction time, which is similar to a free-radical ring-opening polymerization.[74]   The advantage of using a monofunctional phenoxy potassium salt was justified by its ability to obtained controlled molecular weight polymers [55b], while bifunctional initiators can cause chain extension which leads to high molecular weight and low conversion.

Single sized cyclic(arylene thioether) Cy59 underwent rapid ROP (360 °C, 10 min) in the presence of sodium phenoxide to form a linear high molecular weight poly(arylene thioether) **(η_{inh} = 2.98 dL/g).[75]** In contrast to cyclic(arylene ether)s, cyclic(arylene thioether)s underwent ROP even in the absence of any electron withdrawing activating groups. For example, cyclic PPS oligomers underwent rapid ROP to form high molecular weight PPS in the presence of different kinds of anionic initiators, such as alkali phenoxides or alkali thiophenoxides.[76]

9.5.2. Cationic ring-opening polymerization reaction

In a patent application, cyclic(arylene thioether)s have been reported to undergo ROP in the presence of cationic initiators, such as trifluoroacetic acid, aluminum chloride, or trimethyl oxonium tetrafluoroborate.[76] However, from the examples given, ROP of cyclic(PPS) initiated by cationic initiators is not as effective as by anionic initiators.

9.5.3. Free-radical ring-opening polymerization reaction

A recent report showed that cyclic PPS undergoes ROP even in the absence of any initiators to give a low molecular weight polymer.[77] The same phenomenon has also been observed for the case of Cy12.5.[67] The mechanism proposed involved a homolytic cleavage of the C-S bond to form aryl and thiyl radicals (Scheme 18). However, catalytic amounts of free-radical initiators enhance the free-radical ROP of cyclic(arylene thioether)s .[61, 66, 67] They undergo efficient ROP in the presence of free-radical initiators, such as elemental sulfur and aryl disulfides. The free-radical nature of the polymerization reaction has been confirmed by electron paramagnetic resonance spectroscopy (EPR). Although the cyclic(arylene thioether)s undergo ROP in the absence of catalyst, large amounts of cyclics

342

remain (~ 33 %). The introducion of catalytic amounts of sulfur or aryl disulfides significantly improves the efficiency of ROP in term of conversion of cyclics.
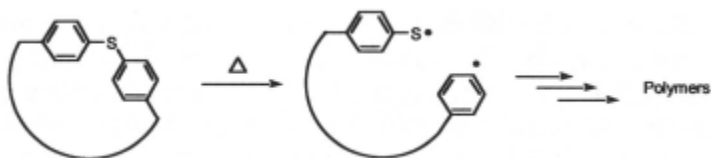
Scheme 18. ROP of cyclic(arylene thioether)s in absence of initiators.

9.6. Conclusions

Efficient methods for preparation of cyclic(arylene ether)s and cyclic(arylene thioether)s have provided a very attractive approach for increasing the processability of high performance polymers. Cyclomer technology can provide materials free from any salt contamination which may be of use in the electronics area. The significantly lower melt visicosity of cyclomers faciliates the processing which should be attractive for fabrication of advanced composite structures free of voids and residual stresses. Synthesis of block copolymers by ROP is still an unexploited area. The synthesis and ROP of cyclomers as precursors to high performance polymers will remain an active research area.

9.7. References and Notes

[1]   J. U. Otaigbe, Trends Polym. Sci., **5**,17 (1997).

[2]   D. J. Brunelle, E. P. Boden and T. G. Shannon, J. Am. Chem. Soc., **112**, 2399 (1990).

[3]   D. J. Brunelle and T. G. Shannon, Macromolecules, **24**, 3035 (1991).

[4]   D. J. Brunelle and M. F. Garbauskas, Macromolecules, **26**, 2724 (1993).

[5]   D. J. Brunelle, H. O. Krabbenhoft and D. K. Bonauto, Polym. Prepr. (Am. Chem. Soc., Div. Polym. Chem.), **34**, 73 (1993).

[6]   D. J. Brunelle, in *Ring-Opening Polymerization: Mechanisms, Catalysis, Structure, Utility*; Brunelle, D.J., Ed.; Hanser Publishers: New York, 1993, p. 310.

[7]   D. J. Brunelle, Trends Polym. Sci., **3**,154 (1995).

[8]   M. J. Mullins, E P. Woo, D. J. Murray and M. T. Bishop, CHEMTECH, 25 (1993).

[9]   M. J. Mullins, *et al.*, Polym. Prepr. (Am. Chem. Soc., Div. Polym. Chem.), **32(2)**, 174 (1991).

[10]   J. A. Cella, J. Fukuyama and T. L. Guggenheim, Polym. Prepr. (Am. Chem. Soc., Div. Polym. Chem.), **30(2)**, 142 (1989).

[11]   K. P. Chan, Y.-F. Wang, A. S. Hay, X. L. Hronowski and R. J. Cotter, Macromolecules, **28**, 6705 (1995).

[12]   K. P. Chan, Y.-F. Wang and A. S. Hay, Polym. Prepr. (Am. Chem. Soc., Div. Polym. Chem.), **36(2)**, 132 (1995).

[13]   Y.-F. Wang, K. P. Chan and A. S. Hay, J. Appl. Polym. Sci., **59**, 831 (1996).

[14]   T. L. Guggenheim, *et al.,* Polym. Prepr. (Am. Chem. Soc., Div. Polym. Chem.), **30(2)**, 579 (1989).

[15]   H. Jiang, T. Chen and J. Xu, Macromolecules, **30**, 2839 (1997).

[16]   W. Memeger, J. Lazar, D. Ovenall, A. J. Arduengo and R. A. Leach, Polym. Prepr. (Am. Chem. Soc., Div. Polym. Chem.), **34(1)**, 71 (1993).

[17]   W. Memeger, J. Lazar, D. Ovenall and R. A. Leach, Macromolecules, **26**, 3476 (1993).

[18]   R. N. Johnson, A. G. Farnham, R. A. Clendinning, W. F. Hale and C. N. Merriam, J. Polym. Sci. Part A-1, **5**, 2375 (1967).

[19]   R. N. Johnson and A. G. Farnham, *Polyarylene Polyethers* (Union Carbide Corp., U. S., 1978).

[20]   P. M. Hergenrother, B. J. Jensen and S. J. Havens, Polymer, **29**, 358 (1988).

[21]   R. Singh and A. S. Hay, Macromolecules, **25**, 1017 (1992).

[22]   T. E. Attwood, *et al.,* Polymer, **22**, 1096 (1981).

[23]   I. Fukawa and T. Tanabe, *Process for preparing crystalline aromatic polyetherketone* (Asahi Kasei Kogyo Kabushiki Kaisha, U. S., 1988).

[24]   P. Knops, N. Senhoff, H. B. Mekelburger and F. Vögtle, Topics in Current Chemistry, **161**, 1 (1991).

[25]   L. Rossa and F. Vögtle, Topics in Current Chemistry, **113**, 1 (1983).

[26]   J. A. Cella, J. J. Talley and J. M. Fukuyama, Polym. Prepr. (Am. Chem. Soc., Div. Polym. Chem.), **30(2)**, 581 (1989).

[27]   Y.-F. Wang, K. P. Chan and A. S. Hay, React Function. Polym., **30**, 205 (1996).

[28a] Y.-F. Wang, K. P. Chan and A. S. Hay, J. Poly. Sci., Polym. Chem. Ed., **34**, 378 (1996).

[28b] H. Jiang, T. Chen, S. Bo and J. Xu, Macromolecules, **30**, 7345 (1997).

[28c] H. Jiang, T. Chen, Y. Qi and J. Xu, Polymer J., **30**, 300 (1998).

[29]   Y.-F. Wang, M. Paventi, K. P. Chan and A. S. Hay, J. Poly. Sci., Polym. Chem. Ed., **34**, 2135 (1996).

[30]   Y. F. Wang, M. Paventi and A. S. Hay, Polymer, **38**, 469 (1997).

[31]   Y.-F. Wang, K. P. Chan and A. S. Hay, Polym. Prepr. (Am. Chem. Soc., Div. Polym. Chem.), **36(2)**, 130 (1995).

[32]   Y. Ding and A. S. Hay, Macromolecules, **29**, 3090 (1996).

[33]   C. Gao and A. S. Hay, Polymer, 4141 (1995).

[34]   Y.-F. Wang, M. Paventi and A. S. Hay, Polym. Prepr. (Am. Chem. Soc., Div. Polym. Chem.), **36(2)**, 128 (1995).

[35]   Y. Ding and A. S. Hay, J. Poly. Sci., Polym. Chem. Ed., **36**, 519 (1998).

[36]   D. Xie and H. W. Gibson, Polym. Prepr. (Am. Chem. Soc., Div. Polym. Chem.), **35(1)**, 401 (1994).

[37]   D. Xie and H. W. Gibson, Makromol. Chem., **197**, 2133 (1996).

[38]   D. Xie, Q. Ji and H. W. Gibson, Macromolecules, **30**, 4814 (1997).

[39]   M. Chen, F. Fronczek and H. W. Gibson, Makromol. Chem., **197**, 4069 (1996).

[40]   M. Chen and H. W. Gibson, Macromolecules, **29**, 5502 (1996).

[41]   D. J. Brunelle, *Preparation of macrocyclic polyetherimide oligomers from substituted bisphthalimides* (G. E., U. S., 1996).

[42]   T. Takekoshi and J. M. Terry, J. Poly. Sci., Polym. Chem. Ed., **35**, 759 (1997).

[43]   H. R. Kricheldorf, J. Meier and G. Schwarz, Makromol. Chem., Rapid Commun., **8**, 529 (1987).

[44]   H. R. Kricheldorf and P. Jahnke, Makromol. Chem., **191**, 2027 (1990).

[45]   H. M. Colquhoun, C. C. Dudman, M. Thomas, C. A. O'Mahoney and D. J. Williams, J. Chem. Soc., Chem. Commun., 336 (1990).

[46]   J. B. Rose, in *High Performance Polymers: Their Origin and Development*; Seymor, R.B. & G. S, K., Ed.; Elsevier: New York, 1986, p. 169.

[47]   J. B. Rose, in *High Performance Polymers: Their Origin and Development*; Seymor, R.B. & G. S, K., Ed.; Elsevier: New York, 1986, p. 187.

[48]   M. Chen, I. Guzei, A. L. Rheingold and H. W. Gibson, Macromolecules, **30**, 2516 (1997).

[49]   A. Ben-Haida, *et al.*, Chemical Communication, 1533 (1997).

[50]   I. Fukawa and T. Tanabe, J. Poly. Sci., Polym. Chem. Ed., **31**, 535 (1993).

[51]   C. A. Martínez and A. S. Hay, J. Poly. Sci., Polym. Chem. Ed., **35**, 1781 (1997).

[52]   Y. Imai, H. Ishikawa, K.-H. Park and M.-A. Kakimoto, J. Poly. Sci., Polym. Chem. Ed., **35**, 2055 (1997).

[53]   A. Jonas and R. Legras, Macromolecules, **26**, 2674 (1993).

[54]   H. M. Colquhoun and D. J. Williams, Macromolecules, **29**, 3311 (1996).

[55a]   M. F. Teasley, D. Q. Wu and R. L. Harlow, Macromolecules, **31**, 2064 (1998).

[55b]   M. F. Teasley and B. S. Hsiao, Macromolecules, **29**, 6432 (1996).

[56]   M. Kaplan and W. Reents, Tetrahedron Letters, **23**, 373 (1982).

[57]   V. Sergeev. *et al.*, Bull. Acad. Sci. USSR, **39**, 763 (1990).

[58]   C. E. Ash and W. A. S. Laurent, *Recovery of cyclic arylene sulfide oligomers* (Phillipps Petroleum Co., U. S., 1995).

[59]   Y. E. Ovchinnikov, V. I. Nedel'kin, S. I. Ovsyannikova and Y. T. Struchkov, Russ. Chem. Bull., **43**, 1384 (1994).

[60]   Z. Y. Wang and A. S. Hay, Polymer, **33**, 1778 (1991).

[61]   Y.-F. Wang and A. S. Hay, Macromolecules, **29**, 5050 (1996).

[62]   Y. F. Wang and A. S. Hay, Macromolecules, **30**, 182 (1997).

[63]   A. C. Archer and P. A. Lovell, Polymer, **36**, 4315 (1995).

[64]   A. C. Archer and P. A. Lovell, Polymer, **36**, 4327 (1995).
[65]   J. R. Babu, A. E. Brink, M. Konas and J. S. Riffle, Polymer, **35**, 4949 (1994).
[66]   Y.-F. Wang, K. P. Chan and A. S. Hay, Macromolecules, **28**, 6371 (1995).
[67]   Y.-F. Wang, K. P. Chan and A. S. Hay, Macromolecules, **29**, 3717 (1996).
[68a]   K. Miyatake, Y. Yokoi, K. Yamamoto, E. Tsuchida and A. S. Hay, Macromolecules, **30**, 4502 (1997).
[68b]   E. Tsuchida, K. Miyatake, K. Yamamoto, and A. S. Hay, Macromolecules, **31**, 6469 (1998).
[69]   D. W. Armstrong and R. E. Boehm, J. Chromatogr. Sci., **22**, 378 (1984).
[70]   K. P. Chan, *Cyclic Aryl Ethers: New Intermedietes for High Performance Polymers* (McGill University, Montreal, 1995).
[71]   F. A. Bottino, L. Grimaldi and A. Mamo, Makromol. Chem., Rapid Commun., **13**, 299 (1992).
[72]   P. O. Danis, D. E. Karr, W. J. SimonsickJr and D. T. Wu, Macromolecules, **28**, 1229 (1995).
[73]   J. J. Hagen and C. A. Monnig, Anal. Chem., **66**, 1877 (1994).
[74]   Y. Ding and A. S. Hay, Polymer, **38**, 2239 (1997).
[75]   H. M. Colquhoun, D. F. Lewis, R. A. Fairman, I. Baxter and D. J. Williams, Journal of Material Chemistry, **7**, 1 (1997).
[76]   H. Miyata, H. Inoue and A. Akimoto, *Polyarylene sulfide and preparation thereof* (Tosoh Corp., U.S., 1995).
[77]   D. A. Zimmerman, J. L. Koenig and H. Ishida, Polymer, **37**, 3111 (1996).

CHAPTER 10
ORGANIC CYCLIC POLYMERS

Jacques Roovers,
National Research Council, Canada

10.1 Introduction

The absence of end-groups and the equivalence of all monomer units in a cyclic polymer are predicted to lead to new insights in the fundamental properties of polymers. The synthesis of all-carbon main chain cyclic polymers, however, appears to be one of the great challenges in polymer chemistry. As this review will show, this challenge has not yet been met completely satisfactorily and newer synthetic and analytical techniques will be required in the future in order to make further rewarding progress.

The cyclization of a polymer chain with formation of a carbon-carbon bond is an irreversible process. It can involve either any two monomer units along the polymer chain or the reaction between two functional groups. The latter may be placed randomly along the chain or exclusively in specific positions. The cyclization is very often performed with two end-standing functional groups. Early attempts have been made to produce loops by intramolecular reactions of functional groups on linear polymers. The oldest study involved a copolymer of propylene and allylsilane $(CH_2=CH-CH_2SiH_3)$ [1]. On warming the polymer in alkali/alcohol mixtures Si-O-Si bonds are formed. When the reaction is performed at high dilution, the intrinsic viscosity of the sample does not increase [1], indicating that no intermolecular linkages are produced. It was speculated that the loops that are formed are probably small, i.e. that nearest neighbours on the chain are favoured and that small loops have little effect on the intrinsic viscosity. In a subsequent study [2], a random copolymer of styrene and methylacrylate was intramolecularly cyclized with 9,10-disodio-9,10-dihydroanthracene and a poly(styrene-co-vinylalcohol) was cyclized with 2,4-toluenediisocyanate. The concentration of the crosslinker in the polymers can be determined spectroscopically and can be compared with the reduction in the intrinsic viscosity due to loop formation at constant molecular weight.

These experiments were repeated in a very controlled manner [3-5]. High molecular weight (MW) narrow molecular weight distribution (MWD) linear polystyrene was chloromethylated to low levels and reacted with n-butylamine.
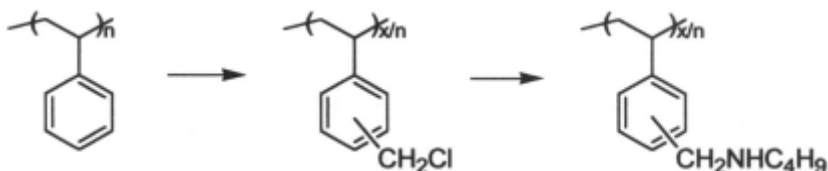
The secondary amine groups are then reacted with a small excess of hexamethylene diisocyanate in very dilute solution (1 g in 5 L of cyclohexane at 34°C). A careful chemical analysis of the polymer has been made from which the number of loops per chain could be calculated. Osmotic and light scattering measurements indicated that the MW of the polymer stays unchanged. The size of the polymers was determined mostly by intrinsic viscosity (IV) measurements. In order to compare the decrease in the IV with the theoretical model [4] values of IV must be converted to radii of gyration (R_g). It was observed that the experimentally observed shrinkage due to loop formation is smaller that the theoretical one based on the Gaussian chain model [5]. There may be many reasons for the qualitative discrepancy. As will be shown later, the main one may well be that the authors assumed that Φ in the Flory relation

$$[\eta] = 6^{3/2} \, \Phi \, R_g^3 / M \qquad (1)$$

is a constant independent of chain topology. As will be shown $\Phi(ring) = 1.8$ $\Phi(lin)$ and the use of a constant value leads to an overestimation of R_g. Martin and Eichinger used a Friedel-Crafts cyclization of monodisperse polystyrene with p-dichloromethylbenzene [6]. They showed clearly that ring size weighting is very important when every monomer is a potential cyclization site. Small rings are preferred and the effect of multiple cyclizations on the polymer dimensions is much smaller than when only randomly placed groups participate in loop formation.

In principle step growth polymerization processes are suitable for the preparation of ring polymers because they leave end-standing groups on the polymer. However, the presence of heteroatoms in the main chain and the wide MWD of such polymers introduce undesirable complications. Living polymerization reactions yielding narrow MWD polymers are generally preferred for cyclization precursors polymers. Two different approaches must be distinguished. The polymer to be cyclized has either two identical functional groups or to different end-standing groups, one derived from the initiator the other the active end group of the polymerization or a derivative. In the first case, cyclization requires a bifunctional "coupling" agent. Schematically,

$$X-R_n-X \ + \ A-B-A \ \longrightarrow \ X-R_n-B-A \ \longrightarrow \ \boxed{-R_n-B-} \ + \ 2 \ X-A$$
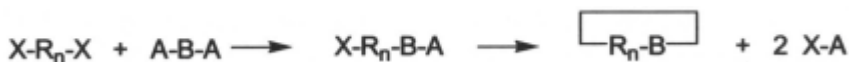
and the second step is the intramolecular cyclization. Several intermolecular side reactions can be written

$$X-R_n-X \ + \ 2 \ A-B-A \ \longrightarrow \ A-B-R_n-B-A$$
$$\searrow$$
$$\longrightarrow \ A-B-R_n-B-R_nB-R_n-X$$
$$2 \ X-R_n-X \ + \ A-B-A \ \longrightarrow \ X-R_nB-R_n-X \ \nearrow$$

$$2 \ X-R_n-B-A \ \longrightarrow \ X-R_n-B-R-R_n-B-A \ \longrightarrow \ \boxed{-R_nB-R_nB-}$$
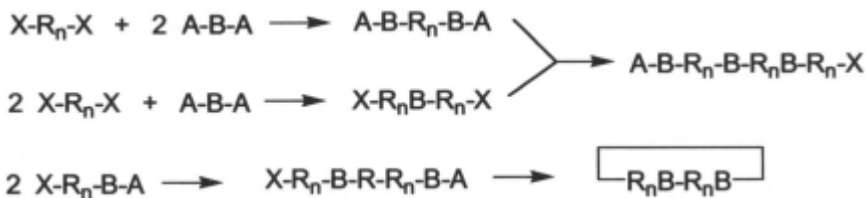
leading mostly to undesirable linear high MW "polycondensates" and possibly also to cyclic multiples.

In the second case, the cyclization requires some type of activation

$$X-R_n-Y \ + \ Z \ \rightarrow \ [\,X-R_n\text{----}\,Y-Z\,] \ \rightarrow \ R_n \ + \ X-Y \ + \ Z$$
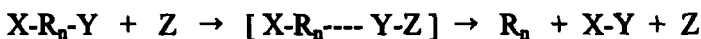
This process has several advantages [7]. The concentration of each functional group is only one half that of the first case, thereby reducing the probability of intermolecular side reactions. Furthermore, Z may be present in a catalytic amount allowing for control over the reaction rate. Most importantly, the stringent stoichiometry required in the first process is non-operative.

The competition between intramolecular cyclization and intermolecular chain extension involves identical chemical reactions. The probability of the reactions then depends on their effective concentration with regard to a reacting group [8]. The probability of finding the ω-end of a chain within a small reaction volume v_s around the α-end is given by

$$P_r \ = \ (3/2\pi)^{3/2} \ v_s \, / \, \langle r^2 \rangle^{3/2} \tag{2}$$

where $\langle r^2 \rangle$ is the mean square end-to-end distance of the chain in the reaction medium. On the other hand the probability of finding the chain end of another polymer within that same reaction volume is

$$P_2 \ = \ (\,N_A \, c \, / \, M\,) \ v_s \,. \tag{3}$$

If each chain contains two reactive groups a factor of two is added in Eq. (3). The concentration at which intra- and intermolecular reactions are equally likely $(P_r = P_2)$ is

$$c_{equal} = (3/2\pi \langle r^2 \rangle)^{3/2} M / N_A \qquad (4)$$

In principle the concentration for any theoretical fractional cyclization yield can be calculated from c_{equal} according to

$$\text{cyclization yield} = c_{equal} / (c_{equal} + c). \qquad (5)$$

This equation embodies the rule of thumb that the more dilute the polymer solution the higher the yield of cyclics. Note that $\langle r^2 \rangle \propto M$ in a θ solvent and that c_{equal} is proportional to $M^{-1/2}$. In a good solvent $\langle r^2 \rangle \propto M^{1.2}$ and $c_{equal} \propto M^{-1.8}$. Some realistic estimates of c_{equal} and the required living end group concentration of the polymer have been made as a function of MW of two-ended polystyrene [9]. Several theoretical studies of the intra/intermolecular competition have been made [10-13].

Several strategies have been tested in attempts to override the statistics of the cyclization step. The first that deserves mention is a possible ring expansion polymerization. The method is based on the repetitive insertion of monomers into a initiating ring structure with a propagating active link. This method has been attempted for the carbocationic polymerization of isobutylene by **γ-tolyl-γ-valerolactone/BCl₃** in CH_3Cl or CH_2Cl_2 at –30 °C [14]. However, detailed further study of end-groups and polymer characteristics indicates that the integrity of the cyclic complex is not maintained during the polymerization and termination step [15]. A similar approach used magnesiacyclohexane in HMPA to anionically prepare oligomers of **α**-methylstyrene [16]. It is thought that the two ends of the growing chain will stay together on the same metal counterion, and that on reaction with dimethyldichlorosilane the two ends in close proximity would preferentially lead to cyclic products. However, the stoichiometry of the polymerization reaction, side reactions and the low incorporation of Si (25%) suggest that little or no cyclic product was obtained. Ishizu et al. describe an interfacial ring closure [17,18]. A narrow MWD polystyrene **(MW = 7 000)** terminated at both ends with bromobutyl groups is dissolved in toluene: DMSO (75:25). The ring closing reagent hexamethylenediamine is dissolved in 50 % aqueous NaOH. The reagents are dilute and the reaction proceeds with rapid stirring at 80 °C within 12 hrs. The resulting mixture contains cyclic and linear polymer of identical molecular weight and possibly some polycondensates.

10.2 Synthesis

10.2.1. Cyclization of homodifunctional polymers

The formation of cyclic polymers by the reaction of a bifunctional living polymer with a bifunctional electrophile was first proposed by Casassa [19]. The practical realization has been outlined [20]:

1. the preparation of a monodisperse bifunctional living polymer e.g. polystyrene initiated by sodium naphthalene
2. the reaction of the living polymer with a difunctional reagent in equimolar amount under high dilution
3. the use of excess cyclizing agent and chain extension with a high molecular weight linear polymer
4. fractionation.

With minor modifications these steps have been followed by all groups who have subsequently prepared cyclic organic polymers. There are many advantages to these procedures. First of all, the living polymer is highly monodisperse and completely bifunctional when prepared with care. The linear parent polymer can be sampled before the cyclization step and, after protonation, it is the perfect linear homologue that facilitates the characterization of the cyclic polymer. Furthermore, the carbanionic end groups of the living polystyrene absorb strongly in the UV-Vis region and the equimolar addition of the cyclizing reagent can be monitored visually as in a titration. Essentially, two types of cyclizing reagents have been used: dichloro- [20] and dibromo-p-xylene [8,21] or dimethyldichlorosilane [9]. No real advantage of either one has been found except that the chlorosilane can be distilled slowly into the dilute living polymer solution.

The high dilution required for high yield cyclization usually limits the amount of polymer that can practically be produced. Vollmert and Huang [22] cyclized 3.6 g of polystyrene in 2.5 L of purified THF in one step. The high dilution problem is almost always solved by dropwise addition of equimolar amounts of living polymer and cyclizing agent to a large reservoir of purified solvent. If stirring is adequate and the addition slower than the cyclization reactions, then the actual concentration of the reagents, although ill defined, can be kept sufficiently low. Nevertheless, the consecutive additions lead to a steadily increasing concentration of linear polycondensates and decreasing yield of cyclics. The chain extension of residual linear polymer described under step 3 above is not much practiced although it has obvious advantages in separating the molecular weight of linear and ring polymers as shown in the SEC traces in reference [23]. The reason for its omission is that it has been observed that the

linear polycondensates continue to grow and, usually, have molecular weights several fold larger than the desired cyclic polymer [8,9,21,22].

After step 3 the crude product is recovered. Geiser and Höcker [20] have described the logical further approach to recover and analyse the cyclic fraction. The first step is a SEC analysis of the crude product. It allows the determination of a crude yield of the cyclization. The separation of the (linear) polycondensate from the cyclic product is by fractional precipitation. Detailed examples have been given by Hild [24] and Roovers [9], It has been observed that cyclic polymers have a lower θ temperature than linear polymers [9,25]. This makes it possible to remove linear from cyclic polymer with identical molecular weight but not without some loss of cyclic material. However, no means has been found to separate cyclics from linear polymer with half the MW. Small amounts of such impurity can only be found by ultracentrifugation analysis [9]. The separation of cyclic from linear polymers must be monitored by SEC. Two features of the SEC traces are important. The delay of the elution of the cyclic relative to that of the linear parent, and the shape of the cyclic elution peak. The latter should be identical to that of the parent polymer, ensuring that no linear polymer contaminates the sample and no fractionation of the cyclics has occurred. The lack of complete resolution of linear and cyclic polymers by standard SEC equipment is at the origin of much confusion. After fractionation and SEC analysis an absolute MW determination of the cyclic polymer should confirm that it is identical to that of the linear parent. The absolute MW determination is followed by the measurement of one or more physical properties of the cyclic sample. The intrinsic viscosity is the dilute solution property most easily measured that is quite sensitive to the polymer topology.

Hild et al. [8] have introduced some variations into the basic process. Instead of making one batch of polymer they repeatedly alternated the polymerization and cyclization steps in one large volume of solvent. Working at a 0.5% (w/v) polymer concentration they obtained 30% cyclization of a polystyrene with MW = 10 000 This procedure was also used for the preparation of 40 g of cyclic polystyrene (20% yield) with MW = 100 000 [22]. Roovers and Toporowski used mixtures of benzene and THF to prepare the bifunctional polystyrene and in some experiments used cyclohexane as the solvent for the cyclization. The use of cyclohexane at room temperature has been questioned [26,27] because the θ temperature for the system is at 34.5 C. This could lead to permanent "knots" in the cyclized polymers. However, no clear experimental evidence in support of this conjecture has been forthcoming. A back of the envelope calculation [9] indicates that knotting, considered as

intramolecular entanglements, would only be observable in cyclics when $MW \geq 10^6$.

The existence of higher multiple cyclics, i.e. dimeric and trimeric cyclics of the parent linear polymer are clearly recognizable in SEC traces [22,23]. Others have denied their existence [8,24]. In any case they have not been properly isolated and studied. The formation of catenated species has been proposed by Vollmert based on the very **low [η]/M** ratio of very small fractions (0.7 %) of very high MW material **(7.10^6),** that was not completely free from gel [22]. Note that the conditions of the cyclization (58 consecutive additions of 3.6 g of polymer in 2.5 L THF) leads to a final 8.3 % solution of polymer in which the smallest **MW = 10^5.** This could conceivably lead to catenanes in the final stage of the cyclization.

Cyclic polybutadiene (62% 1,2) has been prepared with potassium naphthalene in THF/n-hexane (1.35/1) at −1.5°C [28]. The cyclization is performed by slowly adding the living polymer into a large volume of cyclohexane at 0°C with concurrent distillation of dichlorodimethylsilane. The pale yellow color of the living polymer solution is used as an indicator of the reagents stoichiometry. A battery of SEC columns specific to the MW range was used to analyze the ring polymers. This provides better resolution between ring and linear precursor and a quantitative estimate (to within 5 %) of linear contamination.

Madani et al. prepared ring polyisoprene [29]. The two-ended high 1,4-polyisoprene was prepared from a dilithium initiator in hydrocarbon medium. The cyclization was performed in the presence of 15 % THF at -40°C. SEC analysis indicated that a high yield **(> 90 % @ MW = 5000; > 80 % @ MW = 30 000)** was achieved. The authors suggested that the possible association of the lithium carbanions under the cyclization conditions favors the intramolecular reaction.

Poly(2-vinylpyridine) was prepared from the dilithium living precursor polymer in THF [30] and the cyclization was performed by dropwise addition of the living polymer and either 1,4- or 1,2-di(bromomethyl)benzene to a large volume of purified THF at low temperature. Crude yields between 70 and 40 % are observed that decrease with increasing MW.

10.2.2 Cyclization of heterodifunctional polymers.

Deffieux and his collaborators have pioneered the preparation of cyclic polymers from heterodifunctional polymers [7]. The preparation of heterodifunctional polymers starts from a heterodifunctional initiator. The principle is outlined in Scheme 1 for the case of the cationic polymerization of 2-chloroethyl vinyl ether. The **iodo-ZnCl₂** complex promotes the polymerization of vinyl ethers at -40°C while the styrenic double bond is unaffected. The linear polymer can be sampled for later comparison with the cyclic polymer. Cyclization is effected at –10°C by dropwise addition of the living polymer to a solution of **SnCl₄** in toluene. **SnCl₄** activates the α-iodoether function and causes addition to the styrenic double bond. The reaction is terminated by methoxide/methanol. SEC analysis shows 80% Cyclization. The cyclic product is identified by the absence of the styrenic double bond and
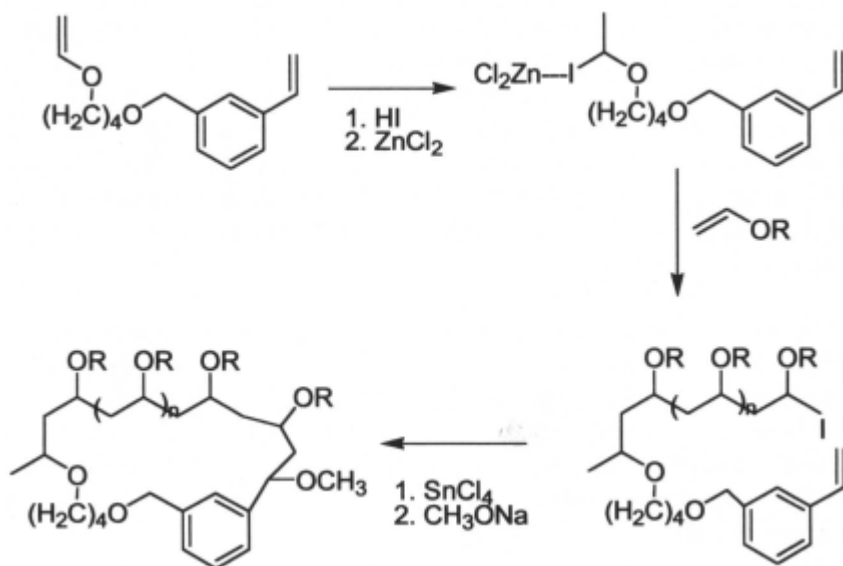
SCHEME 1.

acetal group typical of linear polymer. Poly(2-chloroethyl vinyl ether) and its cyclic isomer can be subjected to a variety of chemical modification reactions [31,32].

Narrow MWD **α,ω-heterodifunctional** polystyrene is prepared anionically starting from 3-lithiopropionaldehyde diethylacetal [33]. After conversion of the styryl anion to the less reactive diphenylethenyl anion, the

polymer is reacted with p-chloromethylstyrene. MWs are in the range from 2000 to 6700. The acetal group is converted into the **α**-iodo ether group with trimethylsilyliodide. The cyclization is performed as shown in Scheme 1. The yield of the cyclic polymer varies from 80 to 85 %. The presence of 10% linear polymer is recognized by the aldehyde group in the NMR spectrum and higher MW polycondensates (10-20 %) are quantified by SEC. The ring closure has also been performed with **TiCl₄** and with trimethylsilyltriflate [31].

Recently, Pasch and Deffieux have been able to analyze linear and cyclic polystyrenes with very similar MWs by means of liquid chromatography at the critical point. At the critical point the elution volume is sensitive to architectural features and functional groups on the polymer [34]. Complete resolution of linear and cyclic polystyrene mixtures is achieved. Several linear species with differing end-groups and at least two cyclic species with different ring closure groups are also separated. After careful quantification of the elution traces it was concluded that the cyclization yields are indeed very high (> 90 %) when the polystyrene MW is less than 8000 but that the yield decreases for higher MW polymers. For example, at **MW = 25 000** the cyclization yield is 57%, which is still very good when compared to the yields of other methods. The structure of the cyclic polystyrene has been confirmed by their MALDI-TOF spectra [35].

Macrocyclic polystyrene with **DP = 20, 30** and 35 have been prepared from **α-carboxyl-ω-amino** bifunctional linear polystyrene [36]. The linear polymer is prepared from 3-lithiopropionaldehyde diethylacetal as the protected functional initiator and 2,2,5,5-tetramethyl-1-(3-bromopropyl)-1-aza-2,5-disila-cyclopentane as the protected bifunctional terminating agent. Accordingly,

is obtained. The preparation of the linear polymer for the cyclization involves five steps and four purifications on silica gel to give

The cyclization step proper involves the formation of an amide bond at high dilution. After silica gel chromatography the cyclic fraction is isolated with an overall yield between 30 and 35 %.

10.2.3 Cyclic diblock copolymers

The obvious interest in cyclic block copolymers is in the comparison of their microphase morphology with the morphology of linear di- and triblock copolymers homologues. Cyclic polymers can only form double loops in strongly segregated microphases while linear triblock copolymers form loops and bridges. The earliest synthesis of a synthetic cyclic block copolymer predates the systematic studies of the 1980s [37]. An original combination of living anionic polymerization and equilibration cyclization was used. The isolated polystyrene containing fraction is a mixture of general formula
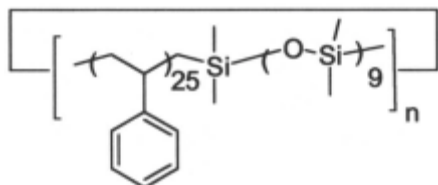
where n varies between 1 and 4. A more rigorous synthesis of cyclic PS-PDMS has been given recently [38,39]. The two-ended poly(dimethylsiloxane-b-styrene-b-dimethylsiloxane) (PDMS-PS-PDMS) is prepared with the Lithium counterion in THF. Dichlorodimethylsilane is the cyclizing agent. It is worth mentioning that alternative approaches were unsuccessful [38,39]. Nevertheless, with the adopted method it is still difficult to produce high MW monodisperse PDMS blocks. At high conversion and long polymerization times redistribution reactions begin to dominate the hexamethylcyclotrisiloxane polymerization [40]. The PDMS content is varied between 5 and 73 %. The cyclic nature of the diblock copolymer is deduced from the delayed elution in SEC. The ^{13}C and ^{29}Si NMR spectra do not show resonances for end groups. It is likely that the higher MW samples are contaminated by linear homologues due to inadvertent termination reactions. In the same studies the synthesis of a

linear CBABC and the corresponding cyclic ABCB polymer is described. In these polymers A is PS, B is 2,2,5,5-tetramethyl-2,5-disila-1-oxacyclopentane and C is PDMS.

Ma and Quirk have synthesized cyclic poly(styrene-b-butadiene)s [41,42]. They used 1,3-bis(1-phenylethylenyl)benzene (DPPE) to prepare a dilithium initiator for the consecutive polymerization of butadiene and styrene in benzene in the presence of excess lithium alkoxide. The triblock copolymer was diluted 10-fold in cyclohexane and cyclized with dichlorodimethylsilane or with DPPE. The cyclic polymer was isolated and identified by its reduced intrinsic viscosity.

Deffieux et al. made poly(styrene-b-2-chloroethyl vinyl ether) copolymers from an anionically prepared **α-styrenyl-ω-acetal** polystyrene [43]. They converted the acetal to an **α-iodo** ether function with trimethylsilyliodide and then polymerized the 2-chloroethyl vinyl ether monomer cationically. Ring closure was catalyzed by **SnCl₄**. Cyclic block copolymers of MWs between 4000 and 7500 were obtained [43].

Ishizu and Ichimura prepared poly(isoprene-b-styrene-b-isoprene) and **α,ω-end** capped the copolymer with 3-bromopropyl groups [18]. An interfacial cyclization technique was used to prepare the diblock ring. No rigorous proof of the final structure was given. The morphology of a number of cyclic diblock copolymers and their linear triblock parent polymers has been compared in the medium **χN<100** and strong **χN>100** segregation regime [44]. The lamellar spacing of the cyclic copolymers is 0.91 to 0.95 time smaller than the linear copolymer spacing. Such small difference is in agreement with theory but requires that utmost experimental care be used.

10.2.4 Tadpole or semicyclic polymers

Tadpole polymers are hybrid polymers consisting of a cyclic and one or more linear fragments. The homopolymer tadpole with one linear branch is completely defined by the mass fraction in the ring. In the case of block copolymer tadpoles several topological isomers are possible depending on the location of the different blocks in the polymer. Not all possibilities have been experimentally explored to date. Quirk and Ma prepared a cyclic polybutadiene with two linear polystyrene chains [41]. They coupled living polystyryllithium with DPPE. The still living polymer is used to initiate two chains of polybutadiene which are cyclized with dichlorodimethylsilane.
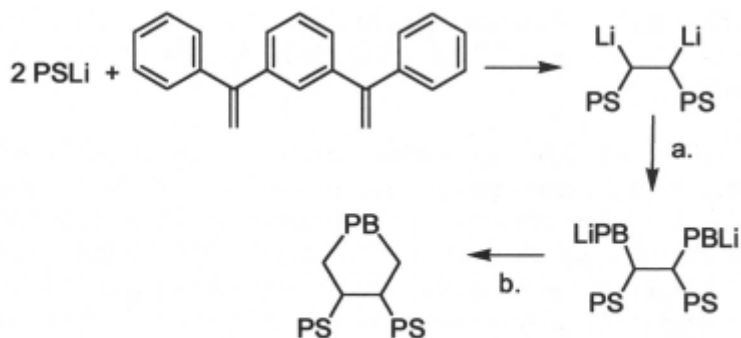
a. Butadiene; b. $(CH_3)_2SiCl_2$.

It is acknowledged that the SEC properties of such polymers will depend considerably on the mass fraction in the cyclic segment. The separation from the linear or branched homologue is smaller the smaller the ring fraction in the polymer.

Deffieux et al. worked out a strategy to prepare cyclic poly(2-chloroethyl vinyl ether) with a polystyrene tail [45]. See Scheme 2.
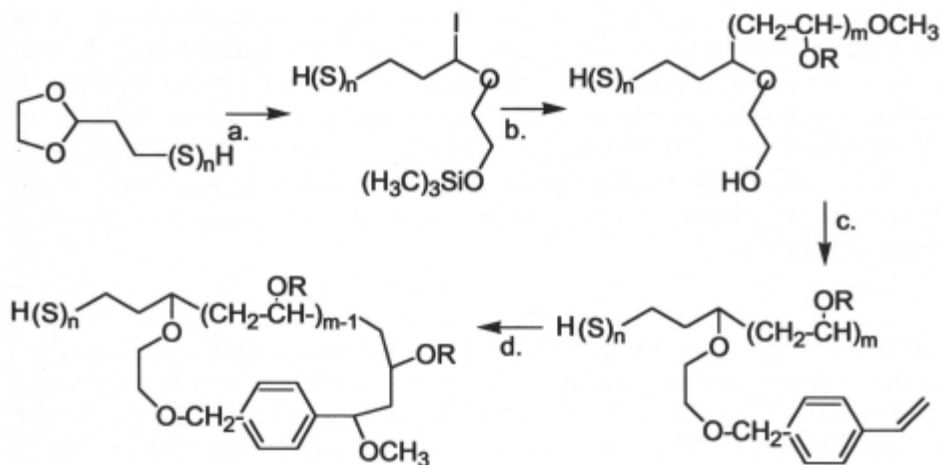
a. Me$_3$Sil ; b. vinylether, H$^+$; c. NaH, p-chloromethylstyrene ; d. SnCl$_4$

SCHEME 2.

The cyclization was achieved with **TiCl$_4$**. The total molecular weight is in the range 6000 to 9000. More recently Kubo et al. were able to attach a linear polystyrene onto a preformed cyclic polystyrene [46]. The amide bond formed in the ring closure was used to react with an **α**-carboxyl polystyrene. Schematically,
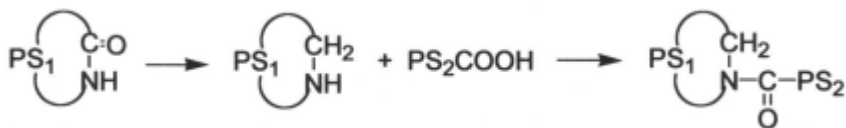
10.2.5 Bicyclic and tricyclic polymers

It is obvious that the synthetic control required for producing a sizable quantity of bicyclic polymer is even greater than for the cyclic polymer. Nevertheless, several groups took on this challenging synthesis. Antonietti and Fölsch prepared difunctional living polystyrene from sodium naphthalene in THP at -40°C [47]. The double cyclization is performed with 1,2-bis(dichloromethylsilyl)ethane. The cyclic yield is about 30% when the cyclization is performed in a 0.5 % solution on a polymer with **MW = 5600.** SEC analysis is inconclusive. However, the doubling of the molecular weight was proved by light scattering and osmotic pressure measurements. The small size of the bicyclic polymer prevented accurate size determination. Some geometric restriction is also seen in the broadened **^{1}H NMR** spectrum of the bicyclic relative to the linear polymer. Madam et al. reacted two-ended living

polyisoprene with **SiCl₄ [29].** From the SEC analysis a polymer contraction was observed but the product seems not to have been isolated and further characterized. The association of the lithium carbanion in the cyclization medium is held responsible for the exceptionally good yield of the bicyclic polyisoprene. Kudo at al. followed a more classic organic chemistry approach [46]. Their anionically prepared polystyrene ring is closed by an amide bond and this was reduced to a secondary amine. Two rings are then linked through a glutaric acid bridge.

Deffieux and his collaborators approached the synthesis of bicyclic polymer differently. They started from a tetrafunctional initiator with two acetal and two styrenic functional groups. Two acetal functions are used to produce two-ended poly(2-chloroethyl vinyl ether) by cationic polymerization [48]. In the cyclization step, the acetal ends of the precursor are activated to a carbocationic group that rapidly reacts with the two remaining styrenic groups of the initiator. The linear and cyclic polymer can be isolated and their properties can be compared. Relatively small bicyclic polymers of 2500 < MW<6500 have been prepared in order to analyze the fragments of the functional groups in the polymer by NMR. The important reactions are outlined in Scheme 1.

A tricyclic poly(2-chloroethyl vinyl ether) was synthesized based on the same principles [49]. The procedure started with the synthesis of an initiator molecule containing three styrenic and three vinyl ether double bonds. The latter are reacted with HI and activated with **ZnCl₂** to initiate the polymerization of 2-chloroethyl vinyl ether (DP = 15 to 45). The end-standing living carbocations are the activated with **SnCl₄** in toluene. They react intramolecularly with the styrenic double bonds of the initiator. The NMR spectra show poor resolution and it is not clear that the tricyclic polymer is not contaminated with dicyclic polymer carrying one linear tail and monocyclic polymer with two linear tails.

10.2.6 Cyclic Alkanes

Cyclic oligomers of cyclododecene with 12<n<96 carbon atoms are prepared by metathesis polymerization in very dilute (0.1 M) solution in cyclohexane in order to promote the formation of cyclic material [50,51].
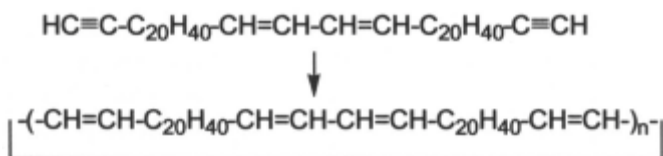
The remaining double bonds in the cyclics are hydrogenated. Seven fractions have been obtained chromatographically.

Lee and Wegner succeeded in expanding the synthesis and isolation of cycloalkanes to compounds with up to 288 carbon atoms. The polymers were obtained by Eglinton coupling of 1,23-tetraeicosadiyne under very dilute conditions [52] according to

$$HC{\equiv}C\text{-}C_{20}H_{40}\text{-}C{\equiv}CH \longrightarrow [(\text{-}CH{=}CH\text{-}C_{20}H_{40}\text{-}CH{=}CH\text{-})_n]$$

where n varies from 1 to 4 and **n=2** is usually the mayor product. The different fractions are separated by adsorption chromatography and hydrogenated over Pd/C. Similarly, linear oligomers are prepared at high concentration. The linear dimer of 1,23 tetraeicosadiyne has subsequently been used to make larger amounts of cyclic tetramer and hexamer

$$HC{\equiv}C\text{-}C_{20}H_{40}\text{-}CH{=}CH\text{-}CH{=}CH\text{-}C_{20}H_{40}\text{-}C{\equiv}CH$$

$$\downarrow$$

$$[(\text{-}CH{=}CH\text{-}C_{20}H_{40}\text{-}CH{=}CH\text{-}CH{=}CH\text{-}C_{20}H_{40}\text{-}CH{=}CH\text{-})_n\text{-}]$$

Cyclics with **n=8** and **n=12** were obtained from the linear tetramer. This geometric growth process assures better separation between the high molecular weight homologues.

10.3. Dilute Solution Properties of ring polymers

In Section 2.1 the necessity of proof of the topology of a ring polymer sample by one or, preferably, more physical properties sensitive to topological effects has been pointed out. Dilute solution properties, when properly extrapolated to zero concentration, are preferred because they are characteristic of the individual polymer chains and devoid of effects due to complex intermolecular interactions. In this section the experimental results of a few important dilute solution properties obtained on ring polymer samples are reviewed. Other techniques, e.g. column chromatography at the critical point [34,53,54] and MALDI-TOF [35] are good candidates for further development with respect to the identification of ring polymers. Selective adsorption on surfaces [55] and trapping in networks [56-58] may also contribute.

10.3.1 The θ temperature

In order to determine the θ temperature of a polymer, the second virial coefficient (A_2) is measured as a function of temperature. The temperature at which $A_2 = 0$ defines the θ temperature. All studies [9,25,59,60] of A_2 versus temperature on ring polystyrene in cyclohexane agree on a θ temperature lowering of about 6 °C relative to linear polystyrene (28.5 vs. 34.5 °C). The θ temperature lowering is independent of the MW of the rings in the range $20.10^3 < MW < 400.10^3$ within the experimental error of $\pm$ 1 °C. Smaller θ temperature depressions have also been observed [61]. It was shown [25] that these results can not be explained by introducing a three body contact term. A three body contact term is effective in explaining the θ temperature depression and its MW dependence in star and comb polymers [62] that also have a higher segment density than linear polymers. The following explanation has been given by Iwata [63]. At the θ temperature of the linear polymer a balance of interactions makes linear polymers thermodynamically invisible and allows them to intermingle freely with each other. However, at the same condition, the number of possible intermingling states for a pair of ring polymers is reduced because of the ring topology. This is an entropic effect equivalent to residual excluded volume for a pair of rings. On lowering the temperature, polymer-polymer interactions are obtained that compensate for this topological effect and make A_2 go to zero. Both Iwata [63] and Tanaka's [64] theories indicate that $\Delta\theta$ is relatively constant over the experimental MW range. Iwata [63] also showed that A_2 at the Flory θ temperature for the linear polymer decreases very slowly with MW in agreement with experimental results[9].

10.3.2 A_2 in good solvents

Values of A_2 for ring polystyrene in good solvents have been published by four laboratories [65-68]. Accurate measurements of A_2 are difficult and small discrepancies in absolute values are noted. This may be due in part to the concentration range used in the determination of A_2 as well as to the method used to derive A_2 from the experimental data. Values of the ratio

$$g_{A2} = (A_2)_r / (A_2)_l \qquad (6)$$

are in the range 0.84 to 0.93 [65], 0.86 to 0.90 [66] and 0.90 [67] for polystyrene in toluene. In THF g_{A2} varies between 0.72 and 0.94 [68]. In making the comparison between ring and linear polymer properties data sets of the respective laboratory have been used. The experimental values are all slightly higher than the $g_{A2} = 0.81$ calculated by the approximate method outlined by Yamakawa [69]. A normalization group theory prediction gives g_{A2}

$\approx 0.87_9$ [67]. The second virial coefficient can not be used as a reliable property to identify cyclic polymers because of the small difference between values of A_2 of linear and cyclic polymers. The dependence of A_2 on the composition of linear and cyclic polymer blends is not known.

10.3.3 Radii of gyration

The fact that the θ temperature measured by A_2 of linear and ring polymers is not identical has caused some concern about the significance of conformational and hydrodynamic properties obtained on cyclic polymers at the Flory θ temperature of linear polymers. It should be recalled that the studies of Iwata and Tanaka identify topological effects between *pairs* of polymer chains as the main cause for the different θ temperatures of linear and ring polymers. There is therefore no reason to believe a priori that θ_{A2} is also the θ temperature for other properties of the isolated ring polymer. In recent simulations Rubio et al. have shown that the conformational θ temperature of ring and linear polymers are identical [70]. It seems therefore best to compare conformational and hydrodynamic properties of ring and linear polymers at the Flory θ temperature.

The available experimental data of the radii of gyration of cyclic polystyrenes are plotted double logarithmically in Figure 1. The results, in the θ state and in the good solvents are obtained by SANS [65,71,72] or by light scattering [72]. The θ condition results can be summarized by

$$<Rg^2> = 0.039_7 \, Mw \quad (\text{Å}^2) \tag{7}$$

that, with $<Rg^2>_l = 0.079 \, M$, yields $g=<Rg^2>_r /<Rg^2>_l = 0.50_3$. The accuracy of values of $<Rg^2>$ and MW cannot be considered better than 5% and the agreement of the experimental value of g with the theoretical ½ [73] is better than can be hoped for and does not allow any further comment.

The case of the good solvent is more complex. The data of Ragnetti et al. [65] deal with samples with MW<30 000. In this MW range the dimensions of polystyrene in a good solvent and in a θ solvent approach each other and the MW dependence becomes variable [69]. The high molecular weight limiting slope is of real interest and only two data points are relevant. (See Figure 1). Using $<Rg^2>_l = 0.0166 \, M^{1.17} \, (\text{Å}^2)$ for linear polystyrene [67] $g = 0.47_5$ and 0.51_9 is obtained for the two samples. These values with their large error margin do not allow to pronounce on whether polystyrene rings are more or less expanded than linear polymers in a good solvent. It appears that the radius of gyration at the θ temperature is the superior physical property to characterize
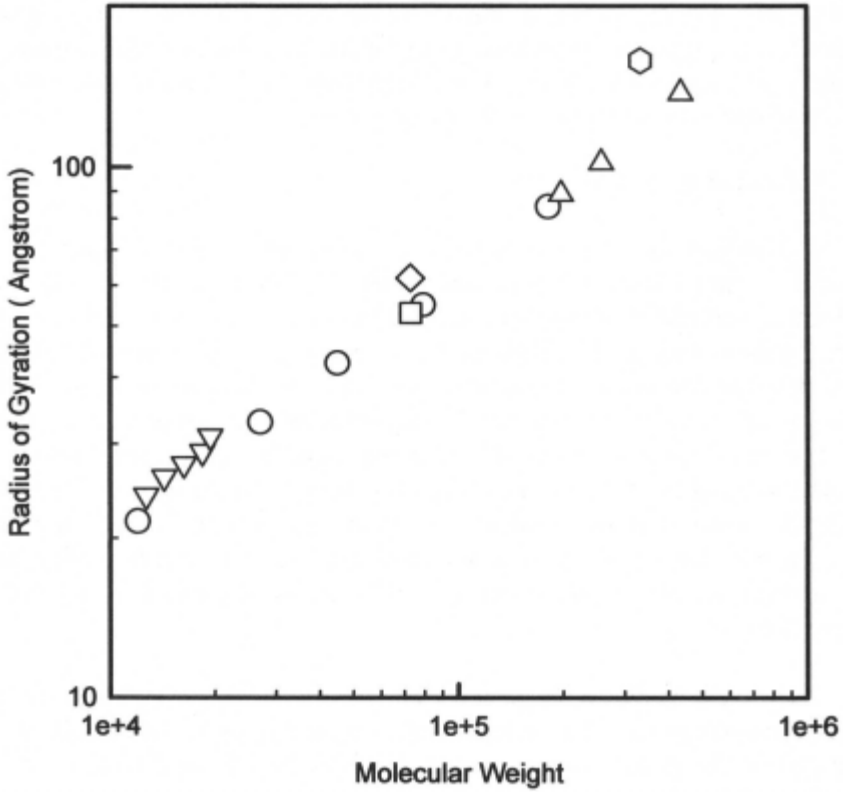
Figure 1-Double logarithmic plot of radii of gyration of cyclic polystyrenes against molecular weight, θ condition : cyclobexane O SANS [71]; □SANS [72]; ▲LS [25]. Good solvent : toluene ∇ SANS [65); ◇ SANS [72]; LS [25].

cyclic polymers. The ratio g is considerably different from unity and probably constant over a wide MW range. Furthermore g is sensitive to the presence of linear polymer because the z-average radius is measured. Unfortunately, for low MW polymers with Rg<200 Å SANS experiments are required. When Rg>200Å modem light scattering may provide acceptable accuracy. Analysis of the angular dependence of the scattered intensity may also help in identifying the ring structure [71,74].

10.3.4 Hydrodynamic radii

Measurements of hydrodynamic radii reinforce what we have observed in the case of the radii of gyration. In the θ state,

$$R_h = 0.20_2 \ Mw^{0.5} \ (\text{Å}) \tag{8}$$

i.e. the hydrodynamic radius is 1.12 times smaller for the cyclic than for the linear polymer. Individual laboratories found $g_h = (R_h)_r / (R_h)_l = 0.89$ [71], $g_h = 0.89$ to 0.86 [25] under θ conditions. In the good solvents, the high molecular weight dependence in THF follows $M^{0.545}$ [68] where samples with MW < 30 000 have been omitted and $g_h = 0.85$. In toluene $g_h = 0.84$ [25] and 0.86 [75] have been obtained. The small range of molecular weights over which the high MW limit has been investigated and the small number of samples make it difficult to determine the solvent dependence of g_h.

10.3.5 Intrinsic viscosity

Intrinsic viscosities of cyclic polystyrene samples have been studied very extensively, because it is the property that combines ease of measurement with sensitivity to topological differences. Its exclusive use as the litmus test [23-25,61,76,77] for the purity of cyclic fractions has been questioned, however.

Data in cyclohexane at 35°C have been obtained by four different laboratories and are summarized in Figure 2. A statistical analysis of all data in Figure 2 yields

$$[\eta] = 5.34 \ 10^{-2} \ Mw^{0.50} \ (\text{mL/g}) \tag{9}$$

for MWs between 7 000 and 500 000. Based on $[\eta]_l = 8.3 \ 10^{-2} \ Mw^{0.5} \ g' = [\eta]_r / [\eta]_l = 0.64_4$. From Figure 2 it can be seen that the agreement between the different laboratories is excellent for low MW ring polymers that are relatively easy to prepare and purify. Discrepancies are observed when the MW > 100000
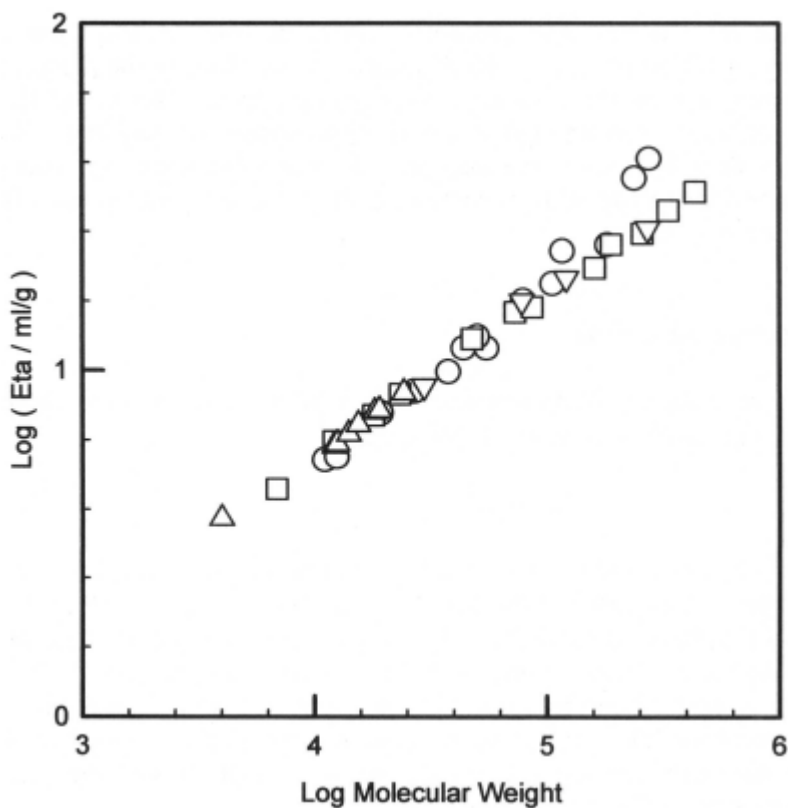
Figure 2-Double logarithmic plot of Intrinsic viscosity against molecular weight of cyclic polystyrene in cyclohexane at 35 °C : O [24,60,76]; □ [25]; Δ [23]; ∇ [77].

Positive deviations are ascribed to the presence of linear material of the same (or higher) MW [9,61] that can be fractionated out. Some single source data [25] suggest that g' slowly decreases with increasing MW. It has been suggested that the high MW samples showing low values of g' contain an appreciable fraction of permanently knotted cyclic polymer. This suggestion goes back to a computer simulation on phantom polymers [26].

In toluene, a good solvent for polystyrene (either at 25 or 35°C) the exact θ temperature has a negligible effect on the polymer conformation and behavior characteristic of long chains is expected when MW > 30 000. Below this molecular weight, the properties of the polymers in good solvents approach θ condition values[78]. The number of cyclic polystyrene samples is much reduced by this unavoidable low MW limit. The data presented are based on measurements in three laboratories [23,25,77] and are summarized by

$$[\eta] = 6.53 \times 10^{-3}\, Mw^{0.73}\ (mL/g) \qquad (10)$$

which, with $[\eta]_l = 1.02\ 10^{-2}\, Mw^{0.73}$ yields $g' = 0.64$. Analysis of the results obtained on matched pairs of linear and cyclic samples yields g' values between 0.64 and 0.68 [76]. Values of $g' > 0.70$ should be considered as indicative of considerable contamination with linear material. Results on ring polystyrene samples in THF [24,60] are slightly more scattered but nothing indicates that g' has a different value in that solvent. As in cyclohexane, one set of ring polystyrenes [25] shows decreasing values of g' with increasing molecular weight. The question whether ring polymers expand more or less than linear polymers when placed in a good solvent cannot be answered on the basis of the available $[\eta]$ results. The available experimental results suggest that, whatever the difference of expansion, it will be small. Subtle changes in the solvent draining through the linear and cyclic polymer coils may also affect the intrinsic viscosity ratios in different solvents.

10.3.6 Comparison with theoretical predictions and simulations

Some basic theoretical predictions on the dilute solution properties of ring polymers are summarized

$$g = <Rg^2>_r/<Rg^2>_l = 0.5 \quad [73,78] \qquad (11)$$

$$g_h = [f]_r/[f]_l = 8/3\pi \quad [79] \qquad (12)$$

$$g' = [\eta]_r/[\eta]_l = 0.662 \quad [80] \qquad (13)$$

All these ratios apply at the θ condition. The first ratio is exact and experimental results confirm its validity. Equations 12 and 13 are discussed in Yamakawa's book [19] together with probable good solvent values for each ratio. A thorough discussion of the significance of the present results on ring polymers in relation to theory is given by Fujita [81].

The approximations involved in the evaluation of the ratios in Equations 12 and 13 have since stimulated Freire and his collaborators to perform several sophisticated computer simulations on ring polymers [70,82-84]. They were encouraged by the excellent agreements their simulations provided in the case of star polymers. In ref. [84] they give an extensive comparison of their results with the experimental data in a good solvent and in ref. [70] they deal with the θ condition. It is remarkable that their value of g' in the limit of high molecular weight is less that 0.60 for all methods and all assumptions. This is in agreement with only one set of experimental results [25].

10.4. Bulk properties

10.4.1 Glass transition temperature

The experimental procedures significantly affect the resulting values of Tg. In order to consider the results obtained by different laboratories it is, therefore, better to consider $\Delta\mathbf{Tg} = \mathbf{Tg_\infty} - \mathbf{Tg}$ data, where $\mathbf{Tg_\infty}$ is the limiting high MW value. It is thereby assumed that a consistent experimental method has been used for all samples. In Figure 3 $\Delta\mathbf{Tg}$ data of cyclic polystyrene and, for comparison, of linear samples are collected. The MW dependence for linear samples can be expressed by

$$\Delta\mathbf{Tg} = -10^5 / \mathbf{Mn} \tag{14}$$

In contrast, $\Delta\mathbf{Tg}$ results for cyclic samples with MW > 7000 show a very small dependence on MW [85]. The slope for the cyclic samples in Figure 3 is 3-4 times smaller than for linear polystyrene. This conclusion is indirectly supported by the viscoelastic studies of McKenna [61,76]. The temperature dependence of the melt viscosity of cyclic polystyrenes with 11 000< Mw <185 000 was in all but one case identical to the temperature dependence of high MW linear polystyrenes. Indeed the Vogel parameters in the relation
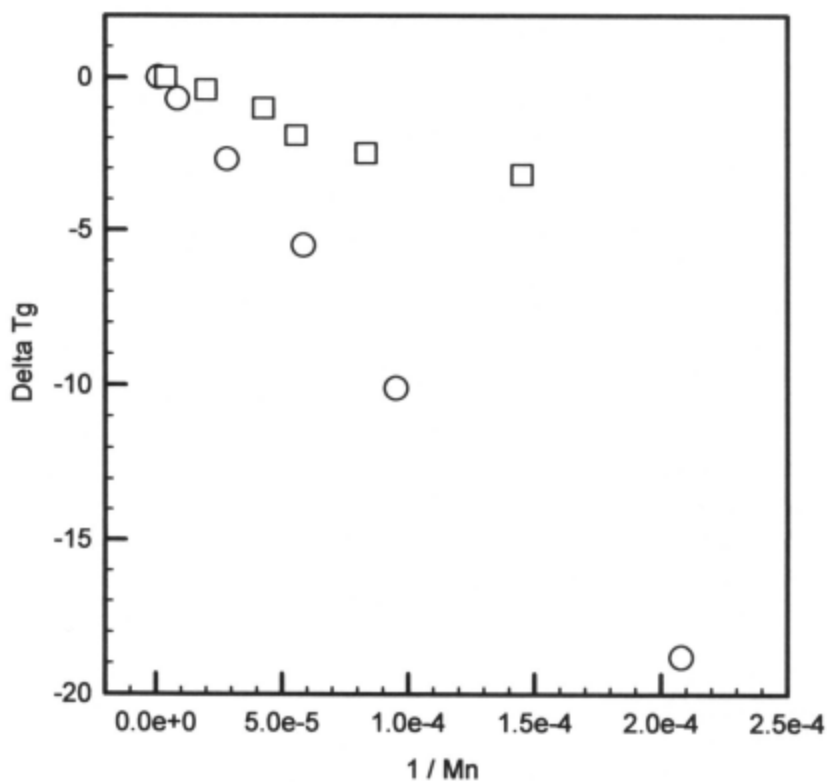
$$\mathbf{Log}\ \eta_0 = \log A' + B /(T - T_\infty) \tag{15}$$

Figure 3-ΔTg = Tg-Tg∞ against the inverse of molecular weight for linear (O) and cyclic (☐) polystyrenes.

are practically identical for all the polystyrenes. Unpublished results quoted in [76] confirm that DSC measurements of the ring polymers are within ±1°C identical with Tg_∞. Liu et al. have published DSC data on ring and linear polystyrene [86]. A minimum is observed for rings with **MW = 5000.** At lower MWs the Tg increases. These results are difficult to reconcile with the other published data but can be easily rationalized by assuming increase linear contamination with increasing MW. Gan et al. report that cyclic polystyrene with Mw > 4000 have Tg equal to Tg_∞ [87]. Recent studies by Deffieux also agree with a small ΔTg at low MW [33].

Cyclic poly(2-vinylpyridine) has been the subject of several Tg studies [30,87]. The original study of Tg of cyclic poly(2-vinylpyridine) revealed that the glass transition temperature increases substantially [30] with decreasing MW to values 18 °K above the Tg_∞ and 40 °K above the Tg of the linear polymer with the same MW. A very careful and detailed study clearly showed that this increase is largely due to the presence of LiBr, produced in the cyclization step [87]. Precipitation of the polymer in water removed the LiBr. The purified poly(2-vinylpyridine) samples have Tgs which vary little in the MW range from 1900 to 19 000. It can be concluded that Tg of cyclic polymers is much less dependent on MW than the Tg of linear polymers. This result lends support to the free chain end effect on Tg. Physicists however search for a deeper understanding of the glass transition phenomenon. An entropic theory of Tg [88] predicts that low MW cyclic polymers should have $Tg > Tg_\infty$. This has not been observed in cyclic organic polymers. It can not be excluded that very small cyclic polymers containing only a few Kuhn steps can only exist with an abnormal set of conformations and that they adopt a different packing in the amorphous state. Furthermore, the ring closing unit as well as the initiator fragment constitute abnormal segments that may affect Tg and obscure the sought-after phenomena.

10.4.2 Viscoelastic properties of the melt of cyclic polymers

The incentive for the study of the viscoelastic properties of cyclic polymers is the conjecture that without chain ends cyclic polymers can not effectively reptate in the same sense as linear polymers. However, the study of the melt properties of ring polymers has turned out to be much more difficult and controversial than anticipated. This became clear from results showing that the melt viscosity of ring polymers is strongly affected by the presence of even

small amounts of linear polymer with the same MW [89]. This results has been confirmed and shown to be true also for other properties such as the plateau modulus and zero-shear recoverable compliance [90]. We now realize that the dilute solution characterization techniques that are commonly used ([η] measurements in combination with SEC, see Section *3.5)* are insufficiently sensitive to detect linear polymer contamination to the level required for valid melt property studies.

Numerous studies have established that the temperature dependence of the zero shear viscosity of ring polystyrene is identical to that of the linear polymer [76,85]. Taking into account differences in the molecular weight dependence of Tg the thermal expansion coefficient of the fractional free volume, α_f, are the same for ring and linear polymer.

The zero-shear melt viscosity of cyclic polymers is best discussed in two MW ranges. Low MW ring polymers are unentangled and, as for linear polymers, their melt viscosity at constant friction coefficient i.e. at **(T - Tg) =** Constant, depends linearly on MW [61,85]. This is shown in Figure 4. The ratio $(\eta_0)_r/(\eta_0)_l = 1/2$ is in agreement with the Rouse model [80] for the relaxation of unentangled ring polymers. The relaxation is essentially an intramolecular process, the medium contributing only through the friction coefficient. It is quite possible that the Rouse region for cyclics extends to higher MWs than for the linear polymers (See Figure 4). A corollary of the Rouse behavior of low MW ring polymer melts is that the zero-shear recoverable compliance $(Je^0)_r = \frac{1}{2}(Je^0)_l$ as observed for at least one sample [85]. At **MW_r = 20 000, $(Je^0)_r \approx (Je^0)_l$** is obtained by two groups [61,85]. The low MW ring polymer results are probably secure since contamination with linear material is less likely, and would presumably have a small linear effect on the melt properties. Furthermore, similar melt properties have been observed for low MW poly(dimethylsiloxane) rings [91].

When considering the melt properties of high MW ring polymers, the first question concerns the entanglement state of ring polymers. Characterized by the entanglement molecular weight, Me, this properties is experimentally derived from either an integration under the loss modulus [92]

$$G_N^0 = (2/\pi)\int_{-\infty}^{+\infty} [G''(\omega) - G_s''(\omega)] \, d \ln \omega \qquad (16)$$

where contributions from the glass transition Gs" are subtracted or from the plateau compliance
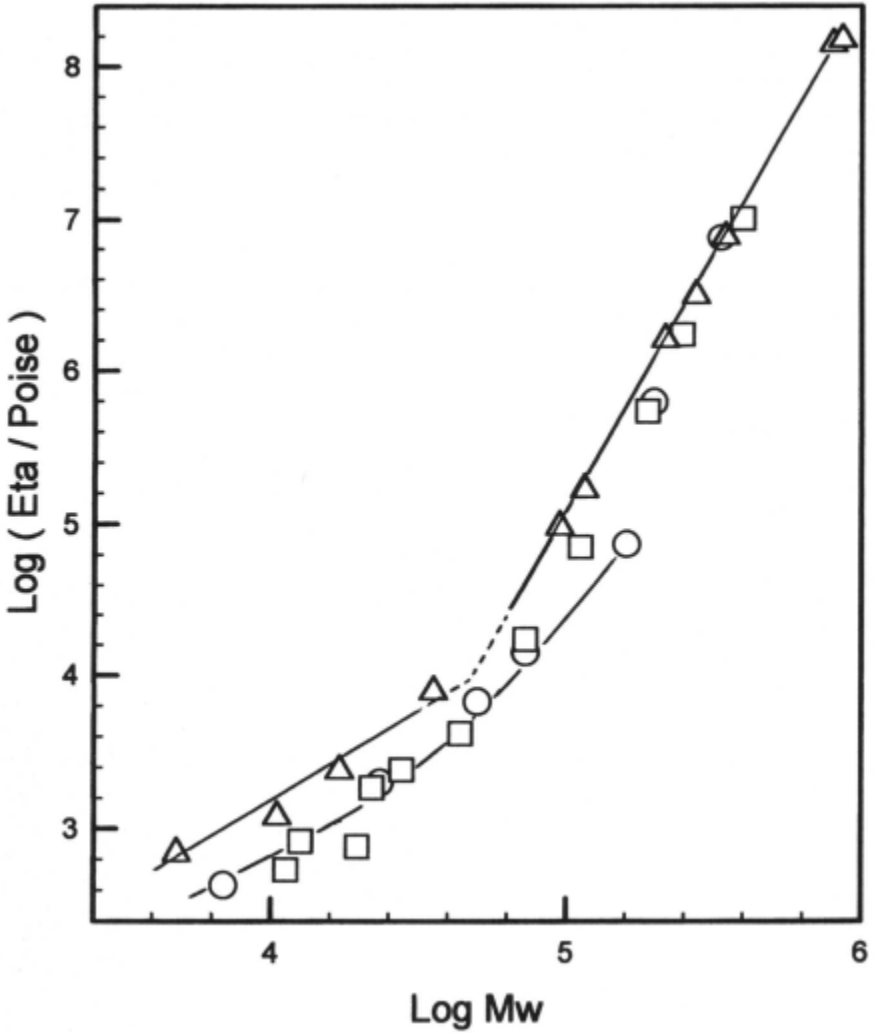
$$G_N^0 = 1 / (J_N^0). \qquad (17)$$

Figure 4-Double logarithmic plot of the melt viscosity against molecular weight at Tg + 69.5 °C. Linear △ [85]; cyclic polystyrenes O [85]; □ [61,76].

In both methods, accurate values of G_N^0 can only be derived for high MW monodisperse samples. McKenna's results indicate that G_N^0 of high MW ring polystyrene is lower than for linear polystyrene but G_N^0 data are not quantified [61]. The results are in qualitative agreement with $(G_N^0)_r = 1/2 (G_N^0)_l$ measured for one high MW polystyrene [85]. A later study of a cyclic polybutadiene [90], however, showed that $(G_N^0)_r \approx 1/6 (G_N^0)_l$. See Figure 5. It is not known whether $(G_N^0)_r$ is molecular weight dependent. However, it is clearly shown that $(G_N^0)_r$ increases approximately linearly in mixture with linear polymer of the same MW [90]. These observations are important. According to the theory of rubber elasticity, Me is given by [92]

$$Me = \rho\, RT\, /\, G_N^0 \tag{18}$$

where ρ is the melt density, R the gas constant and T in °K. The low value of G_N^0 implies that $(Me)_r > (Me)_l$, i.e. each ring polymer is less effectively entangled with other rings than the linear in linear polymer. This situation is unique. For example, branched polymers with many different architectures have G_N^0 equal to or slightly larger than $(G_N^0)_l$. It is tempting to relate the low level of entanglements of rings in rings to theories and computations that suggest that rings in rings are partially collapsed and that v in $R \sim M^v$ is 0.4 [93] or 0.45 [94-96] rather than 0.5 as for linear polymers. Simulations [96] suggested that $(Me)_r / (Me)_l = 3.9$. At this point it is of some interest to make a conjecture. If the entanglement state of cyclic polymers is very different from that of linear polymers and if simple reptation as in linear polymers would still apply then $(\eta_0)_r$ is at least ten times smaller than $(\eta_0)_l$. Since this is not observed in Figure 4 their relaxation mechanism is likely more complex. This can also be deduced from the very different shape of the $G''(\omega)$ curves of the cyclic and linear polybutadienes in Figure 5.

The high MW melt viscosities of ring polymers have been interpreted in two different ways. McKenna et al. [61] omitted the three high MW data of Roovers and concluded that ring melt viscosities scale as

$$(\eta_0)_r \propto Mw^{3.9} \tag{19}$$

for the range $4.8\ 10^4 < Mw < 3.9\ 10^5$. They placed thereby enormous confidence in two high MW samples $(Mw = 2.5\ 10^5$ and $3.9\ 10^5$ resp.) of dubious cyclic content. Indeed these samples are characterized by $[\eta]_r / [\eta]_l = 1.0 \pm 0.1$ in cyclohexane at 32.4 °C and in toluene. Their argument in favor of the cyclic nature of these polymers rests on $(G_N^0)_r = \frac{1}{2} (G_N^0)_l$ and $(Je^0)_r \leq 2$
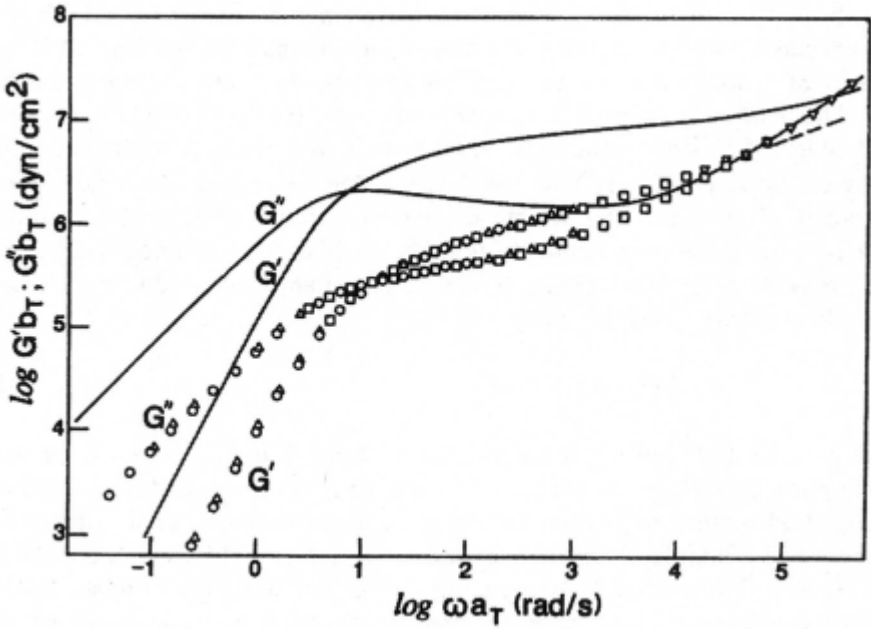
Figure 5-Comparison of the loss G'' and storage G' master curves of linear(solid lines) and ring (symbols) polybutadienes [90]. With permission of the American Chemical Society.

$(Je^0)_l$. The latter relation was used by McKenna et al. as an *a priori* criterion to select "good" cyclic samples. It has since been shown that blends of rings and their linear homologues have a large range of composition $0.9 < \phi_r < 0.75$ for which $(\eta_0)_{blend} \approx (\eta_0)_l$, $(G_N^0)_{blend} \approx (G_N^0)_l$ and $(Je^0)_{blend} \approx 2\text{-}3\ (Je^0)_l$ [90]. See Figure 6. It is therefore most likely that these samples were contaminated with at least 10 to 20 % linear polystyrene. Because the 3.9 power law in Eq.(19) is little different from the classical 3.4 power law for linear polymers it was proposed that this is evidence for reptation dominated relaxation of ring polymers. However, it has been shown in the case of a cyclic polybutadiene that a high value of $(Je^0)_r$ is consistent with a low value of $(\eta_0)_r$. In blends Je^0 decreases rapidly and η_0 increases rapidly with the addition of less than 15 % linear homologue [90]. See Figure 6. Roovers preferred to draw a curve through the experimental data as shown in Figure 4 suggesting that the melt viscosity of rings possibly increases exponentially with MW [85]. In the original paper this curve was continued to cross the line for linear polymers. It seems now prudent to limit the known MW dependence to MW $< 2\ 10^5$ as shown in Figure 4 in view of the uncertain quality of the cyclic samples with MW $> 3\ 10^5$. It can be safely argued that simple reptation of cyclic polymers in the melt is unlikely to be the dominant relaxation mechanism as suggested by relation (19). A quick comparison of $G''(\omega)$ curves of ring and linear polymers in Figure 5 shows that the maximum in the terminal region, characteristic of relaxation dominated by reptation, is absent in the cyclic loss modulus-frequency curve.

The study of blends of ring with their linear homologue has revealed that in a large composition range $0 < \phi_r < 0.80$ the melt viscosity of the blend is higher than that of each component separately. At the maximum $(\eta_0)_{blend} \approx 2.3$ $(\eta_0)_l$ [90]. See Figure 6. This result appears to be unique among blends of polymers of different architecture. Although there are very different "blending" rules according to the types of polymers in the blend [97], the melt viscosity is always intermediate between that of the pure components. The 2.3-fold increase of the melt viscosity of the linear polymer on addition of rings is approximately what is expected when tube renewal effects are eliminated from the relaxation of linear polymers [98], or when linear polymers relax in networks [92]. There are various models on how linear and ring polymers entangle. For example, one has to distinguish entanglements interior and exterior to the ring [99,100]. They will have different "retarding" effects on the ring and on the linear polymer dynamics but are not worked out to this date.
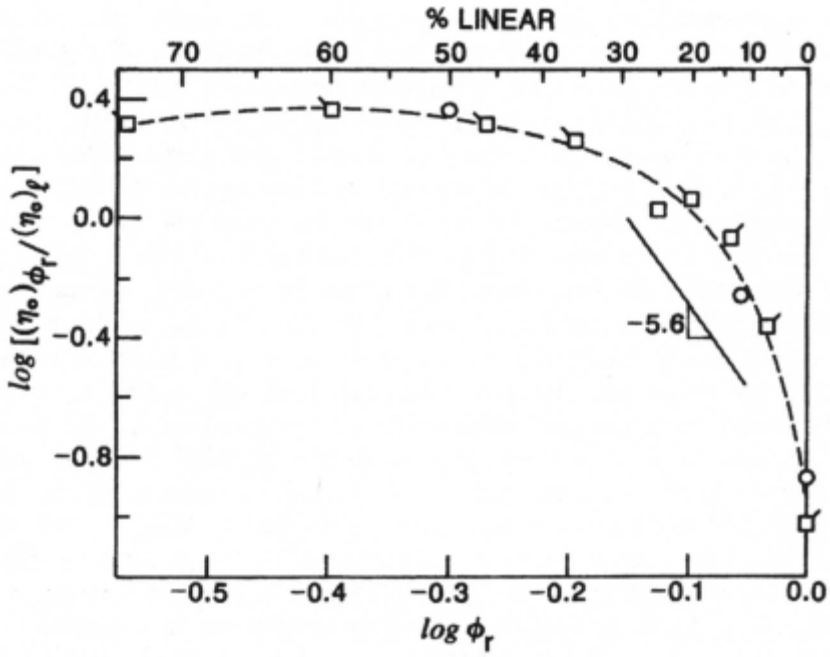
Figure 6-Double logarithmic plot of the melt viscosity against the cyclic fraction in blends of linear and cyclic polybutadiene [90]. With permission of the American Chemical Society.

10.4.3 Diffusion involving ring polymers

The diffusion of ring polymers has been studied under different conditions. The first experiments involved the diffusion of labeled ring polymer in a high MW linear matrix [101]. The method of blending was found to influence the diffusion rate of the ring polymer. When the two polymers are coprecipitated the diffusion rate $(D_r \sim 4.3 \ 10^{-11} \ cm^2/s)$ is comparable to that of linear polymer of the same MW. When the two polymers are mixed by slow solvent evaporation, the labeled ring polymer associates leading to no observable diffusion. Other experiments involve the interdiffusion of two polystyrene layers. In the first series of experiments ring polymers were allowed to diffuse into a thick layer of deuterated linear matrices [100]. For low MW ring polystyrene $(M=10\ 000)$ the diffusion rate is independent of the linear matrix and numerically equal to the diffusion rate of a linear polymer with the same MW. As the MW of the ring polymer increases the diffusion rate decreases below the linear polymer reptation rate and becomes more dependent on the matrix MW. However, at no time does the diffusion rate become as slow as when it would be dominated by constraint release alone. The experimental results could be matched to a model in which restricted reptation is active for unthreaded low MW rings. High MW rings diffuse mostly by means of a fraction of once-threaded rings that slide along the primitive path of the linear matrix chains. These mechanisms are derived from a theoretical proposal by Klein [99].

The diffusion of linear polystyrene in a matrix of ring polystyrene has also been investigated and compared with the diffusion in linear polymer matrices [102]. The cyclic matrices were limited to polymers with MW $\leq 1.8 \ 10^5$. In this range of MW the diffusion of the linear chains into the ring matrices was due to the sum of reptation and constraint release and indistinguishable from diffusion in linear matrices. This is a curious result if the constraint release process is driven by reptation of the ring matrix, a process that is expected to be slower or non-existent in the rings. While it has been argued that the very low melt viscosity of the ring polymers in itself does not control the diffusion, this low viscosity may be indicative of conformational and entanglement characteristics specific to rings in rings that are different from those of rings in linear polymers. This may lie at the origin of the dissymmetry between the diffusion of rings in linear and linear in ring polymers.

10.4.4 Semicrystalline cycloalkanes

The interest in cycloalkanes stems from their potential as model compounds for the adjacent re-entry type chain folding in linear polyethylene lamellae. Indeed, the cycloalkanes have built-in loops (g,g,t,g,g) which connect all-trans stems in the crystal lamellae. The thermal properties of cycloalkanes have been classified into three groups of increasing chain length [103]. The melting temperature, T_m, of low MW cycloalkanes 12<n<24 varies very irregularly with the number of carbon atoms, n, in the ring due to severe conformational constraints [50,103]. These cycloalkanes also show a low temperature solid-solid transition beside the melting process. Between the two temperatures they are plastic deformable. The entropy increase due to the solid-solid transition can reach 80% of the entropy of melting, indicating the high degree of disordering at the solid-solid transition. Medium size rings with 24<n<48 show a single T_m that smoothly increases with MW [50,52,103]. See Figure 7. The T_m of cycloalkane is always several degrees lower than of the corresponding linear alkane. When n > 48 the type of unit cell and T_m depend on the crystallization history [103,104]. The solution crystallized samples are monoclinic, the melt crystallized samples are orthorhombic. The T_m of the latter is a few degrees lower than that of the former. The orthorhombic form has a solid-solid transition a few degrees below the melting temperature when a pseudo-hexagonal structure is formed [52,103]. In the limit of high MW, n > 96, the entropy of melting per CH_2 becomes constant $(8.0 \text{ J K}^{-1} \text{ mol}^{-1})$ [103] although 8.7 has also been given [50]. These values are 10-20 % lower than the best value $9.9 \text{ J K}^{-1} \text{mol}^{-1}$ for polyethylene and are ascribed to less regular lateral packing of cycloalkanes in the lamellae [103].

Some thermal properties of the cycloalkanes can be correlated with ^{13}C CP/MAS data and their thermal variation [103]. Low alkanes have a single ^{13}C peak in the melt that only splits into two (n=12) or more (n=14) peaks at the solid-solid transition temperature in agreement with the high disorder in the plastic intermediate phase [103,105]. However, c-C_{24} has a single ^{13}C peak above the solid-solid temperature (at 30.50 ppm) and in the melt (29.62 ppm) but five peaks in the crystalline state. The major peak accounts for 8 carbons and the smaller peaks account for 4 carbons each. The major peak is assigned to carbons surrounded on both sides by two trans configurations and the other peaks are assigned to the various carbons near and in the g,g,t,g,g loop [105,106]. The all-trans carbons of the longer stems become more prominent in c-C_{36} and c-C_{48} crystals [103]. In c-C_{72}, c-C_{80} and c-C_{96} the crystal morphology is either monoclinic or orthorhombic that affect the ^{13}C peak positions and the peak widths [105,106]. The ^{13}C spectra of the orthorhombic form are more diffuse, indicating that the carbon atoms lie in less well defined positions.
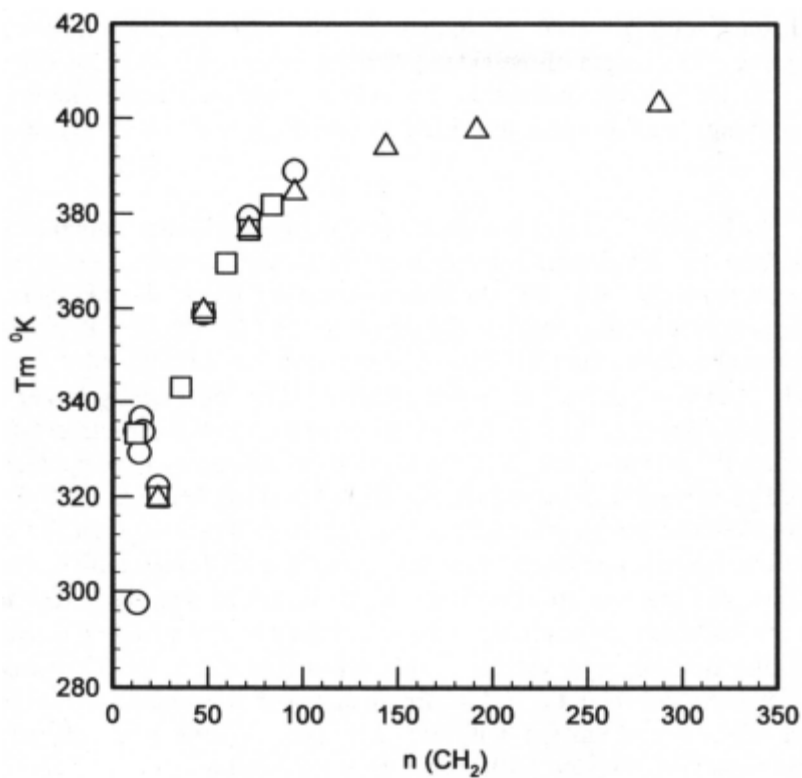
Figure 7-Dependence of the melting temperature on the number of methylene groups in cycloalkanes. O [103];□ [50]; ▲ [52].

Cycloalkanes with n ≥ 144 crystallize in the orthorhombic unit cell of polyethylene. The length of the extended all-trans stem for **n=144** is calculated to be 9.1 nm [52]. X-ray diffraction data indicate a characteristic spacing of that length proving that the stems are oriented perpendicular to the surface of the lamellae.

The length of the all-trans conformation in polyethylene lamellae is also derived from the longitudinal acoustic mode (LAM) frequency observed by Raman spectroscopy [30]. As Strobl has shown for linear alkanes there is no direct inverse relationship between the frequency and the lamellar thickness due to interlamellar interaction [108]. A correction for interlamellar forces is required. It is **v = 2.2 cm⁻¹** for linear alkanes [108] and slightly larger **v = 5 cm⁻¹** for cycloalkanes [52,109]. After such correction to the experimental LAM frequencies, the effective length of the crystalline sequence of the cycloalkanes is in good agreement with the calculated length obtained from n/2 x 1.275 Å. In fact, the calculated length is usually a little too large indicating that the carbon skeleton has a small number of torsions around the all-trans configuration. It should be noted that the effective stem length increases linearly with n to **n = 288** for cycloalkanes. In contrast, linear alkanes show chain folding (dependent on crystallization history) when **n $\geq$ 168**. Of course chain folding breaks the inverse relation between the LAM frequency and the alkane chain length. Unfortunately, a cycloalkane with **n= 2 x 168** carbons has not yet been synthesized and investigated for its possible chain folding.

The forced chain folding in cycloalkanes introduces several irregularities in the crystallites that are not seen in linear polyethylene. Möller has pointed out [110] that the direct transposition of the results obtained with cycloalkanes to polyethylene is not possible. The cycloalkanes have some specific differences in their crystalline morphology, e.g. the distance between the nearest stems, and are generally more complex. A specific signature for adjacent re-entry that would be useful in the study of linear polyethylene lamellae has not been found. Polyethylene has other structural irregularies, e.g. cilia, that are not found in cyclic alkanes and that influence its crystallization and can not be clarified by the study of cycloalkanes.

10.5.Conclusions

It has been shown that several alternative routes to organic cyclic polymers are now well established. However, the synthesis of ring polymers with MW > 100 000 has not been completely successful. This synthesis is a challenge at the edge of present day controlled macromolecular engineering. At this level there is a lack of synthetic precision, of good separation techniques and of sufficiently discriminating analytical methods. As a result, the dilute solution properties of ring polymers are not yet firmly established in the high MW limit that is of fundamental importance in polymer science. For the same reasons, the melt properties, especially diffusion and viscoelastic properties of ring polymers, are only marginally explored despite the importance of the ring polymer properties to the entanglement concept and reptation model. On the other hand, the study of Tg and the lamellar structure of truly monodisperse cycloalkanes are well advanced. As indicated in this review, it can be foreseen that new separation methods and new powerful analytical methods will most likely contribute to further advances in the study of organic ring polymers.

Acknowledgements

382

References

1.   P.Longi,F.Greco and U.Ro8si,Makromol.Chem.,**116**,113(1968).
2.   P.Longi,F.Greco and U.Rossi,Makromol.Chem.,**129**,157(1969).
3.   G.Allen,J.Burgess,S.F.Edwards and O.J.Walsh,Proc.R.Soc.London,**A334**,453(1973).
4.   G.Allen,J.Burges8,S.F.Edwards and O.J.Walsh,Proc.R.Soc.London,**A334**,465(1973).
5.   G.Allen,J.Burgess,S.F.Edwards and O.J.Walsh,Proc.R.Soc.London,**A334**,477(1973).
6.   J.E.Martin and B.E.Eichinger, Macromolecules,**16**,1345,1350(1983).
7.   M.Schappacher and A.Deffieux,Makromol.Chem.,Rapid Commun.,**12,**447(1991).
8.   G.Hild,A.Kohler and P.Rempp,Eur.Polym.J.,**16,**843(1983).
9.   J.Roovers and P.M.Toporowski,Macromolecules,**16,**843(1983).
10. H.Morawetz and N.Goodman,Macromolecules,**3,**699(1970).
11. M.Szwarc,Makromol.Chem.,**190,**567(1989).
12. G.Ercolani and P.Mencarelli.Macromol.Theory Simul.,**6,**1139(1997).
13. D.Dong,T.E.Hogen-Esch and J.S.Shaffer,Macromol.Chem.Phys.,**197,**3397(1996).
14. A.F.Fehérvari,R.Faust and J.P.Kennedy,Polym.Prepr.,**28,**382(1987).
15. A.F.Fehérvari,R.Faust and J.P.Kennedy,Polym.Bull.**23,**525(1990).
16. N.Yamazaki,S.Nakahama and A.Hirao,J.Macromol.Sci.-Chem.,**A9,**551(1975).
17. K.Ishizu and H.Kanno.Polymer,**37,**1487(1996).
18. K.Ishizu and A.Ichimura,Polymer,**39,**6555(1998).
19. E.F.Casassa,J.Polym.Sci.,Part A,**3,**605(1965).
20. D.Geiser and H.Höcker,Polym.Bull.,**2,**591(1980).
21. B.Vollmert and J.-X.Huang,Makromol.Chem.,RapidCommun.,**1,**333(1980).
22. B.Vollmert and J.-X.Huang,Makromol.Chem.,Rapid Commun.,**2,**467(1981).
23. D.Geiser and H.Höcker,Macromolecules,**13,**653(1980).
24. G.Hild,C.Strazielle and P.Rempp,Eur.Polym.J.,**19,**721(1983).
25. J.Roovers,J.Polym.Sci.:Polym.Phys.Ed.,**23,**117(1985).
26. G.ten Brinke and G.Hadziioannou,Macromolecules,**20,**480(1987).
27. P.-G.de Gennes,C.R.AcadSci.Paris,**310,**Série II,1327(1990).
28. J.Roovers and P.M.ToporowskiJ.Polym.Sci.rPart B:Polym.Phys.,**26,**1251(1988).
29. A.E.Madani,J.-C.Favier,P.Hémery and P.Sigwalt,Polym.Int.,**27,**53(1992).
30. T.E.Hogen-Esch,J.Sundararajan and
     W.Toreki,Makromol.Chem.,Macromol.Symp.,**47,**23(1991),
31. A.Deffieux and M.Schappacher,Polym.Adv.Techn.,**7,**122(1995).
32. A.Deffieux and M.Schappacher, in *Macromolecular Engineering Recent
     Advances.*ed.by M.Mishra,Plenum Press,N.Y.1995.
33. L.Rique-Lurbet,M.Schappacher and A.Deffieux,Macromolecules,**27,**6318(1994).
34. H.Pasch,A.Deffieux,I.Henze,M.Schappacher and L.Rique-
     Lurbet,Macromoleculcs,**29,**8776(1996).
35. H.Pasch,A.Deffieux,R.Ghahary,M.Schappacher and L.L.Rique-
     Lurbet,Macromolecules40,98(1997).
36. M.Kubo,T.Hayashi,H.Kobayasshi,K.Tsuboi and T.Itoh,Macromolecules,**30,**2805(1997).
37. F.R.Jones,Eur.Polym.J.,**10,**249(1974).
38. R.Yin and T.E.Hogen-Esch,Macromolecule8,**26,**6952(1993).
39. R.Yin,E.J.Amis and T.E.Hogen-Esch,Macromol.Symp.,**85,**217(1994).
40. J.-G.Zilliox,J.Roovers and S.Bywater,MacromolecuIes,**8,**573(1975).
41. J.Ma,Macromol.Symp.**91,**41(1995).
42. R.P.Quirk and J.Ma,Polym.Prepr.,**29,**10(1988).
43. A.Deffieux,M.Schappacher and L.Rique-Lurbet,Poymer,**35,**4562(1994).
44. R.L.Lescanec,D.A.Hajduk,G.Y.Kim,Y.Gan,R.Yin,S.M.Gruner,T.E.Hogen-Esch and
     E.L.Thomas,MacromolecuIes,**28,**3485(1995).
45. S.Beinat,M.Schappacher and A.Deffieux,Macromolecules,**29,**6737(1996).

46. M.Kubo,T.Hayashi,H.Kobayashi and T.Itoh,Macromolecules,**31,**1053(1998).
47. M.Antonietti and K.J.Fölsch,Makromol.Chem.,RapidCommun.,**9,**423(1988).
48. M.Schappacher and A.Deffieux,Macromolecules,**28,**2629(1995).
49. M.Schappacher and A.Deffieux,Macromolecules,**25,**6744(1992).
50. H.Höcker and K.Riebel,Makromol.Chem.,**178,**3101(1977).
51. H.Sato,K.Okimoto and Y.Tanata,J.Macromol.Sci.,Chem.,**11,**767(1977).
52. K.S.Lee and G.Wegner,Makromol.Chem.,Rapid Commun.,**6,**203(1985).
53. I.V.Blagodatskikh and A.V.Gorshkov.Vysokomol.Soed.,Series A,**39,**l681(1997).
54. A.A.Gorbunov and A.M.Skvortsov,Polym.Sci.,USSR,**29,**1025(1987).
55. G.K.Stratouras and M.K.Kosmas,Macromolecules,**24,**6754(1991);**25,**3307(1992).
56. B.R.Wood,S.J.Joyce,G.Scrivens,J.A.Semlyen,P.Hodge and
    R.O'Dell,Polymer,**34,**3059(1993).
57. L.C.DeBolt and J.E.Mark,Macromolecules,**20,**2369(1987).
58. V.Galiatsatos and B.E.Eichinger.PolymerCommun.,**28,**182(1987).
59. J.Huang,J.Chen,C.Li and D.Lin,Makromol.Chem.,**192,**1249(1991).
60. P.Lutz,G.B.McKenna,P.Rempp and C.Strazielle,Makromol.Chem.,Rapid
    Commun.,**7,**599(1986).
61. G.B.McKenna,B.J.Hostetter,N.Hadjichristidis,L.J.Fetters and
    D.J.Plazek,Macromolecules,**22,**1834(1989)
62. F.Candau,P.Rempp and H.Benoit,Macromolecules,**5,**627(1972).
63. K.Iwata,Macromolecules,**18,**115(1983);**22,**3702(1989).
64. F.Tanaka,J.Chem.Phys.,**87,**4201(1987).
65. M.Ragnetti,D.Geiser,H.Höcker and R.C.Oberthur,Makromol.Chem.,**186,**1701(1985).
66. J.Huang,C.Li,G.Chen,D.Zhu,J.Chen and D.Liu,Makromol.Chem.,**192,**l237(1991).
67. J.F.Douglas,J.Roovers and K.F.Freed,Macromolecules,**23,**4168(1990).
68. M.Duval,P.Lutz and C.Strazielle,Makromol.Chem.,RapidCommun.,**6,**71(1985).
69. H.Yamakawa,*Modern Theory of Polymer Solutions*, Harper and Row,Evanston(1972).
70. A.M.Rubio,J.J.Freire,M.Bishop and J.H.R.Clarke,Macromolecules,**28,**2240(1995).
71. G.Hadziioannou,P.M.Cotts,G.ten Brinke,C.C.Han,P.Lutz,C.Strazielle,P.Rempp and
    A.J.Kovacs, Macromolecules,**20,**493(1987).
72. G.Hadziioannou and J.Roovers, unpublished results.
73. H.A.Kramers,J.Chem.Phys.,**14,**415(1946).
74. E.F.Casassa,J.Polym.Sci.,A,**3,**605(1965).
75. J.Huang.C.Li and B.He,Makromol.Chem.,**187,**149(1986).
76. G.B.McKenna,G.Hadziioannou,P.Lutz,G.Hild,C.Straziell,C.Straupe,P.Rempp and
    A.J.Kovacs, Macromolecules,**20,**498(1987).
77. Z.He,M.Yuan,X.Zhang,X.WangX.Jin,J.Huang,C.Li and
    L.Wang,Eur.Polym.J.,**22,**597(1986).
78. B.H.Zimm and W.H.StockmayerJ.Chem.Phys.,**17,**1301(1949).
79. M.Fukatsu and M.Kurata,J.Chem.Phys.,**44**4539(1966).
80. V.A.Bloomfield and B.H.Zimm,J.Chem.Phys.,**44,**315(1966).
81. H.Fujita, *Polymer Solutions,*Elsevier,Amsterdam(1990).
82. J.M.Garcia Bernal,M.M.Tirado,J.J.Freire and J.Garcia de la
    Torre,Macromolecules,**23,**3357(1990).
83. A.Rey,J.J.Freire and J.Garcia de la Torre,Macromolecules,**23,**3953(1990).
84. J.M.Garcia Bemal,M.M.Tirado,J.J.Freire and J.Garcia de la
    Torre,Macromolecules,**24,**593(1991).
85. J.Roovers,Macromolecules,**18,**1359(1985).
86. X.Liu,D.Chen,Z.He,H.Zhang and H.Hu,Polym.Commun.,**32,**123(1991).
87. Y.Gan,D.Dong and T.E.Hogen-Esch,Macromolecules,**28,**383(1995).
88. E.DiMarzio and C.Guttman,Macromolecules,**30,**1403(1997).
89. G.B.McKenna,D.J.Plazek,Polym.Commun.,**27,**304(1986).

384

90.   J.Roovers,Macromolecules,**21,**1517(1988).
91.   K.Dodgson,D.J.Bannister and J.A.Semlyen,Polymer,**21,**663(1980).
92.   J.D.Ferry,*Viscoelastic Properties of Polymers,*J.Wiley & Sons Inc.,N.Y.(1980).
93.   M.E.Cates,J.M.Deutsch,J.Phys.(Les Ulis),**47,**2121(1986).
94.   S.Geyler and T.Pakula,Makromol.Chem.,Rapid Commun.,**9,**617(1988).
95.   T.Pakula and S.Geyler,Macromolecules,**21,**1665(1988).
96.   J.Skolnich and A.Kolinski,Adv.Chem.Phys.,**78,**23(1990).
97.   T.M.C.McLeish and S.T.Milner,Adv.Polym.Sci.,in press.
98.   W.W.Graessley and M.Struglinski,Macromolecules,**19,**1754(1985).
99.   J.Klein,Macaromolecules,**19,**105(1986).
100.   P.J.Mills,J.W.Mayer,E.J.Kramer,G.Hadziioannou,P.Lutz,C.Strazielle,P.Rempp and
       A.J.Kovacs,Macromoleculcs,**20,**513(1987).
101.   M.Antonietti,J.Coutandin,R.Grütter and H.Sillescu,Macromolecules,**17,**798(1984).
102.   S.F.Tead,E.J.Kramer,G.Hadziioannou,M.Antonietti,H.Sillescu,P.Lutz and
       C.Strazielle,Macromolecules,**25,**3942(1992).
103.   H.Drotloff.D.Emeis.R.F.Waldron and M.Mõller,Polymer,**28**1200(1987).
104.   K..-S.Lee,G.Wegner and S.L.Hsu,Polymer,**28,**889(1987).
105.   M.Mõller,W.Gronski,H.-J.Cantow and H. Hacker,J.Am.Chem.Soc,**106,**5093(1984).
106.   I.Ando,T.Yamanobe,T.Sorita,T.Komoto,H.Sato,K.Deguchi and
       M.Imanari,Macromolecules,**17,**1955(1984).
107.   M.Tasuni,T.Shimanouchi and R.F.Schaufele,Polymer J.,**2,**740(1971).
108.   G.R.Strobl and R.Eckel,J.Polym.Sci.,Polym.Phys.Ed.,**14,**913(!976).
109.   T.Trzeboiatovski,M.Dräger and G.R-Strobl,Makromol.Chem.,**183,**731(1982).
110.   M.Möller,R.F.Waldron,H.Drotloff and ögler,Intcgr.Fund.Polym.Sci.Techn,**2,**334(1987)
       publ.(1988).

CHAPTER 11

NEUTRON SCATTERING AND NUCLEAR MAGNETIC RESONANCE INVESTIGATIONS OF CYCLIC POLYMERS

Peter C. Griffiths

Cardiff University, UK

Over the last twenty years or so, the techniques of small-angle neutron scattering (SANS) and nuclear magnetic resonance (NMR) have emerged as almost unrivalled for studying polymer containing systems, in terms of the structural diversity and detail they furnish.

The structures within crystalline, amorphous and liquid crystalline polymers have characteristic dimensions within the 1-100 Å range, comparable to the wavelengths of neutrons and X-rays. These materials can therefore be studied *via* scattering techniques employing these radiation sources. X-rays are scattered by the electron clouds associated with an atom and accordingly the scattering intensity depends on atomic number - heavier elements scatter much more strongly than lighter ones, with the consequence that protons are often invisible. By contrast, neutrons are scattered by the nucleus and the scattering intensity varies randomly with atomic number. Interestingly, the proton and deuterium have very different neutron - nucleus interactions which leads to an experimental feature known as "contrast matching". To the experimentalist this is invaluable as a suitable mixture of the protonated and deuterated forms of a solvent may be used to remove the scattering from a particular facet or component of the system. More importantly perhaps, is the fact that the energies of neutrons are much less than those of X-rays and thus, neutrons can be considered a non-perturbing probe. In this Chapter, sufficient scattering theory will be outlined to facilitate discussion of experimental studies but the

reader is referred to the excellent text by Higgins and Benoît [1] for a complete description of scattering theory. To facilitate such comparisons, the style and nomenclature of that text will be adopted in this Chapter.

The dynamics of polymers are also complex, ranging from the relatively rapid motions of pendant- or side-groups to the slow conformational rearrangements of the polymer backbone. The characteristic time- and length-scales involved in these processes can be probed by NMR studies; the overall size of the polymer coil determines its diffusion coefficient whilst the mobility of the segments affect the NMR relaxation time or line-width. Both of these approaches will be discussed.

To date, more SANS studies of cyclic polymers have been published and it is therefore pertinent that this Chapter starts there. Wherever possible, direct comparisons between cyclic and linear polymers will be made to emphasis the similarities and differences of the two molecular architectures. The examples chosen are intended to be indicative of the type of experiment possible and to hopefully highlight those areas where the current understanding is not yet complete.

11.1 Small-Angle Neutron Scattering

The basis of the scattering experiment involves extracting information about the polymer from the wave-vector dependent intensity of the scattered radiation which occur as a result of the scattering event. The wave-vector can be defined in an analogous manner to the constructive interference condition in the classical Bragg law;

$$n\lambda = 2d \sin\left(\frac{\theta}{2}\right) \tag{1}$$

where n is an integer representing the order of interference, λ is the wavelength, d is the crystal spacing and θ is the scattering angle. The analogous relationship in neutron scattering is shown in Figure 1. The collision between the nucleus and the neutron is "elastic" since no change in energy, and hence wavelength,
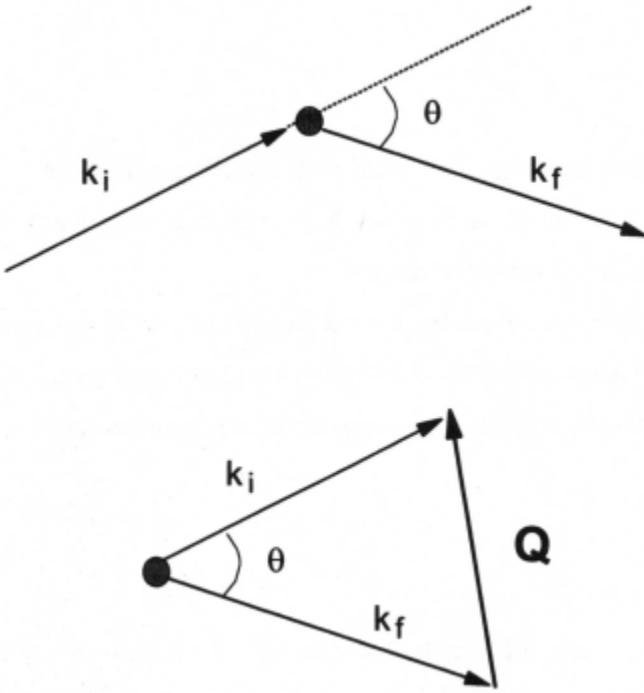
Figure 1; The Wave-vector, Q

occurs. The magnitudes of the initial k_i and final k_f wave-vectors are therefore equal ($k_i = k_f = 2\pi/\lambda$). Defining the wave-vector q as $q = k_f - k_i$;

$$|q| = q = \left(\frac{4\pi}{\lambda}\right)\sin\left(\frac{\theta}{2}\right) \tag{2}$$

Combining equations 1 and 2 yields

$$\frac{2\pi}{q} = \frac{d}{n} \tag{3}$$

which illustrates one important feature of scattering experiments - the inverse relationship between d and q *i.e.* the scattering associated with "large" dimensions occurs at small "q" values.

The energies of neutrons used in typical scattering experiments are much smaller than nuclear binding energies and thus, the scattering interaction can be described by a single parameter, the scattering cross-section, σ;

$$\sigma = 4\pi b^2 \tag{4}$$

where b is the scattering length. Each scattering nucleus effectively acts as a source for each new scattered wave, and b characterises the amplitude of this wave. For a collection of nuclei, *i.e.* a molecule, one must calculate an average scattering cross-section; for instance $\sigma_{H2O} = 167.15 \times 10^{-24}$ cm^2 whilst $\sigma_{D2O} = 19.41 \times 10^{-24}$ cm^2. (Values of scattering length and cross-section are tabulated in reference [1]).

11.1.1 What is measured in a SANS experiment ?

The information about the spatial arrangement of N scattering nuclei is represented by the differential cross-section per atom relative to a given scattering angle, $\frac{d\sigma}{d\Omega}$;

$$\frac{d\sigma}{d\Omega} = \frac{1}{N}\left|\sum_n b_n \exp(i q . R_n)\right|^2 \tag{5}$$

which for an incompressible, two component system at small scattering vectors and considering only the coherent scattering component[†], is given by;

$$\left(\frac{d\sigma}{d\Omega}\right)^{coherent} = \left(\overline{b_1} - \overline{b_0}\right)^2 S_{11}(q) \tag{6}$$

$\overline{b}$ represents the coherent scattering length density of the polymer (subscript 1) or solvent (subscript 0) and $S_{11}(q)$ represents the structure of the scattering species. Convention dictates that $S_{11}(q)$ is usually broken down into two components, $P_1(q)$ and $Q_1(q)$. Taking into account that the N polymer molecules each contain z segments, it can be shown that;

$$S_{11}(q) = Nz^2 P_1(q) + N^2 z^2 Q_1(q) \tag{7}$$

[†] See Ref. [1] for a description of the origins and significance of the coherent and incoherent scattering terms.

The former component, $P_1(q)$, characterises the scattering arising from different parts of the same scattering species - the intramolecular scattering. It is this term that most frequently contains the information desired by the experimentalist - the size and shape of the scattering species. The latter term $Q_1(q)$ characterises the interference pattern arising from scattering from different species. For dilute samples, $Q_1(q)$ may often be neglected.

Once $P_1(q)$ has been isolated, analytical or exact functions can be used to interpret the $P_1(q)$ term. There are several methods for isolating $P_1(q)$ from $S_{11}(q)$. For instance, $P_1(q)$ is obtained directly from scattering experiments on protonated and deuterated mixtures of polymers.

11.1.2 Single Component Linear and Cyclic Polymer Systems
11.1.2.1 Direct Measurement of the Form Factor

The most common method for obtaining the form factor involves measurement of the scattered intensity for a series of samples, extrapolating the data to infinite dilution. Re-writing Eqns. 6 and 7 as the scattering per unit volume;

$$\frac{I(q)}{V} = b_v^2 \, \phi \, V_1 \left[P_1(q) + N Q_1(q) \right] \tag{8}$$

$I(q)$ denotes the measured q-dependent intensity. Knowing that $b_v = \dfrac{b_1}{V_1} - \dfrac{b_o}{V_o}$, where $\dfrac{b_i}{V_i}$ are the scattering lengths per unit volume of the polymer (subscript 1) and solvent (subscript 0) and dividing through by ϕ, the polymer volume fraction *viz*;

$$\frac{I(q)}{\varphi V} = b_v^2 V_1 \left[P_1(q) + N Q_1(q) \right] \qquad (9)$$

and since $\dfrac{N V_1}{V} = \varphi$, one arrives at a linear function in φ;

$$\frac{I(q)}{\varphi V} = b_v^2 V_1 \left[P_1(q) + \frac{\varphi V}{V_1} Q_1(q) \right] \qquad (10)$$

Thus, extrapolation of the I(q) data for a series of samples to $\varphi \to 0$, and removing the $b_v^2 V_1$ term yields $P_1(q)$.

11.1.2.2 Using the Form Factor to obtain the Radius of Gyration

The form factor is defined as;

$$P_1(q) = \frac{1}{z^2} \sum_{i=1}^{z} \sum_{j=1}^{z} \left\langle \exp\left(-i\, q \cdot r_{ij}\right) \right\rangle \qquad (11)$$

where r_{ij} is the vector joining scattering points i and j, averaged over all orientations and conformations. This may be expanded as a power series;

$$P_1(q) = 1 - \frac{q^2}{6z^2} \sum_{i=1}^{z} \sum_{j=1}^{z} \left\langle r_{ij}^2 \right\rangle + \frac{q^4}{5!\, z^2} \sum_{i=1}^{z} \sum_{j=1}^{z} \left\langle r_{ij}^4 \right\rangle \ldots\ldots \qquad (12)$$

The second term in this series is essentially the square of the radius of gyration;

$$\overline{R}_g^2 = \frac{1}{2z^2} \sum_{i=1}^{z} \sum_{j=1}^{z} \left\langle r_{ij}^2 \right\rangle \tag{13}$$

Therefore, the form factor can always be written in a general form;

$$P_1(q) = 1 - \frac{q^2}{3} \overline{R}_g^2 + \dots \tag{14}$$

and thus, the initial slope of an $I(q)$ *versus* q^2 plot is equal to $\dfrac{\overline{R}_g^2}{3}$, (provided

$\dfrac{z\overline{l}^2 q^2}{6} < 1$ where $\overline{l}^2$ is the average square segment length) [2]. For a linear

polymer whose spatial distribution of segments follows Gaussian statistics

$$\overline{R}_g^2 = \frac{z\overline{l}^2}{6} \tag{15}$$

By contrast, for a cyclic polymer;

$$\overline{R}_g^2 = \frac{z\overline{l}^2}{12} \tag{16}$$

i.e. half the value obtained for an equivalent molecular weight linear polymer. These predictions have been largely verified by studies on poly(dimethylsiloxane), PDMS and poly(phenylmethylsiloxane) PPMS [3], [4], [5], [6].

11.1.2.3 Limiting Behaviour of the Form Factor

The complete form factor may also be used to extract information regarding the conformation of the cyclic polymer, and an informative comparison is that with an equivalently sized linear polymer.

The complete form factor for a Gaussian linear chain can be derived, starting from Eqn 11 by averaging over all orientations and distances. When z is large and $\dfrac{\bar{l}^2 q^2}{6} < 1$, one arrives at the familiar Debye equation;

$$P_1(q) = \frac{2}{\bar{R}^2 q^2}\left[\bar{R}^2 q^2 - 1 + \exp\left(-\bar{R}^2 q^2\right)\right] \tag{17}$$

(remembering that $\bar{R}^2 = \left(\dfrac{z\bar{l}^2}{6}\right)$).

A Zimm approach may be invoked by inverting Eqn. 8, setting $N = c N_A / M_w$, $z = M_w / m$ and substituting in Eqn. 10, $i.e.$;

$$\frac{Kc}{I(q)} = \frac{1}{M_w\, P_1(q)} + 2 A_2\, c \tag{18}$$

where M_w is the polymer molecular weight, c is the polymer concentration in g/cm^{-3}, m is the monomer molar mass, N_A is Avogadro's number, A_2 is the second virial coefficient and K contains the scattering cross-sections and other constants. Substituting in various limiting behaviours for $P_1(q)$ into Eqn. 18,

allows several key predictions to be tested. For instance, in the low-q region of the scattering data *i.e* $\overline{R_g}\, q << 1$;

$$\frac{Kc}{I(q)} = \frac{q^2\, \overline{R_g^2}}{3 M_w} + 2 A_2\, c + \frac{1}{M_w} \qquad (19)$$

whereas for the high-q region *i.e* $\overline{R_g}\, q \approx 1$;

$$\frac{Kc}{I(q)} = \frac{q^2\, \overline{R_g^2}}{2 M_w} + 2 A_2\, c \qquad (20)$$

Hence, the ratio of the final to initial slopes (Eqn. 20 divided by Eqn. 19) of a plot of $I(q)^{-1}$ *versus* q^2 for a linear polymer should be 3/2 at infinite dilution.

It has already been shown (Eqn. 15 and 16), that $\overline{R_g^2}$ for a cyclic polymer is half that of a linear polymer. So when $\overline{R_g}\, q << 1$ the initial slope of the $I(q)^{-1}$ *versus* q^2 plot would be half that for the linear polymer. However, when $\overline{R_g}\, q \approx 1$

$$\frac{Kc}{I(q)} = \frac{q^2\, \overline{R_g^2}}{2 M_w} + 2 A_2\, c - \frac{1}{M_w} \qquad (21)$$

and thus, the final slope of the equivalent $I(q)^{-1}$ *versus* q^2 plot for the cyclic polymer will be the same as the linear polymer. The final slope is governed by the local conformation of the polymer molecule and is dominated by bond angle and length constraints. For a sufficiently large polymer, these constraints

should be independent of whether the first and final segments are connected. Therefore, the ratio of the final to initial slopes of the $I(q)^{-1}$ *versus* q^2 plots should increase to 3 at infinite dilution.

Two large PDMS samples have been studied [7], a linear with $M_z = 20,880$ g/mol and a cyclic with $M_z = 20,210$ g/mol which show ratios close to these predictions, 1.2 for the linear (prediction = 1.5) and 2.6 for the cyclic (prediction = 3.0).

11.1.2.4 Analytical Approaches to Interpreting the Form Factor

The complete form factor for a cyclic polymer can also be compared to the linear one by means of a Kratky plot, $q^2 I(q)$ *versus* qR_g. As just shown, the cyclic and linear form factors have the same asymptotic behaviour at high q once the differences in R_g have been accounted for. However, due to the more compact conformation of the cyclic polymer, the number of pairs of segments at a distance R_g will be greater than for a linear polymer. Hence, around $qR_g = 1$, the intensity for a cyclic polymer is expected to be higher than for a linear and a maximum displayed in the Kratky plot. The equivalent plot for a linear polymer would merely attain a plateau value around this q value. These features are indeed present in the experimental data, figure 2. Furthermore, linear polymers could be adequately described by models using Gaussian statistics. By contrast, theoretical calculations based on Gaussian statistics [8],[9] for cyclic polymers with $z \leq 100$ are only in broad agreement with the experimental data - the predicted maximum intensity occurs at the correct qR_g value but its magnitude is poorly reproduced.
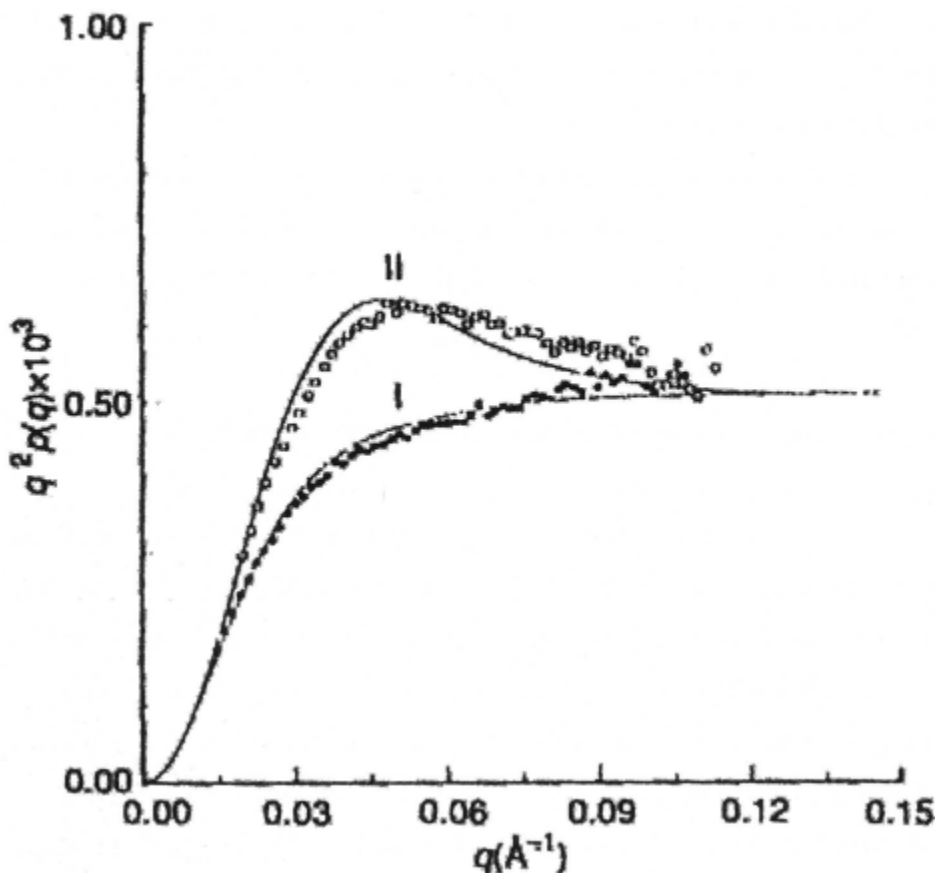
Figure 2; Kratky plot for linear (I) and cyclic (II) polystyrene samples in d_{12}-cyclohexane. The solid lines are calculated as In Section 11.1.2.4. Reprinted with permission from Hadziioannou *et al.* Macromolecules 20, 493 1987, Copyright (1987) American Chemical Society.

However, a Monte Carlo simulation [10] using a RIS model of the PDMS ring which does not invoke Gaussian statistics, better describes the experimental scattering - the location and magnitude of the maximum was accounted for, but the simulated data exhibit a limiting slope and shallow minimum that are not present in the experimental data, figure 3.

Indeed, for a small ring, a second maximum is predicted. These shortcomings, which are not yet fully understood, are thought to be due to the annular nature of the smaller rings.
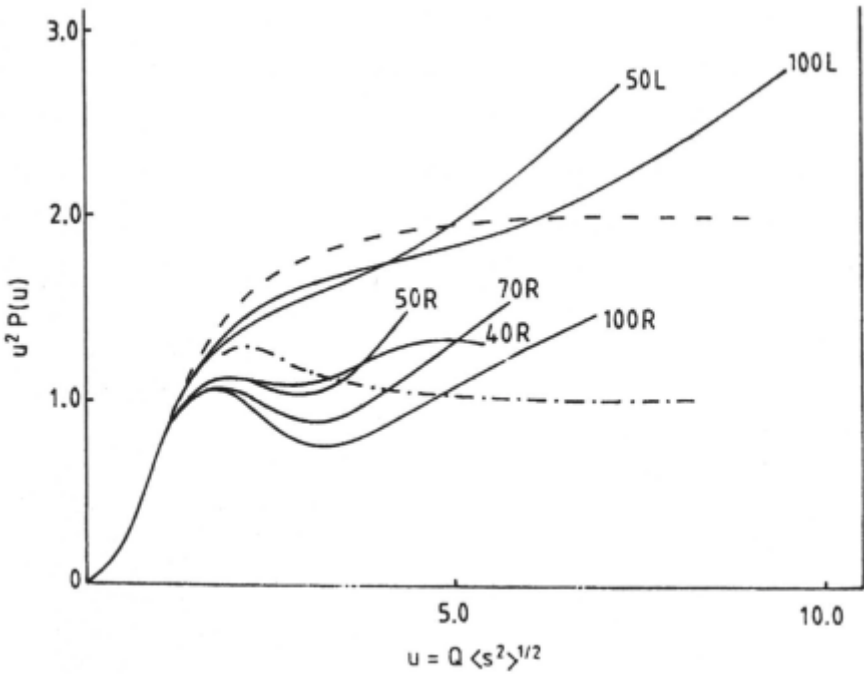
Figure 3; Theoretical Kratky plots, based on the RIS model of the PDMS chain, for linear (L) and cyclic (R) PDMS samples (solid lines). The number proceeding the R or L signifies the number of bonds. The broken lines correspond to Gaussian approximations to $P_1(q)$; dashed Is the linear predictions dash-dotted the cyclic. Reprinted with permission from *Cyclic Polymers Ed. 1,* Copyright (1991) Elsevier Science.

For very high molecular weights, the Monte Carlo simulations suggest that the only difference between the linear and cyclic architectures is a more spherical conformation for the cyclic with a higher average segment density [11].

11.1.3   Linear - Cyclic Polymer Blend Systems

The annular nature of small rings raises the possibility that a linear polymer could "thread" a cyclic, a suggestion supported by viscosity studies [12]. SANS plays a significant role in these sorts of studies due to the ability to render one polymer invisible *via* contrast matching *i.e.* the form factor of a cyclic polymer can be recorded in the presence or absence of a second polymer such that the second polymer contributed little or nothing to the measured scattering. Such a study [13] has been performed recently at ISIS on the LOQ instrument using poly(ethylene oxide) as the polymer dissolved in D_2O/H_2O mixtures.
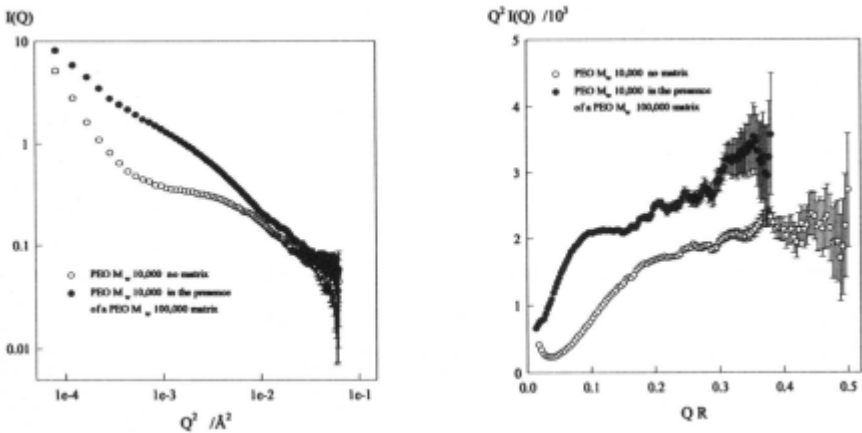
Figure 4; Guinier and Kratky representations of the scattering from aprotonated cyclic M_w = 10,000 PEO in the presence and the absence of a matrix of linear deuterated PEO, M_w = 100,000 under conditions of near contrast match for the linear polymer.

The raw data for the scattering of a protonated cyclic M_w = 10,000 PEO is shown in figure 4 in the Guinier and Kratky representations. The scattering has

been recorded in the presence and the absence of a matrix of linear deuterated PEO, $M_w = 100,000$, under conditions of near contrast match for the linear polymer. The Guinier representation shows quite clearly that the cyclic polymer in the absence of the linear matrix has a larger R_g (a more rapid decay of the scattering) but the Kratky plot does not show clearly the presence of the expected maximum. Analogous behaviour was observed for a smaller cyclic PEO ($M_w = 6,000$). It is clear that the cyclic polymer adopts a very different conformation in the presence of the linear matrix. However, in order to fully analyse the data, we need to introduce terms to account for the (very small) residual scattering from the polymer matrix and an interference term. Currently, this is underway.

11.2 NMR Studies of Linear and Cyclic Polymers

The dynamics of linear polymer molecules in solution and the melt have been studied extensively. Generally, due to its ease of interpretation, the diffusion coefficient has been principally considered.

11.2.1 Dilute and Semi-dilute Polymer Solutions

In solution, the *self*-diffusion coefficient is related to the inverse of the friction opposing the motion of the polymer. The simplest representation of this behaviour is;

$$D_s = \frac{kT}{f} \tag{22}$$

where k is the Boltzman constant, T is the absolute temperature and f is the friction term. For dilute or "moderately" semi-dilute polymer solutions, a power series often adequately represents the observed behaviour,

$$f = f_o \left(1 + k_f^{(1)} c + k_f^{(2)} c^2 + \ldots\right) \tag{23}$$

$k_f^{(1)}$ and $k_f^{(2)}$ are molecular weight dependent coefficients which define the concentration behaviour of the self-diffusion coefficient. f_o is the friction at infinite dilution;

$$f_o = 6\pi\eta_o R_h \tag{24}$$

where η_o is the solvent viscosity and R_h is the time-averaged hydrodynamic radius of the polymer. Above some critical concentration denoted c*, adjacent polymer coils overlap and the dynamics of the polymer solution becomes far more complex. In particular, the friction term becomes far more sensitive to concentration *i.e.* the molecular weight dependence of the $k_f^{(i)}$ terms increase. For more concentrated polymer solutions, "blob" theories [14] propose a steeper concentration dependence of the self-diffusion coefficient;

$$D_s \propto c^{\left(\frac{v-2}{3v-1}\right)} \tag{25}$$

where v is the Flory index. For theta solvents $(v = 0.5)$ $D_s \propto c^{-3.0}$ whilst for good solvents $(v = 0.6)$; $D_s \propto c^{-1.75}$. This behaviour has been verified for a range of linear polymer systems [15].

The self-diffusion coefficients of two linear and one cyclic poly(ethylene oxide) PEO samples dissolved in D_2O [16] have been measured, figure 5. The behaviours of the linear polymer with molecular weight 6,000 and the cyclic polymer with molecular weight 10,000 over the entire concentration range studied were rather similar, and considerably different to the linear molecular
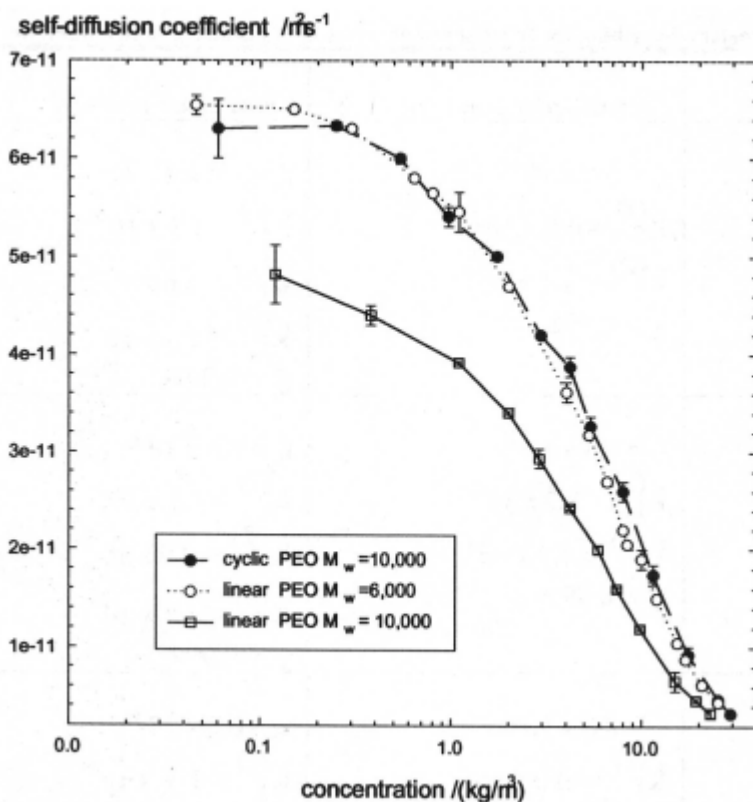
Figure 5; Self-diffusion coefficients of two linear (M_w 6,000 and 10,000) and one cyclic (M_w 10,000) poly(ethylene oxide) PEO samples dissolved In D_2O as a function of concentration. Reprinted with permission from [16], Copyright [1995] American Chemical Society.

weight 10,000 polymer. At infinite dilution, the linear 6,000 and cyclic 10,000 samples have a similar value of the self-diffusion coefficient, and hence, hydrodynamic radius. The linear 10,000 data follow the same general form as the cyclic 10,000 and linear 6,000, but its self-diffusion coefficient is, at any given concentration, always smaller than both the linear 6,000 and cyclic 10,000, consistent with a greater size. At higher concentrations, the self-diffusion

Table 1; **Parameters describing the friction power series fits to the data shown in Figure 5**

	Second order power fit	*Third order power fit*
linear 6,000	$f_o = 6.9 \times 10^{-11}$ $k_f^{(1)} = 4.5 \times 10^{-3}$ $k_f^{(2)} = 1.4 \times 10^{-4}$ $\chi^2 = 0.998$	$f_o = 6.4 \times 10^{-11}$ $k_f^{(1)} = 1.3 \times 10^{-2}$ $k_f^{(2)} = 6.6 \times 10^{-5}$ $k_f^{(3)} = 2.3 \times 10^{-7}$ $\chi^2 = 0.999$
linear 10,000	$f_o = 9.3 \times 10^{-11}$ $k_f^{(1)} = 8.5 \times 10^{-3}$ $k_f^{(2)} = 1.6 \times 10^{-4}$ $\chi^2 = 0.999$	$f_o = 8.6 \times 10^{-11}$ $k_f^{(1)} = 1.5 \times 10^{-2}$ $k_f^{(2)} = 9.9 \times 10^{-5}$ $k_f^{(3)} = 1.9 \times 10^{-7}$ $\chi^2 = 0.999$
cyclic 10,000	$f_o = 8.0 \times 10^{-11}$ $k_f^{(1)} = -4.0 \times 10^{-3}$ $k_f^{(2)} = 1.5 \times 10^{-4}$ $\chi^2 = n/a$	$f_o = 6.3 \times 10^{-11}$ $k_f^{(1)} = 1.6 \times 10^{-2}$ $k_f^{(2)} = -8.4 \times 10^{-6}$ $k_f^{(3)} = 4.3 \times 10^{-7}$ $\chi^2 = 0.999$

coefficient behaviour for all three polymers approach the asymptotic theoretical prediction, $D_s \propto c^{-3.0}$, for semi-dilute solutions under theta conditions. There are subtle differences in the friction behaviour, notably that whereas the linear samples could be adequately described by a second order power series, the cyclic polymer data set could not. Comparing the $k_f^{(1)}$ parameters for the various samples highlights these subtle differences. $k_f^{(1)}$ for cyclic 10,000 is greater than for the linear 6,000 indicating a greater sensitivity of the cyclic species to concentration. Interestingly, the linear 6,000 and cyclic 6,000 samples have comparable $k_f^{(1)}$ parameters but this parameter is largely determined over the lower concentration region and it may be concluded that this parameter is predominantly influenced by the number of segment - solvent interactions. Hence, the magnitude of the friction and thus, self-diffusion coefficient is dominated by the f_0 parameter. More work is required to properly understand these effects, especially using larger cyclic molecules.

The time-averaged hydrodynamic radii for the various polymers calculated from the f_0 parameter are $R_h = 5.2 \, (\pm \, 0.2)$ nm for the cyclic 10,000, $R_h = 5.6 \, (\pm \, 0.2)$ nm for the linear 6,000 sample and the larger value of $7.1 \, (\pm \, 0.2)$ nm for the linear 10,000. The theoretical predictions as discussed in the earlier part of this Chapter, predict $\dfrac{\langle R_{g,l}^2 \rangle}{\langle R_{g,c}^2 \rangle} = 2.0$. $\langle R_s^2 \rangle$ is the mean square radius of gyration and the subscripts 1 and c refer to linear and cyclic species respectively of equivalent molecular weight. Assuming that the radius of gyration is related to the hydrodynamic radius by a molecular weight independent term equivalent for both architectures, the PEO results are in good

agreement with this prediction: $\dfrac{\left\langle R^2_{h,1} \right\rangle}{\left\langle R^2_{h,c} \right\rangle} \simeq 1.9 \ (\pm 0.1)$. These diffusion data

are therefore, in good agreement with the SANS data, the theoretical predictions and other quasi-elastic light scattering (QELS) [17], quasi-elastic neutron scattering (QENS) [18] and boundary spreading diffusion studies on PDMS solutions [19].

11.2.2 Polymer Melts

It is of great importance to be aware of the many differences in the physical properties of cyclic and linear molecules when interpreting their dynamics; for example, linear PDMS polymers of the same molar mass have slightly lower densities than the cyclic polymers[20] - this effect is most pronounced for oligomers and can be explained by the more efficient packing of the disc-like structures that the cyclics can adopt in their all *trans* conformation. These variations affect the dynamics of the system.

11.2.2.1 Diffusion

The theory of the dynamics of highly concentrated or melt linear polymer systems has received considerable attention in recent years, the theories of Rouse [21] and Edwards [22] in particular being most widely referred to. For molecular weights below the so-called critical molecular weight for entanglement $M_w < M_{crit}$, the diffusion may be represented by the simple Rouse model. In this model, it is assumed that segments move isotropically and therefore, the self-diffusion coefficient scales inversely with molecular weight.

The Edwards theory for high molecular weight linear chains above the critical molecular weight for entanglement, models motions by means of macroscopic deformations travelling along a curvilinear tube; this tube is formed by the constraints of the neighbouring molecules. This motion is referred to as "reptation" and starts at a chain end. Cyclic polymers, on this basis, cannot formally reptate since they have no "free chain end". For reptative behaviour to be observed, the motion along the backbone must be highly correlated and is characterised by an inverse square law dependence of the self-diffusion coefficient on chain length.

Experimentally, these two types of diffusion behaviour have been confirmed for a series of linear polymers - entangled systems such as polyethylene (PE), polystyrene (PS) and poly(ethylene oxide) (PEO) all show the reptation exponent above M_{crit}, whilst below M_{crit}, PS, PE, PEO, polypropylene oxide) PPO and PDMS all show the Rouse exponent (see discusson in ref. 26). Corrections must often be applied to this sort of data before unequivocal observation of these exponents are seen. The need for-, and the magnitude of, any correction is related to chain flexibility.

Diffusion results [23] for both cyclic and linear PDMS are shown in figure 6. The lower molecular weight linear species follow the Rouse model. The diffusion of the small cyclics is enhanced compared to the linears due to the increased rigidity of the ring and the concomitant reduction in size.

In the diffusion data for the rings there is a marked change in slope at $M_w = 1,700$ and a "plateau" region extending to $M_w \approx 5,000.$ One possible interpretation is that some cyclic molecules can "thread" through others. These associations will be rather weak. For $M_w > 1,000,$ D_{linear} is always greater than D_{cyclic}. The absolute values of the molecular weight exponents for both linear and cyclic for $M_{crit} > M_w > 5,000$ are in excellent agreement with the Rouse prediction. Above M_{crit}, there is no apparent increase in the molecular weight

exponent for the cyclics or the linears The similarity of the diffusion data for the two forms can be understood in terms of the flexible nature of the backbone and, therefore, the inherently small free volume. Fleischer [24], however, focusing on
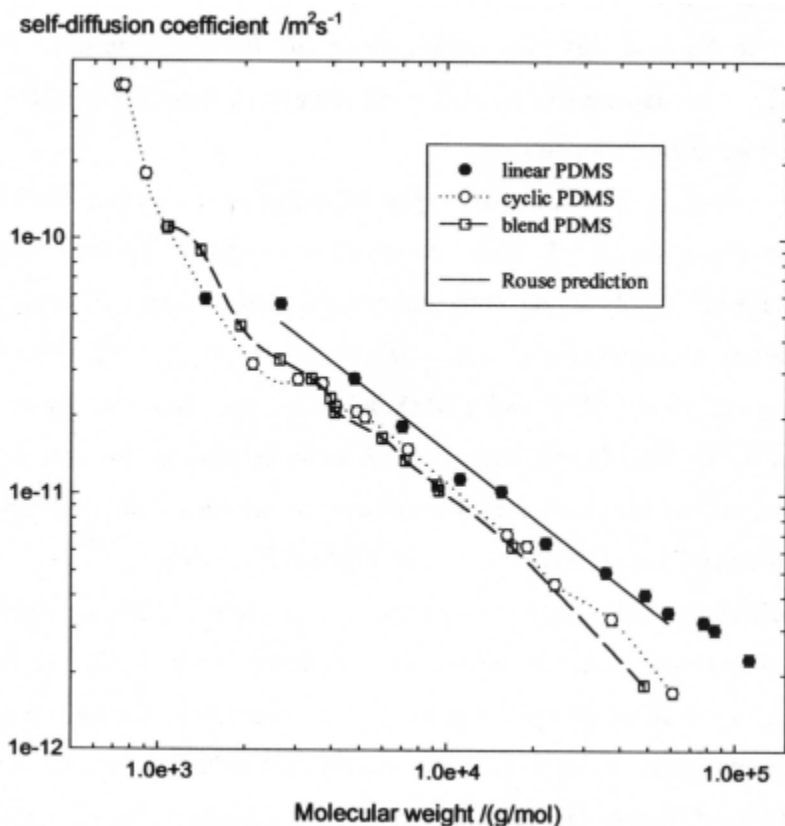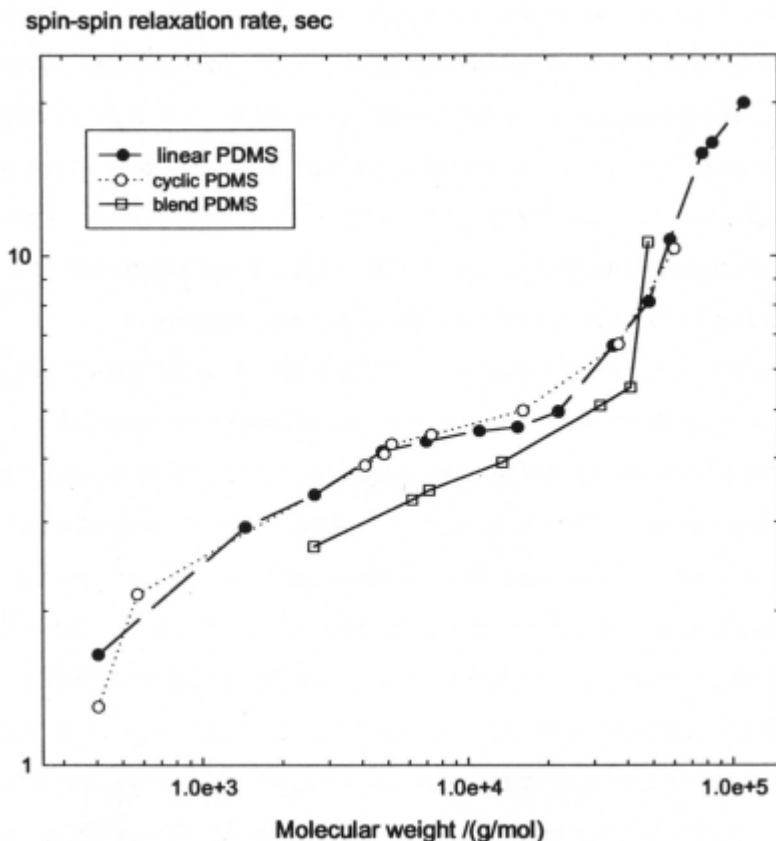

Figure 6; Self-diffusion coefficient versus molecular weight for three different PDMS series; linear, cyclic and equi-mass blends of linear and cyclic samples. Reprinted with permission from [26], Copyright [1996] American Chemical Society, and Polymer 37, Cosgrove *et al.* 1535, Copyright (1996) with permission from Elsevier Science.

linear PDMS at higher temperatures did observe the reptation exponent but only above $5M_{crit}$ - he proposed that the entanglement tubes are incompletely formed below a molecular weight equivalent to $5M_{crit}$.

Three possible molecular configurations for linear and cyclic blends exist [25] each with rather different diffusion possibilities; (a) the cyclic polymer is threaded by linear chains and has a rather extended conformation - the cyclic polymer may only rotate around the linear chains that thread it and cannot translate without their removal (b) the cyclic polymer is unthreaded, and has large loops extending into the surrounding media, and (c) the cyclic polymer is again unthreaded but has no loops and adopts a rather compact configuration. For these last two cases, the diffusion can be described as a "wriggling" process between the linear chains, analogous to reptation. In particular, case (b) may be compared to the diffusion of a star polymer and case (c) contrasted with the diffusion of a much smaller linear polymer.

The self-diffusion coefficients of the blend PDMS samples are also plotted in figure 6 as a function of the reciprocal number-average molecular weight [26]. The blend data crosses the cyclic data at a molecular weight of approx. 3,000 and for molecular weights below this value, the self-diffusion coefficient of the blend lies between the linear and cyclic forms but closer to the cyclic - the slower component. Above this molecular weight, the diffusion of the blend data is always slower than both the cyclic and linear forms.

The ring threading mechanism is proposed to occur for ring sizes greater than $M_w = 2,500$. This corresponds to the plateau in the self-diffusion and viscosity behaviour of the single component cyclic form. As may be seen in figure 6, this also corresponds to the (average) molecular weight where the blend diffusion becomes slower than either of the two single component forms. These observations lend support to the ring threading mechanism. If a cyclic chain has been threaded by only one linear molecule, the diffusion of the linear

chain can only occur if the chain end passes out through the cyclic polymer. This does not contradict the observation of Rouse motion since any of the segments can initiate this motion and can thus explore the local environment in an isotropic manner. The centre-of-mass motion will, of course, be somewhat retarded, in agreement with the experimental observations.

11.2.3 NMR Relaxation

Spin-spin or transverse relaxation, compared to diffusion, operates over a much shorter distance scale and therefore is sensitive to the segmental motions of the polymer. A theory, enveloping a general hierarchy of polymer chain dynamics, has been proposed to quantify Rouse behaviour [27]. The theory is based on the scale-invariant model of dipolar interactions responsible for transverse relaxation and for non-entangled chains predicts exponential relaxation functions of the form;

$$G(t) = \exp(-t/T_2) \tag{27}$$

with the relaxation rate, $\dfrac{1}{T_2} = \alpha \ln M_w + \beta$. The parameters α and β are related to the size of the Rouse unit such that β/α is proportional to the logarithm of the number of monomer units in a Rouse sub-unit. The behaviour above the critical molecular weight is more complex; non-exponential relaxation curves are proposed with much greater relaxation rates. The non-exponentiality, which increases with molecular weight, is attributed to a distribution of mobilities related to the proximity of entanglement points and the greater mobility associated with chain ends.

spin-spin relaxation rate, sec

Figure 7; Spin-spin relaxation rate versus molecular weight for three different PDMS series; linear, cyclic and equi-mass blends of linear and cyclic samples. Reprinted with permission from [26], Copyright (1996) American Chemical Society, and Polymer 37. Cosgrove *et al.* 1535, Copyright (1996) with permission from Elsevier Science.

Spin-spin relaxation times for PDMS samples [26] as a function of molecular weight are shown in figure 7. A sharp break indicative of the critical molecular weight at $M_w = 36,500$ is observed which agrees very well with the value obtained from the viscosity data. For non-entangled polyethylene melts,

the Brereton model yield values, $\alpha = 0.89s^{-1}$ and $\beta = -4.94s^{-1}$. The linear and cyclic PDMS data give $\alpha = 0.90s^{-1}$ and $\beta = -3.5s^{-1}$. The predicted non-single exponential relaxation curves were indeed observed for the higher molecular weight samples. Unlike the viscosity data and diffusion data, there is no obvious difference between the linear and cyclic forms indicating a comparable degree of segmental motion and thereby highlighting the subtle differences in the physical processes that the two measurements are sensitive to.

Stepto [28], re-considering the Graessley-Edwards theory [29], has proposed a modification to account for the common features of the two architectures. With the exception of the small rings, the principal conclusion is that since segmental mobility is insensitive to long range chain connectivity (as shown by a rotational-isomeric-state (RIS) model of the two species), the critical molecular weight for entanglement is more sensitive to the flexibility of the chain rather than the mobility of the whole chain: the presence of entanglements depends only on the localised segment density (which is independent of chain connectivity). This is not applicable to the case of small rings where there is a tendency to form disc-like molecules, resulting in the higher diffusion coefficient and lower viscosity.

The spin-spin relaxation rates, T_2^{-1}, for the pure linear and cyclic melts as a function of molecular weight are displayed in Figure 7 according to the model of Brereton *et al.* The blend data show many similarities with the pure component data. The higher molecular weight samples, above the critical molecular weight, show (a) a strong dependence of the relaxation rate on molecular weight which is equivalent not only for the linear and cyclic forms, but also for the blend data, (b) the actual values of the relaxation rates for the blend and single component samples at an equivalent weight-average molecular weight are also comparable and (c) the onset of this steeper dependence,

characteristic of the critical molecular weight for entanglement in the pure systems, is the same for the blend and single component data.

The spin-spin relaxation data for the melt blends are plotted as a function of weight-average molecular weight, M_w. Below the critical molecular weight, the similarity between the blends and pure components is limited only to the molecular weight dependence - the actual relaxation rates for the blend samples are smaller than for the pure components.

A simple inspection of the single component and blend data below the critical molecular weight for entanglement shows that for the blend data, β must be smaller than in the single component case. α, given by the slope of the molecular weight dependence, is the same for both cases. From the ratio of the β values for the blend data, it is possible to conclude that the effective sub-unit size in the blend is five times larger. A similar conclusion was drawn from the preliminary analysis of the PEO blend SANS data (Section 11.1.3)

The relaxation data for the blend samples strongly suggest some form of entanglement unrelated to conventional entanglement is present over the entire molecular weight range studied. The smallest ring studied by relaxation was $M_w = 2,700$ approximately the minimum size required for ring threading. The diffusion and viscosity data also support the occurrence of an entanglement, unrelated to the conventional type, which starts at the critical ring size.

Acknowledgements

References

1   J.S. Higgins and H.C. **Benoît** *Polymers and Neutron Scattering* Oxford University Press, 1994

2   A. Guinier *Theorie et technique de la radiocristallographie* Dunod, Paris 1956

3   J.S. Higgins, K. Dodgson and J.A. Semlyen   Polymer **20,** 553, 1979

4   S.J. Clarson, J.A. Semlyen and K. Dodgson   Polymer **28,** 189, 1987

5   S.J. Clarson Ph.D. Thesis University of York 1985

6   S. J. Clarson, J.A. Semlyen and K. Dodgson Polymer **32,** 2823, 1991

7   K. Dodgson and J.S. Higgins *Cyclic Polymers* Ed J.A. Semlyen

8   E.F. Casassa J. Polym. Sci. A., **3,** 605, 1965

9   W. Burchard and M. Schmidt Polymer **21,** 745, 1980

10   C.J.C. Edwards, R.W. Richards, R.F.T. Stepto, K. Dodgson, J.S. Higgins and J.A.Semlyen Polymer   **25,** 365, 1984

11   C.J.C. Edwards, D. Rigby, R.F.T. Stepto and J.A. Semlyen Polymer **24,** 395, 1983

12   S.J. Joyce, R.E. Hubbard and J.A.Semlyen European Polymer Journal **29,** 305, 1993

13   P.C. Griffiths *et al* (Unpublished)

14   P.G. de Gennes Macromolecules **9,** 587, 1976

15   P.C. Griffiths and T. Cosgrove   Polymer **35,** 509, 1994.

16   P.C. Griffiths, P. Stilbs, G.E. Yu, and C. Booth J. Phys. Chem. **99,** 16752, 1995

17   C.J.C. Edwards, S. Bantle, W. Burchard, R.F.T. Stepto and A.J. Semylen Polymer **23,** 873, 1982

18   J.S. Higgins, K. Ma, L.K. Nicholson, J.B. Hayter, K Dodgson, and A.J. Semylen Polymer **24,** 793, 1983

19   C.J.C. Edwards, R.F.T. Stepto and A.J. Semylen Polymer **23,** 865, 1982

20   D.J. Orrah, J.A. Semlyen and S.B. Ross-Murphy   Polymer **29,** 1452, 1988

21   P.E. Rouse J. Chem. Phys. **21,** 1272, 1953

22   S.F. Edwards and M. Doi *The Theory of Polymer Dynamics* Oxford University Press 1986

23   T. Cosgrove, P.C. Griffiths, J. Hollingshurst, R.D.C. Richards and J.A. Semlyen Macromolecules **25,** 6761,1992

24   M. Appel and G. Fleischer Macromolecules **26,** 5520, 1993

25   J. Klein   Macromolecules **19,** 105, 1995

26   T. Cosgrove, M.J. Turner, P.C. Griffiths, J. Hollingshurst, M.J. Shenton and J.A. Semlyen Polymer   **37,** 1535, 1996

27 M.G. Brereton, I.M. Ward, N. Boden, P. Wright Macromolecules **24,** 2068, 1991

28 R.F.T. Stepto European Polymer Journal **29,** 415, 1993

29 S.F. Edwards and W.W. Graessley Polymer **22,** 1329, 1980

Harry W. Gibson and Eric J. Mahan

Department of Chemistry

Virginia Polytechnic Institute & State University, USA

12.1 Introduction

Since the first experimental evidence appeared over 30 years ago, the field of rotaxanes has grown considerably. The name rotaxane is derived from the Latin words for 'wheel' and 'axle', [1] and describes a compound that consists of a linear and cyclic species bound together in a threaded structure by non-covalent forces. A low molar mass rotaxane is depicted by structure **1**. To prevent diffusional loss of the cyclic species, bulky groups, often called 'blocking groups', 'knots', or 'stoppers', are attached to the ends of the linear component. The resulting structure **2** is the typical representation for a rotaxane. Although structure **1** also meets the definition for a rotaxane, it is now commonly referred to as a 'pseudorotaxane' because of its potential to disassemble to the individual cyclic and linear components. The composition of the rotaxane is indicated with a number in a bracket, a method of nomenclature reported by Stoddart some time ago. [2] Thus, **2 (x=1)** is a [2]rotaxane; the "2" designates the total number of species involved. So, **2 (x=2)** is a [3]rotaxane, **2 (x=3)** is a [4]rotaxane, etc. This nomenclature, while convenient in simplicity, is ambiguous because a [3]rotaxane can also consist of two linear components in a single cyclic species, as discussed below.
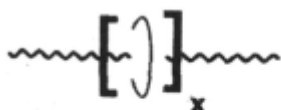
1
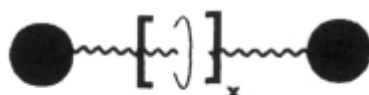
2

Although discussion of rotaxanes may have taken place as early as 1900 [3], the concept did not appear in publication until 1961 when Frisch and Wasserman [4] first proposed the existence of rotaxanes and interlocked rings known as catenanes. It was not until 1967, however, that rotaxanes became a reality with the introduction of experimental evidence of their existence by Harrison and Harrison [5] and Schill and Zöllenkopf. [1] Although these discoveries were nearly simultaneous, the routes used to obtain the rotaxanes were radically different. Since these initial breakthroughs, rotaxanes have evolved from an architectural curiosity to become an integral part of the fields of molecular recognition and self-assembly. The last 30 years, therefore, has seen the development of many new rotaxane systems as well as new methods for their synthesis. As these various rotaxanes have become more accessible and more easily synthesized, the focus has begun to shift towards the development of applications for these unique materials.

The growth of this field has resulted in a number of reviews on the progress made in rotaxane synthesis. As a pioneer, Schill [6] described the early status of the field and summarized further progress in a later review [7]. During the 1980's, Walba [8] and Lipatov [9] included rotaxanes and their macromolecular analogs in their respective reviews. More recently, in 1994 Gibson *et al.* [10] discussed low and high molar mass rotaxanes and included a detailed historical overview in a later review. [11] A number of other reviews have also appeared in the last few years as a result of the continued growth of the field. [12a-e] In addition to the general reviews of the field by Stoddart, [12a-c], the specific area of cyclodextrin-based rotaxanes has recently been reviewed by several authors. [12d] Finally, the topic of photo- and redox-active rotaxanes was recently covered by Benniston. [12e]

Considering these recent detailed reviews, the goal of this chapter is to focus largely on recent developments in rotaxane synthesis and applications. For a more historical perspective of the field, readers are referred to the latter

review by Gibson, [11] that covers developments in rotaxanes through August 1995. This review will therefore continue from that date and consider progress in the field through the end of 1998 for both low and high molar mass rotaxanes. Although an attempt will be made to provide a comprehensive list of new systems synthesized in this time frame, the entire scope of synthetic details will not be provided due to space limitations. For additional information, the reader is referred to these earlier reviews and the specific literature references noted in the tables below.

   The chapter is divided into two major sections. The first section will cover the synthetic methods used in rotaxane formation, while the second will present the properties and applications of these systems. In each section, the discussion will be further divided into low molar mass and polymeric systems, using an arbitrary value of approximately 4 kg $\textbf{mol}^{-1}$ for the linear component as a means of distinguishing between the two areas.

12.2 Rotaxane Synthesis
12.2.1 Structural Requirements of Components

   In the years since the report of the first rotaxane, the structural requirements for both the cyclic and linear components have been investigated and documented. [13-16] The simplest possible linear component is a polymethylene segment, possessing a cross-sectional diameter of approximately 4.5 Å. If a cyclic species is to be threaded by this component, it must contain at least 22 carbon, oxygen, or nitrogen atoms in the ring to provide a cavity of sufficient diameter. Clearly, other linear components are also used in rotaxane synthesis, and as the diameter of these species increases larger rings must also be used to accommodate this size increase. In addition, the size of the stopper or blocking group needed to prevent diffusion of the cyclic species from the pseudorotaxane structure must also be considered. Unlike the linear component, the stopper must have a cross-sectional area larger than the cavity

of the cyclic molecule that it is intended to block. For rings with 28 atoms or less, the trityl group is a sufficient stopper, while the tris(tert-butylphenyl)methyl unit will prevent loss of rings containing up to 42 atoms. [11] Finally, the bis(cyclohexyl)methyl group can act as a stopper of intermediate size, blocking rings of 27 atoms or smaller. [11]

12.2.2 Synthetic Methods for Low Molar Mass Rotaxanes

The three basic approaches generally applied to the synthesis of low molar mass rotaxanes are directed synthesis, threading of preformed cyclic and linear species, and the formation of the cyclic species in the presence of the linear component, otherwise known as 'clipping'.

12.2.2.1 The 'Directed' or 'Chemical Conversion' Approach

This method was introduced by Schill and coworkers [1] in their original rotaxane synthesis and involves designing a central platform covalently bonded to all of the components, followed by selective cleavage of bonds to produce the desired structure. Although the method is elegant and of great historical significance, this method has not been widely used in recent years and no examples have been reported within the time frame of this review. The directed synthesis is hindered by the large number of synthetic steps needed to obtain the product and the resulting low overall yields. Further details of this method can be found in an earlier review [11] and the original literature [1].

12.2.2.2 Statistical Threadings

Like the directed approach, this is also one of the original methods for rotaxane synthesis, in this case employed by Harrison and Harrison [5]. In this approach, the enthalpic interactions between the cyclic and linear components are negligible and formation of the rotaxane is driven primarily by entropic effects. As a result, equilibrium constants for the formation of rotaxanes from
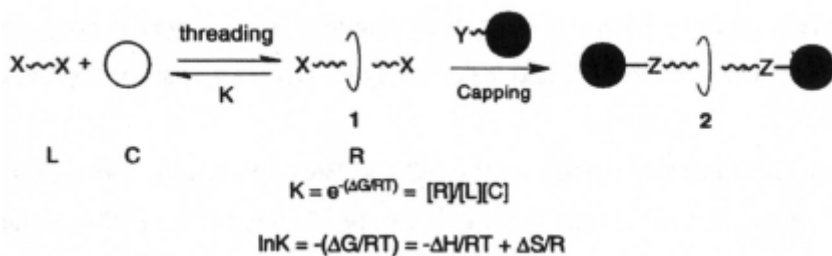
Scheme 1. Threading approach to form pseudorotaxane followed by end-capping to produce rotaxane.

the individual components are low, but the application of leChatelier's principle (neat systems or an excess of one component) or the use of repeated threadings using a polymeric support [5] can be used to effect rotaxane formation.

In addition to the employment of sequential threading and blocking steps by statistical methods, the equilibrium between an end-blocked linear component and a rotaxane by reversible detachment of the stoppers in the presence of a cyclic species can also be used as outlined in Scheme 2a.
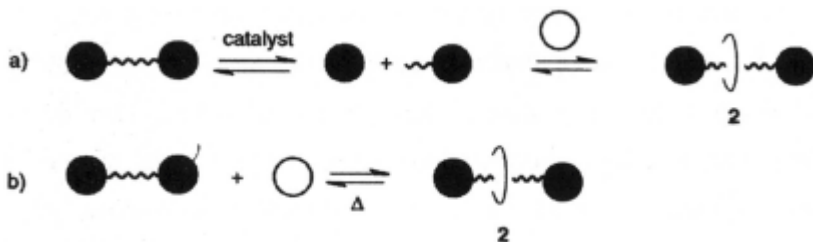
Scheme 2. Rotaxane formation from 'stoppered' linear species: (a) by reversible detachment of the stopper and (b) 'slippage' of cyclic species over the stopper

Like the directed approach, the use of statistical threading methods has rarely been employed in the synthesis of low molar mass rotaxanes in recent years. In the slippage method thermal motions are used to "slip" the cyclic species over the stoppers, while the lack of thermal energy upon cooling prevents the loss of the cyclic species if the stopper is of sufficient size. While the slippage method

(Scheme 2, pathway b) is still used, this technique is employed in conjunction with other synthetic methods and is not solely based on a statistical approach.

12.2.2.3 Enthalpically Driven or Host-Guest-Based Rotaxane Syntheses

Improvement of rotaxane yields can be obtained if the enthalpic factor of the equilibrium shown in Scheme 1 is considered. If an enthalpic driving force, i.e., a negative **ΔH,** is utilized, the equilibrium is shifted towards rotaxane formation and yields can be increased substantially from those obtained by statistical methods. The efforts to provide such driving forces have drawn on concepts from the field of host-guest chemistry, resulting in the close association between the two fields that is seen today. A variety of intermolecular attractive forces have been exploited to produce rotaxanes, and these will be discussed below.

12.2.2.3.a Hydrogen Bonding

The interaction of crown ethers with various linear components through hydrogen bonding has been studied extensively in recent years. Although the original workers did not realize it, this phenomenon was observed for the threading of crown ethers by oligo(ethylene glycol)s [17], when rotaxane yields greater than those expected for statistical threading were observed. The hydroxyl end groups of the glycol can be 'captured' through hydrogen bonding interactions with the crown ether, increasing the likelihood of the formation of a threaded structure when the hydroxyl group is coupled to a bulky "stopper" molecule. As has been noted previously [11], this technique was used to prepare a number of rotaxanes and polyrotaxane systems based on polyester and polyurethane backbones.

More recently, the ability of ammonium ions to hydrogen bond with a variety of crown ethers has been employed for rotaxane formation by both

Kolchinski *et al.* [18] and Stoddart and co-workers. [19] Unlike the glycol systems, the ammonium ion guest site is located at the center of the linear species, rather than at the chain end. This directly promotes the formation of the rotaxane structure, while the chain ends are removed from the site of threading and are thus accessible to further functionalization.

The equilibrium constants for pseudorotaxane complex formation between crown ethers and ammonium ions was found to be quite high for these systems, [19] making them quite efficient for the formation of rotaxanes. Since this initial discovery, the ammonium ion motif has been developed extensively from simple systems to those of increasing complexity. Tables 1 and 2 summarize the various systems that have been employed, including yields or association constants where applicable.

Table 1. Low Molar Mass Pseudorotaxanes From Ammonium Ion Type Linear Systems with Hexafluorophosphate Counterions Formed by Threading

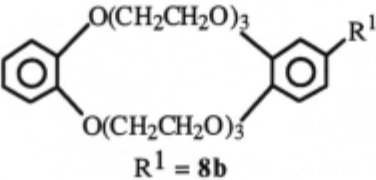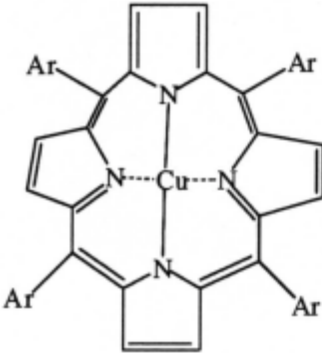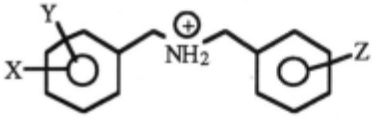| Linear Component (L)	Cyclic Component (C)	Stoichiometry L:C	Yield (%) or K (L mol^{-1})	Ref.
	3	1:1	$\approx 10^4$ a $\approx 50\text{-}70^b$	20,22
	$\left[\text{ArO}(\text{CH}_2\text{CH}_2\text{O})_3\right]_2$ Ar = $m\text{-}C_6H_4$	1:1	g	21
$\overset{\oplus}{\text{C}_6\text{H}_5\text{CH}_2\text{NH}_2\text{CH}_2\text{C}_6\text{H}_5}$	3	1:1	0^c 360^d $420^{b,e}$ 1700^f $27{,}000^a$	20,22 20,22 20,22,34 20,22 20,22
"	4	1:1	0^c 310^d 360^b $22{,}000^a$	20,22
"	5	2:1	-	20,22

Table 1 Continued. Low Molar Mass Pseudorotaxanes From Ammonium Ion Type Linear Systems with Hexafluorophosphate Counterions Formed by Threading
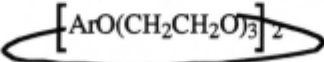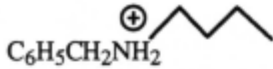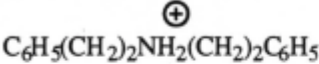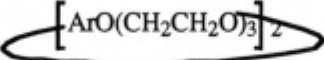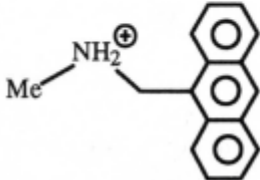
Linear Component (L)	Cyclic Component (C)	Stoichiometry L:C	Yield (%) or K (L mol^{-1})	Ref.
"	**6**	2:1	$5\pm2(M^{-2})^b$	21
"	$\left[ArO(CH_2CH_2O)_3\right]_2$ Ar = m-C$_6$H$_4$	1:1	g	21
C$_6$H$_5$CH$_2$NH$_2^{\oplus}$ ∿	**3**	1:1	-	20,22
C$_6$H$_5$(CH$_2$)$_2$NH$_2^{\oplus}$(CH$_2$)$_2$C$_6$H$_5$	**6**	2:1	-	21
"	$\left[ArO(CH_2CH_2O)_3\right]_2$ Ar = m-C$_6$H$_4$	1:1	g	21
Me—NH$_2^{\oplus}$—CH$_2$—(anthracene)	**3**	1:1	-	37

Table 1 Continued. Low Molar Mass Pseudorotaxanes From Ammonium Ion Type Linear Systems with Hexafluorophosphate Counterions Formed by Threading
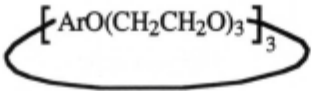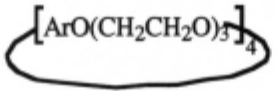
Linear Component (L)	Cyclic Component (C)	Stoichiometry L:C	Yield (%) or K (L mol^{-1})	Ref.
$C_6H_5CH_2NH_2CH_2C_6H_5$ (⊕)	$\left[ArO(CH_2CH_2O)_3\right]_3$ Ar = p-C_6H_4	3:1	-	24,35
"	$\left[ArO(CH_2CH_2O)_3\right]_4$ Ar = p-C_6H_4	4:1	-	24,35

$C_6H_5\left[CH_2-\overset{\oplus}{NH_2}CH_2-p-C_6H_4\right]_x H$

x = 2	3	1:2	-	20,22
x = 2	4	1:2	-	20,22
x = 2	5	1:2 [h]	-	20,22
		2:2 [I]		
x = 3	3	1:3	-	24
x = 4	3	1:4	-	24

Table 1 Continued. Low Molar Mass Pseudorotaxanes From Ammonium Ion Type Linear Systems with Hexafluorophosphate Counterions Formed by Threading

Linear Component (L)	Cyclic Component (C)	Stoichiometry L:C	Yield (%) or K (L mol^{-1})	Ref.
$C_6H_5\left[CH_2-\overset{\oplus}{N}H_2CH_2-p-C_6H_4\right]_x H$				
7	$R^1 = 8b$	1:3	93%	27
7	5	2:3	-	29

Table 1 Continued. Low Molar Mass Pseudorotaxanes From Ammonium Ion Type Linear Systems with Hexafluorophosphate
Counterions Formed by Threading
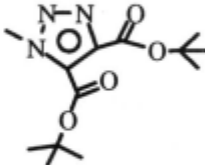
Linear Component (L)	Cyclic Component (C)	Stoichiometry L:C	Yield (%) or K (L mol^{-1})	Ref.
Ar = p-C$_6$H$_4$-CH$_2$NH$_2$$^+CH_2$Ph	5	2:4	-	31
9	-	1:1	j	32

Table 1 Continued. Low Molar Mass Pseudorotaxanes From Ammonium Ion Type Linear Systems with Hexafluorophosphate Counterions Formed by Threading

Linear Component (L)	Cyclic Component (C)	Stoichiometry L:C	Yield (%) or K (L mol^{-1})	Ref.
X = p-COOH, Y = Z = H	3 5	1:1 2:1	610^f -	34 34
X = m-COOH, Y = Z = H	3 5	1:1 2:1	480^f -	34 34
X = Z = p-COOH, Y = H	3	1:1	950^f	34
X = Z = m-COOH, Y = H	3	1:1	880^f	34
X = Y = m-COOH, Z = H	3 5	1:1 2:1	1500^f -	34 34

[a] CDCl$_3$ at 25°C. [b] MeCN at 25°C. [c] DMSO at 25°C. [d] CH$_3$COCH$_3$ at 25°C. [e] MeCN at 20°C. [f] 1:1 MeCN/CHCl$_3$ at 25°C.

[g] Determined in gas phase by HRFABMS. [h] Determined in solution and gas phase by ^{1}H-NMR and mass spectrometry respectively.

[I] Determined in solid phase from crystal structure. [j] Cyclic species determined in gas phase by LSI-MS and in solid phase by crystal structure.

Table 2. Low Molar Mass Rotaxanes From Ammonium Ion Type Linear Systems with Hexafluorophosphate Counterions (Unless noted)
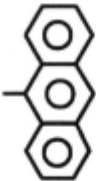
Linear Component	Cyclic Component	"Stopper" (Z)	Method	Stoichiometry L:C	Yield (%) or K (L mol^{-1})	Ref.
$(I^-)_2$ $\left[SCH_2CH_2\overset{\oplus}{N}H_2CH_2-Z\right]_2$	3		threading	1:2	84%	36
$\overset{\oplus}{N}H_2\left[CH_2-\langle O \rangle-Z\right]_2$	3	i-Pr	slippage	1:1	2870[a] 2470[b]	26 26
"	3	t-Bu	slippage	1:1	0	26

Linear Component	Cyclic Component	"Stopper" (Z)	Method	Stoichiometry L:C	Yield (%) or K (L mol^{-1})	Ref.
"	3		threading	1:1	31%	23
"	4	"	threading	1:1	24%	23
$p-C_6H_4\left[CH_2\overset{\oplus}{N}H_2CH_2-\bigcirc-Z \right]_2$						
	3	"	threading	1:2	10%	23

Table 2 Continued. Low Molar Mass Rotaxanes From Ammonium Ion Type Linear Systems with Hexafluorophosphate Counterions (Unless noted)

Linear Component	Cyclic Component	"Stopper" (Z)	Method	Stoichiometry L:C	Yield (%) or K (L mol^{-1})	Ref.
$\overset{\oplus}{NH_2}(CH_2Z)_2$						
	3	n=1	slippage	1:1	290[a]	26
	3	n=1	slippage	1:1	110[b]	26
	3	n=2	slippage	1:1	110[b]	26
$R{\left[CH_2\overset{\oplus}{NH_2}CH_2Z\right]}_2$						
$R = p\text{-}C_6H_4$	5	$3,5\text{-}C_6H_3(Bu\text{-}t)_2$	threading	1:1	-	25
$R = 2,6\text{-}C_{10}H_6$	5	"	threading	1:1	-	25
$R = (CH_2)_3$	5	"	threading	1:1	-	25
$R = (CH_2)_4$	5	"	threading	1:1	-	25

[a] 3:1 CHCl$_3$/MeCN at 20°C.   [b] 3:1 CHCl$_3$/MeCN at 40°C.

Interest quickly grew from the ability of ammonium ions, e.g., the dibenzyl ammonium ion, to form 1:1 complexes, i.e., [2]pseudorotaxanes, with smaller crown ethers such as dibenzo-24-crown-8 (DB24C8, 3) and its asymmetric isomer (asymDB24C8, 4) [20] and 2:1 complexes, i.e., [3]pseudorotaxanes, with larger crowns such as bis(p-phenylene)-34-crown-10 (BPP34C10, 5) [20] and bis(m-phenylene)-32-crown-10 (BMP32C10, 6). [21]

O(CH$_2$CH$_2$O)$_x$

O(CH$_2$CH$_2$O)$_y$
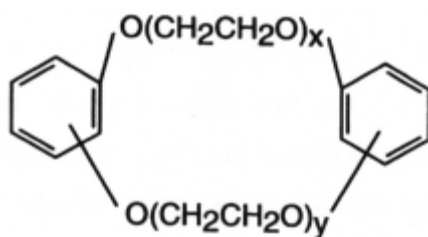
3: o-, o- ; x=y=3
4: o-, o- ; x=2, y=4
5: p-, p- ; x=y=4
6: m-, m- ; x=y=4

Extended linear species that were composed of two or more ammonium ions were used in the creation of [2]-, [3]-, [4]-, and even [5]rotaxanes as reported by Stoddart and co-workers. [22-24] The diammomum ions were also used in conjunction with **5** to create 2:2 complexes, or with bulky end groups and the appropriate spacer group between the ions, a "doubly-docked" pseudorotaxane in which one diammomum ion occupied both complexation sites of **5**. [25] The ammonium ion system has also been utilized as a driving force for the slippage technique [26], and this system was used to test the ability of a variety of stoppers to block DB24C8.

The ammonium ion system has also been used in the formation of larger, extended rotaxane assemblies. Using a branched trifunctional dibenzylammonium salt **7** as a core molecule, Gibson and co-workers [27] assembled dendritic pseudorotaxanes by complexing the core molecule with various dendrons possessing DB24C8 moieties at the focal point. While the generation 3 Fréchet-type dendron [28] is shown in structure **8**, the generation 1 and 2 dendrons coupled to DB24C8 were also employed.

This tritopic salt was also employed by Stoddart and co-workers in the formation of a supramolecular cage assembly. [29,30] The assembly of two tritopic salt molecules **7** with the ditopic crown ether BPP34C10 yields a five-component 2:3 complex in the solid state. A similar idea was employed by Stoddart and Nolte and co-workers, [31] when a porphyrin functionalized with four dibenzylammonium arms was used. When macrocycle **5** was mixed with this compound, a 2:4 complex formed in which the two porphyrin units were stacked in a cofacial orientation similar to the photosynthetic reaction center.

An extended linear system has been envisioned through the use of a self-complexing AB type system that contains the linear and cyclic component in the same molecule. Using a DB24C8 derivative containing a dibenzylammonium sidearm (**9**), Stoddart and co-workers [32] have observed the formation of the cyclic dimer of this species. The assembly of this molecule into linear arrays, however, was not detected. Assembly of a linear array using other types of rotaxane-forming systems will be discussed further in later sections.

A final example of extended supramolecular systems employing ammonium ion complexation has recently been demonstrated. [33,34] Ammonium ions containing carboxylic acid functionalities have been threaded through DB24C8 and BPP34C10. Subsequent intramolecular hydrogen bonding by these carboxylic acid groups assembled the pseudorotaxanes into an interwoven superstructure in the solid state.

The progression from a 1:1 complex between the dibenzylammonium ion and DB24C8 to a 2:1 complex with BPP34C10 has also been further extended to larger cyclic systems. Using tris(p-phenylene)-51-crown-15 and tetrakis(p-phenylene)-68-crown-20, Stoddart and co-workers [24,30,35] have reported the detection of 3:1 and 4:1 complexes, respectively.

In addition to the systems discussed above, ammonium ion-based motifs have been used for the assembly of [3]rotaxanes in high yield [36] and the construction of a pseudorotaxane equilibrium that alternates between the threaded and unthreaded states depending on the counter ion present in the system. [37]

Like ammonium ions, another hydrogen bonding motif for the assembly of rotaxanes has gained much attention in recent years. Using amide-containing macrocycles **10**, Vögtle and co-workers [38-42] have prepared a number of amide-based [2]- and [3]rotaxanes and rotaxane assemblies. The variety of rotaxanes made by this technique is summarized in Table 3. The driving force for rotaxane assembly appears to be the ability of the amide units in the macrocycle to hydrogen bond with complementary functionalities in the linear component as well as potential p-p stacking interactions between the cyclic and linear components when aromatic structures are present in each. Leigh and co-workers [43-45] have also prepared several amide-based [2]rotaxanes, some containing short peptide residues in the linear segment [44,45], through a combination of these hydrogen-bonding template effects and the clipping protocol.

es via threading (unless noted) and hydrogen bonding interactions
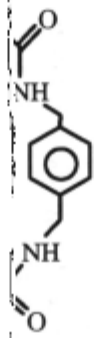
nent	"Stopper" (Z)	Linear: Cyclic	Yield (%)	Ref.

| | COCHPh$_2$ | 1:1[a] | 28% | 43 |
| | COCHPh$_2$ | 1:1[a] | 13% | 43 |

Table 3 Continued. Synthesis of amide-based low molar mass rotaxanes via threading (unless noted) and hydrogen bonding interactions
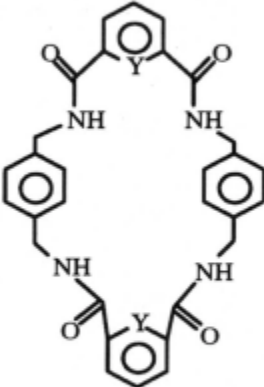
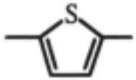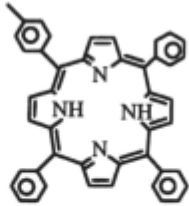| Linear Component	Cyclic Component	"Stopper" (Z)	Linear: Cyclic	Yield (%)	Ref.
$ZNH_2CH_2CONHCH_2COOZ'$		$Z = COCHPh_2$ $Z' = CH_2CHPh_2$			
		$Y = CH$	$1:1^a$	62	45
		$Y = N$	$1:1^a$	34	45
$X\text{--[OOCCH}_2NHCOCH_2NHZ]_2$	"				
$X = (CH_2)_8$	$Y = CH$	$COCHPh_2$	$1:1^a$	30%	44
$X = (CH_2)_{16}$	$Y = CH$	$COCHPh_2$	$1:1^a$	28%	44
$X = (CH_2)_3S(CH_2)_3$	$Y = CH$	$COCHPh_2$	$1:1^a$	36%	44

Table 3 Continued. Synthesis of amide-based low molar mass rotaxanes via threading (unless noted) and hydrogen bonding interactions

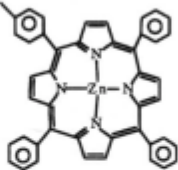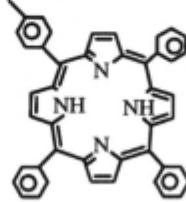| Linear Component	Cyclic Component	"Stopper" (Z)	Linear: Cyclic	Yield (%)	Ref.
$R\text{-}[CONHZ]_2$					
R = p-C$_6$H$_4$	10a	$3,5\text{-}C_6H_3(Bu\text{-}t)_2$	1:1	-	40
R = p-C$_6$H$_4$-p-C$_6$H$_4$	10b	"	1:1	3%	40
R = p-C$_6$H$_4$-p-C$_6$H$_4$	10c	"	1:1	8%	40
R = m-C$_6$H$_4$	10a	$p\text{-}C_6H_4CPh_3$	1:1	11%	39
R =	10a	"	1:1	19%	39
R =	10a	"	1:1	6%	39
R = p-C$_6$H$_4$	10a	"	1:1	7%	39

Table 3 Continued. Synthesis of amide-based low molar mass rotaxanes via threading (unless noted) and hydrogen bonding interactions

Linear Component	Cyclic Component	"Stopper" (Z)	Linear: Cyclic	Yield (%)	Ref.
$R = p\text{-}C_6H_4$	$\left[CH_2OCH_2CH_2B\right]_2$ B = 10d	"	2:1	-	41
$R = p\text{-}C_6H_4$	$1,3,5\text{-}C_6H_3\left[C_6H_4CH_2B\text{-}p\right]_3$ B = 10d	"	3:1	35%	41
$R = m\text{-}C_6H_4$	10a		1:1	-	42
$R =$	10a	"	1:1	-	42
$R =$	10a	"	1:1	-	42

Table 3 Continued. Synthesis of amide-based low molar mass rotaxanes via threading (unless noted) and hydrogen bonding interactions
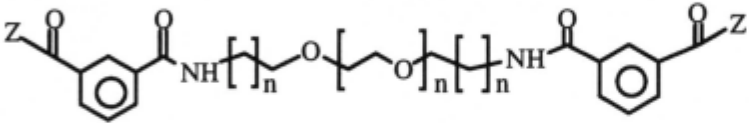
Linear Component	Cyclic Component	"Stopper" (Z)	Linear: Cyclic	Yield (%)	Ref.
R =	10a		1:1	-	42
R$\left[CONHZ\right]_2$					
R =	10a	Z' = p–C$_6$H$_4$CPh$_3$	1:1	-	42

Table 3 Continued. Synthesis of amide-based low molar mass rotaxanes via threading (unless noted) and hydrogen bonding interactions

| Linear Component	Cyclic Component	"Stopper" (Z)	Linear: Cyclic	Yield (%)	Ref.
$R-[NHZ]_2$					
$R = SO_2C_6H_4CO-m$	**10a**	"	1:1	41%	39
$R = p\text{-}C_6H_4(SO_2)_2-$	**10a**	"	1:1	4%	39
"	$p-C_6H_4[CONH(CH_2CH_2O)_2CH_2CH_2B]_2$				
	B = **10d**	"	1:1	13%	41
$R = p\text{-}C_6H_4(CO)_2-$					
$R = SO_2C_6H_4CO-m$	"	"	1:1	28%	41

Table 3 Continued. Synthesis of amide-based low molar mass rotaxanes via threading (unless noted) and hydrogen bonding interactions

Linear Component	Cyclic Component	"Stopper" (Z)	Linear: Cyclic	Yield (%)	Ref.
R =		"			
n = 1	10a	"	1:1	15%	38
n = 2	10a	"	1:1	6%	38
n = 2	10a	"	1:2	2%	38

a Formed by clipping method. b First linear component threads one macrocycle while second linear component threads the other.

7
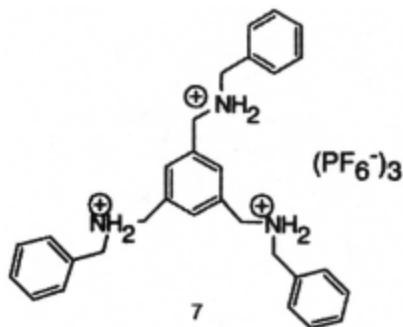
12.2.2.3.b Cyclodextrin Inclusion Complexes and Other Hydrophobic Interactions

The cyclic oligosaccharides, known as cyclodextrins (CD), are able to form inclusion complexes with a number of linear species as a result of both their geometry and functionality. The cyclodextrins form cylindrical cavities that possess hydroxyl functionalities on the rim and hydrocarbon and ether moieties in the interior of the cavity. The three most commonly used cyclodextrins are shown below with the cavity size increasing from a- (**11**) to ß-(**12**) to g-CD (**13**). Also commonly used are the more hydrophobic derivatives of **ß-cyclodextrin,** in which two, **DM-ß-CD** (**14a**), or three, **TM-ß-CD** (**14b**), of the hydroxyl groups

Bn=Benzyl

8a, X = CH$_2$
8b, X = COOCH$_2$
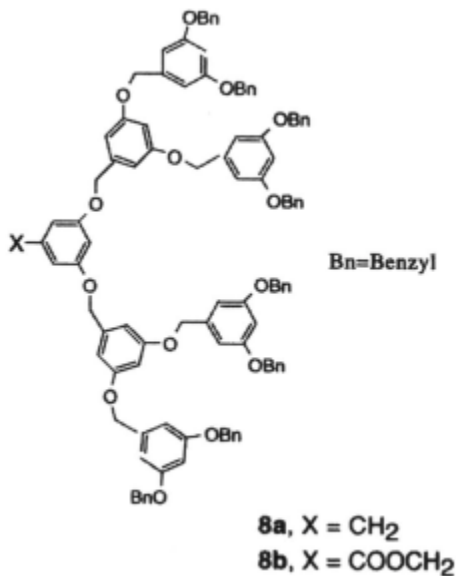
have been methylated. The cyclodextrins are therefore selective in their binding abilities with linear species, and in aqueous solution various inclusion complexes can be formed with the hydrophobic segment of the linear species residing within the hydrophobic cavity of the cyclodextrin. From this complex, a variety of rotaxanes have been formed. With consideration of the recent reviews of this particular subdivision of rotaxane chemistry [12d] and the historical overview presented in past reviews by Gibson, [10,11] only recent developments in this area will be summarized.

Harada has shown previously [46] that CD will selectively bind a series of oligomeric species. Oligo(ethylene glycol)s form 1:1 complexes with a-CD and 2:1 complexes with g-CD but do not complex significantly with **ß-CD,** while propylene glycol oligomers selectively complex with **ß-CD,** and to a lesser extent g-CD, only. While these results have been further documented [47-51], it has also been demonstrated that short chains of poly(isobutylene) bind selectively to g-CD, while squalane complexes with **ß-CD** with some preference versus g-CD. [48] More recently, a- and g-CD were reported to form

inclusion complexes in high yields with aliphatic polyesters such as poly(ethylene adipate), poly(trimethylene adipate), and poly(l,4-butylene adipate) while yields with **ß-CD** are not as high. [52]

The formation of rotaxanes from various a-CD complexes has recently been studied Harada has shown that using oligoethylene compounds with DM-a-CD (**14c**) and TM-a-CD (**14d**) and trinitrophenyl groups as stoppers produces the [2]rotaxanes in high yield. [53] Macartney [54] has also investigated the complexation of a-CD with oligoethylene linear species, showing that longer, more hydrophobic chains slow the kinetics of dissociation of the pseudorotaxane. The kinetics of pseudorotaxane formation, meanwhile, were found to decrease dramatically as the size of the end groups in the linear component increased from trimethylammonium to ethyldimethylammonium. The diethyl and triethyl functional end groups prevented complex formation while the trimethylphosphonium end group only produced pseudorotaxanes at elevated temperatures through a slippage mechanism.

Kaifer and co-workers [55] and Nakashima *et al.* [56] have both used linear components that possess viologen containing end groups. In each case, inclusion complexes were formed with a-CD, but it was the central hydrophobic segment of the linear species that resided within the CD cavity. In further experiments using **ß-CD** or **DM-ß-CD,** Mitzoian and Kaifer [57] showed that the viologen-containing segment of linear guests form weak inclusion complexes in the reduced form and strong complexes in the two-electron, fully-reduced form.

In other work with CD-inclusion complexes, Wenz [58] has reported the formation of complexes between a-CD and a,w-amino acids that contain long hydrophobic segments. A polyamide can then be formed through the polycondensation of the amino acids complexed within the CD cavity. An inclusion complex between **triacetyl-ß-CD** and 11-amino-N-[p-(triphenylmethyl)phenyl]undecanamide has been coupled to the side chain

carboxyl groups of a functionalized poly(ether sulfone). This route has been used by Born and Ritter [59] to obtain polyrotaxanes containing CD units in the side chains.

Although cyclodextrin is the host used most often for inclusion complexes involving hydrophobic interactions, other materials have also been used. Kim and co-workers [60] have investigated the binding between the cyclic amide cucurbituril (**15**) and N,N'-bis(4-pyridylmethyl)-l,4-diaminobutane dihydronitrate. Like cyclodextrin, cucurbituril also has a hydrophobic cavity that can bind the hydrophobic segment of the linear guest.

9
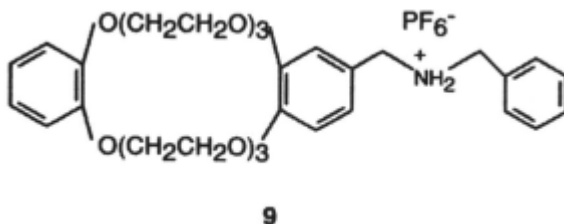
Mixing this complex with platinum ethylenediamine dinitrate led to the formation of a cyclic oligorotaxane or molecular necklace. This simple molecular necklace [4]MN consists of three cucurbituril rings threaded onto the larger ring formed by the three linear segments coordinated to the metal center. Kim [61] has also shown that when the cucurbituril complex is mixed with silver tosylate, a one-dimensional coordination polymer is formed with the linear segments linked together by coordination to silver and threaded by cucurbituril. If silver nitrate is used in lieu of the tosylate, a two-dimensional polymeric network is formed instead. Complexation of cucurbituril with a 1,6-hexanediammonium salt followed by amide formation with a bulky acid chloride group has been used by Buschmann [62] to form rotaxanes. The use

of a difunctional acid chloride has also been used to generate oligo- and polyamide-cucurbituril rotaxanes. [62]

10a. Y=H, X=CO
10b. Y=t-Bu, X=CO
10c. Y=H, X=SO$_2$
10d. Y=bond, X=SO$_2$
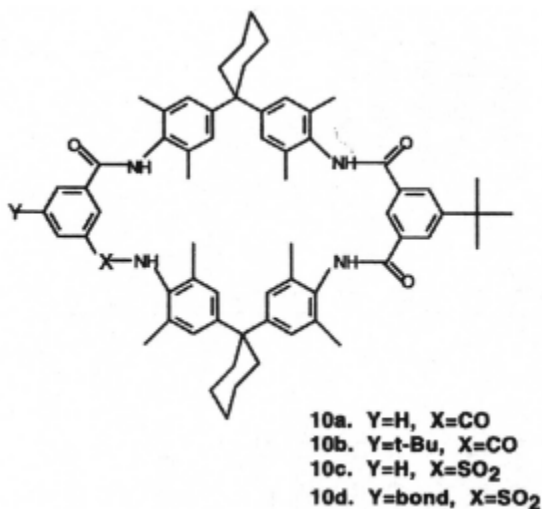
A final example of the use of hydrophobic interactions in the formation of rotaxanes is derived from the use of the cyclophane **16**. Anderson and Anderson et al. [63,64] used this cyclophane to complex an alkyne-containing linear segment in the formation of a conjugated [3]rotaxane. This cyclophane was also used for the formation of an azo dye rotaxane. [65] These rotaxanes and others synthesized by the use of cyclodextrin inclusion complexes and hydrophobic interactions are summarized in Tables 4 and 5.

12.2.2.3.c Metal Templates

Sauvage and Dietrich-Buchecker [66] have pioneered the use of a metal template, particularly Cu(I), in the efficient synthesis of rotaxanes and interlocked ring systems, also known as catenanes. Copper is able to form tetrahedral complexes with 1,10-phenanthrolines. Through the incorporation of the phenanthroline moiety into both a macrocycle (as in structure **17**) and a linear

Table 4. Low Molar Mass Pseudorotaxanes by threading from Cyclodextrins and Hydrophobic Interactions in Aqueous Solutions
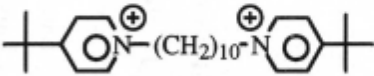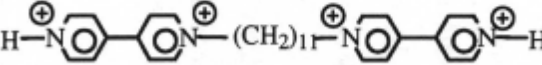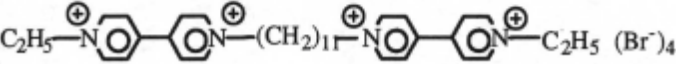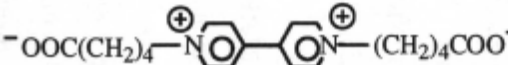
Linear Component	Cyclic Component	Stoichiometry L:C	Yield (%) or K (L mol^{-1})	Ref.
$[Me_3N(CH_2)_8NMe_3]^{2+}$ $(Br^-)_2$	α-CD (**11**)	1:1	44±5 [a]	54
$[Me_3N(CH_2)_9NMe_3]^{2+}$ $(Br^-)_2$	α-CD (**11**)	1:1	240±50 [a]	54
$[Me_3N(CH_2)_{10}NMe_3]^{2+}$ $(Br^-)_2$	α-CD (**11**)	1:1	1360±290 [a]	54
$[Me_3N(CH_2)_{11}NMe_3]^{2+}$ $(Br^-)_2$	α-CD (**11**)	1:1	3170±970 [a]	54
$[Me_3N(CH_2)_{12}NMe_3]^{2+}$ $(Br^-)_2$	α-CD (**11**)	1:1	6760±850 [a]	54
$[Me_2EtN(CH_2)_{10}NEtMe_2]^{2+}$ $(Br^-)_2$	α-CD (**11**)	1:1	-	54
$Me_3P(CH_2)_{10}PMe_3]^{2+}$ $(I^-)_2$	α-CD (**11**)	1:1	-	54

	α-CD (**11**)	1:1	-	54

	α-CD (**11**)	1:1	580[b]	55

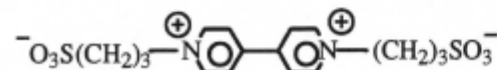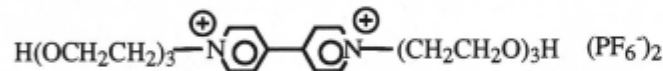|	α-CD (**11**)	1:1	230[c]	55

Table 4 Continued. Low Molar Mass Pseudorotaxanes by threading from Cyclodextrins and Hydrophobic Interactions in Aqueous Solutions

Linear Component	Cyclic Component	Stoichiometry L:C	Yield (%) or K (L mol^{-1})	Ref.
+e$^-$	ß-CD (12)	1:1	9×10^1 d	57
	DM-ß-CD (14a)	1:1	1×10^2 d	57
+2e$^-$	ß-CD (12)	1:1	2×10^9 d	57
	DM-ß-CD (14a)	1:1	7×10^9 d	57

H(OCH$_2$CH$_2$)$_3$—N⊕O—O⊕N—(CH$_2$CH$_2$O)$_3$H   (PF$_6^-$)$_2$

+e$^-$	ß-CD (12)	1:1	5×10^1 d	57
	DM-ß-CD (14a)	1:1	5×10^1 d	57
+2e$^-$	ß-CD (12)	1:1	6×10^3 d	57
	DM-ß-CD (14a)	1:1	2×10^4 d	57

$^-$O$_3$S(CH$_2$)$_3$—N⊕O—O⊕N—(CH$_2$)$_3$SO$_3^-$

+e$^-$	ß-CD (12)	1:1	5×10^1 d	57
	DM-ß-CD (14a)	1:1	7×10^1 d	57

448

Table 4 Continued. Low Molar Mass Pseudorotaxanes by threading from Cyclodextrins and Hydrophobic Interactions in Aqueous Solutions
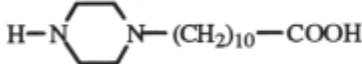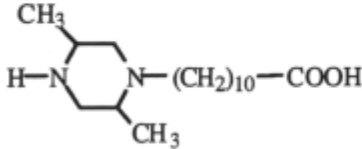
Linear Component		Cyclic Component	Stoichiometry L:C	Yield (%) or K (L mol^{-1})	Ref.
$+2e^-$		ß-CD (**12**)	1:1	7×10^3 d	57
		DM-ß-CD (**14a**)	1:1	1×10^4 d	57
$^+NH_3$-R-NH_3^+ (Cl$^-$)$_2$		cucurbituril (**15**)			
R = (CH$_2$)$_n$ n=4-12			1:1	-	62
= -C$_6$H$_4$-			1:1	-	62
R'-CO-NH-R-NH-CO-R'		cucurbituril (**15**)		-	62
R = (CH$_2$)$_n$ n=4-12	R' = -(CH$_2$)$_n$CH$_3$ n=4-12		1:1	-	62
R = (CH$_2$)$_n$ n=4-12	= -Ph		1:1	-	62
R = (CH$_2$)$_n$ n=4-12	= -C$_6$H$_4$CH$_3$		1:1	-	62
R = (CH$_2$)$_n$ n=4-12	= - C$_6$H$_4$OCOCH$_3$		1:1	-	62
R = (CH$_2$)$_n$ n=4-12	= -C$_6$H$_2$(OCH$_3$)$_3$		1:1	-	62
R = (CH$_2$)$_n$ n=4-12	= -CH$_2$C(Ph)$_3$		1:1	-	62
R = (CH$_2$)$_n$ n=4-12	= -C$_{10}$H$_7$		1:1	-	62
R = -C$_6$H$_4$-	R' = -(CH$_2$)$_n$CH$_3$ n=4-12		1:1	-	62
R = -C$_6$H$_4$-	= -Ph		1:1	-	62
R = -C$_6$H$_4$-	= -C$_6$H$_4$CH$_3$		1:1	-	62
R = -C$_6$H$_4$-	= - C$_6$H$_4$OCOCH$_3$		1:1	-	62
R = -C$_6$H$_4$-	= -C$_6$H$_2$(OCH$_3$)$_3$		1:1	-	62
R = -C$_6$H$_4$-	= -CH$_2$C(Ph)$_3$		1:1	-	62
R = -C$_6$H$_4$-	= -C$_{10}$H$_7$		1:1	-	62

Table 4 Continued. Low Molar Mass Pseudorotaxanes by threading from Cyclodextrins and Hydrophobic Interactions in Aqueous Solutions

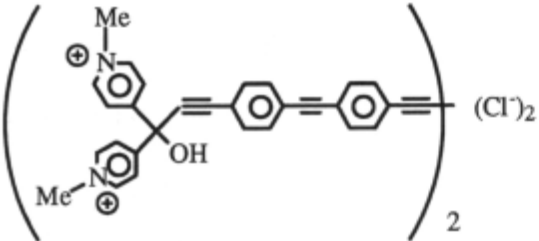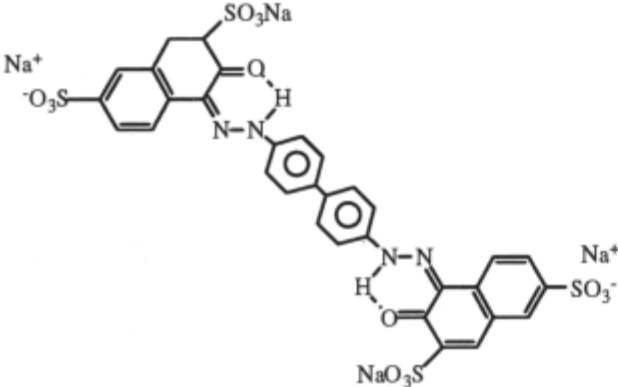| Linear Component	Cyclic Component	Stoichiometry L:C	Yield (%) or K (L mol^{-1})	Ref.
$NH_2-(CH_2)_{10}-COOH$	α-CD (**11**)	1:1^e	53%	58
	2 α-CD (**11**)	1:2^e	65%	58
$H-N\overset{\frown}{\underset{\smile}{\,}}N-(CH_2)_{10}-COOH$	α-CD (**11**)	1:2^e	56%	58
$\underset{CH_3}{\overset{CH_3}{H-N\overset{\frown}{\underset{\smile}{\,}}N-(CH_2)_{10}-COOH}}$	α-CD (**11**)	1:2^e	17%	58
$p-H_2NC_6H_4COOH$	β-CD (**12**)	1:1^e	67%	58
$H_2N-(CH_2)_{10}NH_2$, $HOOC-(CH_2)_8-COOH$	β-CD (**12**)	2:4^e	38%	58

Table 4 Continued. Low Molar Mass Pseudorotaxanes by threading from Cyclodextrins and Hydrophobic Interactions in Aqueous Solutions

Linear Component	Cyclic Component	Stoichiometry L:C	Yield (%) or K (L mol^{-1})	Ref.
	16	1:2	30%	63,64
	16	1:1	-	65

Table 4 Continued. Low Molar Mass Pseudorotaxanes by threading from Cyclodextrins and Hydrophobic Interactions in Aqueous Solutions

Linear Component	Cyclic Component	Stoichiometry L:C	Yield (%) or K (L mol^{-1})	Ref.
$\left(\text{CH}_2\text{CH}_2\text{O}\right)_n$ n=22	α-CD (11)	1:2	92%	47,49
$\left(\text{CH}_2\text{CHO}\right)_n$ CH$_3$ n=17	β-CD (12)	1:2	96%	47,49
	γ-CD (13)	1:2	80%	47,49
R$\left(\text{CH}_2\text{CHO}\right)_nCH_2$—CHR CH$_3$ ... CH$_3$ n=34				
R = OH	β-CD (12)	1:2	50%	47,49
R = NH$_2$	β-CD (12)	1:2	70%	47,49
R$\left(\text{CH}_2\text{CHO}\right)_nCH_2$—CHR CH$_3$ ... CH$_3$ n=34				
R = OH	γ-CD (13)	1:2	31%	47,49
R = NH$_2$	γ-CD (13)	1:2	50%	47,49

Table 4 Continued. Low Molar Mass Pseudorotaxanes by threading from Cyclodextrins and Hydrophobic Interactions in Aqueous Solutions

Linear Component		Cyclic Component	Stoichiometry L:C	Yield (%) or K (L mol^{-1})	Ref.
$-(CH_2CH_2O)_n$ n = 20		α-CD (**11**)	1:2	63%	48
		β-CD (**12**)	1:2	0	48
		γ-CD (**13**)	1:2	0	48
$(CH_2-CHCH_2CH_2)_n$ MW = 423 (with CH₃ substituent)		α-CD (**11**)	1:2	0	48
		β-CD (**12**)	1:2	62%	48
		γ-CD (**13**)	1:2	24%	48
$(CH_2-C)_n$ MW = 800 (with two CH₃ substituents)		α-CD (**11**)	1:2	0	48
		β-CD (**12**)	1:2	8%	48
		γ-CD (**13**)	1:2	90%	48

Table 4 Continued. Low Molar Mass Pseudorotaxanes by threading from Cyclodextrins and Hydrophobic Interactions in Aqueous Solutions

Linear Component	Cyclic Component	Stoichiometry L:C	Yield (%) or K (L mol^{-1})	Ref.

$$\left[\!\!\!-O(CH_2)_xO_2C(CH_2)_4CO-\!\!\!\right]_n$$

Linear Component	Cyclic Component	Stoichiometry L:C	Yield (%) or K (L mol^{-1})	Ref.
x=2, MW ≈ 840-1000	α-CD (11)	1.3:2	≈70%	52
x=3, MW ≈ 840-1000	α-CD (11)	1.3:2	≈70%	52
x=4, MW ≈ 840-1000	α-CD (11)	1.3:2	≈75%	52
x=2, MW ≈ 840-1000	γ-CD (13)	1.5:1	≈70%	52
x=3, MW = 840-1000	γ-CD (13)	1.5:1	≈80%	52
x=4, MW ≈ 840-1000	γ-CD (13)	1.5:1	≈75%	52

[a] D_2O at 25°C. [b] water, pH = 1, at 25°C. [c] water, pH = 7 at 25°C. [d] 0.1 M phosphate buffer at 25°C. [e] Inclusion complexes of the low molar mass compounds could also be polymerized to form polyamide inclusion complexes (M_n) not reported.

Table 5. Low Molar Mass Rotaxanes by Threading from Cyclodextrins and Hydrophobic Interactions in Aqueous Solution.
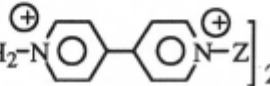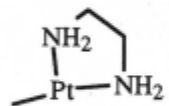
Linear Component	Cyclic Component	"Stopper" (Z)	Stoichiometry L:C	Yield (%) Or K (L mol^{-1})	Ref.
$\left[(CH_2)_6NHZ\right]_2$	DM-α-CD (**14c**)	2,4,6-C$_6$H$_2$(NO$_2$)$_3$	1:1	42%	53
	TM-α-CD (**14d**)	2,4,6-C$_6$H$_2$(NO$_2$)$_3$	1:1	48%	53
$\left[N\!-\!p\!-\!C_6H_4OCH_2CH_2\!-\!N^{\oplus}\!\!\bigcirc\!\!\bigcirc\!N^{\oplus}\!-\!Z\right]_2$ (ClO$_4^-$)$_4$					
	α-CD (**11**)	2,4,6-C$_6$H$_2$(NO$_2$)$_3$	1:1	30%	56
$\left[CH_2CH_2N^{\ominus}H_2CH_2\!-\!\bigcirc\!N\!-\!Z\right]_2$ [(H$_2$O)$_2$NO$_3$]$_2$					
	cucurbituril (**15**)	Pt(NH$_2$–CH$_2$CH$_2$–NH$_2$)	1:1	90%	60
$\left[CH_2CH_2N^{\ominus}H_2CH_2\!-\!\bigcirc\!N\!-\!Z\right]_2$ [(H$_2$O)$_2$NO$_3$]$_2$					
	cucurbituril (**15**)	network with AgNO$_3$	1:1	37%	61

Table 5 Continued. Low Molar Mass Rotaxanes by Threading from Cyclodextrins and Hydrophobic Interactions in Aqueous Solution.

Linear Component	Cyclic Component	"Stopper" (Z)	Stoichiometry L:C	Yield (%) Or K (L mol⁻¹)	Ref.
$+CH_2CHO+_n CH_2-CH-$ $\quad\; CH_3 \qquad\qquad CH_3$ n=34	β-CD (12)	$3,5-NH-C_6H_3(NO_2)_2$	1:2	<1%	47,49
	β-CD (12)	"	1:2	<1%	47,49
$+CH_2CHO+_n CH_2-CH-$ $\quad\; CH_3 \qquad\qquad CH_3$ n=34	γ-CD (13)	"	1:2	12%	47,49
	γ-CD (13)	"	1:2	11%	47,49

species, complexation with the copper template can be used to direct rotaxane formation.

11, x = 6
α-cyclodextrin

12, x = 7
β-cyclodextrin

13, x = 8
γ-cyclodextrin
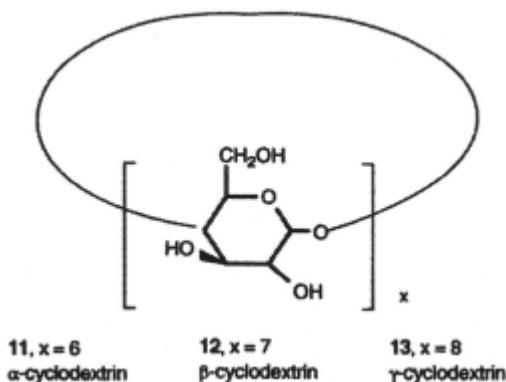
This approach has been used to generate a pseudorotaxane structure, followed by conversion to the rotaxane with the use of a variety of blocking groups as shown in Table 6. In addition to the use of fullerene blocking groups [67,68], Sauvage and co-workers have also employed linear components with terminal terpyridine functionalities. [69,70] Addition of Ru(II) results in coordination of the metal to the terpyridine end groups and effectively blocks the loss of the macrocyclic species.

Porphyrin groups have also been effectively used as blocking groups as well. If the linear species is functionalized with terminal aldehyde groups, these functionalities can be used in the construction of a porphyrin stopper *in*

In one example of this approach [68,71], a preformed porphyrin unit was included in the cyclic component as well, generating a [2]rotaxane possessing 3 porphyrin components. When the linear species contains two phenanthroline moieties, a [3]rotaxane [72] is formed with two terminal porphyrin stoppers. If the experimental conditions are adjusted, a [5]rotaxane structure can be formed. A pair of bis-phenanthroline linear segments is connected by a bridging porphyrin, creating a longer linear component. This linear species is complexed

with four cyclic units to generate the [5]pseudorotaxane, while porphyrin units again compromise the stoppers in the final rotaxane structure.

Another interesting rotaxane structure has been generated from a linear segment that possesses two different coordinating units. In addition to the commonly-used phenanthroline moiety, the linear component also contains a terpyridine functionality that is capable of complexing with copper (II). A pseudorotaxane structure can then be generated in which the oxidation state of the metal will determine which site the macrocycle will complex. This unique thread has been used to form both the pseudorotaxane [73] and the stoppered [2]rotaxane. [68,74,75]

12.2.2.3.d Complexation of Crown Ethers with 4,4'-Bipyridinium Salts and Similar Compounds

Unlike the more recently developed ammonium ions systems discussed previously, the ability of 4,4'-bipyridinium salts to complex effectively with crown ethers and subsequently form rotaxanes has been known for more than a decade. [76-78] The threading process in these systems is driven by a combination of charge-transfer, p-p, hydrogen bonding, and dipole-dipole interactions. Since rotaxanes of this type have existed for some time, the focus in recent years has been on applications for these systems and the development of more complex motifs. Recent developments in this area are summarized in Tables 7 and 8.

One aspect of these systems that has been explored in more detail is their ability to form multi-component rotaxane complexes. Using linear components that contain up to three 4,4-bipyridinium units, Stoddart and co-workers [79] have assembled [2]-, [3]-, and [4]rotaxanes with these systems. The ability to effectively block these systems has also been investigated extensively.

Table 6. Low molar mass pseudorotaxanes and rotaxanes derived from metal complexation by threading.

Linear Component	Cyclic Component	Stopper (Z)	Stoichi- ometry L:C	Yield	Ref.
p–CH$_3$OC$_6$H$_4$–Phen(CH$_2$)$_4$TerOCH$_3$Cl[a]	17	None	1:1	75%	73,75
ZOCH$_2$CH$_2$O–p–C$_6$H$_4$Phen(CH$_2$)$_4$TerCH$_2$CH$_2$OZ[a] 17		p–C$_6$H$_4$C(p–C$_6$H$_4$–t–Bu)$_3$	1:1 [b]	40%	74,75
Phen$\left[p\text{–C}_6\text{H}_4\text{O(CH}_2)_3\text{Z} \right]_2^{\text{a}}$	17	$-$TerCH$_3$ [a]	1:1	75%	69,70
"	17	$-$TerRuTer [a]	1:1	33%	69,70
Phen$\left[p\text{–C}_6\text{H}_4\text{OCH}_2\text{C}\equiv\text{CZ} \right]_2^{\text{a}}$	17	$-$C$\equiv$ C(C$_{60}$)C$\equiv$ CSi(Pr–i)$_3$	1:1	15%	67

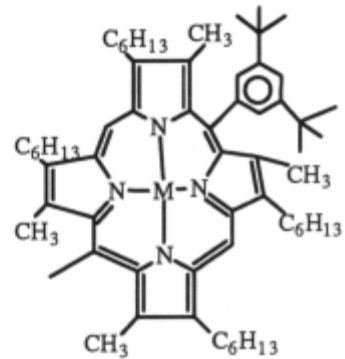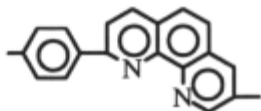Table 6 Continued. Low molar mass pseudorotaxanes and rotaxanes derived from metal complexation by threading.
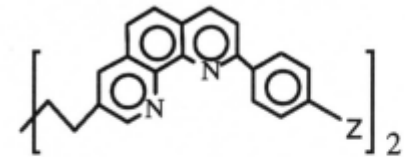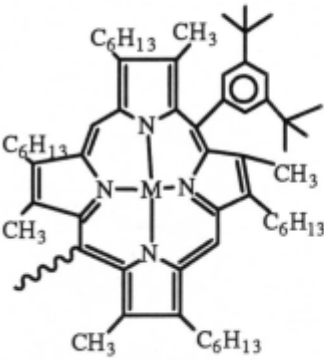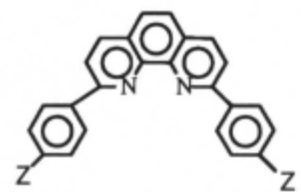
Linear Component	Cyclic Component	Stopper (Z)	Stoichiometry L:C	Yield	Ref.
	17	 M = 2H	1:2	34%	72

Table 6 Continued. Low molar mass pseudorotaxanes and rotaxanes derived from metal complexation by threading.
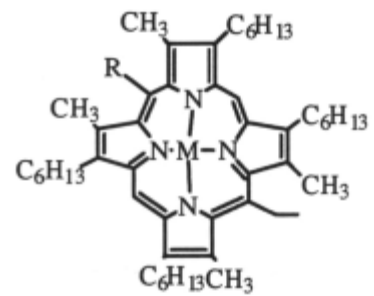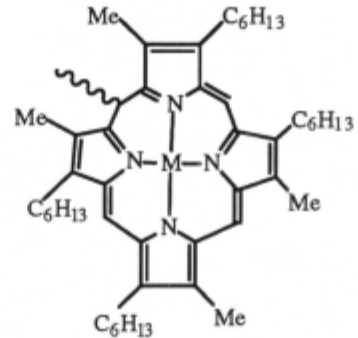
Linear Component	Cyclic Component	Stopper (Z)	Stoichiometry L:C	Yield	Ref.
	17		1:4	8%	72

R = ⟹ (CH₂)₄ ⟸ Z

⟹ =

M = 2H

Linear Component	Cyclic Component	Stopper (Z)	Stoichiometry L:C	Yield	Ref.
			1:1	13%	71

[a]Phen = 1,10-phenanthrolinyl, Ter = 2,5,2'5,2",5"-terpyridyl.
[b]Macrocycle complexes at phenanthroline unit when metal is Cu(I) and at terpyridine site when metal is Cu(II).

Table 7. Low Molar Mass Pseudorotaxanes from Bipyridinium Type Systems with Hexafluorophosphate Counterions by Threading
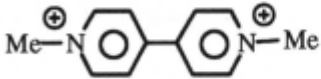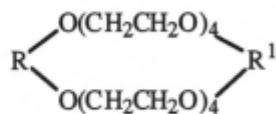
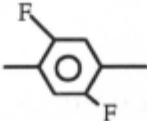| Linear Component	Cyclic Component	Stoichiometry L:C	Yield (%) or K (L mol^{-1})	Ref.
"	R = R^1 = p-C$_6$H$_4$	1:1	730[a] 240[b]	79-82 86
"	R = p-C$_6$H$_4$ R^1 = 1,5-C$_{10}$H$_6$	1:1	919[a]	79-82
"	R = p-C$_6$H$_4$ R^1 = 2,7-C$_{10}$H$_6$	1:1	414[a]	79-82
"	R = R^1 = 1,5-C$_{10}$H$_6$	1:1	1190[a]	79-82, 86
"	R = 1,5-C$_{10}$H$_6$ R^1 = 2,7-C$_{10}$H$_6$	1:1	852[a]	79-82
"	R = R^1 = 2,7-C$_{10}$H$_6$	1:1	970[a]	79-82

Linear Component	Cyclic Component	Stoichiometry L:C	Yield (%) or K (L mol^{-1})	Ref.
"	$R = R^1 = 1,6\text{-}C_{10}H_6$	1:1	472[a]	86
"	$R = R^1 = 2,6\text{-}C_{10}H_6$	1:1	-	86
"	$R = R^1 =$	1:1	-	86

"	$R = R^1 = p\text{-}C_6F_4$	1:1	0[a]	86
"	**5**	1:1	730[c]	84
	$OOC(CH_2CH_2O)_4$	1:1	73[c]	84

$R = R^1 = p\text{-}C_6H_4$

Table 7 Continued. Low Molar Mass Pseudorotaxanes from Bipyridinium Type Systems with Hexafluorophosphate Counterions by Threading

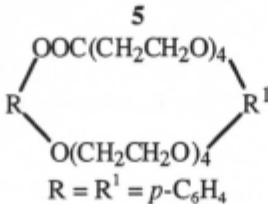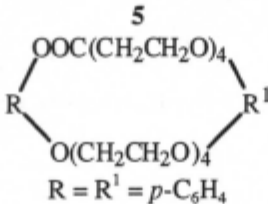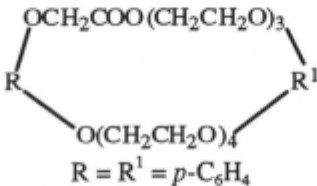| Linear Component	Cyclic Component	Stoichiometry L:C	Yield (%) or K (L mol^{-1})	Ref.
"	$OCH_2COO(CH_2CH_2O)_3$ ... $O(CH_2CH_2O)_4$ R, R^1 $R = R^1 = p\text{-}C_6H_4$	1:1	5 [c]	84
"	$O(CH_2)_2OCH_2COO(CH_2CH_2O)_2$ ... $O(CH_2CH_2O)_4$ R, R^1 $R = R^1 = p\text{-}C_6H_4$	1:1	8 [c]	84

Linear Component	Cyclic Component	Stoichiometry L:C	Yield (%) or K (L mol^{-1})	Ref.
"	$S(CH_2CH_2O)_3CH_2CH_2S$ R R^1 $S(CH_2CH_2O)_3CH_2CH_2S$ $R = R^1 = p\text{-}C_6H_4$	1:1	7[a]	85
"	$S(CH_2CH_2O)_3CH_2CH_2S$ R R^1 $S(CH_2CH_2O)_3CH_2CH_2S$ $R = R^1 = 1,5\text{-}C_{10}H_6$	1:1	17[d]	85

Table 7 Continued. Low Molar Mass Pseudorotaxanes from Bipyridinium Type Systems with Hexafluorophosphate Counterions by Threading

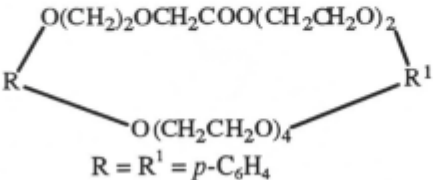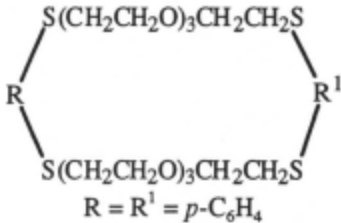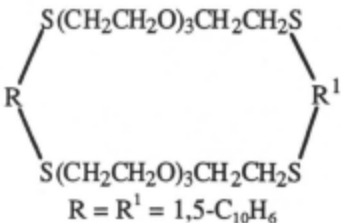| Linear Component	Cyclic Component	Stoichiometry L:C	Yield (%) or K (L mol^{-1})	Ref.
"	S(CH$_2$CH$_2$O)$_4$ R—R^1 S(CH$_2$CH$_2$O)$_4$ $R = R^1 = 1,5\text{-}C_{10}H_6$	1:1	79[a]	85
"	S(CH$_2$CH$_2$O)$_4$ R—R^1 S(CH$_2$CH$_2$O)$_4$ $R = 1,5\text{-}C_{10}H_6$ $R^1 = p\text{-}C_6H_4$	1:1	40[a]	85
"	S(CH$_2$CH$_2$O)$_4$ R—R^1 S(CH$_2$CH$_2$O)$_4$ $R = p\text{-}C_6H_4$ $R^1 = 1,5\text{-}C_{10}H_6$	1:1	59[a]	85

Linear Component	Cyclic Component	Stoichiometry L:C	Yield (%) or K (L mol^{-1})	Ref.
"	S(CH$_2$CH$_2$O)$_4$ / S(CH$_2$CH$_2$O)$_4$ with R, R^1; R = R^1 = p-C$_6$H$_4$	1:1	35[a]	85
"	R = Ph; R = p-C$_6$H$_4$CH$_3$	1:1	57 x 10^3 [a]	88
		1:1	20 x 10^3 [c]	88

467

Table 7 Continued. Low Molar Mass Pseudorotaxanes from Bipyridinium Type Systems with Hexafluorophosphate Counterions by Threading
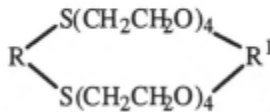
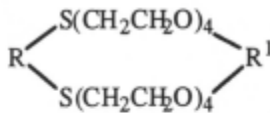| Linear Component	Cyclic Component	Stoichiometry L:C	Yield (%) or K (L mol^{-1})	Ref.
"		1:1	6.0 ± 0.9 $\times10^5$ e	87,88
	"			
X = (CH$_2$)$_2$OH		1:1	$7.4\pm0.8\times10^5$ e	87,88
X = (CH$_2$)$_3$NH$_2$		1:1	$9.0\pm1\times10^5$ e	87,88

Table 7 Continued. Low Molar Mass Pseudorotaxanes from Bipyridinium Type Systems with Hexafluorophosphate Counterions by Threading
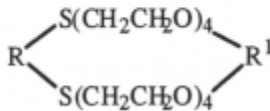
Linear Component	Cyclic Component	Stoichiometry L:C	Yield (%) or K (L mol^{-1})	Ref.

X = Me

| | **3** | 1:1 | 840 ± 51 [a] | 91 |

R = R^1 = 2,3-C$_{10}$H$_6$

X = CH$_2$C$_6$H$_5$ (with cyclic component above): 1:1, -, 92

R = R^1 = 1,5-C$_{10}$H$_6$

X = CH$_2$C$_6$H$_5$ (with cyclic component above): 1:1, 3×10^5 [a], 93

Table 7 Continued. Low Molar Mass Pseudorotaxanes from Bipyridinium Type Systems with Hexafluorophosphate Counterions by Threading
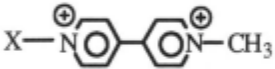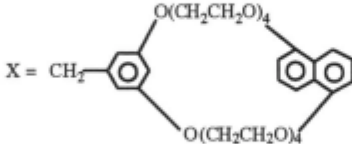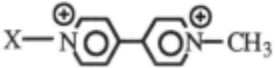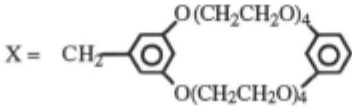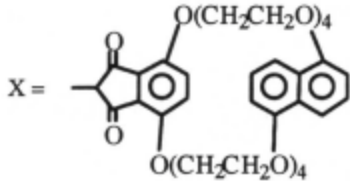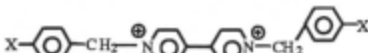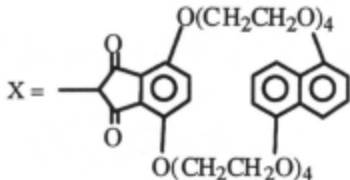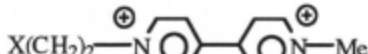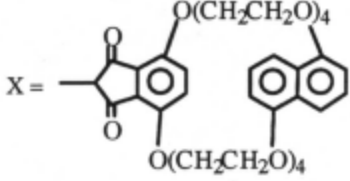
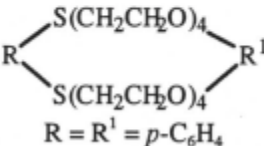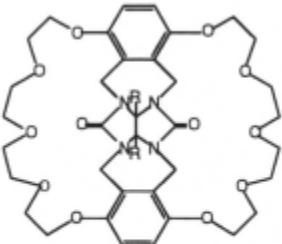| Linear Component	Cyclic Component	Stoichiometry L:C	Yield (%) or K (L mol^{-1})	Ref.

R = R^1 = 1,5-C$_{10}$H$_6$

Linear Component	Cyclic Component	Stoichiometry L:C	Yield (%) or K (L mol^{-1})	Ref.
X = $-$(CH$_2$)$_4$$-$N⊕⟨O⟩⟨O⟩N⊕$-C_2H_5$		1:1	2×10^4 f	94
X =	$-$O(CH$_2$CH$_2$O)$_2$$-$	1:1	7×10^5 g	94
X$-$N⊕⟨O⟩⟨O⟩N⊕$-$CH$_3$	X = CH$_2$	"1:1" pentamer	-	90
X$-$N⊕⟨O⟩⟨O⟩N⊕$-$CH$_3$	X = CH$_2$	"1:1" polymer n = 50	-	89

Table 7 Continued. Low Molar Mass Pseudorotaxanes from Bipyridinium Type Systems with Hexafluorophosphate Counterions by Threading
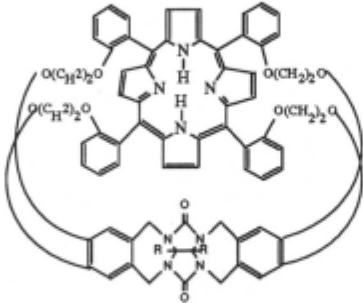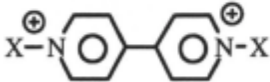
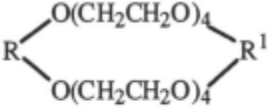| Linear Component	Cyclic Component	Stoichi-ometry L:C	Yield (%) or K (L mol^{-1})	Ref.
		"1:1" tetramer	-	90
		"1:1" tetramer	-	90
		"1:1" pentamer	-	90

[a] MeCN at 25° C. [b] MeCN at 27° C. [c] CH_3COCH_3 at 25°C. [d] 7:3 MeCN/CH_2Cl_2 at 25°C. [e] 1:1 MeCN/CHCl$_3$ at 25°C
[f] EtOH and MeCN at 25°C. [g] EtOH at 25°C

Table 8. Low Molar Mass Rotaxanes From Bipyridinium Type Systems with Hexafluorophosphate Counterions
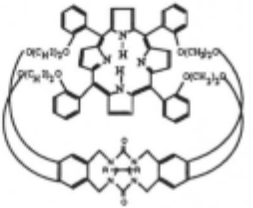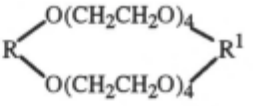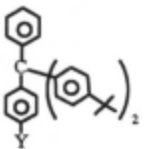
Linear Component	Cyclic Component	"Stopper" (Z)	Method	Stoichiometry L:C	Yield (%) or K (L mol^{-1})	Ref.
		$-COCH_2C(C_6H_5)_3$				
X = $-(CH_2)_3NHZ$			threading	1:1	30%	87,88
X= p-CH$_2$C$_6$H$_4$(OCH$_2$CH$_2$)$_2$OZ						
"	R = R^1 = p-C$_6$H$_4$	Y = H	slippage	1:1	52%	79-82
"		Me	slippage	1:1	45%	79-82
"		Et	slippage	1:1	47%	79-82
"		i-Pr	slippage	1:1	0	79-82
"	R= R^1 = 1,5-C$_{10}$H$_6$	Y = i-Pr	slippage	1:1	57%	79-82
"	R = R^1 = p-C$_6$H$_4$	Y = H	slippage	1:1	-	79-82
		Me	slippage	1:1	-	79-82
		Et	slippage	1:1	-	79-82
		i-Pr	slippage	1:1	-	79-82

Table 8 Continued. Low Molar Mass Rotaxanes From Bipyridinium Type Systems with Hexafluorophosphate Counterions

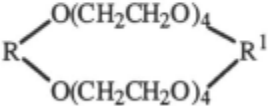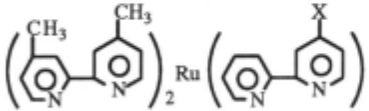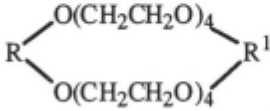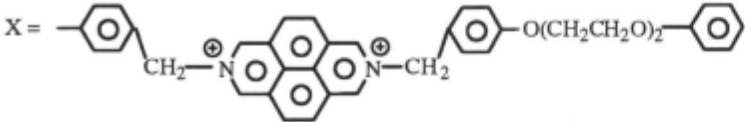| Linear Component	Cyclic Component	"Stopper" (Z)	Method	Stoichi-ometry L:C	Yield (%) or K (L mol^{-1})	Ref.
"	$R = p\text{-}C_6H_4$ $R^1 = 1,5\text{-}C_{10}H_6$	$Y = H$	slippage	1:1	-	79-82
		Me	slippage	1:1	-	79-82
		Et	slippage	1:1	-	79-82
		i-Pr	slippage	1:1	-	79-82
"	$R = p\text{-}C_6H_4$ $R^1 = 2,7\text{-}C_{10}H_6$	$Y = H$	slippage	1:1	-	79-82
		Me	slippage	1:1	-	79-82
		Et	slippage	1:1	-	79-82
		i-Pr	slippage	1:1	-	79-82
"	$R = R^1 = 1,5\text{-}C_{10}H_6$	$Y = H$	slippage	1:1	-	79-82
		Me	slippage	1:1	-	79-82
		Et	slippage	1:1	-	79-82
		i-Pr	slippage	1:1	-	79-82
"	$R = 1,5\text{-}C_{10}H_6$ $R^1 = 2,7\text{-}C_{10}H_6$	$Y = H$	slippage	1:1	-	79-82
		Me	slippage	1:1	-	79-82
		Et	slippage	1:1	-	79-82
		i-Pr	slippage	1:1	-	79-82
"	$R = R^1 = 2,7\text{-}C_{10}H_6$	$Y = H$	slippage	1:1	-	79-82
		Me	slippage	1:1	-	79-82
		Et	slippage	1:1	-	79-82
		i-Pr	slippage	1:1	-	79-82

Table 8 Continued. Low Molar Mass Rotaxanes From Bipyridinium Type Systems with Hexafluorophosphate Counterions
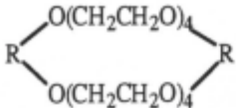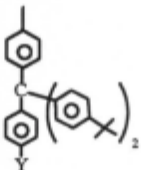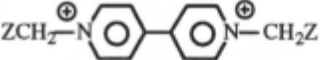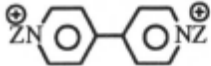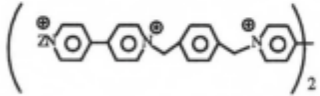
Linear Component	Cyclic Component	"Stopper" (Z)	Method	Stoichiometry L:C	Yield (%) or K (L mol^{-1})	Ref.

	R = p-C$_6$H$_4$	Y = i-Pr	threading	1:1	19%	79-82
	R = 1,5-C$_{10}$H$_6$		slippage	1:2	49%	79-82
	5	3,5–C$_6$H$_3$[Bu–t]$_2$	threading	1:1	-	25
	5	8a	threading	1:1	27%	83

Table 8 Continued. Low Molar Mass Rotaxanes From Bipyridinium Type Systems with Hexafluorophosphate Counterions

Linear Component	Cyclic Component	"Stopper" (Z)	Method	Stoichiometry L:C	Yield (%) or K (L mol^{-1})	Ref.
	5	8a	threading	1:2 1:1	23% 5 %	83
	5	8a	threading	1:3 1:2 1:1	25% 15% 4%	83
	5	X = t–Bu	slippage	1:1	26%	79
	5 1.5 equiv.	"	slippage slippage	1:1 1:2	18% 3%	79 79

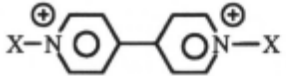Table 8 Continued. Low Molar Mass Rotaxanes From Bipyridinium Type Systems with Hexafluorophosphate Counterions

Linear Component	Cyclic Component	"Stopper" (Z)	Method	Stoichi-ometry L:C	Yield (%) or K (L mol^{-1})	Ref.
	5 4 equiv.	"	slippage slippage	1:1 1:2	5% 33%	79 79
"	5 4 equiv.	"	slippage slippage	1:1 1:2	31% 8%	79 79
"	5 10 equiv.	X = H X = H	slippage slippage	1:1 1:2	20% 55%	79 79
	5 2.2 equiv.	"	threading threading threading	1:1 1:2 1:3	< 1% 1% 3%	79 79 79
"	5 2 equiv.	"	slippage slippage slippage	1:1 1:2 1:3	19% 10% 4%	79 79 79
"	5 20 equiv.	"	slippage slippage slippage	1:1 1:2 1:3	2% 12% 19%	79 79 79

The slippage methodology was used to test the kinetics of [n]rotaxane formation as well as the effectiveness of a variety of blocking groups. [79-82] Although not performed by the slippage route, the use of the Fréchet type dendrons (as seen in structure **8**) [83] as blocking groups was also investigated.

The equilibrium constants for the binding of the N,N'-dimethyl-4,4'-bipyridinium hexafluorophosphate salt (paraquat) with numerous crown ethers have also been determined, [84-86] including some thiacrown ethers [85] and fluorinated hydroquinol crowns. [86] The variation of the equilibrium constant for a series of isomeric crown ethers has also been explored. [84,86] Nolte and Rowan and co-workers [87] have also investigated the binding of 4,4'-bipyridinium salts, using a novel host derived from a molecular clip that contains ethylene glycol units and is capped by a porphyrin. Similar results were also seen for a basket-shaped molecule that contained crown ether moieties. [88]

The ability to use the 4,4'-bipyridinium complexation in the formation of extended linear systems has been investigated as well. Using an AB system derived from BMP32C10 and paraquat (structure **18**), Gibson and co-workers [89] have demonstrated that **18** can assemble to form polymeric linear arrays in solution with up to 50 repeat units in the structure. Evidence from ^{1}H-NMR and solution viscosity measurements support formation of the arrays in solution, while mass spectrometry was able to detect species as high as the tetramer; fibers can also be pulled from a concentrated solution, indicating that polymeric species are present. Stoddart and co-workers [90] have also synthesized a series of self-complementary monomers for the formation of extended linear systems as seen in Table 7. Although linear polymeric species have not been detected in solution, a cyclic dimer of one of the monomers has been isolated by crystallization and mass spectrometry studies have indicated that two of the monomers are able to form pentamers.

While the systems based on 4,4'-bipyridinium salts have been well-characterized, some additional systems which behave in similar fashion have recently been developed. Salts derived from the diazapyrenium moiety have been shown to complex with a number of crown ethers [91-94] and rotaxanes based on this system have been constructed. Another interesting system that is similar to the paraquat systems has been developed recently by Loeb and Wisner. [95] Based on the fact that paraquat complexes more effectively with larger crown ethers such as BPP34C10 [96,97] and little with smaller crown ethers such as DB24C8, [91,98] Loeb has reduced the intramolecular charge separation by utilizing the isomeric 1,2-bis(pyridinium)ethane (BPE) dication. While the charge separation in paraquat is 7.00 Å, the charge separation in BPE is only 3.75 Å, and Loeb has demonstrated that this cation does form strong complexes with DB24C8 and other derivatives of 24-crown-8. This system provides some exciting possibilities because, unlike paraquat, the BPE dication can be easily reduced to the neutral system. At the same other functionalities can be introduced at the 4-positions of the pyridine rings, further expanding the versatility of this system. These systems are summarized in Table 9.

Finally, some interesting developments have come from the creation of hybrid complexation systems shown in Table 10. Stoddart and co-workers [98-101] have synthesized linear species that possess both ammonium ion and 4,4'-bipyridinium sites. The bipyridinium sites can be used to selectively bind larger crown ethers such as BPP34C10 while the ammonium ions can bind other cyclic species such as DB24C8. Using this approach, a number of unique [n]rotaxanes with interesting properties have been constructed.

Table 9. Low Molar Mass Pseudorotaxanes From N,N'-Dipyridylethane Type Systems with Tetrafluoroborate Counterions
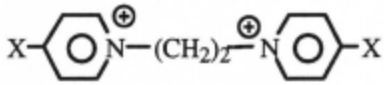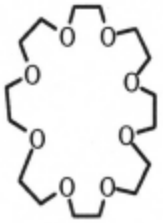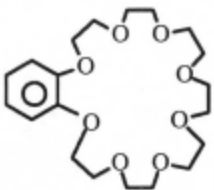
Linear Component	Cyclic Component	Method	Stoichiometry L:C	Yield (%) or K (L mol^{-1})	Ref.
		threading			95
X = H			1:1	165[a]	
Me			1:1	105[a]	
Ph			1:1	160[a]	
CO$_2$Et			1:1	320[a]	
		threading			95
X = H			1:1	195[a]	
Me			1:1	205[a]	
Ph			1:1	300[a]	
CO$_2$Et			1:1	740[a]	

Table 9 Continued. Low Molar Mass Pseudorotaxanes From N,N'-Dipyridylethane Type Systems with Tetrafluoroborate Counterions

Linear Component	Cyclic Component	Method	Stoichiometry L:C	Yield (%) or K (L mol^{-1})	Ref.
	3	threading			95
X = H			1:1	180[a]	
Me			1:1	230[a]	
Ph			1:1	320[a]	
CO$_2$Et			1:1	1200[a]	

[a] MeCN at 25°C.

Table 10. Low Molar Mass Pseudorotaxanes and Rotaxanes by Threading from Mixed Systems with Hexafluorophosphate Counterions
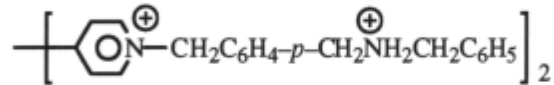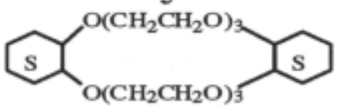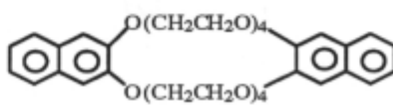
Linear Component	Cyclic Component	"Stopper" (Z)	Stoichiometry L:C	Yield (%)	Ref.
	3	none	1:2	-	100, 101
	3, 5	none	$1:2:1^a$	-	100
	5	none	1:1	-	100, 101
	5	none	a	-	100
		none	1:2	-	101
		none	1:1	-	101

481

Table 10 Continued. Low Molar Mass Pseudorotaxanes and Rotaxanes by Threading from Mixed Systems with Hexafluorophosphate Counterions
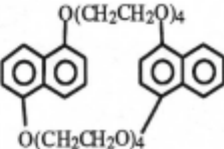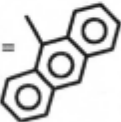
Linear Component	Cyclic Component	"Stopper" (Z)	Stoichiometry L:C	Yield (%)	Ref.
"		none	1:1	-	101
$ZCH_2\overset{\oplus}{N}H_2CH_2CH_2C_6H_4\text{-}p\text{-}CH_2\text{-}N$ ⊕ ⊕ $N\text{-}CH_2Z$					
	3	$C_6H_3(Bu\text{-}t)_2$	1:1	38%	98, 99

Table 10 Continued. Low Molar Mass Pseudorotaxanes and Rotaxanes by Threading from Mixed Systems with Hexafluorophosphate Counterions

Linear Component	Cyclic Component	"Stopper" (Z)	Stoichiometry L:C	Yield (%)	Ref.

ZCH$_2$NH$_2$CH$_2$C$_6$H$_4$-p-CH$_2$-N⊕◯◯⊕N-CH$_2$Z'

3

Z =

Z' = C$_6$H$_3$(Bu-t)$_2$

| | | | 1:1 | 30% | 98, 99 |

[a] Bipyridinium moiety forms a 1:1 complex with one equivalent of **5**; the ammonium ions from two different linear species also form 2:1 complexes with **5** when **5** an excess of **5** is added.

12.2.2.3.e   Complexation of Macrocycles Containing 4,4-Bipyridinium Units

These systems have been made by reversing the methodology used for the complexation of 4,4'-bipyridinium salts discussed above. The p-electron deficient macrocycle **19** was prepared by Stoddart and co-workers [102] and stable rotaxane species could be formed when this cyclic species was combined with p-electron rich species such as aromatic ethers. [103]   Since this development, a number of rotaxanes have been prepared using this method, as demonstrated in Tables 11 and 12.

The association constants for several series of donor species have been determined by Stoddart and co-workers [84-86] and by Kaifer and co-workers [104], and like the crown ether/bipyridinium systems, many of these systems form strong complexes. As a result, a number of rotaxanes that possess one, [105-110] or several, [111,112] aromatic donor sites have been prepared by Stoddart and co-workers. A unique [2]pseudorotaxane has also been prepared by Kimura and co-workers. [113] The donor species for this structure is a zinc phthalocyanine with four polyether substituents containing p-electron rich hydroquinone segments. These substituents are able to complex effectively with macrocycle **19.** While the complexation of each individual substituent resembles a [2]pseudorotaxane, they are all connected to the central zinc phthalocyanine so the formation of a 1:4 complex with the macrocycle is actually observed.

This complexation motif has also been used by Stoddart and co-workers [114] to make hydrogen bonded superstructures similar to those used in the ammonium ion systems. [33,34] In this case macrocycle **19** forms a complex with an aromatic ether donor species that has terminal carboxylic acid groups.   The formation of intermolecular hydrogen bonds between these carboxyl   functionalities   generates   a   non-covalently   bonded "pseudopolypseudorotaxane".

Table 11. Bipyridinium Macrocycle-Based Low Molar Mass Pseudorotaxanes

Linear Component		Cyclic Component	Method	Stoichiometry L:C	Yield (%) or K (L mol^{-1})	Ref.

X	Y	Cyclic Component	Method	Stoichiometry L:C	Yield (%) or K (L mol^{-1})	Ref.
OH	OH	**19**	threading	1:1	18[a]	104
O(CH$_2$)$_2$OH	O(CH$_2$)$_2$OH	**19**	threading	1:1	340[a]	104
(OCH$_2$CH$_2$)$_2$OH	(OCH$_2$CH$_2$)$_2$OH	**19**	threading	1:1	3400[a]	104
			threading	1:1	2200[a]	86
O(CH$_2$)$_2$OCH$_3$	O(CH$_2$)$_2$OCH$_3$	**19**	threading	1:1	290[a]	104
(OCH$_2$CH$_2$)$_2$OCH$_3$	(OCH$_2$CH$_2$)$_2$OCH$_3$	**19**	threading	1:1	3200[a]	104
			threading	1:1	3800[a]	84
OCH$_2$CH$_2$CH$_3$	OCH$_2$CH$_2$CH$_3$	**19**	threading	1:1	28[a]	104
O(CH$_2$)$_2$OCH$_2$CH$_2$CH$_3$	O(CH$_2$)$_2$OCH$_2$CH$_2$CH$_3$	**19**	threading	1:1	320[a]	104
O(CH$_2$)$_2$O(CH$_2$)$_2$SH	O(CH$_2$)$_2$O(CH$_2$)$_2$SH	**19**	threading	1:1	180[a]	104
O(CH$_2$)$_5$OH	O(CH$_2$)$_5$OH	**19**	threading	1:1	54[a]	104
CH$_2$O(CH$_2$CH$_2$O)$_2$H	CH$_2$O(CH$_2$CH$_2$O)$_2$H	**19**	threading	1:1	3200[a]	104
O(CH$_2$)$_5$CH$_3$	O(CH$_2$)$_5$CH$_3$	**19**	threading	1:1	22[a]	104
O(CH$_2$CH$_2$O)$_2$CH$_2$CH$_2$SH	O(CH$_2$CH$_2$O)$_2$CH$_2$CH$_2$SH	**19**	threading	1:1	1200[a]	104
OBn	(OCH$_2$CH$_2$)$_2$OH	**19**	threading	1:1	75[a]	105

Table 11 Continued. Bipyridinium Macrocycle-Based Low Molar Mass Pseudorotaxanes
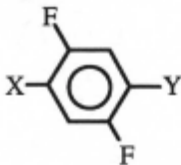
Linear Component		Cyclic Component	Method	Stoichiometry L:C	Yield (%) or K (L mol^{-1})	Ref.
X	Y					
$(OCH_2CH_2)_2OCH_2COOH$	$(OCH_2CH_2)_2OCH_2COOH$	19	threading	1:1	-	114
$(OCH_2CH_2)_3OCH_2COOH$	$(OCH_2CH_2)_3OCH_2COOH$	19	threading	1:1	-	114
$OOCCH_2O(CH_2)_2OMe$	$OOCCH_2O(CH_2)_2OMe$	19	threading	1:1	320[a]	84
$OCH_2COO(CH_2)_2OMe$	$OCH_2COO(CH_2)_2OMe$	19	threading	1:1	520[a]	84
$O(CH_2)_2OOCCH_2OMe$	$O(CH_2)_2OOCCH_2OMe$	19	threading	1:1	130[a]	84
$O(CH_2)_2OCH_2COOMe$	$O(CH_2)_2OCH_2COOMe$	19	threading	1:1	1000[a]	84
$(OCH_2CH_2)_2OCH_2COOMe$	$(OCH_2CH_2)_2OCH_2COOMe$	19	threading	1:1	2400[a]	84
$(OCH_2CH_2)_3OCH_2COOMe$	$(OCH_2CH_2)_3OCH_2COOMe$	19	threading	1:1	4300[a]	84
$OOCCH_2O(CH_2)_2OMe$	$(OCH_2CH_2)_2OCH_3$	19	threading	1:1	300[a]	84
$OCH_2COO(CH_2)_2OMe$	$(OCH_2CH_2)_2OCH_3$	19	threading	1:1	680[a]	84
$O(CH_2)_2OOCCH_2OMe$	$(OCH_2CH_2)_2OCH_3$	19	threading	1:1	430[a]	84

X—◯—Y   X = Y = $(OCH_2CH_2)_2OH$, with F substituents on the benzene ring   19   threading   1:1   15[a]   86

$p-C_6F_4[(OCH_2CH_2)_2OH]_2$ 19   threading   1:1   0[a]   86

Table 11 Continued. Bipyridinium Macrocycle-Based Low Molar Mass Pseudorotaxanes

Linear Component		Cyclic Component	Method	Stoichi-ometry L:C	Yield (%) or K (L mol^{-1})	Ref.

$1,5–X, Y–C_{10}H_6$

X	Y					
$(OCH_2CH_2)_2OH$	$(OCH_2CH_2)_2OH$	19	threading	1:1	>5000[a]	86
$S(CH_2)_2O(CH_2)_2OCH_3$	$S(CH_2)_2O(CH_2)_2OCH_3$	19	threading	1:1	1010[a]	85
$(OCH_2CH_2)_2OCH_3$	$(OCH_2CH_2)_2OCH_3$	19	threading	1:1	>5000[a]	85
$(OCH_2CH_2)_2SCH_3$	$(OCH_2CH_2)_2SCH_3$	19	threading	1:1	1430[a]	85
$O(CH_2)_2S(CH_2)_2OCH_3$	$O(CH_2)_2S(CH_2)_2OCH_3$	19	threading	1:1	184[a]	85
OBn	$(OCH_2CH_2)_2OCH_2R$	19	threading	1:1	910[a]	105
	R = 18-crown-6					
$1,6–C_{10}H_6[(OCH_2CH_2)_2OH]_2$		19	threading	1:1	378[a]	86
$2,6–C_{10}H_6[(OCH_2CH_2)_2OH]_2$		19	threading	1:1	177[a]	86
$2,7–C_{10}H_6[(OCH_2CH_2)_2OH]_2$		19	threading	1:1	221[a]	86

Table 11 Continued. Bipyridinium Macrocycle-Based Low Molar Mass Pseudorotaxanes
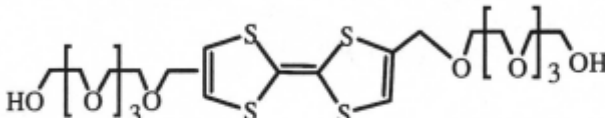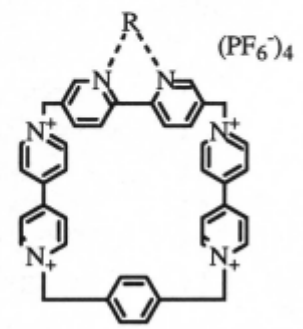
Linear Component	Cyclic Component	Method	Stoichi-ometry L:C	Yield (%) or K (L mol^{-1})	Ref.
	19	threading	1:1	5×10^{4a}	107
1,5–$C_{10}H_6[(OCH_2CH_2)_2OH]_2$		clipping clipping clipping	1:1 1:1 1:1	$4.4 \times 10^{3\,b}$ $7.1 \times 10^{4\,b}$ $5.1 \times 10^{3\,a}$	106 106 106

$R = Re(CO)_3Cl$
$=$ no metal
$=$ no metal

Table 11 Continued. Bipyridinium Macrocycle-Based Low Molar Mass Pseudorotaxanes

Linear Component	Cyclic Component	Method	Stoichiometry L:C	Yield (%) or K (L mol^{-1})	Ref.
$R_1 = O(CH_2CH_2O)_3C_6H_4\text{-}p\text{-}(OCH_2CH_2)_3OCH_3$ $R_2 = OCH_3$	**19**	threading	1:4	1200 ± 200^a	113
		clipping	1:1	24%	108
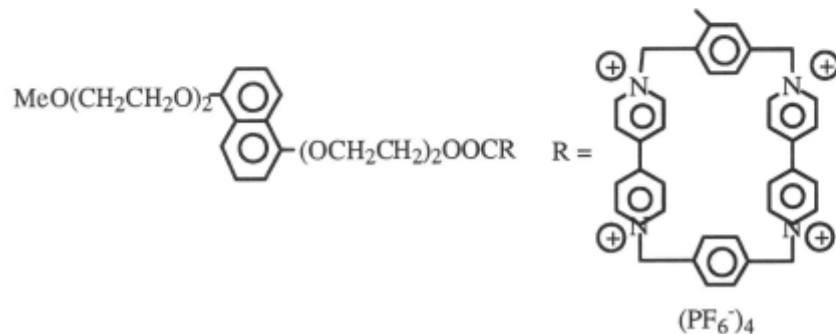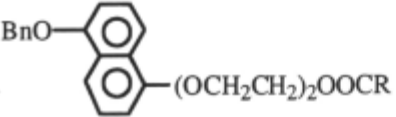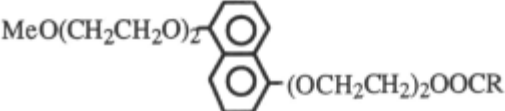
Table 11 Continued. Bipyridinium Macrocycle-Based Low Molar Mass Pseudorotaxanes

Linear Component	Cyclic Component	Method	Stoichi-ometry L:C	Yield (%) or K (L mol⁻¹)	Ref.

Linear Component:

BnO—(O)(O)—(OCH$_2$CH$_2$)$_2$OOCR

| | R = " | clipping | 1:1 | 7% | 108 |

MeO(CH$_2$CH$_2$O)$_2$—(O)(O)—(OCH$_2$CH$_2$)$_2$OOCR

| | R = " | clipping^c | 1:1 | 30% | 108 |

^{a} MeCN at 25°C. ^{b} H$_2$O at 25°C. ^{c} Macrocycle is formed by the clipping procedure; self-association of the aromatic moiety of R with the bispyridinium units during the clipping process yields the rotaxane.

Table 12. Bipyridinium Macrocycle-Based Low Molar Mass Rotaxanes
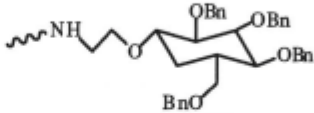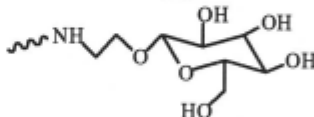
Linear Component	Cyclic Component	"Stopper" (Z)	Method	Stoichiometry L:C	Yield (%) or K (L mol^{-1})	Ref.
$p\text{-}C_6H_4\!\left[(OCH_2CH_2)_3OCH_2COZ\right]_2$	19		Clipping	1:1	7%	110
"	19		Slippage	1:1	-	110
$O\!\left[(CH_2CH_2O)_nCH_2C_6H_4\text{-}p\text{-}CH_2(OCH_2CH_2)_3OZ\right]_2$						
n = 2	19	$-Si(iPr)_3$	Clipping	1:1	32%	112
n = 3	19	$-p\text{-}C_6H_4CPh_3$	Clipping	1:1	8%	112
$ZO(CH_2CH_2O)_3C_6H_4\text{-}p\text{-}O(CH_2CH_2O)_3C_6H_4\text{-}m\text{-}O(CH_2CH_2O)_3Z$						
	19	"	clipping	1:1	11%	111

As seen in Table 12, many of these rotaxanes have been synthesized by the third method for rotaxane formation known as 'clipping'.

Table 12 Continued. Bipyridinium Macrocycle-Based Low Molar Mass Rotaxanes
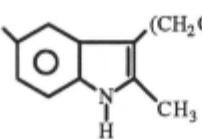
Linear Component	Cyclic Component	"Stopper" (Z)	Method	Stoichiometry L:C	Yield (%) or K (L mol⁻¹)	Ref.

$$m-C_6H_4\left[O(CH_2CH_2O)_3C_6H_5-p-O(CH_2CH_2O)_3Z\right]_2$$

| | 19 | " | clipping | 1:1 | 12% | 111 |

$$p-C_6H_4\left[O(CH_2CH_2O)_3C_6H_5-m-O(CH_2CH_2O)_3Z\right]_2$$

| | 19 | " | clipping | 1:1 | 14% | 111 |

ZO(CH₂CH₂O)₃ — (CH₂CH₂O)₄C₆H₄–p– (OCH₂CH₂)₃OZ

| | 19 | " | Clipping | 1:1 | 9% | 112 |

Linear Component	Cyclic Component	"Stopper" (Z)	Method	Stoichiometry L:C	Yield (%) or K (L mol^{-1})	Ref.

(OCH$_2$CH$_2$)$_6$OC$_6$H$_4$ –p–O(CH$_2$CH$_2$O)$_3$Z
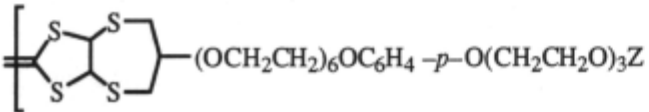
	19	"	Clipping	1:1	8%	112
p–C$_6$H$_4$[O(CH$_2$CH$_2$O)$_2$Z]$_2$	**19**	12-crown-4	slippage	1:1	610[a]	109
"		15-crown-5	slippage	1:1	5100[a] 370[b] 180[c]	109
"		18-crown-6	clipping	1:1	10%	109
p–C$_6$H$_4$[(OCH$_2$CH$_2$)$_2$OCH$_2$COZ/Z']$_2$	**19**	Z = Z' = –NH	clipping	1:1	6%	109

Table 12 Continued. Bipyridinium Macrocycle-Based Low Molar Mass Rotaxanes
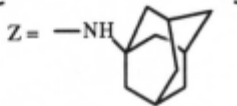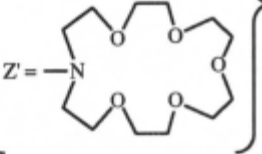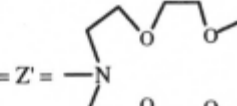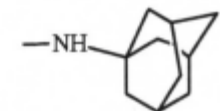
Linear Component	Cyclic Component	"Stopper" (Z)	Method	Stoichiometry L:C	Yield (%) or K (L mol^{-1})	Ref.
"	19	Z = —NH (adamantyl) Z' = —N (crown)	slippage	1:1	86%	109
"	19	Z = Z' = —N (crown)	slippage	1:1	80%	109
1,5–C$_{10}$H$_6$[(OCH$_2$CH$_2$)$_3$COZ]$_2$	20	—NH— (adamantyl)	clipping	2:1	7%	115

Linear Component	Cyclic Component	"Stopper" (Z)	Method	Stoichiometry L:C	Yield (%) or K (L mol^{-1})	Ref.
$1,5-C_{10}H_6 \left[(OCH_2CH_2)_3OCZ \right]_2$	$(PF_6^-)_4$		clipping[d]	1:1	13%	108

[a] MeCN at 25°C. [b] MeCN at 50°C. [c] MeCN at 75°C. [d] Macrocycle is formed by the clipping procedure; self-association of the naphthyl moiety of R with the bispyridinium units during the clipping process yields the rotaxane.

In this procedure, the bipyridinium ring is synthesized in the presence of the linear species, with the linear component serving as a template for the cyclization process (Scheme 3).
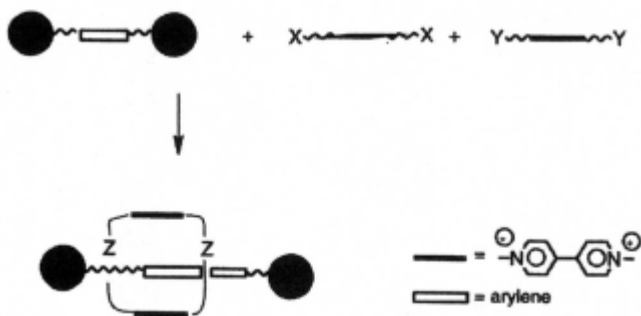
Scheme 3. "Clipping" method of rotaxane synthesis using the stoppered linear species as a template for cyclization.

As noted, a number of rotaxanes have been synthesized by this approach, but a unique example is the bis[2]rotaxane synthesized by Stoddart and co-workers. [115] The bismacrocycle **20**, which is assembled around two linear aromatic ethers by the clipping method, is shown below.

15
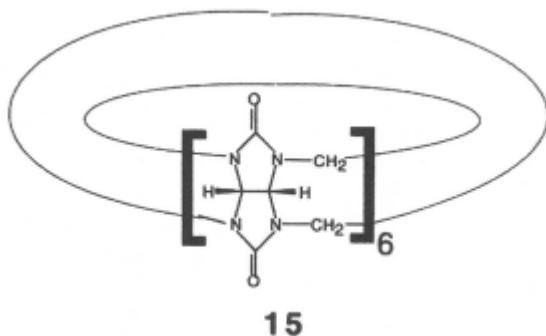
12.2.3 Synthetic Methods for High Molar Mass Rotaxanes (Polyrotaxanes)

When rotaxane structures are incorporated into polymers, a wide range of architectures is possible. As the location of the rotaxane units is varied, the physical and chemical properties of the polymer can be changed dramatically. To provide some clarity, the possible polymer architectures that can be constructed are divided into two main categories: main-chain and side-chain systems. As the name implies, main-chain systems are those in which the rotaxane unit is incorporated directly into the polymer backbone. Consequently, in side-chain polyrotaxanes, the rotaxane structure is part of the polymer side chains. The various polymer architectures that can be obtained are pictured in Scheme 4. Systems that contain blocking groups or stoppers **(a)**, i.e., true polyrotaxanes and those that do not **(b)**, i.e., polypseudorotaxanes, are both represented.
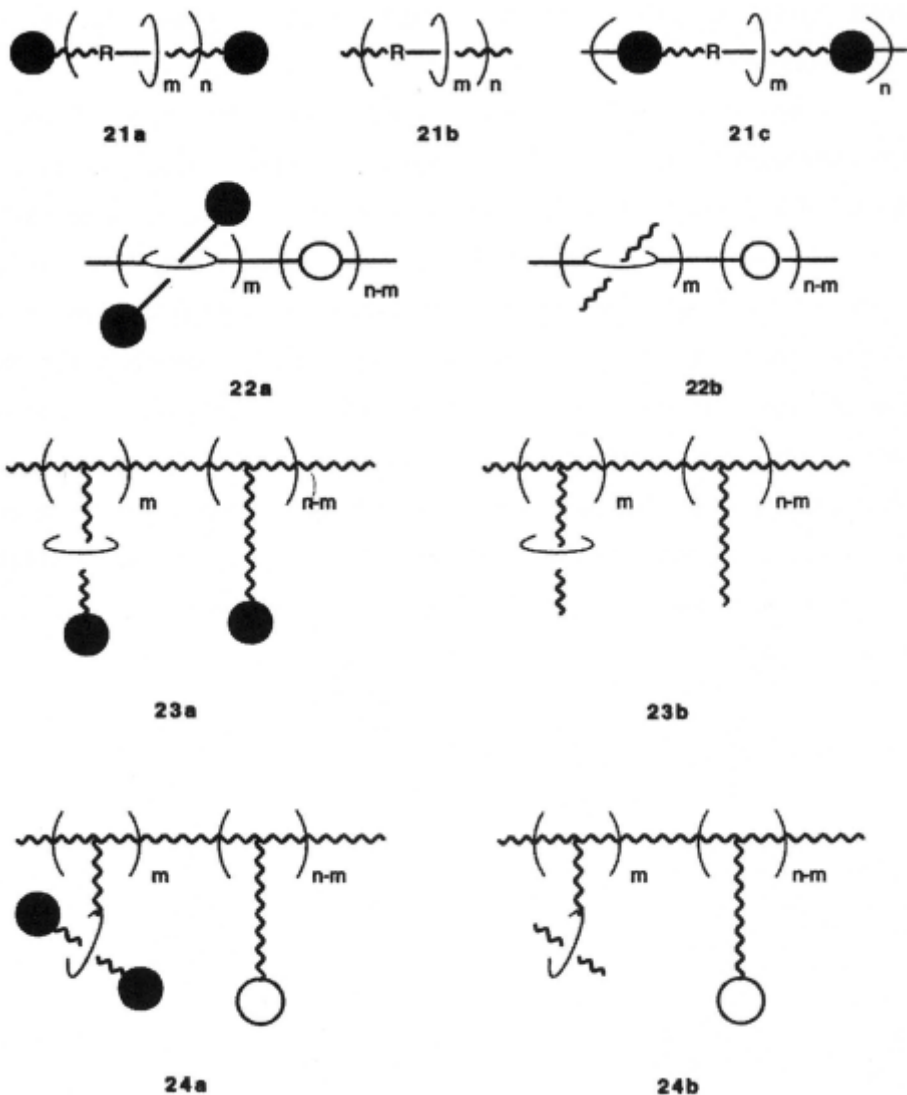
Scheme 4. Various types of polyrotaxane architectures: Main chain

(21 and 22) and side chain (23 and 24) with stoppers (a,c) and without (b)

For each type of polymer depicted in Scheme 4, there are a number of possible routes to the final structure. Scheme 5 demonstrates the methods that can be utilized to form main-chain polypseudorotaxanes (21b) in which the

linear unit is polymeric and the cyclic unit is of low molar mass. Conversely, the cyclic unit can be incorporated into the polymer backbone and a linear species of low molar mass can be used to form the rotaxane. Synthetic routes to polyrotaxanes of this type **(22)** are depicted in Scheme 6. The side-chain polyrotaxane systems can also have either the linear component **(23)** or the cyclic component **(24)** attached to the polymer. The rotaxane structure is then completed when the other low molar mass component, cyclic or linear respectively, is introduced. Methods of preparation for these side-chain polyrotaxanes are shown in Schemes 7 (type **23)** and 8 (type **24)**. Although many of these routes are still largely unexplored, the reported syntheses of polyrotaxanes from the last three years will be discussed in the next section. As an arbitrary means of comparison, the rotaxane content will be reported in terms of the number of cyclics per repeat unit, m/n, when possible.

500

1. **Chemical Conversion**
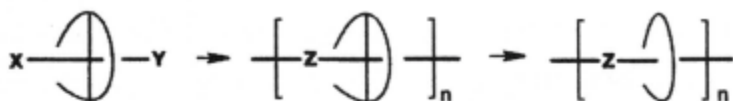
2. **Cyclization in presence of linear macromolecule (clipping)**
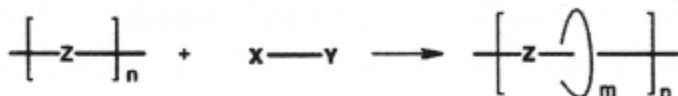
3. **Polymerization of monomeric rotaxane**
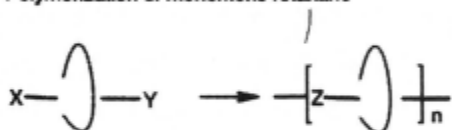
4. **Threading of preformed linear macromolecule through preformed macrocycle**
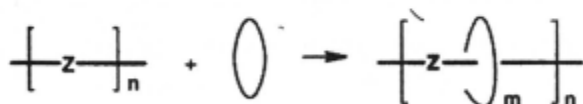
5. **Production of linear macromolecule in the presence of preformed macrocycle**
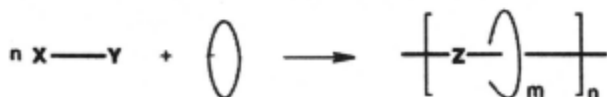
Scheme 5. Potential routes to main-chain polyrotaxanes of type **21b** in which functional groups X and Y react to form Z.

1. Chemical Conversion
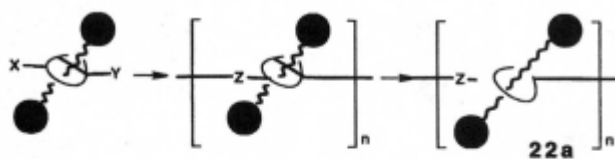
2. Polymerization of Preformed Rotaxane
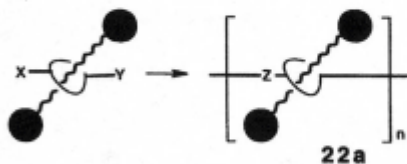
3. Threading of Linear Molecule Through Preformed Polymacrocycle
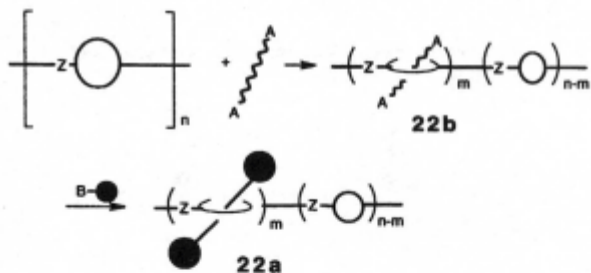
4. Polymerization of Macrocycle in Presence of Linear Species
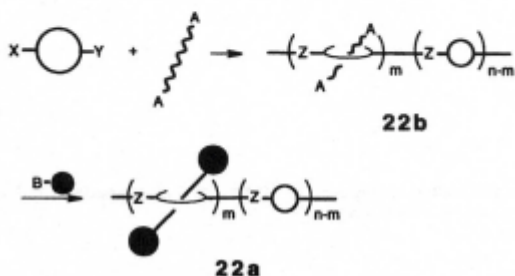
Scheme 6. Potential routes to main chain polyrotaxanes of type **22** in which functional groups X and Y react to form Z moieties and A and B also form covalent bonds

502

Scheme 7. Potential routes to side chain polyrotaxanes of type **23** in which functional groups X and Y react to produce Z moieties and A and B also form covalent bonds.

1. Chemical Conversion
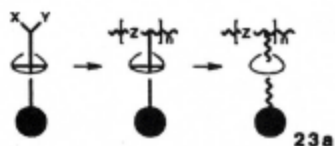
2. Threading of Preformed Graft Copolymer or Pendant Polymacrocycle
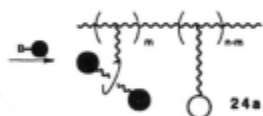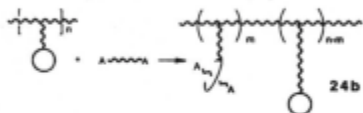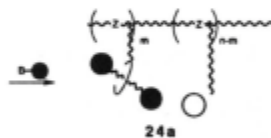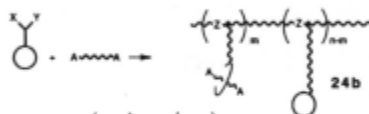
3. Grafting in Presence of Linear Species

4. Grafting of Preformed Rotaxane

5. Polymerization in Presence of Linear Species
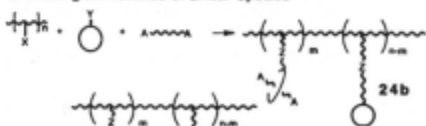
6. Polymerization of Preformed Rotaxane

Scheme 8. Potential route to side chain polyrotaxanes of type **24** in which functional groups X and Y react to form Z moieties and A and B also form covalent bonds.

12.2.3.1 The 'Directed' or 'Chemical Conversion' Approach
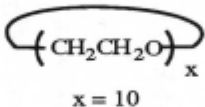
As with the low molar mass rotaxanes, this approach has not been used in the synthesis of any polyrotaxanes during the time frame that is being reviewed here. In fact, it has previously been reported [11] that this approach has not ever been used in the synthesis of polyrotaxanes. This is most likely due to the complex chemistry and large number of synthetic steps that would be needed to efficiently produce polyrotaxanes by this route.

12.2.3.2 Statistical Threadings

Repeating the trend seen with low molar mass rotaxanes, the search for more efficient routes to rotaxanes and polyrotaxanes has led to the increased use of methods that are enthalpically driven and a decrease in the use of the statistical threading method. As summarized in Table 13, only a few examples of polypseudorotaxanes of type **21b** produced in the latter manner have been reported. In these cases, the use of statistical threadings has generally been necessitated by the fact that the use of an enthalpic interaction to drive complexation was not possible.

Gibson and co-workers [116,117] have reported further work on the synthesis of polystyrene by free radical methods using a bulky, blocking group initiator. The initiator is azo-based, but contains a bulky tri- or tetraarylmethyl unit that is designed to block the chain ends once the polymerization is terminated, and therefore prevent dethreading. These initiators were shown to be effective for the homepolymerization of styrene. When the polymerization was conducted in the presence of smaller crown ethers such as BPP34C10 (5) or 30-crown-10 to produce polyrotaxanes of type **21a**, the m/n value corresponded to approximately one cyclic per polymer chain. Use of a mixture of larger crown ethers produced higher m/n values corresponding to approximately 4 cyclics per chain.

Table 13. Main Chain Polyrotaxanes of Type **21** From Statistical Threading

Linear Component	Cyclic Component	"Stopper"	Method	M_n(kg·mol^{-1})	m/n	Mass % Cyclic	Ref.
polystyrene	**5**	a	a	16.4[b]	c	<1	117
				9.6[b,d]	c	3.0	
				12.4[b,d]	c	3.5	
polystyrene	$\text{--}(CH_2CH_2O)\text{--}_x$ x = 10	e	e	27.7	c	1.4	117
polystyrene	$\overline{x} = 30$	f	f	23.4	≈ 0.02	21	116
polystyrene	$\overline{x} = 54.5$	f	f	23.4[b,d]	0.04	21	117
				49.3[b,g]	0.008	2.6	
				23.8[b,g,h]	0.02	12	
				18.5[b,d]	0.025	13	
				2.6[b,d]	0.06	26	

[a] Initiation with $[(Ar)_2(C_6H_4\text{-}p\text{-})C(CH_2)_3OOC(CH_2)_2C(CH_3)(CN)N]_2$ in the presence of crown ether; $Ar = p\text{-}C_6H_4\text{-tBu}$.
[b] varying feed ratio of crown ether
[c] less than one cyclic per macromolecule. [d] toluene as solvent. [e] Initiation with $[Ar_3CC_6H_4\text{-}p\text{-}OOC(CH_2)_2C(CH_3)(CN)N]_2$ in the presence of crown ether; $Ar = p\text{-}C_6H_4\text{-tBu}$. [f] Initiation with $[Ar_3CC_6H_4\text{-}p\text{-}OOC(CH_2)_2C(CH_3)(CN)N]_2$ in the presence of a mixture of crown ethers; $Ar = p\text{-}C_6H_4\text{-tBu}$. [g] benzene as solvent.
[h] AIBN as initiator

These results follow the expected trend for a statistical threading as the ring size is increased.

Gibson and Bheda [118] also report the synthesis of a styrene monomer that contains the tetraarylmethyl blocking group. This monomer was shown to polymerize effectively under free radical conditions, generating a polystyrene backbone with the bulky blocking groups as side chains. Polymerization of the monomer in the presence of a crown ether (Scheme 7, method 6) could produce side-chain polyrotaxanes of type **23a**, but this has yet to be reported.

Finally, Pugh and co-workers [119,120] have suggested a novel approach to the formation of homopolyrotaxanes of poly(ethylene oxide). The cyclic species in this approach is an amphiphilic crown ether with an average ring size of 42 atoms attached to a hydrophobic 12-carbon tail. This macrocycle can organize to form columnar micelles in benzene or toluene in the presence of water. When a poly(ethylene oxide) derivative with low water solubility is added, the polymer can be threaded through the micelles, and hence solubilized. The end groups can then be capped with a bulky blocking group to yield the homopolyrotaxane. Although evidence of this end-capping reaction has been observed, the polyrotaxane product was not isolated.

12.2.3.3 Enthalpically Driven or Host-Guest-Based Polyrotaxane Syntheses
12.2.3.3.a Hydrogen Bonding

In the discussion of low molar mass rotaxanes, it was demonstrated that hydrogen bonding between the hydroxyl groups of alcohols and crown ethers could provide an enthalpic driving force for rotaxane formation. This principle can also be applied to the synthesis of polyrotaxanes. In the synthesis of polyesters and polyurethanes, the hydroxyl groups of the glycol monomers can also associate with crown ethers. When this occurs, subsequent reaction to form the ester or urethane linkage traps the cyclic species and leads to the formation of the polyrotaxane. The use of this technique in the formation of

polyrotaxanes, generally of types **21a** and **b**, has previously been used and reported. [11]

The new polyrotaxanes that have been synthesized by this method are summarized in Table 14. Gibson and co-workers [121-126] have reported further efforts in the synthesis of poly(ester rotaxane)s, particularly those in which a difunctional alcohol containing a bulky blocking group is used as a monomer to generate polyrotaxanes of type **21c**. In the preparation of a sebacate-based poly(ester 30-crown-10 rotaxane), the threading efficiency, m/n, was found to be 5 times higher in the presence of a diol blocking group. [123] The threading efficiency for the formation of poly(ester rotaxane)s could be improved even further if both the dialcohol and the diacid monomers incorporated blocking groups. These polyrotaxanes, which contained two blocking groups per repeat unit, had threading efficiencies almost 14 times as high as polyrotaxanes that did not contain a blocking group. [126]

Using this trapping methodology, Gibson and Gong [125] were able to compare the threading efficiencies for different macrocycles. Polyrotaxanes were synthesized using 30-crown-10, a mixture of 30-crown-10 and BPP34C10 (**5**), and a mixture of 30-crown-lO and DB24C8 (**3**) as solvent. From these reactions it was determined that BPP34C10 had a relative threading efficiency of 1.4 compared to 30-crown-lO, while that of DB24C8 was only 0.84 under these polymerization conditions.

The combination of blocking groups and hydrogen bonding interactions has also been used for the synthesis of poly(urethane/crown ether rotaxane)s. [127,128] For these polymers it was found that the threading efficiencies were better than those for poly(ester rotaxane)s. Because the crown ether can form hydrogen bonds with in-chain NH groups, the rate of dethreading is slowed with respect to the polyester, thus leading to the greater threading efficiency. In another example of polyrotaxanes of type **21a** made by this method, Gibson and

Table 14. Polyrotaxanes of Types 21 and 22 From Hydrogen-Bonding Interactions

Backbone Component	Cyclic Component	"Stopper"	Method	M_n(kg·mol^{-1})	m/n	Ref.
$y = 4$	$\overline{x} = 14$	none	a	29.5	0.32	122,124
$y = 6$	$\overline{x} = 14$	none	a	8.3	0.30	122,124
$y = 10$	$x = 10$	none	a	32.8	0.012	122,124
	$\overline{x} = 12$	none	a	14.3	0.22	122,124
	$\overline{x} = 14$	none	a	8.3	0.29	122,124
	$\overline{x} = 16$	none	a	11.4	0.34	122,124
	$\overline{x} = 20$	none	a	10.7	0.36	122,124
$-[COO(CH_2)_8COORO]_n-$	$x = 10$	built-in				
$R = C(p-C_6H_4C_4H_9-t)_2\,[p-C_6H_4(OCH_2CH_2)_2]_2-$			b	6.0	0.019	126
				12.0	0.083	126

Table 14 Continued. Polyrotaxanes of Types **21** and **22** From Hydrogen-Bonding Interactions

Backbone Component	Cyclic Component	"Stopper"	Method	$M_n(kg\cdot mol^{-1})$	m/n	Ref.

$$-\left\{\left[OROOC(CH_2)_8CO\right]_y\left[O(CH_2)_{10}OOC(CH_2)_8CO\right]_{1-y}\right\}_n-$$

$$R = C(p-C_6H_4C_4H_9-t)_2\left[p-C_6H_4(OCH_2CH_2)_2\right]_2$$

y=0	x = 10	none	c	32.8	0.012	121
y=1	"	built-in	c	16.5	0.061	121,123
y=0.1	"	built-in	c	17.2	0.021	121
y=0.4	"	built-in	c	22.4	0.035	121
y=0.7	"	built-in	c	17.2	0.050	121

Table 14 Continued. Polyrotaxanes of Types 21 and 22 From Hydrogen-Bonding Interactions

Backbone Component	Cyclic Component	"Stopper"	Method	$M_n(kg \cdot mol^{-1})$	m/n	Ref.
$\left[O-R_1-OOC-R_2-COO \right]_n$	d	built-in	e	-	d	125

$R_1 = C(p-C_6H_4C_4H_9-t)_2 \left[p-C_6H_4(OCH_2CH_2)_2 \right]_2$

$R_2 = C(p-C_6H_4C_4H_9-t)_2 \left[p-C_6H_4(OCH_2CH_2)_5 \right]_2$

"	f	built-in	e	-	f	125
.						
"	$(CH_2CH_2O)_{10}$	built-in	g	-	0.11	125
			h	9.0	0.043	126
			h	8.9	0.155	126
			h	25.2	0.173	126

Table 14 Continued. Polyrotaxanes of Types 21 and 22 From Hydrogen-Bonding Interactions

Backbone Component	Cyclic Component	"Stopper"	Method	M_n(kg·mol^{-1})	m/n	Ref.

$$\text{---}\left[\text{OCH}_2\text{CH}_2\text{OOCNH(CH}_2)_6\text{NHCO}\right]_n$$

| | | none | i | 20.0 (M$_w$) | - | 130 |

$$\text{---}\left[(\text{OCH}_2\text{CH}_2\text{O})_4\text{OCNHC}_6\text{H}_4 \text{ --}p\text{--CH}_2\text{C}_6\text{H}_4\text{--}p\text{-- NHCO}\right]_n\text{---}$$

$$\left(\text{CH}_2\text{CH}_2\text{O}\right)_x$$

	$\overline{x} = 20$	none	j	8.03	0.89	129
	"	none	j	7.5	0.58	129
	"	none	j	-	0.34	129
	$\overline{x} = 14$	none	j	19.3	0.29	129
	$\overline{x} = 12$	none	j	7.24	0.16	129

Table 14 Continued. Polyrotaxanes of Types **21** and **22** From Hydrogen-Bonding Interactions
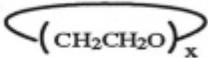
Backbone Component	Cyclic Component	"Stopper"	Method	$M_n(kg \cdot mol^{-1})$	m/n	Ref.
"	$(CH_2CH_2O)_x$					
	$\overline{x} = 14$	none	k	16.6 (backbone)	0.092	131
	"	none	k	16.6 (backbone)	0.178	131
	"	none	k	16.6 (backbone)	0.192	131
	"	none	k	16.6 (backbone)	0.201	131
	$\overline{x} = 10$	none	k	16.6 (backbone)	0.065	131
	$\overline{x} = 14$	none	1	16.6 (backbone)	0.085	131

Table 14 Continued. Polyrotaxanes of Types **21** and **22** From Hydrogen-Bonding Interactions
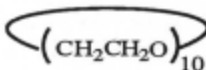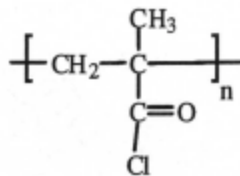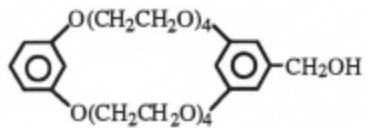
Backbone Component	Cyclic Component	"Stopper"	Method	M_n(kg·mol^{-1})	m/n	Ref.

$$\left[\!\left[OR''OOCNHR'NHCO \right]_x\!\left[OROOCNHR'NHCO \right]_{1-x}\right]_n$$

R = $-(CH_2CH_2O)_3CH_2CH_2-$; R' = $p-C_6H_4CH_2-p-C_6H_4$; R'' = $C\,(p-C_6H_4C_4H_9-t)_2\!\left[p-C_6H_4(OCH_2CH_2)_2 \right]_2$

	$(CH_2CH_2O)_{10}$	built-in	m	17.8	0.032	127,128
	"	built-in	m	22.6	0.036	127,128
	"	built-in	m	12.4	0.040	127,128
	"	built-in	m	18.7	0.045	127,128
	"	built-in	m	23.4	0.49	127,128

$$\left[CH_2-\overset{\overset{\displaystyle CH_3}{|}}{\underset{\underset{\displaystyle Cl}{\overset{|}{C=O}}}{C}} \right]_n$$

Cyclic component: O(CH₂CH₂O)₄ ... O(CH₂CH₂O)₄ bridged diphenyl with –CH₂OH

			n	o	102.8	n	133
					135.5	n	133

513

Table 14 Continued. Polyrotaxanes of Types **21** and **22** From Hydrogen-Bonding Interactions

Backbone Component	Cyclic Component	"Stopper"	Method	$M_n(kg \cdot mol^{-1})$	m/n	Ref.

X = (backbone structure with $O(CH_2CH_2O)_4$ groups)

$X = COO$—(phenyl)—$C(CH_3)_2$—(phenyl)—OOC
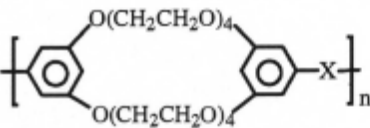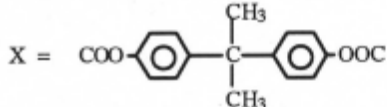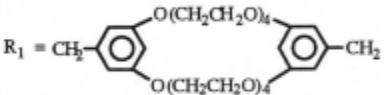
| | self-threaded | self-threaded | p | 49.4 | q | 134 |

$X = CH_2OOC(CH_2)_8COOCH_2$

| | self-threaded | self-threaded | r | s | s | 134 |

Table 14 Continued. Polyrotaxanes of Types **21** and **22** From Hydrogen-Bonding Interactions

Backbone Component	Cyclic Component	"Stopper"	Method	M_n(kg·mol^{-1})	m/n	Ref.

$$+[(OR_1O\,OCNHR_3NHCO)_x\,(OR_2O\,OCNHR_3NHCO)_{1-x}]_n+$$

$R_1 = CH_2$— (aromatic ring) —O(CH$_2$CH$_2$O)$_4$ ... O(CH$_2$CH$_2$O)$_4$ — (aromatic ring) —CH$_2$

$R_2 = (CH_2CH_2O)_3CH_2CH_2$

$R_3 = p\!-\!C_6H_4CH_2C_6H_4\!-\!p$

Cyclic Component	"Stopper"	Method	M_n(kg·mol^{-1})	m/n	Ref.
self-threaded	self-threaded	t	8.5	-	132
self-threaded	self-threaded	t	8.0	-	132
self-threaded	self-threaded	t	6.6	-	132
self-threaded	self-threaded	u	11.3	-	132
self-threaded	self-threaded	v	cross-linked	-	132

[a]Polymerization of diol and sebacoyl chloride in the presence of crown ethers at 80° C. [b]Polymerization at 153°C with 30C10/diol ratio of 2/1 or at 63°C with ratio of 4/1. [c]Polymerization of sebacoyl chloride, 1,10-decanediol, and blocking group diol with 30C10 as solvent at 63° C. [d]Polymerization in the presence of 30C10 and **5**; m/n for 30C10 was 0.051 while that for **5** was 0.069. [e]Polymerization in presence of 30C10 plus other macrocycle at 105°C for 2 days. [f]Polymerization in the presence of 30C10 and **3**; m/n for 30C10 was 0.055 while that for **3** was 0.046. [g]Polymerization in the presence of 30C10 at 105° C for 2 days. [h]Polymerization at 153°C with 30C10/diol ratio of 2/1 or at 63°C with ratios of 4/1 and 5/1. [i]Polymerization in presence of 30C10 with diglyme as cosolvent at 60° C for 12 hours. [j]Polymerization with crown ether as solvent at 90° C. [k]Threading onto performed polymer at crown/repeat unit ratios of 1/1 3/1, 5/1, 6/1 for 42C14 and 5/1 for 30C10 at 80°C for 3 days. [l]Threading onto performed polymer at 3/1 ratio and diglyme as cosolvent at 80° C for 3 days. [m]Polymerization of MDI, diol, and blocking group diol with 30C10 in varying ratios of blocking group diol at 96°C in DMF. [n]Self-threading led to branched or cross-linked structures, m/n not determined. [o]Reaction of poly(methacroyl chloride) with macrocyclic alcohol at varying feed ratios in pyridine. [p]Higashi method. [q]Threading not detected by ^{1}H-NMR NOESY experiments. [r]Bulk polymerization at 140°C. [s]Insoluble material, mechanically cross-linked. [t]Polymerization at 96°C with varying ratio of blocking group diol. [u]Polymerization of blocking group diol and MDI in diglyme at 96° C. [v]Bulk polymerization of blocking group diol and MDI at 96° C.

co-workers [129] report the synthesis of polyurethanes in the presence of crown ethers. As might be expected, the m/n value also increases as the ring size of the crown ether increases. Furthermore, infrared studies allowed an estimate of the strength of intra-annular hydrogen bonding of the crown ether with the methane moieties.

Although blocking groups were not utilized, Beckham and co-workers [130] have also synthesized an aliphatic poly(urethane rotaxane). Although threading efficiencies were not reported, it can be expected that the hydrogen bonding interactions would again result in higher values than seen for statistical threadings. The unique synthesis of a poly(urethane pseudorotaxane) by threading of a preformed polymer with the crown ether (Scheme 5, method 4) in the melt phase has been performed by Gibson and co-workers. [131] Once again, hydrogen bonding interactions contributed to high threading efficiencies.

In the formation of polyrotaxanes of type **22** using a difunctional hydroxy or carboxylic acid macrocycle, hydrogen bonding interactions have led to branched and cross-linked polyrotaxane structures [132-136] generated by self-threading interactions in situ. Like any alcohol or carboxylic acid, the hydroxyl functionality of one macrocycle can participate in hydrogen bonding with the crown ether oxygens of another macrocycle. If the bonded hydroxyl group is then incorporated into the polymerization, a self-threaded structure is generated, leading to branched or cross-linked structures. These polyrotaxanes are examples of type **22a** because, even though typical blocking groups are not present, the cross-linked or branched structures effectively prevent dethreading once self-threading has occurred.

12.2.3.3.b Cyclodextrin Inclusion Complexes

Polyrotaxanes based on cyclodextrins have been known for quite some time and were the basis of the first reported polyrotaxanes. [137] Despite being the oldest of the polyrotaxanes, a number of polyrotaxanes based on cyclodextrin inclusion complexes and hydrophobic interactions have recently been synthesized and are summarized in Tables 15 and 16.

In one series of papers, Yui and coworkers [138-140] prepared main chain polyrotaxanes of type **21a** by forming an inclusion complex between a-CD and poly(ethylene glycol) (Scheme 5, method 4). The end groups were then capped with phenylalanine to generate the polyrotaxane. Because the blocking groups are biodegradable and the threaded CD can then be released, it was hoped that these polyrotaxanes could be used for drug delivery applications. While several other CD-based polyrotaxanes have been prepared by the threading of preformed polymers, [141,142] the polymerization of a preformed inclusion complex (Scheme 5, method 3) has also generated polyrotaxanes of type **21a**. [143,144]

Side-chain polyrotaxanes of type **23** have also been prepared recently, using a variety of methods. Harada and co-workers [145] have measured the association constants for a number of polymers of type **23b** that had been formed via the inclusion complex between a-, **ß-,** and g-CD and the alkyl side chains of copolymers of acrylamide and the alkyl methacrylates (Scheme 7, method 3).

By performing the grafting of side chains in the presence CD (Scheme 7, method 4), side-chain polyrotaxanes of type **23a** have recently been prepared by Ritter [146] and Yamamoto and co-workers. [147] Ritter et al. have also reported the preparations of side-chain polyrotaxanes (type **23a**) based on cyclodextrin through the grafting of a preformed rotaxane species [148] (Scheme 7, method 5) and by the polymerization of a semi-rotaxane monomer (Scheme 7, method 6). [149,150]

Table 15. Cyclodextrin and Cucurbituril-based main-chain polypseudorotaxanes and polyrotaxanes of type **21**.
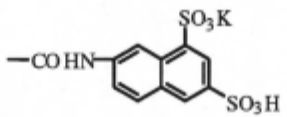
Linear Component	Cyclic Component	"Stopper" (Z)	Method	M_n (kg·mol^{-1})	m/n	Ref.
$Z-(CH_2CH_2O)_n-CH_2CH_2Z$		$-NHCOCH(Bn)NHCOOBn$				
n = 105	α-CD (**11**)	Bn = CH$_2$PH	threading[a]	4.6[b]	≈ 0.095	140
n ≈ 45	α-CD (**11**)[c]	"	threading[d]	2[e]	0.4-0.45[f]	138
n ≈ 90	α-CD (**11**)[c]	"	threading[d]	4[e]	0.4[f]	138
n ≈ 45	α-CD (**11**)[c]	"	threading[d]	2[g]	0.29[f]	139
n ≈ 90	α-CD (**11**)[c]	"	threading[d]	4[g]	0.32[f]	139
$Z-NH(CH_2)_3-[(CH_2)_3NCHC_6H_4\text{-}p-CHN(CH_2)_3]_n-(CH_2)_3NHZ$						
	α-CD (**11**)	$p-C_6H_4C(C_6H_5)_3$	threading[h]	11.2	0.17	144
	ß-CD (**12**)	"	threading[h]	?	0.14	144
$(PO)_y-[(EO)_x]_2-Z$						
x = 22 EO = CH$_2$CH$_2$O y = 39 PO = CH$_2$C(CH$_3$)O	ß-CD (**12**)	—COHN— (naphthalene with SO$_3$K and SO$_3$H)	threading	4.25[i]	0.50[j]	141
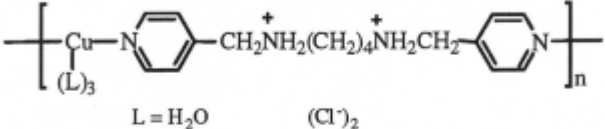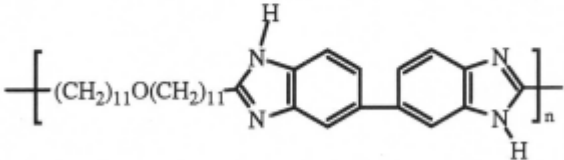
Linear Component	Cyclic Component	"Stopper" (Z)	Method	M_n (kg·mol^{-1})	m/n	Ref.

L = H$_2$O   (Cl$^-$)$_2$

| | cucurbituril (**15**) | none | threading | ? | 1 | 151 |

	α-CD (**11**)	none	k	1	0.10	143
	α-CD (**11**)	none	k	4.3	0.13	143
	α-CD (**11**)	none	k	4.0	0.14	143
	ß-CD (**12**)	none	k	4.2	0.09	143

Table 15 Continued. Cyclodextrin and Cucurbituril-based main-chain polypseudorotaxanes and polyrotaxanes of type **21**.

Linear Component	Cyclic Component	"Stopper" (Z)	Method	M_n (kg·mol^{-1})	m/n	Ref.

$$-\!\!\left[\!(R-\overset{\oplus}{N}Me_2-R_1-\overset{\oplus}{N}Me_2)\right]_{0.13}\!\!\left[\!(R-\overset{\oplus}{N}Me_2R_2-\overset{\oplus}{N}Me_2)\right]_{0.87}\!\!\Big]_n$$

$R = (CH_2)_6$, $R' = CH_2C_6H_4\text{-}p\text{-}CH=CHC_6H_4\text{-}p\text{-}CH_2$, $R_2 = (CH_2)_{10}$

$\overset{\ominus}{Br}$ counterions

| | $\left\{\begin{array}{c} \beta\text{-CD (12)} \\ + \gamma\text{CD (13)} \end{array}\right\}$ | none^1 | threading | - | $\left\{\begin{array}{c} 0.87^m \\ 0.13^m \end{array}\right\}$ | 142 |

Table 15 Continued. Cyclodextrin and Cucurbituril-based main-chain polypseudorotaxanes and polyrotaxanes of type **21**.

Linear Component	Cyclic Component	"Stopper" (Z)	Method	M_n (kg·mol^{-1})	m/n	Ref.
—(NHRNHCOR'CO)$_n$—	cucurbituril (**15**)					
R = (CH$_2$)$_n$- n=4-12; R' = -(CH$_2$)$_n$- n=4-6		none	m	-	-	62
= -C$_6$H$_4$		none	m	-	-	62
= –C$_{10}$H$_6$		none	m	-	-	62
R = -C$_6$H$_4$; R' = -(CH$_2$)$_n$- n=4-6		none	m	-	-	62
= -C$_6$H$_4$-		none	m	-	-	62
= -C$_{10}$H$_6$-		none	m	-	-	62

[a]Threading of preformed polymer in aqueous solution, addition of stoppers performed in DMF. [b]Backbone value for M_n, in vivo degradation showed ca. 10 α-CD per chain. [c]α-CD was hydroxypropylated by treatment with propylene oxide (ca. 9 per α-CD) after polyrotaxane formation. [d]Threading of preformed polymer in aqueous solution, addition of stoppers performed in DMSO. [e]Backbone M_n values, ≈ 35-39 and 18-22 α-CD units per chain for M_n 4000 and 2000 respectively based on ^{1}H-NMR. [f]Using average value from number of threaded α-CD. [g] Backbone M_n values, = 22-35 and 11-15 α-CD units per chain for M_n 4000 and 2000 respectively based on ^{1}H-NMR. [h] Polycondensation with terephthalaldehyde after formation of inclusion complex between 1,6-hexamethylene diamine and α-CD or ß-CD. [i] Backbone M_n values, ^{1}H-NMR estimates of ≈ 20 ß-CD units per chain. [j]Based on PPG segments only. [k]Reaction of 3,3'-diaminobenzidine, 1,12-dodecanediol, and CD in the presence of RuCl$_2$(PPh)$_3$. [l]Converted to polyrotaxane by photochemical dimerization of stilbene units with 4,4'-bis(dimethylaminomethyl)stilbene, which occupies a part of the cavity of each γ-CD. [m]ß-CD occupies (CH$_2$)$_{10}$ sites predominantly. [n]γ-CD occupies the polymeric stilbene sites along with the monomeric stilbene. [o]Polycondensation of diamine/cucurbituril complex with diacid chloride.

Table 16. Cyclodextrin-based side-chain polypseudorotaxanes and polyrotaxanes of type **23**.

Linear Component	Cyclic Component	"Stopper" (Z)	Method	M_n (kg·mol^{-1})	m/n	Ref.

	Cyclic Component	"Stopper" (Z)	Method	M_n	m/n	Ref.
R = *n*-butyl	α-CD (**11**)	none	threading	-	-	145
	ß-CD (**12**)	none	threading	-	-	145
	γ-CD (**13**)	none	threading	-	-	145
R = *t*-butyl	α-CD (**11**)	none	threading	-	-	145
	ß-CD (**12**)	none	threading	-	-	145
	γ-CD (**13**)	none	threading	-	-	145
R = *i*-butyl	α-CD (**11**)	none	threading	-	-	145
	ß-CD (**12**)	none	threading	-	-	145
	γ-CD (**13**)	none	threading	-	-	145
R = *n*-hexyl	α-CD (**11**)	none	threading	-	-	145
	ß-CD (**12**)	none	threading	-	-	145
	γ-CD (**13**)	none	threading	-	-	145
R = *i*-octyl	α-CD (**11**)	none	threading	-	-	145
	ß-CD (**12**)	none	threading	-	-	145
	γ-CD (**13**)	none	threading	-	-	145
R = dodecyl	α-CD (**11**)	none	threading	-	-	145
	ß-CD (**12**)	none	threading	-	-	145
	γ-CD (**13**)	none	threading	-	-	145

Linear Component	Cyclic Component	"Stopper" (Z)	Method	M_n (kg·mol^{-1})	m/n	Ref.
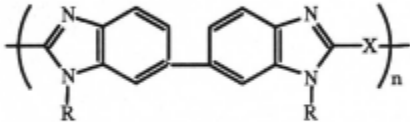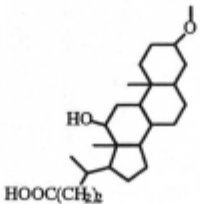
Linear Component	Cyclic Component	"Stopper" (Z)	Method	M_n (kg·mol^{-1})	m/n	Ref.
R = H (0.09) or $(CH_2)_{12}OOCZ$ (0.91) X = -p-C$_6$H$_4$-	TM-ß-C (**14b**)	—CH$_2$CPh$_3$	a	30.8	b	147
X = -$(CH_2)_8$-	TM-ß-C (**14b**)		a	15.9	b	147
R = H(0.15) or $(CH_2)_{12}OOCZ$ (0.85) X = -$(CH_2)_{11}$-O-$(CH_2)_{11}$ (0.91) or —$(CH_2)_{10}$- (0.09)	TM-ß-C (**14b**)	—CH$_2$CPh$_3$	a	7.0	b	147

Table 16 Continued. Cyclodextrin-based side-chain polypseudorotaxanes and polyrotaxanes of type **23**.

Linear Component	Cyclic Component	"Stopper" (Z)	Method	M_n (kg·mol^{-1})	m/n	Ref.

$$-NH(CH_2)_3CONHC_6H_4-p-C(C_6H_5)_3$$

R = -(CH$_2$)$_{10}$CO[O(CH$_2$)$_{11}$CO]$_z$Z y/x = 5

Linear Component	Cyclic Component	"Stopper" (Z)	Method	M_n (kg·mol^{-1})	m/n	Ref.
z = 1.1	DM-ß-CD(**14a**)		c	-	-	146
z = 5.8	"		c	-	-	146
z = 7.9	"		c	-	-	146

R = (CH$_2$)$_{10}$CONH –1,3,5– C$_6$H$_3$[CONH(CH$_2$)$_{10}$COZ]$_2$ —NH(CH$_2$)$_3$CONHC$_6$H$_4$–p–C(C$_6$H$_5$)$_3$

Linear Component	Cyclic Component	"Stopper" (Z)	Method	M_n (kg·mol^{-1})	m/n	Ref.
	DM-ß-CD (**14a**)		c	?	-	148

Table 16 Continued. Cyclodextrin-based side-chain polypseudorotaxanes and polyrotaxanes of type 23.

Linear Component	Cyclic Component	"Stopper" (Z)	Method	M_n (kg·mol^{-1})	m/n	Ref.

Linear Component (first row):
$$\left(\!CH_2\!-\!\underset{\underset{CONH(CH_2)_{10}COZ}{|}}{\overset{\overset{CH_3}{|}}{C}}\!\right)_{\!n}$$

DM-ß-CD (**14a**) — d — 42 — - — 149

Linear Component (second row):
$$\left[o\!-\!C_6H_4\!-\!p\!-\!SO_2C_6H_4\!-\!p\!-\!OC_6H_4\!-\!p\!-\!\underset{\underset{(CH_2)_2CONH(CH_2)_{10}COZ}{|}}{C(Me)}\!-\!C_6H_4\!-\!p\right]$$

—NHC$_6$H$_4$–p–C(C$_6$H$_5$)$_3$

2,3,6-tri-O-acetyl-ß-CD — e — - — ≈ 0.80 — 59

[a] N-alkylation of imidazole ring in the presence of TM-ß-CD. [b] Percentage of overall N sites that were alkylated and threaded were 6, 23, and 62 respectively. [c] Reaction of polymer side chain with stopper in the presence of DM-ß-CD. [d] Polymerization of inclusion complex formed from monomer and DM-ß-CD. [e] Formation of side-chain in the presence of CD compound.

As seen with low molar mass rotaxanes, hydrophobic interactions can also be used to form inclusion complexes with cucurbituril (**15**). An example of a polyrotaxane (type **21b**) has also been reported based on this unique cyclic species. [151] From a preformed complex of N,N'-bis(4-pyridylmethyl)-l,4-diaminobutane dihydrochloride and cucurbituril (**15**), the addition of copper (II) results in coordination polymerization to form the polyrotaxane (Scheme 5, method 3).
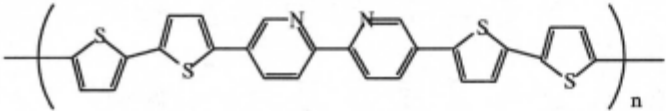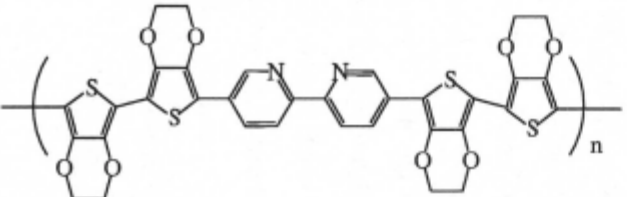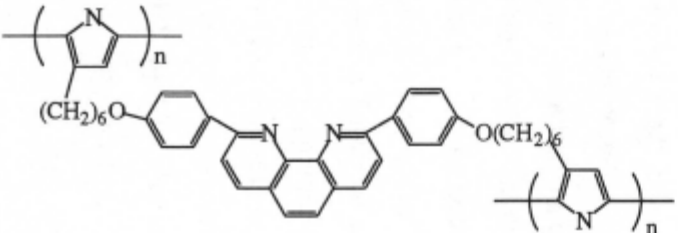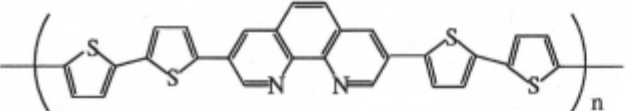
12.2.3.3.c Metal Templates

The exciting developments in the formation of low molar mass rotaxanes using metal templates have recently been extended to the realm of polyrotaxanes. Sauvage et al. [152, 153] have reported the formation of polyrotaxanes from the phenanthroline-based low molar mass rotaxanes discussed above. To achieve the network polyrotaxanes (type **21b**), linear phenanthroline components that possessed pyrrole [152] or thiophene [153] end groups were electrochemically polymerized (Scheme 5, method 3).

Swager and co-workers [154,155] have also recently reported polyrotaxanes of this type using thiophene derivatives as the polymerizable ligand. One other difference in these polymers is that 2,2-bipyridine was used as the metal coordinating ligand in the linear component of the rotaxane as opposed to the phenanthroline functionality employed by Sauvage.

Although not formed by these methods, a two-dimensional polyrotaxane network based on metal coordination has also been reported recently by Robson and co-workers. [156] This structure is based on the coordinating ligand 1,4-bis(imidazol-l-yhnethyl)benzene. When the dihydrate of this ligand is mixed with silver nitrate, the metal can coordinate to the imidazole nitrogens, resulting in a 2D-network of interpenetrating polyrotaxanes. This structure and the other polyrotaxanes made using metal templates are shown in Table 17.

Table 17. Insoluble Main Chain Network Polyrotaxanes of Type 21 Derived from Metal Complexation with Macrocycle 17.

Backbone Species	Method	Ref.
	a	154,155
	a	155
	a	152
	a	153

[a] Electrochemical polymerization

12.2.3.3.d Complexation of Crown Ethers with 4,4'-Bipyridinium salts

Despite the number of studies with low molar mass rotaxanes based on this complexation method, very few examples of polyrotaxanes have been reported recently, as seen in Table 18. Swager and co-workers [157] reported further studies of side-chain polyrotaxanes of type **24b**. Based on polythiophene, the cyclic species is a crown ether attached directly to the polymer backbone. Threading of the cyclic species by paraquat was quite effective in forming the polypseudorotaxane structure.

A few main-chain polyrotaxanes of type **22b** have been developed by Gibson and co-workers. [158,159] The crown ether, incorporated into the backbone of a polyester, forms the pseudorotaxane complex when a compound containing the 4,4'-bipyridinium moiety is added. Although the association constant for complexation is lower than that of the model low molar mass system [159], high degrees of threading efficiency [158,159] were obtained.

The diol containing the 4,4'-bipyridinium moiety was also included in the polymerization of a linear polyurethane [160], thus incorporating the bipyridinium unit into the polymer backbone. As with the low molar mass compound, the bipyridinium units of this polymer complex with the macrocycle in the polyester, generating a mechanically linked branched polymer (**25**) through the "knitting" of the two polymer chains. If the molecular weight of the polymer chains was increased, a cross-linked system resulted.

In addition to forming low molar mass rotaxanes with paraquat, [88] the basket-shaped molecules prepared by Nolte et al. were also found to form complexes with polymeric derivatives of paraquat. This resulted in the formation of polyrotaxanes of type **21b** by threading of the basket-shaped molecule onto the polymer backbone.

Table 18. Polyrotaxanes of Types **22** and **24** from Crown Ether-Paraquat Complexations with Hexafluorophosphate Counterions. (PQ = dimethyl viologen)

Cyclic Component	M_n (kg·mol^{-1})	Guest	K (L mol^{-1})	Ref.
	14.9	PQ	58.0 ± 5.5 [a]	158,159
			42.8 ± 2.2 [b]	158,159
			30.8 ± 2.4 [c]	158,159
			24.9 ± 2.3 [d]	158,159
			20.4 ± 3.0 [e]	158,159
	6.5	PQ	-	157
	3.8	PQ	-	157

Table 18 Continued. Polyrotaxanes of Types **22** and **24** from Crown Ether-Paraquat Complexations with Hexafluorophosphate Counterions. (PQ = dimethyl viologen)

Cyclic Component	M_n (kg·mol^{-1})	Guest	K (L mol^{-1})	Ref.
	8.01	f	-	160

[a] Average of results in acetone at 21.8° C. [b] Average of results in acetone at 30.0° C. [c] Average of results in acetone at 38.0° C. [d] Average of results in acetone at 46.0 ° C. [e] Average of results in acetone at 54.0° C.

f

Ar = p–C$_6$H$_4$CH$_2$C$_6$H$_4$–p

12.2.3.3.e Complexation of Macrocycles Containing 4,4-Bipyridinium Units

While the preparation of polymers using this complexation motif had been unexplored [11], several systems using this method have been reported in the last three years and are noted in Table 19.

A series of polyethers containing hyrdoquinol ether units linked by ethylene glycol segments was synthesized by Hodge and Owen. [161] Using the paraquat-based cyclophane **19**, the polymers were then threaded (Scheme 5, method 4) to form polyrotaxanes of type **21b**. Threading efficiencies, m/n, of approximately 0.5 were obtained for polymers containing shorter ethylene glycol segments, while those with longer segments had m/n values as high as 0.94. [161]

A similar polymer backbone using alternating hydroquinol and 1,5-dinaphthol ethers connected by ethylene glycol spacers was utilized by Parsons and co-workers. [162,163]. This polymer was also threaded by macrocycle **19** to yield the polyrotaxane (type **21b**). Threading efficiencies for this polyrotaxane were higher at room temperature, m/n approximately 0.5, and decreased with increasing temperature. [163]

Cyclophane **19** has also been used by Gibson and co-workers [164] to study the threading of polyurethanes. It was shown that the molecular weight of the polymer could be estimated from an **^{1}H-NMR** analysis of the proportion of cyclic species that was threaded but exchanging rapidly (near the chain ends) versus those that were threaded but exchanging slowly, i.e., those complexed at interior sites of the polymer. This end group analysis method was also used to determine the fraction of polymer between a branch point and a terminus for branched polyurethane systems. Additionally, bisphenol A units were shown to be slippage blocking groups for **19**. [164]

Table 19. Main Chain Polypseudorotaxanes of Type **21** Derived from Complexation with Cyclophane **19**.

$$-\left[(CH_2CH_2O)_x-p-C_6H_4O\right]_n-$$

Backbone Species	Method	$M_n(kg \cdot mol^{-1})$	m/n or $K_a\ (M^{-1})$	Ref.
x = 3	a	11.3	$\approx 0.5^b$	161
x = 4	a	3.5	$\approx 0.7^b$	161
x = 5	a	7.1	$\approx 0.94^b$	161

$$-\left[p-C_6H_4-OCH_2COO(CH_2CH_2O)_2OC(CH_2)_2\right]_n-$$

	Method	$M_n(kg \cdot mol^{-1})$	m/n or $K_a\ (M^{-1})$	Ref.
	a	18.6	$\approx 0.55^b$	161

$$-\left[1,5-C_{10}H_6(OCH_2CH_2)_3-p-C_6H_4O(CH_2CH_2)_3O\right]_n-$$

	Method	$M_n(kg \cdot mol^{-1})$	m/n or $K_a\ (M^{-1})$	Ref.
n = 7	c	3.6	≈ 0.49	162
n = 12	c	6.1	≈ 0.56	162
n = 24	c	12.0	≈ 0.59	162
n = 6	d	3.1	0.49	163
n = 10	d	5.0	0.54	163
n = 24	d	12.0	0.59	163

Table 19 Continued. Main Chain Polypseudorotaxanes of Type 21 Derived from Complexation with Cyclophane 19.

Backbone Species	Method	$M_n(\text{kg}\cdot\text{mol}^{-1})$	m/n or K_a (M^{-1})	Ref.

$\text{MDI} = -\text{CONHC}_6\text{H}_4\text{CH}_2\text{C}_6\text{H}_4\text{NHCO-}$

	Method	M_n	m/n or K_a	Ref.
	e	2.8	71[f]	164
	e	4.4	96[f]	164
	e	11.5	51[f]	164
	e	15.2	35[f]	164

Glyc =

	Method	M_n	m/n or K_a	Ref.
x = 0	e	11.4	g	164
x = 0.014	e	12.2	g	164
x = 0.032	e	12.0	g	164
x = 0.060	e	12.2	g	164
x = 0.120	e	14.6	g	164

Table 19 Continued. Main Chain Polypseudorotaxanes of Type **21** Derived from Complexation with Cyclophane **19**.

Backbone Species	Method	M_n(kg·mol^{-1})	m/n or K_a (M^{-1})	Ref.

x = 0	e	18.8	27.7[h]	164
x = 0.125	e	17.2		
x = 0.250	e	17.8	h	164
x = 0.500	e	23.9	h	164
x = 1	e	21.1	h	164

[a] Addition of cyclophane **19** to solutions of polymers in MeCN at 20° C. [b] Maximum threading achieved by addition of cyclophane **19** as determined by ^{1}H-NMR (MeCN-d3) at −40° C. [c] 1:1 mixture (cyclophane **19**:polymer repeat unit) in DMSO. [d] Addition of cyclophane **19** to polymer solution in DMSO or MeCN at room temperature. [e] Addition of cyclophane **19** to solutions of polymers in DMSO. [f] The association constant was found to decrease with an increase in M_n. [g] The fraction of bound cyclic was found to decrease with an increase in the number of branching points in the polymer. [h] Association constant determined for polymer with no BPA units; as fraction of BPA units increases, the amount of bound cyclic decreases.

12.2.3.3.f Other Complexation Processes

Although the formation of polyrotaxanes from poly(acrylonitrile) and poly(phenylene vinylene) with crown ethers was previously known [11], no new polyrotaxanes based on these complexation processes have been reported. Gibson and Beckham [165] have conducted solid-state NMR studies of poly[(acrylonitrile)-rotaxa-(60-crown-20)], but this polyrotaxane was already known. [11]

12.2.3.3.g 'Clipping' Approach to Polyrotaxanes

In the time covered by this review, no examples of polyrotaxanes formed by this method (analogous to Scheme 3 for low molar mass rotaxanes) have been reported. In fact, no polyrotaxanes formed in this manner have been reported to date. [11] In principle, main-chain (**21**) or side-chain (**23**) polyrotaxanes could be formed when the components used to form the cyclic species are both of low molar mass. For the other main-chain (**22**) and side-chain (**24**) systems, one of the components used in the 'clipping' methodology would be polymeric. In these cases, cross-linking of the system would be likely and isolation of the product difficult.

12.3 Properties of Rotaxanes
12.3.1 Low Molar Mass Rotaxanes
12.3.1.1 Structure Proof

There are a number of techniques that can be used to characterize low molar mass rotaxanes. Although more classical methods such as chromatography and melting point determination can be used to identify rotaxanes, other methods have become standards for the elucidation of rotaxane structures, especially in recent years. Nuclear magnetic resonance spectroscopy (NMR), X-ray crystallography, and newer methods of mass spectrometry that are capable of detecting larger molar masses (on the order of tens of thousands)

have become the most popular methods of structural determination for rotaxanes and will be discussed below.

Ultimately, structural proof can be obtained from X-ray crystallography. Thus, for many of the rotaxanes listed in this chapter, crystal structures have been determined (e.g., Refs 20, 21, 79). In addition to providing structural evidence for the rotaxane, the crystal structure can also furnish important information about the intermolecular interactions that are present in the complex. Hydrogen bonds and other non-covalent bonding interactions, both inter- and intra-molecular, can be visualized and provide important direction for further studies.

To supplement crystal structure data, or provide confirmation of the structure when a crystal can't be obtained, mass spectrometric techniques are frequently used. Methods such as fast atom bombardment (FAB), electrospray, plasma desorption, and matrix assisted laser desorption ionization (MALDI) can determine the molar mass for compounds up to several thousands. Thus, for most low molar mass rotaxanes, the total mass of the rotaxane can be observed. In most cases, the individual linear and cyclic components are the next largest fragments that can be observed (e.g., Refs 18, 19), although the bipyridinium systems can also show the sequential losses of the PF_6 anion and neutral species from the parent rotaxane peak (e.g., Refs 166-168)

In the solution phase, NMR has also been widely used for the characterization of rotaxanes. For some systems, such as those with aliphatic linear and cyclic components [14] and linear oligo(ethyleneoxy) compounds with crown ethers, [17] the chemical shifts of the species are not greatly affected, if at all. For other systems, however, particularly those with aromatic components, the chemical shifts of the protons and carbons of the linear and cyclic components can be changed dramatically when association to form the rotaxane takes place. These chemical shift changes can be observed for cyclodextrin-based systems (e.g., Refs 169, 170), bipyridinium-based rotaxanes

(e.g., Ref 166), and those containing ammonium ions (e.g., Refs 20, 21). Nuclear Overhauser effect (NOE) measurements have also been used to determine the structrues of rotaxanes (e.g., Refs. 63,64). This makes NMR an effective tool in rotaxane characterization for a number of systems.

Although these techniques are the most common, other means of analysis can also be used in the characterization of rotaxanes. The presence of a charge-transfer band in the UV-Visible spectrum of the bipyridinium-benzo crown ether and phenanthroline-Cu(I) systems is evidence for the formation of the rotaxane and the removal of copper respectively (e.g., Ref 171). For cyclodextrin systems, optical activity can also be used to monitor rotaxane formation. When threading takes place, induced circular dichroism in the absorption bands of the linear species can be observed (e.g., Ref 172).

12.3.1.2 Solubility

In many cases, the solubilities of rotaxanes differ significantly from those of the linear and cyclic components that compose them. For example, due to their charged nature, the ammonium ion salts [20] and 4,4'-bipyridinium salts [166] are often insoluble in some organic solvents. Addition of the cyclic component, however, leads to formation of the rotaxane and the salts are then solubilized. This phenomenon can also be seen in cyclodextrin-based systems. While the oligo(ethylene glycol)-a-CD rotaxanes made by Harada and co-workers [173] are insoluble in dimethylformamide and water, both of the individual components are soluble in these media.

12.3.1.3 Stability

The stability of low molar mass rotaxanes has previously been alluded to in the synthesis section. Many of the early rotaxanes, synthesized by methods such as statistical threading or chemical conversion, do not possess a strong attractive force between the components. Few rotaxanes have been

synthesized by these methods in recent years and the stabilities of systems of this type have been discussed previously. [11]

As shown previously (section 2.3.3), recent syntheses of rotaxanes have relied on the use of an enthalpic driving force to promote their formation. In addition to producing higher yields of rotaxanes, these driving forces also lead to increased stabilities once the product is formed. Nevertheless, the rotaxane systems are still susceptible to conditions that can disrupt the enthalpic driving force and promote dethreading.

Pseudorotaxanes based on the 4,4'-bipyridinium salts such as **26** can be dethreaded by treatment with dipolar aprotic solvents such as dimethylsulfoxide, as demonstrated by Gibson and co-workers. [174,175] The color indicative of the threaded state disappears and the NMR spectrum returns to that of the individual linear and cyclic components. The ammonium ion systems are also susceptible to dethreading. In this case, the addition of a base causes deprotonation of the ammonium ion. The neutral structure no longer has a driving force for threading, and the dethreading of the pseudorotaxane is observed. [98] Prodi and Montalti [37] have shown that pseudorotaxane formation for ammonium salts can also be affected by the counterion. The addition of a chloride salt led to the formation of a strong ion pair with the ammonium ion thread and pseudorotaxane formation was disrupted. If an ammonium-based salt with a hexafluorophosphate counterion was then added, the pseudorotaxane could again be formed.

The dethreading of rotaxanes based on metal templates has also been studied. Chambron *et al.* [176] have shown that the phenanthroline-based [3]pseudorotaxanes were disrupted by the addition of cyanide ion. Rapid removal of one copper ion, followed by slower removal of the second was observed by monitoring the metal to ligand charge-transfer absorptions in the UV-Visible spectrum, providing an indirect method for detecting the dethreading process.

12.3.1.4 Dynamics of Motion in Solution

As both the efficiency of rotaxane synthesis and the complexity of the resulting systems have grown, the study of the motion of the cyclic species within the rotaxane has intensified. With the development of linear components that contain multiple recognition sites for the cyclic component, the ability of the cyclic component to shuttle between these sites has been investigated. In the peptide-based rotaxanes (Table 3) prepared by Leigh and co-workers [44], the location of the macrocycle was found to be solvent dependent. In halogenated solvents, the macrocycle can form hydrogen bonds with the peptide residues and is found at these sites. In dimethylsulfoxide, these bonding interactions are disrupted and the macrocycle is instead found at the lipophilic spacer group.

A series of rotaxanes was analyzed by Stoddart and co-workers [111] to determine how subtle changes in the recognition site would effect the shuttling of the cyclic. It was found that the cyclic component displayed a marked selectivity for recognition sites in which the aromatic ether was based on hydroquinone as opposed to resorcinol. In another study of similar rotaxane shuttles, Stoddart and co-workers [112] observed that the hydroquinone moiety was favored over p-xylene for complexation, but was less favored versus the tetrathiafulvalene unit. An indole-based moiety was also expected to have greater selectivity versus hydroquinone-based sites, but steric factors reversed this selectively.

Stoddart and co-workers [98,99] also demonstrated that the shuttling process could also be chemically controlled using a rotaxane that contained a linear component with an ammonium ion and a bipyridinium-based complexation site. The cyclic component, DB24C8 **3**, was selective for the ammonium site, but when base was added to deprotonate the ammonium ion, **3**

was found to reside at the bipyridinium site. Addition of acid caused reprotonation, and the selectivity for the ammonium site returned.

The shuttling process has also been observed in cyclodextrin-based systems. Nakashima and co-workers [56] constructed a rotaxane based on a-CD and a linear component that contained an azo-benzene unit. They showed that a-CD was selective for the azo-benzene unit when it was in the trans conformation. If the molecule was irradiated to induce conversion to the cis isomer, the a-CD then resided on the methylene spacer.

12.3.1.5 Electron Transfer Processes

The incorporation of photo- and electro-active elements into the rotaxane structure has led to the investigation of the electronic properties of these systems. In some cases, these processes can be intimately connected with the molecular dynamics of the system and can be used to control the motion of the cyclic component.

Sauvage and co-workers [73-75] have constructed a rotaxane based on a metal-template in which the linear component contains two binding sites. The phenanthroline-based site is selectively complexed when copper (I) is the metal used in the system. If the metal is oxidized to copper (II), the macrocycle shifts to the second binding site based on the terpyridine unit. Reduction of the metal back to copper (I) results in a return to the phenanthroline-macrocycle complex.

It has also been demonstrated that complete rearrangement of the multiporphyrinic rotaxane prepared by Sauvage and co-workers [71] can occur when the rotaxane is demetallated. The macrocycle in this rotaxane contains a gold porphyrin while the linear segment is terminated with two zinc porphyrins. In the presence of copper, the rotaxane is threaded such that the terminal porphyrins are pointed away from the gold porphyrin in the macrocycle. After removal of the copper, weak forces favour an attractive interaction that causes

the rotaxane to rearrange so that the gold porphyrin is sandwiched between the two zinc porphyrins.

It has also been demonstrated that electronic processes can be used to induce motions via the threading and dethreading of a rotaxane. Stoddart and co-workers have used this idea to prepare systems in which the threading process is driven by photochemical [94,106,108] or electrochemical [107,108] stimuli. They propose that these systems could be used for the development of molecular machines.

Basic electron transfer processes have also been observed in rotaxane systems that have been designed for this purpose. When Sauvage and co-workers [67] attached C_{60} groups to the linear component of their phenanthroline-copper rotaxane systems, the photoinduced electron transfer from copper-complexed core to the fullerene stoppers was observed. Similarly, when the tetra-armed phthalocyanine was complexed with cyclophane **19**, fluorescence quenching of the zinc-phthalocyanine was observed. [113] Finally, Anderson and co-workers [63,64] have reported the synthesis of conjugated rotaxanes that are water soluble with the goal of using these materials as molecular wires.

12.3.2 High Molar Mass Rotaxanes (Polyrotaxanes)
12.3.2.1 Structure Proof

Techniques to provide structural proof for polyrotaxanes are often less direct than those for low molar mass rotaxanes. Particularly, when the polyrotaxane formation occurs via polymerization in the presence of a macrocyle, a control experiment is needed. Conducting the polymerization in the presence of a similar cyclic species that is too small to form a rotaxane can prove that the cyclic species is not being introduced by other means. For example, when Gibson and co-workers [117] prepared polyrotaxanes from the polymerization of styrene in the presence of crown ethers they also used 18-

crown-6, which is too small to be threaded, as a control. Isolation of the homopolymer of styrene, with little to no incorporation of the 18-crown-6, showed that the larger cyclics were not introduced by chain-transfer reactions or other processes and that the unthreaded cyclic materials could also be effectively removed by precipitation or dialysis of the polymer. Analysis of the polyrotaxane by a technique such as gel permeation chromatography (GPC), can be used to verify that the unthreaded cyclic material has been removed. Because the polyrotaxane and the low molar mass cyclic have markedly different retention times, the two species can easily be identified and the absence of low molar mass cyclic can be confirmed.

The polyrotaxane architectures of types **21** and **23** can also be confirmed by degradation of the polymer to recover the intact cyclic compound. The hydrolysis of poly(ester rotaxane)s of these types [123,177] is an example of how this technique can be used to confirm the polyrotaxane structure.

NMR spectroscopy can also be used to confirm polyrotaxane structure but, like some low molar mass systems, changes in the chemical shift values are not always observed when threading occurs. [123,177] In polyrotaxanes based on the bipyridinium moiety, [158,159,161-164] the chemical shift changes can be observed and used to confirm the presence of the rotaxane structure. As seen with low molar mass rotaxanes, NOE measurments can also be used to determine the structure of polyrotaxanes (e.g., Ref. 132). As another alternative, Gibson and co-workers [128] have measured the spin-lattice relaxation times (T_1) for the macrocycle in poly(urethane/crown ether) rotaxanes. Although the T_1 value for 30-crown-10 was smaller in a favorable solvent for complexation (chloroform) versus a non-favorable solvent (dimethylsulfoxide), both values were significantly smaller than that for free 30-crown-10. Measurement of the spin-lattice relaxation time as well as NOE measurements can therefore serve as an effective means of characterizing polyrotaxane formation.

12.3.2.2 Stability

Many of the early polyrotaxanes did not contain stoppers that could constrain the cyclic species. Although the potential for these 'polypseudorotaxanes' to be dethreaded has previously been discussed, [11] Gibson and co-workers have recently shown that the half-life of the polyrotaxane can be quite long, on the order of one year. [124] Thus, even without a blocking species, the 'polypseudorotaxane' structure is quite stable.

In many of the more recent systems, blocking groups have been incorporated into the polyrotaxane to prevent loss of the cyclic components and increase the stability. A number of side-chain polyrotaxanes based on cyclodextrin have included stoppers to prevent dethreading. [146-148] In the main-chain polyrotaxane that utilized cucurbituril as the cyclic species, [143] a blocking group was incorporated into every repeat unit.

Many advances have also recently been made in improving the ability to include blocking groups in polyester and polyurethane rotaxanes. Using diols that contained a blocking group spacer, Gibson and co-workers have synthesized poly(ester rotaxane)s [121-123] and poly(urethane rotaxane)s [127,128] that had improved threading efficiencies. The use of both a blocking diol and a blocking diacid chloride, [126] resulted in even greater threading efficiencies. In the case of self-threading systems [132-134], the formation of branched and cross-linked systems serves as an effective means to prevent dethreading.

There are cases, however, when only temporary stability of the system is desired. In polyrotaxane systems based on poly(ethylene glycol) and a-CD prepared by Yui and co-workers [138-140], phenylalanine was utilized as the stopper. In the presence of an enzyme, the stoppers can be degraded and the cyclodextrin was released. The polyrotaxanes were designed to behave in this manner so that they might be used as potential drug delivery systems.

12.3.2.3 Phase Behaviour

Polyrotaxanes have been found to display significant differences in phase behavior as compared to the parent polymer backbone.

12.3.2.3.a Solubility and Surfactant Behaviour

The solubility of many polymers can be changed significantly by incorporation into polyrotaxanes. Side-chain polyrotaxanes based on trimethyl-**ß-CD** and poly(benzimidazole)s showed considerably higher solubility in a variety of organic solvents when compared with the parent polymers. [147]

In main-chain polyrotaxanes of type **22b**, complexation with 4,4'-bipyridinium salts resulted in solubility changes from the parent polymer. For poly(ester/crown ether) rotaxanes, [158,159] the parent polymers were generally insoluble in acetone, but complexation with the linear species led to a soluble species. Similar behavior was also observed in acetonitrile. Conversely, the bipyridinium species is insoluble in tetrahydrofuran, while the parent polymer is soluble. Formation of the polyrotaxane led to enhanced solubility of the linear species, although some insoluble material was still detected. [159]

The 'dispersion' polymerization of styrene can be carried out in methanol or water in the presence of large crown ethers. [117] When smaller crown ethers such as 18-crown-6 or poly(ethylene oxide) of low molecular weights were substituted, emulsions were not formed, indicating that the presence of the rotaxane was promoting emulsion formation.

12.3.2.3.b Glass Transitions

The glass transition temperature (T_g) represents the point at which a polymer undergoes a conversion from a glassy amorphous state to a rubbery amorphous state upon heating. The formation of a polyrotaxane can cause a

change in the T_g depending on the miscibility of the cyclic and linear components. If the phases are miscible, a single glass transition can be observed for the combination of the two phases. If the phases are not miscible, the T_g of the polymer will be unchanged, while a second T_g may also be present if the cyclic species is able to exist in an amorphous state.

For poly[(styrene)-rotaxa-(crown ether)]s [117], the linear and cyclic phases are not miscible. As a result, glass transition temperatures are seen for both the polymer backbone and the cyclic species. Similarly, in the case of poly(ester rotaxane)s [122,124] phase separation can occur. The crown ethers are highly mobile and can move along the polymer backbone to aggregate in a separate phase. The result is that in some cases the glass transition can be observed for the cyclics. A second T_g for the backbone is not observed because the parent homopolymer is highly crystalline and thus does not exhibit a glass transition. [124]

Conversely, the poly(urethane/crown ether rotaxane)s have a higher degree of miscibility and only one glass transition temperature is observed. [127,130,131] Hydrogen bonding interactions between the crown ether and in-chain NH groups in the polyurethane backbone reduce the mobility of the cyclic species and lead to this result. [129] The T_g is dependent on both the threading efficiency, m/n, and the presence of blocking groups within the polymer. [127] As the percentage of cyclic species increases, i.e., a higher m/n value, the glass transition temperature decreases. But, the presence of blocking groups, which add to the rigidity of the backbone, cause an increase in the T_g. In the case of the branched poly(urethane/crown ether rotaxane)s formed by self-threading interactions [132,133] a single glass transition is also observed.

For polyrotaxanes of type **22b**, the cyclic component is included in the polymer backbone. The glass transition temperatures of these systems increase upon the formation of N,N'-dialkyl-4,4'-bipyridinium polypseudorotaxanes.

[158,159] The presence of the cyclic component in the backbone results in a somewhat flexible backbone for the homopolymer. When complexation with the 4,4'-bipyridinium salt occurs, however, the system becomes more rigid and the resulting T_g is therefore higher.

12.3.2.3.c Phase Transitions, Crystallization, and Melting Points

When threading efficiencies are high enough, crystalline domains resulting from the cyclic components can be observed. If the cyclic components are able to move along the backbone, they can aggregate and crystallize into separate domains. It is possible then, in some systems, to observe two crystalline melting points, one for the cyclic crystalline domain and one for the polymer backbone.

For the poly(ester rotaxane)s [122,124], as mentioned with the glass transition above, two crystalline domains were present. As a result, two separate crystalline melting points were determined. When the polymer backbone was instead a polyurethane [127,131], the mobility of the cyclic species was decreased. Hydrogen bonding between the crown ethers and NH groups in the polymer backbone prevented the organization of the crown ethers into crystalline domains. As a result, no melting point was observed for these amorphous polyrotaxanes.

As a means of comparison, the polyrotaxanes based on polystyrene and crown ethers can be considered. Prepared by a statistical method, these polymers had relatively low degrees of threading. [117] Despite the fact that the crown ethers would be mobile in this system, a separate melting point for the cyclic domain was not observed. This is due to the facts that 1) there are not enough cyclic species present in the polymer to aggregate into crystalline domains and 2) the crown ether and polystyrene are immiscible.

12.3.2.4 Viscosity and Hyrdrodynamic Volume

In the past three years, further studies have yielded more information regarding the viscosity and hydrodynamic volumes of polyrotaxanes to supplement what was previously known. [11]

When compared with the parent polymer backbone the poly(ester rotaxane)s of type **21b** have higher intrinsic viscosities, attributable to an increased hydrodynamic volume due to the presence of the cyclic species. [124,135] The viscosity was found to be solvent dependent, resulting from differential solvation of the linear and cyclic components. In tetrahydrofuran (THF), an effective solvent for both components, the intrinsic viscosity was higher than that for the parent polymer of a similar molecular weight. [124] This again confirmed the fact that the polyrotaxane possessed a greater hydrodynamic volume. In addition to tetrahydrofuran, the intrinsic viscosity of the polyrotaxane was also measured in varying mixtures of methanol and tetrahydrofuran. Methanol is a good solvent for the crown ether but a poor solvent for the polymer backbone. Upon changing the solvent from THF to a mixture of THF and methanol (10:1), the intrinsic viscosity decreased, while the intrinsic viscosities of the parent homopolymer and a copolymer with poly(ethylene oxide) were unaffected by the solvent change. This shows that the effects on the intrinsic viscosity were directly attributed to the polymer topology.

Studies were also performed on polyrotaxanes formed by threading crown ethers onto a preformed polyurethane. It was found that the polyrotaxane had a higher intrinsic viscosity but a lower Huggins constant than the model polyurethane. [131] The presence of the cyclic species causes the polyrotaxane to adopt an expanded conformation, resulting in a greater hydrodynamic volume and thus, a higher intrinsic viscosity. The model polymer, meanwhile, was a random coil that became more expanded upon dilution leading to a higher Huggins constant. The polyrotaxane, however, was

already expanded, even at higher concentrations, so the dependence of the chain conformation on concentration, and hence the Huggins constant was reduced.

Gibson and co-workers [159] have also measured the viscosities of polyrotaxanes of type **22b**, formed by the threading of a poly(ester/crown ether rotaxane) with a 4,4'-bipyridinium salt. It was found that as the degree of threading, m/n, increased, the intrinsic viscosity also increased. As the complexation increased, the solvated volume of the polymer would also increase and lead to the higher viscosity. The chain extension could also be attributed to ionic repulsion between the complexed bipyridinium guests. As the extent of threading increases, these repulsive forces would also be more prevalent. This effect could also contribute to the increase in intrinsic viscosity.

In contrast to the intrinsic viscosity, the melt viscosity of a poly(ester rotaxane) of type **21b** was found to be less than that of the parent polymer. [124,135] In fact, the melt viscosity for the polyrotaxane was found to be equal to that of the model polymer of approximately 40 percent its molecular weight. This effect is explained by the fact that the cyclic species prevent chain entanglements in the melt phase, thereby reducing the viscosity.

12.3.2.5 Electronic properties

The development of conducting systems based on polyrotaxanes remains largely unexplored. A few of the systems that have been developed have previously been reported and documented. [11] In the subsequent years, Swager and co-workers [154] have reported further on conducting polymetallorotaxanes, demonstrating that these systems can reversibly bind zinc and copper ions and exhibit conductivity profiles characteristic of localized redox conductors. A similar system has been reported by Sauvage and co-workers [153], but the ability to rebind copper ions is lost after

demetallation. If the demetallation is performed in the presence of lithium ions, the overall structure can be retained and remetallation with copper can be performed. Electroactive films based on a polypyrrollic rotaxane-containing network have also been reported. [152] This system can also retain its structure after demetallation, allowing for the metal to be reintroduced to the system.

12.4 Potential Applications of Rotaxanes
12.4.1 Low Molar Mass Rotaxanes

Based on the properties discussed above, many potential applications have been envisioned for low molar mass rotaxanes. These include use as potential photo- and electro-active sensitizers and switches, information storage devices, and as chemoselective sensors on the basis of changes in fluorescence or electrochemical response. Other proposed uses include the development of rotaxanes as part of photosensitizers and as components of molecular machines such as molecular abacae.

12.4.2 Polyrotaxanes

Polyrotaxanes have also been proposed for many applications. These include shear-sensitive viscosity control, solubility and viscosity improvement for the synthesis and processing of rigid rod polymers, controlled drug delivery, control of glass transition temperatures, and introduction of crystallinity from the macrocycle to yield new classes of thermoplastic elastomers. Other ideas include solid-state electron- and energy-transfer systems, blending agents, novel surfactants, information storage devices, molecular weight and structure probes, and chemoselective sensors on the basis of conductivity or fluorescence changes.

550

12.5 Conclusions

Although the rotaxane field is barely more than 30 years old, it is growing rapidly. Indeed, the literature produced in the past three years, and reviewed in this chapter, is almost equal to that produced over the previous three decades! Many novel concepts have been used to obtain greater yields of rotaxanes and systems that are more and more complex in structure. The focus continues to shift from simply the design of novel architectures to the development of practical applications for these architectures. As the field continues to grow and expand, the possibilities that can be achieved are endless.

12.6 Acknowledgements

12.7 References

1. G.Schill and H.Zöllenkopf,Nachr.Chem.Techn.,**79**,149(1967);G.Schill and H.Zöllenkopf,Ann.Chem.,**721**,53(1969)

2. P.L.Anelli, P.R.Ashton, R.Ballardini, V.Balzani, M.Delgado, M.T.Gandolfi, T.T.Goodnow, A.E.Kaifer, D.Philp, M..Slawin, N.Spencer, J.F.Stroddart, C.Vincent and D.J. Williams, J.Am.Chem.Soc., **114**, 193 (1992)

3. See footnote in reference 3

4. H.L.Frisch and E.Wasserman,J.Am.Chem.Soc.,**83**,3789(1961)

5. I.T.Harrison and S.Harrison,J.Am.Chem.Soc.,**89**,5723(1967)

6. G. Schill,*Catenanes,Rotaxanes,and Knots*,Academic Press,NY, 1971

7. G.Schill,E.Logemann and W.Littke,Chemie Unserer Zeit,**18**,129(1984)

8. D.Walba,Tetrahedron,**41**,3161(1985)

9. Y.S.Lipatov,T.E.Lipatova and L.F.Kosyanchuk,Adv.Polym.Sci.,**88**,49 (1989)

10. H.W.Gibson,M.C.Bheda and P.T.Engen,Prog.Polym.Sci.,**19**,843(1994)

11. H.W.Gibson.in J . A . S e m e l y n (E d .) , *Large Ring Molecules*,John Wiley & Sons,NY,1996,pp.l91-262

12. (a)D.A.Ambalino and J.F.Stoddart ,Chem.Rev., **95**, 2725(1995); (b) D.Philp and J.F.Stoddart, Angew.Chem.Int.Ed.Engl. ,**35**,1154 (1996); (c) F.M.Raymo and J.F.Stoddart ,Chem.Rev.,in press; (d)S.A.Negopodiev and J.F. Stoddart, Chem.Rev.,**98**,1959(1998); A.Harada, Adv.Polym.Sci.,**133**, 141(1997);A.Harada,Acta Polym.,**49**,3(1998);A.Harada,Coord.Chem.Rev., **148**,115(1996);L.Huang and A.E.Tonelli,J.Macromol.Sci.,Rev.Macromol.Chem. Phys.,**C38**,781(1998);(e)A.C.Benniston,J.Chem.Soc.,Chem.Rev.,**25**,427(1996)

13. I.T.Harrison,J.Chem.Soc.,Chem.Commun.,231(1972)

14. I.T.Harrison,J.Chem.Soc.,Perk.Trans.l,301(1974)

15. G.Schill,W.Bcckmann,N.Schweickert and H.Fritz,Chem.Ber.,**l19**,2647(1986)

16. G.Schill,G.Doerjer,E.Logemann and W.Vetter,Chem.Ber.,**l13**,3697(1980)

17. G.Agam,D.Gravier and A.Zilkha,J.Am.Chem.Soc.,**98**,5206(1976); G.Agam and A.Zilkha,J.Am.Chem.Soc.,**98**,5214(1976)

18. A.G.Kolchinski,D.H.Busch and N.W.Alcock,J.Chem.Soc.,Chem. Commun.,1289(1995)

552

19. P.R.Ashton,P.J.Campbell,E.J.T.Chrystal,P.T.Glink,S.Menzer,D.Philp,N. Spencer,J.F.Stoddart,P.A.Tasker and D.J.Williams,Angew.Chem.,Int.Ed. Engl.,*34*,1865(1995);P.R.Ashton,E.J.T.Chrystal,P.T.Glink,S.Menzer,C. Schiavo,J.F.Stoddart,P.A.Tasker and D.J.Williams,Angew.Chem.Int.Ed. Engl.,*34*,1869(1995)

20. P.R.Ashton,E.J.T.Crystal,P.T.Glink,S.Menzer,C.Schiavo,N.Spencer,J.F. Stoddart,P.A.Tasker,AJ.P.White and D.J.Williams,Chem.Eur.J.,**2**,709 (1996)

21. W.S.Bryant,I.A.Guzei,A.L.Rheingold,J.S.Merola and H.W.Gibson,J.Org. Chem.,**63**,7634(1998)

22. P.T.Glink,C.Schiavo,J.F.Stoddart and D.J.Williams,Chem.Commun., 1483(1996)

23. P.R.Ashton,P.T.Glink,J.F.Stoddart,P.A.Tasker,A.J.P.White and D.J. Williams,Chem.Eur.J.,**2**,729(1996)

24. P.R.Ashton,M.C.T.Fyfe,P.T.Glink,S.Menzer,J.F.Stoddart,A.J.P.White and D.J.Williams,J.Am.Chem.Soc.,**119**,12514(1997)

25. P.R.Ashton,M.C.T.Fyfe,M.-V.Martínez-Díaz,S.Menzer,C.Schiavo,J.F. Stoddart,A.J.P.White and D.J.Williams,Chem.Eur.J.,**4**,1523(1998)

26. P.R.Ashton,I.Baxter,M.C.T.Fyfe,F.M.Raymo,N.Spencer,J.F.Stoddart,A.J.P.White and D.J.Williams,J.Am.Chem.Soc.,**120**,2297(1998)

27. N.Yamaguchi,L.M.Hamilton and H.W.Gibson,Angew.Chem.Int.Ed.,**37**,3275(1998)

28. K.L.Wooley,C.J.Hawker and J.M.J.Fréchet,J.Am.Chem.Soc.,**113**,4252(1991)

29. P.R.Ashton,A.N.Collins,M.C.T.Fyfe,P.T.Glink,S.Menzer,J.F.Stoddart and D.J.Williams,Angew.Chem.Int.Ed.Engl.,**36**,59(1997)

30. M.C.T.Fyfe and J.F.Stoddart,Acc.Chem.Res.,**30**,393 (1997)

31. M.C.Feiters,M.C.T.Fyfe,M.-V.Martínez-Díaz,S.Menzer,R.J.M.Nolte,J.F. Stoddart,P.J.M.vanKan and D.J.Williams,J.Am.Chem.Soc.,**119**,8119 (1997)

32. P.R.Ashton,I.Baxter.S.J.Cantrill.M.C.T.Fyfe.P.T.Glink,J.F.Stoddart,A.J.P.White and D.J.Willliams,Angew.Chem.Int.Ed.,**37**,1294(1998)

33. P.R.Ashton,A.N.Collins,M.C.T.Fyfe,S.Menzer,J.F.Stoddart and D.J. Williams,Angew.Chem.Int.Ed.Engl.,**36**,735(1997)

34. P.R.Ashton,M.C.T.Fyfe,S.K.Hickingbottom,S.Menzer,J.F.Stoddart,A.J.P.White and D.J.Williams,Chem.Eur.J.,**4**,577(1998)

35. M.C.T.Fyfe,P.T.Glink,S.Menzer,J.F.Stoddart,A.J.P.White and D.J. Williams,Angew.Chem.Int.Ed.Engl.,**36**,2068(1997)

36. A.G.Kolchinski,N.W.Alcock,R.A.Roesner and D.H.Busch,J.Chem. Soc.,Chem.Commun.,1437(1998)

37. M.Montaldi and L.Prodi,J.Chem.Soc.,Chem.Commun., 1461(1998)

38. F.Vögtle,T.Dünwald,M.Händel,RJäger,S.Meier and G.Harder,Chem.Eur. J.,**2**,640(1996)

39. F.Vögtle,R.Jäger,M.Händel,S.Ottens-Hildebrandt and W.Schmidt,Synthesis, 353(1996)

40. M.Händel,M.Plevoets,S.Gestermann and F.Vögtle,Angew.Chem.Int.Ed. Engl.,**36**,1199(1997)

41. T.Dünwald,R.Jäger and F.Vögtle,Chem.Eur.J.,**3**,2043(1997)

42. R.Jäger and F.Vögtle,Angew.Chem.Int.Ed.Engl.**36**,930(1997)

43. A.G.Johnston,D.A.Leigh,A.Murphy,J.P.Smart and M.D.Deegan,J.Am. Chem.Soc.,**118**,10662(1996)

44. A.S.Lane,D.A.Leigh and A.Murphy,J.Am.Chem.Soc.,**119**,11092(1997)

45. D.A.Leigh,A.Murphy,J.P.Smart and A.M.Z.Slawin,Angew.Chem.Int.Ed Engl.,**36**,728,(1997)

46. A.Harada and M.Kamachi,J.Chem.Soc.,Chem.Commun., 1322(1990)

47. A.Harada,M.Okada,J.Li and M.Kamachi,Macromolecules,**28**,8406(1995); A.Harada,J.Li and M.Kamachi,Polym.Adv.Tech.,**8**,241(1997);A.Harada, Carbohydrate Polym.,**34**,183(1997)

48. A. Harada,Supramol.Sci.,**3**,19(1996)

49. A. Harada,Am.Chem.Soc.Div.Polym.Chem.,Polym.Prepr.,**36**,570 (1995)

50. A.Harada,in,J.C.Salamone(Ed.),*Polymeric Materials Entyclopedia*,CRC Press,NY,1996,pp.3899-3903.

51. A.Harada,in,J.C.Salamone(Ed.),*Polymeric Materials Encyclopedia*,CRC Press,NY,1996.pp.1697-1702.

52. A.Harada,T.Nishiyama,Y.Kawaguchi,M.Okada and M.Kamachi, Macromolecules,**30**,7115(1997)

53. A.Harada,J.Li and M.Kamachi,J.Chem.Soc.,Chem.Commun.,1413(1997)

54. A.P.Lyon.N.J.Banton and D.H.Macartney,Can.J.Chem.,**76**,843(1998)

55. R.Castro,L.A.Godínez,C.M.Criss and A.E.Kaifer,J.Org.Chem.,**62**,4928 (1997)

56. H.Murakami,A.Kawabuchi,K.Kotoo,M.Kunitake and N.Nakashima,J.Am. Chem.Soc.,**119**,7605(1997);N.Nakashima,A.Kawabuchi and H.Murakami, J.Include.Phen.Molec.Recog.Chem.,**32**,363(1998)

57. A.Mirzoian and A.E.Kaifer,Chem.Eur.J.,**3**,1052(1997)

58.   M.B.Steinbrunn and G.Wenz,Angew.Chem.Int.Ed.Engl.,**35**,2139(1996)

59.   M.Born and H.Ritter,Macromol.Rapid Commun.,**17**,197(1996)

60.   D.Whang,K.M.Park,J.Heo,P.Ashton and K.Kim,J.Am.Chem.Soc.,**120,** 4899(1998)

61.   D.Whang and K.Kim,J.Am.Chem.Soc.,**119**,451(1997)

62.   C.Meschke,H.J.Buschmann and E.Schollmeyer, Macromol. Rapid Commun., **19**, 59 (1998)

63.   S.Anderson and H.L.Anderson,Angew.Chem.Int.Ed.Engl.,**35**,1956(1996)

64.   S.Anderson,R.T.Aplin,T.D.W.Claridge,T.Goodson III,A.C.Maciel,G. Rumbles,J.F.Ryan and H.L.Anderson,J.Chem.Soc.,Perkin Trans. 1,2383 (1998)

65.   S.Anderson,W.Clegg and H.L.Anderson,J.Chem.Soc.,Chem.Commun., 2379 (1998); S.Anderson,T.D.W.Claridge and H.L.Anderson,Angew. Chem.Int.Ed.Engl.,**36**,1310(1997)

66.   J.-P.Sauvage and C.O.Dietrich-Buchecker,Tetrahedron Lett.,**24**,5095 (1983)

67.   N.Amaroli,F.Diederich,C.O.Dietrich-Buchecker,L.Flamigni,G.Marconi,J.F. Nierengarten and J.-P.Sauvage,Chem.Eur.J.,**4**,406(1998)

68.   J.C.Chambron and J.-P.Sauvage,Chem.Eur.J.,**4**,1362(1998)

69.   D.J.Cárdenas,P.Gaviña and J.-P.Sauvage,J.Chem.Soc.,Chem.Commun., 1915(1998)

70.   D.J.Cárdenas,P.Gaviña and J.-P.Sauvage,J.Am.Chem.Soc.,**119**,2656 (1997)

71.   M.Linke,J.C.Chambron,V.Heitz,J.-P.Sauvage and V.Semetey,J.Chem. Soc.,Chem.Commun.,2469(1998)

72.   N.Solladié,J.C.Chambron,C.O.Dietrich-Bucheckcr and J.-P.Sauvage, Angew.Chem.Int.Ed.Engl.,**35**,906(1996)

73.   J.P.Collin,P.Gaviña and J.-P.Sauvage,J.Chem.Soc.,Chem.Commun., 2005(1996)

74.   P.Gaviña and J.-P.Sauvage,Tetrahedron Lett.,**38**,3521(1997)

75.   J.P.Collin,P.Gaviña and J.-P.Sauvage,New J.Chem.,**21**,525(1997)

76.   B.L Allwood,N.Spencer,H.Shahriari-Zavareh,J.F.Stoddart and D.J. Williams,J.Chem.Soc.,Chem.Commun.,1058(1987)

77.   B.L.Allwood,N.Spencer,H.Shahriari-Zavareh,J.F.Stoddart and D.J. Williams,J.Chem. Soc.,Chem.Commun., 1061(1987)

78.   J.-Y.Ortholand,A.M.Z.Slawin,W.Spencer,J.F.Stoddart and D.J.Williams, Angew.Chem.Int.Ed.Engl.,**28**,1394(1989)

79. P.R.Ashton,R.Ballardini,V.Balzani,M.Behloradsky,M.T.Gandolfi,D.Philp, L.Prodi,F.M.Raymo,M.V.Reddington,N.Spencer,J.F.Stoddart,M.Venturi and D.J.Williams,J.Am.Chem.Soc.,**118**,4931(1996)

80. F.M.Raymo and J.F.Stoddart,Pure Appl.Chem.,**69**,1987(1997)

81. M.Asakawa,P.R.Ashton,R.Ballardini,V.Balzani,M.Belohradsky,M.T. Gandolfi,O.Kocian,L.Prodi,F.M.Raymo,J.F.Stoddart and M.Venturi,J.Am. Chem.Soc.,**119**,302(1997)

82. F.M.Raymo,K.N.Houk and J.F.Stoddart,J.Am.Chem.Soc.,**120**,9318(1998)

83. D.B.Amabilino,P.R.Ashton,V.Balzani,C.L.Brown,A.Credi,J.M.J.Fréchet,J. W.Leon,F.M.Raymo,N.Spencer,J.F.Stoddart and M.Venturi,J.Am.Chem. Soc.,**118**,12012(1996)

84. M.Asakawa,C.L.Brown,S.Menzer,F.M.Raymo,J.F.Stoddart and D.J. Williams,J.Am.Chem.Soc.,**119**,2614(1997)

85. M.Asakawa,P.R.Ashton,W.Dehaen,.G.L'abbé,S.Menzer,J.Nouwen,F.M. Raymo,J.F.Stoddart,M.S.Tolley,S.Toppet,A.J.P.White and D.J.Williams, Chem.Eur.J.,**3**,772(1997)

86. R.E.Gillard,F.M.Raymo and J.F.Stoddart,Chem.Eur.J.,**3**,1933(1997)

87. A.E.Rowan,P.P.M.Aarts and K.W.M.Koutstaal,J.Chem.Soc.,Chem. Commun.,611(1998);A.E.Rowan,N.A.J.Sommerdijk,J.N.H.Reek,B. Zwanneburg,M.C.Feiters and R.J.M.Nolte,Macromol.Symp.,**117**,291 (1997)

88. A.P.H.J.Schenning,B.deBruin,A.E.Rowan,H.Kooijman,A.L.Spek and R.J.M.Nolte,Angew.Chem.Int.Ed.Engl.,**34**,2132(1995)

89. N.Yamaguchi,D.S.Nagvekar and H.W.Gibson,Angew.Chem.Int.Ed.,**37**,2361(1998)

90. P.R.Ashton,I.W.Parsons,F.M.Raymo,J.F.Stoddart,A.J.P.White,D.J. Williams and R.Wolf,Angew.Chem.Int.Ed.,**37**,1913(1998)

91. P.R.Ashton,S.J.Langford,N.Spencer,J.F.Stoddart,A.J.P.White and D.J. Williams,J.Chem.Soc.,Chem.Commun.,1387(1996)

92. A.Credi,V.Balzani,S.J.Langford and J.F.Stoddart,J.Am.Chem.Soc.,**119**, 2679(1997)

93. R.Ballardini,V.Balzani,A.Credi,M.T.Gandalfi,S.J.Langford,S.Menzer,L. Prodi,J.F.Stoddart,M.Venturi and D.J.Williams,Angew.Chem.Int.Ed.Engl., **35**,978(1996)

94. P.R.Ashton,R.Ballanlini,V.Balzani,E.C.Constable,A.Credi,O.Kocian,S.J. Langford,J.A.Preece,L.Prodi,E.R.Schofield,J.F.Stoddart and S.Wagner, Chem.Eur.J.,**4**,2413(1998)

556

95. S.J.Loeb and J.A.Wisner,Angew.Chem.Int.Ed.,**37**,2838(1998)

96. B.L.Allwood,N.Spencer,H.Shahriari-Zavareh,J.F.Stoddart and D.J. Williams,J.Chem.Soc.,Chem.Commun., 1064(1987)

97. P.R.Ashton,A.M.Z.Slawin,N.Spencer,J.F.Stoddart and D.J.Williams,J. Chem.Soc.,Chem.Commun.,1066(1987)

98. M.-V.Martínez-Díaz,N.Spencer and J.F.Stoddart,Angew.Chem.Int.Ed. Engl.,**36**,1904(1997)

99. P.R.Ashton,R.Ballardini,V.Balzani,I.Baxter,A.Credi,M.C.T.Fyfe,M.T. Gandolfi,M.Gómez-López,M.-V.Martínez-Díaz,A.Piersanti,N.Spencer, J.F.Stoddart,M. Venturi,A.J.P.White and D.J.Williams,J.Am.Chem.Soc., **120**,11932(1998)

100. P.R.Ashton,P.T.Glink,M.-V.Martínez-Díaz,J.F.Stoddart,A.J.P.White and D.J.Williams,Angew.Chem.Int.Ed.Engl.,**35**,1930(1996)

101. P.R.Ashton,R.Ballardini,V.Balzani,M.C.T.Fyfe,M.T.Gandolfi,M.-V.Martínez-Díaz,M.Morosini,C.Schiavo,K.Shibata,J.F.Stoddart,A.J.P.White and D.J.Williams,Chem.Eur.J.,**4**,2332(1998)

102. B.Odell,M.W.Reddington,A.M.Z.Slawin,N.Spencer,J.F.Stoddart and D.J. Williams,Angew.Chem.Int.Ed.Engl.,**27**,1547(1988)

103. P.R.Ashton,B.Odell,M.W.Reddington,A.M.Z.Slawin,J.F.Stoddart and D.J. Williams,Angew.Chem.Int.Ed.Engl.,**27**,1550(1988)

104. R.Castro,K.R.Nixon,J.D.Evanseck and A.E.Kaifer,J.Org.Chem.,**61**,7298 (1996)

105. M.Asakawa,S.Iqbal,J.F.Stoddart and N.D.Tinker,Angew.Chem.Int.Ed Engl.,**35**,976(1996)

106. P.R.Ashton,V.Balzani,O.Kocian,L.Prodi,N.Spencer and J.F.Stoddart,J. Am.Chem.Soc.,**120**,11190(1998)

107. M.Asakawa,P.R.Ashton,V.Balzani,A.Credi,G.Mattersteig,O.A.Matthews, M.Montalti,N.Spencer, J.F.Stoddart and M.Venturi,Chem.Eur.J.,**3**,1992 (1997)

108. P.R.Ashton,R.Ballardini,V.Balzani,S.E.Boyd,A.Credi,M.T.Gandolfi,M. Gómez-López,S.Iqbal,D.Philp,J.A.Preece,L.Prodi,H.G.Ricketts,J.F. Stoddart,M.S.Tolley,M.Venturi,A.J.P-White and D.J.Williams,Chem.Eur. J.,**3,**152(1997)

109. M.Asakawa,P.R-Ashton,S.Iqbal,A.Quick,J.F.Stoddart,N.D.Tinker,A.J.P. White and D.J.Williams,Israel J.Chem.,**36**,329(1996)

110. P.R.Ashton,S.R.L.Everitt,M.Gómez-López,N.Jayaraman and J.F.Stoddart, Tetrahedron Lett.,**38**,5691(1997)

111. D.B.Amabilino,P.R,Ashton,S.E,Boyd,M.Gómez-López,W.Hayes and J.F. Stoddart,J.Org.Chem.,**62**,3062(1997)

112. P.-L.Anelli,M.Asakawa,P.R.Ashton,R.A.Bissell,G.Clavier,R.Górski,A.E. Kaifer,S.J.Langford,G.Mattersteig,S.Menzer,D.Philp,A.M.Z.Slawin,N. Spencer,J.F.Stoddart,M.S.Tolley and D.J.Williams,Chem.Eur.J.,**3**,1113 (1997)

113. M.Kimura,Y.Misawa,Y.Yamaguchi,K.Hanabusa and H.Shirai,J.Chem. Soc.,Chem.Commun.,2785(1996)

114. M.Asakawa,P.R.Ashton,G.R.Brown,W.Hayes,S.Menzer,J.F.Stoddart,A.J. P.White and D.J.Williams,Adv.Mater.,**8**,37(1996)

115. P.R.Ashton,J.Huff,S.Menzer,I.W.Parsons,J.A.Preece,J.F.Stoddart,M.S. TolleyAJ-P.White and D.J.Williams,Chem.Eur.J.,**2**,31(1996)

116. S.-H.Lee,P.T.Engen and H.W.Gibson,Macromolecules,**30**,337(1997)

117. H.W.Gibson,P.T.Engen and S.-H.Lee,Polymer,**40**,l823(1999)

118. H.W.Gibson and M.Bheda,Polymer,**36**,2615(1995)

119. C.Pugh,J.-Y.Bae,J.R-Scott and C.L.Wilkins,Macromolecules,**30**,8139 (1997)

120. J.-Y.Bae,B.Narayanswamy and C.Pugh,Am.Chem.Soc.Div.Polym. Chem.,Polym.Prepr.,**37**,618(1996)

121. C.Gong and H.W.Gibson,Macromol.Chem.Phys.,**198**,2321(1997)

122. H.W.Gibson and S.Liu,Macromol.Symp.,**102**,55(1996)

123. C.Gong and H.W.Gibson,Macromolecules,**29**,7029(1996)

124. H.W.Gibson,S.Liu,C.Gong,Q.Ji and E.Joseph,Macromolecules,**30**,3711 (1997)

125. C.Gong and H.W.Gibson,Macromolecules,**30**,8524(1997)

126. C.Gong,Q.Ji,T.E.Glass and H.W.Gibson,Macromolecules,**30**,4807(1997)

127. C.Gong,T.E.Glass and H.W.Gibson,Macromolecules,**31**,308(1998)

128. C.Gong and H.W.Gibson,Angew.Chem.Int.Ed.Engl.,**36**,2331(1997)

129. E.Marand,Q.Hu and H.W.Gibson,Macromolecules,**29**,2555(1996)

130. J.Hunt,K.Nagapudi and H.W.Beckham,Am.Chem.Soc.Div.Polm.Chem., Polym.Prepr.,**38**,84(1997)

131. C.Gong,Q.Ji,C.Subramaniam and H.W.Gibson,Macromolecules,**31**,1814 (1998)

558

132. C.Gong and H.W.Gibson,J.Am.Chem.Soc.,**119**,8585(1997)

133. C.Gong and H.W.Gibson,J.Am.Chem.Soc.,**119**,5862(1997)

134. H.W.Gibson,D.S.Nagvekar,J.Powell,C.Gong and W.S.Bryant,
Tetrahedron,**53**,15197(1997)

135. H.W.Gibson,C.Gong,S.Liu and D.S.Nagvekar,Macromol.Symp.,**128**,89
(1998)

136. C.Gong and H.W.Gibson.Curr.Opinion Solid State Mater.Sci.,**2**,647
(1997)

137. N.Ogata,K.Sanui and J.Wada,J.Polym.Sci.,Polym.Lett.Ed.,**14**,459(1975)

138. T.Ooya and N.Yui,J.Biomater.Sci.,Polym.Ed.,**8**,437(1997);T.Ooya,T.Kumeno and
N.Yui,J.Biomater.Sci.,Polym.Ed.,**9**,313(1998)

139. T.Ooya and N.Yui,Macromol.Chem.Phys.,**199**,2311(1998);N.Yui,T.Ooya and
T.Kumeno,Bioconj.Chem.,**9**,118(1998);W.Kamimura,T.Ooya and N.Yui,J.
Contr.Rel.,**44**,295(1997)

140. T.Ooya,H.Mori,M.Terano and N.Yui,Macromol.Rapid Commun.,**16**,259
(1995)

141. H.Fujita,T.Ooya,M.Kurisawa,H.Mori,M.Tenaro and N.Yui,Macromol.Rapid
Commun.,**17**,509(1996)

142. W.Hermann,M.Schneider and G.Wenz,Angew.Chem.Int.Ed.Engl.,**36**,
2511(1997)

143. I.Yamaguchi,K.Osakada and T.Yamamoto,J.Am.Chem.Soc.,**118**,1811
(1996)

144. C.I.Simionescu,M.Grigoras,A.Farcas and A.Stoleru,Macromol.Chem.
Phys.,**199**,1301(1998)

145. A.Harada,H.Adachi,Y.Kawaguchi and M.Kamachi,Macromolecues,**30**,
5181(1997)

146. O.Noll and H.Ritter,Macromol.Rapid Commun.,**18**,53(1997)

147. I.Yamaguchi,K.Osakada and T.Yamamoto,Macromolecules,**30**,4288
(1997)

148. M.Born and H.Ritter,Adv.Mater.,**8**,149(1996)

149. O.Noll and H.Ritter,Macromol.Chem.Phys.,**199**,791(1998)

150. J.Jeromin,O.Noll and H.Ritter,Macromol.Chem.Phys.,**199**,2641(1998)

151. D.Whang,Y.-M.Jeon,J.Heo and K.Kim,J.Am.Chem.Soc.,**118**,11333
(1998)

152. J.-M.Kern,J.-P.Sauvage,G.Bidan,M.Billon and B.Divisia-Blohorn,Adv. Mater.,**8**,580(1996);G.Bidan,M.Billon,B.Divisia-Blohorn,J.M.Kern,L.Raehm and J.-P.Sauvage,New J.Chem.,**22**,1139(1998)

153. P.L.Vidal,M.Billon,B.Divisia-Blohorn,G.Bidan,J.M.Kern and J.-P.Sauvage, J.Chem.Soc.,Chem.Commun.,629(1998)

154. S.S.Zhu,P.J.Carroll and T.M.Swager,J.Am.Chem.Soc.,**118**,8713(1996)

155. S.S.Zhu and T.M.Swager,J.Am.Chem.Soc.,**119**,12568(1997)

156. B.F.Hoskins,R.Robson and D.A.Slizys,J.Am.Chem.Soc.,**119**,2952(1997)

157. M.J.Marsella,P.J.Carroll and T.M.Swager,J.Am.Chem.Soc.,**117**,9832 (1995)

158. C.Gong and H.W.Gibson,Angew.Chem.Int.Ed.,**37**,310(1998)

159. C.Gong,P.B.Balanda and H.W.Gibson,Macromolecules,**31**,5278(1998)

160. C.Gong and H.W.Gibson,Macromol.Chem.Phys.,**199**,l801(1998)

161. G.J.Owen and P.Hodge,J.Chem.Soc.,Chem.Commun.,11(1997)

162. P.E.Mason,J.W.Parsons and M.S.Tolley,Angew.Chem.Int.Ed.Engl.,**35**, 2238(1996)

163. P.E.Mason,I.W.Parsons and M.S.Tolley,Polymer,**39**,3981(1998)

164. P.E.Mason,W.S.Bryant and H.W.Gibson,Macromolccules,in press

165. K.Nagapudi,J.Leisen,H.W.Beckham and H.W.Gibson,Macromolecules,in press

166. P.-L.Anelli,P.R.Ashton,R.Ballardini,V.Balzani,M.Delgado,M.T.Gandolfi, T.T.Goodnow,A.E.Kaifer,D.Philp,M.Pietraszkiewicz,L.Prodi,M.V. Reddington,A.M.Z.Slawin,N.Spencer,J.F.Stoddart,C.Vincent and D.J. Williams,J.Am.Chem.Soc.,**114**,193(1992)

167. Y.X.Shen,P.T.Engen,M.A.G.Berg,J.S.Merola and H.W.Gibson, Macromolecules,**25**,2786(1992)

168. P.R.Ashton,D.Philp,N.Spencer and J.F.Stoddart,J.Chem.Soc.,Chem. Commun.,1124(1992)

169. T.V.S.Rao and D.D.Lawrence,J.Am.Chem.Soc.,**112**,3614(1990)

170. R.Wylie and D.Macartney,J.Am.Chem.Soc.,**114**,3136(1992)

171. C.O.Dietrich-Buchecker,A.K.Khemiss and J.-P.Sauvage,J.Chem.Soc., Chem.Commun.,1376(1986)

172. G.Wenz,E.Bey and L.Schmidt,Angew.Chem.Int.Ed.Engl.,**31**,783(1992); G.Wenz,F.Wolf,M.Wagner,and S.Kubik,New J.Chem.,**17**,729(1993)

173. A.Harada,J.Li and M.Kamachi,Macromolecules,**27**,4538(1994);A.Harada
and M.Kamachi,Macromolecules,**23**,2821(1990);A.Harada,J.Li and M.
Kamachi,Macromolecules,**26**,5698(1993);A.Harada,J.Li and M.Kamachi,
Nature(London),**356**,325(1992)

174. M.C.Bheda,Ph.D.Dissertation, Virginia Polytechnic Institute and State
University,Blacksburg,VA,1992

175. Y.X.Shen,Ph.D.Dissertation, Virginia Polytechnic Institute and State
University,Balcksburg,VA,1992

176. J.-C.Chambron,C.O.Dietrich-Buchecker,J.-F.Nierangarten,J.-P.Sauvage,
N.Soladie,A.-M.Albrecht-Gary and M.Meyer,New J.Chem.,**19**,409(1995)

177. H.W.Gibson,S.Liu,P.Lecavalier,C.Wu and Y.X.Shen,J.Am.Chem.Soc.,
117,852(1995)

CHAPTER 13
OLIGOMERIC AND POLYMERIC CATENANES

David A. Leigh, Richard A. Smith,
University of Warwick, UK

13.1 Introduction - New architectures for old monomers

One of the great assets that polymers possess is their versatility and scope for property tuning. The range of functional groups which can be incorporated into their structures together with the many different ways of fabricating them has led to multi-billion dollar industries and the employment of polymers as the key components in products as diverse as vinyl records, bullet proof vests and artificial organ implants [1][2]. In determining what leads to these vast property ranges, it has long been recognised that in addition to simple chemical composition, both the structural conformation of single chains and the interactions between those chains are inextricably linked to the properties of polymer-based materials. Given the nature of industrial production processes and the high cost of introducing new chemical building blocks, it seems likely that the new polymers of the next century will be derived primarily from the ever-decreasing pool of perhaps a dozen existing cheap monomers [3]. An attractive strategy towards meeting future demands for materials with enhanced properties is thus to assemble these existing building blocks in new ways thus exploiting novel molecular-level architectures rather than the nature of the 'bricks' from which they are built.

13.1.1 Mechanical linkages at the molecular level

Consider the analogy of a molecular level and a macroscopic rod of metal. Different chemical compositions of the polymer can be used to tailor some of its properties (strength, melting point, chemical stability *etc*) in a similar way to using different alloys of the metal in the rod. However, by changing the *architecture* of the metal object from a solid rod to a chain, fundamental changes in other properties (*e.g.* flexibility) of the system may be altered whilst retaining many of the fundamental characteristics (*e.g.* strength) of the original structure. This concept is leading chemists to wonder about the properties of an interlocked chain at the molecular level - a linear mechanically linked polymer (*e.g.* **A**, Figure 1) - or even a polymer made up solely of interlocked rings (e.g. **G**, Figure 1). Incorporating flexible (architecture **A-D**, **F**, **G**) or co-conformationally switchable linkages (architecture **E**) into polymer backbones could generate a range of unusual and potentially useful properties at the macroscopic level including improved solubility, processibility, chemical compatibility, novel rheological properties, variable surface properties, low

temperature stability, shock absorbance, elasticity and so on. Supporting this theory is the wealth of knowledge concerning the physical properties of interpenetrating polymer networks [4] which are dictated by the mechanical entanglement of the polymer chains, suggesting that the properties of polycatenanes should also be greatly influenced by their mechanical linkages.

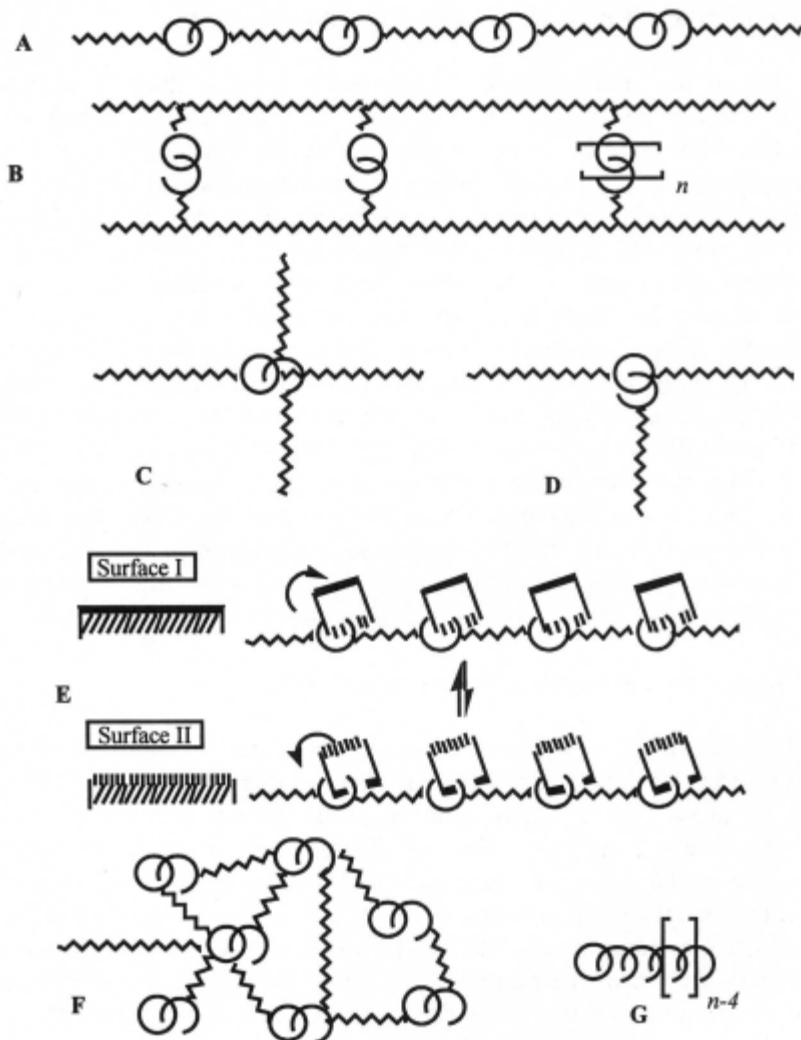Figure 1 - Possible types of polymers based upon catenane architecures: A Linear mechanically-linked polymers; B mechanically cross-linked polymers; C stars with a flexible, potentially switchable, catenane core; D combs with catenane linkages; E main chain catenanes with switchable surface properties; F highly mechanically-crosslinked networks; G poly- or [n]catenanes. Only examples of types A and F have thus far been prepared.

13.1.2 Catenanes: Functional as well as aesthetically pleasing molecular level architectures

Synthetic chemistry research is undertaken for a variety of reasons. Developing methodology in order to overcome a difficult synthetic problem can be motivation in itself, or the target molecule may be expected to exhibit properties of particular appeal. Historically, the preparation of aesthetically pleasing molecules (dodecahedrane, cubane, molecular shuttles, wheels, gears and switches *etc*) has always attracted special interest. The comparison between molecular level architectures and everyday symbols and objects can aid the understanding of what can otherwise appear complex situations. Molecular level observations backed up by pictorial illustrations from the macrocscopic world include features such as the 'chair' and 'boat' forms of cyclohexane, **C₆₀** as a 'football', DNA's **α-helical** 'spiral staircase' and dendritic 'molecular trees'. But what if synthetic molecular versions of macroscopic entities also emulated some of the physical characteristics of their larger cousins?

Catenanes [5] (Figure 2), from the Latin 'catena' meaning 'chain', are molecules containing two or more rings threaded one through the other so that they are inseparable without the breaking of at least one covalent bond.

Figure 2 – General structure of a [2]catenane.

The synthesis of mechanically interlocked ring systems was undoubtedly initially driven by their being a challenging, structurally elegant, target. However, the potential scope for exploiting the unique nature of mechanical linkages through their incorporation into polymeric materials was also almost immediately recognised (Figure 1). Unfortunately, due to the low yielding or labour-intensive synthesis of even simple catenanes, the development of polycatenanes has lagged far behind that of polyrotaxanes (where rings are threaded onto a polymer main- or side-chain, see Chapter 12). These have been synthetically accessible for several years and their structure-property relationships are now also beginning to be understood [6]. However, recent advances in synthetic routes to catenanes - including their synthesis in one step

from cheap, commercially available reagents and their near-quantitative synthesis using olefin metathesis technology (see Section 13.2.4) - together with a greatly improved understanding of their dynamic and other physical properties - means that they are now serious potential components for novel macromolecular architectures.

13.2 Synthesis of [2]catenanes

13.2.1 Historical background

Although interlocked molecular rings were discussed as early as 1912 [7], it was not until the 1960's that Frisch and Wasserman prepared the first catenanes and outlined general routes by which such molecules might be accessible [8]. The suggested synthetic strategies (Figure 3) included; (I) statistical threading of one ring by a linear molecule which is to be formed into the second ring (the statistical approach); (II) the construction of the two rings about a central core (the directed approach); and (III) the so-called 'Möbius strip' approach, a particularly elegant strategy which relies on obtaining Möbius strips containing two half-twists and then successfully cutting along the closed strip to give the two mechanically interlocked rings. Only the last approach has yet to prove successful in preparing catenanes. Despite much effort the Mobius strip strategy is limited by the inherent problem in generating the twists required for the catenane precursor [9].
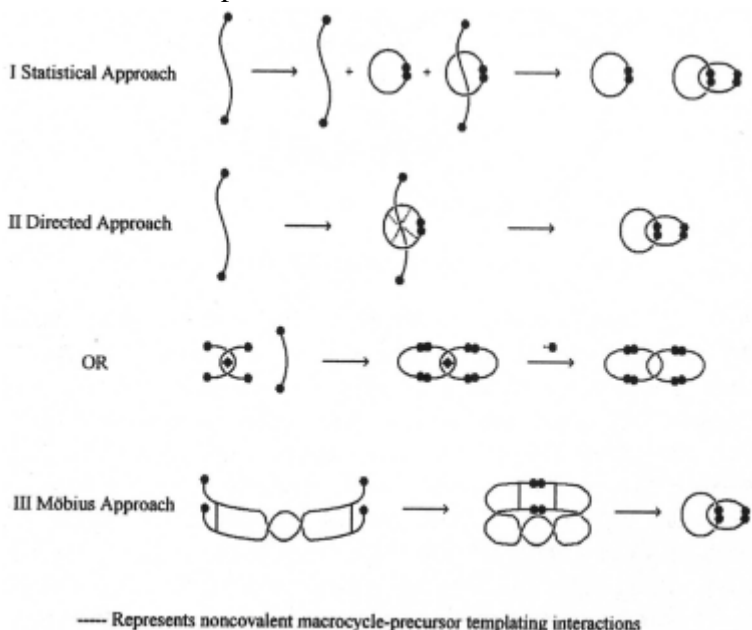

----- Represents noncovalent macrocycle-precursor templating interactions

Figure 3 – Suggested synthetic strategies towards the synthesis of [2]catenanes.

13.2.2 Statistical approach

The first statistical synthesis of a catenane was successfully carried out by Wasserman in 1960 [10]. Later Zilkha and co-workers [11] and Schill *et al.* [12] developed greatly improved preparative statistical syntheses of [2]catenanes (the prefix refers to the number of interlocked components). During the catenane forming reactions a linear precursor is required to thread through a macrocycle before the precursor cyclises. Even using macrocycles as a solvent, the amount of precursor that actually threads is so small that the yields of catenanes obtained were too low for evaluations of any properties induced by the mechanically interlocked architecture.

13.2.3 Directed approach

In order to eliminate the statistical element of the previous strategy, Schill and Lüttringhaus [13] conceived an elegant synthetic pathway utilising the perfect geometry of a functionalised macrocycle to impose intramolecular macrocyclisation in a predetermined way yielding a covalently bound interlocked precursor. Selective cleavage in three positions of this precursor affords the expected [2]catenane. This pathway ensures the formation of interlocked rings but at the heavy price of a multi-step pathway which in itself inhibits the large scale preparation of catenanes.

13.2.4 Noncovalent templating interactions

Clearly, what is required for an efficient route to catenanes is some form of molecular 'glue' which can intertwine and orientate the components of catenane precursors so that they are predisposed - or forced - to interlock before the final cyclisation step. The 'directed approach' was initially used to achieve this using formal covalent bonding strategies. The synthesis of catenanes was revolutionalised in the 1980's, however, by the use of <u>noncovalent</u> bonding to hold components of the catenane precursors in place. Such strategies are now commonplace in catenane synthesis with one or, more often, a combination of the following categories of noncovalent bonding interactions being employed to organise the pre-catenane synthons;

(a)   hydrophobic interactions
(b)   metal-ligand coordination
(c)   **π,π-stacking** of electron rich and electron poor aromatic rings
(d)   complementary donor-acceptor hydrogen-bonding.

13.2.4 (a) Hydrophobic interactions

As early as 1958 Lüttringhaus *et al.* [14] suggested that weak attractive interactions between a linear thread and a macrocycle could be used to overcome the disfavourable entropic contribution to threading which greatly limits the effectiveness of the statistical synthesis of catenanes. To prove the point he tried to utilise the rigid hydrophobic cavity of cyclodextrins (cyclic oligosaccharides) and their ability to bind a linear aliphatic guests in aqueous solution to generate significant concentrations of a threaded catenane precursor. Unfortunately the final cyclisation reactions failed to produce catenane, possibly as a result of an injudicious choice of thread length or conformations being adopted by the threaded component of the complex being adopted which were unfavourable for subsequent cyclisation.

It is testament to this far-sighted strategy, however, that thirty-five years after Lüttringhaus first proposed the idea, the first catenated cyclodextrins were reported by Stoddart [15] who made use of the extended torus-shaped cavity of **heptakis(2,6-di-O-methyl)-β-cyclodextrin** (**1**) (Figure 4). The two [2]catenanes **2** and **3** were obtained in yields of 3.0 and 0.8% respectively in addition to an equimolar mixture of two isomeric [3]catenanes **4** and **5** obtained in 1.1% yield. Developing this theme, using a constitutionally asymmetric diamine as the substrate during the catenane forming reaction, resulted in orientational isomers of a [2]catenane being isolated [16].
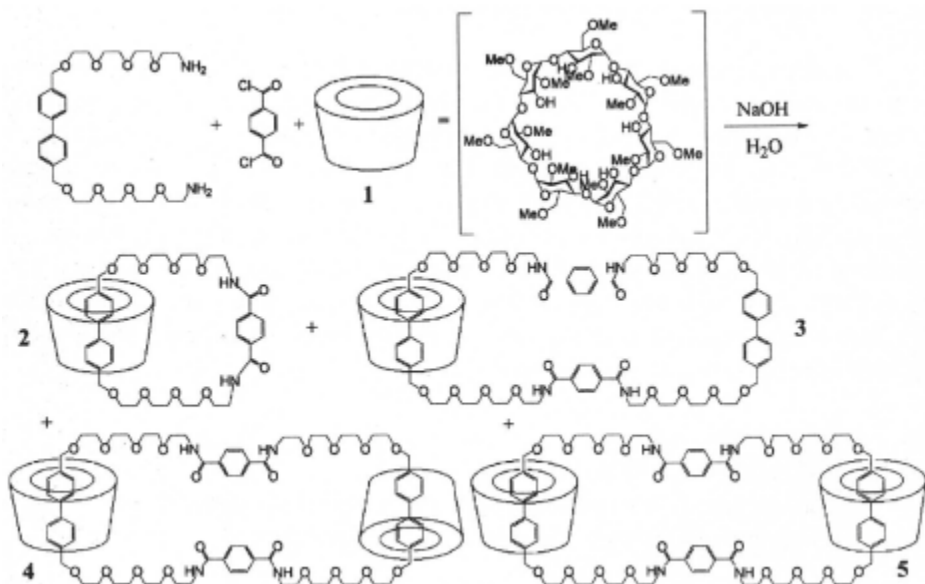

Figure 4 - The synthesis of catenated cyclodextrins.

13.2.4   (b) Metal-ligand coordination

Schill's directed synthesis of catenanes can be considered to consist of a core segment onto which building blocks to the two rings are attached by conventional covalent bonds, elaborated into appropriate precursors, and finally cyclised.   Another type of central unit could be based upon transition metal coordination, with the ligands eventually becoming the two interlocked macrocycles. This approach was originally suggested by Closson to Frisch and Wasserman in 1961 [17] and by Sokolov in 1972 [18], but the remarkable effectiveness of this concept was only demonstrated in 1984 when Sauvage *et al.* found that 2,9-dianisyl-l,10-phenanthroline gives a tetrahedral complex with copper(I) that acts as an excellent catenane-forming template.
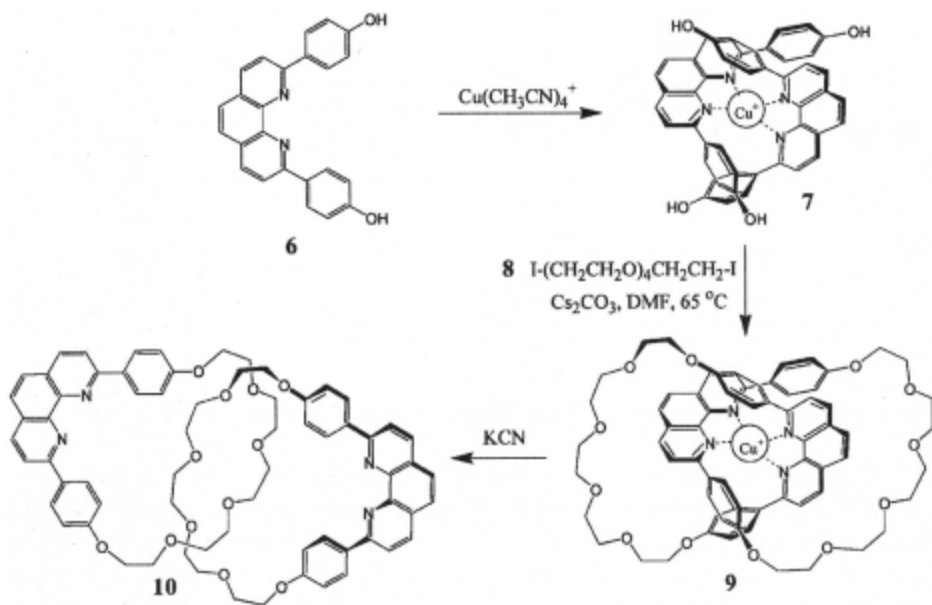

Figure 5 - The supramolecular age of interlocked molecular synthesis arrives: The first catenane synthesised via a transition metal template.

A functionalised version of the phenanthroline ligand (**6**) was prepared (Figure 5) [19][20]. In the presence of $Cu(CH_3CN)_4^+.BF_4^-$, the two ligands (**6**) intertwine through the stable copper(I) complex **7**. The four phenol groups of the complex react with two 1,14-diiodo-3,6,9,12-tetraoxatetradecane (**8**) chains under high dilution conditions (to minimise the amount of intermolecular ring closure) in the presence of a large excess of cesium carbonate in dimethylformamide. The resulting catenate **9** (the term 'catenate' denotes a catenane-metal complex) was obtained in 27% yield using this very convenient

one-pot synthesis which benefits from virtual quantitative interlocking of the catenane precursors. To free the interlocked rings from their metal 'glue' the Cu(I) complex could be demetalated by treatment with potassium cyanide, affording the catenand (free catenane ligand) **10**.
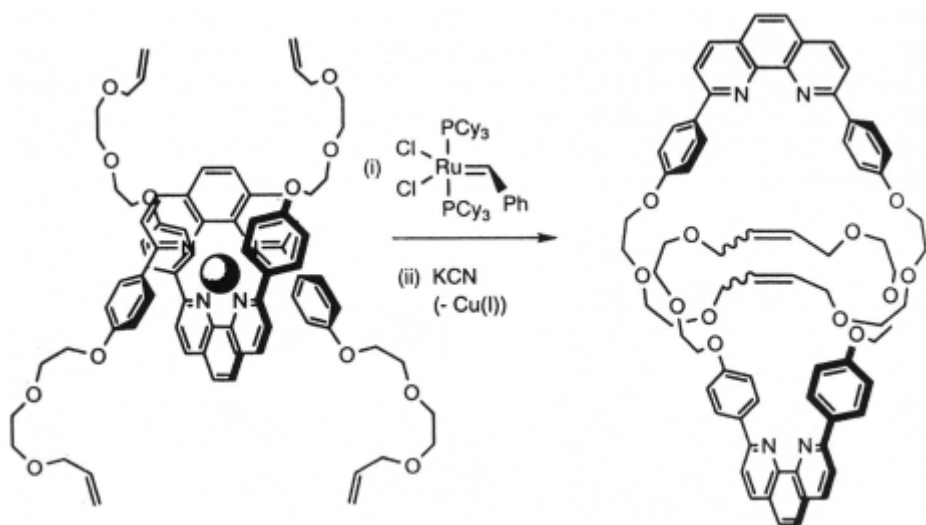

Figure 6 - RCM of an intertwined Cu(I) complex to give, after demetallation, a [2]catenane.

In an exciting recent development, Sauvage has used the synergistic combination [21] of the preorganising Cu(I) template described above with ring closing metathesis (RCM) which is a much more efficient method of closing the catenane precursor complex than phenol alkylation (Figure 6). The yields achieved using this method reach an incredible 92% for the catenate, with the Grubbs RCM catalyst [22] having the additional advantage of being highly substrate-tolerant. The Cu(I) is subsequently easily removed with cyanide ion and the double bonds are available either to be hydrogenated or to be used to further functionalise the free catenane.

Reversible ring closing reactions are potentially even more versatile and offer even higher yields of catenanes than RCM since, if the reactions are under thermodynamic control (favouring catenane formation if attractive intercomponent supramolecular interactions are programmed into their synthesis), the often substantial yields of unwanted macrocyclic non-interlocked 'mistakes' can be 'recycled' (Figure 7).
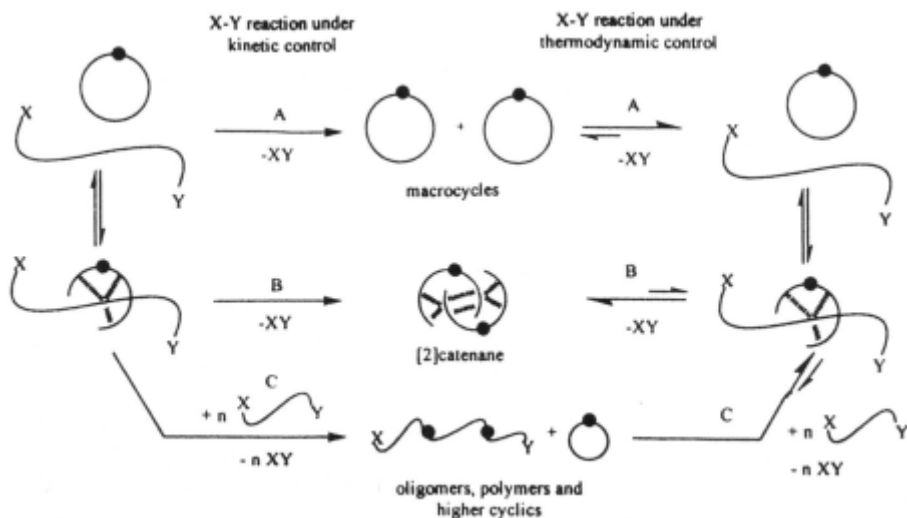
Figure 7 - Catenane synthesis under kinetic (left hand side) and thermodynamic (right hand side) control. Pathway A represents intramolecular cyclisation of unthreaded precursors leading to noninterlocked 'mistakes'; pathway C gives intermolecular oligo- and polymeric condensation products; pathway B affords a [2]catenane with preprogrammed attractive intercomponent Interactions. Reversible ring closure reactions allow conversion of the less stable noninterlocked species through to the [2]catenane.

Fujita *et al.* [23] have used an elegant combination of reversible metal-ligand bonding, **π,π-interactions,** hydrophobic effects and ligand design to obtain a *quantitative(!)* catenane synthesis through self assembly simply by mixing certain bispyridyl ligands with a palladium(II) salt in water (Figure 8). Similarly, Sanders and co-workers [24] have utilised the incorporation of both zinc(II)-bipyridyl ligation and **π-donor (dinaphtho-crown ether)/π-acceptor** (aromatic diimide) stacking interactions to achieve quantitative catenane synthesis under reversible, thermodynamically controlled conditions.
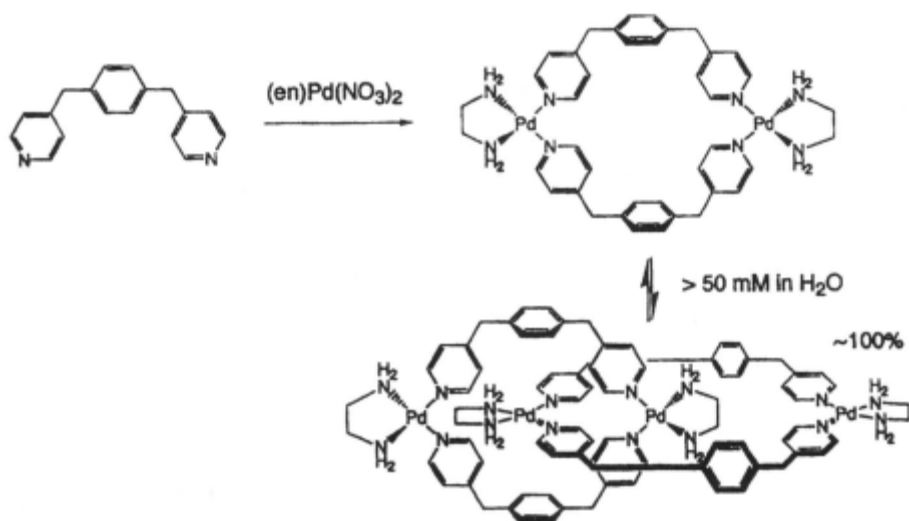
Figure 8 – A thermodynamically controlled route to [2]catenanes containing palladium(II) metal centres.

13.2.4 (c) π,π-stacking of electron rich and electron poor aromatic rings

The use of aromatic stacking interactions to interlock molecular components was pioneered by Stoddart who in 1989 used his understanding of host-guest systems to generate a very successful new type of catenane synthesis [25]. The **π-electron-deficient** cyclobis(paraquat-*p*-phenylene) tetracationic cyclophane (**11**) was threaded and interlocked through the **π-electron-rich** crown ether bis-*p*-phenylene-34-crown-10 (**12**) to give the [2]catenane **13** in 70% yield (Figure 9). The structure contains **π-π** stacking [26][27] between the **π-electron-deficient** and the **π-electron-rich** aromatic rings, as well as hydrogen-bonding interactions [27][28] between the hydrogen atoms attached to the aromatic crown ether and the *p*-xylyl spacers of the cyclophane. Additional hydrogen-bonding interactions [29][30] are present between oxygen atoms of the tetraethylene glycol spacers of the neutral crown ether component and the α-hydrogen atoms of the bipyridinium portions of the tetracationic cyclophane. The generality of this self-assembly process to catenanes has led to many catenanes featuring a variety of different crown ethers [31] and tetracationic cyclophanes [32] together with extensive work surrounding their properties and potential uses [5].
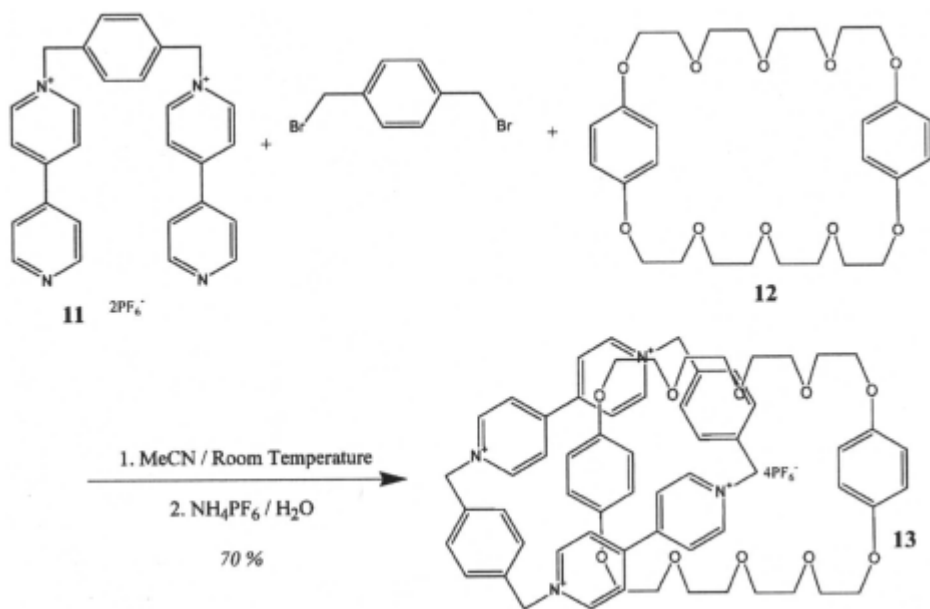
Figure 9 -π,π-Aromatic stacking templated [2]catenane synthesis.

Developing this theme further, Saunders *et al.* recently dimerised bis-acetylenic aromatic diimide precursors in the presence of a dinaphtho-crown ether to afford *uncharged* [2]catenanes through complementary donor-acceptor π-systems in yields of up to 52% [33].

13.2.4 (d) Complementary donor-acceptor hydrogen-bonding and the properties of mechanically interlocked rings

A [2]catenane synthesis based on the self assembly of precursors to interlocked amide containing macrocycles templated by hydrogen bonds and a degree of π-π interactions was independently discovered by Hunter [34] and Vögtle and co-workers [35] in 1992. Hunter's reaction scheme involves the preliminary formation of isophthaloyl bis(diamine) 14 (Figure 10) from the cyclohexylidine-substituted diamine 15 and isophthaloyl dichloride (16) - the reagents used by Vögtle in his one-pot catenane synthesis. When 14 is treated with 16 under high dilution conditions the [2]catenane 17 is formed in 34% yield along with the cyclic dimer 18 (51%) and the cyclic tetramer 19 (5%). In Vögtle's one pot procedure the distribution of the analogous products was 8, 12 and 10% respectively.
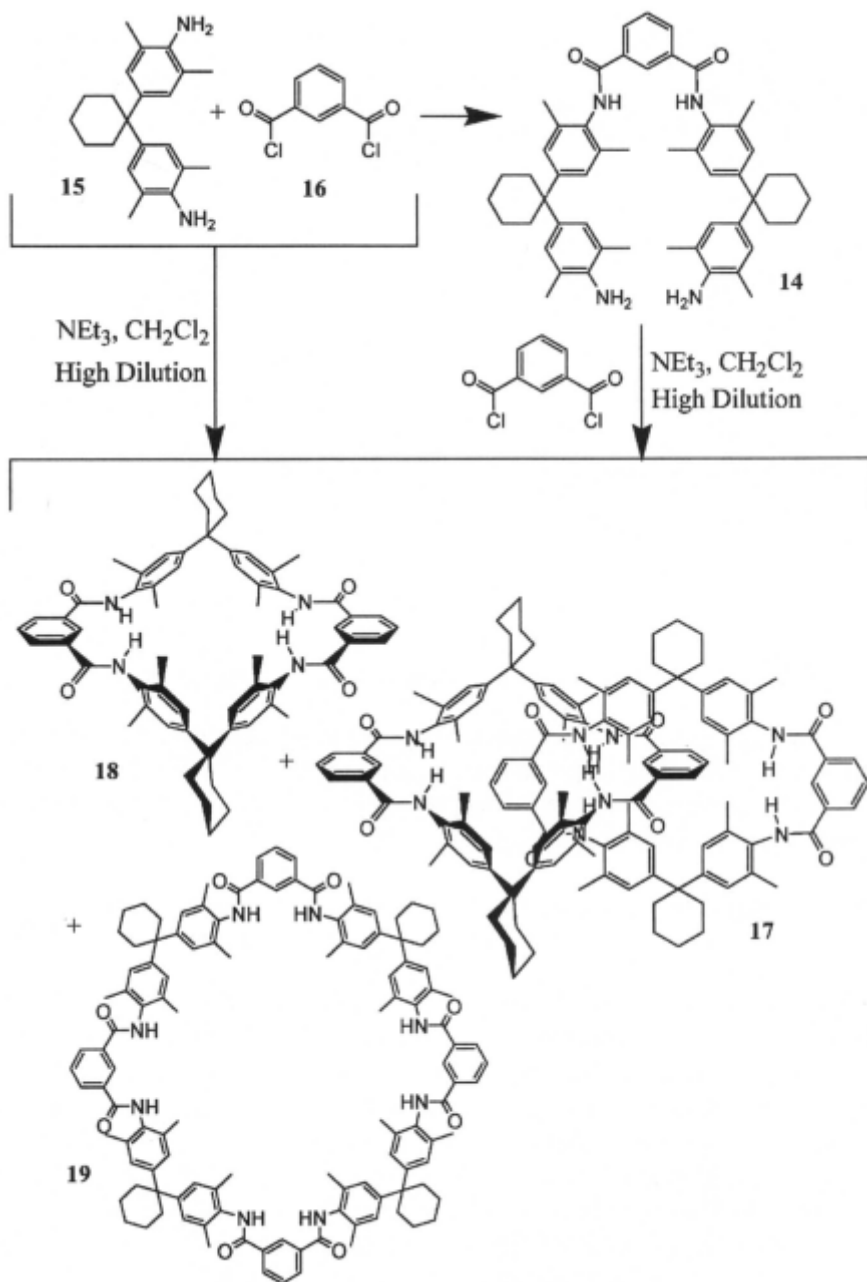
Figure 10 – One- (left) and two-step (right) syntheses of hydrogen-bond templated [2]catenanes and the x-ray crystal structure of [2]catenane 17.

Temperature-dependent NMR studies revealed that the free rotation of the macrocycles in catenane **17** through the centre of the other ('circumrotation'[5]) is prevented by the bulky cyclohexylidene groups. This prevents the inner and outer isophthaloyl units from exchanging their positions and may have consequences for the somewhat limited functionalisation tolerated during this catenane synthesis.

The most practically accessible catenaries on a large scale, however, probably remain benzylic amide catenanes which again utilise the templating power of hydrogen bonding. The simplest of these is prepared directly from commercially available (and cheap!) isophthaloyl dichloride and xylylene diamine in 20% yield following a simple chromatography-free purification procedure (Figure 11) [36][37][38].
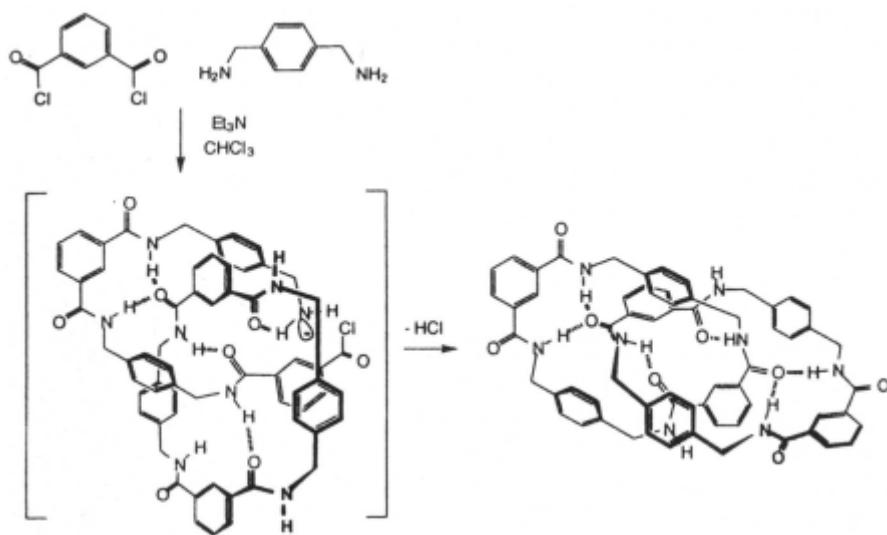
Figure 11 - A one step synthesis of a [2]catenane from commercially available starting materials

The structural versatility and ready availability of this homocircuit (both rings are the same) catenane and its' component macrocycle has made it suitable for the first detailed investigation of the properties of a mechanically interlocked molecule [39][40][41]. Macrocycle circumrotation - the most interesting dynamic feature of catenanes - can be varied in benzylic amide catenanes over *nine(!)* orders of magnitude (from sub-microsecond to many hours for a single circumrotation event) simply by varying the structure of the rings and the polarity of the molecular environment (polar solvents such as dimethyl sulphoxide break up the inter-ring hydrogen which provides the main barrier to ring rotation) [39]. Other unusual properties displayed by benzylic

amide catenanes include that their IR and Raman spectra are unusually matrix dependent (large frequency shifts are observed between KBr and CsI) but matrix insensitive in the case of their non-interlocked macrocyclic components [40]. Similarly, the electrochemistry of catenanes and their components differ, with electrochemically-induced braking of circumrotation a feature in the catenane. The original prototypical benzylic amide catenane can also be sublimed to form high optical quality films of unusually high refractive index (1.6) and of thicknesses **(0.8µm)** sufficient for guided wave applications, indicating considerable promise for these materials as versatile photonic materials [41].

13.3 Higher order catenanes

Our understanding of how to prepare [2]catenanes in an efficient manner is now being translated into the controlled creation of higher order interlocked architectures. One of the challenges in stretching the recently developed templating methodologies to their limit, is the push to add further macrocycles onto the growing mechanically linked chain. Indeed, high molecular weight linear polycatenanes of architecture **G** (Figure 1) can be regarded as something of a 'holy grail' in unnatural product synthesis [42].

13.3.1 [n]Catenanes, adding links to the chain

Since the development of reliable synthetic routes to [2]catenanes the number of examples of [3]catenanes hasn't lagged too far behind. The reason being that a number of routes towards [2]catenanes can be adapted to yield [3]catenanes or, in some cases, [3]catenanes are produced as side products during [2]catenane synthesis. As more efficient, higher yielding templating methodologies are developed the greater the probability that they can be utilised to interlock more than two components at a time. Furthermore, the greater the templating power to hand, the greater the degree of complexity of the structures which can be targeted.

Beneficial to the generation of higher order catenanes has been the discovery that in some cases slight modifications to the structure [43][44][45][46] of the templating macrocycle or reaction conditions [47] can actually disfavour [2]catenane formation in preference to [3]- or higher catenanes [3]. Sanders *et al.* utilised the complimentary of donor-acceptor **π**-systems to template the formation of uncharged catenanes by the oxidative dimerisation of the bis-acetylene-derivatised pyromellitimide **18** in the presence of a dinaphtho-crown ether **19** [33] (Figure 12). This produced the [2]catenane **20** with yields in the range of 25-33%. However, by employing a constrained macrocyclic host **21** for catenane formation both intermolecular and
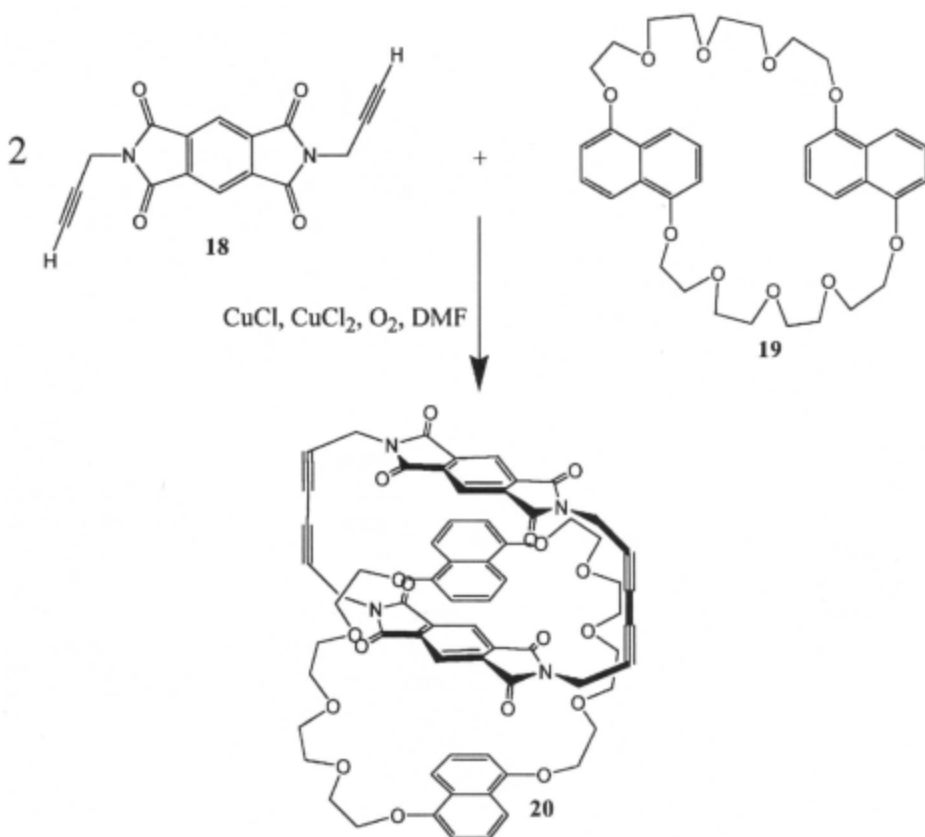
Figure 12 – Synthesis of [2]catenanes from oxidative coupling of **π-stacked** components.

intramolecular ring closure by oxidative coupling of terminal acetylenes of the catenane precursor take place [48] (Figure 13). This observation and rather low yield of [2]catenane (in comparison to **20**) suggest that the macrocyclic cavity of **21** does not provide a particularly efficient template for the cyclisation of the acetylenic catenane forming precursor. Hence, as [2]catenane forms less readily there is a greater chance of intermolecular closing of the precursors leading to the [3]catenane (characterised by mass spectrometry) albeit in a yield of less than 1%.

576
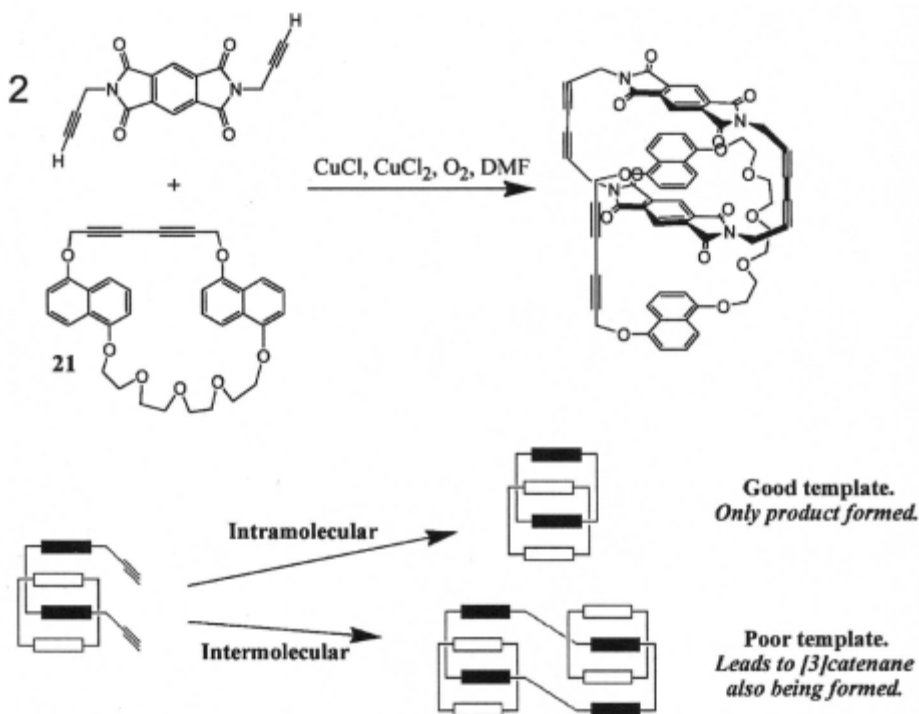
Figure 13 – Favouring [3]catenane formation by using a poor catenane templating
macrocycle.

A similar phenomena is observed with the classic Stoddart system; the use of a poorer crown ether template causes the yields of [3]- and [4]catenanes to rise significantly [45] (Figure 14). Reaction of **22.2PF$_6$** with **23** in acetonitrile in the presence of crown ether **24** afforded, the [2]catenane **25.4PF$_6$** (52%) together with its cyclic dimer, the [3]catenane **26.8PF$_6$** (5%). When the poorer templating, crown ether **27** was reacted under the same conditions, the yield of the [2]catenane **28.4PF$_4$** decreased to 46% while the yield of the [3]catenane **29.8PF$_6$** rose to 7%. In addition, the [4]catenane **30.8PF$_6$,** in which three crown ethers are threaded around a single octactionic cyclophane, was isolated in 3% yield.

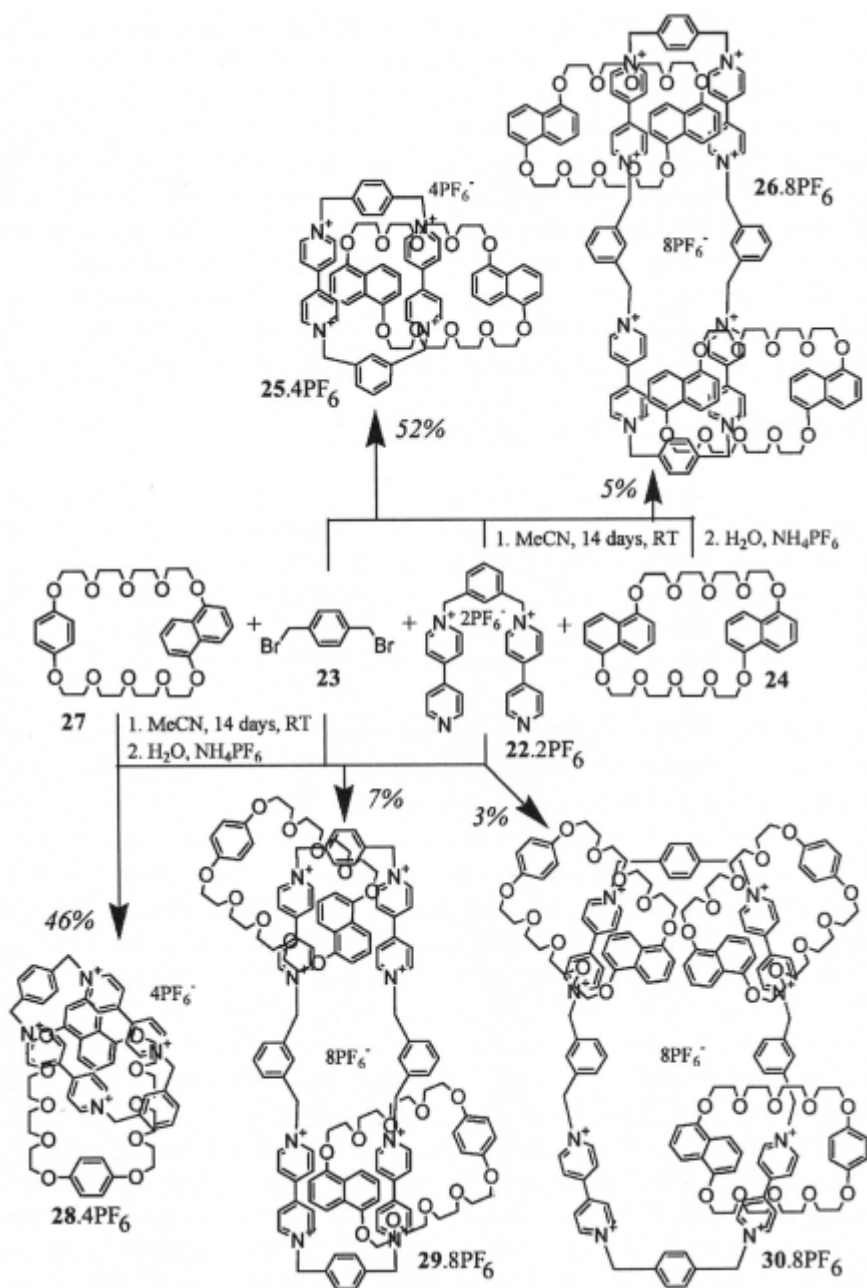**Figure 14** – **Increasing the yields of [3] and [4]catenanes by using poorer macrocyclic catenane templates.**

These effects have shown to be governed by variations in kinetic (covalent bond-forming) and thermodynamic (noncovalent bonding) factors rather than on steric grounds [45]. If the ring closure of the guest is a relatively fast process compared with the intermolecular covalent bond formation, the [2]catenane yield tends to be favoured (note using the π-electron deficient component incorperating two *p*-phenylene spacers gives 83% yield of the [2]catenane with no [3]catenane produced). However, if the kinetics of the ring closure are relatively slow then [3]catenanes and higher aggregates are produced. A significant difference between this system and the observations of Sanders *et al.* is that the templating crown ether **24** does not bind to the catenane precursor **22.2PF₆** under the reaction conditions [49].

13.3.2 'Olympiadane' - a linear [5]catenane

The most impressive oligo-catenane synthesis so far is unquestionably that of the [5]catenane, 'Olympiadane' [50]. Olympiadane, which takes its name from the symbol of the Olympic movement, was synthesised by the Stoddart group employing a [3]catenane as the template on which to clip, in a stepwise manner, smaller tetracationic cyclophanes. The first attempts at such a synthesis culminated in only a trace of the [5]catenane [51], but a superior scheme is shown in figure 15 [46].

Reaction of **31.2PF₆** with equimolar amounts of the dibromide **32** in the presence of an excess of the macrocyclic ether component **33** at ambient temperature and pressure afforded a [3]catenane **34.4PF₆** in 10% yield. The [3]catenane was then 'clipped' at either end through treatment with an excess of **11.2PF₆** and **35** in dimethylformamide, originally at ambient temperature and pressure for fourteen days. The isolated yields obtained were 51% for the [4]catenane **36.8PF₆** and 18% for the [5]catenane **37.12PF₆** [46]. By employing ultra high pressure conditions [50] the yield of the [5]catenane rose dramatically with even higher order species being isolated [46]. At 12 kbar after 6 days no [3]catenane **34.4PF₆** remained and the linear [5]catenane **37.12BF₆,** and branched [6]- and [7]catenanes, **38.16BF₆** and **39.20BF₆** were the major products in yields of 30, 28 and 26% respectively.

The synthesis of Olypiadane is the crowning achievement thus far in the synthesis of interlocked molecules by supramolecular templating strategies. Although it is only five rings long it is clearly a significant step towards achieving polycatenane architectures such as **G** (Figure 1). Unfortunately, as is evident from the examples discussed above, there are major limitations in attempting to extend these kinds of strategies further in that the yields for each further addition of a ring to the growing chain rapidly decrease. Although some headway is possible, for example through the potential further coupling of [5]catenane 'building blocks', this stepwise approach is labour-intensive and

requires many synthetic steps and purification procedures. Looking to the future, traditional stepwise synthetic schemes cannot be a good approach to **G**-type polycatenanes. The goal must be a one pot strategy where all the necessary building blocks self-assemble to form a continuous interlocked chain under thermodynamic control; the question is how to achieve this?
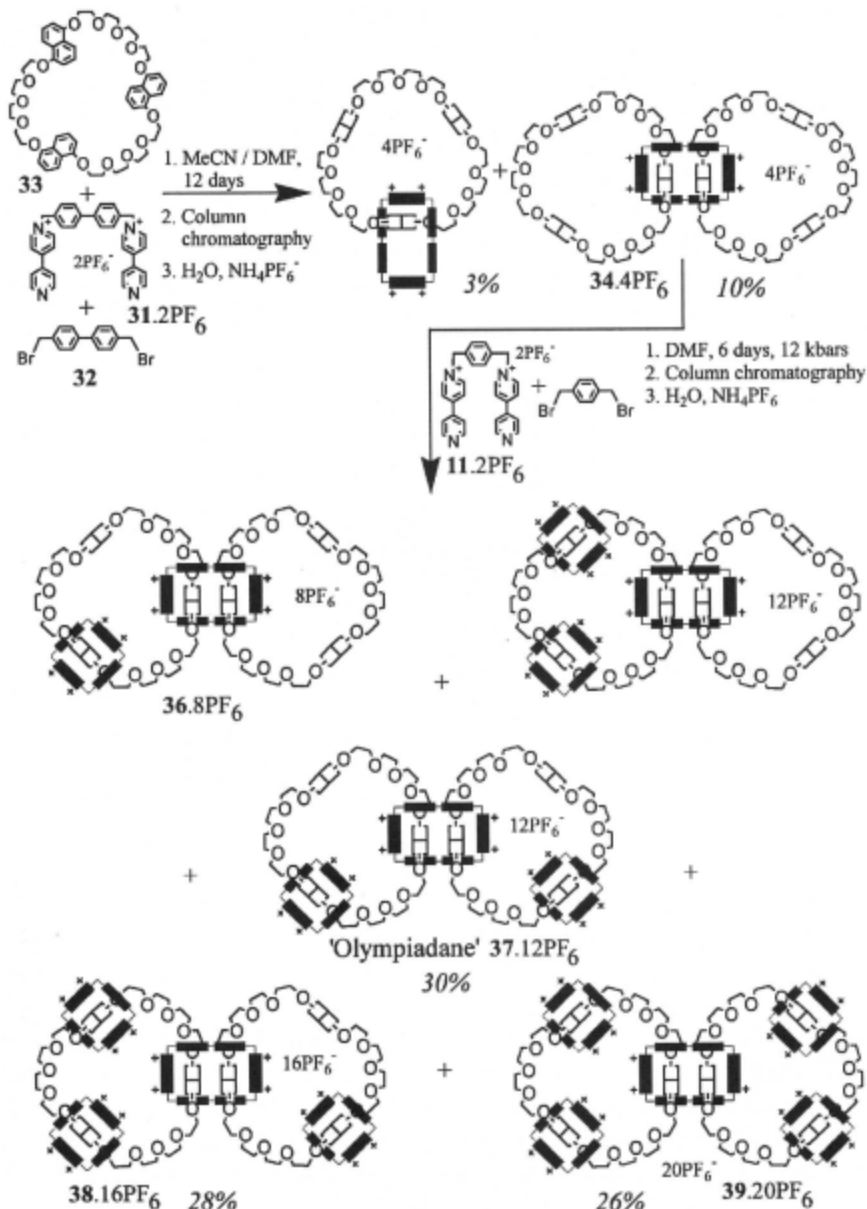

Figure 15 – The synthesis of Olympiadane and higher branched oligomeric [n]catenanes.

13.4 Polycatenanes

13.4.1 In nature

The good news is that polycatenanes are far from an impossible dream. Nature creates its own catenanes from the interlocking of two circular strands of DNA [52]. The existence of catenated circular DNA *in vivo* was discovered by Vinograd and co-workers [53]. The dimeric forms of DNA from mitochondria were separated and viewed under an electron microscope, revealing two circular duplex DNA molecules that were mechanically interlocked. Further studies [54] demonstrated the existance of higher catenanes. In fact, systems containing many thousands of kinetoplast-DNA-catenanes intertwined in a 'chainmail' motif have been identified (Figure 16) [55]. Some of the most stunning electron micrograph images of catenated DNA are of kinetoplast DNA from cells of *Leishmania tarentolae* [56].
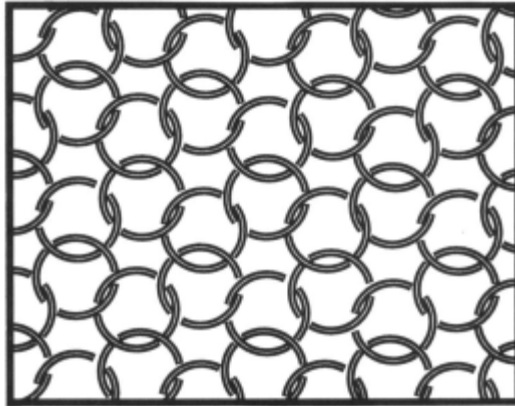
Figure 16 – Network of intertwined kinetoplast-DNA molecules.

During the later stages of the replication of simian virus 40 (SV40) DNA, twenty discrete catenated dimeric species have been identified [57] in which two circular duplex DNAs are linked by one or more intertwining events. The enzymes responsible for the formation of interlocked DNA - *topoisomerases* [58] - are crucial to the replication, transcription and recombination of the genetic information store. In some cases, [59] it is seen that in the catenated state, the DNA double helix becomes slightly unwound compared to the cyclic form, an effect that is believed to be of key importance to the unwinding of DNA during replication [60]. Given their ubiquity in nature, it seems likely that catenated DNA species will be found to play important roles in many biological processes.

13.4.2 Statistical approaches to polycatenanes

Interpenetrating networks (IPN's) [4], *i.e.* the cross linking of a linear macromolecule in the presence of a network polymer, are another important class of polycatenane. Much interest surrounds the effects that the interlocked architectures may have on the various changes in properties observed between the separate polymer networks and IPN's. Unfortunately, the nature of their preparation dictates that there is little control over the number of catenane-type linkages formed and it is difficult to elucidate the nature of the catenane structures that are present.

A route to such polymeric catenanes utilises cyclics that can be entrapped through being threaded within a conventional crosslinked polymer network (Figure 17). In 1975 Frisch and co-workers [61] synthesised a crosslinked polybutadiene containing valinomycin a cyclic depsipeptide suggesting that 0.37% of the resulting polymer contained threaded material. When valinomycin is mixed with a large excess of linear polybutadiene, random threading of the cyclic polypeptide can occur. Subsequent crosslinking of the polymer traps threaded macrocycles on the polymer chain resulting in the polymeric catenane.
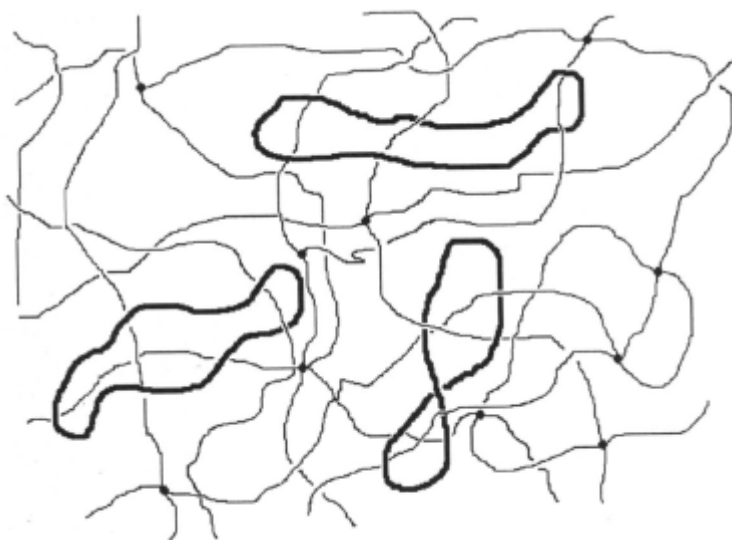

Figure 17 – Cyclics trapped by linear chains which pass through them prior to being end linked into a tetrafunctional network.

In this case no effect on the polymer glass transition was observed. An increase in the elastic modulus was noted however, with the polybutadiene-valinomycin composite appearing to be significantly stiffer than polybutadiene alone. The stiffening of the material might indicate lower segmental mobility and suggest that the threaded rings decrease the number of molecular level conformations allowed.

Semlyen *et al.* [62] have entrapped large cyclics of poly(dimethylsiloxane) **[-Si(CH₃)₂O-]** by end-linking linear poly(dimethylsiloxane) chains in an elastomeric network. Each of three cyclics of varying sizes were mixed with linear polymers of different molecular weights and allowed to interpenetrate for various time periods. After end-linking, the fraction of cyclics trapped was determined by extraction measurements [63][64]. Approximately 25% weight fraction of cyclics were permanently trapped in the networks (by one or more network chains threading through them). Cyclics with Mn <1300 were not trapped by this process since they were too small to be threaded by the polysiloxane chains. Interestingly it was demonstrated that the entrapped cyclics might make a small contribution to the lowering of the deformation modulus of the network polymer [65].

13.4.3 Main chain linear poly[2]catenanes

Although the synthesis of a linear fully interlocked macrocycle chain is plagued by the problem of rapidly decreasing yields for subsequent additions of rings to the ends of the growing polymer chain [50] (Section 13.3.2), the preparation of polymeric [2]catenanes is now achievable [66][70][71][74][75].

13.4.3 (a) Poly[2]catenanes containing metal-ligand coordinated [2]catenanes

The earliest examples of linear polymers bearing [2]catenanes in their backbones (mechanically linked main chain polymers, architecture **A**, Figure 1) were based on the Sauvage transition metal-coordinated catenanes [66]. Polycondensation reactions were carried out between diacid **40** and catenane diols **41** and **42**, affording the poly[2]catenate **43** and poly[2]catenand **44**, respectively (Figure 18). A direct polyesterification method [67] was applied, using *N,N'*-diisopropylcarbodiimide and a 4-(*N,N'*-dimethylamino)pyridine toluene-*p*-sulfonic acid catalyst. Polymerisation was carried out for 3 days at –10°C, 2 days at 0 °C and finally 1 day at room temperature. Large rings were used in the catenand to try to promote mobility of the demetallated system (**44**:M absent) and solubilising groups were required (**41, 42** and the diacid **40**) to counterbalance the high crystallinity of the 1,10-phenanthroline and biphenyl nuclei. The poly[2]catenate **43** and poly[2]catenand **44** polymers were both soluble in chlorinated solvents.

The poly[2]catenate **43** and poly[2]catenand **44** were both analysed by gel permeation chromatography (chloroform, calibration with polystyrene standards), which revealed number-average molecular masses (Mn) and mass-average molecular masses (M_w) of 600,000 and 4,200,000, and 55,000 and 1,800,000, respectively. The additional mass of the copper ions should only contribute slightly to these differences in molecular weight. More significant is the increase in reactivity caused by metal ion-chelation holding the two diol groups on either side of the [2]catenate. From the M_n values, the poly[2]catenand **44** is judged to incorporate an average of 20 mechanical [2]catenand linkages and the poly[2]catenate **43** an average >200. Thermogravimetric analysis showed that poly[2]catenate **43** is stable up to 210 °C, whereas poly[2]catenand **44** exhibited higher thermal stability of up to 300 °C. Second-order transitions, which are attributed to glass transitions, were observed by differential scanning calorimetry at *ca.* 60 and 75 °C for **43** and **44** respectively.
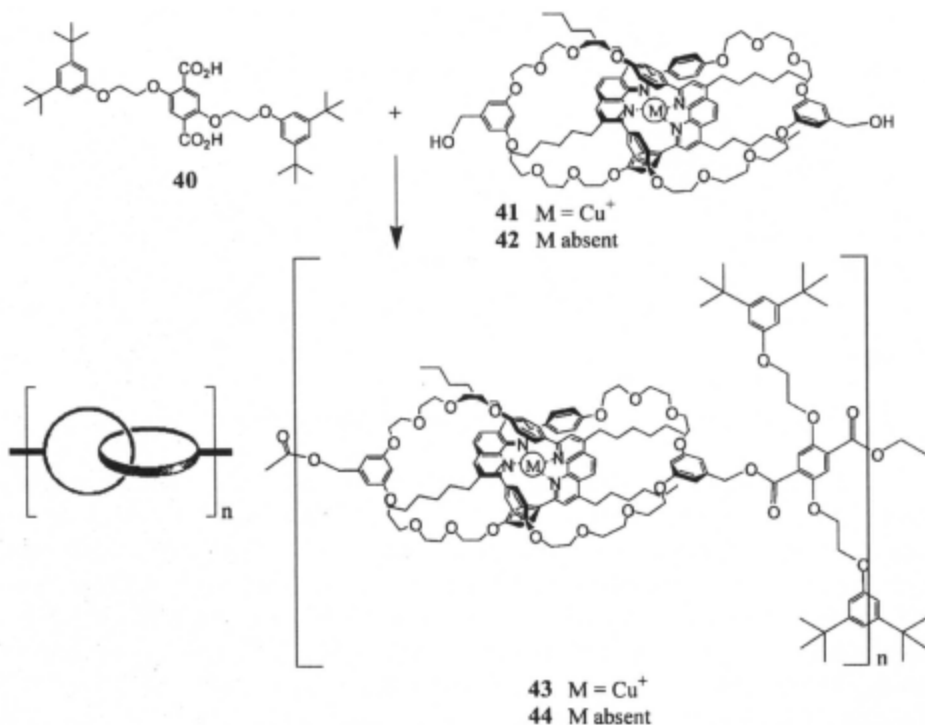

Figure 18 – Synthesis of the first poly[2]catenanes.

A similar system was employed by Shimada and co-workers [68] to synthesise poly[2]catenanes. However, their findings concerning the polymerisation of the free catenand were quite different. The difunctionalised [2]catenate (**46**), incorporating a secondary amine functionality on each ring was synthesised in 30% yield, using an analogous procedure to that of Sauvage by closing the macrocycles with diiodide **45** (Figure 19).
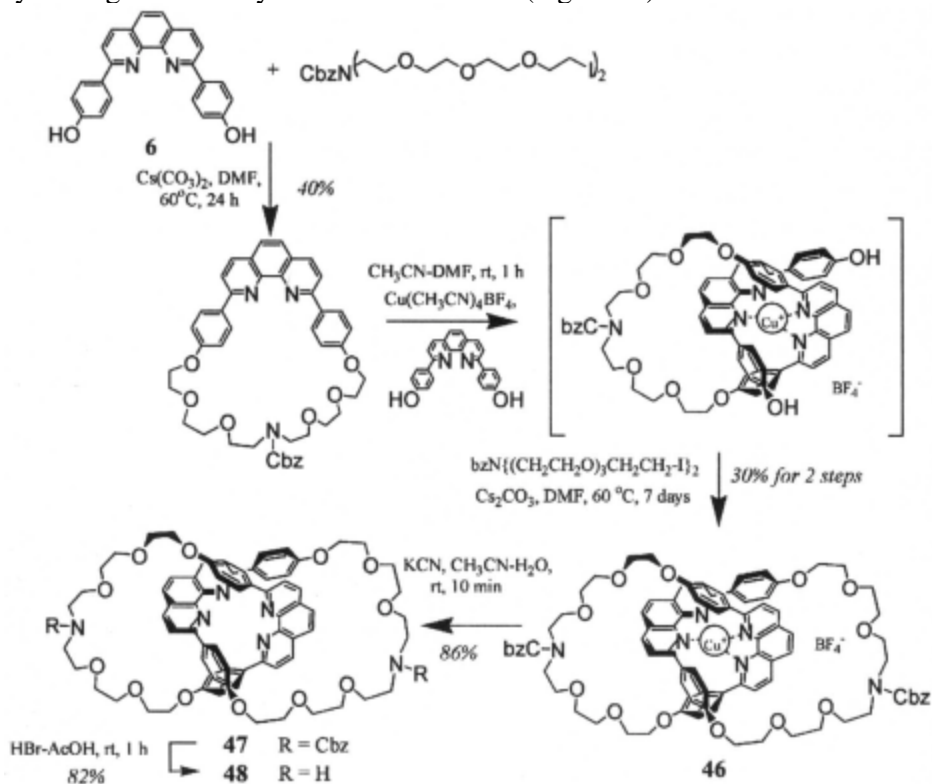
Figure 19 – Synthesis of a diamine functionalised [2]catenane (48).

Remarkably, the diamine [2]catenand **48** was found to preferentially react intramolecularly with adipoyl chloride forming a pretzel-shaped compound **49** [69] rather than polymeric material [68] (Figure 20). However, in the copper(I) catenate complex **50** the two amine groups are held far apart and condensation with adipoyl chloride now affords the poly[2]catenate **51**. The demetallated poly[2]catenand **52** was analysed by GPC (DMF, polystyrene standards), to give an M_n of 810,000 and heterogeneity index M_w/M_n of 4.1 indicating an average of >600 catenane linkages per polymer chain. The significance of these catenane systems is that reactivity can be switched from inter to intramolecular by restricting the rotation of the catenate, imposed by using a copper(I) chelate.
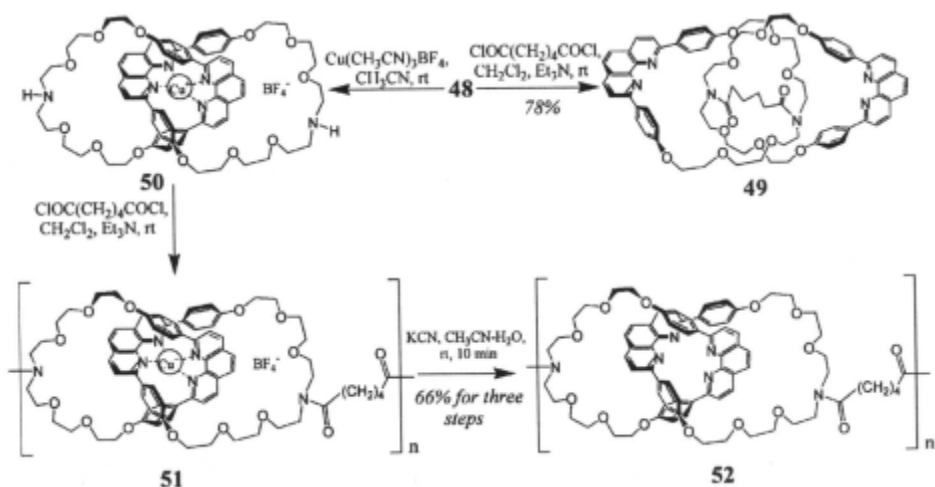
Figure 20 – Condensation polymerisation reaction of diamine [2]catenane 48

13.4.3 (b) Poly/oligo[2]catenanes containing hydrogen bond templated [2]catenanes

Two functionalised [2]catenanes based on the systems developed by Hunter and Vögtle were prepared by Geerts *et al.* [70] **53** and **54** (Figure 21) and used to form poly[2]catenanes. Several attempts at Pd° coupling of **53** with co-monomers **55-58** (Figure 22) were carried out. However, from GPC analysis the reactions with **55** and **56** failed to give even oligomers. In contrast, the use of distannylacetylene or diboronic acid derived comonomers **57** or **58** respectively, successfully led to oligomeric products **59** and **60** (Figure 23).

586

Figure 21 – The synthesis of hydrogen bond templated bromine functionalised [2]catenanes.

Figure 22 – Co-monomers 55-58 used for the Pd° coupling with catenane 53.

Figure 23 – Synthesis of oligo[2]catenanes via Pd° coupling.

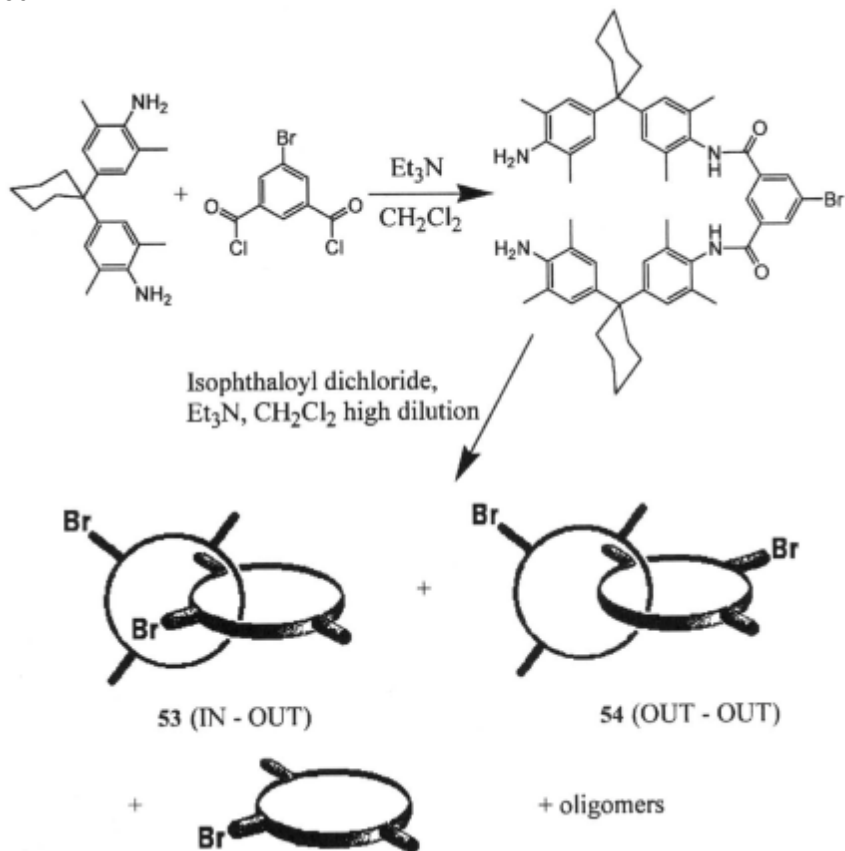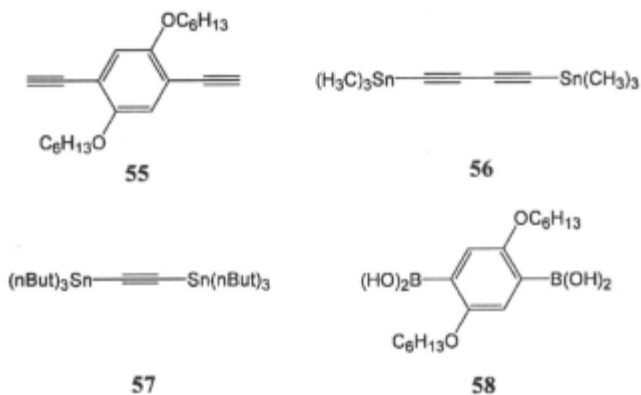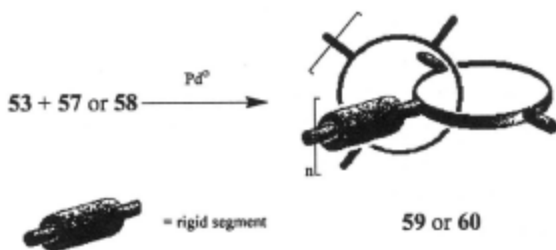GPC (THF, polystyrene standards) gave M_n=3,000, M_w=3,600 for **59** and M_n=3,300, M_w=5,000 for **60**. The GPC data for both oligo[2]catenanes indicates a degree of polymerisation ranging from 1 to 5. Higher oligomers with degrees of polymerisation of 6,7 and 8 were also observed by Fast Atom Bombardment mass spectrometry (FAB-MS). Despite the moderate molecular weight achieved, a glass transition was observed for **60** of 245 °C. The macrocyclic rings in these catenanes are unable to move more than a few degrees, limiting any influences that dynamic mechanical linkages could have on polymer properties.

An even more rigid catenane linkage has been used to prepare poly[2]catenanes [71]. The sterically crowded catenane **61** was copolymerised with a highly soluble terephthalic acid derivative (**40**). A mild polyesterification method was applied at -20 °C for 6 days using *N,N*' diisopropylcarbodiimide as coupling reagent [66][67]. The resulting poly[2]catenane **62** was soluble in a wide variety of solvents and purified by precipitation into methanol. The catenane can be incorporated head-to-head, head-to-tail or tail-tail in the polymer backbone.

The poly[2]catenane **62** was analysed by GPC (THF, polystyrene standards) which showed an M_n of 13,500 and M_w of 29,100, corresponding to a number average degree of polymerisation P_n of 5 and a weight average degree of polymerisation P_w of 11. As is likely the case for all poly[2]catenanes, GPC calibration using polystyrene probably underestimates the true molecular weight as it does not take into account the compact molecular structure of the poly[2]catenane. Indeed, light scattering experiments on **62** indicated higher molecular weights and preliminary GPC results using universal calibration gave indicated a M_w of *ca.* 60,000. MALDI-TOF confirmed the presence of high molecular weights, up to 52,000.

Thermogravimetric analysis (TGA) of the poly[2]catenane **62** showed it possesses excellent thermal stability, with no weight loss being observed below

380 °C. A high glass transition temperature 265 °C was recorded simitar to that (245 °C) for poly[2]catenane **60**.

Care must be taken when making any comparisons between the properties of the poly[2]catenanes **62** and **44** based upon the rigidity of the mechanical catenane linkages. Although both the polymers were prepared in the same manner with the same comonomer the structures of the catenanes macrocycles are radically different.
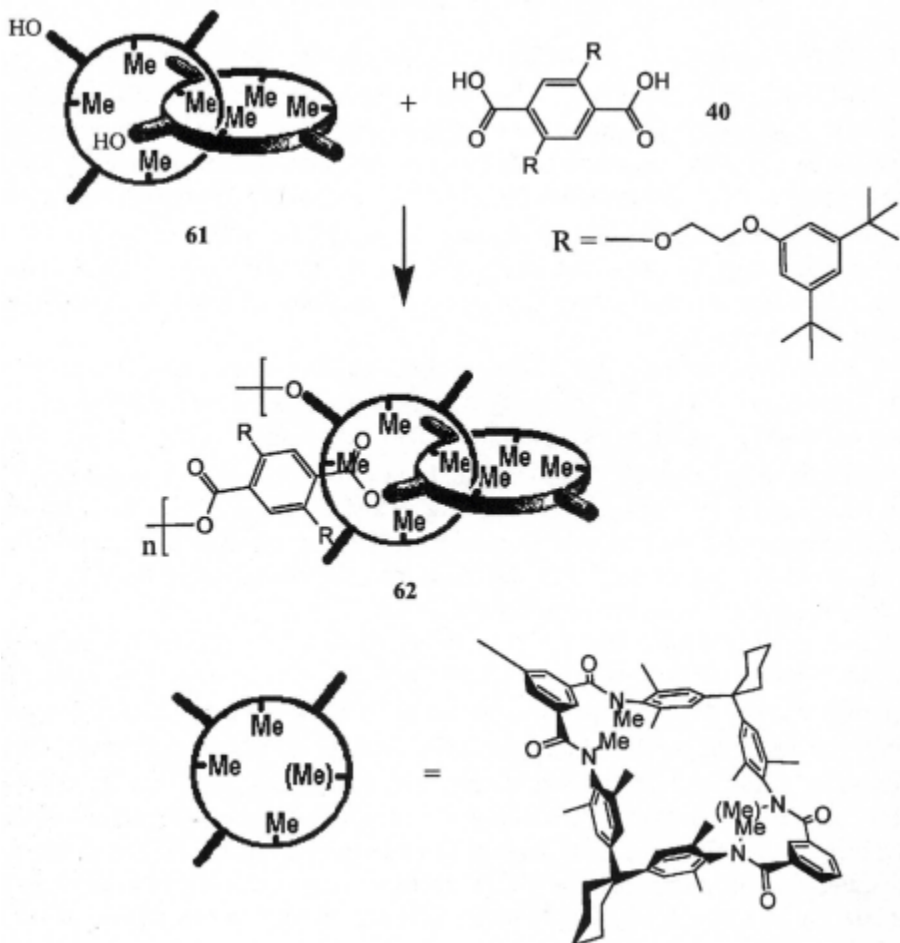
Figure 24 – Synthetic route to a poly[2]catenane containing sterically hindered catenane units.

In complete contrast to Geerts' 'rigid' catenanes, the already rotationally more mobile benzylic amide catenane [36] has been modified to

remove all intramolecular hydrogen-bond interactions by reduction of the amide groups [72] (Figure 25). The enhanced mobility of the reduced system was confirmed by NMR studies and provides an insight into how a poly[2]catenane containing such a unit would have the maximum possible flexibility associated with its mechanical linkages.
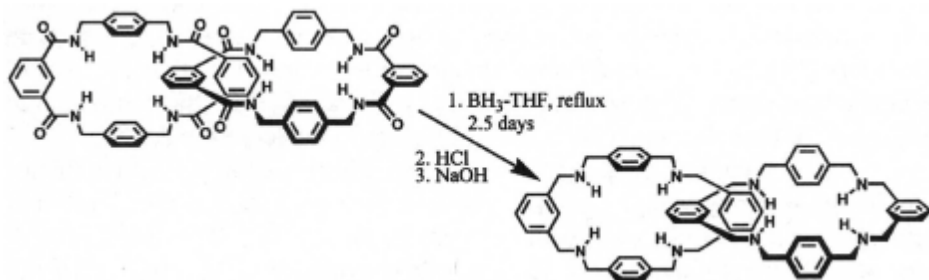
Figure 25 – **Removal of the intramolecular hydrogen bonds of benzylic amide [2]catenane.**

13.4.3 (c) Poly/oligo[2]catenanes containing [2]catenanes templated by π,π-stacking interactions

One way to extrapolate from the synthesis of [2]catenanes to polymers, would be to construct a bifunctionalised monomer capable of polymerisation through self-assembly. A strategy towards this goal was tried by Stoddart *et al.* who synthesised a monomer containing a crown ether which had covalently attached the precursor to a complementry tetracationic bipyridinium-based macrocycle (Figure 26).
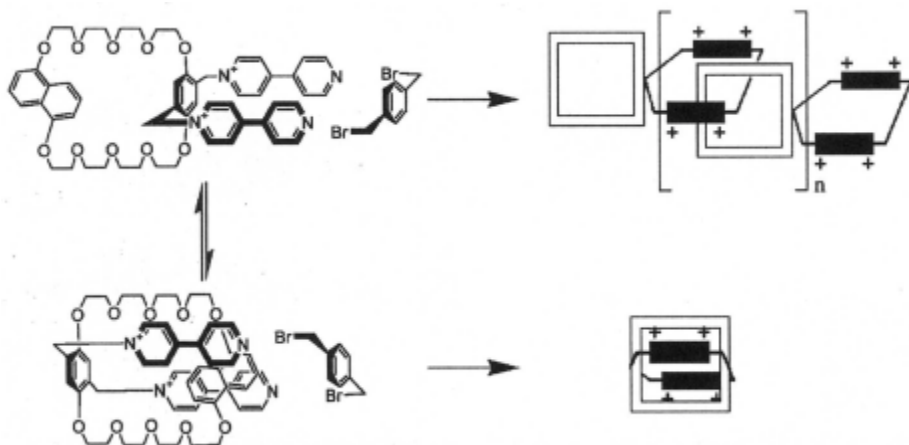
Figure 26 – **Possible self-assembly strategy to poly[2]catenanes.**

In theory this monomer has the potential to polymerise through self-assembly with the bipyridinium units threading the crown ethers and then being closed covalently to give the poly[2]catenane (Figure 26). In practice, however, intramolecular complexation dominates intermolecular complexation and no polymer is observed [73].

A range of functionalised **π-π-assembled** [2]catenanes containing carboxyl and hydroxyl reactive groups were used to form poly[2]catenanes using the Geerts' strategy of polymerising [2]catenanes as AA BB type monomers [74]. The polymerisable functionalities were such that they could be condensed under mild conditions without degradation of the tetracationic component of the catenane which is highly labile to nucleophilic attack.

Early attempts at polymerisation by esterification of [2]catenanes containing hydroxymethyl groups on one macrocyclic component and carboxylic acid residues on the other were unsuccessful. The breakthrough came when a main-chain oligo[2]catenane was synthesised by reaction of the catenane **63.4PF$_6$** with bis(4-isocyanatophenyl)methane, thus affording urethane linkages in a main chain oligo[2]catenane **64.4n(PF$_6$)** [74] (Figure 27).

Figure 27 – Synthetic route to a poly[2]catenane containing catenanes templated by π,π-stacking.

A number-average molecular weight M_n of 26,500 for **64.4*n*(PF$_6$)** was determined by GPC against proteins as standards and from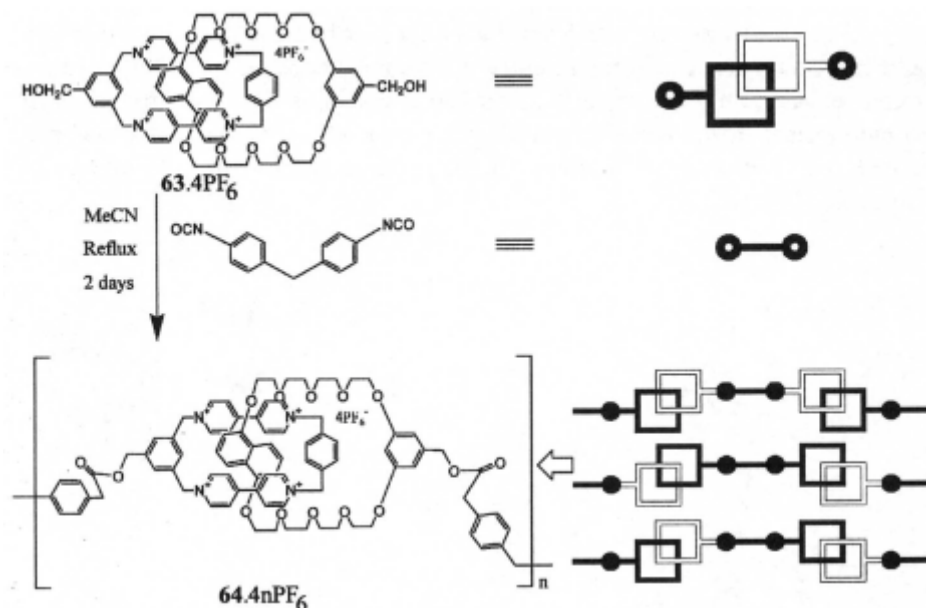 this the oligo[2]catenane was judged to incorporate ~17 [2]catenane repeating units per chain. One drawback of this synthesis is that the exact structure of **64.4*n*(PF$_6$)** is unknown as the polymer main chain can incorporate three different 'bridging motifs' resulting from the unsymmetrical nature of the difunctionalised catenane **63.4PF$_6$**. Thus, the diphenylmethane bridging unit can connect either (a) two identical **π-electron-rich,** (b) two identical **π-electron-deficient** or (c) a **π-electron-rich** to a **π-electron** deficient macrocyclic component of two adjacent [2]catenane repeating units along the oligomer backbone.

Further advances was made by conversion of the **CH$_2$OH** group of **65.4PF$_6$** into a chloromethylene group (Figure 28) [75]. The resulting [2]catenane **(66.4PF$_6$)** could be polyesterified *in situ* to give the poly[2]catenane **67.*n*(4PF$_6$)**. The chloride salt **67.*n*(4Cl$^-$)** was to determine a number-average molecular weight M_n of the polymer of 35,000 by GPC. This value corresponds to a degree of polymerisation of ~25. In this system there is no uncertainty over the exact structure of the polymer backbone.

	R	
65.4PF$_6$	OH	1. 10M HCl$_{aq}$, 50°C, 1 day
66.4PF$_6$	Cl	2. NH$_4$PF$_6$, H$_2$O

1. LiBr, 2,6-Lutidine, MeCN
Reflux, 2 days

2. NH$_4$PF$_6$, H$_2$O

4PF$_6^-$

67.n(4PF$_6$)
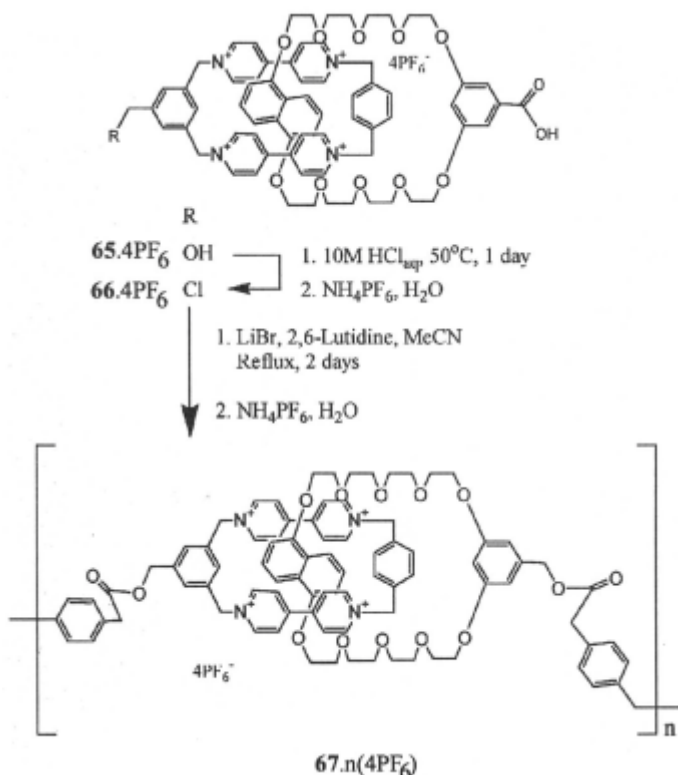
Figure 28 – Synthesis of a polyester-based poly[2]catenane.

13.4.4 Main chain poly(bis[2]catenanes)

An extrapolation on the mechanically linked main chain polymer theme has been the polymerisation of bis[2]catenanes - two [2]catenanes units covalently linked together by a linear spacer unit [76]. The potential advantage of polymerising bis[2]catenanes is that intramolecular cyclisation, such as that seen by Shimada, should be greatly disfavoured The first examples featured monomers with the two monohydroxyl functionalised catenanes connected together with urethane linkages **(71.8PF₆)**. These were polymerised with a bisisocyanate to generate a second generation of urethane linkages between the catenane units in the poly[2]catenane **73.n(8PF₆)**(Figure 29).
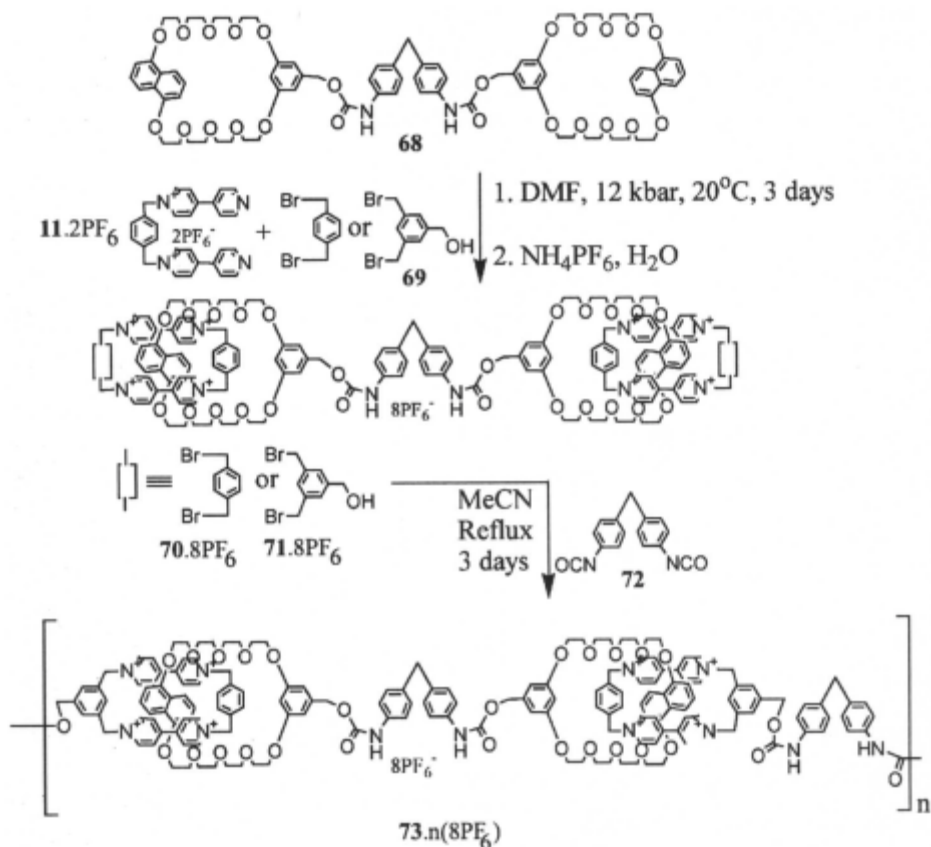
Figure 29 – Synthesis of the main-chain poly(bis[2]catenane) 73.n(8PF₆).

The chloride salt **73.***n***(8C1)** of the poly(bis[2]catenane) was analysed by GPC which revealed an M_n of 45,000 corresponding to a degree of polymerisation of 15. However, since each bis[2]catenane monomer contains two catenane units, the average polymer chain contains approximately 30 mechanical links.

A poly(bis[2]catenane) **78.***n***(8PF$_6$)** containing alternating polyether and urethane connections between the mechanical links has been prepared (Figure 30) by reaction of the bis[2]catenane **77.2PF$_6$** with bis(isocyanate) **72**. The chloride salt **78.***n***(8Cl⁻)** was analysed by GPC which showed an M_n of 45,000 corresponding to a degree of polymerisation of 15 and hence, again, an average of 30 mechanical linkages per polymer chain.
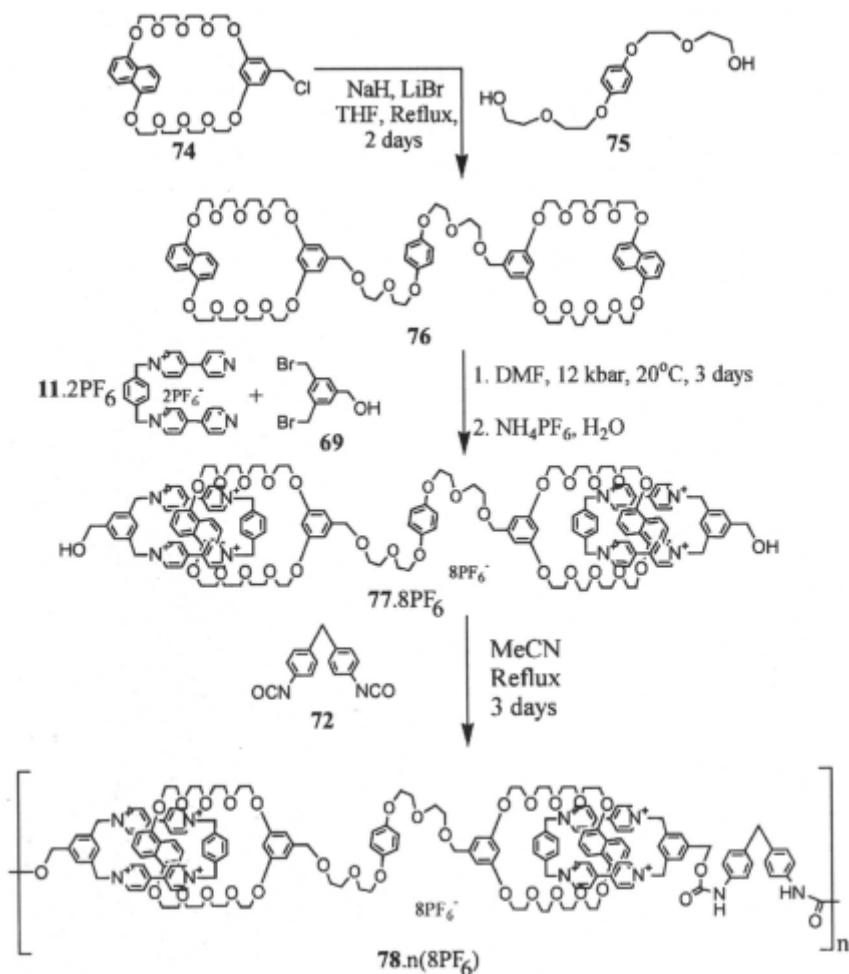
Figure 30 – Synthesis of a poly(bis[2]catenane) with alternating polyether/urethane linkages

A poly(bis[2]catenane) has also been synthesised where half of the intercatenane linkages are formed by chelation to a transition metal leading to a polymer containing alternating -covalent-mechanical-coordination-mechanical-linkages [77] (Figure 31). The urethane-bridged bis[2]catenane **81.8PF$_6$** forms an extended coordination polymer **82.n(PF$_6$)** when treated with one equivalent of silver triflate.

Analysis of the poly(bis[2]catenane) by GPC (NH$_4$PF$_6$ water/acetonitrile 93:7 solution, protein standards) shows an **M$_n$** of 150,000, corresponding to a degree of polymerisation of 40. Therefore each chain of the poly(bis[2]catenane) incorporates an average of 80 [2]catenane mechanical linkages. Clearly, metal ion coordination can provide an efficient method to assemble bis[2]catenanes into regular mechanically linked chains.
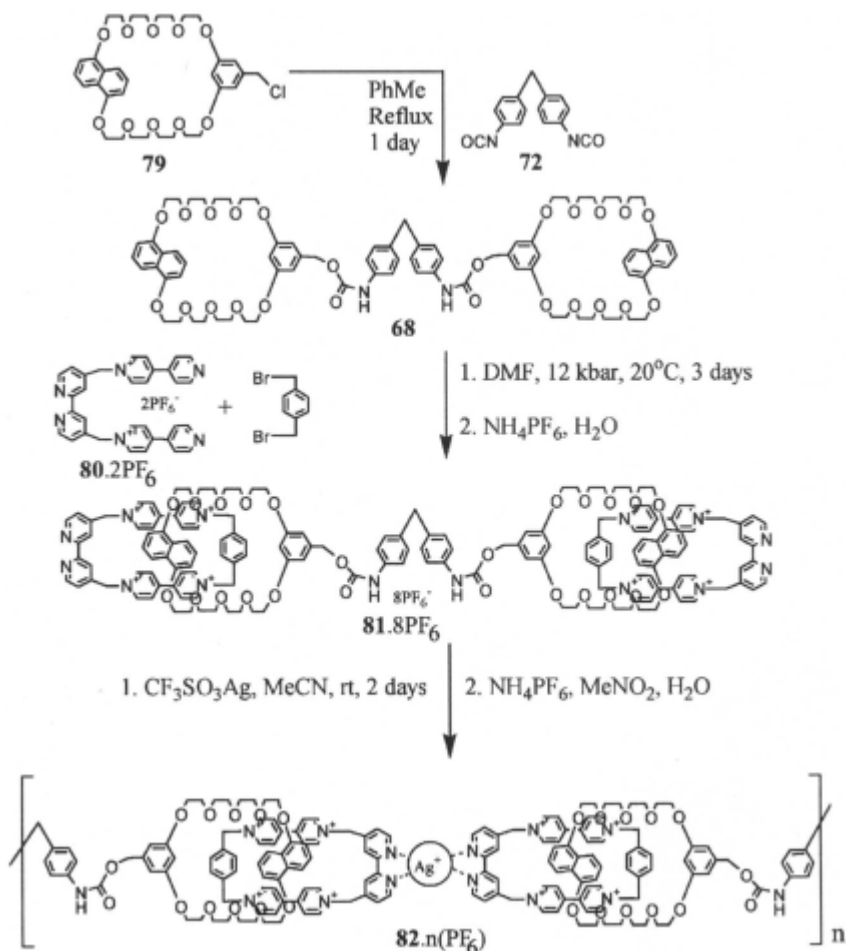
Figure 31 – Synthesis of a poly(bis[2]catenane) with alternating covalent-mechanical-coordination-mechanical linkages.

13.4.5 Side chain poly[2]catenanes

In addition to main chain mechanically linked polymers, catenane linkages can be incorporated as pendant sidechains. This type of architecture has the potential to provide materials with switchable surface properties, if the catenanes incorporated into the are able to 'switch' their orientation in response to an applied external stimuli [78].
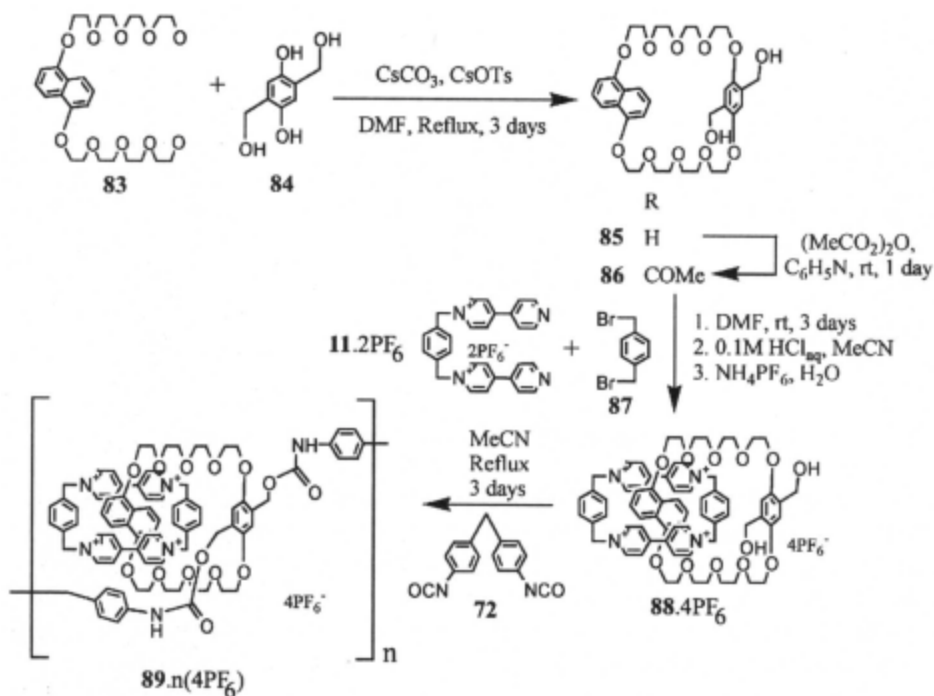
Figure 32 – Synthesis of a side chain poly[2]catenane.

The first side chain poly[2]catenane **89.n(4PF$_6$)** was synthesised by Stoddart *et al.* in 1998 [75] (Figure 32). The chloride salt **89.n(4Cl⁻)** gave an M$_n$ of 27000 by GPC, corresponding to a degree of polymerisation of 20.

13.4.6 [2]catenands built into poly(ethylenimine)
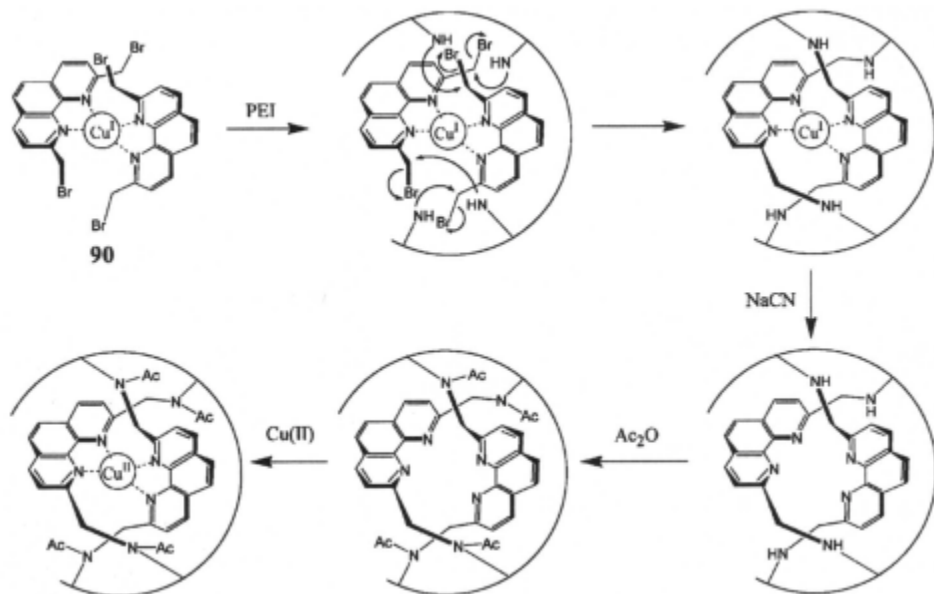
Figure 33 – [2]Catenands for crosslinking poly(ethylenimine).

In an interesting potential use of catenane mechanical linkages, the copper(I)catenate precursor **90** (Figure 33), [119] was crosslinked into a highly branched, water soluble, poly(ethylenimine) (PEI), in an attempt to establish a methodology to be utilised in the design of biomimetic functional molecules [79], The Cu(I) ions were subsequently removed by treatment with NaCN and the amine groups acylated with acetic anhydride. Ionisation constants for the phenanthroline moieties and formation constants for the Cu(II) complex were measured for the PEI derivatives. The experimental results strongly suggest that each catenane precursor cross-links with only one PEI chain. Thus, pretzel-like and fused entwining macrocycles are formed as opposed to any cross-linking of the polymer by the catenanes.

13.5   Conclusions

Mechanically interlocked molecular level architectures ranging from naturally occurring DNA catenanes to the random entrapment of macrocycles within cross linked polymers and poly[2]catenane macromolecules are beginning to capture the imagination of scientists from all disciplines.   The recent improvements in methods for [2]catenane synthesis mean that interlocked structures are now becoming increasingly available as building blocks and cores for novel macromolecular materials.   As yet few examples exist of high mass 'material like' polycatenane structures, much of the work to date has been on a steep learning curve which suggests that exciting times lie ahead in developing novel materials.   Many new mechanically linked architectures and polymer systems will undoubtedly be developed over the next few years. Despite the wealth of suggestions concerning the possible properties that such structures may possess, there is little experimental evidence yet to either support or reject whatever claims are made.   As characterisation and structure-property relationships of these materials begin to unfold and, in turn, are used to develop further synthetic programmes, the answers to these questions will be resolved and the effects of mechanical linkages on bulk and surface properties will begin to be understood.

13.6   References

1.   J.M.G.Cowie in *Chemistry and Physics of Modern Materials*, Blackie Academic & Professional, 2nd edition, 1991.
2.   J.McMurry in *Organic Chemistry*, Brooks/Cole, 2nd edition, 1988.
3.   G.J. Clarkson, D.A. Leigh and R.A. Smith, Curr. Opin. Solid State & Mater. Sci., **3**, 579 (1998).
4.   (a) L.H.Sperling in *Interpenetrating Polymer Networks*, Plenum, NY, 1981; (b) J.E. Mark, Acc. Chem. Res., **18**, 202 (1985); (c) H.L.Frisch, Br. Polym. J., **17**, 149 (1985); (d) J.E. Mark, New J. Chem., **17**, 703 (1993); (e) S.J. Clarson, New J. Chem., **17**, 711 (1993); (f) L.H. Sperling in *Polymeric multicomponent materials: an introduction*, Wiley, NY, 1997.
5.   D.B. Amabilino and J.F.Stoddart, Chem.Rev., **95**, 2725 (1995).
6.   H.W.Gibson in *Large Ring Molecules*, ed. J.A. Semlyen, J. Wiley and Sons, NY, 1995.
7.   (a) G.Schill in *Catenanes Rotaxanes and Knots*, Academic Press, NY, 1971; (b) H.L. Frisch and E.Wasserman, J. Am. Chem. Soc., **83**, 3790 (1961).
8.   H.L. Frisch and E. Wasserman, J. Am. Chem. Soc., **83**, 3789 (1961).
9.   D.M. Walba, R.M. Richard and R.C. Haltiwanger, J. Am. Chem. Soc., **104**, 3219 (1982).
10.   E. Wasserman, J. Am. Chem. Soc., **82**, 4433 (1960).
11.   (a) G. Agam, D. Graiver and A. Zilkha, J. Am. Chem. Soc., **98**, 5206 (1976); (b) G. Agam and A. Zilkha, J. Am. Chem. Soc., **98**, 5214 (1976).
12.   G. Schill, N. Schweickert, H. Fritz and W. Vetter, Angew. Chem, Int. Ed. Engl., **22**, 889 (1983).
13.   (a) G. Schill and A. Lüttringhaus, Angew. Chem., **76**, 567 (1964); (b) G. Schill, Chem. Ber., **100**, 2021 (1967).

14. A. Lüttringhaus, F. Cramer, H. Prinzbach and F. M. Henglein, Liebigs Ann. Chem., **613**, 185(1958).

15. (a) D. Armspach, P.R. Ashton, C.P. Moore, N. Spencer, J.F. Stoddart, T.J. Wear and D.J. Williams, Angew. Chem., Int. Ed. Engl. **32**, 854 (1993); (b) D. Armspach, P.R. Ashton, N. Spencer, J.F. Stoddart and D.J. Williams, J. Pestic. Sci., **41**, 232 (1994).

16. D.Armspach, P.R. Ashton, R. Ballardini, V. Balzani, A. Godi, C.P. Moore, L. Prodi, N. Spencer, J.F. Stoddart, M.S. Tolley, T.J. Wear and D.J. Williams, Chem. Eur. J., **1**, 27 (1995).

17. Ref.8, 3790, footnote.

18. V.I. Sokolov, Russ. Chem. Rev., **42**, 452 (1973).

19. C.O. Dietrich-Buchecker and J-P. Sauvage, Tetrahedron Lett., **24**, 5091 (1983).

20. (a) C.O. Dietrich-Buchecker, J-P. Sauvage and J.M. Kern, J. Am. Chem. Soc., **106**, 3043 (1984); (b) C.O. Dietrich-Buchecker and J.P. Sauvage, Tetrahedron, **46**, 503 (1990).

21. B. Mohr, M. Weck, J-P. Sauvage and R.H. Grubbs, Angew. Chem., Int. Ed. Engl., **36**, 1308(1997).

22. R.H. Grubbs and S. Chang, Tetrahedron, **54**, 4413 (1998).

23. (a) M. Fujita, F. Ibukuro, H. Hagihara and K. Ogura, Nature, **367**, 720 (1994); (b) M. Fujita, M. Aoyagi, F. Ibukuro, K. Ogura and K. Yamaguchi, J. Am. Chem. Soc., **120**, 611 (1998).

24. A.C. Try, M.M. Harding, D.G. Hamilton and J.K.M. Sanders, J. Chem. Soc., Chem. Commun., 723 (1998).

25. P.R. Ashton, T.T. Goodnow, A.E. Kaifer, M.V. Reddington, A.M.Z. Slawin, N. Spencer, J.F. Stoddart, C. Vincent and D.J. Williams, Angew. Chem., Int. Ed. Engl., **28**, 1396 (1989).

26. M.H. Schwartz, J.Incl.Phenom., **9**, 1 (1990).

27. P.L. Aneli, P.R. Ashton, R. Ballardini, V. Balzani, M. Delgado, M.T. Gandolfi, T.T. Goodnow, A.E. Kaifer, D. Philip, M. Pietraszkiewicz, L. Prodi, M.V. Reddington, A.M.Z. Slawin, N. Spencer, J.F. Stoddart, C. Vincent and D.J. Williams, J. Am. Chem. Soc., **114**, 193 (1992).

28. M. Nishio and M. Hirota, Tetrahedron, **45**, 7201 (1989).

29. M. Etter, Acc. Chem. Res., **23**, 120 (1990).

30. C. A. Hunter and D.H. Purvis, Angew. Chem., Int Ed. Engl., **31**, 792 (1992).

31. (a) P.R. Ashton, R. Ballardini, V. Balzani, M. Blower, M. Ciano, M.T. Gandolfi, C.H. McLean, D. Philip, L. Prodi, N. Spencer, J.F. Stoddart and M.S. Tolley ,New J. Chem., **17**, 689 (1993); (b) M.J. Gunter, D.C.R. Hockless, M.R. Johnston, B.W. Skelton and A.H. White, J. Am. Chem. Soc., **116**, 4810 (1994); (c) D.B. Amabilino, P.R. Ashton, G.R. Brown, W. Hayes, J.F. Stoddart, M.S. Tolley and D.J. Williams, J. Chem. Soc., Chem. Commun., 2479 (1994).

32. (a) F.Vögtle, W.M. Müller, U.Müller, M.Bauer and K.Rissanen, Angew. Chem., Int. Ed. Engl., **32**, 1295 (1993); (b) D.B. Amabilino, P.R. Ashton, J.F. Stoddart, M.S. Tolley and D.J. Williams, Angew. Chem., Int. Ed. Engl., **32**, 1297 (1993); (c) P.R. Ashton, J.A. Preece, J.F. Stoddart, M.S. Tolley, A.J.P. White and D.J. Williams, Synthesis, 1344 (1994); (d) P.R .Ashton, L.Pérez-Garcia, J.F. Stoddart, A.J.P. White and D.J. Williams, Angew. Chem., Int. Ed. Engl., **34**, 571 (1995).

33. D.G. Hamilton, J.K.M. Sanders, J.E. Davies, W. Clegg and S.J. Teat, J. Chem. Soc., Chem. Commun., 897 (1997).

34. C.A. Hunter, J. Am. Chem. Soc., **114**, 5303 (1992).

35. F. Vögtle, S. Meier and R. Hoss, Angew. Chem., Int. Ed. Engl., **31**, 1619 (1992).

36. A.G. Johnston, D.A. Leigh, R.J. Pritchard and M.D. Deegan, Angew. Chem., Int. Ed. Engl., **34**, 1209 (1995).

37. A.G. Johnston, D.A. Leigh, A. Murphy, J.P. Smart and M.D. Deegan, J. Am. Chem. Soc., **118**, 10662 (1996).
38. D.A. Leigh, A. Murphy, J.P. Smart and A.M.Z. Slawin, Angew. Chem., Int. Ed. Engl., **36**, 728 (1997).
39. D.A. Leigh, A.Murphy, J.P. Smart, M.S. Deleuze and F. Zerbetto, J. Am. Chem. Soc., **120**, 6458 (1998).
40. M. Fanti, C-A. Fustin, D.A. Leigh, A. Murphy, P. Rudolf, R. Caudano, R. Zamboni and F. Zerbetto, J. Phys. Chem. A., **102**, 5782 (1998).
41. T. Gase, D.Grando, P.A. Chollet, F. Kajzar, A, Lorin, D. Tetard and D.A. Leigh, Photonics Sci. News, **3**, 16 (1998).
42. J.F. Stoddart, Nature, **334**, 10 (1988).
43. D.G. Hamilton, N. Feder, L. Prodi and J.K.M. Sanders, Chem. Euro. J., **4**, 608 (1998).
44. M. Asakawa, P.R. Ashton, C.L. Brown, M.C.T. Fyfe, S. Menzer, D. Pasini, C. Scheuer, N. Spencer, J.F. Stoddart, A.J.P. White and D.J. Williams, Chem. Eur. J., **3**, 1136 (1997).
45. D.B. Amabilino, P.R. Ashton, J.F. Stoddart, A.J.P. White and D.J. Williams, Chem. Eur. J., **4**, 460 (1998).
46. D.B. Amabilino, P.R. Ashton, V. Balzani, S.E. Boyd, A. Credi, J.Y. Lee, S. Menzer, J.F. Stoddart, M. Venturi and D.J. Williams, J. Am. Chem. Soc., **120**, 4295 (1998).
47. P.R. Ashton, S.E. Boyd, C.G. Claessens, R.E. Gillard, S. Menzer, J.F. Stoddart, M.S. Tolley, A.J.P. White and D.J. Williams, Chem. Eur. J., **3**, 788 (1997).
48. D.G.Hamilton, N.Feder, L.Prodi, S,J, Teat, W. Clegg and J.K.M. Sanders, J. Am. Chem. Soc., **120**, 1096 (1998).
49. C.L. Brown, D. Philip, N. Spencer and J.F. Stoddart, Isr. J. Chem., **32**, 61 (1992).
50. D.B. Amabilino, P.R. Ashton, A.S. Reder, N. Spencer and J.F. Stoddart, Angew. Chem., Int. Ed. Engl., **33**, 1286 (1994).
51. D.B. Amabilino, P.R. Ashton, A.S. Reder, N. Spencer and J.F. Stoddart, Angew. Chem., Int. Ed. Engl., **33**, 433 (1994).
52. J.C. Wang, Acc. Chem. Res., **6**, 252 (1973).
53. B. Hudson and J. Vinograd, Nature, **216**, 647 (1967).
54. D.A. Clayton and J. Vinograd, Nature, **216**, 652 (1967).
55. (a) J. Chen, C.A. Rauch, J.H. White, P.T. Englund and N.R. Cozzarelli, Cell, **80**, 61 (1995); (b) J. Chen, P.T. Englund and N.R. Cozzarelli, EMBO J., **14**, 6339 (1995); (c) D.E. Adams, E.M. Shekhtman, E.L. Zechiedrich,M.B. Schmid and N.R. Cozzarelli, Cell, **71**, 277 (1992).
56. L. Simpson and A. Da Silva, J. Mol. Biol, **56**, 43 (1971).
57. O. Sundin and A.Varshavsky, Cell, **21**, 103 (1980).
58. (a) J.C. Wang, J. Biol. Chem., **266**, 6659 (1991); (b) M. Gellert, Annu. Rev. Biochem., **50**, 879 (1981); (c) J.C. Wang, Annu. Rev. Biochem., **54**, 665 (1985); (d) T. Uemura and M. Yanagida, EMBO J., **3**, 1737 (1984).
59. W.M. Stark, C.N. Parker, S.E. Halford and M.R. Boocock, Nature, **368**, 76 (1994).
60. S.A. Wasserman, J.H. White and N.R. Cozzarelli, Nature, **334**, 448 (1988).
61. D. Callahan, H.L. Frisch and D. Klempner, Polym. Eng. Sci., **15**, 70 (1975).
62. L. Garrido, J.E. Mark, S.J. Clarson and J.A. Semlyen, Polym. Comm., **26**, 53 (1985).
63. J.E. Mark and Z-M. Zhang, J. Polym. Sci., Polym. Phys. Edn., **21**, 1971 (1983).
64. L. Garrido, J.E. Mark, S.J. Clarson and J.A. Semlyen, Polym. Comm., **25**, 218 (1984).
65. L. Garrido, J.E. Mark, S.J. Clarson and J.A. Semlyen, Polym.Comm.,**26**, 55 (1985).
66. J-L. Weidmann, J-M. Kern, J-P. Sauvage, Y. Geerts, D. Muscat and K. Müllen, J. Chem. Soc., Chem. Commun., 1243 (1996).
67. J.S. Moore and S.I. Stupp, Macromolecules, **23**, 65 (1990).
68. S. Shimada, S. Ishikawa and N. Tamaoki, Acta. Chem. Scand., **52**, 374 (1998).
69. R. Jäger, T. Schmidt, D. Karbach and F. Vögtle, Synlett, **8**, 723 (1996).

70. Y. Geerts, D. Muscat and K. Müllen, Macromol. Chem. Phys., **196**, 3425 (1995)
71. D. Muscat, A. Witte, A. Köhler, K. Müllen and Y. Geerts, Macromol. Rapid Commun., **18**, 233 (1997).
72. T. Takata, J. Shoji and Y. Furusho, Chem. Lett., **9**, 881 (1997).
73. R. Wolf, M. Asakawa, P.R. Ashton, M. Gómez-López, C. Hamers, S. Menzer, I.W. Parsons, N. Spencer, J.F. Stoddart, M.S. Tolley and D.J. Williams, Angew. Chem., Int. Ed. Engl., **37**, 975 (1998).
74. S. Menzer, A.J.P. White, D.J. Williams, M. Belohradsky, C. Hamers, F.M. Raymo, A.N. Shipway and J.F. Stoddart, Macromolecules, **31**, 295 (1998).
75. C. Hamers, F.M. Raymo and J.F. Stoddart, Eur. J. Org, Chem, 2109 (1998).
76. (a) P.R. Ashton, J.A. Preece, J.F.Stoddart and M.S. Tolley, Synlett, 789 (1994); (b) P.R. Ashton, A.S.Reder, N. Spencer and J.F. Stoddart, J. Am. Chem. Soc, **115**, 5286 (1993); (c) M.B. Nielsen, Z.T. Li and J. Becher, J. Mater. Chem., **7**, 1175 (1997); (d) P.R. Ashton, T. Horn, S. Menzer, J.A. Preece, N. Spencer, J.F. Stoddart and D.J. Williams, Synthesis, **4**, 480 (1997); (e) P.R. Ashton, J. Huff, S. Menzer, I.W. Parsons, J.A. Preece, J.F. Stoddart, M.S. Tolley, A.J.P. White and D.J. Williams, Chem.Eur.J, **2**, 31 (1996); (f) P.R. Ashton, V. Balzani, A. Credi, O. Kocian, D. Pasini, L. Prodi, N. Spencer, J.F. Stoddart, M.S. Tolley, M. Venturi, A.J.P. White and D.J. Williams, Chem. Eur. J, **4**, 590 (1998).
77. C. Hamers, O. Kocian, F.M. Raymo and J.F. Stoddart, Adv. Mat, **10**, 1366 (1998).
78. (a) D.A. Leigh, K. Moody, J.P. Smart, K.J. Watson and A.M.Z. Slawin, Angew. Chem, Int. Ed. Engl, **35**, 306 (1996); (b) M. Asakawa, P.R. Ashton, V. Balzani, A. Credi, C. Hamers, G. Mattersteig, M. Montalti, A.N. Shipway, N. Spencer, J.F. Stoddart, M.S. Tolley, M. Venturi, A.J.P. White and D.J. Williams, Angew. Chem, Int. Ed. Engl., **37**, 306(1998).
79. J.Suh, S.H. Lee, J. Org. Chem, **63**, 1519 (1998).

CHAPTER 14

CYCLIC INORGANIC OLIGOMERS AND POLYMERS

Ionel Haiduc

Universitatea "Babes-Bolyai" Cluj-Napoca, Romania

14.1 Introduction

The formation of cyclic oligomers and polymers with an inorganic backbone is an important subject of study, of both academic and applicative interest. Inorganic rings of various compositions and structures are well known and new ones are frequently described. Their chemistry has been reviewed in several monographs [1]. The inorganic rings raise interesting questions of structure and bonding and quite often they challenge the theory. Their applicative interest is related to their use as precursors for thermally stable polymers, ceramics, semiconductors, catalyst supports or various other advanced materials [2].

Inorganic chemistry displays a rich diversity of ring structures in terms of bond types. The obvious and most important are the cyclic molecules formed through **covalent bonds**. Inorganic ring structures can be built by catenation of identical atoms (inorganic homocycles) or by combining a number of various *building blocks (synthons)* made up from different elements, connected through covalent bonds.

Inorganic ring and polymer formation is not limited to covalent bonding. It can also be achieved by assembling supramolecular structures from molecular units *(tectons)* connected through noncovalent **intermolecular forces** (dative bonds, secondary bonds, ionic interactions or hydrogen bonds) [3]. This is the field of *supramolecular chemistry* and the spontaneous process leading to such structures is called *self-assembly* or *self-organisation*.

Since reference was made to supramolecular chemistry, perhaps it is useful to remember some definitions. Supramolecular chemistry is "*the chemistry of molecular assemblies and of the intermolecular bond*". It is "*the chemistry beyond the molecule*" and deals with "*organized entities of higher complexity that result from the association of two or more chemical species held together by intermolecular forces*" [4, 5].

There are two types of subjects in supramolecular chemistry: a) the *supramolecular assemblies* or systems, also called supramolecular arrays, i.e. "*polymolecular entities that result from the spontaneous association of a large*

undefined number of components", and   b) *supermolecules*, i.e. "*well-defined discrete oligomolecular species that result from the intermolecular association of a few components* [6]. In this chapter we will be more interested in discrete oligomeric cyclic supermolecules than in supramolecular arrays of undefined size.

In principle, there are four main ways of preparing inorganic oligomers and polymers: a) polymerization of double (or triple) bond monomers; b) condensation of functional derivatives, c) ring opening polymerization; and e) ring-ring interconversion. Some of these are equilibrium reactions and are strongly dependent of thermodynamic and kinetic factors.
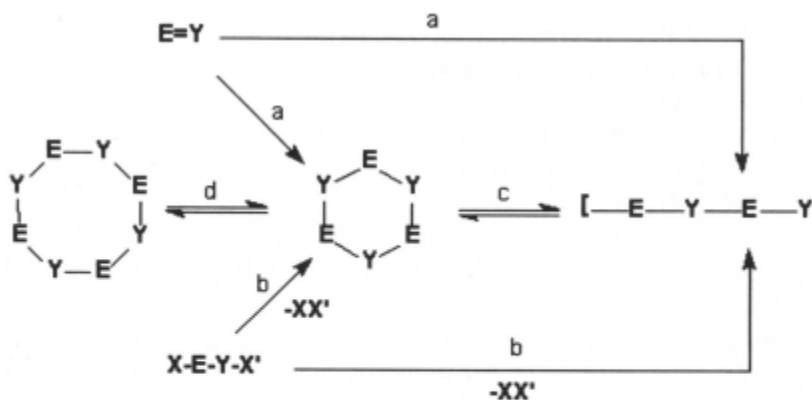
a - double bond monomer polymerisation
b - polycondensation
c - ring opening polymerisation
d - ring-ring equilibration

A peculiar aspect of inorganic chemistry is the general lack of polymerizable monomers, which could be starting materials for carbon-free backbone polymers. Although inorganic compounds containing element-

element double bonds are well known [7] these cannot (or rarely) serve as monomers for the synthesis of inorganic backbone polymers. Thus, the compounds of non-metals in their highest oxidation state, e.g. Group 15 and 16 element derivatives containing $P^V=O$, $P^V=N$, $P^V=S$, $As^V=O(N,S)$ or $S^{VI}=O$, $S^{VI}=N$ cannot be polymerized (unless they contain more than one double bond, e.g. $O=P=O$, $O=P=N$, $N=P=N$, etc. one being polymerizable); those in lower oxidation state are unstable as double bond monomers and tend to form cyclic oligomers or even polymers. The same is true for other double bond monomers, with $B=Y$, $Ge=Y$, $Sn=Y$, $P^{III}=Y$, $As^{III}=Y$, $Sb^{III}=Y$, $S^{II}=Y$, $Se^{II}=Y$ bonds ($Y = O$, N, S, Se). Attempts to prepare such monomers usually lead to cyclic (oligomeric) or polymeric species containing the corresponding repeating units E-Y ($E = B$, Ge, Sn, P, As, Sb, S, Se). Other "inorganic double-bond monomers" such as disilenes, $R_2Si=SiR_2$, iminosilanes, $R_2Si=NR'$, and silathiones, $R_2Si=S$, can be isolated if sterically protected by voluminous (bulky) organic substituents (e.g. R = mesityl). Silanones, $R_2Si=O$, were detected only as short-lived intermediates. Practically all reactions which could be expected to produce such monomers give rise to cyclic (oligomeric) or polymeric species, unless bulky substituents prevent oligomerization or polymerization.

The propensity for catenation of chemical elements varies greatly and it appears that no other non-metal can fully imitate carbon. Inorganic catenated structures (rings or polymeric chains) usually need to be protected by organic groups and - unlike hydrocarbons - the kinetic stability of catenated hydrides of elements other than carbon is low. Therefore, cyclic or polymeric polysilanes $(SiR_2)_n$, polygermanes $(GeR_2)_n$, or polystannnanes $(SnR_2)_n$, are much more stable with R = alkyl or aryl instead of R = H.

The building block approach allows for the synthesis of a broad variety of inorganic backbones for cyclic and polymeric systems. Identical or differing (EY, EY', E'Y) units (where $E = B$, Al, Ga, In, Si, Ge, Sn, P, As, Sb and $Y = O$, N, S, with element E being less electronegative than Y) can be intercombined in various ways to form cyclic or polymeric species.

The term *synthon* is more familiar to organic chemists and describes fragments from which various molecules can be built by synthetic procedures through covalent bonds. Sometimes the term was also used to describe "*structural units within supermolecules which can be formed and/or assembled by known or conceivable synthetic operations involving intermolecular interactions*" [8]. To avoid confusion, the term *tecton* was introduced to describe the molecular units of supramolecular structures assembled through non-covalent forces. Thus, the *tecton* has been defined as "*any molecule whose interactions are dominated by particular associative forces that induce self-assembly of an organized network*" [9, 10]. Here, we will use the term *synthon* for the fragments of covalent molecules and the term *synthon* for the molecular

building blocks of supermolecules self-assembled through non-covalent interactions.

14.2. Covalent ring systems

14.2.1. General aspects

The closest similarity between organic and inorganic cyclic structures is displayed by the *covalent rings*. These include both homo- and heterocycles. Homocycles contain identical atoms; in heterocycles the constituent atoms are different. Basically, covalent inorganic rings are formed by non-metals and Main Group metals, but transition metals are not excluded. To participate in covalent ring formation an atom should be able to form at least two covalent bonds, i.e. to be at least a divalent element. This condition is satisfied by numerous elements of the Periodic Table and therefore a great *variety of compositions* can be expected.

In the organic rings (homo- and heterocycles) the carbon atoms are constantly tetravalent and display sp^3 (tetrahedral), sp^2 (trigonal planar) or sp (linear) hybridizations with the corresponding bonding geometries. The most common heteroatoms are oxygen, sulfur and nitrogen. Inorganic chemistry operates with all elements of the Periodic Table and consequently it can operate with a broader range of possibilities in terms of hybridizations of atomic orbitals, coordination geometries and also oxidation states. Thus, a much broader *variety of structures* can be expected for inorganic cyclic structures.

The inorganic rings formed through covalent bonds are the real counterparts of organic cyclic molecules and illustrate the ability of other elements to imitate carbon. Although characteristic to elements close to carbon in the Periodic Table (in particular boron, silicon, germanium, phosphorus, arsenic, antimony, sulfur and selenium, alone or in association with oxygen, nitrogen or sulfur) this ability is not restricted to non-metals and covalent rings containing metals, e.g. aluminum, gallium, tin or lead, as well as transition metals, are also well known.

There are two types of covalent inorganic rings:

a) *homocyclic ring systems* – consisting of catenated identical atoms, and

b) *heterocyclic ring systems* – containing different elements.

Inorganic homocycles containing three, four, five, six, seven, eight or more identical atoms are known for various elements.
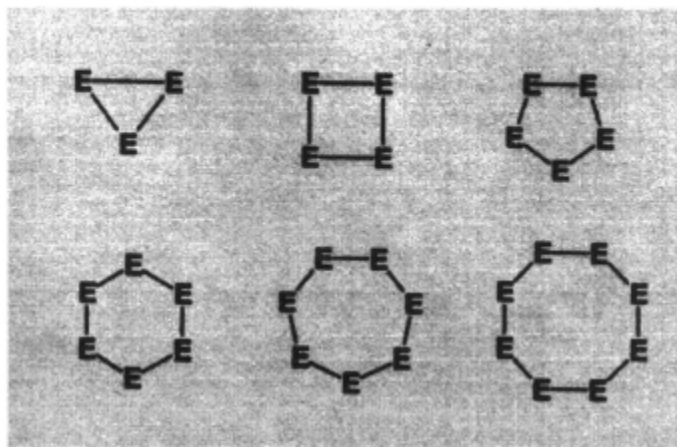
A probably incomplete list includes the following homocyclic rings E_n:

|									
-	Si_3	Ge_3	Sn_3	N_3	P_3	As_3	Sb_3	Bi_3	-
-	Si_4	Ge_4 -	Sn_4 -	N_4	P_4	As_4	Sb_4	Bi_4	-
-	Si_5	Ge_5 -	Sn_5 -	N_5	P_5	As_5	Sb_5	-	-
B_6	Si_6	Ge_6	Sn_6	N_6	P_6	As_6	Sb_6	-	S_6
	Se_6	Te_6							
					P_9	As_8			S_7
	Se_7	-				As_9			S_8
	Se_8	Te_8				As_{10}			S_n
	Se_{12}								$(n > 8)$

The most recent are the cyclotri- and -tetrabismuthanes [11] and the cyclotetradecasulfane, S_{14} [12].

Inorganic heterocycles can be formally generated in three different ways:

a) by *insertion* of one or more heteroatoms in a parent homocycle and maintaining some E-E bonds (between identical atoms) to form rings of the type E_mY_n (m and n differing);

b) by *regular alternation* of two different elements E and Y *i.e.* by combining a discrete number of *identical EY repeating units (synthons)* to form rings of the type **(EY)$_n$ (n = 2, 3, 4, 5, 6...)**

c) by combining a number of *different repeating units,* EY and E'Y or
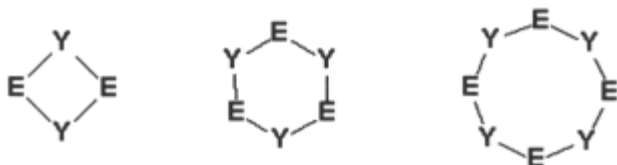
EY', to form rings of the type **(EY)$_m$(E'Y)$_n$** or **(EY)$_m$(EY')$_n$** or even **(EY)$_m$(E'Y')$_n$** (e.g. Scheme 3).
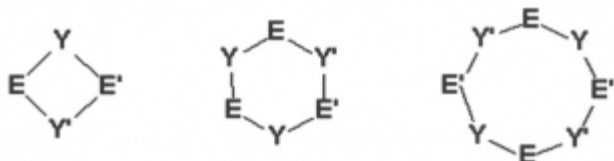
Usually E and Y are elements of different electronegativities and the best combinations are obtained when E is less electronegative (i.e. more electropositive) than carbon (i.e. B, Al, Si, Ge, Sn, Pb, P, As, Sb, Se, Te) in association with an element Y which is more electronegative than carbon (O, N, S).

We will deal here mostly with rings formed from identical repeating units or synthons (type b) which also have chain polymeric correspondents, often as a direct result of ring opening polymerization. Since many inorganic rings, but not all, can undergo ring opening polymerization they can serve as real "monomers" or precursors for the synthesis of inorganic (carbon-free) backbone polymers.

14.2.2. Ring-chain and ring-ring equilibria

The relation between inorganic rings and polymers is often an equilibrium transformation. Depending upon the nature of the repeating building units, such equilibria can be shifted much in favor of the ring (indicating a high tendency of cyclisation and little or no propensity for polymerisation) or in favor of the polymer, under appropriate conditions. In the later case large ring (macrocyclic) oligomers and chain polymers with inorganic

backbones, built upon the principle of repeating building units, can be readily obtained.

The knowledge of equilibrium constants in ring-chain equilibria can give important information upon the propensity of certain inorganic cyclic structures for ring opening polymerization. The simplest way to determine such equilibrium constants is to investigate systems consisting of difunctional units (or "middle groups," able to act as repeating units in the ring and polymeric chain) and monofunctional units (or "end groups", which terminate the chain growth (see ref. [13]). The random probability of ring formation in a system consisting only of mono- and difunctional synthons is described by a set of equilibrium constants [14]. Systems with large values of these cyclisation equilibrium constants will have great tendency to form rings and little propensity for ring-opening polymerization, and *vice-versa*, small values of the cyclisation equilibrium constants correspond to rings which be easily polymerized. A list of such equilibrium constants is given in Table 1, in which some organic rings have also been included for comparison. Indeed, the rings in the top of the column have not been polymerized by ring opening, whereas those at the bottom are known as readily polymerizable inorganic rings. Even if the polymers can be obtained by some other than the ring opening polymerisation, thermodynamics will favor the chain disintegration into small rings.

Table 1   Cyclisation constants for six-membered rings $(AB)_3$

Repeating unit (AB)	K_3
$-Me_2Si-S-$	3000
$-CH_2-CH_2-$	1200
$-Me_2Si-NMe-$	300
$-Me_2Ge-S-$	50
$-ClAs-NMe-$	15
$-CH_2-O-$	4
$-Me_2Ge-O-$	0.9
$-Cl_2P=N-$	0.1
$-O_2S-O-$	0.1
$-(NaO)PO_2-$	0.09
$-Me_2Si-O-$	0.03
$-FAs-NMe-$	0.05
$-S-S-$	0.05

The equilibrium cyclisation constants explains the difference between siloxanes and silazanes in terms of the propensity for ring opening polymerization, based upon investigations of among others, polysiloxane **[Me₂SiO]₄/ₓ** (polymerisable ring) [15]) and polysilazane **[Me₂SiNMe]₃/ₓ** (non-polymerisable ring) systems [16].

The ring-chain equilibria have been investigated for several systems based upon inorganic building units, and methods for calculating the concentration of cyclic oligomers have been proposed for several systems[17]. There are several known examples of interconversion of inorganic rings of various sizes, *i.e.* the redistribution of difunctional synthons, including both ring contractions and ring expansions. Some of such rearrangements are reversible, and can also be described as equlibria, characterised by equilibrium constants.

The knowledge of these equilibrium constants provides information about the preferred ring size for a given repeating unit, or the distribution of building units between rings consisitg of non-identical building units. Among the ring-ring equilibria investigated in some detail, with determination of the equilibrium constants, several can be cited: silicon-sulphur dimer-trimer **[Me₂SiS]₂/₃** (trimer predominant) [18], germanium-oxygen trimer-tetramer **[Me₂GeO]₃/₄** (tetramer predominant) [19], or silazane-silthiane **[Me₂SiNMe]₃**-**[Me₂SiS]₃** [20], silthiane-germathiane **[Me₂SiS]₃-[Me₂GeS]₃** [21]. Unfortunately, only few inorganic ring systems have been subjected to this type of investigations.

## 14.2.3. Homoatomic cyclic oligomers and polymers

14.2.3.1. Polysilanes

Polysilanes are formally the polymers of disilenes, **RR'Si=SiRR'.** Such monomers have been obtained only with very bulky organic groups [22] and cannot serve as precursors for polymeric materials. Cyclic and polymeric polysilanes, based upon silicon-silicon bond backbones, are known as stable compounds mainly as organo-substituted derivatives, **(SiR₂)ₙ** [23]. They are usually prepared by dehalogenation of diorganodichlorosilanes, either with alkali metals (Wurtz coupling) or by electrochemical reduction. In most cases, the major product is the pentamer **(n = 5)** and/or hexamer **(n = 6),** but larger ring oligomers have been obtained in certain cases, e.g. with **R = Me (n = 9, 1%** yield; **n = 10-19,** 0.09-0.26 % yield) in addition to the pentamer (12%), hexamer (59%), heptamer (3%) and octamer (1.8%). All members of the series of cyclic oligomers up to **n = 35** have been separated by column

chromatography and the members up to 19 silicon atoms have been isolated as individual compounds [24]. The nature of products formed depends greatly on the solvent and the presence of complexing agents (e.g. crown ethers to solvate the alkali metal salt) [25].

R = Me, Ph, etc.
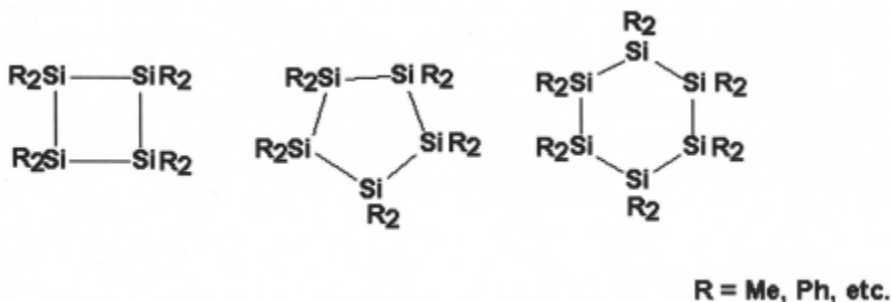
The molecular structures of several cyclosilanes, e.g. $(Me_2Si)_n$ (n = 4, 6 and 7) [26] and $(Ph_2Si)_n$ (n = 4, 5 and 6) [27] and also of the large ring compounds $(SiMe_2)_{13}$ and $(SiMe_2)_{16}$ have been established by single crystal X-ray diffraction [28]. The macrocycles display an irregular conformation.

(SiMe2)16   (SiMe2)16
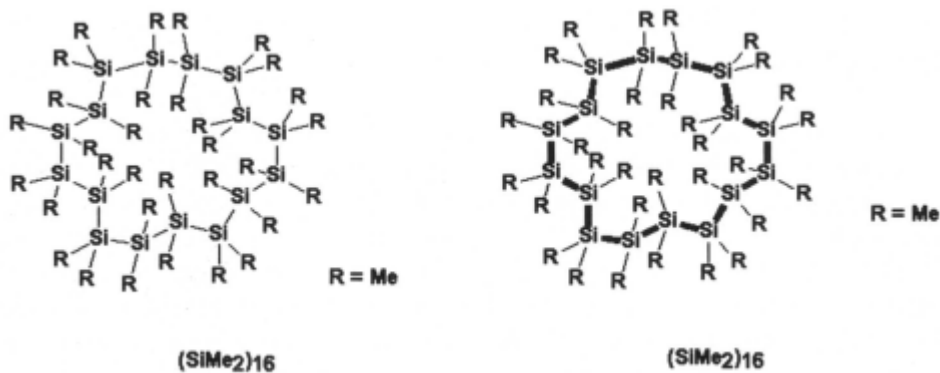
In the case of **MePhSiCl₂** the Wurtz coupling dehalogenation produces three fractions, containing low molecular weight cyclics, intermediate molecular weight cyclic oligomers and high polymeric materials [29].

A more recent development is the catalytic dehydrogenative coupling of silanes **RSiH₃,** leading directly to linear polysilanes (oligomers and polymers) but small amount of cyclics (0.5-4.6 %) are also formed when **R = Me [30].** Diorganosilanes can also be prepared by dehydrogenative coupling of **RR'SiH₂** initiated by **Pt(COD)₂** [31].

The cyclopolysilanes $(Me_2Si)_n$ (n = 5-12) cannot be readily subjected to ring opening polymerization, as they are thermodynamically stable or tend to

undergo Al(Fe)Cl$_3$ catalysed rearrangements with formation of branched cyclopenta- and cyclohexasilanes [32]. However, **(MePhSi)$_4$** has been thermally polymerized in the presence of carbanionic and silyl anionic initiators up to molecular weights in the range from 50000 to 100000. It seems that cyclization to macrocycles also occurs in the process [33]. The cyclotetrasilanes **(MePrSi)$_4$** and **(MeHexSi)$_4$** have been thermally polymerized (to molecular weights of **2.10^6**) but several catalysts attempted failed to initiate polymerization [34]. Transition metal compounds as catalysts in the ring opening polymerization of cyclosilanes have also been investigated [35]. The main interest in polysilanes resides in their use as silicon carbide ceramic precursors [36].

14.2.3.2. Polygermanes

Polygermanes are prepared by methods similar to those used for polysilanes, e.g Wurtz dehalogenative coupling [37]. Cyclogermanes **(R$_2$Ge)$_n$** with **n = 3,** 4 and 5 can be isolated and a low molecular weight polymeric fraction (perhaps cyclic oligomer) can be detected. The alkylpolygermanes are soluble and thermochromic [38].

14.2.3.3. Polystannanes

Polystannanes, **(SnR$_2$)$_n$,** including rings containing from 3 to 9 tin atoms [39], but also polymers of much higher nuclearity, have been described in the literature [40] and were prepared from diorganotin dihalides with alkali metals (Wurtz coupling) [41] or from diorganotin hydrides by dehydrogenative coupling [42], by coupling with diorganotin amides [43], by electrochemical reduction of diorganotin dihalides [44] or by reduction with samarium diiodide [45], In the absence of any obvious monofunctional terminal groups, the polymers might be very large ring species rather than open-end linear polymers, as suggested by their molecular weight. Among these, the dibutyltin **(Bu$^n_2$Sn)$_n$** **(M$_w$** from 0.6 to **1.2x10^4, M$_w$/M$_n$** from 1.3 to 2.6) and dioctyltin **(Oct$_2$Sn)$_n$ (Mw 0.6x10^4, M$_w$/M$_n$ 0.6)** prepared electrochemically, are mentioned.

Cyclic polystannanes have been well studied, and these include dialkylstannanes **(R$_2$Sn)$_n$ (R = Et, n = 6-9; R = Cy, n = 5; R = Bu, n = 5** and 6; **R = Bz, n = 4** and 6) [46] and diarylstannanes, e.g. **(Ph$_2$Sn)$_6$** [47]. Even three-membered ring cyclotristannanes (with bulky substituents, and consequently non-polymerizable) have been synthesized [48].

14.2.3.4. Polyphosphanes

Monomers **R-P=P-R** with voluminous organic groups have been prepared [49] but with common organic sustituents (alkyl, phenyl) only small and regular ring cyclopolyphosphanes **(PR)$_n$ (n = 3-6)** are well known [50]; larger cyclic oligomers are stabilized only as transition metal complexes, e.g. **[M$_2$(CO)$_6$(PMe)$_9$]** (**M = Cr, Mo, W**) and are formed in reactions involving ring expansion rearrangements [51].
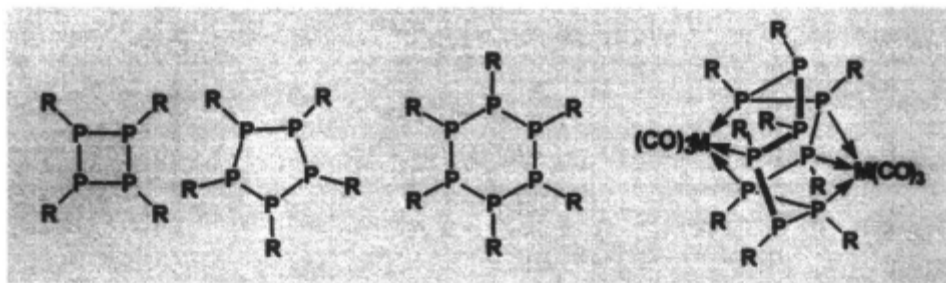
Ring opening polymerization of cyclophosphanes to give linear polyphosphane polymers does not seem to be feasible as the rings are thermodynamically stable.

14.2.3.5. Polyarsanes

Double bond monomers **R-As=As-R** are known only with bulky organic groups [52] and cannot serve as precursors for cyclic oligomers and polymers with As-As backbones. Such compound are formed with common organic groups (alkyl, aryl). Thus, cyclopolyarsanes of small and regular size, **(AsR)$_n$** with **n = 3-6** are well documented [53] and macrocyclic oligomers are formed in ring expansion reactions with metal carbonyls and stabilised as metal complexes. Thus, nine-membered rings **(AsR)$_9$** (with **R = Me** or Ph) and ten-membered rings **(AsMe)$_{10}$** are formed (and stabilized as metal complexes) from the corresponding cyclic hexamers in reactions with chromium and molybdenum hexacarbonyls [54].
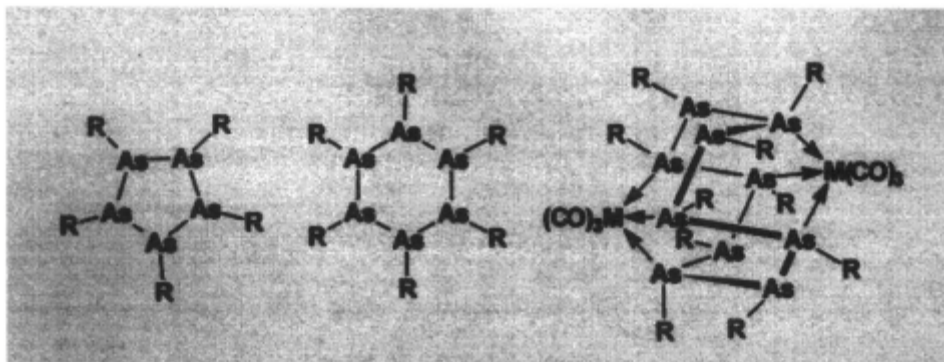
It appears that ring opening polymerization of cyclopolyarsanes has little chances and probably nothing more than ring expansion can be expected with this class of rings.

14.2.3.6. Polysulfanes

Elemental sulphur displays a great propensity for catenation and polysulphur rings (cyclopolysulfanes) of various ring sizes are known as allotropic forms of elemental sulphur [55].

Currently all cyclic sulphur molecules S_n with $n = 6,$ 7, 8, 9, 10, 11,12, 13, 14, 15, 18, 20, 25 are known and single-crystal X-ray diffraction determinations of the molecular structure are available for S_6 [56], S_7 [57], S_8 [58], S_{10} [59], S_{11} [60], S_{12} [61], S_{13} [60a], S_{14} [62], S_{18} [63] and S_{20} [64]. All these rings are puckered.
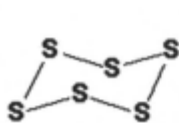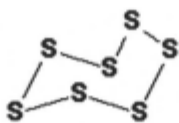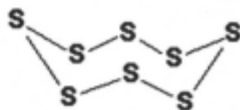
S6   S7   S8
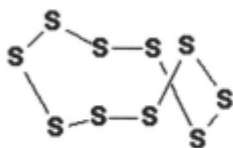
S10   S11   S12
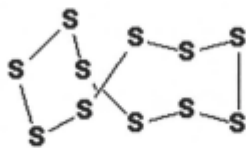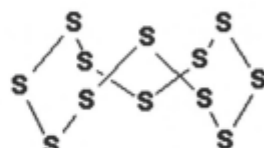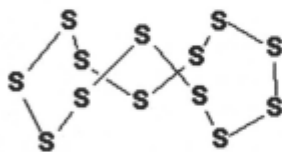
S13   S14
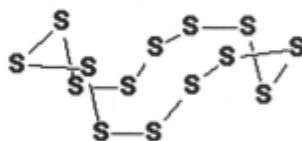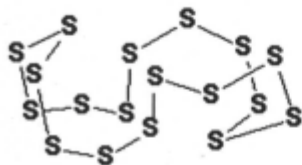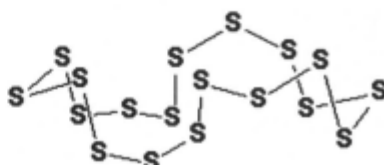
α—S18   β—S18

Most cyclic sulphur oligomers have been synthesised by reacting $(C_5H_5)_2TiS_5$ with appropriate open-chain polysulphur dichlorides (α,ω-dichloropolysulfanes); the complex mixtures formed contain various cyclic oligomers which can be separated with the aid of high-performance liquid chromatography [65].

The thermodynamically stable form is the eight-membered ring S_8 and all other cyclic allotropes undergo molecular rearrangements with formation of the octamer. Ring opening polymerization of cyclosulphanes is also possible and occurs on heating above the melting temperature. The ring-ring and ring-chain equilibria in sulphur melts have been theoretically investigated and the concentration of cyclic species were calculated [66]. It is quite probable that the sulphur melt contains a large proportion of cyclic sulphur polymers.

14.2.4. Heteroatom cyclic oligomers and polymers

14.2.4.1. Borazanes and other boron oligomers

In association with nitrogen, oxygen, sulphur and selenium, boron tends to form six-membered rings $(BY)_3$ $(Y = N, O, S, Se)$, although four- and eight-membered rings are known with the same synthons. Ring opening polymerization is not characteristic for these rings and they are best described as heterocycles rather than oligomers in a homologous polymeric series. Their chemistry has been reviewed [67, 68].

The boron-nitrogen rings are probably stabilized through some electron donation from nitrogen. Four-, six- and eight membered rings consisting of RB-NR' synthons are known and some interconversions have been reported. The corresponding monomers (iminoboranes) bearing sterically demanding organic groups can be isolated, but the cyclic oligomers are much easier to obtain [69].
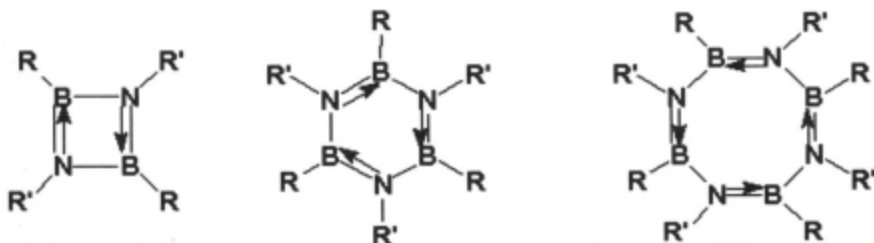
In the six-membered ring B_3N_3 of borazine, the electron delocalization leads to bond equalization, but in the eight-membered ring the B-N bonds display differing bond lengths, which is reminiscent of the situation in the carbon isoelectronic rings (benzene and cyclooctatetraene). Probably because of this quasi-aromatisation the borazine ring cannot be readily subjected to ring opening polymerization, although insoluble, macromolecular polyminoboranes $(-RB-NR'-)_x$ are known, but they have been prepared by a different route, e.g.

thermolysis of diorganoboron azides. Thus, **(EtBNEt)$_x$** is readily depolymerized to the cyclic trimer **(EtBNEt)$_3$** at 150°C. The *iso*-butyl derivative is also known in trimeric and polymeric form [70].

The boron-nitrogen rings can serve as intact building units in macromolecular polycyclic structures [71]. Thus, simple heating of borazine **(HBNH)$_3$** (in the presence of dimethyltitanocene catalyst) produces polymers consisting of chains of linked **B$_3$N$_3$** rings, which at 1200°C produce cubic boron nitride [72].
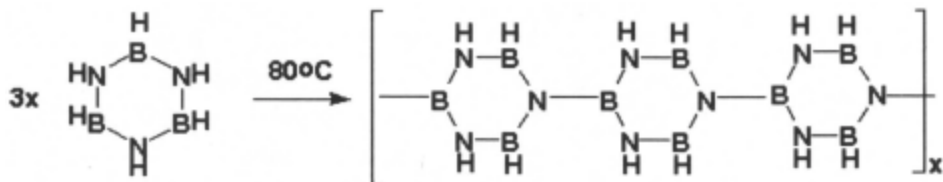
Another way to incorporate borazine rings in polymeric structures is to polymerize vinylborazine (which yields a "semi-inorganic polystyrene" with borazine side groups) [73], or to interconnect borazine rings through polysilazane chains [74].
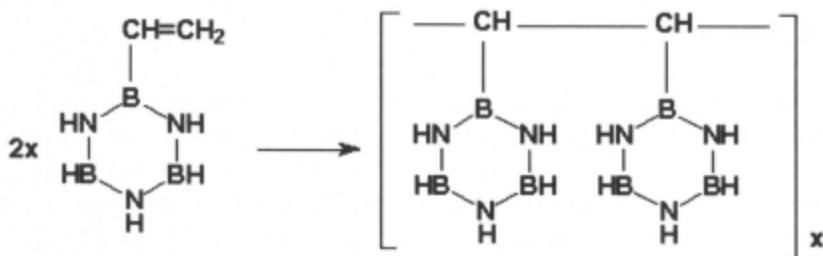
The six-membered boron-oxygen ring, **B$_3$O$_3$,** is present intact as a building unit in numerous polymeric borates, which have been thoroughly reviewed in the Gmelin Handbook [75]. Organosubstituted cyclotriboroxanes (boroxines), **(RBO)$_3$,** are also well known [76], but they do not undergo ring-opening polymerization.

Boron-sulfur [77] and boron-selenium rings also do not undergo ring opening polymerization, but can be incorporated intact in numerous inorganic polymeric structures [78].

We also mention here the organoiminoalanes, **RAl=NR',** which have not been isolated in a monomeric state. The **Al=N** double bond shows a strong

tendency to polymerize (no such monomer isolated so far), but very seldom this results in heterocyclic alazanes containing tricoordinate aluminum. Thus, an aluminum-nitrogen Al_3N_3 ring compound, **[MeAlN(2,6-Pr$^i_2$C$_6$H$_3$)]$_3$,** containing a planar Al_3N_3 heterocycle, can be regarded as a borazine analogue [79].
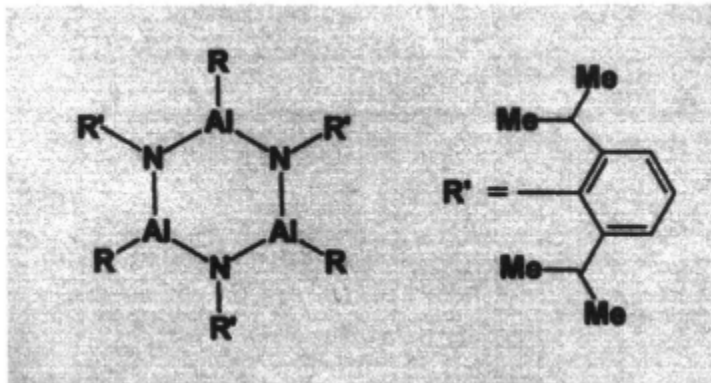
Most frequently, cubane or other aluminum-nitrogen cage supermolecules are formed [80].

14.2.4.2. Silazanes

The silicon-nitrogen pair displays a great tendency of ring formation and stable small and regular size, i.e. four-membered, six-membered and eight-membered rings are well known. Some silicon-nitrogen double bond monomers have been isolated as stable compounds [81] but the presence of bulky substituents prevents cyclization or polymerization by opening the double bond. With "normal" organic substituents, e.g. methyl, other alkyls, phenyl, only cyclosilazanes are formed in all reactions leading to Si-N bond formation. Thus, organocyclosilazanes can be readily obtained by ammonolysis of diorganodichlorosilanes, **R$_2$SiCl$_2$,** but the reaction produces only cyclotri- and cyclotetrasilazanes, **(R$_2$SiNH)$_n$ (n = 3, 4)** [82]. In no case cyclic oligomers higher that the tetramer have been detected in the reaction mixture. Cyclodisilazanes are usually obtained by condensation or coupling reactions, with elimination of amines [from diorganodiaminosilanes, **R$_2$Si(NHR')$_2$]** or metal halides [from **R$_2$Si(NLiR')$_2$** and **R$_2$SiCl$_2$].** The best known are cyclodisilazanes, cyclotrisilazanes and cyclotetrasilazanes [83]. Many have been structurally characterized, but we cite here only the methyl trimer **(Me$_2$SiNH)$_3$** [84], the tetramer **(Me$_2$SiNH)$_4$** (both ammonolysis products of dimethydichlorosilane) and **(Me$_2$SiNMe)$_4$** [85]. The ammonolysis of

organotrichlorosilanes yields cage and polymeric (probably polycyclic) silazanes, and one such structure (a SiN prismane **[Me₆Si₆(NH)₉]**) has been demonstrated by X-ray diffraction [86].
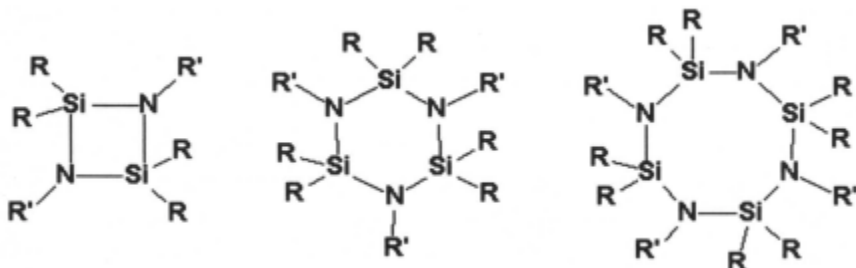
Unlike cyclosiloxanes (see bellow), cyclosilazanes show little tendency to undergo ring opening polymerizations and practically no straightforward polymerization of organocyclosilazanes **(R₂SiNH)ₙ** or **(R₂SiNR')ₙ** to give a linear polysilazane has been achieved so far. The ring-chain equilibrium constants in equilibration reactions indicate a great tendency of ring formation and suggest little chance of obtaining linear polymers by ring opening polymerization. Various polymeric materials based upon silicon-nitrogen frameworks are however known, but they seem to contain intact cyclosilazane rings as building units, or are prepared by other methods [87]. These are important precursors for silicon-nitride ceramics.

Tetrameric **[H₂SiNMe]₄** and short-chain linear polysilazanes **MeNH(H₂SiNMe)ₙH** (average **n = 10)** were described as products of the reaction between **H₂SiCl₂** and **MeNH₂** [88] and a thermal ring opening polymerisation of **[Me₂SiNH]₄** in the presence of **(Me₃Si)₂NH** catalysed by **Ru₃(CO)₁₂,** has been reported [89]. Ring opening polymerisation of cyclosilazanes (mainly dimeric) initiated by various anionic and cationic reagents **(LiR, NaC₁₀H₈, CF₃SO₃SiMe₃, CF₃SO₃Me)** has been recently reported to give high molecular weight polymers [90]. In no case, however, elastomeric polysilazanes, comparable to the corresponding polysiloxanes, have been obtained.

Germanium-nitrogen monomers **R₂Ge=NR'** are known [91] and some germanium-nitrogen ring chemistry has been developed [92], but no polymers based upon a Ge-N skeleton seem to have been obtained so far.

14.2.4.3. Siloxanes

The siloxanes are among the most important inorganic cyclic oligomers and polymers and they deserve a more detailed treatment (see the chapter by S.J. Clarson in this volume). Only a brief presentation is made here in relation with other inorganic ring oligomers. Siloxanes are formally polymers of "silanones" $R_2Si=O$, but such double-bond monomers have been identified only as transient species [93].

Cyclosiloxanes $(R_2SiO)_n$ are formed in the hydrolysis of diorganodichlorosilanes, and cyclic oligomers and polymers of a broad range of n values are present in the product. Catalytic ring opening polymerization of small and regular size organocyclosiloxanes (trimers and tetramers) produce larger ring cyclosiloxanes which can be separated from the mixtures, which also containing linear elastomeric polyorganosiloxanes. The most common and best studied are the poly(dimethylcyclosiloxanes), $(Me_2SiO)_n$, a family of compounds of great industrial importance as precursors of silicone materials [94].

A careful study of the hydrolysis of H_2SiCl_2, $MeHSiCl_2$ and Me_2SiCl_2, using gas chromatography, mass spectrometry and NMR spectroscopy, revealed that oligomeric cyclosiloxane $(H_2SiO)_n$ (up to $n = 23$), $(MeHSiO)_n$ (up to $n = 19$) and $(Me_2SiO)_n$ (up to $n = 17$) can be detected in the hydrolysis product [95]. Oligomeric rings containing from 5 to 8 Me_2SiO units have been separated from the hydrolysis product of Me_2SiCl_2 by traditional procedures of fractional distillation [96].

Several diorganocyclosiloxanes have been structurally characterised by X-ray diffraction, and the conformation of their rings is thus known. Among these, hexamethylcyclotrisiloxane $(Me_2SiO)_3$ contains a planar six-membered ring Si_3O_3 [97], octamethylcyclotetrasiloxane $(Me_2SiO)_4$ contains a non-planar eight-membered ring Si_4O_4 [98], and larger rings, e.g. $(Me_2SiO)_5$ [99] and $(Me_2SiO)_8$ [100], have also been analysed. Large stereoregular cyclosiloxanes $[Ph(Me_3SiO)SiO]_n$ ($n = 6$ and 12) have been synthesized by an indirect route and structurally characterized [101]. The first members of the series, non-polymerizable cyclodisiloxanes (with bulky organic groups) have been obtained by oxidation of disilenes and structurally characterized by X-ray diffraction [102].
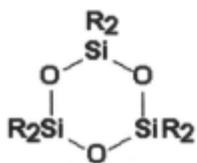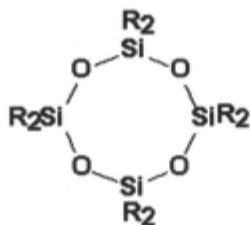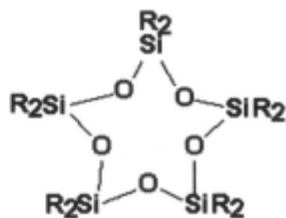
(R2SiO)3   (R2SiO)4   (R2SiO)5
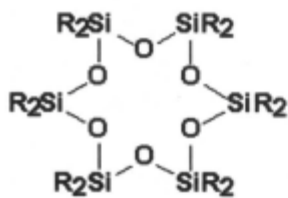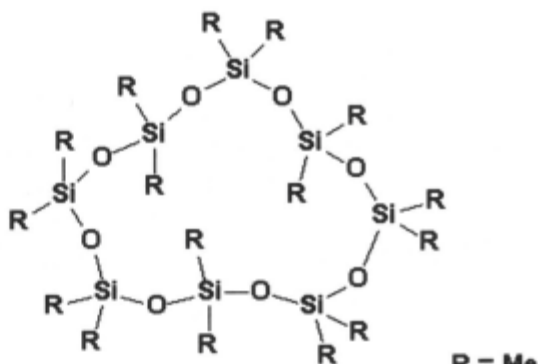
(R2SiO)6   (R2SiO)8   R = Me

Catalytic equilibrations involving ring opening polymerization of cyclosiloxanes, e.g. of the tetramer $(Me_2SiO)_4$, produced mixtures containing cyclosiloxane oligomers and polymers $(Me_2SiO)_n$ with $n = 5\text{-}25$ (KOH used as catalyst) [103] and an extensive study of this type of reaction revealed that cyclic poly(dimethylsiloxanes) with up to $n = 1000$ can be thus obtained, by using a variety of basic or acidic catalysts [104]. The reaction has been extensively investigated and reviewed [105]. In the case of larger ring cyclosiloxanes $(Me_2SiO)_n$, with $n = 4$, 5, 6 and 7, the rate of the cationic polymerization increases with the ring size; in the polymerization of the trimer $(Me_2SiO)_3$ high polymers and cyclic 3x multiples are formed simultaneously under kinetic control [106].

Cyclic polydimethylsiloxanes can be distinguished from the linear polymers of the same composition according to some specific properties such as viscosity [107], glass transition temperature [109] and adsorbtion on silica surfaces [108].

In addition to poly(dimethylsiloxanes) other cyclic oligomers and polymers investigated include methylhydrogensiloxanes **(HMeSiO)$_n$** [110], methylvinylsiloxanes **(MeViSO)$_n$** [111], and methylphenylsiloxanes **(MePhSiO)$_n$** [112].

Germanium analogues of cyclosiloxanes reported to date include **(R$_2$GeO)$_n$** trimers, tetramers and polymers (e.g. with **R = Me,** Et, Pr, Ph, etc.) [113] but they did not attract as much interest as their silicon relatives, although some equilibration reactions have been investigated [114].

14.2.4.4. Phosphazenes and phosphazanes

Phosphazenes are an important class of inorganic rings and polymers, based upon an alternation of phosphorus(V) and nitrogen, i.e. the **-P=N-P=N-** sequence. The general formula **(R$_2$PN)$_n$** covers a large family in which **R =** halogen, functional group (alkoxo, amino, thiolato, etc.) or organic group (alkyl, aryl). The chemistry of cyclic and polymeric phosphazenes has been extensively covered in several reviews and books [115]. The six- and eight-membered rings are the most important members of this class, and their chemistry is quite comprehensive. Larger cyclic oligomers have also been investigated.

Usually the entry into phosphazene chemistry is based upon the formation of perchlorocyclophosphazenes, **(Cl$_2$PN)$_n$,** which are readily prepared by reacting phosphorus pentachloride with ammonium chloride in refluxing tetrachloroethane or other organic solvent. The major products are the trimer and the tetramer, but larger ring oligomers with **n = 5-8** have also been isolated [116].
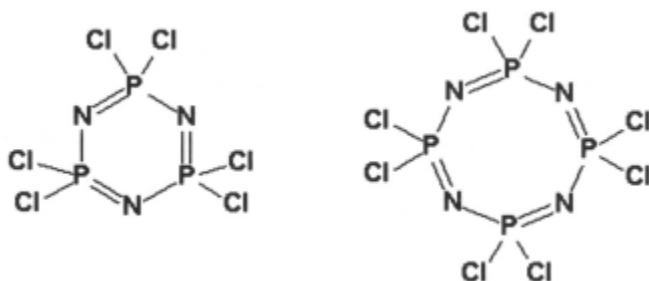
The crude mixture also contains larger rings, as demonstrated by fluorination with potassium fluoride in liquid sulfur dioxide at 90-125° under pressure, producing cyclic oligomers **(F$_2$PN)$_n$** with **n = 3-17,** which can be separated by a

combination of fractional distillation and vapour-phase chromatography [117]. Cyclic bromophosphazenes $(Br_2PN)_n$ witn $n = 3-6$ have also been obtained [118].

The halogens can be readily replaced by various functional groups, e.g. alkoxy and aryloxy, to give $[(RO)_2PN]_n$ ($R = Me$, CH_2CF_3, Ph; $n = 3-8$) and dimethylamino groups to give $[(Me_2N)_2PN]_n$ ($n = 3-8$) [119], or with organic groups, to give $(Me_2PN)_n$ ($n = 3-10$) [120].
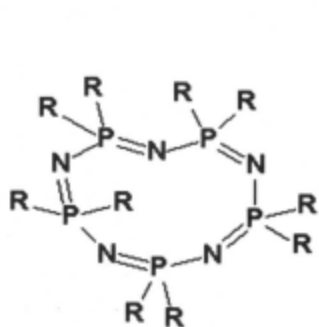
(Me$_2$PN)$_5$
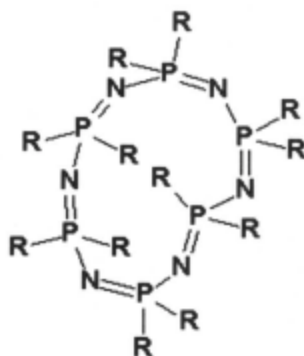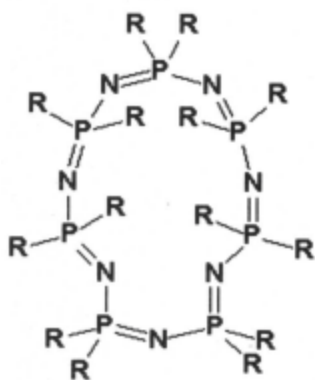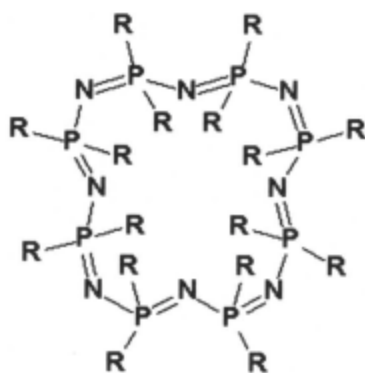
(Me$_2$PN)$_6$

(Me$_2$PN)$_7$

(Me$_2$PN)$_8$

Alkaline hydrolysis of perchlorocyclophosphazenes produces salts of cyclophosphazanic acids, $M^I_n[(O_2PNH)_n]$, $n = 3-8$, with preservation of the ring size and $(PN)_n$ cyclic skeleton, but involves an $[-(HO)_2P=N-]/[-(HO)(O)P-NH-]$ tautomerization [121].

Numerous single crystal X-ray diffraction studies confirmed the structures of cyclophosphazenes, and we mention here only those dealing with larger rings, i.e. **($F_2PN)_5$ [122], ($Cl_2PN)_5$ [123], ($Br_2PN)_5$ [124], ($Me_2PN)_5$ [125], ($Me_2PN)_6$ [126], ($Me_2PN)_7$ [120b], ($Me_2PN)_8$ [127]** and **($Me_2PN)_n$ (n = 9-12) [128]**. The crystal and molecular structures of the hexamers **[(MeO)_2PN]_6** [129] and **[(Me_2N)_2PN]_6** [130], and octamers **[(MeO)_2PN]_8** [131] and **[(Me_2N)_2PN]_8 [132]** have also been reported.

The conformations of these large rings are irregular and demonstrate the flexibility of the phosphazene chains, which allows the formation of cyclic oligomers of practically any size.
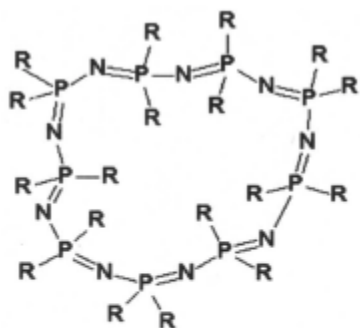
(Me2PN)9
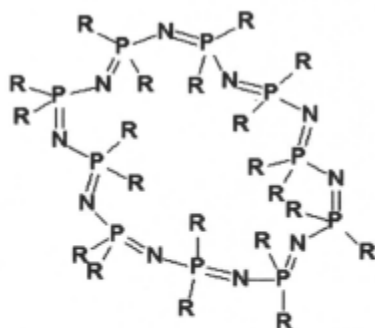
(Me2PN)10
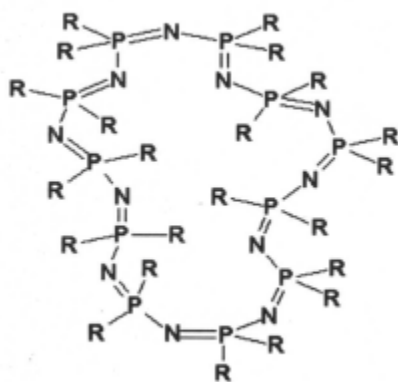
(Me2PN)11
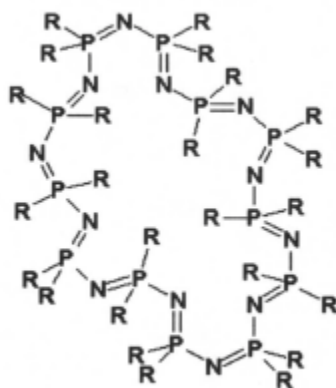
(Me2PN)12

Cyclophosphazenes undergo both thermal ring-opening polymerization (with formation of linear polymers) and ring-ring equilibria (resulting in ring expansion).
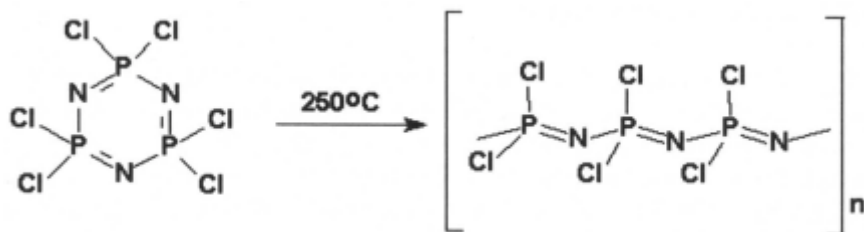
The six-membered ring can expand to 8-, 10- and 12 membered rings (and larger) and a polymerization mechanism has been suggested in which the first step is the conversion of the six-membered ring into a 12-membered ring [133].
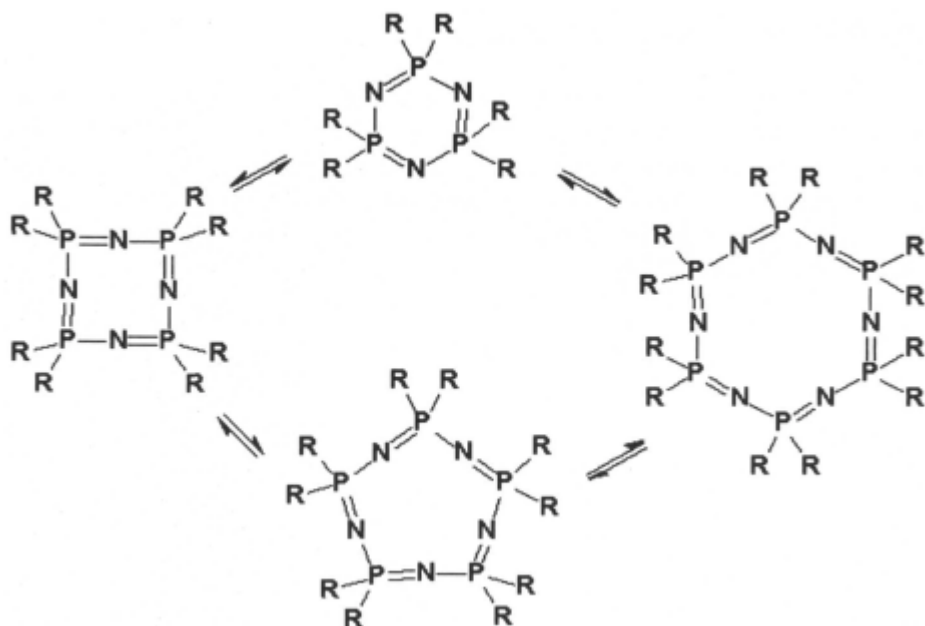
It is quite probable that in many cases the so-called "linear polymers" are in fact very large ring molecules, containing hundreds or thousands of R_2PN units, especially in very pure systems where no monofunctional chain-terminating groups are present. Moisture sensitive polychlorophosphazenes, $(Cl_2PN)_x$, obtained by ring-opening polymerization of the trimer $(Cl_2PN)_3$, can

be modified by substitution of the chlorine atoms with suitable nucleophilic reagents, to give a broad range of hydrolytically very stable functional or organic substituted polymers [134]. Alternatively, some substituted cyclotriphosphazenes can be directly obtained by ring opening polymerization of substituted cyclic trimers [135].

It has been found that some cyclotriphosphazenes, mostly those bearing organic substituents, do not polymerize and undergo only thermal ring expansion through ring-ring equilibria. This is the case with hexamethylcyclotriphospnazene $(Me_2PN)_3$ (trimer-tetramer ring-ring equilibrium) [136], hexaphenylcyclotriphosphazene $(Ph_2PN)_3$ (trimer-tetramer ring-ring equilibrium) [137], hexakis-(trifluoroethoxy)cyclotriphosphazene $[(CF_3CH_2O)_2PN]_3$ (ring expansion to an equilibrium mixture of tetramer, pentamer and hexamer) [138], and hexaphenoxycyclotriphosphazene $[(PhO)_2PN]_3$. Thus, the trimer $(Me_2PN)_3$ and the tetramer $(Me_2PN)_3$ participate in a ring-ring equilibration $(\Delta H = 10.2 \ kcal.mol^{-1}, \ \Delta S = 14.3 \ e.u.)$ and are interconvertible at temperatures between 200 and 350°C, but they do not polymerize; the reaction is catalysed by base [136].

Ring expansion occurs during the thermolysis of the six-membered ferrocenyl derivative bearing phenoxy groups, $1,3,5,5-(PhO)_4(1,3-Fc)P_3N_3$, with the formation of the twelve-membered cyclophosphazene $(PhO)_8(1,3-Fc)_2P_6N_6$. Some transannular substituted cyclotriphosphazenes bearing ferrocenyl readily expand the ring and polymerize thermally, probably due to the strain induced by the 1,3-substitution [139].
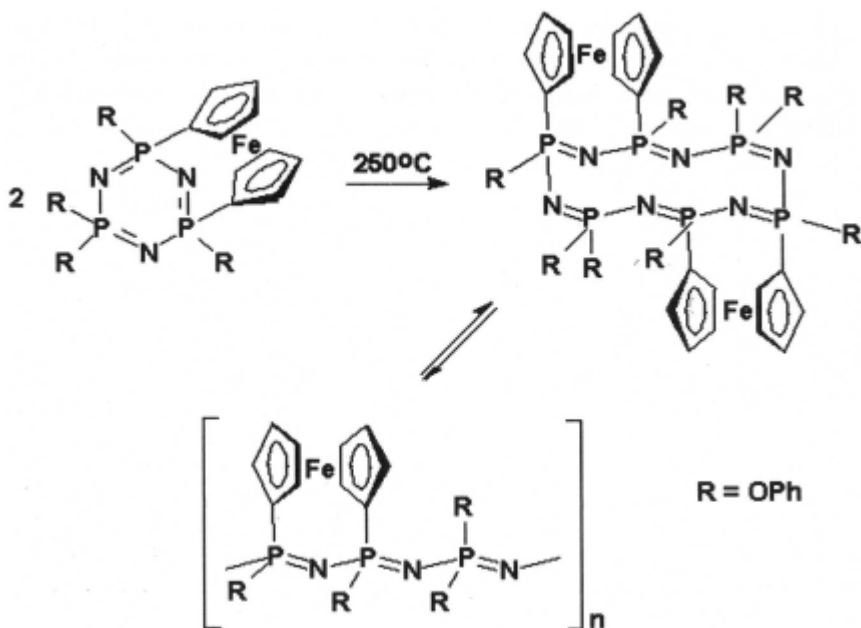
1,2-Dioxyphenyl, 2,2'-dioxybiphenyl, 1,8-dioxynaphtyl and 1,8-diaminonaphtyl, or the related spirocyclic cylotriphosphazene derivatives with 2,2'-dioxybiphenyl, 1,8-dioxynaphtyl and 1,8-diaminonaphtyl substitutents, also undergo thermal ring expansion in addition to polymerization [140].
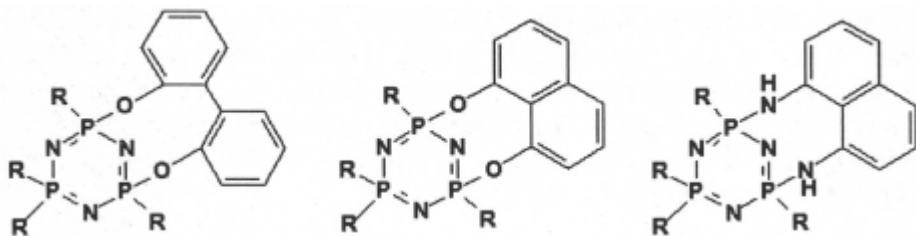
The 2,2'-dioxybiphenyl cyclotriphosphazene 1,3-$(C_{12}H_8O_2)(CF_3CH_2O)_4P_3N_3$ at 200°C or higher temperatures undergoes exclusively ring expansion with formation of the higher cyclic oligomers, ranging from cyclotetraphosphazene $(C_{12}H_8O_2)(CF_3CH_2O)_4P_4N_4$ to cyclododecaphosphazene $(C_{12}H_8O_2)_4(CF_3CH_2O)_{16}P_{12}N_{12}$ in addition to some linear polymer (in the absence or presence of 1% $(Cl_2PN)_3$ as polymerization initiator). The ratio of cyclic oligomers to polymer was 6:1 [140]. The 1,8-naphtalenedioxy derivative $1,3-(C_{10}H_6O_2)(CF_3CH_2O)_4P_3N_3$ above 200°C

undergoes ring expansion and polymerization (cyclic species to polymer ratio 1:1) with formation of 4-, 5-, and 6-membered ring derivatives. Similar results have been obtained with the other transannular derivatives of cyclotriphosphazenes, as well as the spirocyclic derivatives, shown below.
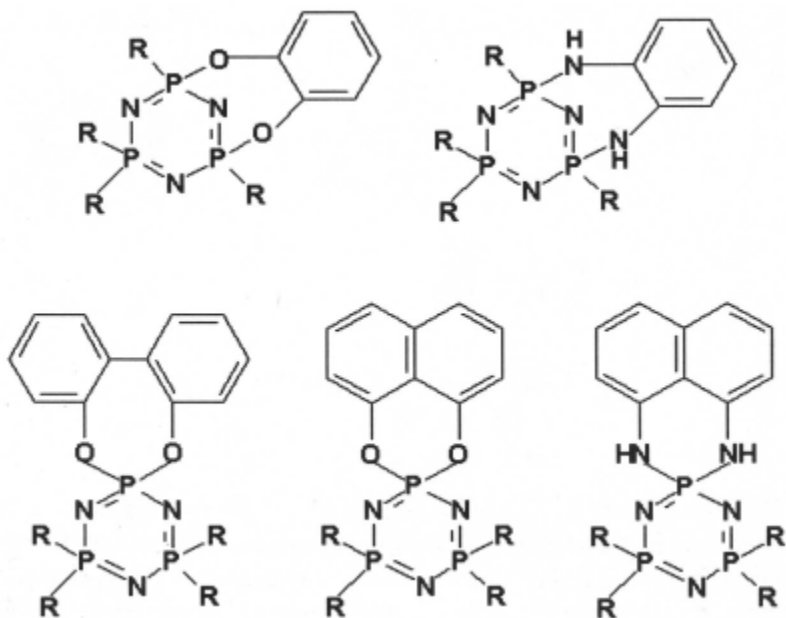
Ring opening polymerization was significant on thermolysis of these strained compounds, and gave low molecular weight polymers. The balance between ring-opening polymerization and ring-ring equilibration (ring expansion) can be correlated with the ability of the transannular organic groups to induce ring strain in the cyclotriphosphazene ring and destabilize the cyclic trimer with respect to the linear polymer [140].

To summarize, the varying effects of heating upon different cyclotriphosphazenes, reflecting their propensity for polymerization or ring-ring equilibration, are presented in Table 2 (with data compiled from [134d]).

Condensation reactions, e.g. **R$_2$P(OR)=N-SiMe$_3$** (with elimination of **Me$_3$SiOR** at 190°C) [141] or **Cl$_3$P=N-SiMe$_3$** (with elimination of **Me$_3$SiCl** at 25°C) [142]) lead directly to polyphosphazenes, which might be large ring polymers.
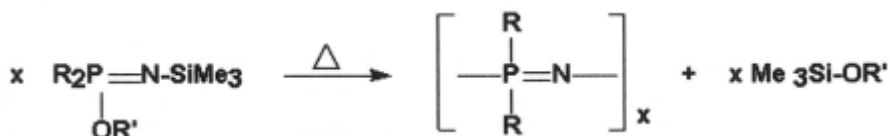
In some cases this procedure may have some advantages, allowing the synthesis of organosubstituted polyphosphazenes which cannot be obtained by substitution.

Table 2 Effect of heating upon cyclotriphosphazenes

Effect	Compounds

Polymerize on heating:

$(F_2PN)_3$; $(Cl_2PN)_3$; $(Br_2PN)_3$; $[(SCN)_2PN]_3$; $(Cl_3P=N)Cl_5P_3N_3$; *gem*-$(Cl_3P=N)_2Cl_4P_3N_3$;$RCl_5P_3N_3$ (R = Me, Et, Pr_n, Bu_n, CH_2Bu^t,CH_2SiMe_3); 1,1-$Me(Me_3SiCH_2)Cl_4P_3N_3$; $FcF_5P_3N_3$ (Fc = ferrocenyl); *gem*-$(Me_3SiCH_2)_2Cl_4P_3N_3$; $1,3$-$FcF_4P_3N_3$;1.3-$Fc(CF_3CH_2O)4P_3N_3$

Polymerize and copolymerize with $(Cl_2PN)_3$:

$PhCl_5P_3N_3$; $PhBr_5P_3N_3$

Polymerize and undergo ring expansion:

PhF_5PN_3; *nongem*-$Me_3Cl_3P_3N_3$; $RF_5P_3N_3$ (R = Me, Et, Bu^t, Ph); *nongem*-$R_2Cl_4P_3N_3$ (R = Me, Et)

Do not polymerize but copolymerize with $(Cl_2PN)_3$ and undergo ring expansion:

$RF_5P_3N_3$ (R = Ph, Bu^t); *gem*- and *nongem*-$Ph_2F_4P_3N_3$; *gem*-$Ph_2Cl_4P_3N_3$; *nongem*-$R_3Cl_3P_3N_3$ (R = Et, Ph)

Do not polymerize, undergo ring expansion:

$(Me_2PN)_3$; $(Ph_2PN)_3$; $[(PhO)_2PN]_3$; *gem*-$Ph_4Cl_2P_3N_3$; $PhCl_5P_3N_3$

Inert, do not polymerize, do not undergo ring expansion:

$(Me_3SiCH_2)_6P_3N_3$

14.2.4.5. Thiaphosphazenes

The first cyclic oligomers and polymers made from phosphorus-nitrogen-sulphur synthons were prepared from ammonia and sulfur by thermal ring opening polymerisation of $Cl_5P_2SN_3$ (at 90°C), followed by substitution of chlorine with phenoxy groups, to increase hydrolytical stability [143].
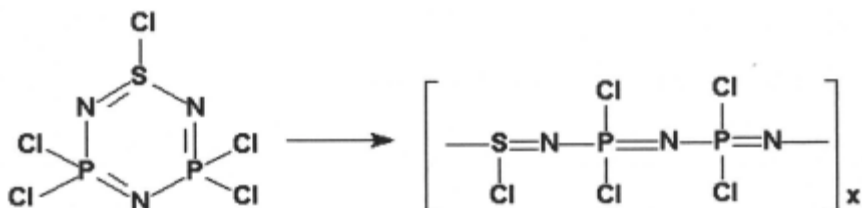
The six-membered ring compound $Cl_5(O)P_2SN_3$ can also undergo ring opening polymerisation, and the resulting hydrolytically sensitive polymers (molecular weights in the range 10^3-10^5) can be made hydrolytically stable by replacing the chlorine substituents with amino, phenoxy or fluoroalkoxy groups.
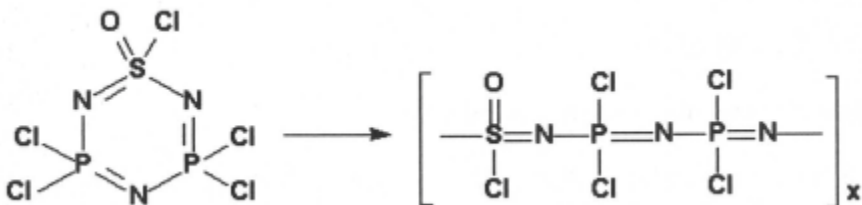
In this polymerization small amounts of macrocyclic oligomers have been found [144]. They have been successfully isolated and structurally characterised by single crystal X-ray analysis [145], which is a real achievement for this type of compound.
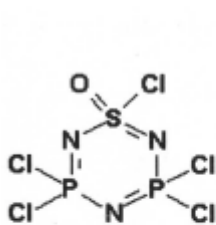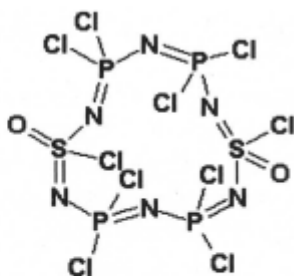
CL4P2(O)SN3   cis-[CL4P2(O)SN3]2   trans[CL4P2(O)SN3]2
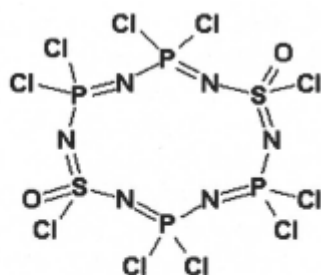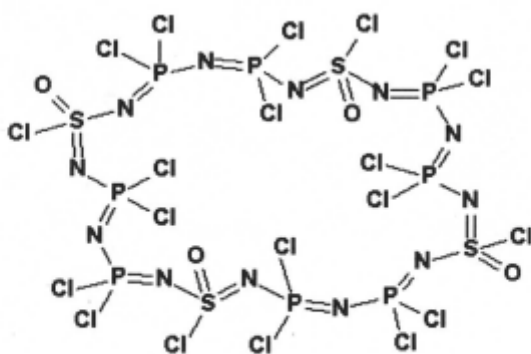
[CL4P2(O)SN3]4

The formation of the macrocyclic oligomers throws some light upon the mechansim of the ring opening polymerization.

A comprehensive review on phosphorus-nitrogen-sulphur polymers is recommended for further details [146].

14.2.4.6. Phosphates and phosph(III)oxanes

The most important cyclic oligomers based upon phosphorus-oxygen backbones are the so-called metaphosphates or cyclophosphates. They contain $[PO_3]_n^{n-}$ ring anions of various sizes, from $n = 3$ to $n = 12$ (isolated and structurally characterised) [147]. The trimers and tetramers are readily obtained

and have been thoroughly investigated, but it took considerable skill to isolate the higher members of the series.

The conformation of higher cyclic oligomers is irregular and the structure diagrams shown below try to illustrate this. Cyclotri- and tetraphosphates have been known since the previous century (see [148] for earlier literature). The cyclohexaphosphates have been isolated next, as sodium, potassium and ammonium salts [149] (and now many others are known) and has been followed by isolation and characterisation of cyclooctaphosphates [150], cyclodecaphosphates [151] and cyclododecaphosphates [152]. Cyclopenta- and cycloheptaphosphates are much more difficult to obtain [153].

$(PO_3)_5^{5-}$
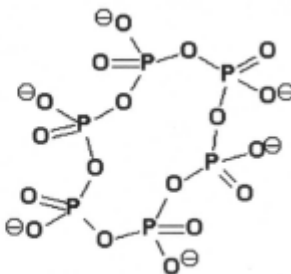
$(PO_3)_6^{6-}$
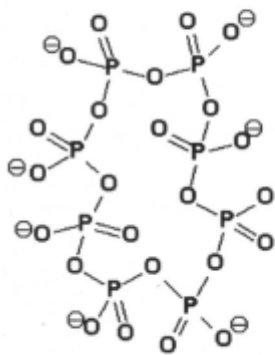
$(PO_3)_8^{8-}$

$(PO_3)_{10}^{10-}$

Oligomeric cyclic phosphates can be readily interconverted and undergo thermal ring opening polymerisation. In fact, this is the reason for the difficulties in isolating the macrocyclic oligomers. The ring-chain equilibria of oligomeric phosphates have been investigated [154].

Phosphorus(III) cyclic oligomers **(RPO)$_n$ (R = NPr$^i_2$, n = 4 and 5)** can be stabilised as metal complexes, but so far have not been isolated in free state [155].

14.2.4.7. Arsazanes, arsoxanes, arsathianes; antimony analogues

Although cycloarsazene trimers and tetramers, **(R$_2$AsN)$_n$ (R = Ph, n = 3 and 4)** are well known [156], larger cyclic oligomers or polymers (polyphosphazene analogues) have not been identified so far. The only oligomeric cycloarsazane reported is an ill-characterised hexamer **(MeAsNH)$_6$,** obtained by ammonolysis of **MeAsCl$_2$ [157].**
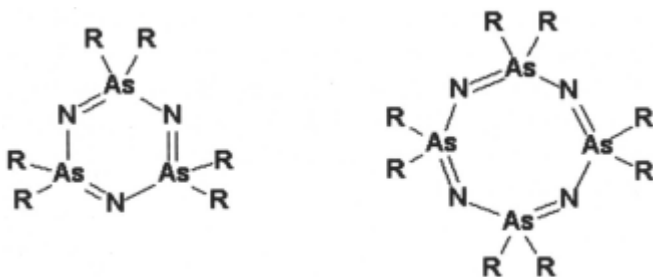
Organoarsenic oxides, **(RAsO)$_n$,** are readily interconvertible cyclic oligomers. According to ^{1}H NMR data, the methyl and ethyl arsoxanes **(R =Me, Et)** are mixtures of cyclic oligomers **(n = 2-5)** with the trimer and tetramer predominating [158]. Crystalline **(MeAsO)$_4$** and **(MesAsO)$_4$** hvae been structurally characterised by X-ray difraction [159]. The arsoxane rings are very labile and readily interconvertible. Ring expansion readily occurs and various ring sizes can be stabilised by complexation. Thus, crown ether-type complexation of sodium stabilises the tetramer whereas potassium and caesium stabilise the pentamer as **[Na(EtAsO)$_4$]$^+$** and **[M(EtAsO)$_5$]$^+$ (M = K, Cs),** respectively [160]. Copper complexes of **(MeAsO)$_4$** are also known [161]. Alkylcycloarsoxane hexamers **(RAsO)$_6$ (R= Me, Et)** have been stabilised as chromium, molybdenum [162], rhenium, ruthenium and copper [163] complexes. The methyl octamer **(MeAsO)$_8$** can be stabilised as ruthenium or osmium complexes [164].
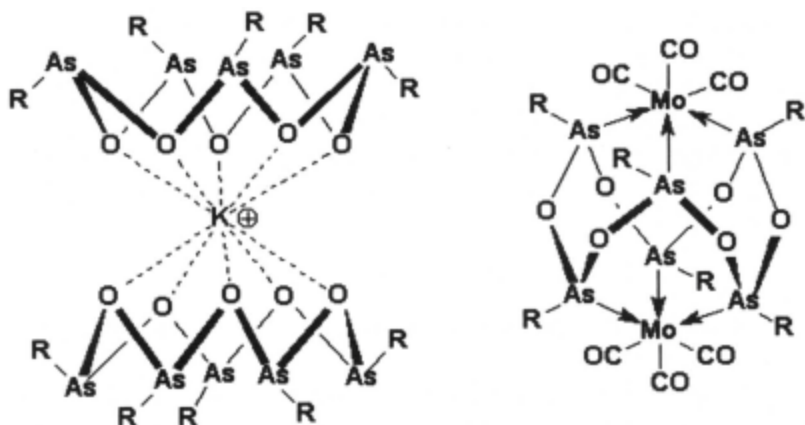
Obviously, the ring conformation is imposed by the coordination pattern of the metal.

A hexameric ethylarsathiane **(EtAsS)₆** is mentioned in the older literature [165]. Only metal complexes of cycloarsathianes have been structurally characterised, and these include a tetramer **(EtAsS)₄** (as ruthenium complex) [166] and the methyl cyclic oligomers **(MeAsS)ₙ** with **n = 4, 5** and 6 (as chromium and molybdenum complexes), the later starting from a trimer-tetramer equilibrium mixture **(MeAsS)ₙ, n = 3** and 4 [167]. The structure of the pentamer complex is shown here.
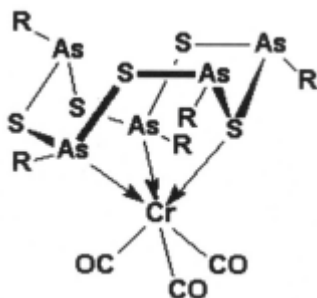
These examples not only indicate an interesting chemistry of arsenic(III) rings but also illustrate their versatility as macrocyclic ligands. It is important to underscore that the coordinated ligand is formed in a metal induced ring expansion of the smaller ring precursors. Surprisingly, no similar cycloarsazane chemistry has been reported so far.

Related antimony chemistry is less developed. A macrocyclic oligomer, a "ring of rings", containing six four-membered cyclic **Sb₂N₂** synthons, has

been formed in the reaction of 2-methoxyaniline with **Sb(NMe₂)₃** and the compound was structurally characterised [168].

R = [2-methoxyphenyl group, MeO]
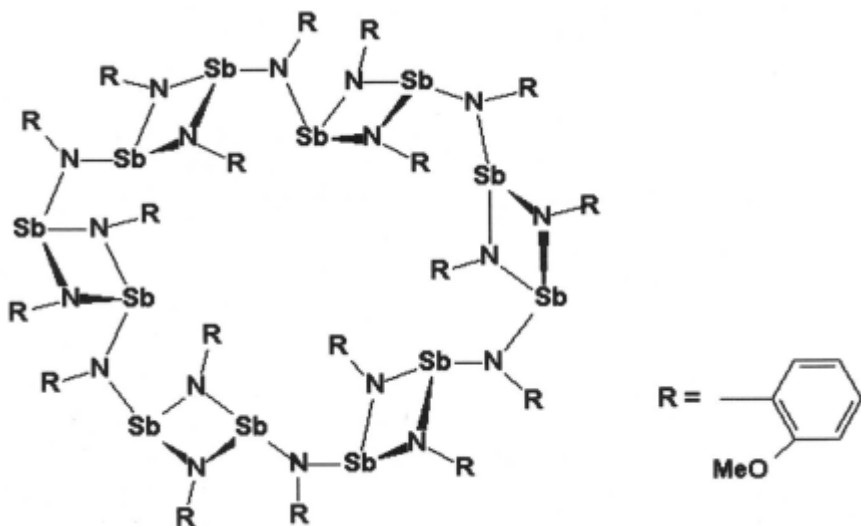
Curiously, such a large macrocycle, **Sb₁₂N₁₂,** containing 24 atoms, is planar. The small Sb₂N₂ subunits are oriented perpendicularly to the macrocycle, and the result is a toroidal structure. Trimeric and tetrameric organoantimony oxides **(RSbO)ₙ (n = 3 and 4)** and sulfides, **(RSbS)ₙ (n = 2, 3 and 4)** have been prepared and some were structurally characterised [169].

14.2.4.8. Thiazenes

The unsubstituted sulphur-nitrogen pair forms a series of cyclic oligomers, which include the dimer, **S₂N₂,** the tetramer, **S₄N₄,** as well as the macromolecular chain **(SN)ₓ ,** a metallic, superconducting polymer [170]. The pentamer is known only in cationic form **S₅N₅⁺** [171] and no unsubstituted trimeric **S₃N₃** ring compound is known. The formal average oxidation state of sulphur in these compounds is S(III).

In substituted form, sulphur(IV) gives rise to a series of trimeric and tetrameric **[XSN]ₙ (X = F, Cl, etc., n = 3 and 4)** cyclic oligomers, and similarly, sulphur(VI) forms trimeric and tetrameric **[X(O)SN]ₙ (n = 3 and 4).** There is an extensive chemistry of these rings, which will not be covered here, since it is well reviewed in some monographs [172]. Only data relevant to inorganic polymer formation will be mentioned.

A fluoro-oxothiazene polymer, **[F(O)SN]ₓ,** has been prepared by dehydrofluorination of **HN=SOF₂** or by reacting **SOF₄** with ammonia [173]. Organo-substituted similar polymers (molecular weights up to **4.10⁵)** were synthesised by polycondensation reactions [174].
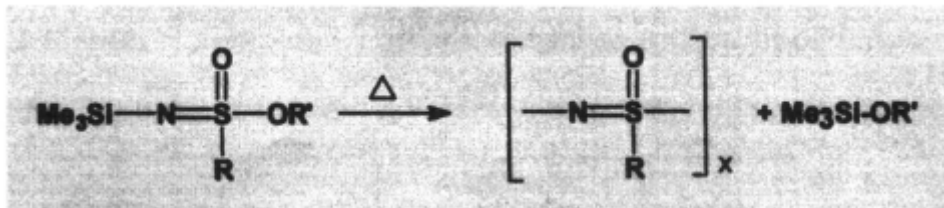
These polymers are soluble in some polar solvents (DMF, DMSO, nitromethane) and even in hot water. Theoretical calculations indicate a cis-trans helical conformation to be the most stable for this type of polymers.

14.2.4.9. Other Main Group covalent rings

In addition to the cyclic oligomers discused, other AB synthons form inorganic ring based upon the principle of repeating units. Only those bearing some relationship with inorganic polymers have been considered in the previous sections.

Among the rings ignored, there are germanium-, tin-, lead-, antimony-, bismuth, selenium- and tellurium-containing inorganic rings. They are generallly limited to a few regular size rings (four-, six- or eight-membered, i.e. made up of two, three and four repeating units, respectively). There is an interesting chemistry related to these rings, but they are outside of the scope of this chapter. The literature before 1980 is covered in a monograph [175]. Unfortunately, the new information about such rings is scattered in various journals and a review would be timely.

14.2.4.10. Covalent rings containing transition metals

There are numerous inorganic (carbon-free) rings containing transition metal atoms and they cannot be covered here comprehensively. We will present only a few selected examples, to illustrate the principles of their structure and formation.

Transition metals can be incorporated in covalent rings, as components of repeating building units. There are three possible ways: a) formation of rings from repeating units made up by regular alternation of a transition metal with an electronegative atom, e.g. nitrogen, oxygen, sulfur, just as in the previous cases discussed above for non-metals and main group metals; b) incorporation of the transition metal as heteroatom into a non-metal inorganic ring; and c) formation of covalent rings based upon metal-metal bonds, and containing only metal atoms in the ring.

Case a) mentioned is illustrated by some ring and polymeric species in which the metal atoms alternate with oxygen. Thus, cyclopentadienyltitanium oxide trimers and tetramers **(e.g. [Cp*TiX(μ-O)]$_n$ (n = 3 or 4, X = F, Cl, Br)** [176], the vanadium analogues **[Cp*VCl(μ-O)]$_4$** [177] or the organozirconium oxide **[Cp$_2$Zr(μ-O)]$_3$** [178] fit into this category. These cyclic and related polycyclic cage organometallic oxides have been reviewed [179].
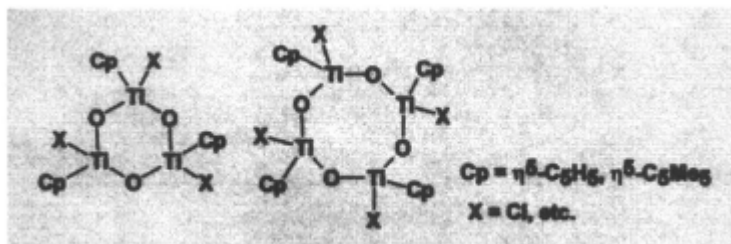
Similarly, three cyclopentadienyltantalum-nitrogen synthons combine to form a six-membered ring, which can be polymerized [180].
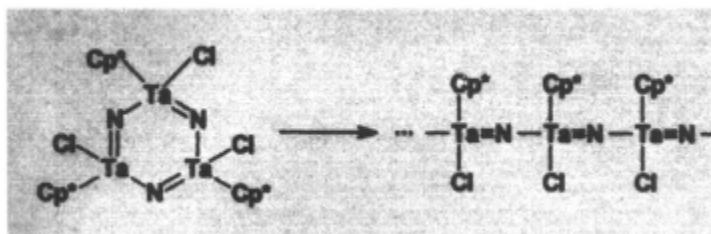
A second possibility, mentioned above, is the incorporation of the metal as heteroatom into covalent non-metal rings, to give e.g. metallacyclophosphazenes [181], metallacyclosiloxanes [182], metallacyclosilazoxanes [183], metallacyclothiazenes [184], metallaborazines [185], etc. Many such rings are known (for reviews see [186, 187]), but only a few can be induced to undergo ring-opening polymerisation, e.g. the

molybdenum- and tungsten-phosphazene heterocycles. The polymers obtained thermally, have molecular weights in the range 12,000-34,500 for **M = Mo** and 17,000–68,000 for **M = W [188].**

M = Mo, W

The third type of transition metal-containing rings is illustrated by a spectacular metal-metal bond, planar 12-membered ring, made of six **-Os(CO)₄-SnPh₂-** repeating units (obtained from **Ph₂SnCl₂** and the **[Os(CO)₄]²⁻** anion) [189].

Another hexamer, based upon iron-tellurium alternation and containing four-membered rings as building units of the macrocycle, has been identified by X-ray diffraction in the compound **[Fe(CO)₂(μ-TePh)₂]₆** [190].

R = Ph

The chemistry of inorganic metal-containing heterocycles is too extensive to be covered here, and the reader is referred to the reviews cited for further examples.

14.3. Supramolecular cyclic self-assembly

14.3.1. General aspects

Supramolecular cyclic self-assembly in a number of organometallic compounds will be illustrated with selected examples. By no means this presentation tends to be exhaustive. Only monocyclic species will be presented, although various cage-like polycyclic oligomers perhaps could also be regarded as cyclic oligomers. For a more comprehensive presentation see ref. [191].

14.3.2. Supramolecular cyclic self-assembly through dative bonds

Among the chemical bonds acting in inorganic chemistry, very important are the *dative bonds*. Unlike normal covalent bonds, which are formed by pairing of electrons with a one-electron contribution from each atom, dative bonds are two-electron bonds formed by "donation" of an electron pair from one atom to another. There is a general tendency to assume that the two-electron bonds between a certain pair of atoms (*e.g.* boron and nitrogen in H_2B-NH_2 and H_3B<-NH_3) are identical, regardless of the origin of electrons (i.e.

covalent and dative), but it has been pointed out that a distinction between the two types should be made [192, 193].

The normal covalent and dative bonds differ at least in three major aspects:

a) the nature of the fragments formed when the bonds are broken;

b) the nature of the bond rupture process;

c) the magnitude of the bond cleavage enthalpy.

Thus: a) free radicals are formed by breaking covalent bonds and neutral molecules result by breaking dative bonds; b) the covalent bond rupture is a homolytic process, whereas the cleavage of a dative bond is a heterolytic process; c) cleavage of a covalent bond requires a significantly larger enthalpy then the cleavage of a comparable dative bond. This can be illustrated with the case of two isoelectronic molecules: ethane, H_3C-CH_3, and amine-borane, $H_3B<-NH_3$. The normal covalent C-C bond ruptures homolytically and the neutral species formed are $^.CH_3$ (paramagnetic) free radicals, with an energy of $89.8 \text{ kcal.mol}^{-1}$ spent in the process. The dative $N->B$ bond rupture proceeds heterolytically, with formation of neutral diamagnetic molecules, BH_3 and NH_3, and only $31.1 \text{ kcal.mol}^{-1}$ are spent in the process. Note that the cleavage of the dative bond requires only about one third of the energy needed for the cleavage of a normal covalent bond.

When an electron donor and an electron acceptor site are present in the same molecule, intermolecular association may occur with formation of cyclic species. This process is called *self-assembly*. Self-assembly is defined as *a spontaneous association of molecules under equilibrium conditions into stable aggregates held together by non-covalent forces* [194]. For a more detailed discussion' see ref. [195]. The resulting species is a *supermolecule* (see above). Thus, aminoboranes, $R_2B-NR'_2$, (containing boron -i.e. electron pair acceptor sites and nitrogen - electron pair donor sites) can exist in monomeric molecular form, in oligomeric form as dimeric, trimeric cyclic supermolecules or as polymeric arrays (depending upon the nature of R and R') [196]. Dative bond self-assembly is not limited to amino derivatives. Halogen or chalcogen bridging can induce similar effects and numerous organometallic fluorides [197] and chalcogenolates [198] can also form cyclic supermolecules.

14.3.2.1. Group 12 organometallic oligomers

In mono-organozinc compounds, RZnX, the metal is coordinatively unsaturated, and if X is a functional group possessing lone electron pairs, self assembly through dative bonds may occur. There are numerous examples of halides, alkoxides, thiolates, amides and other derivatives, which are associated

in solution and in solid state. A few examples will be cited, preferrably illustrated for structures confirmed by X-ray diffraction.

Organozinc halides, such as EtZnX **(X = Cl, Br)** are tetrameric in organic solvents [199], and the iodide EtZnI is polymeric in solid state [200]. Recently a dodecanucear oligomer **[ClZn-CHMe-PEt$_2$-N(SiMe$_3$)$_2$]$_{12}$** formed through **Cl->Zn** donation, has been structurally characterised by single crystal X-ray diffraction [201]. This suggests that many more organozinc cyclic oligomeric structures can be expected.

Organozinc-oxygen compounds, e.g. hydroxides and alkoxides self-assemble as cyclic dimers and trimers. Several organozinc alkoxides, RZnOR', form trimeric oligomers in benzene solutions [202, 203]. Crystal structure determinations reveal the existence of dimeric, trimeric and tetrameric organozinc alkoxides. Thus, **[EtZn-OC$_6$H$_2$Bu$^t_2$-2,6]$_2$** [204] and **[Me$_3$SiCH$_2$Zn-OC$_6$H$_3$Pr$^i_2$]$_2$** [205] are self-assembled cyclic dimers, containing a **Zn$_2$O$_2$** planar four-membered ring.
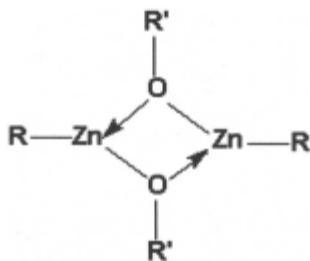
A six-membered zinc-oxygen ring has been identified in pyrazolylborato-zinc hydroxide, **[{η^2−H$_2$B(3-Bu^{t}Pz)$_2$}Zn(μ-OH)}]$_3$** , which is a cyclic trimer [206].
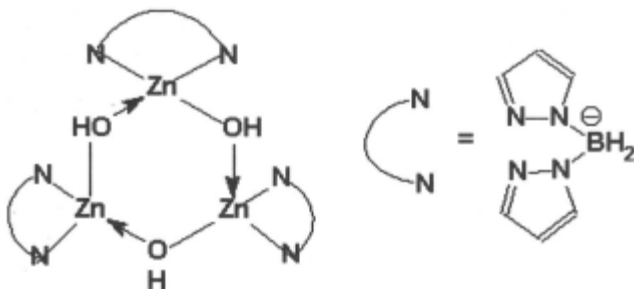
A monocyclic eight-membered **Zn$_4$O$_4$** ring system is present in the aminovinyl alcohol derivative of composition **[EtZnOC(OMe)=CH-NBu^{t}Me]$_4$** [207].
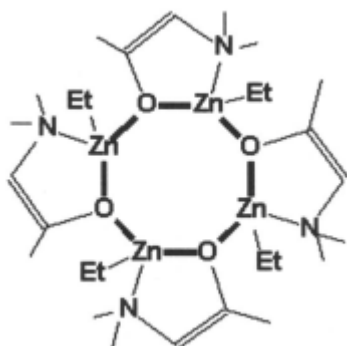
but in hydrocarbon solutions the tetramer is in equilibrium with the corresponding dimer, indicating facile dissociation.
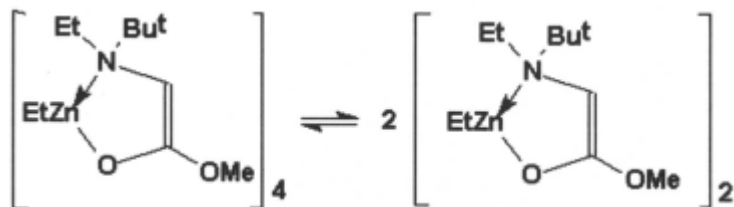
Other self-assembled tetrameric organozinc alkoxides form cubane structures, based upon a Zn_4O_4 cage [208].

In a similar manner, organozinc-sulfur compounds such as thiolates, dithiocarbamates and others, self-assemble into cyclic oligomers. Thus, $Me_3SiCH_2Zn-SCPh_3$ is a dimer containing a planar rhomboidal ring; the cyclic trimers $[Me_3SiCH_2Zn-SC_6H_2Pr^i_3-2,4,6]_3$ and $[Me_3SiCH_2Zn-SC_6H_2Bu^t_3-2,4,6]_3$, both contain planar Zn_3S_3 six-membered rings [209]. A trimeric organozinc-selenium compound, $[Me_3SiCH_2Zn-SeC_6H_2Bu^t_3-2,4,6]_3$ contains a twisted six-membered ring [210].
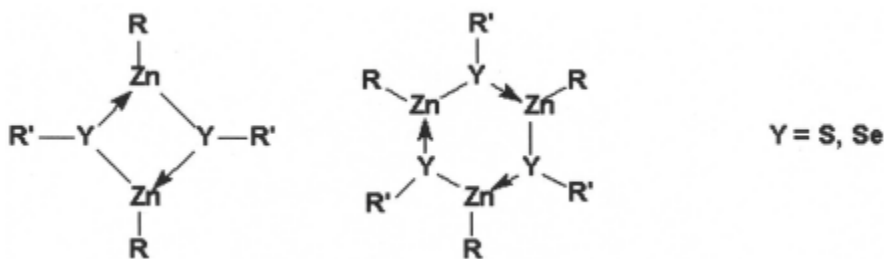
Organozinc thiolates with less bulky organic groups self-assemble into cage like oligomers, such as pentameric **[MeZn-SBu^i]$_5$** and octameric **[MeZn-SPr^i]$_8$** [211]. Interconversion of the cage oligomers in benzene solution has been observed.

Self-assembly through zinc-nitrogen bonds occurs in numerous compounds. They can be illustrated by cyclic dimers **[RZn-NR'$_2$]$_2$ (R =Me** or Et, **R' = Ph)** [212]. A trimer **[RZn-NHR']$_3$.3THF (R = Et, R' = 1-naphtyl)** contains a chair-shaped six-membered **Zn$_3$N$_3$** ring [213].
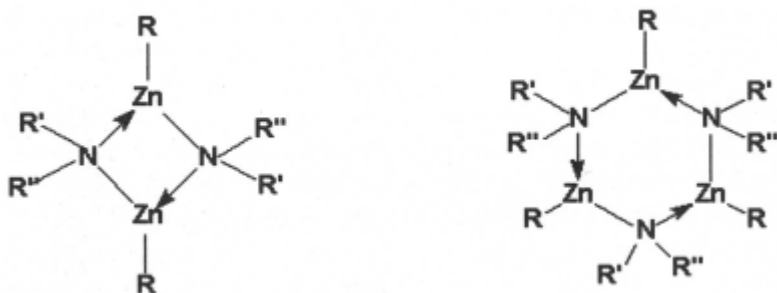
Monorganocadmium compounds, RCdX, like their zinc counterparts, undergo self-assembly with formation of oligomeric and polymeric species. The halides tend to be insoluble in organic solvents, indicating a high degree of association, but some dimeric and tetrameric structures have been established for compouds with bulkier organic groups, e.g. the cyclic dimer **[(Me$_3$Si)$_3$C-CdBr]$_2$** and the cubane tetramer **[(Me$_3$Si)$_3$C-CdCl]$_4$** [184].

From the numerous other organocadmium oligomers we cite here only a trimeric derivative **[MeCd-PBu$^t_2$]$_3$** with trigonally planar coordinated cadmium, as this compound is a useful precursor for cadmium phosphide **(Cd$_3$P$_2$)** nanoparticles [185].
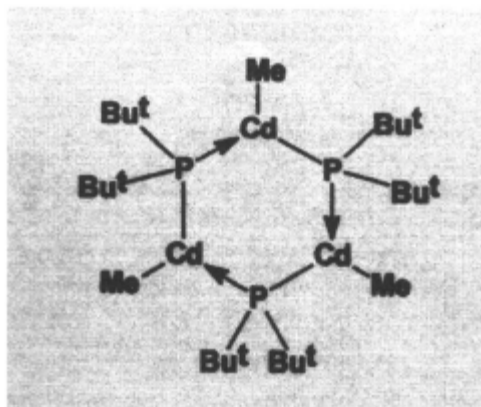
14.3.2.2. Group 13 Organometallic Oligomers

Group 13 organometallics R_2MX and RMX_2 are coordinatively unsaturated and the vacant valence orbital of the metal is able to accept electron pairs from almost any donor atom. If X is a functional group containing lone electron pairs they tend to undergo supramolecular self-assembly, with formation of cyclic oligomers more often than polymeric arrays. Diorgano derivatives, R_2M-X, will generaly form cyclic dimers, trimer and tetramers, if X = halogen (halides), OH (hydroxides), OR' (alkoxides), SR' (thiolates), NHR' and NR'R'' (amides), PHR' and PR_2' (phosphides), AsR_2' (arsenides), etc. and numerous examples are known. Monoorgano derivatives, RMX_2 and RMY (Y = O, S, Se, NR, PR, etc.) tend to self-assemble into polycyclic cage structures [217]. These compounds are of considerable interest as precursors for electronic materials [218].

Numerous self-organised supramolecular organoaluminum halides are known as cyclic dimers, trimers or tetramers.

M = Al, Ga, In, Tl   X = halogen
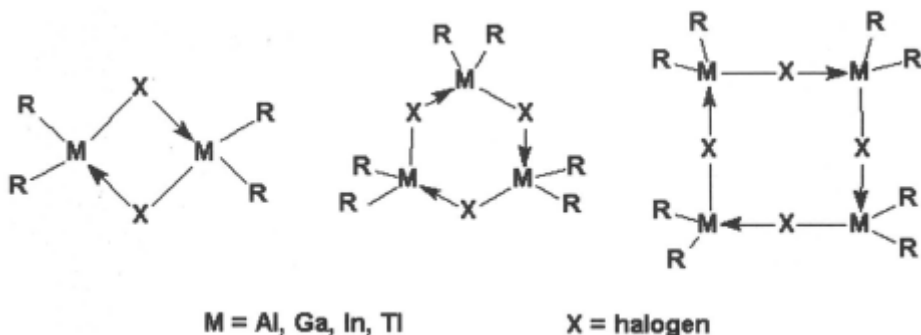
Thus, dimethylaluminum halides, **Me$_2$AlX** are dimers **(X = Cl, Br, I))** while the fluorides, **R$_2$AlF,** are trimers or tetramers, **(R = Me, Et, Pr^n, Bu^i, Bu^t; X = F)** in solution, all associated through halogen bridging [219]. Single crystal X-ray diffraction analysis of **[Me$_2$AlCl]$_2$** [220], **[Bu$^t_2$Al(μ-Cl]$_2$** [221] and other organoaluminum halides have been reported.

Surprisingly, even organoaluminum halides containing bulky organic groups tend to self-assemble into cyclic oligomers. Thus, the structurally characterised bromide, **(Trip)$_2$AlBr** (where **Trip = 2,4,6-Pr$^i_3$C$_6$H$_2$**) [222], and the chlorides **[(C$_5$Me$_5$)(R)AlCl]$_2$** **(R = Me, Bu^i),** **[η^5-C$_5$Me$_5$AlCl(μ-Cl)]$_2$** and **[(η^5-C$_5$Me$_4$Et)AlCl(μ-Cl)]$_2$** [224] are all dimeric.

Organoaluminum-oxygen derivatives (alumoxanes) are important compounds in Ziegler-Natta polymerization of olefins and molecular precursors for ceramic materials [225]. A large body of experimental data indicate association (self-assembly) in solution and solid state [226] and in recent years considerable advances have been made in the elucidation of their structures.

Organoaluminum alkoxides self-assemble through Al-O dative bonds to form dimeric and trimeric cyclic supermolecules.

Thus, dimers **[R$_2$AlOR']$_2$** with **R = Me, R' = Bu^t, SiMe$_3$, SiPh$_3$,** and R = **Et, R' = Et, Bu^t, Ph, CH$_2$C$_6$H$_2$Bu$^t_3$,** have been identified and trimers **[R$_2$AlOMe]$_3$** **(R = Me, Et)** have also been detected by molecular weight determinations in solution [227].

The cyclic structures of some alumoxane oligomers have been confirmed by X-ray single crystal structure analysis of **[Bu$^t_2$Al(μ-OH)]$_3$** [228], **[Me$_2$AlOSiMe$_3$]$_2$** [229], **[Me$_2$AlOC$_6$F$_5$]$_2$** [230] and **[Bu$^t_2$Al(μ-OPr^n)]$_2$** [231] which can be cited as examples.

Organoaluminum thiolates self-assemble into dimeric, trimeric and tetrameric supramolecular oligomers, or may form polymeric supramolecular arrays. Thus, **Me$_2$Al-SMe** is a chain polymer in the solid state, while in the gas-phase it is a dimer [232]. Other dimeric species are **[R$_2$AlSR'] (R = Me, R' =**

C$_6$F$_5$, SiPh$_3$, R = Mes, R = Bz, Ph and others [233]. Trimeric cyclic oligomers, with chair or twisted boat conformation, include structurally characterised [R2AlSR'] with **R = Me, R' = 2-Pr^{i}C$_6$H$_4$, 2-Bu^{t}C$_6$H$_4$, 2-Me$_3$Si-C$_6$H$_4$** and R **=Bu^i, R' = C$_6$H$_2$Pr$^i_3$-2,4,6.** Only a tetramer **(R = Me, R' = C$_6$H$_3$Me$_2$-2,6)** has been reported [234],

The supramolecular association is preserved in solution, and the dimer-trimer equilibria were investigated by NMR spectroscopy.

$$2 \ [Me_2Al\text{-}SMe]_3 \ \longleftrightarrow \ 3 \ [Me_2Al\text{-}SMe]_2$$

In solutions of **[Me$_2$Al-SMe]$_n$** the trimer predominates, and *syn-anti* isomers have been detected.

Although monomeric representatives are known, most aminoalanes self-assemble into cyclic oligomers, and dimeric or trimeric supermolecules **[R$_2$AlNR'R"]$_n$ (n = 2 or 3)** are formed, depending mostly on the steric properties of the organic groups. Numerous examples can be found in the monographic literature and the subject continues to focus interest [235].
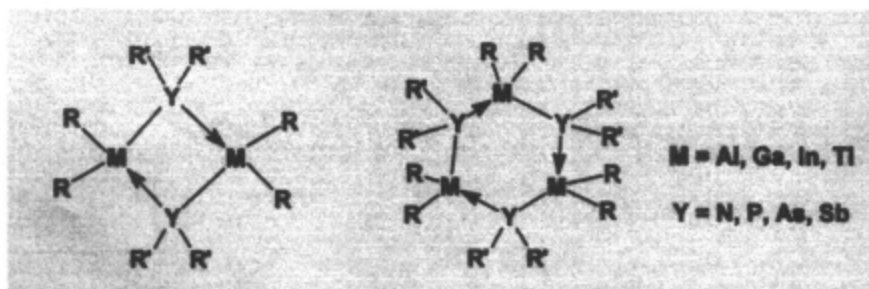
The aluminum-nitrogen rings display variable conformations. Thus, the four-membered **Al$_2$N$_2$** ring can be planar or folded, depending on the nature of organic groups. The six-membered **Al$_3$N$_3$** ring may occur in a skew boat (in **[Me$_2$Al-NH$_2$]$_3$),** planar (in **[Bu$^t_2$Al-NH$_2$]$_3$)** [236] or chair conformation (in *cis*-**[Me$_2$Al-NHMe]$_3$)** [237]. Bulky substituents prevent supramolecular self-assembly and some monomer aminoalanes are known, e.g. **Mes$_2$Al-N(SiMe$_3$)$_2$, Bu$^t_2$Al-N(Mes)$_2$** and **Bu$^t_2$Al-N(SiPh$_3$)$_2$** [238].

Organolaluminum azides are trimeric oligomers **[R$_2$Al-N$_3$]$_3$** and are excellent precursors for AlN semiconducting materials [239].

Phosphinoalanes, **R$_2$Al-PR'R",** also undergo supramolecular self-assembly to form cyclic oligomers. Dimers **[R$_2$Al-PR'R"]$_2$ (R = Me, R' = Ph** or **SiMe$_3$)** and trimers **[R$_2$Al-PR'$_2$]$_3$ (R = Me, R' = Me, Et)** have been observed by molecular weight determinations in solution [240] and some were structurally

characterised by X-ray diffraction, *e.g.* **[(Me₃Si)₂Al-PPh₂]₂** and **[(Me₃Si)₂Al-P(SiMe₃)]₂** [241].

    Similar aluminum-arsenic cyclic dimers and trimers **(M = Al, Y = As)**, and also linear polymers, have been reported. Thus, **[Me₂Al-AsMe₂]ₙ** is polymeric in the solid state and trimeric in solution [240c].

    Organogallium compounds behave very much like organoaluminum compounds and their functional derivatives, **R₂GaX,** are associated self-assembled supermolecules. The functional group X can be halogen, OH, OR', SR', NHR', etc.

    Organogallium halides are known as dimers **(M = Ga, R = Me₃SiCH₂, X = Br** [242]; **R = C₅Me₅, X =Cl** [243] and **R = Mes, X = Cl** [244]. The dichloro derivative is a chain polymer **[MesGaCl(μ-Cl)]ₓ.**

    Dimethylgallium hydroxide has been cited as a trimer **[Me₂GaOH]₃** in solution, but single crystal X-ray analysis revealed a tetramer in the solid state [245]. Finally, a trimer **[Buⁱ₂Ga-OH]₃** containing a planar **Ga₃O₃** ring, has been structurally characterised [246].

    The rings **(Me₂GaOH)₃** and **(Me₂GaOH)₄** sandwiched between two oxa-aza crown ethers, in an unprecedented supramolecular structure, were formed from trimethylgallium in reactions with the crown ethers [247].

    Gallium-oxygen cages are present in tetranuclear, adamantane-like oligomer **[R₄Ga₄(μ-O)₂(μ-OH)₄]** where **R = C(SiMe₃)₃** [248] and in the hexanuclear oligomer **[Mes₆Ga₆(μ³-O)₄(μ³-OH)₄.4THF].6THF** [249].

    Monomeric species **Buⁱ₂Ga-OCPh₃** [250] and **Buⁱ₂Ga-OC₆H₂Buⁱ₃-2,4,6** [251] are known and illustrate the role of bulky substituents in preventing supramolecular self-assembly. Otherwise, most diorganogallium alkoxides are self-assembled dimers **[R₂GaOR']₂** with **M = Ga, R = Me, R' = Me, Prⁿ, Bu, CH₂Buⁱ,** Ph, etc.[252] and **R = σ-C₅Me₅, R' = Et** [253].

    Organogallium phosphinates **[R₂GaO₂PR'₂]₂ (R = Me, Et, Buⁱ, R' = Ph)** are also self-assembled cyclic dimers [254].

M = Al, Ga
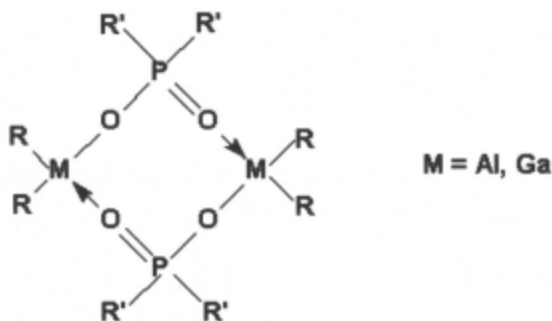
Molecular weight determinations show that dimeric self-assembly occurs in diorganogallium thiolates **[R₂Ga-SR']₂.** Several structurally characterised solid state dimers are known **(R = Me, R' = C₆F₅ , R = Ph, R' = Et** and others) [255]. A tetramer **[Me₂Ga-SC₆H₃Me₂-2,6]₄** has also been reported [256].

Like their sulphur analogues, diorganogallium selenols undergo self-assembly in solution with formation of dimeric supermolecules, e.g. **[R₂Ga-SeR']₂,** e.g. **R = Buᵗ = Buᵗ, R = Ph, R' = Me** and **R = Me₃SiCH₂ R = SiMe₃** [257]. A cyclic trimer **[Prⁱ(Br)Ga-SeEt]₃** is also known [258].

Dimeric self-assembly in solutions of diorganogallium amides is suggested by molecular weight determinations [259]. Trimeric supermolecules with **R = Me, R' = NH₂** or NHMe have been reported [260]. Some derivatives, e.g. **[Me₂Ga-NHBuᵗ]₂, [Me₂Ga-NHPh]₂, [Me₂Ga-N(CH₂Ph)₂]₂** and others have been structurally characterised by X-ray diffraction [261]. The di-*tert*-butylgallium amide is a self-assembled cyclic trimer **[Buᵗ₂Ga-NH₂]₃** and the trimer **[Me₂GaNH₂]₃** containing a planar six-membered **Ga₃N₃** ring is also known. Cubane-like gallium-nitrogen tetramers, e.g. **[MeGa-NC₆F₅]₄,** and a hexaprismane oligomer **[MeGa-NC₆F₅]₆.7THF** have also been structurally characterised [262].

Dimeric and trimeric organogallium phosphides and arsenides have been extensively investigated as precursors for gallium phosphide and gallium arsenide semiconductors [263]. Numerous compounds have been structurally characterised [264]. The association degree depends upon the steric bulkiness of the organic groups.

Numerous monoorganoindium derivatives which contain donor functional groups are self-assembled into cyclic oligomers or high polymers. Thus, dimesitylindium fluoride is a cyclic trimer **[Mes₂InF]₃** [265] whereas the corresponding chloride and iodide are dimers **[Mes₂InX]₂ (X = Cl, I)** [266]. A saw-tooth polymeric chain was found in di-*tert*-butylindium chloride, **[Buᵗ₂InCl]ₓ** [267].

Like their aluminum and gallium analogues, diorganoindium alkoxides and other derivatives containing an indium-oxygen bond tend to self-assemble, mainly into dimeric supermolecules, both in solution and solid state [268]. The same is valid for diorganoindium thiolates, dimers and trimers being known [269].

Numerous dimeric diorganoindium amides, **[R₂In-NR']₂ (R = Me, R' = Me, Et, Prⁱ, etc.)** [270] have been have been structurally characterised by X-ray diffraction.

The diorganoindium phosphides **[Me₂In-PR₂]** are associated in solution as dimers and trimers [271] and numerous crystal structure determinations confirmed their four- or six-membered cyclic structures [272]. These

compounds are precursors for CVD indium phosphide III-V semiconductors [273]. Related indium-arsenic are also well known [274].

14.3.2.3. Group 14 organometallic oligomers

Triphenyltin hydroxide [275] and benzyldimethyltin hydroxide, which are associated through hydroxo bridges display a zig-zag chain structure in the solid state. Cryoscopic measurements show that the latter compound is dimeric in benzene solution [276]. Larger ring oligomers have not been reported.

$$R = R' = Ph$$
$$R = Me, R' = PhCH_2$$
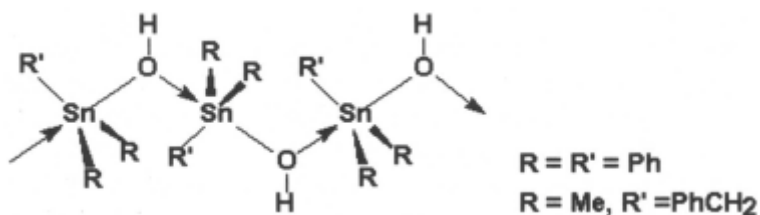
Other triorganotin hydroxides, containing bulky substituents, such as trineophyltin hydroxide [277] and trimesityltin hydroxide [278] are monomeric, non-associated, molecular species.

Sometimes unexpected associations leading to oligomeric complex structures may occur, like in the case of the hydrolysis products of bis(dichloroalkylstanyl)ethanes **[R = CH(Me₃Si)₂]** [279].
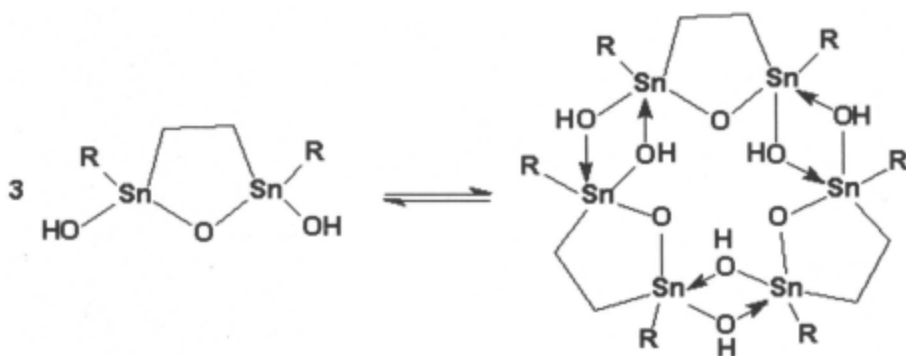
Alkoxo-triorganotin derivatives form zig-zag chains. Thus, trimethyltin methoxide, **Me₃SnOMe,** is a polymer with alternating **Me₃Sn** moieties [280] but cyclic oligomers have not been so far reported.

R = Me
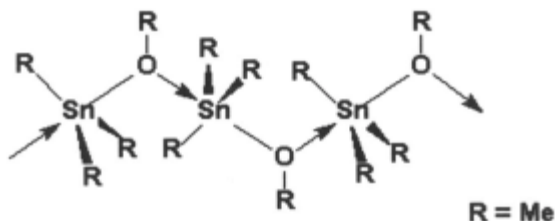
Supramolecular structures based upon oxygen-tin donation include organotin carboxylates. Some are cyclic oligomers, and are only briefly mentioned here, since the ring contains carbon atoms of the carboxylato groups.

Depending on the bulkines of the organic groups, triorganotin carboxylates, **$R_3Sn-OOCR'$,** are either monomers or linear polymers [281]. One example of a cyclic tetrameric structure, namely **$[Bu_3SnOOC-C_6H_3F_2-2,6]_4$,** and a cyclic hexamer, are known [282]. Diorganotin carboxylates **$R_2Sn(OOCR')_2$** are usually monomers, but the products of their partial hydrolysis, the oxocarboxylates are tetrameric supramolecular compounds **$[R_2Sn(O)(OOCR')]_4$** [283].

Several diorganotin derivatives of carboxylic acids are cyclic oligomers. Thus, di-*n*-butyltin thiosalicylate molecules are self-organized into hexameric supermolecules [284].

R = Buⁿ
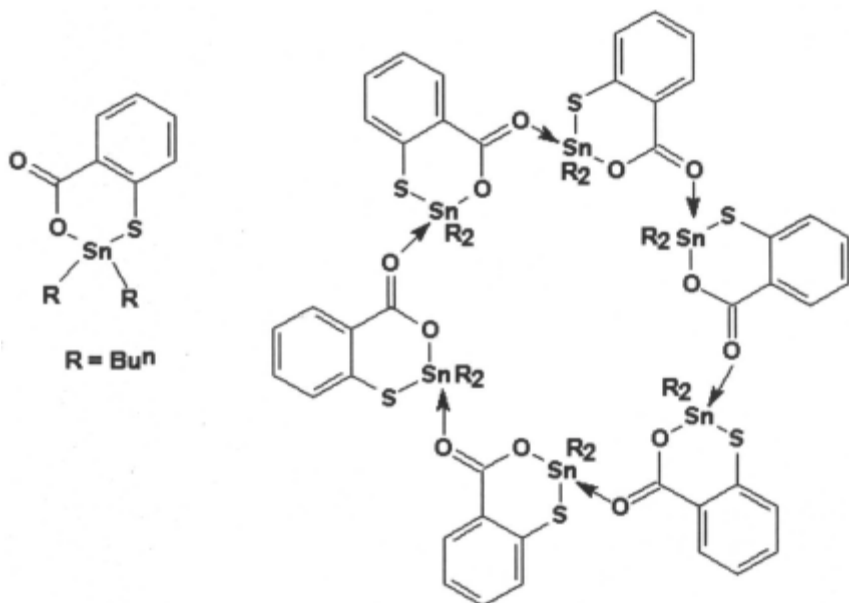
Di-*n*-butyltin 3-thiolopropionate also forms hexameric aggregates in the solid state through tin-oxygen donation [285]. The compound is monomeric in solution.

R = Bu^n
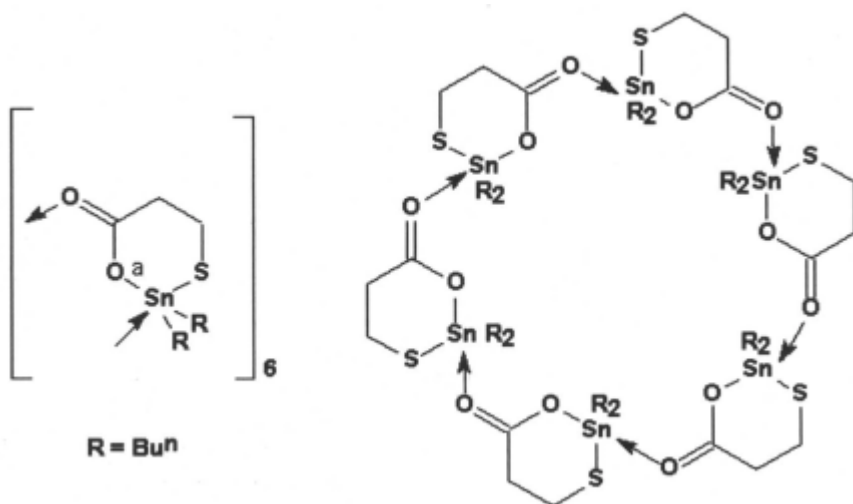
Supramolecular structures are formed in organotin derivatives of some organophosphorus acids. Thus, triphenyltin diphenylphosphate, **Ph$_3$SnO$_2$P(OPh)$_2$** [286], and triphenyltin (O-methyl)methyl-phosphonate, **Ph$_3$SnO$_2$P(OMe)Me** [287] are cyclic hexamers and trimetyltin diphenylphosphinate, **Me$_3$SnO$_2$PPh$_2$** [288] is a cyclic tetramer.

R = Ph, R' = R" = OPh

R = Ph, R' = Me, R" = OMe

R = Me, R' = Ph
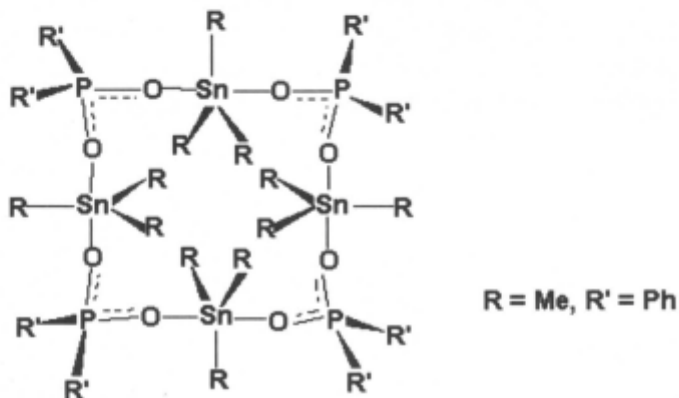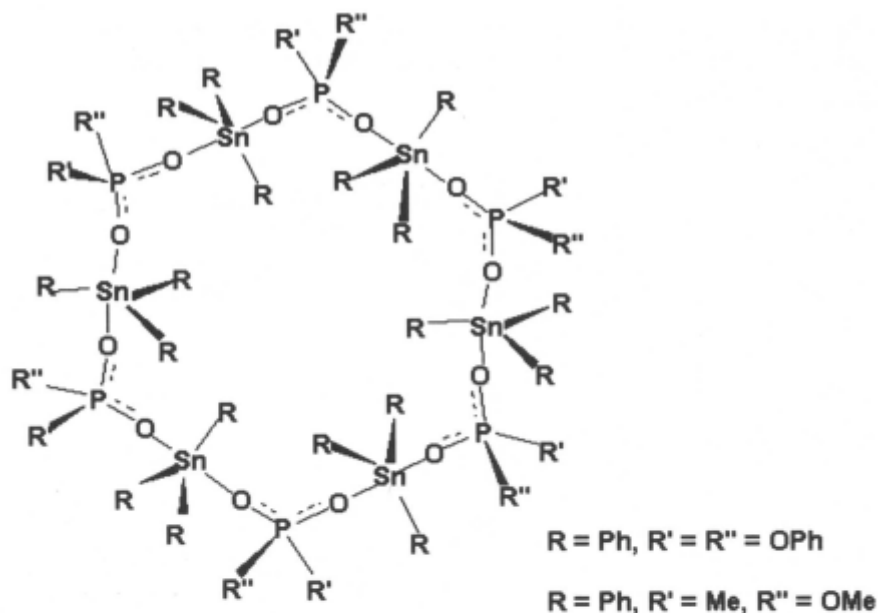
Other triorganotin phosphinates are self-assembled into chain-like, supramolecular helical arrays; these include trimethyltin dimethylphosphinate, **Me₃SnO₂PMe₂**, and dichlorophosphate, **Me₃SnO₂PCl₂**, and tri-n-butyltin diphenylphosphinate, **Bu₃SnO₂PPh₂** [289]. The self-assembly of tributyltin derivatives of phosphorus oxyacids (orthophosphates, phosphonates and phosphinates), **(Bu₃Sn)ₙOₙP(O)Ph₃₋ₙ, n = 0 - 2,** has been investigated with the aid of ¹¹⁹Sn, ³¹P NMR and ¹¹⁹ᵐSn Mossbauer spectroscopy, indicating intermolecular association both in solution and solid state [290]. Associated structures in the solid state and solution, based upon spectroscopic evidence,

have also been suggested for triorganotin O-alkyl phosphonates, **R₃SnOP(O)H(OR')** **(R = Me, Buⁿ, Ph; R' = Me and Et)** [291]. There are no clear criteria to explain the formation of cyclic oligomers in some cases and polymeric arrays in others.

14.3.3. Supramolecular cyclic self-assembly through secondary bonds

The of *"secondary bond"* concept has been introduced by N.W. Alcock [292] to describe *interactions characterised by interatomic distances longer than single covalent bonds but shorter than Van der Waals interatomic distances.* Although these interactions are weaker than covalent or dative bonds, they are strong enough to influence the coordination geometry of the atoms involved, and to hold together pairs of atoms, leading to intermolecular association or self-assembly, with formation of oligomeric or polymeric structures. Usually secondary bonds are not strong enough to survive in solution, especially in coordinating solvents, but they can have spectacular effects in the building a crystal, by creating the secondary structure which defines the supramolecular system in the solid state.

There is a formal similarity between secondary bonding and hydrogen bonding. Secondary bonding interaction occurs as a basically linear X-A...Y system, in which A-X is a normal covalent bond and A...Y is the secondary bond. Thus, like a hydrogen bond, this system is linear and asymmetric, although exceptions can also exist in both cases (see also ref. [293]):

$$\text{X—A} \cdots\cdots \text{X} \qquad\qquad \text{X—H} \cdots\cdots \text{X}$$

normal	*secondary*	*normal*	*hydrogen bond*
covalent		*covalent*	

e.g.   X = Hg, Tl, Sn, Sb, Te   X = F, O, N
        A = S, Se, etc.

The explanation advanced by Alcock [294] suggests that the secondary bond is formed either by donation from the lone pair of X into an *s** orbital of the A-Y bond, or (alternatively and equivalently) as an asymmetric three-center system, with three *s* symmetry atomic orbitals on A, X and Y, combined to form three molecular orbitals: one filled bonding molecular orbital located between A and X, one filled non-bonding or weakly bonding orbital located between A and Y and one empty antibonding orbital (see also [294]). It seems that such secondary interactions are associated with a high electron density at the acceptor binding site (e.g. due to the presence of one or more lone pairs of

electrons). The strength of the secondary bonds is comparable to that of hydrogen bonds.

Secondary bonds are particularly important and frequently occur in compounds of heavier Main Group elements [295] and many examples of supramolecular self-assembly through secondary bonds are known [296]. Only a few examples will be given here to illustrate the concept of inorganic oligomer and polymer formation via secondary bonds.

Tetramethyldiarsane, **Me₂As-AsMe₂,** is associated in the solid state, forming chains of alternating primary covalent As-As bonds (2.43 Å) with weak secondary As...As bonds (3.70A) whereas tetraphenyldiarsane, **Ph₂As-AsPh₂** [297] and **(Me₃Si)₂As-As(SiMe₃)₂** [298] are monomeric and unassociated.

```
        R   R              R   R
         \ /                \ /
---- As —— As ------ As —— As ------
        / \                / \
       R   R              R   R
```
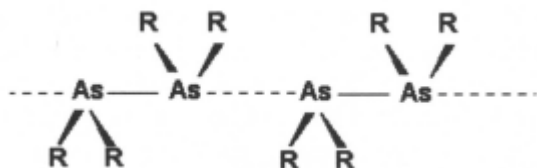
A similar self-assembly is observed in tetraorganodistibanes. Thus, in the solid state the **Me₂Sb-SbMe₂** molecular tectons are self-organised through Sb...Sb secondary bonding interactions (3.645 Å) which alternate with primary bonds (Sb-Sb 2.862 A) in a linear chain (Sb-Sb...Sb 179.2°) [299]. Several other distibanes are similarly associated (for a review see ref. [300]). Among these, the trimethylsilyl derivative, **(Me₃Si)₂Sb-Sb(SiMe₃)₂** (Sb-Sb 2.867 Å, Sb...Sb 3.99 Å), the trimethylgermyl derivative, **(Me₃Ge)₂Sb-Sb(GeMe₃)₂,** the trimethylstannyl derivative, **(Me₃Sn)₂Sb-Sb(SnMe₃)₂** (Sb...Sb 3.879 and 3.81.1 Å at -120°C; 3.890 Å at room temperature) are all self-assembled in chain-like structures, but tetraphenyldistibane, Ph₂Sb-SbPh₂, (with Sb...Sb contacts at 4.29 Å) is molecular, monomeric and unassociated [301].

```
        R   R              R   R
         \ /                \ /
----Sb —— Sb ------ Sb —— Sb -------
        / \                / \
       R   R              R   R
```

In Group 16 the tendency of self-assembly increases from sulfur to heavier elements. Thus, the molecular tectons of dimethyldiselane, MeSe-SeMe, and dimethylditellane, MeTe-TeMe, are associated in chains (packed in turn as sheets) with stronger intermolecular secondary bonds (Se-Se 2.31 Å,

Se...Se 3.55 Å and Te-Te 2.71 Å, Te...Te 3.74 Å, respectively). By contrast, diphenyldisulfane, PhS-SPh and diphenyldiselane, PhSe-SePh are discrete isolated molecules in the crystal, with no secondary association. Diphenylditellane, PhTe-TePh is also a molecular, unassociated compound [302].

Gold-gold interactions, known as aurophilicity [303] lead to the formation of supramolecular chains in isonitrile gold(I) chlorides **[Au(CNBuᵗ)Cl]** (Au...Au 3.695 Å), nitrates **[Au(CNBuᵗ)(NO₃)]** (Au...Au 3.295 and 3.324 Å), cyanides [Au(CNBut)(CN)] (Au...Au 3.568 Å) or to the formation of a gold catenane in **[{Au₆(CCBuᵗ)₆}₂]** [304].
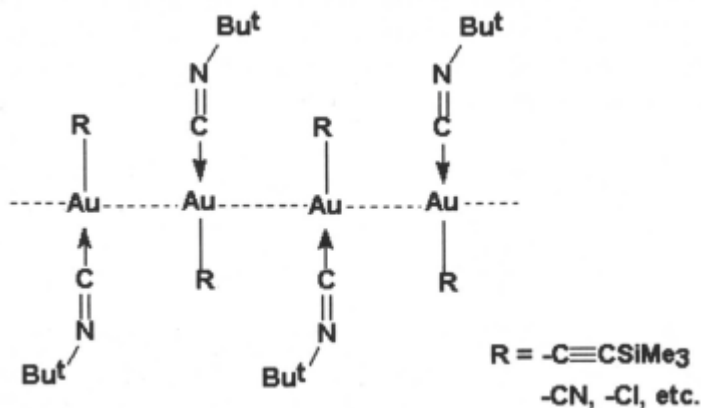
There are numerous examples of secondary bonds in organomercury chemistry. The structural chemistry of mercury(II) is dominated by its tendency to maintain the linear coordination resulted from *sp* hybridization, and to use the nonhybridized vacant p orbitals in further bonding. Secondary bonds to mercury will distort this linearity, but not to a great extent.

A mercury-chlorine eight-membered quasicycle formed through secondary bonds is present in the tetrameric organosilyl-substituted σ-cyclopentadienylmercury chloride, **[BuᵗMe₂Si(Me)₄C₅HgCl]₄** (Hg-Cl 2.33 A, Hg...Cl 3.11 A) [305].
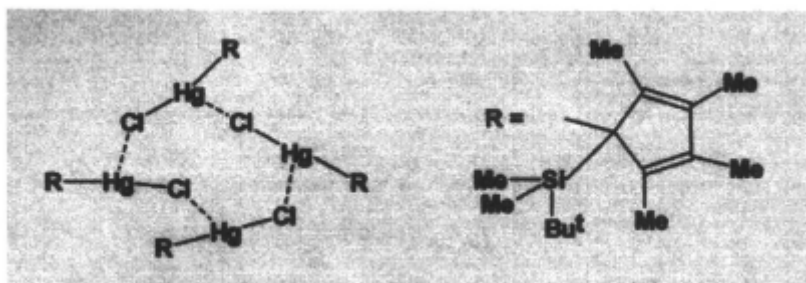
A ladder-like supramolecular array containing Hg-Cl primary bonds (2.329 and 2.345 Å) and secondary Hg...Cl bonds (3.303-3.566 Å) has been established in **meso-α,α-bis(chloromercurio)-α,α′-**bis(trimethylsilyl)-*m*-xylene [306]

R = CH(SiMe3)2
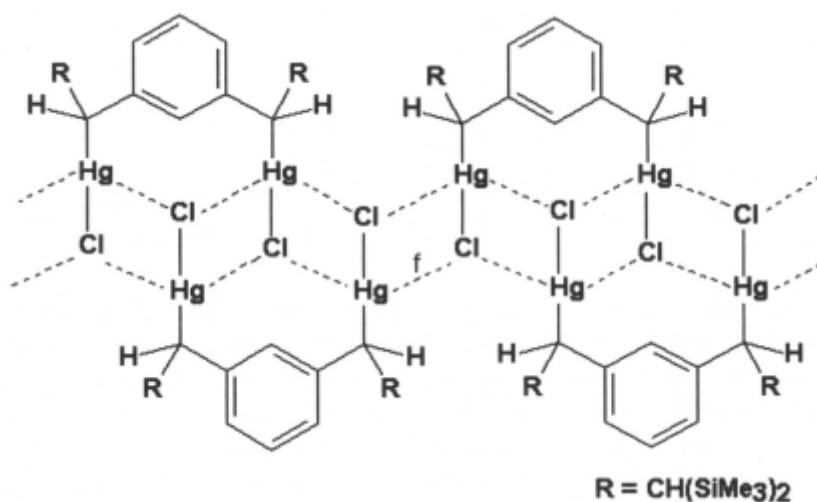
A beautiful self-organized supramolecular structure is shown by methylmercury(II) diphenylmonothiophosphinate, **Me-HgSP(=O)Ph₂.** associated through Hg...O secondary bonds into quasi-cyclic dimers, which are further connected through secondary Hg...O bonds into double chains [307].
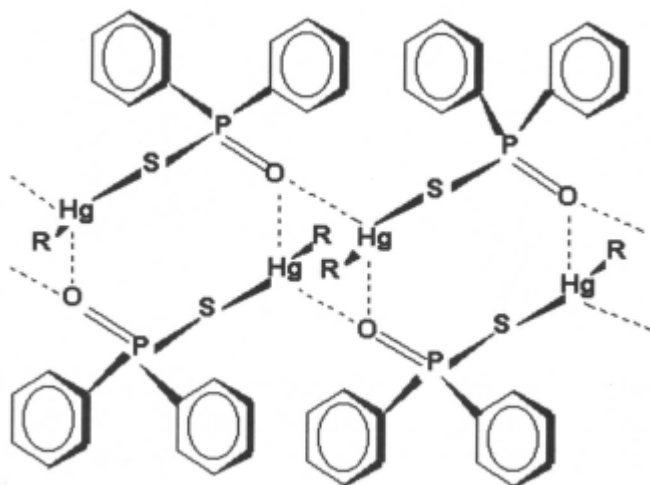
A series of self-organized oligomers and polymers include organomercury dithiophosphates and dithiophosphinates. Thus, phenylmercury diethyldithiophosphate, **PhHgS$_2$P(OEt)$_2$** (Hg-S 2.383 Å; Hg...S 3.323 Å) [308], and methylmercury(II) diphenyldithio-phosphinate, **MeHgS$_2$PPh$_2$** (Hg-S 2.379 Å, Hg...S 3.152 Å) [309] are centrosymmetric quasi-cyclic dimers, whereas phenylmercury(II) diethyldithiophosphinate, **PhHgS$_2$PEt$_2$,** is a polymer (Hg-S 2.375 Å, Hg...S 3.183 Å) [310].
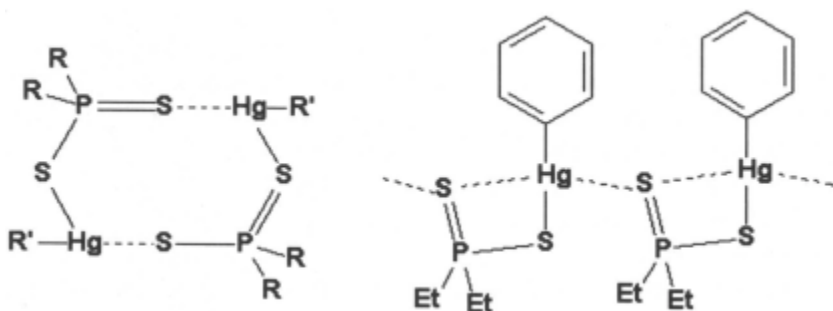
From organoindium chemistry we cite the neopentyl-trimethylsilyl derivative **[(Bu^{t}CH$_2$)(Me$_3$SiCH$_2$)InCl]$_n$** in which dimeric tectons formed through dative bonds (In-Cl 2.572 and 2.659 Å) are further self-organized in ladder supramolecular arrays through secondary bonds (In...Cl 3.528 Å) [311].
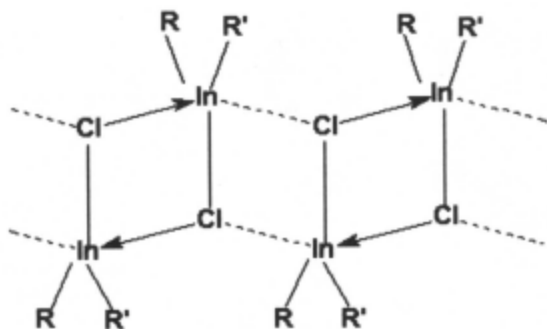
A similar, but slightly different structural motif is observed in the solid state structure of **[MeInCl₂]ₓ,** where the supramolecular self-assembly is maintained only by secondary In...Cl bonds to form the ladder-type ribbon [312].
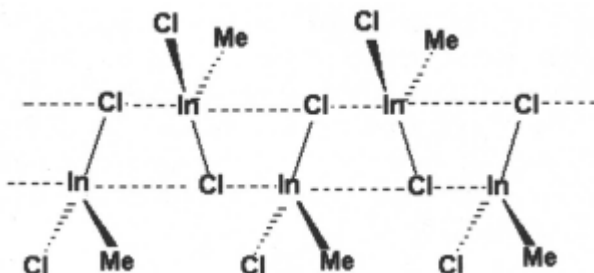
Supramolecular self-assembly is frequent in organothallium chemistry. Only a few examples will be given. Examples include organothallium(III) dithiophosphates and dithiophosphinates such as dimethylthallium diethyldithiophosphinate, **Me₂TlS₂PEt₂** (Tl-S 2.981 and 2.991 Å, Tl...S 3.334 Å), dimethylthallium diphenyldithiophosphinate, **Me₂TlS₂PPh₂,** and diphenylthallium(III) dicyclohexyldithiophosphinate, **(Ph₂TlS₂PCy₂)₂** . An illustration is provided for **(Ph₂TlS₂PCy₂)₂,** which forms double bridged ladders, but other modes of self-organisation have also been observed [313].
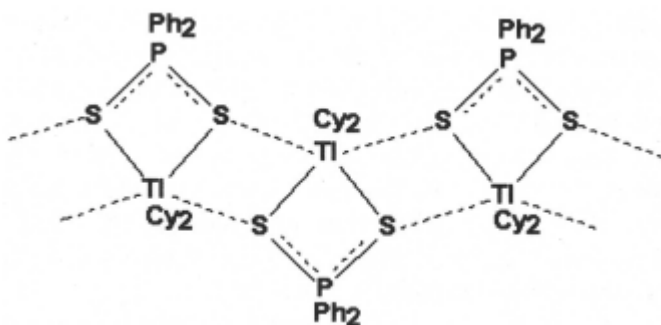
Polymeric ribbons of self-assembled chelate molecules with participation of dative thallium-oxygen and secondary thallium-sulphur intermolecular bonds are present in diphenylthallium(III) diphenylmonothiophosphinate, **Ph₂Tl[S(O)PPh₂]** [314].
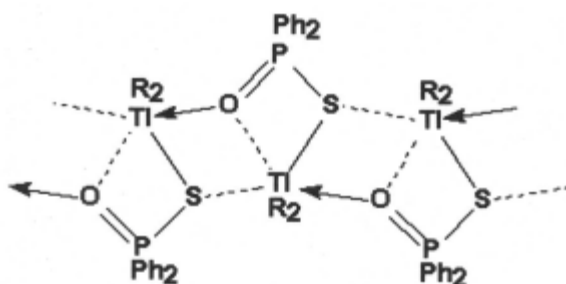
Organotin halides (except organotin fluorides) tend to self-associate in the solid state through secondary bonds, unless bulky substituents hinder the process. With small substituents linear polymeric chains are formed. In the supramolecular polymers the tin atom is five-coordinate with the halogen atoms in axial positions of a trigonal bipyramidal geometry.
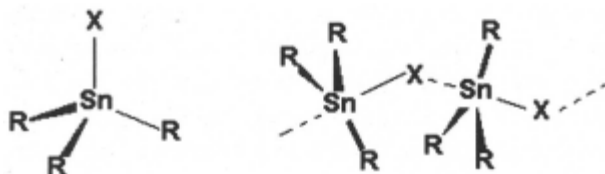
Trimethyltin chloride displays a self-organised bent chain structure with a bending angle Sn-Cl...Sn of 150.5°, and basically linear Cl-Sn...Cl (176.85°) coordination. The tin-chlorine interatomic distances are distinctly

different (Sn-Cl 2.430 Å and Sn...Cl 3.269 Å) [315] the longer one being significantly shorter than the sum of van der Waals radii (estimated as 3.85 Å). Tribenzyltin chloride, **(PhCH₂)₃SnCl** (Sn-Cl 2.387 Å, Sn...Cl 3.531 Å and Cl-Sn...Cl 180°) [316] and **Cyh₃SnCl** (Sn-Cl 2.407 Å, Sn...Cl 3.306 Å, Cl-Sn...Cl 180°) [317] are also supramolecular chains in the solid state, self-organized through secondary bonds. Not all triorganotin monochlorides are associated in the solid state. Thus, triphenyltin monochloride (Sn-Cl 2.353 A), tris(*m*-tolyl)tin chloride (Sn-Cl 2.379 A) and tris(3,5-dimethylphenyl)tin chloride (Sn-Cl 2.357 A) are discrete molecular monomers [318].

In the solid state, several diorganotin dichlorides are self-organised chain polymers, with a strongly distorted octahedral coordination geometry at tin. The tin atoms are connected by double bridges of chlorine atoms. The double bridge consists of a primary Sn-Cl and a secondary Sn...Cl bond. This type was found in dimethyltin dichloride (Sn-Cl 2.40 Å; Sn...Cl 3.54 Å) [319]. Similar structures have been reported for **R₂SnX₂** with **R = Et, X = Cl** and Br [320] ; **R =Buⁿ, X = Cl** [321], **R = Cyh, X = Cl** and Br [322] and also **MePhSnCl₂** [323].

The second structural type, in which both primary Sn-Cl bonds in the bridge are attached to the same chlorine atom, was found in **(ClCH₂)₂SnCl₂ (Sn-Cl 2.37 Å, Sn...Cl 3.71 Å)** [324].

Dioxastannolannes (a class of antitumor-active compounds), containing tin-oxygen bonds in a saturated five-membered ring tend to self-assemble through intermolecular tin-oxygen bonds [325]. This tendency is influenced by steric factors. 2,2-Di-*n*-butyl-l,3,2-dioxastannolane exists as a dimer in solution, but the monomer and higher oligomers have also been detected [326]. In the solid state the compound is associated through tin-oxygen bonds, to form an infinite ribbon. Within the five-membered ring the Sn-O bonds are short (2.097 Å) as expected for covalent single bonds, and the intermolecular contacts are significantly longer (2.495 and 2.520 Å) [327], indicating strong secondary bonds.
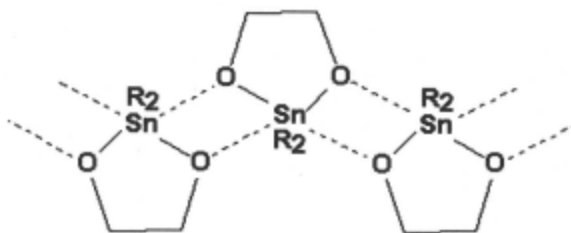
Solution and solid state studies of these compounds, using ^{119}Sn and ^{13}C NMR and Mössbauer spectroscopy [328], established that dimeric, trimeric, tetrameric and even pentameric oligomers exist.
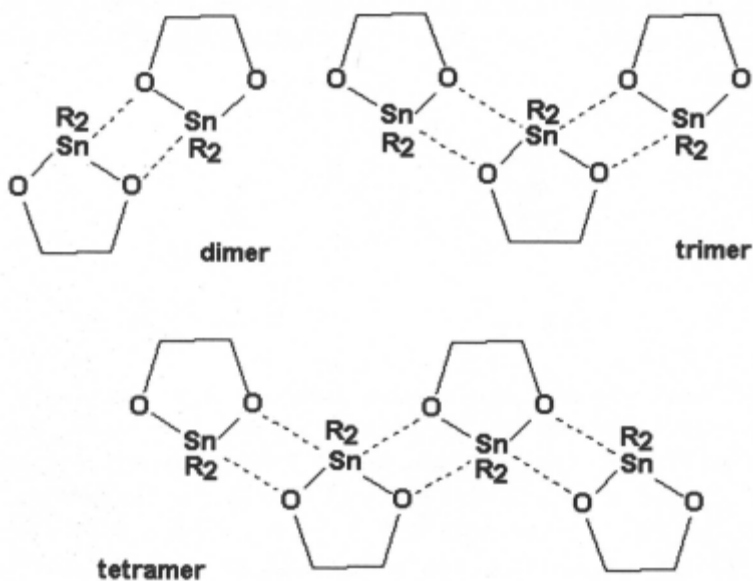
Self-assembly through secondary Sn...S bonds occurs in several sulphur-containing organotin compounds. Diorganodithiastannolanes, $R_2Sn(SCH_2CH_2)_2$, can be cited as examples. Thus, 2,2-dimethyl-1,3,2-dithiastannolane molecules are associated in infinite arrays through secondary Sn...S bonds (3.181 Å) [329].
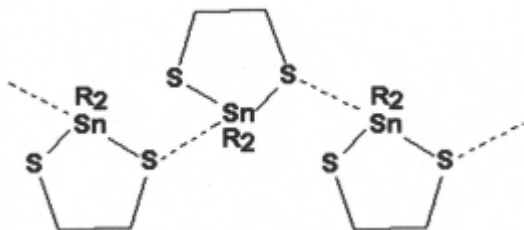
The di-n-butyl analogous derivative is also associated, but the Sn...S secondary bonds are weaker (3.688 Å) and the five membered rings are doubly connected via secondary bonds. Comparison of solution and solid state ^{13}C and ^{119}Sn NMR spectra show that the ethyl and isopropyl analogues are also associated in the solid state but are monomeric in solution. The *tert*-butyl derivative is monomeric, molecular both in solution and crystalline state [330].

Self-assembly through secondary bonds in organolead compounds is quite frequent. Thus, several organolead halides have been structurally characterised. Trimethyllead chloride, Me₃PbCl forms zig-zag chains with Pb-Cl 2.764 Å and Pb...Cl 2.814 Å [331]. Similarly, trimethyllead iodide molecules, **Me₃PbI,** are self-organised in zig-zag chains, with linear I-Pb-I moieties (176.25°) as parts of a trigonal bipyramid, and bent Pb-I...Pb fragments (primary Pb-I 3.038 Å, secondary Pb...I 3.360 Å) [332].
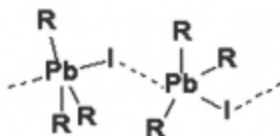
Similar chain association has been also reported for triphenyllead chloride, **Ph₃PbCl** (Pb-Cl 2.706 Å, Pb...Cl 2.947 Å) and bromide, **Ph₃PbBr (Pb-**Br 2.852 Å, Pb...Br 3.106 Å) and benzyldiphenyllead bromide, **BzPh₂PbBr** (Pb-Br 2.885 Å, Pb...Br 2.985 Å) [333].

Diphenyllead dichloride, **Ph$_2$PbCl$_2$,** is associated in doubly bridged chains (Pb-Cl 2.795Å) [334].
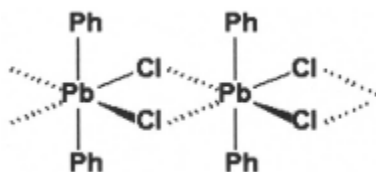
Supramolecular self-assembly occurs in some organolead-sulfur compounds. Thus, triphenyllead(IV) dimethyldithiophosphinate, **Ph$_3$PbS$_2$PMe$_2$,** forms a linear array, with bridging dithiophosphinato groups linking the molecular tectons through secondary Pb...S bonds [335].
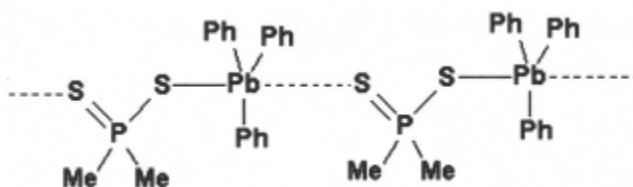
All structurally characterised lead(II) dithiophosphates and dithiophosphinates display various modes of supramolecular self-organizations in the solid state (see ref. [336] for review). Lead(II) bis(dimethyldithiophosphinate), **Pb(S$_2$PMe$_2$)$_2$,** and lead(II) bis(diphenyldithiophosphinate), **Pb(S$_2$PPh$_2$)$_2$,** [337] are interesting examples. In these compounds the molecules form quasi-cyclic dimers, further assembled in infinite chains.

Diorganoantimony(III) dithiophosphates and dithiophosphinates display various self-organized structures. Thus, dimeric diphenylantimony(III) diphenyldithiophosphinate, **[Ph$_2$SbS$_2$PPh$_2$]$_2$,** as well as the dithioarsinate analogue, **[Ph$_2$SbS$_2$AsPh$_2$]$_2$** self-organise into quasi-tricyclic systems. Dimeric bis(p-tolyl)antimony(III) diethyldithiophosphinate, **[(4-MeC$_6$H$_4$)$_2$SbS$_2$PEt$_2$]$_2$,** has a larger transannular antimony-sulphur distance and should be regarded as a quasi-monocyclic eight-membered ring. A similar structure was found in **[Ph$_2$SbS$_2$PMe$_2$]$_2$ [338].**
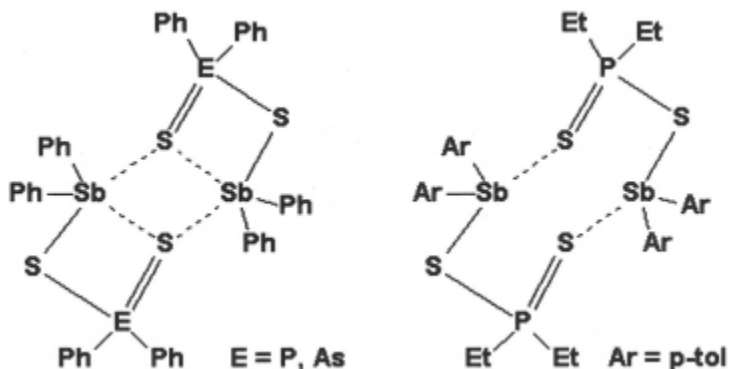
Other analogous compounds self-organise into helical chain-like arrays. Thus, diphenylantimony(III) isopropyldithiophosphate, **Ph₂SbS₂P(OPrⁱ)₂,** dimethylantimony(III) dimethyldithiophosphinate, **Me₂SbS₂PMe₂,** as well as the related dimethyldithioarsinate, **Ph₂SbS₂AsMe₂,** are all helical polymers [339].
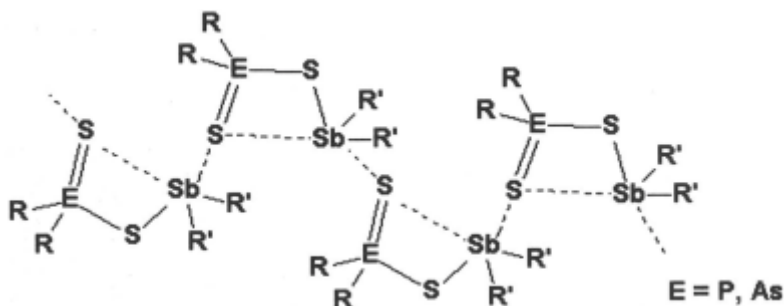
Secondary bond self-assembly is very common in tellurium compounds. Several structurally characterised organotellurium halides are associated in the solid state. Thus, α-dimethyltellurium dichloride, **Me₂TeCl₂,** forms a polymeric array (Te-Cl 2.541 and 2.480 Å; Te...Cl 3.46 and 3.52 Å) [340] and **α-Me₂TeI₂** is also a self-organized polymer (Te-I 2.854-2.994 Å, Te...I 3.659-4.030 Å) [341].

Diphenyltellurium dihalides, **Ph₂TeX₂,** with **X = F** (Te-F 2.006 Å, Te...F 3.208 Å), **X = Cl** (Te-Cl 2.482 and 2.529 Å, Te...Cl 3.677 Å), **X = Br** (Te-Br 2.682 Å, Te...Br 3.93 Å), and **X = I** (Te-I 2.928 Å, Te...I 3.955 Å), bis(pentafluorophenyltellurium) dihalogenides, **(C₆F₅)₂TeX₂,** with **X = F** (Te-F 1.990 Å, Te...F 2.952 Å), **X = Cl** (Te-Cl 2.485 Å, Te...Cl 3.589 Å) and **X = Br** (Te-Br 2.650 Å and Te...Br 3.848 Å), are self-organised into polymeric arrays and contain distinct primary and secondary tellurium-halogen bonds [342].

Tellurium-sulfur secondary bonds can also induce supramolecular self-organisation [343]. Thus, aryltellurium(II) dimethyldithiophosphates, **ArTe[S₂P(OMe)₂],** where **Ar = 4-MeOC₆H₄-** and **EtOC₆H₄-** are assembled into chain structures via dithiophosphate bridging [344].
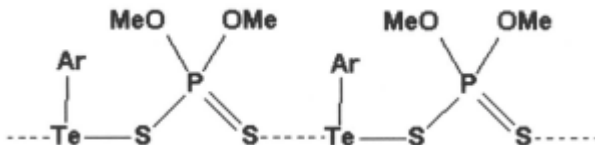
Thermochromic phenyltellurium(II) diphenyldithiophosphinate, **PhTeS₂PPh₂,** contains zig-zag chains assembled through Te...S secondary bonding (Te...S 3.383 Å in the yellow form and Te...S 3.422 Å in the red form)[345].
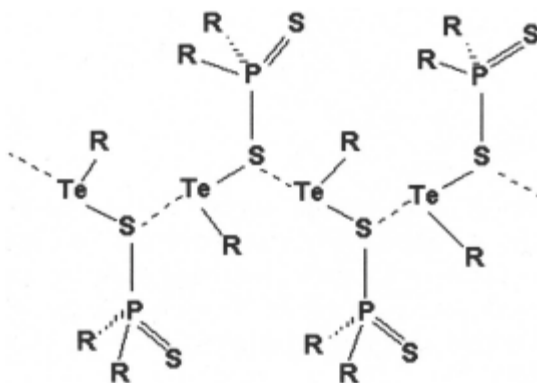
The examples cited represent only a minor selection of known cases of secondary-bond self-assembly.

14.3.4. Supramolecular cyclic self-assembly through hydrogen bonds

The formation of cyclic oligomers and polymeric structures with inorganic backbones, based on hydrogen bonds is a frequent phenomenon in compounds containing OH groups, like water, alcohols, oxoacids, etc. The supramolecular structure of water in various aggregation states is complex due to hydrogen-bond self-assembly [346].

Self-assembly through hydrogen bonds with formation of oligomeric and polymeric supermolecules is well established for primary alcohols. Thus,

methanol forms zig-zag chains in the crystalline state [347], contains cyclic and perhaps linear oligomers **(MeOH)$_n$** with **n = 3-20** in the liquid state (apparently with the hexamer predominating [348]), and tetrameric oligomers are the major form in the vapour phase at room temperature [349]. A hexameric oligomer of methanol trapped in a hydrophobic cavity has been confirmed by X-ray diffraction [350] and a hexameric tris(trifluoromethyl)phenol, 2,4,6-**(CF$_3$)$_3$C$_6$H$_2$OH,** has been structurally characterised in the solid state [351]. Alkynols and their **π-**complexes were recently shown to form eight-membered hydrogen-bond **O$_4$H$_4$** rings, twelve-membered **O$_6$H$_6$** rings and also polymeric chains in self-assembled supramolecular structures [352].
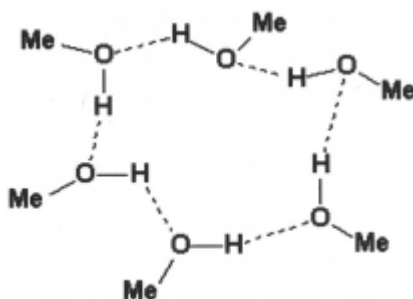
Other examples of hydrogen-bond self-assembly leading to the formation of cyclic supermolecules are provided by organosilanols. The silanols are organosilicon compounds containing Si-OH groups, and thus they represent silicon analogues of alcohols. Numerous organosilanols have been isolated in the solid state and their structures have been determined by X-ray diffraction [353, 354].

The pattern of hydrogen-bond self-assembly in silanols depends greatly on the number of Si-OH functions in the molecule and the number and size of organic groups attached to silicon. Supramolecular arrays (linear polymeric chains, bidimensional sheets or layers, tridimensional networks) are frequently observed, but bulky organic groups hinder the formation of extended structures, and these are limited to dimeric, tetrameric or hexameric oligomeric cyclic supermolecules.

Triorgano-monosilanols, **R$_3$Si-OH,** associate as dimers, tetramers or polymers.
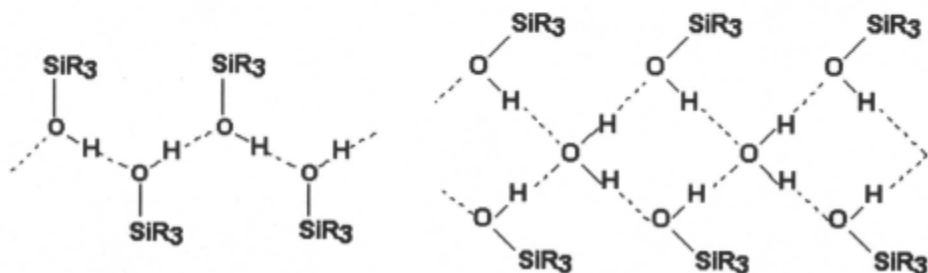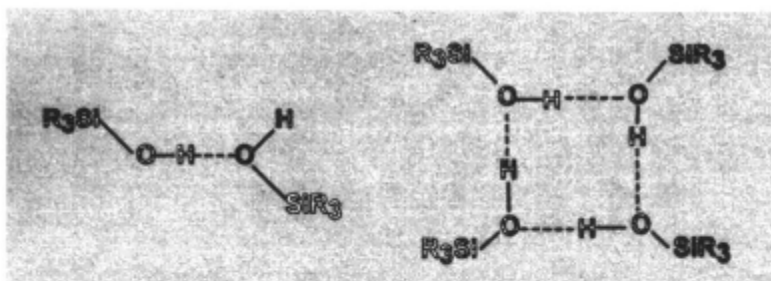
The cyclic tetrameric structure is illustrated by triphenylsilanol, **Ph₃SiOH,** [355] and di(*tert*-butyl)fluorosilanol, **Bu$_2^t$Si(F)OH,** [356]. The structures of these two silanol tetramers are similar to that of triphenylmethanol, **Ph₃C-OH,** which is also a tetramer [357].

A hemihydrate of *tert*-butyldimethylsilanol, **Bu^{t}Me₂Si-OH.0.5H₂O,** displays a unique structure with the participation of water molecules. The assembly is a chain polymer of self-assembled rhombs.

Diorganosilanediols, **R₂Si(OH)₂,** self-assemble into quasi-cyclic dimeric or tetrameric supermolecules, or single and double strand supramolecular arrays.
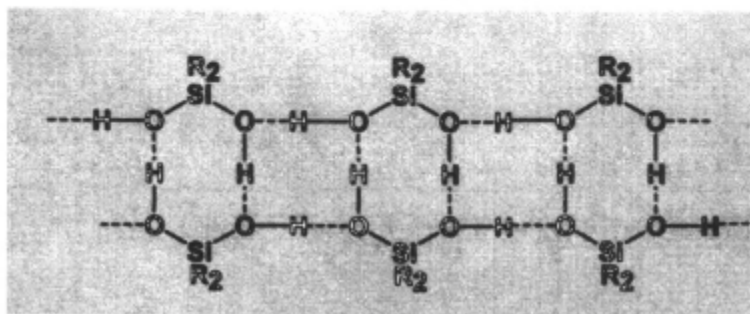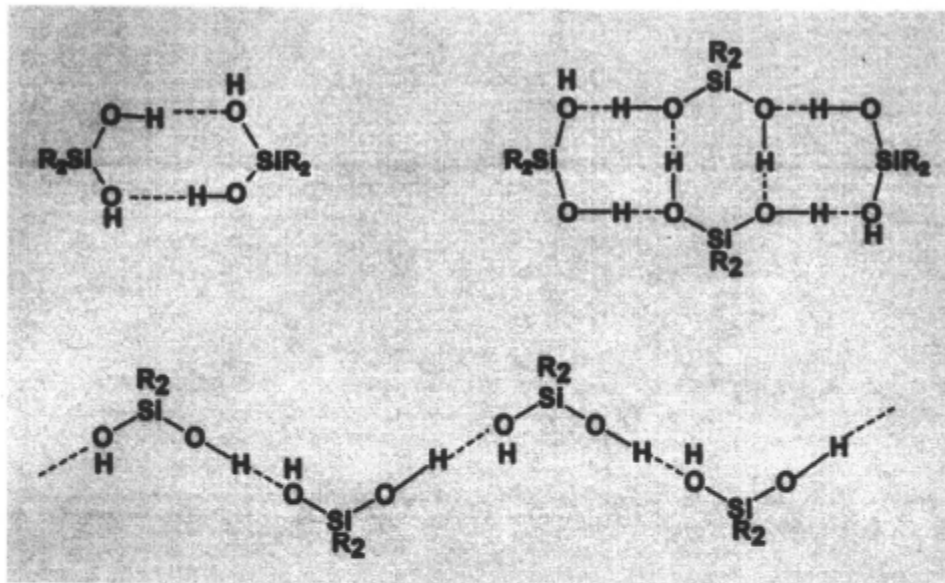
Monoorganosilanetriols, **RSi(OH)₃,** generate more intricate hydrogen-bond assemblies. Thus, hexameric cages were found in **(Me₃Si)₃C-Si(OH)₃** and **(Me₃Si)₃Si-Si(OH)₃** [359]. Tetrameric and octameric aggregates were found in some other organosilanetriols [360].

Hydroxy organogermanium compounds show similar patterns of hydrogen bond self-organization. Thus, triphenylgermanium hydroxide, **Ph₃Ge-OH,** is a hydrogen-bonded tetramer [361], just like its isomorphous organosilicon analogue, and di-*tert*-butylgermanium dihydroxide, **Buᵗ₂Ge(OH)₂,** forms dimeric quasicycles, associated into double chains [362].
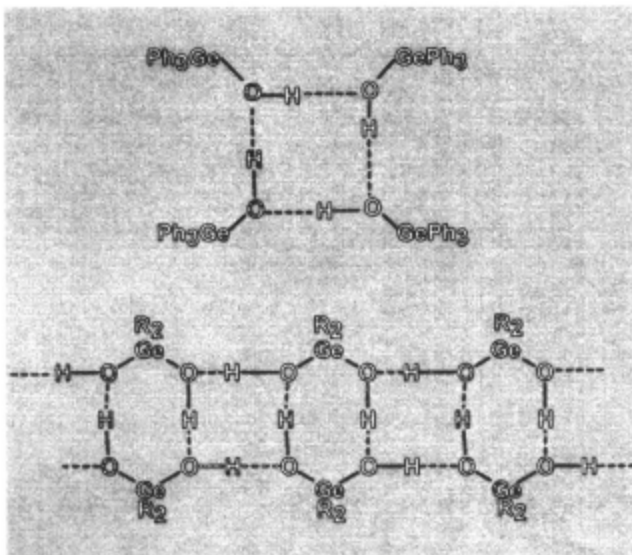
Numerous examples of hydrogen bond self-assembly are provided by organotin compounds. To cite only one, we mention here the primary hydrolysis products of diorganotin halides, **Bu$^t_2$Sn(OH)X** (X = F, Cl, Br), which are dimers (five-coordinate tin) associated in the solid state through X...H-O hydrogen bonds, to form a double chain [363].
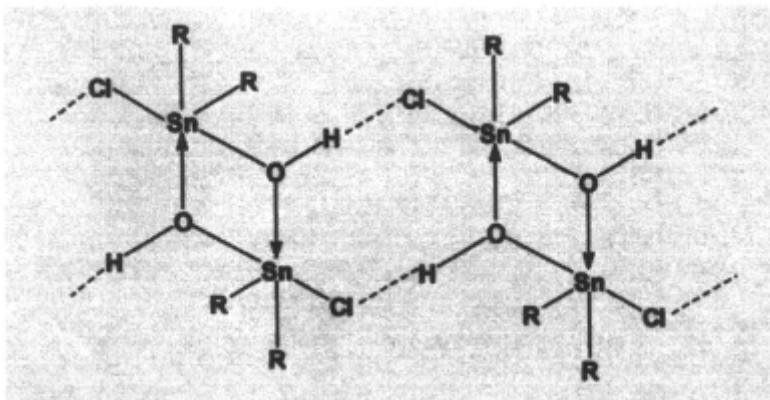
Many other compounds containing OH or NH groups will associate through hydrogen bonds, and the dimeric cyclic motifs analogous to those of carboxylic acids are present in phosphorus and arsenic compounds [364].
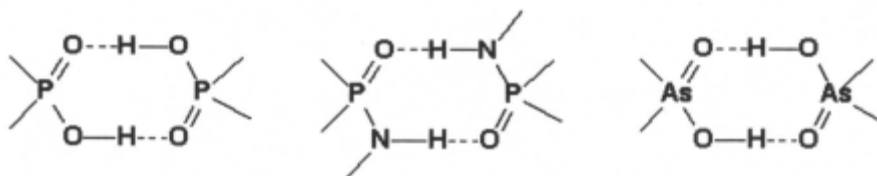
In organoarsenic compounds hydrogen bond self-organization can be illustrated by diorganoarsinic acids, which are hydrogen bonded dimers (R = Me, *tert*-Bu [365]) or infinite helical chains (R = vinyl or phenyl). An unusual tetranuclear aggregate, consisting of two molecules of diphenylarsinic and two molecules of diphenylmonothioarsinc acid, held together by hydrogen bonds, has also been identified by X-ray crystallography[366].
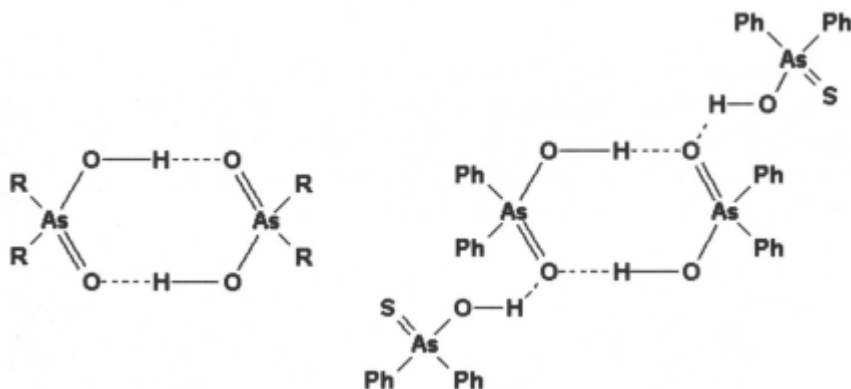
The organoantimony hydroxophosphinate **[Me₃Sb(OH)(O₂PPh₂)]** is a chain-like supramolecular array formed through P=O...H-O hydrogen bonds [367].
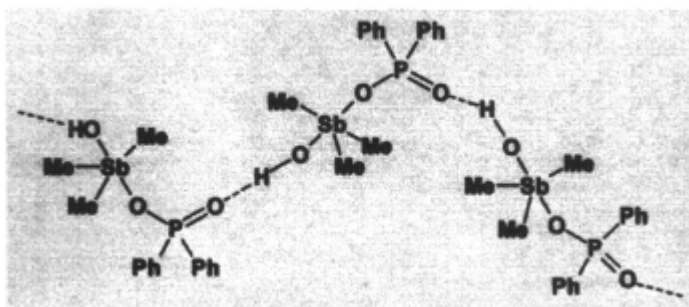
Transition metal organometallics display a broader diversity of hydrogen bonds. Thus, **X-H···π** (where X = O, N, C) hydrogen bonds to electron rich **π**-ligands (alkynes, arenes, cyclopentadienyls) [368] and **M-H···H-C** intermolecular interactions [369] play an important role. A recent development was the recognition of C-H...O weak hydrogen bonding, which play a significant role in the supramolecular self-organization of metal carbonyl organometallic compounds of transition metals [370]. Negatively charged O-H···O⁻ and charge-assisted **C-H$^{\delta+}$···O$^{\delta-}$** hydrogen bonds are particularly strong and allow for the design of organometallic supramolecular crystals with preestablished structures [371].

Hydrogen bonding is an important feature in organic chemistry; the phenomenon is quite well understood now and can be manipulated to build pre-established crystal architectures [372]. This is called *crystal engineering.* The term *crystal engineering* has been defined as "*the planning of a crystal structure from its building blocks, i.e. molecules or ions chosen on the basis of their size, shape and extramolecular bonding capacities*" [373]. So far this is best achieved by rational manipulation of hydrogen bonding capabilities of molecules. Hydrogen bond self-assembly and self-organization is also a quite general phenomenon in inorganic and organometallic compounds, leading to the formation of oligomeric structures.

14.3.5. Supramolecular cyclic self-assembly through ionic interactions

Cyclic self-assembly of inorganic oligomers occurs in some cases with the aid of ionic (electrostatic) interactions. Numerous alkali metal and alkaline earth molecular compounds fall into this category. These include three types of associated, oligomeric or polymeric compounds: a) alkali metal and alkaline earth alkyl and aryl derivatives, in which the metal-carbon bond is essentially ionic; b) alkali and alkaline earth metal amides, phosphides, arsenides, alkoxides, thiolates, etc., i.e. compounds not containing a direct metal-carbon bond; c) organometallic compounds which contain functional groups with mobile hydrogen, which can be readily displaced by an electropositive metal, to form cation-anion ion pairs (e.g. metal silanolates). There are several relevant reviews [374]. In the ionic alkali metal cyclopentadienyls probably **π**-complexation is also important (see Section 14.3.6).

One simple example of cyclic oligomers formed through ionic interactions is the trimer of lithium bis(trimethylsilyl)amide, **[LiN(SiMe₃)₂]₃** [375]. More intricate cage, ladder and polymeric structures are formed in various other compounds [376].
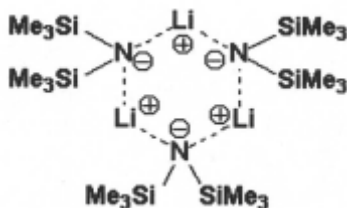
The sodium analogue, **[NaN(SiMe₃)₂]₃** has a similar structure [377], and the lithium phosphide, **[LiPBu$^t_2$(THF)]₄** is a tetramer [378]. Oligomeric alkoxides can be illustrated by trimeric **[Li{OC₆H₂(CH₂NMe₂)₂-2,6-Me-4}]₃,** hexameric **[NaOBu^t]₆** and nonameric **[NaOBu^t]₉** [379]. Thiolates can be trimeric, e.g. **[Li(SC₆H₂Bu$^t_3$-2,4,6)(THF)]₃** [380] and a larger ring (twelve-membered **Li₆S₆)** is found in hexameric **[LiSC₆H₃(CH₂NMe₂)₂-2,6]₆ [381].**

Numerous other examples are cited in ref. [382].

14.3.6. Supramolecular cyclic self-assembly through π-bonds

Thre are some spectacular cyclic oligomers formed with participation of π-bonds between cyclopentadienyl rings and a metal. One example is bis(cyclopentadienyl) lead(II) which exists both in a cyclic hexameric form and in two open-chain polymeric forms (zig-zag in the nonsolvated compound and sinusoidal in the toluene solvate) [383]. The monomeric form exists in the gas phase.
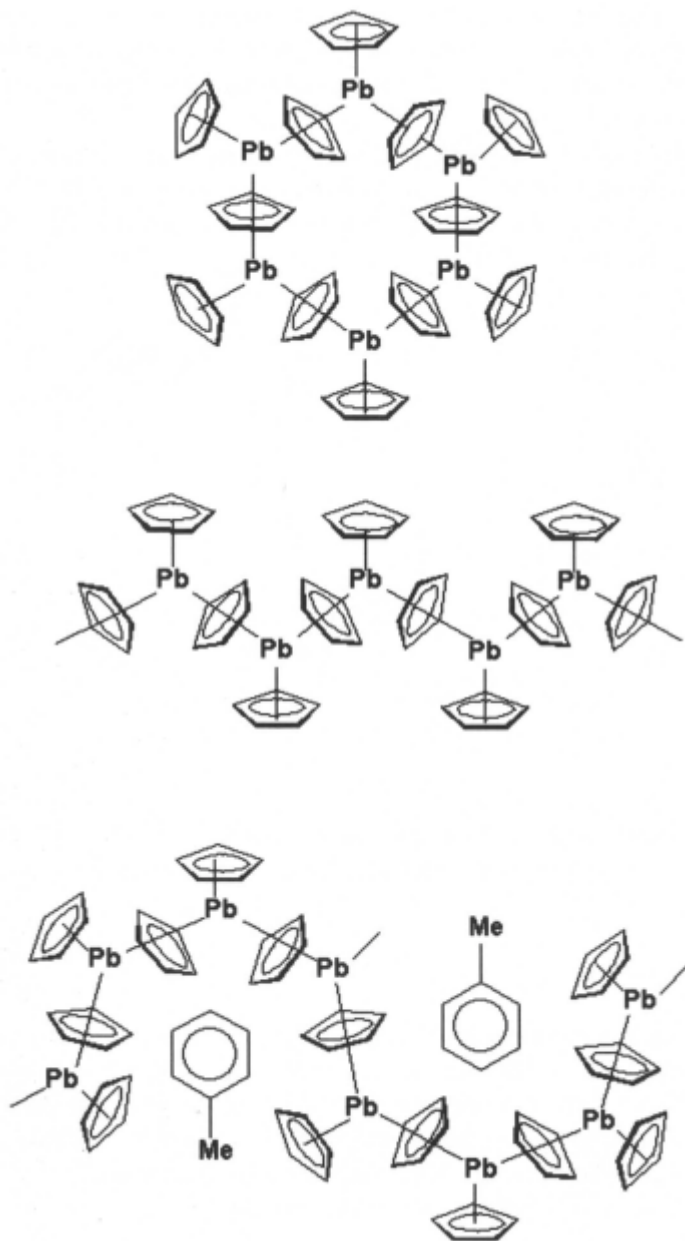
Polymeric chains, probably involving a strong ionic component of the interaction between metal and the cyclopentadienyl rings has been established in CsC_5H_5 [384], $Ca(C_5H_5)_2$ [385], $Ba(C_5Me_5)_2$ [386], $Yb[C_5H_3(SiMe_3)_2]_2$ and $Eu[C_5H_3(SiMe_3)_2]_2$ [387], $Mn(C_5H_5)_2$ [388], and other metal cyclopentadienyls.

672

Oligomeric, stacked multidecker sandwich complexes of lanthanides with cyclooctatetraene have also been described, with 1-5 metal atoms sandwiched between planar C_8H_8 rings. The compounds are described as ionic charge transfer complexes [389].

Another π-bonded cyclic oligomer is the ferrocenyl heptamer, obtained from the dilithium derivative of disilaindacene and iron(II) chloride. The molecular structure of this unusual compound has been established by single crystal X-ray diffraction [390].
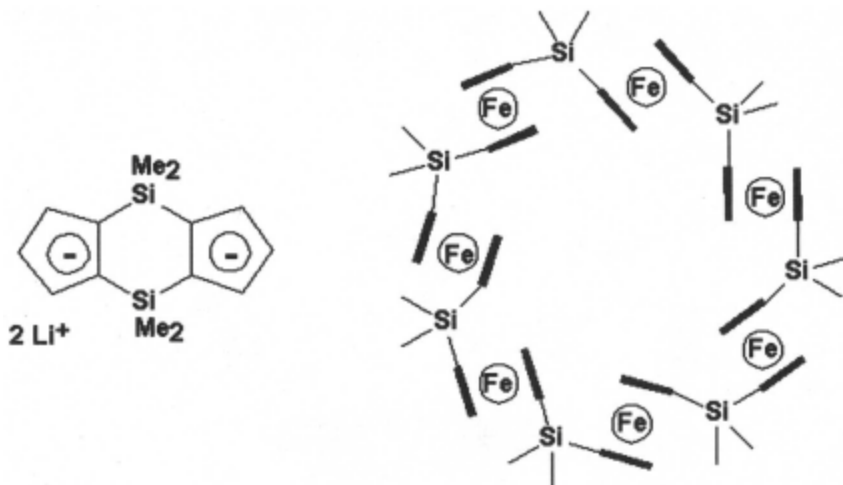
Although the number of known examples is limited, the potential of building cyclic oligomers with the aid of π-bonds should be not neglected.

Acknowledgement

References

1. (a) I. Haiduc, *The Chemistry of Inorganic Ring Systems*, Wiley-Interscience, London, 1970 (2 volumes); (b) I. Haiduc and D.B. Sowerby (Editors), *The Chemistry of Inorganic Homo- and Heterocycles*, Academic Press, London, 1987 (2 volumes); (c) H.W. Roesky (Editor), *Rings, Clusters and Polymers of Main Group and Transition Elements*, Elsevier, Amsterdam, 1989; (d) R. Steudel (Editor), *The Chemistry of Inorganic Ring Systems*, Elsevier, Amsterdam, 1992.

2. (a) R.M. Laine and J.F. Harrod (Editors), *Inorganic and Organometallic Oligomers and Polymers*, Kluwer, Dordrecht, 1991; (b) J.E. Mark, H.R. Alcock and R. West (Editors), *Inorganic Polymers,* Prentice Hall, Englewood Cliffs, 1992; (c) I. Manners, Angew. Chem. **108**, 1712 (1996), Angew. Chem. Int. Ed Engl. **35**, 1602 (1996); (d) M. Zeldin, K.J. Wynne and H.R. Allcock (Editors), *Inorganic and Organometallic Polymers* (ACS Symposium Series Nr. 360) American Chemical Society, Washington DC 1988; (e) *Inorganic and Organometallic Polymers II* (ACS Symposium Series Nr. 572), American Chemical Society, Washington DC 1994.

3. I. Haiduc and F.T. Edelmann, *Supramolecular Organometallic Chemistry*, Wiley-VCH, Weinheim, 1999.

4. J.M. Lehn, *Angew. Chem.* **100**, 91 (1988); A*ngew. Chem. Int. Ed. Engl.* **27**, 89 (1988).

5. J.M. Lehn, *Supramolecular Chemistry. Concepts and Perspectives,* VCH Weinheim, 1995.

6. J.M. Lehn, J.L. Atwood, J.E.D. Davies, D.D. MacNicol and F. Vögtle (Editors), *Comprehensive Supramolecular Chemistry,* Pergamon Press, Oxford, 1996.

7. (a) F.G.A. Stone and R. West (Editors), *Multiply Bonded Main Group Metals and Metalloids* (Advances in Organometallic Chemistry, vol. 39), Academic Press, New York, 1996; (b) P.P. Power, J. Chem. Soc. Dalton **1998**, 2939; (c) A. Meller and W. Maringgele in W. Siebert (Editor), *Advances in Boron Chemistry* (Royal Chemical Society Special Publication vol. 201), Royal Chemical Society, London, 1997, p. 224.

8. G.R. Desiraju, *Angew. Chem.* **107**, 2541 (1995); *Angew. Chem. Int. Ed. Engl.*, **34**, 2311 (1995).

9. S. Simard, D. Su and J.D. Wuest, *J. Am. Chem. Soc.* **113**, 4696 (1991).

10. M.C.T. Fyfe and J.F. Stoddart, *Acc. Chem. Res.* **30,** 393 (1997).

11. H.J. Breunig, R. Rosler and E. Lork, Angew. Chem., **110**, 3361 (1998).

12. R. Steudel, O. Schumann, J. Buschmann and P. Luger, Angew. Chem. **110**, 2502 (1998).

13. I. Haiduc, *The Chemistry of Inorganic Ring Systems*, Wiley-Interscience, London, 1970, vol. 1, p.39.

14. (a) K. Moedritzer, Organomet. Chem. Rev. **1**, 179 (1966); (b) J.R. Van Wazer, J. Macromol. Chem. A, **1**, 29 (1967); (c) J.R. Van Wazer and K. Moedritzer, Angew. Chem. **78**, 401 (1966), Angew. Chem. Int. Ed Engl. **5**, 341 (1966).

15. (a) J.F. Brown and G.M. Sluszarchuk, J. Am. Chem. Soc. **87**, 931 (1965); (b) J.B. Carmichael and R. Winger, J. Polym. Sci. **A3**, 971 (1965); (c) D.W. Scott, J. Am. Chem. Soc. **68**, 2294 (1946).

16. J.R. Van Wazer and K. Moedritzer, J. Chem. Phys. **41**, 3122 (1964).

17. J.A. Semlyen (Editor), *Large Ring Molecules*, Wiley, Chichester, 1996.

18. K. Moedritzer, J.R. Van Wazer and C.H. Dungan, J. Chem. Phys. **42**, 2478 (1965).

19. K. Moedritzer, J. Organomet Chem. **5**, 254 (1967)

20. K. Moedritzer and J.R. Van Wazer, J. Phys. Chem. **70**, 2030 (1966).

21. K. Moedritzer and J.R. Van Wazer, Inorg. Chim. Acta **1**, 152 (1967).

22. (a) R.West, M.J. Fink and J. Michl, Science **214**, 1343 (1981); (b) R. West, Angew. Chem. **99**, 1231 (1987), Angew. Chem. Int. Ed. Engl. **26**, 1201 (1987); (c) R. Okazaki and R. West, Adv. Organomet. Chem. **39**, 231 (1996);

23. (a) R. West, J. Organomet. Chem. **300**, 327 (1986); (b) R.D. Miller and J. Michl, Chem. Rev. **89**, 1359(1989).

24. (a) K.. Matsumura, L.F. Brough and R. West, J. Chem. Soc. Chem. Commun. **1978**, 1092; (b) L.F. Brough, K. Matsumura and R. West, Angew. Chem. Int. Ed. Engl. **18**, 955 (1979); (c) L.F. Brough and R. West, J. Organomet Chem, **194**, 139 (1980); (d) L.F. Brough and R. West, J. Am. Chem. Soc. **103**, 3049 (1981).

25. Z. Pawelec and W. Wojnowski, J. Inorg. Organomet Polym. **5**, 163 (1995).

26. (a) C. Kratky, H.G. Schuster and E. Hengge, J. Organomet Chem. **247**, 253 (1983); (b) H.L. Carrell and J.D. Donohue, Acta Cryst. **B 28**, 1566 (1972); (c) F. Shafiee, J.R. Damewood, K.J. Haller and R. West, J. Am. Chem. Soc. **107**, 6950 (1985).

27. (a) L. Parkanyi, K. Sasvari and J. Batha, Acta Cryst. **B 34**, 883 (1978); (b) L. Parkanyi, K. Sasvari, J.P. Declerc and G. Germain, Acta Cryst. **B 34**, 3678 (1978); (c) M. Drager and K.G. Walker, Z. Anorg. Allg. Chem. **479**, 65 (1981).

28. F. Shafiee, K.J. Haller and R. West, J. Am. Chem. Soc. **108**, 5478 (1986)

29. R.G. Jones, W.K.C. Wong and S.J. Holder, Organomtallics, **17**, 59 (1998).

30. (a) C.T. Aitken, J.F. Harrod and E. Samuel, J. Am. Chem. Soc. **108**, 4059 (1986); (b) T.D. Tiley and H.G. Woo, in *Inorganic and Organometallic Oligomers and Polymers*, Edited by J.F. Harrod and R.M. Laine, Kluwer, Dordrecht, 1991, p.3; (c) Y. Mu and J.F. Harrod, *ibid.* p.23;

31. B.P.S. Chaudhan, T. Shimizu and M. Tanaka, Chem. Lett. **1997**, 785.

32. T.A. Blinka and R. West, Organometallics **5**, 128 (1986).

33. (a) R. Matyaszewski, J. Inorg. Organomet. Polym. **1**, 463 (1991); (b) K. Matyaszewski, Y.L. Chen and H.K. Kim, ACS Symp. Ser. **360**, 78 (1980); (c) M. Cypiyk, Y. Gupta and K. Matyaszewski, J. Am. Chem. Soc. **113**, 1046 (1991); (d) E. Fossum and K. Matyaszewski, Macromolecules **28**, 1618 (1995).

34. S. Gautier and D.J. Worsfold, in *Inorganic and Organometalllc Oligomers and Polymers*, Edited by J.F. Harrod and R.M. Laine, Kluwer, Dordrecht, 1991, p. 37.

35. M. Cypryk, J. Chrusciel, E. Fossum and K. Matyaszewski, Makromol. Chem., Makromol. Symp. **73**, 167(1993).

36. M. Scarlete, S. Brienne, I.S. Butler and J.F. Harrod, Chem. Mater. **6**, 977 (1994) and references therein.

37. (a) P. Trefonas and R. West, J. Polym. Sci., Polym. Chem. Ed. **23**, 2099 (1985); (b) R.D. Miller and R. Sooriyakumaran, J. Polym. Sci. Polym. Chem. Ed. **25**, 111 (1987).

38. I. Haiduc and M. Drager, in I. Haiduc and D.B. Sowerby (Editors), *The Chemistry of Inorganic Homo- and Heterocycles*, Academic Press, London, 1987, Vol. 1, p. 361.

39. (a) W.P. Neumann and J. Pedain, Liebigs Ann. Chem. **672**, 34 (1964); (b) R. Sommer, W.P. Neumann and B. Schneider, Tetrahedron Lett. **1964**, 3875.

40. (a) L.R. Sita, Adv. Organomet. Chem. **38**, 189 (1995); (b) L.R. Sita, Acc. Chem. Res. **27**, 191 (1994).

41. (a) N. Devilder, M. Hill, K.C. Molloy and G.J. Price, Chem. Commun. **1996**, 711; (b) W. Zhou and N.L. Yang, Am. Chem. Soc., Div. Polym. Chem., **33**, 188 (1992).

42. (a) T. Imori and T.D. Tilley, J. Chem. Soc. Chem. Commun. **1993**, 1607; (b) T. Imori, V. Lu, H. Cai and T.D. Tilley, J. Am. Chem. Soc. **117**, 9931 (1995).

43. B. Watta, W.P. Neumann and J. Sauer, Organometallics **4**, 1954 (1985).

44. M. Okano, N. Matsumoto, M. Arakawa, T. Tsuruta and H. Hamano, Chem. Commun. **1998**, 1799.

45. K. Mochida, M. Hayakawa, T. Tsuchikawa, Y. Yokoyama, M. Wakase and H. Hayashi, Chem. Lett. **1998**, 91.

46. (a) W.P. Neumann and K. Konig, Liebigs Ann. Chem. **677**, 12 (1964); (b) W.P. Neumann and J. Pedain, Liebigs Ann. Chem. **672**, 34 (1964); (c) W.P. Neumann, J. Pedain and R. Sommer, Liebigs Ann. Chem. **694**, 9 (1966); (d) B. Jausseaume, N. Nonet, M. Pereyre, A. Saux and J.M. Frances Organometallics **13**, 1034 (1994); (e) H. Puff, C. Bach, H. Reuter and W. Schuh, J. Organomet Chem. **277**, 17 (1984);

47. (a) W.P. Neumann and K. Konig, Angew. Chem. Int.Ed. Engl. **1**, 212 (1962); (b) M. Drager, B. Mathiasch L. Ross and M. Ross, Z. Anorg. Allg. Chem. **506**, 99 (1983); (c) D.H. Olson and R.E. Rundle, Inorg. Chem. **2**, 1310 (1963).

48. (a) S. Masamune, L.R. Sita and D.J. Williams, J. Am. Chem. Soc. **105**, 630 (1983); (b) S. Masamune and L.R. Sita, J. Am. Chem. Soc. **107**, 6390 (1985); (c) L.R. Sita and R.D. Bickerataff, J. Am. Chem. Soc. **111**, 3769 (1989); (d) A. Schafer, M. Weidenbruch, W. Saak, S. Pohl and H. Harsmann, Angew. Chem. Int. Ed. Engl. **30**, 834 (1991); (e) F.J. Brady, C.J. Cardin, D.J. Cardin, M.A. Convey, M.M. Devereux and G.A. Lawless, J. Organomet. Chem. **241**, 199 (1991).

49. M. Yoshifuji, I. Shima, N. Imamoto, K. Hirotsu and T. Higuchi, J. Am. Chem. Soc. **103**, 4587 (1981).

50. (a) M. Baudler and M. Glinka, in I. Haiduc and D.B. Sowerby (Eds), *The Chemistry of Inorganic Homo- and Heterocycles*, Academic Press, London, 1987, vol. 2, p. 423, (b) M. Baudler, Angew. Chem. **99**, 429 (1987), Angew. Chem. Int. Ed. Engl. **26**, 419 (1987).

51. P.S. Elmes, B.M. Gatehouse and B.O. West, J. Organomet Chem. **82**, 235 (1974).

52. (a) A.H. Cowley, J.G. Lasch, N.C. Norman and M. Pakulski, J. Am. Chem. Soc. **103**, 5506 (1983; (b) A.H. Cowley, N.C. Norman and M. Pakulski, J. Chem. Soc. Dalton Trans. **1985**, 383.

53. (a) A.J. DiMaio and A.L. Rheingold, Chem. Revs. **90**, 169 (1990); (b) I. Haiduc and D.B. Sowerby in I. Haiduc and D.B. Sowerby (Eds), *The Chemistry of Inorganic Homo- and Heterocycles*, Academic Press, London, 1987, vol. 2, p. 701.

54. (a) P.S. Elmes, B.M. Gatehouse, D.J. Lloyd and B.O. West, J. Chem. Soc. Chem. Commun. **1974**, 953; (b) P.S. Elmes, B.M. Gatehouse and B.O. West, J. Organomet. Chem. **82**, 235 (1974); (c) A.L. Rheingold, M.L. Fountain and A.J. Di Maio, J. Am. Chem. Soc. **109**, 141 (1987).

55. (a) B. Meyer (Ed), *Elemental Sulfur. Chemistry and Physics*, Interscience, New York, 1965; (b) R. Steudel, in A. Muller and B. Krebs (Eds), *Sulfur: Its Significance for Chemistry, for Geo-, Bio- and Cosmosphere and Technology,* Elsevier, Amsterdam, 1984, p. 3; (c) R. Steudel, in I. Haiduc and D.B. Sowerby (Eds), *The Chemistry of Inorganic Homo- and Heterocycles*, AcademicPress, London, 1987, vol. 2, p. 737; (d) R. Steudel, in R. Steudel (Ed.) *The Chemistry of Inorganic Ring Systems*, Elsevier, Amsterdam, 1992, p. 233; (e) R.S. Laitinen, P. Pekonen and R.J. Suontamo, Coord. Chem. Revs. **130**, 1 (1994).

56. J. Steidel, J. Pickardt and R. Steudel, Z. Naturfosch., **33 b**, 1554 (1978).

57. (a) R. Steudel, R. Reinhardt and F. Schuster, Angew. Chem. **89**, 756 (1977), Angew. Chem. Int. Ed. **16**, 715 (1977), (b) R. Steudel, J. Steidel, J. Pickardt, F. Schuster and R. Reinhardt, Z. Naturfosrsch. **35b**, 1378 (1980).

58. (a) Y. Watanabe, Acta Ciystallogr, **B 30**, 1396 (1974); (b) L.K. Templeton, D.M. Templeton and A. Zalkin, Inorg. Chem **8**, 1999 (1876); (c) L.M. Goldschmidt and C.E. Strouse, J. Am. Chem. Soc. 99, 7580 (1977); (d) P. Coppens, Y.W. Yang, R.H. Blessing, W.F. Cooper and F.K. Larsen, J. Am. Chem. Soc. **99**, 760 (1977).

59. (a) R. Reinhardt, R. Steudel and F. Schuster, Angew. Chem. **90**, 55 (1978): Angew. Chem. Int. Ed. Engl. **17**, 57 (1978); (b) R. Steudel, Z. Naturfosch. **38b**, 543 (1983).

60. (a) J. Steidel and R. Steudel, J. Chem. Soc. Chm. Commun. **1982**, 1312; (b) R. Steudel, J.

Steidel and T. Sandow, Z. Naturforsch. **41b**, 958 (1986).

61. J. Steidel, R. Steudel and R. Kutoglu, Z. Anorg. Allg. Chem. **476**, 171 (1981).

62. R. Steudel, O. Schumann, J. Buschmann and P. Luger, Angew. Chem. **110**, 2502 (1998).

63. (a), T. Debaerdemaker, E. Hellner and A. Kutoglu, Z. Anorg. Allg. Chem. **405**, 153 (1974); (b) T. Debaerdemaker and A. Kutoglu, Naturwiss. **60**, 49 (1973); (c) T. Debaerdemaker and A. Kutoglu, Cryst. Struct. Commun. **3**, 611 (1974).

64. T. Debaerdemaker, E. Hellner, A. Kutoglu, M. Schrnidt and E. Wilhelm, Naturwiss. **60**, 300 (1973).

65. (a) R. Steudel, H.J. Mausle, D. Rosenbauer, H. Mockel and T. Freyholt, Angew. Chem. **93**, 402 (1981), Angew. Chem. Int. Ed. Engl. **20**, 394 (1981); (b) R. Steudel and R. Strauss, Z. Naturforsch. **37b**, 1219 (1982); (c) F.N. Tebbe, E. Wasserman, W.G. Peet, A. Vatvars and A.C. Hayman, J. Am. Chem. Soc. **104**, 4971 (1982).

66. (a) J.A. Semlyen, Trans. Faraday Soc. **63**, 743, 2342 (1967); (b) J.A. Semlyen, Trans. Faraday Soc. **64**, 1396 (1968).

67. *Gmelin Handbuch der Anorganischen Chemie, Borverbindungen, Teil 17, Borazin und seine Derivate*, Springer Verlag, Berlin, 1978; see also *Gmelin Handbuch der Anorganischen Chemie, Boron Compounds. 1ˢᵗ Supplement,* Vol. 2, Boron and Nitrogen, Springer Verlag, Berlin, 1980, p. 110.

68. W. Maringgele, in I. Haiduc and D.B. Sowerby (Editors), *The Chemistry of Inorganic Homo- and Heterocycles*, Academic Press, London, 1987, Vol. 1, p. 17.

69. (a) P. Paetzold, Adv. Inorg. Chem. **31**, 141 (1987); (b) H. Noth, Angew. Chem. **100**, 1664 (1988), Angew. Chem. Int. Ed. Engl. **27**, 1603 (1988); (c) G. Elter, M. Neuhaus, A. Meller, D. Schmidt-Bose, J. Organomet. Chem. **381**, 299 (1990); (d) W. Luthin, G. Elter, A. Heine, D. Stalke, G.M. Sheldrick and A. Meller, Z. Anorg. Allg. Chem. **608**, 147 (1992); (e) G. Elter, M. Geschwendter and A. Meller, Z. Anorg. Allg. Chem. **619**, 1474 (1993); (f) T. Albrecht, G. Elter and A. Meller, Chem. Commun. **1998**, 2583; (g) H. Noth, B. Rasthofer, S. Weber, C. Narula and A. Konstantinov, Pure appl. Chem. 55, 1453 (1983).

70. (a) P. Paetzold and T. von Bennigsen-Mackiewic, Chem. Ber. **114**, 298 (1981); (b) H.U. Meier, P. Paetzold and E. Schroder, Chem. Ber. **11**, 1954 (1984).

71. (a) L.G. Sneddon, in E. Siebert (Editor), *Advances in Boron Chemistry*, The Royal Society of Chemistry, London, 1997, p. 491; (b) R.T. Paine and L.G. Sneddon, ACS Symp. Ser. **572**, 358 (1994); (c) K.L. Paciorek, W. Krone-Schmidt, D.H. Harris, R.H. Kratzer and K.J. Wynne, ACS Symp. Ser. **360**, 392 (1988); (d) L.G. Sneddon, K. Su, P.J. Franzen, A.T. Lynch, E.E. Remsen and J.S. Beck, in J.F. Harrod and R.M. Laine (Editors), *Inorganic and Organometallic Oligomers and Polymers*, Kluwer Academic Publishers, Dordrecht, 1991, p. 199.

72. (a) P.J. Fazen, J.S. Beck, A.T. Lynch, E.E. Remsen and L.G. Sneddon, Chem. Mater. **2**, 96 (1990); (b) P.J. Fazen, E.E. Remsen, P.J. Carrol, J.S. Beck and L.G. Sneddon, Chem. Mater. **7**, 1942 (1995).

73. (a) A.T. Lynch and L.G. Sneddon, J. Am. Chem. Soc. **111**, 620 (1989) ; (b) K. Su, E.E. Remsen, H. Thomson and L.G. Sneddon, Macromolecules, **24**, 3760 (1991).

74. K. Su, E.E. Remsen, G.A. Zank and L.G. Sneddon, Chem. Mater. **5**, 547 (1993).

75. *Gmelin Handbuch der Anorganischen Chemie, Borverbindungen,* Teil 7, Springer Verlag, Berlin, 1975.

76. I. Haiduc, in I. Haiduc and D.B. Sowerby (Editors), *The Chemistry of Inorganic Homo- and Heterocycles*, Academic Press, London, 1987, vol.1, p. 109.

77. W. Siebert, in I. Haiduc and D.B. Sowerby (Editors), *The Chemistry of Inorganic Homo- and Heterocycles*, Academic Press, London, 1987, vol.1, p. 143.

78. O. Conrad, C. Jansen and B. Krebs, Angew. Chem. Int. Ed. Engl. **37**, 3208 (1998).

79. (a) K.M. Waggoner, H. Hope and P.P. Power, Angew. Chem. Int. Ed. Engl. **27**, 1699 (1988); (b) K.M. Waggoner and P.P. Power, J. Am. Chem. Soc. **113**, 3385 (1991).

80. M. Cesari and S. Cuccinela, in I. Haiduc and D.B. Sowerby (Editors), *The Chemistry of Inorganic Homo- and Heterocycles*, Academic Press, London, 1987, vol. 1, p. 167.

81. (a) N. Wiberg, K. Schurz and G. Fischer, Angew. Chem. Int. Ed. Engl. **24**, 1053 (1985); (b) R. Boese and U. Klingebiel, J. Organomet. Chem. **315**, C17 (1986); for review see I. Hemme and U. Klingebiel, Adv. Organomet Chem. **39**, 159 (1996).

82. D.A. Armitage, in S. Patai and Z. Rappoport (Editors), *The Silicon-Heteroatom Bond,* J.Wiley & Sons, Chichester, 1991, p.365.

83. U. Klingebiel, in I. Haiduc and D.B. Sowerby (Editors), *The Chemistry of Inorganic Ring Systems,* Academic Press, London, 1987, Vol.1, p. 221.

84. B. Rozsondai, I. Hargittai, A.V. Golubinskii, L.V. Vilkov and V.S . Mastryukov, J. Mol. Struct. **28**, 339 (1975).

85. (a) G.S. Smith and L.E. Alexander, Acta Cryst. **16**, 1015 (1963); (b) B.P.E Edwards, W. Harrison, I.W. Novell, M.L. Post, H.M.M. Shearer and J. Trotter, Acta Cryst. **B 32**, 648 (1976).

86. B. Rake, H.W. Roesky, I. Uson and P. Muller, Angew. Chem. **110**, 1508 (1998).

87. (a) D. Seyfert and G. Wísseman, J. Am. Ceram. Soc. **67**, C 132 (1984); (b) D. Seyferth, ACS Symp. Ser. **360**, 143 (1988); (c) D. Seyferth, in J.M. Zeigler and F.W.G. Fearon (Editors), *Silicon-Based Polymer Science* (Adv. Chem. Ser. vol. 224), American Chemical Society, Washington DC, 1990, p. 565; (d) H.N. Han, D.A. Lindquist, J.S. Haggerty and D. Seyferth, Chem. Mater. **4**, 705 (1992); (e) Y.D. Blum, G.A. McDermott and A.S. Hirschon, in J.F. Hatred and R.M. Laine, *Inorganic and Organometallic Oligomers and Polymers*, Kluwer Academic Publishers, Dordrecht, 1991, p. 161; (f) K.E. Gonsalves, ibidem p. 177; (g) M. Birot, J.P. Pillot and J. Donogues, Chem. Rev. **95**, 1443 (1995); (h) D. Seyferth, G.H. Wisseman, C.A. Poutarse, J.M. Schwark and Y.F. Yu, Polym. Prepr. **38**, 389 (1987); (i) R-M. Stewart, N.R. Dandoi, D. Seyferth and A.J. Perrotta, Polym. Prepr. **32**, 569 (1991); (j) N.R. Dando, A.J. Perrotta, C.

Strohmann, R.M. Stewart and D. Seyferth, Chcm. Mater. **5**, 1624 (1993); (k) M. Birot, J.P. Pillot and J. Donogues, Cheat. Rev. **95**, 1443 (1995).

88. D. Seyferth and G.H. Wiseman, Polymer Prepr. **25**, 10 (1984).

89. (a) R.M. Laine, Y.D. Blum, D. Tse and R. Geaser, ACS Symp. Ser. **360**, 124 (1988); (b) Y.D. Blum, G.A. McDermott, R.B. Wilson nd A.S. Hirschon, Polym. Prepr. **32**, 548 (1991).

90. (a) E. Duguet, M. Schappacher and A. Soum, Organometallics **25**, 4835 (1992); (b) E. Duguet, M. Schappacher and A. Soum, Polym. Int. **33**, 129 (1994); (c) D. Seyferth, M.J. Schwark and M.K. Stewart, Organometallics **8**, 1980 (1989).

91. (a) J. Pfeiffer, W. Maringgele, M. Noltemeyer and A. Meller, Chem. Ber. **122**, 245 (1989); (b) A. Meller, G. Ossig, W. Maringgele, D. Stalke, R. Herbst-Irmer, S. Freitag and G.M. Sheldrick, J. Chem. Soc. Chem. Commun. **1991**, 1123; (c) C. Glidewell, D. Lloyd, K.W. Lumbard and J.S. McKechnie, J. Chem. Soc. Dalton Trans. **1987**, 2981.

92. I. Haiduc in I. Haiduc and D.B. Sowerby (Editors), *The Chemistry of Inorganic Homo- and Heterocycles*, Academic Press, London, 1987, Vol. 1, p. 368.

93. (a) C.A. Arrington, R. West and J. Michl, J. Am. Chem. Soc. **105**, 6176 (1983); (b) V.N. Khabashesku, Z.A. Kerzina, K.N. Kudin and O.M. Nefedov, J. Organomet. Chem. **566**, 45 (1998); (c) for review see also G. Raabe and J. Michl, Chem. Rev. **85**, 419 (1985).

94. E.G. Rochow, *Silicon and Silicones*, Springer, Heidelberg, 1987.

95. D. Seyferth, C. Proud'home and G.H. Wiseman, Inorg. Chem. **22**, 2163 (1983)

96. (a) W.I. Patnode and D.F. Wilcock, J. Am. Chem. Soc. **68**, 358 (1946); (b) M.J. Hunter, J.F. Hyde, E.L. Warrick and H.J. Fletcher, J. Am. Chem. Soc. **68**, 667 (1946); (c) D.F. Wilcock, J. Am. Chem. Soc. **68**, 691 (1946); (d) R.O. Sauer and D.J. Mead, J. Am. Chem. Soc. **68**, 1794 (1946).

97. G. Peyronel, Atti Acad. Naz. dei Lincei, Rend. Cl. Fis. Mat. Nat. **16**, 231 (1954).

98. H. Steinfink, B. Post and I. Fankuchen, ActaCryst. **8**, 420 (1955).

99. A.F. Skryshevskii, V.P. Klochkov and Yu. V. Pasenchik, Zh. Strukt. Khim. **2**, 140 (1961).

100. N.L. Paddock, S.J. Rettig and J. Trotter, Can. J. Chem. **61**, 541 (1983).

101. O.I. Shchegolikhina, V.A. Igonin, Yu.A. Molodtsova, Yu.A. Pozdnikova, A.A. Zhdanov, T.V. Strelkova and S.V. Lindeman, J. Organomet. Chem. **562**, 141 (1998).

102. M. Michalczuk, M.J. Fink, K.J. Haller, R. West and J. Michl, Organometallics **5**, 531 (1986).

103. J.F. Brown and G.M.J. Slusarczuk, J. Am. Chem. Soc. **87**, 931 (1965)

104. (a) S.J. Clarson and J.A. Semlyen (Eds.) *Siloxane Polymers*, Prentice Hall, Englewood

Cliffs, NJ, 1993, Ch. 3; (b) P.V. Wright and M.S. Beevers, in J.A. Semlyen (Ed), *Cyclic Polymers*, Elsevier, London, 1986, Ch. 3; (c) J.A. Semlyen, Adv. Polym. Sci. **21**, 41 (1976); (d) J.A. Semlyen, Pure Appl. Chcm. **53**, 1797 (1981); (e) D.W. Scott, J. Am. Chem. Soc. **68,** 2294 (1946); (f) J.B. Carmichael and J. Heffel, J. Phys. Chem. **69**, 2218 (1965); (g) J.B. Carmichael and R. Winger, J. Polym. Sci. **B 3**, 473 (1965); (h) P.J. Flory and J.A. Semlyen, J. Am. Chem. Soc. **88**, 3209 (1966); (i) J.B. Carmichael, D.J. Gordon and F.J. Isackson, J. Phys. Chem. **71**, 2011 (1967); (j) J.A. Semlyen and P.V. Wright, Polymer, **10**, 543 (1969); (k) P.V. Wright, J. Polym. Sci. Polym. Phys. Ed. **11**, 51 (1973); (1) J. Chojnowski, M. Scibiorek and J. Kowalski, Makromol. Chem. **178**, 1351 (1977); (m) K. Dodgson and J.A. Semlyen, Polymer, **18**, 1265 (1977); (n) K. Dodgson, D. Sympson and J.A. Semlyen, *Polymer*, **19**, 1285 (1978); (o) C.J.C. Edwards, S. Bantle, W Burchard, R.F.T. Stepto and J.A. Semlyen, *Polymer*, **23**, 873 (1982).

105. (a) Yilgor and J.E. McGrath, Adv. Polym. Sci. **86**, 1 (1988); (b) S. Chojnowski, in *Siloxane Polymers*, Edited by J.A. Semlyen and S.J. Clanon, Prentice Hall, Englewood Cliffs, 1991; (c) S. Penczek and P. Kubisa, in *Ring-Opening Polymerization. Mechanism, Catalysis, Structure, Utility,* Edited by D.J. Brunelle, Hansen Publishers, Munich, 1993, p. 72; (d) R.P. Quirk and J. Kim, *ibid.* p. 272; (e) P.V. Wright, in *Ring Opening Polymerization.* Edited by K.J. Ivin and T. Saegusa, Elsevier Applied Science Publishers, London, 1984, Vol. 2, p. 1055; (f) T.C. Kendrick, B.M. Parbhoo and J.H. White, in Sir Geoffrey Allen and J.C. Bevington (Editors), *Comprehensive Polymer Science,* Edited by, *Vol. 4. Chain Polymerization II*, (Volume Editors G.C. Eastwood, A. Ledwith, S. Russo and P. Sigwalt), Pergamon Press, Oxford, 1989, Chapter 25, p. 525; (g) J. Chojnowski, J. Inorg. Organomet. Polym. **1**, 299 (1991); (h) G.J. Out, A.A. Teretskii, M. Moller and D. Oelfin, Macromolecules **27**, 3310 (1994).

106. P. Sigwalt, M. Masure, M. Moreu and R. Bischoff, Makromol. Chem., Makromol Symp. **73**, 147 (1993).

107. D.J. Orrah, J.A. Semlyen and S.B. Ross-Murphy, Polymer, **29**, 1452 (1988).

108. S.J. Clarson, K. Dodgson and J.A. Semlyen, Polymer, **26**, 930 (1985).

109. A.Patel, T. Cosgrove and J.A. Semlyen, Polymer, **32**, 1313 (1991).

110. (a) R.D.C. Richards, W.D. Hawthorne, J.S. Hill, M.S. White, D. Lacey, J.A. Semlyen, G.W. Gray and T.C. Kendrick, J. Chem. Soc. Chem. Common. **1990,** 95; (b) R.D.C. Richards, J. Hollingshurst and J.A. Semlyen, Polymer, **34**, 23, 4965 (1993).

111. T.R. Formory and J.A. Semlyen, Polymer Commun. **30**, 86 (1989).

112. (a) S.J. Clarson and J.A. Semlyen, Polymer, **27**, 1633 (1986); (b) S.J. Clarson, K. Dodgson and J.A. Semlyen, Polymer, **28**, 189 (1987).

113. (a) M.P. Brown and E.G. Rochow, J. Am. Chem. Soc. **72**, 2089 (1950); (b) H.A. Anderson, J. Am. Chem. Soc. **72**, 2089 (1950); **74**, 2370 (1952); (c) I. Ross and M. Drager, Z. Naturforsch. **39b**, 868 (1984); (d) K. Haeberle and M. Drager, Z. Anorg. Allg. Chem. **55**, 116 (1987).

114. (a) K. Moedritzer and J.R. Van Wazer, Inorg. Chem. **4**, 1753 (1965); (b) K. Moedritzer and J.R. Van Wazer, J. Polym. Sci., Polym. Chem. Ed. **6**, 547 (1968).

115. C.W. Alien, in I. Haiduc and D.B. Sowerby, *The Chemistry of Inorganic Homo- and*

Heterocycles, Academic Press, 1987, Vol. 2, p. 115.

116. N.L. Paddock,T.N. Ranganathan and J.N. Wingfield, J. Chem. Soc. Dalton Trans. **1972**, 1578.

117. A.C. Chapman, N.L. Paddock, D.H. Paine, H.T. Searle and D.R. Smith, J. Chem. Soc. **1960**, 3608.

118. (a) G.E. Coxon, D.B. Sowerby and G.C. Tranter, J. Chem. Soc. **1965**, 5679; (b) G.E. Coxon and D.B. Sowerby, J. Chem. Soc. A, **1967**, 1566.

119. G. Allen, D.J. Oldfield, N.L. Paddock, F. Rallo, J. Serregi and S.M. Todd, Chem. Ind. (London) **1965**, 1032.

120. (a) N.L. Paddock, T.N. Ranganathan and S.M. Todd, Can. J. Chem. **49**, 164 (1971); (b) K.D. Gallicano, R.T. Oakley, N.L. Paddock, S.J. Rettig and J. Trotter, Can. J. Chem. **55**, 304 (1977).

121. F.H. Pollard, G. Nickless and R.W. Warrender, J. Chromatogr. **9**, 513, (1962); **10**, 73, 78 (1953).

122. J.G. Hartsuiker and A.J. Wagner, J. Chem. Soc. Dalton Trans. **1978**, 1425.

123. A.W. Schlueter and R.A. Jacobson, J. Chem. Soc. **A1968**, 2317.

124. J.G. Hartsuiker and A. J. Wagner, J. Chem. Soc. Dalton Trans. **1968**, 1069.

125. M.W. Dougill and B. Sheldrick, Acta Crystallogr. **B 33**, 295 (1977).

126. R.T. Oakley, N.L. Paddock, S.J. Rettig and J. Trotter, Can. J. Chem. **55**, 3118 (1977).

127. R.T. Oakley, N.L. Paddock, S.J. Rettig and J. Trotter, Can. J. Chem. **55**, 2530 (1977).

128. R.T. Oakley, S.J. Rettig, N.L. Paddoc and J. Trotter, J. Am. Chem. Soc. **107**, 6923 (1985)

129. M.W. Dougill and N.L. Paddock, J. Chem. Soc. **1974**, 1022.

130. A.J. Wagner and A. Vos, Acta Crystallogr. **B 24**, 1423 (1968).

131. N.L. Paddock, J. Trotter and S.H. Whitlow, J.Chem. Soc. A, **1968**, 2227.

132. H.P. Calhoun, N.L. Paddock and J. Trotter, J. Chem. Soc. Dalton Trans. **1976**, 38.

133. H.R. Allcock, in R. Steudel (Ed.), *The Chemistry of Inorganic Ring Systems*, Elsevier, Amsterdam, 1992, p. 145.

134. (a) H.R. Allcock, *Phosphorus-Nitrogen Compounds*, Academic Press, New York, 1972; (b) H.R. Allcock, Makromol. Chem. **4**, 3 (1981); (c) H.R. Allcock, in M. Zeldin, K.J. Wynne and H.R. Allcock (Eds.), *Inorganic and Organometallic Polymers* (ACS Symposium Series, vol. 360), American Chemical Society, Washington DC, 1988, p. 250; (d) H.R. Allcock, in D.J. Brunelle (Editor), *Ring Opening Polymerization*, Hanser Publishers, Munich, 1993, Ch. 7, p.

217; (e) H.R. Allcock, in Sir Geoffrey Allen and J.C. Bevington (Editors) *Comprehensive Polymers Science, Volume 4. Chain Polymerization* (G.C. Eastwood, A. Ledwith, S. Russo and P. Sigwalt, Volume Editors), Pergamnon Press, Oxford, 1989, Ch. 26, p. 525; (f) H.R. Allcock, J. Inorg. Organomet. Polym. **2**, 197 (1992); (g) H.R. Allcock, Chem. Mater. 6, 1476 (1994); (h) H.R. Allcock, Adv. Mater. **6**, 106 (1994).

135. (a) H.R. Allcock, Acc. Chem. Res. **12**, 357 (1979); (b) H.R. Allcock, J.L. Desorscie and G.H. Riding, Polyhedron **6**,119 (1985).

136. H.R. Allcock and D.B. Patterson, Inorg. Chem. **16**, 197 (1977).

137. H.R. Allcock, and G.Y. More, Macromolecules **8**, 377 (1975).

138. H.R. Allcock, J.L. Schmutz and K.M. Kosydar, Macromolecules **11**, 179 (1978).

139. (a) I. Manners, G.H.Riding, J.A. Dodge and H.R. Allcock, J. Am. Chem. Soc. **111**, 3067 (1989); (b) H.R. Allcock, J.A. dodge, I. Manners and G.H. Riding, J. Am. Chem. Soc. **113**, 9596 (1991).

140. H.R. Allcock and M.L. Turner, Macromolecules **26,** 3 (1993).

141. R.H. Neilson and P. Wisian-Neilson, Chem. Rev. **88**, 541 (1988).

142. (a) C.H. Honeman, I. Manners, C. Morrissey and H.R. Allcock, J. Am. Chem. Soc. **117**, 7035 (1995); (b) M.J. Begley, D.B. Sowerby and R.J. Tillott, J. Chem. Soc., Dalton Trans. **1974**, 2527; (c) L.K. Krannicck, H. Thewalt, W.J. Cook, S.R. Jain and H.H. Sisler, Inorg. Chem. **12**, 2304(1973).

143. (a) J.A. Dodge, I. Manners, G. Renner, H.R. Allcock and O. Nuyken, J. Am. Chem. Soc. 1990, **112**, 1268; (b) H.R. Allcock, J.A. Dodge and I. Manners, Macromolecules **26**, 11 (1993).

144. (a) D.P. Gates, M. Edwards, L.M. Liable-Sands and A.L. Rheingold, J. Am. Chem. Soc. **120**, 3249 (1998); (b) D.P. Gates, A.R. McWIlliams and I. Manners, Macromolecules **31**, 3494 (1998); (c) M. Liang and I. Manners, J. Am. Chem. Soc. **113**, 4044 (1991); (d) M. Liang and I. Manners, Makromol. Chem. Rapid Commun. **12**, 613 (1991); (d) Y. Ni, A. Stammer, M. Liong, J. Massey, G.J. Vancso and I. Manners, Macromolecules **25**, 7119 (1992); (e) Y. Ni, P. Park, M. Liang, J. Massey, C. Waddling and I. Manners, Macromolecules **29**, 3401 (1996).

145. Y. Ni, A.J. Lough, A.L. Rheingold and I. Manners, Angew. Chem. **107**, 1079 (1995); Angew. Chem. Int. Ed. Engl. **34**, 998 (1995).

146. I. Manners, Coord. Chem. Rev. **137**, 109 (1994).

147. (a) A. Durif, *Crystal Chemistry of Condensed Phosphates*, Plenum Press, New York, 1995; (b) A. Durif, in I. Haiduc and D.B. Sowerby (Editors), *The Chemistry of Inorganic Homo- and Heterocycles*, Academic Press, London, 1987, Vol. 2, p. 659; (c) M.T. Averbuch-Pouchot and A. Durif, in P. Zanello (Editor), *Stereochemistry of Organometallic and Inorganic Compounds*, *Vol.5*, *Chains, Clusters, Inclusion Compounds*, Elsevier, Amsterdam, 1994, p. 3.

148. I. Haiduc, *The Chemistry of Inorganic Ring Systems,* Wiley-Interscience, London, 1970, vol. 2, p. 819.

149. (a) E. Thilo and U. Schulke, Angew. Chem. **75**, 1175 (1963); (b) K.H. Jost, Acta Crystallogr. **19**, 555 (1965); (c) E.J. Griffith and R.I. Buxton, Inorg. Chem. **4**, 549 (1965).

150. (a) U. Schulke, Angew. Chem. **7**, 71 (1967); (b) U. Schulke, Z. Anorg. Allg. Chem. **360**, 231 (1968); (c) U. Schulke and N.N. Chudinova, Izv. Akad. Nauk SSSR, Neorg. Mater. **10**, 1697 (1974), Inorg. Mater. (Engl. transl.) **10**, 1459 (1974).

151. (a) M. Bagieu-Boucher, A. Durif and J.C. Guitel, J. Solid State Chem. **40**, 248 (1981), **45**, 159 (1982); (b) U. Schulke, M.T. Averbuch-Pouchot and A. Durif, Z. Anorg. Allg. Chem. **612**, 107 (1992), **620**, 545 (1994); (c) M.T. Averbuch-Pouchot, A. Durif and U. Schulke, J. Solid State Chem. **97**, 299 (1992)

152. (a) A.V. Lavrov, M.Ya. Voitenkov and E.G. Tselebrovskaya, Izv. Akad. Nauk SSSR, Neorg. Mater. **17**, 99 (1981); (b) I. Grunze and N.N. Chudinova, Izv. Akad Nauk SSSR, Neorg. Mater. **24**, 988(1988).

153. (a) S. Ohashi, G. Kura, Y. Shimada and M. Kara, J. Inorg. Nucl. Chem. **39**,1513 (1977); (b) K.H. Jost, Acta Crystallogr. **B 28**, 732 (1972).

154. (a) D.R. Cooper and J.A. Semlyen, Polymer, **13**, 414 (1972); (b) J.A. Semlyen (Editor), *Cyclic Polymers*, Elsevier, London, 1986, Ch.1.

155. (a) E.H. Wong, X.Y. Sun, E.J. Gabe, F.L. Lee and J.P. Charland, Organometallics **10**, 3010 (1991); (b) H. Yang, E.H. Wong, A.L. Rheingold, B.E. Owens-Watermire and B.S Haggerty, Organometallics **13**, 4825 (1994).

156. (a) W.T. Reichle, Tetrahedron Lett. **1962**, 51; (b) H.H. Sisler and C. Stratum, Inorg. Chem. **5**, 2003 (1966); (c) M.J. Begley, D.B. Sowerby and R.J. Tillott, J. Chem. Soc. Dalton Trans. **1974**, 2527; (d) L.K. Krannick, H. Thewalt, W.J. Cook, S.R. Jain and H.H. Sisler, Inorg. Chem. **12**, 2304(1973).

157. W. Ipatiew, G. Razuvaev and V. Stromski, Ber. Dtsch. Chem. Ges. **62**, 598 (1929).

158. (a) H.C. Marsmann and J.R. Van Wazer, J. Am. Chem. Soc. **92**, 3969 (1970); (b) M. Durand and J. P. Laurent, J. Organomet. Chem. **77**, 225 (1974) ; (c) W.S. Sheldrick and T. Hausler, Z. Naturforsch. **48b**, 1069 (1993)

159. (a) A.J. DiMaio and A.L. Rheingold, Organometallics **10**, 3764 (1991); (b) A.M. Arif, A.H. Cowley and M. Pakulski, J. Chem. Soc. Chem. Coomun. **1987**, 165.

160. (a) W.S. Sheldrick and T. Hausler, Z. Anorg. Allg. Chem. **619**, 1984 (1993); (b) T. Hausler and W.S. Sheldrick, Chem. Ber. **130**, 371 (1997); (c) W.S. Sheldrick, Coord. Chem. Rev. 182, 125 (1999).

161. I.M. Miller and W.S. Sheldrick, Z. Naturforsch. **52b**, 951 (1957).

162. (a) A.L. Rheingold and A.J. DiMaio, Organometalllics **5**, 393 (1986); (b) T. Hausler and W.S. Sheldrick, Chem. Ber. **129**, 131 (1996).

684

163. T. Hausler and W.S. Sheldrick, Z. Naturforsch. **52b**, 1997, 679.

164. I.M. Muller and W.S. Sheldrick, Eur. J. Inorg. Chem. **1998**, 1999.

165. A.E. Kretov and A.J. Berlin, Zh. Obshch. Khim. **1**, 411 (1931).

166. T. Hausler and W.S. Sheldrick, Chem. Ber. **129**, 131 (1996).

167. O.M. Kekia and A.L. Rheingold, Organometallics **17**, 726 (1998).

168. M.A. Beswick, M.K. Davies, M.A. Paver, P.R. Raitby, A. Steiner and D.S. Wright, Angew. Chem. **108**, 1660 (1996); Angew. Chem. Int. Ed. Engl. **35**, 1518 (1996).

169. (a) H.J. Breunig, M.A. Mohamed and K.H. Ebert, Z. Naturforsch. **49b**, 877 (1994); (b) M.A. Mohamed, K.H. Ebert and H.J. Breunig, Z. Naturforsch. **51b**, 149 (1996).

170. (a) M.M. Labes, P. Love and L.F. Nichols, Chem. Revs. **79**, 1 (1979); (b) A.J. Banister and I.B. Gorel, Adv. Mater. **10**, 1415 (1998).

171. A.J. Bannister, P.J. Dainty, A.C. Hazzell, J.G. Lomberg, Chem. Comrnun. **1969**, 1187.

172. (a) T. Chivers, in I. Haiduc and D.B. Sowerby, *The Chemistry of Inorganic Homo- and Heterocycles*, Academic Press, London, 1987, p. 793; (b) I. Haiduc, *The Chemistry of Inorganic Ring Systems*, Wiley-Interscience, London, 1970, vol. 2, p. 913, 942, 949 and references therein.

173. G.W. Parshall, R. Cramer and R.E. Foster, Inorg. Chem. **1**, 677 (1962).

174. (a) A.K. Roy, J. Am. Chem. Soc. **114**, 1530 (1992); (b) A.K. Roy, G.T. Burns, G.C. Lie and S. Grigoras, J. Am. Chem. Soc. **115**, 2604 (1993).

175. I. Haiduc and D.B. Sowerby (Editors), *The Chemistry of Inorganic Homo- and Heterocycles*, Academic Press, London, 1987.

176. (a) H.W. Roesky, I. Leichtweis and M. Noltemeyer, Inorg. Chem. **32**, 5102 (1993); (b) F. Palacios, P. Royo, R. Serrano, J.L. Balcazar, I. Fonseca and I. Florencio, J. Organomet. Chem. **375**, 51 (1989); (c) T. Carofiglio, C. Floriani, A. Sgamellotti, M. Rosi, A.Chiesi-Villa and C. Rizzoli, J. Chem. Soc. Dalton Trans. **1992**, 1081; (d) S. Cirueles, T. Cuenca, J.C. Flores, R. Gomez, P. Gomez-Sal and P. Royo, Organometallics **12**, 944 (1993).

177. F. Bottomley, J. Darkwa, L. Sutin and P.S. White, Organometallics **5**, 2165 (1986)

178. G. Fachinetti, C. Floriani, A. Chiesi-Villa and C. Guastini, J. Am. Chem. Soc. **101**, 1767 (1979).

179. (a) F. Bottomley and L. Sutin, Adv. Organomet. Chem. **28**, 339 (1988); (b) F. Bottomley, Polyhedron **11**, 1707(1992).

180. H. Plenio, H.W. Roesky, M. Noltemeyer and G.M. Sheldrick, Angew. Chem. **100**, 1377 (1988); Angew. Chem. Int. Ed. Engl. **27**, 1330(1988).

181. (a) H.W. Roesky, P. Olms, R. Hasselbring, N. Winkhofer, F.Q. Liu and M. Noltemeyer,

Phosphorus, Sulfur & Silicon, **76**, 255 (1993); (b) P. Olms, H.W. Roesky, K. Keller, M. Noltemeyer, R. Bohra, H.G. Schmidt and D. Stalke, Chem. Ber. **124**, 2655 (1991); (c) R. Hasselbring, H.W. Roesky and M. Noltemeyer, Angew. Chem. **104**, 613 (1992); (d) S.K. Pandey, A. Steiner, H.W. Roesky and D. Stalke, Inorg. Chem. **32**, 5444 (1993); (e) A. Haoudi-Mazzah, A. Mazzah, H.G. Schmidt, M. Noltemeyer and H.W. Roesky, Z. Naturforsch. **46b**, 587 (1991); (f) F.Q. Liu, H.G. Schmidt, M. Noltemeyer, C. Freire-Erdbrugger, G.M. Sheldrick and H.W. Roesky, Z. Naturforsch. **47b**, 1085 (1992); (g) H.J. Gosink, H.W. Roesky, H.G. Schmidt, M. Noltemeyer, E. Inner and R. Herbst-Irmer, Organometallics **13**, 3420 (1994); (h) F.Q. Liu, I. Uson and H.W. Roesky, Z. Anorg. Allg. Chem. **622**, 819 (1996); (i) K. Dehnicke and J. Strahle, Polyhedron **8**, 707 (1989).

182. (a) H.W. Roesky, Synlett **1990**, 651; (b) T. Lubbeen, M. Witt, H.W. Roesky, M. Noltemeyer and H.G. Schmidt, Inorg. Chem. **34**, 4275 (1995); (c) F.Q. Liu, I. Uson and H.W. Roesky, J. Chem. Soc. Dalton Tram. **1995**, 2453; (d) F.Q. Liu, I. Uson, H.W. Roesky, Z. Anorg Allg. Chem. **622**, 819 (1996); (e) A. Haoudi-Mazzah, A. Mazzah, H.G. Schmidt, M. Noltemeyer and H.W. Roesky, Z. Naturforsch. **46b**, 587 (1991); (f) F.Q. Liu, H.G. Schmidt, M. Noltemeyer, C. Freire-Erdbrugger, G.M. Sheldrick and H.W. Roesky, Z. Naturforsch. **47b**, 1085 (1992).

183. (a) A.J. Elias, H.G. Schmidt, M. Noltemeyer and H.W. Roesky, Eur. J. Inorg. Solid State Chem. **29**, 23 (1992); (b) A.J. Elias, H.W. Roesky, W.T. Robinson and G.M. Sheldrick, J. Chem. Soc. Dalton Trans.**1993**, 495.

184. H.W. Roesky, in H.W. Roesky (Editor), *Rings, Clusters and Polymers of Main group and Transition Elements*, Elsevier, Amsterdam, 1989, p. 394.

185. H.J. Koch, H.W. Roesky, R. Bohra, M. Noltemeyer and H.G. Schmidt, Angew. Chem. **104**, 612 (1992); Angew. Chem. Int. Ed. Engl. **31**, 598 (1992);

186. (a) H.W. Roesky, Synlett **1990**, 651; (b) H.W. Roesky, P. Olms, R. Hasselbring, N. Winkhofe, F.Q. Liu and M. Noltemeyer, Phosphorus, Sulfur & Silicon, **76**, 255 (1993); (c) M. Shakir and H.W. Roesky, Phosphorus, Sulfur & Silicon, **93-94**, 13 (1994); (d) H. Plenio, M. Witt, F.T. Edelmann, T. Henkel, M. Noltemeyer, F. Pauer, D. Stalke, G.M. Sheldrick and H.W. Roesky, Phosphorus, Sulfur & Silicon **41**, 335 (1989); and references therein.

187. M. Witt and H.W. Roesky, Chem. Rev. **94**, 1163 (1994).

188. H.W. Roesky and M. Lucke, Angew. Chem. **101**, 480 (1989); Angew. Chem. Int. Ed. Engl. **28**, 493 (1989).

189. W.K. Leong, R.K. Pomeroy, R.J. Batchelor, F.W.B. Einstein and C.F. Campana, Organometallics **16**, 1079 (1997).

190. M. Bettenhausen and D. Fenske, Z. Anorg. Allg. Chem. **625**, 13 (1999).

191. I. Haiduc and F.T. Edelmann, *Supramolecular Organometallic Chemistry*, Wiley-VCH 1999, Chapter 3.

192. A. Haaland, *Angew. Chem.* 1989, **101**, 1017; *Angew. Chem. Int. Ed. Engl.* 1989, **28**, 992.

193. A. Haaland, in G.H. Robinson (Editor), *Coordination Chemistry of Aluminum*, VCH

Publishers, Weinheim, 1993, Chapter 1, p.1.

194. B. König, *Europ. Chem. Chronicle* 1998, **3**, 17.

195. J.M. Lehn, *Supramolecular Chemistry.Concepts and Perspectives,* VCH Weinheim, 1995, Chapter 9.

196. (a) E. Wiberg and K. Schuster, Z. Anorg. Allg Chem. **213**, 77, 89 (1935); (b) H. Noth and H. Vahrenkamp, Chem. Ber. **100**, 3353 (1967); (c) W. Maringgelle, in I. Haiduc and D.B. Sowerby (Editors), *The Chemistry of Inorganic Homo- and Heterocycles*, Academic Press, London, Vol. 1, p. 74.

197. (a) M.G. Walawalkar, R. Murugavel and H.W. Roesky, Eur.J. Solid State Inorg. Chem. **33**, 943 (1996); (b) E.F. Murphy, R. Murugavel and H.W. Roesky, Chem. Rev. **97**, 3425 (1997); (c) B. Neumuller, *Coord. Chem. Rev.* 1997, **158**, 69; (d) H. Dorn, E.F. Murphy, S.A.A. Shah and H.W. Roesky, J. Fluorine Chem. **86**, 121(1997); (e) B.R. Jagirdar, E.M. Murphy and H.W. Roesky, Progr. Inorg. Chem. in press.

198. (a) G.H. Robinson (Editor), *Coordination Chemistry of Aluminum*, Wiley-VCH, New York, 1993; (b) J.P. Oliver, *J. Organomet. Chem.* 1995, **500**, 269.

199. J. Boersma and J.G. Noltes, Tetrahedron Letters, **1966**, 1521.

200. P.T. Moseley and H.M.M. Shearer, J. Chem. Soc. Dalton Trans. **1973**, 65.

201. A. Muller, B. Neumuller and K. Dehnicke, Angew. Chem. **109**, 244 (1997); Angew. Chem. Int. Ed. Engl. **36**, 2350 (1997).

202. G.E. Coates and D. Ridley, J. Chem. Soc. A, **1966**, 1064.

203. J.G. Noltes and J. Boersma, J. Organomet Chem. **12**, 425 (1968).

204. M. Parvez, G.L. BergStresser and H.G. Richey, Acta Cryst **C 48**, 641 (1992).

205. M.M. Olmstead, P.P. Power and S.C. Shoner, J. Am. Chem. Soc. **113**, 3379 (1991).

206. I.B. Gorrell, A. Looney, G. Parkin and A.L. Rheingold, J. Am. Chem. Soc. **112**, 4068 (1990).

207. F.H. Van der Steen, J. Boersma, A.L. Spek and G. Van Koten, J. Organomet. Chem. **390**, C21 (1990); Organometallics **10**, 2467 (1991).

208. W.A. Hermann, S. Bogdanovich, J. Behm and M. Denk, J. Organomet. Chem. **430**, C33 (1992).

209. M.M. Olmstead, P.P. Power and S.C. Shoner, J. Am. Chem. Soc. **113**, 3379 (1991).

210. K. Ruhlandt-Senge and P.P. Power, Inorg. Chem. **32**, 4505 (1993).

211. (a) G.W. Adamson, N.A. Bell and H.M.M. Shearer, Acta Cryst **B 38**, 462 (1982);
 (b) G.W. Adamson and H.M.M. Shearer, Chem. Commun. **1969**, 897.

212. (a) J.G. Noltes and J. Boersma, J. Organomet Chem. 1969, **16**, 345; (b) N.A. Bell, H.M.M. Shearer and C.B. Spencer, Acta Cryst. **C 39**, 1182 (1983).

213. M.G. Davidson, D. Elilio, S. Liless, A. Martin, P.R. Raithby, R. Snaith and D.S. Wright, Organometallics **12**,1 (1993).

214. S.S. Al-Juaid, N.H. Buttrus, C. Eaborn, P.B. Hitchcock, J.D. Smith and K. Tavakkoli, J. Chem. Soc. Chem. Commun. **1988**, 1389.

215. (a) B.L. Benac, A.M. Cowley, R.A. Jones, C.M. Nunn and T.C. Wright, J. Am. Chem. Soc. **111**, 4986 (1989); (b) M. Green and P.O'Brien, Advan. Mater. **10**, 527 (1998).

216. (a) G.H. Robinson (Editor), *Coordination Chemistry of Aluminum*, VCH, Weinheim, 1993; (b) A.J. Downs (Editor), *Chemistry of Aluminum, Gallium, Indium and Thallium*, Chapmann & Hall, London, New York, 1993; (c) C.E. Holloway and M. Melnik, J. Organomet. Chem. **543**, 1 (1997); (d) B. Neumuler, Coord. Chem. Rev. **158**, 69 (1997); (e) J.P. Oliver, J. Organomet Chem. **500**, 269 (1995); (f) I. Haiduc, *The Chemistry of Inorganic Ring Systems*, Wiley-Interscience, London, 1970; (g) I. Haiduc and D.B. Sowerby (Editors), *The Chemistry of Inorganic Homo and Heterocycles*, Academic Press, London, 1987.

217. (a) Y. Yang, H.G. Schmidt, M. Noltemyer, J. Pinkas and H.W. Roesky, J. Chem. Soc. Dalton Trans. **1996**, 3609; (b) M.G. Walawalkar, R. Murugavel, H.W. Roesky and H.G. Schmidt, Inorg. Chem. **36**, 4202 (1997); (c) Y. Yang, M.G. Walawalkar, J. Pinkas, H.W. Roesky, H.G. Schmidt, Angew. Chem. **110**, 101 (1998); Angew. Chem. Int. Ed. Engl. **37**, 96 (1998); (d) M.R. Mason, J. Cluster. Sci. **9**, 1 (1998); (e) A. R. Barton, Chem. Soc. Rev. **22**, 93, 1993; (f) C.J. Harlan, M.R. Mason and A.R. Barron, Organometallics, **13**, 2957 (1994); (g) C.J. Harlan, E.G. Gillan, S.G. Bott and A.R. Barron, Orgnometallics **15**, 5479 (1996); (h) M.B. Power, J.W. Ziller and A.R. Barron, Organometallics **11**, 2783 (1992); (i) M.D. Healy, .B. Power and A.R. Barron, Coord. Chem. Rev. **130**, 63; (j) A.R. Barron, Comments Inorg. Chem. **14**, 123 (1993); (k) M. Cesari and S. Cucinella, in vol. *The Chemistry of Inorganic Homo- and Heterocycles*, I. Haiduc and D.B. Sowerby (Editors), Academic Press, London, 1987, Vol.1, Chapter 6, p. 167.

218. (a) T.D. Getman and G.W. Franklin, Comments Inorg. Chem. **17**, 79 (1995); (b) S.M. Stuczynski, R.L. Opila, P. Marsh, J.G. Brennan and M.L. Steigerweld, Chem. Mater. **3**, 379 (1991).

219. (a) J.J.Eisch and W.C. Kaska, J. Am. Chem. Soc. **88**, 2976 (1966); (b) J. Weidlein and V. Krieg, J. Organomet Chem. **17**, 41 (1969); (c)V. Krieg and J. Weidlein, **21**, 281 (1970).

220. K. Brendhaugen, A. Haaland and D.P. Novak, Acta Chem.Scand. **28A**, 45 (1974).

221. C.N. McMahon, J.A. Francis and A.R. Barron, J. Chem. Cryst. **27**, 191, 1997.

222. M.A. Petrie, P.P. Power, H.V. Rasika Dias, K. Ruhlandt-Senge, K.M. Waggoner and R.J. Wehmschulte, Organometallics, **12**, 1086 (1993).

223. P.R. Schonberg, R.T. Paine, C.F. Campana and E.N. Duesler, Organometallics, **1**, 799 (1982).

224. H.J. Koch, S.Schultz, H.W. Roesky, M. Noltemeyer, H.G. Schmidt, A. Heine, R. Herbst-

Irmer, D. Stalke and G.M. Scheldrick, Chem. Ber. **125**, 1107 (1992)

225. (a) A.W. Apblett, A.C. Warren and A.R. Barron, J. Mater. Chem. **3**, 597 (1993); (b) C. Landry, J.A. Davis, A.W. Apblett and A.R. Barren, J. Mater. Chem. **3**, 597 (1993).

226. J.P. Oliver and R. Kumar, Polyhedron **9**, 409 (1990); (b) S. Pasynkiewicz, Polyhedron **9**, 429 (1990).

227. (a) B. Cetinkaya, P.B. Hitchcock, H.A. Jasim, M.F. Lappert and H.D. Williams, Polyhedron **9**, 239 (1990); (b) R. Kumar, M.L. Sierra, V. Srini, J. de Mel and J.P. Oliver, Organometallics **9**, 484 (1990).

228. M.R. Mason, J.M. Smith, S.G. Bott and A.R. Barren, J. Am. Chem. Soc. **115**, 4971 (1993).

229. P.J. Wheatley, J. Chem. Soc. **1963**, 2562.

230. D.G. Hendershot, R. Kumar, M. Barber and J.P. Oliver, Organometllics 1991, **10**, 1917.

231. C.N. McMahon, S.G. Bott and A.R. Barton, J. Chem. Soc. Dalton Trans. **1997**, 3129.

232. A. Haaland, O. Stokkeland and J. Weidlein, J. Organomet Chem. **94**, 353 (1975).

233. V.J.S. De Mel, R. Kumar and J.P. Oliver, Organometallics **9**, 1303 (1990).

234. M. Tagiof, M.J. Heeg, M. Bailey, D.G. Dick, P. Kumar, D.G. Hendershot, H. Raibanoohi and J.P. Oliver, Organometallics **14**, 2903 (1995).

235. (a) S.D. Waeszada, F.Q. Liu, E.F. Murphy, H.W. Roesky, M. Treichert, I. Uson, H.G. Schmidt, T. Albers, E. Parisini and M. Noltemeyer, Organometallics, **16**, 1260, 1997; (b) S.D. Waeszada, C. Rennekamp, H.W. Roesky, C. Ropken and E. Parisini, Z. Anorg. Allg. Chem. **624**, 987 (1998); (c) D.C. Bradley, I.S. Harding, I.A. Maia and M. Motevalli, J. Chem. Soc. Dalton Trans. **1997**, 2969; (d) S. Kuhner, K.W. Klinkenhammer, W. Schwarz and J. Weidlein, Z. Anorg. Allg. Chem. **624**, 1051 (1998).

236. L.V. Interrante, G.A. Sigel, M. Garbauskas, C. Hejna and G.A Slack, Inorg. Chem. **28**, 252 (1989).

237. G.M. McLaughlin, G.A. Sim and J.D. Smith, J. Chem. Soc. Dalton Trans. **1972**, 2197.

238. (a) D.A. Atwood and D. Rutherford, Main Group Chem. **1**, 431 (1996); (b) M.A. Petrie, K. Ruhland-Senge and P.P. Power, Inorg. Chem. **32**, 1135 (1993).

239. A. Miehr, O. Ambacher, T. Metzger, E. Born and A. Fischer, Chem. Vap. Deposition **2**, 51 (1996).

240. (a) G.E. Coates and J. Graham, J. Chem. Soc. **1963**, 233; (b) E. Hey-Hawkins, M.F. Lappert, J.L . Atwood and S.G. Bott, J. Chem. Soc. Dalton Trans. **1991**, 939; (c) O.T. Beachley and G.E. Coates, J. Chem. Soc. **1965**, 3241.

241. J.F. Janik, E.N. Duesler, W.F. McNamara, M. Westerhausen and R.T. Paine,

Organometallics **8**, 506 (1989).

242. A.P. Purdy, R.L. Wells, A.T. McPhail and C.G. Pitt, Organomctallics **6**, 2099 (1987)

243. O.T. Beachley Jr, R.B Hallock, H.M. Zhang and J.L. Atwood, Organomctallics **4**, 1675 (1985).

244. D. C. Bradley, H. Chudzynska, M.M. Factor, D.M. Frigo, M.B. Hursthouse, B. Hussein and L.M. Smith, Polyhedron, **7**, 1289 (1988).

245. (a) M.E. Kenney and A.W. Laubengayer, J. Am. Chem. Soc. **76**, 4839 (1954); (b) G.S. Smith and J.L. Hoard, J. Am. Chem. Soc. **81,** 3907 (1959).

246. (a) A.A. Naiini, V. Young, H. Han, M. Akinc and J.G. Verkade, Inorg. Chem. **32**, 3781 (1993); (b) D.A. Atwood, A.H. Cowley, P.R. Harris, R.A. Jones, S.U. Koschmieder, C.M. Nunn, J.L. Atwood and S.G. Bott, Organometallics **12**, 24 (1993).

247. Q. Zhao, H. Sun, W. Chen, C. Duan, Y. Liu, Y. Pan and X. You, Organometallics **17**, 156 (1998).

248. C. Schnitter, H.W. Roesky, T. Albers, H.G. Schmidt, C. Ropken, E. Parisini and G.M. Sheldrick, Chem. Eur. J. **3**, 1783 (1997).

249. J. Storre, T. Belgardt, D. Stalke and H.W. Roesky, Angew. Chem. **106**, 1365 (1994); Angew. Chem. Int. Ed. Engl. **33**, 1244 (1994).

250. W.M. Cleaver and A.R. Barron, Organometallics **12**, 1001 (1993).

251. M.A. Petrie, M.M. Olmstead and P.P. Pwer, J. Am Chem. Soc. **113**, 8704 (1991).

252. (a) H. Schmidbaur and F. Schindler, Chem. Ber. **99**, 2178 (1966); (b) M.B. Power, W.M. Cleaver, A.W. Apblett, A.R. Barron and J.W. Ziller, Polyhedron **11**, 477 (1992; (c) W.M. Cleaver, A.R. Barron, A.R. McGuffey and S.G. Bott, Polyhedron **13**, 2831 (1994).

253. A.H. Cowley, S.K. Mehrotra, J.L. Atwood and W.E. Hunter, Organometallics **4**, 1115 (1985).

254. (a) D.J. Browning, J.M. Corkers and M. Webster, Acta Crystallogr. **C 52**, 882, 1996;

(b) C.C. Landry, A. Hynes, A.R. Barron, I. Haiduc and C. Silvestru, Polyhedron 1996, **15**, 391.

255. (a) D.G. Hendershot, R. Kumar, M. Barber and J.P. Oliver, Organometallics **10**, 1917 (1991); (b) A. Boardman, S.E. feffs, R.W.H. Small and I.J. Worrall, Inorg. Chim. Acta **1985**, L 39; (c) S.U. Ghazi, M.J. Heeg and J.P. Oliver, Inorg. Chem. **33**, 4517 (1994).

256. M.B. Power, J.W. Ziller and A.R. Barron, Organometallics **11**, 2783 (1992).

257. (a) R. Kumar, D.G. Dick, S.U. Ghazi, M. Taghiof, M.J. Heeg and J.P. Oliver, Organometallics **14**, 1601 (1995); (b) H. Rahbarnoohi, R.L. Wells, L.M. Liable-Sands, G.P. Yap and A.L. Rheingold, Organometallics **16**, 3959 (1997).

258. G.C. Hoffmann and R. Fischer, Inorg. Chem. **28**, 4165 (1989).

259. (a) K.M. Waggoner and P.P. Power, J. Am. Chem. Soc. **113**, 3385 (1991); (b) S.J. Schauer, C.H. Lake, C.L. Watkins, L.K. Krannich and D.H. Powell, J. Organomet. Chem. **549**, 31 (1997); (c) M.A. Banks, O.T. Beachley Jr., H.J. Gysling and H.R. Luss, Organometallics **9**, 1979 (1990).

260. (a) D.A. Atwood, A.H. Cowley, P.R. Harris, R.A. Jones, S.U. Koschmieder, C.M. Nunn, J.L. Atwood and S.G. Bott, Organometallics **12**, 24 (1993); (b) A. Storr, J. Chem. Soc. A **1968**, 2605.

261. (a) K.M. Waggoer and P.P. Power, J. Am. Chem. Soc. **113**, 3385 (1991); (b) S.J. Schauer, C.H. Lake, C.L. Watkins, L.K. Krannich and D.H. Powell, J. Organomet. Chem. **549**, 31 (1997); (c) J.T. Park, Y. Kim, J. Kim, K. Kim and Y. Kim, Organometallics **11**, 3320 (1992); (b) O.T. Beachley Jr., M.J. Noble, M.R. Churchill and C.H. Lake, Organometallics **11**, 1051 (1992;

262. (a) T.Belgardt, H.W. Roesky, M. Noltemeyer and H.G. Schmidt, Angew. Chem. **105**, 1101 (1993), Angew. Chem. Int. Ed Engl. **32**, 1056 (1993); (b) C. Schnitter, S.D. Waeszada, H.W. Roesky, M. Teichert, I. Uson and E. Parisini, Organometallics **16**, 1197 (1997).

263. (a) A.H. Cowley and R.A. Jones, Angew. Chem. **101**, 1235 (1989), Angew. Chem. Int. Ed Engl. **28**, 1208 (1989); (b) A.H. Cowley, J. Organomet. Chem. **400**, 71 (1990): (c) R.L. Wells, Cord Chem. Rev. **1992**, 273; (d) Y. Pan and P. Boudjouk, Main Group Chem. **1**, 61 (1995).

264. (a) D.A. Atwood, A.H. Cowley, P.R. Harris, R.A. Jones, S.U. Koschmieder and C.M. Nunn, J. Organomet Chem. **449**, 61 (1993); (b) O.T. Beachley Jr., J.D. Maloney and R.D. Rogers, J. Organomet Chem **449**, 69 (1993); (c) A.H. Cowley, R.A. Jones, M.A. Mardones and C.M. Nunn, Organometallics **10**, 1635 (1991); (d) R.L. Wells, A.P. Purdy, A.T. McPhail and C.G. Pitt, J. Organomet Chem. **308**, 281 (1986); (e) R.L. Wells, J.W. Pasterczyk, A.T. McPhail, J.D. Johansen and A. Alvanipour, J. Organomet Chem. **407**, 17 (1991) and references therein.

265. T. Krauter and B Neumuller, Z. Anorg. Allg. Chem. **621**, 597 (1995).

266. (a) J.T. Leman and A.R. Barron, Organometallics **8**, 2214 (1989); (b) J.T. Leman, J.W. Ziller and A.R. Barron, Organometallics **10**, 1766 (1991).

267. S.L. Stoll, S.G. Bott and A.R. Barron, Polyhedron **16**, 1763 (1997).

268. [1] D.C. Bradley, D.M. Frigo, M.B. Hursthouse and B. Hussain, Organometallics **7**, 1112 (1988).

269. H. Rahbarnoohi, M. Taghiof, M.J. Heeg, D.G. Dick and J.P. Oliver, Inorg. Chem. **33**, 6307 (1994).

270. (a) J.D. Aitchison, J.D.J. Backer-Dirs, D.C. Bradley, M.M. Faktor, D.M. Frigo, M.B. Hursthouse, B. Hussain and R.L. Short, J. Organomet Chem. **366**, 11 (1989); (b) G. Rossetto, D.A.N. Brianese, U. Casellato, F. Ossola, M. Porchia, A. Vitadini, P. Zanella and R. Graziani, Inorg. Chim Acta **170**, 95 (1990); (c) M. Trapp. H.D. Hausen, G. Welckler and J. Weidlein, J. Organomet Chem. **450**, 53 (1993); (d) B. Neumuller, Chem. Ber. **122**, 2283 (1989); (e) B. Neumuller, Z. Naturforsch. **45b**, 1559 (1990).

271. A.H. Cowley, R.A. Jones, M.A. Mardones and C.M. Nunn, Organometallics **10**, 1635

(1991).

272. (a) O.T. Beachley Jr., J.D. Maloney, M.A. Banks and R.D. Rogers, Organometallics **14**, 3448 (1995); (b) R.L. Wells, A.T. McPhail, L.J. Jones, and M.F. Self, J. Organomet. Chem. **449**, 85 (1993); (c) R.L. Wells, A.T. Mc Phail, L.J. Jones, and M.F. Self, Polyhedron **12**, 141 (1993); (d) B. Werner and B. Neumuller, Organometallics **15**, 4258 (1996) and references therein.

273. (a)T. Douglas and K.H. Theopold, Inorg. Chem. **30**, 594 (1991); (b) S.M. Stuczynski, R.L. Opila, P. Marsh, J.G. Brennan and M.L. Steigerwald, Chem. Mater. **3**, 379 (1991).

274. (a) R.L. Wells, L.J. Jones, A.T. McPail and A. Alvanipour, Organometallics **10**, 2345 (1991); (b) R.L. Wells, A.T. McPhail, L.J. Joes and M.F. Self, Polyhderon **12**, 141 (1993); (c) A. Dashti-Mommertz, B. werner and B. Neumuller, Polyhedron **17**, 525 (1998); (d) A.H. Cowley, R.A. Jones, K.B. Kidd, C.M. Nunn and D.L. Westmoreland, J. Organomet. Chem., **341**, Cl (1988).

275. C. Glidewell and D.C. Liles, Acta Crystallogr. **B 34**, 129 (1978).

276. U. Wannagat,V. Damrath, V. Huch, M. Veith and U. Harder, J. Organomet. Chem. **443**, 153 (1993).

277. T.P. Lockhart, J. Organomet. Chem. **287**, 179 (1985).

278. H. Reuter and H. Puff, J. Organomet. Chem. **379**, 223 (1989).

279. B. Zobel, M. Schurmann, K. Jurkschat, D. Dakternieks and A. Duthie, Organometallics **17**, 4096 (1998).

280. A.M. Domingos and G.M. Sheldrick, Acta Crystallogr. **B 30**, 519 (1974).

281. (a) E.R.T. Tiekink, Trends Organomet. Chem. **1**, 71 (1994); (b) D.R. Smyth and E.R.T. Tiekink, Z. Kristallogr. **213**, 605 (1998).

282. (a) M. Gielen, A. El Khloufi, M. Biesemans, F. Kayser, R. Willem, B. Mahieu, D. Maes, J.N. Lisgartea, L. Wyns, A. Moreira, T.K. Chattopadhay and R.A. Palmer, Organometallics **13**, 2849 (1994); (b) S.W. Ng, V.G. Kumar Das, G. Pelizzi and F. Vitali, Heteroatom Chem. **1**, 433 (1990).

283. E.R.T. Tiekink, Appl. Organomet. Chem. **5**, 1 (1991).

284. J. Meunier-Piret, M. Boualam, R. Willem and M. Gielen, Main Group Chem. **16**, 329 (1993).

285. T.P. Lockhart, Organometallics **7**, 1438 (1989).

286. K.C. Molloy, F.A.K. Nasser, C.L. Barnes, D. van der Helm and J.J. Zuckerman, Inorg. Chem. **21**, 960 (1982).

287. J.G. Masters, F.A.K. Nasser, M.B. Hossain, A.P. Hagen, D. van der Helm and J.J. Zuckerman, J. Organomet. Chem. **39**, 385 (1990).

288. M.G. Newton, I. Haiduc, R.B. King and C. Silvestru, J. Chem. Soc., Chem. Commun. **1993**, 1229.

289. (a) F. Weller and A.F. Shihada, J. Organomet. Chem. 322, 185 (1987); (b) A.F. Shihada and F. Weller, Z. Naturforsch. **50b**, 1343 (1995).

290. S.J. Blunden, R. Hill and D.G. Gillies, J. Organomet. Chem. **270**, 39 (1984).

291. J.N. Pandey and G. Srivastava, J. Organomet. Chem. **354**, 301 (1988).

292. (a) N.W. Alcock, Adv. Inorg. Chem. Radiochem. **15**, 1 (1972); (b) N.W. Alcock and R.M. Contryman, J. Chem. Soc. Dalton Trans. **1977**, 217.

293. G.A. Landrum and R. Hoffmann, Angew. Chem. **110**, 1989 (1998); Angew. Chem. Int. Ed. Engl. **37**, 1887 (1998).

294. N.W. Alcock, *Bonding and Structure. Structural Principles in Inorganic and Organic Chemistry.* Ellis Horwood, New Yoek, London, 1993, p. 195.

295. I Haiduc, Coord. Chem. Rev. **158**, 325 (1997).

296. I. Haiduc and F.T. Edelmann, *Supramolecular Organometallic Chemistry*, Wiley-VCH, Weinheim, 1999, Chapter 4.

297. G. Becker and O. Mundt, in B. Krebs (Editor), *Unkonventionelle Wechselwirkungen in der Chemie metallischer Elements*, VCH Winhem, 1992, p. 199.

298. G. Becker, G. Gutenkunst and C. Witthauer, Z. Anorg. Allg. Chem. **486**, 90 (1982).

299. (a) G. Mundt, H. Riffel, G. Becker and A. Simon, Z. Naturforsch. **B 39**, 317 (1984); (b) A.J. Ashe III, E.G. Ludwig Jr., J. Oleksyszyn and J.C. Huffman, Organometallics **3**, 337 (1984).

300. A.J. Ashe III, Adv. Organomet. Chem. **30**, 77 (1990).

301. (a) G. Becker, H. Freundenblum and C. Witthauer, Z. Anorg. Allg. Chem. **492**, 37 (1982); (b) S. Roller, M. Drager, H.J. Breunig, M. Ates and J. Gulec, J. Organomet. Chem. **378**, 327 (1989); (c) S. Roller, M. Drager, H.J. Breunig, M. Ates and J. Gulec, J. Organomet. Chem. **329**, 319 (1989); (d) G. Becker, M. Meiser, O. Mundt and J. Weidlein, Z. Anorg. Allg. Chem. **569**, 62 (1989); (e) K. von Deuten and D. Render, Cryst. Struct. Commun. **9**, 167 (1980).

302. (a) J.D. Lee and M.W.R. Bryant, Ada Crystallogr. **B 55**, 2094 (1969), (b) R.E. Marsh, Acta Crystallogr. **5**, 458 (1952).

303. (a) H. Schmidbaur, Chem. Soc. Rev. **24**, 383 (1995); (b) D.M.P. Mingos, J. Chem. Soc. Dalton Trans. **1996**, 561.

304. D.S. Egleton, D.F. Chodosh, R.L. Webb and L.L. Davies, Acta Crystallogr. **C 42**, 36 (1986); (b) T.J. Mathieson, A.G. Landon, N.B. Milestone and B.K. Nicholson, Chem. Commun. **1998**, 371; (c) C.M. Che, H.K. Yip, W.T. Wong and T.F. Lai, Inorg. Chim. Acta **197**, 177 (1992);

(d)D.M.P. Mingos, S. Menzer, D.J. Williams and J. Yau, Angew. Chem. **107**, 2045 (1995), Angew. Chem. Int. Ed. Engl. **34**, 1894 (1995).

305. P. Hitchcock, J.M. Keats and G.A. Lawless, J. Am. Chem. Soc. **120**, 599 (1998).

306. M. Tschinkl, A. Schier, J. Reide, G. Mehltretter and F.P. Gabbai, Organometallics **17**, 2924 (1998).

307. J.S. Casas, A. Castineiras, I. Haiduc, A. Sanchez, J. Sordo and E.M. Vazquez-Lopez, Polyhedron **16**, 781 (1997).

308. E.M. Vazquez-Lopez, A. Castineiras, A. Sanchez, J. Casas and J. Sordo, J. Cryst. Spectr. Res. **22**, 403 (1992).

309. J. Zukerman-Schpector, E.M. Vazquez-Lopez, A. Sanchez, J.S. Casas and J. Sordo, J. Organomet. Chem., **405**, 67 (1991).

310. J.S. Casas, A. Castineiras, A. Sanchez, J. Sordo and E.M. VBazquez-Lopez, J. Organomet. Chem. **468**, 1 (1994).

311. O.T. Beachley Jr., J.D. Maloney, M.R. Churchill and C.H. Lake, Organometallics **10**, 3568 (1991).

312. K. Mertz,. Schwarz, F. Zettler and H.D. Hausen, Z. Naturforsch. **30 b**, 159 (1975).

313. (a) R. Carballo, J.S. Casas, E.E. Castellano, A. Sanchez, J. Sordo, E.M. Vazquez-Lopez and J. Zukerman-Schpector, Polyhedron **16**, 3609 (1997); (b) J.S. Casas, A. Sanchez, J. Sordo, E.M. Vazquez-Lopez, E.E. Castellano and J. Zukerman-Schpector, Polyhedron **11**, 2889 (1992); (c) J.S. Casas, E.E. Castellano, A. Castineiras, A. Sanchez, J. Sordo, .M. Vazquez-Lopez and J. Zukerman-Schpector, J. Chem. Soc. Dalton Trans. **1995**, 1403.

314. J.S. Casas, A. Castineiras, I. Haiduc, A. Sanchez, J. Sordo and E.M. Vazquez-Lopez, Polyhedron **13**, 1805 (1994).

315. (a) J.L. Lefferts, K.C. Molloy, M.B. Hoassain, D. Van der Helm and J.J. Zuckerman, J. Organomet. Chem. **240**, 349 (1982); (b) M.B. Hossain J.L. Lefferts, K.C. Molloy, D. van der Helm and J.J. Zuckerman, Inorg. Chim. Acta **36**, L 409 (1979).

316. S.W. Ng, Acta Crystallogr. **C 53**, 56 (1997).

317. S. Calogero, P. Gans, V. Peruzzo and G. Tagliavini, J. Organomet. Chem. **179**, 145 (1979).

318. J.S. Tse, F.L. Lee and E.J. Gabe, Acta Crystallogr. **C 42**, 1876 (1986).

319. A.G. Davies, H.J. Milledge, D.C. Puxley and P.J. Smith, J. Chem. Soc. A, **1970**, 2862.

320. N.W. Alcock and J.F. Sawyer, J. Chem. Soc. Dalton Trans. **1977**, 1090

321. J.F. Sawyer, Acta Crystallogr. **C 44**, 633 (1988).

322. P. Ganis, G. Valle, D. Furlani and G. Tagliavini, J. Organomet. Chem. **302**, 165 (1986).

694

323. M.M. Amini, E.M. Holt and J.J. Zuckerman, J. Organomet. Chem. **327**, 147 (1987).

324. N.G. Bokii and Yu. T. Struchkov, J. Struct Chem. USSR (Engl. Trans.) **13**, 619 (1972), Zh. Strukt. Khim. 13, 665 (1972).

325. S.W. Ng, P.G. Parsons, K.Y. Sim, C.J. Tranter, R.H. White and D.J. Young, Appl. Organomet. Chem. **11**, 577 (1997).

326. (a) R.C. Mehrotra and V.D. Gupta, J. Organomet. Chem. **4**, 145 (1965); (b) W.J. Considine, J. Organomet. Chem. **5**, 263 (1966); (c) J.C. Pommier and J. Valade, J. Organomet. Chem. **12**, 433 (1968); (d) G. Domazetis, R.J.Magee and B.D. James, J. Inorg. Nucl. Chem. **41**, 1546 (1979).

327. (a) A.G. Davies, A.L. Price, H.M. Daves and M.B. Hursthouse, J. Organomet. Chem. **270**, Cl (1984); (b) A.G. Davies, A.L. Price, H.M. Daves and M.B. Hursthouse, J. Chem. Soc. Dalton Trans. **1986**, 297.

328. (a) T.B.Grindley, R.E. Wasylishen, R. Thangarasa, W.P. Power and R.D. Curtis, Can. J. Chem. **70**, 205 (1992); (b) T.B. Gridley and Thangarasa, J. Am. Chem. Soc. **112**, 1364 (1990); (c) R.H. Herber, A. Shanzer and J. Libman, Organometallics **3**, 586 (1984).

329. (a) M. Drager, Z. Anorg. Allg. Chem. **477**, 154 (1981); (b) A.S. Secco and J. Trotter, Acta Crystallogr. **C 39**, 451 (1983).

330. (a) A.G. Davies, S.D. Slater, D.C. Povey and G.W. Smith, J. Organomet. Chem. **352**, 283 (1988); (b) P.A. Bates, M.B. Hursthouse, A.G. Davies and S.D. Slater, J. Organomet. Chem. **363**, 45 (1989).

331. D. Zhang, S.Q. Du and A. Weiss, Z. Naturforsch. **46a**, 337 (1991).

332. R. Hillwig, F. Kunkel, K. Harms, B. Neumuller and K. Dehnicke, Z. Naturforsch. **52b**, 149 (1997).

333. (a) H. Preut and F. Huber, Z. Anorg. Allg. Chem. **435**, 234 (1977); (b) U. Fahrenkampf, M. Schurmann and F. Huber, Acta Crystallogr. **C 50**, 1252 (1994).

334. M. Mammi, V. Busetti and A. Del Pra, Inorg. Chim. Acta **1**, 419 (1967).

335. F.T. Edelmann, I. Haiduc, C. Silvestru, M.Schmidt and M. Noltemeyer, Polyhedron **17**, 2943 (1998).

336. (a) I. Haiduc, D.B. Sowerby and S.F. Lu, Polyhedron **14**, 3389 (1996); (b) I. Haiduc and D.B. Sowerby, Polyhedron **15**, 269 (1996).

337. (a) C. Silvestru, I. Haiduc, R. Cea-Olivares and S. Hernandez-Ortega, Inorg. Chim. Acta **233**, 151 (1995); (b) K.H. Ebert, H.J. Breunig, C. Silvestru, I. Stefan and I. Haiduc, Inorg. Chem. **33**, 1695 (1994).

338. (a) C. Silvestru, L. Silaghi-Duitrescu, I. Haiduc, M.J. Begley, M. Nunn and D.B. Sowerby, J. Chem. Soc. Dalton Trans. **1986**, 1031; (b) C. Silvestru, I. Haiduc, R. Kaller, K.H. Ebert and H.J.

Breunig, Polyhedron **12**, 2611 (1993); (c) M.N. Gibbons, D.B. Sowerby, C. Silvestru and I. Haiduc, Polyhedron **15**, 4573 (1996).

339. (a) C. Silvestru, M. Curtui, I. Haiduc, M.J. Begley and D.B. Sowerby, J. Organomet. Chem. **426**, 49 (1992); (b) K.H. Ebert, H.J. Breunig, C. Silvestru and I. Haiduc, **13**, 2531 (1994); (c) D.B. Sowerby, M.J. Begley, L. Silaghi-Dumitrescu, I. Silaghi-Dumitrescu and I. Haiduc, J. Organomet. Chem. **469**, 45 (1994)

340. G.D. Christopherson, R.A. Sparks and J.D.McCullough, Acta Crystallogr. **11**, 782 (1958).

341. L.Y.Y. Chan and F.W.B. Einstein, J. Chem. Soc. Dalton Trans. **1972**, 316.

342. (a) F. Berry and A.J. Ewards, J. Chem. Soc. Dalton Trans. **1980**, 2306; (b) N.W. Alcock and W.D. Harrison, J. Chem. Soc. Dalton Trans. **1982**, 251; (c) G.D.Christopherson and J.D. McCullough, Acta Crystallogr. **11**, 249 (1958); (d) N.W. Alcock and W.D. Harrison, J. Chem. Soc. Dalton Trans. **1984**, 869; (e) J. Aramini, R.J. Batchelor, C.H.W. Jones, F.W.B. Einstein and R.D. Sharma, Can. J. Chem. **65**, 2643 (187); (f) D. Naumann, L. Ehmanns, K.F. Tebbe and W. Crump, Z. Anorg. Allg. Chem. **619**, 1269 (1993).

343. I. Haiduc, R.B. King and M.G. Newton, Chem. Rev. **94**, 301 (1994).

344. (a) S. Husebye, K. Maartmann-Moe and O. Mikalsen, Acta Chem. Scand. **43**, 868 (1989); 44, 464 (1990).

345. A. Silvestru, I. Haiduc, K.H. Ebert and H.J. Breunig, Inorg. Chem. **33**, 1253 (1994); J. Organomet. Chem. **482**, 253 (1994).

346. see for example G. Corongiu and E. Clementi, in G. Wipff (Editor), *Computational Approaches in Supramolecular Chemistry* (NATO ASI Series, Series C, Vol. 426), Kluwer Academic Publishers, Dordrecht, 1994, and references therein.

347. J.K. Tauer and W.N. Lipscomb, Acta Cryst. 5, 606 (1952).

348. (a) M. Magini, G. Paschina and G. Piccaluga, J. Chem. Phys. **77**, 2051 (1982); (b) A.N. Narten and A. Habenschuss, J. Chem. Phys. **80**, 3387 (1984); (c) S. Sarkar and R.N. Joarder, J. Chem. Phys. **99**, 2032 (1993).

349. W. Weltner and K.S. Pitzer, J. Am. Chem. Soc. **73**, 2606 (1951).

350. F.N. Penkert, T. Weyhermuller and K. Wieghardt, Chem. Commun. **1998**, 557.

351. F.T. Edelmann, ACS Symp. Ser. **555**, 309 (1994).

352. D. Braga, F. Grepioni, D. Walther, K. Heubach, A. Schmidt, W. Imhof, H. Gorls and T. Klebke, Organometallics **16**, 4910 (1997) and references therein.

353. P.D. Lickiss, Adv. Inorg. Chem. **42**, 147 (1995).

354. (a) R. Murugavel, V. Chandrasekar and H.W. Roesky, Acc. Chem. Res. **29**, 183 (1996), (b) R. Murugavel, A. Voigt, M.G. Walawalkar and H.W. Roesky, Chem. Rev. **96**, 2205 (1996).

355. H. Puff, K. Braun and H. Reuter, J. Organomet. Chem. **409**, 119 (1991).

356. N. Buttrus, C. Eaborn, P.B. Hitchcock and A. Saxena, J. Organomet. Chem., **287**, 157 (1985).

357. G. Fergusson, J.F. Gallagher, C. Glidewell, J.N. Low and S.N. Scrimgeour, Acta Crystallogr. **C 48**, 1272 (1992).

358. P.D. Lickiss and K.M. Stubbs, J. Organomet. Chem. **421**, 171 (1991).

359. (a) N.H. Buttrus, R.I. Damja, C. Eaborn, P.B. Hitchcock and P.D. Lickiss, J. Chem. Soc. Chem. Commun. **1985**, 1385; (b) S.S: Al-Juaid, N.H. Buttrus, R.I. Damja, Y. Derouiche, C. Eaborn, P.B. Hitchcock and P.D. Lickiss, J. Organomet. Chem. **371**, 287 (1989).

360. H.W. Roesky, Chem. Ber. **129**, 391 (1996).

361. G. Fergusson, J.F. Gallagher, D. Murphy, T.R. Spalding, C. Glidewell and H.D. Holden, Acta Crystallogr. **C 48**, 1228 (1992).

362. H. Puff, S. Franken, W. Schuh and W. Schwab, J. Organomet. Chem. **254**, 33 (1983).

363. H. Puff, H. Hevendehl, K. Hofer, H. Reuter and W. Schuh, J. Organomet. Chem. **287**, 163 (1985).

364. F.H. Allen, P.R. Raithby, G.P. Sjields and R. Taylor, Chem. Commun. **1998,** 1043.

365. M.R. Smith, R.A. Zingaro and E.A: Meyers, J. Organomet. Chem. **20**, 105 (1969).

366. L. Silaghi-Dumitrescu, I. Silaghi-Dumitrescu, J. Zukerman-Schpector, I. Haiduc and D.B. Sowerby, J. Organomet. Chem. **517**, 101 (1996).

367. C. Silvestru, A. Silvestru, I. Haiduc, D.B. Sowerby, K.H. Ebert and H.J. Breunig, Polyhedron **16**, 2643 (1997)

368. D. Braga, F. Grepioni and E. Tedesco, Organometallics **17**, 2669 (1998).

369. D. Braga, P. De Leonardis, F. Grepioni, E. Tedesco and M.J. Calhorda, Inorg. Chem. **37**, 3337 (1998).

370. (a) G.R. Desiraju, Acc. Chem. Res. **24**, 290 (1991); (b) D. Braga and F. Grepioni, Acc. Chem. Res. **27**, 51 (1994); (c) D. Braga, F. Grepioni and G.R. Desiraju, J. Organomet. Chem. **548**, 33 (1997); (d) D. Braga, F. Grepioni and G.R. Desiraju, Chem. Rev. **98**, 1375 (1998).

371.. D. Braga, A. Angeloni, E. Tagliavini and F. Grepioni, J. Chem. Soc. Dalton Trans. **1998**, 1961

372. G. Desiraju, *Crystal Engineering. The Design of Organic Solids,* Elsevier, Amsterdam, 1989

373. D. Braga and F. Grepioni, Comments Inorg. Chem. **19**, 185 (1997).

374. (a) E. Weiss Angew. Chem. **105**, 1565 (1993), Angew. Chem. Int. Ed. Eng. **32**, 1501, 1993;

(b) M. Driess, Adv. Organomet. Chem. **39**, 193 (1996); (c) T.P. Hanusa, Chem. Rev. **93**, 1023 (1993); (d) J.D. Smith, Adv. Organomet. Chem. **43**, 267 (1999).

375. R.D. Rogers, J.L. Atwood and R. Gruning, J. Organomet. Chem. **157**, 229 (1978).

376. (a) A.M. Sapse and P.von Rague-Schleyer (Editors), *Lithium Chemistry. A Theoretical and Experimental Overview,* J. Wiley and Sons, New York, 1995; (b) K. Gregory, P. von Rague-Schleyer and R. Snaith, Adv. Inorg. Chem. **37**, 48, 1991; (c) R.E. Mulvey, Chem. Soc. Rev. **27**, 339 (1998), (d) R.E. Mulvey, Chem. Soc. Rev. **20**, 167 (1991); (e) D.B. Collum, Acc. Chem. Res. **25**, 448 (1992); (f) L.M. Jackman, D. Cizmeciyan, P.G. Williard and M.A: Nichols, J. Am. Chem. Soc. **115**, 6262 (1993); (g) S. Chadwick, U. Englich and K. Ruhland-Senge, Organometallics **16**, 5792 (1997).

377. M. Driess, H. Pritzkow, M. Skipinski and U. Winkler, Organometallics **16**, 5108 (1997).

378. R.A. Jones, A.L. Stuart and T.C. Wright, J. Am. Chem. Soc. **105**, 7459 (1983).

379. (a) T. Greiser and E. Weiss, Chem. Ber. **110**, 3388 (1977); (b) J.E. Dvies, J. Kopf and E. Weiss, Acta Crystallogr. **B 38**, 1982, 2251.

380. (a) K. Ruhland-Senge, U. Englich, M.O. Senge, S.O. Chadwick and P.P. Power, Inorg. Chem. **32**, 4505 (1993); Inorg. Chem. **35**, 5820 (1996).

381. M.D. Janssen, E. Rijberg, C.A. de Wolf, M.P. Hogerheiode, D. Kruis, H. Kooijman, A.L. Spek, D.M. Grove and G. vn Koten, Inorg. Chem. **35**, 6735 (1996).

382. I. Haiduc and F.T. Edelmann, *Supramolecular Organometallic Chemistry,* Wiley-VCH, Weinheim, 1999, Chapter 6.

383. (a) C. Panattoni, G. Bombieri and U. Croatto, Acta Cryst. **21**, 823 (1966); (b) M.A. Beswick, C. Lopez-Casideo, M.A. Paver, P.R. Raithby, C.A Russell, A. Steiner and D.S. Wright, Chem. Commun. **1997**, 109; (c) J.S. Overby, T.P. Hanusa and V.G. Young Jr., Inorg. Chem. **37**, 163 (1998).

384. (a) S. Harder and M.H. Prosenec, Angew. Chem. Int. Ed. Engl. **35**, 97 (1996); (b) R.E. Dinnebier, U. Behrens and F. Olbrich, Organometallics **16**, 3855 (1997).

385. R. Zerger and G. Stucky, J. Organomet. Chem. **80**, 7 (1974).

386. R.A. Williams, T.P. Hanusa and J.C. Huffman, Organometallics **9**, 1128 (1990).

387. P.B. Hitchcock, J.A.K. Howard, M.F. Lappert and S. Prashar, J. Organomet. Chem. **437**, 177 (1992).

388. W. Binder and E. Weiss, Z. Naturforsch. **33**, 1235 (1978).

389. T. Kurikawa, Y. Negishi, F. Hayakawa, S. Nagao, K. Miyajima, A, Nakajima and K. Kaye, J. Am. Chem. Soc. **120**, 11766 (1998).

390. B. Grossmann, J. Heinze, E. Herdtweck, F.H. Kohler, H. Noth, H. Schwenk, M. Spiegler, W. Wachter and B. Weber, Angew. Chem. **109,** 384 (1997); Angew. Chem. Int. Ed. Engl. **36,** 387 (1997).

CHAPTER 15

CYCLISATION AND THE FORMATION, STRUCTURE AND PROPERTIES OF POLYMER NETWORKS

Robert F.T. Stepto, David J.R. Taylor
Polymer Science & Technology Group, Manchester Materials Science Centre,
UMIST & University of Manchester, Manchester M1 7HS, UK

List of Symbols

c_a, c_b	instantaneous concentrations of **A**- and **B**-groups
c_{a0}, c_{b0}	initial concentrations of **A**- and **B**-groups
$c_{ext,a}, c_{ext,b}$	instantaneous concentrations of **A**- and **B**-groups external to a given molecule
$c_{int,a}, c_{int,b}$	instantaneous concentrations of **A**- and **B**-groups on a given molecule
f	chemical functionality of the reactant molecules in a self-polymerisation
f_a, f_b	chemical functionalities of $\mathbf{RA}_{fa}$ and $\mathbf{R'B}_{fb}$ monomer units in a two-monomer polymerisation
f_n, f_w	number-average and weight-average functionalities in a polymerisation involving reactant species of mixed functionalities
i	number of repeat units in a loop (or ring) structure
n_{a0}, n_{b0}	initial numbers of **A-** and **B**-groups
$n_{a,ch}, n_{b,ch}$	numbers of **A**- and **B**-groups on a chosen (*ch*) molecule in a simulation
$n_c^{\,0}$	number of chains per unit volume, in a perfect network
$n_r(i)$	number fraction of loop structures with i repeat units
	extent of reaction in a self-polymerisation
p^*	conjugate (or sol) extent of reaction after the gel point, in a self-polymerisation
p_a, p_b	extents of reaction of **A**- and **B**-groups in a two-monomer polymerisation
p_{re}	total extent of ring-forming reaction at the end of a polymerisation
$p_{re,1}, p_{re,i>1}$	extents of ring-forming reaction giving smallest loops ($i = 1$) and larger loops ($i > 1$), at the end of a polymerisation $[p_{re,1} + p_{re,i>1} = p_{re}]$

$\langle r^2 \rangle^{\frac{1}{2}}$	root mean-square end-to-end distance of the subchain forming the smallest loop structure ($i = 1$)
u_g, u_s	unit fractions of gel and sol
u_x	unit fraction of x-mers
x	degree of polymerisation; average fractional loss of entropy per chain from loops of size $i > 1$
x_n, x_w	number-average and weight-average degrees of polymerisation
$x_{n,red}, x_{w,red}$	reduced number-average and weight-average degrees of polymerisation in a simulation, evaluated over all species *except* the largest molecule
A	front factor in the theory of rubber elasticity, relating the concentration of elastic chains to the shear modulus
G	actual shear modulus of the bulk network material
G^0	shear modulus of the bulk, perfect network material
M_c	number-average molar mass of elastic chains in a network
M_c^0	molar mass of elastic chains in a perfect network
N_a, N_b	number of **A**- and **B**-bearing monomer units in a polymerisation simulation
N_{Av}	Avogadro's number
N_c^0	number of chains in a perfect network
N_c^I	number of elastically ineffective chains
N_i	number of opportunities of forming a loop structure of i repeat units
N_J	number of junctions (or branch points) in a network structure
$N_r(i)$	number of loop structures of i repeat units
N_{re}	total number of loop structures at the end of the polymerisation
N_x	number of x-mers
P_{ab}	mutual concentration of pairs of reactive groups on the same molecule, which can react intramolecularly to form the smallest loop structure ($i = 1$)
$P_{ab,i}$	mutual concentration of reactive groups on the same molecule, which can react intramolecularly to form a loop structure of i repeat units
$P(\underline{r} = \underline{0})$	probability per unit volume that the ends of a subchain forming the smallest loop are coincident ($\underline{r} = \underline{0}$)
R	gas constant
T	absolute temperature
T_g	glass transition temperature
α	product of extents of reaction in a two-monomer polymerisation ($= p_a p_b$)
α^*	conjugate (or sol) extent-of-reaction product after the gel point, in a two-monomer polymerisation ($= p_a^* p_b^*$)

β	$= p(1-p)^{f-2}$ in a self-polymerisation, or $= \alpha(1-\alpha)^{f-2}$ in a two-monomer polymerisation (involving a single branched species)
λ	an instantaneous ring-forming parameter for a given molecule $[= c_{int}/(c_{int}+c_{ext})]$
$\lambda_{a0}, \lambda_{b0}$	initial ring-forming parameters, $\lambda_{a0} = P_{ab}/c_{a0}$, $\lambda_{b0} = P_{ab}/c_{b0}$
ν	number of bonds in the subchain which can form the smallest loop structure
ρ	density of a bulk network material

15.1 Introduction

This chapter considers nonlinear polymerisations through the reaction of functional groups and the structures, or chemical connectivities, and resulting mechanical properties of the networks formed at the ends of such polymerisations. There are important general relationships between (*a*) reactant structures (molar mass, chemical functionalities (*f*), chain stiffness) and reaction conditions (dilution and ratio of reactive groups) and (*b*) the network structure and network properties, that can be defined. Such relationships enable more accurate predictions of network properties, such as rubbery modulus, and T_g, to be made, directly from the initial, reaction formulations used. They also provide a deeper *molecular* understanding of network behaviour.

Gelation and network formation from nonlinear polycondensations and polyadditions can result in elastomeric networks[1], in vitrification[2] and also in microgel formation[3]. Many polymerisation formulations exist in which random (intermolecular) reaction between reactive groups means that reaction proceeds homogeneously throughout the volume of the polymerising mixture. Such polymerisations may be used to form model (but not perfect) elastomeric networks, whose properties can be predicted and interpreted in molecular terms with more certainty than those prepared *via* the crosslinking of polymer chains[4].

The chemical reactions used for network formation are often the conventional condensation and addition reactions met in linear polycondensations and polyadditions to form, for example, polyesters, polyamides, polyurethanes, polysiloxanes. The difference is that at least *one* of the reactants carries more than two reactive groups, that is, $f > 2$. This property leads to branched molecular structures and, under conditions that can be defined precisely for idealized polymerisations, to network formation, namely, macroscopic molecular growth limited only by the size of the reaction volume. Often the reactive groups are at the ends of chains or sub-chains, giving rise to the term "endlinking" (nonlinear polymerisation).

It is well established[5] that the occurrence of intramolecular reaction during nonlinear, network-forming polymerisations gives rise to loop structures in the resulting network topology. It is evident that a *distribution* of loop sizes will exist in a network structure, the details of which are largely inaccessible to experimental analysis. Such loop structures are associated with a reduction in the rubbery shear modulus of the network material relative to that expected for the hypothetical, perfect network, in which all network chains are assumed to be elastically effective. However, the relative contributions to the observed modulus-reduction, from loop structures of various sizes, are still not known[6]. It is clear that the formation of the smallest possible loop structure will render a fixed number of chains elastically ineffective[6] (the number being dependent upon the branch-point functionality), whereas the influence of larger loops is, at present, unclear.

The present account concentrates on results obtained using a new Monte-Carlo (M-C) polymerisation algorithm[7] to simulate the formation of a series of polyurethane (PU) network materials. The connectivities in the simulated network structures were recorded as functions of extent-of-reaction, *p*. By correlating the detailed structural information from the M-C simulations with *experimentally-measured* reductions in moduli[5,8], the loss in network elasticity due to larger loop structures can be estimated.

15.2 Formation of polymer networks according to Flory-Stockmayer (F-S) statistics

The molecular changes underlying the phenomenon of gelation in nonlinear polymerisations were first described quantitatively by Flory[9,10,11] and by Stockmayer[12,13]. The gel point is that point in a polymerisation where continuing structures first occur with unit probability.

For an $\mathbf{RA}_{f_a} + \mathbf{R'B}_{f_b}$ polymerisation the F-S gel point is simply[10-13]

$$(f_a - 1)p_a(f_b - 1)p_b = 1$$

Equation 15.2-1

where p_a and p_b are the extents of reaction of **A-** and **B-**groups, namely, the fractions of the two types of groups which have reacted. The assumptions leading to **Equation 15.2-1** are that intramolecular reaction does not occur and that all **A-** and all **B-**groups have the same probabilities of being reacted, namely, p_a and p_b. In the sense of a polycondensation proceeding by random (intermolecular) reactions of pairs of groups, such polymerisations may be termed *random polymerisations*[14,15]. The factor $(f_a - 1)$ in **Equation 15.2-1** is the number of paths which can lead from a randomly chosen **A-**group on an

RA_{fa} unit to an adjoining $R'B_{fb}$ unit and p_a is the probability per path. Similarly, $(f_b - 1)$ is the number of paths which can lead from the $R'B_{fb}$ unit, and p_b is the probability per path.

Another basic type of network-forming polymerisation is the RA_f self-polymerisation, where A-groups react with each other, as, for example, in the preparation of polysiloxanes. The condition for gelation in this case is

$$(f-1)p_a = 1$$

Equation 15.2-2

As may be expected, the occurrence of infinite species at the gel point is accompanied by a divergence of the molar-mass distribution, or, more fundamentally, the degree-of-polymerisation (DP) distribution, in that the mass average and higher averages become infinite. The expression for the number-average DP, denoted x_n, for an $RA_{fa}+R'B_{fb}$ polymerisation is simply derived, independent of the distribution.

$$x_n = \frac{\text{number of units}}{\text{number of molecules}} = \frac{\sum x N_x}{\sum N_x}$$

Equation 15.2-3

where N_x is the number of molecules with degree of polymerisation x. In the absence of intramolecular reaction, the number of molecules is the initial number (*i.e.* the number of monomer units) less the number lost (*i.e.* the number of A-groups or B-groups reacted $= n_{a0}\,p_a = n_{b0}\,p_b$). Hence,

$$x_n = \frac{N_a + N_b}{N_a + N_b - n_{a0} \cdot p_a}$$

Equation 15.2-4

N_a and N_b denote the numbers of RA_{fa} and $R'B_{fb}$ units, respectively.

The expression for the weight-average DP, denoted x_w, which requires an expression for the distribution of species, is due to Stockmayer[16], namely,

$$x_w = \frac{\sum x^2 N_x}{\sum x N_x} = 1 + \frac{p_a p_b f_{an} f_{bn} [p_a (f_{aw} - 1) + 2]}{(p_a f_{an} + p_b f_{bn})[1 - p_a p_b (f_{aw} - 1)(f_{bw} - 1)]}$$

Equation 15.2-5

where f_n and f_w represent the number-average and weight-average functionalities, respectively.

For an **RA$_f$** self-polymerisation, the expressions for x_n and x_w are

$$x_n = \frac{1}{1 - (f_n \cdot p / 2)}$$

Equation 15.2-6

and

$$x_w = \frac{1 + p}{1 - p(f_w - 1)}$$

Equation 15.2-7

In this case, the number of molecules lost is one-half of the number of **A**-groups reacted.

The preceding equations relate to changes from the beginning of a polymerisation up to the gel point. As discussed in detail by Flory[9], the infinite species which occur from the gel point to complete reaction cannot be enumerated as individual molecules. The sum of reactant units which have joined together to form infinite species is the gel fraction, namely, the unit fraction[5] of gel, u_g. This fraction increases monotonically from zero at the gel point until complete reaction. For stoichiometric formulations, $u_g = 1$ at complete reaction. The complementary quantity, the unit fraction of sol, u_s, can be evaluated directly by summing over the units in finite species knowing the DP distribution. For example, for an **RA$_f$** self-polymerisation,

$$u_s = \sum_{x=1}^{x} u_x = 1 - u_g$$

Equation 15.2-8

where u_x is the fraction of reactant molecules (or units) in the species with degree of polymerisation x. The detailed expression for u_x is

$$u_x = \frac{x(1-p)^2}{p} \cdot \frac{f[x(f-1)]!}{[x(f-2)+2]!x!} \cdot \beta^x$$

Equation 15.2-9

where

$$\beta = p(1-p)^{f-2}$$

Equation 15.2-10

The combinatorial factor relates to the number of distinguishable isomers of molecules of x units with $x(f - 2) + 2$ unreacted groups. The expression for u_s is

$$u_s = \frac{(1-p)^2 p^*}{(1-p^*)^2 p}$$

Equation 15.2-11

where p $(0 \le p \le 1)$ is the extent of reaction and p^* is the lowest value of p which satisfies **Equation 15.2-11** for a given value of β.

For $RA_2 + RB'_{fb}$ polymerisations, expressions of the same forms as in **Equation 15.2-6** to **Equation 15.2-11** apply for x_n, x_w and u_s, provided these quantities are defined on the basis of the branch units, RB'_{fb}, only, irrespective of how many RA_2 residues are in a given molecule, and p is replaced by $\alpha = p_a p_b$. Free RA_2 monomer is then excluded from considerations. Expressions for complete molecular species, including the counting of RA_2 units, are available[17] but are more complex and are not often needed. It is the branch-point or 'complexity' distribution that is of prime importance[9].

15.3 Intramolecular reaction

There are two fundamental assumptions of F-S statistics as applied to network-forming polymerisations – the random reaction of pairs of functional groups, and the exclusion of intramolecular reaction between finite (sol) species. For nonlinear polymerisations, however, the increasing numbers of reactive groups per molecule, together with the spatial correlations between

groups on the same mlecule, mean that intramolecular reaction *cannot* generally be neglected.

The effects of reactant structure on intramolecular reaction are parameterised in terms of P_{ab} for the smallest loop[5,18,19]:

$$P_{ab} = \frac{P(r = 0)}{N_{Av}}$$

Equation 15.3-1

where $P(r = 0)$ is the probability-density of a zero end-to-end vector between reactive groups. P_{ab} thus represents the mutual concentration of **A-** and **B-** groups at the ends of the shortest sub-chain, which can react intramolecularly. The structure of this sub-chain, consisting of v skeletal bonds, and whose root-mean-square end-to-end distance is $\langle r^2 \rangle^{1/2}$, is shown in **Figure 15.3-1.**
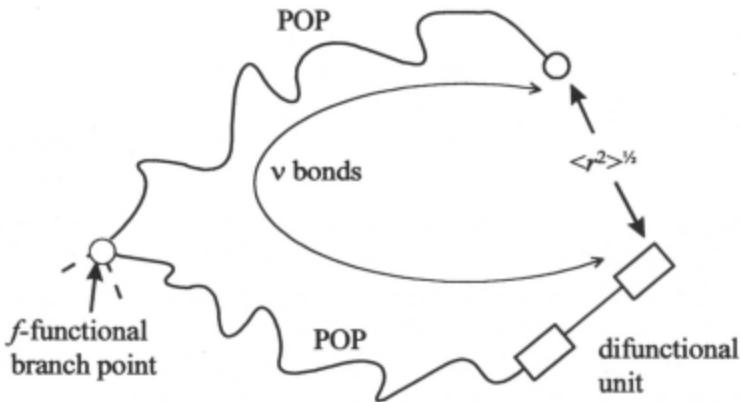
Figure 15.3-1 : schematic diagram of a sub-chain forming a smallest loop structure illustrated with respect to a polyurethane-forming polymerisation. The diagram shows the two arms of a polyoxypropylene (POP) star polyol, one arm having reacted with a difunctional monomer (a diisocyanate in the case of polyurethane formation); the root-mean-square distance of the chain of v between the terminal groups is $\langle r^2 \rangle^{1/2}$.

If it assumed that the network-chain end-to-end distance distribution can be represented by a Gaussian function with mean-square end-to-end distance, $\langle r^2 \rangle$, P_{ab} is given by

$$P_{ab} = \frac{1}{N_{Av}} \left\{ \frac{3}{2\pi <r^2>} \right\}^{3/2}$$

<div align="right">**Equation 15.3-2**</div>

Since the units of P_{ab} are moles per unit volume, it can be described as the mutual *concentration* of pairs reactive groups on the same molecule which can react intramolecularly, and is said[20] to define an *internal* concentration of reactive groups, c_{int}. This is shown schematically in **Figure 15.3-2** for a particular **A**-group, where the competition between intramolecular and intermolecular reaction with a specific **B**-group is due to the relative concentrations of **B**-groups on the same molecule (described by $c_{b,int}$) and of **B**-groups on *other* molecules, or the so-called external concentration[20], $c_{b,ext}$. The latter quantity may be approximated by the simple expression

$$c_{b,ext} = c_b = c_{b0}(1 - p_b)$$

<div align="right">**Equation 15.3-3**</div>

where c_b is the instantaneous concentration of reactive groups (at extent of reaction p_b). An analogous expression exists for the reaction of a **B**-group:

$$c_{a,ext} = c_a = c_{a0}(1 - p_a)$$

<div align="right">**Equation 15.3-4**</div>
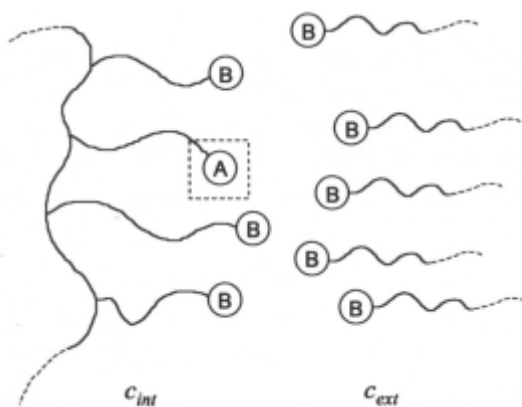
Figure 15.3-2 - diagram illustrating the concepts of internal and external concentrations of **B**-groups around a chosen **A**-group, leading, respectively, to intramolecular and intermolecular reaction

It must be noted that a key assumption of F-S statistics is implicit in the use of such a scheme: intermolecular reactions must occur randomly.

Intramolecular reaction between the pendant **A**- and **B**-groups at each end of a sub-chain of the type shown in **Figure 15.3-1** would result in the formation of the smallest possible loop structure. However, it is apparent that all manner of loop sizes, consisting of larger numbers of monomer units, are possible, resulting in ring-structures with integer multiples of ν bonds. If all such subchains in a polymerisation mixture are assumed to obey Gaussian statistics, the P_{ab} parameter for the formation of the ith loop size can be evaluated using a more general form of **Equation 15.3-2:**

$$P_{ab,i} = \left(\frac{3}{2\pi i < r^2 >} \right)^{\frac{3}{2}} \frac{1}{N_{Av}} = P_{ab} i^{-\frac{3}{2}}$$

Equation 15.3-5

It is assumed that the presence of i branch points in a subchain forming a loop of size i does not affect the subchain conformational statistics. The total value of c_{int} is formed by the sum over all possible (N_i) pairs of groups which can react intramolecularly to form loops of size i:

$$c_{int} = \sum_i c_{int,i} = P_{ab} \sum_i N_i i^{-\frac{3}{2}}$$

Equation 15.3-6

Intramolecular reaction is therefore governed principally by $P_{ab,i}$, which decreases with increasing i (or increasing $i<r^2>$), and the numbers of opportunities, N_i, of forming loops of size i, which will increase as the reaction proceeds (due to the increase in the number of reactive groups per molecule). These two factors can be combined to define a *ring-forming parameter*[5,20], λ:

$$\lambda = \frac{c_{int}}{c_{int} + c_{ext}}$$

Equation 15.3-7

which describes the proportion of reactions which occur intramolecularly. It is clear that λ will be affected by the detailed molecular structure of the sub-chains (through c_{int}), and also by the overall concentration of reactive groups, c_{ext}. The

dependence of λ upon c_{int} is itself determined by a number of factors, including the flexibilities and lengths of the subchains (through P_{ab} in **Equation 15.3-2**), and by the changing graph topologies[21] of the collection of structures in the reaction mixture (through N_i in **Equation 15.3-6**). The influence of c_{ext} means that λ is larger for less concentrated polymerisation systems, and will increase as the reaction proceeds.

A useful measure of a the inherent propensity of a given system to intramolecular reaction is given by λ_{a0}, in terms of the initial concentration of A-groups[5,19,20,22]:

$$\lambda_{a0} = \frac{P_{ab}}{c_{a0}}$$

Equation 15.3-8

(an analogous expression exists for λ_{b0}, in terms of c_{b0}). For stoichiometric polymerisation reactions, $c_{a0} = c_{b0}$, and

$$\lambda_{a0} = \lambda_{b0} = \frac{2P_{ab}}{(c_{a0} + c_{b0})}$$

Equation 15.3-9

The concept of a ring-forming parameter captures the combined effects of reactant structure and reactive-group concentration, and provides a measure of the initial propensity for intramolecular reaction in a nonlinear polymerisation system. Decreases in chain length or chain stiffness result in an increase in P_{ab} and, hence, in the probability of intramolecular reactions forming loop structures. Similarly, decreasing the concentration of reactive groups also enhances the probability of intramolecular reaction.

15.4 Elasticity of perfect network structures

A precise knowledge of the reactant structures used in endlinking polymerisations can be used to calculate the shear modulus, G^0, of the bulk, hypothetically perfect network material, in which *every* chain is assumed to be elastically effective.

$$G^0 = A n_c^0 kT = A \frac{\rho RT}{M_c^0}$$

Equation 15.4-1

ρ is the density of the network, T the absolute temperature and n_c^0 the number of elastically effective chains per unit volume of the network. A is the so-called "front factor"[23] in the theory of rubber elasticity, whose value depends upon the assumption of the deformation mechanism for the junction points. For affine deformation $A=1$, or for phantom deformation $A = 1\text{-}2/f$, for f-functional junction points. M_c^0 is the network-chain molar-mass expected on the basis of the reactant structures (*i.e.* assuming a perfect network structure is formed).

The shear modulus, G, from small-strain uniaxial compression measurements[24] can be expressed by

$$G = A \frac{\rho RT}{M_c}$$

Equation 15.4-2

where M_c is the actual (number-) average molar mass of elastic chains over the mass of the whole network[5]. Hence,

$$\frac{M_c}{A} = \frac{\rho RT}{G}$$

Equation 15.4-3

This equation is independent of the assumptions of affine versus phantom deformation, and shows that M_c/A can be evaluated from experimental stress-strain measurements.

It is widely acknowledged[5,6,8,19,20,22] that loop structures formed both pre-gel and post-gel will reduce the concentration of elastic chains in the final network, and thus the experimentally measured modulus of the bulk network, G, will be less than G^0. The relative reduction in modulus, G/G^0, can be quite considerable, and has obvious technological implications in terms of the mechanical properties expected for particular polymer networks, based on the reactant structures. The relative reduction in modulus can also be expressed as M_c/M_c^0.

15.5 Experimental analyses of polyurethane (PU) networks

The data to be discussed in the present chapter come from six series of PU-network materials, formed via stoichiometric $RA_2 + R'B_f$ polymerisations of hexamethylene diisocyanate (HDI) and star polyoxypropylene (POP) polyols, and using various initial dilutions of reactive groups (in nitrobenzene)[8,22]. The structure of the polyol $(R'B_f)$ was varied, in order to test the effects of branch-point functionality (f) and network-chain length (v) on the moduli of the resulting networks. The six reaction systems are listed in **Table 15.5-1,** where M_c^0 is the network-chain molar mass (that for a chain of v skeletal bonds between branch points) and is defined by the reactant structures. It is easy to deduce that v is also the number of skeletal bonds in a sub-chain forming the smallest possible loop structure[22] (see **Figure 15.3-1**). The corresponding values of the mean-square end-to-end distance, $<r^2>$, are also shown. The latter quantities were calculated[25] via detailed conformational analyses of the branched chain structures of the type shown in **Figure 15.3-1**.

System	f	v	M_c^o /g mol^{-1}	$<r^2>$ /nm^2
1. HDI + POP triol	3	35	635	3.718
2. HDI + POP triol	3	62	1168	6.877
3. HDI + POP tetrol	4	28	500	2.753
4. HDI + POP tetrol	4	32	586	3.628
5. HDI + POP tetrol	4	43	789	4.605
6. HDI + POP tetrol	4	65	1220	6.581

Table 15.5-1 - functionalities, f, and elastic chain molar masses in the perfect network, M_c^0, for six series of PU-forming, nonlinear polymerisations[22]. The calculated values[25] of the mean-square end-to-end distance, $<r^2>$, for subchains forming the smallest possible loop are also shown.
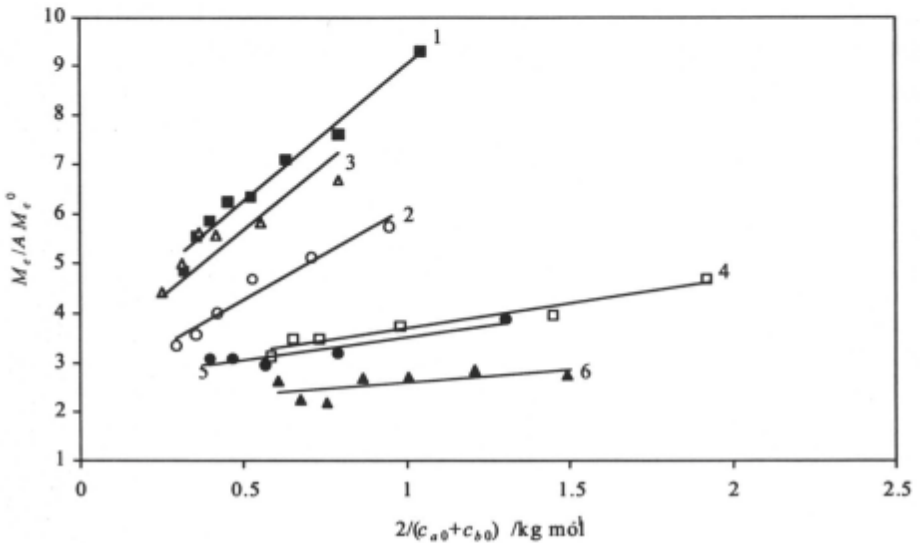
Figure 15.5-1 - experimentally-determined[22] values of M_c/AM_c^0, as functions of the initial dilution of reactive groups, $2/(c_{a0}+c_{b0})$, for six series of polyurethane networks analysed at complete reaction

The plot in **Figure 15.5-1** shows the experimentally-determined values of M_c/A relative to M_c^0 for the perfect networks (M_c/AM_c^0), as functions of the initial dilution of reactive groups, $2/(ca_0+cb_0)$, for the six series of PU networks at complete reaction. For each experimental system, an increase in the initial dilution of reactive groups results in greater reductions in moduli, consistent with increased incidence of intramolecular reaction, and the formation of inelastic loop structures. The positive slopes of the plots in **Figure 15.5-1**

indicate that direct relationships exist between intramolecular reaction (which increases with reactant dilution) and the network defects at complete reaction. This in itself suggests that the dominant network defects are inelastic loop structures, which can form both pre-gel and post-gel.

The plots in **Figure 15.5-1** clearly show that the magnitudes of the experimentally observed reductions in modulus are by no means insignificant. If perfect networks are formed and they behave affinely, *as expected* at the small strains studied, then $M_c/AM_c^0 = 1$. Hence, on an affine basis, there is a ten-fold decrease in modulus in the case of the dry (bulk) network formed from the short-chain triol **(system 1; $M_c^0 = 635$ g mol^{-1}),** at the highest initial dilution of reactive groups. For a given branch-point functionality, an increase in subchain length **(v)** results in a decrease in M_c/AM_c^0, due to the decrease in the probability of loop formation (since $<r^2>$ in **Equation 15.3-2** increases). However, the reductions in moduli for the tetrafunctional networks are considerably less than those of the corresponding trifunctional structures. To a first approximation, this can be understood[6], on the basis of the different effects of the smallest loops that can form during $f = 3$ and $f = 4$ polymerisations, as will now be discussed.

It should be noted that if, at the other extreme, the perfect networks were to exhibit phantom rather than affine behaviour, then for $f = 3$, $M_c/AM_c^0 = 3$ and for $f = 4$, $M_c/AM_c^0 = 2$. The observed values of M_c/AM_c^0 are greater, therefore, than those for perfect networks assuming either affine *or* phantom behaviour.

15.6 General effects of loops on elasticity[5,6]

The effect of the smallest loop structures on the loss of network elasticity is shown diagrammatically in **Figure 15.6-1(a),** for networks of trifunctional and tetrafunctional branch points. In perfect f-functional networks, each junction provides $f/2$ elastic chains. In the case of $f = 3$, each loop structure renders two branch points inelastic (shown as ☐ in the diagram), which is equivalent to the loss of three elastic chains. For the network with tetrafunctional branch points, the effect is reduced - each loop is associated with the loss of a single elastic branch point, or two elastic chains. As a result, trifunctional networks are expected to be more sensitive to loop defects than are tetrafunctional networks, and the decrease in modulus for the latter is expected to be less than that of the corresponding trifunctional network, consistent with the experimental data in **Figure 15.5-1**.

However, it is clear that there will be a *distribution* of loop sizes in the completely-reacted network structure, which is likely to be broad owing to the presence of the large loops which are formed post-gel, resulting from intramolecular reaction between pairs of groups on the gel molecule. Unlike the smallest loops, larger loop structures do not disrupt the continuity of the

network structure, and therefore the network chains in larger loops *are* capable of supporting a load. Examples of the two-membered loop structures for the trifunctional and tetrafunctional networks are shown in **Figure 15.6-1(b)**. The question as to *how* the larger loop-structures contribute to the decrease in network elasticity remains unanswered The conformational entropy of a large loop-structure will be reduced[5,7,26] relative to that of an unperturbed, free linear chain of the same number of skeletal bonds, due to the decrease in the total number of possible chain conformations resulting from the constraints imposed by the branch points along the chain and at the two chain ends. However, in a completely reacted network structure, *every* chain (except those in smallest loops) must form part of a topological circuit, and will therefore be subject to some degree of entropy loss. Since the origin of rubber-like elasticity lies in the conformational entropy of the network chains, any decrease in entropy should manifest itself as a decrease in the elasticity of the real network structure relative to that of the hypothetical, perfect one, whose network chains are assumed to be indistinguishable from the corresponding set of unperturbed (free) chains.
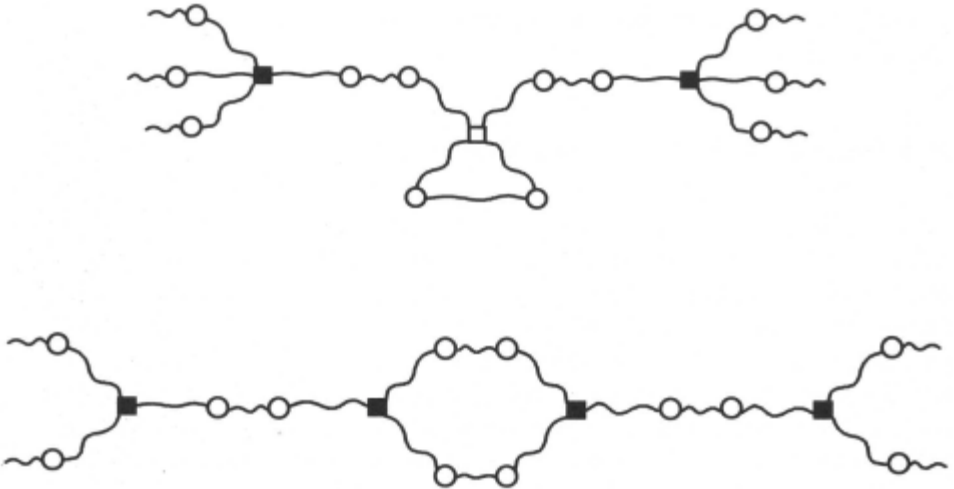
Figure 15.6-1 - **(a)** smallest-loop structures and **(b)** two-membered loop structures for networks of trifunctional and tetrafunctional branch points. O represents a reacted pair of groups; ■ denotes a fully-elastic junction point; ▪ denotes a junction point of reduced elasticity; □ denotes an elastically-inactive junction point.

15.7 Total proportions of loop structures of *all* sizes in nonlinear polymerisations obeying F-S statistics

Post-gel intramolecular reaction must occur between reactive groups on the gel molecule, even during an ideal network-forming polymerisation obeying F-S statistics. The extent of gel-gel (and thus loop-forming) reaction in random, RA_f and $RA_2+R'B_f$ polymerisations at complete reaction has been evaluated by Stepto[27], and the results are shown in **Table 15.7-1**.

f	RA_f	$RA_2+R'B_f$
3	1/3	1/6
4	1/2	1/4
5	3/5	3/10
10	8/10	4/10

Table 15.7-1 - calculated[27] maximum extents of intramolecular reaction for hypothetical, nonlinear polymerisations obeying F-S statistics

For RA_f polymerisations, the formation of each loop corresponds to the reaction between two branch units on the gel molecule, and thus the extent of gel-gel reaction in the perfect network is simply equal to the cycle rank[23], $\xi = 1 - 2/f$. In the case of $RA_2 + R'B_f$ systems, a loop is closed *only* via a difunctional unit, requiring two reactions of pairs of groups, of which only one is intramolecular. As a result, the total extent of gel-gel reaction is half that of the corresponding RA_f system. However, in a real nonlinear polymerisation, spatial correlations between reactive groups on the largest molecule mean that smaller loops are more likely to form (both pre- and post-gel), and thus the distribution of loop sizes at complete reaction will not be the same as that resulting from the random gel-gel reactions allowed by F-S theory after the gel point.

15.8 Smallest-loop analysis of extents of loop-formation at complete reaction

The effects of loop size in $RA_2+R'B_3$ polymerisations were previously investigated[6] via the introduction of a parameter, p_{re}, denoting the extent of intramolecular reaction at the end (e) of the polymerisation[6,20] which contributes to the loss in network elasticity. For an initial number, N_b, of $R'B_f$ branch units, the number of loops formed at complete reaction is given by fN_bp_{re}. Considering first the case of an $RA_2+R'B_3$ polymerisation, and assuming for a moment that the entropy loss due to loop structures of *all* sizes can be treated using the analysis applied to smallest loops (recall **Figure 15.6-1(a)**), the number of branch points rendered inelastic is equal to twice the number of

loops, *i.e.* $2fN_b p_{re} = 6N_b p_{re}$. The number of branch points remaining elastic is therefore $N_b(1 - 6p_{re})$, and the *fraction* of branch points (or chains) remaining elastic is given by $(1 - 6p_{re})^{-1}$. Hence, the effective network-chain molar mass, M_c, is given by

$$M_c = \frac{M_c^{\,0}}{1 - 6p_{re}}$$

<div align="right">**Equation 15.8-1**</div>

Rearrangement of **Equation 15.8-1** yields

$$\frac{M_c}{M_c^{\,0}} = \frac{1}{1 - 6p_{re}}$$

<div align="right">**Equation 15.8-2**</div>

Similar reasoning follows for the $RA_2 + R'B_4$ case, in which only one branch point is lost per loop (recall **Figure 15.6-1a**)), yielding an analogous expression for $M_c/M_c^{\,0}$

$$\frac{M_c}{M_c^{\,0}} = \frac{1}{1 - 4p_{re}}$$

<div align="right">**Equation 15.8-3**</div>

The forms of **Equation 15.8-2 and Equation 15.8-3** indicate that if it is assumed that *all* loop structures contribute to the loss of elastic chains, then the total amounts of post-gel reaction calculated on the basis of F-S statistics (**Table 15.7-1**) would result in a *total* loss of network elasticity (*i.e.* an infinite reduction in modulus).

The evaluations[6] of p_{re} derived from the experimentally-measured values of $M_c/AM_c^{\,0}$, amount to equating the *total* entropy loss (due to smallest- and larger-loop structures) with an *equivalent* number of smallest loops only. These evaluations showed that affine behaviour ($A = 1$) was the only way of interpreting the values of $M_c/AM_c^{\,0}$ to give acceptable values of p_{re}. However, from the Monte-Carlo simulations to be descibed in the following section, it is now known that the key to a *full* understanding of the relationship between stress-strain behaviour and network topology is the identification of how various types of loop structure contribute differently to experimentally-observed reductions in modulus.

15.9 Monte-Carlo polymerisation algorithm[7,28,29]

Theories to predict the modulus of a network material must begin by constructing a realistic model of the network structure (including defects). The elastically ineffective portions of the structure can be identified and excluded from the elasticity calculations, which are usually based on a contribution per elastically-effective chain in the network. Detailed characterisation of the connectivity, or topology, of a network structure via conventional, experimental means is impossible. In order to investigate the effects of network topology on elastomeric properties one must therefore resort to numerical simulations of nonlinear polymerisations, which have the potential to provide this detailed structural information. It is important to correctly account for the formation of loop-structures of various sizes (resulting from intramolecular reactions), correctly weighted according to their probabilities of formation.

To these ends, a Monte-Carlo (M-C) nonlinear polymerisation algorithm, originally devised by Dutton *et al.*[7] has been further developed. The M-C method has been used to generate realistic representations of the PU networks, listed in **Table 15.5-1**, based on the knowledge of reactant structures and reactive-group concentrations.

The M-C network polymerisation algorithms, for single- and two-monomer reactions, are based on a perturbation to F-S random-reaction statistics. For a finite population of reactant molecules, the algorithm simulates, as a function of extent-of-reaction, the formation of *all of the connections* in a reaction mixture. Intramolecular reactions are allowed by assigning probabilities for intermolecular and intramolecular reaction, weighted, respectively, according to the initial concentrations of reactive groups in the system, and the detailed conformational statistics of subchains separating pairs of reactive groups on the same molecule (**Equation 15.3-5** to **Equation 15.3-8**). However, reactions are not currently weighted according to the sizes of the molecules to which specific reactive groups are attached. The M-C algorithm therefore does not take account of diffusion effects.

The new algorithm has so far been designed to simulate self-polymerisations $(\mathbf{RA_f})$, and two-monomer, stoichiometric polymerisations of the general type $\mathbf{RA_2 + R'B_f}$. During the course of a simulated polymerisation, populations of monomer units are connected together according to the relative probabilities for intramolecular and intermolecular reactions. The connectivity is recorded as a function of extent of reaction of $\mathbf{A}$- or $\mathbf{B}$-groups, along with the calculated sol and gel fractions, and average degrees of polymerisation.

15.9.1 Input parameters

The algorithm requires an initial number of **A**- and **B**-bearing reactants, $N_a + N_b$ (where $n_{a0} = f_a N_a = n_{b0} = f_b N_b$, for stoichiometric reactions), with functionalities of $f_a = 2$ and $f_b = 3,4$ for the systems discussed in this chapter. The initial concentrations of reactive groups, $c_{a0} + c_{b0}$, are also specified (which effectively defines a reaction volume, or reactant molar masses). The final parameter characterising the reactants is P_{ab}, the mutual concentration of **A**- and **B**-groups on adjacent, connected monomer units ($i = 1$), as defined in **Equation 15.3-2**.

15.9.2 Choosing a pair of groups to react

The first (**A** or **B**) group in a reacting pair is chosen randomly from the total number of unreacted groups $(n_a + n_b)$ at a particular extent of reaction. If the chosen group belongs to a monomer unit, any subsequent reaction must be intermolecular, and the algorithm skips directly to the random choice of a reaction partner from amongst the unreacted groups (of the opposite type, **B** or **A**) on *other* molecules. However, if the group chosen first is attached to a larger molecule, intramolecular reaction may also be possible, and its associated probability must be enumerated. This involves scanning the entire structure of the chosen molecule, to identify the numbers and "locations" (relative to the chosen group) of all groups of the opposite type, which can react intramolecularly. This is achieved by using a graph-theoretical algorithm known as "MINPATH"[30]. The MINPATH algorithm performs an efficient, systematic search through the structure, and tabulates the shortest connected distances ("paths") between a given vertex and all of the others. This logic is applied as part of the nonlinear polymerisation algorithm to find the spanning numbers of bonds between the branch unit to which the first chosen group is attached, and all other branch units on the same molecule. The total internal concentration of reactive groups, c_{int}, relative to the chosen group is then calculated from the sum of $P_{ab,i}$ contributions from groups on the same molecule **(Equation 15.3-5)**.

The external concentration, c_{ext}, of groups on *other* molecules at a given extent of reaction is enumerated from the total number of unreacted (**A** or **B**) groups, n_a or n_b, the number of unreacted groups on the chosen molecule, $n_{a,ch}$ or $n_{b,ch}$, and the initial concentrations of reactive groups, c_{a0} and c_{b0}:

$$c_{ext,a} = \frac{(n_a - n_{a,ch})}{n_{a0}} \cdot c_{a0}$$

Equation 15.9.2-1

or

$$c_{ext,b} = \frac{(n_b - n_{b,ch})}{n_{b0}}.c_{b0}$$

<div align="right">**Equation 15.9.2-2**</div>

In the case of an unreacted B-group, for example, a random number in the range $0 \rightarrow 1$ is used to choose intermolecular or intramolecular reaction, based on the values of $c_{int,b}$ and $c_{ext,b}$. If intramolecular, a second random number is used to pick the specific monomer unit, or residue, on the same molecule, to react, weighted according to the individual $P_{ab,i}$ components of c_{int}. If intermolecular, a second random number is used to pick the second group to react randomly according to the numbers of unreacted groups on *other* molecules.

15.9.3 Updating of connectivity records and averages

After each reaction the functionalities of the two monomer units, and the numbers of reactive groups, n_a and n_b, are decreased by 1. The extents of reaction p_a and p_b are recalculated, using

$$p_a = \frac{(n_{a0} - n_a)}{n_{a0}}, \qquad p_b = \frac{(n_{b0} - n_b)}{n_{b0}}$$

<div align="right">**Equation 15.9.3-1**</div>

The connectivity is updated, the largest molecule identified, and, if the reaction was intramolecular, the loop-size distribution updated. In the two-monomer simulations, the sol fraction and degrees of polymerisation were calculated on the bases of the numbers of branch units (*i.e.* the number of difunctional monomers is assumed to contribute zero to the degree of polymerisation). In a numerical simulation (with finite system size) the sol fraction, u_s, is defined as the proportion of branch units which are *not* connected to the largest molecule, and u_g is calculated as $1-u_s$. Also, the average degrees of polymerisation, x_n and x_w, are updated. For comparison with conventional F-S theory, the *reduced*, average degrees of polymerisation $(x_{n,red}, x_{w,red})$, described[28] by Eichinger *et al.*, are also calculated by averaging over all molecules except the largest one. As described[28], these reduced degrees of polymerisation are equivalent to the values of x_n and x_w for the sol fraction only.

Whilst there are unreacted groups still remaining, the procedure described in **Section 15.9.2** is repeated, and the calculated values of u_s, $x_{n,red}$, $x_{w,red}$, and the ring-size distribution are printed out at regular extent-of-reaction intervals.

15.9.4 Modified polymerisation algorithm to mimic F-S statistics

In order to check the calculations performed by the M-C algorithm, it was modified so that it would mimic F-S statistics. The P_{ab} input parameter was disregarded, and all intramolecular reaction prior to the F-S gel point was disallowed. After the gel point, intramolecular reaction was allowed only between randomly-chosen pairs of groups on the largest (*i.e.* the gel) molecule. Series of F-S simulations were performed with increasing numbers of starting units to investigate any system-size effects. Since F-S theory allows random, intramolecular reaction between groups attached to the gel molecule after the F-S gel point, the distribution of post-gel loop-sizes was also investigated using the numerical F-S algorithm.

The M-C results were compared with the predictions of F-S statistics using the equations described in **Section 15.2,** for **RA**$_f$ self-polymerisations. For **RA$_2$+R′B**$_f$ polymerisations, the predictions of F-S theory were calculated as functions of the extent-of-reaction product, $\alpha = p_a p_b$, in the range $0 \rightarrow 1$. α at the F-S gel point was calculated from **Equation 15.2-1**. As described earlier, in **Section 15.2**, for a self-polymerisation, the conjugate extent of reaction, p^*, must be calculated in order to evaluate post-gel properties. For a two-monomer polymerisation, the corresponding quantity is α^*, which is calculated as before. The same equations are used, with p^* replaced by α^*. The values of u_s, $x_{n,red}$ and $x_{w,red}$ are then calculable in terms of the numbers of branch units **(R′B**$_f$**)** only, using **Equation 15.2-4** to **Equation 15.2-11**, again replacing p^* with α^* (= α prior to the F-S gel point).

15.10 Simulations according to F-S statistics – **RA**$_f$ self-polymerisations

The F-S algorithm was used to simulate self-polymerisations of trifunctional, tetrafunctional and pentafunctional monomers, with 500, 1000 and 3000 starting units.

The calculated values of u_s for two **RA**$_4$ systems are plotted as functions of extent-of-reaction, p, in **Figure 15.10-1.** The plot for $N_a = 1000$ shows how the numerically-determined sol fraction begins to decrease *prior* to the F-S gel point, since the size of the largest molecule existing pre-gel is a significant quantity compared to the remaining number of monomers in the *finite* monomer population. However, increasing the initial system size, as shown by the plot for 3000 starting units, can reduce this effect. The F-S gel point, characterised by

the sudden decrease in u_s (at $p = 1/(f-1) = 0.333$), is not particularly well reproduced by the M-C data points for the run with the smaller sample size.
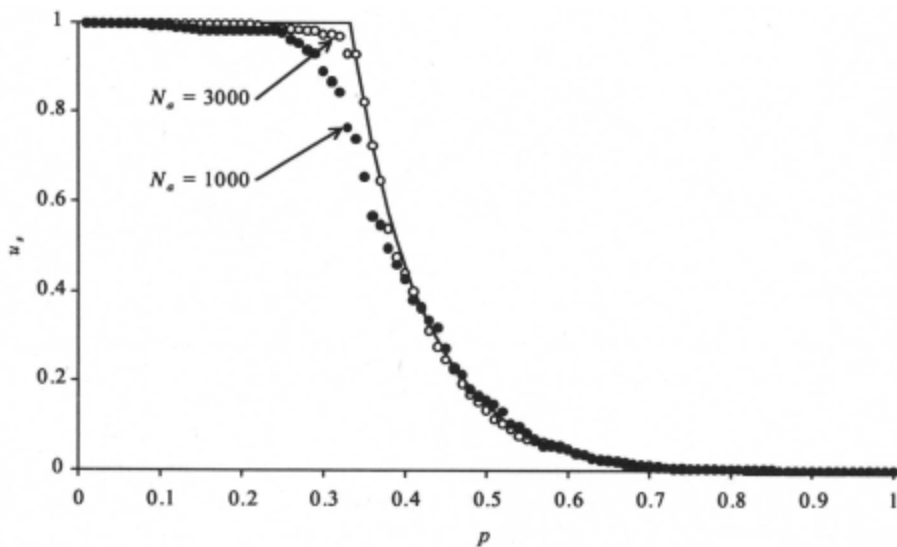
Figure 15.10-1 - **RA₄** simulations: sol fractions, u_s, versus extent of reaction, p, calculated using the F-S simulation algorithm; the continuous plot, calculated directly from F-S theory, is also shown for comparison.

The values of $x_{n,red}$ were also calculated during the course of the F-S simulations, and the results are plotted alongside the analytical predictions of F-S theory in **Figure 15.10-2**. Again, there is considerable scatter of the M-C data points about the analytical F-S plots, particularly in the post-gel region ($p > 0.333$) due to the decrease in the number of molecules as the simulated reaction proceeds towards completion. The scatter is reduced by increasing the system size. The extent of reaction at which $x_{n,red}$ falls to zero corresponds to the point at which *all* of the monomer units in the M-C simulation have joined to form a single network molecule, and there are no sol molecules remaining over which to perform the averaging. This phenomenon is a feature of using finite systems.
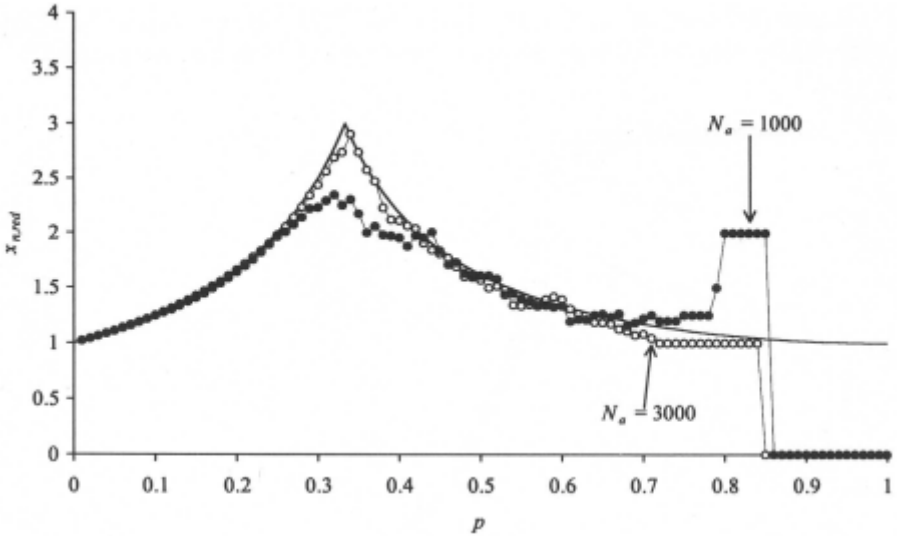
Figure 15.10-2 - **RA₄** simulations: reduced number-average degree of polymerisation, $x_{n,red}$, versus extent of reaction, p, calculated using the F-S simulation algorithm; the continuous plot, calculated directly from F-S theory, is also shown for comparison.

The reduced weight-average degree of polymerisation, $x_{w,red}$, is plotted in **Figure 15.10-3.** Due to the finite numbers of monomer units in the M-C simulations, the calculated values of $x_{w,red}$ remain finite throughout the course of the simulations, although they pass through a maximum at an extent of reaction slightly greater than the F-S gel point. This maximum becomes better defined as the system size is increased. Even in simulations with $N_a = 3000$, a general characteristic of the F-S simulations is that the maximum in $x_{w,red}$ occurs slightly later than the F-S gel point (by *ca.* 10% in p_a). It may be noted that Eichinger and coworkers[28] used the maximum in $x_{w,red}$ to define a *lower* bound for the extent of reaction at gel in their M-C polymerisation simulations, using systems of up to 10000 branch units. The scatter in the M-C data points is most pronounced in the post-gel region, as expected, and is greater than the scatter in the calculated values of $x_{n,red}$, since the weight-average is a higher moment of the degree-of-polymerisation distribution than the number-average.
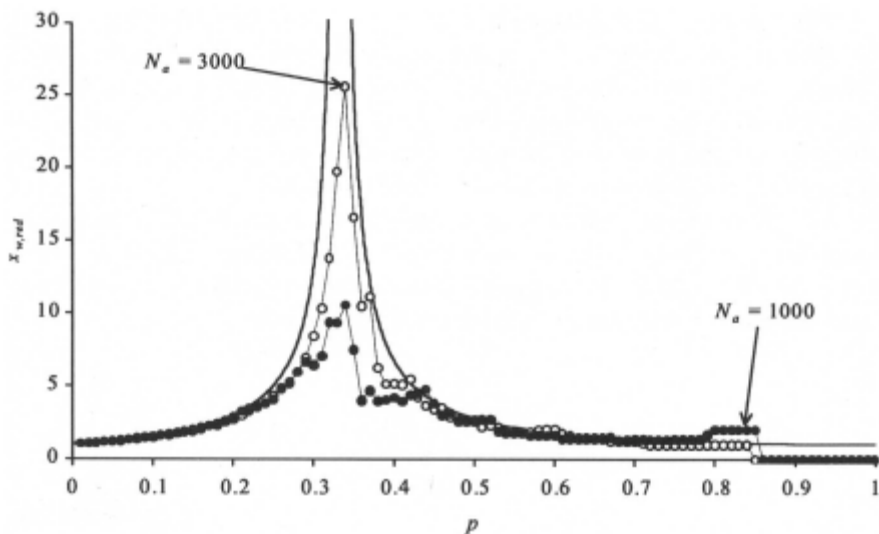
Figure 15.10-3 - **RA₄** simulations: reduced weight-average degree of polymerisation, $x_{w,red}$, versus extent of reaction, p, calculated using the F-S simulation algorithm; the continuous plots, calculated directly from F-S theory, are also shown for comparison.

A principal strength of the M-C approach lies in its ability to record the structural details of the molecules formed. In the numerical F-S simulations, intramolecular reactions leading to the formation of loop structures are allowed on the largest (*i.e.* gel) molecule only after the F-S gel point. At complete reaction, the extents of intramolecular reaction, and hence the numbers of loops for a given number of branch units, can be derived directly from F-S statistics[27](see **Table 15.7-1**). These values are compared with the corresponding values from the **RA₄** simulations in **Table 15.10-1.**

no. of units, N_a	no. of reactive groups $(= f.N_a)$	total no. of pair-wise reactions $(= \frac{1}{2}f.N_a)$	Total no. of loop-forming reactions, N_{re} (M-C)	Total no. of loop-forming reactions, N_{re} (F-S)
500	2000	1000	501	500
1000	4000	2000	1001	1000
3000	12000	6000	3001	3000

Table 15.10-1 - RA₄ polymerisations: numbers of loop structures at complete reaction, N_{re}, predicted[27] by F-S theory $[= \frac{1}{2}f.N_a(1-2/f)]$ (*cf.* **Table 15.7-1**), and calculated by M-C simulations obeying F-S statistics.

The data in **Table 15.10-1** indicate that an extra loop is formed in the numerical (M-C) simulations relative to the analytical predictions of F-S theory. The extra loop is a result of intramolecular reaction between the last two groups to react; a reaction which, in the case of an infinite system, is negligible. It may be noted that the total of extent of ring-forming reaction in **RA₄** self-polymerisations is equal to $(1-2/f) = 1/2,$ as shown earlier in **Table 15.7-1**.

The normalised distributions of loop sizes in completely reacted **RA₃**, **RA₄** and **RA₅** systems of 3000 units, are plotted in **Figure 15.10-4**. In order to compare systems with different functionalities, the ordinate axis is expressed in terms of the number fraction of loop structures, $n_r(i)$, where

$$n_r(i) = \frac{N_r(i)}{\sum_i N_r(i)}$$

Equation 15.10-1

and $N_r(i)$ denotes the number of loop structures consisting of i repeat units. As noted previously[7], the distributions are broad, as loop structures with a wide range of sizes are formed.
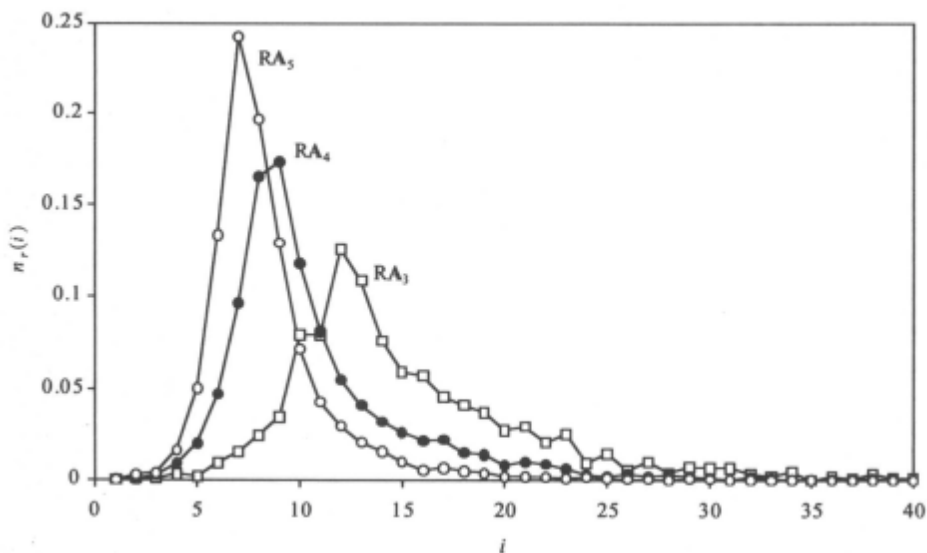
Figure 15.10-4 - the distribution of loop sizes in completely-reacted **RA₃**, **RA₄** and **RA₅** network structures consisting of 3000 branch units; $n_r(i)$ denotes the number fraction of loops containing i repeat units.

Since the formation of loop structures is not weighted in the F-S algorithm the numbers of smallest loops are negligible, and the maxima in the distributions reflect the different numbers of opportunities for forming loop structures of various sizes, integrated over all post-gel reaction. An increase in the branch-unit functionality yields a narrower loop-size distribution, whose maximum appears to shift towards smaller loop sizes. The maxima in the distribution functions in **Figure 15.10-4** occur at $i = 12,$ 9 and 7, for RA_3, RA_4 and RA_5 systems, respectively. The decrease in the scatter of the distributions with increasing functionality is due to an increase in the numbers of opportunities to form loops of the optimum size, and also due to the improvements in M-C averaging over the larger numbers of reactive groups (and hence greater numbers of loops).

The loop-size distributions, as functions of the extent of reaction, were recorded using the M-C algorithm, and the results for the largest RA_4 system $(N_{a0} = 3000)$ are shown in **Figure 15.10-5.** There are several points of interest. The first appearance of loop structures occurs in the interval $p_a = 0.35 - 0.40,$ immediately after the F-S gel point. Prior to this point, no intramolecular reaction is allowed, and hence no loop structures are formed. Loops up to maximum size of $i = 63$ were formed during this particular simulation, and it is interesting to note that the larger loops appear to form relatively early in the post-gel regime. As post-gel reaction continues, the proportion of smaller loops increases rapidly, and the well-defined maximum in the loop-size distribution begins to form. It is notable that there are no smallest loops $(i = 1)$ in this particular case, even at complete reaction.
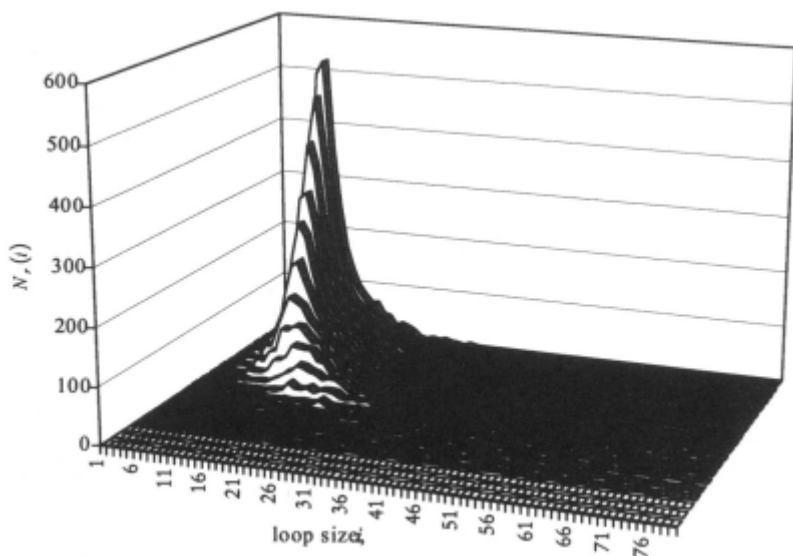
Figure 15.10-5 - cascade plot showing the change in the loop-size distribution with increasing extent of reaction for an **RA₄** simulation obeying F-S statistics **(N_a = 3000).** Loop size is expressed as the number of monomer units per loop, i, and the number of loops of size i as **$N_r(i)$;** the reaction is separated into 20 intervals from **$p = 0 \rightarrow 1$,** with the distribution furthest from the observer corresponding to complete reaction.

The results presented in this section show that the modified M-C algorithm is capable of reproducing F-S statistics for self-polymerisations, allowing for simulation scatter and system-size effects, and serves as a useful check that the numerical algorithm is able to correctly simulate the polymerisation of a population of monomer units.

15.11 Simulations according to F-S statistics – $RA_2+R'B_f$, two-monomer polymerisations

Two-monomer polymerisations of difunctional monomer plus trifunctional or tetrafunctional monomer units were simulated with various numbers of starting units. For illustration, the results for a stoichiometric **$RA_2+R'B_4$** simulation consisting of 1000 branch units (a total of $n_{a0}+n_{b0} = 8000$ reactive groups) are shown in **Figure 15.11-1.** Due to the presence of two monomer species, the abscissa is expressed in terms of the extent-of-reaction product, α.

The development of the loop-size distribution during the course of the simulation is shown in **Figure 15.11-1.** It should be noted that the loop size, i, now describes the number of **–ARA–BR'B–** dimer residues between a pair of

groups reacting to close a loop. Compared to the corresponding plot for the **RA₄** self-polymerisation **(Figure 15.10-5),** the loop-size distribution for the two-monomer system is broader.
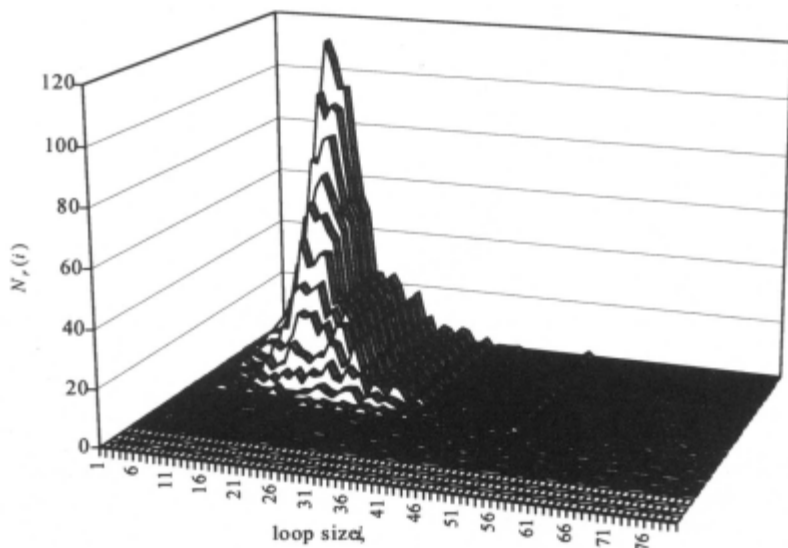
Figure 15.11-1 - cascade plot showing the change in the loop-size distribution with increasing extent of reaction for an **RA₂+R′B₄** simulation obeying F-S statistics $(n_{a0} + n_{b0} = 8000)$. Loop size is expressed as the number of dimer residues per loop, i, and the number of loops of size i as $N_r(i)$; the reaction is separated into 20 intervals from $\alpha = 0 \to 1$, with the distribution furthest from the observer corresponding to complete reaction.

In addition, the maximum in the distribution at complete reaction is shifted towards a larger loop size in the two-monomer system, compared with the self-polymerisation **(Figure 15.10-5).**

It appears that the most probable loop size is closely related to the functionalities of the reactant species, with increases in functionality being associated with decreases in the optimum loop size. In fact, the *average* functionality per reactive group appears to determine the shape of the loop-size distribution. This is demonstrated in **Figure 15.11-2,** where the average distribution from four **RA₂+R′B₄** simulations (whose stoichiometric quantities of reactive groups have an average functionality of 3) is compared with the average distribution from four **RA₃** F-S simulations. Allowing for simulation scatter, the distributions are indistinguishable from each other.
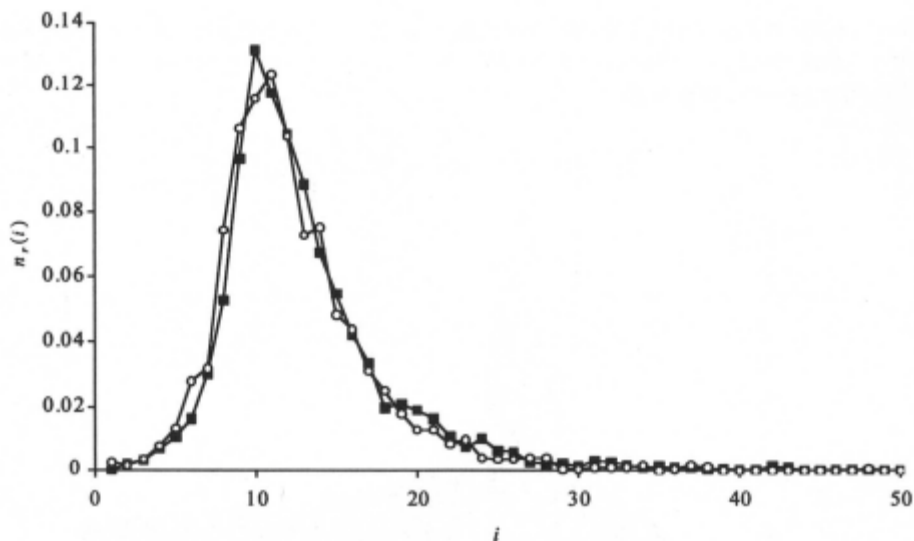
Figure 15.11-2   **RA₃** and **RA₂+R′B₄** simulations at complete reaction; a comparison of the average number-fraction loop-size distributions averaged over four M-C runs, each of 1000 branch units. **(-----) RA₃, (——) RA₂+R′B₄**

15.12 RA₂+R′B_f simulations with pre-gel and post-gel intramolecular reaction

The inclusion of pre-gel intramolecular reaction, weighted according to the size of the loop being formed, is expected to have significant effects on the network structures generated using the M-C polymerisation algorithm. Since the smallest loops are most likely to form (both pre-gel and post-gel), they are expected to dominate in the resulting loop-size distribution. Also, the fact that intramolecular reaction is also likely to occur between groups attached to *sol* molecules may yield a finite sol fraction at complete reaction, due to the formation of completely-reacted, discrete sol species.

A series of simulations were carried out for **RA₂+R′B₃** and **RA₂+R′B₄** systems, using various ring-forming parameters, λ_{a0}. The ranges of values of λ_{a0} covered are those corresponding to the values of $<r^2>$ and $2/(c_{a0}+c_{b0})$ (see **Equation 15.3-2** and **Equation 15.2-9**) for the experimental PU-forming polymerisations (see **Table 15.5-1**). The values of λ_{a0} required to cover the values of $<r^2>$ and reactant concentrations for all the polymerisations lay in the range 0.01 to 0.1 for $f = 3$ and $f = 4$. Initially, therefore, the M-C simulations were performed using this range of values of λ_{a0}.

The development of the loop-size distributions (averaged over the whole reaction mixture), for $RA_2+R'B_4$ systems with $\lambda_{a0} = 0.01$ and $\lambda_{a0} = 0.1$ are plotted in **Figure 15.12-1** and **Figure 15.12-2,** respectively.
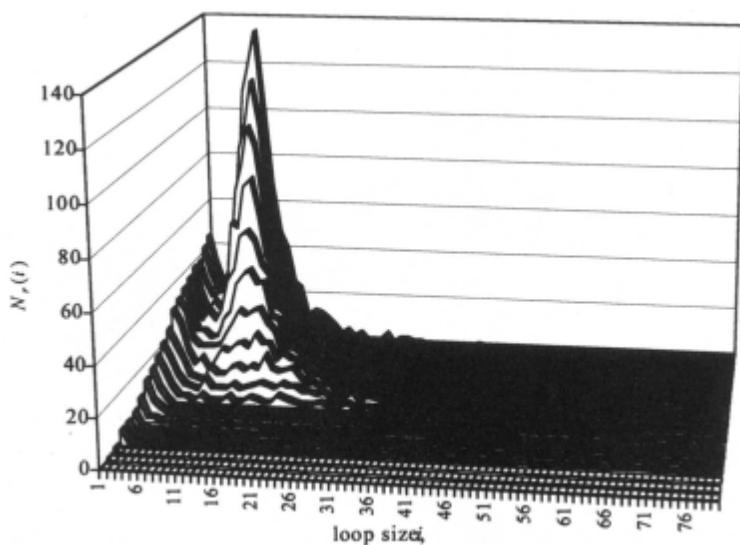
Figure 15.12-1 - $\lambda_{a0} = 0.01$: cascade plot showing the changes in the loop-size distribution (averaged over the whole reaction mixture) with increasing extent of reaction, for an $RA_2+R'B_4$ simulation $(n_{a0} + n_{b0} = 8000)$. Loop size is expressed as the number of dimer residues per loop, i, and the number of loops of size i as $N_r(i)$; the reaction is separated into 20 intervals from $\alpha = 0 \rightarrow 1$, with the distribution furthest from the observer corresponding to complete reaction.
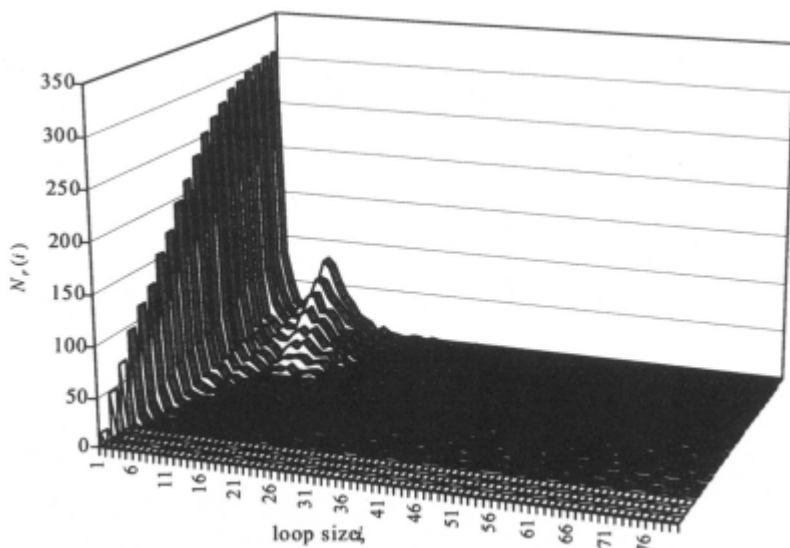
Figure 15.12-2 - as for **Figure 15.12-1**, but with $\lambda_{a0} = 0.1.$

Even though the sol fraction and average degrees of polymerisation (as functions of extent of reaction) calculated during the M-C simulation with $\lambda_{a0} = 0.01$ do not differ significantly from F-S values, the distributions plotted in **Figure 15.12-1** show that, due to the competition between pre-gel and post-gel intramolecular and intermolecular reaction, and the probabilities of forming loops of various sizes, a significant proportion of smallest-loop structures are formed. Peaks in the distributions at intermediate loop sizes, which are characteristic of the loop populations formed according to F-S statistics (see **Figure 15.11-1),** are also present in **Figure 15.12-1.** It may also be noted that larger loops $(i \approx 40)$ are formed relatively early in the simulation. As the reaction nears completion, smallest loops and loops with sizes around the optimum begin to dominate.

Increasing λ_{a0} from 0.01 to 0.1 has a dramatic effect on the loop-size distribution, as shown in **Figure 15.12-2.** The distributions are almost totally dominated by smallest-loop structures. The small numbers of larger loops do not form until much later in the polymerisation. At complete reaction with $\lambda_{a0} = 0.1$ there are approximately four times more smallest loops compared to the simulation with $\lambda_{a0} = 0.01,$ and the characteristic peak in the distribution at intermediate loop-sizes is much smaller.

The distributions at complete reaction for the F-S simulation and the simulations with $\lambda_{a0} = 0.01$ and 0.1 are compared in **Figure 15.12-3.** The dominance of smallest loops as λ_{a0} increases can be clearly seen. Also, it can be

seen that the peak is shifted to slightly lower loop sizes in the simulations using λ_{a0} compared with those using F-S statistics. This is to be expected since intramolecular reactions are then biased towards the formation of smaller loops.
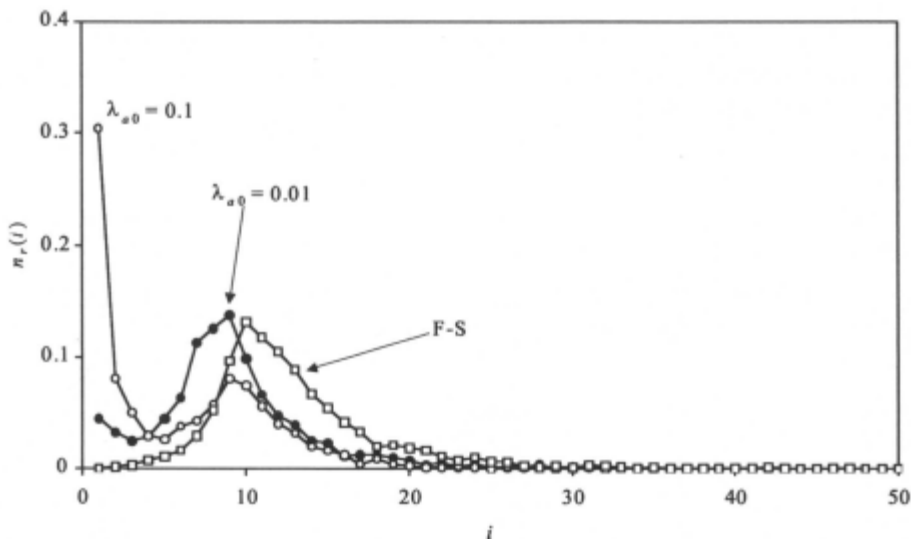
Figure 15.12-3 - $RA_2+R'B_4$ simulations at complete reaction; a comparison of the average number-fraction loop-size distributions for **F-S, $\lambda_{a0} = 0.01$** and $\lambda_{a0} = 0.01$ simulations, each of 1000 branch units.

15.13 Extents of intramolecular reaction – effects of increasing λ_{a0}

It should be stressed that the loop-size distributions presented in the previous two sections are averaged over the *whole* polymerisation mixture. However, it has been shown that for larger values of λ_{a0} there may be a finite number of discrete sol molecules remaining at the end of the simulated polymerisation, which must also contain loop structures. Due to the sizes of these sol species, they are likely to contain a disproportionate amount of small loops. The mechanical properties of elastomeric network materials are usually made *after the removal of any residual sol fraction.* Therefore, in order to compare the simulated network structures with experimental modulus measurements, it is important to differentiate between the loop-structures on the gel molecule and those in sol species.

The changes in the calculated loop-size distributions in the gel molecule with increasing λ_{a0} can be characterised by calculating extents of reaction resulting in smallest loops, $p_{re,1}$, as a function of λ_{a0}, since the exact effects of

smallest loops on network elasticity can be deduced (see **Section 15.6, Figure 15.6-l(a))**. The complementary quantity, $p_{re,\triangleright1}$, the extent of reaction resulting in the formation of *larger* loops may also be calculated. Series of stoichiometric simulations with 1000 branch units were performed with λ_{a0} in the range 0.01 to 0.40.

For illustration, the results for the series of stoichiometric $RA_2+R'B_3$ simulations involving 1000 branch units, with λ_{a0} in the range 0.01 to 0.30, are listed in **Table 15.13-1.**

λ_{a0}	u_g (complete reaction)	$p_{re,1}$	$p_{re,\triangleright1}$	$p_{re,total}$
0.01	1.000	0.0127	0.1543	0.1670
0.03	0.998	0.0224	0.1446	0.1670
0.05	0.994	0.0349	0.1321	0.1670
0.10	0.952	0.0490	0.1180	0.1670
0.15	0.926	0.0695	0.0976	0.1671
0.20	0.828	0.0741	0.0930	0.1671
0.25	0.652	0.0838	0.0833	0.1671
0.30	0.416	0.0979	0.0696	0.1675

Table 15.13-1 - extents of intramolecular reaction leading to the formation of smallest loops, $p_{re,1}$, larger loops, $p_{re,\triangleright1}$, and the total extent of intramolecular reaction, $p_{re,total}$, on the gel molecule at complete reaction, for stoichiometric $RA_2+R'B_3$ simulations. The gel fractions, u_g, at complete reaction are also shown.

The data in **Table 15.13-1** show the decrease in the gel fraction at complete reaction with increasing λ_{a0}. The total extents of intramolecular reaction in the gel molecule are those expected[27]. For an infinite $RA_2+R'B_3$ system, $p_{re,total}$ is given by $\frac{1}{2}(1-2/f) = 1/6$ (see **Table 15.7-1**). The finite size of the simulated systems results in an extra loop structure per molecule at complete reaction, and thus $p_{re,total}$ is slightly increased relative to the ideal case (0.1667). As λ_{a0} is increased, and the gel molecule at complete reaction decreases in size, the extra loop forms a larger proportion of the *total* number of loops in the gel molecule, and $p_{re,total}$ increases. For values of λ_{a0} between 0.3 and 0.4, the size of the gel molecule does not decrease significantly. As expected, the proportion of smallest loops also increases with increasing λ_{a0}, and for $\lambda_{a0} \geq 0.30$, smallest loops account for *ca.* 60% of all loop structures formed on the gel molecule. The values of $p_{re,1}$ and $p_{re,\triangleright1}$ are plotted as functions of λ_{a0} in **Figure 15.13-1.**
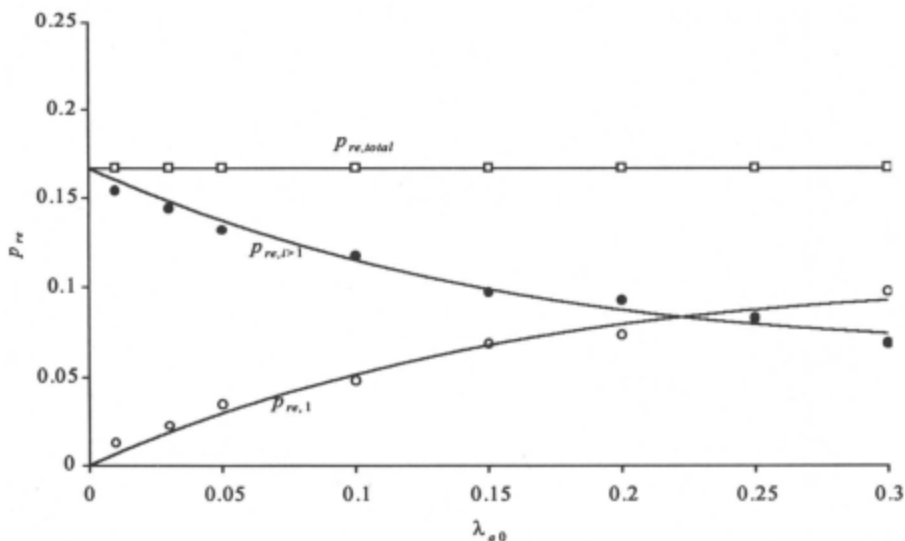
Figure 15.13-1 - $p_{re,1}$ and $p_{re,\triangleright 1}$ versus λ_{a0} for **RA₂+R′B₃** simulations with 1000 branch units at complete reaction

A similar set of stoichiometric **RA₂+R′B₄** simulations were performed, again using system sizes of 1000 branch units. The proportion of smallest loops increases with increasing λ_{a0}, and at $\lambda_{a0} = 0.30$, smallest loops account for *ca.* 50% of all loop structures formed on the gel molecule. In the case of an infinite **RA₂+R′B₄** system[27], $p_{r,total}$ is given by $\frac{1}{2}(1-2/f) = 1/4$ (see **Table 15.7-1**). The values of $p_{re,1}$ and $p_{re,\triangleright 1}$ are plotted as functions of λ_{a0} in **Figure 15.13-2.**
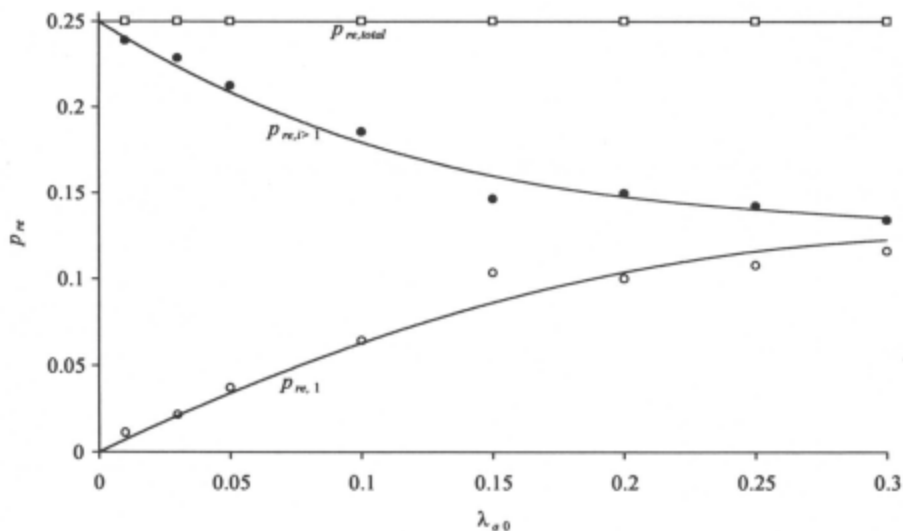
Figure 15.13-2 - $p_{re,1}$ and $p_{re,\triangleright 1}$ versus λ_{a0} for **RA$_2$+R'B$_4$** simulations with 1000 branch units at complete reaction.

The plots in **Figure 15.13-1** and **Figure 15.13-2** show that the incidence of smallest loops $(p_{re,1})$ is negligible when $\lambda_{a0} = 0$. Essentially, in agreement with F-S statistics, all intramolecular reaction then occurs *after* the gel point, resulting in larger loop structures. However, as λ_{a0} increases, $p_{re,1}$ increases, at the expense of the proportion of larger loop structures $(p_{re,\triangleright 1})$, since $p_{re,total}$ remains constant, as dictated by the cycle ranks of the networks at complete reaction. For a given value of λ_{a0}, the tetrafunctional systems give rise to more loop structures than the trifunctional systems, simply due to the greater number of opportunities for loop-formation in the former case. However, relative to the *total* number of loop structures, the proportion of smallest loops appears to be fairly insensitive to the branch-point functionality.

15.14 Correlation of model network topologies with experimental network modulus measurements

The experimental results from six series of PU networks, with trifunctional and tetrafunctional junction points, were described in **Section 15.5** (see **Table 15.5-1**). Generally, there are $f/2$ network chains emanating from an f-functional branch point. In a perfect network, all such chains would be elastically effective; *i.e.* they would be connected to fully elastically effective branch points at both ends. However, in the case of real networks, the formation

of loops causes a reduction in the elasticity of the structure, reducing the modulus relative to that of the perfect network. In the case of network structures with trifunctional and tetrafunctional branch points, the formation of a *smallest* loop renders a fixed number of branch points elastically ineffective, as discussed in **Section 15.6 (Figure 15.6-1a)).** When larger loop structures are considered, the associated loss in elasticity is not immediately evident **Figure 15.6-1b)).** For the present correlation with experimental data, it is assumed that the branch points in larger loops are, on average, of *reduced* elasticity.

The effects of the loop structures on the experimental reductions in moduli can be taken into account, approximately, by basing the numbers of elastically effective chains on the corresponding to the values of $p_{re,1}$ and $p_{re,i>1}$ (taken from the M-C simulations). The numbers of elastic chains, N_c^0, in a hypothetical, perfect network of N_J junctions or branch points is simply given by

$$N_c^{\,0} = \frac{N_J f}{2}$$

Equation 15.14-1

If the number of chains rendered elastically ineffective, N_c^I, can also be estimated, the reduction in modulus, or increase in M_c, can be calculated using

$$\frac{M_c}{M_c^{\,0}} = \frac{N_c^{\,0}}{N_c^{\,0} - N_c^{\,I}}$$

Equation 15.14-2

The quantity N_c^I may be estimated as follows. For the simulated trifunctional networks of N_J branch units, the numbers of smallest loops are given by $3N_J p_{re,1}$, which equates to a loss of elastic chains equal to $3 \times 3N_J p_{re,1}$. However, the $3 \times 3N_J p_{re,i>1}$ chains in *larger* loops are subject only to a partial loss in elasticity, and may be taken as equivalent to $x \times 3 \times 3N_J p_{re,i>1}$ chains, where x is the fractional loss in elasticity per chain in a larger loop structure, ($x = 1$ corresponds to a *total* loss in elasticity, seen in the case of smallest loops only.) Hence, for $f = 3$

$$N_c^{\,I} = \frac{3N_J}{2}\left\{ 6N_J p_{re,1} + x.6 p_{re,i>1} \right\}$$

Equation 15.14-3

and substituting the results from **Equation 15.14-1** and **Equation 15.14-3** into **Equation 15.14-2** yields

$$\frac{M_c}{M_c^0} = \frac{1}{1 - 6p_{re,1} - x.6p_{re,i>1}}$$

<div align="right">**Equation 15.14-4**</div>

A similar expression can be derived for tetrafunctional network structures:

$$\frac{M_c}{M_c^0} = \frac{1}{1 - 4p_{re,1} - x.4p_{re,i>1}}$$

<div align="right">**Equation 15.14-5**</div>

15.14.1 Correlation of simulated loop distributions and experimental modulus measurements

The experimentally determined values of M_c/AM_c^0 (see **Figure 15.5-1**) for the series of PU networks listed in **Table 1** were used in conjunction with simulated values of $p_{re,1}$ and $p_{re,i>1}$ to estimate x, the fractional loss of elasticity for chains larger loop structures, using **Equation 15.14-4** and **Equation 15.14-5**, assuming $A = 1$. However, since $p_{re,1}$ and $p_{re,i>1}$ calculated via M-C are dependent upon P_{ab}, values of M_c/M_c^0 depend on both x and P_{ab}. Correlations between M-C calculations and experimental data were therefore performed in two ways:

i) bivariate least-squares fitting, to evaluate x and P_{ab} simultaneously;

ii) monovariate least-squares fitting, to evaluate x using P_{ab} values calculated *ab initio,* via chain-conformational analyses[25].

Two examples of the fitted experimental M_c/AM_c^0 data with $A = 1$ are shown in **Figure 15.14.1-l(a)** and **Figure 15.14.1-1(b),** for PU systems 1 and 3. In both cases, the bivariate fitting procedure results in very good fits to the experimental data, as expected. M_c/AM_c^0 was also calculated using the *ab initio* values of P_{ab}, but assuming that $x = 0$ (*i.e.* no additional loss in elasticity from larger loop structures), and these values are plotted, for comparison. It is obvious that the neglect of the elasticity loss in larger loop structures results in a *gross underestimation* of the experimentally observed reductions in moduli. The effects of the values used for P_{ab} are secondary compared with the effects of assuming $x = 0$.
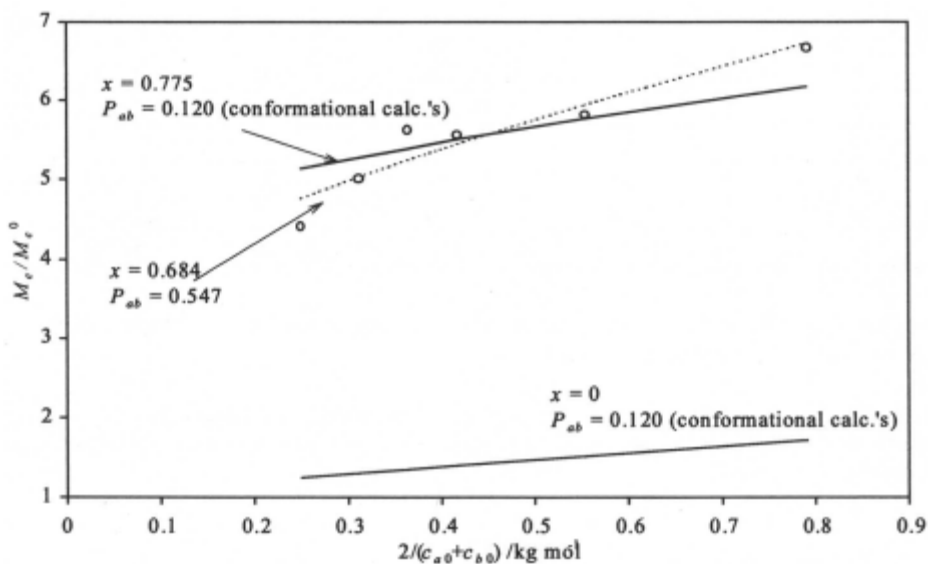
Figure 15.14.1-1 - experimental and calculated (**Equation 15.14-4** and **Equation 15.14-5**) plots of relative reduction in modulus on an affine basis, M_e/M_c^0, versus initial dilution of reactive groups, $2/(c_{a0}+c_{b0})$: (a) PU system **1** ($f = 3$); (b) PU system **3** ($f = 4$)

The calculated values of x and P_{ab}, using monovariate and bivariate analyses, for PU systems 1 to 6 are listed in **Table 15.14.1-1**. Using the bivariate fitting method, it can be seen that values of x in the range 0.67 to 0.60 are required to reproduce the experimental modulus reductions for the trifunctional PU networks (systems 1 and 2), and 0.68 to 0.48 for the tetrafunctional PU networks (systems 3 to 6). In both cases, an increase in the size of the smallest loop structure results in a decrease in x, indicating less elasticity lost. However, the values of P_{ab} estimated from bivariate fitting are much higher than those calculated via $<r^2>$ for the sub-chain structures, and thus the monovariate fitting required larger values of x (0.82 - 0.69, for $f = 3$, and 0.78 - 0.56 for $f = 4$). The unrealistically high values of P_{ab} from the bivariate fitting were required in order to match the slopes of the experimental M_e/M_c^0 plots, which were larger than those calculated using P_{ab} values from chain-conformational analyses.

PU system	f	x^a	$P_{ab}{}^a$ /mol l^{-1}	x^b	$P_{ab}{}^b$ /mol l^{-1}
1	3	0.667	0.538	0.816	0.076
2	3	0.599	0.103	0.690	0.030
3	4	0.684	0.547	0.775	0.120
4	4	0.638	0.457	0.730	0.079
5	4	0.582	0.129	0.637	0.055
6	4	0.481	0.088	0.559	0.032

[a] bivariate fitting

[b] monovariate fitting; P_{ab} values were calculated *ab initio*, via chain-conformational analyses using $\langle r^2 \rangle$ values from **Table 15.5-1**

Table 15.14.1-1 - values of x and P_{ab} based on correlations of experimentally-measured reductions in moduli for PU networks, and extents of intramolecular reaction calculated from M-C simulations

15.15 **Discussion**

The "book-keeping" performed by the M-C nonlinear polymerisation algorithm has been validated by modifying the connection criteria in line with the basic assumptions of F-S polymerisation statistics. The numerical simulation results were found to be in good agreement with the analytical predictions of F-S theory, subject to the usual M-C scatter and finite system-size effects. Furthermore, the major strength of an M-C approach has been illustrated, in that it is able to elucidate the detailed structure of the gel molecule.

Detailed structural information, including the distribution of loop sizes, for polymer network materials is generally inaccessible via experiment. However, correlations between experimentally-measured network moduli and extents of loop-forming reaction calculated via M-C simulation, suggest that larger loop structures ($i>1$) contribute significantly to the observed loss of elasticity (relative to that of a perfect network).

The account of the nonlinear polymerisation algorithm, and simulation results, presented in this chapter demonstrate that a method has been developed to systematically connect up a population of reactant molecules, according to the calculated probabilities of intermolecular and intermolecular reaction. The polymerisation algorithm provides a means of generating realistic model network structures, whose topologies are known in full detail. Although the incidence of unreacted chain ends in a network material can, in principle, be quantified experimentally, enumerating the other significant types of network defect, namely loop structures, remains experimentally intractable. The M-C

simulation approach, in which the numbers of loop structures are weighted according to the molecular structures of the reactants, can provide this detailed information.

Current work is focusing on the direct calculation of the entropies of larger loop structures and more exact calculation of P_{ab} for sub-chains in branched structures. From such calculations, moduli can be predicted more accurately *directly* from reactant structures and reaction conditions.

References

1   J.E. Mark, B.E. Erman, in *Polymer Networks - Principles of Their Formation, Structure and Properties,* ed R.F.T. Stepto, Blackie Academic & Professional, London (1998); chap. 7

2   R.J.J. Williams, *ibid.*, chap. 4

3   N.B. Graham, C.M.G. Hayes, *Macromol. Symp.*, **93,** 293 (1995)

4   K. Dušek in *Polymer Networks - Principles of Their Formation, Structure and Properties,* ed R.F.T. Stepto, Blackie Academic & Professional, London (1998); chap. 3

5   R.F.T. Stepto, *ibid.* chap. 2

6   R.F.T. Stepto, B.E. Eichinger, in *Elastomeric Polymer Networks*, eds. J.E. Mark, B. Erman, Prentice-Hall, Englewood Cliffs, New Jersey (1992); chap. 18

7   S. Dutton, R.F.T. Stepto, D.J.R. Taylor, *Angew. Makromol. Chem.*, **240**, 39 (1996)

8   J.L. Stanford, R.F.T. Stepto, in *Elastomers and Rubber Elasticity, Amer. Chem. Soc. Symp. Series 193,* eds. J.E. Marie, J. Lal, American Chemical Society, Washington D.C. (1982); chap. 20

9   P.J. Flory, *Principles of Polymer Chemistry,* Cornell University Press, Ithaca (1953)

10   P.J. Flory, *J. Amer. Chem. Soc.*, **63**, 3083, 3091, 3097 (1941)

11   P.J. Flory, *Chem. Revs.*, **39**, 137 (1946)

12   W.H. Stockmayer, *J. Chem. Phys.*, **11**, 45 (1943)

13   W.H. Stockmayer, *J. Chem. Phys.*, **12,** 125 (1944)

14   J.L. Stanford, R.F.T. Stepto, *J. Chem. Soc.*, *Faraday Trans. 1,* **71**, 1292 (1975)

15   J.L. Stanford, R.F.T. Stepto, D.R. Waywell, *J. Chem. Soc.*, *Faraday Trans. 1,* **71**, 1292 (1975)

16   W.H. Stockmayer, J. *Polymer Sci* **9**, 69 (1952); **11**, 424 (1953)

17   H. Rolfes, Ph.D. Thesis, University of Manchester (1992)

18   H. Jacobson, W.H. Stockmayer, J. Chem. Phys., **18**, 1600 (1950)

19   S.B. Ross-Murphy, R.F.T. Stepto, in *Large Ring Molecules,* ed J.A. Semlyen (1996); chap 16

20   R.F.T. Stepto, in *Comprehensive Polymer Science,* **1ˢᵗ** Suppl.,(eds. S.L. Aggarwal, S. Russo), Pergamon Press, Oxford, 1992; chap. 10

21   for example, see R.J. Wilson, *Introduction to Graph Theory,* 3rd ed, Longman, London (1985)

22   see R.F.T. Stepto, *Intramolecular Reaction and Network Formation and Properties,* in *Biological and Synthetic Polymer Networks,* ed O. Kramer, Elsevier Applied Science, Barking, 1988; chap. 10

23   J.E. Mark, *Adv. Polymer Sci.*, **44**, 1 (1982)

24   A.B. Fasina, R.F.T. Stepto, *Makromol. Chem.*, **182**, 2479 (1981)

25   D.J.R. Taylor, R.F.T. Stepto, to be published

26   W.W. Graessley, *Macromolecules,* **8**(2), 186, 865 (1975)

27   R.F.T. Stepto, *Polym. Bull. (Berlin),* **24,** 53 (1990)

28   for example, see K-J Lee, B.E. Eichinger, *Polymer,* **31**, 406, 414 (1990)

29   J. Somvársky, K. Dušek, *Polymer Bull,* **33**, 369, 377 (1994)

30   E.S. Page, L.B. Wilson, "*An Introduction to Computational Combinatorics*", Cambridge University Press (1979); p. 74 *et seq.*

CHAPTER 16

THEORETICAL ASPECTS OF CYCLIC POLYMERS: EFFECTS OF EXCLUDED VOLUME INTERACTIONS

Mustapha Benmouna[a)] and Ulrich Maschke[b)]

a) Université Aboubakr Belkaïd, Institut de Physique et Chimie, Bel Horizon, BP119,13000 Tlemcen, Algeria

b) Université des Sciences et Technologies de Lille, Laboratoire de Chimie Macromoléculaire, CNRS UPRESA N° 8009, Bâtiment C6, 59655 Villeneuve d'Ascq Cedex, France

16.1. Introduction

Cyclic polymers provide the ideal conditions for studying the statistics of long polymer chains. Terminal ends in linear chains introduce defects from the statistical point of view since the translational invariance along the chain is suddenly interrupted. This is not the case for ring polymers where all the monomers are identical. This translational invariance along ring homopolymers is very attractive from the theoretical point of view and attributes to this class of polymers with special features as compared to their linear counterparts [l]-[2]. These features were the subject of intensive investigations both from the theoretical [3]-[8] and the experimental [9]-[13] points of view. It has been recognized long time ago that the theta temperature of dilute solutions of ring polymers undergoes a shift downward due to chain closure [11]. The second virial coefficient obtained either from light scattering or osmotic pressure is found to be positive at the ordinary theta temperature $(T=\Theta)$ corresponding to linear chains where normally it should be zero [11] [12] [14] [15]. The size of a ring polymer such as the radius of gyration is more than 40% lower than its linear counterpart for the same molecular weight and temperature only because of chain closure. Under good solvent conditions however, some models predict that cyclic polymers swell more than linear chains. Interestingly enough, many properties of cyclic chains are found to be similar to those of branched polymers. This observation may indicate that the reason for discrepancies between cyclic and linear chains should be the same than that distinguishing linear from branched polymers of the same molecular weight [17]. Since the relatively higher monomer density around the center of mass for branched polymers is responsible for discrepancies with the linear chains, the same interpretation should hold for cyclic polymer systems where the monomer density is slightly higher around the center of mass. This is supported by similarities observed between the properties of cyclic and branched polymers as compared to linear chain systems. The argument of enhanced density used to explain discrepancies between linear and cyclic polymers has been disputed by others who support rather the point of view that such discrepancies are due to

topological constraints [18]-[20]. Topological constraints are certainly responsible for many of die peculiar properties of cyclic polymers but their effects are probably more important in the case of more complex rings presenting multiple knots, catenanes, Olympic rings and others [21] (see Figure 1).
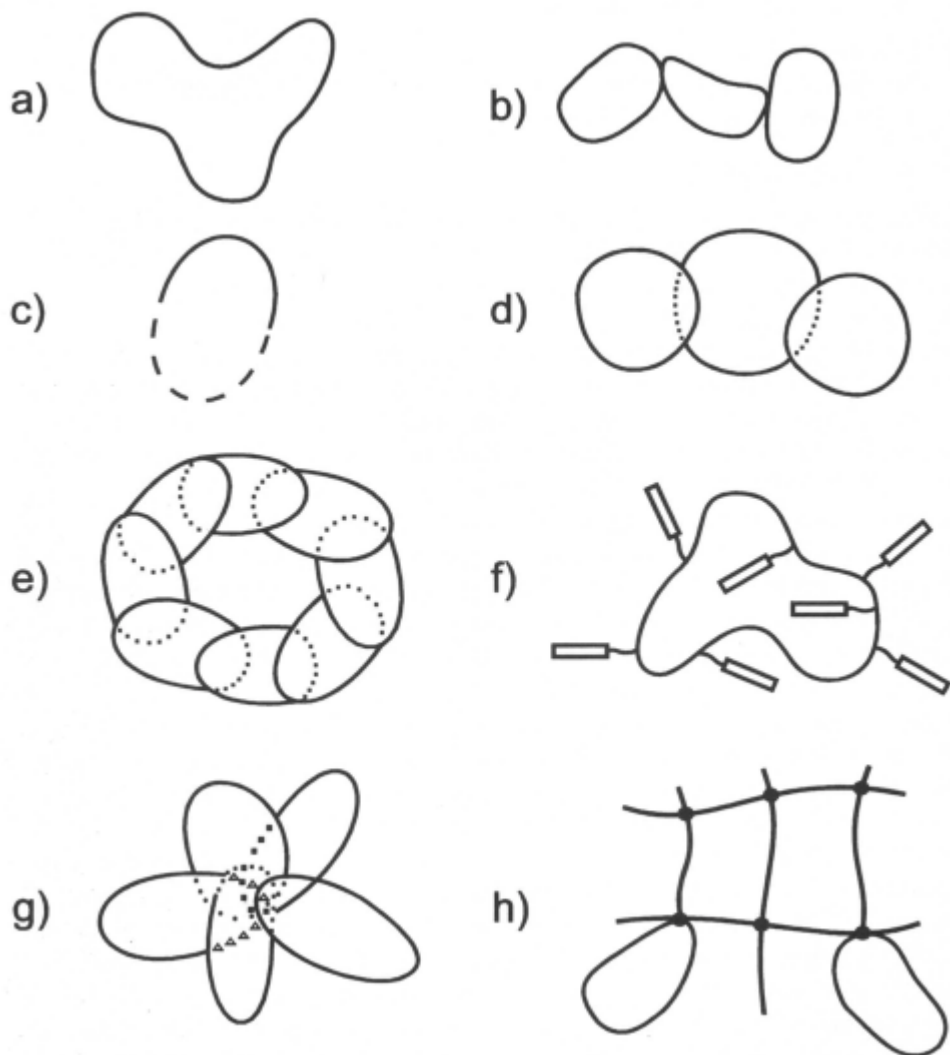
Figure 1 - Examples of ring polymers :a) Simple ring b) Knotted ring c) Cyclic Diblock copoiymer d) Catenanes e) Olympic ring f) Side chain liquid crystal ring g) Micellar ring h) Network polymer with rings

Moreover, their impacts are more sensitive when one looks at bulk properties rather than single chains in solution. To have an idea about the complexity and the large variety of systems involving cyclic polymers, we give in Figure 1 examples of these systems.

In this chapter, we review some properties of cyclic chains underlying their special features by comparing with the results obtained from linear chains. We focus on the simplest case of homopolymers both in theta solvent and in dilute solutions. In section 2, we examine thermodynamics of ring polymers. The shift in the theta temperature due to chain closure is discussed together with the second virial coefficient. The enhanced compatibility of polymer systems in the presence of rings is also invoked. The entropy reduction of cyclic chains in solvent is given within the Flory-Huggins lattice model as suggested by Leonard [22]-[24]. In section 3, structural properties of cyclic chains in solution are reviewed. The radius of gyration and some related quantities are discussed both in theta solvent conditions and under the influence of excluded volume interactions. A particular emphasis is put on the ratio of square radii of gyration of linear and cyclic chains. This ratio is known to have the value 2 under theta solvent conditions whereas field theoretical calculations suggest a slightly lower value in the presence of excluded volume interactions indicating that ring polymers swell more in good solvents than their linear counterparts. Several models predicting more or less consistent results of chain swelling are reviewed. In the same section, the single chain form factor under various conditions of solvent quality and the structure factor in dilute solutions are also examined. In section 4, the dynamical properties of cyclic polymers in solution are discussed. The calculation of the single chain intermediate scattering function is described using both Rouse and Rouse-Zimm eigenmodes. Differences between linear and cyclic chains are highlighted in the calculation of eigenmodes. Hydrodynamic radii in the presence of long range backflow effects are discussed. The effects of excluded volume and hydrodynamic interactions on the intrinsic viscosity are also calculated. The scaling of bulk viscosity in terms of molecular weight is briefly discussed in connection with the reptation model of chains in dense media.

16.2   Thermodynamic properties

16.2.1   Entropy reduction and compatibility enhancement

Studies of the thermodynamic properties of cyclic polymers are scarce as compared to those of linear chain systems. They are relatively less understood and sometimes even fundamental quantities such as the free energy of cyclic polymers in solution or blends involving cyclic polymers are not completely known. One knows that there is entropy reduction due to chain closure but only few attempts were made to evaluate such a reduction. For

example, Leonard [23]-[24] proposed to extend the Flory-Huggins [22] lattice model to mixtures containing cyclic chains. The free energy density in units of thermal energy $k_B T$ is

$$f = \frac{\Delta F}{k_B T} = \frac{\Delta U - T\Delta S}{k_B T} \tag{1}$$

where k_B is the Boltzman constant, T the absolute temperature and ΔU the enthalpy density

$$\frac{\Delta U}{k_B T} = \chi \varphi_s \varphi_i \quad (i = 1, c) \tag{2}$$

χ is the Flory-Huggins interaction parameter, φ_s and φ_i are the volume fractions of solvent s and polymer i, respectively; the polymer being either cyclic (i=c) or linear (i=l); ΔS is the entropy change which for the case of linear chains of degree of polymerization N_1 is given by

$$\frac{\Delta S}{R} = \left(1 + \varphi_1 \left(N_1^{-1} - 1\right)\right)^{-1} \left[\varphi_s \ln \varphi_s + \frac{\varphi_1}{N_1} \ln \varphi_1\right] \tag{3}$$

while, for a solution of rings of degree of polymerization N_c, it is

$$\frac{\Delta S}{R} = \left(1 + \varphi_c \left(N_c^{-1} - 1\right)\right)^{-1} \left[\frac{E^{N_c} + 1}{N_c} \varphi_s \ln \varphi_s + \frac{\varphi_c}{N_c} \ln \varphi_c\right] \tag{4}$$

R is the ideal gas constant. The subscripts s, c and 1 stand for solvent, cyclic and linear chains, respectively. The difference between the entropy changes for cyclic and linear chain solutions with the same degree of polymerization is the factor $\left(E^{N_c} + 1\right)/N_c$ on the right hand side (RHS) of eq. (4). In this factor, the quantity E^{N_c} is given in terms of the tabulated function [25] $\psi(x)$ as follows

$$E^{N_c} = \frac{N_c(N_c - 2)}{N_c - 1}\left[1 - \frac{\Psi\left(\frac{N_c^2 - N_c - 1}{N_c - 1}\right) - \Psi\left(\frac{2N_c - 3}{N_c - 1}\right)}{N_c - 1}\right] \quad (5)$$

For N_c exceeding roughly 20 which is normally the case for polymers, E^{N_c} can be simplified using the approximate form

$$\frac{E^{N_c} + 1}{N_c} \approx 1 - \frac{\ln N_c - 0.4228}{N_c} \quad (6)$$
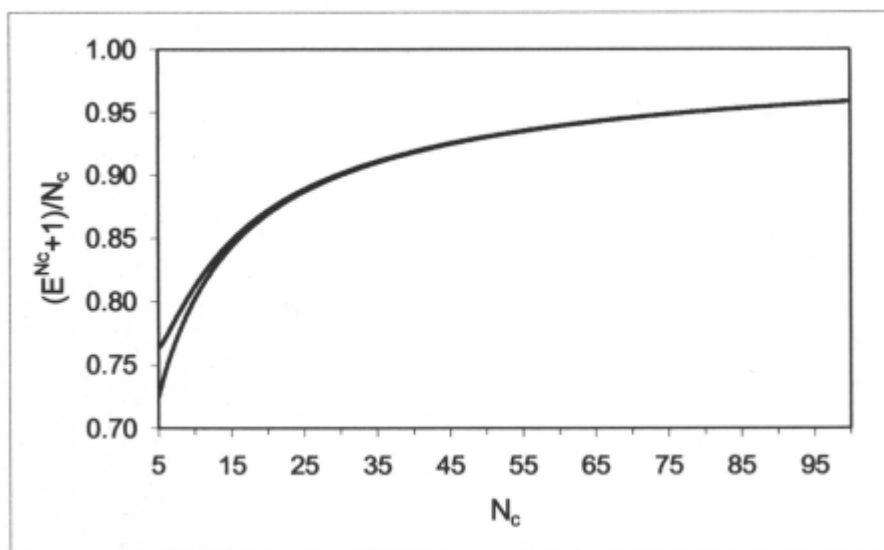
Figure 2 - Representation of $(E^{N_c} + 1)/N_c$ versus N_c (see eqs (4, 6)). This quantity describes the effect of chain closure on the entropy of mixing of polymer/solvent solutions. N_c is the degree of polymerization of the ring. For $N_c \to \infty$, the linear chain limit where $(E^{N_c} + 1)/N_c$ goes to 1 is reached. The lower curve Is the exact result (Eq. (5)). The upper curve is the approximate result (Eq. (6)).

Figure 2 shows the variation of $\left(E^{N_c} + 1\right)/N_c$ as a function of N_c in the exact and approximate forms (eqs. (5) and (6), respectively). Within a very good accuracy, one can safely replace E^{N_c} by the approximate and much simpler form given by eq. (6) as soon as N_c increases above 20. Above $N_c = 100$, the quantity in eq. (6) tends to the asymptotic limit 1 where linear and cyclic chain entropy changes are the same and chain closure is irrelevant. The entropy

reduction due to chain closure represented by the factor $\left(E^{N_c} + 1\right)/N_c$ in eq. (4) is illustrated in Figure 3 for $N_c=N_l=50$. This Figure shows the variation of $\Delta S/R$ versus φ_c and φ_l as given in eqs. (3) and (4). Although small, the entropy reduction in this case cannot be neglected completely. This reduction is observed practically at all polymer volume fractions and reaches a maximum for $\varphi_c \approx 0.9$ in the case under consideration. The effects of chain closure on the enthalpic free energy is even less known than the entropy. Dudowicz and Freed [26] investigated the changes in the Flory-Huggins interaction parameter χ due to crosslinking and chemical bound between different blocks in a block copolymer and in cyclic chains. To evaluate the effects of chain ends, these authors used a generalized lattice cluster theory of polymers, and found that the χ-parameter contains a correction term inversely proportional to the degree of polymerization N_l. In cyclic chains, this term is identically zero.
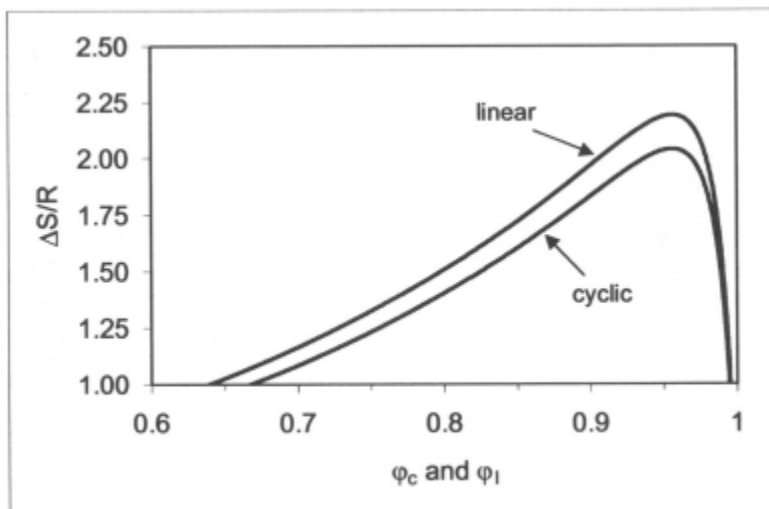
Figure 3 - The entropy of mixing $\Delta S/R$ versus polymer composition φ_c or φ_l. The upper curve corresponds to linear chains (eq (3)) and the lower curve to cyclic chains (eq.(4)) with $N_c=50$.

Khokhlov and Nechaev [27] addressed the problem of mixtures of linear and cyclic polymers by looking to the compatibility enhancement using a generalization of the Flory-Huggins lattice model. Their argument is that restrictions to ring entanglements lead to restrictions on their conformation and hence to a loss of entropy. The total free energy for this system is the standard Flory-Huggins free energy to which a term representing topological constraints through N_e is added, where N_e is the average distance between neighboring entanglement points. The new free energy term reminescent of the ring is

proportional to φ_c/N_e and results into a shift in the critical interaction parameter for a mixture of linear and cyclic polymers

$$\chi_c \sim 1/\sqrt{N_e N_c} \tag{7}$$

while for a blend of linear chains, the critical interaction parameter is

$$\chi_c \sim N_c^{-1} \tag{8}$$

16.2.2. The theta temperature and the second virial coefficient

To our best knowledge, it was Candau et al. [11] who for the first time showed that the theta temperature for cyclic chains in solution undergoes a shift downward. Their observation was made by light scattering of polystyrene (PS) in various solvents. The same result was later confirmed by others [1] [2] [16] [28]. For example, PS in decaline shows a theta temperature at 15°C for the cyclic polymer while for the linear polymer it is 19°C. In cyclohexane, the theta temperature is 34.5°C for linear PS whereas for cyclic PS, this temperature decreases to 28°C. In deuterated cyclohexane, these temperatures are 33°C for ring PS and 40°C for linear PS. One could use these results to assume that at a given temperature, excluded volume effects are more important for cyclic chains than for analogous linear polymers and the swelling is more pronounced, which would be consistent with the field theoretical calculation of Prentis [29]. This author suggested that the ratio of square radii of gyration $\beta = R_{gl}^2 / R_{gc}^2$ should be slightly lower than 2 in the presence of excluded volume effects.

For a dilute solution of linear chains at the theta temperature, the chain size is not perturbed by excluded volume interactions and the second virial coefficient A_{2l} is zero. Using perturbation theory, Zimm et al. [30] [31] derived a relationship between second virial coefficients and swelling factors for linear and cyclic chains. This relationship can be written as follows for linear chains

$$A_{2l} = 2.91 \frac{N_{Av} l^2}{n_0 M} \left(\alpha_l^2 - 1 \right) \tag{9}$$

while for cyclic chains the result is

$$A_{2c} = 2.36 \frac{N_{Av} l^2}{n_0 M} \left(\alpha_c^2 - 1 \right) \tag{10}$$

where N_{Av} is the Avogadro number, M is the molecular weight of the polymer, n_o and 1 the mass and length of a monomeric unit, respectively. The swelling factors α_l and α_c describe the increase of radii of gyration at a temperature T above Θ due to the excluded volume interactions.

$$\alpha_l = \frac{R_{gl}(T)}{R_{gl}(\Theta)} \qquad\qquad \alpha_c = \frac{R_{gc}(T)}{R_{gc}(\Theta)} \qquad\qquad (11)$$

Eqs. (9) and (10) indicate that the second virial coefficient A_2 vanishes at the theta temperature for both linear and cyclic chains. This is a well known behavior for linear chain solutions but it is not completely clear whether it should apply to cyclic chain solutions as well. The theta temperature is defined as the temperature at which the second virial coefficient as measured by light scattering or osmotic pressure vanishes for both linear and cyclic chains. However, in the latter case the polymer size does not seem to follow Gaussian statistics with $v=0.5$ as in the case of linear chains (i.e. $R_{gl} \sim N^{0.5}$). Moreover, the second virial coefficient is known to depend upon molecular weight. As the mass of the polymer becomes larger, the second virial coefficient decreases but differently depending on the chain architecture. It is found that for cyclic polymers, this decrease is faster as compared to linear chain systems [32]-[36].

16.2.3. The critical exponent v

The critical exponent v has been examined extensively by computer simulations [37]-[51] looking at the variation of the radius of gyration versus molecular weight. Most often however, simulations are performed in the bulk state. For linear chains, the exponent is $v_l=0.5$ indicating Gaussian statistics and absence of excluded volume interactions. For cyclic chains, different results are obtained and exponents between 0.4 and 0.45 are observed indicating deviations from Gaussian statistics.

The presence of knots makes the chains more compact and their size increases in the sense that the exponent v is slightly higher than for unknotted rings. Pakula and Geyler [37] reported computer simulations on mixtures of cyclic and linear chains and found that the radius of gyration of linear chains remains independent of composition while that of cyclic chains, the rings show a compact configuration in the presence of a small amount of linear chains. In a concentrated system of linear chains, rings swell considerably. In a system of exclusively cyclic chains, there is a maximum contraction and $v_c=0.45$, which is slightly higher than 0.4 found by others. In dilute mixtures of rings and linear chains, the maximum swelling takes place and leads to an exponent characteristic of Gaussian statistics with $v_c=0.5$.

Muller et al. [39] performed computer simulations on ring polymers and observed that the exponent ν_c depends on the degree of polymerization N. The following relationship was proposed

$$\nu_c \approx 0.386 + \frac{0.327}{N^{0.39}} \tag{12}$$

In the infinite chain limit ν_c goes to 0.386 while for finite chain length ν_c increases slightly.

Jagodzinski et al. [40] investigated the universal shape properties of linear and cyclic chains in the presence of excluded volume interactions using renormalization group theory and Monte Carlo simulations. Considering the scaling of the radius of gyration with the degree of polymerization N they found the critical exponent $\nu{=}0.591$ while by examining the variation of the form factor in the intermediate q range they obtained an exponent $\nu{=}0.587$. They examined the ratio $R_{gl}^2 / (N^{2\nu}l^2)$ and found for linear chains 6.249 which is higher than 6 known theoretically under the theta conditions and lower than 7.042 obtained under good solvent conditions for $\nu{=}0.6$ or 6.9 for $\nu{=}0.587$ knowing that

$$\frac{R_{gl}^2}{N^{2\nu}l^2} = \frac{1}{2(\nu+1)(2\nu+1)} \tag{13}$$

For cyclic chains, the theoretical ratio $R_{gc}^2 / R_{1/2}^2$ is equal to $1/3$ under theta solvent conditions while in the presence of excluded volume, one needs to specify the model for the mean square distance between two points along the chain separated by n monomers as we shall discuss in the forthcoming sections. Note that Monte Carlo simulations of Jagodzinski et al. give 3.217 a slightly higher value than the theta solvent prediction.

16.3   Structural properties

16.3.1 Radii of gyration and related quantities

The radius of gyration can be calculated for both linear and cyclic chains using the general definition

$$R_g^2 = \frac{1}{2N^2} \sum_{ij} \langle r_{ij}^2 \rangle \tag{14}$$

where $\left\langle r_{ij}^2 \right\rangle$ is the mean square distance between monomers i and j along the chain and $\langle ... \rangle$ means the ensemble average. In the continuous limit and for large N, discrete sums can be approximated by an integral and one obtains the following result after replacing double sums by single ones,

$$R_g^2 \approx \frac{1}{N^2} \int_0^N dn(N-n)\left\langle r_n^2 \right\rangle \tag{15}$$

where $|i-j| \equiv n$ and use has been made of the fact that $\left\langle r_n^2 \right\rangle$ depends only on $|i-j| = n$ and not on i and j separately. This is an important simplification which is rigorously valid only in the case of cyclic chains because of translational invariance. In linear chains, the conformation near terminal ends is different from that near the center but nevertheless such a simplification is usually made although the resulting error is not exactly known when one considers measurable quantities such as the radius of gyration.

16.3.1.1 Theta solvent conditions

For a linear Gaussian flexible chain in a theta solvent, the mean square distance between two points along the chain separated by n monomers is approximated by

$$\left\langle r_n^2 \right\rangle = nl^2 \quad (\text{linear}, T = \Theta) \tag{16}$$

where the length of the unit segment 1 is of the order of 10Å but could be much higher for stiff polymers. Substituting eq. (16) into (15) after some straightforward manipulations yields the known result

$$R_{gl}^2 = \frac{Nl^2}{6} \quad (\text{linear}, T = \Theta) \tag{17}$$

For a Gaussian ring, the closure condition requires that $\left\langle r_N^2 \right\rangle = 0$ and $\left\langle r_{N-n}^2 \right\rangle \equiv \left\langle r_n^2 \right\rangle$. The first condition simply states that the two ends are connected and the second condition represents the circularity requirement.

Therefore, the mean square distance between two monomers separated by a chemical distance n becomes

$$\left\langle r_n^2 \right\rangle = nl^2 \left(1 - \frac{n}{N}\right) \tag{18}$$

Use of eqs. (18) and (15) also yields the known result

$$R_{gc}^2 = \frac{Nl^2}{12} \quad \text{(cyclic, } T = \Theta\text{)} \tag{19}$$

Taking the ratio of eqs. (17) and (19) gives

$$\beta = \frac{R_{gl}^2}{R_{gc}^2} = 2 \quad (T = \Theta) \tag{20}$$

This result shows that for Gaussian unperturbed chains of the same degree of polymerization, the radius of gyration of a linear chain is 40% higher than that of the corresponding ring at $T=\Theta$. In the rest of this chapter, the temperature Θ will be assumed equal for linear and cyclic polymers. In the next section, we will see how the above results are modified in the presence of excluded volume effects under good solvent conditions.

16.3.1.2 Good solvent conditions for linear chains

For linear chains, swelling under the effects of excluded volume interaction is characterized by several models. Perturbation theory [16] [46]-[48] gives the following result

$$R_{gl}^2 = \frac{Nl^2}{6}\left[1 + 1.276\, Z\right] \tag{21}$$

where Z is the excluded volume parameter

$$Z = \left(\frac{3}{2\pi l^2}\right)^{3/2} \vartheta \sqrt{N} \tag{22}$$

expressed in terms of ϑ the binary cluster integral

$$\vartheta = \int a^3 r \left[g(r) - 1 \right] \tag{23}$$

and g(r), the pair correlation function. The swelling factor for linear chains α_l is defined by

$$\alpha_l^2 = \frac{R_{gl}^2}{(Nl^2/6)} \tag{24}$$

and is given by the following equations within the perturbation theory

$$\alpha_l^2 = 1 + 1.276 Z \tag{25}$$

When Z becomes higher than 1, other models are available and are valid beyond the range of perturbation theory. One of them is given by the classical Flory equation

$$\alpha_l^5 - \alpha_l^3 = 1.276 Z \tag{26}$$

This equation satisfies the perturbation theory when α_l is close to 1 and Z is smaller than 1. When Z is larger, α_l becomes higher than one and eq. (27) gives the scaling behavior

$$R_{gl}^2 \approx N^{2\nu} l^2 \quad \left(\nu = \frac{3}{5} \right) \tag{27}$$

The temperature blob model due to de Gennes, Daoud and Jannink [49]-[52] may also describe the swelling behavior of linear chains under the influence of excluded volume interactions. This model is expressed as follows (see Figure 9) for linear chains

$$\left\langle r_n^2 \right\rangle = nl^2 \quad \text{for } n \le N_\tau \tag{28}$$

$$\left\langle r_n^2 \right\rangle = \left(\frac{n}{N_\tau} \right)^{2\nu} \xi_\tau \quad \text{for } n \rangle N_\tau \tag{29}$$

where $\mathbf{N_\tau}$ is the number of monomers within a blob and $\mathbf{\xi_\tau}$ is the end-to-end distance of the blob. $\mathbf{N_\tau}$ varies with temperature as $\mathbf{N_\tau \sim (T{-}\Theta)^{-2}}$. $\mathbf{\xi_\tau}$ and $\mathbf{N_\tau}$ are related by

$$\xi_\tau = N_\tau l^2 \tag{30}$$

Long ago, independently Peterlin [53] and Loucheux, Weill and Benoit [54] suggested the same model for chain swelling of linear polymers under good solvent conditions. They wrote the mean square distance between two points along the chain separated by n monomers as follows

$$\left\langle r_n^2 \right\rangle = n^{1+\varepsilon} l^2 \tag{31}$$

where $\boldsymbol{\varepsilon}$ is a smallness parameter comprised between 0 and 0.2. Using this expression into the definition of the radius of gyration yields

$$R_{gl}^2 = \frac{N^{1+\varepsilon} l^2}{(2+\varepsilon)(3+\varepsilon)} \tag{32}$$

or letting $\mathbf{2v{=}1{+}\varepsilon}$ gives the equivalent result

$$R_{gl}^2 = \frac{N^{2v} l^2}{2(2v+1)(v+1)} \tag{33}$$

In the following section we consider the generalization of these considerations to the case of cyclic chains under similar conditions.

16.3.1.3   Good solvent conditions for cyclic chains

The effects of excluded volume interactions on the swelling of cyclic chains are not well understood. Few attempts were made to elucidate this problem and are briefly reviewed here.

First, it is interesting to note that the field theoretical calculations of Prentis [29] have shown that the ratio $\beta = R_{gl}^2 / R_{gc}^2$ in good solvents should be 1.847 which is slightly lower than 2 indicating that rings swell more than linear chains under the effects of excluded volume interactions. At a given temperature, these interactions should be stronger for cyclic chains in comparison with the case of linear chains. Furthermore it is usually admitted

[39] [55] [29] that in infinitely dilute solutions the critical exponent for chain swelling v is the same for linear and cyclic polymers and is close to 0.6, the critical exponent first predicted by Flory for linear chains. Therefore, we shall adopt the following values in the applications below

$$v_c = v_l = \begin{cases} 0.5 \text{ for } T = \Theta \\ 0.6 \text{ for } T \gg \Theta \end{cases} \tag{34}$$

16.3.1.3.1   Perturbation theory

Following the method applied for linear chains, deviations from unperturbed dimensions of ring polymers due to excluded volume were evaluated using perturbation theory and the result is

$$R_{gc}^2 = \frac{Nl^2}{12}\left[1 + \frac{\pi}{2}Z\right] \tag{35}$$

which corresponds to the swelling factor α_c

$$\alpha_c^2 \equiv \frac{R_{gc}^2}{Nl^2/12} = 1 + \frac{\pi}{2}Z \tag{36}$$

Eqs. (24), (25) and (36) show that cyclic chains swell more than linear chains in the presence of excluded volume. Taking the ratio of eqs. (24) and (36) yields

$$\beta = \frac{R_{gl}^2}{R_{gc}^2} = 2\frac{\alpha_l^2}{\alpha_c^2} \tag{37}$$

or, using eq. (25)

$$\beta = 2\frac{1 + 1.276\,Z}{1 + (\pi/2)Z} \tag{38}$$

For small Z, one obtains the perturbation theory result

$$\beta = 2[1 - 0.274\,Z] \tag{39}$$

showing that β decreases slightly under the influence of excluded volume interactions. This result is consistent with the field theoretical calculations of Prentis. However, these calculations were performed in the asymptotic good solvent limit while the perturbation calculations are valid for small deviations from the unperturbed theta state where Z is small compared to 1.

16.3.1.3.2   Flory Model

If excluded volume interactions are strong, one should use a more appropriate model and the Flory equation provides a possible candidate. Assuming that the excluded volume parameter Z is the same for linear and cyclic chains, the only difference between the two systems is the constant in front of Z in eq. (26).
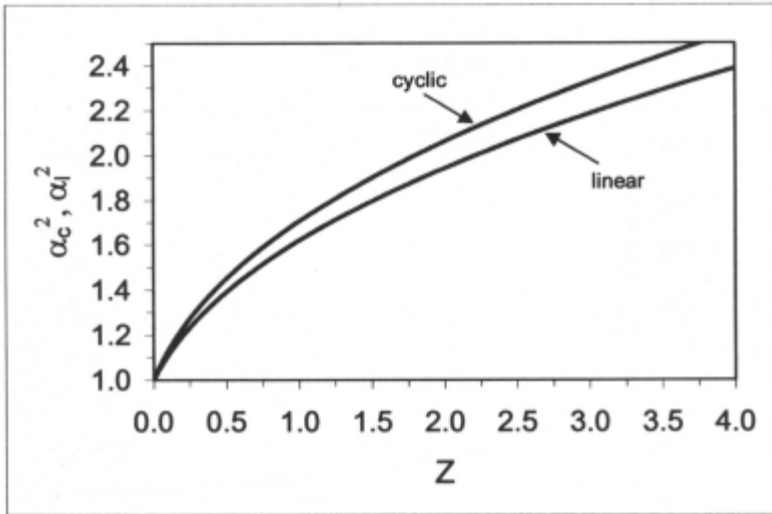
Figure 4 - The swelling factors $\alpha_c^2 = R_{gc}^2/(Nl^2/12)$ and $\alpha_l^2 = R_{gl}^2/(Nl^2/6)$ versus Z, the excluded volume parameter following Flory's equation (eq (26)) for linear chains and for cyclic chains (eq (40)). The upper curve corresponds to cyclic chains. The lower curve corresponds to linear chains.

For cyclic polymers, this constant is $\pi/2$ and the Flory equation becomes

$$\alpha_c^5 - \alpha_c^3 = \frac{\pi}{2} Z \qquad (40)$$

For small excluded volume parameters $Z \ll 1$, α_c is close to 1 and eq. (40) is consistent with the perturbation theory result (see eq (35)). In the asymptotic good solvent limit, α_c increases with Z following the scaling law

$$\alpha_c \to \left(\frac{\pi}{2} Z\right)^{1/5} \tag{41}$$

while for linear chains, this limit gives

$$\alpha_1 \to (1.276 \, Z)^{1/5} \tag{42}$$

Both limits imply that R_{gc} and R_{gl} scale with the degree of polymerization according to
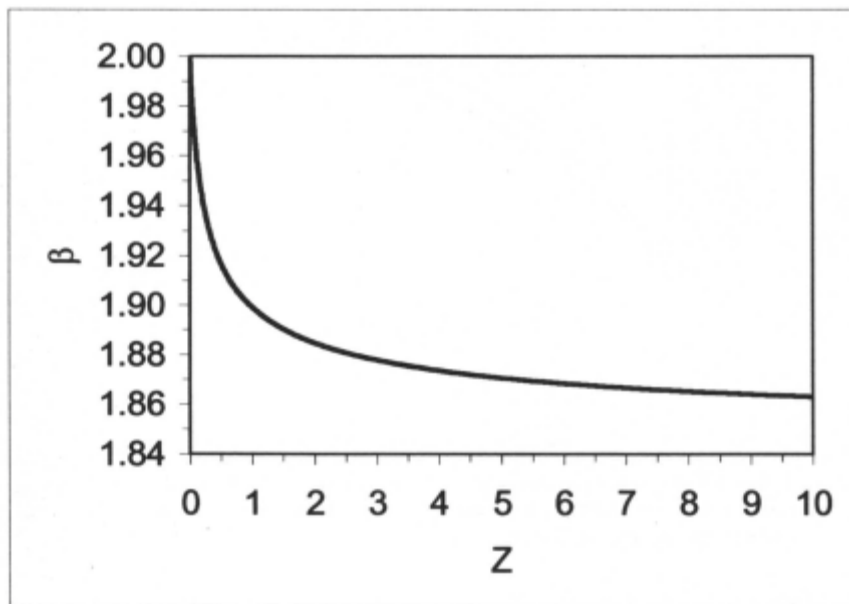
Figure 5 - The ratio $\beta = R_{gl}^2/R_{gc}^2 = 2\alpha_1^2/\alpha_c^2$ versus Z following Flory's equation.

Figure 4 shows the variations of α_c^2 and α_1^2 as a function of Z predicted by eqs. (40) and (26), respectively. Both swelling factors increase rapidly with Z but α_c is slightly higher showing that rings are more sensitive to

excluded volume interactions. The increase for $0<Z<1$ is faster than for $Z>1$. This means that when the temperature increases above Θ, excluded volume interactions develop quickly in both systems and the swelling factor increases linearly with Z. For high values of Z, the asymptotic chain swelling gets slower and follows the power law $\alpha_c \sim \alpha_l \sim Z^{1/5}$ for both species differing only via the constant in front. Likewise Figure 5 represents the ratio $\beta \equiv R_{gl}^2 / R_{gc}^2$ with Z in the same model. Recalling that $\beta = 2\alpha_l^2 / \alpha_c^2$ it is expected to see β decreasing with the excluded volume parameter if cyclic chains indeed swell more than linear chains. The asymptotic limit when Z is large is

$$2\left(\frac{1.236}{1.57}\right)^{2/5} = 1.816$$ slightly lower than the field theoretical result of Prentis

which is 1.847. Other models are available enabling one to account for chain swelling under the effects of excluded volume interactions. We shall review few of them by selecting those that are based upon assumption for the mean square distance between two points separated by n monomers.

16.3.1.3.3   Bloomfield-Zimm model [56]

According to these authors, the swelling of cyclic chains is governed by the following form of the mean square distance

$$\left\langle r_n^2 \right\rangle = l^2 \frac{n^{1+\varepsilon}(N-n)^{1+\varepsilon}}{n^{1+\varepsilon} + (N-n)^{1+\varepsilon}} \tag{44}$$

or equivalently, using $1+\varepsilon=2\nu$,

$$\left\langle r_n^2 \right\rangle = l^2 \frac{n^{2\nu}(N-n)^{2\nu}}{n^{2\nu} + (N-n)^{2\nu}} \tag{45}$$

Figure 6 represents the variation of $\left\langle r_n^2 \right\rangle / \left(N^{2\nu} l^2\right)$ versus n/N according to different models and in particular according to eq. (44) for $\varepsilon=0.1$ and 0.2 (see curves 3a and 3b). Comparing these curves with those of the linear chains 1a and 1b one observes that for small values of n/N the linear chain curves are only slightly higher but for n/N higher than 0.5, there is a larger difference with increases with n/N.
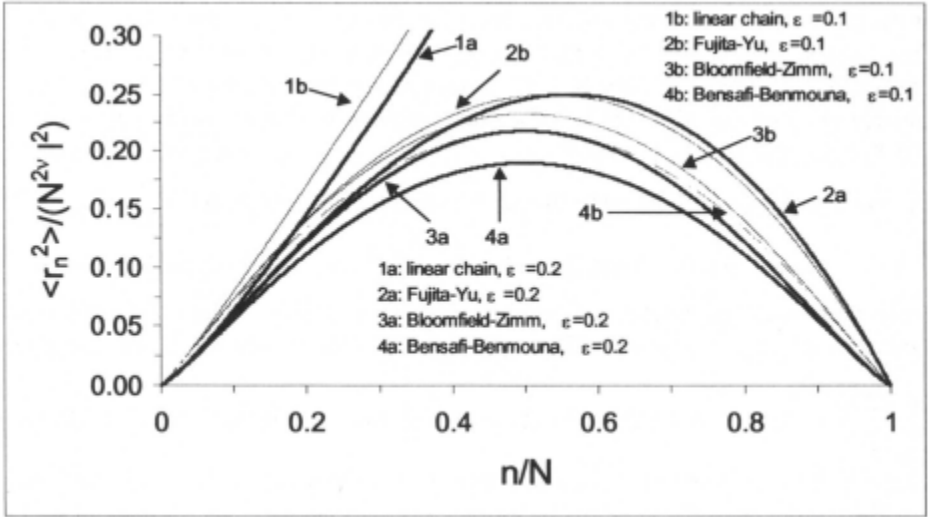
Figure 6 - The mean square distance between two points along the ring polymer separated by n monomers $\langle r_n^2 \rangle$ normalized with $N^{2\nu}l^2$ versus n/N, N being the degree of polymerization for different models of excluded volume Interactions. Thin curves correspond to $\varepsilon = 2\nu-1 = 0.1$ and thick curves correspond to $\varepsilon = 0.2$. In the descending order for thin and thick curves: Fujita-Yu model - Bloomfield-Zimm model - Bensafi-Benmouna model. The curves on the left hand side represent the case of a linear chain.

Substituting eq. (44) into (15) yields

$$R_{gc}^2 = l^2 N^{1+\varepsilon} \int_0^1 dx \frac{x^{1+\varepsilon}(1-x)^{2+\varepsilon}}{x^{1+\varepsilon} + (1-x)^{1+\varepsilon}} \tag{46}$$

The swelling factor is obtained as

$$\alpha_c^2 = 12 N^\varepsilon \int_0^1 dx \frac{x^{1+\varepsilon}(1-x)^{2+\varepsilon}}{x^{1+\varepsilon} + (1-x)^{1+\varepsilon}} \tag{47}$$

Taking the ratio of eqs. (32) and (46) gives

$$\beta = \frac{1}{(2+\varepsilon)(3+\varepsilon)} \frac{1}{\int_0^1 dx \frac{x^{1+\varepsilon}(1-x)^{2+\varepsilon}}{x^{1+\varepsilon} + (1-x)^{1+\varepsilon}}} \tag{48}$$

Figure 7 represents the swelling factor α_c^2 versus ε in different models and curve 2 corresponds to the Bloomfield-Zimm model. There is a continuous increase of α_c^2 with ε. When ε increases from 0 to 0.1, α_c^2 undergoes 50% increase. This model predicts that the swelling factor is slightly lower than in the case of linear chains as excluded volume interactions increase with ε. This is in discrepancy with the model of Flory whose results are shown in Figure 4 in terms of the excluded volume parameter Z.
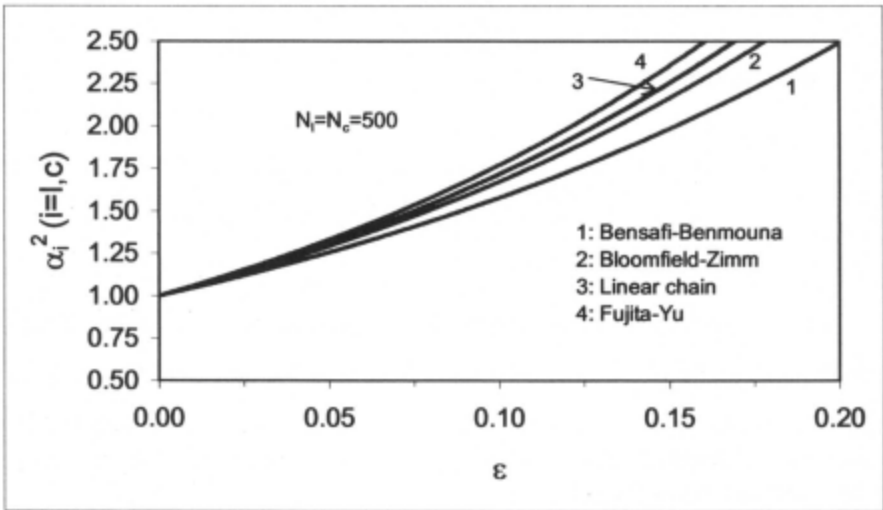
Figure 7 - The swelling factor for cyclic α_c^2 and linear chains α_l^2 versus ε with $N_c = N_l = 500$ for linear chains and three models of excluded volume interactions of cyclic chains. In the descending order : Fujita-Yu model of cyclic chains - Linear chains - Bloomfield-Zimm model of cyclic chains - Bensafi-Benmouna model of cyclic chains.

16.3.1.3.4   Yu-Fujita model [57]

The Yu-Fujita model is different from the previous one and assumes that $\left\langle r_n^2 \right\rangle$ is given by

$$\left\langle r_n^2 \right\rangle = l^2 n^{1+\varepsilon}\left[1-\left(\frac{n}{N}\right)^{1+\varepsilon}\right] \qquad (49)$$

Following the same procedure one obtains

$$R_{gc}^2 = 1^2 N^{1+\epsilon} \int_0^1 dx(1-x)(1-x^{1+\epsilon})x^{1+\epsilon} \tag{50}$$

and the swelling factor is

$$\alpha_c^2 = 12 N^\epsilon \int_0^1 dx(1-x)(1-x^{1+\epsilon})x^{1+\epsilon} \tag{51}$$

and the ratio β

$$\beta = \frac{1}{(2+\epsilon)(3+\epsilon)} \frac{1}{\int_0^1 dx(1-x)(1-x^{1+\epsilon})x^{1+\epsilon}} \tag{52}$$

This model has a major drawback since it does not satisfy the circularity condition $\langle r_n^2 \rangle = \langle r_{N-n}^2 \rangle$ and therefore, it cannot be considered as a reliable model for cyclic chains swelling under the influence of excluded volume interactions. Nevertheless, we shall present its predictions for the sake of comparison with other models.

16.3.1.3.5   Bensafi-Benmouna model [4]

In this model, the mean square distance $\langle r_n^2 \rangle$ is only slightly changed from the Fujita-Yu model as one can see from the following equation to meet the requirement of chain closure

$$\langle r_n^2 \rangle = 1^2 n^{1+\epsilon}\left[1 - \frac{n}{N}\right]^{1+\epsilon} \tag{53}$$

The lowest two curves in Figure 6 show the variation of $\langle r_n^2 \rangle / \left(N^{2\nu} 1^2 \right)$ as a function of n/N for two values of ϵ. It predicts lower values as compared to the Bloomfield-Zimm model in the whole range of n/N. The gap between the two models decreases with ϵ. In this case, one can easily check that the radius of gyration is

$$R_{gc}^2 = 1^2 N^{1+\epsilon} \int_0^1 dx\, x^{1+\epsilon}(1-x)^{2\left(1+\frac{\epsilon}{2}\right)} \quad (54)$$

The swelling factor reads

$$\alpha_c^2 = 12\, N^\epsilon \int_0^1 dx\, x^{1+\epsilon}(1-x)^{2\left(1+\frac{\epsilon}{2}\right)} \quad (55)$$

while the ratio β is

$$\beta = \frac{1}{(2+\epsilon)(3+\epsilon)} \frac{1}{\displaystyle\int_0^1 dx\, x^{1+\epsilon}(1-x)^{2\left(1+\frac{\epsilon}{2}\right)}} \quad (56)$$
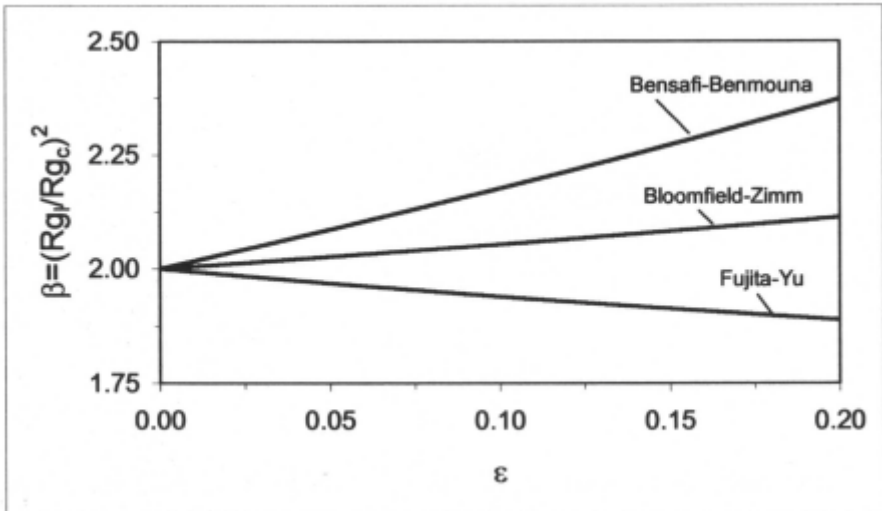
Figure 8 - $\beta = R_{gl}^2/R_{gc}^2$ versus ϵ In the descending order : Bensafi-Benmouna model - Bloomfield-Zimm model - Fujita-Yu model.

The lowest curve in Figure 7 shows the variation of α_c^2 versus ϵ in this model and indicates that the swelling is moderate as compared to Bloomfield-Zimm model (the curve immediately above). Both models predict lower swelling than linear chains. Another appropriate comparison between the

swellings of linear and cyclic chains is provided by the ratio β. This quantity is plotted against ε in Figure 8 and reveals an increase with the excluded volume interaction. This means that linear chains swell more than rings under the effects of excluded volume which is in discrepancy with the Fujita-Yu model and with the field theoretical calculations of Prentis.

16.3.1.3.6 The Blob model [58]

Figure 9 gives schematic representations for the blobs in cyclic (Figure 9a) and linear (Figure 9b) chains. This scheme shows the increased density of monomers in the vicinity of polymer center in the cyclic case. The number of blobs and their size depend upon temperature $T-\Theta$ as indicated earlier. Within a blob, the chain is not sensitive to excluded volume effects and satisfies Gaussian unperturbed statistics while between blobs, excluded volume effects are important. A quantitative implementation of the blob picture is made through the mean square distance $\left\langle r_n^2 \right\rangle$

$$\left\langle r_n^2 \right\rangle = l^2 n \left(1 - \frac{n}{N}\right) \quad ; n \leq N_\tau \tag{57}$$

$$\left\langle r_n^2 \right\rangle = \xi_\tau^2 \frac{n^{1+\varepsilon}\left(1 - \frac{n}{N}\right)^{1+\varepsilon}}{N_\tau^{1+\varepsilon}\left(1 - \frac{N_\tau}{N}\right)^{1+\varepsilon}} \quad ; n \geq N_\tau \tag{58}$$

with

$$\xi_\tau^2 \equiv l^2 N_\tau \left(1 - \frac{N_\tau}{N}\right) \tag{59}$$

For small N_2, the quantity $\left\langle r_n^2 \right\rangle \left(N^{2\nu} l^2\right)$ is similar to the lowest curves of Figure 6. The radius of gyration has two contributions depending on whether excluded volume effects are more or less important. Letting $N_\tau/N=y$ one can easily verify that

$$\frac{R_{gc}^2}{Nl^2} = \frac{y^2}{2}\left(1 - \frac{4y}{3} + \frac{y^2}{2}\right) + \frac{\displaystyle\int_0^1 dx\, x^{1+\varepsilon}(1-x)^{2\left(1+\frac{\varepsilon}{2}\right)}}{y^\varepsilon(1-y)^\varepsilon} \tag{60}$$

The swelling factor in the blob model is found as

$$\alpha_c^2 = 6y^2\left(1 - \frac{4y}{3} + \frac{y^2}{2}\right) + \frac{\displaystyle 12\int_0^1 dx\, x^{1+\varepsilon}(1-x)^{2\left(1+\frac{\varepsilon}{2}\right)}}{y^\varepsilon(1-y)^\varepsilon} \tag{61}$$
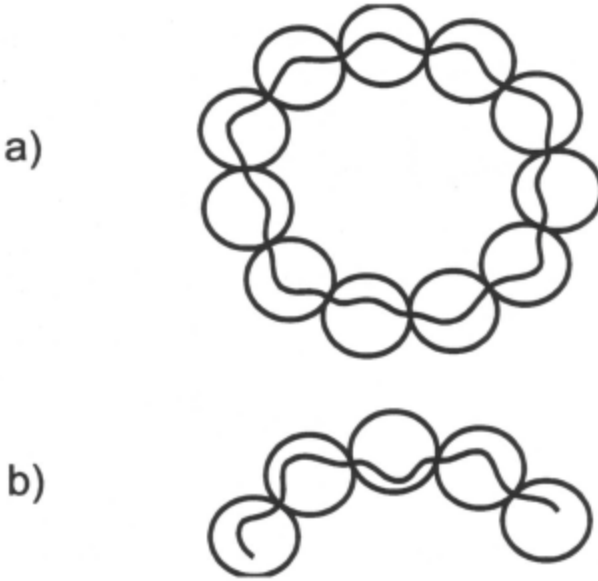
Figure 9 - Schematic representation of the blob model a) cyclic chain b) linear chain

This model is given to complete the discussion of the swelling factor and the ratio β which gives a direct comparison of the swelling behavior of cyclic and linear chains. The former models describe the extend to which chains swell under the effects of excluded volume interactions by fixing the value of exponent ν or ε while in the Flory model, the strength of excluded volume is represented by Z which is proportional to the binary cluster integral which in turn is proportional to $T-\Theta$. The blob model enables one to include the selective

sensitivity of chain to excluded volume depending upon whether one looks at the chain as a whole or at small sections corresponding to chemical lengths lower than the total degree of polymerization. The important feature of the blob model is the possibility it offers to use either of the models presented above. One could choose the model that fits best to the experimental conditions.

16.3.2 The form factor and the structure factor

The calculation of the form factor for a single chain follows a similar procedure as the radius of gyration. The calculation proceeds from the definition of the form factor $P(q)$:

$$P(q) = N^{-2} \sum_{ij} \exp\left(iq r_{ij}\right) \tag{62}$$

where the factor N^{-2} in front is chosen to have the renormalization $P(q{=}0){=}1$. Using the Gaussian approximation, one obtains

$$\left\langle \exp\left(iq r_{ij}\right)\right\rangle \approx \exp\left(-\frac{q^2}{6}\left\langle r_{ij}^2\right\rangle\right) \tag{63}$$

Transforming double sums into single ones and replacing discrete sums by integrals yields

$$P(q) = \frac{2}{N^2} \int_0^N dn\,(N-n)\exp\left(-\frac{q^2\left\langle r_n^2\right\rangle}{6}\right) \tag{64}$$

where terms of the order of N^{-1} are neglected compared to 1. This result shows that the models discussed previously for excluded volume interactions can be applied to the calculation of the form factor.

It is known that under theta conditions, the form factor is given by the following function first derived by Casassa [59]

$$P_c(q) = \frac{2\exp(-u/4)}{\sqrt{u}} \int_0^{\sqrt{u}/4} dt\,\exp\left(t^2\right) \tag{65}$$

where use has been made of $u \equiv q^2Nl^2/6$. If the temperature is only slightly higher than theta, one could introduce the excluded volume effects as a perturbation in the radius of gyration assuming that the form factor is given by eq. (65). To do this, it would be sufficient to let $u = 2q^2R_{gc}^2$ with $R_{gc}^2 = \left(Nl^2/12\right)[1 + (\pi/2)Z]$. If the temperature is much higher than theta and excluded volume interaction is strong, then the form factor of the ring cannot be described by the simple Casassa function. One should find a more appropriate expression taking into account not only the swelling of the radius of gyration but also the chain deformation. This extension could be implemented using an appropriate form for the mean square distance $\left\langle r_n^2 \right\rangle$. One of the models discussed previously could be a candidate. We limit ourselves to the model of Bensafi-Benmouna [4] given by eq. (53). Combining eqs. (55) and (64) yields

$$P_c(q) = 2\int_0^1 dx\,(1-x)\exp\left(-u\,x^{1+\varepsilon}(1-x)^{1+\varepsilon}\right) \qquad (66)$$
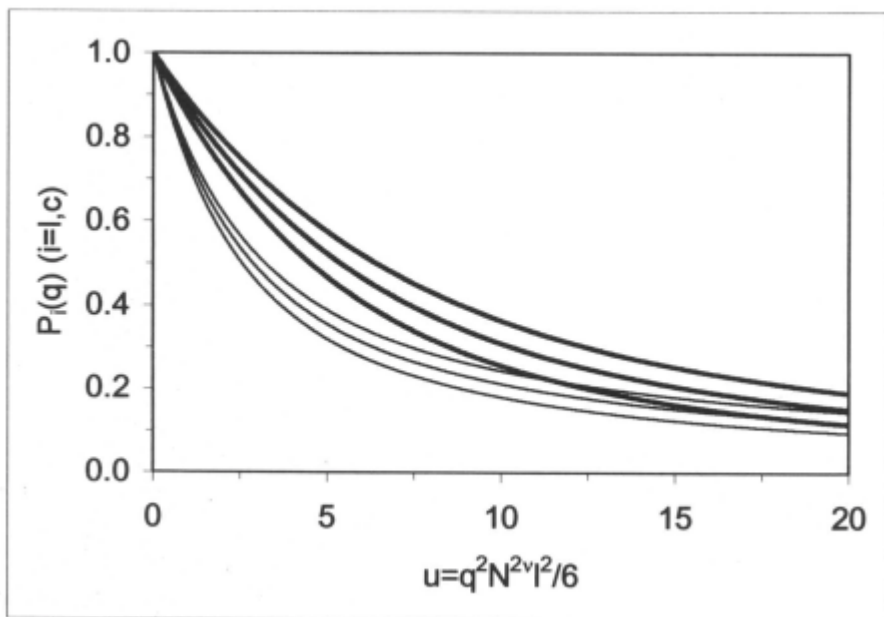
Figure 10 - uP(q) versus $u=q^2N^{2\nu}l^2/6$ for linear and cyclic polymers and three values of the excluded volume exponent $\varepsilon=2\nu-1$. Thick curves represent cyclic chains and thin curves are for linear chains. In the descending order $\varepsilon=0.2$, $\varepsilon=0.1$ and $\varepsilon=0$ (theta solvent). For cyclic chains we use the Bensafi-Benmouna model of chain swelling.

In the presence of excluded volume interactions u becomes

$$u = \frac{q^2 l^2}{6} N^{1+\varepsilon} \tag{67}$$

Figure 10 gives the variation of $P_c(q)$ versus $u \equiv q^2 N^{2\nu} l^2 / 6$ for both linear and cyclic chains and two values of $\varepsilon=0.1$ and 0.2 to describe the effects of excluded volume interactions. Here we choose one model of chain swelling for shortness but it is a straightforward task to extend these calculations to the other models. In the range of u<10, P(q) decays faster for linear chains with and without excluded volume. As excluded volume interactions develop more, the decay of P(q) with u slows down.
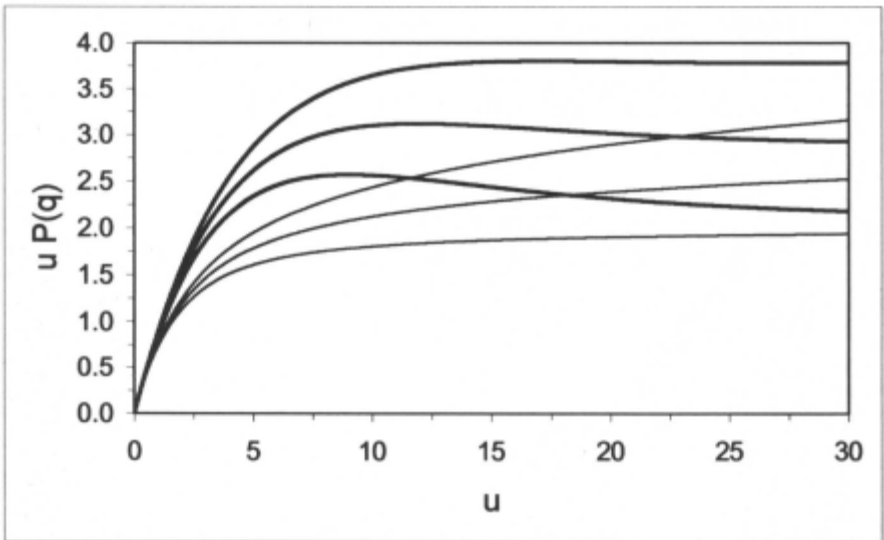
Figure 11 - The same as Figure 10 in the Kratky representation.

Another illustration of these results is given in Figure 11 in the Kratky representation. This representation is useful because it shows the qualitative differences between cyclic and linear chains. The Kratky plots corresponding to cyclic chains under Θ-conditions show a maximum which is not observed in the case of linear chains. This is shown clearly in Figure 11 where u P(q) is plotted versus u for linear (thin lines) and cyclic chains (thick lines) and three values of ε. These values are 0 (Θ - solvent), 0.1 and 0.2 in the ascending order. The maxima in the curves corresponding to cyclic chains tend to disappear when ε decreases as excluded volume interactions become weaker.

The structure factor $S(q)$ is a quantity which is directly accessible by scattering of radiation since it is proportional to the scattered intensity $\Delta I(q)$. One could obtain this quantity in a scattering experiment from a Zimm plot analyzis by writing

$$\frac{K}{\Delta I} = \frac{1}{S(q)} = \frac{1}{M c P_c(q)} + 2A_2 \tag{68}$$

or

$$S(q) = \frac{M c P_c(q)}{1 + 2A_2 M c P_c(q)} \tag{69}$$

where K is a constant depending on the experimental setup and c is the polymer concentration in g/cc. Knowing $P_c(q)$ and A_2, one could easily deduce the properties of the structure factor $S(q)$ in Θ - solvent conditions and in the presence of excluded volume interactions. In good solvent conditions the form factor can be calculated within one of the models for excluded volume interactions described in the preceeding section. In Θ - solvents, the Cassassa function is known to be a good representation of $P_c(q)$. With regards to the second virial coefficient, there is comparatively little information as one can see from our discussions in the first part of this chapter.

16.4   Dynamical properties

16.4.1 The intermediate scattering function

The intermediate scattering function $S(q,t)$ is a quantity that contains information on the time and space correlations of concentration fluctuations [60] - [62]. As such, it gives a direct information of the chain dynamics. It is directly accessible by quasi elastic light scattering (QELS) by using the Siegert relationship between $S(q,t)$ and the field autocorrelation function $g(q,t)$ [60].

$$g(q,t) = 1 + \beta S(q,t) \tag{70}$$

where β is a constant related to the scattering volume. The intermediate scattering function is also accessible by neutron scattering either indirectly from the inverse Fourier transform of the dynamic structure factor $S(q,\omega)$ where ω is the frequency, or directly by neutron spin echo (NSE) technique [63] [64]. To analyze either QELS or NSE measurements of $S(q,t)$ one needs a theoretical expression both in time t and space q. Several theoretical methods are available for the calculation of $S(q,t)$. One of them is the Mori-Zwanzig projection operator technique derived from the linear reponse theory [65]. This method

was further developed in the case of polymer solutions by Akcasu and coworkers [66] - [68]. In the projection operator formalism, S(q,t) satisfies the following integro-differential equation

$$\frac{\partial}{\partial t}S(q,t) + \Omega(q)S(q,t) - \int_0^t du\, \varphi(t-u,q)S(u,q) = 0 \qquad (71)$$

where $\underline{\Omega(q)}$ is the first cumulant or the characteristic relaxation frequency

$$\Omega(q) = \frac{qq : \sum_{ij} \left\langle \underline{D}_{ij} \exp\left(iqr_{ij}\right)\right\rangle}{\sum_{ij}\left\langle \exp\left(iqr_{ij}\right)\right\rangle} \qquad (72)$$

Double dots mean tensor product, the denominator is the form factor $N^2P(q)$ and $\underline{D}_{ij}$ is a diffusion tensor

$$\underline{D}_{ij} = \frac{k_BT}{\xi}\underline{I}\,\delta_{ij} + k_BT\,(1-\delta_{ij})\,\underline{T}_{ij} \qquad (73)$$

δ_{ij} is the Kronecker delta function, $\underline{I}$ the unit tensor, ξ the friction coefficient of a monomer and $\underline{T}_{ij}$ the Oseen tensor describing long range hydrodynamic interactions.

$$\underline{T}_{ij} = \frac{1}{8\pi\eta r_{ij}}\left[1 + \frac{r_{ij}r_{ij}}{r_{ij}^2}\right] \qquad (74)$$

η is the solvent viscosity and the relationship $\xi = 6\pi\eta l$ will be assumed. In eq. (71), $\varphi(t,q)$ represents the memory function which accounts in particular for deviations from single exponential decay functions in the long time limit of S(q,t). Eqs. (71) to (74) are valid whether one deals with linear or cyclic chains. It provides a general formalism for the calculation of S(q,t) and hence it could be of value in the interpretation of QELS and NSE data [63] [64] [67] [68]. However this method is extremely difficult because of the memory function. If one is interested on the initial decay of S(q,t) only and if the memory effects could be neglected, then the first cumulant $\underline{\Omega(q)}$ is sufficient

and leads to quite useful information about chain dynamics in the initial stages. The calculation of the first cumulant defined by eqs. (72) through (74) can be performed by specifying the equilibrium distribution represented by the symbol <...>.

Other methods are available for the calculation of the intermediate scattering function S(q,t) starting from the general definition

$$S(q,t) = \sum_{ij} \left\langle \exp\left(q\left[\underline{r}_i(0) - \underline{r}_j(t)\right]\right)\right\rangle \tag{75}$$

where $\underline{r}_i(0)$ and $\underline{r}_j(t)$ are the position coordinates of monomer i at $t=0$ and monomer j at time t, respectively. This calculation proceeds by using a transformation from the space coordinate $\underline{r}_i$ to normal coordinates $\underline{x}_k$ using the transformation matrix

$$\underline{r}_i = Q_{ik} \underline{x}_k \tag{76}$$

where implicit summation over k is used, i and k run over chain monomers from 1 to N. This transformation allows decoupling of chain dynamics into independent normal modes. A closed chain with nearest neighbor interaction is characterized by the circular matrix $\mathbf{A}$

$$\mathbf{A} = \begin{pmatrix} 2 & -1 & 0 & 0 & - & - & - & -1 \\ -1 & 2 & -1 & 0 & - & - & - & 0 \\ - & - & - & - & - & - & - & - \\ - & - & - & - & - & - & - & - \\ -1 & 0 & 0 & - & - & - & -1 & 2 \end{pmatrix} \tag{77}$$

The transformation matrix $\mathbf{Q}$ diagonalizes the interaction matrix $\mathbf{A}$. The eigenvalues μ_j and eigenvectors Q_{jl} of $\mathbf{A}$ are given by

$$\mu_j = 2\left(1 - \cos\frac{2\pi}{N}j\right) \quad \text{(closed chain)} \tag{78}$$

$$Q_{jl} = \frac{1}{\sqrt{N}}\exp\left(i\frac{2\pi}{N}jl\right) \tag{79}$$

The eigenvalues satisfy the circularity condition $\mu_k = \mu_{N-k}$. For open chains, $\mathbf{A}$, μ_j and Q_{jl} are slightly different. In particular, the eigenvalues μ_j are

$$\mu_j = 2\left(1 - \cos\frac{\pi k}{N}\right) \quad \text{(linear chain)} \tag{80}$$

The time dependent distribution function necessary to solve the integral eq. (75) is split into normal coordinates according to

$$\psi(\underline{x},t) = \psi_0(\underline{x}_0,t)\,\psi_1(\underline{x}_1,t)\,\psi_2(\underline{x}_2,t)\,\ldots\psi_N(\underline{x}_N,t) \tag{81}$$

In the Rouse-Zimm hydrodynamic model, these distribution functions satisfy the decoupled dynamical equations

$$\frac{\partial\psi_0}{\partial t} = \frac{k_B T}{\xi}v_0\frac{\partial^2\psi_0}{\partial x_0^2} \tag{82}$$

$$\frac{\partial\psi_j}{\partial t} = \frac{k_B T}{\xi}\left[v_j\frac{\partial^2\psi_j}{\partial x_j^2} + \frac{3}{l^2}\mu_j\frac{\partial}{\partial x_j}\left(x_j\psi_j\right)\right] \tag{83}$$

where $j=1,2,\ldots N$; ξ is the friction coefficient per monomer; v_j are the eigenvalues of the hydrodynamic matrix $\underline{H}_{ij}$ which is related to the diffusion matrix $\underline{D}_{ij}$ via the relationship

$$\underline{D}_{ij} = \frac{k_B T}{\xi}\underline{H}_{ij} \tag{84}$$

Note that v_0 is the hydrodynamic eigenvalue related to the center of mass diffusion coefficient

$$v_0 = \frac{1}{N}\sum_{ij}H_{ij} \tag{85}$$

$$H_{ij} = \delta_{ij} + (1-\delta_{ij})\frac{\xi}{\sqrt{6\pi\pi}l}\frac{1}{\sqrt{|i-j|\left[1-\frac{|i-j|}{N}\right]}} \tag{86}$$

where the second term in the RHS is just the angular preaveraged form of the Oseen tensor in eqs. (73) and (74) for cyclic chains. For linear chains, one finds

$$\nu_{0l} = 1 + \sqrt{\frac{2N}{3\pi}}\left(\frac{\xi}{\eta l}\right) \tag{87}$$

while for cyclic chains, the result is

$$\nu_{0c} = 1 + \frac{8}{3\pi\sqrt{6\pi}}\sqrt{N}\left(\frac{\xi}{\eta l}\right) \tag{88}$$

This gives the center of mass diffusion coefficient which for cyclic chains, is

$$D_c = \frac{k_B T}{N\xi}\left[1 + \sqrt{\frac{N}{6\pi}}\frac{\xi}{\eta l}\right] \tag{89}$$

and for linear chains,

$$D_l = \frac{k_B T}{N\xi}\left[1 + 0.195\sqrt{N}\frac{\xi}{\eta l}\right] \tag{90}$$

After some lengthy but straightforward calculations, one finds the following result for the intermediate scattering function

$$S(q,t) = \exp\left(-Dq^2 t\right)\sum_{ij}\exp\left(-\frac{q^2 l^2}{6}\sum_{k=1}^{N}F_k(t)\right) \tag{91}$$

with

$$F_k(t) = \frac{|Q_{ki}|^2 + |Q_{kj}|^2 - 2\mathrm{Re}(Q_{ki}Q_{ik})\exp(-\varpi\nu_k t)}{\mu_k} \tag{92}$$

where Re means real part and ϖ is the monomer jump frequency

$$\varpi \equiv \frac{3k_B T}{\xi l^2} \tag{93}$$

Using the eigenvalues μ_k corresponding to cyclic chains yields

$$S(q,t)= \exp\left(-Dq^2t\right)\sum_{ij}\exp\left(-\frac{q^2l^2}{6N}\sum_{k=1}^{N}\frac{\left[1-\cos\left(|i-j|\frac{2\pi k}{N}\right)\exp(-\varpi v_k t)\right]}{\mu_k}\right)\quad (94)$$

Using the following approximation valid for large N

$$\frac{1}{2N}\sum_{k=1}^{N}\frac{1-\cos|i-j|\frac{2\pi k}{N}}{1-\cos\frac{2\pi k}{N}}\approx|i-j|\left[1-\frac{|i-j|}{N}\right]\quad (95)$$

gives

$$S(q,t)=\exp\left(-Dq^2t\right)\sum_{ij}\exp\left(\frac{-q^2l^2}{6}\left\{\begin{array}{l}|i-j|\left(1-\frac{|i-j|}{N}\right)\\+2\sum_{k=1}^{N}\frac{\left(-\exp(-\varpi v_k t)\right)\cos\frac{2\pi}{N}k(i-j)}{\mu_k}\end{array}\right\}\right)$$

$$(96)$$

For linear chains, the result is slightly different

$$S(q,t)=\exp\left(-Dq^2t\right)$$

$$\sum_{ij}\exp\left(\frac{-q^2l^2}{6}\left\{|i-j|+\frac{4}{\pi}\sum_{k=1}^{N}\frac{1-\exp(-\varpi v_k t)}{\mu_k}\cos\frac{\pi k}{N}\left(i-\frac{1}{2}\right)\cos\frac{\pi k}{N}\left(j-\frac{1}{2}\right)\right\}\right)$$

$$(97)$$

Similar results were obtained by Pecora et al. [69]-[71] in the Rouse limit and by Akcasu et al. for linear and cyclic polymers with and without hydrodynamic interactions. In the infinite chain length limit, the circularity condition is irrelevant and one recovers the results of de Gennes [72] for Rouse dynamics and Dubois-Violette and de Gennes [73] including the effects of hydrodynamic interactions via angular preaveraged Oseen tensor. In the presence of hydrodynamic interaction, the asymptotic form of the intermediate scattering function is

$$S(q,t) = \int_0^\infty du \exp\left(-u\left[+h\left(u\tau^{-2/3}\right)\right]\right) \tag{98}$$

where h(u) is given by

$$h(u) = \frac{4}{\pi} \int_0^\infty dx \frac{\cos x^2}{x^3}\left[-\exp\left(-x^2 u^{-3/2}\right)\right] \tag{99}$$

$$\tau = \frac{k_B T}{6\sqrt{2\pi}} q^3 t \tag{100}$$

It is interesting to note that the initial slope of S(q,t) given by the derivative $-\left.\dfrac{\partial S(q,t)}{\partial t}\right|_{t=0}$ is nothing else but $\Omega(q)$ given by

$$\Omega(q) = \frac{k_B T}{6\pi} q^3 t \tag{101}$$

which is a well known result for chains in the intermediate asymptotic q range defined by $ql \to 0$ and $qR_g \to \infty$.

16.4.2 Diffusion coefficients, hydrodynamic radius and corresponding quantities

The diffusion coefficient neglecting memory effects can be calculated from the first cumulant in the $q=0$ limit

$$D = \lim_{q \to 0} \frac{\Omega(q)}{q^2} = \frac{1}{N^2}\sum_{ij}\left\langle \underline{\underline{D}}_{ij}^{33}\right\rangle \tag{102}$$

where $\left\langle \underline{\underline{D}}_{ij}^{33}\right\rangle$ is the component of the diffusion tensor along the direction of q averaged over the equilibrium distribution function. Using eqs. (72) through (74) together with eq. (102) yields the diffusion coefficient

$$D = \frac{k_B T}{N\xi}\left[1 + \frac{\xi}{6\pi\eta N}\sum_{ij}\left(1 - \delta_{ij}\right)\left\langle\frac{1}{r_{ij}}\right\rangle\right] \qquad (103)$$

The first term in the RHS of this equation represents the Rouse contribution while the second one is due to hydrodynamic interactions as already mentioned before. This result can be used to define various hydrodynamic radii for the chain. The Stokes-Einstein radius R_l is defined as

$$R_l = \frac{k_B T}{6\pi\eta D} \qquad (104)$$

The hydrodynamic radius in the free draining limit (Rouse dynamics) R_f assuming that the relationship between friction coefficient ξ and viscosity η is

$$\xi = 6\pi\eta l \qquad (105)$$

yields

$$R_f = Nl = N\left(\frac{\xi}{6\pi\eta}\right) \qquad (106)$$

The effective impermeable radius R_e is defined by

$$R_e^{-1} = \frac{1}{N^2}\sum_{ij}\left(1 - \delta_{ij}\right)\left\langle\frac{1}{r_{ij}}\right\rangle \qquad (107)$$

Eq. (103) can be written in terms of these hydrodynamic radii as

$$R_h^{-1} = R_f^{-1} + R_e^{-1} \qquad (108)$$

For large N, the free draining radius becomes small and R_h is comparable to R_e. The value of this radius depends on both hydrodynamic model and the equilibrium distribution function with and without excluded volume interactions. The results are also sensitive to the chain architecture and should differ whether one considers linear or cyclic polymers. The free draining radius R_f is the same for linear and cyclic polymers but the impermeable radius shows a strong influence of chain architecture. Neglecting the Rouse term, one obtains the ratio

$$\frac{D_l}{D_c} = \frac{8}{3\pi} = 0.849 \tag{109}$$

which is valid in the absence of excluded volume interactions. The hydrodynamic radius can be calculated using

$$R_h^{-1} = N^{-2} \sum_{ij} \left\langle r_{ij}^{-1} \right\rangle \tag{110}$$

The Gaussian approximation yields

$$\left\langle r_{ij}^{-1} \right\rangle \approx \sqrt{\frac{6}{\pi}} \left\langle r_{ij}^2 \right\rangle^{-1/2} \tag{111}$$

Combining these two eqs., one gets

$$R_h^{-1} = 2\sqrt{\frac{6}{\pi}} N^{-2} \int_0^N dn \, (N-n) \left\langle r_n^2 \right\rangle^{-1/2} \tag{112}$$

which can be used for linear and cyclic chains as well.

16.4.2.1   Theta solvent conditions

In a theta solvent, excluded volume interactions are negligible and the mean square distance is $\left\langle r_n^2 \right\rangle = nl^2$ while for cyclic chains, one has $\left\langle r_n^2 \right\rangle = n(1 - n/N)l^2$. Performing some straightforward mathematical manipulations, one obtains

$$R_{hl} = \frac{3}{8}\sqrt{\frac{\pi N}{6}} \, l \tag{113}$$

$$D_l = \frac{8}{3\pi\sqrt{6\pi}} \frac{k_B T}{\eta\sqrt{N} \, l} \tag{114}$$

$$R_{hc} = \frac{1}{\sqrt{6\pi}} \sqrt{N} \, l \tag{115}$$

$$D_c = \frac{1}{\sqrt{6\pi}} \frac{k_B T}{\eta \sqrt{N} l} \tag{116}$$

Considering the ratios of these equations yields

$$\frac{R_{hl}}{R_{hc}} = \frac{D_c}{D_l} = \frac{3\pi}{8} \tag{117}$$

This means that diffusion of cyclic chains is faster than that of corresponding linear chains under theta solvent conditions assuming that both species have the same degree of polymerization. Accordingly, the hydrodynamic radius of cyclic chains is lower. This is consistent with the ratio of radii of gyration if one recalls that under theta conditions $R_{gl} = \sqrt{2} R_{gc} = l\sqrt{N/6}$ and therefore $R_{gl}/R_{gc} = \sqrt{2}$. The following ratios are also useful

$$\frac{R_{gc}}{R_{hc}} = \sqrt{\frac{\pi}{2}} = 1.253 \tag{118}$$

$$\frac{R_{gl}}{R_{hl}} = \frac{8}{3\sqrt{\pi}} = 1.508 \tag{119}$$

The ratio of the radius of gyration and the hydrodynamic radius is higher for linear chains.

16.4.2.2 Good solvent conditions

The above results are modified by the excluded volume interactions present in good solvent conditions. Theoretically, the effects of these interactions could be introduced following different schemes as discussed earlier. In the present section, we examine the increase in hydrodynamic radii or equivalently the decrease in diffusion coefficient due to excluded volume effects within the same schemes. In addition, we need to include the effects of long range hydrodynamic interactions.

16.4.2.2.1 Perturbation theory

Application of perturbation theory to the calculation of the hydrodynamic radius has given the following result [46]-[47]

$$R_{hc} = \sqrt{\frac{N}{6\pi}} \, l \, [1 + 0.63 \, Z]$$
(120)

which corresponds to the diffusion coefficient

$$D_c = \frac{1}{\sqrt{6\pi}} \frac{k_B T}{\eta \, l \sqrt{N}} [1 - 0.63 \, Z]$$
(121)

Under the effects of excluded volume interactions, the hydrodynamic radius increases less rapidly than the radius of gyration since according to eq. (35) $R_{gc} = \sqrt{\frac{N}{12}} \, l \, [1 + 0.785 \, Z]$. This increase in the hydrodynamic size means that chain diffusion gets slower as a result of excluded volume interactions. A similar trend is observed for linear chains where one has

$$R_{hl} = \frac{3}{8} \sqrt{\frac{\pi}{6}} \sqrt{N} \, l \, [1 + 0.609 \, Z]$$
(122)

corresponding to the diffusion coefficient

$$D_l = \frac{8}{3\pi \sqrt{6\pi}} \frac{k_B T}{\eta \, l \sqrt{N}} [1 - 0.609 \, Z]$$
(123)

Considering eqs. (120) through (123), one can form the following characteristic ratios

$$\frac{R_{hl}}{R_{hc}} = \frac{D_c}{D_l} = \frac{3\pi}{8} \frac{1 + 0.609 \, Z}{1 + 0.63 \, Z}$$
(124)

or approximately

$$\frac{R_{hl}}{R_{hc}} = \frac{D_c}{D_l} \approx 1.178 \, [1 - 0.021 \, Z]$$
(125)

The ratio of linear and cyclic chain hydrodynamic radii decreases slightly with excluded volume interactions. This means that cyclic chains swell more in the presence of these interactions and hence ring polymers diffusion tends to slow down in good solvent conditions. This increased sensitivity of the rings to excluded volume interactions is also observed in the radii of gyration within the perturbation scheme. Indeed, if one considers the ratio of the radii of gyration, it is found that

$$\frac{R_{gl}}{R_{gc}} = 1.414 \left[1 - 0.141 Z \right] \tag{126}$$

The decrease of this ratio with Z is larger than for the ratio of hydrodynamic radii. The sensitivity of the ring radius of gyration is not only larger as compared to the radius of gyration of the corresponding linear chain, but this sensitivity to excluded volume interactions is much stronger than in the case of hydrodynamic radii. This would mean that the hydrodynamic interactions tend to reduce the effects of excluded volume interactions. To our knowledge, such observation has not been made before. Another quantity of interest is the ratio of the radius of gyration and the hydrodynamic radius of cyclic chains. Within perturbation theory, this ratio is given by

$$\frac{R_{gc}}{R_{hc}} \approx 1.253 \left[1 + 0.155 Z \right] \tag{127}$$

In general, regardless of the architecture the radius of gyration of a given chain is higher than the hydrodynamic radius. This is the case of eq. (127). In addition, unlike the other two ratios considered above, one observes that R_{gc}/R_{hc} increases sharply with Z confirming the much higher sensitivity of radii of gyration to excluded volume interactions as compared to hydrodynamic radii.

Similar conclusions are reached by considering other models of chain swelling under good solvent conditions. We shall briefly review hereafter three of them by giving only the final results for hydrodynamic radii and corresponding diffusion coefficients for linear and cyclic chain systems. Prior to this discussion and in order to compare with the results for linear chains, we should first give the hydrodynamic radius and diffusion coefficient for the latter system in the presence of excluded volume interactions. This is immediately obtained by combining eq. (112) and the mean square distance for linear chains $\left\langle r_n^2 \right\rangle = n l^2$.

The result is

$$R_{hl} = \sqrt{\frac{\pi}{6}} \frac{(1-\nu)(2-\nu)}{2} N^\nu 1 \tag{128}$$

which by virtue of eq. (104) yields the diffusion coefficient

$$D_1 = \frac{k_B T}{\eta 1 N^\nu} \frac{1}{\pi} \sqrt{\frac{2}{3\pi}} \frac{1}{(1-\nu)(2-\nu)} \tag{129}$$

16.4.2.2.2 Bloomfield-Zimm model

The hydrodynamic radius for a cyclic polymer in a good solvent within the Bloomfield-Zimm model is obtained as

$$R_{hc} = \frac{1}{2}\sqrt{\frac{\pi}{6}} \frac{N^\nu 1}{\int_0^1 dx \frac{(1-x)^{1-\nu}}{x^\nu}\sqrt{x^{2\nu}+(1-x)^{2\nu}}} \tag{130}$$

corresponding to the diffusion coefficient

$$D_c = \frac{k_B T}{\eta 1 N^\nu} \frac{1}{\pi}\sqrt{\frac{2}{3\pi}}\int_0^1 dx \frac{(1-x)^{1-\nu}}{x^\nu}\sqrt{x^{2\nu}+(1-x)^{2\nu}} \tag{131}$$

and the ratio

$$\frac{R_{hc}}{R_{hl}} = \frac{D_1}{D_c} = \frac{1}{(1-\nu)(2-\nu)\int_0^1 dx \frac{(1-x)^{1-\nu}}{x^\nu}\sqrt{x^{2\nu}+(1-x)^{2\nu}}} \tag{132}$$

16.4.2.2.3   Yu-Fujita model

The form of the hydrodynamic radius in this model is only slightly different from eq. (130) and is given by

$$R_{hc} = \frac{1}{2}\sqrt{\frac{\pi}{6}}\frac{N^{\nu}1}{\int\limits_{0}^{1}dx\dfrac{1-x}{x^{\nu}\sqrt{1-x^{2\nu}}}} \tag{133}$$

while the diffusion coefficient is

$$D_c = \frac{k_BT}{\eta 1 N^{\nu}}\frac{1}{\pi}\sqrt{\frac{2}{3\pi}}\int\limits_{0}^{1}dx\frac{1-x}{x^{\nu}\sqrt{1-x^{2\nu}}} \tag{134}$$

and the ratio of these equations and eqs. (128), (129) yields

$$\frac{R_{hc}}{R_{hl}} = \frac{D_1}{D_c} = \frac{1}{(1-\nu)(2-\nu)\int\limits_{0}^{1}dx\dfrac{1-x}{x^{\nu}\sqrt{1-x^{2\nu}}}} \tag{135}$$

Here, we present the equations without further comments. The results of different models can be easlily compared by giving a value to the exponent ν or **ε** and evaluating the integrals numerically.

16.4.2.2.4   Bensafi-Benmouna model

Since the results are similar to those of the above two models, we write them without further comments

$$R_{hc} = \frac{1}{2}\sqrt{\frac{\pi}{6}}\frac{N^{\nu}1}{\int\limits_{0}^{1}dx\dfrac{(1-x)^{1-\nu}}{x^{\nu}}} \tag{136}$$

$$D_c = \frac{k_BT}{\eta 1 N^{\nu}}\frac{1}{\pi}\sqrt{\frac{2}{3\pi}}\int\limits_{0}^{1}dx\frac{(1-x)^{1-\nu}}{x^{\nu}} \tag{137}$$

and

$$\frac{R_{hc}}{R_{hl}} = \frac{D_l}{D_c} = \frac{1}{(1-\nu)(2-\nu)\int\limits_0^1 dx \frac{(1-x)^{1-\nu}}{x^\nu}} \tag{138}$$

These models correspond to different ways of accounting for excluded volume interactions under good solvent conditions. All the formulae are written in terms of the exponent ν or $\varepsilon=2\nu-1$ to allow for a direct comparison between different models. It is sufficient to give a value to ν and ε and to perform numerical integration to make such a comparison. It would be interesting to compare these model predictions with experimental data when they become available or if some computer simulations can be performed to explore the effects of hydrodynamic and excluded volume interactions on the hydrodynamic radii, diffusion coefficients and related quantities.

16.5   Viscosity of cyclic polymers

16.5.1 Intrinsic viscosity

16.5.1.1   Rouse dynamics under theta solvent conditions

The measurement of the intrinsic viscosity is a useful way to characterize with a high accuracy the shape, architecture and size of polymers. It may yield even more precise data than other techniques such as light scattering. The intrinsic viscosity under oscillatory shear of frequency ω is [16] [17] [74]

$$[\eta] = \frac{RT}{2\omega M \eta} \sum_{k=1}^N \frac{1}{\mu_k [1+\omega\tau_k]} \tag{139}$$

M is the molecular weight, R is the ideal gas constant, and τ_k is the Rouse relaxation time of the mode of order k. For large N, the eigenvalues μ_k can be approximated by

$$\mu_k \text{ (cyclic)} \cong \frac{4\pi^2 k^2}{N^2} \tag{140}$$

$$\mu_k \text{ (linear)} \cong \frac{\pi^2 k^2}{N^2} \tag{141}$$

The intrinsic viscosities at zero frequency $(\omega=0)$ are easily obtained from the above equations as

$$[\eta]_l = \frac{RT}{12\varpi} \frac{N^2}{M\eta} \tag{142}$$

$$[\eta]_c = \frac{RT}{24\varpi} \frac{N^2}{M\eta} \tag{143}$$

Their ratio is

$$\frac{[\eta_l]}{[\eta_c]} = 2 \tag{144}$$

According to Flory, the intrinsic viscosity is within a constant factor given by $[\eta] = R_g^3 / M$ for both cyclic and linear chains. However, it is worthnoting that from this expression one would obtain a ratio of intrinsic viscosities equal to $2\sqrt{2} = 2.8$ which is quite high as compared to eq. (144). A more precise form of the intrinsic viscosity including hydrodynamic interaction is $[\eta] = R_h R_g^2 / M$ which would give a ratio $[\eta_l]/[\eta_c] = \frac{R_{hl}}{R_{hc}} \frac{R_{gl}^2}{R_{gc}^2} = \frac{3\pi}{4} = 2.355$ closer to the result in eq. (144). The application of the latter formula to the study of intrinsic viscosities in the presence of hydrodynamic and excluded volume interaction is presented in the following section.

16.5.1.2 Effects of hydrodynamic and excluded volume interactions

Viscosity measurements [15] [28] [75] on binary solutions of PS and cyclohexane at 34.5°C (theta temperature) and in THF (good solvent) have revealed significant deviations from the ratio $[\eta_c]/[\eta_l] = 0.5$. For example, the ratio for PS/cyclohexane is 0.66 while in THF it is even higher and equal to 0.73. These results indicate that cyclic chains swell more than linear counterparts under the influence of excluded volume interactions.

The results in eqs. (142) and (143) are valid neither qualitatively nor do they yield the proper scaling of $[\eta]$ versus N. Other expressions should be found to account for hydrodynamic interactions and excluded volume. One could use the following expression which is good within a numerical factor

$$[\eta] = \frac{R_h R_g^2}{M} \qquad (145)$$

This expression is quite convenient from a theoretical point of view. It allows one to include both hydrodynamic backflow effects through R_h and excluded volume interactions through both R_h and R_g. The models of excluded volume introduced earlier could be particularly useful for this purpose.

16.5.1.2.1   Perturbation theory

Combining eq. (145) with the expression of R_g (eq. (21)) and R_h (eq. (122)) yields

$$[\eta] = \frac{3}{48}\sqrt{\frac{\pi}{6}}\frac{N^{3/2}l^2}{M}[1 + 1.885\,Z] \qquad (146)$$

while combining of eqs. (35), (120) and (145) yields the intrinsic viscosity for rings in the perturbation limit

$$[\eta]_c = \frac{3}{12\sqrt{6\pi}}\frac{N^{3/2}l^2}{M}[1 + 2.20\,Z] \qquad (147)$$

In the absence of excluded volume where $Z=0$, one obtains $\dfrac{3\pi}{4} = 2.355$ as indicated earlier. In the perturbation limit, one has

$$\frac{[\eta_l]}{[\eta_c]} = \frac{3\pi}{4}[1 + 3.085\,Z] \qquad (148)$$

This result shows that hydrodynamic and excluded volume both contribute to increase the ratio $[\eta_l]/[\eta_c]$ in discrepancy with the experimental data of Lutz et al. which indicate that this ratio should be lower than 2.

If Z increases, the Flory equation for chain swelling is useless since the hydrodynamic radii are not available. Other models such as the ones described

earlier in this chapter should be used. We briefly illustrate the application of three of them to the calculation of the intrinsic viscosity.

16.5.1.2.2   Bloomfield-Zimm model

In the previous sections, we calculated both the radius of gyration and the hydrodynamic radius in the Bloomfield-Zimm model of ring swelling under the influence of excluded volume interactions. Therefore all the ingredients are available to compute the intrinsic viscosity according to eq. (145). Combining equations (46), (129), and (145) yields for the cyclic chains

$$[\eta]_c \cong \frac{N^{3\nu} l^3}{2M} \sqrt{\frac{\pi}{6}} \frac{\displaystyle\int_0^1 dx \frac{x^{2\nu}(1-x)^{1+2\nu}}{x^{2\nu}+(1-x)^{2\nu}}}{\displaystyle\int_0^1 dx \frac{(1-x)^{1-\nu}}{x^{\nu}}\sqrt{x^{2\nu}+(1-x)^{2\nu}}} \tag{149}$$

while for the linear polymer, the intrinsic viscosity is obtained from eqs. (32), (130) and (145)

$$[\eta] = \frac{N^{3\nu} l^3}{4M} \sqrt{\frac{\pi}{6}} \frac{(1-\nu)(2-\nu)}{(1+\nu)(1+2\nu)} \tag{150}$$

Taking the ratio of these two results yields

$$\frac{[\eta]}{[\eta]_c} = \frac{(1-\nu)(2-\nu)}{2(1+\nu)(1+2\nu)} \frac{\displaystyle\int_0^1 dx \frac{(1-x)^{1-\nu}}{x^{\nu}}\sqrt{x^{2\nu}+(1-x)^{2\nu}}}{\displaystyle\int_0^1 dx \frac{x^{2\nu}(1-x)^{1+2\nu}}{x^{2\nu}+(1-x)^{2\nu}}} \tag{151}$$

16.5.1.2.3 Bensafi-Benmouna model

A similar procedure can be repeated in the case of another model of chain swelling. For example, the Bensafi-Benmouna model introduced earlier yields

$$[\eta]_c \cong \frac{N^{3\nu} l^3}{2M} \sqrt{\frac{\pi}{6}} \frac{\int_0^1 dx \, (1-x)^{1+2\nu} x^{2\nu}}{\int_0^1 dx \, \frac{(1-x)^{1-\nu}}{x^\nu}} \qquad (152)$$

while the linear chain result is given in eq. (150). The ratio of intrinsic viscosities in the present case is

$$\frac{[\eta]}{[\eta]_c} = \frac{(1-\nu)(2-\nu)}{2(1+\nu)(1+2\nu)} \frac{\int_0^1 dx \, \frac{(1-x)^{1-\nu}}{x^\nu}}{\int_0^1 dx \, (1-x)^{1+2\nu} x^{2\nu}} \qquad (153)$$

Comparison of these results requires a numerical calculation of these integrals which can be performed quite easily by choosing a value for the exponent ν.

16.5.1.2.4 Blob model

Dodgson and Semlyen [76] reported data of $[\eta_l]$ and $[\eta_c]$ for PDMS in various theta and good solvents and observed different behaviors depending upon molecular weight. For short chains, they observed that $[\eta]$ is not sensitive to the excluded volume but for long chains, the swelling is important under good solvent conditions. One could attempt to account for this selective sensitivity to excluded volume with regards to the molecular weight by using the blob picture whereby excluded volume effects are important only if the molecular weight is higher than a certain value M_τ and neglegible below. The square radius of gyration within the blob model is given by eq. (60) in terms of $y = N_\tau / N$ and $\varepsilon \equiv 2\nu - 1$ while the hydrodynamic radius can be easily deduced from eqs. (57), (58) and (112). Therefore, one could deduce immediately the intrinsic viscosity using eq. (145) and the remaining task is to perform numerical calculations if one knows N_τ / N and ε and if one chooses a model for the mean square distance between two points separated by a chemical

distance n exceeding N_τ. For more details on the blob model one could refer to the paper by Larabi et al. [58].

16.5.2 Viscosity of dilute and strong polymer solutions

The intrinsic viscosity is related to the specific viscosity η_{sp} by the known definition

$$[\eta] = \lim_{c \to 0} \frac{\eta_{sp}}{c} = \lim_{c \to 0} \frac{\eta - \eta_0}{\eta_0 \, c} \qquad (154)$$

The specific viscosity is determined in dilute solution if the intrinsic viscosity $[\eta]$ and Huggins coefficient k_H are known.

$$\frac{\eta_{sp}}{c} = [\eta] + k_H [\eta] c + \dots \qquad (155)$$

The Huggins coefficient depends upon interactions and hydrodynamic backflow effects. For dilute solutions, it is sufficient to know k_H to determine the variation of η_{sp}/c with concentration to the first order.

The problem of the dependence of η_{sp} on molecular weight and concentration of linear and cyclic chains is still unsolved. Two regimes are distinguished. In the dilute regime, it is sufficient to consider the first order concentration and determine the Huggins coefficient k_H. Different models are available for linear chains and could be extended to the case of cyclic polymers if chain closure is accounted for properly. In the highly entangled regime, the viscosity scales with molecular weight following the scaling law for cyclic and linear chains as $\eta \sim M^{3.4}$. This indicates that the threshold molecular weight M_c above which entanglement takes place is a property of segment rather than a property of the chain as a whole. This analogous behavior of linear and closed polymers would point out to a similar dynamic mechanism of reptation which would be surprising. Relaxation of the constraints in the reptation mechanism takes place only at the terminal ends and becomes ambiguous for closed chains. Therefore cyclic polymers cannot reptate according to a constraint release mechanism. Slower dynamics of rings would be an immediate consequence of these observations.

In fact similar scaling laws are found for the viscosity of linear and cyclic chains versus molecular weight. Below the entanglement molecular weight M_c, the viscosity increases following the scaling law $\eta \sim M^{1.5}$ which is

larger than the ideal Rouse law $\eta \sim M$. Above M_c, the viscosity increases more rapidly for both linear and cyclic polymers $\eta \sim M^{3.4}$. The threshold molecular weight for entanglement M_c is found to be higher for cyclic polymers. The reason is not quite clear but it is argued that it could be due to the fact that chain conformation in the bulk is partially collapsed and hence rings are less effective in forming entanglements.

16.6 Conclusions

Various properties of cyclic polymers are discussed in this work. In many ways, they are found quite distinct from those of linear chains. From a thermodynamic point of view, this distinction is characterized by compatibility enhancement due to a loss of entropy as a result of chain closure. A shift in the theta temperature of dilute solutions of cyclic polymers in solvents is observed. Excluded volume effects are stronger for cyclic chains in solution as compared to those of corresponding linear chains of the same mass at the same temperature. The mean square radius of gyration for linear chains is twice the corresponding quantity for rings under theta solvent conditions. In good solvents, several models are available for the description of chain swelling of rings and linear polymers. They do not predict similar tendencies. Perturbation calculations, Flory equation of swelling and field theoretical calculations predict that the ratio $\beta \equiv R_{gl}^2 / R_{gc}^2$ decreases under good solvent conditions and becomes lower than 2, the value obtained under theta conditions in the absence of excluded volume interactions. Bloomfield-Zimm, Yu-Fujita and Bensafi-Benmouna models predict higher values. Existing data obtained from scattering experiments and computer calculations are not sufficient to draw a definite conclusion about the real tendencies although they favor a reduction of β in good solvents. Moreover, the scattering signal from cyclic chains in solution is more enhanced than that of the corresponding linear chains under the same conditions. This enhancement could be attributed to the fact that monomer density is higher around the center of mass of cyclic chains and therefore, it is observed under theta and good solvent conditions. The ratio of square hydrodynamic radii of cyclic and linear chains under theta conditions is about 1.4 which is much lower than the ratio of square radii of gyration. Moreover, the radius of gyration is 50% larger than the hydrodynamic radius for linear chains whereas it is only 25% higher for cyclic chains. Generally, the geometric sizes are much higher than hydrodynamic sizes and the difference is enhanced for linear chains as compared to their cyclic counterparts. In the presence of excluded volume interaction, the geometric size swell even more than the hydrodynamic sizes and this swelling is quite stronger for cyclic chains. These observations are also reflected in the intrinsic viscosities since this is

788

proportional to the product of the hydrodynamic radius and the square radius of gyration. Since the sizes of linear chains are higher than corresponding cyclic chains, the intrinsic viscosities are higher by a factor of 2 or more. The intrinsic viscosity of cyclic chains increases more than corresponding open chain systems under the effects of excluded volume interaction. The ratio of intrinsic viscosities of linear and cyclic polymer solutions increases strongly with excluded volume interactions.

References

1. J.A.Semlyen,*Cyclic PoIymers,*Chapter 1,Elsevier,London,1986.

2. J. A.Semlyen, *Large Ring Polymers,*Wiley,Chichester, 1996.

3. M.Benmouna,A.Bensafi,T.A.Vilgis,U.Maschke,B.Ewen,Recent Res. Devel. in Polymer Science,**1**,175(1997).

4. A.Bensafi, U. Maschke, M. Benmouna, Polymer International, Volume 49, 1-9 (2000).

5. M.Benmouna,R.Borsali,H.Benoit,J.PhysiqueIIFrance,**3**,1041(1993).

6. M.Brereton,T.A.Vilgis,J.Phys.A :Math.Gen.,**28**,1149(1995).

7. A.K.Kholodenko,T.A.Vilgis,J.Phys.A :Math.Gen.**29**,939(1996).

8. H.Benoît,J.F.Joanny,G.Haziioannou,B.Hammouda,Macromolecules,**26**,5790(1993).

9. R.Weill,J.Vingrad,Proc.Natl.Acad.Sci.(USA),**50**,730(1965).

10. G.Hadziioannou,D.Cotts,G.tenBrinke,C.C.Han,P.Lutz,C.Strazielle,P.Rempp,A.Kovacs, Macromolecules,**20**,493(1987).

11. F.Candau,P.Rempp,H.Benoît,Macromolecules,**5**,627(1972).

12. E.J.Amis,D.F.Hodgson,W.Wu,J.Polym.Sci.,Polym.Phys.Ed.,**31**,2049(1993).

13. A.C.Dagger,J.A.Semlyen,Polym.Prepr.,ACS,Div.Polym.Chem.,**39**(1),579(1998).

14. G.Hild,C.Strazielle,P.Rempp,Eur.Polym.J.,**16**,843(1983).

15. G.B.McKenna,G.Hadziioannou,P.Lutz,A.J.Kovacs,Macromolecules,**20**,498(1987).

16. H. Yamakawa,*Modern Theory of Polymer Solutions*,Harper and Row,NY,1971**.**

17. W.Burchard in *Cyclic Polymers,* ed. by J.A.Semlyen,Elsevier,London,1986.

18. A.V.Vologodskii,A.V.Lukshin,M.D.Frank-Kamenetskii,V.V.Anshelevich,Sov.Phys. JETP,**39**,1059(1974).

19. A.V.Vologodskii,A.V.Lukshin,M.D.Frank-Kamenetskii,Sov.Phys.JETP,**40**,932(1975).

20. M.D.Frank-Kamenetskii,A.V.Lukshin,A.V.Vologodskii,Nature,**258**,398(1975).

21. W.Burehard,E.Michel,V.Trappe,Macromolecules,**29**,5934(1996).

22. P.J.Flory, *Principles of Polymer Chemistry*, Cornell University Press,Ithaca,NY,1956.

23. J.Leonard,J.Polym.Sci.,Polym.Phys.Ed.,**31**,1496(1993).

24. J.Leonard,J.Phys.Chem.**93**,4346(1989).

25. M.Abramowitz,I.A.Stegun,in *Handbook of Mathematical Functions*,Dover Publications Inc., NY,1972.

26. J.Dudowicz,K.F.Freed,Macromolecules,**24**,5076(1991).

27. A.R.Khokhlov,S.K.Nechaev,J.Phys.IIFrance,**6**,1547(1996).

28. P.Lutz,G.B.McKenna,P.Rempp,C.Strazielle,Makromol.Chem.Rapid Com.**7**,599(1986).

29. J.J.Prentis,J.Chem.Phys.**76**,1574(1982).

30. B.H.Zimm,W.H.Stockmayer,M.Fixmann,J.Chem.Phys.**21**,1716(1953).

31. B.H.Zimm,W.H.Stockmayer,J.Chem.Phys.,**17**,1301(1949).

32. C.J.C.Edwards,R.F.T.Stepto,J.A.Semlyen,Polymer,**21**,781(1980).

33. C.J.C.Edwards,R.F.T.Stepto,J.A.Semlyen,Polymer,**23**,869(1982).

34. M.B.Huglin,M.B.Sokro,Polymer,**21**,651(1980).

35. J.S.Higgins,K.Dodgson,J.A.Semlyen,Polymer,**20**,553(1979).

36. K.Kuwahara,T.Okasawa,M.Kanako,J.Polym.Sci.,Part C,**23**,543(1968).

37. T.Pakula,S.Geyler,Macromolecules,**21**,1665(1988).

38. M.E.Cates,J.M.Deutsch,J.Phys.(Paris),**47**,2121(1986).

39. M.Muller,J.P.Wittmer,M.E.Cates,Phys.Rev.E,**53**,5063(1996).

40. O.Jagodzinski,E.Eisenriegler,K.Kremer,J.Phys.I,France,**2**,2243(1992).

41. T.Pakula,Macromolecules,**20**,2909(1987).

42. S.Geyler,T.Pakula,Makromol.Chem.RapidCom.**9**,617(1988).

43. J.desCloizeux,M.L.Metha,J.Phys.(Paris),**40**,667(1979).

44. C.A.Croxton,Macromolecules,**25**,4352(1992).

45. C.A.Croxton,Macromolecules,**24**,537(1991).

46. W.Burchard,M.Schmidt,**21**,745(1980).

47. M.Fukatsu,M.Kurata,J.Chem.Phys.**44**,4539(1966).

48. W.Stockmayer,A.C.Albrecht,J.Polym.Sci.,**32**,215(1958).

49. P.G.de Gennes,*Scaling Concepts in Polymer Physics*,Cornell University Press,Ithaca, NY,1979.

50. J.des Cloiseaux,G.Jannink,*Polymers in solution,*Clarenton Press,Oxford(1990).

51. M. Daoud,PhD-Thesis,Université Paris VI(1977).

52. B.Farnoux,Ann.Phys.**1**,73(1976).

53. A.Peterlin,J.Chem.Phys.**23**,2464(1955).

54. G.Weill,C.Loucheux,H.Benoît,J.Chim.Phys.**55**,540(1958).

55. T.Pakula,K.Jeszka,"Simulation of single complex macromolecules",reprint 1998.

56. V.Bloomfield,B.H.Zimm,J.Chem.Phys.,**41**,315(1966).

57. H.Yu,H.Fujita,J.Chem.Phys.,**52**,1115(1970).

58. L.Larabi,A.Bensafi,T.A.Vilgis,U.Maschke,M.Benmouna,in preparation.

59. E.F.Casassa,J.Polym.Sci.,Part A,**3**,605(1965).

60. B.Berne,R.Pecora,*Dynamic Light Scattering*,Wiley,New York,1976.

61. W.Brown,*Dynamic Light Scattering - the method and some applications,*Clarendon Press, Oxford,1993.

62. M.Doi,S.F.Edwards,*The Theory of Polymer Dynamics,*Clarendon Press,Oxford,1986.

63. F.Mezei in *Neutron Spin Echo,*ed. by F.Mezei,Lecture Notes in Physics,**122**, Springer Verlag,Berlin,1980.

64. B.Ewen,D.Richter,*Neutron Spin Echo Investigations on the Segmental Dynamics of Polymers in Melts, Networks and Solutions,* Adv.Polym.Sci.,**134**,1(1997).

65. R.Zwanzig, Lectures in Theoretical Physics, Eds. W.E. Brittin, Downsand J.Downs, NY, 1961.

66. Z.Akcasu,H.Gurol,J.Polym.Sci.,Polym.Phys.Ed,**14**,1(1976).

67. Z.Akcasu,M.Benmouna,C.C.Han,Polymer,**21**,866(1980).

68. M.Benmouna,Z.Akcasu,Macromolecules,**11**,1187(1978).

69. J.Seils,R.Pecora,Macromolecules,**25**,350(1992).

70. J.Seils,R.Pecora,Macromolecules,**25**,354(1992).

71. R.Pecora,J.Chem.Phys.,**49**,1032(1968).

72. P.G.deGennes,Physics,**3**,37(1967).

73. E.Dubois-Violette,P.G.deGennes,Physics,**3**,181(1967).

74. W.Burchard,M.Schmidt,Polymer,**21**,745(1980).

75. M.Duval,P.Lutz,C.Strazielle,Makromol.Chem.,**6**,71(1985).

76. K.Dodgson,J.A.Semlyen,Polymer,**21**,663(1980).